



IMPERIAL INSTITUTE
OF
AGRICULTURAL RESEARCH, PUSA.

PROCEEDINGS

OF THE

ROYAL SOCIETY OF LONDON

SERIES A

CONTAINING PAPERS OF A MATHEMATICAL AND
PHYSICAL CHARACTER.

VOL. CXXXIX.

LONDON:

PRINTED FOR THE ROYAL SOCIETY AND SOLD BY
HARRISON AND SONS, LTD., ST. MARTIN'S LANE,
PRINTERS IN ORDINARY TO HIS MAJESTY.

MARCH, 1933.

LONDON:

HARRISON AND SONS, LTD., PRINTERS IN ORDINARY TO HIS MAJESTY,
ST. MARTIN'S LANE

CONTENTS.

SERIES A. VOL. CXXXIX.

No. A 837.—January 2, 1933.

	PAGE
Address of the President, Sir F. Gowland Hopkins, at the Anniversary Meeting, November 30, 1932	1
Sedimentation Equilibrium in the Ultracentrifuge: Types Obtained with Soap Solutions. By J. W. McBain, F.R.S., and M. E. Laing McBain	26
On the Electromagnetic Fields due to Variable Electric Charges and the Intensities of Spectrum Lines According to the Quantum Theory. By G. A. Schott, F.R.S.	37
Gaseous Combustion at High Pressures. Part XIV.—Explosions of Hydrogen-Air and Carbonic Oxide-Air Mixtures at Initial Pressures up to 1000 Atmospheres. By W. A. Bone, F.R.S., D. M. Newitt and D. T. A. Townend	57
Gaseous Combustion at High Pressures. Part XV.—The Formation of Nitric Oxide in Carbonic Oxide-Oxygen-Nitrogen Explosions. By D. T. A. Townend and L. E. Outridge. Communicated by W. A. Bone, F.R.S.	74
Gaseous Combustion at High Pressures. Part XVI.—Nitric Oxide Formation in Continuous High-Pressure Flames of Carbonic Oxide in Oxygen-Nitrogen Atmospheres. By D. M. Newitt and F. G. Lamont. Communicated by W. A. Bone, F.R.S.	83
On the Surface Potentials of Unimolecular Films of Ergosterol -The Photochemical Formation of Vitamin D. By R. J. Fosbinder. Communicated by E. K. Rideal, F.R.S.	93
The Theory of the Crystal-Photoeffect. By H. Teichmann. Communicated by R. H. Fowler, F.R.S.	105
Electron Scattering in Helium. Absolute Measurements at 90° and 45°. By S. Werner. Communicated by N. Bohr, For. Mem. R.S.	113
A New Primary Standard Barometer. By J. E. Sears, Junr., and J. S. Clark. Communicated by Sir Joseph Petavel, F.R.S. (Plate I)	130
The Combination of Hydrogen and Oxygen Photosensitised by Nitrogen Peroxide. By R. G. W. Norrish and J. G. A. Griffiths. Communicated by Sir William Pope, F.R.S.	147
Applications of the Method of Impact Parameter in Collisions. By E. J. Williams. Communicated by R. H. Fowler, F.R.S.	163
The Collision of Slow Electrons with Atoms. II.—General Theory and Inelastic Collisions. By H. S. W. Massey and C. B. O. Mohr. Communicated by R. H. Fowler, F.R.S.	187

	PAGE
Interferential Comparison of the Red and other Radiations emitted by a New Cadmium Lamp and the Michelson Lamp. By J. E. Sears, Junr., and H. Barrell. Communicated by Sir Joseph Petavel, F.R.S. (Plate 2)	202
The Thermodynamics of Adsorption at the Surface of Solutions. By E. A. Guggenheim and N. K. Adam. Communicated by F. G. Donnan, F.R.S.....	218

No. A 838.—February 1, 1933.

On the Flow of Electric Current in Semi-Infinite Stratified Media By L. V. King, F.R.S.	237
The Air Pressure on a Cone Moving at High Speeds—I and II. By G. I. Taylor, F.R.S., and J. W. Maccoll (Plates 3 and 4)	278
A Theoretical Investigation of the Oxygen Atom in various States of Ionisation. By D. R. Hartree, F.R.S., and M. M. Black	311
The Corpuscular X-Ray Spectra of the Radio-Elements. By C. D. Ellis, F.R.S. (Plate 5)	336
The Concepts of Inverse Probability and Fiducial Probability Referring to Unknown Parameters. By R. A. Fisher, F.R.S.	343
On the Foundations of the Electron Wave Equation. By S. R. Milner, F.R.S.....	349
The Internal Conversion of the γ -Rays and Nuclear Level Systems of the Thorium B and C Bodies. By C. D. Ellis, F.R.S., and N. F. Mott....	369
On the Arc Spectrum of Iodine By S. C. Deb Communicated by M. N. Saha, F.R.S. (Plate 6)	380
On the Absorption Spectra of Some Higher Oxides. By A. K. Dutta and P. K. Sen Gupta. Communicated by M. N. Saha, F.R.S. (Plates 7 and 8).....	397
The Kinetics of Electrode Processes. Part II—Reversible Reduction and Oxidation Processes. By J. A. V. Butler and G. Armstrong Communicated by J. Kendall, F.R.S.	406
The Stark Effect for Xenon. By H. W. Harkness and J. F. Heard. Communicated by A. S. Eve, F.R.S. (Plates 9-12)	416
The Efficiency of Secondary Electron Emission By S. R. Rao. Communicated by O. W. Richardson, F.R.S.	436
The Beneficial Effect of Oxidation on the Lubricating Properties of Oil. By R. O. King. Communicated by H. T. Tizard, F.R.S. (Plate 13)	447
The Atomic Scattering Factor for X-Rays in the Region of Anomalous Dispersion. By D. Coster and K. S. Knol. Communicated by W. L. Bragg, F.R.S.....	459
The Application of Quantum Mechanics to Chemical Kinetics. By R. P. Bell. Communicated by C. N. Hinshelwood, F.R.S.	466

No. A 839.—March 3, 1933.

On the Calculation of Stresses in Braced Frameworks. By R. V. Southwell, F.R.S.	475
Fluorescent Excitation of Mercury by the Resonance Frequency and by Lower Frequencies.—V. By Lord Rayleigh, For. Sec. R.S. (Plate 14)	507

	PAGE
On the Refractivity of Para-Hydrogen. By Clive Cuthbertson, F.R.S., and Maude Cuthbertson	517
X-Ray Study of Copper-Cadmium Alloys. By E. A. Owen and L. Pickup. Communicated by Sir William Bragg, F.R.S. (Plates 15 and 16)	526
The Photochemistry of Phosphine. By H. W. Melville. Communicated by J. Kendall, F.R.S.	541
The Relationship between Viscosity, Elasticity and Plastic Strength of a Soft Material as Illustrated by some Mechanical Properties of Flour Dough —II. By R. K. Schofield and G. W. S. Blair. Communicated by Sir John Russell, F.R.S.....	557
The Parent of Protactinium. By O. A. Gratias and C. H. Colhe. Communicated by F. A. Lindemann, F.R.S.	567
Thermal Decomposition and Detonation of Mercury Fulminate. By W. E. Garner and H. R. Hales. Communicated by Sir Robert Robertson, F.R.S.	576
On the Diffuse Double Layer. By J. Lens. Communicated by F. G. Donnan, F.R.S.	596
The Positive Ion Work Function of Tungsten for the Alkali Metals. By R. C. Evans. Communicated by Lord Rutherford, O.M., F.R.S.	604
Analysis of α -Rays by an Annular Magnetic Field. By Lord Rutherford, O.M., F.R.S., C. E. Wynn-Williams, W. B. Lewis, and B. V. Bowden. (Plate 17) ...	617
The Relative Velocities of the Alpha-Particles from Thorium X and its Products and from Radium C'. By G. H. Briggs. Communicated by Lord Rutherford, O.M., F.R.S.	636
The Maximum Energy of the β -Rays from Uranium X and other Bodies. By B. W. Sargent. Communicated by C. D. Ellis, F.R.S.	659
The Hyperfine Structure of the Lines of the Arc Spectrum of Rubidium. By D. A. Jackson. Communicated by F. A. Lindemann, F.R.S.	673
The Broadening of the Ultraviolet Absorption Bands of Xenon under Pressure. By J. C. McLennan, F.R.S., and R. Turnbull. (Plates 18-20)	683
Some Photographs of the Tracks of Penetrating Radiation. By P. M. S. Blackett and G. P. S. Occhialini. Communicated by Lord Rutherford, O.M., F.R.S.	699
Index	727

PROCEEDINGS OF THE ROYAL SOCIETY.

SECTION A.—MATHEMATICAL AND PHYSICAL SCIENCES.

Address of the President, Sir Frederick Gowland Hopkins, at the Anniversary Meeting, November 30, 1932.

In accordance with pious custom I will begin my Address by recalling the losses that the Society has sustained during the year behind us. Two of our Foreign Members have passed away and fourteen of our Fellows :—

I will speak first of the former :

KARL RITTER VON GOEBEL. Von Goebel was supreme in the field of plant morphology, and played a leading part in guiding that branch of science on to modern lines. His influence was exerted in bringing the circumscribed and formal studies of morphology into closer contact with experiment and relating them with function. He gave to the subject a philosophical outlook. While a learned student of Form, he was also himself an experimentalist, and one less concerned with the construction of phylogenetic theories than with the study of causation. In illustration his experiments dealing with the effect of environment on symmetry may be quoted. His contributions to science were extensive and various, ranging in their date of publication from 1877 until near his death. His encyclopædic book, "*Organographie der Pflanzen*," exerted a great influence upon the thought of others. Of von Goebel an informed writer has said that "he leaves behind the memory of a gracious personality to whom the science of botany owes a supreme debt, not only as a great observer, but also as a safe guide to correct channels of thought."

GRAHAM LUSK. Lusk devoted the whole of his active life, from early manhood to its end, to patient studies of the problems of animal nutrition. As a student he worked successively with Carl Voit and Max Rubner, and in his own work he most profitably combined the methods of both of these investigators; the chemical studies which derived from the former were checked and extended by the calorimetric technique of the latter. Lusk contributed much of importance to our knowledge of nutrition and metabolism, and especially to that of the intermediary stages in the metabolism of the main foodstuffs. His book, "*The Science of Nutrition*," exerted a wide influence. He was one of the American representatives on the Inter-Allied Scientific Food Commission in 1917, and his wide knowledge was of great

service to that body. Lusk was a man who stood for the highest standards in science, conduct, and all things else, and won the deep respect of all scientific circles in America. He had many friends in this country, and his friendship was a gift enjoyed by all who possessed it. The circumstances of his election to our Membership were sad. He had received news of it with deep gratitude, and then before many days had passed he was no more.

I will speak of the Fellows in the order of their demise :

ALFRED FERNANDEZ YARROW. A great marine engineer and shipbuilder ; a great benefactor to science, and a great-hearted man. Lady Yarrow in her biography of her husband quotes his first schoolmaster as saying that he " was born with two leading features—a talent for engineering and a thirst for affection—to give and to receive." The talent and the thirst remained with him throughout a long life, the latter being sometimes revealed even to the least intimate of his friends. How early the talent was displayed is made evident in the biography, and it is of interest to recall how as a boy he constructed and installed with the aid of a friend the first private overhead telegraph in London. He was apprenticed to a London shipbuilding firm before he was sixteen, and at the end of that apprenticeship, finding the firm unwilling to help him, and having collected a little capital, he determined to be independent, and, together with a friend called Hadley, started ship-building works of his own on the Thames. These works rapidly became a centre of great activity and obtained a reputation which may be measured by the fact that, when Yarrow determined to move to the Clyde in 1905-6, over 400 invitations were received from various local authorities, all anxious that so flourishing an enterprise should come into their midst. It is impossible to give here even a bare list of Yarrow's successes in developing speed and efficiency in ships. His reputation especially grew during the period when he was busy constructing fast torpedo boats and destroyers, but he built many other types of vessel, and many which possessed qualities quite remarkable in their day. In his efforts to increase speed he contrived, and after many years of expensive experiment, constructed the water-tube boiler with which his name will always be associated ; this, however, was but one out of many successes which he fathered.

It was in 1923 that Yarrow handed to the Royal Society £100,000 for the furtherance of research, with the one stipulation that none of it should be employed in expensive building. He was entirely satisfied with the policy which led to the foundation of the Research Professorships carrying his name. Characteristic of him was the modesty which led to his surprised gratification

on his election to the Fellowship in 1922. He retained great activity of mind and an adventurous spirit up to his last and ninetieth year.

WILLIAM DAVID DYE, an experimentalist of the very highest rank, began his all too short scientific career as Student Assistant at the National Physical Laboratory. In that home of precision, where the attainment of ultimate accuracy is ever sought, he found an atmosphere entirely suited to his genius. He came under the influence of Mr. Albert Campbell, the beauty of whose experimental work stimulated Dye and started him in the employment of his own talent for the development of new methods. He soon gained a reputation for highly accurate work on the primary electrical standards and units. After the war he succeeded Dr. F. E. Smith as head of the Electrical Standards Division of the Laboratory, and continued to develop methods of great accuracy in such fields as terrestrial magnetism and radio frequency. In everything related to Radio Standards he became a recognised authority. He was elected Fellow of the Society in 1928.

JAMES MERCER. Mercer was a mathematician who did brilliant work while holding a research Fellowship at Trinity College, Cambridge. In subsequent years other claims upon his time, and unsatisfactory health, limited his output. His original work extended and illuminated the Theory of Integral Equations and covered other ground of much importance in pure mathematics. A paper on the Limits of Real Variants which he published in 1906 has inspired quite recent work. Another in 1909 describes work which led to the result known as Mercer's Theorem. He held the post of Assistant Lecturer at Liverpool University and later became Fellow and Lecturer of Christ's College, Cambridge. He was elected to the Society in 1922.

Sir FREDERICK ANDREWES. Andrewes was a pathologist, more especially concerned with bacteriology, who always kept in close touch with the clinician. It was his constant desire that his science should serve the immediate needs and promote the current progress of practical medicine. This did not involve a lack of interest in the wider problems of bacteriology as a branch of biology, but it perhaps led to the circumstance that his scientific work, though always significant, greatly helpful, and covering a wide field, was for the most part concerned with practical details. Of wide interest, however, were studies such as that carried out with T. J. Horder, which provided a basis for the classification of pathogenic streptococci, and the serological analysis of dysentery and the typhoid group of organisms which he pursued during the war. Andrewes was a man of wide culture and a charming companion. He was elected to our Fellowship in 1915.

GEORGE CLARIDGE DRUCE. Although engaged in the exacting business of a retail pharmacist throughout his life, his innate love of Nature in the wild, displayed from his boyhood onwards, led Druce to become a leading authority on the British flora. Of this he possessed an intimate personal knowledge gained by frequent visits to all parts of the country. His book "The Flora of Buckinghamshire" of which the last edition was published as late as 1930, is a classic of its kind. He wrote much upon other local floras and kept in constant touch with every advance in field botany. His business was in Oxford, and he enjoyed close association with University authorities. In 1895 he was made Curator of the Fielding Herbariums, and was attached to Magdalen College with an honorary M.A. degree. Later he became D.Sc. The life of Druce was of a quality which the Society did well to honour. He was elected to the Fellowship in 1927.

ERNEST HOWARD GRIFFITHS. Griffiths had been for some years a private science tutor at Cambridge before he displayed the urge for research. In 1887 he started work in the Sidney College Laboratory, almost in solitude, and began an attack on the problem which directly, or indirectly, occupied most of his years as an investigator. This was to determine Joule's Constant with the electrical method raised to a high degree of accuracy. The needs of this problem led him to investigate platinum thermometers and the measurement of platinum temperature as introduced by Callendar, and he published several papers on the subject. His publication "On the Value of the Mechanical Equivalent of Heat" which appears in the 'Philosophical Transactions' for 1893, is of permanent importance. In 1901 he became Principal of University College of South Wales, and the duties of that post interrupted his research activities for several years. Later, however, when a research laboratory was built at his University, he did further work, and just before the war published, along with Dr. Ezer Griffiths, papers upon the heat capacity of metals. He passed his later years in retirement at Cambridge, suffering unfortunately from bad health, but retaining all his scientific interests. He became a Fellow in 1895, and was later awarded the Hughes Medal.

SIR HORACE PLUNKETT was one whose qualifications for sharing our Fellowship were other than those most commonly recognised. He had no close knowledge of science or its methods, and perhaps no special interest in it for its own sake. He recognised, however, that science could help towards the accomplishment of the great aim of his life, and realised this perhaps more and more during the progress of his efforts. Moreover he saw, as a sympathetic biographer has remarked, that science applied to things must be controlled

by science applied to men. As is well known, the object of his ambition was the regeneration of Irish rural life. To this end he started a great movement which was to unite all classes, creeds and parties in an endeavour to promote economic and social progress in his native country, and particularly to secure higher standards of living and enterprise among those who cultivated her soil. Under his inspiration the Irish Agricultural Organisation Society which he started in 1894 secured the unity he hoped for, and the result was a new and real co-operation among agriculturists. At a later date the disintegrating forces of politics interfered with his beneficent policy, and the sad aftermath of the war led to the destruction of his home in Dublin. He resumed his efforts, however, when thereafter resident in England, and continued them to the end. Surely, if indirectly, he did much for the advancement of agricultural science, and his services were recognised by his election to the Society in 1902.

SIR WILLIAM WATSON CHEYNE. The science of Pathology towards the end of the last century stood deeply in debt to this distinguished surgeon. While himself a pioneer in bacteriological research he did more perhaps than anyone else during the eighteen seventies and eighties to make known in this country the bacteriological researches which were proceeding so rapidly in Germany and France and to interpret their results. English pathologists enmeshed in the details of morbid anatomy, and more used to descriptive than to experimental methods, were then contributing little or nothing to bacteriology. The influence of Watson Cheyne, however, greatly stimulated interest and research in the subject. In his younger days he wrote and worked under the inspiration of Lord Lister, whom he served as House Surgeon, first at Edinburgh and later at King's College, London. Had he possessed independent means, then very necessary for complete devotion to pathology, there is little doubt that he would have chosen a scientific career; but he was compelled to earn his living as a surgeon, and in that calling he attained to eminence. He was elected to the Fellowship in 1894.

JOHN WALTER GREGORY. It has been justly claimed that Gregory of all British geologists was the most widely known. Urged by a natural lust for travel, but always in pursuit of significant knowledge, he explored the world. That he was a geographer as well as a geologist explained, perhaps, the nature of his special interests; but it must not be forgotten that he was incidentally also a palaeontologist, petrologist and mineralogist. He was well equipped, therefore, to appreciate all the evidence concerning earth structure and earth history that travel presents to eyes and mind. He knew Spitzbergen and no

less Thibet. The face of nearly every inhabitable country was familiar to him, and he himself was well known at every centre where the subjects of his interest were being studied. Gregory began his scientific career as an assistant at the British Museum. Later he became Professor of Geology in Melbourne, and finally, for a quarter of a century held the chair of that subject in Glasgow. As a teacher of the subject he was highly successful. All who knew him well testify to his great and accurate erudition, and to that originality of outlook which is manifest in his writing. Some two hundred published papers bear witness to his intellectual fertility. Though 68 years old he was yet on a venturesome quest when an unhappy accident led to his death. He was drowned last June by the overturning of his canoe when on the River Urubamba in Northern Peru. He was elected a Fellow in 1901.

SIR RICHARD THRELFALL One might be content to describe Threlfall as one of the greatest of electro-chemists ; as one who, combining chemical insight with the aptitudes of an engineer, and much scientific acumen, notably promoted the progress of industrial chemistry. Such a description would, however, be inadequate. In more than common measure personality and character contributed to Threlfall's influence. Contact with him was for his contemporaries a refreshing stimulus, for younger workers it meant sure help and encouragement. While bent on successful accomplishment for himself, he loved success in others.

In his student days at Cambridge, he was an athlete of note. Many will have enjoyed the tale, as told by Sir Joseph Thomson and others, of his successful fight for the recognition of Rugby football as a sport entitled to the award of "Blues"

After acting as Demonstrator in the Cavendish Laboratory he went to Sydney as Professor of Physics. In 1889 he returned to England and joined the firm of Albright and Wilson, the great producers of phosphorus, at Oldbury. Among the most interesting and enterprising of his researches while at Sydney was his comparison of values for gravity at different places by means of a quartz thread balance. He was able to claim high accuracy for these determinations. During his later years he did further work with the same balance. It remained at Sydney after Threlfall resigned his Chair there, until, in 1923, at the suggestion of Sir Frank Smith, it was brought to this country for study. Its subsequent history is told in a fascinating paper by Threlfall and A. J. Dawson in our 'Philosophical Transactions' of the current year. In his earlier years he invented the rocking microtome, an instrument which has been of priceless value to many branches of biological study. He himself

recently discussed the history of the instrument in the 'Biological Reviews,' published by the Cambridge Philosophical Society. I have referred to his dealings with these two very diverse instruments of precision in illustration of the breadth of Threlfall's interests. On his triumphs in industrial chemistry I need not dwell. The debt that we owe to him, however, cannot be made clear without reference to his war work. The nation's needs were greatly served by his experience and his qualities. The Army, Navy and Air Force all alike benefited by the response of his practical genius to the call of some of their most urgent needs. Threlfall in recent years made a point of attending the Society's meetings as often as was possible, and was our frequent and ever welcome companion at Club dinners. He will be greatly missed. He was elected a Fellow in 1899.

JOHN CHARLES FIELDS. Fields was a highly gifted mathematician well known in particular for his famous treatise on the "Theory of the Algebraic Functions of a Complex Variable." He came early in life under the influence of distinguished German teachers and acquired a deep desire to do, and to encourage original and creative work in his subject. This enthusiasm he brought to his Chair in the University of Toronto where he always advocated, and in every way promoted, the claims of research. It was largely due to his influence that the Legislature of the Province came to make annual grants to the University ear-marked for the encouragement of original work, and he initiated a movement in the direction of having research professorships attached to the Royal Canadian Institute similar to those administered by ourselves. In the teaching of mathematics in Canada and the United States his influence helped to bring about successful reforms. He became a Fellow in 1913.

SIR RONALD ROSS. It has been given to few as it was given to Ross to produce in a few patient years a great gift for humanity; a gift at once complete, straightway ready for use, and of incalculable benefit. Ross, like many other discoverers, was fortunate in his times and contacts. Contemporary thought and knowledge had shaped a course for him, and no man's work could owe more to the inspiration of another man than that of Ross to Manson. Nevertheless Manson himself declared that his own chief claim to a share in the discovery of the secrets of malarial transmission was his discovery of Ross. It required indeed the special gifts of Ross, his fine technique, his determination, and his patient and observant eye to establish so conclusively, and in what was relatively so short a time, the evil influence of *Anopheles*. Let us recognise the happiness of the circumstance that brought the older and the younger man

together. It is impossible in brief paragraphs to follow the stages of Ross's investigation. It offered many difficulties; there were misleading assumptions to disprove as well as new facts to discover. In particular there was long delay from the circumstance that the delinquent sought, the true carrier of the organism, was a mosquito of no common species: in India its number amounted to no more than a fraction of 1 per cent. of those which swarmed round the investigator. In little more than two years, however, the work in essentials was complete. It only remained for good administration to make use of the results. Though this has not always been forthcoming, yet much has been done, and the world, and especially the British Empire, has received a priceless favour. Ross became a Fellow of the Society in 1901, was Vice-President 1911-15, and received the Royal Medal in 1909.

ALFRED CHASTON CHAPMAN. Chapman's activities were exceptional in that, although engaged from his student days onwards in a professional practice, which grew to be large and exacting, he made time for personal researches which contributed not a little to the advance of pure science. He was deeply interested in some of the wider issues of both chemistry and biology, and he formed independent views concerning them. At the same time he took pride in his profession, and did all he could to promote within it high standards of education and practice. In Presidential Addresses to the Society of Public Analysts, after stating his belief in the educational value of the subject, he urged that Chairs of Analytical Chemistry, directed to giving sound technical training to future professional chemists, should be established in Universities. His interest in mycology and applied bacteriology and a belief in the practical importance of these led him to advocate with equal conviction the foundation of an Institute of Microbiology, which unfortunately this country still lacks.

Chapman gave his time unsparingly to enterprises in which he believed, and he was a highly useful member of a great number of Boards and Committees. He became President of the Institute of Chemistry, of the Society of Public Analysts, and of the Royal Microscopical Society. His personality, unique in many ways, carried a charm which none could fail to recognise. He was elected in 1920.

Sir DUGALD CLERK was a man of great inventive power, whose researches on internal combustion engines and on every aspect of the use of gaseous fuels have contributed greatly to the progress of industry and to human comfort and enjoyment. His work on the specific heat of gases, and that on explosion pressures, are instances of his important contributions to pure science. In

the War he served as Director of Engineering Research at the Admiralty, and was Chairman of the Internal Combustion Engine Committee of the Air Ministry. He was elected to our Fellowship in 1908, and received a Royal Medal in 1924.

The sum total of accomplishment involved in the work of all these, our comrades who are no more, is surely great and worthy of all remembrance.

Mr. Aldous Huxley, writing in just praise of the literary, as distinct from the scientific, work of his grandfather, remarks that Thomas Henry Huxley *was* a hero of science; but *is*, and will remain, a hero of literature. He develops the theme that individual scientific accomplishment, unlike literary accomplishment, is fated to be forgotten, because it is always but a step in progress, and loses its importance as knowledge grows and widens. The truth of this view is, I think, but limited. Great personal accomplishment in science is not forgotten, even if for obvious reasons it is stored in fewer memories than is great literature. Yet I think the historians of science should meet with all encouragement, and not alone because of their piety towards past labours. The perspective of history is illuminating and a corrective at all times. It is especially valuable in maintaining sound judgments in times of revolution; and science to-day is revolutionary. I hope that you will agree with me that Chairs in the History of Science are among the needs of our time.

Whatever of truth there may be in Mr. Huxley's dictum is illustrated *mutatis mutandis* by the life of Christopher Wren. By the majority of his fellow-countrymen Wren is remembered as the great architect, relatively few have kept in memory his greatness as a pioneer in experimental science. But we of the Royal Society in the year of the tercentenary of his birth should surely have in mind his services to the Society, at its birth, and during its infancy. No one who has read our early history, or who alternatively is familiar with the life story of Wren, can doubt that the measure of those services was truly great. You will remember how that group of enthusiasts who had the advance of experimental science at heart attended together a lecture by Wren at Gresham College, and immediately after it sat down to plan for the future. At this meeting, for which attendance at Wren's lecture had served as a sort of ceremony of dedication, the formation of our Society was, in principle at least, decreed. All concerned doubtless felt the refreshing quality of Wren's optimism. Once the actual work of the Society began, his activity inspired every meeting. His keen but rational delight in experiments of all kinds, his mechanical and artistic skill, his quite extraordinary versatility and, not less important, his lovable nature and unselfish helpfulness: all these qualities he

brought to the service of the infant Society to its immense advantage. Wren's own original work was, it is true, not fated to influence the future of science as did that, say, of his contemporary, Robert Boyle, but his personal qualities were exactly adjusted to the service of experimental science when making its first tentative endeavours.

We have arrived at a period when the tercentenaries of the birth of original Fellows, and of those elected early, have occurred, or will occur, frequently in the course of a small span of years. It is beyond our power and resources to organise a public celebration for each such case, however great the desire to do so. But on right occasions our own memories should wake.

And this year we should have specially in mind one other of our early Fellows, the dates of whose birth and death nearly coincided with those of Wren, but whose whole personality differed widely from his save in the fertile curiosity concerning Nature which they equally shared. There would be, in any case, small need to remind you of Antony van Leeuwenhoek's happy relations with this Society. The need is the less because the pious and prolonged labours of our Fellow, Mr. Clifford Dobell, have given us a book in which we may find the quaint, lovable and altogether remarkable personality of the man made for us almost a living figure. You will recall that Leeuwenhoek in 1673 got into touch with Oldenburg, our active Secretary of those days, and then, for fifty years, constantly transmitted to the Society all his microscopical observations and discoveries. Very numerous papers and letters from him are preserved in our archives. His skill in making lenses, by methods which he kept secret, was almost miraculous. Those who were fortunate enough to attend a recent meeting of the Society when Professor D'Arcy Thompson gave a demonstration, saw proof that one of these simple biconvex lenses could show the structure of a diatom with a definition equal to that given by a modern compound microscope. Leeuwenhoek was elected a Fellow of the Society in 1679.

Allow me yet a reference to one other among the great men whose association with the Society illumined its past. Elected in 1688 was Marcello Malpighi, the manuscripts of whose contributions to our early Transactions are another of the great treasures of our archives. In contrast to Leeuwenhoek, who made and used his microscopes as an amateur, Malpighi held Chairs of Anatomy in several of the great Italian schools of medicine, and was physician to the Pope of his day. His researches covered a wide range in the comparative anatomy of animals and plants, and his richly illustrated accounts of the development of the chicken in the incubated egg, of which the original

manuscripts and drawings are, let me remind you, in our library, made him the founder of the science of embryology. He also first saw the connexion of arteries and veins by the network of capillary vessels, though a clearer account of these and of the blood corpuscles passing through them was given by Leeuwenhoek. The Society may well be proud that these two great pioneers in biology and in the use of the microscope were enrolled among its early Fellows, and that its Transactions gave many of their greatest discoveries to the world.

The Report of Council contains the customary account of the activities of the Society during the year. I will refer here to a few items of special interest.

An important benefaction has increased our opportunities for supporting the work of highly qualified investigators. The late Mr. Gordon Warren, shortly before his death, placed at the disposal of the Society the sum of £1,400 annually for a period of seven years for the purpose of maintaining a Research Professorship or two Research Fellowships. Council gratefully accepted the proposal, and the first two Warren Research Fellows, Dr. A. J. Bradley and Dr. W. Hume-Rothery, were appointed in June.

Mr. Warren's death occurred with tragic suddenness while he was considering further plans for the benefit of scientific research. In his will he left a large sum in the hands of his bankers, which, subject to a life interest, will ultimately be devoted to the purpose of science. It was his expressed wish that the Royal Society should be consulted in the matter of its disposal, because of his conviction, which most will feel to be justified, that the Society is especially well qualified to advise on such matters.

The award of a Messel Research Fellowship to Mr. C. N. Hinshelwood, who was elected to the Fellowship of the Society three years ago, will, I believe, give general satisfaction. The Society is fortunate when it is able by such appointments to secure for distinguished investigators increased opportunities for research.

Various grants from our Trust Funds are enumerated in Council's Report. I may mention that the Royal Society Mond Laboratory at Cambridge, towards the building of which we provided £15,000 from the Mond Fund, is now practically complete and will be opened early in February next.

As the result of the Government's Conversion Scheme, and for other reasons, important changes have been made in our holdings of Stocks. The result has been a slight reduction in the income of some of our Trust Funds, but Council are convinced that the changes will be to the advantage of the future financial position of the Society.

I would draw attention, as important to all Fellows, to the Report of the Library Committee which has been adopted by Council. In particular I will emphasize the desire of the Committee that the Library should possess a copy of every book of importance written by a Fellow of the Society. It is hoped that authors will look upon the presentation of such books as a normal obligation.

An event of the year with which the Society is deeply concerned is the retirement of Sir Richard Glazebrook from the Chair of the Executive Committee of the National Physical Laboratory. Sir Richard's services in that capacity, continuing those he rendered as first Director of the laboratory, are of national importance, and their value cannot be overestimated. For the labours which have contributed so much to the creation and development of one of this country's most valuable assets the Royal Society, because of its responsibilities, must ever be especially grateful. The gratitude, however, like the services, should be national.

In now attempting a brief review of some few aspects of scientific progress, I should like to refer, for my text as it were, to the two organised discussions which were held during the current year. The success of these has further justified, I feel, the policy which decided that such discussions should be organised from time to time. In particular they are valuable when they tempt distinguished workers from abroad to visit the Society as contributors to debate. It might be well, I think, if we agreed to break with tradition and on these occasions extend the hours of meeting. I should have found it impossible, in any case, to omit some reference to the discussion, opened by Lord Rutherford in person, on the structure of atomic nuclei. The occasion was remarkably timely, for after a date was fixed for it, but before that date arrived, certain pregnant researches had brought forth supremely important data, with a final rapidity which I think had been unexpected by all concerned. The revelation of these new experimental results and of their great significance gave a dramatic character to the discussion which was felt by all who were present. The atomic nucleus for a long time had seemed to be an impregnable fortress. but missiles of high destructive power have been gradually contrived by almost magical skill in the army of attack, and the fortress, in spite of its formidable potential barrier, is crumbling. It is interesting for the spectator to realise how much is learnt by the commanders of the attack from the nature of the missiles (parts of itself) with which the fortress replies to the bombardment. Even were it within my ability this is, of course,

not the place for an attempt to summarize the discussion. One cannot help recalling, however, the sense of progressive accomplishment which was conveyed in Lord Rutherford's opening address, as for instance when he dealt with the nuclear origin of the γ -rays. Nor can one forget moments of actual excitement as when, recalling a twelve years old prophecy of his own respecting the probable existence of neutrons, he referred to Dr. Chadwick's recent success in producing these entities (of which the mass is unity and the charge zero) by bombarding beryllium with α -particles from polonium. During the discussion a full account of this success was heard for the first time. Exciting again was the moment when your ex-President at the close of his remarks referred to the striking results obtained by J. D. Cockcroft and E. T. S. Walton, also in the Cavendish Laboratory, and but a very short time before the meeting. These investigators (as is by now well known) having constructed an apparatus capable of providing a steady stream of protons, of energy up to 600 thousand volts, successfully employed the stream in the disintegration of the lithium nucleus. "The simplest assumption to make (I quote Lord Rutherford) being that the lithium nucleus of mass 7 captures a proton, and the resulting nucleus of mass 8 breaks up into two α -particles. On this view the energy emitted corresponds to about 16 million electron volts . . ."

It is not unjustifiable to say that before the moment of Cockcroft and Walton's success, man did not know how to release atomic energy on his own initiative, whereas now, though doubtless in a limited sense, he possesses that power. At the same time the phenomenon of transmutation seems to be at hand in full reality. The occasion of this discussion cannot fail to stand out as of much significance in the annals of the Royal Society and in the history of this country's contributions to science. Hence I think my reference to it is fully justified.

The second discussion dealt with the growth of knowledge at a different level of present accomplishment; but with phenomena that are highly significant. It was concerned with recent studies of the nature and properties of those highly active catalysts—the enzymes—the presence of which in each living unit converts a system, which without them would be static, into an organism which is so characteristically dynamic. Anyone who reads in succession the records of these two discussions as found in our 'Proceedings,' will perhaps be tempted to wonder how soon, if ever, intellectual concepts, based upon the phenomena which were the subject of the first, are fated to invade, and perhaps revolutionize thought in the great field of which the second covered part. Will the data of atomic physics ultimately illuminate the processes of life? An interesting question for all biologists. At present we know nothing to

suggest a certain answer. I have indeed met not a few who had a strong *a priori* conviction that life, in some way, in some limited sense at least, makes use of atomic energy, that such ability might indeed be the special stamp of life. Some twelve years ago a distinguished Dutch physiologist, the late Professor Zwaardemaker, thought he had proved that the weak radioactivity of potassium is an indispensable stimulus to certain vital activities; but the importance of this influence would seem to be at most very small. Even Zwaardemaker did not hold that it conditioned life. Its radioactivity is certainly not the main reason for the indispensability of potassium in living systems.

Although they bear very remotely, if at all, on the question I just now raised, it may be logical here to mention certain recent experimental studies which seem to have proved that living tissues may be the seat of radiations able to produce effects at a distance, and to suggest that certain activities in one cell of a tissue can thus influence activities in neighbouring cells. It was claimed some time ago by Gurvitch, a Russian biologist, that when growing cells divide they emit rays which accelerate the processes of division in other cells. The existence of these mitogenetic rays, so called because of the claim mentioned, met at first with general disbelief, and a year ago I might have been disinclined to mention the subject; but work by many during the last year seems to have brought satisfactory proof that chemical reactions in living tissues are indeed accompanied by radiations, and that events in one cell may thus influence other cells without material transmission. The phenomena as described are doubtless related to that of chemiluminescence, which many non-biological reactions display, and may perhaps have affinities with the emission of more intensive radiations by specialised cells in the luminiferous organs of animals or by luminiferous bacteria. The much more general invisible radiations under reference have been now studied by physical methods. Their emission from active cells has been (it is claimed) demonstrated by means of Geiger's Counter; their wave-length measured, and by methods which I must not stop to describe, their specific spectra in various cases duly mapped. It has even been claimed, for instance, that a characteristic spectrum of a radiation from a tetanised muscle is identical with that yielded *in vitro* by a reaction (the breakdown of creatin phosphate) known to occur in active muscle. Many published statements of this kind must be received with hesitation until fully confirmed; but that activities in living cells may be accompanied by radiations recognisable by physical means is now, I think, a fact which is proved. This alone will certainly lead to many fresh lines of enquiry. It is

not yet proved, however, that the phenomena as described, are of fundamental importance, nor even that they are associated with all forms of life.

What, on the other hand, we do know for certain, is that in all living systems in which dynamic events have been adequately studied, the influence of colloidal catalysts is found to be dominant. These catalysts ("enzymes" if you will) exert a specific control over complex chemical reactions, of which the exact co-ordination in time and space is one of the primary characteristics of an organism. It is, I think, difficult to exaggerate the importance to biology, and I venture to say to chemistry no less, of extended studies of enzymes and their action. Of the chemical reactions displayed in an organism few, if any, proceed uncatalysed, while they are reactions so completely and harmoniously organised that all are maintained in complex dynamic equilibrium. If chemical thought is to function with effect in helping towards a description of living systems, it must dwell especially on this chemical co-ordination which, like other aspects of organisation, illustrates that subservience of parts to the whole which characterises an organism. The organising potentialities inherent in highly specific catalysis have not, I believe, been adequately appraised in chemical thought. The concentration of a catalyst or, alternatively, the extent of its active surface will determine the velocity of changes due to its influence, but highly specific catalysts determine in addition just what particular materials, rather than any others, shall undergo change. In this respect they are like the living cell itself, for they select from their environment. Finally the specific catalyst, in virtue of its own intimate structure, determines which among possible paths the course of change shall follow. It has directive powers. Even in a cell juice, or in an extract from living tissues from which all cell structure is absent, experiment has shown that a group of contributory reactions, including syntheses, may proceed in due and just sequence and so lead to the same end result as is normally reached in the intact living system. A striking degree of organisation may indeed be attained in such preparations under the directive influence of the more soluble enzymes derived from the cell or tissue. Much more than must a structured colloidal system, like the intact cell, in which a number of catalysts with such controlling powers are present in circumstances exactly adjusted to a final result, be one in which reactions are conditioned and organised to a high degree without the aid of unknown, or any other influences. I do not expect that all will feel able to admit as much as I myself would like to claim, namely, that the control of events by intracellular enzymes, exerted in the specialised colloidal apparatus of the cell by itself secures the status of the cell as a system which can maintain itself

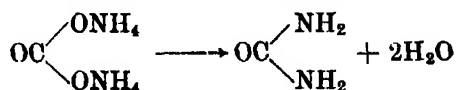
in dynamic equilibrium with its environment. I am not denying for a moment that the cell has esoteric qualities which may call for organising influences of a greatly different kind, exerted maybe at some higher level. It is at any rate sure that the inter-related activity of highly specific catalysts represents a notable device of Nature which has supported during the course of evolution those dynamic manifestations which characterise living things.

The discussion on enzymes greatly profited from the presence of Professor Willstätter, who, together with members of his school, has done so much to advance our knowledge of these agencies. I have sometimes heard it suggested that the advance in question, from a chemical standpoint at any rate, represents a relative failure, apparently because no enzyme has yet been isolated in a state to conform with the classical criteria of "purity." If this be the reason for any suggestion of failure, there is surely some misunderstanding. Isolation, individualisation and purity are words which, if used at all in this domain, may well need to be given meanings differing not a little from those which are applicable in classical organic chemistry. Few will doubt to-day that the specific influence of a catalyst is due to its specific structure. All indications, however, point to the circumstance that the active structure of an enzyme is supported by a colloidal "carrier" which stabilizes it. It is indeed likely that in very many cases, if not in all, the active catalytic mechanism is a specific configuration at part of the surface of a colloidal particle, or, alternatively, part of a structural surface in the histological sense. If so we should no more expect to isolate them in a pure state than so to isolate the active areas on a catalytic metallic surface. It is true that enzymic activity may be displayed by agencies which are not all strictly of one type. It is not unlikely that in certain cases the specifically active groups may be inherent in the structure of a complex but relatively stable molecule, such as that of an exceptional protein. Cases are known indeed in which a protein many times recrystallised retains specific enzymic activity. As was pointed out in the discussion, however, in one such case at least it has been shown that the protein structure can be to a large extent destroyed without disappearance of the activity. Crystallisation in such a case does not yield an entity which would reveal its active structure to the ordinary methods of organic chemistry. What is essential for enzyme studies at their present stage is an assurance that a single entity alone is responsible for this or that observed activity. To this end the technique developed by the school of Willstätter has greatly helped. While we are waiting for the knowledge which may ultimately yield, on lines acceptable to current chemical thought, a method for characterising these exceptional

entities as units, the actual configuration which confers activity on this or that enzyme can be, and in many cases no doubt soon will be, determined by indirect methods. The future of such methods was at least foreshadowed during the discussion, for instance in the contributions of Professor Waldschmidt-Leitz, and Dr. J. H. Quastel.

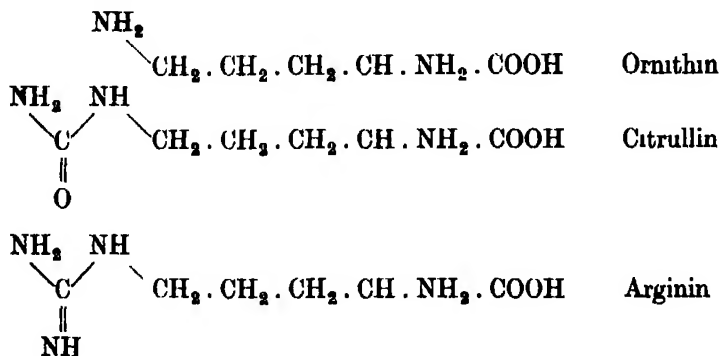
I would like now to illustrate a little further the nature of current progress in animal biochemistry by a reference to investigations dealing with related, but somewhat different aspects of the control of dynamic phenomena in living tissues.

From the researches published during the year I might select many to show that efforts to disentangle the complexities of these phenomena can in their own way be as profitable as any branch of chemical endeavour. I think it will be more useful, however, if you will allow me to refer more particularly to one research which is typical of many in respect of its methods and its success. In this the investigator approached on new lines a fundamental problem which for the last sixty years has been the subject of speculation, and no less of experiments which up to a point were informative. The problem was to discover the nature of the final chemical steps which lead to the production of urea in the animal body. That the mammalian liver can convert ammonium carbonate into urea has been many times experimentally proved, and it is equally sure that ammonia and, of course, carbon dioxide are continuously produced in metabolism. Therefore most of us have long been content to believe that urea arises by the direct removal of the elements of water from the molecule of ammonium carbonate on the lines of the simplest of reactions :



That urea does indeed arise in the liver by a synthesis from ammonia and carbon dioxide remains certain ; but the research under reference, brilliantly carried out by Krebs of Freiburg-im-Brisgau, has shown that its production is on no such simple lines as those mentioned. It calls for a mechanism involving a most interesting interplay among activated molecules. The facts as revealed have just that degree of unexpectedness—if I may use the phrase—which was to be expected in a biochemical phenomenon. I often find myself compelled to assert that though biochemical events are, of course, limited by chemical possibilities, they are not safely to be predicted by chemical probabilities, even when these are strong. That is why experimental biochemistry must remain an independent scientific discipline.

In order to make clear to you the essential results of Krebs' research, omitting of necessity most details, I will ask you to consider the molecular structure of three biological substances : Ornithin, Citrullin and Arginin :—



Note first the structure of ornithin : α — δ — amino valeric acid. In the presence of ammonia and carbon dioxide, and when activated by agencies in the hepatic tissue, ornithin is converted into citrullin, which, as a ureido-acid, already carries the carbamide structure. Urea does not arise directly from this, however, another stage intrudes.

Citrullin takes up another molecule of ammonia (with elimination of water as at the first stage) and the structure of arginin with its guanidin grouping is thus established. Now arginin is the normal substrate for the well-studied and very active hepatic enzyme, arginase ; and under its influence the guanidin group is hydrolysed. Urea thereupon splits off from the arginin molecule and ornithin is reproduced. The sequence is then re-established. Urea is thus produced continuously from the ammonia which arises in the deamination of the amino acids of protein, and from the carbon dioxide of metabolic oxidations in general, but on lines which may seem strangely complex. It would be too much to say at present that this is the only line of origin for urea in the body, but we know now that it is the main line. In maintaining the sequence of reactions, ornithin can function in minute amounts ; acting therefore essentially as a catalyst. The nature of the relations involved in this mechanism is characteristic of the living cell. Analogies may be found, for instance, in those fundamental oxidation-reduction systems which were mentioned in my Address last year.

In another respect the example I am putting before you illustrates the nature of current biochemical studies. The data were obtained by the methods of micro-analysis and only a few milligrammes of hepatic tissue were employed in

individual experiments. Yet the results were consistent and reproducible and experimental errors well under control. The high accuracy to be obtained in ordinary organic analysis by micro methods is now well recognised, but it is becoming clear that technique is so developing that kinetic studies can be made equally accurate on a similar scale. To studies of living systems this offers advantages which cannot be overestimated. One further point : it is becoming more and more a matter for confidence that when tissues with cells intact are quickly removed from the animal after its death and placed straightway in a fluid medium of carefully proved adequacy it only remains to provide an adequate supply of oxygen which shall reach each unit of the tissue, to secure the continuance of the events which had been proceeding *in vivo*. Indeed we are gaining sufficient knowledge of the requirements of such excised tissues to justify the claim that the course of metabolism observed in them during extensive periods of survival need differ in no way from the normal. All such requirements so far as they are known, were provided in the typical research to which your attention has been turned.

I would point out then that we can proceed from the study of tissue extracts in which it is easy to deal with the kinetics of isolated reactions, each determined by its appropriate catalyst, to studies of other tissue extracts, made with discrimination, in which the progress of a variety of reactions retains not a little of the organisation which characterised them during life, and thence to other studies in which we follow the kinetics of reactions controlled by the intact and still living tissues or cells. Thus and otherwise has biochemistry escaped from the dilemma voiced in earlier dogma, namely that since chemical methods must at the very moment of their application convert the living into the dead, they can do nothing to elucidate the dynamic events of life. The escape is more real than may seem on a superficial view, and especially real perhaps to those who are themselves applying modern chemical methods in the biological field.

Statement of Award of Medals, 1932

The Copley Medal is awarded to Dr. George Ellery Hale, For. Mem R.S.

Dr. Hale's first notable achievement was in 1892, when he brought the spectroheliograph to success. This instrument gives a picture of the sun by the light of one spectrum line, and allows the bright clouds of hydrogen and calcium in the upper regions of the sun's atmosphere to be photographed as

projected on the disc. The idea had been suggested and tried much earlier, but Hale was the first to make a workable automatic instrument of this kind. [H. Deslandres was also working with great success on similar lines. Nothing would be gained by a minute analysis of questions of priority, which are not of primary importance. We may compare the case with that of Darwin and Wallace, or with that of Janssen and Lockyer.]

About the year 1895 Hale organised the building of the Yerkes Observatory and of the great refracting telescope there, to which an improved spectroheliograph was adapted. To this period belongs also a masterly investigation of the spectra of certain faint red stars.

The organisation of the Yerkes Observatory would have exhausted the activities of many men. In Dr. Hale's case it was only the precursor of a much larger enterprise, the Mt. Wilson Observatory, with many unique instruments, such as the 150-foot tower telescope and the 100-inch diameter reflector.

At the Mt. Wilson Observatory Dr. Hale made his great discovery of the Zeeman effect in sunspots by observing the circular polarisation of the edges of the broadened spectrum lines, where they cross the spot. Regions of thousands of miles across were thus shown to be the seat of intense magnetic forces, comparable in strength with those used in the dynamo machine. This discovery had been developed in many important directions.

In recent years Dr. Hale has developed the spectrohelioscope, an instrument depending on the persistence of vision which allows us to observe transient phenomena scarcely accessible to the spectroheliograph. We may confidently expect that it will contribute to clearing up the mysterious relations between terrestrial magnetism and solar phenomena.

The Rumford Medal is awarded to Professor Fritz Haber.

For nearly forty years Fritz Haber has been renowned the world over as a leader in the field of physical chemistry. Alike at Karlsruhe, where he went in 1894, and at Dahlen from 1911 to the present time, he has been famed as an ideal Director of Research, inspiring schools of great and highly productive activity. His own early studies of the oxidation and reduction of organic substances by electrochemical methods, and the numerous electrochemical studies which followed this important work; such as his researches on gas cells, on the rate of ionic reactions, on the electrolysis of solid salts, on the velocity of reaction at electrodes, and on the use of the glass electrode, have enormously advanced progress in this branch of science.

His profound study of the thermodynamics of gas reactions culminated in his brilliant researches on the synthetic production of ammonia. With van Oort, Haber had commenced to carry out a preliminary investigation on the ammonia equilibrium, but owing partly to discrepancy with figures obtained by application of the Nernst Theorem, further experiments were made with le Rossignol in 1906. In 1908 satisfactory catalysts had been found and the synthesis of ammonia achieved. The far-reaching technical results of these careful thermodynamical studies are in themselves a monument to Fritz Haber; one of the German factories alone can produce more than 1,000 tons of ammonia daily. The influence of this on the food supply of the world is of the highest importance.

Haber's wide interest, combined with his insight and grasp, made possible application of modern physical principles to a wide range of problems of physical chemistry, such as the determination of molecular structure and calculation of lattice energies, the nature of the amorphous state, chemiluminescence, reaction kinetics and electron emission during chemical reaction. During the past few years Haber has been successfully making manifest the rôle of the hydrogen atom in combustion processes.

By the application of thermodynamical principles in the realm of chemistry Haber has thus not only enriched the mass of human knowledge, but also added to the general welfare of mankind.

A Royal Medal is awarded to Professor Robert Robinson, F.R.S.

Professor Robert Robinson has won world-wide distinction by his work in many branches of organic chemistry, particularly by his elucidation of the structure of plant products and of their phytochemical synthesis. His experimental work covers a wide field of endeavour and is especially noteworthy for its sustained successes. No living organic chemist has displayed a greater versatility of thought and of method. His more recent researches on the distribution, the constitution and the laboratory synthesis of the anthocyanins, the pigments of flowers, fruits and berries have excited the keenest interest of chemists and biologists. His work on the structure of alkaloids and the syntheses to which it has led him are classical in character. The synthesis of tropinone has been referred to as the most elegant synthesis in chemical literature. On the mechanism of chemical reaction he has contributed theoretical ideas which, of interest both to chemists and physicists, have opened new avenues of investigation.

A Royal Medal is awarded to Professor Edward Mellanby, F.R.S.

Professor Edward Mellanby's chief claim is based on his proof that the central factor in the development of rickets is a defective diet. He introduced experimental methods, produced rickets by feeding animals on a deficient diet, and showed that the missing factor was of the nature of a fat-soluble vitamin. Previously only clinical observations had been recorded, on the effect of sunlight, and on other supposed factors; there was no sound evidence before his researches that a material substance regulates the calcification of bone. It was Mellanby's fundamental work which during the last decade made possible numerous and important researches by others, culminating a year ago in the recognition of the material substance (Vitamin D) as an isomeride of ergosterol.

A further claim to the award may be based on Mellanby's later researches, which suggest hitherto unsuspected problems, though their very novelty has so far precluded the clear definition and finality which is now the outcome of his earlier works. Thus he has shown the adverse effect, under certain circumstances, of an excessive amount of cereal germs. In the absence of vitamin A the latter, and particularly ergot of rye, produce a degeneration of the spinal cord. Incidentally, this observation provides a satisfactory explanation of the peculiar and hitherto obscure incidence of convulsive ergotism in man. Mellanby has thus indicated the presence, in one of the chief articles of diet, of a substance of general and unsuspected importance. Because of its fundamental nature Mellanby's experimental work may well rank with the best descriptive work in the biological sciences.

The Davy Medal is awarded to Professor Richard Willstätter, For. Mem. R.S.

Richard Willstätter is recognised by all as among the greatest of organic chemists. In a period extending over a little less than forty years he has given ever clearer proofs of his experimental genius.

His earlier studies gave us our present complete knowledge of the molecular structure of atropine and cocaine, and his analytic and synthetic studies of these alkaloids have had important sequels in systematic organic chemistry and in pharmacology. He then proceeded to a series of ingenious researches bearing on the problem of quinonoid character and on the benzene theory and these led in succeeding years to further work on cyclic compounds of much general interest. He early showed himself to be a master of method in organic chemistry.

Probably Willstätter's name will, in the future, bring most readily to mind

the discovery of magnesium in chlorophyll, and this, along with the painstaking and monumental investigations of the structure of chlorophyll and the blood pigment, represents perhaps the high-water mark of his achievement. Coupled with this work was a series of valuable contributions to the study of carbon assimilation. Equally novel and brilliant were his researches on the anthocyanin pigments of flowers and blossoms; a whole new chapter of organic chemistry was written.

Finally, the studies on the enzymes have added greatly to our positive knowledge, enabled us fully to estimate the difficulty of the task, and laid down the lines on which future work must proceed.

It is impossible in a few words to discuss or adequately appraise Willstätter's outstanding services to science; nothing has been said of lignin, the polysaccharides, or the carotinoids and many other fields in which he laboured with great success. It is clear, however, that he has always attacked the more difficult and fundamental problems relating to the intricacies of complex natural products. Although all his work bears on biochemistry, his methods and outlook were those of the organic chemist.

The Darwin Medal is awarded to Dr. Carl Erich Correns.

Dr. Correns was one of the three botanists (the other two being Tschermak and de Vries) who in 1900 independently brought to the notice of biologists the fundamental work of Mendel, which had remained neglected since 1865. From 1900 till the present time Correns has been actively engaged in developing the science of genetics. Some of his more fundamental discoveries are here mentioned.

In 1902 he was the first to elucidate the remarkable phenomenon of the production of red flowers in the first cross between two white-flowered races of *Mirabilis*. He was also the first to show in the crossing of two species of *Mirabilis* that if very numerous genetic factors relating to small morphological differences are present it is impossible to establish segregation in the F_2 generation, unless very large numbers are available. This explains the appearance of supposed "constant" hybrids, as has since been shown by other observers in numerous instances.

Correns was also the first experimenter clearly to establish inheritance which did not follow Mendelian rules. Thus he showed in *Mirabilis* and other plants that variegation of the leaves depending on the failure to develop chlorophyll, is inherited only through the mother because the plastids which carry the chlorophyll are present in the egg cell and not in the sperm. Again,

he demonstrated that paternal characters shown by extra-embryonal parts of fruits produced by crossing (so-called "xenia") were always limited to the endosperm, *i.e.*, to the food tissue formed by the fusion of a second sperm with nuclei belonging to the maternal parent.

But his most important work is probably the elucidation of the inheritance of sex. By crossing a monoecious with a dioecious species of *Bryonia* he showed in 1907 that the females were all homozygous and the males heterozygous for the sex factor. The generalisation that one sex is always homozygous and the other heterozygous corresponds with the normal approximately equal distribution of the sexes in the offspring of unisexual individuals and with the differences between the chromosomes of the sex-cells, and is now well-established doctrine. Deviation from the equal distribution of the sexes Correns showed to be due in *Melandrium* to the more rapid action of the male-determining sperms, and this is a principle of wide application. Again, he was the first to explain the differential fertility of a generation of plants with their parents and with one another by the assumption of two distinct and inherited inhibiting substances in the stigmata of the flowers.

From 1900, when he helped to found the science of genetics on the basis of Mendel's work, for more than thirty years Correns' work, by its sureness in the perception of fundamental problems and by the excellence of its execution, has been that of a master, and several of the key discoveries in the subject are due to him.

The Buchanan Medal is awarded to Professor Thorvald Madsen.

Dr. Madsen has given distinguished service in advancing the Science and Practice of Hygiene for many years up to the present time. His best known scientific work has been on the toxins and anti-toxins of diphtheria and tetanus bacilli and on other animal, vegetable and bacterial toxins and antigens and their antibodies. He initiated and published with Arrhenius, classical work on the theory of toxin and anti-toxin combination, showing that the process resembled the combination of a weak acid and base rather than the union of a strong acid and base, as had been held by Ehrlich.

Madsen was largely concerned with the origin of the Commission on Hygiene, which he directed in Eastern Europe during the latter part of the War.

Since then he has been President of the Health Committee of the League of Nations and President of the Permanent International Committee on Biological Standards, which was in great part due to his initiative, and has served to promote united action in this sphere by the chief countries of Europe.

The Hughes Medal is awarded to Dr. James Chadwick, F.R.S.

Dr. Chadwick is distinguished for his contributions to Radio-activity and Nuclear Physics. Amongst a number of other investigations on α , β and γ rays he was the first to show explicitly about 1920 that the charge on the nucleus was equal to the atomic number, by a quantitative study of the large angle scattering of α -particles by selected elements (Cu, Ag, Au), thus verifying by direct experiment the correctness of Moseley's deduction. He was associated with Rutherford, 1922-1930, in a long series of investigations (1) on the anomalous scattering of α -particles by light elements, which threw the first light on the size and structure of the nucleus, and (2) on the artificial transmutation of the elements by α -ray bombardment. These experiments showed that at least twelve of the lighter elements were transmuted with the ejection of a proton, and laid the foundations of a study which has recently so rapidly accelerated.

In 1928 efforts were started to improve the technique of these experiments by using automatic electrical counting, and methods were perfected by the end of 1930. Dr. Chadwick took an active part in this work and applied the new methods to a more detailed study of the groups of disintegration protons, especially from boron and aluminium, for which he established clearly for the first time the existence of definite nuclear α -particle and proton levels. Finally, this year, when the observations by M. and Mme. Curie-Joliot had indicated certain curiosities, produced by the supposed γ -radiation from beryllium bombarded by α -particles, Dr. Chadwick immediately recognized that the effects observed could only be adequately explained by the assumption that the radiation from beryllium was of a new type—the ejection of a neutron; by a brilliant series of experiments he confirmed this conjecture, and with the collaboration of Dee and Feather was able to establish its essential properties.

The experiments of Dr. Chadwick are characterised by scrupulous accuracy of measurement and interpreted with great care and critical judgment. They form a striking contribution to science. He has also in virtue of his position played a great part in directing and supervising a large number of other important researches in the same field.

Sedimentation Equilibrium in the Ultracentrifuge; Types Obtained with Soap Solutions.

By JAMES W. McBAIN, F.R.S., and M. E. LAING McBAIN, D.Sc., Stanford University, California.

(Received September 6, 1932).

The centrifuge has been used in the study of the constitution of solutions by a number of investigators. Des Coudres and Tolman* used it with electrolytes to measure the initial tendency towards sedimentation without, however, prolonging the experiment sufficiently to allow the sedimentation to take place, but measuring the e.m.f. instantaneously set up in a centrifugal as in a gravitational field. Work on ordinary electrolytes has been in abeyance for twenty years.

To Svedberg is due the remarkable achievement of realising centrifuges of high power in which the process and attainment of sedimentation may be observed by optical methods throughout the operation of the centrifuge. This introduces a new and invaluable quantitative instrument of singular power for the examination of innumerable problems in colloid and chemical science.

Since Svedberg's use of the ultracentrifuge has been largely confined to such materials as proteins, cellulose, and colloidal gold, it may not be generally realised that substances of ordinary molecular weight are accessible to study by the ultracentrifuge, and in the particularly favourable case of mercuric chloride, even in one of the small ultracentrifuges.

We have been accorded by Professor Svedberg the great privilege of using his unique ultracentrifuge and the other facilities of his especially equipped laboratories in order to study the behaviour of a series of typical soap solutions in a centrifugal field (about 100,000 times gravity). For this we express our grateful thanks, especially in view of the extensive programme of work contemplated for his equipment.

The study of colloidal electrolytes involves an extension of the theory so far used for the ultracentrifuge. The theory of the simplest case of sedimentation equilibrium is well known. The concentration gradient of a neutral molecule such as sucrose, mercuric cyanide, or any colloid consisting solely of independent

* For bibliography and references to theoretical treatment see 'J. Amer. Chem. Soc.', vol. 33, p. 122 (1911).

primary particles at the isoelectric point, depends entirely upon the effective molecular weight (activity), and the product of the density of the solution and the change in volume of a large amount of solution when to it is added 1 gm. of the substance in question (partial specific volume of the solute). The gradient may be expressed as

$$\frac{RT}{\omega^2 x} \cdot \frac{d \ln c}{dx} = M (1 - \bar{v} \rho),$$

where c is the concentration, x the distance from the axis of rotation, M the effective molecular weight, \bar{v} the partial specific volume, and ρ the density of the solution. ω is the angular velocity (2π times the number of revolutions per second). For the expression $1 - \bar{v} \rho$, we shall use the symbol " g ," which is a specific property of the substance named.

This formula seems to be of general applicability when applied to the solution of any substance as a whole if all the constituents in the solution are in equilibrium with each other. For example, it might be applied to such a complex system as a soap solution in spite of the numerous constituents present, *provided* that the equilibrium between them is instantaneously and constantly maintained. The value of M employed must be that corresponding, for example, to the actual lowering of freezing point.

The extent to which sedimentation should take place with typical solutions in the oil turbine ultracentrifuge (Svedberg, 1927) with 700 r.p.s. and an average radius of $x = 5$ cm., may be illustrated by the numerical examples in Table I.

Table I.—Sedimentation of Typical Solutions in an Oil Turbine Ultracentrifuge.

	Solution, per cent.	Increase per centimetre per cent.
Sucrose	1	66
Potassium chloride	1	10
Sodium sulphate	1	24
Mercuric chloride	1	280
Potassium laurate	1	24

What soap actually does will be described below.

The increase of 2.8-fold in concentration between $x = 4.5$ and $x = 5.5$ cm. for mercuric chloride is seen to be so great in spite of the low molecular weight of 270 that the effect should be accessible to observation in a small ultracentrifuge, although with the latter a long time would be necessary for attainment of equilibrium. This substance possesses the advantage that it is almost entirely in the form of strictly isoelectric molecules, and it should serve as an

exceptionally favourable material for testing the operation of any ultra-centrifuge. The time taken for the practical attainment of such equilibria cannot be quantitatively evaluated by the formulæ in current use but might lie between a day or less for mercuric chloride and a week for sucrose, for, although the molecular weights are small, the diffusion constant is in every case large.

Interest frequently centres exclusively upon the sedimentation of certain colloidal particles, which if charged must be regarded as polyvalent ions. If no other electrolytes are present, the solution is to be regarded as that of an electrolyte consisting of the colloidal particles and the corresponding ions of opposite charge. It is the custom in papers on centrifugal action to make the simplifying assumptions that the electrolytes are completely dissociated and that colloidal particles and ions follow the perfect gas laws, their activities being set equal to their concentrations.

Sedimentation of a single ion in a solution containing only one kind of positive ion and one kind of negative ion has been discussed in some detail by Svedberg,* and the more general formulation is given by Evans and Cornish.†

Thus for a cation we may write

$$\frac{RT}{\omega^2 x} \cdot \frac{d \ln c_1}{dx} = M_1 g_1 - n_1 \frac{96490 \cdot 10^7}{\omega^2 x} \cdot \frac{dE}{dx}$$

and for an anion

$$\frac{RT}{\omega^2 x} \cdot \frac{d \ln c_2}{dx} = M_2 g_2 + n_2 \frac{96490 \cdot 10^7}{\omega^2 x} \cdot \frac{dE}{dx}$$

n_1 is the number of charges on the cation and n_2 the number of charges on the anion.

By adding these equations, we may eliminate from them the slope of potential within the solution, dE/dx , which Svedberg and his collaborators refer to as the "Donnan effect."

It is of doubtful advantage to rename this slope of potential within the solution "Donnan effect." It occurs with ordinary ions just as well as with colloids. Tiselius‡ has suggested that it should be measured in a series of experiments with membranes.§ As is pointed out in the early work, at equilibrium no external e.m.f. can be observable between a pair of reversible elec-

* 'Kolloid-Z.,' vol. 36, *Ergänzungsband*, p. 64 (1925)

† 'J. Amer. Chem. Soc.,' vol. 52, p. 1009 (1930).

‡ 'Z. phys. Chem.,' vol. 124, p. 458 (1926).

§ For complete references to the theoretical treatment of the electrical potential, see Tolman, 'J. Amer. Chem. Soc.,' vol. 33, p. 121 (1911).

trodes of any one kind placed at two levels in the solution.* The potential difference which exists between each electrode and the part of the solution with which it is in contact will be different at the two levels, but this difference will be accurately compensated by the slope of potential within the solution between these two points. No matter what the nature of the reversible electrodes employed, the same slope of potential is concerned, and the potential difference will be equal to that for a concentration cell of any other ions present in the solution, all yielding an identical result. If the sedimentation equilibrium of, say, one of the ions, as, for example, a protein ion, is known, the sedimentation gradient of all other ordinary ions in that solution is likewise determined and yields the value dE/dx for the potential gradient within the concentration cell. Tolman and Des Coudres were careful not to study equilibrium but instead to measure the real external e.m.f. which is instantaneously set up while the solution is still in its initial homogeneous state.

Since, to a very high degree of approximation, no separation of oppositely charged ions can occur and both ions must sediment equally, at any level $n_1c_1 = n_2c_2$, and for this simple case $d \ln c_1 = d \ln c_2$. Hence we obtain

$$\frac{RT}{\omega^2 x} \cdot \frac{d \ln c_1}{dx} = \frac{n_2 M_1 g_1 + n_1 M_2 g_2}{n_1 + n_2}.$$

Inspection of this formula shows that any electrolyte such as potassium chloride, sodium sulphate, or a colloidal particle with its opposite ions exhibits an apparent molecular weight of the undissociated substance, divided by the total number of ions into which the molecule dissociates; or, accurately, the molecular weight is reduced in proportion to the arithmetic mean of the values of Mg of all of the ions formed by the dissociation of 1 molecule (2 for potassium chloride, 3 for sodium sulphate, 41 for a proteinion of valency 40). This is the deduction already made when considering the solution as a whole.†

* This is true only of a closed system with such electrodes as hydrogen or iodine as used in Tolman's study; it is not true where an indefinitely large store of electrode material may pass through the system, continually displacing the sedimentation equilibrium of the solution itself.

† The *ad hoc* suggestions of McBain, Donnan, Porter and others in explanation of the discrepancy between observation and theoretical sedimentation equilibrium of colloidal particles are seen to be erroneous (McBain, 'Kolloid-Z.', vol. 40, p. 1 (1926); 'Colloid Sym. Mon.', vol. 4, p. 10 (1926)). See Johnston and Howell, 'Phys. Rev.', (2) vol. 35, p. 274 (1930); McDowell and Usher, 'Proc. Roy. Soc.,' A, vol. 138, p. 133 (1932). However, the objection by McBain, that the effect of the charges known to be present, and of the opposite ions accompanying the particles, has always been ignored, still stands. It is seen to be of serious import.

Svedberg considers that in many cases $n_1 M_2 g_2$ may be neglected in comparison with $n_2 M_1 g_1$. For a typical protein of molecular weight 40,000 and valency 40 and a partial specific volume 0.75, $n_2 M_1 g_1$ is approximately equal to $1 \times 40,000 \times 0.2 = 8000$. For monovalent ions of opposite sign such as chlorine ions, if \bar{v} be taken to be equal to that of potassium chloride, $n_1 M_2 g_2$ equals $40 \times 35.5 \times 0.38 = 540$, a correction of 7 per cent.

This expression may be written

$$\frac{RT}{\omega^2 x} \cdot \frac{d \ln c_1}{dx} = M_1 g_1 - \frac{n_1}{n_1 + n_2} \cdot (M_1 g_1 - M_2 g_2),$$

or

$$\frac{RT}{\omega^2 x} \cdot \frac{d \ln c_1}{dx} = M_1 g_1 - n_1 \frac{M_1 g_1 n_2 c_1 - M_2 g_2 n_2 c_2}{n_1^2 c_1 + n_2^2 c_2}$$

For one cation with two anions, we obtain for the cation

$$\frac{RT}{\omega^2 x} \cdot \frac{d \ln c_1}{dx} = M_1 g_1 - n_1 \frac{M_1 g_1 n_2 c_1 - M_2 g_2 n_2 c_2 - M_3 g_3 n_3 c_3}{n_1^2 c_1 + n_2^2 c_2 + n_3^2 c_3}.$$

Inspection of this equation shows that the sedimentation of a single kind of ion or charged colloid is not essentially affected by the presence of several ions of opposite sign instead of only one.

For two cations and one anion such as a protein in the presence of an acid or if the concentration of (H^+) may be neglected in the presence of a salt, the formula becomes

$$\frac{RT}{\omega^2 x} \cdot \frac{d \ln c_1}{dx} = M_1 g_1 - n_1 \frac{M_1 g_1 n_2 c_1 + M_2 g_2 n_2 c_2 - M_3 g_3 n_3 c_3}{n_1^2 c_1 + n_2^2 c_2 + n_3^2 c_3}.$$

At the isoelectric point the normal molecular weight M will be observed, since $n_1 = 0$ and the influence of all ions is cancelled. However, away from the isoelectric point where n_1 might be, for example, as much as 40, if the protein ion is in the presence of a salt like potassium chloride (or any buffer of equivalent properties), the influence of the second term can be formidable, being, as shown before, 97.5 per cent. for no buffer but still possibly as much as 30 per cent. when the concentration of the salt is 1 N. The valency mentioned may be extreme, but for any value the correction is not negligible. Since all of the experimental work of Svedberg and his collaborators on sedimentation equilibria of proteins has been calculated on the assumption that the second term on the right-hand side of the general equation could be neglected, it is concluded that all of the results apart from those obtained at the isoelectric

point stand in need of appreciable correction. Application of the correction would reduce the molecular weights yielded by the experiment.* Were it possible for the protein ions to sediment very rapidly in a salt mixture as compared with other ions present, the corrections would be lessened, but the principle of electric neutrality has to be observed which would necessitate either the bringing down of compensating ions to the same extent or the forcing up of like ions to a corresponding extent in a direction opposite to their normal sedimentation.

Likewise, important corrections have to be applied to the usual conclusions regarding the sedimentation of all charged particles such as gamboge or gold in a gravitational field, since in every case their sedimentation must be accompanied by an equal sedimentation of their oppositely charged ions. It is one of the outstanding problems of colloid science to determine the magnitude of these effects and the real degree of independence of ions at a small but real distance (say 10 Å) from a surface.

In the present communication discussion is confined to sedimentation equilibrium whereas much of the work with the ultracentrifuge has been concerned with sedimentation velocity. It has been considered chiefly as the result of Svedberg and Chirnoaga† and of Stamm‡ that sedimentation velocity continues to follow simple theory when diffusion becomes complicated and abnormal. However, sedimentation equilibrium consists of the dynamic equilibrium between sedimentation velocity in one direction and diffusion in another, and both opposing processes must be exactly equally simple or equally complicated. An exact analogy is to be found in any chemical equilibrium where the equilibrium law may be simple but each of the opposing rates very complicated, the complications and catalyses exactly balancing.§ Diffusion in mixtures is known to be complicated, since diffusing substances interfere with each other. It is even possible to reverse the direction of one substance by a heavy diffusion column of another in a liquid analogy of the Langmuir diffusion pump for gases.||

* This will, therefore, not help to explain the fact that in Svedberg's interpretation of his results, there is no appreciable amount of ions, undissociated acids or salts (that is, other than fully dissociated ions) contained in or sorbed by the protein, contrary to such results as those of Pauli and his collaborators where the sorption of ions has been followed electrometrically; possibly the per cent. by weight falls within the experimental error.

† 'J. Amer. Chem. Soc.,' vol. 50, p. 1399 (1928).

‡ 'J. Amer. Chem. Soc.,' vol. 52, p. 3055 (1930).

§ Cf. Roebuck, 'J. Phys. Chem.,' vol. 6, p. 365 (1902).

|| Cf. McBain and Liu, 'J. Amer. Chem. Soc.,' vol. 53, p. 59 (1931).

In all the foregoing treatment of individual sedimentations the possibility of chemical transformation of one kind of sedimenting material into another has been ignored or expressly excluded. This assumption cannot be maintained when dealing with such cases as weak electrolytes, soap solutions, etc. For all such cases further restrictions must be laid upon the independent sedimentation of the constituents.* For example, with a weak electrolyte such as acetic acid, at every level the mass law equation must be satisfied; thus,

$$\frac{\text{HAc}}{(\text{H}^+)(\text{Ac})} = K.$$

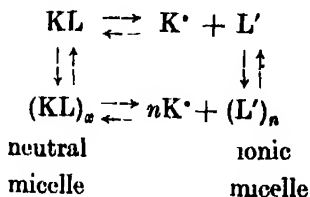
Again, for a soap solution,† where above a certain concentration there is only colloidal electrolyte, for every level,

$$\frac{\text{Ionic micelle}}{\text{Neutral micelle}} = K.$$

Similar equations, empirical or otherwise, must be written for all possible equilibria between constituents of the solution.

Experiments with Soap Solutions.

We have seen that with such a system as soap solutions there are two extreme possibilities. The first is sedimentation of the solution as a whole, provided that all the equilibria are instantaneously restored and constantly maintained. These equilibria are:



where KL denotes the undissociated simple molecules, K* and L' the ordinary ions (L' standing for laurate ion, for example), and the two kinds of colloidal particles present are named above. Experiments in the oil turbine ultra-centrifuge should in this case exhibit no boundary of sedimenting particles as is customary with proteins, but the solution would slowly change as a whole towards the logarithmic distribution of concentration already considered.

* Tiselius ('Z. phys. Chem.,' vol. 124, p. 455 (1926), equation (17)) has discussed exactly how these may be automatically fulfilled, and the extent to which the equilibrium constant K is altered through differences in partial specific volumes.

† For references, see 'Int. Crit. Tables,' vol. 5, p. 460 (1929).

This equilibrium would not be even approximately attained in the 4 hours duration of each of our experiments. The result would, therefore, be that the solution at the end of the experiment would still appear essentially uniform.

The other extreme possibility would have been observed if the equilibria could have been completely "frozen" so that in 4 hours no transformation of neutral colloid into potassium ions and ionic micelle, or *vice versa*, would occur. The result would be completely independent sedimentation of neutral micelle and of ionic micelle, and the sedimentation of the former at least would be rapid and quite like that of a protein. However, it is well known that hours are not required for the substantial attainment of equilibrium within a soap solution, and such complete separation is impossible.

The expected result is, therefore, that some intermediate sedimentation equilibrium will be observed where a dynamic balance is maintained between the intrinsically rapid sedimentation of neutral micelle, and its continued formation in the more dilute regions, and its continued resolution into simpler forms in the more concentrated regions.

We may term this new type of sedimentation equilibrium "snowfall equilibrium" on account of the many superficial analogies between it and the falling of snow. In both cases there is no sharp upper boundary of falling particles but more are being produced from the water vapour or soap solution, respectively. In both cases the observed upper level of the accumulated particles is rising or moving in the opposite direction to that of the particles themselves. We thus picture, as the centrifuging of a soap solution proceeds, a gradual building up of the concentration of the soap solution at the end of the cell towards which the soap is sedimenting, becoming more and more marked over a wider range of levels as sedimentation proceeds until ultimately sedimentation equilibrium would be attained throughout.

The direction in which sedimentation occurs depends upon the respective partial specific volumes of the neutral micelle and ionic micelle and the density of the solution as a whole. We shall describe cases in which sedimentation is wholly downwards, others in which it is wholly upwards, and yet others in which it is both upwards and downwards, revealing the two kinds of colloidal particles present.

Density of Soap Solutions.

There is a dearth of numerical information with regard to the densities of soap solutions,* and we have, therefore, determined a further series.

* 'Int. Crit. Tables,' vol. 5, p. 447 (1929).

For potassium laurate, $1/D_4^{18^\circ} = 1.00138 - 0.00098x$ where x is per cent. by weight of solution up to 20 per cent. Further, $D_4^{18^\circ} = 1.0364$ for 29.4 per cent. ($1.800 N_w$). The specific volumes, except for sodium oleate, are linear over a wide range of concentration and may be expressed as follows. For potassium laurate containing $1.000 N_w$ potassium chloride, $1/D_4^{18^\circ} = 0.9587 - 0.00045x$ up to $x = 20$ per cent. of potassium laurate by weight of solution. For potassium laurate containing $2.000 N_w$ potassium chloride, $1/D_4^{18^\circ} = 1.0840 \pm 0.0000x$ up to $x = 12.3$ per cent. ($0.5862 N_w$ potassium laurate). For lauryl sulphonic acid, $1/D_4^{18^\circ} = 1.00138 - 0.00029x$ up to $x = 15$ per cent.

Hence the partial specific volumes of the $0.5 N_w$ soap solutions employed are :—

Potassium laurate in water	0.904
" " " 1.0 N_w KCl	0.914
" " " 2.0 N_w KCl	0.923
Lauryl sulphonic acid in water	0.972
Sodium oleate in water	0.94

That for $0.25 N_w$ sodium oleate in water is 0.96.

In all cases, if instantaneous chemical equilibrium is maintained of the soap sedimenting as a whole, sedimentation should be downwards (zero in the solution containing $2.0 N_w$ KCl), but the observed change in concentration should be inappreciable in the 4 hours allowed.

Snowfall Sedimentation in Soap Solutions.

Ten runs were made, comprising duplicates with $0.5 N_w$ potassium laurate, the same in the presence of $1.0 N_w$ KCl, $0.5 N_w$ lauryl sulphonic acid,* $0.25 N_w$ sodium oleate, and one each of $0.5 N_w$ potassium laurate with $2.0 N_w$ KCl, and $0.5 N_w$ sodium oleate. The duplicates in each case gave qualitatively the same result. Kahlbaum's purest paraffin oil was employed to seal the cell, it being apparently without effect on soap solutions even after weeks of contact. A 2-mm. cell was employed. Difficulty was experienced in getting it completely clean on account of the comparative inaccessibility of its interior, since the ultracentrifuge cells are not designed to be taken apart for cleaning. Usually the solution was seen to settle bodily when the full centrifugal force was applied, owing to the filling of some inaccessible cavity, but since the

* Specially prepared and purified by Dr. C. R. Noller and J. Gordon at Stanford University.

depth of liquid thereafter remained constant, the progress of sedimentation could be followed without further disturbance. Numerous tests were made for sources of error which might affect the results. As far as possible the routine procedure of the laboratory was followed.

Although the results, owing to the nature of the sedimentation and the unexpected course of the absorption of ultraviolet light, do not lend themselves to quantitative calculation,* they are of such interest in demonstrating the occurrence of the types of equilibria discussed above that they may be briefly displayed. Four of the tracings of the curves of density of the photographic plate corresponding to the light passing through at different levels in the cell are chosen for reproduction in fig. 1. In each experiment such a density curve was taken every half-hour on two independent photographic plates, making four such records for each solution. The curves are so drawn that concentrations, corresponding to increase of absorption of light, are read upwards.

It is at once seen that three new types of curve have been obtained :—

- (a) Sedimentation upwards ; with $0.25 N_w$ sodium oleate.
- (b) Sedimentation downwards ; with $0.5 N_w$ potassium laurate.
- (c) Sedimentation both upwards and downwards ; with $0.5 N_w$ lauryl sulphonic acid and also with $0.5 N_w$ potassium laurate containing $1.0 N_w$ potassium chloride.

$0.5 N_w$ sodium oleate and $0.5 N_w$ potassium laurate containing $2.0 N_w$ potassium chloride are both highly viscous. With the former there was slight sedimentation upwards and with the latter only the slightest indication of sedimentation (upwards) in the 3 hours available.

The results of type (c) are naturally of the greatest interest. They constitute very direct confirmatory evidence of both neutral micelle and ionic micelle as separate entities in soap solutions, the former rising to the top and the latter sinking to the bottom.† The direction is entirely a matter of relative density. Each solution is of especial interest. With the laurate the addition of the potassium chloride has increased the density just enough to float the

* The disconcerting fact was discovered that just in the middle of the range of concentration employed Beer's law was found not to apply, absorption of light being for the middle range almost independent of concentration. This will be further investigated.

† This controverts the statement of Kruyt ("Colloids," p. 241 (1927)) "that this dualistic representation is superfluous." He thus ignored or overlooked the fact that any other interpretation is incompatible with the migration data of one of us (Laing, 'J. Phys. Chem.,' vol. 28, p. 673 (1924)), and also the direct experimental separation of the two kinds of colloidal particle in sodium oleate by ultrafiltration (McBain and Jenkins, 'J. Chem. Soc.,' vol. 121, p. 2325 (1922)).

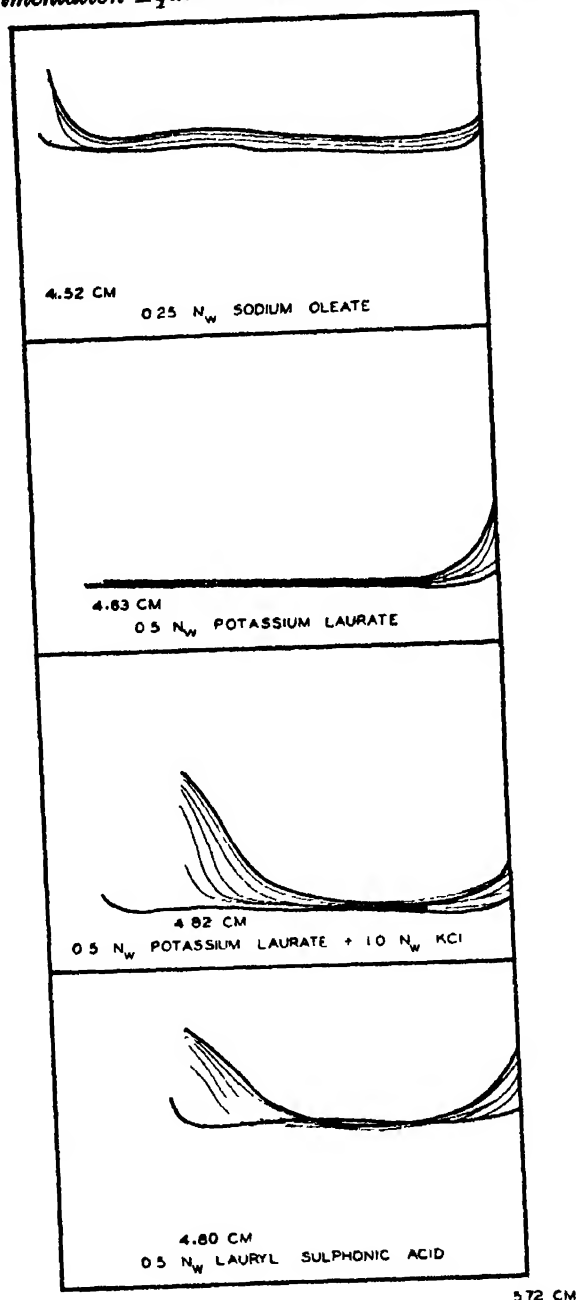


FIG. 1.—Graphs of microphotometric tracings of photographs at one-half hour intervals, showing concentration upwards as ordinates and distances from the axis of rotation as abscissae. In all cases the bottom of the cell, which was 5.72 cm. from the axis of rotation, is the right-hand edge of the diagram. The position of the meniscus when it had settled down under rotation is indicated by the dotted line for each group.

neutral micelle and not the ionic micelle. The experiments with the hydrogen soap, lauryl sulphonic acid, demonstrate that the phenomena are not due to hydrolysis.

Summary.

The sedimentation equilibrium of charged colloids and of electrolytes has been discussed.

Experiments have been carried out on a series of different soap solutions in the oil turbine ultracentrifuge at Uppsala, Sweden, through the courtesy of Professor The Svedberg. These have yielded new types of equilibrium and confirm the independent existence of neutral micelle and ionic micelle in soap solutions.

On the Electromagnetic Fields due to Variable Electric Charges and the Intensities of Spectrum Lines According to the Quantum Theory.

By G. A. SCHOTT, F.R.S., University College of Wales, Aberystwyth.

(Received September 20, 1932.)

1. The procedure usually adopted in the Quantum Theory for the estimation of the intensities of a spectrum line includes two stages: (1) the electric moment, p , of the distribution responsible for the spectrum line is calculated by means of Schrodinger's integrals or some equivalent method; (2) the rate of loss of energy due to radiation is calculated by the classical formula due to H. Hertz, viz., $2\dot{p}^2/3c^3$, just as if the distribution were concentrated in a dipole of precisely the same moment p . The first stage involves no difficulties beyond those met with in the evaluation of the integrals or matrices with which we are concerned, the only principles needed being those of the particular quantum theory adopted. But the second stage is open to grave objections and can only be justified on the ground of necessity owing to the absence of any completely satisfactory quantum theory of the electromagnetic field. Sometimes an appeal is made to Bohr's Correspondence Principle, but this itself involves a somewhat hazardous extrapolation from infinitely large down to small quantum numbers and cannot take the place of a rigorous calculation.

A logically consistent method is possible, based on Maxwell's theory as represented by his electromagnetic equations and their solutions in terms of the classical retarded potential integrals. It may be objected that we do not

know how far Maxwell's equations can be applied to the interiors of atoms, in particular to distributions like those of Schrodinger, but precisely the same objection applies to the customary use of the classical expression for the radiation from an oscillating dipole. Moreover, the attempts made by Heisenberg and Pauli, Dirac and others to formulate a quantum theory of the electromagnetic field have all been based on the assumption that such a theory must be consistent with Maxwell's equations. The direct application of the methods of classical electromagnetic theory to Schrodinger's distributions can be justified at least as a rigorous attempt to determine their electromagnetic field and the radiation from them, and the validity of the procedure will have to be judged by the agreement, or otherwise, of the results obtained with experience. In this way we avoid the assumption that a spatially extended distribution can be treated as if its electric moment were concentrated in a point; in fact, the results obtained in this paper for the more important spectrum line series show definitely that the assumption is false, because it leads to results in many cases quite inconsistent with a rigorous application of Maxwell's theory.

The procedure adopted in the following investigation, apart from the fundamental hypothesis of the applicability of the retarded potential integrals employed, makes no initial assumptions respecting the rate of change and spatial extent and configuration of the electric distribution whose field is to be found. It is applied for the sake of illustration to a simple Schrödinger distribution capable of generating spectrum lines, and for the sake of definiteness Schrodinger's definitions of electric density and current are used. But since the wave function ψ determines both the scalar and vector potentials without ambiguity, there is a complete correlation between the electric and magnetic forces of the resulting electromagnetic field. Consequently there seems to be no good reason against interpreting ψ as a probability amplitude as Born does, so that the distant electric and magnetic forces and the radiation obtained in this investigation can be regarded as averages, either for a large number of independent, similar, closely contiguous atoms, or for a single atom over a considerable interval of time. For the sake of simplicity the usual assumption is made that the wave function is a simple harmonic function of the time, although this is inconsistent with the existence of radiation in the absence of a continuous supply of energy from outside, and with the empirically known fact that the radiation in spectrum lines is emitted in wave trains with a finite length, or at least with a definite beginning and gradual extinction by damping. These more general cases involve some difficult questions of principle, and I hope to consider them at a later date. I also propose to extend the

investigation to other problems, such as the intensities of lines in band spectra and the radiation from wave packets.

2. *Integral Expressions for the Potentials and Forces of the Field.*—The method employed is based on certain integrals given by me on previous occasions*

$$\phi = \int d\Omega \int_{-\infty}^{\infty} \int_{-\infty}^{\infty} e^{i\mu(t-R-\tau)} \rho d\tau d\mu / 2\pi R, \quad (1)$$

$$\mathbf{a} = \int d\Omega \int_{-\infty}^{\infty} \int_{-\infty}^{\infty} e^{i\mu(t-R-\tau)} \mathbf{C} d\tau d\mu / 2\pi R, \quad (2)$$

where ρ and \mathbf{C} are the electric density and current at the volume element $d\Omega$ at the time τ , and R is the distance of the fieldpoint from $d\Omega$. The expressions have been modified slightly by the introduction of \mathbf{C} in place of $\rho\mathbf{v}$, so as to include the Schrödinger distributions, and by the omission of c , the velocity of light, which amounts to taking as unit of time the time required by light to traverse unit length.

We must consider briefly the character of these integrals and the validity of the transformations to be performed on them. They have been derived from the retarded potential integrals of Lorentz by substituting for the retarded values of ρ and \mathbf{C} in those integrals in each fixed volume element $d\Omega$ their Fourier integral expressions in terms of the time τ and the parameter μ . This process is well known to be valid (1) if ρ and \mathbf{C} have only a finite number of maxima and minima in every finite interval of τ , (2) if, when they become infinite at any instant of time, the integrals $\int \rho d\tau$ and $\int \mathbf{C} d\tau$ converge at this instant, (3) if the integrals $\int \rho d\tau/\tau$ and $\int \mathbf{C} d\tau/\tau$ converge absolutely for $\tau = \pm \infty$.† Further, if ρ and \mathbf{C} become discontinuous at any time, the Fourier integrals must be interpreted to mean the arithmetic means of ρ and \mathbf{C} just before and just after the instant in question. In actual practice no difficulties arise from these conditions except the third; in fact, as regards (1), a moving charge gives rise to only one or two maxima, and periodic distributions, such as those of Schrödinger, always possess finite periods; as regards (2), infinities only arise from moving surface distributions, and in these cases the integrals $\int \rho d\tau$ and $\int \mathbf{C} d\tau$ are of the order of the surface density and

* 'Ann. Physik,' vol. 24, p. 637 (1907); 'Electromagnetic Radiation,' chap. II, § 9, equations (8) and (9).

† Riemann-Weber, 'Partielle Differentialgleichungen,' § 17 (1900).

finite ; the last condition, concerning discontinuities, only concerns interpretation. On the other hand, condition (3) involves real difficulties : even for the variable parts of Schrodinger distributions, which are proportional to $\cos(2\pi\nu\tau + \epsilon)$, the integrals $\int \rho d\tau/\tau$ and $\int C d\tau/\tau$ for infinitely large positive and negative values of τ behave like the integral $\int_0^\infty \sin b\tau d\tau/\tau$, which converges at infinity, but only conditionally, not absolutely as the condition requires, even in the less stringent form quoted above. For distributions like the various electron models the difficulty is greater still, for in these cases the integrals do not converge at all, not even conditionally. In spite of this difficulty we know from experience that the expressions (1) and (2) actually do lead to generally accepted results, such as the point potentials and the usual expressions for the energy, momentum and electromagnetic mass of the electron, some of which have been verified by other methods. Thus we have every reason to expect that they will give correct results for the Schrödinger distributions, for which the convergence difficulty is less serious. If it were worth while, the difficulty could be avoided altogether by introducing rapidly converging factors, such as $e^{\pm\epsilon\tau}$ according as τ is negative, or positive ; in some respects the resulting expressions, $e^{\pm\epsilon\tau} \cos(2\pi\nu\tau + \epsilon)$ would afford a better representation of experience than the usual simple harmonic expression, in so far as they would provide for a gradual increase of intensity during generation, and for damping during extinction of the spectrum line. But for the illustration of the method I prefer to sacrifice a little rigour for the sake of comparative simplicity.

In order to determine the electric and magnetic forces, \mathbf{d} and \mathbf{h} , we must differentiate the expressions (1) and (2) once with respect to a co-ordinate or the time. Lorentz has shown that this is permissible under the volume integration for the retarded potential integrals ; it is also permissible for (1) and (2) under the signs of integration for τ and μ , if the integrals $\int_{-\infty}^\infty \int_{-\infty}^\infty \rho d\tau d\mu$ and $\int_{-\infty}^\infty \int_{-\infty}^\infty C d\tau d\mu$ converge absolutely at the upper and lower limits ; as regards τ these conditions can be satisfied when necessary by the introduction of the exponentials $e^{\pm\epsilon\tau}$ already mentioned ; as regards μ it will appear below that the conditions are satisfied for the Schrödinger distributions. Often it will be more convenient to defer the actual differentiations to a later stage of the development.

Lastly we shall need to change the order of integration, integrating first

over the volume $d\Omega$, then with respect to μ and last of all with respect to τ . This is permissible if each of the integrals (1) and (2) converges absolutely at the infinite limits, or if the integrals obtained from them by changing the order of integration have this property. In this case each integral is equal to its transformed; we shall usually find *a posteriori* that the second of the two alternative conditions is true.

3. To effect the necessary transformations we choose spherical polar co-ordinates with any convenient pole, initial line and initial plane. Let the co-ordinates of the field point be (r, θ, ϕ) and of the volume element $d\Omega$ (s, χ, ψ) , so that we have

$$R = \sqrt{r^2 + s^2 - 2rs \cos \gamma}, \quad \cos \gamma = \cos \theta \cos \chi + \sin \theta \sin \chi \cos (\psi - \phi). \quad (3)$$

The addition theorem of the general Bessel function gives*

$$\begin{aligned} \frac{e^{-i\mu R}}{R} &= \frac{\sqrt{(\frac{1}{2}\pi\mu)} H_{\frac{1}{2}}^{(2)}(\mu R)}{i\sqrt{R}} \\ &= \frac{\pi}{2i} \sum_{n=0}^{\infty} (2n+1) \frac{H_{n+\frac{1}{2}}^{(2)}(\mu R) J_{n+\frac{1}{2}}(\mu s)}{\sqrt{r}\sqrt{s}} P_n(\cos \gamma) \end{aligned} \quad (4)$$

The series converges absolutely when $r > s$, when $r < s$, we must interchange r and s . As usual $J_{n+\frac{1}{2}}$ denotes the Bessel function of the first kind, $H_{n+\frac{1}{2}}^{(2)}$ the second Hankel function, both of half-integral order $n + \frac{1}{2}$, and $P_n(\cos \gamma)$ the zonal harmonic of the first kind of integral order n . We multiply (4) by $d\Omega = ds d\omega$, where $d\omega$ is the element of solid angle $\sin \chi d\chi d\psi$, and integrate term by term between the proper limits. Substituting the result in (1) and assuming provisionally that we can change the order of integration we obtain

$$\begin{aligned} \phi &= \int_{-\infty}^{\infty} \int_{-\infty}^{\infty} e^{i\mu(t-\tau)} d\tau d\mu \sum_{n=0}^{\infty} \frac{2n+1}{4i} \left\{ \frac{H_{n+\frac{1}{2}}^{(2)}(\mu r)}{\sqrt{r}} \right. \\ &\quad \times \int_0^r \int \int J_{n+\frac{1}{2}}(\mu s) P_n(\cos \gamma) \rho s^{3/2} ds d\omega + \frac{J_{n+\frac{1}{2}}(\mu r)}{\sqrt{r}} \\ &\quad \times \left. \int_r^{\infty} \int \int H_{n+\frac{1}{2}}^{(2)}(\mu s) P_n(\cos \gamma) \rho s^{3/2} ds d\omega \right\}. \end{aligned} \quad (5)$$

From (2) we obtain a similar expression for \mathbf{a} with \mathbf{C} in place of ρ .

4. As we are mainly concerned with the method of development and are interested chiefly in the radiation problem, for which we only need the infinitely

* G. N. Watson, 'Bessel Functions,' 11.41, equation (4) with $r = \frac{1}{2}$, $\pi = \mu R$.

distant field, we shall in the present investigation simplify (5) by neglecting all but the largest terms. Thus we shall put*

$$\sqrt{(\frac{1}{2}\pi\mu r)} H_{n+\frac{1}{2}}^{(2)}(\mu r) = i^{n+\frac{1}{2}} e^{-i\mu r}. \quad (6)$$

Moreover, we shall only deal with distributions which are either entirely at a finite distance from the origin, like the classical electron models, or of order $e^{-\alpha r}$ at great distances, where α is positive, like the Schrödinger distributions. Thus the second volume integral in (5) can be made zero, or at least negligible, by choosing r large enough, and then the upper limit of the first integral can be taken as infinity. Thus we get

$$\begin{aligned} \phi = \frac{1}{2\sqrt{(2\pi)}} \int_{-\infty}^{\infty} \int_{-\infty}^{\infty} \frac{e^{i\mu(t-\tau-r)}}{r\sqrt{\mu}} d\tau d\mu \sum_{n=0}^{\infty} (2n+1) i^n \\ \times \int_0^{\infty} \int J_{n+\frac{1}{2}}(\mu s) P_n(\cos \gamma) \rho s^{3/2} ds d\omega \end{aligned} \quad (7)$$

with a similar expression for \mathbf{a} .

In order to find the electric and magnetic forces, \mathbf{d} and \mathbf{h} , to the same approximation from the usual equations (in our units)

$$\mathbf{d} = -\text{grad } \phi - \dot{\mathbf{a}}, \quad \mathbf{h} = \text{rot } \mathbf{a} \quad (8)$$

we need only differentiate the exponential, bearing in mind that $\text{grad } r = \mathbf{r}_1$ the unit vector along r . Thus we obtain

$$\begin{aligned} \mathbf{d} = \frac{1}{2\sqrt{(2\pi)}} \int_{-\infty}^{\infty} \int_{-\infty}^{\infty} \frac{e^{i\mu(t-\tau-r)}}{r} \sqrt{\mu} d\tau d\mu \sum_{n=0}^{\infty} (2n+1) i^{n+1} \\ \times \int_0^{\infty} \int J_{n+\frac{1}{2}}(\mu s) P_n(\cos \gamma) \{\rho \mathbf{r}_1 - \mathbf{C}\} s^{3/2} ds d\omega \end{aligned} \quad (9)$$

$$\begin{aligned} \mathbf{h} = \frac{1}{2\sqrt{(2\pi)}} \int_{-\infty}^{\infty} \int_{-\infty}^{\infty} \frac{e^{i\mu(t-\tau-r)}}{r} \sqrt{\mu} d\tau d\mu \sum_{n=0}^{\infty} (2n+1) i^{n+1} \\ \times \int_0^{\infty} \int J_{n+\frac{1}{2}}(\mu s) P_n(\cos \gamma) \{-[\mathbf{r}_1 \mathbf{C}]\} s^{3/2} ds d\omega. \end{aligned} \quad (10)$$

It should be noted that \mathbf{h} can be got from \mathbf{d} by forming the vector product of \mathbf{d} by \mathbf{r}_1 , not directly, but under the sign of integration with respect to τ , for \mathbf{r}_1 in general depends on τ , but not on μ , s or ω .

5. *Axiosymmetrical Schrödinger Distribution in a Fixed Hydrogen Atom.*—As an illustration we shall apply our formulæ to the simplest case, in which a

* Watson, *loc. cit.*, 7.2, equation (6), with $z = \mu r$.

centrosymmetrical distribution with principal quantum number l coexists with an axiosymmetrical distribution with principal quantum number k and azimuthal quantum number 2. Then the part of the wave function corresponding to these two coexistent distributions is of the form*

$$\psi = A e^{-r/a} L'_l \left(\frac{2r}{al} \right) e^{2\pi i \nu_l t + s_l} + B (\mathbf{r} \mathbf{p}_1) e^{-r/ak} L'''_{k+1} \left(\frac{2r}{ak} \right) e^{2\pi i \nu_k t + s_k}, \quad (11)$$

where $A, B, \vartheta_l, \vartheta_k$ are real constants, \mathbf{p}_1 is a constant unit vector along the axis of symmetry of the distributions, $a = \hbar^2/4\pi^2 m e^2$ is the radius of the first Bohr orbit of hydrogen, $\nu_l = 2\pi^2 m e^4/\hbar^3 l^2$ and $\nu_k = 2\pi^2 m e^4/\hbar^3 k^2$ are the characteristic frequencies of the two distributions and L_l is the Laguerre polynomial of order l and L'_l its first derivative, with a similar meaning for L'''_{k+1} .

The variable part of the electric density ρ due to the coexistence of the two distributions is given by

$$\rho = e\psi\bar{\psi} = 2eAB \cos(2\pi\nu t + \varepsilon) (\mathbf{r} \mathbf{p}_1) e^{-ar} L'_l \left(\frac{2r}{al} \right) L'''_{k+1} \left(\frac{2r}{ak} \right), \quad (12)$$

where

$$\alpha = \frac{l+k}{lka}, \quad \nu = \nu_l \sim \nu_k = \frac{2\pi^2 m e^4}{\hbar^3} \frac{(l^2 \sim k^2)}{k^2 l^2}, \quad \varepsilon = \vartheta_l - \vartheta_k. \quad (13)$$

The electric moment due to the coexistence of the two distributions is in the direction \mathbf{p}_1 by symmetry and is given by

$$\begin{aligned} p &= \iiint \rho(\mathbf{r} \mathbf{p}_1) r^2 dr d\omega \\ &= \frac{4}{3} \pi eAB \cos(2\pi\nu t + \varepsilon) \int_0^\infty e^{-ar} L'_l \left(\frac{2r}{al} \right) L'''_{k+1} \left(\frac{2r}{ak} \right) r^4 dr, \end{aligned} \quad (14)$$

for $(\mathbf{r}_1 \mathbf{p}_1)$ is a zonal harmonic of the first kind of order one, so that the mean value of its square is $\frac{1}{3}$, and that of $(\mathbf{r} \mathbf{p}_1)^2$ is $\frac{1}{3} r^2$. The integral with respect to r will be evaluated below.

Again the current \mathbf{C} due to the coexistence of the two distributions is given by the usual formula

$$\begin{aligned} \mathbf{C} &= \frac{\hbar e}{4\pi m i} \{ \psi \text{grad } \bar{\psi} - \bar{\psi} \text{grad } \psi \} \\ &= \frac{\hbar eAB}{2\pi m} \sin(2\pi\nu t + \varepsilon) e^{-ar} \{ L'_l L'''_{k+1} \mathbf{p}_1 + [2L'_l L''_{k+1} - 2kL''_l L'''_{k+1} \\ &\quad - (l-k)L'_l L'''_{k+1}] (r/ka) (\mathbf{r}_1 \mathbf{p}_1) \mathbf{r}_1 \}, \end{aligned} \quad (15)$$

* Schrödinger, 'Ann. Physik,' vol. 79, p. 361 (1926); vol. 80, p. 483 (1926).

where the arguments of L_l and L_{k+1} are $2r/al$ and $2r/ak$ respectively, whilst accents denote differentiations with respect to the respective arguments as before.

6. In order to obtain the electric and magnetic forces at a great distance by means of (9) and (10) we need the value of $\rho \mathbf{r}_1 - \mathbf{C}$ at the volume element $ds d\omega$, whose radius vector is \mathbf{s} , and at the time τ . It is convenient to express it in terms of spherical surface harmonics S_m corresponding to the unit vector \mathbf{s}_1 , in particular in terms of the three zonal harmonics: \mathbf{p}_1 of order zero, $m = 0$, $(\mathbf{s}_1 \mathbf{p}_1)$ of order one, $m = 1$, and $(\mathbf{s}_1 \mathbf{p}_1) \mathbf{s}_1 - \frac{1}{3} \mathbf{p}_1$ of order two, $m = 2$. We find from (12) and (15)

$$\rho \mathbf{r}_1 - \mathbf{C} = \cos(2\pi\nu\tau + \epsilon) \cdot F(\mathbf{s}_1 \mathbf{p}_1) \mathbf{r}_1 \\ - \sin(2\pi\nu\tau + \epsilon) \{G \mathbf{p}_1 + H \{(\mathbf{s}_1 \mathbf{p}_1) \mathbf{s}_1 - \frac{1}{3} \mathbf{p}_1\}\}, \quad (16)$$

where F , G , and H are scalar functions of s given by

$$F = 2eABe^{-as} L'_l L'''_{k+1} \cdot s \\ G = \frac{heAB}{2\pi m} e^{-as} \{L'_l L'''_{k+1} + [2lL'_l L''_{k+1} - 2kL''_l L'''_{k+1} \\ - (l-k)L'_l L'''_{k+1}](s/3kla)\} \\ H = \frac{heAB}{2\pi m} e^{-as} [2lL'_l L''_{k+1} - 2kL''_l L'''_{k+1} - (l-k)L'_l L'''_{k+1}](s/kla) \quad (17)$$

where now the arguments of L_l and L_{k+1} are $2s/la$ and $2s/ka$.

In (9) and (10) $P_n(\cos \gamma)$ is a biaxial harmonic of order n with its axes along \mathbf{r}_1 and \mathbf{s}_1 ; hence, if S_m is a zonal harmonic of order m with its axis along \mathbf{s}_1 , as is the case above, we have

$$(2n+1) \iint P_n(\cos \gamma) S_m d\omega = 4\pi R_m \quad \text{when } n = m,$$

where R_m is the same harmonic as S_m , but with \mathbf{s}_1 replaced by \mathbf{r}_1 ; the surface integral vanishes when $n \neq m$.

Moreover, since both the centre and axis of the atom are fixed, the vectors \mathbf{r} and \mathbf{p}_1 are independent of τ , and therefore any quantities depending on them can be taken outside the signs of integration. Consequently we obtain from (9), (10) and (16)

$$\mathbf{r} \mathbf{d} = I \mathbf{p}_1 + J(\mathbf{r}_1 \mathbf{p}_1) \mathbf{r}_1, \quad \mathbf{r} \mathbf{h} = r[\mathbf{r}_1 \mathbf{d}] = I[\mathbf{r}_1 \mathbf{p}_1], \quad (18)$$

where

$$I = - \int_{-\infty}^{\infty} \int_{-\infty}^{\infty} e^{i\mu(t-r-\tau)} \sqrt{(2\pi\mu)} d\tau d\mu \sin(2\pi\nu\tau + \varepsilon) \\ \times \int_0^{\infty} \{GJ_{1/2}(\mu s) + \frac{1}{2}HJ_{5/2}(\mu s)\} s^{3/2} ds \quad (19)$$

$$J = \int_{-\infty}^{\infty} \int_{-\infty}^{\infty} e^{i\mu(t-r-\tau)} \sqrt{(2\pi\mu)} d\tau d\mu \left\{ -\cos(2\pi\nu\tau + \varepsilon) \int_0^{\infty} FJ_{3/2}(\mu s) s^{3/2} ds \right. \\ \left. + i \sin(2\pi\nu\tau + \varepsilon) \int_0^{\infty} HJ_{5/2}(\mu s) s^{3/2} ds \right\}. \quad (20)$$

The radial component of the Poynting vector is given by

$$\Pi_r = \frac{c}{4\pi} (\mathbf{r}_1 d\mathbf{h}) = cI^2 [\mathbf{r}_1 \mathbf{p}_1]^2 / 4\pi r^2. \quad (21)$$

The rate of loss of energy due to radiation is

$$R = \iint \Pi_r r^2 d\omega = \frac{2}{3} c I^2 \quad (22)$$

in our units, since $[\mathbf{r}_1 \mathbf{p}_1]^2 = 1 - (\mathbf{r}_1 \mathbf{p}_1)^2$, and the mean value of $(\mathbf{r}_1 \mathbf{p}_1)^2$ is one-third. Hence to find the radiation we need calculate only the function I , which is given by (19) and (17), and to express it in terms of the electric moment \mathbf{p} we need (14) also.

7. The expression for I can be simplified considerably; in the first place we see from (17) that

$$G = \frac{hcAB}{2\pi m} e^{-as} L'_l L''_{k+1} + \frac{1}{2} H. \quad (23)$$

Thus in the s -integral in I the factor of Hds becomes

$$\frac{1}{2} \{J_{1/2}(\mu s) + J_{5/2}(\mu s)\} s^{3/2} = J_{3/2}(\mu s) s^{1/2} / \mu$$

by the recurrence formula of the Bessel functions, and by (17) and (23) the integral reduces to

$$\frac{hcAB}{2\pi m} \int_0^{\infty} e^{-as} \{L'_l L''_{k+1} J_{1/2}(\mu s) + [2lL'_l L''_{k+1} - 2kL''_l L''_{k+1}] \\ - (l-k) L'_l L''_{k+1}\} J_{3/2}(\mu s) / \mu k l a \} s^{3/2} ds.$$

But bearing in mind that $\alpha = (k+l)/kla$, that the arguments of L_l and L_{k+1} are $2s/la$ and $2s/ka$ respectively and lastly that

$$J_{1/2}(\mu s) s^{3/2} = d\{J_{3/2}(\mu s) s^{3/2}\} / d\mu s$$

we see that

$$e^{-as} \{L'_l L''_{k+1} J_{1/2}(\mu s) + [2lJ'_l J''_{k+1} + 2kJ''_l J''_{k+1}] \\ - (l+k) L'_l L''_{k+1}\} J_{3/2}(\mu s) / \mu k l a \} s^{3/2} = \frac{d}{d\mu s} \{e^{-as} L'_l L''_{k+1} J_{3/2}(\mu s) s^{3/2}\}.$$

The quantity inside the last bracket vanishes at both limits of the s -integral, so that the corresponding part of the integral vanishes identically, and the remaining part reduces to

$$\frac{h e A B}{\pi m a l \mu} \int_0^{\infty} e^{-as} (L'_1 - 2L''_1) L'''_{k+1} J_{3/2}(\mu s) s^{3/2} ds.$$

Moreover, by (13) we have

$$h/\pi m a = 8\pi v a k^{3/2}/(l^2 \sim k^2).$$

Hence substituting in (19) we obtain

$$I = -\frac{8\pi e A B v a k^{3/2}}{l^2 \sim k^2} \int_{-\infty}^{\infty} \int_{-\infty}^{\infty} e^{i\mu(t-r-\tau)} \sin(2\pi v\tau + \varepsilon) \sqrt{\frac{2\pi}{\mu}} Q d\tau d\mu, \quad (24)$$

where

$$Q = \int_0^{\infty} e^{-as} \left\{ L'_1 \left(\frac{2s}{al} \right) - 2L''_1 \left(\frac{2s}{al} \right) \right\} L'''_{k+1} \left(\frac{2s}{ak} \right) J_{3/2}(\mu s) s^{3/2} ds. \quad (25)$$

Similarly we may write (14) in the form

$$p = 4\pi e A B \cos(2\pi v\tau + \varepsilon) \cdot P, \quad (26)$$

where

$$P = \int_0^{\infty} e^{-as} L'_1 \left(\frac{2s}{al} \right) L'''_{k+1} \left(\frac{2s}{ak} \right) s^4 ds. \quad (27)$$

Thus the expression for the radiation R in terms of the electric moment p by means of (22) and (24), . . . (27) turns on the evaluation of the integrals I and P . This evaluation can be effected by means of a method developed by Schrodinger,* which is based on the expression of the Laguerre polynomial by means of a generating function.

8. *Generating Functions for the P and I Integrals.*—With the appropriate substitutions Schrodinger's equation (112) gives

$$\left. \begin{aligned} \sum_{l=1}^{\infty} L'_1 \left(\frac{2s}{al} \right) \frac{v^{l-1}}{l!} &= -e^{-\frac{2vs}{(1-v)al}} / (1-v)^2 \\ \sum_{l=2}^{\infty} L''_1 \left(\frac{2s}{al} \right) \frac{v^{l-1}}{l!} &= e^{-\frac{2vs}{(1-v)al}} v / (1-v)^3 \\ \sum_{l=1}^{\infty} \left\{ L'_1 \left(\frac{2s}{al} \right) - 2L''_1 \left(\frac{2s}{al} \right) \right\} \frac{v^{l-1}}{l!} &= -e^{-\frac{2vs}{(1-v)al}} (1+v) / (1-v)^3 \\ \sum_{k=2}^{\infty} L'''_{k+1} \left(\frac{2s}{ak} \right) \frac{u^{k-2}}{(k+1)!} &= -e^{-\frac{2us}{(1-u)ak}} / (1-u)^4 \end{aligned} \right\} \quad (28)$$

* *Ann. Physik*, vol. 80, p. 485 (1926), equation (112).

Multiply the first and last equation together and then multiply the product by $e^{-as}s^4 ds$ and integrate term by term with respect to s from 0 to ∞ , which is permissible, because we can always choose u and v small enough to secure absolute convergence for every value of s . On the left-hand side by (27) we obtain a double series involving P integrals, such as $P(l, 1: k+1, 3)$, where the indices have all been put in evidence explicitly. On the right-hand side we obtain an integral which reduces to a gamma function of order 5. Using (13) we write

$$\gamma = \alpha + \frac{2u}{(1-u)ak} + \frac{2v}{(1-v)al} - \frac{w}{(1-u)(1-v)kla} \quad \left. \vphantom{\frac{2u}{(1-u)ak}} \right\} \quad (29)$$

$$w = (l+k)(1-uv) + (l-k)(u-v)$$

Then we find

$$\sum_{k=2}^{\infty} \sum_{l=1}^{\infty} \frac{u^{k-2} v^{l-1}}{(k+1)! l!} P(l, 1: k+1, 3) = \frac{\int_0^{\infty} e^{-\gamma s^4} ds}{(1-u)^4 (1-v)^2}$$

$$= \frac{24k^5 l^5 a^5 (1-u)(1-v)^3}{w^5}.$$

Expand the right-hand side in ascending powers of u and v , and for convenience sake write

$$X = \frac{(1-u)(1-v)^3}{w^5}, \quad X_{k-2, l-1} = \left(\frac{\partial^{k+l-2} X}{\partial u^{k-2} \partial v^{l-1}} \right)_{u=0, v=0}, \quad (30)$$

where it is to be understood that u and v are to be put equal to zero after all differentiations have been performed. Equating coefficients on both sides we obtain

$$P(l, 1: k+1, 3) = 24(k^2-1) k^5 l^5 a^5 X_{k-2, l-1}. \quad (31)$$

Substituting this value in (26) we obtain for the electric moment of the combined distributions with principal and azimuthal quantum numbers $\{l, 0\}$ and $\{k, 1\}$ respectively the expression

$$p(l, 1: k+1, 3) = 64\pi eABa^5 \cos(2\pi\nu t + \varepsilon) \cdot (k^2-1) k^5 l^5 X_{k-2, l-1}. \quad (32)$$

Thus the calculation of the electric moment is reduced to the evaluation of the successive differential coefficient $X_{k-2, l-1}$.

9. The process of finding $I(l, 1: k+1, 3)$ follows similar lines, but naturally is more complicated. We multiply the third and last of equations (28) together and then multiply their product by $e^{-as} J_{3/2}(\mu s) s^{3/2} ds$ and integrate with respect to s from 0 to ∞ in accordance with (25). On the left-hand side we obtain a

double series as before with the P-functions replaced by Q-functions. On the right-hand side we obtain by (29)

$$\frac{1+v}{(1-u)^4(1-v)^3} \int_0^\infty e^{-\gamma s} J_{3/2}(\mu s) s^{3/2} ds.$$

The integral is a special case of the Lipschitz-Hankel integral,* and its value is

$$\frac{(2\mu)^{3/2}}{(\gamma^2 + \mu^2)^2 \sqrt{\pi}}.$$

Hence the resulting equation becomes

$$\sum_{l=2}^{\infty} \sum_{l=1}^{\infty} \frac{u^{l-2} v^{l-1}}{(k+1)! l!} Q(l, 1: k+1, 3) = \frac{1+v}{(1-u)^4(1-v)^3} \frac{(2\mu)^{3/2}}{(\gamma^2 + \mu^2)^2 \sqrt{\pi}}.$$

In accordance with (24) we multiply this equation by

$$- \frac{8\pi eAB\alpha v k^2 l}{l^2 - k^2} e^{i\mu(t-r-\tau)} i \sin(2\pi v\tau + \epsilon) \sqrt{\frac{2\pi}{\mu}} d\tau d\mu$$

and integrate with respect to μ and τ from $-\infty$ to ∞ ; thus we obtain

$$\left. \begin{aligned} \sum_{k=2}^{\infty} \sum_{l=1}^{\infty} \frac{u^{k-2} v^{l-1}}{(k+1)! l!} I(l, 1: k+1, 3) \\ = -32\pi eAB\alpha v \frac{k^2 l (1+v)}{(l^2 - k^2)(1-u)^4(1-v)^3} J \end{aligned} \right\} \quad (33)$$

where

$$J = \int_{-\infty}^{\infty} \int_{-\infty}^{\infty} e^{i\mu(t-r-\tau)} \frac{i\mu \sin(2\pi v\tau + \epsilon)}{(\gamma^2 + \mu^2)^2} d\tau d\mu$$

To evaluate J rigorously note that γ can be made positive by choosing u and v small enough. Beginning with the μ -integral we change the sign of μ in the lower half and obtain

$$- \int_0^\infty \frac{2\mu \sin(t-r-\tau) d\mu}{(\gamma^2 + \mu^2)^2} = -(t-r-\tau) \int_0^\infty \frac{\cos(t-r-\tau) \mu}{\gamma^2 + \mu^2} d\mu,$$

by an integration by parts. Putting $\mu = \gamma x$ we obtain

$$- \frac{t-r-\tau}{\gamma} \int_0^\infty \frac{\cos \gamma(t-r-\tau) x}{1+x^2} dx = - \frac{\pi(t-r-\tau)}{2\gamma} e^{-\gamma|t-r-\tau|}.$$

This expression must be multiplied by $\sin(2\pi v\tau + \epsilon) d\tau$ and integrated with respect to τ , best in two stages; we write

$$\tau = t-r+\xi \text{ from } \tau = t-r \text{ to } \infty, \quad \tau = t-r-\xi \text{ from } \tau = -\infty \text{ to } t-r.$$

* Watson, *loc. cit.*, 13.2, equation (5) with $t=s$, $a=\gamma$, $b=\mu$, $v=3/2$.

In both stages ξ is positive, ranging from 0 to ∞ , and is equal to $|t - r - \tau|$; hence we obtain

$$\begin{aligned} J &= \frac{\pi}{2\gamma} \int_0^\infty \xi e^{-\gamma\xi} \{ \sin [2\pi\nu(t-r) + \varepsilon + 2\pi\nu\xi] - \sin [2\pi\nu(t-r) + \varepsilon - 2\pi\nu\xi] \} d\xi \\ &= \frac{\pi}{\gamma} \cos [2\pi\nu(t-r) + \varepsilon] \int_0^\infty \xi e^{-\gamma\xi} \sin 2\pi\nu\xi d\xi \\ &= \frac{4\pi^2\nu}{(\gamma^2 + 4\pi^2\nu^2)^2} \cos [2\pi\nu(t-r) + \varepsilon]. \end{aligned} \quad (34)$$

A quicker, but not rigorous, method is to substitute for $i\mu$ in J , where it occurs outside the exponential, the operator D , or $\partial/\partial t$ in our units, $\partial/c\partial t$ in the usual units, and let the resulting functional operator, in the present case $D/(\gamma^2 - D^2)^2$, operate on the exponential. Assuming differentiation with respect to t under the signs of integration to be permissible, we can take the functional operator outside the double integral, which then reduces to a Fourier integral for $\sin [2\pi\nu(t-r) + \varepsilon]$, and gives (34) at once. But differentiation with respect to t under the signs of integration in general is only permissible for absolutely convergent integrals; although the Fourier integral is not absolutely convergent, the method gives the correct result in our case. This suggests that it can be used tentatively in other cases, where a rigorous method has not been found.

Bearing (29), (30), (33) and (34) in mind we shall write

$$Y = \frac{1+v}{k^4 l^4 a^4 (1-u)^4 (1-v)^3 (\gamma^2 + 4\pi^2\nu^2)^2} = \frac{1-v^2}{w^4 (1+\theta^2)^2} \quad (35)$$

where

$$\theta = \frac{2\pi\nu a k l (1-u)(1-v)}{w} = \frac{2\pi\nu a k l (1-u)(1-v)}{(l+k)(1-uv) + (l-k)(u-v)} \quad (36)$$

The expression for Y can be simplified without appreciable error; in fact, we find from (36)

$$\frac{\partial\theta}{\partial u} = -\frac{4\pi\nu a k l^2 (1-v)^2}{w^3}, \quad \frac{\partial\theta}{\partial v} = -\frac{4\pi\nu a k^2 l (1-u)^2}{w^3},$$

both of which are essentially negative. Hence θ is greatest when $u = v = 0$ and then it is equal by (13) and (36) to

$$\frac{2\pi\nu a k l}{l+k} = \frac{\pi e^2 (l \sim k)}{c h k l} = \alpha \frac{l \sim k}{2 k l},$$

where α now denotes the fine structure constant $2\pi e^2/ch$, whose value is 1/137.

The smallest possible values of k and l are 1 and 2 for the Lyman series, so that the greatest possible value of θ is $\frac{1}{4}\alpha$, or about $1/550$. If we neglect θ^2 in (35), we only commit a relative error in Y of about 7.10^{-6} . Accordingly we shall write

$$Y = \frac{1 - v^2}{w^4}, \quad Y_{k-2, l-1} = \left(\frac{\partial^{k+l-2} Y}{\partial u^{k-2} \partial v^{l-1}} \right)_{u=0, v=0}. \quad (37)$$

From (33), (34), (35) and (37) we obtain as before

$$I(l, 1 : k+1, 3) = -128\pi^2 e A B a^5 v^2 \cos[2\pi v(t-r) + \varepsilon] \frac{(k^2-1) k^7 l^6 Y_{k-2, l-1}}{l^2 \sim k^2}. \quad (38)$$

Comparing (32) and (38) we can write

$$\left. \begin{aligned} I(l, 1 : k+1, 3) &= \ddot{p}(t-r)/f(l, 1 : k+1, 3) \\ \text{where} \quad f(l, 1 : k+1, 3) &= \frac{2(l^2 - k^2) X_{k-2, l-1}}{k Y_{k-2, l-1}} \end{aligned} \right\}. \quad (39)$$

Substituting from (39) in (22) and returning to the usual units by putting α for l and $\dot{p}(t-r/c)/c^2$ for $\ddot{p}(t-r)$ we obtain for the radiation due to the coexistence of the l th centrosymmetrical and k th axiosymmetrical states considered

$$R = \frac{2 \{ \ddot{p}(t-r/c) \}^2}{3c^3} / \{ f(l, 1 : k+1, 3) \}^2. \quad (40)$$

The first factor is the classical expression for the radiation from a dipole of electric moment p , usually employed in the estimation of the intensity of a spectrum line in quantum theory investigations. The second factor is a correction factor whose value is to be calculated by means of (30), (37) and (39). This value will determine how far the usual procedure is consistent with the classical electromagnetic theory on which in part it is based.

10. *The Correction Factor f.*—In order to simplify the calculation of the reduction factor f we shall write

$$[m, n, p] = \left(\frac{\partial^{m+n} w^{-p}}{\partial u^m \partial v^n} \right)_{u=0, v=0}. \quad (41)$$

Applying Leibnitz' theorem to (30) and (37) we obtain

$$\begin{aligned} X_{k-2, l-1} &= [k-2, l-1, 5] - 3(l-1)_1 [k-2, l-2, 5] \\ &\quad + 6(l-1)_2 [k-2, l-3, 5] - 6(l-1)_3 [k-2, l-4, 5] \\ &\quad - (k-2) \{ [k-3, l-1, 5] - 3(l-1)_1 [k-3, l-2, 5] \\ &\quad + 6(l-1)_2 [k-3, l-3, 5] - 6(l-1)_3 [k-3, l-4, 5] \}. \end{aligned} \quad (42)$$

$$Y_{k-2, l-1} = [k-2, l-1, 4] - 2(l-1)_2 [k-2, l-3, 4]. \quad (43)$$

These equations reduce the calculation of f to that of $[m, n, p]$. Since by (29) we have $w = (l+k)(1-uv) + (l-k)(u-v)$, we find

$$\begin{aligned} \left(\frac{\partial^m w^{-p}}{\partial u^m} \right)_{u=0} &= \frac{(p+m-1)!}{(p-1)!} \frac{\{(l+k)v - (l-k)\}^m}{\{l+k - (l-k)v\}^{p+m}} \\ &= (-1)^m \frac{(p+m-1)!}{(p-1)! (l-k)^p} \frac{\{\xi(\xi-v) - (\xi^2-1)\}^m}{(\xi-v)^{p+m}} \\ &= (-1)^m \frac{(p+m-1)!}{(p-1)! (l-k)^p} \sum_{s=0}^m (-1)^s m_s \frac{\xi^{m-s} (\xi^2-1)^s}{(\xi-v)^{p+s}}, \end{aligned}$$

where we have written ξ for $(l+k)/(l-k)$ for the moment. We obtain from (41)

$$\begin{aligned} [m, n, p] &= (-1)^m \frac{(p+m-1)!}{(p-1)! (l-k)^p} \sum_{s=0}^m (-1)^s m_s (p+s)(p+s+1) \\ &\quad \dots (p+s+n-1)(1-\xi^{-2})^s \\ &= (-1)^m \frac{(p+m-1)! (p+n-1)! (l-k)^{m-n}}{\{(p-1)!\}^2 (l+k)^{m-n+p}} \sum_{s=0}^m (-1)^s m_s \\ &\quad \times \frac{(p+n)(p+n+1) \dots (p+n+s-1)}{p(p+1) \dots (p+s-1)} \left(\frac{4kl}{(k+l)^2} \right)^s. \quad (44) \end{aligned}$$

By differentiating with respect to v first we obtain similarly

$$\begin{aligned} [m, n, p] &= (-1)^m \frac{(p+m-1)! (p+n-1)! (l-k)^{m-n}}{\{(p-1)!\}^2 (l+k)^{m-n+p}} \sum_{s=0}^m (-1)^s n_s \\ &\quad \times \frac{(p+m)(p+m-1) \dots (p+m+s-1)}{p(p+1) \dots (p+s-1)} \left(\frac{4kl}{(k+l)^2} \right)^s. \quad (45) \end{aligned}$$

We use (44) when m is small and (45) when n is small. The following table gives the values calculated by means of these equations of the functions $[m, n, p]$ needed for the Lyman, Balmer and Paschen series.

$$\left. \begin{aligned} [0, l-1, 4] &= \frac{(l+1)!}{3!} \frac{(l-2)^{l-1}}{(l+2)^{l+2}} \\ [0, l-3, 4] &= \frac{l!}{3!} \frac{(l-2)^{l-2}}{(l+2)^{l+1}} \\ [0, l-1, 5] &= \frac{(l+3)(l+1)!}{4!} \frac{(l-2)^{l-1}}{(l+2)^{l+3}} \\ [0, l-2, 5] &= \frac{(l+1)!}{4!} \frac{(l-2)^{l-2}}{(l+2)^{l+2}} \\ [0, l-3, 5] &= \frac{(l+1)!}{4!} \frac{(l-2)^{l-3}}{(l+2)^{l+2}} \\ [0, l-4, 5] &= \frac{l!}{4!} \frac{(l-2)^{l-4}}{(l+2)^{l+1}} \end{aligned} \right\}, \quad (46)$$

$$\left. \begin{aligned}
 [1, l-1, 4] &= 4 \frac{(l+2)!}{3!} \frac{(l-3)^{l-2}}{(l+3)^{l+3}} (2l-3) \\
 [1, l-3, 4] &= 4 \frac{l!}{3!} \frac{(l-3)^{l-3}}{(l+3)^{l+2}} (2l+3) \\
 [1, l-1, 5] &= \frac{(l+2)!}{4!} \frac{(l-3)^{l-2}}{(l+3)^{l+4}} (7l^2 + 18l - 45) \\
 [1, l-2, 5] &= \frac{(l+2)!}{4!} \frac{(l-3)^{l-3}}{(l+3)^{l+3}} (7l-15) \\
 [1, l-2, 5] &= \frac{(l+1)!}{4!} \frac{(l-3)^{l-3}}{(l+3)^{l+3}} (7l+15) \\
 [1, l-4, 5] &= \frac{l!}{4!} \frac{(l-3)^{l-5}}{(l+3)^{l+2}} (7l^2 - 18l - 45)
 \end{aligned} \right\}, \quad (47)$$

$$\left. \begin{aligned}
 [k-2, 0, 4] &= \frac{(k+1)!}{3!} \frac{(k-1)^{k-2}}{(k+1)^{k+2}} \\
 [k-2, 0, 5] &= \frac{(k+2)!}{4!} \frac{(k-1)^{k-2}}{(k+1)^{k+3}} \\
 [k-3, 0, 5] &= \frac{(k+1)!}{4!} \frac{(k-1)^{k-3}}{(k+1)^{k+2}}
 \end{aligned} \right\}, \quad (48)$$

$$\left. \begin{aligned}
 [k-2, 1, 4] &= 4 \frac{(k+1)!}{3!} \frac{(k-2)^{k-2}}{(k+2)^{k+2}} \\
 [k-2, 1, 5] &= \frac{(k+1)!}{4!} \frac{(k-2)^{k-2}}{(k+2)^{k+3}} (3k+10) \\
 [k-3, 1, 5] &= \frac{(k+1)!}{4!} \frac{(k-2)^{k-4}}{(k+2)^{k+2}} (3k-10)
 \end{aligned} \right\}, \quad (49)$$

$$\left. \begin{aligned}
 [k-2, 2, 4] &= 4 \frac{(k+1)!}{3!} \frac{(k-3)^{k-3}}{(k+3)^{k+3}} (11k^2 - 45) \\
 [k-2, 2, 5] &= 6 \frac{(k+2)!}{4!} \frac{(k-3)^{k-3}}{(k+3)^{k+4}} (5k^2 + 12k - 45) \\
 [k-3, 2, 5] &= 6 \frac{(k+1)!}{4!} \frac{(k-3)^{k-4}}{(k+3)^{k+3}} (5k^2 - 12k - 45)
 \end{aligned} \right\}. \quad (50)$$

11 We shall now use these values of $[m, n, p]$ for the calculation of the reduction factors f for the more important spectrum line series by means of (39) combined with (42) and (43).

Lyman Series.—One of the principal numbers is unity, and the corresponding distribution is of necessity centrosymmetrical and that of lowest energy.

Thus it must correspond to $l = 1$, whilst the distribution of higher energy must be axiosymmetrical and correspond to $k \geq 2$. Thus we must use (48) with (42) and (43) and obtain with (39)

$$\begin{aligned} X_{k-2,0} &= [k-2, 0, 5] - (k-2)[k-3, 0, 5] \\ &= \{(k+2)(k-1) - (k-2)(k+1)\} \frac{(k+1)!}{4!} \frac{(k-1)^{k-3}}{(k+1)^{k+3}} \\ &= \frac{1}{2}k \frac{(k+1)!}{3!} \frac{(k-1)^{k-3}}{(k+1)^{k+3}}, \\ Y_{k-2,0} &= [k-2, 0, 4] = \frac{(k+1)!}{3!} \frac{(k-1)^{k-2}}{(k+1)^{k+2}}, \\ f(1, 1: k+1, 3) &= \frac{2(k^2-1)X_{k-2,0}}{kY_{k-2,0}} = 1. \end{aligned} \quad (51)$$

Balmer Series.—One principal quantum is two, corresponding to the distribution of lower energy, whilst the other is three or more, corresponding to the distribution of higher energy. There are two modes of generation according as the smaller quantum number is l as before, or k .

(1) $l = 2, k \geq 3$.—We use (49) with (42), (43) and (39) and obtain

$$\begin{aligned} X_{k-2,1} &= [k-2, 1, 5] - 3[k-2, 0, 5] - (k-2)\{[k-3, 1, 5] \\ &\quad - 3[k-3, 0, 5]\} \\ &= [k-2, 1, 5] - (k-2)[k-3, 1, 5] - 3X_{k-2,0} \\ &= 2k \frac{(k+1)!}{3!} \left\{ \frac{(k-2)^{k-3}}{(k+2)^{k+3}} - \frac{1}{2} \frac{(k-1)^{k-3}}{(k+1)^{k+3}} \right\}, \\ Y_{k-2,1} &= [k-2, 1, 4] = 4 \frac{(k+1)!}{3!} \frac{(k-2)^{k-2}}{(k+2)^{k+2}}, \\ f(2, 1: k+1, 3) &= \frac{2(k^2-4)X_{k-2,1}}{kY_{k-2,1}} = 1 - \frac{3}{4} \frac{(k+2)^{k+3}(k-1)^{k-3}}{(k-2)^{k-3}(k+1)^{k+3}}. \end{aligned} \quad (52)$$

(2) $k = 2, l \geq 3$.—We use (46) with (42), (43) and (39) and obtain :

$$\begin{aligned} X_{0,l-1} &= [0, l-1, 5] - 3(l-1)_1[0, l-2, 5] + 6(l-1)_2[0, l-3, 5] \\ &\quad - 6(l-1)_3[0, l-4, 5] \\ &= \frac{l!}{4!} \frac{(l-2)^{l-3}}{(l+2)^{l+3}} \{(l+1)(l+3)(l-2)^2 - (l-1)(l-3)(l+2)^2\} \\ &= 2l \frac{l!}{3!} \frac{(l-2)^{l-3}}{(l+2)^{l+3}}, \\ Y_{0,l-1} &= [0, l-1, 4] - 2(l-1)_2[0, l-3, 4] = -2l \frac{l!}{3!} \frac{(l-2)^{l-2}}{(l+2)^{l+2}}, \\ f(l, 1: 3, 3) &= \frac{(l^2-4)X_{0,l-1}}{Y_{0,l-1}} = -1. \end{aligned} \quad (53)$$

Paschen Series.—One principal quantum number is three, the other is four or more; there are two modes of generation:—

(1) $l = 3, k \geq 4$.—We use (50) with (42), (43) and (39) and obtain:

$$\begin{aligned} X_{k-2,2} &= [k-2, 2, 5] - 6[k-2, 1, 5] + 6[k-2, 0, 5] \\ &\quad - (k-2) \{ [k-3, 2, 5] - 6[k-3, 1, 5] + 6[k-3, 0, 5] \} \\ &= [k-2, 2, 5] - (k-2) [k-3, 2, 5] - 6X_{k-2,1} - 12X_{k-2,0} \\ &= \frac{1}{2} k(k+1)! \left\{ (7k^2 - 27) \frac{(k-3)^{k-4}}{(k+3)^{k+4}} - 4 \frac{(k-2)^{k-3}}{(k+2)^{k+3}} + \frac{(k-1)^{k-2}}{(k+1)^{k+2}} \right\}, \end{aligned}$$

$$\begin{aligned} Y_{k-2,2} &= [k-2, 2, 4] - 2[k-2, 0, 4] \\ &= \frac{1}{2} (k+1)! \left\{ (2(11k^2 - 45)) \frac{(k-3)^{k-3}}{(k+3)^{k+3}} - \frac{(k-1)^{k-2}}{(k+1)^{k+2}} \right\}, \end{aligned}$$

$$\begin{aligned} f(3, 1: k+1, 3) &= \frac{2(k^2-9)X_{k-2,2}}{kY_{k-2,2}} \\ &= 3 \frac{7k^2 - 27 - 4 \frac{(k+3)^{k+4}(k-2)^{k-3}}{(k-3)^{k-4}(k+2)^{k+3}} + \frac{(k+3)^{k+4}(k-1)^{k-2}}{(k-3)^{k-4}(k+1)^{k+3}}}{2(11k^2 - 45) - \frac{(k+3)^{k+3}(k-1)^{k-2}}{(k-3)^{k-3}(k+1)^{k+2}}}. \quad (54) \end{aligned}$$

(2) $k = 3, l \geq 4$.—We use (47) with (42), (43) and (39) and obtain:

$$\begin{aligned} X_{1,l-1} &= [1, l-1, 5] - 3(l-1)_1 [1, l-2, 5] + 6(l-1)_2 [1, l-3, 5] \\ &\quad - 6(l-1)_3 [1, l-4, 5] - [0, l-1, 5] + 3(l-1)_1 [0, l-2, 5] \\ &\quad - 6(l-1)_2 [0, l-3, 5] + 6(l-1)_3 [0, l-4, 5] \\ &= \frac{l! (l-3)^{l-4}}{4! (l+3)^{l+4}} \{ (l+1)(l+2)(l-3)^2 (7l^2 + 18l - 45) \\ &\quad - 3(l^2 - 1)(l^2 - 9)(7l - 15) + 3(l^2 - 1)(l^2 - 9)(7l + 15) \\ &\quad - (l-1)(l-2)(l+3)^2 (7l^2 - 18l - 45) \} - X_{0,l-1} \\ &= l.l! \left\{ (7l^2 - 27) \frac{(l-3)^{l-4}}{(l+3)^{l+4}} - \frac{1}{2} \frac{(l-2)^{l-3}}{(l+2)^{l+3}} \right\}, \end{aligned}$$

$$\begin{aligned} Y_{1,l-1} &= [1, l-1, 4] - (l-1)(l-2) [1, l-3, 4] \\ &= 4 \frac{l! (l-3)^{l-3}}{3! (l+3)^{l+3}} \{ (l+1)(l+2)(l-3)(2l-3) \\ &\quad - (l-1)(l-2)(l+3)(2l+3) \} \\ &= -4l.l! \frac{(l-3)^{l-3}}{(l+3)^{l+3}} (l^2 - 3), \end{aligned}$$

$$f(l, 1: 4, 3) = \frac{2(l^2-9)X_{1,l-1}}{3Y_{1,l-1}} = - \frac{7l^2 - 27 - \frac{1}{2} \frac{(l+3)^{l+4}(l-2)^{l-3}}{(l-3)^{l-4}(l+2)^{l+3}}}{6(l^2-3)}. \quad (55)$$

12. *Discussion.*—A study of the correction factors f given by (51) ... (55) for the Lyman, Balmer and Paschen series, in the cases when they are due to the coexistence of a centrosymmetrical with an axiosymmetrical distribution, shows that these factors generally differ from unity. In fact, we see from (51) and (53) that the factors are equal to unity in only two cases, viz., the Lyman series on the one hand, and the Balmer series, for the mode of generation by a centrosymmetrical high energy and an axiosymmetrical low energy distribution, on the other. In order to obtain some idea of the magnitudes involved in general we shall give some numerical values calculated by means of (52), (54) and (55). In the first place we find by (52) and (54) for the mode of generation by an axiosymmetrical high energy and centrosymmetrical low energy distribution ($k > l$):—

k	3	4	5	6	∞
Balmer ($l = 2$)					
$f(2, 1 : k + 1, 3)$	-1.86	-3.03	-3.58	—	-4.54
$\{f(2, 1 : k + 1, 3)\}^2$	3.5	9.2	12.8	—	20.6
Paschen ($l = 3$)					
$f(3, 1 : k + 1, 3)$	—	-2.00	-2.21	-2.41	-2.95
$\{f(3, 1 : k + 1, 3)\}^2$	—	4.0	4.9	5.8	8.7

The classical expression for the radiation is seen from (40) to be f^2 times the rigorous expression obtained by our method from Maxwell's equations. We see from the numbers just given that the usual method of calculation gives much too great an intensity, and that the discrepancy in any one series increases as the principal quantum number k increases, just the opposite to what we should expect from Bohr's Correspondence Principle.

Secondly, we find for the mode of generation by a centrosymmetrical high energy and axiosymmetrical low energy distribution by (55) ($l > k$):—

l	4	5	6	∞
Paschen ($k = 3$)				
$f(l, 1 : 4, 3)$	-0.91	-0.86	-0.83	-0.76
$\{f(l, 1 : 4, 3)\}^2$	0.83	0.74	0.69	0.57

For this mode of generation the classical expression gives too small a value for the intensity, and as before the discrepancy increases as the principal quantum number l increases.

Our final conclusion is that the usual classical expression for the radiation is unreliable and often leads to very great discrepancies from a rigorous formula.

Summary.

The object of the preceding investigation is to develop a rigorous method of calculating the electromagnetic fields of variable electric charges on the basis of the classical electromagnetic theory without making any such assumptions respecting the spatial extent or the rate of variation of the electric distributions considered as those which limit the applicability of the existing point charge formulæ for the potentials and forces and the Liénard expression for the radiation. The resulting formulæ are illustrated by applying them to simple Schrodinger distributions and calculating their distant electromagnetic fields and the radiation of energy from them. The expressions thus obtained for the intensities of the lines of the Lyman, Balmer and Paschen series and the numerical values calculated from them show that the usual practice of determining the electric moment of a distribution by means of Schrodinger's integrals, or some equivalent method, and then applying the classical expression for the radiation from a dipole of equal moment, is liable to lead to gross errors.

[*Note added in proof, November 12, 1932.*—Since this paper was written my attention has been called to a series of papers by A. Rubinowicz, commencing in the 'Phys. Z.,' vol. 29, p. 817 (1928) on the "Forbidden" Hydrogen lines. He, like myself, employs the Bessel function expansion (4) and the method of generating functions used in § 8, but his method is confined to distributions which are simple harmonic functions of the time, whilst mine, dating from 1907, applies to *all* variable distributions. Moreover his object is to discuss the forbidden lines, whilst the object of my illustration is to show the danger attending the usual method of calculating the intensity of dipole radiation.]

Gaseous Combustion at High Pressures, Part XIV. Explosions of Hydrogen-Air and Carbonic Oxide-Air Mixtures at Initial Pressures up to 1000 Atmospheres.

By WILLIAM A. BONE, D.Sc., F.R.S., D. M. NEWITT, D.Sc.,
and D. T. A. TOWNEND, D.Sc.

(Received August 19, 1932)

Introduction.

In the previous papers of this series have been described explosions of theoretical hydrogen-air, carbonic oxide-air, etc., mixtures in spherical steel enclosures at initial pressures up to 175 atmospheres, and in 1929 our collected researches on the subject were published in a separate volume entitled "Gaseous Combustion at High Pressures," in which their theoretical implications were fully considered in the light of the experimental evidence as a whole.

Without recapitulating all the many points of interest established during the work, there was one of outstanding importance which should now be recalled, namely, the discovery, attested by an overwhelming mass of cumulative evidence, which is set forth in Chapters IX to XIII (pp. 120 to 208) of our book, of N_2 -activation in $CO-O_2-N_2$ explosions at high initial pressures due to an absorption by N_2 -molecules of the radiation emitted by the burning carbonic oxide. In theoretical CO -air explosions this was marked by (i) a continuously increasing "lag" in the time taken for the attainment of maximum pressure, as the density of the medium was increased from $P_1 = 10$ to $P_1 = 175$ atmospheres, and (ii) a strong exothermic effect during the subsequent "cooling period" (*without there having been any corresponding suppression of kinetic energy during the explosion itself*), as the activated N_2 molecules slowly reverted to their normal condition. Moreover in explosions of $CO-O_2-N_2$ mixtures containing oxygen in excess of that required for the complete combustion of the carbonic oxide, the so-activated nitrogen reacted with the excess of oxygen with the production of large quantities of nitric oxide.

From careful comparative measurements made on the various pressure-time records obtained during explosions of $2CO + O_2 + 4R$ (where $R = N_2$, CO or O_2) mixtures at initial pressures between 3 and 150 atmospheres, as well as from data obtained from explosions of $2CO + 3O_2 + 2N_2$ mixtures at initial pressures between 3 and 75 atmospheres, it was deduced that

(i) while the N_2 -activation effect in a theoretical CO-air explosion increased with the density of the medium up to a steady maximum value with $P_i = 150$ atmospheres, its intensity relative either to the density of the medium or to the total kinetic energy developed on explosion reached a maximum at $P_i = 75$ to 100 atmospheres when it was equivalent to as much as nearly 25 per cent. of the total energy developed, (ii) that in $2CO + 3O_2 + 2N_2$ explosions at $P_i = 75$ atmospheres the nitric oxide surviving in the cold products (namely 3 per cent.) was about *half* the maximum amount actually formed during the explosion itself.*

In view of the theoretical interest of such deductions and their obvious bearing upon technical problems of nitrogen-fixation, it was decided to carry out further experiments upon (i) explosions of theoretical H_2 -air and CO-air, etc., mixtures at much higher initial pressures than hitherto attempted, (ii) nitric oxide formation in $2CO + 3O_2 + 2N_2$ explosions at $P_i = 50$ to 90 atmospheres under conditions such as would ensure a much more rapid cooling, and therefore a greater NO-survival, than in our former experiments, and (iii) nitric oxide formation in continuous CO-flames maintained at controlled steady high pressures in various O_2 - N_2 atmospheres.

For the achievement of these objectives it was necessary to design and install in our laboratories new high-pressure vessels and ancillary appliances at considerable expense; but thanks to the generosity of Imperial Chemical Industries, Ltd., we were enabled to do so in 1928, since which time the work has steadily progressed. And in this and the following two papers are described the principal new results obtained up to date.

EXPERIMENTAL.

A.—*The New Bomb to withstand Explosion Pressures up to 10,000 Atmospheres.*

For the experiments contemplated under (i), it was necessary to design a new bomb (No. 5 of those used in these researches) capable of withstanding maximum explosion pressures up to 10,000 atmospheres (= 65.6 tons per square inch). And after consultation with Sir George Hadcock, F.R.S., who kindly helped us with his great experience of gun-design, it was decided to employ a cylindrical explosion chamber 7.5 cm. long by 3.75 cm. diameter (capacity = 116 c.c.) closed at either end by screwed fittings, the one carrying the necessary inlet valve with ignition device and the other a Petavel mano-

* The evidence for this is set forth in Table XXX, p. 162 and pp. 161–173 of our book (*q.v.*).

meter. At 10,000 atmospheres pressure, the walls would then have to withstand a load of 917 tons, and each end plug one of 115.5 tons. And in order to ensure a relatively uniform distribution of stress in the walls, it was decided to have a comparatively thin walled inner barrel suitably reinforced by wire-winding as in naval gun construction. The bomb was subsequently constructed for us by Messrs. Armstrong, Whitworth & Co., at their Elswick Works, Newcastle-on-Tyne.

The Bomb Body (fig. 1).—The cylindrical barrel (A) of the bomb, machined out of a forging of nickel-chromium molybdenum steel ($C = 0.32$, $Ni = 2.50$,

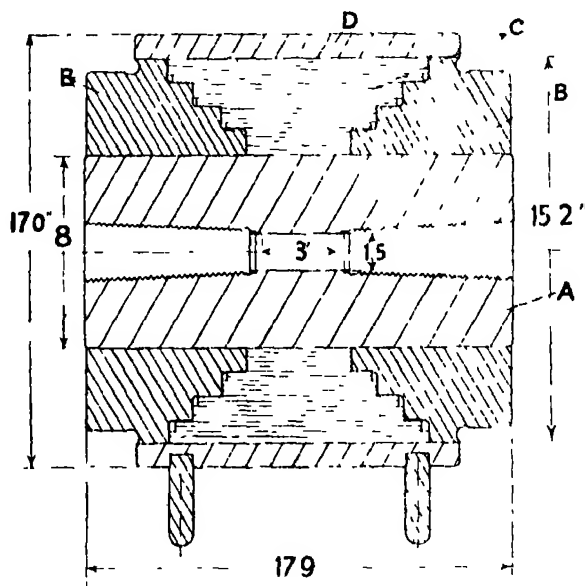


FIG 1.

$Cr = 0.58$, $Mo = 0.65$, $Mn = 0.55$, $Si = 0.16$, $S = 0.032$, and $P = 0.02$ per cent.) was 18.1 inches long by 8 inches external diameter, with a cylindrical explosion chamber 3 inches long by $1\frac{1}{2}$ inches diameter. Each of the end plugs was 6.45 inches long, with 4 threads per inch and tapered from 2.3 inches at the inner to 2.784 inches at the outer end. It was calculated that an explosion pressure of 10,000 atmospheres in the chamber would subject the thread to a shearing stress of 2.7 tons per square inch.

A nickel-steel collar (B) was shrunk on to each end of the barrel A, and 95 layers of steel wire of section 0.25 inch by 0.04 inch were wound round its middle section as shown at C, this winding being protected by a nickel-steel jacket D, of thickness 1.03 inches. The whole bomb with its end plugs

was mounted on ball bearings in a massive cast-iron stand, bolted to a concrete foundation, in such wise that it could be readily rotated about its axis.

The Inlet Valve with Ignition Device.—In order to avoid drilling a separate hole into the explosion vessel for an ignition plug, a combined inlet valve and ignition device (fig. 2) was designed. The ignition device consisted of a steel rod A terminating in a conical boss insulated from the main body of the plug by a thin compressed mica cone B. A gas-tight joint was made between the cone and the plug by tightening the nut C. Ignition was effected by electrically fusing a thin platinum wire stretching between the insulated rod A and the body of the plug.

In designing the valve special precautions had to be taken to protect its seating from the corrosive action of the hot explosion products. The seating

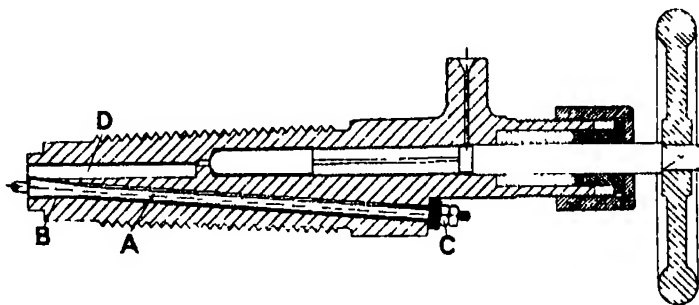


FIG. 2

was therefore made in the interior of the plug $4\frac{1}{2}$ inches away from the explosion cavity. As it was impossible to drill a hole through this length of hard steel sufficiently small to prevent the access of hot gas to the seating, a $\frac{3}{8}$ -inch diameter steel plug (D) on the side of which a fine V groove had been machined, was driven into the end of the plug and extended to within $\frac{1}{2}$ inch of the seating. The narrow gas passage thus produced admirably protected the seating, whilst at the pressures employed no difficulty was experienced in forcing the gas through it into the bomb. The valve spindle was $\frac{3}{8}$ inch in diameter and was turned by a 3-foot tommy bar.

The Petavel Gauge carried by the other screwed end-fitting was similar in design to that employed in our former experiments.

The copper washers originally employed for the obturation of the inlet valve and Petavel gauge fittings proved unsuitable for explosions at initial pressures exceeding 500 atmospheres; accordingly for use at such higher pressures the design had to be modified, a procedure which necessitated shorten-

ing the length of the cylindrical explosion chamber from 3 inches to $2\frac{1}{2}$ inches without altering its diameter.

The Hydraulic Intensifier used in Calibrating the Petavel Manometer.—In order to calibrate the Petavel gauge for the pressures generated during the explosions, it was necessary to produce and maintain hydraulically for some time in the explosion chamber static pressures up to 10,000 atmospheres. For this purpose a special "intensifier" (fig. 3) was designed. It consisted essentially of a high pressure piston A of $\frac{1}{8}$ -inch diameter closely fitting into a steel plug which could be screwed into the valve opening of the bomb.

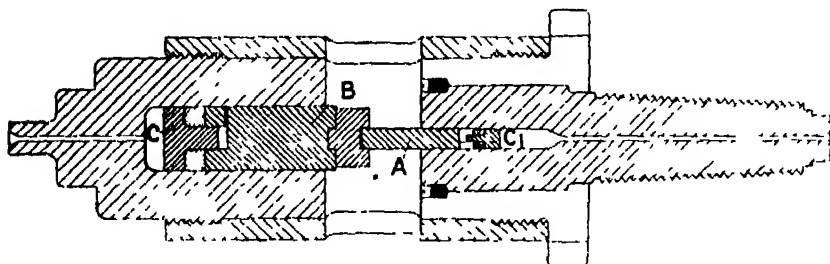


FIG. 3

In making the calibration, the explosion cavity of the bomb was completely filled with vaseline, and then the piston A was forced inwards by means of pressure applied hydraulically to the larger piston B, of 10 times the sectional area of A, abutting on its opposite end, the pressure so applied being measured by a standard Bourdon-tube gauge.

In order to ensure a liquid-tight-joint between the pistons and cylinder walls, each piston had a false-head (C and C') between which and the piston proper was a soft rubber packing ring. This made a self-tightening packing which proved perfectly satisfactory up to the highest pressure reached in the experiments.

The Filling System and Experimental Procedure.—In order that the experimental data may be rightly understood, some reference must be made to the "filling system" for mixing and introducing the gases into the bomb explosion-chamber and to the subsequent general experimental procedure. The filling system, shown diagrammatically in fig. 4 consisted essentially of the following items: (1) A series of high-pressure steel cylinders (*e.g.* C) into which the highly purified single gases had been separately compressed to pressures between 400 and 500 atmospheres; (2) two standard Bourdon gauges, G_1 , G_2 , having pressure-ranges (a) 0–250, and (b) 0–2000 atmospheres respectively; (3) a glass-lined steel tube D, one-half filled with "active" coconut charcoal, for

the removal of any iron-carbonyl possibly present in the compressed carbonic oxide used, and the other half with specially purified and re-distilled phosphoric anhydride, to ensure a uniform degree of drying of the gases passing through it ; (4) a compression cylinder, B, in which the gases were finally compressed hydraulically over clean, dry mercury, into the explosion bomb.

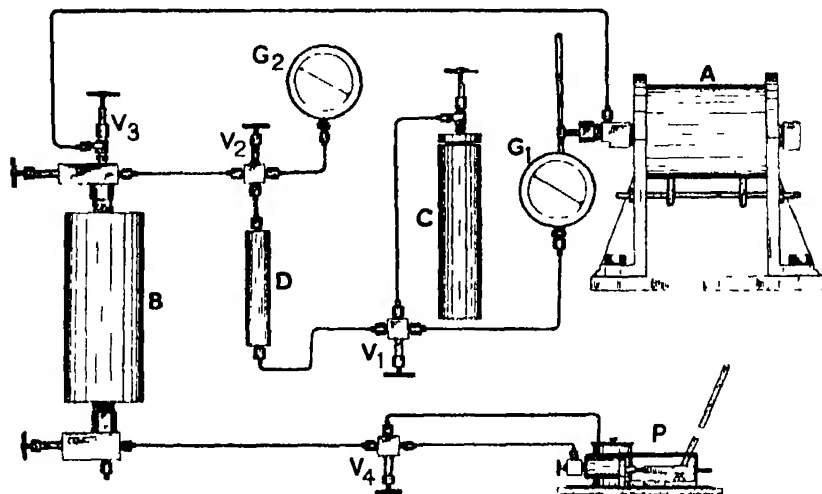


FIG. 4.

Passage of the gases was controlled by means of the standard three-way nickel-steel valves V_1 , V_2 , V_3 , all connections being of drawn steel fine-bore tubing screwed into mild steel union nipples and rendered gas-tight by silver brazing.

Procedure.—In making an experiment, the compressed constituents of the particular explosive mixture were separately introduced in proper proportions, slowly through D, into the compression cylinder B and bomb chamber A, and from 12 to 24 hours allowed for mixing, after which the final compression to just above the pressure desired for the subsequent explosion was effected by means of the mercury hydraulic pump P. This being accomplished, a final mixing of the gases in the explosion chamber was effected by rotating the bomb on its bearings, the mixture was then sampled for analysis, and its pressure finally accurately adjusted to the desired point (P_i) after which it was fired in the usual manner with the Petavel manometer and recorder in action.

B.—Corrections of the Initial and Maximum Explosion Pressures (P_i and P_m) for Deviations from the Gas Laws.

(1) P_i .—At the higher initial pressures employed in these experiments, the deviations of the gaseous media from the gas-laws became considerable, and

in each case were directly determined beforehand in our compressibility apparatus by the method already described in detail on pp. 50 to 54 of our book (*q.v.*). The relationships between the gauge-pressure (P_g) actually employed and the corresponding "corrected" pressures (P_{ab}) for each explosive medium at each of the various experimental explosion pressures were as follows.

Table I.

Explosive medium.	Initial explosion pressure P_g as indicated by the gauge (atmospheres).					
	75	250	350	500	750	1000
	Ascertained "corrected" pressure P_{ab}					
$2H_2 + O_2 + 3.76N_2$	74.2	238	305	392	485	580
$2CO + O_2 + 3.76N_2$	76.2	243.5	312.5	388.5	460	520
$2CO + O_2 + 3.76CO$	76.2	245	320	392	—	—

It is thus seen how far at such higher pressures the actual rate of increase in the density of each particular medium lagged behind the increase in its corresponding pressure as observed on the gauge. Thus, for example, a doubling of the latter from 500 to 1000 atmospheres increased the density of the theoretical hydrogen-air medium by 1.43 and of the theoretical CO-air medium by 1.34 only, and it is clear that beyond 1000 atmospheres a further large increment in the gauge-pressure would have had a disproportionately small effect upon the density of such media.

P_m .—A co-volume correction was applied to the observed maximum explosion pressure in each case on the assumption that the space occupied by a gas molecule is proportional to the third power of its effective molecular diameter and that the variation of the latter with the absolute temperature is in accordance with the mean values calculated (1) on the assumption that it is proportional to nearly the first power of the absolute temperature, and (2) according to Sutherland's formula. The basis of such "correction" is discussed on pp. 252–254 of our book, and the so-corrected value will be referred to as P_{mb} .

The Pressure-Time Explosion Records and the "Cooling Correction" for P_m .—It should always be remembered that the pressure-time records obtained in such explosions are influenced by the shape and capacity of the particular explosion chamber used, and especially by the ratio between its wall-surface

and total volume which largely determines the cooling factor. Therefore the explosion data actually observed with any given mixture at a particular initial pressure and temperature will vary with changes in the explosion chamber, and their significance in any case will be relative to the particular chamber used. Hence it follows that while the data from a series of explosions of a particular mixture over a wide range of different initial pressures in one and the same explosion vessel may be regarded as quite comparable amongst themselves, they are not so with the corresponding data from a similar series of explosions of that mixture in another chamber of different size and contour unless, what is always difficult, correlating factors between the two series can be deduced experimentally.

In comparing the data from these new experiments with those from our previous ones, it should be remembered that whereas formerly a spherical explosion chamber of *circa* 240 c.c. capacity with a surface/volume ratio *circa* 0.78 was employed, we were now using a cylindrical chamber of *circa* 116 c.c. capacity with a surface/volume ratio *circa* 1.17, the firing point in all cases being at one side or end so that the flame always had the same horizontal run to the head of the recording pressure gauge.

In our theoretical H_2 -air explosions, where the explosion-times were so rapid that the pressure-rises on the pressure-time records were almost vertical, any direct estimation of the proper "cooling-correction" applicable to the P_{mb} values was impracticable, and therefore not attempted. In the slower CO-air, etc., explosions, such "cooling corrections" were deduced and applied as described on pp. 245-247 of our book (*qv*) and the fully-corrected maximum explosion pressures will be referred to as P_{mbe} .

Experimental Comparisons between New and Old Conditions.—In order to establish as far as possible a basis of correlation between the conditions of the old and new experiments, respectively, a preliminary series of theoretical H_2 -air, CO-air and $2CO + O_2 + 3.76/CO$ explosions was made at $P_i = 75$ atmospheres in the new cylindrical bomb (No. 5) for comparison with previous similar explosions at the same initial pressure in the old spherical bombs Nos. 2 and 3. It should, however, be noted that whereas the diluent in the latter was $4(N_2 \text{ or } CO)$ in the former it was $3.76(N_2 \text{ or } CO)$.

The results, as detailed in Table II, showed that whereas with slow explosions in the new bomb the explosion time (t_m), if anything, tended to be shorter, the cooling effect of the walls was so much greater that the observed maximum explosion pressures and temperatures were only about 0.86 those formerly obtained in the spherical bomb. In this, and all other tabulations:—

Table II.—Explosions at $P_t = 75$ Atmospheres in Different Bombs.

Mixture exploded :	$2H_2 + O_2 + 4N_2$	$2H_2 + O_2 + 3 \text{ } 76N_2$	$2CO + O_2 + 4N_2$	$2CO + O_2 + 3 \text{ } 76N_2$	$2CO + O_2 + 4CO$	$2CO + O_2 + 3 \cdot 76CO$
In bomb of capacity c.c. :	No. 2 spherical 240.	No. 3 spherical 240	No. 5 cylindrical 116	No. 2 spherical 240	No. 3 spherical 240.	No. 5 cylindrical 116.
P_a , atmospheres	74.2	74.2	74.2	76.2	76.2	76.2
t_m , seconds	0.005	0.005	0.005	0.30	0.015	0.01
P_m , atmospheres	635	625	545	635	720	650
P_{mb} , atmospheres	608	597	518	605	683	611
P_{mb}/P_a	8.19	8.05	6.98	7.94	8.96	8.02
P fall in 1 sec. after t_m —						
Atmospheres	320	385	415	125	223	370
Per cent.*	54	66	83	22	34	64
T_m , K°	2750°	2705°	2345°	2660°	3020°	2725°
T_m in cylindrical bomb						
T_m in spherical						

* i.e., the percentage of the total possible P -fall between T_m and room temperature.

- P_i = observed initial pressure in atmospheres at the actual firing temperature.
 P_{ib} = ditto "corrected" for ascertained deviations from the gas laws.
 t_m = time in seconds from commencement of pressure-rise to the attainment of maximum pressure (also referred to as the "explosion time" in the text).
 P_m = observed maximum pressure in atmospheres.
 P_{mb} = ditto "corrected" for estimated deviation from Boyle's Law (i.e., co-volume correction).
 P_{mbc} = ditto also for cooling during t_m .
 T_m = mean maximum temperature K° actually attained on explosion.
 P_f = observed final pressure in atmospheres of the cold explosion products at room temperature 0.
 P_{fb} = ditto "corrected" for ascertained deviations from the gas laws.

The explosive mixtures were always fired at room temperature, which varied between 15° and 17° . At all initial pressures up to and including 500 atmospheres several experiments were carried out with each particular mixture, with results which invariably agreed within about 2 per cent. ; at still higher initial pressures we were content with two well-agreeing experiments at each particular pressure. In the present publication, however, we have restricted ourselves to detailing the results of what we consider the best representative experiment with each mixture at each selected initial pressure.

D.— $2H_2 + O_2 + 3.76N_2$ *Explosions at Initial Pressures between 250 and 750 Atmospheres.*

In this series of experiments, theoretical hydrogen-air ($2H_2 + O_2 + 3.76N_2$) mixtures were fired in the cylindrical bomb at initial pressures of 250, 350, 500 and 750 atmospheres respectively. Up to $P_i = 500$ atmospheres the explosions were all well under control and went off normally without damaging the bomb, but at $P_i = 750$ atmospheres detonation was set up instantaneously and so violently as to lift both the Petavel manometer and the inlet valve from their respective seatings, whereby hot gaseous products got past them with consequential considerable damage to the screw threads adjacent to the bomb cavity, which in parts were completely melted. As this entailed undue risk to the operators, it was decided not to proceed to any higher pressure.

Satisfactorily complete records, as detailed in Table III, were obtained at all initial pressures up to and including 500 atmospheres, from which it will be seen that both the explosion time (t_m), the P_{mb}/P_0 ratios (and consequently the T_m also), while tending to increase with the density of the medium, had become nearly constant after the latter exceeded that corresponding with $P_0 = 350$ atmospheres. From the pressure-time records reproduced in fig. 5, *a*, *b* and *c*, it will be seen how sudden was the pressure rise on ignition and

Table III.— $2H_2 + O_2 + 3.76N_2$ Explosions in Cylindrical Chamber
 7.5×3.75 cm.; capacity = 114 c.c.

P_0 atmospheres	350	350	500
P_{0b} atmospheres	238	305	392
t_m seconds	0.015	0.02	0.022
P_m atmospheres	2130	2950	4100
P_{mb} atmospheres	1810	2390	3075
P_b atmospheres	132	170	215
P fall in 1 second— Atmospheres	1450	1780	2100
Per cent.	72.5	64	54
P_{mb}/P_{0b}	7.61	7.83	7.85
T_m K°	2560°	2830°	2840°

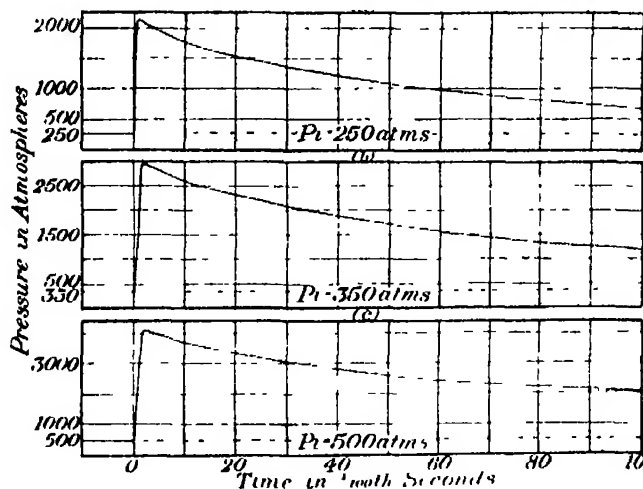


FIG. 5.

how abruptly the "cooling" period succeeded the attainment of the maximum pressure. In each case the rate of cooling followed Newton's law throughout showing it to be uncomplicated by any exothermic effects; and from calculations it would appear that the amount of H_2O -dissociation at T_m was always less than 0.5 per cent., or a quite negligible amount so far as its possible effect on the cooling curves.

E.— $2\text{CO} + \text{O}_2 + 3.76\text{N}_2$ *Explosions at Various Initial Pressures up to 1000 Atmospheres.*

In this series of experiments explosions of theoretical CO-air ($2\text{CO} + \text{O}_2 + 3.76\text{N}_2$) mixtures were successfully carried out at initial pressures of 250, 350, 500, 750 and 1000 atmospheres, respectively. Up to and including 500 atmospheres the original length of the cylindrical bomb cavity, namely, 7.5 cm., was used; but a change in the copper washers, and the damage done to the end fittings by the H_2 -air detonation at $P_i = 750$ atmospheres, necessitated certain alterations before higher pressures were attempted, which reduced the length but *not* the diameter of the explosion chamber to 6.25 cm. Consequently the explosions at $P_i = 750$ and 1000 atmospheres, respectively, were carried out in the so-reduced chamber; and in order to correlate the two sets of results, an explosion was carried out in it at $P_i = 500$ atmospheres also.

The experimental results, which are detailed in Table IV, entirely support the conclusions drawn from our previous experiments that absolutely the N_2 -activation effect in such explosions was rapidly approaching a maximum when the density of the medium exceeded that corresponding with $P_i = 150$ atmospheres. Thus the fact of there being neither any increased "lag" in the "explosion time" (t_m) nor yet any further increase in the estimated exothermic effect during the first second of the "cooling period," after the initial pressure exceeded 350 atmospheres, may be regarded as conclusive evidence of there having been no further increase in the N_2 -activation after such point had been passed.

As might be expected, the P_{mb}/P_{i0} ratios steadily increased from 7.89 to 9.00, corresponding with a rise of from 2650 to just under 3000° K. in the mean maximum "explosion temperature," as the initial pressure was increased from 250 to 1000 atmospheres, and the calculated degree of CO_2 -dissociation at the maximum temperature correspondingly increased from about 2.5 to 5.5 per cent.

It should also be observed that at no time was there the slightest sign of any "carbon deposition" during any of the explosions, an important consideration especially in view of what was found during the next series of explosions with $2\text{CO} + \text{O}_2 + 3.76\text{CO}$ media in which the nitrogen in the air had been replaced by its equivalent of carbonic oxide.

From the pressure-time records reproduced in fig. 6, *a*, *b*, *c* and *d*, it will be observed that (unlike similar records obtained when these mixtures were

Table IV.— $2\text{CO} + \text{O}_2 + 3.76\text{N}_2$ Explosions

P_i atmos.	P_0 atmos.	t_m secs.	P_m atmos.	P_{mb} atmos.	P_{mbc} atmos.	P_b atmos.	P-fall in 1 sec after t_m		$P_{mb} P_b$	T_m K°.	P-equivalent of exothermic effect in 1 sec after t_m	Calculated CO_2 -dissociated at T_m , per cent
							atmos.	Per cent				
Explosion Chamber, 7.5×3.75 cm.												
250	243.5	0.28	2290	1923	2212	205	780	37	7.89	2650°	315	2.4
350	312.5	0.33	3270	2583	3024	269	1060	35	8.26	2760°	326	3.6
500	388.5	0.33	4500	3330	3814	327	1350	32.5	8.57	2860°	—	5.0
Explosion Chamber, 6.25×3.75 cm.												
500	388.5	0.22	4480	3320	—	325	1430	34.5	8.54	2850°	—	5.0
750	490	0.22	5820	4070	—	385	1690	30	8.85	2950°	—	5.5
1000	520	0.24	7100	4690	—	434	1990	30	9.00	2995°	—	5.5

exploded in our spherical bombs) there was always a well-marked "hump" in the rising pressure-curve indicative of some retardation of the flame when it first impinged upon the walls of the cylindrical cavity. This feature was more marked in these comparatively slow explosions than in the next series of more rapid $2\text{CO} + \text{O}_2 + 3.76\text{CO}$ explosions; and in the still more rapid H_2 -air explosions (*q.v.*) it was untraceable. It was due to purely "environmental" circumstances and had no chemical significance.

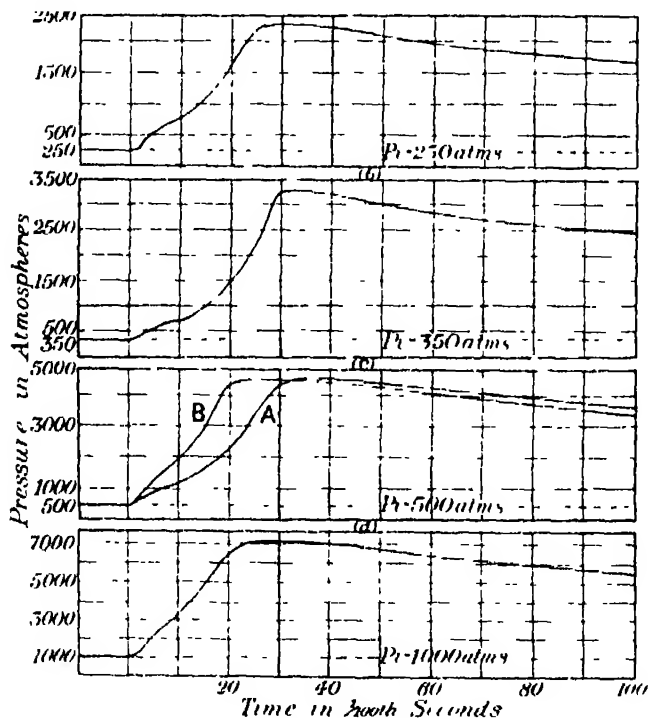


FIG. 6.

F.— $2\text{CO} + \text{O}_2 + 3.76\text{CO}$ Explosions at Initial Pressures between 250 and 500 Atmospheres.

Hitherto in these investigations we had always carried out explosions of $2\text{CO} + \text{O}_2 + 4\text{CO}$ mixtures at initial pressures corresponding with those of our $2\text{CO} + \text{O}_2 + 4\text{N}_2$ explosions in order to obtain data required for the measurement of the N_2 -activation and CO_2 -dissociation effects during the last-named. And it may be recalled how the replacement of N_2 by its equivalent of CO in such explosions not only made the "explosion time" as short as in corresponding $2\text{H}_2 + \text{O}_2 + 4\text{N}_2$ explosions, and eliminated the "exothermic

effect" exerted by the nitrogen during the "cooling period," but also suppressed CO_2 -dissociation altogether. Moreover in none of such $2\text{CO} + \text{O}_2 + 4\text{CO}$ explosions at initial pressures up to 150 atmospheres was there even the slightest deposition of carbon.

Accordingly in these new experiments at still higher initial pressures, we essayed for comparative purposes a corresponding series of $2\text{CO} + \text{O}_2 + 3.76\text{CO}$ explosions at initial pressures of 250, 350, 500, etc., atmospheres. Unfortunately, however, for the strict validity of the comparison, it was found that at all such higher initial pressures slight but unmistakable carbon-deposition occurred during the explosions, a feature which had never been observed at lower initial pressures. Nevertheless the observations were not without interest inasmuch as they showed very clearly how an increase in pressure affects equilibrium in a reversible $\text{CO}-\text{C}-\text{CO}_2$ system in the opposite direction to an increase in temperature. The experimental details are shown in Table V and the corresponding pressure-time records are reproduced in fig. 7, *a*, *b*, and *c*.

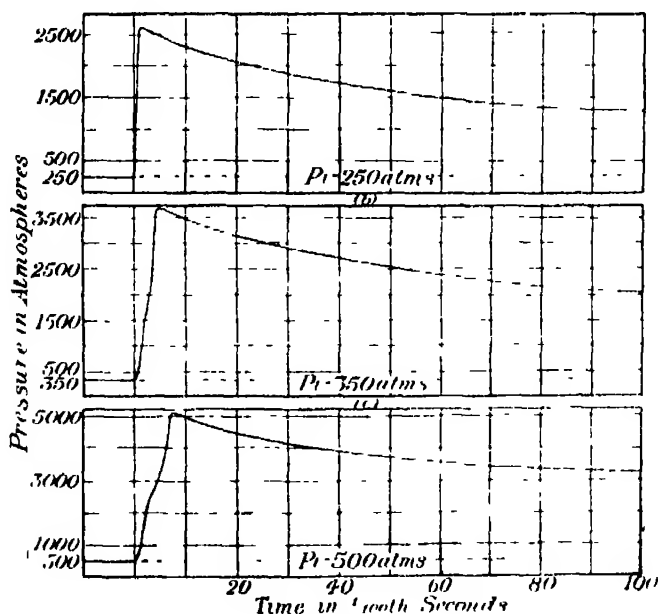


FIG. 7

It will be seen that, in conformity with our previous experience at lower pressures, the "explosion-times" were all considerably less, the mean maximum temperature considerably higher, and the rates of cooling after t_m much faster than in the corresponding $2\text{CO} + \text{O}_2 + 3.76\text{N}_2$ explosions, circumstances

Table V.— $2CO + O_2 + 3.76CO$ Explosions in Cylindrical Chamber, 7.5×3.75 cm.

P_i atmos.	P_{i0} atmos.	t_m secs.	P_m atmos.	P_{m0} atmos.	P_{m0c} atmos.	P fall in 1 sec. after t_m		$P_{m0} P_{i0}$	T_m K°.	Percentage carbon- deposition.
						atmos.	Percent			
250	245	0.015	2800	2132	2172	1350	57	8.70	2955°	0.6
350	320	0.045	3700	2849	2948	1710	50	8.91	3025°	1.3
500	392	0.075	5100	3621	3821	1980	41.5	9.24	3140°	2.3

attributable to the total suppression of both N_2 -activation and CO_2 -dissociation effects by the replacement of N_2 by CO as the diluent

In conclusion we wish to express our best thanks to Imperial Chemical Industries, Ltd., for generous grants out of which both the heavy capital, and running costs of the experiments have been defrayed

Summary

(1) Explosions of $2H_2 + O_2 + 3.76N_2$, $2CO + O_2 + 3.76CO$, and $2CO + O_2 + 3.76N_2$ mixtures have been successfully carried out in a cylindrical bomb chamber 7.5 cm. long by 3.75 cm. diameter, of 114 c.c. capacity at initial pressures up to 500 atmospheres in the first and second and up to 1000 atmospheres in the third case, and complete pressure-time records thereof have been obtained.

(2) Correlating experiments at $P_i = 75$ atmospheres have indicated that whereas the observed explosion times for *quick* explosions were much the same as, or for *slow* explosions a little less than, would have been observed had a spherical bomb chamber of 240 c.c. capacity been employed (as in our previous experiments) the mean maximum temperatures (abs.) were probably *circa* 0.86 those which would have resulted in the latter case.

(3) The effects of the considerable deviations of the explosive media concerned from the gas-laws at the high initial pressure (*i.e.*, over 250 atmospheres) employed are such as involve much smaller actual density increments from given gauge-pressure increments.

(4) With the $2H_2 + O_2 + 3.76N_2$ explosions there was a quite definite increase in the "explosion times" with density at initial pressures over 250 atmospheres; but at 750 atmospheres the detonation, instantaneously set up, was so violent that further work at any higher pressure was impracticable.

(5) In the $2CO + O_2 + 3.76N_2$ explosions, the characteristic lag in the "explosion time," as well as the exothermic effects observed during the "cooling period" after t_m —both of which had hitherto consistently increased with the density of the medium—reached their maxima at a density corresponding with P_i somewhere between 350 to 500 atmospheres, and afterwards remained constant. These circumstances are indicative of the N_2 -activation effect having reached a maximum at such a density of the medium.

(6) The CO_2 -dissociation at the maximum temperature in the $2CO + O_2 + 3.76N_2$ explosions at $P_i = 500$ to 1000 atmospheres was of the order of 5 to 6 per cent.

(7) In the $2\text{CO} + \text{O}_2 + 3.76\text{CO}$ explosions, which were always very much more rapid than the corresponding $2\text{CO} + \text{O}_2 + 3.76\text{N}_2$ explosions, the "explosion times," which up to then had been nearly constant, began definitely to increase with further increments in the density of the medium above $P_1 = 250$ atmospheres, and at about the same point slight carbon-deposition began to be manifested during the explosion, the two circumstances probably being connected. The rates of pressure-fall during the first second of the "cooling periods" immediately after t_m were also always much faster than in the corresponding $2\text{CO} + \text{O}_2 + 3.76\text{N}_2$ experiments.

Gaseous Combustion at High Pressures. Part XV.—The Formation of Nitric Oxide in Carbonic Oxide-Oxygen-Nitrogen Explosions.

By DONALD T. A. TOWNEND, D.Sc., and LIONEL E. OUTRIDGE, B.Sc.

(Communicated by W. A. Bone, F.R.S. —Received August 19, 1932)

Introduction.

In previous papers of this series* it was shown that the secondary formation of nitric oxide in $\text{CO}-\text{O}_2-\text{N}_2$ explosions, when oxygen is present in excess of that required to burn all the carbonic oxide, rapidly increases with the density of the medium, the optimum composition of the medium for the purpose being $2\text{CO} + 3\text{O}_2 + 2\text{N}_2$.

The former experiments were carried out, in bombs Nos. 2 and 3, the 7.5 cm. diameter spherical explosion chambers of which were each of 240 c.c. capacity with a surface/volume ratio 0.78, under conditions permitting of no acceleration in the normal rate of cooling down of the hot products from the maximum explosion temperature.

In such circumstances the amounts of NO_2 surviving in the *cold* products of

* 'Proc. Roy. Soc.,' A, vol. 105, p. 426 (1924); vol. 108, p. 415 (1925); and vol. 115, p. 45 (1927); also "Gaseous Combustion at High Pressures," chap. XII, pp. 174-190 (1929).

a $2\text{CO} + 3\text{O}_2 + 2\text{N}_2$ explosion increased with the density of the medium as follows:—

P_i atmos.	t_m sec	P_m atmos.	T_m K°	Per cent. NO_2^* in cold products.	$\text{NO}_2/\text{CO}_2 \times 10^2$.
3.0	0.065	—	—	0.3	0.9
25.0	0.060	—	—	0.8	2.4
50.0	0.035	422	2685°	1.8	5.4
75.0	0.030	675	2800°	3.0	9.0

* Although the oxide of nitrogen actually formed during the explosion is nitric oxide during the subsequent cooling it combines with the excess of oxygen present forming the peroxide which is what survives and is estimated at the end of the experiment

From thermodynamical considerations and data published by W. Nernst and his co-workers,† it was deduced that, owing to its endothermic character, (a) no large NO-formation would be expected in such explosions unless the maximum temperature exceeds 2500° K. except under conditions of a prior N_2 -activation depending more on the density of the medium than its temperature, and (b) but little of it would survive decomposition unless the subsequent cooling from T_m down to well below 2500° K. is exceedingly rapid.

The combined evidence of the pressure-time and spectrographic records obtained during the former experiments, together with the estimations of NO_2 surviving in the cold products, pointed unmistakably to the following sequence of events in such explosions at high initial pressures, namely, (i) an instantaneous primary N_2 -activation by radiation from the main CO-combustion; (ii) a slower secondary NO-formation from such "activated" N_2 and any excess-oxygen present; (iii) an adjustment (never complete) towards equilibrium in the $2\text{NO} \rightleftharpoons \text{N} + \text{N} + \text{O} + \text{O}$ system—together with (possibly) some N_2 -“deactivation”—as the products cool down, and (iv) towards the end of the “cooling period” the conversion of any surviving NO into the peroxide. Of these stages (i) would occur during the “combustion period” only, but (ii) might occur either *before* or *after* t_m , according to circumstances, it being largely a question of temperature, time and the ratio between the nitrogen and *excess* oxygen in the medium (1 : 1 being the most favourable), while (iii) and (iv) would occur mainly or wholly after t_m , i.e., during the “cooling period.”

Apart from such considerations, however, it can be shown experimentally that the secondary NO-formation is not instantaneous, but requires an

† ‘Z. anorg. Chem.,’ vol. 45, p. 46 (1905) and vol. 46, p. 212 (1906).

appreciable time which diminishes rapidly as the maximum temperature rises, and only becomes negligible at temperatures above 2500° K. Fortunately at any given temperature its rate of decomposition is always many times less than its rate of formation, so that the faster the cooling after T_m in the explosion the greater the chance of oxides of nitrogen surviving in the cold products. And from the pressure-time records, etc., of former experiments during these investigations it was calculated, on certain very reasonable assumptions, that probably about *half* of the nitric oxide actually formed during the explosion had so survived.

The matter being not only of considerable theoretical interest, but also of possible importance as regards the technical fixation of nitrogen, *i.e.*, as an alternative to synthetic ammonia processes, it was discussed with the technical staff of Imperial Chemical Industries who saw commercial possibilities in it provided that a *minimum* surviving NO-yield at $P_i = 75$ atmospheres of about 10 per cent. could be assured. Consequently arrangements were made with Professor W. A. Bone whereby we were enabled to carry out under his supervision the further experiments described herein, which were designed greatly to accelerate the normal cooling down of the explosion products in a closed chamber in the expectation that considerably more oxides of nitrogen would actually be found surviving in the cold products than was the case in the former experiments.

EXPERIMENTAL.

A.—*The Explosion Bomb (No. 6)*

The object of the experiments being, not only to determine how much the NO_2 -survival in the *cold* final products of $2\text{CO} + 3\text{O}_2 + 2\text{N}_2$ explosions at high initial pressures could be increased by accelerating to the utmost their cooling-down from T_m , but if possible to explore the rate of NO-formation throughout the whole "explosion period," and to ascertain at what points on the pressure-time record it reached a maximum, it was decided, after due consideration of other alternative means, to adopt the principle of exploding the medium at a series of selected high initial pressures ranging between about 40 and 90 atmospheres in a steel enclosure. One end of this was separated by a metal disc of variable resisting strength from a larger cast-iron "expansion chamber" into which the explosion products were rapidly released (and thereby suddenly chilled) at the moment when the disc burst during the explosion, which could be approximately predetermined by suitably regulating its resisting-strength. Accordingly, after some preliminary trials upon the

bursting of such discs during explosions, the apparatus shown in fig. 1 was designed, and afterwards constructed for us in the workshops of Synthetic Ammonia and Nitrates, Ltd., at Billingham-on-Tees.

The body of the apparatus comprised three main metal sections X_1 , X_2 and X_3 , forming two enclosures, namely (a) an "explosion chamber," A, separated by the metal disc, D, from a much larger "expansion chamber," B. The "explosion chamber" was cylindrical, $4\frac{1}{2}$ inches long by $4\frac{1}{2}$ inches diameter and of 990 c.c. capacity with a surface/volume ratio 0.55, and machined out of a nickel-steel forging, suitable openings in it being provided for an inlet valve V_1 , a Petavel manometer, M, and an ignition plug, P. The disc, D, was held gas-tight in recesses turned on one side from the body, X_1 , of the explosion chamber, A, and on the other from the central conical nickel-steel

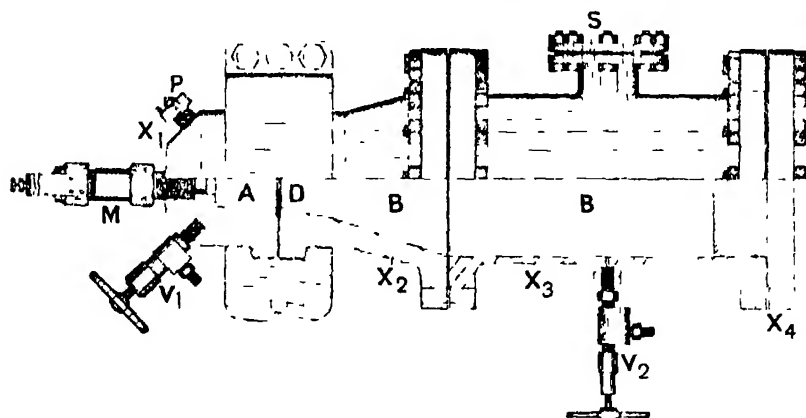


FIG. 1

section, X_2 , $12\frac{1}{2}$ inches long by $4\frac{1}{2}$ inches tapering outwards to $11\frac{1}{2}$ inches diameter, which formed part of the expansion chamber, B. A gas-tight joint was effected by means of "Klingerit" washers, the two sections X_1 and X_3 being held rigidly together by a series of six $1\frac{1}{4}$ -inch bolts operating on two semi-circular clamps E_1 and E_2 . The main shell, X_3 , of the "expansion chamber," B, was a cylindrical iron casting, 16 inches long by $11\frac{1}{2}$ inches internal diameter, bolted to the central conical section, X_2 , by means of a series of sixteen 1-inch bolts passing through suitable flanges. The end-plate, X_4 , suitably bolted to X_3 , was furnished with a bed of lead, 4 inches thick, for the safe reception of projectiles from the bursting discs. A "safety disc," S, 6 inches in diameter, was also bolted to the expansion chamber in order to safeguard against any too dangerously rapid rise of pressure therein. The valve, V_2 , which was kept closed during an explosion, served for the withdrawal of samples of the cold

released explosion-products for analysis at the conclusion of each experiment. The total volume of the expansion chamber, B, was 38.4 times that of the explosion chamber, A.

The chief difficulty encountered during the experiments was the designing of discs so as to ensure each bursting during an explosion at some predetermined point anywhere along the pressure-time record. After many trials, the design, shown in fig. 2 was adopted, the shaded part showing the disc intact *before* and the unshaded the bulged-out part remaining *after*, an explosion. The discs were of mild steel, $5\frac{1}{4}$ inches in diameter and between 0.3 and 0.4 inch thick according to the initial explosion pressure employed; and by narrowing

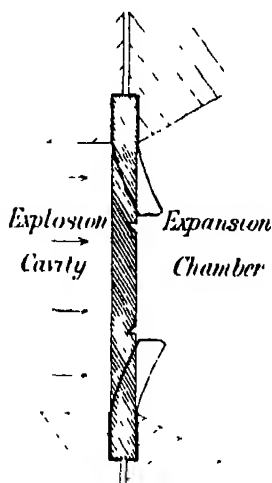


FIG. 2.

the diameter at the "circle of shear" considerably below that at which a disc was firmly clamped, as shown in the diagram, its bursting in an explosion was delayed by its prior "dishing" as a whole. By using this delay it was found possible so to control the moment of sudden release of the explosion products as to time it approximately for any particular pre-determined point on the pressure-time record during *either* the "explosion period" (i.e., the pressure-rise), or at P_m , or even during the subsequent "cooling-period" as required.

B.—Procedure.

The Explosions.—The compressed constituents of the explosive medium under investigation were each separately and slowly admitted from storage cylinders into the explosion chamber, A, through a 12-inch glass lined steel tube filled as to one half with "activated" coconut-shell charcoal (for the removal of any possible traces of iron carbonyl from the carbonic oxide) and as to the other half with purified phosphoric anhydride. The proportions of each constituent were regulated so as to produce in A a mixture of the desired composition at a pressure somewhat higher than that at which it was subsequently fired. After allowing several hours for their complete mixing, a sample of the medium was withdrawn for the checking of its composition by analysis. Finally, when the pressure had been correctly adjusted to the desired initial point (P_i) the mixture was fired, and a pressure-time record of the explosion taken by means of the Petavel manometer in the usual manner.

In a control series of explosions of a $2CO + 3O_2 + 2N_2$ medium at selected

different initial pressures, the discs fitted between A and B were purposely made strong enough to withstand the force developed without bursting in order to obtain a typical series of unbroken pressure-time records from beginning to end of the respective explosions for reference purposes. Subsequently the main series of explosions with the same medium was carried out, in three groups, so as to cover the principal ranges of initial pressures, namely, 40 to 45 atmospheres, 68 to 72 atmospheres, and 88 to 90 atmospheres,* respectively, the strengths of the discs used in each case being suitably adjusted so as to ensure its bursting at *approximately* the right point—the exact position of which was automatically registered on the resulting pressure-time record—and suddenly releasing the products of explosion into the “expansion chamber,” B, which until then had contained only air at the room temperature and pressure. The effect of such release, as proved by the pressure-time record, was to cool the hot products down to room temperature in less than 0.005 second.

Estimation of NO₂ in the Explosion Products.—Immediately after each explosion a sample of the cold expanded products was withdrawn from B, through the valve V₂, into a pyrex-glass sampling vessel of 500 c.c. capacity and the percentage of NO₂ therein subsequently estimated by the phenol disulphonic acid method. On multiplying this result by a pre-determined factor so as to “correct” it for the dilution of the cold explosion products in each case by air in the expansion chamber (e.g., at 50 atmospheres the factor was 1.9) the actual percentage of NO in the products at the moment of the disc bursting was obtained.

C.—Results.

(i) $2\text{CO} + \text{O}_2 + 3.76\text{N}_2$ *Explosions with Discs Unburst.*—(a) A few trial explosions of theoretical H₂-air and CO-air mixtures at initial pressures of 50 atmospheres, the explosion chamber A being fitted with a disc strong enough to withstand the force developed so that the products were retained therein throughout, showed that the explosion-times (t_m) were approximately twice as long as, and the rates of cooling after T_m only slightly less than, those observed in similar explosions at the same initial pressures in the No. 2 spherical bomb (capacity 240 c.c.) used in these researches.

(b) For comparison with the subsequent main series of $2\text{CO} + 3\text{O}_2 + 2\text{N}_2$ explosions, where the secondary NO-formation would reach a maximum, a

* It was found necessary in each experiment to adjust the initial pressure to some suitable point within one or other of the given ranges so as to ensure the particular disc used bursting just at the desired point on the pressure-time curve.

special series of $2\text{CO} + \text{O}_2 + 3.76\text{N}_2$ explosions, in which it was negligibly small (i.e., not exceeding 0.05 per cent.), were next carried out at initial pressures of 40, 50 and 90 atmospheres, respectively, with the following results :

Table I.— $2\text{CO} + \text{O}_2 + 3.76\text{N}_2$ Explosions in Bomb with Disc Unburst.

P_i , atmospheres	40	50	90
t_m , seconds	0 24	0 35	0 65
P_m , atmospheres	320	425	775
P_m/P_i	8 0	8 5	8 6
P-fall in 1 second after P_m —			
Atmospheres	70	90	145
Per cent *	21 5	23 5	20 7
T_m , K°	2620°	2720°	2800°

* I.e., of the total possible between P_m and P_i

Such results are indicative of considerable N_2 -activation during the explosions ; thus, for example, the t_m 's materially increased with the density of the medium, and the average rates of cooling during the first second after t_m were only 0.6 those observed in corresponding $2\text{CO} + \text{O}_2 + 3.76\text{CO}$ explosions.

(2) $2\text{CO} + 3\text{O}_2 + 2\text{N}_2$ Explosions with Disc Unburst.—In order to establish data for the normal course of events in $2\text{CO} + 3\text{O}_2 + 2\text{N}_2$ explosions at various initial pressures between 35 and 90 atmospheres when the products were prevented from escaping from the explosion chamber, A, we next proceeded with a series of such explosions in which the disc D was purposely made strong enough to withstand without bursting the force developed. The following typical results were obtained.

Table II — $2\text{CO} + 3\text{O}_2 + 2\text{N}_2$ Explosions with Disc Unburst.

	(1)	(2)	(3)	(4)
P_i , atmospheres	35	60	70	90
t_m , seconds	0 20	0 20	0 24	0 20
P_m , atmospheres	290	535	635	840
P_m/P_i	8 5	8 9	9 07	9 33
P-fall in 1 second after P_m —				
Atmospheres	80	115	140	162
Per cent	31.0	24.8	24.4	21.5
T_m , K°	2600°	2800°	2830°	2920°
In cold products—				
Percentage NO_2	0.6	1.0	1 0	1.25
$\text{NO}_2/\text{CO}_2 \times 10^3$	1 8	3.0	3.0	3.75

In fig. 3 is reproduced the pressure-time record of experiment (3) at $P_i = 70$ atmospheres ; the vertical arrows show the various points at which, in the

second group of the subsequent main series of experiment, the disc burst in explosions with the same mixture at approximately the same initial pressure, the vertical dotted line indicating how abrupt was the pressure-fall when the disc burst in the last of them.

From the foregoing results it will be seen that the explosion times (t_m) were materially shorter, and the P_m/P_i ratios rather higher, than in the corresponding $2\text{CO} + \text{O}_2 + 3.76\text{N}_2$ explosions, and that the percentage of NO_2 found in the cold products increased from 0.6 to 1.25 as P_i was raised from 35 to 90 atmospheres.

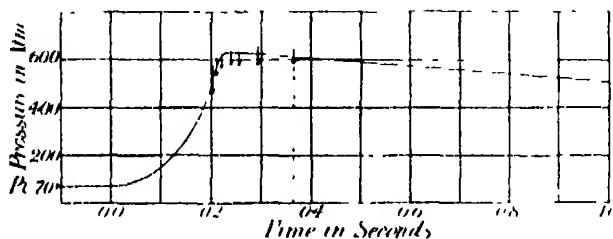


FIG. 3.

(3) *The Main Series of $2\text{CO} + 3\text{O}_2 + 2\text{N}_2$ Explosions with Bursting Discs.*—

The main series of experiments comprised three groups in which $2\text{CO} + 3\text{O}_2 + 2\text{N}_2$ mixtures were fired in the explosion chamber of the bomb at initial pressures of 40 to 50, 68 to 72, and 88 atmospheres, respectively, the strengths of the discs being so graduated as to ensure bursts at several different points—both *before* and *after* the attainment of maximum pressure—on the pressure-time record.

The results, as detailed in Table III, showed in each case (i) the time of the disc bursting as a fraction of a second *before* or *after* (— or +) what would have been or was t_m , the moment of maximum pressure; (ii) the mean pressure, P_b , of the medium at the moment when the disc burst; and (iii) the NO_2 -yield as a volumetric percentage of the final products. Also, in all cases when the disc burst *after* t_m are added; (iv) the T_m in $^\circ\text{K}$; and (v) the $\text{NO}_2/\text{CO}_2 \times 10^2$ ratio in the final products.

In regard to the NO -formation, the results as a whole show not only the beneficial influence of pressure thereon, but also that it begins during the “combustion period” and continues far beyond P_m into the “cooling period” in such explosions. Indeed we are satisfied that only in the second group of experiments had the NO -formation certainly attained a maximum; in both the other two groups it seems probable that, had we succeeded in getting a

Table III.— $2\text{CO} + 3\text{O}_2 + 2\text{N}_2$ Explosions with Bursting Discs.

P_i (atmos.).	P_b when disc burst atmos	Time of burst in seconds <i>before</i> or <i>after</i> P_m .	T_m K°	On cold products.	
				Percentage NO_2 .	$\text{NO}_2/\text{CO}_2 \times 10^3$
First Group. $P_i = 40$ to 45 atmospheres.					
40 0	325	-0 05	—	1 8	—
45 5	350	-0 05	—	2.2	—
40 0	335	+0 01	2600°	2.2	6 6
43 0	350	+0 05	2500°	2 6	7.8
45 5	380	+0 05	2585°	2 4	7 2
Second Group. $P_i =$ approximately 70 atmospheres.					
70	520	-0 03	—	3.3	—
69	510	-0 02	—	3 3	—
68	505	-0 01	—	3 3	—
70	650	+0 01	2895°	3 3	9 9
68	635	+0 02	2915°	4 5	13 5
70	620	+0 06	2815°	5 4	16.2
72	630	+0 13	2815°	5 4	16.2
Third Group. $P_i = 88$ atmospheres.					
88	800	-0 05	—	3 0	—
88	800	-0 04	—	3 0	—
88	825	At P_m	2920°	5 1	15.3
88	830	At P_m	2930°	4 5	13 5

disc to burst further along the pressure-time record than it actually did, a somewhat higher NO_2 -yield would have resulted

As it was, the largest NO_2 -yields actually attained were 2.6 per cent. at $P_i = 43$ atmospheres in the first group, 5.4 per cent. at $P_i = 70$ atmospheres in the second, and 5.1 per cent. at $P_i = 88$ atmospheres in the third group. In the last named, at least, where we did not succeed in getting a disc to burst *after* the moment of maximum pressure, P_m , the maximum NO -formation had certainly never been reached, but had we so succeeded, the NO_2 -yield would probably have exceeded 6.0 per cent.

Not only do the NO -yields greatly exceed any previously obtained in such explosions, but the experimental results as a whole afford further strong support for the view that there is a primary N_2 -activation followed by a secondary NO -formation as set forth in our introduction.

Moreover, from the results of the second group of the main series of the present experiments, combined with those of the previous $2\text{CO} + \text{O}_2 + 4\text{N}_2$

explosions set forth in Table XXX (p. 162) of "Gaseous Combustion at High Pressures," it would seem that most probably the energy represented by the heat of formation of the nitric oxide actually formed in our $2\text{CO} + 3\text{O}_2 + 2\text{N}_2$ explosion at $P_1 = 70$ atmospheres represented about half of that previously expended in activating the nitrogen.

In conclusion, we have pleasure in thanking Professor W. A. Bone and Messrs. M. P. Appleby and William Rintoul, of Imperial Chemical Industries, Ltd., for their advice in connection with the apparatus and procedure.

Gaseous Combustion at High Pressures, Part XVI.—Nitric Oxide Formation in Continuous High-Pressure Flames of Carbonic Oxide in Oxygen-Nitrogen Atmospheres.

By DUDLEY M. NEWITT, D.Sc., and FRANK G. LAMONT, M.Sc.

(Communicated by W. A. Bone, F.R.S.—Received August 19, 1932)

As it seemed desirable to supplement the experiments dealt with in Part XV by a systematic study of nitric oxide formation in steady flames of carbonic oxide continuously maintained at high pressures in atmospheres composed of oxygen and nitrogen in various pre-determined proportions, at Professor Bone's request we undertook to do so, with results which are set forth herein.

In 1909 Haber and Coates published experiments* in which steady flames of carbonic oxide were maintained in oxygen-nitrogen atmospheres at various steady pressures up to 45 atmospheres. Their apparatus consisted of a bronze cylinder in which carbonic oxide was burnt under pressure at a steatite orifice, an electrically-glowed platinum wire being used for ignition, and the products of combustion were lead away by a small quartz cap terminating in a platinum tube (which higher up was water-cooled).

In one series of experiments, Table I, in which the supporting atmosphere was a $50\text{O}_2/50\text{N}_2$ "Linde-air," the NO-yields were found to vary with the pressure.

Haber and Coates, while recognising that an increase in pressure is much more effective than a considerable increase in temperature in promoting NO-formation in the flame, concluded that little benefit results from increasing the pressure beyond a certain point, which from the results in Table I seemed

* 'Z. phys. Chem.', vol. 69, p. 337 (1909).

Table I.—Haber and Coates' Results for CO-flames in $50\text{O}_2/50\text{N}_2$ Atmospheres.

Pressure (atmos.).	Percentages in products.			$\text{NO}/\text{CO}_2 \times 10^2$.
	CO_2 .	O_2	NO	
5	51.9	11.2	0.68	1.31
5	51.05	10.2	0.78	1.47
9	31.6	26.6	0.98	3.09
9	32.8	25.4	1.05	3.21
13	20.6	35.0	0.87	4.22
13	21.6	34.3	0.87	3.98
17	15.3	39.2	0.67	4.38
45	8.93	--	0.418	4.68

to be about 13 atmospheres. They remarked that the NO-yields actually obtained were materially higher than those calculated for the then known Nernst figures for a purely thermal equilibrium, and thought that, besides thermal factors, "ionisation" in the flame plays an important part.

According to the views established by this series of investigations in Professor Bone's laboratories there seems no reason why the beneficial effect of increasing pressure upon NO-formation in such circumstances should cease at so low a point as supposed by Haber and Coates, and from our re-investigation of the matter it seems that on this point they erred.

In comparing the results of such experiments with those of $2\text{CO}-\text{O}_2-\text{N}_2$ explosions it should be borne in mind that whereas in the former combustion proceeds steadily under conditions of "constant pressure" in a more or less heterogeneous "shell" of flame, in the latter it occurs in a homogeneous medium under conditions intermediate between those of "constant pressure" and "constant volume," and approximates more nearly to the last-named the quicker and more homogeneously the enclosure is filled with flame. Consequently, the mean maximum flame temperature attained in such an explosion at a given initial pressure will be higher than that of a CO-flame steadily maintained at the same pressure in a similar O_2-N_2 atmosphere; some direct measurements in our laboratories have generally confirmed this, though it has not been possible to deduce an exact comparison therefrom.

Seeing that in the previous parts of this investigation it has been shown that N_2 -activation in $\text{CO}-\text{O}_2-\text{N}_2$ explosions only becomes manifest at initial pressures of 10 atmospheres, and does not assume practical importance until still higher pressures—being chiefly operative at those exceeding 50 atmospheres—it was deemed necessary for us to have an apparatus in which CO-flames could be steadily maintained in selected O_2-N_2 atmospheres at all

pressures up to 100 atmospheres ; the design of such a one formed an important part of the work and will now be described.

EXPERIMENTAL.

Apparatus.—The apparatus, shown in section in fig. 1, consisted of a mild steel cylinder, A, closed by flanged end-plates carrying the gas inlet and outlet pipes. It was fitted with two plugs holding conical quartz windows capable of withstanding pressures up to 100 atmospheres, through which the flame could be observed and adjusted during an experiment. The cylinder

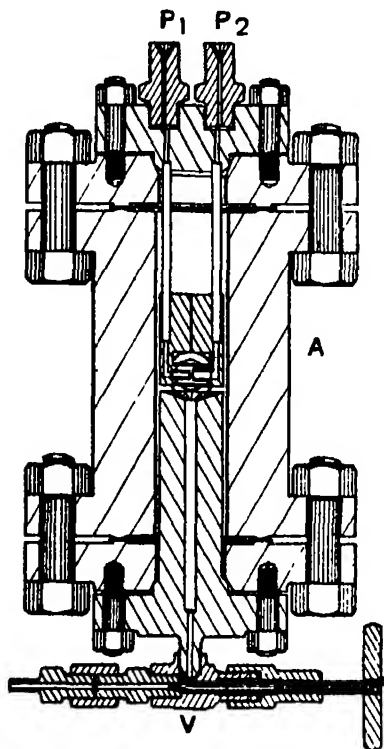


FIG. 1.

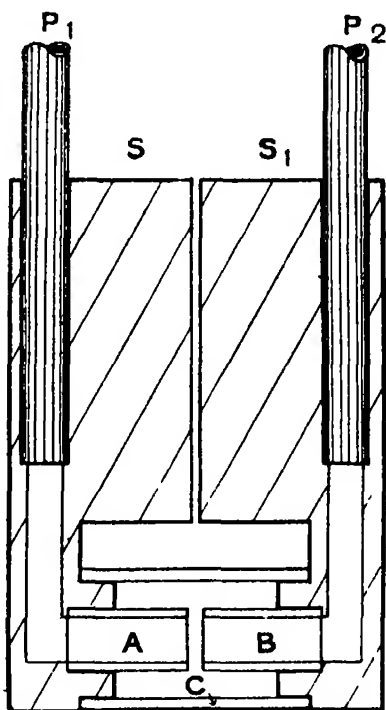


FIG. 2.

was 1 foot in length, with an internal diameter of 2 inches and with walls $1\frac{1}{2}$ inches thick ; it was lined throughout with stainless steel of a quality resistant to the action of hot oxides of nitrogen.

The combustible gas and the O_2-N_2 mixture entered the cylinder separately through the pipes P_1 and P_2 , and the products of combustion passed out through the stainless steel valve V. At the outset the designing of a burner capable of giving a steady flame proved a difficult matter. Finally, after many trials, the design, shown in fig. 2, was found most suitable.

It consisted of two blocks of stainless steel S, S_1 , connected to the inlet pipes P_1 and P_2 for the carbonic oxide and supporting "air" respectively, and drilled to receive two silica jets A and B. These jets faced one another at a distance of 2 mm. apart and were surrounded by a transparent silica tube C, in which were cut two vertical slits facing the quartz windows of the pressure vessel. Such device enabled a vertical disc of flame to be maintained mid-way between A and B.

The flame was started at room pressure by a taper inserted through one of the window-plug openings. The plug was then replaced, and the pressure

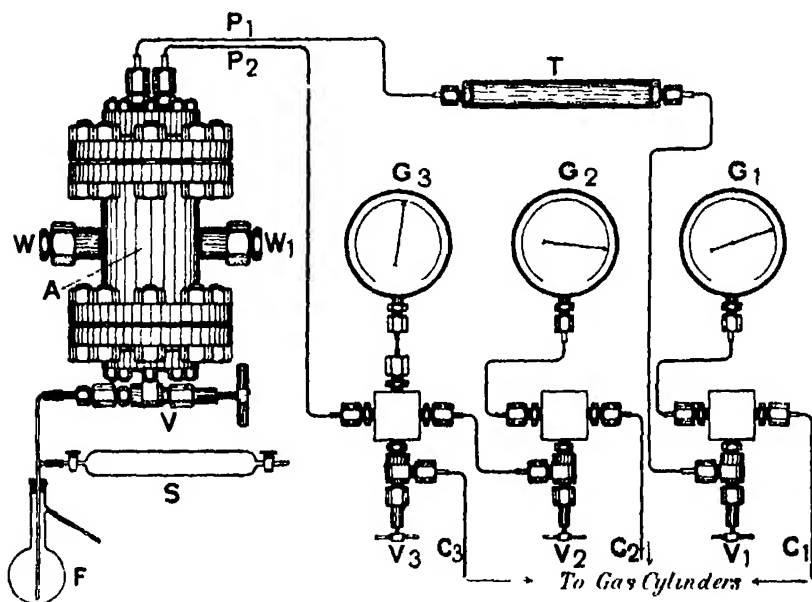


FIG. 3.

inside the vessel increased to the desired experimental point by regulating the valve V

The general arrangement of the apparatus with its control valves and gauges is shown diagrammatically in fig. 3. The cylinder C_1 , containing the combustible gas at a high pressure was connected to the inlet pipe P_1 , through the control valve V_1 . A bronze tube T containing activated charcoal interposed between the valve and the inlet pipe served for the removal of any possible traces of iron-carbonyl possibly present in the compressed carbonic oxide. The mixture of oxygen and nitrogen constituting the "supporting atmosphere" for the CO-flame was contained under pressure in the cylinder

C₂, whence it passed through a control valve, V₂, and the valve V₃, on to the inlet pipe P₂. Two Bourdon gauges G₁ and G₂ indicated the pressures in the two supply cylinders, respectively, while a third gauge G₃ showed that in the combustion chamber, from which the products of combustion passed outwards through the valve V₄ and the flask, F.

Procedure.—Each series of experiments consisted in maintaining a steady flame of carbonic oxide at some pre-determined pressure (either 10, 30, or 100 atmospheres) in a particular supporting atmosphere of oxygen and nitrogen in some constant proportion, then varying the ratio between the CO burnt and the supporting atmosphere. Gas samples of the escaping products of combustion were taken at suitable intervals so timed as amply to allow each change in ratio to exercise its full effect upon the composition of the products. The rate of combustion was, however, so regulated as always to ensure the same quantity of the combustible gas being consumed in the flame in unit time.

The NO₂-content of the gaseous products was determined on half-litre samples, by the phenol-disulphonic acid method.

Characteristics of Pressure Flames of Carbonic Oxide—In the type of burner employed in these experiments the effect of pressure on a carbonic oxide flame is very pronounced. With the combustion chamber open to the air, the flame completely filled the space between the two jets and had a characteristic blue colour. On closing the vessel and progressively increasing the pressure the flame soon contracted to a thin disc of intensely luminous burning gas, the plane of the disc being at right angles to the axis of the jets, the hot products of combustion streamed out through the slits in the outer quartz tube (C. fig. 2) and were rapidly cooled by contact with the cold walls of the pressure vessel.

When the supporting atmosphere of the flame contained nitrogen, oxides of nitrogen were immediately formed, and with increase of pressure, the products as seen through the quartz windows of the combustion chamber assumed a deep red colour.

It is exceedingly difficult to maintain a carbonic oxide flame burning in atmospheric air (*i.e.*, O₂ + 3.76N₂) at high pressures, and we only succeeded in doing so by first establishing a flame in an enriched "air" (O₂ + 2N₂) and then slowly substituting ordinary air in its place. The difficulty, which was not encountered when working with atmospheres richer in oxygen may be ascribed to the relative "dryness" of the compressed gases used; the flame, when formed, was very sensitive and "flickered" rapidly as though maintained by an intermittent series of small explosions.

With enriched "airs" the flame was comparatively steady although it still exhibited occasional signs of "flickering." Attempts to measure the temperatures of such pressure-flames spectroscopically were unsuccessful; but in most cases they exceeded 2500° K.

Results.

Four principal series of experiments were carried out with carbonic oxide flames burning in atmospheres composed of $70\text{O}_2/30\text{N}_2$, $50\text{O}_2/50\text{N}_2$ ("Linde-air"), $33\cdot3\text{O}_2/66\cdot7\text{N}_2$ and $20\cdot9\text{O}_2/70\cdot1\text{N}_2$ (ordinary air), respectively. In each series, except that with ordinary air, the percentages of NO_2 in the exit gases were determined for various ratios between the combustible gas and the supporting atmosphere supplied to the flame when burning steadily at pressures of 10, 30 and 100 atmospheres, respectively. The O_2/N_2 ratios in each supporting atmosphere, though not always absolutely constant, varied but little from the mean values of 2.345 in the first, 0.99 in the second, 0.51 in the third, and 0.258 in the fourth series.

The experimental results are summarised in Tables II to V in which are shown (i) the ratios between (a) O_2 and CO, and N_2/CO supplied to the flame; (ii) the ratio between the N_2 supplied and the CO_2 formed therein; (iii) the percentage composition of the cold exit gases; and (iv) the $\text{NO}_2/\text{CO}_2 \times 10^3$ ratio therein.

In each series the experiments fall into three groups according to the pressure maintained in the combustion chamber; in each group the individual experiments are recorded in order of their O_2/CO ratios, beginning with the lowest, an arrow indicating the point where the theoretical $\text{O}_2/\text{CO} = 0.5$ ratio would be, and an asterisk the maximum NO_2 -yield obtained.

Owing to the difficulties encountered in maintaining steady flames in the fourth series of experiments with ordinary air as the supporting atmosphere, the results of only three experiments, all at $P = 100$ atmospheres, are detailed, namely, one with the theoretical, and two others with excessive, air supply. The very low NO_2 -yields obtained, however, diminished their importance save for comparative purposes.

In no case was combustion complete in the sense of the products being entirely free from *either* combustible *or* oxygen, though in most cases when they contained much oxygen, their content of carbonic oxide was very small. This feature of the experiments, however, does not necessarily imply that *within the flame itself* combustion was never complete, because conceivably

small amounts of either oxygen or combustible gas might have been swept outwards mechanically along with the escaping products without ever having actually been in the flame. Moreover combustion would always be impeded by the relative dryness of the compressed gases delivered to the flames, the small volume of which would favour their escape unburnt. Indeed, it is perhaps more remarkable that the combustion was so well maintained as it was in such a relatively dry medium.

In all cases, and even when considerable amounts of carbonic oxide were present in the exit gases, oxides of nitrogen were visibly produced; and in each group of each series the $\text{NO}_2/\text{CO}_2 \times 10^2$ ratios in the exit gases—which, under corresponding conditions, was greatest in the “Linde-air” series—not only steadily increased with the N_2/CO_2 ratio, even long past the point when the O_2/CO ratio was the theoretical 0.5, but in corresponding circumstances were always materially increased by pressure.

Thus, for example, in the “Linde-air” series (Table III) the highest $\text{NO}_2/\text{CO}_2 \times 10^2$ ratios observed were —

$$\text{O}_2/\text{CO} \quad \text{N}_2/\text{CO}_2$$

At P = 10 atmospheres, 2.15 with 0.84 and 0.87

At P = 30 atmospheres, 4.95 with 2.28 and 3.15

At P = 100 atmospheres, 8.46 with 1.71 and 1.81.

Seeing that in each particular group of experiments presumably the mean flame temperature would pass through a maximum when the O_2/CO ratio was at, or somewhat below, the theoretical 0.5—a point indicated by an arrow in each of the tables—the maximum NO-formation in the flame would appear to depend more upon the ratio between the nitrogen present and the carbonic oxide actually burnt in the flame than upon its mean temperature. And in this connection the fact that in all series of experiments at the highest pressure employed (100 atmospheres) the NO_2/CO_2 ratios in the products materially increased, with the O_2/CO and N_2/CO ratios at the burner, far beyond what might have been expected on purely thermal grounds (indeed only in the $70\text{O}_2/30\text{N}_2$ series was any limit reached at such pressure) seems of considerable significance.

Moreover, there can be no doubt about the favourable influence of pressure upon the NO-formation in all circumstances; for in these experiments, unlike those of Haber and Coates, this was manifested over the whole range (10 to 100 atmospheres) explored. Such beneficial influence may, we think, be

Table II.—Carbonic Oxide Flame in $70\text{O}_2/30\text{N}_2$ Atmospheres.

O ₂ /CO at burner.	N ₂ /CO at burner	N ₂ /CO ₂	Percentage in exit gases					NO ₂ /CO ₂ × 10 ³ .
			CO ₂	CO	O ₂	N ₂	NO ₂	
First Group. P = 10 atmospheres.								
0 258	0 113	0 22	45 2	44 35	0 15	9 95	0 35	0 78
0 446	0 212	0 26	65 5	14 75	2 4	16 65	0 70	1 07
0 635	0 262	0 269	70 3	1 05	9 35	18 4	0 90	1 28
0 958	0 397	0 405	52 8	1 05	24 85	20 95	0 95	1 80
1 54	0 635	0 67	35 35	1 85	38 85	23 20	0 80	2 26
1 92	0 79	0 83	29 55	1 45	14 05	24 15	0 80	2 70
2 57	1 07	1 165	21 90	2 10	50 15	25 12	0 75	3 40*
Second Group. P = 30 atmospheres								
0 375	0 162	0 222	62 85	22 70	0 25	13 75	0 45	0 72
0 45	0 184	0 213	72 20	11 40	0 50	14 85	1 05	1 45
0 538	0 223	0 237	73 40	4 50	4 25	16 85	1 00	1 36
0 833	0 347	0 366	55 65	3 15	20 20	19 95	1 05	1 89
1 68	0 696	0 771	31 00	3 35	41 15	23 35	1 15	3 70*
2 05	0 875	0 98	25 80	3 05	45 40	24 80	0 95	3 60
Third Group. P = 100 atmospheres.								
0 27	0 122	0 232	45 25	43 25	0 45	10 55	0 50	1 08
0 628	0 209	0 27	71 95	0 20	7 60	18 5	1 75	2 43
0 811	0 349	0 35	60 30	0 30	17 50	20 4	1 50	2 49
1 012	0 438	0 412	51 15	0 40	24 90	21 7	1 85	3 02
1 239	0 543	0 522	43 25	0 80	31 20	23 0	1 75	4 05
1 44	0 627	0 633	38 9	0 25	35 35	23 75	1 75	4 50
2 05	0 875	0 915	28 0	1 25	44 3	24 85	1 60	5 70*
2 16	0 931	0 965	27 0	0 90	45 4	23 5	1 40	5 20

attributed more to the increasing density than to any temperature increment in the burning medium

Comparison with Results of Explosion Experiments.—In comparing the results of our "Linde-air" series of experiments (Table III) with those of the $2\text{CO} + 3\text{O}_2 + 2\text{N}_2$ explosions recorded in the previous paper, it will be seen how much more favourable were the conditions of the latter to NO -formation. Thus, for example, whereas in the explosion at $P_1 = 88$ atmospheres the $\text{NO}_2/\text{CO}_2 \times 10^3$ ratio in the suddenly cooled products reached 15.3, the highest ever obtained in our steady flames at $P = 100$ atmospheres was 8.43 only.

Table III.—Carbonic Oxide Flame in 50O₂/50N₂ Atmospheres.

O ₂ /CO at burner	N ₂ /CO at burner.	N ₂ /CO ₂	Percentages in exit gases					NO ₂ /CO ₂ × 10 ³ .
			CO ₂	CO.	O ₂	N ₂	NO ₂ .	
First Group. P = 10 atmospheres.								
0 47	0 50	0 59	54 75	10 03	2 6	31 85	0 75	1 37
0 49	0 48	0 53	60 35	5 75	1 3	31 75	0 85	1 40
0 60	0 60	0 67	51 40	5 80	7 9	34 10	0 80	1 50
0 84	0 83	0 87	44 25	1 60	15 4	37 80	0 95	2 15
1 04	1 06	1 11	36 50	1 65	20 7	40 10	0 75	2 05
1 45	1 43	1 51	28 15	1 35	28 0	41 90	0 65	2 13
1 56	1 54	1 68	25 25	2 20	30 1	42 15	0 30	1 10
Second Group P = 30 atmospheres								
0 38	0 38	0 50	54 50	17 65	6 25	27 30	0 30	0 55
0 55	0 53	0 59	55 75	5 85	4 95	32 55	0 90	1 62
0 66	0 64	0 75	45 8	7 80	11 25	34 15	1 00	2 18
0 72	0 72	0 74	49 65	1 90	11 00	36 35	1 10	2 21
0 78	0 78	0 85	43 90	4 00	14 00	36 85	1 25	2 85
1 05	1 05	1 20	32 85	5 15	22 20	38 80	1 10	3 35
1 25	1 25	1 54	26 40	6 00	26 30	40 15	1 15	4 36
2 28	2 33	3 15	14 15	5 00	35 80	44 35	0 70	4 95*
Third Group. P = 100 atmospheres.								
0 93	1 00	1 02	40 55	0 85	16 20	40 35	2 05	5 06
1 07	1 14	1 16	36 45	0 70	19 40	41 30	2 15	5 90
1 71	1 77	1 81	24 80	0 50	28 80	43 80	2 10	8 46*

Perhaps a still more striking contrast is that afforded between the NO₂/CO₂ × 10³ ratios of 0.72 only obtained in our present experiments when a CO-flame was steadily maintained in excess of ordinary air (O₂/CO₂ being 0.73, *vide* Table V) and the 9.3 obtained in some previous experiments during these investigations when a 2CO + 1.5O₂ + 6N₂ medium was exploded in No. 3 spherical bomb at P₁ = 125 atmospheres †

In conclusion, we desire to thank Professor W. A. Bone for his constant interest and advice, and Imperial Chemical Industries for generous grants towards the heavy cost of the work.

† Part V, 'Proc. Roy. Soc.,' A, vol. 108, p. 415 (1925) and "Gaseous Combustion at High Pressures," p. 187.

Table IV.—Carbonic Oxide Flame in 33·3O₂/66·6N₂ Atmospheres.

O ₂ /CO at burner.	N ₂ /CO at burner	N ₂ /CO ₂	Percentages in exit gases.					NO ₂ /CO ₂ × 10 ³ .
			CO ₂	CO	O ₂	N ₂	NO ₂	
First Group. P = 10 atmospheres.								
0 09	0 18	1 06	14 95	69 50	0 20	15 30	0 05	0 33
0 35	0 66	1 10	35 95	22 50	2 65	38 70	0 20	0 56
0 42	0 81	1 14	37 70	15 60	3 40	42 90	0 40	1 06
0 74	1 40	1 42	37 00	0 80	9 25	52 50	0 45	1 22
0 83	1 52	1 66	32 65	2 10	12 25	52 50	0 50	1 53
0 90	1 81	2 09	26 10	3 90	15 45	54 10	0 45	1 73*
1 17	2 17	2 82	19 35	5 85	19 90	54 70	0 20	1 03
1 21	2 26	4 00	13 55	10 35	22 00	54 00	0 05	0 37
Second Group P = 30 atmospheres.								
0 27	0 52	1 00	34 20	31 30	0 50	33 90	0 10	0 20
0 40	0 80	1 24	34 65	18 65	3 60	42 30	0 30	0 87
0 46	0 92	1 21	37 85	12 25	3 85	45 70	0 35	0 90
0 74	1 58	1 65	33 75	1 40	8 90	55 50	0 45	1 34
1 04	2 23	2 37	24 80	1 50	14 55	58 50	0 65	2 62*
1 21	2 57	2 74	21 90	1 40	16 60	59 60	0 50	2 28
1 52	3 23	3 38	18 10	0 90	19 30	61 25	0 45	2 48
Third Group P = 100 atmospheres.								
0 33	0 63	0 98	39 40	21 00	0 05	38 55	0 40	1 01
0 95	1 75	2 78	18 55	11 05	18 40	51 65	0 35	1 88
0 96	1 83	1 96	28 15	1 95	14 20	54 90	0 80	2 84
1 15	2 19	2 41	23 40	2 40	17 25	56 20	0 75	3 21
1 41	2 80	2 95	19 95	1 30	19 10	58 90	0 75	3 76
2 46	4 88	5 60	11 10	1 60	25 10	61 40	0 60	5 40*

Table V.—Carbonic Oxide Flame in Ordinary Air at P = 100 Atmospheres.

O ₂ /CO at burner	N ₂ /CO at burner	N ₂ /CO ₂	Percentages in exit gases.					NO ₂ /CO ₂ × 10 ³ .
			CO ₂	CO	O ₂	N ₂	NO ₂	
0 18	0 73	2 23	18 70	38 20	1 20	41 85	0 05	0 27
0 20	1 13	2 64	19 35	25 85	3 45	51 30	0 05	0 26
0 38	1 45	3 42	16 25	21 95	6 40	55 35	0 05	0 31
0 60	1 93	2 81	22 10	10 05	5 65	62 10	0 10	0 45
0 52	2 19	3 02	21 35	8 30	5 65	64 00	0 15	0 70
0 72	2 85	3 40	20 10	3 95	7 20	68 60	0 15	0 75*

Summary.

Regarded as a whole, our experimental results, especially in connection with those described in the previous paper, besides showing the favourable influence of pressure on NO-formation in CO-flames continuously maintained in O_2 - N_2 atmospheres, also demonstrate its dependence more upon the N_2/CO_2 ratio than mere temperature in the flame, and bear out generally the views already expressed regarding N_2 -activation. While it may be impossible to appraise the relative influences of the various factors (including those of "thermal" and "mass") involved, undoubtedly N_2 -activation is prominent in steady CO- O_2 - N_2 flames as well as in such explosions at high pressures; and in this connection the invariably marked beneficial effect upon NO-formation by the increase in pressure from 10 to 100 atmospheres in our experiment may be regarded as significant.

On the Surface Potentials of Unimolecular Films of Ergosterol.—The Photochemical Formation of Vitamin D.

By RUSSEL J. FOXBINDER, Cancer Research Laboratories, Graduate School of Medicine, University of Pennsylvania.

(Communicated by E. K. Rideal, F.R.S.—Received June 14, 1932—Revised October 21, 1932).

The mechanism of the photochemical conversion ergosterol into vitamin D is not known, but two interesting views, supported by experimental evidence, have been offered in explanation. While both theories suggest that vitamin D is formed as a result of an isomeric change in the ergosterol molecule they differ considerably in that the active product of irradiation is assumed to be a ketone and an alcohol respectively.

The arguments in favour of the ketone formation are dependent on the lability of the hydrogen atoms of the secondary alcohol group. An intra- or inter-molecular dehydrogenation is supposed to occur resulting in the formation of ketones with two or three double bonds of which the former is isomeric with ergosterol. Rosenheim and Adam* have suggested the above mechanism in view of the similarity of the force-area characteristics, also the

* 'Proc. Roy. Soc.,' B, vol. 105, p. 422 (1930).

position of the absorption maxima of oxycholesteriline and a potent vitamin D preparation.

Windaus* and his collaborators have definitely rejected the ketone theory as they found the active irradiation product to be a monohydric alcohol containing three double bonds. The fact that ergosteryl esters such as the allophanate provide vitamin D on irradiation, followed by hydrolysis, suggests that the secondary alcohol group is not concerned in the activation process, but arguments against this assumption are provided by the non-precipitability of the vitamin with digitonin and the observation by Bills and McDonald† that ergosteryl-180ergosteryl ether cannot be activated.

In this investigation a study of the mechanism of the conversion of ergosterol to vitamin D was attempted by examining the behaviour of unimolecular ergosterol films under the influence of ultra-violet radiation. For this purpose two methods were available. The nature of any change in orientation of the molecules may be obtained by a determination of force-area characteristics, while an alteration in the structure of the immersed polar group may be investigated by application of the surface potential method devised by Schulman and Rideal.‡

Experimental Method.

The apparatus employed for the determination of the surface potentials was essentially the same as that described by Schulman and Rideal, but with several modifications. A quartz trough 23 cm. \times 18 cm. \times 2 cm. dimensions, having the top and inside edges ground smoothly and accurately, was used. In the grinding process great care was taken in order to have a surface free from small ridges which would allow leakage of a liquid film past the barriers. The constriction of the area of the film placed upon the aqueous surface was carried out by means of a waxed glass slide operated by a holder to which was attached a graduated scale. The entire apparatus was constructed in such a fashion that all necessary adjustments could be made from the outside after placing a film on the liquid surface. The trough was supported by a heavy copper thermostat which was provided with levelling screws. A Swann type electrometer having a sensitivity of 3 mm./mv. at 1 meter distance was used as a null instrument. After experimenting with various types of air electrodes it was found that a small platinum wire, on which polonium was deposited

* 'Proc. Roy. Soc.,' B, vol. 108, p. 568 (1931).

† 'J. Biol. Chem.,' vol. 87, p. 54 (1930).

‡ 'Proc. Roy. Soc.,' A, vol. 130, p. 259 (1931).

electrolytically, was most suitable. Proper insulation of the polonium coated electrode as well as the lead wire to the electrometer was provided by means of amber. In addition to a vertical adjustment, the electrode holder was constructed to permit both lateral and horizontal displacement, which is a vital necessity if one is to be certain that there is always a uniform film covering a given area. The electrical circuit was completed by means of a calomel cell making contact with the liquid in the trough through a fine syphon, and, to avoid a large liquid-liquid junction potential the substrate was employed in the preparation of the calomel cell. Citric acid-NaOH and phosphate buffers of p_H 6.4 were prepared according to the directions given by Clark ("The Determination of Hydrogen Ions") with freshly redistilled grease-free water. Buffer solutions were employed in order to avoid p_H changes due to (1) adsorption of CO_2 from the air, and (2) added salts. The ergosterol used in the experiments was of a high degree of purity being kindly given by Dr C. E. Bills, who also supplied a small amount of crystalline vitamin D having a potency of 42,000 units per milligram. Solutions of ergosterol were prepared in redistilled *n*-hexane (boiling point 65.5° to 66°), but the limited solubility of vitamin D in hexane necessitated the use of benzene as a solvent. Instead of the usual calibrated dropping pipette a Burroughs & Wellcome micro-syringe was employed in placing a film on the surface. In other respects the technique and precautions described by Schulman and Rideal were carefully followed.

The source of ultra-violet radiation was a Hanovia quartz-mercury arc operating on 100 volts A.C. at 2.5 amperes. Radiation from the arc fell at a rather oblique angle on the film from a distance of approximately 14 inches. At this distance the heat effect from the arc is negligible.

Procedure and Results.

Preliminary experiments indicated the formation by ergosterol of a rather unstable solid condensed film with a limiting area of 41 \AA^2 per molecule on the substrates employed, and irradiation of the film resulted in a progressive increase in the area per molecule.

Under the experimental conditions the molecular areas at the beginning and the end of 20 minutes radiation were 41 \AA^2 and 60 \AA^2 respectively. Thus it was necessary to provide for the increase in molecular area either by continuous adjustment of the trough area, or, if the molecules comprising the film possess sufficient cohesive forces, one could simply move the barrier to a

position corresponding to the limiting area of a solid condensed film at zero compression, subsequently withdrawing it to a position such that free expansion may take place at zero compression up to an area per molecule of 60 \AA^2 . The latter method was finally adopted, as a number of experiments proved that the same result was obtained in either case.

In the first experiments the film of ergosterol was irradiated intermittently in order to determine whether a noticeable difference of potential was produced by the increased ionisation of the air. The results definitely proved that the potential difference due to increased conductivity of the gas space was negligible; accordingly all subsequent experiments were carried out with continuous radiation.

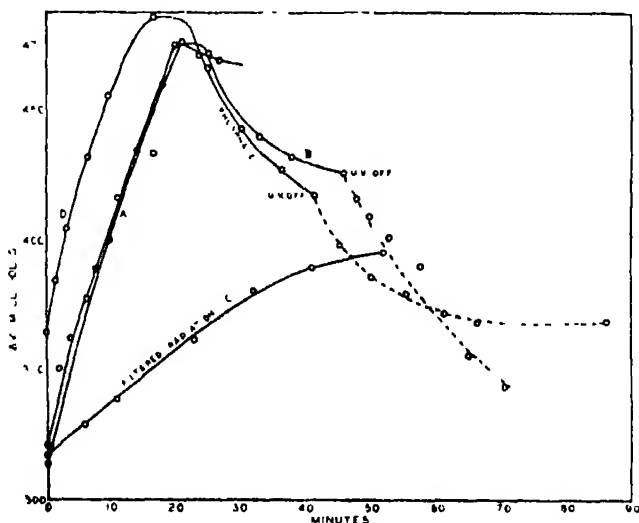


FIG. 1.

In fig. 1 are plotted the values of the change in surface potential, ΔV , against the time of radiation, in every case the number of molecules per square centimetre was identical. Curves A, B and C were obtained on a citric acid substrate, while in D a phosphate buffer was employed. It is to be noted that ΔV increases rather rapidly, to attain a maximum value at a time of approximately 20 minutes. Further the use of weaker radiation resulted in a greatly decreased rate of change in ΔV , due to the decrease in radiation intensity. The dotted portions of the curves represent the fall in ΔV after the source of radiant energy was removed. With due precautions the values given in the curves could be obtained repeatedly, both on phosphate and citric acid buffers. If at any point over a period of time up to and not greatly exceeding

attaining of the maximum, the radiation source was removed, it was found that ΔV fell rather rapidly to the initial value. Following this procedure on the ascending side, application of ultra-violet radiation again resulted in a rapid increase in ΔV , the value passing through the maximum after the proper time had elapsed, but on the descending side if one again applies radiation, the value of ΔV will not exceed that which existed previously.

It is well known that iron and copper salts are quite effective catalysts in solution, particularly in the oxidation of hydroxy organic acids by hydrogen peroxide. If oxidation played a rôle in the formation of vitamin D one would expect to find that the activation would be enhanced in the presence of these

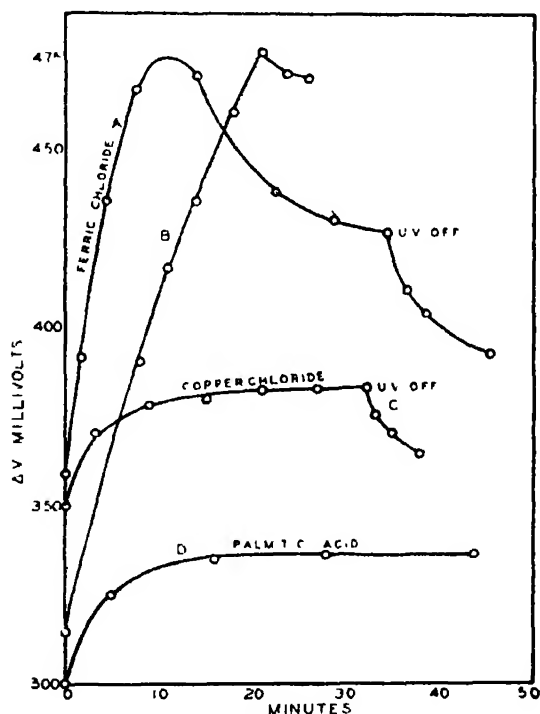


FIG. 2.

catalysts; accordingly, a number of experiments were carried out in which sufficient cupric or ferric chloride was added to the citrate buffer to give a concentration of 1.0 mM/litre. From fig. 2 it will be seen that rather surprising results were obtained. Whilst the ferric ion caused a more rapid attainment in the maximum value of ΔV , the cupric ion absolutely inhibited

the formation of the vitamin as evidenced by the small change in ΔV and also by the fact that no expansion of the molecular area was observed.

On irradiating either a palmitic acid film (see D, fig. 2) or the clean surface of the substrate the value of ΔV and V changed rather rapidly and soon reached constant values, as was to be expected. The result obtained with the palmitic acid film indicated the absorption of the same amount of energy by the substrate whether or not the surface was covered by a film. In the following table are given a series of the maximum values of ΔV and the values for the change in V of the substrate for the same time.

Table I.

Film.	Substrate	1. $\Delta V_{\max} - \Delta V_0$ millivolts	2. $V_{\text{sub}} - V_0$ millivolts	Difference
Ergosterol	Phosphate p_H 6.4	125	22	103
"	Citrate-NaOH p_H 6.4	143	33	110
"	Citrate-NaOH $FeCl_3$	117	37	80
"	Citrate-NaOH $CuCl_2$	32	45	-13
Palmitic acid	Citrate NaOH	34	33	1

There are numerous examples in the literature of the preparation of iso-ergosterols by the catalytic action of organic and inorganic acids on ergosterol. Whilst a few are capable of attaining activity most of the isomers are characterised by their stability toward radiation. It therefore appeared to be of interest to determine the photochemical effect on an ergosterol film on an acetic acid substrate. Fig. 3 shows the type of ΔV , time curve obtained on 0.1 N. HAc. A comparison of the results on this substrate with those obtained on either citrate or phosphate buffers reveals a striking dissimilarity, not only in the form of the curves, but also in the change in ΔV . In fact, one may readily believe that an isomeric form of ergosterol, not easily activated, existed for on placing the ergosterol on the surface an exceedingly rapid reaction appeared to be taking place as a change in potential occurred, the velocity of which was so great that it could not be followed.

The alteration in ΔV cannot be ascribed to a phototropic effect as almost identical potentials were obtained over various sections of the surface occupied by the film during the radiation process.

Since zero pressure was maintained during the process of irradiation there can be no change in the electric moment of the ergosterol molecules which have not suffered change due to absorption of radiation.

The alteration of an interfacial potential difference due to a unimolecular film was shown by Helmholtz to be

$$4\pi n\mu = \Delta V,$$

where the change in potential ΔV is produced by n molecules per square centimetre of the film forming substance, each molecule possessing an average electric moment of effective vertical component μ . Therefore, in order to calculate the change in moment of the ergosterol molecule subjected to radiation it was necessary to determine the variation in the number per square centimetre with the time of irradiation. This was accomplished by con-

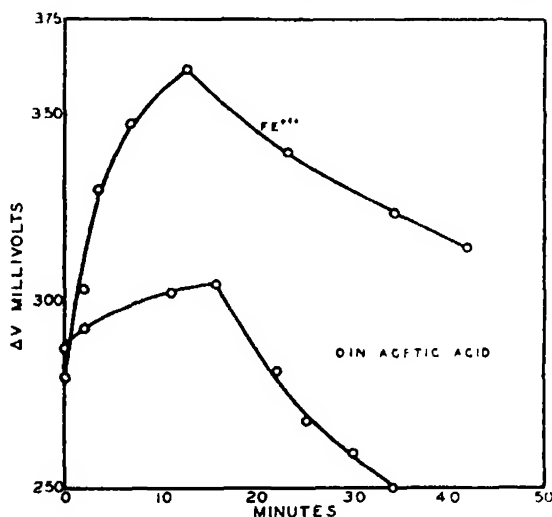


FIG. 3.

structing force-area curves* of ergosterol films which were irradiated for various time intervals on a citrate-NaOH buffer, fig. 4, and subsequently plotting values of the molecular areas at zero compression against the time as shown in fig. 5. The result obtained indicates that the expansion increases approximately linearly with time of exposure. Thus figs. 6 and 7 in which values of the vertical component of the effective electric moment are plotted against irradiation time, were obtained by means of molecular areas interpolated from fig. 5.

We thus obtain the interesting result that on citrate and phosphate buffers the value of μ increased approximately twofold from 3.50 and 3.95×10^{-19}

* The author is indebted to Miss Anna M. Lessig for the force-area determinations.

e.s.u. to 7.25 and 7.45×10^{-10} e.s.u. respectively, for an irradiation time of 20 minutes; thereafter decreasing gradually. With citrate + FeCl_3 the

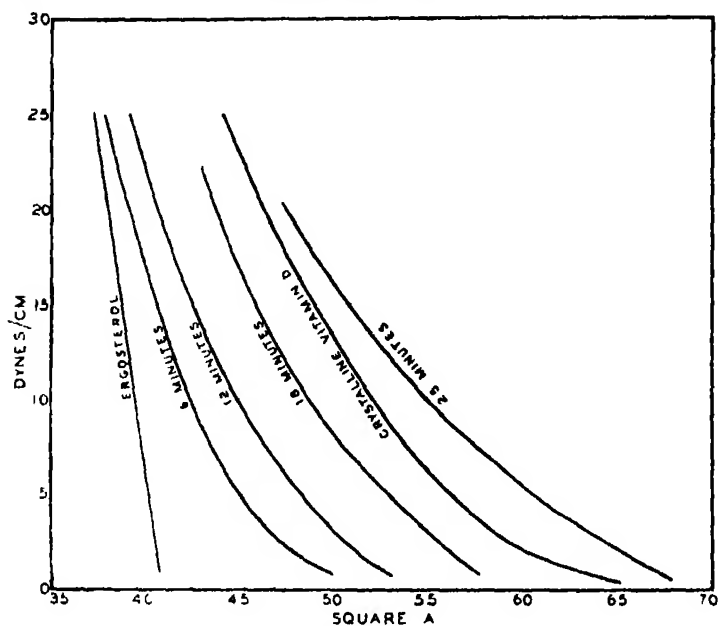


FIG. 4.

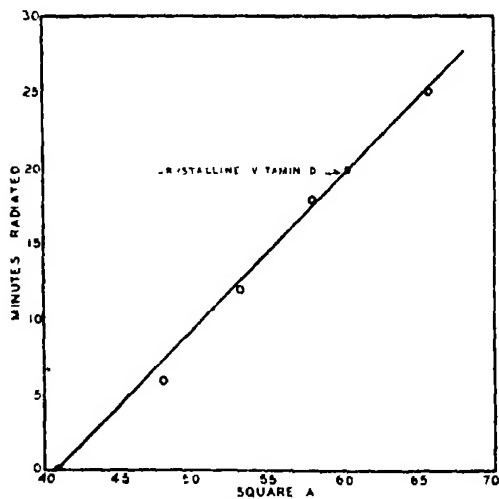


FIG. 5.

initial value of μ was much greater owing to a preliminary partial expansion in the molecular area. An examination of fig. 7 shows that on an acetic acid

substrate the value of μ increased from 3.00 to 4.5×10^{-19} e.s.u. in 15 minutes after which a gradual decrease was observed. The addition of a small amount

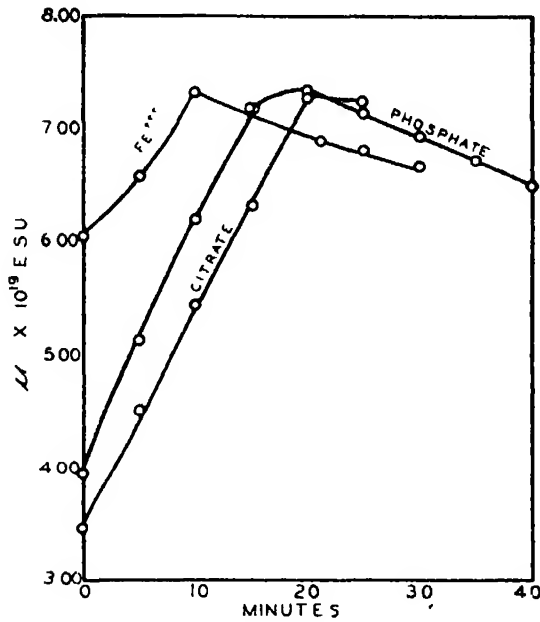


Fig. 6.

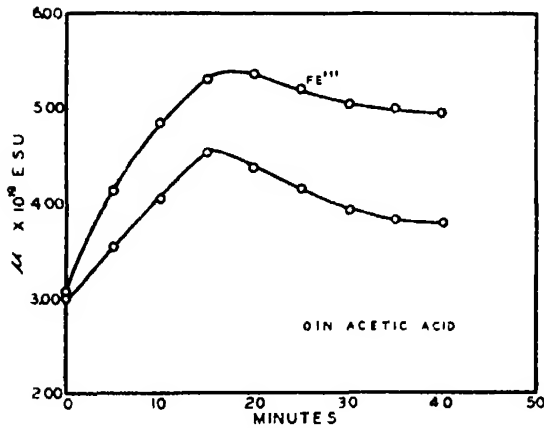


Fig. 7.

of ferric ion resulted in a greater difference in the value of μ , namely, an increase from 3.00 to 5.3×10^{-19} e.s.u.

It appears reasonable to assume that the change in ΔV or μ with time of irradiation represents the actual course of the formation and destruction of

vitamin D, especially in view of the following evidence. Since it was virtually impossible to test the potency of the product obtained by radiation of ergosterol in the film state by means of a biological method an indirect but justifiable procedure was adopted. From the experimental evidence presented, it has been shown that the maximum values of ΔV and μ are attained after an exposure of 20 minutes to ultra-violet radiation under the specified conditions. Now an examination of the force-area curves in fig. 4 (see also fig. 5) reveals that exposure of an ergosterol film to ultra-violet for the above period of time would yield an irradiation product which would give a force-area curve almost identical with that obtained with crystalline vitamin D. Additional evidence for the approximate identity of crystalline vitamin D and the product formed by irradiation of a film of ergosterol for 20 minutes is given from a determination of the contribution of the polar sheet formed by molecules of these materials to the total observed electric moment. Schulman and Rideal have shown that molecules with a polar group immersed at an aqueous surface the effective electric moment is made up of a number of component parts, which include the effect of the displacement of water molecules by the polar group, and the stabilising diffuse ionic double layer which is formed due to the existence of a polar sheet. Thus the equation relating the observed potential difference with the electric moment is

$$\Delta V = 4\pi n\bar{\mu} \pm \Delta V_u,$$

where ΔV_u is the potential due to the diffuse ionic double layer and $4\pi n\bar{\mu}$ the contribution of the polar sheet to the total observed effective moment. In fig. 8 is shown the surface potential differences ΔV due to films of vitamin D in various states of compression on a citrate-NaOH buffer solution of p_H 6.4. The values of the mean electric moment, μ , the true electric moment $\bar{\mu}$,

Table II.

Film material	Mean μ $\times 10^{18}$ e.s.u.	$\bar{\mu}$ $\times 10^{18}$ e.s.u.	$\Delta V\bar{\mu}$ millivolts.
Crystalline vitamin D	4.30	2.91	98
Ergosterol irradiated in film state for 10 minutes	5.00	3.14	114

and ΔV_u the contribution of the underlying double layer to the air-liquid potential difference are given in Table II.

As a result of these observations it would seem reasonable to assume that

the product obtained at the end of 20 minutes irradiation of an ergosterol film is almost identical with crystalline vitamin D.

The Significance of the Results.

From the semi-reversible nature of the change in ΔV and μ , and the permanent increase in the molecular area of the ergosterol molecule on exposure to ultra-violet radiation it appears reasonable to assume that the photochemical

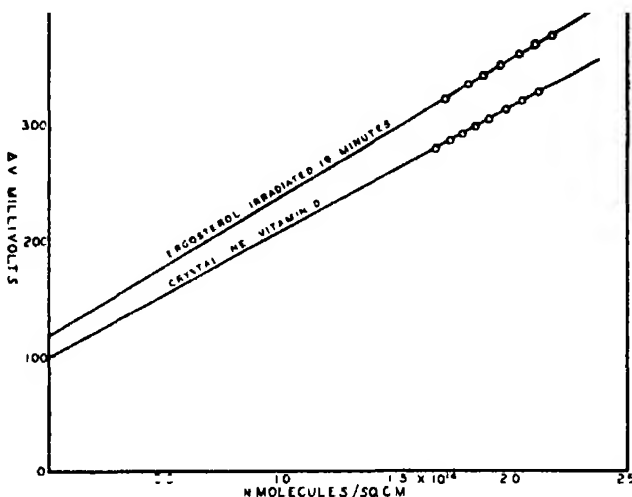


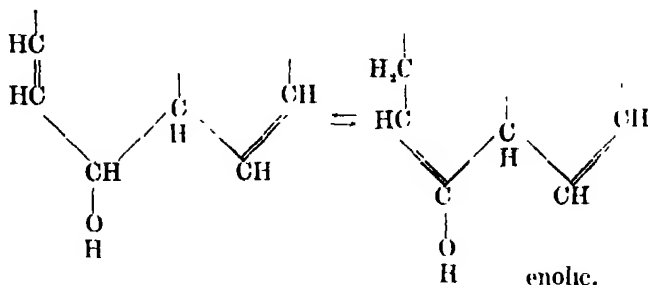
FIG. 8

formation of vitamin D involves at least two distinct reactions, one of which is reversible. Since zero pressure was maintained throughout the time of irradiation, one would expect that a truly reversible reaction would produce, with a given intensity of illumination, a definite stationary state indicated by the attainment of a constant value of ΔV . It was noted, however, that with extended irradiation the value of ΔV passed a maximum and then decreased. This phenomenon may be associated with the accumulation of stable inactive over-irradiated products.

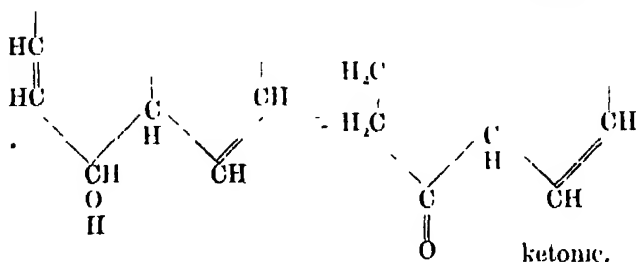
The magnitude of the alteration of the molecular electric moment on absorption of radiation is convincing evidence that the secondary alcohol group suffers a pronounced change in structure, which appears to be the primary process, for the photochemical conversion was completely inhibited by the addition of cupric ions to the substrate. For the primary process two mechan-

isms are possible by which a labile molecule possessing a larger moment may be formed :—

(a)



(b)



The reaction succeeding this elementary process, and which is irreversible, probably involves a steric or structural re-arrangement which is manifested in the adhesion of the CH(OH) group being permanently altered

Although the twofold increase in the value of μ does not permit one to decide which primary process occurs, the observation by Windaus that ergosterol esters may be activated seems to be an argument in favour of mechanism (a). If either type of labile molecule is assumed to be formed then on withdrawing the source of radiation a steric re-arrangement at the CH(OH) group may result, but this is in harmony with the fact that the vitamin does not form a sparingly soluble addition compound with digitonin.

The author is greatly indebted to Professor E. K. Rideal, F.R.S. for his stimulating interest and helpful criticism.

Summary.

The surface potentials and force-area curves of films of ergosterol and its irradiation products on the surface of a citric acid-NaOH buffer have been examined.

From a study of the behaviour of ΔV and μ on irradiation, a suggested mechanism for the photochemical formation of vitamin D is proposed.

The Theory of the Crystal-Photoeffect.

By HORST TEICHMANN.

(Communicated by R. H. Fowler, F.R.S. — Received July 29, 1932.)

Introduction

H. Dember† has observed that the illumination of semi-conductors (cuprite, proustite pyargyrite) produces a new photoelectric effect. If both sides of the crystal are connected by a circuit containing a galvanometer, fig. 1, a photoelectric current arises in such a direction that electrons in the semi-conductor move always in the direction of the incident light; the current can be measured without application of any accelerating potential. He has found a negative charge on the back of the single-crystal when the potential was measured by a compensation-method, or directly with an electrometer, even if the electrodes had been prevented from touching the semi-conductor, fig. 2.

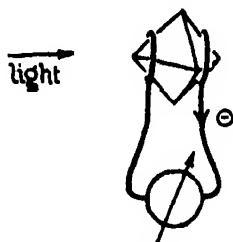


FIG. 1

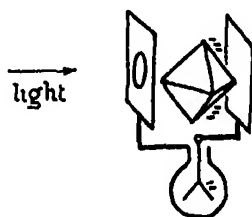


FIG. 2

H. Dember has given to this phenomenon the name *Crystal-Photoeffect* in order to distinguish it from the other photoelectric effects, especially from the "Sperrschicht"-Photoeffect. The latter is caused by photo-electrons excited near the boundary between a semi-conductor and a metal and can be explained by the unipolar conduction of the contact.

The crystal-photoeffect has been observed recently also on diamonds by R. Robertson, J. J. Fox and A. E. Martin.‡

H. Dember remarks that the crystal-photoeffect is most probably caused by the exponential decrease of the concentration of electrons due to the absorption of light within the semi-conductor and by the pressure of the light.

† 'Phys. Z.', vol. 32, p. 554 (1931); vol. 32, p. 856 (1931), vol. 33, p. 207 (1932)
Dember and Teichmann, *Fortschr. Min.*, vol. 16, p. 57 (1931).

‡ 'Nature,' vol. 129, p. 579 (1932).

In the following sections we shall show that the existence of a difference in the electron-concentration between different parts of the crystal in connection with the quantum-mechanical model of a semi-conductor developed by A. H. Wilson† postulates the existence of the crystal-photoeffect and gives a satisfactory explanation of the experimental facts.

The Model of a Semi-conductor.

The characteristic of a semi-conductor is that the continuum of electron-states begins with an energy-level E_2 lying above the critical level E_0 of the Fermi-distribution. In a pure substance the energy-level E_0 is situated within a band of disallowed energies, which separates the first band of allowed energies E_1 filled up entirely with electrons from the second band beginning with the energy-level E_2 , fig. 3. If there are some impurities, the existence of a number of discrete levels in the interval is possible. That means that the average energy-difference which must be overcome by an electron to reach the second band of allowed energies has become smaller, or in other words the energy-level E_2 is nearer to E_0 , fig. 4

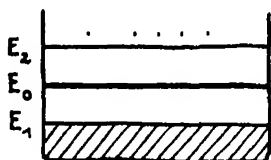


FIG. 3

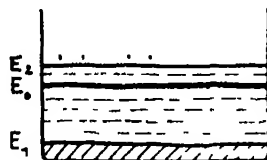


FIG. 4.

It has been remarked by L. Nordheim‡ that the band of disallowed energies can act as a potential-hill. If we bring a piece of impure substance in contact with a piece of pure substance (for instance Cu_2O), the energy-level E_{0i} and E_{0p} lie at the same height in the equilibrium state, fig. 5. We notice that the

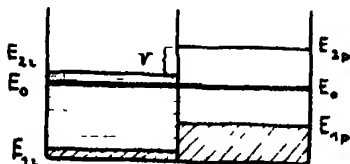


FIG. 5.

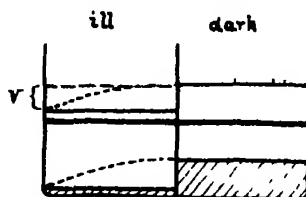


FIG. 6

† 'Proc. Roy. Soc.,' A, vol 133, p. 458 (1931); vol 134, p 277 (1931).

‡ 'Z. Physik,' vol. 75, p 434 (1932)

continuum of electron-states begins with a higher energy-level E_{2p} in the pure substance than in the impure E_{2i} . The value of the potential-jump V is given by the difference: $V = E_{2p} - E_{2i}$. It is clear that we also get a potential-hill if one of the substances is not pure but has another concentration of impurities than the other.

Action of Light on a Semi-conductor.

Light absorbed by a semi-conductor (for instance (Cu_2O) produces in its interior an inner photoelectric effect. Electrons bound on an atom (of the pure substance or of an impurity) are raised to higher energy-levels, greater than E_2 . They cause a magnification of the electron-concentration in the upper energy-band. As in the case considered at the end of the last section the energy-level E_2 of the illuminated part of the semi-conductor is lowered relative to that of the dark part, fig. 6. Because of the exponential decrease of the light-intensity caused by the absorption this potential-hill is in reality no sudden jump but has a certain inclination (dotted line). For a first approximation it is sufficient to work with a potential-jump. This will agree the better with the experimental facts the greater the value of the absorption-coefficient. We can say that this jump is due to a charging process in which the illuminated part loses electrons and that its height gives us the potential we measure.

The electrons in the energy-band E_2 can diffuse and recombine. The diffusion occurs in the direction of the decrease of the electron-concentration. It produces the photoelectric current in the dynamical case. The recombination can take place either directly with the vacancies which arise in the lower energy-levels or in two (or more) stages by interaction with the impurities. We shall see that the dependence of the average electron-concentration in the upper level on the illumination will give us some hints for a discrimination between these two cases. We can suppose that the recombination is relatively small because of the existence of the band of disallowed energies separating the energy-level E_1 from E_2 . It will increase with the electron-concentration till it reaches such a magnitude that in the unit of time the number of electrons excited is equal to the number of electrons that recombine. This happens in the equilibrium state.

The Equilibrium State.

Now, it is necessary to calculate the amount of the lowering of the upper level E_2 by the illumination. We have seen in the last section that this value must be equivalent to the measured potential.

Because the distribution in the continuum of electron-states in the upper level is a Maxwellian one, we can get the potential V , fig. 6, from the Boltzmann equation which gives the condition of equilibrium between two energy-levels with the energy-difference V and the electron concentration n_1 and n_2 respectively. If $n_1 > n_2$ we can write it in the form

$$n_1 : n_2 = e^{\epsilon V/kT}, \quad (1)$$

where ϵ is the electron charge, k the Boltzmann constant, and T the absolute temperature.

In our case the smaller electron concentration in the dark part (n_2) is equal to the number of thermally excited electrons per unit volume (n_T) and the bigger concentration in the illuminated part consists of a sum of thermally excited electrons and those of photoelectric origin ($n_1 = n_P + n_T$). Therefore the Boltzmann equation (1) gives the following value of the potential

$$V = \frac{kT}{\epsilon} \log \left(1 + \frac{n_P}{n_T} \right). \quad (2)$$

The average electron concentration in the upper level n_P produced by light is a function of the illumination I . According to our considerations at the end of the last section the form of this function depends on the kind of excitation and recombination. It turns out that if the excitation and recombination is a one-stage process we can obtain no agreement between theory and observation. Let us assume therefore that these processes happen in two stages.† If n_P denotes the average electron concentration in the upper level E_2 , n_0 that in the ground level and n_i the concentration of electrons in the intervening impurity-levels, fig. 7

$$\begin{array}{l} N_2 = K'n_i I \uparrow \downarrow R_2 = K''n_P \quad n_i \\ \hline N_1 = K n_0 I \uparrow \downarrow R_1 = K'''n_i (n_i + n_P) \quad n_0 \end{array}$$

FIG. 7

† It is known that for such crystals as sodium chloride the action of light of two different wave-lengths is necessary to produce the inner photoelectric effect (see B. Gudden, 'Handbuch der Physik,' vol. 13). This has been shown clearly by R. Hilsch and R. W. Pohl ('Z. wiss. Photogr.,' vol. 30, p. 255 (1930)) using KBr crystals. It may be that cuprous oxide behaves in the same way, but that the two wave-lengths necessary are very close together. (Also the note added to the summary at the end of this paper).

where $N_{1,2}$ is the number of excited electrons, $R_{1,2}$ the number of recombined electrons, and K_1, K', K'', K''' are constants, the condition of equilibrium is given by the following equations :

$$\left. \begin{aligned} N_1 &= R_1 \\ N_2 &= R_2 \end{aligned} \right\} \text{ i.e., } \left. \begin{aligned} n_0 I &= \kappa n_i (n_i + n_p), \\ n_i I &= \kappa' n_p \end{aligned} \right\} \quad (3)$$

We can use for the recombination currents R_1 and R_2 the equations written down in fig. 7 because for the first stage the number of levels available is equal to $n_i + n_p$ the number of excited electrons, and for the second stage the number of impurity-levels is large compared with those already occupied, n_i in number.

By multiplication of the equations (3) with one another and eliminating of n_i we get

$$I^2 = C^2 n_p^2 \left(\frac{K'}{I} + 1 \right) \quad (C \text{ constant}), \quad (4)$$

or for the dependence of the average electron concentration in the upper level n_p on the illumination

$$n_p = \frac{CI^{\frac{1}{2}}}{\sqrt{(K' + I)}}. \quad (5)$$

It is probable that $n_i \gg n_p$, therefore we can neglect in equation (4) the unit in comparison with K'/I and we get instead of (5) the approximation

$$n_p = C^* I^{\frac{1}{2}}. \quad (5^*)$$

It is possible to compare this formula with the experimental facts by calculating n_p from the Boltzmann equation (2)

$$n_p = n_T e^{eV/kT} - n_i, \quad (6)$$

using the values V measured by Dember (*loc. cit.*) on single-crystals of Cu_2O with different illuminations. The value of n_T can be calculated from data given by W. Vogt† by the equation

$$n_T = n_\infty e^{-\Delta W/kT}, \quad (7)$$

where $\Delta W \approx e\Phi$ is the width of the band of disallowed energies, n_∞ is the value of the thermally caused electron concentration for $T = \infty$.

If we put $T = 300^\circ$ (room temperature), $\Phi = 0.3$ volt, and $n_\infty = 5.0 \times 10^{18}$ we get

$$n_T = 4.60 \times 10^{13}.$$

In Tables I and II the observed and calculated data are given.†

Table I.

Cu₂O-crystal from Chessy.

I (arbitrary units).	V (volt).	$n_T < 10^{-14}$	$C^* < 10^{-14}$
1	0.046	2.26	2.26
2	0.072	6.97	2.46
4	0.108	29.37	3.67
8	0.156	189.68	8.38

Table II.

Cu₂O-crystal from Tsumeb.

I (arbitrary units)	V (volt)	$n_T < 10^{-14}$	$C^* < 10^{-14}$
1	0.060	4.21	4.21
2	0.088	13.32	4.71
4	0.124	54.91	6.86
8	0.174	381.57	16.86

The values of the illumination are given in arbitrary units. In the first case the illumination $I = 1$ is equivalent to an average number of light-quanta of 4.0×10^{16} in the second case $I = 1$ corresponds to 5.6×10^{16} light-quanta.

We see that our assumption of a recombination process in two states reproduces the experimental facts satisfactorily, but the increase of C^* , which cannot be explained entirely by the neglect of the factor $\sqrt{(K' + 1)}$ in using equation (5*) shows that the recombination process might be still a little more complicated.

Connecting now the equations (1) and (5*) we get for the potential V with which the illuminated part of the crystal is charged up, in dependence on the illumination I :

$$V = \frac{kT}{e} \log (1 + C^* I) \quad (8)$$

If the illumination is not too small we can also write in a first approximation

$$V = \frac{kT}{e} \log C^* I. \quad (8^*)$$

The factor C is no pure constant because it contains n_T which is a function of the temperature (equation (7)). If we take this into account but neglect a possible influence of the temperature on the recombination we can write the potential V in its dependence on the temperature in the form:

$$V = \frac{kT}{e} \log (1 + C^{**} I^3 e^{c/T}). \quad (9)$$

For great values of the illumination I the potential V is nearly a linear function of the temperature T . If the recombination should follow a similar law in its

† I am very much obliged to Professor Dember for communication of his measurements from the graphs published in his papers (*loc. cit.*).

dependence on the temperature to the concentration of the thermally excited electrons we would expect some essential deviations from the formula calculated above.

The variation of the potential V in the direction x of the light penetrating in the crystal follows from the dependence of the illumination I on x . If we use the absorption-law in the form $I = I_0 e^{-\alpha x}$ (α absorption coefficient) equation (8) gives us

$$V = \frac{kT}{e} \log (1 + C''' I' e^{-\alpha x}). \quad (10)$$

In connection with (8*) we get again a linear dependence of V on x for strong illuminations.

The Dynamical State.

If both sides of the single-crystal are connected by a circuit the charging up will arise only to a potential necessary to overcome the ohmic potential-decrease produced by the electron-current in the outer and inner part of the circuit. A part of the electrons reaching the upper energy-level E_2 causes the photoelectric current by diffusion in the x -direction, i.e., the direction of the maximum decrease of the electron concentration in the upper band. If the current were a definite portion of the rate of production of these electrons by light, it would be proportional to the three halves power of the illumination

$$i = \alpha n_i I = \beta I^{\frac{1}{2}}, \quad (11)$$

where i is the photoelectric current and B a constant. This is not in good agreement with the observations, unless we assume that the curvature would appear on stronger illumination. But the equilibrium theory of this note is not deep enough to attack the problem when a current is flowing. The observed current is closely proportional to I , Tables III and IV.

Table III
Cu₂O-crystal from Chessy.

I (arbitrary units).	$i \times 10^{10}$ (amp.).	$i/I \times 10^{10}$
1	60	60.0
2	121	60.5
4	275	68.8
8	594	74.3

Table IV.
Cu₂O-crystal from Tsumeb.

I (arbitrary units)	$i \times 10^{10}$ (amp.)	$i/I \times 10^{10}$
1	121	121.0
2	209	104.5
4	385	96.3
8	825	103.1

The illumination corresponds to the same number of light-quanta respectively given in Tables I and II.

A dependence of the photoelectric current on the temperature which is not yet investigated would allow us to discuss the nature of the temperature-influence on the recombination and on the diffusion in the direction of the light.

Discussion.

H. Dember (*loc. cit.*) has discussed in detail the impossibility of identifying the observed photoelectric phenomena on single-crystals with a "Sperrschicht" effect. And, indeed, the absence of any rectification-effect in the unilluminated arrangement, fig. 1—as was found experimentally—is the best proof that the influence of the contact between the electrodes and the single-crystal cancels out.

The inverse effect measured on poly-crystals shows that in this case the boundary-layers between the different small single-crystals act as "Sperrschichten." That is in agreement with L. Nordheim's model of a potential-hill discussed above. For we may assume that the growing up of a substance in a poly-crystalline form is due to sudden changes of the impurity concentration.

The irregular deviations observable in the tables given above between the results of the theory here developed and the experiments can perhaps be described to errors in the measurements of the magnitude of which the authors have given no account.

The fact that only some semi-conductors show the crystal-photoeffect points to the existence of some especial properties. Indeed, Robertson, Fox and Martin (*loc. cit.*) found the effect only on diamonds with an anomalous transparency. We believe, that these or similar peculiarities are influencing the rate of recombination. In the case of a one-stage recombination the potential arising may be too small to be measured. Only when some circumstances cause a two-stage recombination may the effect become observable because then the recombination is small enough to permit an important accumulation of electrons in the upper energy-level.

I am greatly indebted to Professor R. H. Fowler and Mr. A. H. Wilson for many suggestions and discussions, and I have to express my thanks to the "Jahrhundertstiftung der Technischen Hochschule, Dresden" for enabling me to work at Cambridge.

Summary.

A detailed discussion of the model of a potential-hill within a substance has shown that the quantum-mechanical model of the semi-conductor developed by Wilson postulates the existence of the crystal-photoeffect in single-crystals. Some equations are given showing the potential V which arises in the equilibrium-state as a function of the illumination of the temperature and the thickness of the single crystal. In a following section the dynamical case is discussed. The theoretical considerations are in a good agreement with the experimental results.

[*Note added in proof, September 10th (1932)* Professor Dember has informed me that he has found substances (for instance, zinc-sulphite-crystals) which show no crystal-photo-effect at room temperature, but which become sensitive at high temperatures (about 440°C) This fact proves our assumption of a two-stage process and shows that the impurities are indeed intervening]

*Electron Scattering in Helium. Absolute Measurements
at 90° and 45° .*

By DR. SVEN WERNER, Universitetets Institut for Teoretisk Fysik and Den Polytekniske Læreanstalt, Copenhagen.

(Communicated by N. Bohr, For Mem. R.S.—Received August 5, 1932)

The scattering formula of Rutherford gives an expression for the number $n_1 d\Omega$ of electrons in a gas which are scattered from a beam of electrons over the solid angle $d\Omega$ by impacts with atoms, which are to be found along a certain length l of this beam. If $+Ze$ is the charge of the nucleus of the atoms, $-e$ and m the charge and the mass of the electron, V the potential difference through which the electrons are accelerated, N the number of atoms in unit volume and n_0 the total number of electrons which pass a certain cross-section of the beam, we have the well-known formula

$$n_1 d\Omega = n_0 N l \left(\frac{Ze}{4V} \right)^2 \frac{d\Omega}{\sin^4 \frac{1}{2}\Theta}, \quad (1)$$

where Θ is the angle of scattering. When $n_0 = 1$, $N = 1$, and $l = 1$ the scattering is usually expressed by $I_s d\Omega$, where I_s is the so-called "scattered

intensity. According to Rutherford's formula we get for the classical scattering due to the nucleus.

$$I_0 = \left(\frac{e}{4V} \right)^2 \frac{Z^2}{\sin^4 \frac{1}{2}\Theta}. \quad (2)$$

Taking into consideration the electrons around the nucleus Mott* and Bethe† find :

$$I_0 = \left(\frac{e}{4V} \right)^2 \frac{(Z - F)^2}{\sin^4 \frac{1}{2}\Theta}. \quad (3)$$

where F is the atomic form factor, known from the scattering of X-rays, and also a function of $(V \sin^2 \frac{1}{2}\Theta)$. The values calculated for helium by James have been used for F in this paper.

As previously shown by the author,‡ the scattering of electrons from a beam of electrons in a gas can be determined experimentally by measuring the number of scattered electrons passing through ring-slits arranged round the beam. If a ring-slit has the width b and the distance $OS = R$, fig. 1, then

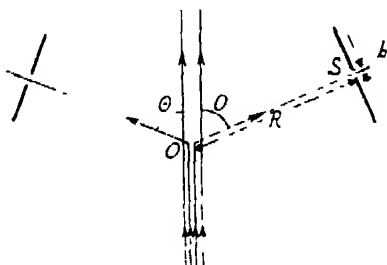


FIG. 1.

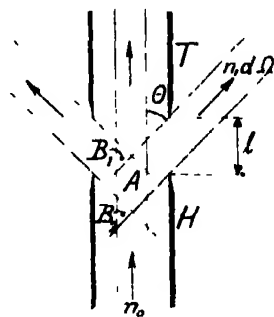


FIG. 2.

$d\Omega = 2\pi \sin \theta d\theta$ and $d\theta = b/R$. The number of electrons passing through the slit is then $n_1 d\Omega = n_0 \cdot N \cdot I_0 \cdot 2\pi \sin \theta \cdot b/R$, and the scattered fraction is

$$\phi = \frac{n_1}{n_0} d\Omega = 2\pi \cdot N \cdot I_0 \cdot \sin \Theta \cdot \frac{b}{R}. \quad (4)$$

When the quantity ϕ is measured, I_0 may be calculated.

Geometrical Considerations.—The following quantities are determined directly by measurements on the apparatus: the width b of the ring-slits, the distance $OS = R$ to the ring-slits and the angle Θ . The length of the electron beam is determined by the distance between the ends of the two tubes H and T , in

* 'Proc. Roy. Soc.,' A, vol. 127, p. 658 (1930).

† 'Ann. Physik,' vol. 5, p. 383 (1930)

‡ 'Proc. Roy. Soc.,' A, vol. 134, p. 202 (1931) (cited as Paper 1).

the interior of which the electron beam is found, fig. 2. The scattered fraction ϕ is found by measurements of the scattered number ($n_1 d\Omega$), when a certain number of electrons (n_0) has passed through the apparatus. The measurement of b , R and Θ is straightforward, but an exact determination of the scattering length of the beam l offers some difficulties. From the atoms in the limited region A , the electrons which are scattered through an angle Θ will reach the ring-slit S without any obstacles. From the atoms in the two regions B_1 and B_2 , which are of equal size, only a fraction of the electrons scattered through the angle Θ will reach the ring-slit and be measured. A simple geometrical consideration shows, however, that the total amount of electrons, which reach the slit S from B_1 and B_2 , corresponds exactly to the half of the total scattering through the angle Θ from both these regions; or to the whole of the scattering from the region B_1 alone. Since the volume $A + B_1$ is equal to the volume of a part of the electron beam, of length equal to the distance between H and T , then the distance $H - T = l$ will be the length of the scattering part of the electron beam. A correction is, however, necessary in that S is a finite distance from $H - T$. In fig. 3 it is seen that from the region A the scattering through the angle Θ is measured without errors just as in fig. 2. The two B -regions are now unequal, it is simple to determine graphically for a certain point in the B -regions, how large a part of the ring-slit S can be seen from this point without being screened by the tubes H or T . The free (visible) part of the ring-slit, expressed in degrees, may be called the free angle. By investigating variations of the free angle for different points along the path of an electron in the beam from B_2 through A to B_1 , one may determine the effective length of the beam — by this is understood the length which, with a constant free angle of 360° would give the same total scattering through the scattering angle Θ . If this is done in the present geometrical circumstances and in different places of the cross-section of the electron beam, a corrected value for the effective length l_e is found. This value is in the experiments only 1 or 2 per cent. different from the length l_1 in fig. 3, which, by the way, is the length of the A -region in the direction of the beam.

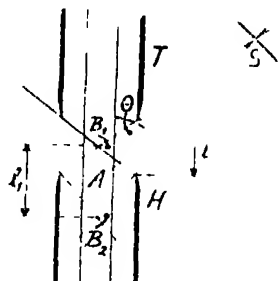


FIG. 3.

In the experiments an apparatus with a ring-slit corresponding to $\Theta = 90^\circ$ (model I), an apparatus with a ring-slit at $\Theta = 45^\circ$ (model II), and an apparatus with two ring-slits at $\Theta = 90^\circ$ and $\Theta = 45^\circ$ (model III) has been used. With the latter it was possible in the same series of observations to find

the scattering through both 90° and 45° . The apparatus, model III, is shown schematically in fig. 6.

It is presumed that the electron beam is cylindrical; actually it is slightly conical (angle 4°), but it has not been necessary to introduce any correction on this account. The finite width of the slit S is also of no importance for the calculation of the length of the beam. In the experiments b/R is very small ($b = 0.5-1.0$ mm. and $R =$ about 30 mm.). The length of the beam l is sometimes rather large compared with R , but this was needed to get sufficient intensity. The value of the angle Θ was, therefore, only defined within certain limits, and the observed scattering is the scattering within a certain interval of angle. In experiments with $l = 5$ mm. these limits were $\Theta = 90^\circ \pm 7^\circ$ and $\Theta = 45^\circ \pm 4^\circ$ respectively, and with $l = 2$ mm. the limits were $\Theta = 90^\circ \pm 3^\circ$

and $\Theta = 45^\circ \pm 2^\circ$ respectively. But the number of electrons, which pass through the ring-slit, is equal to $2\pi I_0 \sin \theta d\theta$, and if we use the theoretical expression (3) for I_0 , it is seen that at the two angles in question ($\Theta = 90^\circ$ and $\Theta = 45^\circ$) and at the velocities used (30-400 volts), this number will vary linearly with the angle Θ approximately, through an interval of $10-15^\circ$. The error made by assuming this linearity in the calculation of I_0 from the experiments is small, about 2 per cent. Experiments with varying l also confirm this.

The determination of $n_1 d\Omega$ is made by collecting the electrons passing through the ring-slit in a Faraday-chamber and measuring the charge by means of an electrometer. Small supports, which carry the upper part of the apparatus, screen parts of the ring-slit, a small correction (2-5 per cent.) is therefore necessary.

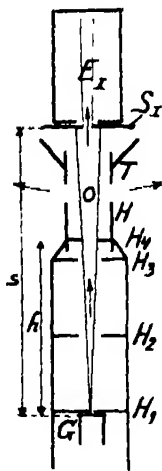


FIG. 4.

In fig. 4 is shown the electron beam. At G is the filament, and between G and H_1 is the accelerating field. Screens with holes H_2 and H_3 stop the scattered electrons, and a circular hole in H_4 , together with H_1 , defines the dimensions of the electron beam. Between H and T —at O —the scattering, which has to be observed, takes place. The screen S_1 has an opening, the radius of which is considerably smaller than that of the beam. The number of electrons passing through S_1 into the Faraday-chamber E_1 , which is connected to an electrometer, will then be proportional to the number n_0 of the electrons of the beam. If q is the fraction of the electrons, which reaches E_1 , q may be expressed by $q = \pi \cdot r_s^2 / \pi \cdot r_B^2$, where r_s and r_B are the radii of the opening S_1 and of the electron beam when it reaches S_1 , respectively. This

latter radius is determined geometrically by the radius (d) of the hole in the screen H_4 together with the distances s and h . We have $r_B = sd/h$. The opening in H_1 is a slit, with a width of 1–2 mm., which is placed perpendicular to the straight filament just above its hottest point. The distance $G-H_1$ is about 1 mm. In the calculation of r_B it is assumed that the electron source is a point. The electrons come from a certain length of the filament depending on the width of the slit H_1 . Geometrical considerations, as well as controlling experiments show that within the limit of experimental error (less than 2 per cent.) the electron source may be considered as a point.

The edges of all the slits and holes were sharpened. This was of great importance, especially for the screens which define the direct beam. Sometimes on the screen S_1 a thin deposit of tungsten, "evaporated" from the filament G was observed. The hole in H_4 was circular, and the tungsten deposit was also circular and with a radius and position exactly corresponding to the geometry of the apparatus. This shows that the tungsten particles move along straight lines from the filament to the screen. But in some experiments the tungsten deposit had, as shown in fig. 5, a very irregular contour. One may conclude that the tungsten particles, when leaving the filament, are electrically charged, and that false electric fields produce irregular deflections. These irregularities occurred together with certain abnormal effects in the scattering, which showed that the electron beam was also exposed to false electric fields, probably situated near the screens. With the sharpening of the slits and careful cleaning these abnormal conditions disappeared. The cause of the irregularities was probably a deposit of tungsten, etc., at the edges.

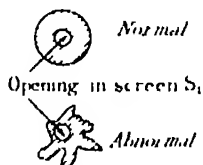


FIG. 5.

The diameter of the holes and the width of the slits were measured by means of a comparator, and all other distances were measured with an accuracy of about 0.1 mm.

Electrical Arrangements.—A diagram of the electrical connections and of the apparatus (model III) is shown in fig. 6. The tungsten filament G is connected with two parallel resistances r and r' . In this way the filament may be kept at a temperature near the emission by a current through r . When additional current is supplied through r' , the filament is heated so as to emit electrons. In the experiments, therefore, it is only necessary to make a small change of the current in this circuit, when the electron beam is wanted. The electrical disturbances arising from this small change are negligible. The electron emission was measured on a microammeter (μA) and in the experi-

ments was found to vary from less than $1 \cdot 10^{-6}$ amp. to $200 \cdot 10^{-6}$ amp. The tensions were taken from storage batteries. The accelerating potential was read at the voltmeter V , the electron-beam passing through H and T , which are at the same potential. A small rise in the potential between T and S_I keeps the positive ions away from S_I . Between S_I and E_I is a strong potential drop, which retards the electrons; and normally only those which have suffered no loss of velocity on their way from G to S_I may pass. Connected with E_I is the Lindemann electrometer L_I .

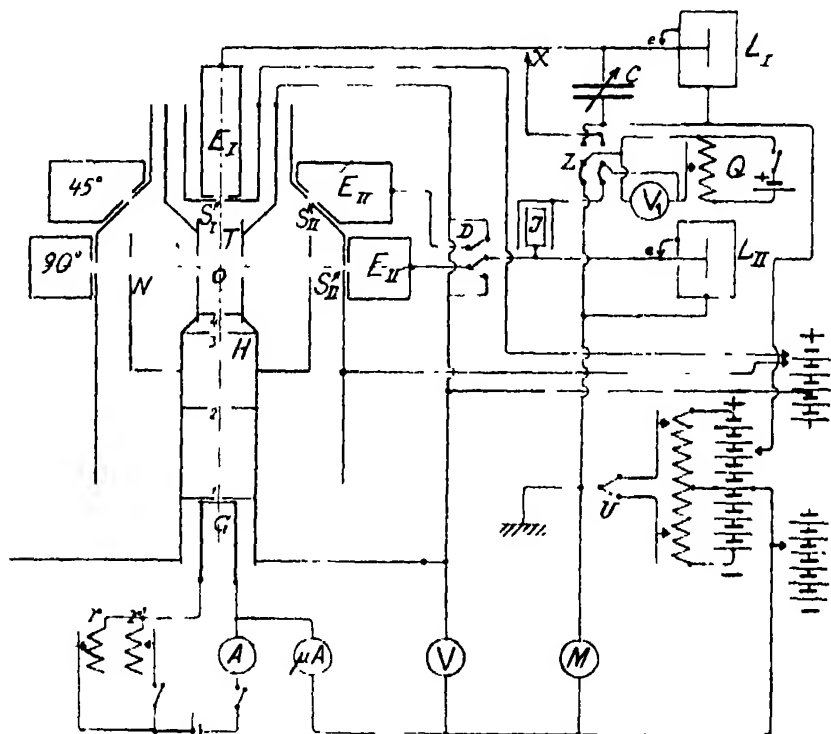


FIG. 6.

The electrons scattered at O may enter E_{II} through S_{II} . In the apparatus shown one may measure the scattering either through 90° or through 45° , for by means of the switch-over D one of the electrodes E_{II} may be earthed and the other connected to the Lindemann electrometer L_{II} . In the figure the switch-over is shown in position for measurements at 90° . In front of the slit S_{II} is the potential rise, which retards the positive ions. The screen N has the same potential as H and T , and it is the purpose of this screen to make the lines of force in the retarding field parallel to the paths of the electrons

entering S_{II} . If this precaution is not taken, electrons on their way from O to S_{II} would possibly be deflected, and a false scattering angle would result.

Between S_{II} and E_{II} is the potential drop, which retards the scattered electrons. By this arrangement one obtains the result that electrons in the direct beam and the scattered electrons pass the same electric fields and are measured as far as possible in the same way. To calibrate the electrometers the circuit Q is used. The potentials for the quadrants in the electrometers are maintained by storage batteries (not shown), and these potentials may be set accurately by means of potentiometers. At e platinum contacts are placed in order to "earth" the electrometers. The circuit consists of a battery, a potentiometer and a voltmeter V_1 (0-0.5 volts). Connected with the electrometer L_I and the electrode E_I is the mica precision condenser C, which may be varied between 0.001 and 2.00 μF . From the circuit Q an accurately known potential may, by means of the switch-over Z, be given to the electrometer at X, and its volt-sensitivity determined. Since the capacity of C is much larger than that of E_I and L_I , the charge-sensitivity of this system is determined by the capacity of C and the volt-sensitivity of L_I . The capacity of the system E_{II} - L_{II} is to be kept as small as possible so as to measure small charges, and the charge-sensitivity of this system is found by means of a Harms' condenser I permanently connected to the system. By means of the switch-over Z (in the position shown) the external cylinder in this condenser may be given a known potential change, if the current in the circuit Q is changed. In this way a known electric charge may be introduced on the system E_{II} - L_{II} . This charge is the product of the induction-coefficient of the Harms' condenser and the voltage change. The sensitivity of L_{II} was rather high and had therefore to be controlled during the measurements. The sensitivities used were, for L_I : $5.00 \cdot 10^{-3}$ volts per scale division, which if $C = 1.00 \mu F$, corresponds to a charge-sensitivity of 15.0 e.s. units per scale division, and for L_{II} : 0.00159 e.s. units per scale division.

For the measurements the filament G was brought to emission, until a certain deflection (usually 40 scale divisions = 0.200 volts) was observed at L_I . The charge, which L_{II} received during the same time, was read (y' scale divisions). This deflection was a measure of the ratio between the electron currents to E_{II} and to E_I . This ratio may vary greatly with the different experimental conditions, and it was found convenient to be able to vary the size of the condenser C and accordingly the charge-sensitivity of L_I . In this way one always obtains sufficient deflections at L_I as well as at L_{II} . All measurements of scattering may be expressed by the number of scale

divisions (y), which L_{II} would show, if E_I had received an electric charge of 300 e.s. units. This charge would raise the potential of E_I 0.100 volts, if $C = 1.00 \mu F$. We have

$$y = \frac{1.00}{C} \frac{0.100}{0.200} y'.$$

To avoid contact potentials and other electrical disturbances the whole apparatus is made of copper, and all parts which may be hit by electrons are covered by a thin layer of lamp black. The apparatus and several of the outer connections are covered with a metal shield, as a protection against disturbances from outside. The electrodes E_I and E_{II} are practically screened, electrostatically, from each other.

Pressure.—Helium, purified by means of charcoal cooled in liquid air, was kept in glass bulbs at a constant pressure. From these the helium passed through a long capillary (in which the pressure under the experimental conditions was reduced to $1/10,000$), again through charcoal in liquid air and into the apparatus, from which it was pumped away by a mercury diffusion pump. The pressure was measured by a large MacLeod manometer directly connected to the apparatus, and which was carefully calibrated and tested by comparison with other manometers. The pressure $1 \cdot 10^{-4}$ mm. Hg corresponds to about 6 mm. difference in the level of the mercury columns. By cooling devices mercury vapour was kept away from the apparatus. The residual gas pressure was very small, usually $1.5 \cdot 10^{-5}$ mm. Hg. In all series of measurements the procedure was the following: the scattering x_1 was measured in helium at high pressure P_1 , then the scattering x_3 in helium at low pressure P_3 and again the scattering x_2 at high pressure P_2 . The exact meaning of the quantity x will be explained later. Since the scattering is proportional to the pressure (compare Paper I) one may calculate from the three measurements the scattering $x = \frac{1}{2}(x_1 + x_2) - x_3$ at the pressure $p = \frac{1}{2}(P_1 + P_2) - P_3$. The ratio between x and p gives the scattering at unit pressure. In all experiments this value for the scattering $(x_0)_p$ is calculated at a pressure equal to $1.00 \cdot 10^{-4}$ mm. Hg.

Controlling Measurements.—A number of different tests were made to ascertain that the apparatus was functioning correctly.

The distribution of velocity among the scattered electrons was found by varying the potential difference between S_{II} and E_{II} (fig. 6). In this way were obtained retarding potential curves, some of which are shown in fig. 7. The abscissa shows both the retarding potential P (the potential difference between

$T - H$ and E_{II}) and the potential M , which is the difference between the accelerating potential V and the retarding potential P . M is read directly at the voltmeter M in fig. 6. The ordinate is the number of scale divisions y , which is observed on I_{II} , when E_I has received a charge of 300 e.s. units. The curves I and II are taken from experiments in pure helium, while curve III shows the retarding potential curve, when impurities are present. It will be seen that the slope of these curves gives a control of the purity of the gas. And it will also be noticed that impurities (air, etc.) increase the scattering

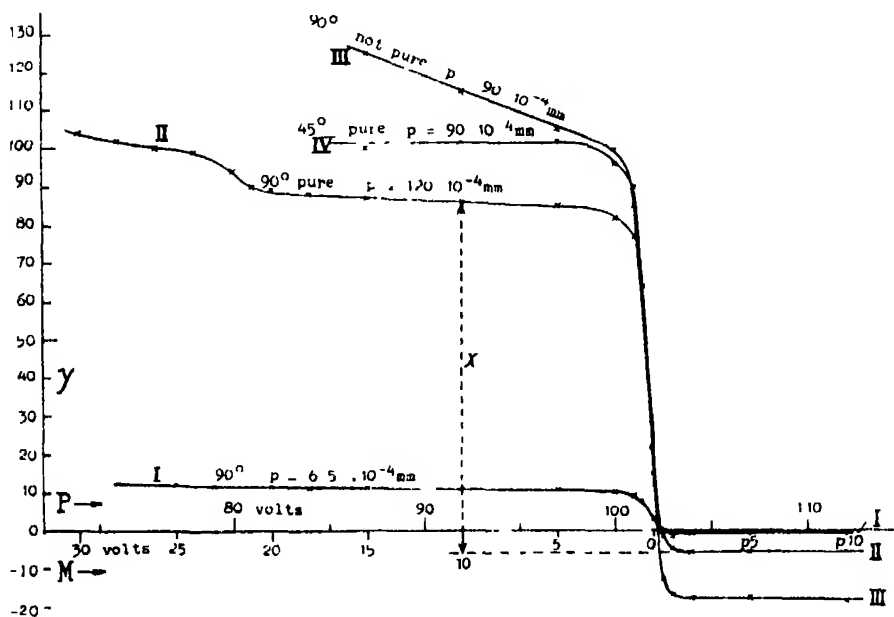


FIG. 7 $-V = 102$ volts.

considerably. Curve IV shows a retarding potential curve for scattering through 45° in pure helium. The run of the curves below the abscissa axis (positive charge on E_{II}) at the retarding potentials larger than the accelerating potential is already mentioned in Paper I. The horizontal line determined by the deflections at these values of the retarding potential defines the zero line of the retarding potential curve. This line has, as will be seen, different positions at different pressures, and it is to be noted, how much impurities shift the position of this line. This is also explained by the view put forward in Paper I, according to which this part of the curves is due to a (photoelectric?) ionisation in the space between S_{II} and E_{II} . Experiments have also shown that when this distance is short, the reversed currents are small.

The retarding potential curves are practically horizontal between $M = 15$ volts and $M = 5$ volts. The difference between the ordinates corresponding to $M = 10$ volts and $M = p5$ volts is therefore a measure for the number of electrons elastically reflected. The expression $p5$ volts means that the retarding potential is 5 volts larger than the accelerating potential. Series of measurements with $M = 4$ and $p2$ volts have been made, and the scattering found was the same as that found with $M = 10$ and $p5$ volts. At accelerating potentials smaller than 80 volts the zero line coincides with the abscissa axis. In order to change easily during the measurements from retarding potentials smaller than the accelerating potential V to retarding potentials larger than V , the switch-over U (fig. 6) was arranged.

The effect of the retarding field in front of S_{II} may be tested by varying the potential of S_{II} . In Table I S_{II} means the potential difference between S_{II}

Table I.

Accelerating potential $V = 40.7$ volts.

$p = 63 \cdot 10^{-4}$ mm. Hg. $\Theta = 90^\circ$.

S_{II} (volts).	y .	y .	x .
	$M = 10$ volts	$M = p5$ volts	
+20	86	-1.3	87
16	84	-1.3	85
10	85	-1.3	86
6	81	-1.3	82
2	78	-2.0	80
0	64	-27.0	91

Accelerating potential $V = 295$ volts.

$p = 64 \cdot 10^{-4}$ mm. Hg. $\Theta = 90^\circ$.

+20	0.7	-2.0	2.7
16	1.8	-1.1	2.9
10	1.9	-0.8	2.7
6	1.6	-1.1	2.7
2	0.2	-2.4	2.6
0	>-130	>-130	—

Accelerating potential $V = 102$ volts.

$p = 2 \cdot 10^{-4}$ mm. Hg. $\Theta = 45^\circ$.

+14	+32	0.0	32
2	24.0	-7.5	31.5
0	-80	-80	—

and N , and y the deflection on L_{II} . x is the difference between the two y -values and accordingly measured the observed scattered amount of electrons. It is seen that x is independent of the potential of S_{II} , when this potential is larger than $+2$ volts, relative to N , T and H . If the potential is smaller, positive ions from O , fig. 6, may enter E_{II} . Usually $S_{II} = +16$ volts.

In the measurement of the direct beam at E_I the fields are arranged as nearly as possible analogous to the fields which are used when measuring the scattered electrons near E_{II} . The difference M_I between the accelerating potential and the retarding potential is therefore usually 10 volts. To keep the positive ions away, the screen S_I has a positive potential relative to T . Experiments show that variations of the potentials M_I and S_I within certain limits are without any influence on the value x of the scattering. In Table II

Table II.

$V = 101$ volts. $p = 95 \cdot 10^{-4}$ mm Hg. $\theta = 90^\circ$.

M_I	S_I (volts).	S_{II} (volts)	M	y .	x
10	16	16	10	157	168
			$p5$	- 11	
6	4	4	6	148	171
			$p3$	-23	
4	2	2	6	141	177
			$p3$	-32	

is given an example of the determination of the scattering using very different values of the potentials M_I , S_I , S_{II} and M . While the agreement between the two first measurements is satisfactory, a small deviation for small values of these potentials is found.

How far the result of the measurements depended on the current i in the electron beam was also investigated. As mentioned, all measurements were made by sending a certain amount of electrons to E_I , and the rate of charge of the electrometer L_I is then proportional to i . The conditions in the direct beam were often the cause of disturbances, and a control had to be made before a reliable series of measurements could be undertaken. If i was not found to be proportional to the current I between the filament G and H_1 (read at μA in fig. 6), false values of the scattering were obtained. The current I was

always kept as small as possible. This error was independent of the pressure, and the cause was probably small impurities at the screens defining the electron beam.

Absolute Measurements. As mentioned in Paper I, the linear dependence of the scattering on the pressure was found to hold up to $p = 100 \cdot 10^{-4}$ mm. Hg. This was again tested and confirmed. At electron velocities of about 30 volts a small deviation from the linearity at the highest pressures was found.

In order to get a determination of the scattering, the observations given in Table III have to be made. From the values of x and p the scattering x_0 at $1.00 \cdot 10^{-4}$ mm. Hg is calculated.

Table III
V = 101 volts.

$\Theta = 45^\circ$.				$\Theta = 90^\circ$.			
M = 10.	y p5 volts.	x	p mm. Hg	M = 10	y p5 volts.	x	p mm. Hg
+150	-2	152	$66 \cdot 10^{-4}$	+49	-5	54	$67 \cdot 10^{-4}$
39	0	39	$6 \cdot 0 \cdot 10^{-4}$	12 0	0	12 0	$6 \cdot 0 \cdot 10^{-4}$
190	-4	194	$87 \cdot 10^{-4}$	60	-6	66	$86 \cdot 10^{-4}$
$x_0 = 1.90$				$x_0 = 0.8$			

By the constant of the apparatus k is understood the factor by which we have to multiply x_0 to get the scattered intensity I_θ . Accordingly $I_\theta = k \cdot x_0$. In formula (4) we have an expression for the scattered fraction of electrons ϕ . This quantity may also be found from the observations. The meaning of x_0 is already explained, and the deflection x_0 indicates an electric charge on E_{II} - L_{II} of $0.00159 \cdot x_0$ e.s. units. Since only the fraction q of the electrons in the beam enters E_I (p. 116) the scattered fraction will be expressed by

$$\phi = x_0 \cdot q \cdot \frac{0.00159}{300} = x_0 \cdot q \cdot 5.3 \cdot 10^{-6},$$

and we therefore get by means of (4)

$$I_\theta = \frac{q \cdot 5.3 \cdot 10^{-6} \cdot R}{2\pi \cdot N \cdot l_k \cdot b \cdot \sin \Theta} x_0 = k \cdot x_0,$$

where N now is the number of atoms per cm^3 at the pressure $1.00 \cdot 10^{-4}$ mm. Hg.

Any change in the geometry of the apparatus (scattering length l , of the beam, the widths of the slits, etc.) will cause a change in the value of k .

Relative measurements of the scattering (i.e., at varying potentials and through a fixed scattering angle) may be made with a good accuracy at a constant value of k . The absolute values of the scattering will furthermore include the errors in the determination of k . While x_0 may be determined with an accuracy of about 5 per cent., the determination of k will need measurements of at least eight different quantities, with errors from 1 to 3 per cent. If I_0 is determined using different values of k , one may test the influence of the dimensions of the apparatus upon the result. In Table IV is shown two measurements at different widths (b) of the slit S_{II} , all other dimensions left unaltered. The scattered intensity I_0 , measured at three different velocities, is found to be independent of the width of the slit

Table IV.

$$\Theta = 90^\circ.$$

$b = 0.50 \text{ mm}$		$b = 1.0 \text{ mm}$	
$k = 0.94 \cdot 10^{-18}$		$k = 0.47 \cdot 10^{-18}$	
V (volts).	$I_0 \cdot 10^{18}$	V (volts)	$I_0 \cdot 10^{18}$
100	1.52	100	1.48
40	6.9	40	7.0
30	10.6	30	10.9

A change in the diameter of electron beam is also without any influence on the experimentally determined value of I_0 .

If the length of that part of the electron beam from which the scattering is observed, is changed by altering the distance T-H ($= l$), it will be seen to be of no influence on the value found for I_0 . At $V = 100$ volts, e.g., one finds for I_0 the values $1.56 \cdot 10^{-18}$, $1.48 \cdot 10^{-18}$ and $1.64 \cdot 10^{-18}$ by single measurements at $l = 10 \text{ mm.}$, 5.0 mm. and 2.0 mm. respectively. If the scattering did not vary linearly with the angle with sufficient approximation, as was previously assumed, this would be discovered here.

Many control measurements were made with wide variations in the dimensions of the apparatus, and always the same values of I_0 were found. It is therefore justifiable to conclude that the electrons on their way through the holes and slits in the experiments follow exactly the ordinary geometric laws of rectilinear propagation.

Results.—The results of the measurements are given in Table V; the values being obtained graphically from curves drawn from a great number of observations. The absolute measurements at 100 volts have been made with special care, and at $\Theta = 90^\circ$ about 20 and at $\Theta = 45^\circ$ about 10 reliable, independent measurements form the basis for the values given in the table. The other

Table V.

V (volts).	Scattered intensity I_θ .	
	$\Theta = 90^\circ$.	$\Theta = 45^\circ$
30 0	11 2 $\cdot 10^{-18}$	25 $\cdot 10^{-18}$
35 0	9 0 $\cdot 10^{-18}$	22 5 $\cdot 10^{-18}$
40 0	7 4 $\cdot 10^{-18}$	20 $\cdot 10^{-18}$
50	5 2 $\cdot 10^{-18}$	15 8 $\cdot 10^{-18}$
60	3 8 $\cdot 10^{-18}$	12 6 $\cdot 10^{-18}$
80	2 3 $\cdot 10^{-18}$	8 6 $\cdot 10^{-18}$
100	1 60 $\cdot 10^{-18}$	6 4 $\cdot 10^{-18}$
150	0 77 $\cdot 10^{-18}$	3 7 $\cdot 10^{-18}$
200	0 45 $\cdot 10^{-18}$	2 4 $\cdot 10^{-18}$
250	0 29 $\cdot 10^{-18}$	1 75 $\cdot 10^{-18}$
300	0 21 $\cdot 10^{-18}$	1 35 $\cdot 10^{-18}$
400		0 85 $\cdot 10^{-18}$

values were obtained from a great number of observations at the accelerating potentials given in the table. The accuracy of the relative scattering at the different potentials is about 5 per cent., but the absolute value is less accurate. The accuracy may here be assumed to be about 10 per cent.

In fig. 8 the scattered intensity I_θ is shown as a function of the accelerating potential V. The diagram is doubly logarithmic. The abscissa is the voltage V, and on the top of the diagram the corresponding velocity of the electrons is given. The ordinate is I_θ . In this representation the Rutherford formula (2) will be a straight line. According to the Mott-Bethe formula (3) I_θ is a function of $(V \sin^2 \frac{1}{2}\Theta)$, just as in formula (2). One may therefore find the scattered intensity at different angles by shifting the curves parallel to the abscissa axis. The curves A represent I_θ calculated from formula (2), the nuclear scattering. The curves B are I_θ from formula (3). The shifts of the A- and B-curves from $\Theta = 90^\circ$ to $\Theta = 45^\circ$ are the same. The curves C are the experimental curves according to Table V. In the figure several observation points are plotted to show the accuracy. Since the figure is doubly logarithmic, the same relative error, e.g., ± 10 per cent., will be represented all over the figure by the same distance. At $\Theta = 90^\circ$ good agreement with the theoretical

formula (3) is found above 150 volts, but at low voltage, as already shown by the measurements of the relative scattering in Paper I, large deviations are found. One may conclude that at $\Theta = 90^\circ$ the Mott-Bethe formula (3) will

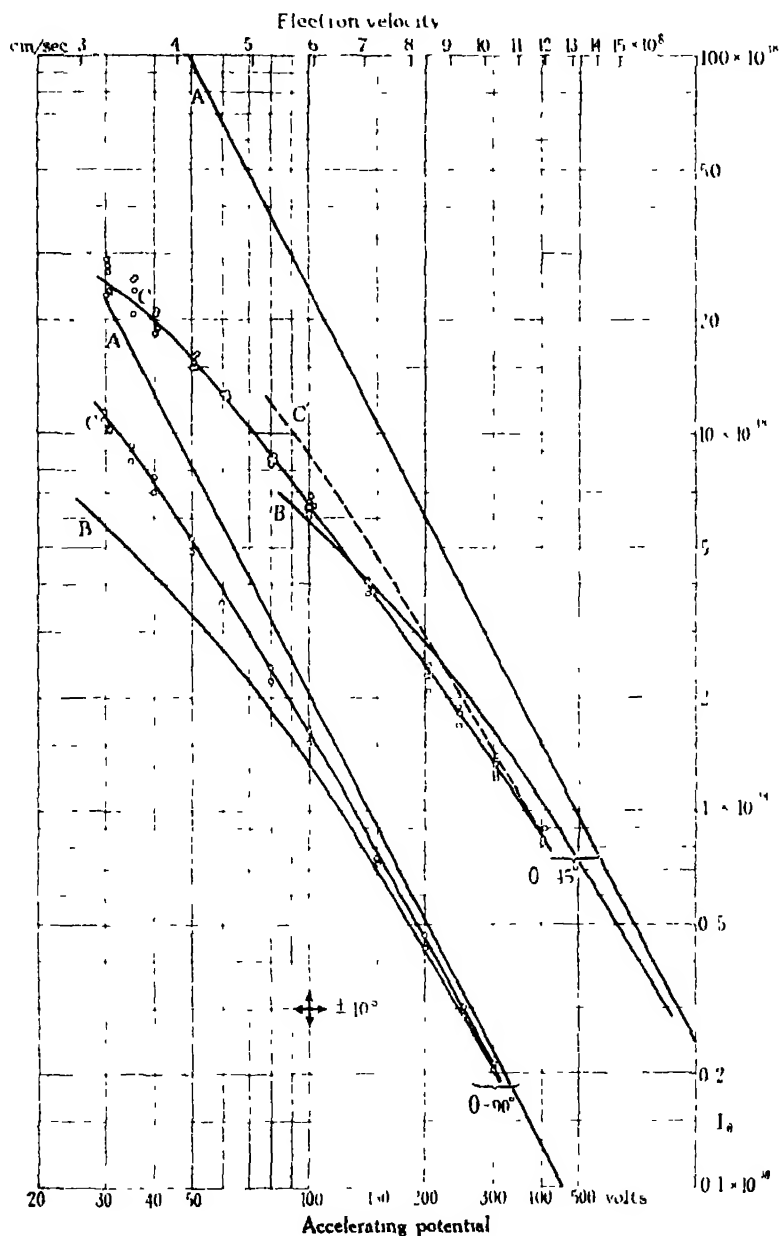


FIG. 8.

express the scattering only when the scattering is less than 20 per cent. smaller than the nuclear scattering.

The agreement between the measurements at $\Theta = 45^\circ$ and the formula (3) is less good. At the smaller angle $\Theta = 45^\circ$ it is, however, to be expected that errors in the angle Θ will manifest themselves far more than at $\Theta = 90^\circ$. The scattering increases very much with decreasing angle; Rutherford's formula gives the relative error $dI_e/I_e = 2d\Theta$ at $\Theta = 90^\circ$, while one gets $dI_e/I_e = 5d\Theta$ at $\Theta = 45^\circ$. Furthermore, on account of the construction of the apparatus used, uncontrollable errors in the definition of the scattering angle will be more probable at 45° than at 90° . It is, therefore, best to estimate the possible error at $\Theta = 45^\circ$ as about 15 per cent. An error of this size would just be able to explain the difference between the experimental curve C and the theoretical curve B in fig. 8 at large velocities. The measurements at 45° , just as at 90° , are partly made as relative measurements, partly as absolute measurements under varying conditions. With the apparatus model III a direct comparison between scattering through 90° and 45° was made. The measurements have, as shown in fig. 8, given fairly coincident results. Only at low voltages (40–30 volts) is the error 15–20 per cent. on a single measurement.

From the different slope of the two C-curves one may conclude that the scattering which, following formula (3) should be a function of $(V \sin^2 \frac{1}{2}\Theta)$ is not solely a function of this quantity. The possibility of such a deviation from formula (3) is also pointed out by Chr. Møller.* If the scattering was a function of $(V \sin^2 \frac{1}{2}\Theta)$, then the two C-curves could be made to coincide by a shift parallel to the X-axis. The curve C' shows C at 90° shifted to coincide with C at 45° and at $V = 400$ volts. It is evident that this conclusion is to a certain degree independent of the eventual errors in the absolute values.

From the absolute values at 45° it can be seen that formula (3) corresponds fairly well with the experiments, when possible errors have been taken into account, at large velocities. At small velocities, however, the deviation, as expected, will be considerably larger.

From experiments by Dymond and Watson† at electron velocities corresponding to 210 volts, Mott concludes that the scattering was a function of $(V \sin^2 \frac{1}{2}\Theta)$. By comparison of the values of the scattering at this voltage with Mott's values (in fig. 8) it will be seen that this conclusion was justified within the error of the experiments of Dymond and Watson.

To compare the predictions of the theory with the results of the experiments

* 'Z. Physik,' vol. 66, p. 513 (1930).

† 'Proc. Roy. Soc.,' A, vol. 122, p. 571 (1929).

the relative deviation Δ_E from the nuclear scattering is calculated in Table VI. Δ_E is the difference between the nuclear scattering and the observed scattering divided by the nuclear scattering.

Table VI.

V (volts).	$\Theta = 90^\circ$.		$\Theta = 45^\circ$.	
	Δ_E .	Δ_T .	Δ_E .	Δ_T .
30 0	0.50	0 74	0 91 (0 90)	—
35.0	0 46	0 70	0 88 (0 87)	—
40 0	0 42	0 66	0 87 (0 85)	—
50	0 37	0.59	0 83 (0 81)	—
60	0 33	0.53	0 81 (0 77)	—
80	0 28	0.44	0.77 (0 73)	0.81
100	0 22	0 34	0.72 (0.68)	0 75
150	0.16	0 24	0 65 (0 59)	0 64
200	0 12	0.16	0 60 (0 52)	0 53
250	0 11	0.12	0 54 (0 45)	0.45
300	0 10	0.10	0 49 (0 39)	0 38
400	—	—	0 43 (0 30)	0.30

In column Δ_T is given the relative deviation from the nuclear scattering, as calculated from the theoretical formula (3). At $\Theta = 45^\circ$ the considerations about a possible error in the value of Θ must be remembered. If coincidence of the experimental scattering and formula (3) is assumed at $V = 400$ volts, one gets the values in brackets at 45° . One may note the agreement between theory and experiment at 90° , and also that the scattering at low velocities is much smaller than the nuclear scattering: at 30 volts only 50 per cent. At 45° the scattering observed at 30 volts is only 9 per cent. of the nuclear scattering.

In conclusion, the author wishes to express his best thanks to Professor Niels Bohr for his great help and interest, and to the Trustees of the " Carlsbergfond " for a grant during the work.

Summary.

The scattered intensity I_s is found experimentally at velocities corresponding to 30–400 volts and at scattering angles $\Theta = 90^\circ$ and 45° . In Table V and fig. 8 the results of the measurements are given. In fig. 8 and Table VI the results of the observations are compared with the nuclear scattering according to the Rutherford formula (2), and with the scattering according to Mott and Bethe's calculations in formula (3). Agreement is found at velocities above 150 volts. Large deviations take place at smaller velocities. The method and details of the experimental arrangement are described.

A New Primary Standard Barometer.

By J. E. SEARS, Jnr., C.B.E., M.A., M.I.Mech.E., and J. S. CLARK, A.R.C.Sc.,
B.Sc., D.I.C., of the National Physical Laboratory.

(Communicated by Sir Joseph Petavel, F R S —Received August 18, 1932.)

[PLATE 1]

1. *Introduction—Historical.*

Several of the national laboratories have, at some time or other, set up "fundamental" or "primary" standard barometers, with the object of measuring atmospheric pressure in absolute value, and with greater precision than is possible with a barometer of the Fortin type. As long ago as 1854, Kew Observatory established a standard barometer which was described by Welsh.* This instrument had a glass tube about 1·1 inches in internal diameter and the height of the mercury column was observed by means of a cathetometer, which was attached to the same supporting wall as the barometer tube itself. The level of the mercury in the cistern was observed by setting the cathetometer microscope on a fiducial mark which was carried on a short steel stem, the lower end of which was ground to a rounded point which could be brought into contact with the surface of the mercury in the cistern. The upper surface of the mercury was observed by setting a horizontal cross line in the cathetometer microscope tangential to the image of the mercury meniscus as seen in the microscope. It is evident that, except for the reduction of the errors due to the variations of the surface tension of mercury, by the provision of a tube of fairly large diameter, this instrument has most of the possibilities of error which may exist in the Fortin type of barometer.

The Bureau International des Poids et Mesures had, in 1880, a "normal" barometer constructed on lines suggested by Wild.† This instrument was superseded by another, described in the *Travaux et Memoires* of the Bureau,‡ and which was of interest because of the provision of a simple method of displacing any gases or vapours which might accumulate in time above the surface of the mercury in the closed limb. In each of these instruments the mercury meniscus was observed directly through the barometer tube by means

* 'Phil. Trans.,' A, vol. 146, p. 507 (1856).

† 'Repertorium Experiment. Physik,' vol. 11, p. 389 (1875).

‡ 'Trav. Bur. int. Pds. Mes.,' vol. 1 (1881).

of a cathetometer and the temperature of the mercury column determined by means of thermometers immersed in mercury near the barometer. Subsequently, another "normal" barometer,* also constructed on the lines suggested by Wild, was set up. This instrument was of interest in that a new method of observing the mercury surfaces, described by Marek,† was employed. This method, which consists in projecting an image of a horizontal wire into the space above the mercury, and reading by means of a microscope the positions of this image and of its reflection in the mercury surface, appears to be entirely satisfactory, and was adopted, with slight modifications, for the primary standard barometer described in this paper.

The work of verifying mercurial and aneroid barometers was carried out in this country at Kew Observatory up to the year 1912, when it was transferred to the National Physical Laboratory at Teddington. A new large bore working standard barometer of the Fortin type was provided for this work at the Laboratory, and was very carefully compared with the old Kew standards before the transfer. The standards themselves were left at Kew, and the late Sir George Beilby, F.R.S., generously gave a sum of £200 for the purpose of constructing a new primary standard for future use at the Laboratory. A design for this was prepared, and a preliminary model of the proposed glass-work was constructed. The work was, however, interrupted by the war, and was not resumed until the year 1921. The model barometer was then filled, and appeared to be quite satisfactory. It was, however, found impracticable to obtain glass tubing optically worked to the accuracy which was desired for the construction of the final instrument, and after considerable delay it was eventually decided to proceed on different lines.

At the present time, it is a comparatively simple matter to produce and maintain a very low pressure (say less than 1 μ of mercury) within an enclosure, by means of any of the modern pumping systems. Hence it is no longer essential to make the barometer of glass tubing sealed off permanently when filled with mercury. A barometer may now be made of steel—a form of construction which makes it possible to have accurately flat and parallel glass windows through which to observe the mercury surfaces, and so avoid errors due to optical distortion caused by observing through glass tubes which are very difficult to obtain straight and parallel. Since the vacuum above the surface of the mercury in such a barometer can be produced and renewed

* *Ibid.*, vol. 3 (1884).

† 'Repertorium Experiment. Physik,' vol. 16, p. 585 (1880); also 'Trav. Bur. int. Pds. Mes.,' vol. 3, D 22 (1884).

whenever required, the instrument can be taken down and cleaned whenever necessary and there is no need to carry out any process of outgassing which is so troublesome in the case of a glass barometer which, after being sealed off, is required to maintain its vacuum unimpaired for an indefinite period.

These possibilities have been made use of in the design of the new primary standard barometer now to be described.

2. Description of New Primary Standard Barometer.

A photograph of the new primary standard barometer, taken before it was surrounded by its glass case, is shown in fig. 1, Plate 1.

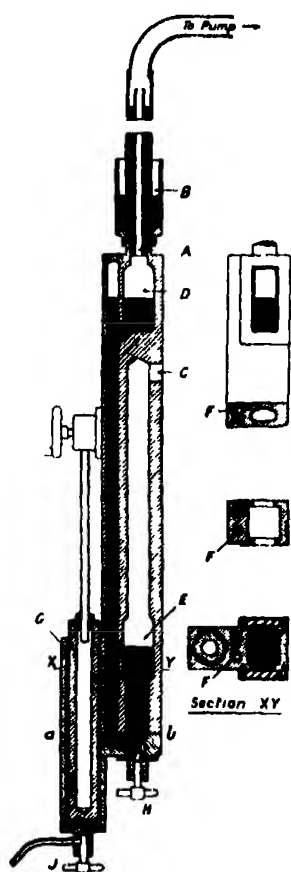


FIG. 2.

The barometer consists essentially of a U-tube bored in a block of stainless steel, as shown diagrammatically in fig. 2. The upper end of one side of the U is connected at A to a mercury vapour condensation pump, whereby the vacuum above the mercury in the barometer is produced and maintained as required. The connection is made through a mercury seal B so as to prevent vibrations being transmitted directly from the vacuum pipe line (which is connected to the wall of the room) to the barometer itself (which is resting on a large concrete base isolated from the floor of the room). The other end of the U is open to the pressure of the air at C. The mercury surfaces within the barometer are observed through optically flat and parallel glass windows placed in pairs, one above the other and 30 inches apart. The measurements of barometric height are referred directly to a line standard placed vertically by the side of the barometric column, by means of micrometer microscopes fixed to brackets carried on a massive vertical column, which can be translated horizontally so that the microscopes come opposite either to the mercury surfaces or to the line standard.

The actual construction of the stainless steel portion of the barometer may be followed in fig. 2. The tubes bored in the solid block of stainless steel are opened out at D and E to form reservoirs each $1\frac{1}{2}$ inches square in section and

of length (in the direction of the axis of the barometer) about 4 inches. These reservoirs form the upper and lower limbs of the barometer. Cross-sections of these reservoirs are shown in fig 2

F, shown in section in fig. 2, is another hole bored throughout the length of the stainless steel block and parallel to the hole connecting the reservoirs D and E. This hole contains mercury, and in it a mercurial thermometer, with a bulb 30 inches in length, is immersed. The 30-inch bulb is arranged to be at the same height as the barometric column and is immersed in mercury up to the level of the top of the bulb, which is very closely the level of the top of the barometric column. This thermometer, being so near the mercury forming the barometric column and being completely immersed in mercury and surrounded by the same mass of steel, should record very closely the mean temperature of the barometric column. The position of the projecting stem of this thermometer is shown at T in fig. 3.

The other cylindrical hole G shown in fig. 2 contains a stainless steel plunger which is used to adjust the levels of the mercury in the barometer, and, by considerably withdrawing the plunger, to allow the mercury levels to sink below the levels of the glass windows when the barometer is not in use.

The lower portion of the barometer, below the line *ab*, fig. 2, consists of another block of stainless steel in which is embodied a 4-way cock H, the extension of the plunger hole, and a draining cock J, in the form of a needle valve. The 4-way cock serves to connect together as required the various parts of the barometer.

The barometer and the line standard, S, fig 3, are mounted side by side on a massive base, and the vertical column K, which carries a pair of micrometer microscopes L disposed vertically one above the other, may be moved sideways, parallel to itself, in V-grooves on the base casting, so that the microscopes may be brought opposite either to the mercury surfaces or to the line standard as required.

The brackets which support the two micrometer microscopes also carry two "collimators," M, fig. 3, each arranged co-axially with its corresponding microscope. The axes of the micrometer microscopes are accurately parallel and as nearly as possible perpendicular to the axis of the barometer itself. The "collimators" enable a real image of a horizontal wire to be formed just above the mercury surface in each reservoir, the images being projected through the rear glass window of each reservoir. This real image and its virtual image formed by reflection in the horizontal surface of the mercury, are visible together in the field of the microscope, and the actual surface of the mercury,

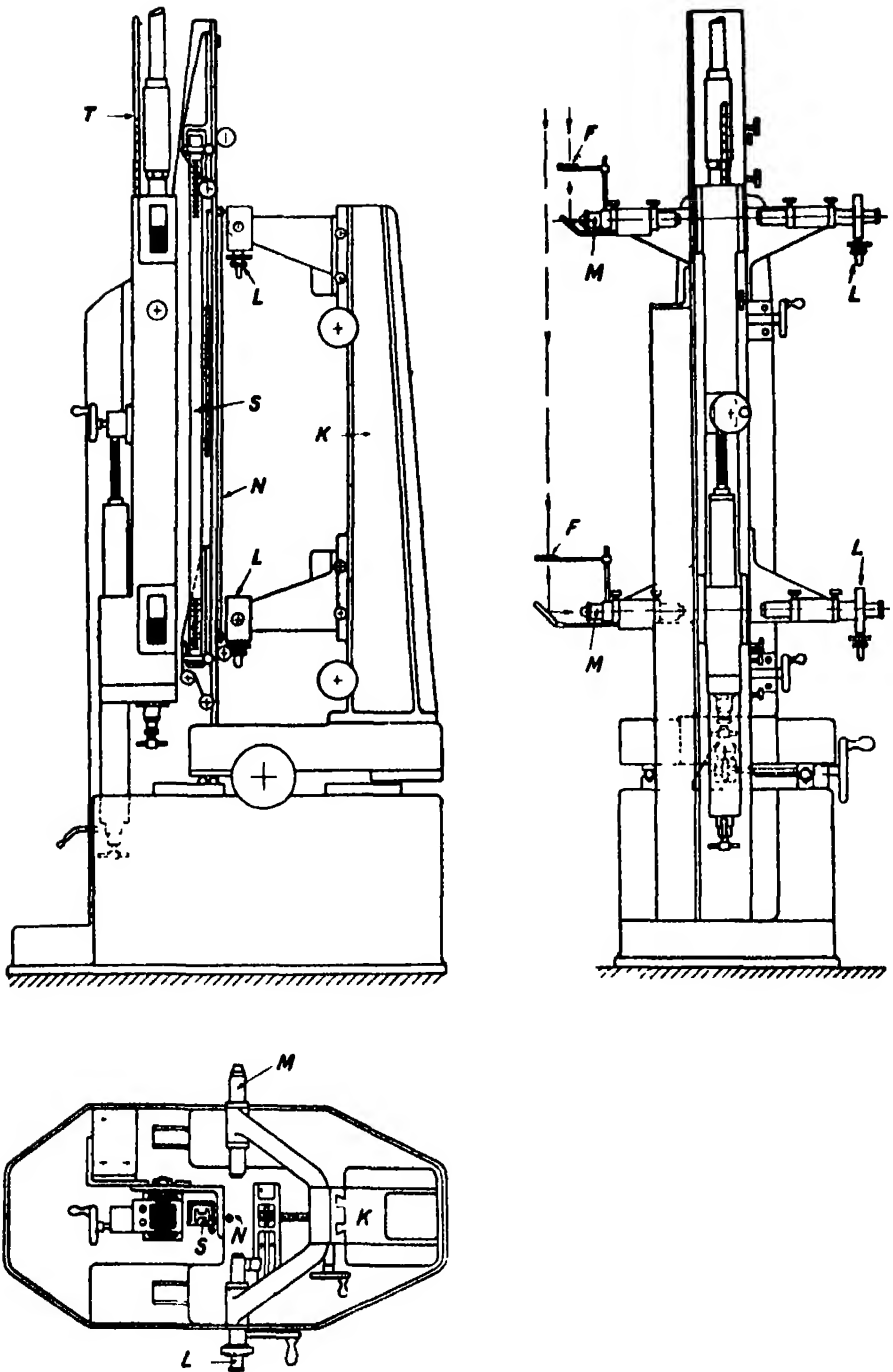


FIG. 3

which is normally invisible in the microscope, is taken to be half way between these images. The horizontal cross wires are illuminated by means of a pointolite lamp, each collimator being provided with a ground glass diffuser and a green filter, F, fig. 3, so that the images appear as black lines on uniformly illuminated green fields.

The glass windows through which these images are formed and observed are sealed on to the stainless steel in such a way that the small quantity of grease necessary to make the seal vacuum-tight cannot come into contact with the mercury. To achieve this the front and rear external surfaces of the walls of the reservoirs are ground flat and parallel to form good bearing surfaces for the glass windows, and on these flat portions a groove of semicircular section and of radius $1/32$ -inch is cut. This groove divides the flat bearing surfaces into two parts. The inner portion (i.e., nearest to the window aperture of the reservoir) is left clean and dry, but the outer portion has placed on it a trace of rubber-tallow grease, which is flattened out into a very thin film when the glass window is pressed against it. This grease film forms an excellent vacuum-tight joint and the groove prevents the excess of grease getting into contact with the mercury. In the case of the lower reservoir, where the internal and external pressures are practically equal, it was not necessary to use any grease and the flat glass was simply held against the flat bearing surface by means of a protective cover. The flat bearing surfaces and grooves are shown in section in fig. 2.

The line standard, S, fig. 3, is provided with two adjustments both at its upper and at its lower ends. These serve to adjust it vertical and to focus the scale divisions. A third adjustment at the lower end enables the scale to be raised or lowered to bring selected scale divisions to suitable positions within the fields of the microscopes. A plumb line N is suspended from the main support of the barometer, and serves as a reference for adjusting the line standard vertical. The micrometer microscopes were first of all set vertically one above the other by observing the plumb line with one microscope clamped first of all in one bracket and then in the other, thin packing pieces being inserted under the vertical column supporting the brackets until the image of the plumb line coincided with the axis of the microscope in both brackets. The second microscope was then replaced in its bracket and both microscopes focussed on the plumb line. By traversing the microscope column to a position opposite the line standard the latter can now be adjusted to verticality by focussing its graduations in the fields of the two microscopes. The adjustment to verticality need not be carried out with very high precision since an error

of 1 mm. in this adjustment only produces an error in the vertical height amounting to about 0.7μ in 76 cm.

The mercury used in the barometer was first of all cleaned by allowing it to trickle slowly through a column of dilute nitric acid (20 per cent. HNO_3). It was then distilled three times whilst a stream of air was bubbled through the still, the air pressure being about 3 cm. of mercury. This process, according to Hulett,* should remove practically the whole of the oxidisable metal likely to exist as impurities in mercury. Finally the mercury was distilled *in vacuo*.

The stainless steel body of the barometer was carefully cleaned inside before sealing on the windows and inserting the mercury. It was first of all washed with hot dilute caustic soda to remove all traces of grease left behind from the machining operations. The whole mass of stainless steel was completely immersed in a bath of hot caustic soda. It was then washed out, first with several washings of hot tap water and finally with hot distilled water, and then allowed to dry. The steel became so hot after being immersed in the boiling distilled water, that it dried naturally by evaporation of the water. The windows were then carefully cleaned and sealed on, and, after assembly in position, the barometer was ready for filling with mercury. The mercury, purified as already described, was carefully poured in through C, sufficient being inserted so that, after the barometer had been evacuated, the mercury level in the open (lower) limb was just half-way up the window of the lower reservoir, the plunger then being within about 1 inch of its lowest position.

The barometer, when completely assembled and connected with the vacuum pipe line, pumps, and McLeod gauge, was surrounded by a glass case which helped to keep uniform the temperature of the air surrounding the barometer. Except while the barometer is actually in use, the plunger is withdrawn so that the mercury in each reservoir falls below the level of the glass window. In this way the glass windows are kept clean and on lowering the plunger the mercury rises and produces a new clean surface whenever required.

Before taking readings of the barometric height, the vacuum is renewed by the pumping system, which consists of an annular jet mercury vapour pump backed by a rotary oil pump. No difficulty whatever is experienced in reducing the residual pressure, as indicated by the McLeod gauge in the vacuum pipe line, to less than 0.1μ of mercury. The vapour pressure of mercury at ordinary temperatures has been investigated by Hill.† It varies from 1μ at 13°C .

* 'Phys. Rev.', vol. 33, p. 307 (1911).

† 'Phys. Rev.', vol. 20, p. 259 (1922).

to $2\ \mu$ at 21°C. , being very closely $1.5\ \mu$ of mercury at 18°C. A residual pressure of the order of $1.5\ \mu$ may therefore always exist above the surface of the mercury in the barometer, although this is not indicated by the McLeod gauge.

3. Optical System for Reading the Barometer.

The method of reading the position of the mercury surface by bisecting the distance between the real and virtual images of a horizontal wire in the collimator depends for its success on several considerations. Only a limited portion of the mercury meniscus is sufficiently flat to form a virtual image reasonably free from distortion, and owing to the obstruction of the mercury column itself, only limited portions of the objectives of the microscopes and collimators are operative in forming the images.

The form of the mercury meniscus can be deduced from consideration of the special case of a large surface of mercury bounded by a plane vertical wall. It may be shown that, for a meniscus height of 1 mm., at a distance of 1 cm. from an infinitely extending wall, the departure from flatness of the meniscus is only $2\ \mu$ and for distances exceeding 1 cm. the departure from flatness is even less. For a 2-mm. meniscus height the departure from flatness is $5\ \mu$ at the distance 1 cm. and $0.5\ \mu$ at 1.5 cm. from the wall. Hence for the usual height of meniscus found in practice in the barometer the surface may be taken to be very closely flat at any distance exceeding 1.5 cm. from the walls of the reservoir.

The actual form of the mercury surface has been calculated for a 1 mm. and a 2 mm. meniscus.* Taking the point of contact of the mercury with the glass wall as the origin and measuring x horizontally and y vertically, the coordinates of the mercury surfaces are given in Tables I and II.

These results when plotted give a meniscus curve of the form shown in fig. 4, which, however, is not drawn to scale, the vertical ordinates y being much exaggerated.

In this figure the optical axis hh' of the collimator (and of the microscope) passes horizontally through the apex of the meniscus. I is the real image of the horizontal cross-wire formed by the collimator. It is evident that all the observable rays contributing to the formation of this image must lie between aIb and cId , which are tangential to the meniscus surface, and the inclination of cId is also limited by the diameters of the lenses. If I is taken on the axis

* The authors are indebted to Mr. F. A. Gould of the National Physical Laboratory for permission to quote from his (unpublished) computations of the form of a mercury meniscus.

Table I.—Meniscus height 1 mm.

x .	y .
cm.	cm.
0.0	0.0
0.078	0.04
0.199	0.07
0.324	0.08
0.364	0.087
0.416	0.090
0.489	0.094
0.614	0.097
0.740	0.0984
0.934	0.0995
1.088	0.0998
1.427	0.09995

Table II.—Meniscus height 2 mm.

x .	y
cm.	cm
0.059	0.08
0.102	0.11
0.169	0.14
0.290	0.17
0.415	0.184
0.455	0.187
0.507	0.191
0.580	0.194
0.705	0.1968
0.831	0.1984
1.026	0.1995
1.519	0.19995

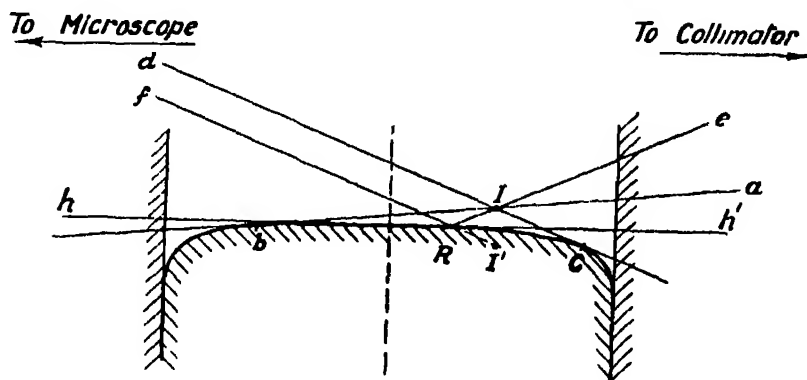


FIG. 4.

of the barometer, these tangents are symmetrical, and since I must not vary far above the mercury surface, only a very narrow beam of light would then contribute to the formation of the image I . In the standard barometer described by Marek (*loc. cit*) the image I was formed actually on the axis of the barometer tube. If, however, I is taken to be on the side of the axis towards the collimator, as shown in fig. 4, then ab is nearly horizontal; but cd is more inclined to the horizontal since the point of contact of the tangent at c is well below the horizontal surface hh' passing through the apex of the meniscus. In this case a wider beam contributes to the formation of I . If now we consider the reflected light which goes to the formation of I' , we see that this is limited by the tangent ib and the lines eIR , Rf which are equally inclined to the surface at R . The inclination of eIR is limited by the aperture of the lens forming the image. Thus the light forming the direct image I and that form-

ing the reflected image I' come from entirely different parts of the collimator objective. Now it is evident that the further R and I are moved towards the collimator the greater is the relative amount of the central flat portion of the meniscus contributing towards the formation of the reflected image I' , and the greater the distance of I above the horizontal the greater the angle of the cone of light forming the direct image I . Hence, in order to obtain the direct and reflected images equally bright and equally well defined a compromise must be made. Experiments were made with the direct image I formed at various distances above the mercury surface and at various horizontal distances from the axis of the barometer. It was found that best results were obtained when the image I was at a distance of about 18 mm behind the axis of the barometer, and that the definition was equally good for both images when the separation of the images was anything between 0.8 and 1.6 mm.

By tracing the rays on a scale drawing of the mercury meniscus, with the images placed 18 mm. behind the axis of the barometer, *i.e.*, about 15 mm. in front of the rear window, it may be seen that the separation of the images is 1.6 mm. when the limiting ray cIR comes from the upper edge of the image-forming lens. Furthermore, it may be seen that, even within the range of separations (0.8 to 1.6 mm.) which gave good definition, an appreciable part of the curved portion of the meniscus on the side towards the microscope contributes towards the formation of the reflected image I' , although apparently not sufficient to cause any obvious lack of definition. It was therefore necessary to determine experimentally whether the bisection of the observed distance II' really represented the position of the apex of the mercury meniscus.

By means of the 4-way cock H , fig. 2, it is possible to shut off either the upper or the lower limb of the barometer so as to render the position of the mercury surfaces independent of the atmospheric pressure. Tests under these conditions were then carried out with each surface in succession. By raising and lowering the brackets carrying the microscopes and collimators it is possible to vary the distance of the image I above the surface. Corresponding readings were taken of the positions of I and I' and of a fixed line on the scale S , and the readings of the apparent position of bisection corresponding with various separations of I and I' were plotted. A typical series of results has been plotted in fig. 5, in which the vertical ordinates represent the distance in microns of the points of bisection from a fixed arbitrary point on the scale S . These results show that, for any separation of the images between about 0.6 and 1.5 mm. the bisection of the apparent distance between I and I' gives a constant reading, and although this is not proof that the reading is really that of the mercury

surface, yet if the optical systems and the separation of the images are kept the same on both upper and lower limbs, the *difference* between the points of bisection must be very closely the true height of the mercury column. It seems that provided I and I' are at a suitable distance from the vertical axis of the barometer and the separation of I and I' is not so large or so small that the definition of one or other of the images is obviously impaired, then the

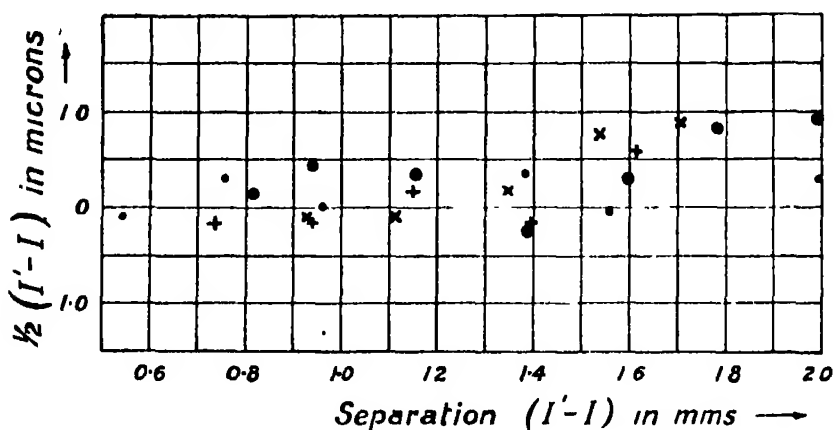


Fig. 5.

curvature of the meniscus does not introduce any error into the apparent position of the surface as determined by bisecting the distance between the images. These tests were repeated, varying the separation of the images by varying the position of the horizontal wires in the collimators and without changing the position of the axis of the microscope in relation to the mercury surface. Similar results were obtained, showing that in practice any separation of the images between 0.8 mm. and 1.5 mm. is permissible.

Although only a little more than one-half the aperture of the microscope objective is used in observing the images, the whole of the lens is used when observing the line standard, since the scale must necessarily be illuminated vertically through the axis of the objective. This cannot be avoided, but since the lenses in both upper and lower microscopes are similar, it is unlikely that any appreciable error is introduced thereby in measurement of *differences* in height. The similarity of the optical qualities of the upper and lower microscopes was confirmed by interchanging them.

The images were observed through the glass windows which were 11 mm. thick and were optically polished flat and parallel. The stainless steel surfaces to which they were sealed were ground and lapped so that the top

and bottom windows were co-planar and the front and rear windows parallel. Any departure from parallelism of the inner and outer surfaces of the windows through which the images are observed would result in displacement of the apparent position of the images. Since the image is at a distance of about 50 mm. behind the inner surface of the window, an error in parallelism of 1 second of arc would produce a vertical displacement of the image amounting to only 0.15μ . The four windows were tested in an interferometer, using circular fringes, and the maximum observed departure from parallelism was 4 seconds of arc in one case. In the other three cases, the surfaces were parallel to within 1 second of arc. Two of these three were chosen for the front windows and the others served for the rear windows, which were only of secondary importance.

The optical and mechanical axes of the micrometer microscopes were found to be coincident and the parallelism of the mechanical axes of the upper and lower microscopes was checked by means of a sensitive spirit-level resting on cylindrical mandrels clamped in each of the brackets. The thickness of each of the glass windows being 11 mm, an error in parallelism of the microscope axes of 50 seconds of arc would produce an error in the apparent barometric height of about 1μ .

4 *Measurement of Temperature.*

The special mercurial thermometer which is placed in F, fig. 2, to determine the mean temperature of the mercury column was made by Messrs. S. & A. Calderara. It has a bulb 76 cm. in length, 8 mm. in internal diameter and walls about 1 mm. thick. The stem is about 42 cm. long and is graduated to show the ice point and the range 15° C. to 23° C., the scale divisions being 0.8 mm. for 0.02° C. The thermometer was calibrated under conditions similar to those in which it is used in the barometer. It was supported vertically in a tube about 2 cm. diameter containing mercury up to the level of the top of the bulb and the whole was immersed in a water bath up to the level of the top of the bulb. The emergent stem was exposed to air temperature. Corrections to the nearest 0.002° C. were determined at the ice point and over the range 15° to 20° C., and the results corrected so as to apply to the condition when the whole of the thermometer, including the emergent stem, was at the temperature indicated by the thermometer.

The approximate coefficient of expansion of mercury is 0.00018 per degree Centigrade. Hence, in order to specify the barometric height to an accuracy

of $1\ \mu$, the mean temperature of the mercury column must be known to an accuracy of 0.007°C .

The standard scale is of invar and its temperature is sufficiently well determined by means of a mercurial thermometer suspended near it.

5 *Density of Mercury.*

A change in density of the mercury in the barometer amounting to 1 part in a million corresponds to an error in the barometric height of $0.8\ \mu$. Now the most reliable determinations of the density of mercury up to the present are those of Marek* obtained at the Bureau International des Poids et Mesures and those of Thiesen, Scheel and Diesselhorst† and of Scheel and Blankenstein,‡ obtained at the Reichsanstalt. These values differ amongst themselves by about 7 parts in a million.

It is unlikely that the density of "pure" mercury can be regarded as constant, at any rate closer than 1 part in 200,000 since it has been shown, by Laby and Mepham§ and by Mulliken and Harkins,|| that the ordinary method of purifying mercury by distillation under reduced pressure results in the partial separation of the isotopes of mercury.

Hence it becomes necessary to know the density of the actual mercury contained in the barometer itself to an accuracy approaching one part in a million in order that no uncertainty exceeding $1\ \mu$ in the barometric height shall be introduced by uncertainty of the density of the mercury used.

At this stage it was not considered necessary to determine the actual density of the mercury used, but at the time of filling the barometer samples of the mercury used were taken and carefully stored away in sealed bottles. A comparison of the density of these samples with the density of the mercury which has been in the barometer should, if carried out at some future date, give some indication whether or not the mercury in the barometer has been contaminated by its contact with stainless steel.

6. *Comparisons with other Standard Barometers.*

The semi-portable standard barometer, described in the Annual Report of the National Physical Laboratory for 1927 (pp. 156-159) was re-erected in

* 'Trav. Bur. int. Poids. Mes.,' vol. 2 (1883).

† 'Z. Instr. Kunde,' vol. 18, p. 138 (1898).

‡ 'Z. Physik,' vol. 31, p. 202 (1925).

§ "Nature," vol. 109, p. 207 (1922).

|| 'J. Amer. Chem. Soc.,' vol. 44, p. 61 (1922).

the same room as the new primary standard barometer, and the readings of the two instruments have been compared. It has been found possible to synchronise very closely the times at which the essential readings on the two instruments were taken, so that the indications of the two instruments were strictly comparable. The cross wires in the micrometer microscopes of the primary standard barometer could be set on the reflected images of the horizontal cross wires of the collimators, without actually reading the micrometers, the total time occupied being 20 to 30 seconds. The micrometer readings corresponding with those settings could be taken subsequently at leisure, together with all the other readings on the direct images of the horizontal cross wire and on the standard scale. The corresponding settings on the other barometer (which may now be called the No. 2 standard barometer) occupied 40 to 50 seconds, and it was therefore possible for two observers, making the first contact on the No. 2 standard barometer about 10 seconds before the first micrometer microscope setting on the primary barometer, to get the mean time of observation on the two instruments very closely synchronous.

The readings of the two instruments were reduced to the same (standard) temperature, and to the same datum level, viz., the level of the middle point of the lower reservoir of the primary standard barometer.

The mean of 55 intercomparisons made between the two barometers gave the result :—

Primary Standard *minus* No. 2 Standard = -0.00002 inch

The individual values of Primary *minus* No. 2 ranged between $+0.0015$ inch and -0.0015 inch, the mean residual ($\pm \Sigma d/n$, where d is the difference between -0.00002 inch and the observed value of Primary *minus* No. 2) being $\pm 0.0005_1$ inch.

These results indicate that, assuming the primary standard barometer to be correct, the "index error" of the No. 2 standard is $+0.00002$ inch, which, for all practical purposes, is zero. It also indicates that the density of the mercury in the primary must be very closely the same as that in the No. 2 standard.

The No. 2 standard barometer was then removed to the barometer test room, set up near the working standard Fortin barometer and the readings of the Fortin barometer were compared with those of the No. 2 standard barometer, the latter being corrected in accordance with its small index error as determined above.

The mean of 77 intercomparisons between these two instruments gave the result :—

No. 2 Standard *minus* Fortin = -0.0013 inch.

The individual values of No. 2 standard *minus* Fortin ranged between $+0.001$ inch and -0.003 inch, and the mean residual was $\pm 0.0007_5$ inch.

Finally, direct simultaneous intercomparisons were made between all three barometers. The Fortin and also the No. 2 standard barometers being now in a room situated about 90 yards away from the primary standard barometer it was only possible to make these intercomparisons when the weather conditions were such that there was no appreciable pressure gradient between the points occupied by the three instruments. The readings of all three instruments were, of course, reduced to the same datum level. Sixty-two such direct intercomparisons were made between the Primary and the Fortin standards, resulting in a mean value .—

Primary standard *minus* Fortin = -0.0015 inch.

The individual values ranged between -0.0001 inch and -0.0029 inch, and the mean residual was $\pm 0.0006_3$ inch.

The corresponding direct intercomparisons between the Primary and No. 2 standards merely confirmed the previously determined index error ($+0.00002$ inch) of the latter.

These results indicate that the index error of the Fortin standard barometer is very closely $+0.0014$ inch, the previously accepted value for this instrument being $+0.002$ inch, with an estimated accuracy of ± 0.001 inch. The new figure is reliable to well within the accuracy with which it is possible to read the Fortin working standard barometer.

7. Estimated Accuracy of Readings.

The mean residuals of the differences obtained in the above three series of intercomparisons are summarised in the following table :—

Intercomparison.	Mean residual.
Primary and No. 2	inch $\pm 0.0005_1$
No. 2 and Fortin	$\pm 0.0007_5$
Primary and Fortin	$\pm 0.0006_3$



FIG. 1.

Hence, if the mean residual errors of single observations of the individual instruments, Primary, No. 2 and Fortin standard barometers, are represented by a , b and c respectively, then we may write:—

$$a^2 + b^2 = (5.1)^2 = 26.01$$

$$b^2 + c^2 = (7.5)^2 = 56.25$$

$$a^2 + c^2 = (6.3)^2 = 39.69$$

from which $a = \pm 2.1$, $b = \pm 4.6$ and $c = \pm 5.9$, the unit being 0.0001 inch. These are, of course, only approximate estimates of the accuracy of the three instruments, but they agree very closely, in the cases of the No. 2 and Fortin barometers, with the accepted accuracies of single readings, which are about ± 0.0004 inch* and ± 0.0006 inch† respectively.

In designing the primary standard barometer, the systematic errors have everywhere been kept well within $\pm 1 \mu$, and results of the type plotted in fig. 5 indicate that the possible errors in the cathetometry are of the order of $\pm 1 \mu$.

The figure of ± 0.00021 inch (5.3μ) for the accuracy of a single observation with this instrument may therefore appear at first sight to be somewhat disappointing. It should, however, be noted that observations of the type plotted in fig. 5 were taken with the cock H closed, so that the mercury column was unaffected by changes of atmospheric pressure. On the other hand, the observations from which the mean residual of ± 0.00021 inch was calculated were subject to the effects of small atmospheric variations, which are always taking place, even when the general barometric pressure is comparatively steady, and although the observations were made only on days when the atmospheric conditions were moderately steady, no attempt was made to limit them strictly to days of *exceptional* steadiness. It is reasonable therefore to suppose that a considerable proportion of the apparent residual really represents, not instrumental error, but actual variations of pressure. In any case it is to be noted that the residual, 0.00021 inch, relates to the uncertainty of a *single* observation, and that the probable error of the mean of a series of observations would be considerably less.

It should also be observed that, as regards the determination of pressure in absolute measure, the possible variation of 7 parts in 10^6 in the density of mercury, already referred to, represents a variation of similar amount (5μ)

* See "Annual Report of the National Physical Laboratory for 1927," p. 159.

† Based on 70 intercomparisons between two Fortin standard barometers by seven different observers.

in the height of the mercury column, so that it will be necessary actually to determine the density of the mercury contained in the barometer before any higher accuracy can be attained with certainty in the measurement of absolute pressure.

8. Acknowledgments

In conclusion the authors desire to record their indebtedness to Sir Joseph Petavel, the Director of the National Physical Laboratory, for his interest and valuable suggestions made during the course of the work, to Mr. A. Turner, who worked out many of the details of the design; and to Mr. J. Simmons, whose very careful workmanship on the actual construction of the metal parts of the barometer contributed much to the successful working of the completed instrument.

Summary.

The paper contains an account of a new primary standard barometer recently installed at the National Physical Laboratory to serve as a basis of reference for all measurements relating to barometric pressures.

The body of the instrument is constructed in stainless steel, with optically flat parallel glass windows through which the mercury surfaces are observed. These windows can be removed, if necessary, for cleaning, and the vacuum can be restored by means of suitable pumps whenever the instrument is required for use. The average temperature of the mercury column is ascertained by means of a mercurial thermometer with a bulb 30 inches long, immersed in mercury in a hole bored in the stainless steel body parallel to the barometric column.

Two micrometer microscopes are fixed, one above the other, to a massive vertical column which can be translated laterally so as to view either the mercury surfaces, or the divisions of a standard invar scale set up at the side of the barometer body. The height of each mercury surface is taken to be the mean of two microscope readings, one of the direct image of a horizontal cross wire projected into the space above the mercury, and one of the reflection of this image in the mercury.

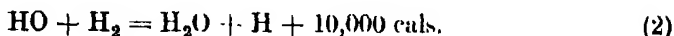
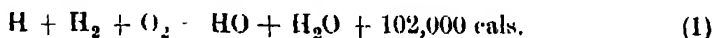
The design and general accuracy of workmanship are such that individual readings should be correct to the order of 0.001 mm. In practice it is found that the mean residual error of a single observation is of the order of 0.005 mm., this being probably attributable in the main to minute fluctuations of barometric pressure which are continually taking place, even when atmospheric conditions are reasonably steady.

The Combination of Hydrogen and Oxygen Photosensitised by Nitrogen Peroxide.

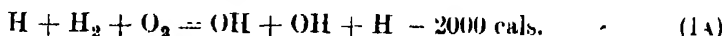
By R. G. W. NORRISH and J. G. A. GRIFFITHS.

(Communicated by Sir William Pope, F.R.S.—Received August 22, 1932.)

The homogeneous reaction between hydrogen and oxygen has been proved by the work of Hinshelwood, of Haber, and of Semenov to be a chain reaction, which under certain conditions of temperature and pressure may pass over into an explosive combination. The reaction is subject to the kinetics characteristic of certain types of chain reactions, in that, for any particular temperature, there are upper and lower pressure limits for explosion, the former controlled by deactivation of the chains in the gas phase, and the latter by their termination at the surface. The conditions further point to a branching chain mechanism; below 300° C. there is no observable propagation of reaction chains. These facts seem to be well represented by the scheme of Bonhoeffer and Haber,* which was put forward on the basis of a spectroscopic study of the dissociation of steam at high temperatures.



reaction (1) sometimes taking the alternative form



which accounts for the branching of the chains. Reaction (2) does not occur appreciably at temperatures below 300° C., but the OH radicals yield hydrogen peroxide which may be detected.

It has been shown that the reaction chains under certain conditions start from the wall of the vessel†; they may, however, also be generated in the homogeneous phase by the artificial introduction of hydrogen atoms, formed in the electric arc,‡ or produced photochemically by the decomposition of ammonia.§ In the latter case, admixture of less than 0.5 per cent. of ammonia

* 'Z. phys. Chem.,' A, vol. 137, p. 263 (1928), 'Z. angew. Chem.,' vol. 42, p. 475 (1929).

† Alyea and Haber, 'Z. phys. Chem.,' B, vol. 10, p. 193 (1930).

‡ Haber and Oppenheimer, 'Z. phys. Chem.,' B, vol. 16, p. 443 (1932).

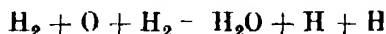
§ Farkas, Haber and Hartek, 'Naturwiss.,' vol. 18, p. 246 (1930); 'Z. Electrochem.,' vol. 36, p. 711 (1930).

(less than 1 mm.) was sufficient to cause explosion above 400° C., when the system was illuminated by short wave-length ultra-violet light. The auto-catalytic character of the reaction, indicating the branching of chains, was also clearly manifest in the considerable induction periods to which the system was subject.

Efforts have been made to initiate reaction artificially by the introduction of oxygen atoms.* There is no theoretical reason why this should not be possible since the reaction

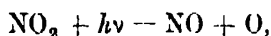


is undoubtedly exothermic, at least to the extent of 4000 cals., while the reaction



is also exothermic by about 15,000 cals. Yet the results recorded in the literature are not conclusive. Haber† throws some doubt on his earlier experiments involving the direct introduction of O atoms from an arc, while efforts to propagate the hydrogen-oxygen chains by the photochemical decomposition of nitrogen peroxide had up to the present not been attended with much success.

Thus, in spite of the fact that the photochemical decomposition of nitrogen peroxide undoubtedly occurs according to the equation



Norrish‡ was unable to record any measurable water formation when 150 mm. of nitrogen peroxide mixed with varying quantities of hydrogen at room temperature were exposed to the full radiation of the mercury lamp, and we have recently confirmed his results for a wide range of pressures of nitrogen peroxide. Similarly, Farkas, Haber and Harteck§ were disappointed in their efforts to use nitrogen peroxide as a photosensitiser for the hydrogen-oxygen reaction. They were indeed able to report a very slight formation of water, both at high temperatures and at room temperature, but the estimated quantum yield of water of 0.01 showed that under their conditions the process was extremely inefficient. Similar results at room temperature were obtained by Schumacher|| for nitrogen peroxide mixed either with hydrogen or with hydrogen

* Harteck and Kopsch, 'Z. Electrochem,' vol. 36, p. 714 (1930).

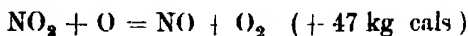
† 'Naturwiss.,' vol. 18, p. 917 (1930).

‡ 'J. Chem. Soc.,' p. 761 (1927).

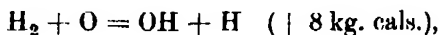
§ 'Z. Electrochem,' vol. 36, p. 711 (1930).

|| 'J. Amer. Chem. Soc.,' vol. 52, p. 2584 (1930).

and oxygen, and both Farkas, Haber and Harteck (*loc. cit.*) and Schumacher (*loc. cit.*) have explained the high inefficiency of the process on the basis of competition between the reactions



and



the former of which, according to Schumacher, probably occurs some 10^4 times more readily than the latter.

Thus although, photochemically, nitrogen peroxide is to be regarded as a source of oxygen atoms, it acts also as an inhibitor in the photosensitised reaction by removing these atoms.

These results are remarkable in view of the existence of a strong thermal catalytic effect of nitrogen peroxide. Thompson and Hinshelwood* have shown that in its presence the explosion of hydrogen and oxygen takes place at temperatures at which they alone are almost completely inert to one another, provided that the concentration of nitrogen peroxide lies in a narrow range between two critical values.

It seemed to us likely that there might be a much closer connection than had previously been supposed between the condition of thermal and photochemical sensitisation of the explosion by nitrogen peroxide, and in the experiments which follow, this view is found to be fully justified.

So far as the thermal data are concerned, our results, in general, support those of Thompson and Hinshelwood. The same sharp upper and lower limits of concentration of nitrogen peroxide were found. In our investigation, however, no explosions were obtained until about 480°C. , the explosions found by Thompson and Hinshelwood at the lower temperatures being replaced by a very rapid but measurable reaction.

This difference in our results, which as is described later was ultimately removed when a small change was made in the dimensions of the reaction vessel, was singularly fortunate from our point of view, since it has made possible a closer kinetic study of the reaction in comparison with the photosensitised reaction—which we have found to occur—than would otherwise have been possible.

When, without other variation of the conditions, the contents of the reaction vessel were submitted to irradiation with light from a mercury vapour lamp an immediate increase in the reaction velocity was observed. In this way we

* · Proc. Roy. Soc. 'A. vol. 124, p 219 (1929).

discovered the optimum conditions of photochemical sensitisation which had previously escaped the notice of other workers. As will be seen the sensitised reaction is subject to precisely the same limits as the thermal reaction, and its nature is such as to leave no doubt that an effect which is already present in the thermal reaction is being enhanced photochemically.

Experimental

The general method of experimentation adopted was similar to that already described by one of us.* The reaction vessel, A, fig. 1, was of quartz, cylindrical in shape and of 150 c.c. capacity. It was connected via a tap to a vertical mercury manometer, M, and to the gas supply tube by ground joints. The reaction vessel was heated in a cylindrical electric furnace F, closed at one

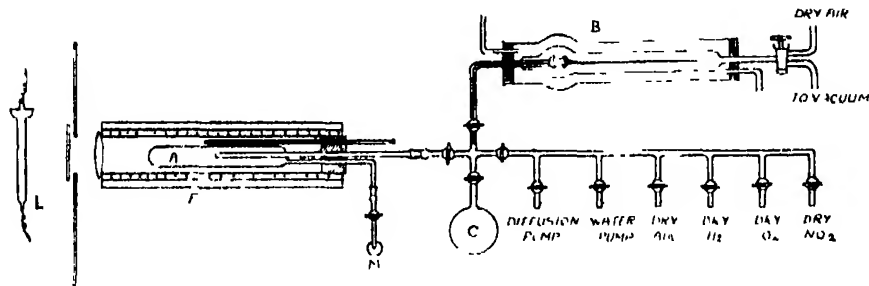


FIG. 1.

end by a quartz lens which focussed light from the mercury vapour lamp L into the reaction vessel. The apparatus could be evacuated first by a water pump and subsequently by a mercury diffusion pump backed by a Toepler pump. The nitrogen peroxide, oxygen, and hydrogen were introduced separately in the order given, the mercury manometer having been previously filled with oxygen at the required pressure to act as a buffer against the nitrogen peroxide. The inlet tube for the gases projected along the axis past the centre of the bulb to ensure adequate mixing. The reaction vessel was also connected with a sensitive Bourdon gauge B in order to measure with precision the pressure of nitrogen peroxide admitted, and also to follow accurately the velocity of combination of the hydrogen and oxygen at temperatures where it proceeded very slowly. The gauge was thermostatted by water at room temperature, and after admitting the nitrogen peroxide, the pressure of oxygen and hydrogen admitted to the system was balanced by admitting air to the outer chamber. When used to measure the pressure of nitrogen peroxide,

* Norrish, 'Proc. Roy. Soc.,' A, vol. 135, p. 334 (1932).

or to follow the course of the reaction, the deflection of the gauge pointer was measured by a microscope with a scale in the eyepiece. In this way pressure changes could be accurately measured to within 0.003 mm. Hg.

The investigations were carried out up to 500° C., the temperature of the furnace being regulated by a variable resistance adjusted by hand, and read by mercury thermometers. It was found possible to achieve thermostatic control to $\pm 0.5^\circ \text{C}$ by this means.

Steady Reaction Catalysed both Thermally and Photochemically After regulation of the furnace to the appropriate temperature, during which the reaction vessel was pumped out to a pressure of less than 10^{-5} mm., the gases were added and the course of the reaction immediately followed, if slow, by the Bourdon gauge, or if fast, by means of the mercury manometer. Thus at 302° C. the pressure changes were followed on the gauge, while at 450° C. the mercury manometer had to be used. During a given experiment the speed of the reaction was alternately measured in the dark and the light by raising and lowering a screen in front of the lamp. In this way, using a constant pressure of a mixture of $(2\text{H}_2 + \text{O}_2)$, pairs of points were obtained for each temperature and pressure of nitrogen peroxide used, these represent respectively the thermal sensitised and the sum of thermal and photosensitised reaction velocities. In fig. 2 are shown specimens of the types of curves

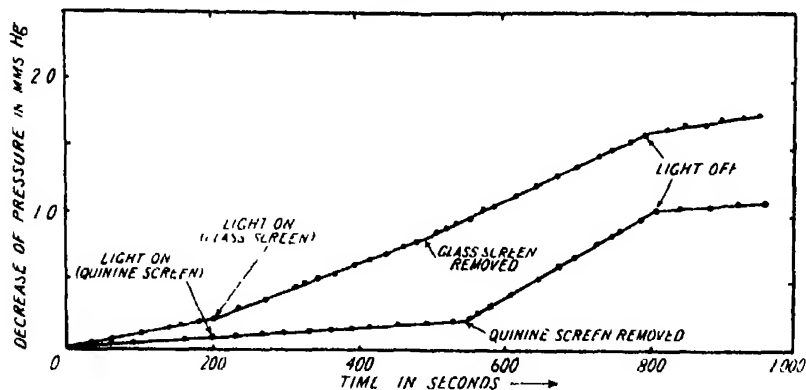
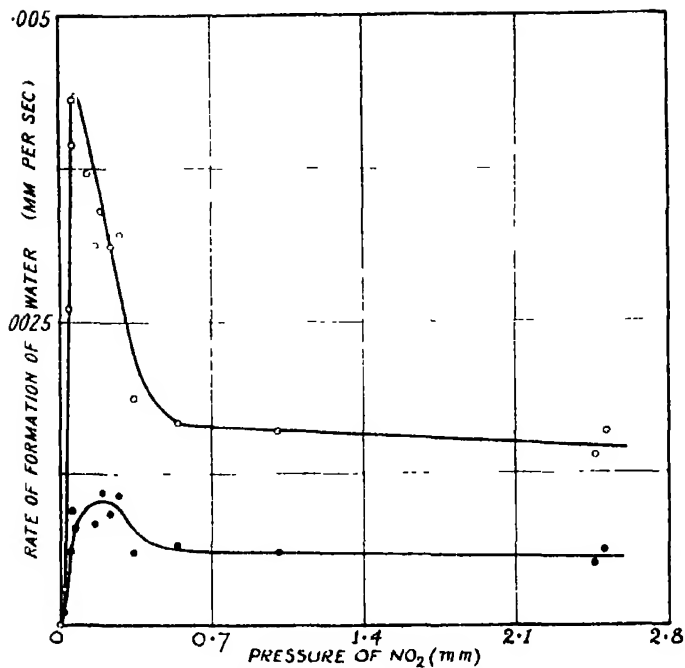


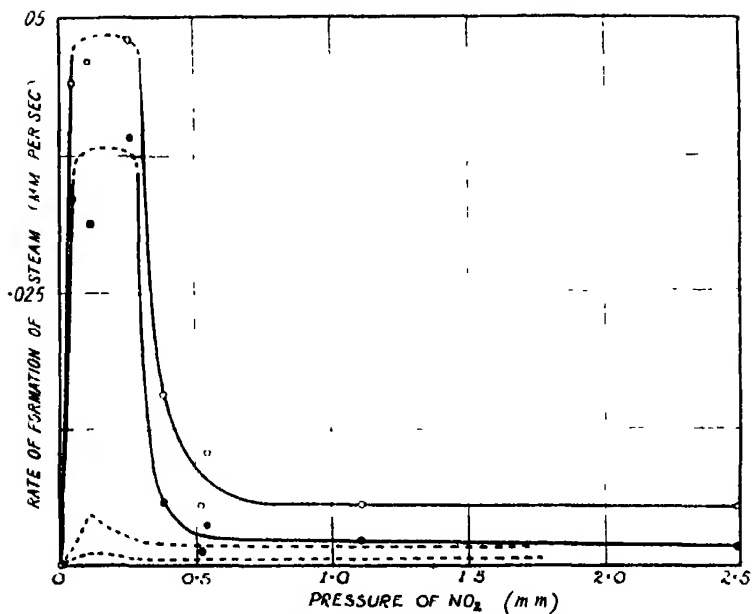
Fig. 2.

obtained. For each particular temperature, a series of pressures of nitrogen peroxide* was taken and in this way the curves shown in figs. 3, 4, 5 and 6

* The pressures of nitrogen peroxide given in the figures are the actual values calculated from the observed pressure of "nitrogen peroxide" and allowing for the dissociation of the peroxide in the presence of 50 mm. of oxygen; the dissociation constants given by Bodenstein and Lindner (*loc. cit.*) were used.

FIG. 3. -302°C . 100 mm. H_2 , 50 mm. O_2 .

○ Reaction in light ● Reaction in dark.

FIG. 4.— -357°C . 100 mm. H_2 , 50 mm. O_2 .

○ Reaction in light ● Reaction in dark.

were derived. All of the velocities recorded were obtained while the pressure of the steam produced was less than 10 mm.

It will be noted that at all temperatures investigated there was a range of pressure of nitrogen peroxide within which the formation of water was markedly catalysed. This range was very sharply bounded at the lower pressure limit, but somewhat less sharply at the upper limit. As the pressure of nitrogen peroxide was increased the reaction never completely disappeared, but in its

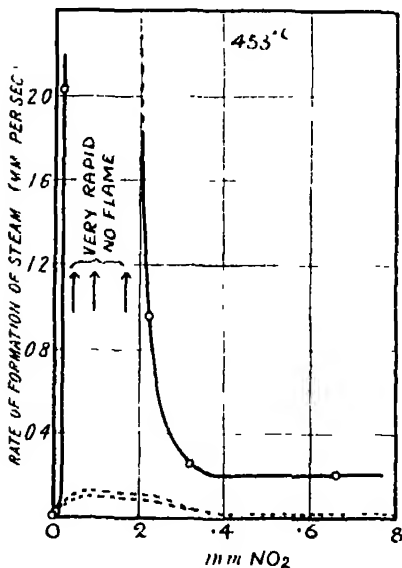


FIG 5.

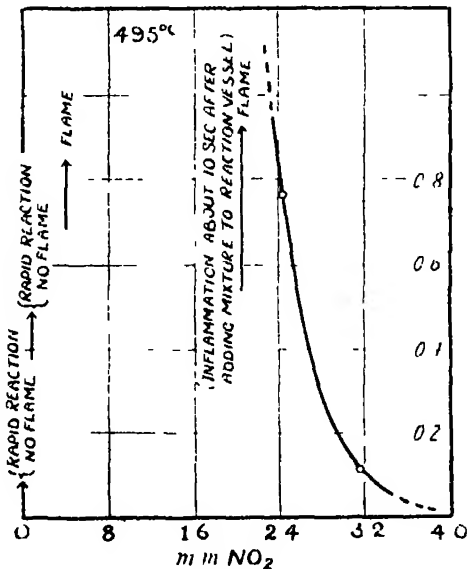


FIG 6

absence up to temperatures of 453° C. there was no detectable change going on.

At the lower temperatures there was a sharp photochemical effect, which was strictly bounded by the same limits as the thermal effect. This is well seen in the curve for 302° C.; here, under optimum conditions of 0.2 mm nitrogen peroxide the velocity was increased some fourfold. As the temperature was increased, both the thermal and photochemical effects were immensely augmented. Thus at 357° C the thermal reaction under optimum conditions was increased some thirty-fold over that at 302° C. The ratio of the photochemical effect to the thermal effect, however, decreased as the temperature was raised, and finally the photochemical effect at 453° C. could not be detected in comparison with the extremely fast thermal reaction. At this temperature the threshold of inflammation appeared to be reached, for at the optimum pressure of nitrogen peroxide (about 0.4 mm.) the gases reacted as fast as

the oxygen could be added. In the absence of nitrogen peroxide, however, there was no detectable reaction. At 495° C. flame or explosions were obtained, but these ceased as the pressure of nitrogen peroxide was increased beyond 10 mm. though in this case no lower limit of nitrogen peroxide could be observed. Essentially similar results to those described above were obtained at all of the temperatures investigated when the three gases were mixed in an auxiliary store bulb C, fig. 1, at room temperature and added rapidly to the hot reaction vessel via taps of wide bore.

Explosion Catalysed Thermally.—There remained the discrepancy, referred to above, between our results and those of Thompson and Hinshelwood (*loc. cit.*), who observed explosion between much the same limits of pressure of nitrogen peroxide as we obtained for the rapid catalysed reaction at similar temperatures. This discrepancy finally disappeared when we removed the internally sealed tube from the axis of our reaction vessel, for with the apparatus so modified we obtained results fully consistent with those of the earlier workers.

In these experiments the mixture of gases was so prepared, at room temperature in the vessel C, that on admitting the mixture rapidly to the reaction vessel at 351° C., the pressures of hydrogen and oxygen were 100 mm. and 50 mm., respectively, and the pressures of nitrogen peroxide were as recorded. (These pressures of nitrogen peroxide here represent the total ($\text{NO}_2 + \text{NO}$) formed by dissociation in the reaction vessel. At 351° C., approximately 30 per cent. of the nitrogen peroxide was dissociated in the presence of 50 mm. of oxygen.)

Table I —Temperature 351° C.

Number of experiment	Observed pressure of "nitrogen peroxide" (mm.)	Rate of formation of water (mm. per sec.).		Comments
		In dark	In light	
100	0.04	0.0012	0.002	
105	0.266	0.0024	0.017	--
91	0.308	Immediate explosion		
92	0.36	Immediate explosion		
96	0.411	Immediate explosion		
95	0.414	Delayed explosion		Induction period 150 seconds (no illumination).
93	0.42	Delayed explosion		Induction period (90 seconds in dark, plus 8 seconds illumination).
97	0.422	Immediate explosion		--
94	0.438	0.0094	0.032	No explosion
106	0.49	0.0034	0.0085	

The lower explosion limit is therefore determined by a critical pressure of nitrogen peroxide between 0.266 and 0.308 mm while the upper limit is realised with 0.41–0.42 mm. of nitrogen peroxide. These points fall reasonably on the curves of Thompson and Hinshelwood (*loc cit*), whilst they are bracketed by the limits of the rapid non-explosive reaction described by us. Similar explosions were obtained at 360° C. and 400° C. though in view of the general similarity with the results of Thompson and Hinshelwood no attempt was made further to determine the critical limits of nitrogen peroxide at these temperatures.

The explosion is thus revealed as dependent either on the internal shape or total surface of the reaction vessel. In the absence of further evidence, we prefer to assume that the conditions of chain propagation are partly controlled by surface deactivation, as has already been found by Hinshelwood and Thompson,* and Gibson and Hinshelwood† in the uncatalysed reaction between hydrogen and oxygen.

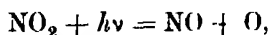
In two experiments recorded in Table I induction periods of some considerable length were noted before explosion occurred in the thermal reaction. It appears that the induction period is shortened by illumination, but in view of the fact that the phenomenon proved difficult to control the point could not be established with certainty. These results recall the similar induction periods obtained by Farkas, Haber and Harteck (*loc. cit.*) for the explosion photosensitised by ammonia, and cited by them as evidence for the autocatalytic character of the reaction.

It seems to be clear that between certain sharp limits of pressure, nitrogen peroxide brings about a strong catalysis of the hydrogen-oxygen reaction, but that there is also an inhibiting effect which becomes predominant beyond the upper limit of pressure. The catalysis is strongly enhanced by illumination of the system by visible light and by light in the near ultra-violet part of the spectrum, and the fact that the thermal and photochemical effects are confined to the same limits of pressure of nitrogen peroxide suggests that they operate essentially by the same mechanism. In view of these facts it may be concluded that the catalytic function of the nitrogen peroxide both thermally and photochemically lies in the provision of centres which constitute the starting-point of the reaction chains, while its inhibitive function is to be ascribed to a simultaneous deactivating influence on the reaction chains, which ultimately becomes predominant as its pressure increases.

* 'Proc. Roy. Soc.,' A, vol. 118, p. 170 (1928)

† *Ibid.*, p. 591.

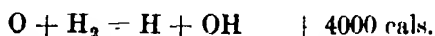
Mechanism of Initiation of Reaction Chains by Nitrogen Peroxide.—A further investigation of the photochemical effect described above, with reference to wave-length, makes possible a decision as to the nature of the reaction centres initiating the chains in the photochemical change. It is now well known that nitrogen peroxide is dissociated photochemically according to the process



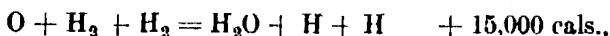
and that there is a sharp photochemical threshold between 436 $\mu\mu$ and 405 $\mu\mu$.* It is possible to separate these two lines of the mercury spectrum by using as a colour filter a 4 per cent. solution of quinine hydrochloride 1 cm. thick, enclosed between glass plates, only the lines of wave-length 436 $\mu\mu$ and longer are then transmitted. Such a filter was used and the results, shown in the graph of fig. 2, demonstrated clearly that light transmitted by the quinine hydrochloride, though strongly absorbed by the nitrogen peroxide, is ineffective within the limits of experimental error. On the other hand the effect is strong in light transmitted by glass plates. It is thus proved that there is a photochemical threshold lying between 436 $\mu\mu$ and 365 $\mu\mu$ which undoubtedly corresponds to the threshold for simple photochemical dissociation of the nitrogen peroxide referred to above. We may therefore take it as established that the oxygen atoms generated photochemically form starting-points for the reaction chains, and that photo-activated as distinct from photo-dissociated nitrogen peroxide is not catalytically active.

General Theoretical Discussion

From these photochemically produced oxygen atoms the Haber chains could readily be generated by either of the reactions



or



which give rise to hydrogen and hydroxyl in the system.

It will be well, however, in attempting to develop a kinetic expression for the process to proceed independently of any particular mechanism of chain propagation. This can be done by means of the conception of the reaction centre, which passing periodically through a series of reactions constitutes the chain. If the concentration of the reactants be maintained constant the

* Dickinson and Baxter, 'J. Amer. Chem. Soc.', vol. 50, p. 774 (1928); Norrish, 'J. Chem. Soc.', p. 1158 (1929)

momentary rate of reaction is proportional to the concentration $[n]$ of these reaction centres, i.e.,

$$d[\text{H}_2\text{O}]/dt = k[n]$$

Now for the pure photochemical reaction these centres are generated from the oxygen atoms in their collision with hydrogen molecules and by the branching of chains, according to the Haber scheme already given

We may thus write

$$dn/dt = k_1[\text{O}] \cdot [\text{H}_2] + k_2[n], \quad (1)$$

where k_2 represents the branching factor.

At the same time, the retarding influence of the nitrogen peroxide is exerted on the chains, so that centres may be assumed to be destroyed by (a) adsorption on the wall, (b) reaction with nitrogen peroxide.*

This gives

$$-dn/dt = k_3[n]S + k_4[n][\text{NO}_2], \quad (2)$$

where S is proportional to the area of deactivating surface.

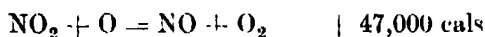
For a stationary velocity, such as we observed

$$dn/dt = -dn/dt \quad (3)$$

and hence

$$n = k_1[\text{O}][\text{H}_2]/(k_3S + k_4[\text{NO}_2] + k_2). \quad (4)$$

In evaluating the concentration of oxygen atoms, $[\text{O}]$, we remember the strong affinity of the reaction

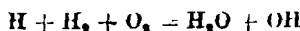


Thus we may write for the rates of reaction at low concentrations of nitrogen peroxide, where the light absorbed is proportional to the pressure,

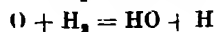
$$+d[\text{O}]/dt = k_0[\text{NO}_2] \quad (5)$$

$$-d[\text{O}]/dt = k_5[\text{NO}_2][\text{O}] + k_1[\text{H}_2][\text{O}]. \quad (6)$$

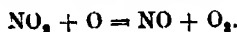
* On the basis of the recent suggestion of Haber and Oppenheimer ('Z. phys. Chem. B, vol. 16, p. 443 (1932)) that the reaction



may be split into two consecutive reactions



the effect of the NO_2 terminating the chains is easily explained by the reaction



And thus at equilibrium

$$[O] = k_0 [NO_2] / (k_5 [NO_2] + k_1 [H_2]). \quad (7)$$

This gives

$$n = \frac{k_1 k_0 [NO_2] [H_2]}{(k_3 S + k_4 [NO_2] - k_2) (k_5 [NO_2] + k_1 [H_2])} \quad (8)$$

and

$$\frac{d[H_2O]}{dt} = \frac{kk_1 k_0 [NO_2] [H_2]}{(k_3 S + k_4 [NO_2] - k_2) (k_5 [NO_2] + k_1 [H_2])}. \quad (9)$$

Since the concentrations of hydrogen and oxygen are kept constant, this reduces to :

$$\frac{d[H_2O]}{dt} = \frac{k' [NO_2]}{(k_3 S + k_4 [NO_2] - k_2) (k_5 [NO_2] + k')} \quad (10)$$

This expression is capable of giving curves of the same type as those observed experimentally. It is of the form

$$y = x/(x + a)(x + b).$$

For a particular temperature "b" is constant, since k' (equation (10)) is constant, while "a" may have positive or negative values according as the surface factor $k_3 S$ is greater or less than the branching factor k_2 . Thus, any circumstance such as increase of temperature which brings about an increase in k_2 , or any diminution of $k_3 S$ such as that effected, in our case, by removing the central tube from the axis of the reaction vessel, will diminish the constant "a," or make it negative

Fig. 7 represents a family of curves all corresponding to a particular temperature, obtained by varying "a" and giving to "b" a constant value of 0.1. If we take a particular value of y (velocity of water formation, represented by AB in fig. 7), as corresponding to explosion,* it is seen that there are three possibilities :—

- (1) There may be no explosion, but only a maximum velocity, as obtained at the lower temperatures indicated (Curves IV, V and VI, fig. 7.) Compare figs. 3 and 4.
- (2) There may be an upper and lower pressure limit as obtained by Thompson and Hinshelwood, and confirmed by us when the total internal surface of our reaction vessel was decreased. (Curve III, fig. 7.)

* This view assumes that when the velocity of the homogeneous chain reaction exceeds a limiting value, the process becomes approximately adiabatic, since the heat of reaction is produced more rapidly than it can be conducted away. In this way the temperature of the system rises very rapidly and inflammation occurs.

- (3) There may be an upper limit but no lower limit, corresponding to a negative value of " a " as obtained by us at 495° (Curves I and II, fig. 7.) Compare fig. 6.

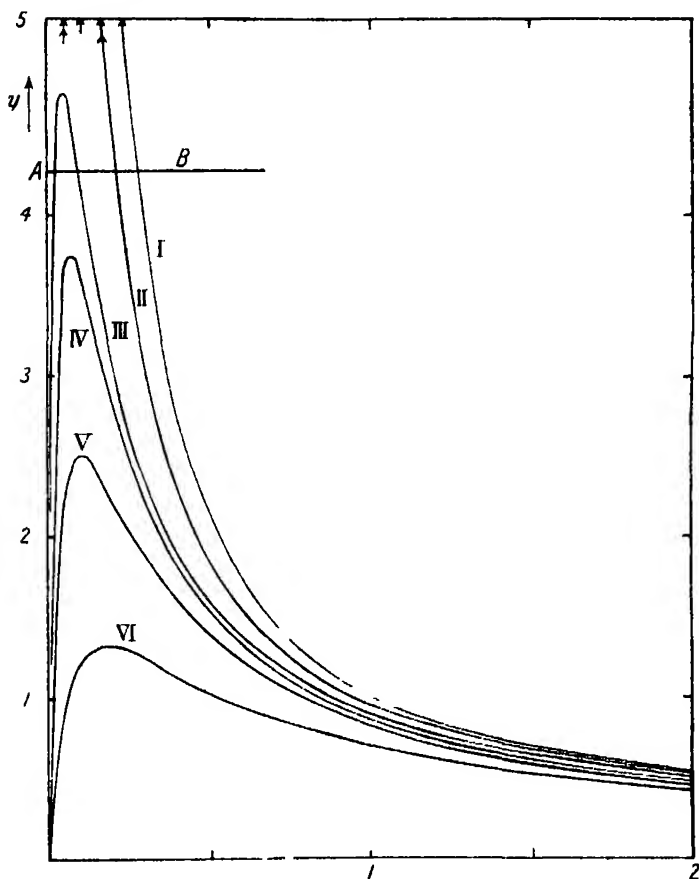


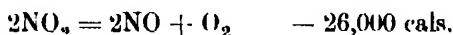
FIG 7.—Graph of function $y = \frac{x}{(x + 0.1)(x + a)}$

I	$a =$	0.1	IV	$a =$	0.04
II		0.05	V		0.1
III		0.02	VI		0.3

These different possibilities have all been realised, and it may be claimed that in all respects equation (10) is capable of a satisfactory description of the results obtained, both in our work and that of Thompson and Hinshelwood.

The parallelism between the photochemical and the thermal effects has been fully brought out in the experimental curves. It is apparent that for a given temperature the maxima in the velocity curves occur at the same pressures of nitrogen peroxide and between the same pressure limits. An equation of

exactly the same form as (9) and differing from it only in the magnitude of k_0 , which defines the speed of generation of oxygen atoms will therefore represent the thermal results. All the other constants remain the same. This being so, since we must accept oxygen atoms as the source of chains in the photochemical change, we cannot escape the conclusion that they are also the source in the thermal reaction, and it is then apparent that the catalytic function of the nitrogen peroxide lies in its power to act as a source of oxygen atoms. The origin of these oxygen atoms in the photochemical decomposition of nitrogen peroxide is reasonably well understood, their origin in the thermal change is more obscure. It has always been supposed that when nitrogen peroxide decomposes it does so by a bimolecular collision

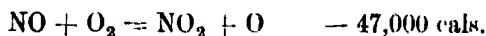


We might now conclude that part of this change—though it may be only a small part—is a process involving the separation of oxygen atoms :

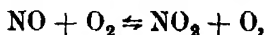


as has been suggested by Schumacher.*

This process, however, would require an energy of activation of at least 70,000 cal., and in measurements of the speed of the dissociation of nitrogen peroxide would be completely undetectable in comparison with the bimolecular decomposition which occurs with an activation of 26,000 cal. Data do not yet exist by which we can test the adequacy of this process to supply the oxygen atoms required for the thermal reaction, and the question must be left undecided for the present. On the other hand, we would draw attention here to at least one other process which is quite possibly a readier source of oxygen atoms than the direct dissociation of nitrogen peroxide envisaged by Schumacher, namely, the reaction



Since this heat of reaction of $-47,000$ cal. is much smaller than the $-70,000$ cal. of the former process, and the respective activation energies therefore quite possibly differ by about 20,000 calories, the latter reaction would appear to have the greater probability. If this is conceded, the thermal catalysis of the hydrogen-oxygen explosion is seen to be dependent on the equilibrium



* 'Nature,' 126, p. 132 (1930), 'Z. phys. Chem.,' B, vol. 10, p. 7 (1930).

the forward reaction controlling the initiation of the chains and the backward reaction their termination.

It is therefore possible that nitric oxide is the true catalyst in the thermal reaction, whilst nitrogen peroxide is an inhibitor, though in the photochemical process, the nitrogen peroxide assumes the rôle of photocatalyst as well, and acts as a source of oxygen atoms.

This conclusion is not out of harmony with the kinetics developed above, for in the presence of a large excess of oxygen the law of mass action leads to the relationship

$$[\text{NO}]/[\text{NO}_2] = \text{Const.}$$

Thus, the speed of generation of O atoms which has been taken for the thermal reaction as proportional to the concentration of nitrogen peroxide (see equation (9)) is equally well represented as proportional to the concentration of nitric oxide without alteration of the validity of the theoretical equation.

Acknowledgments.

Our acknowledgments are due to the Royal Society and the Chemical Society for research grants which defrayed part of the cost of this investigation, and to the Department of Scientific and Industrial Research for the award of a Research Assistantship to one of us.

Summary.

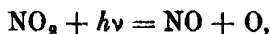
(1) A further study of the reaction between hydrogen and oxygen catalysed by small quantities of nitrogen peroxide has been made at temperatures between 300° C and 500° C and the general results of Thompson and Hinshelwood (*loc. cit.*) confirmed.

The sharp limits of pressure of nitrogen peroxide which in their work defined the explosive reaction, were found in our case to bound a region of strong catalysis exhibiting measurable reaction velocity, inflammation was not obtained till a temperature of 495° C., as compared with 370° C. in the earlier work, had been reached. When the internal surface (surface/volume ratio) of the reaction vessel was diminished, explosion limits similar to those observed by Thompson and Hinshelwood were found at temperatures as low as 350° C. The velocity of the slow combination which occurs outside the limits of rapid or explosive reaction was determined

(2) Under conditions where measurable velocities were obtained the reaction was found to be photochemically sensitive, for on exposure of the reaction

vessel to the rays of a mercury vapour lamp the thermal effect was magnified some fourfold at 300° C., and some twofold at 360° C. ; as the temperature was raised still further the thermal velocity increased greatly until at 450° C. the photochemical effect was not detectable in comparison.

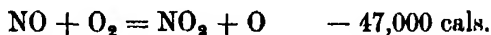
(3) The photochemical catalysis was found to be subject to the same wavelength threshold as the simple photochemical decomposition of nitrogen peroxide,



and it is therefore concluded that oxygen atoms form the starting-point of the reaction chains for the photosensitised reaction.

(4) The photochemical effect is subject to exactly the same limits of pressure of nitrogen peroxide as the thermal catalysis and this is taken as evidence that in the latter also the function of the nitrogen peroxide is to provide atoms of oxygen as the starting-point of the reaction.

(5) A kinetic mechanism has been developed on the basis of the Haber theory of the hydrogen-oxygen explosion, involving the starting of reaction chains on atoms of oxygen and their termination either at the surface or on molecules of nitrogen peroxide. This mechanism explains the form of all the results obtained up to the present time. Photochemically the atoms of oxygen result from the direct dissociation of the nitrogen peroxide. Thermally their origin is more uncertain, but it is considered that the reaction



is more probable than the reaction



as their source.

Applications of the Method of Impact Parameter in Collisions.

By E. J. WILLIAMS, Manchester University.

(Communicated by R. H. Fowler, F.R.S.--Received August 25, 1932 Revised November 7, 1932).

In the application of quantum mechanics to collisions the method of impact parameter has been largely neglected in favour of the more statistical method put forward by Born in 1926. This is mainly because the method of impact parameter is not applicable to all kinds of collisions. It affords, however, a valid treatment of *light* collisions in which the momentum transfer is small compared with the momentum of the primary particle, and its application in these cases proves very fruitful. We shall deal, in this paper, mostly with the problems which eminently lend themselves to treatment by this method and which have not been previously considered. One of these is the spatial distribution with respect to the path of the particle of the atoms ionised and excited by it. The results obtained in this respect show the existence of a radius of action characteristic of the velocity of the particle, and they answer the question of the extent to which the observation of an ionised or excited atom determines the position of the responsible particle. Another problem dealt with is the connection between the perturbation of distant atoms by the field of a moving particle and the perturbation of atoms by radiation—one which bears intimately on the theory of the loss of energy by electric particles put forward by Fermi in 1924.* The problem of the relativity effect in light collisions is also fully discussed, the quantum-mechanical relativity corrections to the primary ionisation and loss of energy in light collisions being deduced. These corrections were put forward by the writer some time ago, and compared with experiment.† Very recently, however, the problem was considered by Bethe,‡ and Møller,§ on the basis of Born's theory, and they arrive at the same results. A feature of the use of the method of impact parameter in this problem, as indeed in others, is that the general physical reasons for the results obtained are readily apparent.

The paper is arranged as follows. For the purpose of the subsequent applications § 1 is devoted to theorems dealing with the perturbation of atoms

* 'Z. Physik,' vol. 29, p. 315 (1924).

† 'Proc. Roy. Soc.,' A, vol. 130, p. 328 (1931); vol. 135, p. 108 (1932)

‡ 'Z. Physik,' vol. 76 (1932).

§ 'Ann. Physik,' vol. 14, p. 531 (1932).

by certain special types of forces, the results obtained forming convenient summaries of some of the requirements of quantum mechanics. § 2 deals with the non-relativity loss of energy in distant collisions, a problem considered by Gaunt* in the only previous application of the method of impact parameter using quantum mechanics. In his calculations Gaunt deals directly with the resultant perturbing force due to the moving particle. In the present calculations we resolve the perturbing force into perpendicular components, and then consider the effects of these separately. This greatly simplifies the problem, and follows closely the classical treatment of the problem by Bohr.† By adopting this procedure the result obtained by Gaunt after somewhat lengthy calculation is readily obtained. § 3 deals with the relativity effect in light collisions, and § 4 with the connection between the theory of collisions put forward by Fermi and quantum mechanics. § 5 deals with the lateral distribution in space of the atoms ionised and excited by a moving particle, and also discusses the general physical reasons for the relativity corrections deduced in § 3.

§ 1. Let us consider a hydrogen atom in the ground state at $t = 0$, and let $u(1)$ be the proper function describing this state. Let $V(t, xyz)$ be a perturbing potential lasting from $t = 0$ to $t = T$. Then according to quantum mechanics, if the perturbation is small, the probability $P(s)$ that at the end of the perturbation the atom is in a new state represented by the proper function $u(s)$, (s summarising the various quantum numbers which characterise the state) is

$$P(s) = (4\pi^2 e^2 / h^2) \left| \int_0^T V(t, xyz) e^{2\pi i \nu s t} u(1) \bar{u}(s) d\tau dt \right|^2 \quad (1)^\ddagger$$

ν_s is the frequency corresponding to the transition $u(s) \rightarrow u(1)$ and is equal to $(W(s) - W(1)) / h = Q/h$, where $W(s)$ is the proper value of the state s , and Q is the energy transfer to the atom. If s is a state in the continuous spectrum then $P(s) dW$ is the probability that the atom is excited to the states s with total energy between W and $W + dW$.

An electric force varying with the time implies the existence of magnetic forces. The effect of these magnetic forces is generally small and of a secondary nature, and equation (1), which neglects them, is accurate enough in all the cases to which it is applied in this paper.

* 'Proc. Camb. Phil. Soc.', vol. 23, p. 732 (1927).

† 'Phil. Mag.', vol. 25, p. 10 (1913), and vol. 30, p. 581 (1915).

‡ Cf. Dirac, 'Quantum Mechanics,' equation (19), p. 166.

The following special types of perturbation will now be considered.

Case (a).—Time T , for which the perturbation lasts satisfies $T \ll 1/\nu_e$.

In this case the variation of $e^{2\pi i \nu_e t}$ during the perturbation is negligible. It can therefore be taken outside the integral in (1) and we have

$$\begin{aligned} P(s) &= (4\pi^2 e^2 / h^2) |e^{2\pi i \nu_e t}|^2 \left| \int_0^T \int V(t, xyz) u(1) \bar{u}(s) d\tau dt \right|^2 \\ &= (4\pi^2 e^2 / h^2) \left| \int A(xyz) u(1) \bar{u}(s) d\tau \right|^2, \end{aligned} \quad (2)$$

where

$$A(xyz) = \int_0^T V(t, xyz) dt. \quad (3)$$

We see that as far as the perturbing potential is concerned its effect depends only on its time-integral, and its actual variation with the time is immaterial. Since the time-integral of the potential is determined by the time-integral of the component forces it follows that the effect of the perturbation under the conditions of this case is also completely determined by the time-integral of the component forces.

Case (b). $-T \ll 1/\nu_e$, as in case (a). Components F_1, F_2, F_3 of perturbing force, F , satisfy $\int F_2 dt = \int F_3 dt = 0$, $\int F_1(t, xyz) dt = I/e$, where I is independent of x, y, z , e = electronic charge.

This is the case of a sudden force applied to the atom such that the time-integral of the force is uniform over the atom. The conditions do not necessarily require the force at any instant to be uniform over the atom. Since $T \ll 1/\nu_e$ the results of (a) apply. (3) of that section, however, simplifies as follows

$$e A(xyz) = e \int V(xyz, t) dt = e \int_0^x \int_0^T F_1(x'yz, t) dx' dt = \int I dx' = Ix + V_0,$$

therefore

$$\begin{aligned} P(s) &= (4\pi^2 / h^2) \left| \int (Ix + V_0) u(1) \bar{u}(s) d\tau \right|^2 \\ &= (4\pi^2 / h^2) I^2 \left| \int x u(1) \bar{u}(s) d\tau \right|^2 = (4\pi^2 / h^2) I^2 |x_{1s}|^2, \end{aligned} \quad (4)$$

x_{1s} is the x -co-ordinate matrix for spontaneous transition from state s to the ground state. Let $|x_{1s}|^2$ denote the summation of $|x_{1s}|^2$ over all the states

with the same proper energy $W(S)$. Then the probability that the perturbed atom acquires energy $W(S) - W(1)$ is

$$P(S) = (4\pi^2/h^2) I^2 |x_{1s}|^2. \quad (5)$$

The total energy acquired by the atom is therefore

$$\bar{Q}_q = (4\pi^2/h^2) I^2 (\Sigma + \int) |x_{1s}|^2 (W(S) - W(1)). \quad (6)$$

The sign \int indicates summation over the states in the continuous spectrum. The summations concerned are involved in the theory of the dispersion and scattering of radiation, and are also dealt with by Bethe in his application of Born's theory of collisions. From these treatments we find

$$(\Sigma + \int) |x_{1s}|^2 (W(S) - W(1)) = h^2/8\pi^2 m, \quad (7)$$

so that

$$\bar{Q}_q = I^2/2m. \quad (8)$$

This is also the energy that would be acquired by a classical free electron. We thus arrive at the simple result that if a sudden impulse is applied to an atomic electron the average energy acquired by it according to quantum mechanics is equal to the energy which would be acquired by a classical free electron. The equivalence is, of course, only statistical. We are dealing with small perturbing forces and the average transfer \bar{Q}_q is much less than the smallest possible finite transfer that can take place. The latter corresponds to the first resonance potential, and for atomic hydrogen is equal to $\frac{3}{2}J$ where J is the ionisation potential.

It is interesting to consider the probability that the atom is left undisturbed by the applied impulse. This probability is $P(1) = 1 - (4\pi^2/h^2) I^2 (\Sigma + \int) |x_{1s}|^2$. From the theory of the Compton effect we find that

$$(\Sigma + \int) |x_{1s}|^2 = h^2/8\pi^2 mJ.*$$

We therefore have

$$P(1) = 1 - (4\pi^2/h^2) (I^2 h^2/8\pi^2 mJ) = 1 - I^2/2mJ = 1 - \bar{Q}_q/J. \quad (9)$$

* From Sommerfeld, "Wave Mechanics," p. 221,

$$(\Sigma + \int) \left| \int e^{i\alpha\tau} u(1) \bar{u}(s) d\tau \right|^2 = 1 - (1 + h^2 \alpha^2/32\pi^2 mJ)^{-4}.$$

Now $\lim_{\alpha \rightarrow 0} e^{i\alpha\tau} = 1 + i\alpha\tau$, retaining 1st order terms. Therefore

$$\alpha^2 (\Sigma + \int) \left| \int x u(1) \bar{u}(s) d\tau \right|^2 = \lim_{\alpha \rightarrow 0} \{1 - (1 + h^2 \alpha^2/32\pi^2 mJ)^{-4}\} = h^2 \alpha^2/8\pi^2 mJ.$$

Dividing by α^2 we have $(\Sigma + \int) |x_{1s}|^2 = h^2/8\pi^2 mJ$.

We may call this the probability of an "elastic" encounter. The probability of an inelastic encounter—resulting in excitation or ionisation—is

$$1 - P(1) = \bar{Q}_e/J. \quad (10)$$

This result means that the average transfer per inelastic encounter is J . The actual distribution about this average of the energy transfers in the inelastic encounters may be obtained from the variation of $|x_{1s}|^2$ with S . We find that $|x_{1s}|^2$ is inappreciable except for v_s close to J/h , so that the energy transfers are concentrated close to J . Actually 41 per cent. of the total energy transfer goes to excite the second energy level for which $Q = \frac{3}{2}J$, 14 per cent. to excite the other discrete levels, and the remaining 45 per cent. in ionisation. In the ionising encounters the probability $\phi(Q)$ of energy transfer, Q , falls off very rapidly with increasing Q , and the total transfer in encounters with Q greater than about $2J$ is insignificant. This result is of importance in connection with the basic assumption that the time of perturbation, T , satisfies $T \ll 1/v_s$. The summation in (6) is over all the continuous spectrum and theoretically extends to indefinitely large values of v_s . $v_s = Q/h$, and the insignificant energy loss in encounters with $Q \gg J$ therefore means that only values of v_s of the order of J/h are of importance. It follows, therefore, that the result (8) is valid provided $T \ll h/J$.

Case (c).—Perturbing force uniform over the atom. Not necessarily true that $T \ll 1/v_s$

Let the force be $F(t)$ parallel to the x axis. Then $V(t, xyz) = V_0 + F(t)x$, and (1) becomes

$$\begin{aligned} P(s) &= (4\pi^2 e^2/h^2) \left| \int_0^T F(t) e^{2\pi i v_s t} x u(1) \bar{u}(s) dt d\tau \right|^2 \\ &= (4\pi^2 e^2/h^2) \left| \int_0^T F(t) e^{2\pi i v_s t} dt \right|^2 \left| \int x u(1) \bar{u}(s) d\tau \right|^2 \\ &= (4\pi^2 e^2/h^2) \left| \int_0^T F(t) e^{2\pi i v_s t} dt \right|^2 |x_{1s}|^2. \end{aligned} \quad (11)$$

This case has already been considered by previous writers,* the same result as (11) being given. The probability of the excitation of any state with proper energy $W(S)$ is

$$P(S) = (4\pi^2 e^2/h^2) \left| \int_0^T F(t) e^{2\pi i v_s t} dt \right|^2 |x_{1s}|^2 \quad (12)$$

* Dirac, 'Quantum Mechanics,' equation (22), p. 168

The average total energy transfer is therefore

$$\bar{Q}_e = (4\pi^2 e^2 / h^2) (\Sigma_s \left| \int_0^T F(t) e^{2\pi i \nu_s t} dt \right|^2 |x_{1s}|^2) (W(s) - W(1)). \quad (13)$$

The energy transfer to a harmonic oscillator according to classical theory is considered in Rayleigh's 'Sound' (vol. 1, p. 74). From the result given there we find that the energy transfer to an elastically bound electron due to the action of an electric force $F(t)$ is

$$Q_{cl} = (e^2 / 2m) \left| \int_0^T F(t) e^{2\pi i \nu t} dt \right|^2, \quad (14)$$

where ν is the natural frequency of the electron. Comparing with (12) we see that the probability of the excitation of any state S on the quantum theory is proportional to the classical energy transfer to an electron with natural frequency, ν_s , equal to $(W(s) - W(1))/h$. This is a reflection of the correspondence principle. An electron with frequency ν_s is the virtual oscillator of the old quantum theory, and the matrix element $|x_{1s}|^2$ in (12) gives the relative weight of this oscillator. An idea of the effective weight of all the virtual oscillators may be obtained if we neglect the variation of $\left| \int_0^T F(t) e^{2\pi i \nu_s t} dt \right|^2$ with ν_s in making the summation in (13), and take an effective value of $\nu_s = \bar{\nu}$. Then

$$\bar{Q}_e = (e^2 / 2m) \left| \int_0^T F(t) e^{2\pi i \bar{\nu} t} dt \right|^2. \quad (15)$$

This is equal to the classical transfer provided we take the natural frequency of the classical electron equal to $\bar{\nu}$. We notice that if $\bar{\nu} \ll 1/T$, as in case (b), (15) immediately gives the result (8) of that section. In this case owing to the independence of $\int_0^T F(t) e^{2\pi i \nu_s t} dt$ of ν_s the approximation underlying (15) leads to no error, and the equivalence between \bar{Q}_e and Q_{cl} is exact.

A simple connection exists between the probability $P(s)$ of excitation of the state s and the Fourier representation of $F(t)$. This was pointed out by Dirac,* and is of interest because it bears on the method used by Fermi for dealing with collisions (considered in § 4). If in the Fourier representation of $F(t)$ we regard the Fourier component of frequency ν as the electric force in a train of

* 'Quantum Mechanics,' *loc cit*

homogeneous radiation then the energy of this equivalent radiation per unit frequency range crossing unit area is

$$E_r = (c/2\pi) \left| \int_0^T F(t) e^{2\pi i \nu t} dt \right|^2. \quad (16)$$

Comparing with (11) we see that

$$P(s) = (8\pi^3/ch^2) |x_{1s}|^2 E_r. \quad (17)$$

This result shows that the probability of any given transition is proportional to the intensity of the Fourier components of the perturbing force which has a frequency equal to that of the virtual oscillator corresponding to the transition concerned.*

Before concluding this section it is necessary for the purpose of the applications to follow to consider one more point. Suppose there are two perpendicular perturbing forces $F_1(t)$, $F_2(t)$, each uniform over the atom. Let $P_1(S)$ and $P_2(S)$ respectively be the probabilities that these forces, when acting separately, excite a state with proper value $W(S)$. We require the probability of this state being excited when the forces act simultaneously on the atom. Since F_1 and F_2 are uniform over the atom, the problem, when the forces are due to radiation, is that of the superposition of two beams of radiation travelling in the same direction and polarised at right angles to one another. In this case we know that the resultant absorption of energy from the radiation is the sum of the energies absorbed from the beams when they act separately. In other words $P(S) = P_1(S) + P_2(S)$.† Now our basic equation (1) makes no distinction between the perturbing effect of the field of an electric particle and that of the field of radiation. It follows that $P(S) = P_1(S) + P_2(S)$ whatever the origin of the perturbing forces F_1 and F_2 .

* It is interesting to notice that in view of this we must regard all transitions induced in an atom as resonance effects. When the perturbation is a sudden impulse, as in case (b), it is difficult to think of the ionisation or excitation as produced by resonance. However, an impulse, I , lasting for an infinitesimal time, gives Fourier components of constant intensity at all frequencies, this intensity being given by $E_r = (c/2\pi) I^2$. These harmonic components then cause transitions by resonance.

† This does not apply to the "proper functions" excited. For example, two beams of radiation polarised at right angles and differing in phase by $\pi/2$ liberate photoelectrons uniformly in all lateral directions. However, if they are in phase this is not so. The "proper functions" excited in the two cases are therefore not the same. The total number of photoelectrons liberated in all directions is, however, the same in both cases. This means that the probability of the excitation of any given proper value is the same in both cases.

§ 2. *Distant Collisions between an Atom and a Moving Particle.*

As mentioned in the Introduction we deal in this paper only with light collisions in which the momentum acquired by the "knocked" atomic electron is small compared with the momentum of the moving particle. In such cases it is legitimate to neglect the reaction on the moving particle during the collision, and to regard it as merely the origin of a Coulombian field of force moving with uniform velocity in a straight line. The perpendicular distance between this line and the nucleus of the perturbed atom is the impact parameter, p , and the probability of any particular excitation of the atom may be obtained by first calculating the perturbation of the atom for a definite value of p and then integrating over all values of p from 0 to ∞ . *

We define the distant collisions considered in this section as those in which the impact parameter is greater than λ where λ is a length appreciably greater than atomic dimensions, σ . In such cases the perturbing force may be assumed to be uniform over the atom, and can be resolved into two components F_1 , F_2 , perpendicular to and parallel to the path of the particle respectively. In fig. 1 AB represents the path of the moving particle, and O the nucleus of the atom. Taking the origin of time as the instant when the moving particle is at N we have

$$F_1 = Ep / (p^2 + v^2t^2)^{3/2} \quad (18A)$$

$$F_2 = Ev / (p^2 + v^2t^2)^{3/2}. \quad (18B)$$

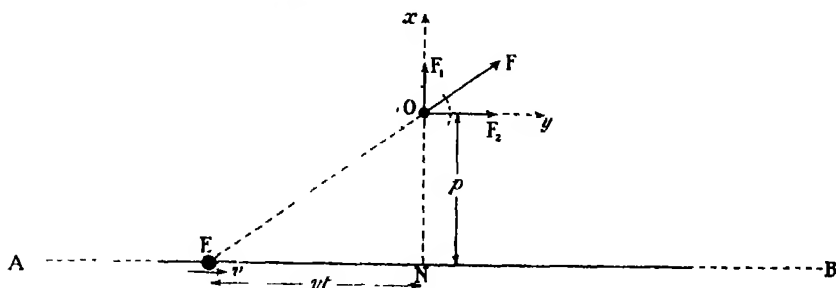


FIG 1.

The effect of a perturbing force uniform over the atom is considered in § 1, case (c). It also follows from the end of that section that the effects of the two components F_1 and F_2 may be considered separately.

* The legitimacy of this procedure and its equivalence to Born's theory of collisions have been shown by Mott ('Proc. Camb. Phil. Soc.', vol. 27, p. 553 (1931)) and Frame ('Proc. Camb. Phil. Soc.', vol. 27, p. 511 (1931)).

We shall first give Bohr's classical expression for the rate of loss of energy, $d^A T/dx$, in distant collisions with $p > \lambda$. This follows from (14), and in the case of a particle traversing an atmosphere containing N electrons per unit volume, each with natural frequency ν , we have

$$(d^A T/dx)_{cl} = (e^2/2m) \int_{\lambda}^{\infty} 2\pi p dp N \left\{ \left| \int_{-\infty}^{+\infty} F_1(t) e^{2\pi i \nu t} dt \right|^2 + \left| \int_{-\infty}^{+\infty} F_2(t) e^{2\pi i \nu t} dt \right|^2 \right\} \quad (19)$$

On the quantum theory there is virtually a multitude of natural oscillators. We must consider each one separately, *i.e.*, consider the probability of the excitation of a given state, and then sum up the dissipations due to transitions to different states. That the resultant average loss of energy must be approximately equal to the classical value follows from the result (15), which expresses the fact that the resultant weight of all the quantum oscillators is approximately equivalent to that of one classical electron. To prove the almost exact equivalence found by Gaunt (*loc. cit.*) between classical theory and quantum mechanics in this respect, it is necessary to consider the requirements of the latter in somewhat greater detail. Using the result (12) we find that the probability that the particle excites an atom to a state with proper value $W(S)$, in 1 cm. of its path, in distant collisions, is

$$P_S^A = (4\pi^2 e^2/h^2) |x_{1S}|^2 \int_{\lambda}^{\infty} 2\pi p dp N \left\{ \left| \int_{-\infty}^{+\infty} F_1(t) e^{2\pi i \nu t} dt \right|^2 + \left| \int_{-\infty}^{+\infty} F_2(t) e^{2\pi i \nu t} dt \right|^2 \right\} \quad (20)$$

The integrals involved in this expression are the same as those in the classical expression (19), and to evaluate (20) we can make use of Bohr's result for (19). In his calculation Bohr makes the simplifying assumption that λ is small compared with v/ν , in which case (19) gives

$$(d^A T/dx)_{cl} = (4\pi N E^2 e^2/mv^2) \log(1.123 v/2\pi\nu\lambda). \quad (21)$$

Making the corresponding assumption that λ is small compared with v/ν_S in (20), we have

$$P_S^A = (4\pi^2 e^2/h^2) |x_{1S}|^2 (8\pi N E^2/v^2) \log(1.123 v/2\pi\nu_S\lambda). \quad (22)$$

Since $|x_{1S}|^2$ is small except for ν_S close to J/h (p. 167) only P_S^A in this region of ν_S is of importance. It follows that the condition $\lambda \ll v/\nu_S$ is effectively satisfied provided $\lambda \ll v\hbar/J$

To find the average loss of energy we multiply (22) by $W(S) - W(1)$ and sum over all S , so that

$$d^2T/dx = (8\pi N E^2/v^2)(4\pi^2 e^2/h^2)(\Sigma + \int)_S (W(S) - W(1)) |x_{1S}|^2 \log(1.123 v/2\pi v_S \lambda).$$

The log term on the right-hand side may be written as the sum of $\log\{1.123 v/2\pi(J/h)\lambda\}$ and $\log\{(J/h)/v_S\}$. The first of these log terms is independent of S so that since $(\Sigma + \int)_S (W(S) - W(1)) |x_{1S}|^2 = h^2/8\pi^2 m$ the contribution to d^2T/dx arising from this term is

$$(4\pi N E^2 e^2/mv^2) \times \log\{1.123 v/2\pi(J/h)\lambda\}$$

As regards the second log term we again recall that $|x_{1S}|^2$ is very small except for a region of values of v_S close to J/h . In the region which matters the argument of the second log term is therefore nearly unity and consequently of little importance compared with the first log term the argument of which is of the order of $vh/J\lambda \gg 1$. Actually the effective value of the argument of the second term, obtained by numerical integration, is 1.10 .* The exact value of the dissipation is therefore

$$d^2T/dx = (4\pi N E^2 e^2/mv^2) \log\{1.123 v/2\pi(1.1 J/h)\lambda\}. \quad (23)$$

Comparing with the classical result (21) we see that provided we take the natural frequency of the electron in the classical problem equal to $1.1 J/h$ the classical dissipation of energy in distant collisions is the same as the quantum-mechanical dissipation. This result is what was found by Gaunt in his treatment of the problem. Gaunt's treatment, however, involves considerable calculation which is avoided here by considering the effects of the component forces separately, and then comparing the unintegrated expressions with the corresponding classical expressions.

It is important to observe that the results (21) and (23) are applicable only to particles with velocities large compared with the orbital velocity, u , of the

* Substituting for the matrix elements $|x_{1S}|$ their actual values we find that the contribution to d^2T/dx arising from the second term is

$$\frac{4\pi N E^2 e^2}{mv^2} \left\{ \sum_{n=1}^{\infty} \left(1 - \frac{1}{n^2}\right) \frac{2^8 n^7 (n-1)^{2n-5}}{3(n+1)^{2n+6}} \log \frac{n^2-1}{n^2} + \int_0^{\infty} \left(1 + \frac{1}{x^2}\right) \frac{2^8 e^{-4x} \cot^{-1} x}{3(1+x^{-2})^3 (1-e^{-2\pi x})} \log\left(1 + \frac{1}{x^2}\right) dx \right\}.$$

By numerical calculation we find, with sufficient accuracy, $\{\Sigma + \int\} = \{-0.132 \pm 0.001\} + \{0.226 \pm 0.003\} = 0.094 \pm 0.003 = \log(1.10 \pm 0.1)$. The same numerical calculation occurs in Gaunt's work who finds the value 0.10_0 . The agreement is satisfactory, so that the present numerical calculation confirms that carried out by Gaunt.

undisturbed atomic electron. This limitation arises from the simplifying assumption that $\lambda \ll vh/J^*$, and also from the fact that our basic equation (1) assumes the perturbation to be small, which is not the case if the particle moves comparatively slowly past the perturbed atom. The limitation $v \gg u$ applies to the results of most calculations which have been made on the dissipation of energy by moving particles, including the recent calculations made by Bethe† using Born's theory of collisions.

The condition $v \gg u$ also ensures that all distant collisions are necessarily light collisions. For the energy transfers in distant collisions are concentrated close to the ionisation potential J , according to practically the same distribution law as that for the energy transfers in a sudden impulse (§ 1 (b)). This is so because, from (5) and (22), the probability of a given energy transfer is, in both cases, very nearly proportional to $|x_{13}|^2$. The momentum acquired by the electron is thus of the order of $\sqrt{(2mJ)} \sim mu$, which is much less than the momentum mv of the primary moving particle provided $v \gg u$.

§ 3. *Relativity Effect in Light Collisions.*

The writer‡ has previously considered the relativity effect in a general way, allowing for it by considering the Fitzgerald contraction of the field of the moving particle and the consequent increase in its "radius of action." (See § 5.) This increase gives rise to an increase in the dissipation of energy and this represents the relativity correction. A more rigorous derivation of this correction, using the results of the previous sections will now be given.

We shall first consider the rate of loss of energy $d_w T/dx$ in light collisions with $Q < W$, where $J \ll W \ll (Jmc^2)^{\frac{1}{2}}$. It is important to know the theoretical relativity correction to this quantity, because in experiments on the behaviour of very fast particles it is the quantity which has been most accurately investigated. The non-relativity value of $d_w T/dx$ according to Bethe's calculations is

$$d_w T/dx = (2\pi N E^2 e^2 / mv^2) \log (2mv^2 W / 1 \cdot 2 J^2). \quad (24)§$$

We shall consider separately the contributions to this quantity from distant

* λ is the lower limit to the impact parameter in distant collisions and is of the order of atomic dimensions, σ . Now $\sigma \sim h/mu$ and $J \sim mu^2$, so that $\lambda \ll vh/J$ is satisfied provided $h/mu \ll vh/mu^2$, i.e., $v \gg u$.

† 'Ann. Physik,' vol. 5, p. 325 (1930).

‡ 'Proc. Roy. Soc.,' A, vol. 130, p. 328 (1931); vol. 135, p. 108 (1932).

§ Williams, 'Proc. Roy. Soc.,' A, vol. 135, p. 125 (1932).

and close collisions. The total non-relativity energy loss in distant collisions is given by (23), viz.,

$$d^A T/dx = (4\pi N E^2 e^2 / m v^2) \log (1.123 \, v h / 2 \cdot 2\pi J \lambda). \quad (23)$$

From the end of the last section $d^A T$ is spent in excitation, and in light ionising collisions with Q very close to J , the loss of energy in quantities appreciably greater than J being negligible. Since $W \gg J$ it follows that the whole of $d^A T/dx$, given by (23), contributes to $d_w T/dx$. The contribution to $d_w T/dx$ from close collisions with $p < \lambda$ is obtained by subtracting (23) from (24) which gives

$$(d_w T/dx)_{p < \lambda} = (2\pi N E^2 e^2 / m v^2) \log (8\pi^2 m W \lambda^2 / 1.3 \, h^2). \quad (25)$$

We now further divide $d^A T/dx$ into the part $d_1^A T/dx$ due to the perturbation of the atom by the component force F_1 , perpendicular to the velocity of the particle, and the part $d_2^A T/dx$ due to the other component, F_2 . From the analysis leading to (23) we find

$$d_1^A T/dx = (4\pi N E^2 e^2 / m v^2) \{ \log (1.123 \, v h / 2 \cdot 2\pi J \lambda - \frac{1}{2}) \} \quad (23A)^*$$

$$d_2^A T/dx = 2\pi N E^2 e^2 / m v^2. \quad (23B)^*$$

In the collisions concerned the velocity acquired by the "knocked" electron is very small compared with that of light since $Q < W \ll (J m_0 c^2)^{\frac{1}{2}}$. In considering the relativity correction we can therefore neglect the effect of the magnetic forces due to the moving particle, and also the relativity correction to the mass of the "knocked" electron. Also since the moving particle has a velocity comparable with that of light—even if it is an electron—the momentum communicated to the "knocked" electron is negligible compared with the momentum of the moving particle. The latter may therefore be assumed to move uniformly in a straight line and the method of impact parameter is applicable to all the collisions concerned. The relativity effect thus reduces to the effect which the relativity modification of the field of a particle moving with uniform velocity has on the perturbation produced by that field. This modification likewise controls the classical relativity correction and was considered by Bohr. The modified values of the component forces F_1 and F_2 are†

$$F_1 = E p (1 - \beta^2) / \{ p^2 (1 - \beta^2) + v^2 t^2 \}^{3/2} = (E / \sqrt{1 - \beta^2}) p / \{ p^2 + (v / \sqrt{1 - \beta^2})^2 t^2 \}^{3/2} \quad (26)$$

$$F_2 = E v t (1 - \beta^2) / \{ p^2 (1 - \beta^2) + v^2 t^2 \}^{3/2} = E (v / \sqrt{1 - \beta^2}) t / \{ p^2 + (v / \sqrt{1 - \beta^2})^2 t^2 \}^{3/2}$$

Comparison with the non-relativity expressions (18) shows that the analysis

* In deducing these use is made of Bohr's classical calculations, 'Phil. Mag.', vol. 30, p. 581 (1915).

† For the necessary formulae for this modification see Richardson, "Electron Theory of Matter," p. 249.

of § 2 for distant collisions will still apply provided, in the case of F_1 , E and v are replaced by $E/\sqrt{1-\beta^2}$ and $v/\sqrt{1-\beta^2}$ respectively, and in the case of F_2 , by E and $v/\sqrt{1-\beta^2}$ respectively. Making these substitutions in the final non-relativity expressions (23) we obtain the corrected values

$$d_1^*T/dx = (4\pi NE^2e^2/mv^2) \{ \log (1 \cdot 123 \, v h / 2 \cdot 2\pi J \lambda \sqrt{1-\beta^2}) - \frac{1}{2} \} \quad (27A)$$

$$d_2^*T/dx = (2\pi NE^2e^2/mv^2)(1 - \beta^2), \quad (27B)$$

which on adding give

$$d^*T/dx = (2\pi NE^2e^2/mv^2) \{ 2 \log (1 \cdot 123 \, v h / 2 \cdot 2\pi J \lambda) + \log (1 - \beta^2)^{-1} - \beta^2 \}. \quad (27)$$

The distribution of this energy loss between different collisions is practically identical with that of the non-relativity loss (23), and it is therefore all to be included in d_w^*T/dx . The correction to the contribution to d_w^*T/dx from distant collisions is thus an increase of

$$dT_R/dx = (2\pi NE^2e^2/mv^2) \{ \log (1 - \beta^2)^{-1} - \beta^2 \}. \quad (28)$$

In the close collisions, since the impact parameter \sim atomic dimensions, σ , and since $v \approx c$, the time of collision, T , is small, and does not exceed σ/c . It follows from § 1, case (a)—which deals with sudden impulses—that provided $\sigma/c \ll 1/v_g = h/Q$, i.e., provided $Q \ll (Jm_0c^2)^{\frac{1}{2}}$, the probability of an energy transfer Q depends only on the time-integral of the perturbing component forces. The expressions (26) show that the time-integral of the perturbing force at any point is unaffected by the relativity modification of the field of the particle. The energy transfers in such close collisions are therefore unaffected and their contribution to d_w^*T/dx is given by the non-relativity expression (25). The correction (28) to distant collisions therefore represents the full relativity correction to d_w^*T/dx . The corrected value is accordingly

$$d_w^*T/dx = (2\pi NE^2e^2/mv^2) \{ \log (2mv^2W/1 \cdot 2 \, J^2) + \log (1 - \beta^2)^{-1} - \beta^2 \}. \quad (29)$$

This formula is exactly the same as that recently deduced by Bethe using a method entirely different from the method of impact parameter used here. The writer has elsewhere compared the relativity corrections in (29), and also the corrections in the formula for the primary ionisation given below, with experiment.* The corrections are in the right direction and of the right order

* The relativity corrections in (29) and (32) were first put forward by the writer in 'Proc. Roy. Soc., A, vol. 130, p. 328 (1931), and their implications regarding the behaviour of ultra-fast particles, such as those associated with penetrating radiation, discussed. Also compared with experiment and discussed in 'Proc. Roy. Soc., A, vol. 135, p. 108 (1932). In the latter term $-\beta^2$ in the corrections is left out. Its effect is small compared with that of the term $\log (1 - \beta^2)^{-1}$, but in so far as it has an effect it reduces the agreement with experiment.

of magnitude. The experiments concerned are, however, not sufficiently accurate to provide a stringent test.

The primary ionisation due to a moving particle is practically entirely dependent on the frequency of light collisions with Q close to the ionisation potential. We have found that the relativity effect in such light collisions is an extra energy loss, dT_R , given by (28). The corresponding increase in the primary ionisation depends upon how dT_R is distributed between different kinds of collisions. This distribution is identical with the distribution of the energy loss when the atom is acted upon by a sudden impulse*. The latter is considered in § 1, case (b), and we find that the average energy spent per ion produced is 3.5 J. The extra primary ionisation per centimetre corresponding to dT_R is therefore

$$I_R = (dT_R/dx) \div 3.5 \text{ J} = 0.285 (2\pi N E^2 e^2 / mv^2 J) \{\log (1 - \beta^2)^{-1} - \beta^2\}. \quad (30)$$

The non-relativity primary ionisation according to Bethe is

$$I = 0.285 (2\pi N E^2 e^2 / mv^2 J) \log (42mv^2/J). \quad (31)$$

The relativity corrected value is therefore

$$I = 0.285 (2\pi N E^2 e^2 / mv^2 J) \{\log (42mv^2/J) + \log (1 - \beta^2)^{-1} - \beta^2\}. \quad (32)$$

It is interesting to notice that since relativity considerations only affect the distant collisions and since these practically all result in energy transfers of the order of J , the frequency $\Phi(Q)$ of light collisions, for which $Q \gg J$ and $Q \ll \sqrt{(Jm_0c^2)^2}$, is unaffected, and is given by the non-relativity expression, viz.,

$$\Phi(Q) = 2\pi N E^2 e^2 / mv^2 Q^2 \quad (33)$$

This result may readily be expressed in terms of scattering, for an energy loss $Q \gg J$ causes a deflection through an angle $\approx (2mQ)^{1/2} \div Mv/(1 - v^2/c^2)^{1/2}$. The resulting scattering formula is the classical non-relativity formula multi-

* The relativity effect on the probability P_s^Λ of the excitation in distant collisions of a state S may be found in exactly the same way as the relativity effect on the dissipation d^2T/dx , and by comparison with (27) we find that the effect is an increase of

$$(4\pi^2 e^2 / \hbar^2) (4\pi N E^2 / v^2) \{\log (1 - \beta^2)^{-1} - \beta^2\} \times |x_{1S}|^2.$$

This increase in P_s^Λ , and the value of $P(s)$ for a sudden impulse (equation (5)), depend on S in exactly the same way, both being proportional to $|x_{1S}|^2$. This means that they have the same distributions.

plied by $(1 - v^2/c^2)$. Since (32) applies only to light collisions this result applies only to small angles of scattering.

It is important to emphasise, before concluding this section, that the relativity corrections to the dissipation in light collisions and to the primary ionisation, are quite independent of any system of relativity quantum mechanics, and depend only on the relativity theory of the field of a particle moving with uniform velocity and upon non-relativity quantum mechanics. This is so because in the collisions concerned the reaction on the moving particle is negligible. The degree of agreement between relativity-corrected formulæ and experiment in the case of primary ionisation and the energy lost in light collisions, can therefore be no criterion of the correctness of any system of relativity quantum mechanics. To test such a theory it is necessary to investigate collisions in which the velocity of the "knocked" electron is not negligible compared with that of light. In this connection it might be mentioned that according to existing data the observed frequency of collisions, in which the "knocked" electron acquires a velocity of the order of $\frac{1}{4}c$, is about twice the value given by (32).^{*} Since the corresponding energy acquired by the "knocked" electron is much greater than its energy of binding to the atom, the collisions concerned are effectively collisions between free electrons. The application of relativity quantum mechanics to such collisions, which have hitherto been made,[†] agree with (32) and are therefore in disagreement with experiment.

§ 4 *Distant Collisions and the Photoelectric Effect of Radiation.*

Equation (17), § 1, shows that the probability that a perturbing force, F , which acts uniformly over the atom, causes a transition from the ground state to a state with total energy $W(S)$, is $\{(8\pi^3/ch^2)|x_{1s}|^2\} \times E_{\nu}$. The quantity within brackets is the coefficient, μ , of photoelectric absorption of radiation of frequency $\nu = (W(S) - W(1))/h$, whilst E_{ν} measures the intensity of the harmonic component of this frequency in the Fourier representation of the perturbing force F . The perturbation of an atom in distant collisions—in which F is, of course, uniform over the atom—is therefore correctly obtained by resolving the perturbing force into its Fourier components and assuming

^{*} Williams and Terroux, 'Proc. Roy. Soc.,' A, vol. 126, p. 289 (1930). Experiments are in progress to check this result.

[†] Møller, 'Z. Physik,' vol. 14, p. 531 (1932). In a recent work ('Proc. Roy. Soc.,' A, vol. 132, p. 688 (September, 1932)) Champion finds that for comparatively large angles of scattering Møller's calculations agree with experiment.

each component to behave like radiation of the same frequency. This is the fundamental idea underlying the theory of the dissipation of energy by moving particles put forward by Fermi in 1924 *. The difference, in the case of distant collisions, between the calculations made by Fermi at that time, and those described in § 2, is that Fermi took the experimental values of the absorption coefficient, μ , whilst in § 2 the quantum-mechanical value $(8\pi^3/ch^2)|x_{12}|^2$ is used. A numerical comparison of the latter with the empirical values used by Fermi shows that they are roughly the same. Therefore in distant collisions—which contribute about half the total stopping power—the dissipation calculated by Fermi necessarily agrees in order of magnitude with the numerical requirements of § 2. In close collisions, with p less than atomic dimensions, Fermi's procedure is very rough because he assumes in such cases that the perturbing force is uniform over the whole atom and equal to the force at the nucleus. This approximation does not, however, alter the order of magnitude of his final results. That Fermi obtained values for the stopping-power roughly in agreement with other theories and with experiment, is therefore what we would expect. As regards the distribution of the energy loss between different kinds of collisions, the very large concentration of collisions with energy losses near the ionisation potential, which is required by quantum mechanics,† is, in terms of Fermi's theory, explained by the very rapid increase in photoelectric absorption which takes place as an absorption limit is approached.

The connection between the perturbation in distant collisions and the photoelectric effect of radiation is more than formal. In the photoelectric effect the momentum of the photoelectron is balanced mostly by recoil of the nucleus, and the reaction on the radiation field, equal to $h\nu/c$, is small in comparison. The state of affairs is the same in distant collisions. By comparing the results of § 5 with results obtained by Bethe, using Born's method, we find that in such collisions the momentum of the ejected electron is balanced by the nucleus, and the deflection of the moving particle is much less than what it would be if the whole reaction of the ejected electron were exerted on it. It is not so with close collisions—in which the moving particle passes "through" the atom. In these the deflection of the moving particle in most cases corresponds to a two-body collision with the ejected electron. Accordingly, if we consider collisions with a given energy transfer, Q ,—not too large compared with the ionisation potential J —some of the collisions will be distant collisions,

* 'Z. Physik,' vol. 29, p. 215 (1924).

† Cf. end of § 2, also Williams, 'Proc. Roy. Soc.,' A, vol. 130, p. 334 (1931).

others close collisions. It follows that in some cases the moving particle will be little deflected, and in others it will suffer the full deflection corresponding to a two-body collision. This reminds one of certain observations by C. T. R. Wilson in which he finds that whilst a "branch track" generally produces the expected deflection of the primary electron it sometimes produces a much smaller deflection. The observed frequency of the latter is, however, much greater than what one would expect from a simple theory using hydrogen-like wave functions.

§ 5. Spatial Distribution of the Excited and Ionised Atoms with respect to the Path of the Particle

We shall first consider what fraction of the non-relativity dissipation takes place in distant collisions. The energy lost in distant collisions is given by (23) and is

$$d^*T/dx = (4\pi N E^2 e^2 / m v^2) \log (1.123 v h / 2 \cdot 2\pi J \lambda), \quad (23)$$

λ is the lower limit to the impact parameter and in our calculations it is assumed to be appreciably greater than atomic dimensions, in order that the perturbing force may be uniform over the atom. However, as λ occurs in the log term in (23) the latter is very insensitive to its value, and we can take λ equal to atomic dimensions. This simplifies the expression of the results without introducing any sensible error. In the case of hydrogen atoms we shall take λ equal to the diameter of the Bohr orbit, viz., $\sqrt{h^2/2\pi^2 m J}$. Substituting this for λ in (23) we have

$$d^*T/dx = (2\pi N E^2 e^2 / m v^2) \log (0.5 m v^2 / J). \quad (34)$$

The total energy lost due to *all* collisions has been calculated by Bethe and is

$$dT/dx = (4\pi N E^2 e^2 / m v^2) \log (1.8 m v^2 / J). \quad (35)$$

Since we are dealing with particles with velocities large compared with the orbital velocities of the atomic electrons traversed, $m v^2 \gg J$. It follows then from (34) and (35) that roughly half the total loss of energy by a moving particle is lost in distant collisions—collisions in which the particle may be said to pass outside the atom. This is not due to the fact that on quantum mechanics the atomic electron may sometimes be found at large distances from the nucleus, because the probability that an electron is at large distances r from the nucleus fall off exponentially with r , whilst as we shall see presently (equation (43)) the probability of an energy transfer falls off only as the inverse square of the distance, p , of the moving particle from the nucleus.

The number, n_i^σ , of inelastic distant collisions per centimetre is obtained by dividing (34) by the average energy transfer per inelastic collision. The latter is J (see end of § 2 and § 1, (b)), so that

$$n_i^\sigma = (2\pi N E^2 e^2 / m v^2 J) \log (0.5 m v^2 / J). \quad (36)$$

The total number of inelastic collisions per centimetre according to Bethe is

$$n_i = (2\pi N E^2 e^2 / m v^2 J) \log (3.1 m v^2 / J). \quad (37)$$

Since $m v^2 \gg J$ it follows that nearly all inelastic collisions are distant collisions. For a 100,000-volt electron, *e.g.*, (36) and (37) show that about 85 per cent of the inelastic collisions occur when the path of the particle is at least 1 Å. unit from the hydrogen nucleus. The previous result that half the total energy loss takes place in close collisions arises from the fact that a close collision when it does occur means much more loss of energy than a distant collision.

To obtain the detailed distribution of the distances of ionised and excited atoms from the path of the particle in distant collisions we must consider the probability of ionisation or excitation for a given impact parameter. We shall here consider separately the probability P_1^s of excitation or ionisation to a state S caused by the component F_1 of the perturbing force, and the probability P_2^s of such excitation or ionisation caused by the other component F_2 . From (12)

$$P_1^s = (4\pi^2 e^2 / \hbar^2) |x_{is}|^2 \left| \int F_1(t) e^{i\pi v t} dt \right|^2. \quad (38)$$

$$P_2^s = (4\pi^2 e^2 / \hbar^2) |x_{is}|^2 \left| \int F_2(t) e^{i\pi v t} dt \right|^2. \quad (39)$$

Since the energy transfers, Q , in distant collisions, are practically confined to a small region of values close to J we can assume that v_s in these expressions is of the order of J/\hbar . The larger the impact parameter the slower F_1 and F_2 vary with the time. The expressions (18) show that they rise from inappreciable values to large values and fall again to inappreciable values in a time of the order of p/v —or if we use the relativity expressions (26), in a time of the order of $(1 - \beta^2)^{1/2} p/v$. We call this the “time of collision,” T . When T is much less than $1/v_s$, *i.e.*, $p \ll \hbar v / J (1 - \beta^2)^{1/2}$, we have the conditions of a sudden impulse dealt with in § 1, (b). In that case the total energy transfer is, from (8), equal to $I^2/2m$, where I is the time integral of the perturbing force. Now, whether we use relativity expressions or not, the time integral of F_1 is $2Ee/pv$, and that of F_2 vanishes (because F_2 is an odd function of the time).

Thus, for collisions with $p \ll \hbar/J(1 - \beta^2)^{\frac{1}{2}} = \rho$, say, the average energy transfer per collision is

$$\bar{Q}_{p < \rho} = I^2/2m = 2E^2e^2/mv^2p^2. \quad (40)$$

Since the average energy transfer per inelastic collision is J the probability of excitation or ionisation for this region of p is

$$P_{p < \rho} = 2E^2e^2/mv^2p^2 J. \quad (41)$$

In other words, if the particle is traversing an atmosphere of hydrogen atoms, containing N atoms per unit volume, the number of atoms excited or ionised at distances from the path of the particle between p and $p + dp$, per centimetre of path, is

$$dn_i = 2\pi p dp N \cdot 2E^2e^2/mv^2p^2 J = (4\pi NE^2e^2/mv^2 J) \frac{dp}{p} \quad (42)$$

whilst the corresponding energy transfer is

$$d(dT/dx) = 2\pi p dp N \cdot 2E^2e^2/mv^2p^2 = (4\pi NE^2e^2/mv^2) dp/p. \quad (43)$$

These expressions apply to $p < \rho$ (and of course p greater than atomic dimensions since we are dealing with distant collisions). If $p > \rho$ the time of collision, $T \sim 1/v$, and the integrals $\int F(t) e^{2\pi i \nu t} dt$ in (38) and (39) are vanishingly small, since $F(t)$ varies very little in one period of $e^{2\pi i \nu t}$. These are the conditions of adiabatic perturbation and the energy transfer is negligible. Ions and excited atoms are thus produced up to distances of the order of ρ from the path of the particle with appreciable frequency, but the number produced beyond this distance is negligible.* For this reason we call ρ the *radius of action* of the particle. The transition to adiabatic conditions takes place gradually, so that the radius of action has no exact value. We can, however, define an exact *effective* value as that of the upper limit, ρ , to p , which gives the correct value of $d^{\lambda}T/dx$ when we assume that the change to adiabatic conditions takes place suddenly at $p = \rho$. Then from (27) and (43) (neglecting the small term $-\beta^2$ in the relativity correction) we have

$$1 \cdot 12 \hbar/2 \cdot 2\pi J \lambda (1 - \beta^2)^{\frac{1}{2}} = \rho/\lambda,$$

so that

$$\rho = 0 \cdot 2 \hbar/J(1 - \beta^2)^{\frac{1}{2}}. \quad (44)$$

It is interesting to consider the interpretation of the radius of action in terms of Fermi's theory (§ 4). For a given impact parameter, p , the spectral

* Actually the probability of excitation or ionisation up to $p \sim \rho$ falls off only as p^{-2} but for $p \gg \rho$ it falls off as p^{-4} .

intensity, E_p , in the Fourier representation of the perturbing force, falls rapidly to insignificant values as v increases beyond $v_m \sim v/(1 - \beta^2)^{1/2} p$, so that v_m is effectively the high frequency limit of the spectrum. For $p \gg \rho \sim \hbar v/J(1 - \beta^2)^{1/2}$, $\hbar v_m \ll J$. The negligible effect for $p \gg \rho$ is thus due to the fact that for such p there are no frequencies in the Fourier spectrum of the perturbing force high enough to excite the atom.

As a numerical example of the above results, we find that for a 100,000-volt electron traversing hydrogen $\rho \sim 1 \times 10^{-8}$ cm. If the hydrogen is at N.T.P. the average number of atoms excited or ionised in this case is 13. Of these, two are situated with their nuclei within 1×10^{-8} cm. of the path of the particle, 4 are between 1×10^{-8} cm. and 5×10^{-8} cm. away from the path of the particle, 4 between 5×10^{-8} cm. and 2.5×10^{-7} cm. away, and the remaining 3 between 2.5×10^{-7} cm. away and the radius of action of about 10^{-6} cm.*

The existence of a radius of action means that the observation of an ionised or excited atom does not locate the responsible particle within atomic dimensions. In the above case of a 100,000 volt electron for example, if a hydrogen atom, A, is observed to be excited or ionised by it, it is certain—and no more is certain—that the path of the electron is within about 10^{-6} cm. of A; there is

* In referring to a radius of action and the spatial distribution of the ions with respect to the path of the ionising particle, we ought to consider the implications of the Uncertainty Principle regarding the definition of the path of a moving particle. In order that the distance p of the ionised or excited atom from the path of the moving particle may have a meaning we must be able to represent the particle for a distance α , large compared with p , by a wave-packet of dimensions δ , small compared with p . The most homogeneous wave-packet of dimensions δ spreads by an amount $\alpha\lambda/\delta$ in travelling a distance α . The value of δ which gives the best definition over a distance α is accordingly $(\alpha\lambda)^{1/2}$. The particle can therefore be represented by a wave-packet of dimensions $(\alpha\lambda)^{1/2}$ over a distance α . The above conditions are therefore satisfied provided $(\alpha\lambda)^{1/2} \ll p < \alpha$, i.e., provided $\lambda \ll p$. We are dealing in this paper with particles with velocity, v , much greater than the orbital velocities, u , of the atomic electrons traversed. This means that even if the moving particle is an electron the de Broglie wave-length, $\lambda = \hbar/mv$ is much less than atomic dimensions σ , which are of the order of \hbar/mu . Therefore in distant collisions with $p > \sigma$ the condition $\lambda \ll p$ is necessarily satisfied. As a corollary it is interesting to notice that the position of a particle for a certain interval of time can be defined with an accuracy, δ , which is very much less than the dimensions of the region within which we may observe atoms being ionised and excited by the particle during that time. For there is no functional relation between δ which defines the locality of the moving particle and p which represents the dimensions of the region within which the ions are produced. δ is measured by $\hbar(1 - \beta^2)^{1/2}/Mv$ whilst p is of the order of $\hbar v/J(1 - \beta^2)^{1/2}$. By adjusting v and M , e.g., we can make δ as small as we please and at the same time make p as large as we please.

a probability of 0.3 that it is between 10^{-6} cm. and 2.5×10^{-7} cm. away from A, a probability of 0.3 that it is between 2.5×10^{-7} and 5×10^{-8} away, a probability of 0.2 that it is between 5×10^{-8} and 1.5×10^{-8} , and a probability of 0.2 that it is within 1.5×10^{-8} cm. of A. In general for a particle of velocity, v , the probability that its path is between p and $p + dp$ away from the atom it excites or ionises is approximately

$$P(p) dp = dn_i/n_i = \{2/\log(3.1 mv^2/J\sqrt{1-\beta^2})\} dp/p. \quad (45)$$

This applies to $p < \rho$ and $p >$ atomic dimensions. The probability that the path is within atomic dimensions of the nucleus of A is small and the probability that it is outside the radius of action is negligibly small.*

The relativity value, ρ , of the radius of action is $(1 - \beta^2)^{-1/2}$ times the non-relativity value, ρ_0 . This difference between ρ and ρ_0 accounts for nearly the whole of the relativity correction (28), for, from (43), it means an extra dissipation of energy equal to

$$\int_{\rho_0}^{\rho} (4\pi N E^2 e^2 / mv^2) dp/p - (2\pi N E^2 e^2 / mv^2) \log(1 - \beta^2)^{-1/2}. \quad (46)$$

The reason for the relativity increase in the radius of action may readily be seen. The Fitzgerald contraction of the field of the moving particle reduces the time of collision for a *given* impact parameter by $(1 - \beta^2)^{-1/2}$, so that the impact parameter corresponding to a *given* time of collision is increased by the same factor. The radius of action, which is the impact parameter corresponding to a time of collision equal to the natural period $1/\nu_s$ of the atomic oscillator, is therefore increased by $(1 - \beta^2)^{-1/2}$. This means that a region of p from ρ_0 to $\rho_0 \times (1 - \beta^2)^{-1/2}$ which, if it were not for relativity effect, would be a region of adiabatic conditions and therefore insignificant energy transfer, is a region in which there is energy transfer to the atomic electron statistically

* Some of the features of these results may also be deduced from Born's theory of collisions. In that theory the moving particle after a collision with an atom, A, is represented by ψ waves spreading from A. A is thus effectively an aperture from which the waves emanate. The extent to which these waves are confined in a forward direction depends upon the radius of this equivalent aperture. Scattering through an angle less than θ corresponds approximately to an aperture of radius, p , $\sim \lambda/\theta$ where λ is the wave-length. The probability of scattering between θ and $\theta + d\theta$ then gives the intensity of the scattered waves emanating from an annulus of radii p and $p + dp$, i.e., it gives the probability that an inelastically scattered particle passes between p and $p + dp$ of the scattering atom A. Using Bethe's scattering formulæ we then find results in accordance with (45). In particular the negligible scattering according to Bethe's formula through angles less than J/mv^2 corresponds to the negligible ionisation and excitation which exists according to the present formulæ outside the radius of action.

equal to the transfer $2E^2e^2/mv^2 p^2$ to a free electron. The average transfer within the radius of action is given by the non-relativity value $2E^2e^2/mv^2 p^2$ because the conditions in this region are those of a sudden impulse, in which case the energy transfer depends only on the time-integral of the perturbing force and this is unaltered by the Fitzgerald contraction of the field.

The extra dissipation (46) due to the increase in the radius of action does not represent the whole of the relativity correction (28), so that our picture of the relativity effect is not quite complete. The part not represented is $(-2\pi NE^2e^2/mv^2)\beta^2$. This arises from the effect of the component, F_2 , of the perturbing force parallel to the motion of the particle. We have seen that because the time-integral of this component vanishes it has no effect for $p \ll \rho$, and because of adiabatic conditions it has no effect for $p \gg \rho$. However, for $p \sim \rho$, $\int F_2 e^{i\pi u t} dt$ is not insignificant. There is accordingly a small dissipation of energy due to F_2 in the region of $p \sim \rho$. Its non-relativity value, given by (23B), is $2\pi NE^2e^2/mv^2$. The increase in ρ due to relativity effect means that, when we take this effect into account, the disturbance due to F_2 takes place at greater distances away from the path of the particle and is therefore feebler. This, however, is cancelled out by the fact that the effect is operative over a correspondingly larger region of p . The relativity decrease in the effect of F_2 is really due to the fact that the Fitzgerald contraction of the field of the particle is not accompanied by a corresponding increase in the intensity of F_2 . As a result the non-relativity value must be multiplied by $(1 - \beta^2)$, and this gives rise to the rest of the relativity correction represented by $(-2\pi E^2e^2/mv^2)\beta^2$.

The following table shows the actual magnitude of the relativity effect in the case of electrons traversing atomic hydrogen at N.T.P. The figures also apply to protons of the same velocity.

Energy (volts)	$\beta = v/c$.	Radius of action, ρ (cm.)	Primary ionisation per cm.
10^5	0.55	1×10^{-8}	6.3
10^6	0.944	3×10^{-8}	2.5
10^7	0.9989	2×10^{-5}	2.9
10^8	0.9988	2×10^{-4}	3.6
10^9	0.9988	2×10^{-3}	4.3
10^{10}	0.9988	2×10^{-2}	5.0
10^{11}	0.9988	2×10^{-1}	5.6
10^{12}	0.9988	2	6.3
10^{13}	0.9988	20	7.0

The change in ionisation with velocity after $\beta \sim 0.99$ is practically all due to the increase in the radius of action. The primary ions represented by the difference between the numbers in the last column are thus produced at distances from the path of the electron between the corresponding values of the radius of action given in the third column.

The calculations which have been made in this paper refer specifically to hydrogen atoms, but the results obtained have a much more general applicability. The characteristics of the special case considered are represented in the calculations by the actual values given to the matrix elements ν_{13} . The calculations may therefore be repeated for any atomic electron, provided in the steps where we have given these matrix elements their special values for hydrogen we leave them undetermined. We then readily find that in the case of the relativity effect, the relativity formulæ for a many-electron atom may be obtained from the relativity formulæ given here for hydrogen, by making the same alterations that are made in Bethe's calculations in order to generalise the non-relativity formula for hydrogen to a many-electron atom. In the case of $d_w T/dx$, for example, we replace $1.1 J$ in (29) by the "mean excitation energy" for the many-electron atom concerned, which can be obtained from Bethe's non-relativity calculations. The results for the spatial distribution of ions (§ 5) are also applicable to any atomic electron provided J is replaced by an energy of the order of the ionisation potential of the electron considered.* Applying these results we find that the primary ionisation in oxygen or nitrogen is about nine times the above values for hydrogen.† The radius of action in these gases depends upon the ionisation potential, J' , of their outer electrons, being $(13.6/J')$ times the values given for hydrogen. Taking J' as 10 volts we see that a 10^{10} volt electron, for example, traversing these gases has a finite thickness of about $\frac{1}{2}$ mm, which should be detectable in a cloud photograph.

I should like to take this opportunity of thanking Professors R. H. Fowler and W. L. Bragg and Mr. N. F. Mott for the interest they have taken in this paper.

Summary.

The method of impact parameter is applied to light collisions, which we define as those in which the momentum transfer is small compared with the

* (43), which does not involve J and its dependent formulæ, has in general to be multiplied by a factor of the order of unity.

† Based on the observed ionisation in those gases at low velocities.

momentum of the moving particle. The main problems considered are the distribution in space of the ions produced by a moving particle, and the relativity corrections to the primary ionisation and to the loss of energy in light collisions. The beginning of the paper is devoted to general theorems concerning the perturbation of an atom by a sudden impulse and other special types of perturbing forces.

[*Note added in proof, November 7, 1932.* —In this paper, and also in the calculations of the relativity effect by Bethe and Møller, no account is taken of the effect of radiative forces. In a recent letter to the 'Physical Review,' W. F. G. Swann, in a discussion of the nature of penetrating radiation, suggests that an electron with energy greater than about 10^9 volts may, on account of radiative forces, not produce any ionisation at all. In his argument Swann appears to assume that it is necessary to have a close classical-like collision in order to produce ionisation. This, however, is not so. On the quantum theory, in the first place, nearly all the ionisation takes place in distant collisions with impact parameter greater than atomic dimensions (equation (35)), whilst secondly the radiative forces have no direct mechanistic influence on the ionisation,—any more than the scattering of radiation has on its photoelectric absorption. If we take these circumstances into account we find that on the quantum theory there is no such effect as that suggested by Swann, and the relativity formulæ given in this paper are not invalidated as a result of the effect of radiative forces.]

The Collision of Slow Electrons with Atoms. II.—General Theory and Inelastic Collisions.

By H. S. W. MASSEY, B.A., M.Sc., Ph.D., Exhibition of 1851 Senior Student, Trinity College, Cambridge, and C. B. O. MOHR, B.A., M.Sc., Trinity College, Cambridge, Exhibition of 1851 Student, University of Melbourne.

(Communicated by R. H. Fowler, F.R.S.—Received August 27, 1932)

Introduction.

Although a satisfactory theory of the collisions of fast electrons with atoms is provided by the method of Born-Dirac, a complete theory of slow collisions has not yet been developed. This is due to the large number of complicating factors which cannot be neglected when the time of interaction between atoms and the incident wave is considerable. These complications include the distortion of the incident and scattered waves by the atomic field, the exchange of electrons between atom and colliding beam, and the disturbance of the atomic wave functions by the incident wave.

The effect of the second of these phenomena was considered in detail to a first approximation by us† and found to be of considerable importance. In this paper, the accuracy of the calculation could not be regarded as high inasmuch as the other disturbing effects were neglected. It was then shown in a later paper‡ how the effect of the disturbance of the incident wave could be included in the calculation, and it was found that for the elastic scattering the agreement with experiment was considerably improved. On applying the method to the calculation of inelastic collision probabilities, the effect of the distortion of the incident wave was found to be small in comparison with, say, the effect of exchange. However, when one considers physically the excitation of an atom by electron impact, it is clear that the distortion of the outgoing wave by the field of the excited atom will be of greater importance than that of the incident wave by the normal atom. This is due to the greater spread of the field of the excited atom and also to the increased wave-length of the outgoing wave. In the same way, the distortion of the outgoing wave may be important in the case of elastic exchange.

In this paper the theory is extended to allow for the distortion of the outgoing wave, and detailed calculations for the excitation probabilities of the

† 'Proc. Roy. Soc.,' A, vol. 132, p. 605 (1931). Referred to later as Paper A.

‡ 'Proc. Roy. Soc.,' A, vol. 136, p. 289 (1932). Referred to later as Paper B.

2^1P and 2^3P states of helium are described. It is shown also that for a considerable range of velocities, the calculations in Paper B of the effect of exchange are valid, this range being that in which the exchanged and directly scattered waves are of comparable intensity and interfere strongly. For the range where the previous calculations need modification, the necessary calculation is given. Further possibility of improvement of the theory is discussed. The disagreement with observation seems to consist in the theory predicting too great an effect at low velocities. This may be due to the neglect of the disturbance of the atomic wave function by the incident electrons.

The theory is also of interest in connection with the diffraction effects observed by Mohr and Nicoll† in the inelastic scattering of electrons of moderate velocity by heavy atoms. In these experiments the angular distributions of the inelastically scattered electrons were found to exhibit maxima and minima at large angles similar to those previously found to occur in the angular distributions of the elastically scattered electrons. These effects are seen to be explicable in terms of the theory developed in this paper.

§ 1. General Theory.

A Elastic Collisions.—It was shown in Paper B, §§ 1 and 2, that the elastic scattering of electrons by atoms of hydrogen and helium may be described by means of two wave functions $F_0(r)$, $G_0(r)$, which have the asymptotic form

$$\left. \begin{aligned} F_0(r) &\sim e^{ikz} + r^{-1} e^{ikr} f(\theta, \phi) \\ G_0(r) &\sim r^{-1} e^{ikr} g(\theta, \phi) \end{aligned} \right\}. \quad (1)$$

The differential cross section for elastic collisions then takes the form

$$\begin{aligned} I(\theta) d\omega &= \left\{ \frac{1}{4} |f+g|^2 + \frac{3}{4} |f-g|^2 \right\} d\omega \text{ for hydrogen} \\ &= |f-g|^2 d\omega \text{ for helium.} \end{aligned} \quad (2)$$

Consider first the simpler case of hydrogen. The functions $F_0(r)$, $G_0(r)$ were shown to satisfy the equations

$$\left. \begin{aligned} [\nabla_1^2 + k^2] F_0(r_1) &= -\frac{8\pi^2 me^2}{\hbar^2} \int \left(\frac{1}{r_1} - \frac{1}{r_{12}} \right) \Psi(r_1, r_2) \psi^*_{*0}(r_2) d\tau_2 \\ [\nabla_2^2 + k^2] G_0(r_2) &= -\frac{8\pi^2 me^2}{\hbar^2} \int \left(\frac{1}{r_2} - \frac{1}{r_{12}} \right) \Psi(r_1, r_2) \psi^*_{*0}(r_1) d\tau_1 \end{aligned} \right\}, \quad (3)$$

where the function $\Psi(r_1, r_2)$ is the solution of the wave equation for the

† 'Proc. Roy. Soc.,' A, vol. 138, pp. 229 and 469, (1932).

complete system. In order to obtain approximate formulæ for $F_0(r_1) \pm G_0(r_1)$ we neglect the effect of the inelastically scattered waves included in Ψ and take

$$\Psi(r_1, r_2) \simeq F_0(r_1) \psi_0(r_2) + G_0(r_2) \psi_0(r_1). \quad (4)$$

In this way we make no initial assumptions as to the relative magnitude of F_0 and G_0 .

Substituting in (3) gives

$$\begin{aligned} \left| \nabla_1^2 + k^2 - \frac{8\pi^2 m}{h^2} V_{00}(r_1) \right| F_0(r_1) \\ = - \frac{8\pi^2 m e^2}{h^2} \int \left(\frac{1}{r_1} - \frac{1}{r_{12}} \right) G_0(r_2) \psi_0(r_1) \psi_0^*(r_2) d\tau_2, \quad (5A) \end{aligned}$$

$$\begin{aligned} \left| \nabla_2^2 + k^2 - \frac{8\pi^2 m}{h^2} V_{00}(r_2) \right| G_0(r_2) \\ = - \frac{8\pi^2 m e^2}{h^2} \int \left(\frac{1}{r_2} - \frac{1}{r_{12}} \right) F_0(r_1) \psi_0(r_2) \psi_0^*(r_1) d\tau_1, \quad (5B) \end{aligned}$$

where

$$V_{00}(r_1) = \int \left(\frac{e^2}{r_{12}} - \frac{e^2}{r_1} \right) |\psi_0(r_2)|^2 d\tau_2$$

Changing the co-ordinates of G_0 to r_1 , we obtain by adding and by subtracting (5B) from (5A), the equations

$$\begin{aligned} \left[\nabla_1^2 + k^2 - \frac{8\pi^2 m}{h^2} V_{00}(r_1) \right] \{F_0(r_1) \pm G_0(r_1)\} \\ = \pm \frac{8\pi^2 m e^2}{h^2} \int \left(\frac{1}{r_1} - \frac{1}{r_{12}} \right) \{F_0(r_2) - G_0(r_2)\} \psi_0(r_1) \psi_0^*(r_2) d\tau_2. \quad (6) \end{aligned}$$

This equation may be converted to an integral equation in the following way. We require a solution of the equation for $F_0(r_1) \pm G_0(r_1)$ which has the asymptotic form

$$F_0(r_1) \pm G_0(r_1) \sim e^{ikr_1} + r_1^{-1} e^{ikr_1} \{f(\theta_1, \phi_1) \pm g(\theta_1, \phi_1)\}. \quad (7)$$

Let us then treat the right-hand side of (6) as a known function $\phi(r_1)$ of r_1 . We may then write

$$\left[\nabla_1^2 + k^2 - \frac{8\pi^2 m}{h^2} V_{00}(r_1) \right] \{F_0(r_1) \pm G_0(r_1)\} = \phi(r_1). \quad (8)$$

The solution of this type of inhomogeneous equation has been discussed by Massey.† If $\mathfrak{F}(r, \theta)$ be the solution of the homogeneous equation

$$\left[\nabla^2 + k^2 - \frac{8\pi^2 m}{h^2} V_{00}(r) \right] \mathfrak{F}(r, \theta) = 0, \quad (9)$$

which has the asymptotic form

$$\mathfrak{F}(r, \theta) \sim e^{ikz} + \frac{e^{ikr}}{2ikr} \sum_{s=0}^{\infty} (2s+1) (e^{2i\eta_s} - 1) P_s(\cos \theta), \quad (10)$$

corresponding to an incident plane wave and a diverging spherical wave, then the asymptotic form of the required solution of (8) is

$$F_0(r) \pm G_0(r) \sim e^{ikz} + \frac{e^{ikr}}{r} \left\{ \sum_s \frac{2s+1}{2ik} (e^{2i\eta_s} - 1) P_s(\cos \theta) \right. \\ \left. \pm \frac{1}{4\pi} \int \phi(r') \mathfrak{F}(r', \pi - \Theta) d\tau' \right\},$$

where Θ denotes the angle between the vectors \mathbf{r}, \mathbf{r}' .

We thus have for the asymptotic form of the solution of (6)

$$F_0(r) \pm G_0(r) \sim e^{ikz} + \frac{e^{ikr}}{r} \left\{ \sum_s \frac{2s+1}{2ik} (e^{2i\eta_s} - 1) P_s(\cos \theta) \right. \\ \left. \pm \frac{2\pi m e^2}{h^2} \int \left(\frac{1}{r_1} - \frac{1}{r_{12}} \right) \{F_0(r_2) - G_0(r_2)\} \psi_0(r_1) \psi_0^*(r_2) \mathfrak{F}_0(r_1, \pi - \Theta_1) d\tau_1 d\tau_2 \right\} \quad (11)$$

The significance of the various terms in this formula is interesting. The first is the incident plane wave, the second the wave scattered by the static field $V_{00}(r)$ of the atom, while the third is the scattered wave due to electron exchange.

We must introduce two further approximations in order to calculate the exchange amplitude. In two cases we may do this without difficulty. They are as follows —

(1) Effect of atomic field small, so that all waves may be taken as approximately plane. In this case we set on the right-hand side of (11)

$$F_0(r_2) - G_0(r_2) = e^{ik\mathbf{n} \cdot \mathbf{r}_2}, \\ \mathfrak{F}_0(r_1, \pi - \Theta_1) = e^{-ik\mathbf{n} \cdot \mathbf{r}_1},$$

† 'Proc. Roy. Soc.' A, vol. 137, p. 447 (1932).

where \mathbf{n}_0, \mathbf{n} are unit vectors in the direction of incidence and observation respectively. This gives for the exchange amplitude

$$\frac{2\pi me^2}{h^2} \int \left(\frac{1}{r_1} - \frac{1}{r_{12}} \right) e^{i(\mathbf{n}_0 \cdot \mathbf{r} - \mathbf{n} \cdot \mathbf{r}_1)} \psi_0(r_1) \psi_0^*(r_2) d\tau_1 d\tau_2, \quad (12)$$

the formula derived by Oppenheimer.

(2) Effect of exchange small compared with direct scattering. In this case we may take

$$F_0(r_2) - G_0(r_2) = \tilde{F}_0(r_2, \Theta_2),$$

and we have for the exchange amplitude

$$\frac{2\pi me^2}{h^2} \iint \left(\frac{1}{r_1} - \frac{1}{r_{12}} \right) \tilde{F}_0(r_2, \Theta_2) \tilde{F}_0(r_1, \pi - \Theta_1) \psi_0^*(r_2) \psi_0(r_1) d\tau_1 d\tau_2. \quad (13)$$

For helium we obtain similar formulæ by following the same method, but as in this case only the antisymmetric cross section is effective it is possible to make a third approximation. If the exchange interference is considerable, then the function $F_0(r_2) - G_0(r_2)$ may approximate to a plane wave and we obtain the exchange amplitude

$$\begin{aligned} \frac{2\pi me^2}{h^2} \iiint \left(\frac{2}{r_1} - \frac{1}{r_{12}} - \frac{1}{r_{13}} \right) e^{i(\mathbf{n}_0 \cdot \mathbf{r}_2)} \\ \times \tilde{F}_0(r_1, \pi - \Theta_1) \psi_0(r_1, r_3) \psi_0^*(r_2, r_3) d\tau_1 d\tau_2 d\tau_3 \end{aligned} \quad (14)$$

Unfortunately it is not always clear when this formula may be applied, as the interference may only be considerable at large distances, and the deviations of $F_0(r_2) - G_0(r_2)$ from a plane wave may still be important in the region of the atom.

Before we proceed to consider the application of the formulæ of this section, we will first consider the approximations involved. Firstly we see that the wave function Ψ must satisfy the orthogonality relations

$$\left. \begin{aligned} \int \{ \Psi - F_n(r_1) \psi_n(r_2) \} \psi_n^*(r_2) d\tau_2 &= 0 \\ \int \{ \Psi - G_n(r_2) \psi_n(r_1) \} \psi_n^*(r_1) d\tau_1 &= 0 \end{aligned} \right\}. \quad (15)$$

for Ψ may be expanded in either of the forms

$$\begin{aligned} \Psi &= \sum_n F_n(r_1) \psi_n(r_2), \\ \Psi &= \sum_n G_n(r_2) \psi_n(r_1). \end{aligned}$$

The approximate expressions for Ψ do not satisfy these conditions and consequently terms appear in the expressions for the scattered amplitudes which would vanish if exact formulæ could be obtained. Thus in expressions (12), (13), and (14) the terms in $1/r_1$ should vanish. For sufficiently high velocities of impact these terms will be small, but for low velocities the errors introduced will be considerable. However, one cannot simply drop the terms in $1/r_1$ in the amplitude integrals as the contribution from the remaining terms would also be different in an exact theory. In order to correct partially for the non-orthogonality it is advisable to retain the terms in $1/r_1$ as was explained in Paper A. Feenberg† has introduced a second method of attempting to correct for the non-orthogonality which may be more accurate. In this method, instead of substituting the approximation $H(r_2)$ (either e^{ikr_2} or $\mathfrak{F}_0(r_2)$) for $F_0(r_2) - G_0(r_2)$ one takes the form

$$H(r_2) - \psi_0(r_2) \int H(r) \psi_0^*(r) d\tau$$

which is orthogonal to $\psi_0(r_2)$. On substitution in (11) we obtain the formulæ (12) and (13) but with

$$\int \frac{1}{r_{12}} |\psi_0(r_2)|^2 d\tau$$

in place of $1/r_1$. This method is partially justified by the fact that if $F_0(r_1) \pm G_0(r_1)$ is a solution of the equation (6), then so also is

$$F_0(r_1) \pm G_0(r_1) + c\psi_0(r_1).$$

The approximation of neglecting the effect of the inelastically scattered waves is connected with the difficulty discussed above, but it will be serious at low velocities in other ways also. In order to include the reaction of the inelastic scattering it is necessary to use a method of approximation which commences from atomic wave functions already perturbed by the interaction with the colliding electron.

† 'Phys. Rev.', vol. 40, p. 40 (1932).

[*Note added in Proof*—While this paper was in course of publication, a second paper has appeared by Feenberg ('Phys. Rev.', vol. 42, p. 17, (1932)), which contains a note added in proof. In this note, Feenberg states that we derive equations "resembling only remotely the equations" found by him. He also states that our equations are "at best of doubtful validity". It will be perfectly obvious from the above that the resemblance between the two sets of equations is by no means remote, and in the voltage range in which Feenberg uses the equations the two methods give results which are almost identical. At voltages below 10 volts neither method can lay claim to accuracy as is clear from comparison with experiment.]

B. Inelastic Collisions.—The scattering of electrons which have excited the n th state of atoms of hydrogen and helium may be described by means of two wave functions $F_n(r_1)$, $G_n(r_2)$ which have the asymptotic form

$$\left. \begin{aligned} F_n(r_1) &\sim r_1^{-1} e^{ik_n r_1} f_n(\theta_1, \phi_1) \\ G_n(r_2) &\sim r_2^{-1} e^{ik_n r_2} g_n(\theta_2, \phi_2) \end{aligned} \right\}, \quad (16)$$

where F and G are combined in the same way as f and g to obtain the cross-section. In Paper B, § 3, these functions are shown to satisfy the equations

$$\left. \begin{aligned} [\nabla_1^2 + k_n^2] F_n(r_1) &= \frac{8\pi^2 m e^2}{\hbar^2} \left\{ \left(\frac{1}{r_1} - \frac{1}{r_{12}} \right) \Psi(r_1, r_2) \psi_n^*(r_2) d\tau_2 \right. \\ [\nabla_2^2 + k_n^2] G_n(r_2) &= \frac{8\pi^2 m e^2}{\hbar^2} \left\{ \left(\frac{1}{r_2} - \frac{1}{r_{12}} \right) \Psi(r_1, r_2) \psi_n^*(r_1) d\tau_1 \right. \end{aligned} \right\}. \quad (17)$$

We neglect the interaction of all states except the initial and n th state, and take

$$\Psi = F_0(r_1) \psi_0(r_2) + F_n(r_1) \psi_n(r_2) + G_n(r_2) \psi_n(r_1), \quad (18)$$

where $F_0(r_1)$ represents the incident and elastically scattered waves and is the solution of the equation

$$\left[\nabla_1^2 + k^2 - \frac{8\pi^2 m}{\hbar^2} V_{00}(r_1) \right] F_0 = 0. \quad (19)$$

This amounts to neglecting in equations (17) all non-diagonal matrix elements of the interaction energy except those which refer to the initial state, as may be seen by substituting the expression (18) for Ψ in equations (17).

On substitution in (17) we obtain, by following a similar procedure to that used in the consideration of the elastic exchange, the equation

$$\left[\nabla_1^2 + k_n^2 - \frac{8\pi^2 m}{\hbar^2} V_{nn}(r_1) \right] \{F_n(r_1) - G_n(r_1)\} = - \frac{8\pi^2 m e^2}{\hbar^2} \left\{ \int \left(\frac{1}{r_1} - \frac{1}{r_{12}} \right) [F_0(r_1) \psi_0(r_2) \psi_n^*(r_2) - F_0(r_2) \psi_0(r_2) \psi_n^*(r_1) - (G_n(r_2) - F_n(r_2)) \psi_n(r_1) \psi_n^*(r_2)] d\tau_2 \right\}, \quad (20)$$

where

$$V_{nn}(r_1) = - \int \frac{e^2}{r_{12}} |\psi_n(r_2)|^2 d\tau_2.$$

We are now in a position to obtain approximate formulæ for the amplitude of the inelastically scattered waves.

Firstly, for high velocities of impact, we have

$$F_0(r_1) = e^{ik_{n0} \cdot r_1}, \quad F_n = 0 \quad (n \neq 0), \quad G_n = 0,$$

on the right-hand side of equation (20) and we neglect the effect of the term V_{nn} . This gives the formula of Paper A, viz.,

$$\left[\nabla^2 + k_n^2 - \frac{8\pi^2 m}{h^2} V_{00} \right] F_0 = 0. \quad (21)$$

Secondly, if the effect of exchange is small, we have

$$\left[\nabla^2 + k_n^2 - \frac{8\pi^2 m}{h^2} V_{nn} \right] [F_n - G_n] = - \frac{8\pi^2 m}{h^2} V_{0n} F_0. \quad (22)$$

We require the asymptotic form of the solution of this equation which satisfies the boundary conditions: (a) $F_n - G_n$ is finite everywhere, (b) $F_n - G_n$ has the asymptotic form

$$r^{-1} e^{ik_n r} f_n(\theta, \phi).$$

It is

$$F_n - G_n \sim r^{-1} e^{ik_n r} \frac{2\pi m}{h^2} \int V_{0n}(r_1) F_0(r_1, \theta_1) \mathfrak{F}_n(r_1, \Theta_1) d\tau_1, \quad (23)$$

where $\mathfrak{F}_n(r, \Theta)$ is that solution of the homogeneous equation

$$\left[\nabla^2 + k_n^2 - \frac{8\pi^2 m}{h^2} V_{nn} \right] \mathfrak{F}_n = 0, \quad (24)$$

which has the asymptotic form

$$\mathfrak{F}_n \sim e^{ik_n r \cos \Theta} + r^{-1} e^{ik_n r} h_n(\theta, \phi),$$

where

$$\cos \Theta = \cos \theta_1 \cos \theta + \sin \theta_1 \sin \theta \cos(\phi_1 - \phi),$$

θ being the angle of scattering.

For this case the scattered amplitude is then

$$\frac{2\pi m}{h^2} \int V_{0n}(r_1) F_0(r_1, \theta_1) \mathfrak{F}_n(r_1, \Theta) d\tau_1. \quad (25)$$

In other cases a satisfactory method of approximation is more difficult to obtain. In dealing with two electron atoms, the interference of F_n and G_n may be such that $F_n(r_2) - G_n(r_2)$ on the right-hand side of (20) may be neglected. We then obtain for the scattered amplitude

$$\frac{2\pi m e^2}{h^2} \int \left(\frac{1}{r_1} - \frac{1}{r_{12}} \right) \{ F_0(r_1) \psi_0(r_2) \psi_n^*(r_2) \mathfrak{F}_n(r_1, \Theta) \\ - F_0(r_2) \psi_0(r_2) \psi_n^*(r_1) \mathfrak{F}_n(r_1, \Theta) \} d\tau_2. \quad (26)$$

When the exchange effect is large there is no satisfactory method of approximation. The procedure followed in this paper is to calculate the probabilities from the formulæ within their range of validity. To obtain some idea of the behaviour beyond this range, the expression (26) is used even when the exchange effect is considerable, *i.e.*, for electron energies just above the excitation potential of the particular level considered. In any case the method is not valid in this region as the expression (18) for Ψ does not satisfy the orthogonality relations (15). The error introduced by neglecting non-diagonal matrix elements is probably considerable and the chief interest of the detailed calculation of the amplitudes (25) and (26) and comparison of the results with experiment is to determine how important these neglected terms are.

§ 2. *Detailed Calculation of Cross Section.*

A. Elastic Scattering.—The method of calculation is very similar to that described in Paper B and it is only necessary to discuss the results. The most important point to establish in connection with elastic exchange in helium and hydrogen is that the voltage at which the peculiar effects first occur in the observed angular distributions (below 15 volts in helium and 5 volts in hydrogen) is that voltage below which exchange becomes important. The use of the formula (26) does not affect the conclusions of Paper B in this respect, the changes introduced for voltages greater than 15 volts in helium being unimportant. At such voltages exchange is so small that it has no appreciable effect on the angular distribution; below 15 volts, however, exchange becomes appreciable just as before.

While discussing the elastic scattering, it is interesting to note the considerable difference between the calculated angular distributions and those observed recently by Hughes, McMillen, and Webb† in helium above 30 volts to as high as 350 volts. These observers find that the angular distributions fall off much more rapidly with increasing angle of scattering at small angles than those calculated from the Born formula. The effect of exchange appears to be much too small at these voltages to explain this effect which must be due to polarisation or some related phenomenon. The deviations which they observe at large angles, where the experimental curves remain fairly flat instead of falling continually as required by the Born formula, are readily explained as due to distortion; the coefficient of the harmonic P_0 only is disturbed, so that the scattering at large angles is practically constant, since $P_0(\cos \theta) = 1$.

† 'Phys. Rev.', vol. 41, p. 154 (1932).

B. *Inelastic Scattering*.—Owing to the very considerable complication of the calculations, the cross-sections for excitation of the 2^1P and 2^3P levels only were computed. For these states the same atomic wave functions as those used in Paper A were taken. These are of the form, using atomic units :

$$\psi_n(r_1, r_2) = Y_1(\cos \theta_2) e^{-2r_1 - 4r_2} \pm Y_1(\cos \theta_1) e^{-4r_1 - 2r_2}, \quad (27)$$

where Y_1 is a normalised surface spherical harmonic of order 1, and the upper and lower signs corresponding to the singlet and triplet levels respectively. Substituting in expression (26) we see that it is necessary to evaluate integrals of the form

$$\int \frac{1}{r_{13}} \psi_0(r_1, r_2) \psi_n^*(r_1, r_2) F_0(r_3) \mathfrak{F}_n(r_3) d\tau_1 d\tau_2 d\tau_3, \quad (28)$$

$$\int \left(\frac{2}{r_1} - \frac{1}{r_{12}} - \frac{1}{r_{13}} \right) \psi_0(r_1, r_2) \psi_n^*(r_2, r_3) F_0(r_3) \mathfrak{F}_n(r_1) d\tau_1 d\tau_2 d\tau_3, \quad (29)$$

where \mathfrak{F}_n is the solution of the equation

$$\left[\nabla^2 + k_n^2 - \frac{8\pi^2 m}{\hbar^2} V_{nn} \right] \mathfrak{F}_n = 0, \quad (30)$$

which is normalised so as to have the asymptotic form

$$e^{-ik_n r \cos \theta} + r^{-1} e^{ik_n r} h_n(0, \phi).$$

The field V_{nn} corresponding to any of the three wave functions (27) with the respective forms $\cos \theta$, $2^{-1} \sin \theta e^{+\phi}$ for the surface harmonic function is not spherically symmetrical, but by averaging over all orientations of the axis of co-ordinates one obtains

$$V_{nn} = \left(\frac{1}{2} r^2 + \frac{1}{4} r + \frac{3}{4} + \frac{1}{r} \right) e^{-r} + \left(2 + \frac{1}{r} \right) e^{-4r}, \quad (31)$$

which is sufficiently accurate. With V_{nn} in this form one may expand \mathfrak{F}_n in harmonics in the form

$$\mathfrak{F}_n = \sum_l A_l \mathfrak{F}_n^{(l)} P_n(\cos \theta), \quad (32)$$

and equation (30) becomes

$$\frac{d^2}{dr^2} (r \mathfrak{F}_n^{(l)}) + \left\{ k_n^2 - \frac{8\pi^2 m}{\hbar^2} V_{nn} - \frac{l(l+1)}{r^2} \right\} (r \mathfrak{F}_n^{(l)}) = 0. \quad (33)$$

The calculation of the \mathfrak{F}_n from this differential equation has been carried out by McDougall† who finds that the terms with $l = 0, 1, 2$ differ appreciably

† 'Proc. Camb. Phil. Soc.', vol. 28, p. 341 (1932).

from plane waves for incident electrons with energies up to 120 volts. In order to satisfy the normalising condition we must have

$$A_l = i^{-l} e^{i\gamma_l} (2l+1), \quad (34)$$

where γ_l is the phase constant which is such that $r \mathfrak{F}_n^l$ has the asymptotic form

$$a_l \sin(k_n r - \frac{1}{2} l \pi + \gamma_l). \quad (35)$$

We may then write

$$\mathfrak{F}_n^l = \sum_l i^{-l} e^{i\gamma_l} (2l+1) \mathfrak{F}_n^l P_l(\cos \theta), \quad (36)$$

where for $l > 2$ we may take

$$\gamma_l = 0, \quad \mathfrak{F}_n^l(r) = \left(\frac{2\pi}{k_n r}\right)^{\frac{1}{2}} J_{l+\frac{1}{2}}(k_n r). \quad (37)$$

Alternatively we may write

$$\mathfrak{F}_n^l(r) = e^{-i k_n r} + \sum_{l=0}^{\infty} i^{-l} e^{i\gamma_l} \left\{ \mathfrak{F}_n^l(r) - \left(\frac{2\pi}{k_n r}\right)^{\frac{1}{2}} J_{l+\frac{1}{2}}(k_n r) \right\} P_l(\cos \theta). \quad (38)$$

The function F_0 , which is the solution of the problem of the elastic scattering by the static field of the normal helium atom, has already been discussed in Paper B where it was shown to have the form

$$F_0(r) = e^{i k_0 r} + e^{i \delta_0} F_0^0(r) - \left(\frac{2\pi}{k r}\right)^{\frac{1}{2}} J_{\frac{1}{2}}(kr). \quad (39)$$

The calculation of the integral (28) is most conveniently carried out by using the expressions (38) and (39), and so obtaining the integral in the form

$$I = I_B + \text{correcting terms in } P_l(\cos \theta),$$

where I_B is the value given by Born's first (plane wave) approximation, which is given in Paper A.

The exchange integral (29) is most easily evaluated by using the expressions (36) and (37).

§ 3. Results and Discussion.

In view of the approximations necessary in deducing the general formulæ, it is unlikely that the calculated cross-sections are correct for energies of impact less than 35 volts, but the calculations have been extended to lower voltages than this in order to see in what direction they are at fault. The results of the calculations are illustrated in figs. 1 and 2. The probabilities of excitation to the 2^1P and 2^3P levels for electrons with incident energies below 100 volts are illustrated in fig. 1, together with the experimental curves for the 3^1P

and 3^3P levels recently obtained by Lees.[†] The dotted portion of the curves indicates the region in which the calculations are probably not accurate. Comparison of these curves with those calculated using Born's approximation (Paper A) shows that the agreement with experiment has been improved to a slight extent, in that the maximum probability of excitation of the singlet level lies at a higher voltage, and the maximum is not so flat as in the calculations of Paper A.[‡] The calculated magnitudes of the $2P$ singlet and triplet excitation probabilities at 100 volts are $0.11 \pi a_0^2$ and $0.0007 \pi a_0^2$ respectively, while the ratio observed by Lees for the $3P$ levels is about 10. The latter figure has to be corrected on account of the various optical transitions which take place in the experiments, before exact comparison with theoretical magnitudes can be made; when this is done, it is found that the calculated

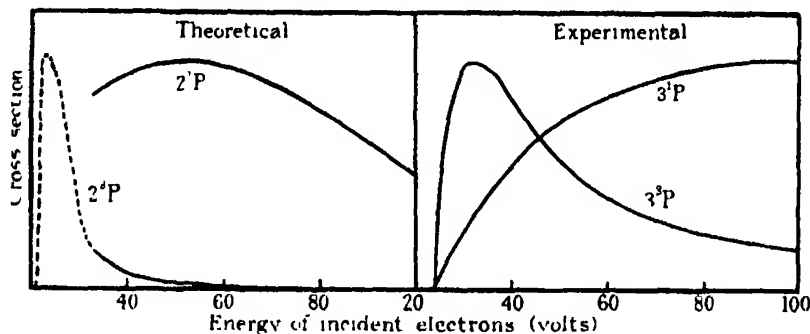


FIG. 1.

ratio of the cross-sections at 100 volts is roughly the value indicated by experiment. The rate of fall of the experimental triplet curve beyond 50 or even 100 volts is much more gradual than for the theoretical triplet curve, which falls off quite rapidly above 50 volts, although the theory should be fairly accurate at such voltages. This will be discussed in a later paper which will contain calculated probabilities for excitation to a number of excited levels for electrons with energies above 50 volts.

With regard to the discrepancy between theory and experiment for electrons of low velocity, one general feature of the excitation curves is seen to be present. In all cases, the theory predicts too large a cross-section for low velocity impacts. This feature occurs particularly in the excitation of optically allowed levels, as in the case of excited singlet P states in two-electron systems, and in

[†] 'Proc. Roy. Soc.,' A, vol. 137, p. 173 (1932).

[‡] In fig. 1, only the forms of the theoretical and experimental curves can be compared, not their absolute magnitudes

the case of ionisation.† This behaviour is probably due to the neglect of the disturbance of the atomic wave functions by the incident electron, and further improvements in the theory must take the form of a perturbation method in which this disturbance of the atom is taken into account in the initial approximation.

The angular distributions of the scattered electrons are illustrated in fig. 2. The form of these curves at large angles is very sensitive to changes in the relative magnitude of the various terms, and we therefore give curves for the case of the 2^1P excitation with and without the effect of exchange.

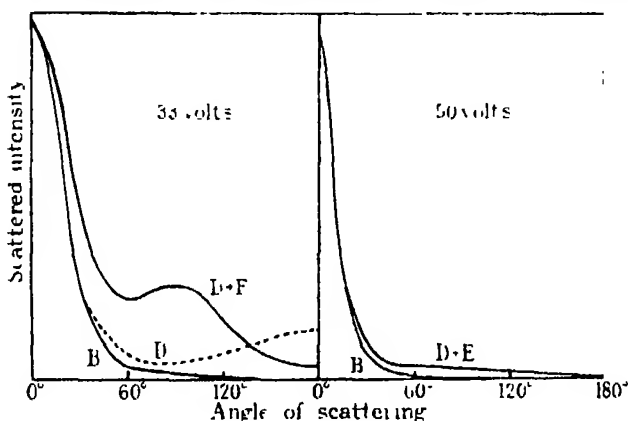


FIG. 2.—Illustrating angular distributions of electrons which have excited the 2^1P state in helium. B denotes curves calculated with the use of Born's formula, D that calculated including the effect of distortion, D + E that calculated including the effect of distortion and exchange.

Angular distributions have been measured by Mohr and Nicoll‡ for the case of those electrons which have excited the atom to the 2^1P level. Their curves for 83 and 120 volt electrons are fairly flat at large angles of scattering, an effect which is easily explained as due to distortion of the zero order wave as in the case of the elastic scattering. Their curve for 54 volt electrons shows indications of the maximum which appears in the calculated curve in fig. 2, as already described.

4. Inelastic Scattering by Heavy Atoms.

We now consider the diffraction effects observed by Mohr and Nicoll‡ in the angular distributions of electrons scattered inelastically by heavy atoms. These inelastic angular distributions are seen to exhibit maxima and minima,

† The subject of ionising collisions will be discussed in a paper to be published shortly.

‡ 'Proc. Roy. Soc.,' A, vol. 138, p. 229 (1932).

the curves being closely similar at large angles and moderate velocities to the corresponding curves for the elastic scattering of electrons of the same incident velocity. In the following discussion, exchange effects are neglected.

In the case of the elastic scattering, the scattered intensity at an angle of scattering θ is given by†

$$I(\theta) = \left| \sum_l \frac{2l+1}{2ik} (e^{2i\eta_l} - 1) P_l(\cos \theta) \right|^2 \quad (40)$$

When the η_l 's are all small compared with unity, this expression reduces to the value given by the Born approximation, and which we shall denote by $I_B^2(\theta)$. We may then write the exact expression (40) in the form

$$I(\theta) = \left| I_B^2(\theta) + \frac{1}{2ik} \sum_l (2l+1) (e^{2i\eta_l} - 1 - 2i\eta'_l) P_l(\cos \theta) \right|^2, \quad (41)$$

where η'_l denotes the value of the phases as given by the Born approximation ‡. For large l , $\eta_l = \eta'_l$. Now the function $I_B(\theta)$ is known to fall off rapidly with increasing θ , while the correcting terms are less dependent on angle, consisting mainly of contributions from the first few harmonics. Therefore the influence of the corrections will be most noticeable at large angles. In the case of helium, it is only the first term of the series in (41) which is important, giving an angular distribution almost constant at large angles as already pointed out in § 3. In the case of heavy atoms, the method has been successful in explaining the observed angular distributions in many cases.

In the case of the scattering of electrons which have excited the n th state of a given atom, we have for the intensity of scattering, by a generalisation of formula (25):

$$I_n^2(\theta) = \left| \frac{k_n}{k} \frac{8\pi^2 m^2}{h^4} \int V_{0n}(r') F_0(r', \theta') \mathfrak{F}_n(r', \pi - \Theta') d\tau' \right|^2, \quad (42)$$

where

$$V_{0n}(r) = \int V(r, r_a) \psi_0(r_a) \psi_n^*(r_a) d\tau_a,$$

the suffix a distinguishing the co-ordinates of the atomic electrons. The functions $F_0(r, \theta)$, $\mathfrak{F}_n(r, \Theta)$ can be written in the form

$$F_0(r, \theta) = e^{ikr \cos \theta} + \sum_l \left\{ F_0^l(r) - \left(\frac{2\pi}{kr} \right)^{\frac{1}{2}} J_{l+\frac{1}{2}}(kr) \right\} (2l+1) i^l P_l(\cos \theta), \quad (43)$$

$$\mathfrak{F}_n(r, \pi - \Theta) = e^{-i k_n r \cos \Theta} + \sum_l \left\{ \mathfrak{F}_n^l(r) - \left(\frac{2\pi}{k_n r} \right)^{\frac{1}{2}} J_{l+\frac{1}{2}}(k_n r) \right\} (2l+1) i^l P_l(\cos \theta), \quad (44)$$

where the first term denotes the plane wave undisturbed by the atomic field, and the series represents the disturbance of the plane waves by the fields of

† 'Z. Physik,' vol. 45, p. 307 (1927).

‡ Mott, 'Proc. Camb. Phil. Soc.' vol. 25, p. 304 (1928).

the normal and excited atom respectively. Substituting in expression (42) we find that $I_n^2(\theta)$ is given by an expression of the form

$$I_n^2(\theta) = \frac{k_n}{k} \frac{8\pi^2 m^2}{h^4} \left| \int V_{0n}(r') \exp. i(kr' \cos \theta' - k_n r' \cos \Theta') d\tau' \right. \\ \left. + \sum_l P_l(\cos \theta) \int V_{0n}(r') H_l(r', \theta', \phi') d\tau' \right|^2. \quad (45)$$

The first integral is just that occurring in Born's formula and its magnitude is small at angles greater than about 30° , so that at large angles the main contribution comes from the series. The number of harmonics important in this series determines the diffraction effects at angles greater than 30° . Now if the energy of the incident electrons is much greater than the excitation energy, $k_n \simeq k$, and the fields of the normal and the excited atom are effectively the same. In this case, the same number of terms in (43) and (44) will be required and they will be of the same relative importance as for the elastic scattering which is described by (41). The diffraction effects will therefore be similar in the two cases, just as has been observed.† For low velocities this will not be true, as the field V_{nn} has a much greater spread than V_{00} and so will affect more harmonics of \mathfrak{F}_n than V_{00} will of F_0 . Also the difference between k_n and k will be important at low velocities. Hence the inelastic and elastic angular distributions should become dissimilar at large angles at sufficiently low velocities, as has been found to be the case experimentally. Detailed calculations are in progress for the case of the inelastic scattering in argon.

Summary.

The theory of collisions of slow electrons with atoms given in a previous paper has been extended to include the effect of the distortion of both the incident and scattered electron waves by the static field of the atom, together with the effect of electron exchange. Using this method the inelastic scattering of slow electrons in helium is considered for the case of the excitation of the 2^1P and 2^3P states of the atom. It is seen that the effect of the distortion does not introduce any great modification of the form of the inelastic cross section curves, and the lack of agreement with experiment at quite low velocities is thought to be due to the neglect of other complicating factors in the theory, in particular the effect of polarisation. The theory is adequate to explain the observed effect of the diffraction of inelastically scattered electrons by heavy atoms.

† If the potential V_{0n} is not spherically symmetrical, extra terms will appear in formula (45) involving the harmonics $P^m(\cos \theta)$. For the excitation of optically allowed levels, the effect of these terms on the general form of the angular distribution does not appear to be great.

*Interferential Comparison of the Red and other Radiations emitted by
a New Cadmium Lamp and the Michelson Lamp.*

By J. E. SEARS, Jnr., C.B.E., M.A., M.I.Mech.E., and H. BARRELL, B.Sc.,
A.R.C.Sc., D.I.C.

(Communicated by Sir Joseph Petavel, F.R.S.—Received September 9, 1932.)

[PLATE 2.]

(1) *Introduction*

It is now generally recognised that future definitions of the units of length will probably be based on the length of a wave of visible light. At present the wave-length of the red radiation of cadmium serves as the basis of all measurements of the lengths of electro-magnetic waves which are perceptible by optical means, and provisional sanction has been given to measurements of length on the same basis, as an alternative to direct reference to the metre.*

Whether the cadmium red radiation provides the best reference standard for all measurements of length has not yet been definitely established. Two international committees, one representing spectroscopists† and the other metrologists,* have sanctioned standard specifications for cadmium lamps of the Michelson type from which the red radiation may be produced. The two specifications differ from one another in certain details, but both are subject to the same objections. These objections are directed partly against the high temperature at which it is necessary to run the lamp and partly against the high voltage required to excite the radiation. Therefore, such hyperfine structure and asymmetry as may be present in the red line of cadmium is likely to be masked in the Michelson lamp by a combination of two phenomena—the enhanced Doppler effect due to the high temperature of the radiating cadmium atoms, and the effect of the moderately high intensity of the electric field. Were this not so, it might be somewhat surprising that no definite evidence of fine structure or asymmetry had so far been observed in the red line from the Michelson lamp, notwithstanding the many careful examinations, with the aid of the most sensitive interferometers, to which this line has been subjected, in view of its importance as the reference standard for all other wave-lengths. Recently Nagaoka and Sugiura‡ have recorded that they have

* “Cté. int. Pds. Mes.; Procès-Verbaux des Séances,” p. 67 (1927).

† ‘Trans. Int. Astron. Union,’ vol. 2, pp. 188, 232 (1925).

‡ ‘Sci. Pap. Inst. Phys. Chem. Res., Tokyo,’ vol. 10, p. 263 (1929).

observed slight evidences of structure in the red radiation when excited under special conditions in which great precautions were taken to ensure extreme sharpness of the line. It is believed, however, that no subsequent confirmation of this effect has yet been published.

There are further minor disadvantages associated with the use of the Michelson lamp, among which is the necessity for an auxiliary furnace to maintain the cadmium in a vaporised state, and this may be additionally inconvenient where constant temperature conditions are desired in the neighbourhood of the spectrograph or interferometer. Also, the lamp is not a particularly intense source of light, and has not, in its standard form, a very long life. Some of the disadvantages of the Michelson lamp have been overcome in a new, high intensity cadmium lamp which has been recently developed at the Osram laboratories in Germany.* So far as is known no description of this lamp has been published, but a sodium lamp of similar type has been described by Reger.† The difficulty of temperature disturbances in the room is not eliminated by using the new lamp, but in other respects the lamp is a much more convenient source of highly monochromatic red radiation than the Michelson lamp. The primary object of the investigation described in this paper has been to effect a comparison between the wave-lengths of the red radiation emitted by the Michelson and Osram lamps, and to examine the red line from the latter for evidences of fine structure. At the same time comparisons of the wave-lengths and fine structure of the green and two blue lines of cadmium have also been made.

(2) Apparatus and Method.

The type of Michelson lamp used in the present work has been described elsewhere.‡ It does not conform with the standard specifications in one important detail, for the lamp, instead of being highly evacuated and sealed, is permanently connected to a large glass bulb containing air at 1 mm. pressure. This modification, which was first suggested and tried by Pérard,§ appears to overcome the disadvantage of the short life of the standard lamp. The normal conditions of excitation of this modified Michelson lamp were temperature 320° C., pressure 1 mm., intensity of current 0·05 amp. per cm.², and potential

* Studien-Gesellschaft für Elektrische Beleuchtung m.b.H.

† 'Z. InstrKunde,' vol. 51, p. 472 (1931).

‡ Sears and Barrell, 'Phil. Trans.,' A, vol. 231, p. 111 (1932).

§ 'Rev. d'Optique,' vol. 7, p. 10 (1928).

difference across the electrodes about 600 volts. Experience with the highly evacuated type of lamp has shown that its internal resistance rapidly increases during the early stages of its life, until a voltage of about 2000 is required to pass the same current. Thus, the modified lamp, in addition to its longer life, has the advantage of consistent conditions of excitation at a much lower potential. The limit of interference in the red line produced from the modified Michelson lamp is about 450,000 waves, corresponding to a path difference of about 300 mm.

The new Osram lamp consists of a sealed cylindrical glass tube, about 10 cm. long and 1.75 cm. diameter, having a coiled filament at each end. The tube contains argon, at low pressure, and cadmium, and is enclosed in an evacuated glass jacket of diameter 3.5 cm and 17 cm. long. The jacket is held at one end in a 4-pin base of the type usually associated with thermionic valves, and the ends of the two filaments are brought out separately through a "pinch" to the four pins.

The lamp is connected in series with a variable resistance and is operated from a 220-volt A.C. supply, capable of delivering 2 amperes. The external connections to the four pins of the lamp are arranged so that the two filaments can be joined in series with one another by closing a switch, the two filaments and the resistance then being all in series with the 220-volt leads. The two filaments quickly become incandescent, and after 20 seconds have elapsed the switch is opened. This action throws the voltage across the argon in the inner tube, the two heated filaments now acting as the two electrodes for this purpose, and a glow discharge is immediately started in the gas. When the value of the resistance is adjusted to 95 ohms (as recommended by the makers), the lamp passes a current of 2 amperes. Within 2 minutes the cadmium in the inner tube becomes partially vaporized, owing to the heat generated by the discharge. Examination of the visible spectrum of the lamp at this stage showed that the intensity of the argon lines gradually diminished, while that of the cadmium lines increased. The green and two blue lines of cadmium first appeared, followed later by the red line, and within 5 minutes of starting the lamp the argon spectrum entirely disappeared.

If the value of the resistance is increased, the lamp can be made to run quite satisfactorily on currents of 1 ampere and lower. It is shown later that some interesting changes take place in the structure and fineness of the cadmium lines when the current through the lamp is increased from 1 to 2 amperes.

Concerning the life of these new cadmium lamps, one of them broke down after about 9 hours running, owing to a mechanical defect, but another has

been used for an aggregate period now exceeding 80 hours, and is still in perfect condition.

The instrument used for the comparison of wave-lengths was a Fabry-Perot interferometer made by Hilger. The distance between the parallel semi-silvered glass plates was variable from 0 to 200 mm. A convergent beam of light from either source could be directed at will, using a reflecting prism, on to a 1 cm. aperture in a screen fixed in front of the movable plate of the interferometer. The light transmitted by the interferometer plates was focussed by an achromatic lens, of 27 cm focal length, on to the wide slit of a small spectrograph having a constant-deviation prism, and produced there a real image of the complex system of circular interference fringes due to the various monochromatic radiations. The dispersive system of the spectrograph produced images of the slit in these radiations at the focal plane of the camera lens, which had a focal length of 46 cm., and each image of the slit was crossed by a diametral section of the circular fringe system produced by the corresponding radiation, see fig. 1, Plate 2. The camera of the spectrograph held a plate of size 6 cm. by $4\frac{1}{2}$ cm., and the dispersion was such that the whole of the visible spectrum could be photographed simultaneously across the shorter dimension of the plate, which was of the type known as Ilford Soft Gradation Panchromatic

The diameters of five bright fringes in each image of the slit were subsequently measured on the plate by means of a travelling microscope, and their values were used to calculate the "excess fractions" in the usual manner by a method of least squares.* The measurements were confined to the four intense radiations at 6438 Å., 5086 Å., 4800 Å., and 4678 Å.

Observations were made on the two sources for a series of 12 path differences, increasing by steps of 20 mm. from 20 mm. to 240 mm. The order of interference for the red line, and incidentally for the other lines, corresponding to the smallest of these path differences, was derived from a preliminary experiment in which the usual "method of coincidences" was applied to the group of excess fractions which were measured in a series of radiations of neon, in addition to those of cadmium, using for the purpose of this method an approximate value of the distance between the interferometer plates obtained from the scale of the interferometer. Having thus established the orders of interference corresponding to a known point on the scale of the instrument, the values of the orders for the four cadmium radiations at greater path differences were quite easily identifiable by the application of the method of coincidences to

* Rolt and Barrell, 'Proc. Roy. Soc.,' A, vol. 122, p. 131 (1929).

the measured excess fractions in these four radiations only. To eliminate any uncertainty due to errors in the scale and micrometer attached to the interferometer, checks were made by additional observations on krypton lines at some of the larger path differences.

The following procedure was adopted at each setting of the interferometer for photographing the interference phenomena in light from the two sources. First an exposure was made with the Michelson lamp. Then two exposures were made in succession with the Osram lamp excited by a current of 1 ampère, and these were succeeded by a further exposure with the Michelson lamp. After this two exposures were made in succession with the Osram lamp excited by a current of 2 amperes, and these were followed by a final exposure with the Michelson lamp.

Suitable exposures for the Michelson lamp varied from 4 minutes at the smaller path differences up to 8 minutes at the larger. It was found necessary to give longer exposures for the red line than for the other lines in the Osram lamp. This was done by dividing symmetrically into three parts the total exposure time required for the red line. During the first part a Wratten filter No. 26, transmitting only the red radiation, was interposed between the Osram lamp and the interferometer; then the filter was removed for the second part to allow the complete spectrum to be photographed; for the third part the filter was again interposed as at first. For the Osram lamp in the 1 ampere condition exposures ranged from $3\frac{1}{2}$ to 5 minutes for the red line, and from 35 to 50 seconds for the other lines, while for the lamp in the 2 ampere condition exposures ranged from 40 to 70 seconds for the red line and from 5 to 10 seconds for the other lines. The difference between the intensities of the sources is clearly demonstrated by comparing these values of the exposure times.

The arrangement of the work described above made it possible to compare, at each path difference, the order of interference for the red line from the Michelson lamp with that from the Osram lamp in the two conditions of exciting current. Thus the mean value derived from the first and second observations with the Michelson lamp was compared with the mean derived from the two interpolated observations with the Osram lamp in the 1 ampere condition, and the mean value from the second and third exposures with the Michelson lamp was compared with the mean from the two interpolated observations with the Osram lamp in the 2 ampere condition.

The accuracy of the above method of comparison depends upon the temperature conditions of the interferometer and the ambient air being constant, or else uniformly changing with time. The room temperature was thermo-

statically controlled during the work by a toluene-mercury thermo-regulator, but its action was not entirely satisfactory owing to the temperature disturbances caused by the presence of the two hot cadmium lamps in the room. Owing to the comparatively high thermal coefficient of expansion of the steel slides and screw of the Fabry-Perot interferometer, the slight departures from linear changes of temperature with time, which sometimes occurred, led to a somewhat lower precision being obtained in the comparisons than had been expected.

In order to reduce the observed orders of interference to values under the usually accepted standard conditions of air, concurrent observations were made, during the photographic work, of the temperature of the air between the interferometer plates and of the barometric pressure and humidity of the air in the room.

The photographic records made for the purpose of comparing the red lines were used also for determining the wave-lengths of the other lines. Having established, as will be seen later in Table I, that the wave-lengths of the red line produced from both sources were identical within the limits of experimental error, it was possible to determine, by the usual methods, the wave-lengths of the other cadmium lines in terms of the accepted value of the wave-length of the red line.

The green and two blue lines of cadmium are known to have fine structure, and some new determinations of the positions of the satellites were made in both sources at the smaller path differences. Fig. 1, Plate 2, is a photograph showing the interference fringes, at a path difference of about 19.4 mm., due to cadmium radiations emitted by the Osram lamp when excited by a current of 2 amperes. It will be noted that the red line is apparently free from structure but that the other lines are each accompanied by one or more satellites. Similar photographs were obtained at the same path difference with the Michelson lamp and with the Osram lamp when excited by a current of 1 ampere.

(3) *Results*

For convenience of reference in the tables and explanatory matter which appear in this section, the following symbols are used. λ_R , λ_G , λ_{B1} and λ_{B2} represent respectively the wave-lengths of the red, green and two blue lines of cadmium. At each path difference over which comparisons were made, M_1 , M_2 and M_3 denote respectively the first, second and third observations on the Michelson lamp; $(O1)_1$ and $(O1)_2$ denote respectively the first and second

observations on the Osram lamp in the 1 ampere condition, while $(O2)_1$ and $(O2)_2$ denote likewise the two observations on the Osram lamp in the 2 ampere condition. Elsewhere the symbols M , $O1$ and $O2$, without suffixes, are used respectively in referring to the Michelson lamp and the Osram lamp in the two conditions of exciting current.

Table I shows the results of comparisons of the red line. The sequence in which the observations on the sources were taken at each path difference was: M_1 , $(O1)_1$, $(O1)_2$, M_2 , $(O2)_1$, $(O2)_2$ and M_3 . The second column of the table gives the mean values of the orders of interference obtained from M_1 and M_2 ,

Table I.—Results of Comparisons of λ_R .

Path difference (mm)	Orders of interference		$(\mu - \nu1)$	Orders of interference		$(\mu - \nu2)$
	Michelson lamp (μ)	Osram lamp, 1 ampere ($\nu1$)		Michelson lamp (μ)	Osram lamp 2 ampere ($\nu2$)	
19.4	30,065.509	30,065.497	+0.012	30,065.571	30,065.558	+0.013
39.1	60,727.872	60,727.866	-0.006	60,727.855	60,727.859	0.004
60.6	94,198.914	94,198.871	+0.043	94,199.025	94,199.019	0.006
78.8	122,344.714	122,344.719	-0.005	122,344.882	122,344.896	-0.014
99.9	155,213.476	155,213.449	+0.027	155,213.696	155,213.605	0.009
118.6	184,247.042	184,247.050	-0.008	184,246.979	184,246.996	-0.017
140.3	217,849.215	217,849.207	+0.008	217,849.316	217,849.294	-0.022
159.6	247,793.711	247,793.679	+0.032	247,793.795	247,793.768	-0.027
179.9	279,476.864	279,476.840	+0.024	279,477.083	279,477.088	-0.005
201.1	312,377.592	312,377.606	-0.014	312,378.260	312,378.278	-0.018
221.1	343,445.437	343,445.406	+0.031	—	—	—
241.1	374,505.558	374,505.551	+0.004	—	—	—

and the third column gives the mean values of the orders obtained from $(O1)_1$ and $(O1)_2$. Similarly the fifth and sixth columns show respectively, for comparison, the mean values of the orders from M_2 and M_3 , and from $(O2)_1$ and $(O2)_2$. All the orders of interference are corrected to values corresponding to the accepted standard conditions, viz., in dry air at 15° C., under a pressure of 760 mm., and containing an assumed normal proportion (0.03 per cent.) of carbon dioxide. For the purpose of these corrections the values of refractive index and dispersion of air given by Pérard* were used.

The comparisons of the red line from M and $O1$ were not extended beyond a path difference of about 240 mm. (although the interference phenomena were still visible at this stage) for the reason that, beyond 240 mm., it was difficult to determine, without ambiguity, the exact orders of interference by

* 'Trav. Bur. int. Pds. Mes.', vol. 18, p. 42 (1929).

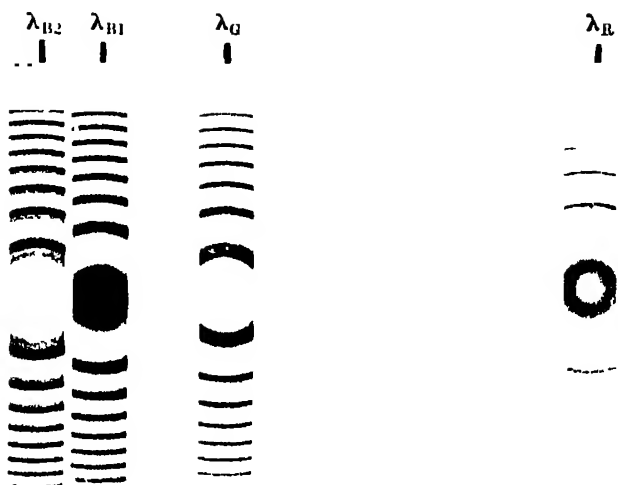


FIG. 1.—Interference fringes in Cadmium radiations at a path difference of 19.4 mm

the method of coincidences, owing to the lack of a sufficient number of suitable auxiliary radiations. The limit of interference in both sources is about 450,000 waves, corresponding to a path difference of about 300 mm.

The visibility of fringes in the red radiation from O2 rapidly declines beyond 200 mm. and subsequent observations were subject to large experimental errors of measurement. They are, therefore, not included in the table. The limit of interference for the red line from O2 is about 500,000 waves. It was observed, however, that as the path difference was increased beyond 200 mm. the fringes completely disappeared over a range extending from about 220 mm. to 245 mm.; then they became just visible again and finally disappeared at about 330 mm. This behaviour indicates certain complexity in the radiation which is not present when it is excited with a current of 1 ampere, and may possibly be due to self reversal.

The algebraic sum of the values of $(\mu - \nu_1)$, given in Table I, is $+0.160$, and that of $(\mu - \nu_2)$ is $+0.001$. The difference is believed to be due to non-linear changes of temperature with time, which particularly affected the interferometer during the earlier portion of certain comparisons, i.e., when M and O1 were being compared. In support of this explanation the relation between path difference (which depends directly on temperature) and time,

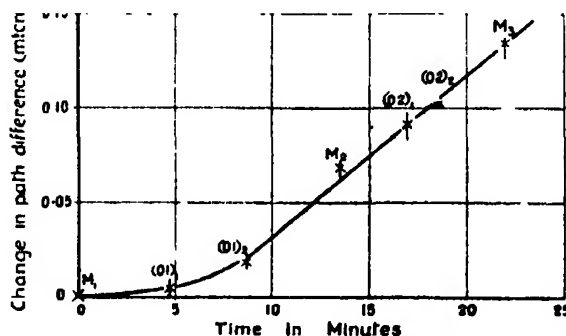


FIG. 2—Relation between change of path difference and time during the comparisons at 60.6 mm.

during the observations at 60.6 mm., is given in fig. 2. For the four radiations observed, results similar to those in Table I were obtained, and assuming, temporarily, on this evidence that the wave-lengths under the three conditions of excitation were in agreement, the changes in path difference with time were derived by calculation from the products of the respective wave-lengths and the observed changes in the corresponding orders

of interference. Each short vertical line in the diagram represents the range covered by the values calculated for the four radiations, and its position on the time scale indicates the mean time of the observation from which the values were calculated. Each cross represents the arithmetical mean of the individual values comprised within the range. The smooth curve drawn through the crosses clearly indicates non-linearity of the relation between path difference (or temperature) and time during the comparison of M and O1. Therefore the large value of $(\mu - \nu_1)$ in this case is at least partially accounted for by non-linear changes of temperature with time, and is certainly not due entirely to a difference between the wave-lengths of the red line from the two sources. Similar examination of the other results produced further evidence that the larger values of $(\mu - \nu_1)$ and $(\mu - \nu_2)$ were generally associated with similar temperature effects. It was also noted that the larger values of these quantities were mostly obtained when the photographic work had been commenced rather soon after the lamps had been started, and before the thermo-regulator had had time to eliminate the consequent disturbances of room temperature.

The values of λ_R for the Osram lamp were calculated in terms of λ_R for the Michelson lamp, assuming the latter to be 6438.4696 Å. The best final value of wave-length was found by assigning to the values determined at the various path differences weights proportional to the orders of interference from which they were calculated, and then abstracting the weighted mean. In this manner the wave-lengths found for the red line from the Osram lamp in the 1-ampere and 2-ampere conditions were, respectively, 6438.4700 Å. and 6438.4696 Å., which values are identical with the wave-length from the Michelson lamp to an accuracy of at least 1 part in 16,000,000.

It is of interest to plot the values of $(\mu - \nu_1)$ and $(\mu - \nu_2)$, given in Table I, against the corresponding values of the order of interference. This has been done in fig. 3, with a view to finding any evidence of difference of structure in the radiation produced from the two lamps. It will be seen that the curve for $(\mu - \nu_2)$ makes one complete oscillation about the axis of abscissæ in a period of about 190,000 waves, and this behaviour might indicate the presence of a very faint satellite to the red line from the Osram lamp at ± 0.034 Å., assuming that the red line from the Michelson lamp were simple and symmetrical. There is, perhaps, a slight suggestion of the same oscillation in the values of $(\mu - \nu_1)$, but it is almost obscured by the irregularities which, as already explained, are probably due to temperature disturbances.

Since it is obviously of the greatest importance to know definitely, both for

the purposes of spectroscopy and metrology, whether the red line of cadmium is a simple and symmetrical radiation, it is intended, shortly, to re-examine the red line emitted by the Michelson and Osram lamps with much greater precision. This is to be done with the aid of an invar Fabry-Perot étalon, of the variable-gap type, which is being constructed for use in an air thermostat in which the temperature may be controlled and measured to an accuracy of $\pm 0.002^\circ \text{C}$.

The wave-lengths of the other cadmium lines were calculated in terms of the wave-length of the red line, assuming for the purposes of calculation that the value of the latter was the same for both sources. Since all the measurements involved in these calculations are obtained from the same

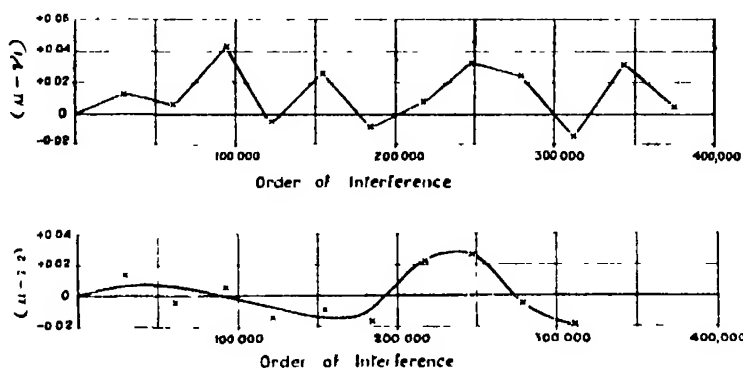


FIG 3 —Relation between $(\mu - \nu)$ and order of interference

negative at a single exposure, the results of this part of the work are unaffected by errors due to temperature changes.

Since

$$(N + \phi)\lambda_R = P\lambda, \quad (1)$$

where N is the order of interference in the red line at a given path difference, and P is the order of interference at the same path difference in one of the other lines whose wave-length is λ . ϕ represents the small difference between the phase changes occurring in reflection of light, of differing wave-lengths λ_R and λ , at the two semi-silvered glass surfaces of the interferometer, expressed in terms of the red line. There are two unknown quantities in equation (1) λ and ϕ , both of which may be completely determined from observations at two differing retardations. Since observations were made at several retardations, the best values of λ and ϕ could be determined from a least squares

solution of the equations, but this would be laborious procedure owing to the large number of significant figures involved

The difficulties of solution may be overcome by modifying equation (1) in the following manner.

Let

$$(N + \phi)\lambda_R = P(\lambda + \delta\lambda), \quad (2)$$

where λ is an approximate value of the required wave-length, and $(\lambda + \delta\lambda)$ is its true value. Suppose that P' is the approximate value of the order of interference calculated from the equation

$$N\lambda_R = P'\lambda, \quad (3)$$

where N , λ_R , and λ are known. If N is eliminated from equations (2) and (3), then

$$\frac{\phi\lambda_R}{P\lambda} = \frac{P - P'}{P} + \frac{\delta\lambda}{\lambda} \quad (4)$$

Since the values of the three terms involved in equation (4) are small, and $N\lambda_R$ is approximately equal to $P\lambda$, equation (4) may be re-written in the form

$$\frac{P - P'}{P} = \frac{\phi}{N} - \frac{\delta\lambda}{\lambda} \quad (5)$$

Equation (5) is linear and of the form $y = ax + b$, where $y = (P - P')/P$, $x = 1/N$, $a = \phi$ and $b = -\delta\lambda/\lambda$, and a series of such equations may be conveniently solved for a and b by the method of least squares, since values of x and y , involving only a limited number of significant figures, are sufficiently accurate to obtain the necessary precision in a and b .

Table II displays the results obtained for the wave-lengths of the principal components of the green and two blue lines. In this table the figures under the columns headed " m " denote the approximate maximum values of the retardations to which the calculated wave-lengths apply. It will be seen that M and O1 produce radiations whose wave-lengths are identical within the limits of experimental error. The only difference between the sources lies in the somewhat smaller range over which λ_Q from O1 has been calculated. It was found that the visibility of fringes in the green line from O1 rapidly declined for retardations greater than 276,000 and thereafter the wave-length calculated from the observed orders of interference was uncertain. The

Table II.—Results for λ_G , λ_{B1} and λ_{B2} .

Series of observations	Green line			First blue line				Second blue line			
	λ_G	ϕ	m	λ_{B1}	ϕ	m	λ_{B2}	ϕ	m		
M_1	A			A			A				
M_2	5085 8210	0 000	395,000	4799 9102	-0 011	419 000	4678 1489	0 010	430 000		
M_3	5085 8213	-0 002	395,000	4799 9106	-0 012	419 000	4678 1495	-0 009	430,000		
	5085 8211	-0 005	395,000	4799 9105	+0 002	419 000	4678 1496	-0 015	430 000		
Mean M	5085 8211			4799 9104			4678 1493				
(01) ₁	5085 8214	-0 004	276,000	4799 9102	-0 018	419 000	4678 1490	+0 013	430,000		
(01) ₂	5085 8212	-0 004	276 000	4799 9106	-0 012	419 000	4678 1497	-0 019	430 000		
Mean (01)	5085 8213			4799 9104			4678 1494				
(02) ₁	{ 5085-8140 5085-8294	{ (-0 001) (-0 001)	{ 395,000 135,000	{ 4799 9073 4799 9153	{ (-0 010) (-0 010)	{ 164,000* 164,000*	4678 1500	{ (-0 013) (-0 013)	441,000		
(02) ₂	{ 5085 8137 5085 8292	{ (-0 001) (-0 001)	{ 395,000 155,000	{ 4799 9066 4799 9147	{ (-0 010) (-0 010)	{ 164 000* 164 000*	4678 1494	{ (-0 013) (-0 013)	441,000		
Mean (02)	{ 5085 8139 5085 8283			{ 4799 9070 4799 9150			4678 1497				

* Doublet in first blue line observed in this retardation only

mean value of λ_G from M and O1 is 5085·8212 Å. The values of this wave-length determined by other observers are :—

5085·8219 Å.	(Michelson*)
5085·8230 Å.	(Meggers and Burns†)
5085·8222 Å.	(The Reichsanstalt‡)
5085 8224 Å	(Pérard§).

The mean value of λ_{B1} from M and O1 is 4799·9104 Å., which may be compared with Michelson's value of 4799·9088 Å. (*loc. cit.*), and Meggers and Burns' value of 4799·9139 Å. (*loc. cit.*). The mean value of λ_{B2} from M and O1 is 4678·1493 Å., for which Meggers and Burns give 4678·1504 Å.

The calculated values of ϕ , given in Table II, do not vary regularly with wave-length, as they would be expected to do, but it will be noted that they are of relatively small magnitude, and that variations in the calculated values of ϕ for a given radiation have little influence on the corresponding values determined for the wave-length. In calculating wave-lengths for O2, it was found more convenient to assume mean values of ϕ derived from the observations on M and O1, and these assumed values are therefore shown bracketed in the table.

An interesting change takes place in the structure of the principal component of both the green and first blue lines when the current through the Osram lamp is increased from 1 ampere to 2 amperes, since each one of them is apparently resolved into a doublet in the latter condition. The structure of these two lines may be observed in the actual process of transformation at suitable retardations if the exciting current is slowly increased from 1·2 to 1·4 ampere. The doublet structure of the green line was clearly visible at path differences of 39·1, 60·6 and 78·8 mm. At 99·9 mm. the interference pattern was faint and much confused, while in the range extending from 118·6 to 201·1 mm., only the component of smaller wave-length was visible. In the first blue line the doublet structure was only identifiable at the retardation of 164,000 (78·8 mm. difference of path) and, therefore, the corresponding value of " m " in Table II is marked with an asterisk. At other path differences the principal component of the first blue line appeared to be simple, but its calcu-

* 'Trav. Bur. Int. Pds Mes', vol. 11, p. 85, (1895). Both the Michelson values given above are corrected to dry air conditions, and are stated in terms of the value 6438·4696 Å for the red line.

† 'Sci. Pap. Bur. Stand. Wash.', vol. 18, p. 186, (1922-1923).

‡ 'Z. InstrKunde', vol. 47, p. 227, (1927)

§ 'Rev. d'Optique,' vol. 7, p. 17, (1928)

lated wave-length varied in a regular manner between the limits defined by the observed doublet separation. The doublet separations in the principal components of the green and first blue lines were 0.0154 Å. and 0.0080 Å. respectively. The mid-points of the doublets lie at 5085.8216 Å. for the former and 4799.9110 Å. for the latter, and these positions are in close agreement with those of the principal components in the other conditions of excitation. From this, and from the fact that the components in each line are of approximately equal intensity, it would seem that these two lines are subject to self-reversal in O2 thereby producing rather the same effect as close doublets. The behaviour of the first blue line clearly confirmed this effect, but that of the green line did not, owing to the fact that little evidence of the presence of the component of longer wave-length was obtained at the greater retardations. The structure of the green and first blue lines discussed here is additional to that, mentioned later, which is common to all conditions of excitation.

The value of λ_{B2} from O2 is closely the same as that from M up to and including retardations of about 341,000.

The results of the measurements of the structure of the green and two blue lines, observed in all conditions of excitation, are collected together in Table III. The positions of the satellites are given with reference to the position of the principal components, and the wave-lengths quoted for the latter are the mean values obtained from M and O1. The results for O2 are referred, where necessary, to the mid-point of the principal doublet, for as this is closely coincident in position with the principal component in the other conditions of excitation, no sensible change in the basis of reference is made thereby. Since some of the satellites were obscured by the principal components at certain retardations, or else were not observed at retardations other than the smallest owing to a presumed lack of homogeneity, it was considered necessary to show in the table the relative weights of individual measurements. These weights are proportional to the sums of the path differences at which the measurements could be made. Thus a weight of 1 indicates measurements that could be made only at the smallest path difference used, namely about 20 mm whereas a weight of 6 indicates measurements made at path differences of about 20, 40 and 60 mm., and so on.

The mean results of the measurements of structure are given in Table IV. The results for the positions of the satellites are in good agreement with those obtained by Fabry,* Nagaoka and Mishima,† Schrammen,‡ and by

* 'C. R. Acad. Sci. Paris,' vol. 138, p. 854 (1904).

† 'Proc. Imp. Acad. Japan,' vol. 2, p. 201 (1926).

‡ 'Ann Physik,' vol. 83, p. 1161 (1927).

Table III—Results of Measurements of the Structure of Cadmium Lines.

Principal component.	Positions of satellites									
	Michelson lamp				Osram lamp (1 amp.)				Osram lamp (2 amps.)	
	M ₁	M ₂	M ₃	Weight.	(01) ₁	(01) ₂	Weight	(02) ₁	(02) ₂	Weight.
A.	A	A	A	1	A	A	1	A	A	1
5085 8212	+0 0746	+0 0783	+0 0778	1	+0 0766	+0 0756	1	+0 0704	+0 0751	1
	-0 0230	-0 0229	-0 0232	6	-0 0238	-0 0246	6	-0 0290	-0 0271	3
	-0 0603	+0 0605	+0 0646	1	+0 0590	+0 0601	1	+0 0577	+0 0570	6
	+0 0151	+0 0150	+0 0148	9	+0 0164	+0 0162	9	+0 0176	+0 0175	5
4799 9104	-0 0297	-0 0304	-0 0289	4	-0 0286	-0 0285	4	-0 0291	-0 0297	4
	-0 0790	-0 0800	-0 0789	1	-0 0796	-0 0807	1	-0 0836	-0 0849	1
	+0 0289	+0 0298	+0 0275	3	+0 0303	+0 0306	3	+0 0308	+0 0318	3
4678 1493	-0 0571	-0 0562	-0 0562	1	-0 0572	-0 0562	1	-0 0551	-0 0528	1

* The measurements leading to the results given in this row would be capable of an alternative interpretation leading to a position for this satellite approximately -0.1 Å from the principal component. The interpretation chosen leads to results in agreement with other observers, and it was not thought necessary, for the purpose of the present investigation, to make additional observations in order to resolve this ambiguity.

Schuler and Keyston* using other sources of cadmium radiations. No measurements of intensity were made in the present work.

Table IV.—Comparison of Measurements of the Structure of Cadmium Lines

Principal component	Michelson lamp.	Osram lamp (1 amp.)	Osram lamp (2 amp.).
A	A	A	A
5085 8212	+0 0769 0 0230	+0 0761 -0 0242	+0 0728 +0 0081 -0 0073 -0 0280
4799 9104	+0 0618 +0 0150 -0 0297 0 0793	+0 0596 +0 0163 0 0286 -0 0802	+0 0571 +0 0176 +0 0046 0 0034 -0 0294 0 0842
1678 1493	+0 0287 0 0565	+0 0304 -0 0567	+0 0313 -0 0540

The authors' acknowledgments are due to the Director of the National Physical Laboratory for permission to publish this paper, and to Mr R. F. Zobel and Miss W. M. Battersby for their assistance in the computations involved

(4) Summary

The wave-length of the red line of cadmium, whether produced from the Michelson lamp or from the Osram lamp, is the same to an accuracy of at least 1 part in 16,000,000. When the Osram lamp is excited with a current of 1 ampere the wave-lengths and structure of the two blue radiations are also identical with those from the Michelson lamp, within the limits of experimental error. In the same condition of the Osram lamp a smaller limit of interference was found for the green line, but up to and including retardations of about 276,000 the wave-length is identical with that from the Michelson lamp. It can be said, therefore, that the Osram lamp, when excited with a current of 1 ampere, is a safe substitute for the Michelson lamp as a standard source of monochromatic red radiation

When the current through the Osram lamp is increased from 1 ampere to 2 amperes, the green and first blue lines show increased complexity which

* 'Z. Physik,' vol. 67, p. 433 (1931).

may possibly be due to self reversal. At the greater retardations the red line also exhibits a variation in visibility which may be due to the same effect. Furthermore, the principal component of the second blue line becomes less homogeneous. Therefore, the Osram lamp, when excited with a current of 2 amperes, is definitely unsuitable as a standard source of monochromatic red radiation.

Some slight evidence was observed, at smaller retardations, of differing structure in the red line as produced from the Michelson lamp and the Osram lamp in the 2-ampere condition. In the case of the comparisons of the Michelson lamp and the Osram lamp in the 1-ampere condition, this effect, if present, was largely masked by incidental temperature disturbances which particularly affected the steel slides and screw of the Fabry-Perot interferometer during these comparisons. The intercomparisons of the red radiation emitted by the two sources are to be repeated with better apparatus and under conditions more suitable for the attainment of the very high precision which is required to discern any small differences of structure which may be present.

The Thermodynamics of Adsorption at the Surface of Solutions.

By E. A. GUGGENHEIM and N. K. ADAM.

(From the Sir William Ramsay Laboratories of Physical and Inorganic Chemistry, University College, London, W C 1, and Imperial Chemical Industries, Ltd.)

(Communicated by F. G. Donnan, F R S — Received September 13, 1932)

Introduction.

In Gibbs'* thermodynamic theory of surfaces, the general equations governing equilibrium at interfaces were given, including equations governing adsorption. He pointed out, that in order to assign definite numerical values to the surface excess Γ of each component, it is necessary to choose a definite position for a certain mathematical surface, placed parallel to, and within, or near to, the inhomogeneous region between the two bulk phases. Gibbs' most general equations apply to any possible position of this surface, but the particular equation commonly known as "Gibbs' adsorption equation" was

* 'Collected Works,' vol. I, p. 219, *et seq.*

deduced by the aid of a particular choice of the position of this mathematical surface, such that the surface excess of one of the components vanished.

The object of this paper is to examine the form taken by Gibbs' general equations, when other conventions relating to the position of this dividing surface are chosen, and to establish the quantitative relations between the values of the surface excess of each component, obtained on the various conventions used. Our aim in doing this is to attempt to remove some of the confusion which has arisen, when interpreting the results of calculations of the Γ in terms of the physical structure of the surface. The particular convention relating to the position of the dividing surface used by Gibbs suffers from the disadvantage that it is not easily visualised in terms of the physical structure of the surfaces, and is also unsymmetrical in respect of the components of the solution. Some of the alternative conventions examined here seem to us more convenient in both these respects, and the values of Γ obtained by their aid are no more difficult to calculate from surface tension and vapour pressure data on solutions.

Confusion is likely to arise from the not uncommon definition of "surface excess per unit area" at the surface of a solution, as the difference between the quantity of solute contained in a given volume of the solution containing unit area of free surface, and that in an equal volume without any free surface. It will be shown in this paper that (except at infinite dilution) the numerical value of the surface excess defined in this manner is not the same as that obtained on the particular conventions used by Gibbs in obtaining the most well-known adsorption equation: indeed equations (39) to (44) show that the ratio of the two numerical values of Γ on Gibbs' convention and on the above definition [$\Gamma^{(v)}$ of our notation] becomes infinite as the solution approaches the composition of the pure second component, whose adsorption is being considered. The papers of Schofield and Rideal* and of Wynne-Jones† are of interest as illustrating the difficulty of forming a definite physical conception of the surface excess as defined on Gibbs' convention [$\Gamma_2^{(1)}$ in our notation].

Dependence of Surface Excess Γ on Position of Geometrical Surface.

The discussion will be confined to systems consisting of two bulk phases in complete thermodynamic equilibrium, separated by a plane surface. In this case, the temperature T , the pressure P , and the chemical potential μ ,

* 'Proc. Roy. Soc.,' A, vol. 109, p. 61 (1925); 'Phil. Mag.,' vol. 13, p. 806 (1932).

† 'Phil. Mag.,' vol. 12, p. 907 (1931).

of every species i will each have a value constant throughout the system. The two bulk phases will be completely homogeneous except in the immediate neighbourhood of the surface. We may therefore imagine a cylindrical column of unit cross-section, with its axis perpendicular to the bounding surface, connecting the homogeneous part of one phase with the homogeneous part of the other phase. This is shown diagrammatically in fig. 1. The first phase denoted by α is completely homogeneous up to and somewhat beyond the surface A and the second phase denoted by β is completely homogeneous, down to and somewhat beyond the surface B. Between the surfaces A and B, somewhere about S and S', is a region which is still homogeneous in the directions perpendicular to the axis of the cylindrical column but is not so in the direction parallel to this axis. The essential feature of Gibbs' treatment

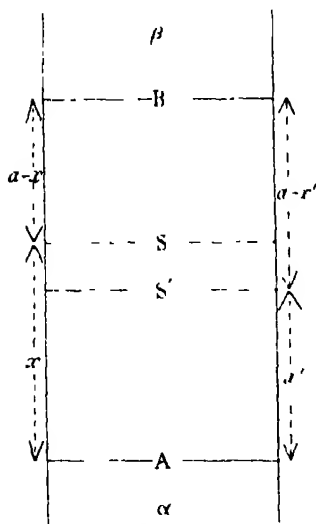


FIG. 1.

is to choose a definite geometrical surface such as S to which the thermo-dynamic properties of the system are referred as follows. Imagine a hypothetical system in which the phase α remains homogeneous right up to the surface S and the phase β remains homogeneous right down to the surface S. In this hypothetical system the number of moles of the species i contained in the column between the surfaces A and B will be

$$xc_i^\alpha + (a - x)c_i^\beta, \quad (1)$$

where a denotes the distance between A and B, x denotes that between A and S, $(a - x)$ that between S and B, while c_i^α, c_i^β denote the number of moles per unit volume in the homogeneous interiors of the phases α and β . In the actual

system the number of moles of the species i contained in the column between the surfaces A and B will in general not be given by the expression (1). We may define quantities Γ_i such that the number of moles of each species i between A and B in the actual system is

$$xc_i^\alpha + (a - x)c_i^\beta + \Gamma_i. \quad (2)$$

The Γ_i may then be positive or negative and are called the "surface excess of the species i ."

For constant temperature and pressure of the whole system variations of

the quantities Γ_i and the surface tension γ are related by the thermodynamic formula*

$$-d\gamma = \sum_i \Gamma_i d\mu_i, \quad (3.1)$$

where μ_i denotes the chemical potential of the species i at any part of the system. Provided the vapours of the various components i obey the laws of perfect gases, we may write as an alternative to (3.1)

$$-d\gamma = RT \sum_i \Gamma_i d \log p_i, \quad (3.2)$$

where R is the gas constant and p_i the partial vapour pressure of the species i at any part of the system.

Suppose now that instead of the surface S we should choose a different surface S' to which to refer the thermodynamic behaviour of the system. Corresponding to this surface we should define quantities Γ'_i such that the number of moles of the chemical species i between A and B is

$$x'c_i^a + (a - x')c_i^b + \Gamma'_i, \quad (4)$$

where x' denotes the distance AS' . Now the actual number of moles of each species i between A and B is obviously independent of a purely conventional choice between the surfaces S and S' . Hence the expressions (2) and (4) must be identical, that is

$$xc_i^a + (a - x)c_i^b + \Gamma_i = x'c_i^a + (a - x')c_i^b + \Gamma'_i \quad (5)$$

or

$$\Gamma'_i = \Gamma_i - (x' - x)(c_i^b - c_i^a). \quad (6)$$

Comparing the relations of the form (6) for the various chemical species present, we obtain

$$\frac{\Gamma'_i - \Gamma_i}{c_i^b - c_i^a} = \frac{\Gamma'_k - \Gamma_k}{c_k^b - c_k^a} = \quad (7)$$

Corresponding to the relations (3.1) or (3.2) we have

$$-d\gamma = \sum_i \Gamma'_i d\mu_i \quad (8.1)$$

$$-d\gamma = RT \sum_i \Gamma'_i d \log p_i. \quad (8.2)$$

For (3) and (8) to be simultaneously true it is necessary that

$$\sum_i (\Gamma'_i - \Gamma_i) d\mu_i = 0 \quad (9.1)$$

or

$$\sum_i (\Gamma'_i - \Gamma_i) d \log p_i = 0. \quad (9.2)$$

* Gibbs, *loc. cit.*, vol. I, equation (508).

Substituting from (6) and (9) we find as necessary conditions

$$(x' - x) \sum_i (c_i^\beta - c_i^\alpha) d\mu_i = 0 \quad (10.1)$$

or

$$(x' - x) \sum_i (c_i^\beta - c_i^\alpha) d \log p_i = 0. \quad (10.2)$$

It is easily seen that equation (10.1) is in accordance with the Gibbs-Duhem* relation when we have at constant temperature and pressure

$$\sum_i c_i^\alpha d\mu_i = 0 \quad (11)$$

$$\sum_i c_i^\beta d\mu_i = 0. \quad (12)$$

Similarly (10.2) is in accordance with the Duhem-Margules relation

$$\sum_i c_i^\alpha d \log p_i = 0 \quad (13)$$

in the phase α , and

$$\sum_i c_i^\beta d \log p_i = 0 \quad (14)$$

in the phase β †

To sum up: when the geometrical surface S is displaced a distance δx , the values of the various Γ_i become altered by amounts $\delta\Gamma_i$ given by

$$\delta\Gamma_i = \delta x \cdot (c_i^\beta - c_i^\alpha) \quad (15)$$

but the expressions

$$\sum_i \Gamma_i d\mu_i \quad (16.1)$$

occurring in (3.1), or

$$\sum_i \Gamma_i d \log p_i \quad (16.2)$$

occurring in (3.2), remain invariant so that the relations

$$-d\gamma = \sum_i \Gamma_i d\mu_i \quad (17.1)$$

$$-d\gamma = RT \sum_i \Gamma_i d \log p_i \quad (17.2)$$

remain unaffected.

Liquid-vapour Interface.—Let us now suppose that the phase α is a slightly volatile liquid and the phase β is vapour. It is generally accepted that the density of matter in the non-homogeneous region is comparable with that in the homogeneous part of the liquid phase while the density in the vapour phase is in comparison negligibly small. In this case some of the above formulæ

* Gibbs, *loc. cit.*, vol. 1, equation (98).

† Cf. Gibbs, *loc. cit.*, vol. 1, pp. 233–237

become simplified, and the physical meaning of the various Γ_i becomes much clearer.

We may in this case neglect c_i^B , omit the index in c_i^A and write

$$x_i c_i + \Gamma_i \quad (18)$$

for the number of moles of the species i above the surface A . It is now possible to redefine the Γ_i in a manner which makes no explicit reference to the geometrical surface S and which makes clearer the physical significance of the Γ_i . If we compare a portion of the liquid containing unit area of surface with another very nearly equal portion in the interior of the liquid then the former will contain Γ_i moles of each species i more than the latter.

The indefiniteness in the values of the Γ_i was according to the original definition due to indefiniteness relating to the exact position of the geometrical surface S . According to the new definition it is due to indefiniteness about the quantity of liquid in the interior with which one compares the portion of liquid containing unit area of surface. According to either definition there is one degree of freedom in the assignment of values to the various Γ_i . The variations $\delta\Gamma_i$ corresponding to changes in position of the dividing surface up to which the hypothetical system remains homogeneous, are subject to the relation

$$\frac{\delta\Gamma_i}{c_i} = \frac{\delta\Gamma_k}{c_k} = \dots \quad (19.1)$$

which is the form now taken by (15). In terms of the mole fractions N_i, N_k, \dots in the interior of the liquid phases this may be written

$$\frac{\delta\Gamma_i}{N_i} = \frac{\delta\Gamma_k}{N_k} = \dots \quad (19.2)$$

It follows that all linear combinations of the form

$$N_k \Gamma_i - N_i \Gamma_k \quad (20)$$

are invariant with respect to displacement of the geometrical surface S .

Alternative Conventions Relating to the Γ_i .—As Gibbs pointed out one may choose the position of the geometrical surface S such that for one component, say 1, the value of Γ_1 shall be zero. According to this convention a portion of the liquid containing unit area of surface contains Γ_i moles of each species i more than a portion in the interior which contains exactly the same quantity of the species 1. The values of the Γ_i corresponding to this convention,

referred to henceforth as convention 1, will be specified by writing $\Gamma_i^{(1)}$ [Gibbs used $\Gamma_{s(1)}$]. We have by definition

$$\Gamma_1^{(1)} = 0. \quad (21)$$

Similarly, if we define Γ_i as the excess number of moles of the species i in a portion of liquid with unit surface area over a portion in the interior *containing exactly the same number of moles of the species 2*, we shall use the notation $\Gamma_i^{(2)}$ and shall refer to this convention as convention 2. We then have by definition

$$\Gamma_2^{(2)} = 0. \quad (22)$$

A convention more symmetrical with respect to the various species present is the following. A portion of the liquid with unit area of surface contains Γ_i moles of each species i more than a portion in the interior *containing exactly the same total number of moles of all species*. Using the notation $\Gamma_i^{(N)}$ for this convention, to be referred to as convention N, we have by definition

$$\sum_i \Gamma_i^{(N)} = 0. \quad (23)$$

According to yet another convention we may define Γ_i as the number of moles of the species i in a portion of the liquid containing unit area of surface more than in a portion in the interior *of exactly the same mass*. Corresponding to this convention, to be referred to as convention M, we shall use the notation $\Gamma_i^{(M)}$ and we have by definition

$$\sum_i m_i \Gamma_i^{(M)} = 0, \quad (24)$$

where m_i denotes the molar mass ("molecular weight") of the species i .

Finally we may define Γ_i as the number of moles of the species i in a portion of the liquid containing unit area of surface more than in a portion in the interior *of exactly the same volume*. This convention will be called convention v, and the notation $\Gamma_i^{(v)}$ will be used. If we may with sufficient accuracy assume the surface tension to be independent of the pressure, it follows thermodynamically that change of surface area takes place without expansion or contraction. In this case the relation between the $\Gamma_i^{(v)}$ is

$$\sum_i v_i \Gamma_i^{(v)} = 0, \quad (25)$$

where v_i denotes the partial molar volume of the species i .

We have cited five alternative conventions for fixing the values of the Γ_i to which correspond respectively the notations $\Gamma_i^{(1)}$, $\Gamma_i^{(2)}$, $\Gamma_i^{(N)}$, $\Gamma_i^{(M)}$, $\Gamma_i^{(v)}$.

Each convention is defined by one of the equations (21) to (25) which are all linear relations of the general form

$$\sum_i \alpha_i \Gamma_i = 0. \quad (26)$$

One of the primary causes of our writing this paper is the common practice of defining Γ_i according to convention v and then applying to the $\Gamma_i^{(v)}$ relations that are exact only for the $\Gamma_i^{(u)}$. It is only with convention v that the geometrical surface S coincides exactly with the physical boundary of the liquid.

Relations between the Γ_i on Different Conventions.

We shall now investigate how the various conventional sets of Γ_i are related one to another. In this investigation we shall confine ourselves to a system of only two components 1 and 2. The relation (26) then becomes

$$\alpha_1 \Gamma_1 + \alpha_2 \Gamma_2 = 0, \quad (27)$$

while the Gibbs formula (3.2) becomes

$$-\frac{1}{RT} d\gamma = \Gamma_1 d \log p_1 + \Gamma_2 d \log p_2 \quad (28)$$

and the Duhem-Margules relation (13) may be written

$$N_1 d \log p_1 + N_2 d \log p_2 = 0 \quad (29)$$

If we eliminate Γ_1 and p_1 from (27), (28), (29) we obtain

$$-\frac{1}{RT} d\gamma = \Gamma_2 d \log p_2 \left\{ 1 + \frac{\alpha_2 N_2}{\alpha_1 N_1} \right\}. \quad (30)$$

If on the other hand we eliminate Γ_2 and p_2 we obtain

$$-\frac{1}{RT} d\gamma = \Gamma_1 d \log p_1 \left\{ 1 + \frac{\alpha_1 N_1}{\alpha_2 N_2} \right\}. \quad (31)$$

From (30) it follows that

$$\Gamma_2 \left\{ 1 + \frac{\alpha_2 N_2}{\alpha_1 N_1} \right\} \quad (32.1)$$

is invariant with respect to displacement of the Gibbs surface S. Similarly from (31) we see that

$$\Gamma_1 \left\{ 1 + \frac{\alpha_1 N_1}{\alpha_2 N_2} \right\} \quad (32.2)$$

is invariant as regards displacement of the surface S.

According to (20) the quantity

$$N_1 \Gamma_2 - N_2 \Gamma_1 \quad (33)$$

is also invariant as regards displacement of the surface S.

The forms taken by (27) and the values of α_1 , α_2 corresponding to the various kinds of Γ_1 , Γ_2 are given by

$$\Gamma_1^{(1)} = 0 \quad \alpha_2 = 0 \quad (34)$$

$$\Gamma_2^{(2)} = 0 \quad \alpha_1 = 0 \quad (35)$$

$$\Gamma_1^{(v)} + \Gamma_2^{(v)} = 0 \quad \alpha_1 = \alpha_2 \quad (36)$$

$$M_1 \Gamma_1^{(u)} + M_2 \Gamma_2^{(u)} = 0 \quad \frac{\alpha_1}{M_1} = \frac{\alpha_2}{M_2} \quad (37)$$

$$V_1 \Gamma_1^{(v)} + V_2 \Gamma_2^{(v)} = 0 \quad \frac{\alpha_1}{V_1} = \frac{\alpha_2}{V_2} \quad (38)$$

Substituting the appropriate values of α_1 , α_2 from relations (34) to (38) into (30), we obtain for conventions 1, N, M, V, the following relations, of which the first is, of course, the ordinary Gibbs adsorption equation

$$\begin{aligned} -\frac{1}{RT} \frac{\partial \gamma}{\partial \log p_2} - \Gamma_2^{(1)} &= \Gamma_2^{(v)} \left\{ 1 + \frac{N_2}{N_1} \right\} \\ -\Gamma_2^{(u)} \left\{ 1 + \frac{N_2}{N_1} \frac{M_2}{M_1} \right\} &= \Gamma_2^{(v)} \left\{ 1 + \frac{N_2}{N_1} \frac{V_2}{V_1} \right\}. \end{aligned} \quad (39)$$

For convention 2, of course, $\Gamma_2^{(2)}$ is zero in accordance with equation (22).

Introducing the mean molar mass \bar{M} and the mean molar volume \bar{V} defined by

$$\bar{M} = N_1 M_1 + N_2 M_2 \quad (40)$$

$$\bar{V} = N_1 V_1 + N_2 V_2 \quad (41)$$

the relations (39) may be written

$$-\frac{N_1}{RT} \frac{\partial \gamma}{\partial \log p_2} = N_1 \Gamma_2^{(1)} = \Gamma_2^{(v)} = \frac{\bar{M}}{M_1} \Gamma_2^{(u)} = \frac{\bar{V}}{V_1} \Gamma_2^{(v)} \quad (42.1)$$

$$\Gamma_2^{(2)} = 0. \quad (42.2)$$

Similarly by substituting from the relations (34) to (38) into (31) we obtain

$$-\frac{N_2}{RT} \frac{\partial \gamma}{\partial \log p_1} = N_2 \Gamma_1^{(2)} = \Gamma_1^{(v)} = \frac{\bar{M}}{M_2} \Gamma_1^{(u)} = \frac{\bar{V}}{V_2} \Gamma_1^{(v)} \quad (43.1)$$

$$\Gamma_1^{(1)} = 0. \quad (43.2)$$

The relations (29), (36), (42) and (43) may all be combined in the form

$$\begin{aligned} -\frac{N_1}{RT} \frac{\partial \gamma}{\partial \log p_2} - \frac{N_2}{RT} \frac{\partial \gamma}{\partial \log p_1} &= \Gamma_2^{(N)} = -\Gamma_1^{(N)} \\ &= N_1 \Gamma_2^{(1)} = -N_2 \Gamma_1^{(2)} = \frac{\bar{M}}{M_1} \Gamma_2^{(M)} = -\frac{\bar{M}}{M_2} \Gamma_1^{(M)} \\ &= \frac{\bar{V}}{V_1} \Gamma_2^{(V)} = -\frac{\bar{V}}{V_2} \Gamma_1^{(V)} \end{aligned} \quad (44.1)$$

$$\Gamma_1^{(1)} = 0 \quad \Gamma_2^{(2)} = 0. \quad (44.2)$$

Equations (44) give the relations between all the Γ for both components.

It is easy to check that (44) is in agreement with the invariance of the expression (33), that is

$$\begin{aligned} \Gamma_2^{(N)} = -\Gamma_1^{(N)} &= N_1 \Gamma_2^{(N)} - N_2 \Gamma_1^{(N)} \\ &= N_1 \Gamma_2^{(1)} = -N_2 \Gamma_1^{(2)} \\ &= N_1 \Gamma_2^{(M)} - N_2 \Gamma_1^{(M)} \\ &= N_1 \Gamma_2^{(V)} - N_2 \Gamma_1^{(V)} \\ &= N_1 \Gamma_2^{(X)} - N_2 \Gamma_1^{(X)} \end{aligned} \quad (45)$$

where the index X refers to any convention for fixing the values of the Γ other than the five conventions 1, 2, N, M, V.

Relations for very Dilute Component.—It is of special interest to consider the behaviour of the various Γ_1 and Γ_2 for mixtures differing only slightly from the pure substances 1 or 2. If the amount of the species 2 is very small compared with that of the species 1, we have approximately

$$N_1 \approx 1 \quad \frac{\bar{M}}{M_1} \approx 1 \quad \frac{\bar{V}}{V_1} \approx 1 \quad (46)$$

and consequently by (41.1)

$$-\frac{1}{RT} \frac{\partial \gamma}{\partial \log p_2} = \Gamma_2^{(V)} = \Gamma_2^{(1)} = \Gamma_2^{(N)} = \Gamma_2^{(V)}. \quad (47)$$

Thus in the immediate neighbourhood of $N_2 = 0$ four of the conventions give identical values for Γ_2 .

For small values of N_2 where the surface film contains relatively few molecules of component 2, it is reasonable to expect that the number of molecules of 2 in the surface which at these great dilutions is practically equal to $\Gamma_2^{(V)}$, and therefore to the other Γ_2 , will be proportional to N_2 . We may consider the surface film as a region in which the molecules have a different energy from

those in the interior, then Boltzmann's distribution law will hold good, the concentrations of component 2 in the surface and the interior bearing a constant ratio to each other, determined by the work of adsorption. Therefore, for small values of N_2

$$\Gamma_2 \propto N_2. \quad (48)$$

This is the analogue of Henry's law and Nernst's distribution law for surface films; it is well known to be verified by experiment

For small values of N_2 we may therefore write

$$\Gamma_2^{(s)} = \Gamma_2^{(l)} = \Gamma_2^{(m)} = \Gamma_2^{(v)} = k_2 N_2, \quad (49)$$

where k_2 is independent of N_2 . Similarly for small values of N_1 we may write

$$-\Gamma_1^{(s)} = -\Gamma_1^{(l)} = -\Gamma_1^{(m)} = -\Gamma_1^{(v)} = k_1 N_1, \quad (50)$$

where k_1 is independent of N_1 .

Relations for almost Pure Component—Formulae (49) and (50) give the behaviour of the various Γ of the dilute component. By comparing these with (44) we can obtain directly the behaviour of the Γ of the almost pure component. We obtain for small values of N_2 using (46)

$$-\Gamma_1^{(s)} = -N_2 \Gamma_1^{(l)} = -\frac{M_1}{M_2} \Gamma_1^{(m)} = -\frac{V_1}{V_2} \Gamma_1^{(v)} = k_2 N_2 \quad (51)$$

from which we see that the values of $-\Gamma_1^{(s)}$, $-\Gamma_1^{(m)}$, $-\Gamma_1^{(v)}$ tend to zero as N_2 tends to zero and N_1 to unity, but $-\Gamma_1^{(l)}$ on the other hand tends towards the constant value k_2 . Similarly in the neighbourhood of $N_1 = 0$ we have the relations.

$$\Gamma_2^{(s)} = N_1 \Gamma_2^{(l)} = \frac{M_2}{M_1} \Gamma_2^{(m)} = \frac{V_2}{V_1} \Gamma_2^{(v)} = k_1 N_1. \quad (52)$$

The Γ N Curves.—From the definitions of $\Gamma^{(s)}$, $\Gamma^{(m)}$ and $\Gamma^{(v)}$ or alternatively from formula (44.1) we see that as long as the two species are of comparable molar mass and molar volume the values of $\Gamma^{(s)}$, $\Gamma^{(m)}$ and $\Gamma^{(v)}$ for each species will at any given composition be of the same order of magnitude. The curves for $\Gamma^{(s)}$, $\Gamma^{(m)}$, $\Gamma^{(v)}$ for each species plotted against the mole fraction N_2 will be qualitatively similar. In particular according to the relations (49), (50), (51), (52), they all pass through both the origins $N_2 = 0$ and $N_1 = 0$ with finite slopes. For $\Gamma^{(v)}$ the geometrical surface S coincides with the physical boundary of the liquid and if the two species are of comparable molar mass and molar volume this will be *approximately* true also for $\Gamma^{(s)}$ and $\Gamma^{(m)}$.

The behaviours of $\Gamma_2^{(u)}$ and of $\Gamma_1^{(u)}$ are, however, quite different. For solutions very dilute with respect to the species 2 there is no appreciable difference between $\Gamma_2^{(u)}$ and the Γ_2 of the other conventions. But for solutions consisting mainly of the species 2, with only a little of the species 1, whereas $\Gamma_2^{(n)}$, $\Gamma_2^{(m)}$, $\Gamma_2^{(v)}$ tend to zero with N_1 , $\Gamma_2^{(u)}$ on the other hand tends to the finite value k_1 . For such solutions the distance between the geometrical surface S and the physical boundary of the liquid is not inappreciable. From the data for the system water-alcohol, discussed in detail below, one finds using (15) that for almost pure alcohol (species 2) containing a little water (species 1) the geometrical surface corresponding to $\Gamma_2^{(u)}$ is distant about 1.3 Å. from the physical boundary of the liquid, a distance which cannot be regarded as negligible compared with the thickness of the non-homogeneous film. In the case of $\Gamma_1^{(u)}$ in the neighbourhood of pure water ($N_1 = 1$) the distance between the geometrical surface S and the boundary is according to (15) about 40 Å. which is possibly even greater than the total thickness of the non-homogeneous film.

The quantities $\Gamma_2^{(u)}$ and $\Gamma_1^{(u)}$ were introduced by Gibbs for mathematical convenience, but those wishing to obtain a physical picture of the "surface excess" Γ will probably find $\Gamma^{(v)}$, $\Gamma^{(m)}$ or $\Gamma^{(n)}$ easier to visualize. Should one, however, prefer to use $\Gamma_2^{(u)}$ and $\Gamma_1^{(u)}$ then in considering the curves obtained by plotting these against the mole-fraction it should be remembered that the conventions 1 and 2 are themselves sufficient to account for the comparatively complicated shapes of the curves, without there being any physical peculiarity in the system. It is to be emphasised that the curves for $\Gamma_2^{(u)}$ and $\Gamma_1^{(u)}$ are thermodynamically associated with curves for the $\Gamma^{(n)}$, $\Gamma^{(m)}$ and $\Gamma^{(v)}$ and the last three will have simpler forms than the first two.

Relationship to Osmotic Pressure.—For a solution of only two components, such as we have been considering, if we choose to regard one component 1 as solvent and the other 2 as solute, we can obtain differential relations between the Γ and the osmotic pressure Π of the solution. The exact thermodynamic relation between the osmotic pressure Π and the partial vapour pressure p_1 of the solvent* is

$$v_1 d\Pi = u_1 dp_1, \quad (55)$$

where u_1 denotes the molar volume of the solvent vapour. Provided the vapour obeys the laws of perfect gases (55) becomes

$$v_1 d\Pi = RT d \log p_1. \quad (56)$$

* Porter, 'Proc. Roy. Soc.,' A, vol. 70, p. 519 (1907).

Substituting from (56) into (44.1) we obtain

$$\begin{aligned}
 \frac{N_2}{v_1} \frac{\partial \gamma}{\partial H} &= \Gamma_2^{(x)} = -\Gamma_1^{(x)} \\
 &= N_1 \Gamma_2^{(1)} = -N_2 \Gamma_1^{(2)} \\
 &= \frac{\bar{M}}{M_1} \Gamma_2^{(M)} = -\frac{M}{M_2} \Gamma_1^{(M)} \\
 &= \frac{\bar{v}}{v_1} \Gamma_2^{(v)} = -\frac{v}{v_2} \Gamma_1^{(v)}.
 \end{aligned} \tag{57}$$

The relation between $\Gamma_2^{(v)}$ and H may be written in a particularly simple form, namely,

$$\Gamma_2^{(v)} = \frac{N_2}{v} \frac{\partial \gamma}{\partial H} = c_2 \frac{\partial \gamma}{\partial H} \tag{58}$$

where c_2 denotes the number of moles of solute in unit volume of solution. Formula (58) has been obtained by Milner,* by an elementary proof involving a reversible cycle, and is generally quoted in text-books. It is, however, not made clear that the simple formula (58) applies only to $\Gamma_2^{(v)}$, whilst the corresponding formulæ for $\Gamma_2^{(1)}$, $\Gamma_2^{(N)}$, $\Gamma_2^{(M)}$ are according to (57) somewhat more complicated.

Application to the System Water-Ethyl Alcohol.

The necessary data have been taken from the surface tension measurements of Bircumshaw† and the vapour pressure measurements of Dobson.‡ Before using Dobson's data, they were examined to see whether the vapour pressure measurements for the two components were compatible with the Duhem-Margules relation (29). It was found that the dotted curves of fig. 2 could be drawn through the experimental points, the tangents (drawn as full lines) being chosen so as to be in exact agreement with the Duhem-Margules relation, the maximum deviation of any experimental point from the curve chosen being 0.5 mm. of mercury pressure and nearly all the points lying within 0.2 mm. of the selected curve.

Table 1 gives the actual data used in calculating the various Γ . The suffix 1 refers to water and 2 to alcohol. Column 1 gives the mole fractions, columns 2 and 3 the vapour pressures used in millimetres of mercury; column 4 the

* 'Phil. Mag.,' vol. 13, p. 96 (1907).

† 'J. Chem. Soc.,' p. 887 (1922).

‡ 'J. Chem. Soc.,' p. 2866 (1925).

values of $\frac{N_1}{p_1} \frac{\partial p_1}{\partial N_1}$ or of $\frac{N_2}{p_2} \frac{\partial p_2}{\partial N_2}$ taken from either curve; as already mentioned the two curves were selected to conform with the thermodynamic requirement

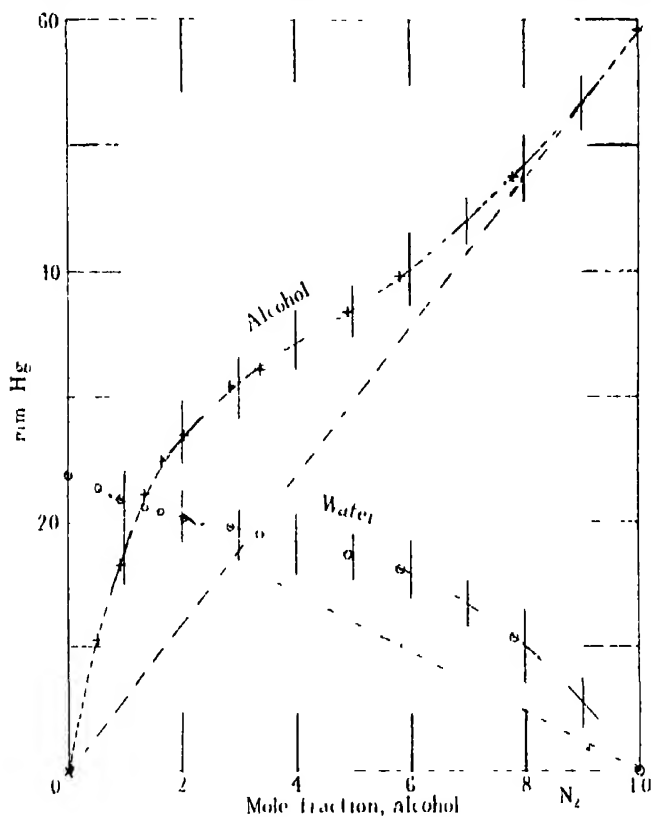


FIG. 2.

Table I

N_1	p_1	p_2	$\frac{N_1}{p_1} \frac{\partial p_1}{\partial N_1}$ $= \frac{N_2}{p_2} \frac{\partial p_2}{\partial N_2}$	γ	$N_2 \frac{\partial \gamma}{\partial N_2}$	$p_2 \frac{\partial \gamma}{\partial p_2}$	$\Gamma_2^{(1)} \times 10^{10}$ in moles/cm ²	$\Gamma_2^{(2)} \times 10^{(3)}$ moles/sq. Å.
0	23.75	0.0	1.00	72.2	0.0	0.0	0.0	0.0
0.1	21.7	17.8	0.76	36.4	11.8	15.6	6.3	3.8
0.2	20.4	26.8	0.41	29.7	6.5	16.0	6.45	3.9
0.3	19.4	31.2	0.37	27.6	5.4	14.6	5.9	3.6
0.4	18.35	34.2	0.355	26.35	4.4	12.6	5.1	3.1
0.5	17.3	36.9	0.41	25.4	4.25	10.5	4.25	2.6
0.6	16.8	40.1	0.53	24.6	4.5	8.45	3.4	2.06
0.7	13.3	43.9	0.655	23.85	4.7	7.15	2.9	1.75
0.8	10.0	48.3	0.77	23.2	4.75	6.2	2.5	1.5
0.9	5.5	53.3	0.915	22.6	5.0	5.45	2.2	1.33
1.0	0.0	59.0	1.00	22.0	5.2	5.2	2.1	1.27

that these quantities should be equal. In the fifth column are given the values of the surface tension, obtained from a large scale plot of Bircumshaw's data.

From this plot we read the values of $-N_2 \partial\gamma/\partial N_2$ given in the sixth column. The values of $-p_2 \partial\gamma/\partial p_2$ were obtained by two methods: either by dividing the values of $-N_2 \partial\gamma/\partial N_2$ by those of $\frac{N_2}{p_2} \frac{\partial p_2}{\partial N_2}$ or by plotting γ against $\log p_2$ and taking the slopes of this curve directly. It is to be observed that if the solutions were ideal, the values of $-p_2 \partial\gamma/\partial p_2$ in column 6 and of $-N_2 \partial\gamma/\partial N_2$ in column 7 would be identical, while the values of $\frac{N_2}{p_2} \frac{\partial p_2}{\partial N_2}$ in column 4 would be unity throughout. The eighth column gives the values of $\Gamma_2^{(1)}$ in moles per square centimetre, obtained by dividing the values in the seventh column by RT which is 2.48×10^{10} ergs. We estimate the uncertainty in calculating the individual values of $\Gamma_2^{(1)}$ to be of the order 0.4×10^{-10} moles per square centimetre, but the smoothed curve given in fig. 3A is probably rather more accurate than this. The last column gives $\Gamma_2^{(1)}$ in molecules per square Å.

Table II shows the values of all the Γ calculated from the values of $\Gamma_2^{(1)}$ given in Table I, by equations (44). The partial molar volumes used in the calculation of the $\Gamma^{(v)}$ were obtained from tables of the density of alcohol-

Table II.

(All the Γ are given in moles/cm² $\times 10^{10}$).

N_2	$\Gamma_2^{(s)}$	$\Gamma_1^{(s)}$	$\Gamma_2^{(w)}$	$\Gamma_1^{(w)}$	$\Gamma_2^{(v)}$	$\Gamma_1^{(v)}$	$\Gamma_2^{(1)}$	$\Gamma_2^{(2)}$
0.0	0.0		0.0	0.0	0.0	0.0	0.0	220
0.05	5.55		5.15	13.2	5.1	14.8	5.85	111
0.1	5.7		4.95	12.6	4.75	14.05	6.3	57
0.2	5.15		3.95	10.1	3.6	11.35	6.45	25.7
0.3	4.15		2.8	7.2	2.45	8.05	5.9	13.75
0.4	3.05		1.9	4.8	1.55	5.3	5.1	7.6
0.5	2.1		1.2	3.05	0.95	3.25	4.25	4.25
0.6	1.35		0.7	1.8	0.55	1.9	3.4	2.25
0.7	0.9		0.4	1.1	0.3	1.1	2.9	1.25
0.8	0.5		0.2	0.55	0.15	0.6	2.5	0.6
0.9	0.2		0.1	0.25	0.05	0.25	2.2	0.25
1.0	0.0		0.0	0.0	0.0	0.0	2.1	0.0

water mixtures. Fig. 3A shows the values of all the different Γ_2 , the adsorption of alcohol; fig. 3B shows the negative adsorption of water $-\Gamma_1$. The following features are to be particularly noted. The four Γ_2 curves all coincide in the neighbourhood of $N_2 = 0$, as also do the four Γ_1 curves in the neighbourhood of $N_1 = 0$. The curves for $\Gamma_2^{(s)}$, $\Gamma_2^{(w)}$, $\Gamma_2^{(v)}$, all approach the $N_1 = 0$ origin

with finite but different slopes, but the $\Gamma_2^{(1)}$ curve approaches the $N_1 = 0$ axis horizontally, cutting it at the height $k_1 = 2.1 \times 10^{-10}$ moles per square centimetre numerically equal to the gradient of the $-\Gamma_1$ curves in the neighbourhood of $N_2 = 1$. Similarly the curves for $-\Gamma_1^{(v)}$, $-\Gamma_1^{(u)}$, $-\Gamma_1^{(w)}$, all approach the $N_2 = 0$ origin with finite but different slopes, while the $-\Gamma_1^{(2)}$ curve cuts the $N_2 = 0$ axis at the height $k_2 = 220 \times 10^{-10}$ equal to the slope

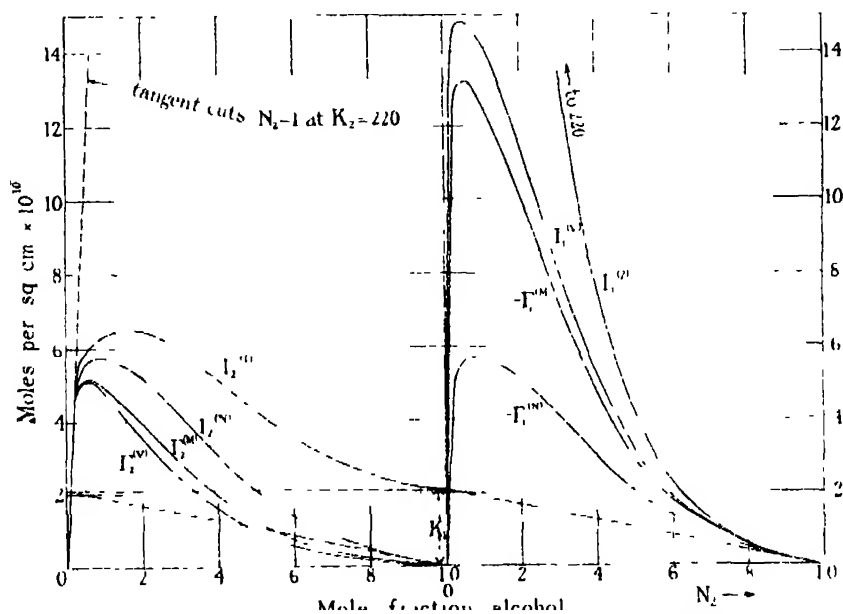


FIG. 3A — Adsorption of Alcohol.

3B.—Adsorption of Water.

of the Γ_2 curves at the $N_2 = 0$ origin. Finally the curves for $\Gamma_2^{(u)}$ and $-\Gamma_2^{(v)}$ are identical.

Seeing that the curves for the $\Gamma^{(u)}$, $\Gamma^{(w)}$, $\Gamma^{(v)}$, must pass through both the origins $N_2 = 0$ and $N_1 = 0$ with finite slopes, the general shape of these curves is of the simplest kind. As already pointed out the somewhat less simple shapes of the $\Gamma_2^{(1)}$ and $\Gamma_1^{(2)}$ curves are entirely due to the peculiarities of the conventions 1 and 2.

A Possible Structure for the Surface of the Water-Alcohol Solutions.

The simplest theory of the structure of the surface is that the non-homogeneous layer is a film only one molecule thick. To investigate this theory it is most convenient to adopt the convention of placing the Gibbs' geometrical surface S so as to separate the homogeneous liquid from the unimolecular

layer outside it. We shall refer to this as convention u and use the notation $\Gamma_1^{(v)}$, $\Gamma_2^{(v)}$. It is obvious that $\Gamma_1^{(v)}$ and $\Gamma_2^{(v)}$ are actually the number of moles of water and alcohol respectively in unit area of the unimolecular layer. The $\Gamma^{(v)}$ unlike the $\Gamma^{(1)}$, $\Gamma^{(2)}$, $\Gamma^{(n)}$, $\Gamma^{(m)}$, $\Gamma^{(v)}$ do not satisfy a relation of the form (27). To deduce the relations between the $\Gamma^{(v)}$ and $\Gamma^{(n)}$ we therefore have to use a procedure somewhat different from our former one. From the relation (45) for $\Gamma_1^{(x)}$ and $\Gamma_2^{(x)}$ we have for $\Gamma_1^{(v)}$ and $\Gamma^{(v)}$

$$-\Gamma_1^{(n)} = \Gamma_2^{(n)} = N_1 \Gamma_2^{(v)} - N_2 \Gamma_1^{(v)}. \quad (59)$$

If in a solution of given composition the areas occupied by a mole of water in the unimolecular layer are A_1 and by a mole of alcohol A_2 then

$$A_1 \Gamma_1^{(v)} + A_2 \Gamma_2^{(v)} = 1. \quad (60)$$

By solving (59) and (60) simultaneously we obtain

$$\Gamma_2^{(v)} = \frac{A_1 \Gamma_2^{(n)} + N_2}{N_1 A_1 + N_2 A_2} \quad (61)$$

$$\Gamma_1^{(v)} = \frac{A_2 \Gamma_1^{(n)} + N_1}{N_1 A_1 + N_2 A_2}. \quad (62)$$

As one would expect in the immediate neighbourhood of $N_2 = 0$

$$\Gamma_2^{(v)} = \Gamma_2^{(n)} = \Gamma_2^{(m)} = \Gamma_2^{(v)} = \Gamma_2^{(1)} \quad (63)$$

and in the immediate neighbourhood of $N_1 = 0$

$$\Gamma_1^{(v)} = \Gamma_1^{(n)} = \Gamma_1^{(m)} = \Gamma_1^{(v)} = \Gamma_1^{(2)}. \quad (64)$$

The values of the $\Gamma^{(v)}$, unlike those of the $\Gamma^{(1)}$, $\Gamma^{(2)}$, $\Gamma^{(n)}$, $\Gamma^{(m)}$, $\Gamma^{(v)}$ cannot be calculated from purely thermodynamic data. For to use (61) and (62) we must know the values of A_1 and A_2 to be inserted at each composition. Actually we know these values only roughly. As an approximation we must assume that A_1 and A_2 are independent of the composition. For the alcohol we may safely assume A_2 to be about 0.12×10^{20} sq. cm. per mole, equivalent to 20 \AA^2 per molecule, this being approximately the area occupied by a long chain aliphatic alcohol molecule orientated perpendicular to the surface in the insoluble unimolecular surface films.* For water it is more difficult to decide on the most likely value for A_1 . If we take as the area occupied by a water molecule that of the side of a cube, whose volume is equal to the mean volume occupied by a single molecule in the liquid state, the relevant value of A_1 is almost exactly one-half that assumed for A_2 .

Since, however, the molecules are presumably not cubic the true value of

* See Adam, "Physics and Chemistry of Surfaces," p. 50 (1930).

Δ_1 may be either greater or smaller according to how the molecules are orientated.

We have made calculations on the three alternative assumptions:—

- (1) Δ_1 equal to one-third of Δ_2 .
- (2) Δ_1 equal to one-half of Δ_2 .
- (3) Δ_1 equal to two-thirds of Δ_2 .

The results of these calculations are given in Table III, which is in three sections corresponding respectively to the three alternative values of Δ_1 . In each section the values of $\Gamma_2^{(v)}$ and of $\Gamma_1^{(w)}$ calculated by means of formulæ (61) and (62) are given in the first and second columns. In the third column in each section are given the values of $\frac{\Gamma_2^{(v)}}{\Gamma_1^{(v)} + \Gamma_2^{(v)}}$, the molecule fraction of alcohol in the unimolecular layer. It will be seen at once that the value assumed for Δ_2 , the area of the water molecule is of small importance. According to each of the three assumptions concerning the value of Δ_1 , as the mole fraction of alcohol in the interior increases to about 0.1 or 0.2 the mole fraction of alcohol in the unimolecular layer increases rapidly to about 0.7. It then remains almost unchanged until the mole fraction in the interior is over 0.5. It then increases steadily to the value of 1.0 in pure alcohol.

The very small apparent decrease in $\Gamma_2^{(v)}$ as N_2 increases from about 0.2 to about 0.4 is probably not real. It is probably due to the use of inexact values for Δ_1 and Δ_2 . It is extremely likely that the true values of Δ_1 and Δ_2

Table III.
(All Γ in 10^{-10} moles/cm²).

N_2	$\Delta_1 = 0.04 \times 10^{10}$ cm ² $\Delta_2 = 0.12 \times 10^{10}$ cm ²			$\Delta_1 = 0.06 \times 10^{10}$ cm ² $\Delta_2 = 0.12 \times 10^{10}$ cm ²			$\Delta_1 = 0.08 \times 10^{10}$ cm ² $\Delta_2 = 0.12 \times 10^{10}$ cm ²		
	$\Gamma_2^{(v)}$	$\Gamma_1^{(w)}$	$\frac{\Gamma_2^{(v)}}{\Gamma_1^{(v)} + \Gamma_2^{(v)}}$	$\Gamma_2^{(v)}$	$\Gamma_1^{(w)}$	$\frac{\Gamma_2^{(v)}}{\Gamma_1^{(v)} + \Gamma_2^{(v)}}$	$\Gamma_2^{(v)}$	$\Gamma_1^{(w)}$	$\frac{\Gamma_2^{(v)}}{\Gamma_1^{(v)} + \Gamma_2^{(v)}}$
0.0	0.0	25.0	0.00	0.0	16.7	0.00	0.0	12.5	0.00
0.05	6.2	6.4	0.49	6.1	4.5	0.57	6.0	3.5	0.63
0.1	6.8	4.6	0.60	6.7	3.3	0.67	6.6	2.6	0.72
0.2	7.25	3.25	0.69	7.1	2.5	0.74	7.0	2.1	0.77
0.3	7.25	3.25	0.69	7.0	2.7	0.72	6.9	2.2	0.76
0.4	7.25	3.25	0.69	6.9	2.9	0.71	6.7	2.4	0.74
0.5	7.3	3.1	0.70	6.9	2.9	0.71	6.7	2.5	0.73
0.6	7.45	2.65	0.74	7.1	2.5	0.74	6.8	2.3	0.75
0.7	7.65	2.0	0.79	7.4	1.9	0.80	7.15	1.8	0.80
0.8	7.9	1.3	0.88	7.65	1.4	0.85	7.5	1.25	0.86
0.9	8.1	0.7	0.94	8.0	0.7	0.92	7.9	0.65	0.93
1.0	8.35	0.0	1.00	8.35	0.0	1.00	8.35	0.0	1.00

depend somewhat on the relative numbers of alcohol and water molecules in the surfaces just as the partial molar volumes v_1 and v_2 vary with the composition of the solution.

In spite of a certain degree of uncertainty as to the exact values of A_1 and A_2 , the results of our calculations do seem to show that our theory that the only part of the liquid that is not homogeneous is a unimolecular layer leads to reasonable results. As the mole fraction of alcohol increases in the interior so it does in the unimolecular layer. The increase is perhaps not as steady as one might have expected, but this departure from the highest conceivable simplicity is not altogether surprising when one compares it with the complicated dependence of the partial vapour pressures or the partial molar volumes on the composition in the water-alcohol system. The alternative assumption made by Schofield and Rideal* that at mole fractions of alcohol greater than about 0.3 the surface contains a complete unimolecular layer of alcohol leads to the conclusion that below this unimolecular film there must be a layer containing excess of water. This theory seems to us unnecessarily complicated.

When our article was ready for the press a paper by Butler and Wightman† appeared with new measurements of the surface tension of water-alcohol mixtures at 25° C confirming the values of Bircumshaw. Values for $\Gamma_2^{(u)}$ are computed, agreeing fairly well with our own computations. Butler and Wightman also discuss the significance of these values in connection with the theory that the non-homogeneous part of the system is a unimolecular layer. Their formula (5) is a special case of our (45) and is equivalent to our (59), while their formula (4) is the same as our (60).

Summary.

The convention commonly used in fixing Gibbs' geometrical dividing surface, in which the surface excess $\Gamma_1^{(u)}$ of one of the components is arbitrarily taken as zero, is ill adapted to forming a physical picture of the structure of the surface. Several other conventions for fixing the interface have been examined. The relations between the values of Γ obtained on these various conventions are derived from Gibbs' general equations and formulæ are given for calculating each one of them.

The structure of the surface of water-alcohol mixtures is calculated approximately from the assumption that the inhomogeneous layer does not extend below the first layer of molecules.

* 'Proc. Roy. Soc.,' A, vol. 109, p. 61 (1925).

† 'J. Chem. Soc.,' p. 2089 (1932).

On the Flow of Electric Current in Semi-Infinite Stratified Media.

By LOUIS V. KING, F.R.S., Macdonald Professor of Physics, McGill University
Montreal, Canada.

(Received August 3, 1932.)

Section 1.—Introduction.

We suppose a semi-infinite medium to be built up of layers in each of which the electrical conductivity is finite. Direct current is introduced at a point electrode on the free surface and flows to a second electrode at a given distance away. It is obvious that the stream-lines and equipotentials accessible to measurements on the free surface will depend on the conductivities, depths and thicknesses of the strata. The problem dealt with in the present paper is to build up a theory of electrical conduction in stratified media which will enable the nature of the stratification to be deduced from measurements of surface potential gradients.

From the mathematical point of view, it is sufficient to obtain a solution for a single electrode from which current flows symmetrically to infinity. When the surface potential has been obtained for this simplified problem, the potential distribution for flow between several electrodes is found by addition.

The present investigation has shown a considerable advantage in the use of the *current function* ψ in solving the single electrode problem, in terms of which surface potentials and gradients may be easily derived, and hence by addition the solution for any stated distribution of electrodes. As far as the writer is aware, this method of treatment is new. It enables solutions for semi-infinite media in which the conductivity is a continuous function of the depth to be obtained and, in general, for discontinuously stratified media in each layer of which the conductivity varies continuously with the depth. These later developments are associated with Sturm-Liouville expansions and with inversion formulæ involving definite integrals of solutions of the Sturm-Liouville differential equation. In fact, the theory of electrical conduction in a semi-infinite medium in which the conductivity varies with the depth gives a physical interpretation of the Sturm-Liouville expansions and actually leads to a large class of inversion formulæ, connected with solutions of the Sturm-Liouville equation, of which Fourier's integral and Hankel's well-known theorem are examples.

In the present paper attention is confined to a number of simple problems of practical interest. It is evident that the results obtained from the theoretical treatment to be dealt with in the following sections have an application to the geophysical problem of determining the stratification constants at a certain locality on the earth's surface by measurements of surface potential gradients, current being introduced at suitably disposed electrodes. This method has now become one of the standard methods of "geophysical prospecting," for a description of which the reader is referred to several well-known treatises.*

While it is comparatively easy to obtain field data, the interpretation of field graphs in terms of stratification is a problem of great difficulty and interest, towards the solution of which it is hoped that the present paper makes a contribution.

The numerical computation of tables from which graphs and nomograms for the analysis of field data has been considered beyond the scope of the present paper. This feature of the work, as well as the design of integragraphs for the machine analysis of field graphs, is more especially the province of geophysical institutes or research organisations in close touch with practical problems of geophysical prospecting.

Section 2.—The Electrical Current Function ψ . The Surface Gradient Characteristic, $\bar{\rho}/\rho$.

We suppose current to be introduced at a theoretical point-electrode at the free surface. We take this to be the origin of a system of cylindrical co-ordinates, (r, z) . The specific resistance ρ is supposed to depend only on the depth z measured from the free surface. The potential V at any point must satisfy the equation of continuity

$$\frac{1}{r} \frac{\partial}{\partial r} \left(\frac{r}{\rho} \frac{\partial V}{\partial r} \right) + \frac{\partial}{\partial z} \left(\frac{1}{\rho} \frac{\partial V}{\partial z} \right) = 0, \quad (1)$$

subject to the various boundary conditions. Since there is no flow of electricity across the plane $z = 0$, we have in all cases,

$$\frac{\partial V}{\partial z} = 0 \quad \text{at} \quad z = 0. \quad (2)$$

* Hummel, "A Theoretical Study of Apparent Resistivity in Surface Potential Methods," Amer. Inst. Min. Metall. Eng. N.Y. Tech. Pub., 418 (1931).

Eve and Keys, "Applied Geophysics in the Search for Minerals," Camb. Univ. Press (1929).

If the resistance changes suddenly over a plane $z = h$, we have to find a solution V of equation (1) for the adjacent medium of specific resistance ρ' subject to the boundary conditions,

$$V = V' \quad \text{and} \quad \frac{1}{\rho} \frac{\partial V}{\partial z} = \frac{1}{\rho'} \frac{\partial V'}{\partial z} \quad \text{at} \quad z = h, \quad (3)$$

with similar conditions at each interface separating media of different conductivities.

It is convenient to introduce an "electrical current function" ψ defined by the equations,

$$u_r = \frac{1}{r} \frac{\partial \psi}{\partial z} = -\frac{1}{\rho} \frac{\partial V}{\partial r} \quad \text{and} \quad u_z = -\frac{1}{\rho} \frac{\partial V}{\partial z} = -\frac{1}{r} \frac{\partial \psi}{\partial r}, \quad (4)$$

where u_r and u_z are the radial and axial components of current flow across unit area.

Eliminating V , it is readily seen that ψ satisfies the differential equation

$$\frac{\partial^2 \psi}{\partial r^2} - \frac{1}{r} \frac{\partial \psi}{\partial r} + \frac{1}{\rho} \frac{\partial}{\partial z} \left(\rho \frac{\partial \psi}{\partial z} \right) = 0, \quad (5)$$

while the boundary conditions (3) are replaced by

$$\psi = \psi' \quad \text{and} \quad \rho \frac{\partial \psi}{\partial z} = \rho' \frac{\partial \psi'}{\partial z} \quad \text{at} \quad z = h. \quad (6)$$

In any plane through the axis of z we draw a curve from a point on the axis to the plane $z = 0$. Consider the flow across the surface of revolution generated by rotating this curve about the axis, between two planes at a distance dz apart, and two axial planes making an angle $d\theta$ with each other. Obviously, referring to fig. 1, the equation of continuity gives for the outward flow δI across the area, $r d\theta \, ds$,

$$\delta I = u_r \cdot r d\theta \cdot dz + u_z \cdot r d\theta \cdot dr,$$

or from (4),

$$= \left(\frac{\partial \psi}{\partial z} dz - \frac{\partial \psi}{\partial r} dr \right) d\theta = \delta \psi \cdot d\theta. \quad (7)$$

Since the co-ordinates of the extremities of ds are (r, z) and $(r + dr, z - dz)$, the result of integrating with respect to θ , and with respect to s along the curve from A to B, gives for the flow across the corresponding portion of the surface

of revolution, $I = 2\pi(\psi_A - \psi_B)$. In particular, if we take $\psi_A = \psi_0$ on the axis of z , and $\psi_B = \psi_s$ on the surface $z = 0$, we may write

$$I = 2\pi(\psi_0 - \psi_s). \quad (8)$$

In the above equation I is obviously the total current introduced at the electrode.

If the element ds of the curve AB is chosen so that there is no flow across it, $\delta\psi = 0$ along it, so that $\psi = \text{constant}$ represents a family of stream-lines.

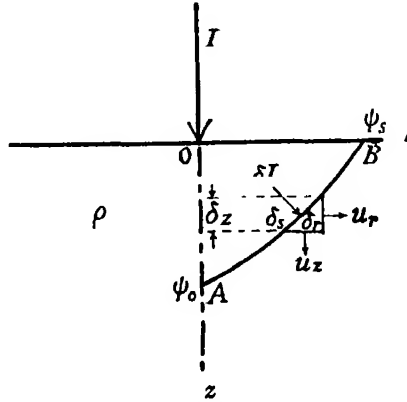


FIG. 1.

Since by (6) ψ is continuous over a surface of discontinuity, it is readily seen that (8) holds generally for all cases where ψ_0 is taken on the axis, even if the medium be discontinuously stratified.

Since I is a constant, it is also evident that the solution of (5) appropriate to a point electrode at the origin must be such that its value ψ_0 on the axis is independent of z , a property of great assistance in finding the requisite solutions.

It is readily seen that the function ψ defined by equations (4) corresponds, in electrical conduction problems, to Stokes's "current function" in hydrodynamics, and that, in general, such a function exists in stratified media in which the specific resistance is a continuous or discontinuous function of the depth z .

The magnetic field H consists of lines of force in circles having their centres on the axis through the electrode. If ψ is the value of the stream function at (r, z) , it follows from Ampere's formula that

$$rH = 4\pi(\psi_0 - \psi),$$

which gives a physical interpretation of ψ in terms of the magnetic work-

function rH , especially useful in solving problems involving the propagation of electromagnetic effects in conducting media.

For a medium of constant specific resistance $\rho = \rho_0$, we at once see that

$$V = \frac{C}{(r^2 + z^2)^{1/2}} = \frac{C}{R}, \quad \text{where} \quad R^2 = r^2 + z^2, \quad (10)$$

is a solution of the equation of continuity (I). By integrating the flow across a hemisphere or cylinder enclosing the electrode, we easily obtain the constant $C = I\rho_0/(2\pi)$. Over the surface $z = 0$, we have,

$$V_s = \frac{I\rho_0}{2\pi} \cdot \frac{1}{r} \quad \text{and} \quad \frac{dV_s}{dr} = -\frac{I\rho_0}{2\pi} \cdot \frac{1}{r^2}. \quad (11)$$

In practice it is not possible to measure the surface potential V_s , but the surface gradient dV_s/dr is easily measurable.

When the medium is stratified or varies continuously in specific resistance, the above laws are departed from, and in general, from (4) we have

$$-\frac{dV_s}{dr} = \frac{\rho_s}{r} \left[\frac{\partial \psi}{\partial z} \right]_{z=0},$$

ρ_s being the specific resistance at the surface $z = 0$.

It is convenient to define by $\bar{\rho}$ the observable combination of quantities,

$$\bar{\rho} = -\frac{2\pi r^2}{I} \frac{\delta V_s}{\delta r} = \frac{2\pi \rho_s}{I} r \left[\frac{\partial \psi}{\partial z} \right]_{z=0}, \quad (12)$$

or

$$\frac{\bar{\rho}}{\rho_s} = \frac{2\pi r}{I} \left[\frac{\partial \psi}{\partial z} \right]_{z=0}. \quad (13)$$

For a homogeneous medium it is evident that $\bar{\rho}/\rho_s = 1$, which when plotted against distance gives a straight line through the point 1 parallel to the r axis. When the medium is stratified we obtain a curve departing from this straight line, from which the nature of the stratification is to be inferred. In geophysical prospecting the curve $\bar{\rho}/\rho_s$ plotted against r may be referred to as the "surface gradient characteristic."* In the following sections, this "gradient characteristic" is worked out for various stratifications. It will be seen that the use of the electrical stream-function ψ leads directly to extremely convergent series or integrals expressing the dependence of $\bar{\rho}/\rho_s$ on the distance from the electrode.

* This name seems to the author preferable to the designation "apparent resistivity" for the quantity $\rho_s/\bar{\rho}$, which has been employed by several writers. This is especially so when media of variable specific resistance are dealt with.

Section 3.—On the Determination of the Current-Function ψ for Stratified Media.

When the specific resistance ρ is constant, the differential equation for ψ is,

$$\frac{\partial^2 \psi}{\partial r^2} - \frac{1}{r} \frac{\partial \psi}{\partial r} + \frac{\partial^2 \psi}{\partial z^2} = 0. \quad (14)$$

Following the usual procedure, we seek solutions of the form

$$\psi = R \cdot Z, \quad (15)$$

where R is a function of r only, and Z depends only on the depth z .

By substituting in (14), it is seen that a solution of the special type (15) is possible if R and Z each satisfy the differential equations,

$$\frac{d^2 R}{dr^2} - \frac{1}{r} \frac{dR}{dr} - \lambda^2 R = 0 \quad \text{and} \quad \frac{d^2 Z}{dz^2} + \lambda^2 Z = 0, \quad (16)$$

where λ is a parameter to be chosen to suit the boundary conditions of the problem.

The equation in R has the solutions $r\lambda K_1(r\lambda)$ and $r\lambda I_1(r\lambda)$, in the standard notation for Bessel functions of imaginary argument.

The K -functions are defined by the definite integrals,

$$K_0(x) = \int_0^\infty e^{-x \cosh \phi} d\phi, \quad K_1(x) = -\frac{d}{dx} K_0(x) = \int_0^\infty \cosh \phi e^{-x \cosh \phi} d\phi, \quad (17)$$

while the I -functions are defined by

$$I_0(x) = \frac{1}{\pi} \int_0^\pi e^{-x \cos \phi} d\phi, \quad I_1(x) = \frac{d}{dx} I_0(x) = -\frac{1}{\pi} \int_0^\pi \cos \phi e^{-x \cos \phi} d\phi. \quad (18)$$

Since the I -functions tend to infinite values as x becomes large, while ψ must have a finite value on the axis, we make use of the one solution

$$R = Ar\lambda K_1(r\lambda), \quad (19)^*$$

* For the reader's convenience a few of the more elementary properties of $K_0(x)$ and $K_1(x)$ are recapitulated in Note (i) of the Appendix. For more detailed properties, the reader is referred to Gray, Mathews and MacRobert, "Treatise on Bessel Functions" (Macmillan & Co., 1922). G. N. Watson, "Theory of Bessel Functions" (Macmillan & Co., 1922). Jahnke und Emde's "Funktionentafeln mit Formeln und Kurven" (Teubner, Berlin, 1923). Here the notation differs somewhat from that of the standard English treatises, e.g., $K_0(x) = \frac{1}{2}\pi i H_0^{(1)}(ix)$, and $K_1(x) = -\frac{1}{2}\pi i H_1^{(1)}(ix)$.

Extensive tables of Bessel Functions are in course of preparation by a Committee of the British Association, useful "Mathematical Tables," vol. 1, (1931) having just been published.

which tends to zero for large values of r , and, in addition, has the convenient property,

$$\lim_{r \rightarrow 0} x K_1(x) = \lim_{r \rightarrow 0} r \lambda K_1(r \lambda) \sim 1. \quad (20)$$

The second equation in (16) has the obvious solutions,

$$Z = \sin \lambda z \quad \text{and} \quad Z = \cos \lambda z.$$

Since the additive constant implicit in a solution of (14) has been chosen to make $\psi = 0$ at the surface $z = 0$, we make use of a solution of the type,

$$\psi = \sum_{\lambda} A_{\lambda} \sin \lambda z \cdot r \lambda K_1(r \lambda) + Cz. \quad (21)$$

The term Cz is a particular solution of the differential equation (14) corresponding to $V = -C\rho \log r + \text{constant}$, which must be included to express the fact that in some cases the distribution of potential at great distances from the electrode approximates to that characteristic of two-dimensional flow, as for instance when the medium is bounded by an insulating plane.

The type of solution (21) is adapted to two special boundary conditions—(i) when the medium is bounded by an insulating plane, and (ii) when the boundary plane is perfectly conducting and therefore an equipotential. In these circumstances the summation is extended over values of λ , given by an *equation of condition* resulting from the boundary conditions, while the coefficients A_{λ} are determined by taking $r = 0$, when, according to (8)

$$\psi = \psi_0 = I/(2\pi), \quad (22)$$

expressing the fact that the flow across the surface of revolution swept out by a plane curve extending from *any* point on the axis to the surface is equal to I , so that ψ_0 is independent of z .

When the medium in question is bounded by an infinitely extended one of finite conductivity, expansions of the type (21) are no longer possible, because the intervals between successive roots of the equation of condition become infinitesimal, in which circumstances the series (21) degenerates into a definite integral of the type

$$\psi = \int_0^{\infty} \phi(\lambda) \sin \lambda z \cdot r \lambda K_1(r \lambda) d\lambda + Cz. \quad (23)$$

Since we are primarily interested in the “surface gradient characteristic” $\bar{\rho}/\rho$, this is immediately given by (18) either in the form of the series,

$$\frac{1}{2\pi} \frac{\bar{\rho}}{\rho} = r \left[\frac{\partial \psi}{\partial z} \right]_{z=0} = \sum_{\lambda} A_{\lambda} r^2 \lambda^2 K_1(r \lambda) + Cr, \quad (24)$$

or as a definite integral

$$\frac{I}{2\pi\rho} = \int_0^\infty \phi(\lambda) r^2 \lambda^2 K_1(r\lambda) d\lambda + Cz. \quad (25)$$

In a later paper we shall consider general methods for determining the coefficients A_s for complex types of stratification, or in the case of infinitely extended media, where conductivity varies continuously with the depth, we shall show how the fundamental *integral equation* of which (23) is a special type may always be solved. For the present we shall illustrate the general procedure just described by determining ψ for a number of simple types of stratifications dealt with in the following sections.

Section 4.—Homogeneous Medium Bounded by Insulating Plane $z = h$.

Following the procedure described in Section 3, we may express ψ in the form,

$$\psi = \sum_s A_s \sin \lambda z \cdot r \lambda K_1(r\lambda) + Cz. \quad (26)$$

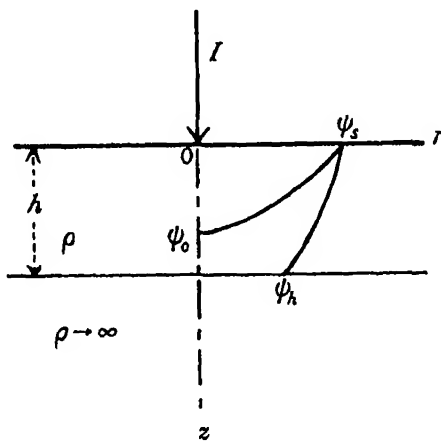


FIG. 2.

Boundary Condition.—Since there is no flow across the plane $z = h$, we evidently have from the definition of ψ ,

$$I/2\pi = \psi_h - \psi_s = \psi_0 - \psi_s \quad \text{for all values of } r. \quad (27)$$

Since $\psi_s = 0$, it follows from (26) that the *equation of condition* is

$$\sin \lambda h = 0, \quad \text{so that} \quad \lambda = s\pi/h, \quad (s = 1, 2, 3, \dots). \quad (28)$$

By taking $r \rightarrow \infty$, it follows that since $r\lambda K_1(r\lambda) \rightarrow 0$,

$$Ch = I/(2\pi).$$

If now we take ψ on the axis $r \rightarrow 0$, it follows from (26) and (27) that for all values of z ,

$$\frac{1}{2\pi} \left(1 - \frac{z}{h} \right) = \sum_s A_s \sin \lambda z, \quad (0 < z < h), \quad (29)$$

which is an ordinary Fourier series for the determination of the coefficients A_s . Multiplying each side of (29) by $\sin \lambda z$ and integrating with respect to z from 0 to h , we find without difficulty that

$$A_s = I/(\pi h \lambda),$$

so that the expression for ψ , satisfying all the conditions of the problem, is,

$$\psi = \frac{1}{2\pi} \left[\frac{z}{h} + \frac{2r}{h} \sum \sin \lambda z K_1(r\lambda) \right], \quad (\lambda = s\pi/h). \quad (30)$$

It now follows from (24) that the surface gradient characteristic is,

$$\frac{\bar{\rho}}{\rho} = \frac{r}{h} + 2 \frac{r}{h} \sum \lambda r K_1(r\lambda) - \frac{r}{h} + 2\pi \left(\frac{r}{h} \right)^2 \sum_{s=1}^{\infty} s K_1 \left(\frac{\pi r}{h} s \right), \quad (31)$$

a rapidly convergent expansion when r/h is of order unity.

When x is small, it is proved in Note (u) of the Appendix that

$$\sum_{s=1}^{\infty} K_0(sx) \sim \frac{1}{2}\pi/x + \frac{1}{2} \log x - \left(\frac{1}{2} \log 4\pi - \frac{1}{2}\gamma \right) + \dots \quad (32)$$

Differentiating with respect to x ,

$$\sum_{s=1}^{\infty} s K(sx) \sim \frac{1}{2}\pi/x^2 - \frac{1}{2}/x + \dots \quad (33)$$

Writing $x = \pi r/h$, the series (31) gives, when $h \rightarrow \infty$, $\bar{\rho}/\rho \sim 1$, as should be the case in a semi-infinite homogeneous medium. The expansion of $\bar{\rho}/\rho$ for small values of r/h is given in Note (iv) of the Appendix.

Section 5.—Homogeneous Medium Bounded by a Perfectly Conducting Plane $z = h$.

As before we express ψ in the form

$$\psi = \sum_s A_s \sin \lambda z \cdot r \lambda K_1(r\lambda) + Cz. \quad (34)$$

Boundary Condition.—Since the stream lines $\psi = \text{constant}$ cut the boundary plane $z = h$ everywhere at right angles, $\partial\psi/\partial z = 0$ at $z = h$ for all values of r , from which it follows at once, by making $r \rightarrow \infty$, that $C = 0$. Furthermore, the equation of condition is

$$\cos \lambda h = 0, \quad \text{so that} \quad \lambda = (s - \frac{1}{2})\pi/h, \quad (s = 1, 2, 3, \dots). \quad (35)$$

If now we take ψ on the axis $r = 0$, where $\psi = \psi_0 = I/(2\pi)$ for all values of z , it follows from (34) and (35) that

$$I/(2\pi) = \Sigma A_s \sin \lambda z, \quad (0 < z < h),$$

a well-known Fourier expansion. We easily find in the usual way that

$$A_s = I/(\pi h \lambda),$$

so that the solution for ψ is

$$\psi = \frac{I}{\pi} \cdot \frac{r}{h} \Sigma \sin \lambda z K_1(r\lambda), \quad (\lambda = (s - \frac{1}{2})\pi/h). \quad (36)$$

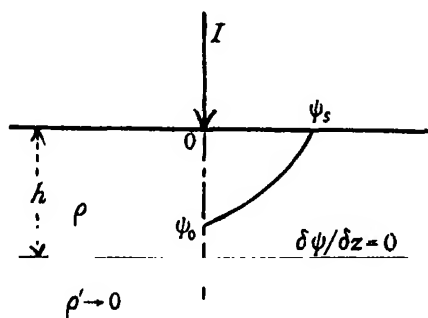


FIG. 3.

From (18) it follows that the "surface gradient characteristic" may be written,

$$\frac{\bar{\rho}}{\rho} = 2 \frac{r}{h} \Sigma \lambda r K_1(r\lambda) = 2\pi \left(\frac{r}{h}\right)^2 \Sigma_{s=1}^{\infty} (s - \frac{1}{2}) K_1 \left\{ \frac{\pi r}{h} (s - \frac{1}{2}) \right\}, \quad (37)$$

a rapidly converging expansion when $r/h \sim 1$.

When x is small, it is proved in Note (iii) of the Appendix that

$$\Sigma_{s=1}^{\infty} K_0 \{(2s - 1)x\} \sim \frac{1}{4}\pi/x + \frac{1}{2} \log 2 + \dots, \quad (38)$$

giving by differentiation,

$$\Sigma_{s=1}^{\infty} (2s - 1) K_1 \{(2s - 1)x\} \sim \frac{1}{4}\pi/x^2 + \dots, \quad (39)$$

from which it follows, writing $x = \frac{1}{2}\pi r/h$ in (37) that when $h \rightarrow \infty$, $\bar{\rho}/\rho \sim 1$, as we should expect in the case of a semi-infinite homogeneous medium. The

detailed expansion of $\bar{\rho}/\rho$ for small values of r/h is considered in Note (iv) of the Appendix.

Section 6.—Two Media in Contact Bounded by Insulating Plane.

Let the upper layer, of specific resistance ρ and thickness h , be in contact with a second layer for which the corresponding quantities are ρ' and h' . This

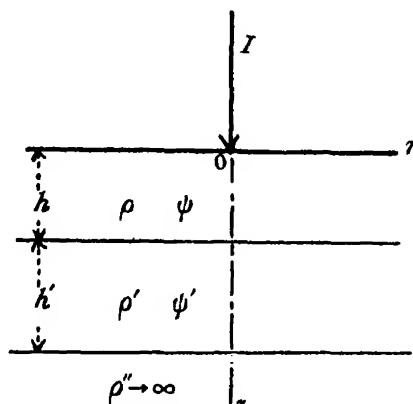


FIG. 4.

layer is bounded by an insulating plane at $z = h + h'$. As in the preceding problems, the current functions ψ and ψ' in each medium may be written,

$$\left. \begin{aligned} \psi &= \Sigma A_s \sin \lambda z \cdot r \lambda K_1(r\lambda) + Cz \\ \psi' &= \Sigma A'_s \sin \lambda(h + h' - z) \cdot r \lambda K_1(r\lambda) + B' + C'z \end{aligned} \right\} \quad (40)$$

The boundary conditions are, at $z = h$,

$$\psi = \psi' \quad \text{and} \quad \rho \partial\psi/\partial z = \rho' \partial\psi'/\partial z$$

for all values of r . As a consequence we have

$$A \sin \lambda h = A' \sin \lambda h' \quad \text{and} \quad \rho A \cos \lambda h = -\rho' A' \cos \lambda h', \quad (41)$$

which give, on eliminating A and A' , the equation of condition

$$\rho' \tan \lambda h + \rho \tan \lambda h' = 0. \quad (42)$$

Furthermore, when $r \rightarrow \infty$, we must have at $z = h$,

$$B' + C'h = Ch \quad \text{and} \quad C\rho = C'\rho'. \quad (43)$$

At the insulating boundary an additional equation results from the fact that the flow across the surface of revolution swept out by a plane curve extending

from any point in the plane $z = h + h'$ to the surface $z = 0$ is $I/(2\pi)$ for all values of r .

When $r \rightarrow \infty$, it is evident from (40) that this results in the equation

$$I/2\pi = (B' + C'h) + C'h',$$

or, making use of (43),

$$Ch + C'h' = I/(2\pi). \quad (44)$$

It is convenient to write

$$\gamma = (h'\rho)/(h\rho'), \quad (45)$$

in terms of which, $C = I/\{2\pi h(1 + \gamma)\}$.

The coefficients A in (40) are determined from the expansion of ψ when $r = 0$, when, according to (22) we have $\psi = \psi_0 = I/(2\pi)$ for all values of z between 0 and h . According to (40) we have

$$\frac{I}{2\pi} = \sum A \sin \lambda z + \frac{I}{2\pi(1 + \gamma)} \frac{z}{h}, \quad (0 < z < h), \quad (46)$$

λ being the roots of the transcendental equation (42).

The general theory of such expansions will be considered in a later communication. For the present we content ourselves by noticing that when the thickness h' of the lower layer is small so that $\lambda h'$ is negligible, while γ remains finite, the equation of condition becomes

$$\tan \lambda h + \gamma \cdot \lambda h = 0, \quad (47)^*$$

one for which expansions of the type (46), were originally considered by Fourier.†

Following the usual procedure, we find

$$A = \frac{I}{\pi \lambda h} \cdot \frac{1}{1 + \gamma \cos^2 \lambda h},$$

and finally, from (24), for the "surface gradient characteristic," the expression,

$$\frac{\bar{p}}{\rho} = \frac{r}{h(1 + \gamma)} + 2 \frac{r}{h} \sum \frac{r \lambda K_1(r \lambda)}{1 + \gamma \cos^2 \lambda h}. \quad (48)$$

It is easily verified that when $\rho' \rightarrow \infty$ or $\rho' > 0$, the formula (48) reduces to (31) and (37) respectively.

* Tables giving the roots of transcendental equation of this type are given by McKay, 'Proc. Phys. Soc. Lond.,' vol. 44, p. 22 (1932).

† Carslaw, "Fourier Series and Integrals" (Macmillan & Co., 1921). Also "Heat Conduction" (Macmillan & Co., 1921), where problems of this type are dealt with.

Section 7.—Two Media Bounded by Insulating Plane.

(i) *Solution in Terms of Definite Integrals involving $J_0(r\lambda)$.*—When the lower medium considered in the problem of the preceding section has an infinite depth, the roots of the equation of condition (42) become separated by infinitesimal intervals. It is instructive in view of later developments to deal with the case of two media bounded by an insulating plane according to a well-known method which enables us to express the surface potential as a definite integral involving $J_0(r\lambda)$.* It is readily seen that the equation (1) for the potential V may be written,

$$\frac{\partial^2 V}{\partial r^2} + \frac{1}{r} \cdot \frac{\partial V}{\partial r} + \frac{\partial^2 V}{\partial z^2} = 0. \quad (49)$$

It is satisfied in each medium by the expressions,

$$V = \frac{I\rho}{2\pi} \int_0^\infty \{e^{z\lambda} + A(\lambda) \cdot \cosh \lambda z\} J_0(\lambda r) d\lambda, \quad (50)$$

and

$$V' = \frac{I\rho}{2\pi} \int_0^\infty B(\lambda) \cosh \lambda (h + h' - z) \cdot J_0(\lambda r) d\lambda \quad (51)$$

where $A(\lambda)$ and $B(\lambda)$ are functions of λ to be determined from the boundary conditions (3) at $z = h$.

Making use of the well-known integral

$$\int_0^\infty e^{-ax} J_0(bx) dx = \frac{1}{(a^2 + b^2)^{1/2}}, \quad (52)$$

it is readily seen that $(\partial V / \partial z) = 0$ at the boundaries $z = 0$ and $z = h + h'$.

The flow across the boundary of a cylinder of radius r and depth h in the first medium is

$$I = \frac{1}{\rho} \int_0^r \frac{\partial V}{\partial z} \cdot 2\pi r dr + \frac{1}{\rho} \int_0^r \frac{\partial V}{\partial r} \cdot 2\pi r dz, \quad (53)$$

which is also satisfied by (50) for all values of r and z . Writing $z = 0$ in equation (50), we see that the surface potential is given by

$$V_s = \frac{I\rho}{2\pi} \int_0^\infty (1 + A) J_0(\lambda r) d\lambda. \quad (54)$$

We find on calculating A and B from the boundary conditions that

$$V_s = \frac{I\rho}{2\pi} \int_0^\infty \frac{\rho \sinh \lambda h \cdot \sinh \lambda h' + \rho' \cosh \lambda h \cdot \cosh \lambda h'}{\rho \cosh \lambda h \cdot \sinh \lambda h' + \rho' \sinh \lambda h \cdot \cosh \lambda h'} \cdot J_0(\lambda r) d\lambda. \quad (55)$$

* Ollendorff, "Erdströme," p. 69 (Springer, Berlin, 1928).

It is possible, by making use of Mehler's integral*

$$\int_0^\infty \frac{x J_0(ax) dx}{x^2 + k^2} = K_0(ak), \quad (56)$$

to develop an integral of the type (55) in a series of K_0 -functions in cases where the coefficient of $J_0(\lambda r)$ is capable of expansion in the form

$$\frac{\phi(\lambda)}{\psi(\lambda)} = \frac{a_0}{\lambda} + \sum \frac{a_u \lambda}{\lambda^2 + \alpha^2}, \quad (57)$$

the summation being extended to include the roots of $\psi(\lambda) = 0$, which, with the exception of a possible zero root, are supposed to be all purely imaginary and different in value.

The coefficients a_u are evidently given by

$$a_0 = \lim_{\lambda \rightarrow 0} \left[\frac{\lambda \phi(\lambda)}{\psi(\lambda)} \right] \quad \text{and} \quad a_u = \lim_{\lambda \rightarrow i\alpha} \left[\frac{2\phi(\lambda)}{\psi'(\lambda)} \right]. \quad (58)$$

Introducing the constant

$$\beta = (\rho' - \rho) / (\rho' + \rho), \quad (59)$$

we may write (55) in the more convenient form,

$$V_r = \frac{I\rho}{2\pi} \int_0^\infty \frac{\cosh \lambda(h+h') + \beta \cosh \lambda(h-h')}{\sinh \lambda(h+h') + \beta \sinh \lambda(h-h')} \cdot J_0(\lambda r) d\lambda. \quad (60)$$

We easily find

$$\left. \begin{aligned} \sigma_0 &= \frac{I}{2\pi} \cdot \frac{\rho\rho'}{\rho h' + \rho' h}, \quad \frac{1}{2}a_u = \frac{I\rho}{2\pi} \cdot \frac{\cos \alpha(h+h') + \beta \cos \alpha(h-h')}{(h+h') \cos \alpha(h+h') + \beta \cos \alpha(h-h')} \\ \text{or} \quad \frac{1}{2}a_u &= \frac{I\rho}{2\pi} \cdot \frac{\sin 2\alpha h'}{h \sin 2\alpha h' - h' \sin 2\alpha h} \end{aligned} \right\} \quad (61)$$

α being the positive root of the equation of condition

$$\sin \alpha(h+h') + \beta \sin \alpha(h-h') = 0 \quad \text{or} \quad \rho' \tan \alpha h + \rho \tan \alpha h' = 0. \quad (62)$$

Since

$$\left. \begin{aligned} \frac{d}{dr} \int_0^\infty \frac{J_0(\lambda r) d\lambda}{\lambda} &= - \int_0^\infty J_1(\lambda r) d\lambda = - \frac{1}{r}, \\ \text{we may write} \quad \int_0^\infty \frac{J_0(\lambda r) d\lambda}{\lambda} &= - \log r + \text{const.} \end{aligned} \right\} \quad (62.1)$$

* Watson, "Theory of Bessel Functions," p. 425 (1922).

Finally, making use of (56), we obtain the following expansion for the surface potential,

$$V_s = -\frac{I\rho}{2\pi} \left[\frac{\rho'}{h\rho' + h'\rho} \log r - \sum \frac{2 \sin 2\alpha h'}{h \sin 2\alpha h' - h' \sin 2\alpha h} \cdot K_0(\alpha r) \right]. \quad (63)$$

It may be verified that when $h = 0$, or $h' = 0$, or $\beta = 0$, or $\beta = 1$, the solution (63) reduces to (30), while the case $\beta = -1$ leads to the expansion (36).

Furthermore, when $\alpha h'$ is small, the equation of condition (62) becomes $\tan \alpha h = -\gamma \cdot \alpha h$, and from (61),

$$\frac{1}{2}a_u = \frac{I\rho}{2\pi} \cdot \frac{2\alpha}{2\alpha h - \sin 2\alpha h} = \frac{I\rho}{2\pi} \cdot \frac{1}{h} \cdot \frac{1}{1 + \gamma \cos^2 \alpha h},$$

which agrees with the expansion (48) already obtained

Of some interest, as admitting of easy computations, is the case $h = h'$, when the equation of condition is

$$\sin 2\lambda h = 0, \text{ so that } \lambda = \frac{1}{2}u\pi/h, \text{ and } \cos 2\lambda h = (-1)^u.$$

Thus

$$a_0 = \frac{I}{2\pi h} \cdot \frac{\rho\rho'}{\rho + \rho'} = \frac{I\rho}{2\pi h} \cdot \frac{1}{2} (1 + \beta), \quad \frac{1}{2}a_u = \frac{1 + (-1)^u \beta}{2h}.$$

Writing $x = \frac{1}{2}\pi r/h$, we have in this particular case

$$V_s = -\frac{I\rho}{2\pi h} \left[\frac{1}{2} (1 + \beta) \log x - \sum_{u=1}^{\infty} \{1 + (-1)^u \beta\} K_0(u\pi) \right] + \text{const.} \quad (64)$$

When the thickness of the medium (ρ' , h') tends to a very large and ultimately infinite value, it is readily seen that the roots of the equation of condition, $\rho' \tan \alpha h + \rho \tan \alpha h' = 0$, become separated by infinitesimal intervals, which ultimately tend to $\delta\alpha = \text{Lt. } (\pi/h')$. In these circumstances, it follows from (61) that

$$\frac{1}{2}a_u = -\frac{I\rho}{2\pi} \frac{\sin 2\alpha h'}{h' \sin 2\alpha h} \quad (64.1)$$

Replacing, ultimately, $1/h'$ by $d\alpha/\pi$, and expressing $\sin 2\alpha h'$ in terms of αh from the equation of condition, we find

$$\text{Lt. } \frac{1}{2}a_u = \frac{\rho\rho'}{\rho^2 \cos^2 \lambda + \rho'^2 \sin^2 \lambda} \cdot \frac{d\alpha}{\pi}.$$

The logarithmic term of (63) disappears, and the summation ultimately becomes an integral between limits zero and infinity, leading to the expression, when h' tends to infinite depth,

$$V_s = \frac{I\rho}{\pi^2} \int_0^{\infty} \frac{\rho\rho'}{\rho^2 \cos^2 \alpha h + \rho'^2 \sin^2 \alpha h} \cdot K_0(\alpha r) d\alpha, \quad (64.2)$$

which reduces, as it should, to $V_s = I\rho/(2\pi r)$ when $\rho = \rho'$. Writing $\alpha h = \frac{1}{2}t$, and $\beta = (\rho' - \rho)/(\rho' + \rho)$, we easily find

$$V_s = \frac{I\rho}{2\pi^2} \cdot \frac{(1 - \beta^2)}{h} \int_0^\infty \frac{K_0(\frac{1}{2}rt/h) dt}{1 - 2\beta \cos t + \beta^2}. \quad (64.3)$$

A result which will be derived independently in the next section.

Section 8—Layer of Thickness h Bounded by Semi-Infinite Medium.

Following the procedure of the preceding section, we write

$$V = \frac{I\rho}{2\pi} \int_0^\infty (e^{-\lambda z} + A \cosh \lambda z) J_0(\lambda r) d\lambda \quad \text{and} \quad V' = \frac{I\rho}{2\pi} \int_0^\infty B \cdot e^{-\lambda z} \cdot J_0(\lambda r) d\lambda,$$

and obtain from the boundary conditions, the constants A and B , so that

$$V_s = \frac{I\rho}{2\pi} \int_0^\infty \frac{\rho \sinh \lambda h + \rho' \cosh \lambda h}{\rho \cosh \lambda h + \rho' \sinh \lambda h} \cdot J_0(\lambda r) \cdot d\lambda, \quad (65)^*$$

equivalent to writing $h' = \infty$ in (55). It is evident that an expansion in K_0 -functions is not possible in this case. In terms of β defined by (59), we may write (65) in the form

$$V_s = \frac{I\rho}{2\pi} \int_0^\infty \frac{1 + \beta e^{-2\lambda h}}{1 - \beta e^{-2\lambda h}} \cdot J_0(\lambda r) dr.$$

Expanding in powers of $e^{-2\lambda h}$, and making use of (52), we readily obtain the expansion, in powers of $\beta = (\rho' - \rho)/(\rho' + \rho)$,

$$V_s = \frac{I\rho}{2\pi} \left[\frac{1}{r} + 2 \sum_{u=1}^\infty \frac{\beta^u}{\{r^2 + (2uh)^2\}^{\frac{1}{2}}} \right] \quad (66)^\dagger$$

an expression easily obtained independently by the method of images, but, unfortunately not satisfactorily convergent for purposes of numerical computation unless β is small.

* By methods of contour integration, of which an example proving independently the equivalence of the integrals (64.2) and (65) is given in Section 10, we may in general expect to replace integrals involving $J_0(\lambda r)$ by much more convergent ones involving $F_0(\lambda r)$.

† This result is easily obtained by the method of images following the procedure developed in an analogous problem by Maxwell ('Electricity and Magnetism,' vol. 1, Chap. XI, 1873). The method of images is the basis of elaborate calculations on electrical conduction in stratified media by Hummel, J. N., published in 'Gerlands Beiträge,' vol. 20, pp. 281-287 (1928). A detailed summary of these investigations is given in a paper by Hummel, *loc. cit.* (1931).

Making use of the integral (20.1) we may write (66) in the form,

$$V_s = \frac{I\rho}{\pi^2} \int_0^\infty K_0(rx) \cdot \left\{ 1 + 2 \sum_{u=1}^\infty \beta^u \cos 2hux \right\} \cdot dx.$$

Since $\beta^2 < 1$, making use of a well-known summation, we obtain the expression

$$V_s = \frac{I\rho}{\pi^2} (1 - \beta^2) \int_0^\infty \frac{K_0(rx) dx}{1 - 2\beta \cos 2hx + \beta^2},$$

or, writing $x = \frac{1}{2}t/h$, we have the convergent integral, well suited to numerical computation,

$$V_s = \frac{I\rho}{2\pi^2} \cdot \frac{(1 - \beta^2)}{h} \int_0^\infty \frac{K_0(\frac{1}{2}rt/h) dt}{1 - 2\beta \cos t + \beta^2}, \quad (67)$$

which agrees with (64.3).

For purposes of computation we may write,

$$V_s = \frac{I\rho}{2\pi^2} \cdot \frac{(1 - \beta^2)}{h} \sum_{n=0}^\infty \int_0^{2\pi} \frac{K_0\{(t + 2u\pi)x\} dt}{1 - 2\beta \cos t + \beta^2}, \quad (68)$$

where we have written $x = \frac{1}{2}r/h$.

The integral is convergent except in the neighbourhood of $\beta = \pm 1$.

As the solution of the problem of the present section represents a state of affairs likely to be met with in practice, when β does not approach closely to ± 1 , it is of some importance to discuss the nature of the gradient $\partial V_s / \partial r$ in some detail. Since observations are confined to the neighbourhood of one electrode, it is most convenient to make use of the expansion (66) which is valid for β positive ($\rho' > \rho$), or β negative ($\rho' < \rho$).

Writing $\xi = \frac{1}{2}r/h$, and denoting

$$\beta_3 = \sum_1^\infty \frac{\beta^u}{u^3}, \beta_5 = \sum_1^\infty \frac{\beta^u}{u^5}, \dots \text{ and generally } \beta_k = \sum_1^\infty \frac{\beta^u}{u^k}, \quad (69)^*$$

we easily obtain from (66) the expression for the gradient—

$$r^2 \frac{dV_s}{dr} = -\frac{I\rho}{2\pi} \left\{ 1 + 2\beta_3\xi^3 - 3\beta_5\xi^5 + \frac{3 \cdot 5}{4} \beta_7\xi^7 - \frac{3 \cdot 5 \cdot 7}{4 \cdot 6} \beta_9\xi^9 + \dots \right\}. \quad (70)$$

It is evident from equation (12) that the term in brackets is the "surface gradient characteristic" $\bar{\rho}/\rho$. It is seen to vary extremely slowly with the distance r from the electrode, rising if β_3 is positive, i.e., if $0 < \beta < 1$, or $\rho' > \rho$, and falling if β_3 is negative, i.e., if $-1 < \beta < 0$, or $\rho' < \rho$.

* The properties of these series are briefly dealt with in Note (iv) of the Appendix.

The series (70) is not sufficiently convergent to discuss the variation of the "surface gradient characteristic" with distance, even for moderate values of $\frac{1}{2}r/h$. For very great distances, it is seen from (66) that expansion in powers of $\frac{1}{2}h/r$ is not legitimate, since a value of u is ultimately reached for which $2uh/r > 1$, after which the expansion must proceed according to powers of $(\frac{1}{2}r/uh)$.

To obtain a convergent expansion of the integral (65), we consider separately the two cases $\rho' < \rho$ and $\rho' > \rho$.

Case (i.) Lower Medium more Highly Conducting, $\rho' < \rho$.—Introducing ζ defined by the equation

$$(1) \quad \tanh \zeta = \rho'/\rho \quad \text{or} \quad 2\zeta = \log \{(\rho + \rho')/(\rho - \rho')\}, \quad (71)$$

we see that (65) take the form.

$$V_s = \frac{I\rho}{2\pi} \int_0^\infty \tanh(\lambda h + \zeta) J_0(\lambda r) d\lambda. \quad (72)$$

Following the method of the preceding section, we make use of an expansion of the form

$$\tanh(\lambda h + \zeta) = \Sigma \left(\frac{a}{\lambda + \alpha} + \frac{b}{\lambda + \beta} \right), \quad (72.1)$$

where α and β are the conjugate roots given by

$$\frac{\alpha}{\beta} = -\frac{\zeta}{h} + (u - \frac{1}{2}) \frac{\pi i}{h}, \quad (72.2)$$

and the summation is extended over values of u from 1, 2, 3, ..., ∞ . We at once find $a = b = 1/h$.

Writing

$$\frac{1}{\lambda + \alpha} = \int_0^\infty e^{-(\lambda + \alpha)t} dt,$$

we have

$$\int_0^\infty \frac{J_0(\lambda r) d\lambda}{\lambda + \alpha} = \int_0^\infty e^{-\alpha t} dt \int_0^\infty J_0(\lambda r) e^{-\lambda t} d\lambda = \int_0^\infty \frac{e^{-\alpha t} dt}{(t^2 + r^2)^{\frac{1}{2}}} = \int_0^\infty e^{-\alpha x} \sinh x dx, \quad (72.3)$$

with a similar expression when α is replaced by β . We obtain, finally, for the surface potential the expression

$$V_s = \frac{I\rho}{\pi h} \sum_{u=1}^\infty \int_0^\infty e^{-(\zeta r/h) \sinh x} \cos \{(\pi r/h)(u - \frac{1}{2}) \sinh x\} dx. \quad (73)$$

When $\zeta = 0$, the exponential vanishes, and since*

$$K_0(z) = \int_0^\infty \cos(z \sinh \phi) \cdot d\phi,$$

we see that the expansion (73) reduces to the type of series already obtained in Section 4.

To obtain the asymptotic expansion for V_s when r/h is large, we find by successive integration by parts of the third integral in (72.3), that

$$V_s = \frac{I\rho}{2\pi} \left[\frac{1}{r} \left(\frac{1}{\alpha} + \frac{1}{\beta} \right) + \sum_{m=1}^{\infty} (-1)^m \frac{\{1^2 \cdot 3^2 \cdot 5^2 \cdots (2m-1)^2\}}{r^{2m+1}} \Sigma \left(\frac{1}{\alpha^{2m+1}} + \frac{1}{\beta^{2m+1}} \right) \right], \quad (74)$$

where the second summation includes the conjugate roots (72.1). We easily find

$$\frac{1}{\alpha} + \frac{1}{\beta} = h \cdot \frac{2\zeta}{\zeta^2 + \{(u - \frac{1}{2})\pi\}^2},$$

and by a well-known summation formula, $\Sigma \left(\frac{1}{\alpha} + \frac{1}{\beta} \right) = \tanh \zeta$, as is easily

verified by writing $\lambda = 0$ on both sides of equation (72.1).

In general we notice that

$$\Sigma \left(\frac{1}{\alpha^{2m+1}} + \frac{1}{\beta^{2m+1}} \right) = (-1)^m \frac{h^{2m}}{(2m)!} \frac{d^{2m}}{d\zeta^{2m}} (\tanh \zeta).$$

We thus have the asymptotic expansion

$$V_s \sim -\frac{I\rho}{2\pi} \left\{ \frac{\tanh \zeta}{r} + \sum_{m=1}^{\infty} \frac{\{1^2 \cdot 3^2 \cdot 5^2 \cdots (2m-1)^2\}}{(2m)!} \frac{h^{2m}}{r^{2m+1}} \frac{d^{2m}}{d\zeta^{2m}} (\tanh \zeta) \right\} \quad (75)$$

The surface potential gradient ultimately tends to the value given by

$$\lim_{r \rightarrow \infty} r^2 \frac{dV_s}{dr} = -\frac{I\rho}{2\pi} \tanh \zeta = -\frac{I\rho'}{2\pi}, \quad (76)$$

by virtue of the relation (71). When ρ approaches ρ' in value, $\zeta \rightarrow \infty$ and, $\tanh \zeta \rightarrow 1$, so that we recover the result for a homogeneous medium.

Case (ii). Lower Medium Less Conducting, $\rho' > \rho$.—In this case it is necessary to write $\tanh \zeta = \rho'/\rho$, or $2\zeta = \log \{(\rho' + \rho)/(\rho' - \rho)\}$. We find for the surface potential the expression

$$V_s = \frac{I\rho}{2\pi} \int_0^\infty \coth(\lambda h + \zeta) \cdot J_0(\lambda r) \cdot d\lambda. \quad (79)$$

* Watson, *loc. cit.*, p. 183.

As before we have

$$\coth(\lambda h + \zeta) = \frac{1}{\lambda h + \zeta} + \frac{1}{h} \sum \left(\frac{1}{\lambda + \alpha} + \frac{1}{\lambda + \beta} \right),$$

where the conjugate roots α and β have the expressions

$$\frac{\alpha}{\beta} = -\frac{\zeta}{h} \pm \frac{i\pi}{h}.$$

The first term contributes the integral

$$\int_0^\infty \frac{J_0(\lambda r)}{\lambda h + \zeta} d\lambda = \frac{1}{h} \int_0^\infty \frac{e^{-i\lambda h} d\lambda}{(t^2 + r^2)^{1/2}} = \frac{1}{h} \int_0^\infty e^{-(\zeta r/h) \sinh x} dx. \quad (80)$$

The first integral shows that when $\zeta \rightarrow 0$, as in (62.1), the contribution to the potential is $-\frac{1}{h} \log r + \text{constant}$.

The third integral in (80) may be written*

$$\int_0^\infty e^{-(\zeta r/h) \sinh x} dx = \frac{\pi}{2} [-Y_0(\zeta r/h) + H_0(\zeta r/h)]. \quad (81)$$

where Y_0 is defined by the expansion

$$Y_0(z) = 2 \{ \gamma + \log(\frac{1}{2}z) \} J_0(z) - 2 \sum_{m=1}^\infty \frac{(-1)^m (\frac{1}{2}z)^{2m}}{(m!)^2} \left\{ \frac{1}{1} + \frac{1}{2} + \dots + \frac{1}{m} \right\}. \quad (82)$$

The function H_0 is defined by the definite integral

$$H_0(z) = \frac{2}{\pi} \int_0^{\pi/2} \sin(z \cos \theta) d\theta.$$

Both functions are tabulated at close intervals in Watson's "Theory of Bessel Functions." Finally, we obtain the expansion of the integral (79) in the form

$$V = \frac{I_0}{2\pi h} \left[\int_0^\infty e^{-(\zeta r/h) \sinh x} dx + 2 \sum_1^\infty \int_0^\infty e^{-(\zeta r/h) \sinh x} \cos \{ (u\pi r/h) \sinh x \} dx, \right] \quad (83)$$

which is easily seen to reduce to the series dealt with in Section 3 when $\zeta \rightarrow 0$. The functions under the summation signs are of the class already considered, and depend for numerical evaluation on tables of Bessel functions of complex argument. For large values of $(\zeta r/h)$, we proceed as in case (1) directly to an asymptotic expansion.

* The notation used is that of Watson, "Bessel Functions," p. 313. The Y-functions of Watson are denoted by N in Jahnke and Emde (*loc. cit.*).

We find

$$\begin{aligned} \frac{1}{\alpha} + \frac{1}{\beta} &= h \sum \frac{2\zeta}{\zeta^2 + u^2\pi^2} = h \left(\cosh \zeta - \frac{1}{\zeta} \right), \\ \frac{1}{\alpha^m} + \frac{1}{\beta^m} &= \frac{(-1)^m h^m}{m!} \cdot \frac{d^m}{d\zeta^m} \left(\cosh \zeta - \frac{1}{\zeta} \right), \end{aligned} \quad (84)$$

and finally, the asymptotic expansion

$$V_s \sim \frac{I\rho}{2\pi} \left[\frac{\cosh \zeta}{r} + \sum_1 \frac{1^2 \cdot 3^2 \cdot 5^2 \cdot \dots (2m-1)^2}{(2m)!} \left(\frac{h}{r} \right)^{2m} \frac{d^{2m}}{d\zeta^{2m}} (\cosh \zeta) \right]. \quad (85)$$

As before, we have

$$\text{Lt.}_{r \rightarrow \infty} r^2 \frac{dV_s}{dr} = - \frac{I\rho}{2\pi} \cosh \zeta = \frac{I\rho'}{2\pi}.$$

According to theory, the general trend of the curves connecting

$$\bar{\rho}/\rho = - \frac{2\pi r^2}{I\rho} \cdot \frac{dV_s}{dr}$$

and r is shown in fig. 5. The determination of ρ'/ρ depends on the trend of the curve for large values of (r/h) . The determination of h depends on the

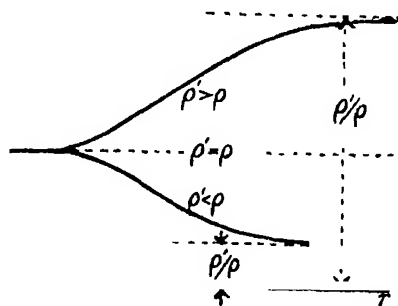


FIG. 5.

identification of an observed curve with one of a family corresponding to that value of ρ'/ρ . Such a family of curves for field use is probably most easily obtained by the graphical computation of the integral (67).

Section 9.—Layer of Thickness t and Specific Resistance ρ' embedded in Semi-infinite Homogeneous Medium.

This represents a case of some importance from a practical point of view. When the last medium extends to infinity, we cannot expect a simple expansion

in terms of K_0 -functions, and so proceed according to the method of the last section, writing

$$\left. \begin{aligned} V &= \frac{I\rho}{2\pi} \int_0^\infty (e^{-\lambda z} + A \cosh \lambda z) \cdot J_0(\lambda r) d\lambda, \\ V' &= \frac{I\rho}{2\pi} \int_0^\infty (Be^{-\lambda z} + Ce^{\lambda z}) \cdot J_0(\lambda r) d\lambda, \\ \text{and} \\ V'' &= \frac{I\rho}{2\pi} \int_0^\infty De^{-\lambda z} \cdot J_0(\lambda r) d\lambda. \end{aligned} \right\} \quad (86)$$

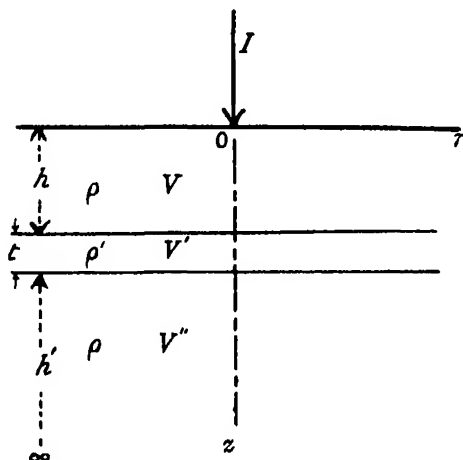


FIG. 6.

The constants A, B, C, D are determined from the boundary conditions at $z = h$ and at $z = h + t$. After some reductions, we obtain the following expressions for the surface potential:—

Case (i). *Insulating Stratum*, $\rho' > \rho$.—Writing $\rho'/\rho = \cosh \zeta$, we obtain

$$V_s = \frac{I\rho}{2\pi} \int_0^\infty \frac{\sinh(2\zeta + \lambda t) + e^{-2\lambda h} \sinh \lambda t}{\sinh(2\zeta + \lambda t) - e^{-2\lambda h} \sinh \lambda t} \cdot J_0(\lambda r) \cdot d\lambda. \quad (87)$$

Case (ii). *Conducting Stratum*, $\rho' < \rho$.—Writing $\rho'/\rho = \tanh \zeta$, we obtain,

$$V_s = \frac{I\rho}{2\pi} \int_0^\infty \frac{\sinh(2\zeta + \lambda t) - e^{-2\lambda h} \sinh \lambda t}{\sinh(2\zeta + \lambda t) + e^{-2\lambda h} \sinh \lambda t} \cdot J_0(\lambda r) \cdot d\lambda. \quad (88)$$

Neither of the expressions (87) or (88) are easily interpreted from the numerical point of view, and little simplification is effected by taking the ratio t/h small.

The denominators of the expressions which have to be integrated will, in general, have complex roots in terms of which the integrals may be expressed

as in the preceding section, as a series of Bessel functions of complex argument. It is always possible, however, to derive an asymptotic expansion for the potential, general methods for doing so being developed in the next section. If we apply the theorem in question, we find that the asymptotic expression

in both cases is $V_s \sim \frac{I\rho}{2\pi} \cdot \frac{1}{r}$, so that $(r^2 \frac{dV_s}{dr}) \sim \frac{I\rho}{2\pi}$, and therefore $(\bar{\rho}/\rho) \sim 1$,

both when r is small and when it is very large. We conclude that in case (i) $(\bar{\rho}/\rho)$ will show a maximum, and in case (ii), a minimum for a value of r which will depend in a complicated way on h, t and (ρ'/ρ) .

The general nature of the theoretical graphs is shown in fig. 7.

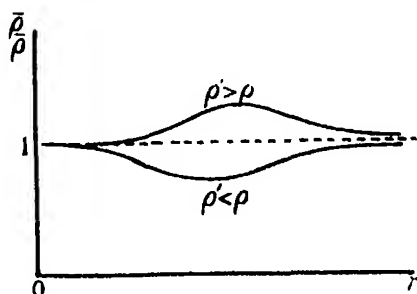


FIG. 7.

Section 10.—General Methods of Approximation. *The Characteristic Function.*

(i) *Asymptotic expansion for surface potential.*—In general the problem of dealing with stratified layers, each supposed to be homogeneous, is capable of being solved, the surface potential being ultimately expressed by an integral of the type

$$V_s = \frac{I\rho}{2\pi} \int_0^\infty F(\lambda, \rho, \rho', \dots, h, h', \dots) \cdot J_0(\lambda r) d\lambda, \quad (89)$$

the characteristics of the medium as regards thicknesses, depths, and specific resistances of the strata being included in the function $F(\lambda, \rho, \rho', \dots, h, h', \dots)$, which may be referred to as the *characteristic function*. We suppose $F(\lambda)$ expressed in the form

$$F(\lambda, \rho, \rho', \dots, h, h', \dots) = \frac{\phi(\lambda)}{\psi(\lambda)} = \sum_n \frac{a_n}{\lambda - \alpha_n}. \quad (90)$$

$\phi(\lambda)$ has no infinities, and $\psi(\lambda)$ has simple zeros at $\lambda = \alpha_1, \alpha_2, \dots, \alpha_n, \dots$,

the roots of $\psi(\lambda) = 0$, in general complex, and supposed in the present case to be all different. As in (74), we have by successive partial integrations

$$\int_0^\infty \frac{J_0(\lambda r) d\lambda}{\lambda + \alpha} = \int_0^\infty \frac{e^{-\alpha t} dt}{(t^2 + r^2)^{1/2}} \sim \frac{1}{r\alpha} + \sum_{m=1}^\infty (-1)^m \cdot \{1 \cdot 3 \cdot 5 \dots (2m-1)\}^2 \left(\frac{1}{r\alpha}\right)^{2m+1}. \quad (90.1)$$

Thus,

$$V_s \sim \frac{1}{r} \sum_n \frac{a_n}{\alpha_n} + \sum_{m=1}^\infty \frac{(-1)^m \{1 \cdot 3 \cdot 5 \dots (2m-1)\}^2}{r^{2m+1}} \sum_n a_n \left(\frac{1}{\alpha_n}\right)^{2m+1}.$$

From (90) we easily see that $\sum \frac{a_n}{\alpha_n} = [F(\lambda)]_{\lambda=0}$, and by successive differentia-

tions, $(2m)! \cdot \sum \frac{a_n}{\alpha_n^{2m+1}} = \left[\frac{\partial^{2m} F}{\partial \lambda^{2m}} \right]_{\lambda=0}$. We thus obtain the asymptotic expansion, in which the successive coefficients may be expressed in terms of successive differentials with respect to λ of the characteristic function $F(\lambda)$, for argument $\lambda = 0$, i.e.,

$$V_s \sim \frac{1}{2\pi} \left[\frac{F(\lambda)}{r} + \sum_{m=1}^\infty (-1)^m \cdot \frac{\{1 \cdot 3 \cdot 5 \dots (2m-1)\}^2}{(2m)!} \left(\frac{\partial^{2m} F}{\partial \lambda^{2m}} \right) \cdot \frac{1}{r^{2m+1}} \right]_{\lambda=0}. \quad (91)$$

When r is large we have from the equation (12) the following asymptotic expression for the "surface gradient characteristic,"

$$\lim_{r \rightarrow \infty} \frac{\bar{\rho}}{\rho} \sim \lim_{r \rightarrow \infty} \frac{2\pi}{1} r^2 \frac{dV_s}{dr} \sim \lim_{\lambda \rightarrow 0} F(\lambda) \quad (92)$$

(ii) *Transformation of Definite Integrals involving $J_0(\lambda r)$ by Contour Integration.*—In problems involving contour integration it is convenient to make use of the functions $H_0^{(1)}(z)$ and $H_0^{(2)}(z)$ defined by the relations

$$H_0^{(1)}(z) = J_0(z) + iY_0(z) \quad \text{and} \quad H_0^{(2)}(z) = J_0(z) - iY_0(z). \quad (92.1)^*$$

and in the present case of the functions

$$H_0^{(1)}(izr) = (2/\pi i)K_0(zr) \quad \text{and} \quad H_0^{(1)}(-izr) = -J_0(zr) + iY_0(zr). \quad (92.2)^*$$

We will suppose that the characteristic function $F(\lambda)$ is expressed in the form (90), $F(\lambda) = \phi(\lambda)/\psi(\lambda)$, and that in general $\psi(\lambda)$ has simple poles of the type

$$\lambda = \alpha \pm i\beta \quad (\alpha > 0, \beta > 0). \quad (92.3)$$

When λ is replaced by $-i\mu$, we will have, in general,

$$F(-i\mu) = A(\mu) - iB(\mu). \quad (92.4)$$

* Watson, "Theory of Bessel Functions," §§ 3.6 (1) and 3.7 (8), pp. 73 and 78.

A useful transformation of integrals of the type (89) to more convergent integrals and expansions results from carrying out the contour integration,

$$\int_0^\infty F(-it) H_0^{(1)}(it\tau) dt, \quad (t = \mu + i\lambda), \quad (92.5)$$

around an infinite quadrant

It follows from (92.3) that, in general, the integrand in (92.5) has poles of the type $\tau = \beta + i\alpha$ in the first quadrant. The corresponding residue is

$$R = \frac{\phi(-i\tau) H_0^{(1)}(i\tau)}{-i\psi'(-i\tau)} = \frac{2}{\pi} \frac{\phi(\alpha - i\beta)}{\psi'(\alpha - i\beta)} K_0(\beta + i\alpha). \quad (92.6)$$

We will suppose that (92.6) may be resolved into real and imaginary parts, so that

$$R = R_r(\alpha, \beta) + i R_i(\alpha, \beta). \quad (92.7)$$

Integrating (92.5) along the real and imaginary axes of the infinite quadrant, the theory of residues gives, since the arc of the infinite quadrant contributes nothing,

$$\int_0^\infty \{A(\mu) - iB(\mu)\} \frac{2}{\pi i} K_0(\mu r) d\mu - \int_0^\infty F(\lambda) \{-J_0(\lambda r) + iY_0(\lambda r)\} i d\lambda \\ = 2\pi i \Sigma [R_r(\alpha, \beta) + i R_i(\alpha, \beta)],$$

which gives, on equating the imaginary parts, the useful transformation,

$$\int_0^\infty F(\lambda) J_0(\lambda r) d\lambda = \frac{2}{\pi} \int_0^\infty A(\mu) K_0(\mu r) d\mu + 2\pi \Sigma R_r(\alpha, \beta), \quad (92.8)$$

where

$$\left. \begin{aligned} R_r(\alpha, \beta) + i R_i(\alpha, \beta) &= \frac{2}{\pi} \frac{\phi(\alpha - i\beta)}{\psi'(\alpha - i\beta)} K_0(\beta + i\alpha). \quad (\alpha > 0, \beta > 0), \\ \text{and} \quad F(i\mu) &= A(\mu) + iB(\mu) \end{aligned} \right\} \quad (92.9)$$

and the summation is extended over those roots, $\lambda = \alpha \pm i\beta$, of $\psi(\lambda) = 0$, for which $\tau = \beta + i\alpha$ lies in the first quadrant of the complex plane, $t = \lambda + i\mu$.

As a simple illustration consider the integral (79) arising in Section 8,

$$V_s = \frac{I\rho}{2\pi} \int_0^\infty \coth(\lambda h + \zeta) \cdot J_0(\lambda r) d\lambda,$$

where

$$\tanh \zeta = \rho/\rho', \quad (\rho < \rho').$$

In this case the poles of $F(\lambda) = \coth(\lambda h + \zeta)$ are evidently given by

$$\sinh(\lambda h + \zeta) = 0 \quad \text{or} \quad \lambda = -\zeta/h \pm \frac{1}{2}s\pi, \quad (s = 1, 2, 3, \dots)$$

so that since ζ is real and positive, $\tau = \frac{1}{2}\pi - i(\zeta/h)$, showing that there are no poles in the first quadrant of the complex plane, from which it follows that $\Sigma R_r(\alpha, \rho) = 0$. Furthermore,

$$F(\mu) = \coth(\zeta + i\mu h) = \frac{\sinh 2\zeta - i \sin 2\mu h}{\cosh 2\zeta - \cos 2\mu h},$$

and (92.8) gives immediately

$$V_s = \frac{I\rho}{2\pi} \int_0^\infty \coth(\lambda h + \zeta) \cdot J_0(\lambda r) d\lambda = \frac{I\rho}{\pi^2} \sinh 2\zeta \int_0^\infty \frac{K_0(\mu r) d\mu}{\cosh 2\zeta - \cosh 2\mu h},$$

(92.10)

or

$$V_s = \frac{I\rho}{\pi^2} \int_0^\infty \frac{\rho\rho' K_0(\mu r) d\mu}{\rho^2 \cos^2 \mu h + \rho'^2 \sin^2 \mu h}$$

in agreement with (64.2).

Similarly in the case $\rho > \rho'$, we write $\tanh \zeta' = \rho'/\rho$, and we then find

$$V_s = \frac{I\rho}{2\pi} \int_0^\infty \tanh(\lambda h + \zeta') \cdot J_0(\lambda r) d\lambda = \frac{I\rho}{\pi^2} \sinh 2\zeta' \int_0^\infty \frac{K_0(\mu r) d\mu}{\cosh 2\zeta' + \cos 2\mu h}.$$

(92.11)

The integrals (92.10) and (92.11) are rapidly convergent, and well suited for numerical computation by quadratures

Section 11 -- Application of Hankel's Inversion Theorem to Analysis of Field Observations.

Practical measurements of surface potentials in the field enable us to compute $\bar{\rho}$ from the definition $I\bar{\rho}/(2\pi) = -r^2 dV_s/dr$, so that (89) gives the relation

$$\frac{1}{r^2} \frac{\bar{\rho}}{\rho} = \int_0^\infty F(\lambda, \rho, \rho', \dots, h, h', \dots) \lambda J_1(\lambda r) d\lambda, \quad (93)$$

where the left-hand side is supposed to be known as the function of r .

A very remarkable theorem, due to Hankel,* states that, subject to suitable restrictions in the form of the function $\phi(x)$, if

$$f(x) = \int_0^\infty \lambda \phi(\lambda) \cdot J_u(\lambda x) \cdot d\lambda$$

(94)

then

$$\phi(\lambda) = \int_0^\infty x f(x) \cdot J_u(\lambda x) \cdot dx.$$

* Watson, *loc. cit.*, § 14 3; Bateman, "Partial Differential Equations," Camb. Univ. Press, § 7.32, p. 409 (1932).

If we apply this theorem to (93), we have

$$F(\lambda, \rho, p', \dots, h, h', \dots) = \int_0^\infty \frac{\bar{\rho}}{\rho} \cdot \frac{J_1(\lambda r)}{r} dr. \quad (95)$$

Thus it is theoretically possible from an observed curve giving $(\bar{\rho}/\rho)$ as a function of r , to determine by a series of graphical integrations the characteristic function $F(\lambda)$. We have seen that corresponding to a given stratification it is always possible to construct the characteristic function, although its integration, when multiplied by $J_0(\lambda r)$, to give surface potentials is, except in a few simple cases, practically impossible. As a method of analysing field observations, it is suggested that characteristic functions corresponding to simple distributions of strata be computed. By comparing these with the experimentally determined $F(\lambda)$, we may obtain some idea of the stratification which gives rise to observed surface potential gradients.

As a test of the applicability of (95) to the problems we have been discussing, we may apply it to determine the characteristic function corresponding to

$$\frac{\bar{\rho}}{\rho} = \frac{4}{\pi} \sum_1^\infty (2u - 1) x^2 \cdot K_1\{(2u - 1)x\}, \text{ where } x = \frac{1}{2}\pi r/h, \quad (96)$$

arrived at in (37).

Equation (95) gives

$$F(\lambda) = \frac{4}{\pi} \sum_1^\infty \int_1^\infty (2u - 1) x \cdot K_1\{(2u - 1)x\} \cdot J_1(2h\lambda x/\pi) \cdot dx. \quad (97)$$

By a partial integration, we find

$$\int_0^\infty t \cdot K_1(at) \cdot J_1(bt) \cdot dt = \frac{b}{a} \int_0^\infty t \cdot K_0(at) \cdot J_0(bt) \cdot dt = \frac{b}{a} \cdot \frac{1}{a^2 + b^2}, \quad (98)$$

making use of a result due to Nicholson *. Applying this to (97) we obtain

$$F(\lambda) = \sum_1^\infty \frac{2\lambda h}{(\lambda h)^2 + (u - \frac{1}{2})^2 \pi^2} = \tanh(\lambda h). \quad (99)$$

Reference to (72) shows that the vertical stratification corresponding to this characteristic function is a homogeneous layer of specific resistance ρ and of depth h bounded by a perfect conductor of infinite depth, since $\zeta = 0$, i.e., $\rho' = 0$, and this we know is correct. The reader will have no difficulty in verifying the solution (31). Thus apart from its possible practical importance in the analysis of surface potential gradients, the theorem (95) affords a valuable

* Watson's *loc cit* § 13.45 (2), p. 41.0

check on theoretical calculations of such gradients, assuming a known stratification.

From a practical point of view, the use of an integrating machine suitable to the graphical determination of the integral (95) would, by bringing out the characteristic function $F(\lambda, \rho, \rho', \dots, h, h', \dots)$ make the interpretation of stratification considerably easier than the attempt to use directly the "surface gradient characteristics" $\bar{\rho}/\rho$ plotted against r .

Section 12.—On the Interpretation of Some Simple Types of Field Graphs.

Assuming constant specific resistance, it is possible to determine the surface gradient by taking two electrodes at a very great distance apart so that the potential distribution at any one of these is practically that corresponding to one electrode. If a current I is introduced into the earth, the potential drop ΔV_s in distance Δr from the electrode may be read on some form of potentiometer. It is convenient to calculate the "surface gradient characteristic," $\bar{\rho}/\rho_s$, according to the formula

$$\frac{\bar{\rho}}{\rho} = \frac{2\pi}{I} \frac{r^2}{\rho} \cdot \frac{\Delta V_s}{\Delta r}, \quad (100)$$

which should be constant for all values of r in the case of a semi-infinite homogeneous earth.* The graph of $\bar{\rho}/\rho$ plotted against r (or some convenient power of r), as determined from field observations should, theoretically, enable us to determine the vertical stratification of electrical resistivity. Unfortunately only a few simple cases are capable of easy solution.

Case (1). Depth of Conducting Stratum covering Insulating Bed Rock.—For comparison with theoretical curves, it is convenient to make a few determinations of earth resistance near the single electrode, so that $\bar{\rho}/\rho$ may be plotted against the distance r . The graph characteristic of highly insulating bed-rock is shown in fig. 8, the curve tending to an asymptote through the origin, whose equation from (31) is seen to be $y = \bar{\rho}/\rho = r/h$. The depth of the insulating bed-rock may be read off the r -axis as the intersection of $\rho/\rho = 1$ with the asymptote.†

* The ratio $\Delta V_s/I$ is most conveniently read off on a "megger." For details of field measurements consult Eve and Keys *loc. cit.*

† The effect of a depth gradient of resistivity is to give a surface gradient characteristic of the type indicated by the dotted curve in fig. 8. In these circumstances it will be shown in a later paper that by drawing the tangent at $\bar{\rho}/\rho = 1$ intersect the asymptotic, a more correct estimate of the depth h may be inferred.

Case (ii). Depth of Conducting Stratum covering Highly Conducting Bed Rock.—The graph characteristic of highly conducting bed-rock is shown in fig. 9. Denoting $y = \bar{\rho}/\rho$, and $x = \frac{1}{2}\pi r/h$, its theoretical equation is

$$y = x^2 \sum_1^{\infty} \lambda K_1(x\lambda), \quad (101)$$

where $\lambda = (2s - 1)$ and $s = 1, 2, 3, \dots$

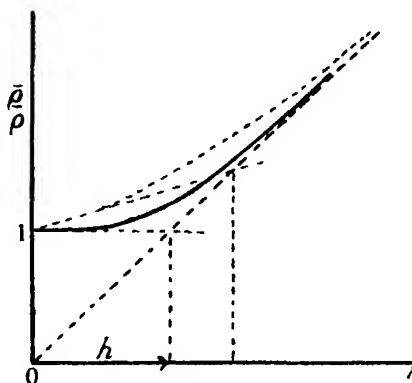


FIG. 8

We easily find

$$\left. \begin{aligned} \frac{dy}{dx} &= \sum [\lambda x K(\lambda x) - \lambda^2 x^2 K_0(\lambda x)], \\ \frac{d^2y}{dx^2} &= \sum [-3x\lambda^2 K_0(\lambda x) + x^2\lambda^3 K_1(\lambda x)]. \end{aligned} \right\} \quad (102)$$

Since $d^2y/dx^2 = 0$ at $x = 0$, it appears that the curve is very flat near the origin, falling away extremely slowly from the horizontal tangent at $x = 0$

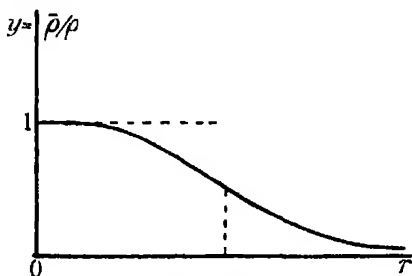


FIG. 9a.

(fig. 9a). The only characteristic from which h may be roughly estimated is the point of inflexion, given by

$$x = \frac{1}{2}\pi r/h = 3 \sum \lambda^2 K_0(\lambda x) / \sum \lambda^3 K_1(\lambda x) \quad (103)$$

Making use of tables we find by interpolation that the point of inflexion occurs for $x = \frac{1}{2}\pi r/h = 2.320$. If the point of inflexion in the field graph occurs at r metres (or feet), it follows that the depth of the highly conducting stratum is given by $h = 0.678r$ in the same units as r .

Since in field observations r is easily determined and accurately known, we may plot $r\bar{\rho}/\rho$ against r . The corresponding theoretical graph has the equation

$$z = x^3 \sum \lambda K_1(\lambda x) \quad (104)$$

and

$$\frac{dz}{dx} = 2x^3 \sum \lambda K_1(\lambda x) - x^3 \sum \lambda^3 K_0(\lambda x). \quad (105)$$

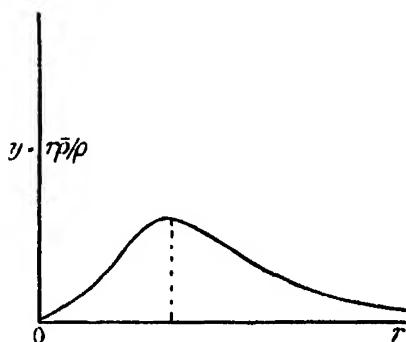


FIG. 9b

The theoretical graph (fig. 9b) now has a pronounced maximum for a value of r given by

$$x = 2\sum \lambda K_1(\lambda x) / \sum \lambda^3 K_0(\lambda x). \quad (106)$$

A rough determination from the tables gives, approximately, $x = \frac{1}{2}\pi r/h = 2.319$, so that if r is the position of the maximum in the field graph $r\bar{\rho}/\rho$ plotted against r , the depth of the highly conducting layer is given by $h = 0.678r$ in the same units.*

The above methods only make use of a few points of the field graph and the value of h thus determined will be correspondingly rough. A better method is to draw accurately the theoretical graph (101) on a sheet of transparent celluloid having the y -axis as one edge. The field graph (100) should be plotted so that the y -ordinate may be superposed on that of the theoretical graph, and having an x -scale so adjusted that by rotating the theoretical curve about the y -axis, and viewing the field graph through it from a distance,

* The approximate numerical agreement with the position of the point of inflexion in fig. 9a is accidental, and would disappear if the calculations were pushed to a higher order of accuracy.

the two curves may be adjusted to fit as closely as possible. Then, corresponding to each value of r in the field graph, the corresponding value of $x = \frac{1}{2}\pi r/h$ may be read off from the theoretical graph, and hence several values of h may be calculated. If the values are consistent, it may be concluded that the bed-rock is relatively highly conducting, if not it must be inferred that conditions do not correspond to the simple theoretical assumption forming the basis of the calculations.

The method just described may be used in connection with field graphs of the type represented in fig. 8 or the modified field graph fig. 9b.

Section 13.—On the Effect of Frequency on Surface Potential Distributions.

We suppose an alternating current I of frequency f to be introduced by an infinitely long straight wire along the z -axis into a semi-infinite medium of constant specific resistance. Since the magnetic field is symmetrical with respect to the axis, the problem is most easily solved in terms of the magnetic work-function $\psi = Hr \sin \theta$. When the Maxwell-Faraday laws are expressed in solid

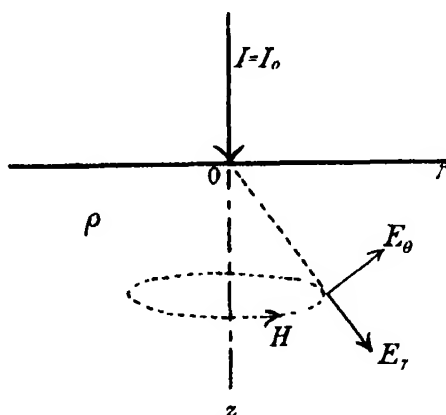


FIG. 10

polar co-ordinates, with the origin at the electrode as shown in fig. 10, the differential equation for ψ expressing electromagnetic wave-propagation is

$$\frac{\partial^2 \psi}{\partial r^2} + \frac{1 - \mu^2}{r^2} \frac{\partial^2 \psi}{\partial \mu^2} = \frac{K}{c^2} \frac{\partial^2 \psi}{\partial t^2} + \frac{4\pi}{\rho} \frac{\partial \psi}{\partial t}, \quad (107)$$

where, as usual, $\mu = \cos \theta$, $c = 3 \times 10^{10}$ cm./sec., and ρ is the specific resistance in e.m. units, while K is the dielectric constant of the medium.

The electric fields E_r and E_θ , expressed in e.s. units, and the magnetic field H , expressed in e.m. units, are given in terms of ψ by the relations,

$$\frac{4\pi}{\rho} E_r + K \dot{E}_r = -\frac{c}{r^2} \frac{\partial \psi}{\partial \mu}, \quad \frac{4\pi}{\rho} E_\theta + K \dot{E}_\theta = -\frac{c}{r \sin \theta} \frac{\partial \psi}{\partial r}, \quad H = \frac{\psi}{r \sin \theta}. \quad (108)$$

If we denote by κ the operational symbol

$$\kappa = \left(\frac{K}{c^2} \frac{\partial^2}{\partial t^2} + \frac{4\pi}{\rho} \frac{\partial}{\partial t} \right), \quad (109)$$

or, in the case of waves of frequency $f = \omega/(2\pi)$,

$$\kappa = \left(-\frac{K}{c^2} \omega^2 + \frac{4\pi i \omega}{\rho} \right), \quad (110)$$

so that the propagation equation may be written

$$\frac{\partial^2 \psi}{\partial r^2} + \frac{1 - \mu^2}{r^2} \frac{\partial^2 \psi}{\partial \mu^2} = \kappa^2 \psi. \quad (111)$$

In practical problems it is convenient to denote by C the "induction constant" of the medium expressed in centimetres by the relation

$$C = \left(\frac{\rho}{4\pi\omega} \right)^{\frac{1}{2}} = \left(\frac{\rho}{8\pi^2 f} \right)^{\frac{1}{2}} = \left(\frac{\rho \text{ (ohms)} \times 10^9}{8\pi^2 f} \right)^{\frac{1}{2}}. \quad (112)$$

For a radiation field of wave-length λ , equation (110) may be written

$$\kappa = \left\{ -\left(\frac{2\pi}{\lambda} \right)^2 + \frac{i}{C^2} \right\}^{\frac{1}{2}}, \quad (113)$$

from which it appears that when λ is very much greater than C , we may neglect propagation-effects and write, approximately,

$$\kappa \sim \sqrt{i}/C = \sqrt{\frac{1}{2}} (1 + i)/C = e^{i\pi/4}/C. \quad (114)$$

In these circumstances the equations (104) become

$$\frac{4\pi}{\rho} E_r = -\frac{c}{r^2} \frac{\partial \psi}{\partial \mu}, \quad \frac{4\pi}{\rho} E_\theta = -\frac{c}{r \sin \theta} \frac{\partial \psi}{\partial r}, \quad \text{and} \quad H = \frac{\psi}{r \sin \theta}, \quad (115)$$

while the current-components u_r and u_θ in e.m. units are given according to Ohm's Law by

$$u_r = E_r/(\rho c) \quad u_\theta = E_\theta/(\rho c). \quad (116)$$

For low frequencies, the boundary conditions are:—

(i) $\psi = 0$ for $\theta = 0$ or $\mu = 1$, since there is no concentration of current in the conducting medium along the axis.

(ii) $u_\theta = 0$ for $\theta = \frac{1}{2}\pi$ or $\mu = 0$, since there is no current flow across the boundary. From (115) and (116) this is equivalent to $\partial\psi/\partial r = 0$ for $\mu = 0$.

(iii) Near the origin, when r is small, $\psi \sim 2(1 - \mu)I$, expressing, according to (115) and (116), the fact that the total current flow across a small hemisphere centred at the origin is equal to the current introduced by the electrode. It is easily seen that these conditions are satisfied by the special solution of the propagation equation (111),

$$\psi = 2I \{e^{-\kappa r} - \mu e^{-\kappa r}\}. \quad (117)$$

It follows from (115) that at the surface $\theta = \frac{1}{2}\pi$ the tangential electric field just inside the medium is given by

$$E_r = \frac{I\rho}{2\pi} \frac{c}{r^2} (\kappa r + e^{-\kappa r}). \quad (\theta = \frac{1}{2}\pi) \quad (118)$$

In any actual measurements, E_r/c is measured in volts per centimetre, expressed as $E_r/c = -\partial V_s/\partial r$. Substituting for κ from (114) and writing $\gamma = r/C\sqrt{2}$, we find on resolving (118) into real and imaginary parts, that corresponding to a current $I = I_0 \cos \omega t$,

$$-r^2 \frac{dV_s}{dr} = \frac{I_0\rho}{2\pi} [(\gamma + e^{-\gamma} \cos \gamma) \cos \omega t - (\gamma - e^{-\gamma} \sin \gamma) \sin \omega t]. \quad (119)$$

We can arrange an A.C. potential measuring apparatus, such as a "megger," so as to determine in various ways the quantity

$$\frac{\bar{\rho}}{\rho} = -\frac{2\pi r^2}{\rho I_0} \frac{dV_s}{dr}. \quad (120)$$

(i) *The inphase component* is given by

$$[\bar{\rho}/\rho]_0 = \gamma + e^{-\gamma} \cos \gamma \quad (\gamma = r/C\sqrt{2}), \quad (121)$$

and its graph when plotted against γ is seen from fig. 11 to oscillate about the asymptote $[\bar{\rho}/\rho]_0 = \gamma$, as indicated in the curve marked (i).

(ii) *The quadrature component* is given by

$$[\bar{\rho}/\rho]_{\frac{1}{2}\pi} = \gamma - e^{-\gamma} \sin \gamma. \quad (\gamma = r/C\sqrt{2}). \quad (122)$$

When plotted against γ its graph is also seen to oscillate about the same asymptote as shown in the curve (ii).

(iii) When the root-mean-square component is considered by utilising A.C. instruments of the dynamometer type for measuring electrode current and voltage gradients, we have in this case

$$[\bar{\rho}/\rho] = \{2\gamma^2 + \gamma e^{-\gamma} (\cos \gamma - \sin \gamma) + e^{-2\gamma}\}^{\frac{1}{2}}, \quad (123)$$

which oscillates about the asymptote, $[\bar{\rho}/\rho] = \gamma \sqrt{2}$. Near the origin $[\bar{\rho}/\rho] \sim 1 + \frac{1}{2}(\gamma/C)^4 + \dots$, deviating very little from a horizontal straight

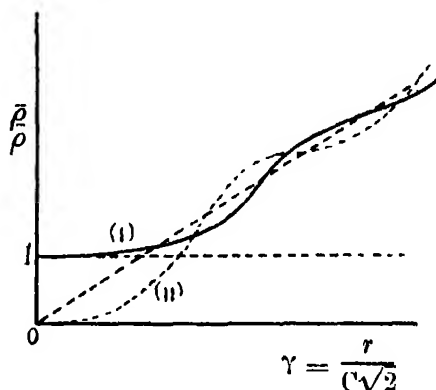


FIG. 11

line through the point $[\bar{\rho}/\rho] = 1$, characteristic of zero frequencies, until r becomes comparable with C . We note that the phase of the voltage gradient is in advance of that of the electrode current by an angle α given by

$$\tan \alpha = (\gamma - e^{-\gamma} \sin \gamma) / (\gamma + e^{-\gamma} \cos \gamma). \quad (124)$$

At great distances from the electrode, it is seen that $\alpha \rightarrow \frac{1}{2}\pi$, while near the origin, $\tan \alpha \sim \gamma^3$.

The asymptotic behaviour of $\bar{\rho}/\rho$ illustrated in fig. 11 is due to the fact that an infinitely long electrode has been used. At low frequencies the field H in air is inversely proportional to the distance along the plane, and its variation with time gives a field promoting radial flow of current near the surface, also falling off inversely with the distance. The case of an electrode of finite length, along which electrical oscillations are maintained, constitutes a much more difficult problem, that of the vertical antenna over an earth of finite conductivity, which the writer hopes to deal with elsewhere.

The illustration chosen in the present section suffices to show, however, that even in a homogeneous earth, frequency has a marked effect on the measurements of voltage gradients at distances from the electrode of the order of, or exceeding the "induction constant" C .

The following table gives a few values of the "induction constant" C at 50 cycles :—

Table of ' Induction Constant ' at 50 Cycles.

ρ (ohms)	1	10^2	10^4	10^6	$C = \frac{\rho \text{ (ohms)} \times 10^9}{8\pi^2 f}$
C (metres)	5	50	500	5000	

We notice from (117) that the amplitude of the magnetic field H falls off rapidly with depth, principally according to the factor $e^{-z/C\sqrt{2}}$.

It also follows that the components of current-density fall off according to the same law, so that all electrical effects become small at depths exceeding a few multiples of C . As a result, apart from the difficulty of interpreting A.C. results, the disturbance of surface potential gradients by underlying changes of electrical conductivity, becomes rapidly less as the frequency is increased, depending on the "induction constant" of the superficial strata. On the other hand, from the practical point of view, a tendency to higher frequencies gives the opportunity for increased sensitiveness of measurement and additional data represented by phase relations. The optimum frequency to be used is that which makes the "induction constant" characteristic of the surface layers approximately equal to the depth which it is hoped to penetrate.

To my colleagues, Dr. A. S. Eve, F.R.S., and Dr. D. A. Keys, the author is indebted for many helpful discussions relating to the practical details of the problems discussed in this paper.

Section 14.—Summary and Conclusions.

(1) By introducing current into the earth by one or more electrodes, and measuring the surface gradients, it is possible to infer the stratification. Assuming strata parallel to the surface, the mathematical theory reduces to working out the problem for a single electrode.

(2) There is considerable advantage in introducing and working with a current-function ψ defining lines of flow, in terms of which the observable surface gradient characteristics may be directly expressed.

(3) Strata, ultimately bounded by media of very high or very low specific resistance, give rise to expressions for the "surface gradient characteristic,"

$\rho/\rho_s = -\frac{2\pi r^2}{I\rho_s} \frac{dV_s}{dr}$, in the form of highly convergent series in $K_1(r\lambda)$, where λ are the roots of an *equation of condition*.

(4) When the strata are ultimately bounded by a semi-infinite medium of finite specific resistance, the surface potentials are more easily expressed in terms of a definite integral involving $J_0(r\lambda)$

(5) In all problems of the type considered the stratification constants appear as a factor $F(\lambda, \rho, \rho', \dots, h, h')$ multiplying $J_0(r\lambda)$ in the definite integral just mentioned.

(6) Methods of deriving asymptotic expansions for the "surface gradient characteristic" $\bar{\rho}/\rho_s$ in terms of the *characteristic function* $F(\lambda)$ are developed. By a process of contour integration the definite integral in $J_0(r\lambda)$ may be transformed into highly convergent integrals and series in $K_0(r\lambda)$.

(7) An application of Hankel's Inversion Theorem enables the characteristic function to be determined by the integration of field graphs, and promises to be of practical use in the deduction of stratification constants.

(8) Practical rules are given for the interpretation of field graphs in the light of theoretical solutions for the surface gradient characteristics corresponding to simple types of stratifications.

(9) The use of alternating current of low frequencies offers many practical advantages as regards accuracy and variety of measurements. On the other hand, the effect of induced currents makes the results of observation more difficult to interpret. The case for an electrode of infinite length introducing alternating current into a semi-infinite medium of constant specific resistance is worked out in detail, neglecting the effects of the wave-propagation of electromagnetic effects.

(10) In an Appendix are discussed points of mathematical interest relating to details of calculation in various sections

APPENDIX.

(1) *Note on the Properties of the Functions $K_0(x)$ and $K_1(x)$.*

When u is an integer, the solution of the equation.

$$\frac{d^2y}{dx^2} - \frac{(2u-1)}{x} \frac{dy}{dx} + y = 0, \quad (i)$$

is known to be

$$y = x^u [AJ_u(x) + BY_u(x)]. \quad (ii)$$

Writing ix for x , the corresponding solution of

$$\frac{d^2y}{dx^2} - \frac{(2u-1)}{x} \frac{dy}{dx} - y = 0 \quad (\text{iii})$$

may be written

$$y = x^u [C I_u(x) + D K_u(x)]. \quad (\text{iv})$$

The solution (19) corresponds to $u = 1$. The solution $I_1(x)$ increases indefinitely with x , and must therefore be rejected. The functions $I_u(x)$ and $K_u(x)$ satisfy the differential equation

$$\frac{d^2y}{dx^2} + \frac{1}{x} \frac{dy}{dx} - \left(1 + \frac{u^2}{x^2}\right) y = 0 \quad (\text{v})$$

For convenience of reference, we note the following formulæ

$$I_0(x) = \frac{1}{\pi} \int_0^\pi \cosh(x \cos \phi) d\phi = 1 + \frac{x^2}{2^2} + \frac{x^4}{2^2 \cdot 4^2} + \frac{x^6}{2^2 \cdot 4^2 \cdot 6^2} + \dots \quad (\text{vi})$$

and

$$K_0(x) = -I_0(x) \left\{ \gamma + \log \frac{1}{2} x \right\} + \frac{x^2}{2^2} + \frac{x^4}{2^2 \cdot 4^2} \left(1 + \frac{1}{2} \right) + \frac{x^6}{2^2 \cdot 4^2 \cdot 6^2} \left(1 + \frac{1}{2} + \frac{1}{3} \right) + \dots \quad (\text{vii})$$

where γ is Euler's constant, $\gamma = 0.57721$.

When x is sufficiently large, we have the asymptotic expansion

$$K_0(x) = \left(\frac{\pi}{2x} \right)^{\frac{1}{2}} e^{-x} \left\{ 1 - \frac{1}{8x} + \frac{1^2 \cdot 3^2}{(8x)^2 \cdot 2!} - \dots \right\} \quad (\text{viii})$$

When x is small, it follows that

$$K_0(x) \sim \{\log 2 - \gamma\} - \log x + \dots, \quad (\text{ix})$$

so that

$$\text{Lt.}_{x \rightarrow 0} [x K_1(x)] = \text{Lt.}_{x \rightarrow 0} \left[-x \frac{d}{dx} K_0(x) \right] \sim 1, \quad (\text{x})$$

as x decreases to zero.

(ii) Expansion of $\sum_1^\infty K_0(ux)$ for Small Values of x .

While the series involving $K_0(ux)$, which occur repeatedly in electrical problems of the type considered in this paper, are extremely convergent for moderate values of x , accurate numerical calculation becomes considerably more difficult for extremely small values of x . In such circumstances we may

advantageously employ Euler's formula* in the form

$$f(x) + f(x+h) + f(x+2h) + \dots + f(x+uh) + \dots \\ = \frac{1}{h} \int_x^{x+uh} f(x) dx + \frac{1}{2} f(x) - \sum_{\kappa=1}^{\infty} (-1)^{\kappa-1} \frac{B_{\kappa} h^{2\kappa-1}}{(2\kappa)!} f^{(2\kappa-1)}(x) + \dots, \quad (i)$$

applicable when $f(x_u) \rightarrow 0$, and the successive derivatives, $f^{(2\kappa-1)}(x_u) \rightarrow 0$ as the integer u increases indefinitely. In the usual notation B_{κ} is the κ th Bernoulli number. If we write $f(x) = K_0(x)$, and $h = x$, we have for small values of x ,

$$K_0(x) = (\log 2 - \gamma) - \log x, \quad K_0'(x) \sim -\frac{1}{x},$$

$$K_0'''(x) \sim -\frac{2!}{x^3}, \quad K_0^{(2\kappa-1)}(x) \sim -\frac{(2\kappa-2)!}{x^{(2\kappa-1)}},$$

where γ is Euler's constant $\gamma = 0.5772 \dots$

We thus obtain by the application of the theorem (i), the following expression for the sum,

$$\sum_1^{\infty} K_0(ux) \sim \frac{1}{x} \int_x^{\infty} K_0(x) dx + \frac{1}{2} K_0(x) + \sum_{\kappa=1}^{\infty} \frac{(-1)^{\kappa-1} B_{\kappa}}{2\kappa(2\kappa-1)} + \dots \quad (ii)$$

Retaining only terms in $1/x$, $\log x$ and a constant term, we easily find in carrying out the integration on the right-hand side of (ii),

$$\sum_1^{\infty} K_0(ux) \sim \frac{1}{x} \left[\frac{\pi}{2} + \frac{1}{2} \log x - \frac{1}{2} (\log 2 - \gamma) \right] + \sum_{\kappa=1}^{\infty} \frac{(-1)^{\kappa} B_{\kappa}}{2\kappa(2\kappa-1)}. \quad (iii)$$

It is somewhat remarkable that the infinite series under the summation sign is capable of being summed. Making use of the definite integral* for B_{κ}

$$B_{\kappa} = 4\kappa \int_0^{\infty} \frac{t^{2\kappa-1} dt}{e^{2\pi t} - 1}, \quad (iv) \dagger$$

we have

$$\sum_{\kappa=1}^{\infty} \frac{(-1)^{\kappa-1} B_{\kappa}}{2\kappa(2\kappa-1)} = 2 \int_0^{\infty} \frac{dt}{e^{2\pi t} - 1} \sum_1^{\infty} \frac{(-1)^{\kappa-1} t^{2\kappa-1}}{2\kappa-1} = 2 \int_0^{\infty} \frac{\tan^{-1} t}{e^{2\pi t} - 1} dt \quad (v)$$

* For a discussion of this formula see Whittaker and Robinson, "The Calculus of Observations," chap. VII, London, (1914).

† Whittaker and Watson, "Modern Analysis," 1915 ed., p. 126.

It so happens that the definite integral (v) has been evaluated in the more general form,*

$$\int_0^\infty \frac{\tan^{-1}(x/p)}{e^{2\pi qx} - 1} dx = \frac{1}{2q} \{ \log T(pq + 1) - \frac{1}{2} \log(2\pi pq) + pq(1 - \log pq) \}. \quad (vi)$$

Writing $p = 1$, $q = 1$ in the above formula, we have

$$\int_0^\infty \frac{\tan^{-1} t}{e^{2\pi t} - 1} dt = \frac{1}{2} (1 - \frac{1}{2} \log 2\pi),$$

and finally we may write (iii) in the form

$$\left. \begin{aligned} \sum_1^\infty K_0(ux) &= \frac{1}{2}\pi/x + \frac{1}{2} \log x - (\frac{1}{2} \log 4\pi - \frac{1}{2}\gamma) + \text{terms in } x^m \text{ and } x^m \log x \\ &= \frac{1}{2}\pi/x + \frac{1}{2} \log x - 0.9769041 + \dots \end{aligned} \right\} \quad (vii)$$

By actual summation of the tabular entries in Jahnke and Emde's tables of $K_0(x)$, the constant term in (vii) was found to be 0.9772 in fair agreement with the actual value determined later by the above application of Euler's summation formula

(iii) *Expansion of $\sum_1^\infty K_0(2u-1)x$ for Small Values of x .*†

If we write $h = 2x$ in Euler's summation formula we easily find

$$\sum_1^\infty K_0(2u-1)x = \frac{1}{2x} \int_0^\infty K_0(x) dx + \frac{1}{2} K_0(x) + \sum_{\kappa=1}^\infty \frac{(-1)^{\kappa-1} B_\kappa 2^{2\kappa-1}}{2\kappa(2\kappa-1)} + \quad (i)$$

$$+ \frac{1}{4}\pi/x - \frac{1}{2} + 2 \int_0^\infty \frac{dt}{e^{2\pi t} - 1} \sum_1^\infty \frac{(-1)^{\kappa-1} (2t)^{2\kappa-1}}{2\kappa-1} + \quad (ii)$$

$$+ \frac{1}{4} \frac{\pi}{x} - \frac{1}{2} + 2 \int_0^\infty \frac{\tan^{-1} 2t}{e^{2\pi t} - 1} dt + \quad (iii)$$

$$+ \frac{1}{4}\pi/x - \frac{1}{2} + \{ \log T(\frac{1}{2}) - \frac{1}{2} \log \pi + \frac{1}{2} (1 - \log \frac{1}{2}) \} + .$$

writing $p = \frac{1}{2}$, $q = 1$ in (vi) g, Note (ii),

$$+ \frac{1}{4}\pi/x + \frac{1}{2} \log 2 + \dots + \text{terms in } x^m \text{ and } x^m \log x \quad (iv)$$

$$+ \frac{1}{4}\pi/x + 0.3465736 + \dots \quad (v)$$

A rough determination of the constant term in (v) by summing the odd entries in Jahnke and Emde's tables of $K_0(x)$ gave the value 0.3473.

* Bierens de Haan, "Nouvelles Tables d'Integrales," Table 282. This integral is known as Binet's "second expression" for $\log T(z)$. Whittaker and Watson, *loc. cit.*, § 12.32.

† The series discussed in Notes (ii) and (iii) have recently been discussed by Watson, 'Quart. J. Math.' See also Bateman, *loc. cit.*, § 7.33, p. 414.

$$(iv) \text{ On the Series } \beta_x = \sum_{n=1}^{\infty} \beta^n / n^x.$$

Appell has studied the above series, which may be expressed as a definite integral, valid for all values of x such that $|x| < 1$ and $R(s) > 0$,

$$\phi(s, x) = \sum_{n=1}^{\infty} \frac{x^n}{n^s} = \frac{1}{\Gamma(s)} \int_0^{\infty} \frac{x z^{s-1} dz}{e^z - x} \quad (i)^*$$

This result enables us to obtain the series (70) directly from either of the integrals (72) or (79). Writing $\coth x = 1 + 2/(e^{2x} - 1)$, we have in the latter case,

$$\int_0^{\infty} \coth(\lambda h + \zeta) J_0(\lambda) d\lambda = \frac{1}{i} + \frac{1}{h} \int_0^{\infty} \frac{x J_0(\xi z) dz}{e^z - x},$$

where we have written

$$\xi = \frac{1}{2}i/h \quad \text{and} \quad x = e^{-2s} = (\rho' - \rho)/(\rho' + \rho) = \beta \quad (ii)$$

It follows from (79) that

$$\frac{\bar{\rho}}{\rho} = \frac{2\pi}{1\rho} r^2 \frac{dV}{dt} = 1 + 2\xi^2 \int_0^{\infty} \frac{x z J_1(\xi z) dz}{e^z - x}.$$

Making use of the expansion

$$J_1(\xi z) = \frac{1}{2}\xi z \left\{ 1 - \frac{1}{1!2!} \left(\frac{\xi z}{2}\right)^2 + \dots + \frac{(-1)^m}{m!(m+1)!} \left(\frac{\xi z}{2}\right)^{2m} + \dots \right\},$$

and utilising Appell's integral (i), we easily deduce that

$$\begin{aligned} \frac{\bar{\rho}}{\rho} = & 1 + 2! \xi^2 \phi(\zeta, \beta) - \frac{4!}{1!2!} \frac{\xi^4}{2^2} \phi(\delta, \beta) + \\ & + \frac{(-1)^m \xi^{2m+2} (2m+2)!}{m!(m+1)! 2^{2m}} \phi(2m+\zeta, \beta) + \dots \end{aligned} \quad (iii)$$

which agrees with (70), since in the notation of that section $\beta_x = \phi(\kappa, \beta)$

The same result is obtained from (72), β being replaced by β' , and ρ and ρ' in (ii) being interchanged.

When $\beta = \pm 1$, (iii) gives the expansion near the origin of the series (31) and (37), in which cases the coefficients in (iii) become Riemann's Zeta Function

* Appell, 'C. R. Acad. Sci. Paris,' vol. 87, p. 874, (1878) referred to by Whittaker and Watson, *loc. cit.*, Ex. 7, p. 274.

defined by $\zeta(s) = \sum_{n=1}^{\infty} \frac{1}{n^s}$ in terms of which it is easily shown that

$$\phi(\kappa, 1) = \zeta(\kappa) \quad \text{and} \quad \phi(\kappa, -1) = -(1-2)^{1-\kappa} \zeta(\kappa) \quad (\text{iv})^*$$

For odd integral values of κ , the function $\zeta(\kappa)$ is most easily computed from the series

$$\zeta(\kappa) (1-2^{-\kappa}) = 1^{-\kappa} + 3^{-\kappa} + 5^{-\kappa} + 7^{-\kappa} + \dots + p^{-\kappa} + \dots, \quad (\text{v})^\dagger$$

where 1, 3, 5, 7, ..., p are odd numbers

We thus have in the case $\beta = 1$, $\rho' \rightarrow \infty$ (homogeneous stratum bounded by insulating plane) the expansion of the series (31) for small values of r/h ,

$$\begin{aligned} \frac{\bar{\rho}}{\rho_0} &= \frac{r}{h} + 2\pi \left(\frac{r}{h}\right)^2 \sum_{s=1}^{\infty} \delta K_1\left(\frac{\pi r}{h} \delta\right) \\ &= 1 + 2! \zeta(3) \left(\frac{r}{2h}\right)^3 + \frac{4!}{1! 2!} \frac{\zeta(5)}{2^2} \left(\frac{r}{2h}\right)^5 + \dots \quad (r/h \rightarrow 0) \end{aligned} \quad (\text{vi})$$

Similarly, the case $\beta = -1$, $\rho' \rightarrow 0$ (homogeneous stratum bounded by perfectly conducting plane), gives the series expansion for (37)

$$\left. \begin{aligned} \frac{\bar{\rho}}{\rho} &= 2\pi \left(\frac{r}{h}\right)^2 \sum_{s=1}^{\infty} \left(\delta - \frac{1}{2}\right) K_1\left\{\frac{\pi r}{h} \left(\delta - \frac{1}{2}\right)\right\} \\ &= 1 - 2! \frac{1}{4} \zeta(3) \left(\frac{r}{2h}\right)^3 + \frac{4!}{1! 2!} \frac{1}{16} \zeta(5) \left(\frac{r}{2h}\right)^5 + \dots \end{aligned} \right\} \quad (\text{vi})$$

We note the numerical values

$$\left. \begin{aligned} \zeta(2) = \phi(2, 1) &= \frac{1}{6} \pi^2 = 1.6459 & \zeta(3) &= 1.2021 \\ \zeta(4) = \phi(4, 1) &= \frac{1}{90} \pi^4 = 1.0823 & \zeta(5) &= 1.0369 \\ \zeta(6) = \phi(6, 1) &= \frac{1}{42} \pi^6 = 1.0173 & \zeta(7) &= 1.0083 \end{aligned} \right\} \quad (\text{vii})^\ddagger$$

* Whittaker and Watson, *Loc. cit.*, Ex. 1, 13, p. 261

† Quoted from Adams's 'Smithsonian Mathematical Tables,' p. 140 (1922)

‡ Whittaker and Watson, *Loc. cit.*, 13.3

The Air Pressure on a Cone Moving at High Speeds.—I.

By G. I TAYLOR, F.R.S., Yarrow Research Professor, and J. W. MACCOLL,
B.Sc., Ph.D.

(Received October 7, 1932)

§ 1. *Introduction and Summary.*

When a body moves through air at a uniform speed greater than that of sound, a shock wave is formed which remains fixed relative to the body. This wave is situated on a surface where a very abrupt change in density and velocity occurs. It can be seen as a sharp line in photographs of bullets in flight. In front of this surface the air is stationary, behind it there is a continuous field of fluid flow which may contain further shock waves. The nature of these shock waves is well known and the equations which govern their propagation were first obtained by Rankine.† The work of Rankine, however, seems to have escaped the notice of subsequent writers and it was not till some years later that they were rediscovered by Hugoniot‡ to whom they are usually attributed. Rankine's equations give the relationship between the conditions in front and behind a plane shock wave. They connect the ratio of the density in front and behind the wave with the components of velocity normal to the wave. They have been applied by Meyer§ to find the flow in the neighbourhood of an inclined plane or wedge moving at high speeds.

Meyer begins with a plane shock wave reduced to rest by giving the whole field a suitable velocity perpendicular to its plane. He then gives the whole field a velocity parallel to the wave front. The system is then a steady one, the shock wave remaining at rest, but the direction of motion of the air, which is now oblique to the wave, suffers an abrupt change at the wave front. By combining two such shock waves intersecting at a point, but not continuing beyond the intersection, a system can be devised in which all the air on one side of the pair of waves is moving with a uniform velocity. The air which passes through one wave is deflected, say, upwards, while that which passes through the other is deflected downwards. This system can evidently be bounded by a solid wedge, the faces of which are parallel to the two parts of the deflected air stream.

† 'Phil. Trans.,' vol. 160, p. 277 (1870).

‡ 'Ec. polyt., Paris,' vols. 57-59, p. 1 (1887-1889).

§ 'Mitt. ForschArb. Ingenieurw. V D.L.,' No. 62 (1908)

Meyer exhibited this solution of the flow near a wedge moving at high speed by means of a series of curves showing the relationships between the pressure, speeds and angle of the wedge. His equations were reproduced by Ackeret† who added a photograph of the flow in the neighbourhood of a wedge showing that Meyer's regime does in fact occur. The solution has certain limitations which are obvious from an inspection of Meyer's curves. These limitations have been treated independently and in greater detail by Bourquard.‡

When the wedge is replaced by a cone no solution exactly similar to Meyer's can be obtained, because after passing obliquely through a conical shock wave the air cannot continue to flow in the direction into which it was first deflected. The pressure behind the shock wave, therefore, cannot be uniform, as it is in the case of the wedge. On the other hand, it turns out that an irrotational solution of the flow in the neighbourhood of a solid cone can be found such that the pressure, velocity and density of the stream is constant over coaxial cones passing through the same vertex.

If a conical shock wave is capable of changing the air from a state of uniform motion parallel to the axis of the cone to a condition which satisfies the irrotational solution mentioned above, then the system so constructed is a possible solution of the problem of flow at high speeds past a cone. That such solutions can be found has been suggested by Busemann,§ who gave a graphical method for obtaining them. In his very short note on the subject no details or results are given so that we cannot make a comparison between his work and ours. It is clear, however, that his graphical method is capable of doing what he claims for it, though we have been unable to find any account of further developments on those lines.

In the present paper it is shown that under certain conditions the conical regime is possible and the complete solution is worked out by numerical integration, for three cones of semi-vertical angles 10° , 20° and 30° .

The calculated pressures at the surface of the cone are compared with observations of pressure made in a high speed wind channel and excellent agreement is found. In one case, that of the 60° cone (i.e., 30° semi-vertical angle), further comparisons are made with photographs of bullets in flight, and it is found that the limitation indicated by mathematical analysis that in this case the conical regime is possible only when the speed is greater than $1.46a$, a being the speed of sound, corresponds with the condition observed

† "Gasdynamik," 'Handbuch der Physik,' vol. 7, chap. 5 (1927)

‡ Bourquard, 'Mémor. Artill. française,' vol. 11, p. 135 (1932).

§ Busemann, 'Z. angew. Math. Mech.,' vol. 9, p. 496 (1929).

$(u_s, 0)$ are the components of velocity at the surface of the solid cone.

p, ρ are the pressure and density of air at any point behind the shock wave.

p_1, ρ_1, a are the pressure, density and velocity of sound in the undisturbed stream.

γ is the ratio of the specific heats so that $a^2 = \gamma p_1 / \rho_1$. The value $\gamma = 1.405$ is used throughout the calculations.

p_2, ρ_2, p_s, ρ_s are the pressure and density immediately behind the shock wave and at the surface of the cone.

p_0, ρ_0 are the pressure and density of air at rest in a reservoir, which could attain the condition p_1, ρ_1, U by flowing in a steady stream under adiabatic conditions. Evidently $p_0 \rho_0^{-\gamma} = p_1 \rho_1^{-\gamma}$.

p_3, ρ_3 are the pressure and density of air at rest corresponding with the conditions behind the shock wave, so that $p_3 \rho_3^{-\gamma} = p_2 \rho_2^{-\gamma}$.

c_1, c are the velocities at which air at rest in the states (p_0, ρ_0) and (p_3, ρ_3) would flow into a vacuum under adiabatic conditions.

a^* is the local speed of sound at any point behind the shock wave. The local speed of sound is the speed at which sound waves would be propagated through air in the condition (p, ρ) ; it is *not* the speed at which sound would be propagated relative to the cone.

α is the angle between the normal to the shock wave and the streamlines in front of it. These are parallel to the axis of the cone so that $\theta_w = \frac{1}{2}\pi - \alpha$.

β is the angle between the normal to the shock wave and the streamlines immediately behind the shock wave.

ϕ is the angle between the streamline at any point and the radius vector from the point of the cone.

The following symbols are used in conformity with Meyer and Ackeret's notation in order to reduce the formulæ to non-dimensional forms:—

$$x = p_2/p_0,$$

$$y = p_1/p_0,$$

$$z = p_3/p_0.$$

Irrotational Motion.—A solution of the equations of fluid flow near a solid cone will be sought in which all the variables, such as pressure, density and velocity, are functions of θ only. In this case the flow must be irrotational and the condition for irrotational flow is

$$\frac{\partial u}{\partial \theta} - v = 0, \quad (1)$$

The condition of continuity is

$$\frac{\partial}{\partial r} (\rho u^2 \sin \theta) + \frac{\partial}{\partial \theta} (\rho v \sin \theta) = 0,$$

and, since $\partial u / \partial r = 0$, this is

$$2\rho u \sin \theta + \frac{d}{d\theta} (\rho v \sin \theta) = 0. \quad (2)$$

Hence, combining (1) and (2),

$$-\frac{v}{\rho} \cdot \frac{d\rho}{d\theta} = \frac{d^2 u}{d\theta^2} + \cot \theta \cdot \frac{du}{d\theta} + 2u. \quad (3)$$

The adiabatic relationship between pressure and density is $p/p_3 = (\rho/\rho_3)^\gamma$ so that Bernoulli's equation is

$$\frac{\gamma p_3 \rho^{\gamma-1}}{(\gamma-1) \rho_3^\gamma} + \frac{1}{2} (u^2 + v^2) = \text{constant} = \frac{1}{2} c^2 = \frac{\gamma}{\gamma-1} \cdot \frac{p_3}{\rho_3}, \quad (4)$$

where c is the velocity which the gas would attain if allowed to flow in steady motion into a vacuum and p_3 , ρ_3 are the pressure and density at points where the velocity is zero.

Differentiating (4) with respect to θ and substituting $du/d\theta$ for v

$$\frac{\gamma p_3}{\rho_3^\gamma} \rho^{\gamma-1} \cdot \frac{d\rho}{\rho d\theta} + u \cdot \frac{du}{d\theta} + \frac{du}{d\theta} \cdot \frac{d^2 u}{d\theta^2} = 0, \quad (5)$$

and substituting for $\frac{1}{\rho} \cdot \frac{d\rho}{d\theta}$ from (3), (5) becomes

$$u \frac{du}{d\theta} + \frac{du}{d\theta} \cdot \frac{d^2 u}{d\theta^2} = \frac{\gamma p_3}{\rho_3^\gamma} \cdot \rho^{\gamma-1} \cdot \left(\frac{d^2 u}{d\theta^2} + \cot \theta \frac{du}{d\theta} + 2u \right). \quad (6)$$

and substituting for $\rho^{\gamma-1}$ from (4), (6) becomes

$$\frac{du}{d\theta} \left(u \frac{du}{d\theta} + \frac{du}{d\theta} \cdot \frac{d^2 u}{d\theta^2} \right) = \frac{1}{2} (\gamma-1) \left\{ c^2 - u^2 - \left(\frac{du}{d\theta} \right)^2 \right\} \left\{ \frac{d^2 u}{d\theta^2} + \cot \theta \cdot \frac{du}{d\theta} + 2u \right\}. \quad (7)$$

This equation may be re-arranged into the more convenient form

$$\begin{aligned} \frac{1}{c} \cdot \frac{d^2 u}{d\theta^2} \left\{ \frac{\gamma+1}{2c^2} \left(\frac{du}{d\theta} \right)^2 - \frac{\gamma-1}{2} \left(1 - \frac{u^2}{c^2} \right) \right\} &= (\gamma-1) \frac{u}{c} \left(1 - \frac{u^2}{c^2} \right) \\ &+ \frac{\gamma-1}{2c} \left(1 - \frac{u^2}{c^2} \right) \cot \theta \cdot \frac{du}{d\theta} - \frac{\gamma u}{c^3} \left(\frac{du}{d\theta} \right)^2 - \frac{\gamma-1}{2c^3} \cot \theta \left(\frac{du}{d\theta} \right)^3. \end{aligned} \quad (8)$$

This equation determines the motion when any initial values of u , v and θ are given.

To determine the pressure at any point when the solution of (8) is known (4) may be used. This may be written in the form

$$\frac{p}{p_3} = \left(1 - \frac{u^2}{c^2} - \frac{v^2}{c^2}\right)^{\frac{\gamma}{\gamma-1}}. \quad (9)$$

The pressure, velocity and direction of motion of the flow behind the shock wave are given by (8) and (9).

In front of the shock wave the velocity is uniform and equal to U while the pressure is p_1 so that the pressure equation equivalent to (9) applicable to that region is

$$y = \left(1 - \frac{U^2}{c_1^2}\right)^{\frac{\gamma}{\gamma-1}}. \quad (10A)$$

where y is written for p_1/p_0 , and p_0 is the pressure in a reservoir from which air could flow with velocity U , pressure p_1 and density ρ_1 . c_1 is the velocity at which gas at pressure p_0 and density ρ_0 discharges into a vacuum.

It is more usual to express velocities in terms of a , the velocity of sound in the undisturbed air. To find c_1/a , equation (4) may be applied to the region in front of the shock wave, thus

$$c_1^2 = \frac{2\gamma}{\gamma-1} \cdot \frac{p_0}{\rho_0} \quad \text{and} \quad a^2 = \gamma \cdot \frac{p_1}{\rho_1},$$

so that

$$\frac{c_1^2}{a^2} = \frac{2}{\gamma-1} \cdot \frac{p_0}{p_1} \cdot \frac{\rho_1}{\rho_0} = \frac{2}{\gamma-1} \left(\frac{1}{y}\right)^{1-\frac{1}{\gamma}}.$$

Substituting this expression in (10A),

$$\frac{U^2}{a^2} = \frac{2}{\gamma-1} (y^{-\frac{\gamma-1}{\gamma}} - 1) \quad (10B)$$

§ 3. Numerical Integration of Equation (8).

It is hardly to be expected that solutions of (8) could be found in finite terms, but on the other hand (8) is in a form suitable for numerical calculation. At the solid surface $\theta = \theta_s$ and $v = du/d\theta = 0$ so that the initial value of $d^2u/d\theta^2$ can be found. It is equal to $-2u_s \ddagger$. If $\delta\theta$ is a small increment in θ , the value

\ddagger A construction involving the use of a hodograph is given by Bourquard ('R. Acad. Sci., Paris, 1932 *loc. cit.*) which is equivalent to this result.

Table I.—Abridged Form of the Calculations for $\theta_s = 30^\circ$, $u_s/c = 0.35$.

$$v_\theta/c = c^{-1} \cdot [du/d\theta]_0 = c^{-1} \cdot \{v_{\theta-30} + \delta\theta \cdot [d^2u/d\theta^2]_{\theta-30}\}$$

$$u_\theta/c = c^{-1} \cdot \{u_{\theta-30} + \delta\theta \cdot [v_M]\}, \quad \text{where } v_M = \frac{1}{2} \{v_\theta + v_{\theta-30}\}$$

$$c^{-1} \cdot d^2u/d\theta^2 = L/M, \quad \text{where } L = c^{-3} \cdot [0.405 \{c^2 - u^2 - v^2\} \{u + \frac{1}{2} v \cdot \cot \theta\} - uv^2]$$

$$\text{and } M = c^{-2} \cdot [0.2025 \{c^2 - u^2\} - 1.2025 v^2]$$

$$p/p_1 = [c^{-2} \cdot (c^2 - u^2 - v^2)]^{3/4} \cdot 0.99$$

$$\tan \phi = v/u \quad \beta - \alpha = 0 + \phi \quad \alpha = \pi/2 - \theta.$$

θ°	30.	33.	36.	39.	42.	45.	48.
$-v/c$	0.0000	0.03665	0.07036	0.10192	0.13182	0.16039	0.18784
u/c	0.3500	0.34904	0.34624	0.34173	0.33561	0.32796	0.31884
$c^{-1} \cdot [c^2 - u^2 - v^2]$	0.8775	0.87683	0.87517	0.87283	0.86999	0.86672	0.86306
$c^{-1} \cdot [u + \frac{1}{2} v \cdot \cot \theta]$	0.3500	0.32082	0.29782	0.27880	0.26241	0.24776	0.23427
L	0.12439	0.11346	0.10385	0.09500	0.08663	0.07853	0.07064
M	0.17769	0.17622	0.17227	0.16636	0.15979	0.14979	0.13948
$-c^{-1} \cdot d^2u/d\theta^2$	0.7000	0.6439	0.6028	0.5711	0.5456	0.5243	0.5065
p/p_1	0.6355	0.6338	0.6297	0.6239	0.6168	0.6088	0.6000

	51.	54.	57.	60.	63.	66.	69.
v/c	0.21436	0.24009	0.26518	0.28984	0.31433	0.33920	0.36502
u/c	0.30831	0.29641	0.28318	0.26865	0.25283	0.23572	0.21727
$c^{-1} \cdot [c^2 - u^2 - v^2]$	0.85699	0.85450	0.84919	0.84382	0.83728	0.82938	0.81911
$c^{-1} \cdot [u + \frac{1}{2} v \cdot \cot \theta]$	0.22152	0.20919	0.19708	0.18498	0.17275	0.16021	0.14710
L	0.06289	0.05530	0.04789	0.04064	0.03360	0.02669	0.01975
M	0.12799	0.11539	0.10170	0.08687	0.07075	0.05289	0.03219
$-c^{-1} \cdot d^2u/d\theta^2$	0.4914	0.4792	0.4709	0.4678	0.4749	0.5046	0.5135
p/p_1	0.5002	0.5796	0.5679	0.5548	0.5400	0.5226	0.5003
$\tan \phi$			0.9364	1.0789	1.2432	1.4390	1.6828
ϕ			43° 07'	47° 10'	51° 11'	55° 12'	59° 17'
Shock wave conditions	$\beta - \alpha$	$\beta - \alpha$	13° 53'	12° 50'	11° 49'	10° 48'	9° 43'
			33° 00'	30° 00'	27° 00'	24° 00'	21° 00'
			0.452	0.489	0.521	0.550	0.574
			0.221	0.248	0.272	0.291	0.308
p_2/p_1			0.064	0.069	0.072	0.075	0.075
			0.469	0.505	0.536	0.564	0.589

Table II—Summary of Results of Calculations

$\theta_s = 10^\circ$										
u_s/c	0.35	0.375	0.40	0.45	0.50	0.60	0.70	0.80	0.90	
$\delta\theta$	3.0°	2.0°	2.0°	1.5°	1.5°	1.5°	1.0°	0.5°	0.5°	
x	0.587	0.536	0.493	0.408	0.325	0.182	0.0802	0.0236	0.00263	
y	0.476	0.504	0.486	0.401	0.316	0.171	0.0700	0.0168	0.00115	
z	0.999	1.000	1.000	1.000	1.000	1.000	1.000	0.992	0.946	
θ_w	87.9°	81.1°	70.3°	55.6°	46.6°	34.4°	26.3°	20.1°	15.4°	
$U^2 a$	1.09	1.04	1.07	1.22	1.39	1.81	2.30	3.33	5.46	
Mach angle	67.1°	74.3°	69.3°	53.0°	45.8°	33.5°	24.8°	17.5°	10.6°	
θ_a	*	*	32.5°	†	†	†	†	†	†	
$(p_s - p_1)/\rho_1 U^2$	0.202	0.114	0.077	0.066	0.030	0.054	0.048	0.045	0.038	
$\theta_s = 20^\circ$										
u_s/c	0.27	0.30	0.35	0.40	0.50	0.60	0.70	0.80	0.90	
$\delta\theta$	3.0°	3.0°	3.0°	2.0°	1.5°	1.5°	1.0°	0.5°	0.5°	
x	0.656	0.619	0.532	0.453	0.363	0.175	0.0781	0.0203	0.502 × 10 ⁻³	
y	0.312	0.385	0.417	0.356	0.219	0.104	0.0339	0.00334	0.293 × 10 ⁻⁴	
z	0.954	0.989	0.999	0.999	0.998	0.987	0.945	0.791	0.170	
θ_w	84.1°	80.4°	69.1°	58.0°	44.4°	36.1°	30.4°	26.2°	22.9°	
$U^2 a$	1.40	1.25	1.19	1.36	1.65	2.13	2.86	4.17	9.74	
Mach angle	45.4°	53.1°	57.1°	50.1°	37.4°	28.0°	20.5°	13.9°	5.9°	
θ_a	*	*	†	32.7°	†	†	†	†	†	
$(p_s - p_1)/\rho_1 U^2$	0.488	0.388	0.263	0.219	0.178	0.159	0.148	0.134	0.128	
$\theta_s = 30^\circ$										
u_s/c	0.27	0.30	0.35	0.40	0.50	0.60	0.65	0.70	0.80	
$\delta\theta$	3.0°	3.0°	3.0°	2.0°	1.0°	1.0°	1.0°	1.0°	0.5°	
x	0.625	0.597	0.524	0.448	0.294	0.154	0.0688	0.0306	0.271 × 10 ⁻³	
y	0.258	0.282	0.274	0.224	0.119	0.0424	0.0216	0.0082	0.122 × 10 ⁻⁴	
z	0.933	0.961	0.972	0.967	0.926	0.815	0.725	0.574	0.0897	
θ_w	76.8°	71.4°	63.3°	56.6°	47.4°	41.3°	39.2°	37.3°	34.2°	
$U^2 a$	1.54	1.47	1.49	1.63	2.05	2.71	3.16	3.85	7.84	
Mach angle	40.6°	42.7°	42.1°	37.8°	29.3°	21.7°	18.5°	15.1°	7.3°	
θ_a	*	*	*	41.0°	†	†	†	†	†	
$(p_s - p_1)/\rho_1 U^2$	0.537	0.477	0.401	0.362	0.318	0.299	0.285	0.278	0.262	

* Speeds behind the shock wave everywhere less than that of sound
† Speeds behind the shock wave everywhere greater than that of sound.

of $du/d\theta$ at $\theta = \theta_s + \delta\theta$ is $-2u_s \cdot \delta\theta$ and the value of u/c is

$$u_s/c + \frac{1}{2}(-2u_s/c) \cdot \delta\theta^2.$$

These values of u/c and $\frac{1}{c} \frac{du}{d\theta}$ may now be inserted in (8) to find the value of $\frac{1}{c} \cdot \frac{d^2u}{d\theta^2}$ at $\theta = \theta_s + \delta\theta$, and this value may again be used to find the values of u/c and $\frac{1}{c} \frac{du}{d\theta}$ at $\theta = \theta_s + 2\delta\theta$. This method of step-by-step calculation will give the solution of (8) when any given initial values of u_s/c and θ_s are chosen.

The accuracy of the method will depend on the magnitude of $\delta\theta$. In some cases sufficient accuracy can be obtained by taking steps of three degrees, while in others smaller intervals must be taken. In some cases it was necessary to proceed by steps as small as 0.5° . The accuracy of the method in any given case may be judged by repeating the process using steps only half as great as those first taken. If there is no change in the results to the order of accuracy required, the steps may be considered as so small that no further diminution in $\delta\theta$ would produce any appreciable change in the result.

To illustrate the method, the complete calculation is given in Table I. for one case, namely, that of a 60° cone ($\theta_s = 30^\circ$) when $u_s/c = 0.35$.

In this case it was found that the interval $\delta\theta = 3^\circ$ was small enough to give the required accuracy. The calculation is carried from $\theta = 30^\circ$ to $\theta = 69^\circ$ and the variations in u/c , v/c with θ are shown in the curves marked $u_s/c = 0.35$ in fig. 2. It will be seen that as θ increases u/c and v/c decrease. The values of p/p_s derived from (9) are given in Table I and are shown in fig. 2.

The method described above was applied to three cones whose vertical angles are 60° , 40° and 20° (so that $\theta_s = 30^\circ$, 20° , 10°). In each case a range of values of u_s/c was chosen so as to cover the whole range in which results of interest might be expected. The actual values taken for u_s/c are shown in the top row of each section of Table II while the interval $\delta\theta$ used in the step-by-step integration is given in the second row.

It seems unnecessary to give in tabular form the details of the solutions obtained. They are set forth, however, in graphical form in figs. 2, 3 and 4 where the variations of u/c , v/c and p/p_s with θ are shown for each cone, for some, but not all, of the values of u_s/c for which the solutions were obtained.

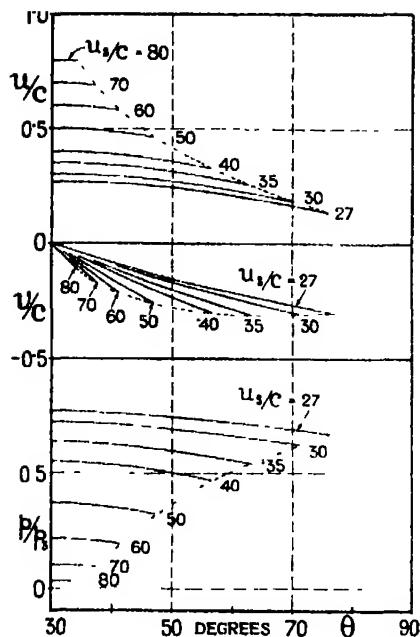


FIG. 2.— u/c , v/c and p/p_3 for 30° cone.

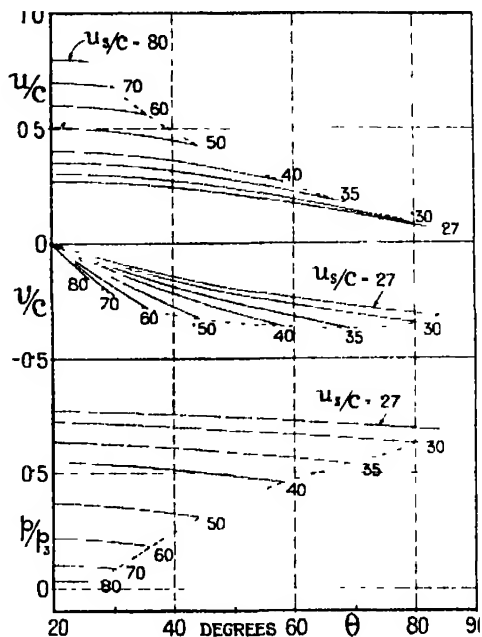


FIG. 3.— u/c , v/c and p/p_3 for 20° cone.

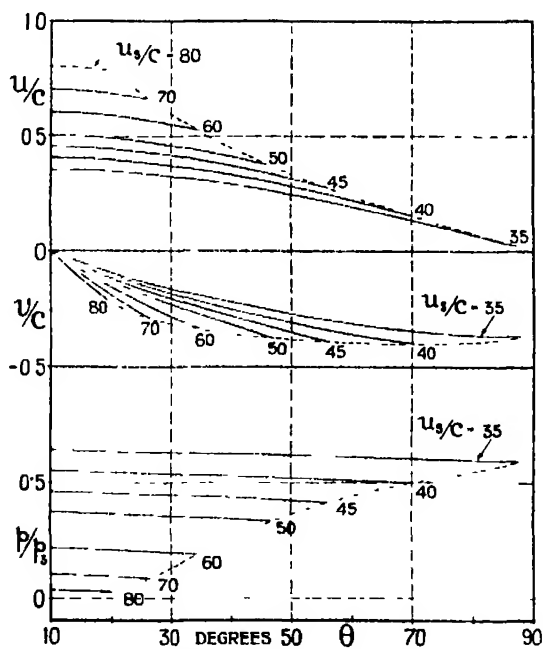


FIG. 4.— u/c , v/c and p/p_3 for 10° cone.

§ 4. Shock Wave Equations.

Meyer's equations governing the conditions on either side of an oblique shock wave are (Ackeret, *loc. cit.*, p. 330)

$$\cos^2 \alpha = \left\{ \frac{(\gamma - 1) + (\gamma + 1)(x/y)}{4\gamma \cdot [(1/y)^{\frac{\gamma-1}{\gamma}} - 1]} \right\} \cdot (\gamma - 1), \quad (11)$$

$$\tan \beta = \frac{(\gamma - 1)y + (\gamma + 1)x}{(\gamma - 1)x + (\gamma + 1)y} \cdot \tan \alpha, \quad (12)$$

where α , β , x , y , γ have the meanings explained in the list of symbols and illustrated in fig. 1.

Our present purpose is to use these equations to find out whether a shock wave is capable of changing the uniform stream at pressure p_1 moving parallel to the axis with velocity U into a stream at pressure p_2 moving at angle $\theta + \phi$ to the axis. For this purpose evidently we must take

$$\frac{1}{2}\pi - \alpha = \theta \quad \text{and} \quad \beta - \alpha = \theta + \phi. \quad (13)$$

These conditions, however, do not suffice to connect the motion at the two sides of the shock wave. The pressure p/p_3 given by (9) must be equal to p_2/p_3 . But $p_2/p_3 = p_2/p_0 \cdot p_0/p_3 = x/z$ so that the pressure condition is

$$p/p_3 = x/z. \quad (14)$$

The method adopted for finding the conditions under which (13) and (14) can be satisfied simultaneously was to find for each value of θ and $\theta + \phi$ in the step-by-step calculation the values of x , y and z in the shock wave equations which correspond with values of α and $\beta - \alpha$ given by (13). The values of p/p_3 obtained in the step-by-step calculation and of x/z were then plotted on a diagram for each value of θ and the point where the two curves cross gives the angle θ_w at which the shock wave can exist so that the required conditions are satisfied. An example of this kind of diagram is shown in fig. 5.

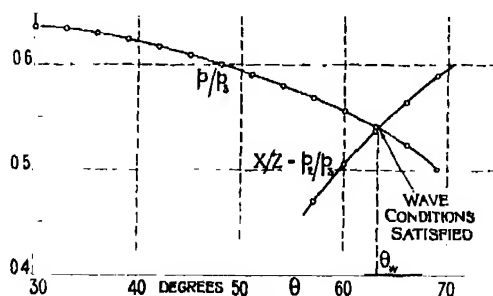


FIG. 5.

In his presentation of the shock wave equations, Meyer calculated the values of α and β from (11) and (12) for a limited number of values of x and y . He then plotted on an x, y diagram three sets of interpolated curves showing the values of x and y for a limited number of values of α , β and $\beta - \alpha$ respectively. To find x and y for given values of α and $\beta - \alpha$ two of these diagrams would have to be superimposed and the co-ordinates of the intersections of the corresponding contours read. This method turns out to involve considerable difficulties in interpolation; accordingly, two new sets of curves were plotted with α and $\beta - \alpha$ as rectangular co-ordinates. One of these, fig. 6, gives the value of x corresponding with any given values of α and $\beta - \alpha$, the other, fig. 7, gives the value of y .† Most of the values of x and y in Table II were found in this way, though in some cases when the points occurred near the limits of the diagram direct calculation was used, (11) and (12) being solved as simultaneous equations in x and y for appropriate values of α and $\beta - \alpha$.

Meyer's equations do not give z directly. This can be obtained by constructing the equation for β which is analogous to the expression (11) giving α in terms of y and x/y . For this purpose it is merely necessary to substitute in (11) β for α , y/x for x/y , and z/x for $1/y$.‡

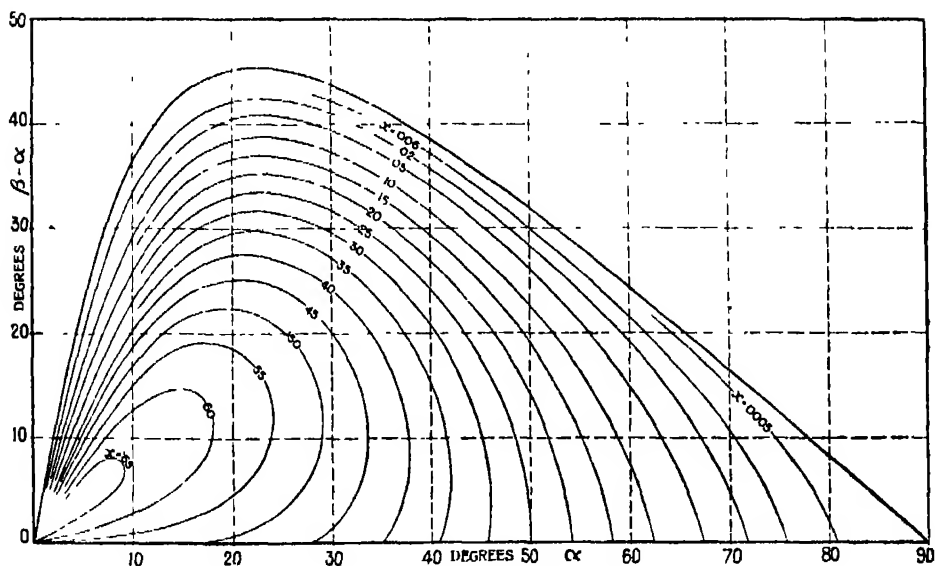


FIG. 6.

† It will be noticed from (12) that the limiting forms of these contours when $x = 0$ or when $y = 0$ are identical, namely, $\tan \beta = \frac{\gamma + 1}{\gamma - 1} \tan \alpha$.

‡ I.e., p_2/p_1 for p_1/p_0

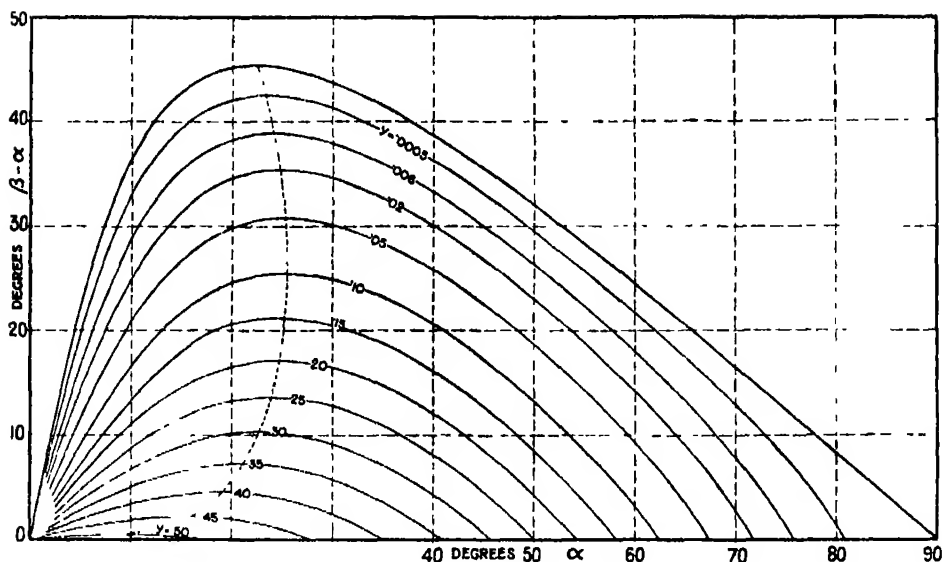


FIG. 7.

The resulting equation can be re-arranged into the form

$$\left(\frac{z}{x}\right)^{\frac{\gamma-1}{\gamma}} = 1 + \frac{\gamma-1}{4\gamma \cos^2 \beta} \{\gamma-1 + (\gamma+1)y/x\}. \quad (15)$$

After the tables for α and β , from which figs. 6 and 7 were prepared, had been made they were used in conjunction with (15) to construct a table giving z in terms of x and y . The diagram of fig. 8 shows how z varies with x for constant values of y .

It will be noticed that this diagram is contained within a certain bounding curve which corresponds with $\alpha = \beta = 0$. The x and z co-ordinates of this curve were calculated separately for various values of y so as to check the calculations. The formulæ used for this purpose were derived by putting $\cos \alpha = \cos \beta = 1$ in (11) and (15). They are

$$\frac{x}{y} = \frac{1}{\gamma^2 - 1} [4\gamma y^{\frac{1-\gamma}{\gamma}} - (\gamma+1)^2]$$

and

$$\left(\frac{z}{x}\right)^{\frac{\gamma-1}{\gamma}} = 1 + \frac{(\gamma-1)^2}{4\gamma} + \frac{(\gamma^2-1)^2}{16\gamma^2 \cdot \left(y^{\frac{1-\gamma}{\gamma}} - \frac{(\gamma+1)^2}{4\gamma}\right)}.$$

The values of x and y derived from figs. 6 and 7 and entered in Table I were used in conjunction with fig. 8 to find the values of z given near the foot of the

table. The values of x/z found in this way are plotted in fig. 5 as a function of θ .

The position of the shock wave is determined by the intersection of the

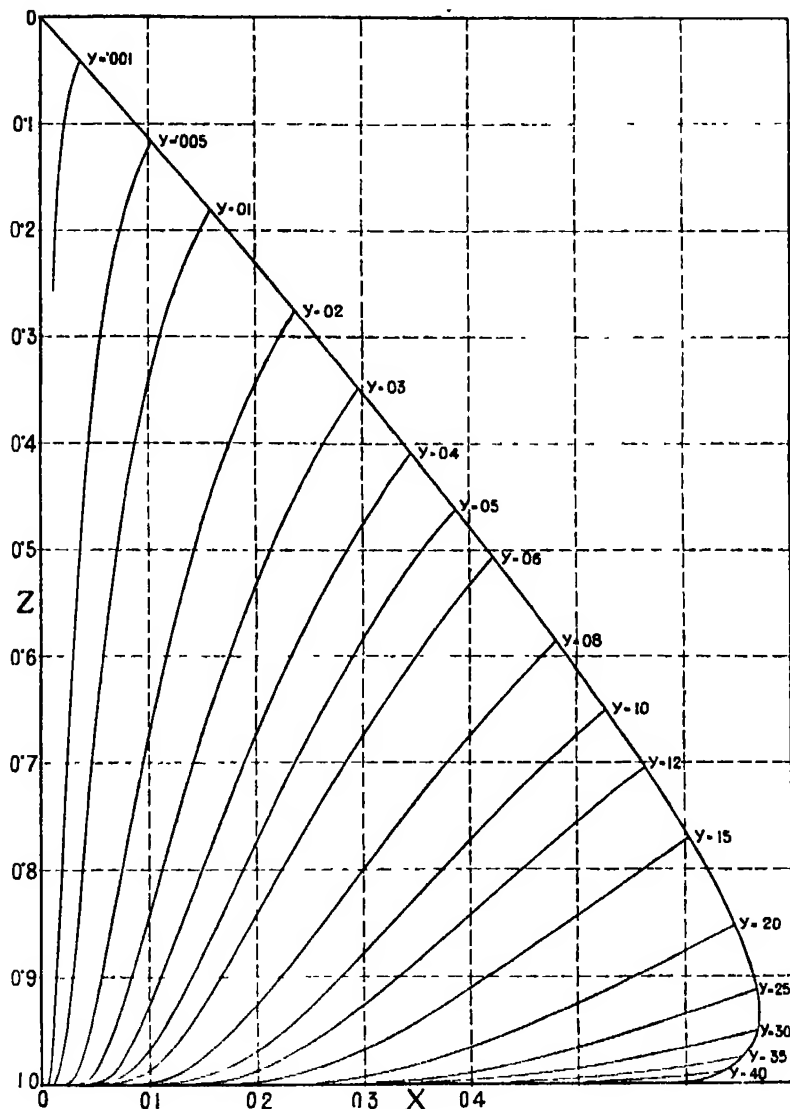


FIG. 8.

curves for x/z and p/p_3 . In the particular case $\theta_s = 30^\circ$, $u_s/c = 0.35$ which is shown in fig. 5 the intersection occurs at $\theta = 63.3^\circ$, and this value is entered as θ_w in Table II.

The same process was repeated for each of the other initial conditions, and the results set forth in Table II.

Graphical Representation of Solutions.—To gain a clearer understanding of the manner in which the various physical quantities occurring in the solution depend on the speed and vertical angle of the cones, the values of x , y and z have been plotted as functions of u_s/c for each of the cones. The resulting curves are shown in figs. 9, 10 and 11.

In the limiting case of a cone of very small vertical angle, *i.e.*, when $\theta_s \rightarrow 0$ the disturbance is very small so that $U = u_s$, $x = y$, $c = c_1$ and $z = 1$. The relation (10A) thus becomes

$$y : \left[1 - \left(\frac{u_s}{c} \right)^2 \right]^{\frac{1}{\gamma-1}} \quad (16)$$

The limiting curves for $\theta_s = 0$ are plotted in figs. 9 and 10 by means of equation (16).

§ 5. Reduction of Results to Familiar Forms.

It remains to reduce the results summarised in Table II to a form convenient for comparison with observation. The velocity of the undisturbed stream (corresponding with the speed of a bullet when considered relative to still air) is found by inserting the value of y given in Table II in equation (10B). The values of U/a so found are also given in Table II.

The pressure at any point is derivable from the values for p/p_3 given by (9). In this form, however, it is not available for comparison with experimental results which are usually given in the form $\frac{p-p_1}{\rho_1 U^2}$. This is connected with p/p_3 by means of the formula

$$\frac{p-p_1}{\rho_1 U^2} = \left(\frac{pz}{p_3 y} - 1 \right) \cdot \frac{a^2}{\gamma U^2}. \quad (17)$$

The physical quantity which can most easily be measured is p , the pressure at the surface of the cone. The calculated values of $\frac{p-p_1}{\rho_1 U^2}$ are given in Table II and are shown as functions of U/a in fig. 12.

Another physical quantity that can be measured is θ_w . This is the angle which the shock wave makes with the axis of a pointed bullet at its point. It can be measured in a bullet photograph which shows the wave of compression. θ_w has, therefore, been plotted in fig. 13 as a function of U/a for each of the three cones.

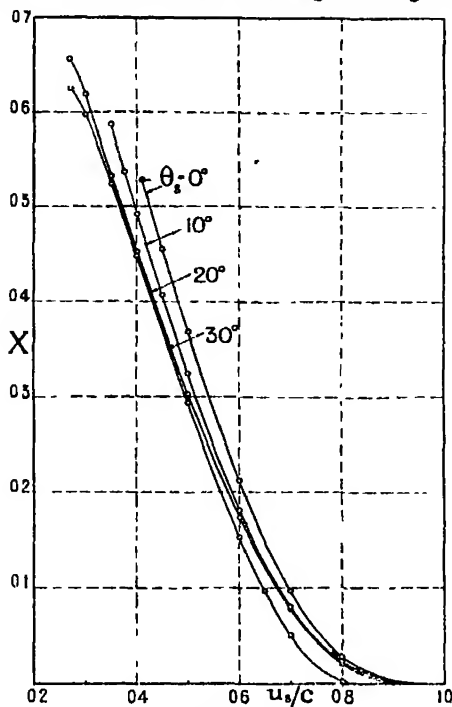


FIG 9.

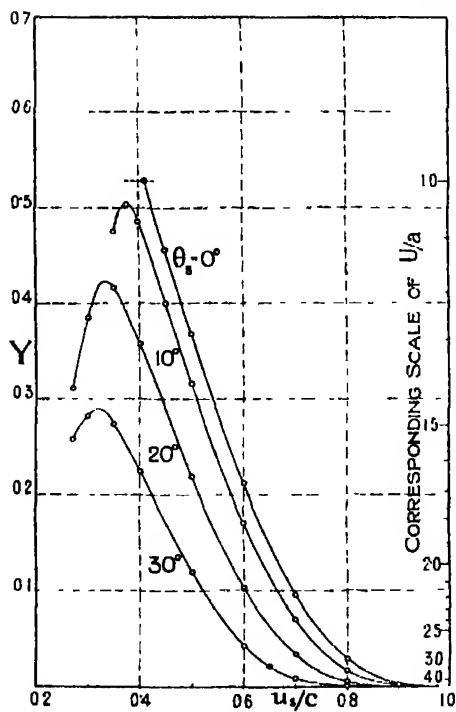


FIG 10.

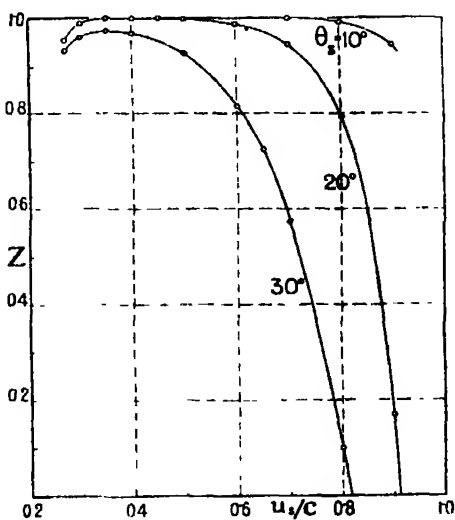
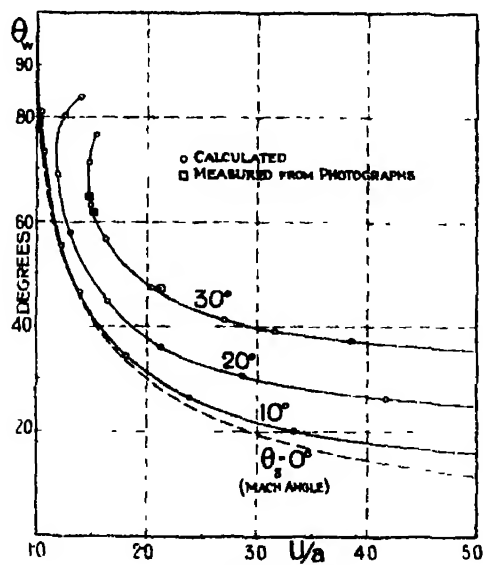
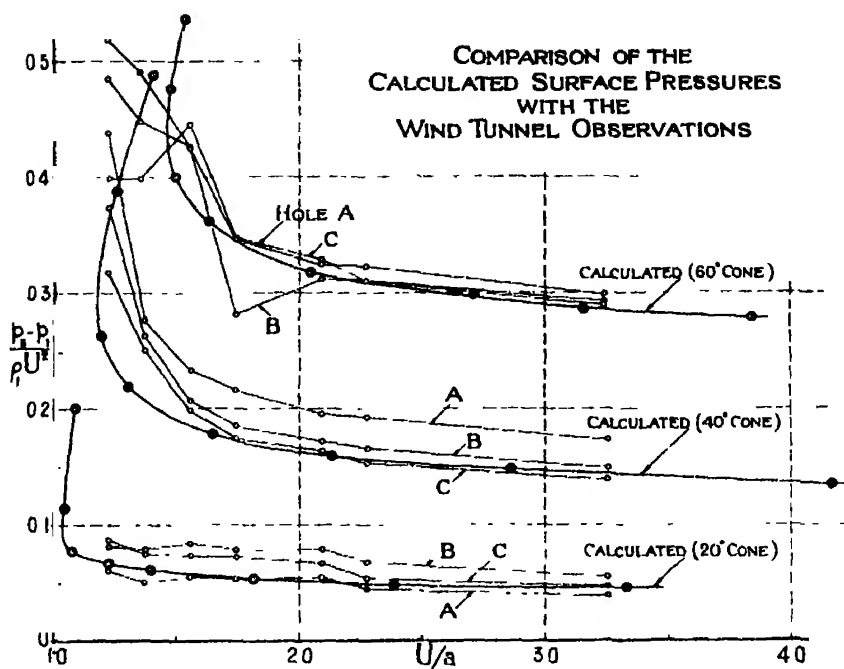


FIG. 11.



The limiting value of θ_w when $\theta_s \rightarrow 0$ is evidently the Mach angle $\sin^{-1} a/U$, so that the equation to the limiting curve for $\theta_s = 0$ is $U/a = \operatorname{cosec} \theta_w$. This is plotted as a broken line in fig. 13.

A point which seems worth noticing in connection with these solutions is that in some of them the speed of flow behind the shock wave is everywhere lower than the local speed of sound. In some it is everywhere higher. In the remaining cases the speed of flow is greater than that of sound immediately behind the shock wave, but it decreases till at the surface of the cone it is less than that of sound. In these cases the speed of flow is equal to the local speed of sound at some value θ_a which is intermediate between θ_w and θ_s . The various cases are distinguished in Table II and the values of θ_a are given when this symbol has a physical meaning.

The ratio of the speed to the local speed of sound is a function of p/p_s only. If q represents the speed while a^* is the local speed of sound at a point where the velocity is q

$$1 + \left(\frac{p_s}{p} \right)^{\frac{\gamma-1}{\gamma}} = 1 \quad (18)$$

so that $q = a^*$ when $\left(\frac{p_s}{p} \right)^{\frac{\gamma-1}{\gamma}} = \frac{\gamma+1}{2}$. Under these conditions

$$\frac{q}{a} = \sqrt{\frac{\gamma-1}{\gamma+1}} = 0.41. \quad (19)$$

Since the minimum velocity occurs at the surface of the solid cone this implies that if $u_s/c > 0.41$ the speed is everywhere greater than that of sound. In the case of the 60° cone (it can be seen in fig. 10) $u_s/c = 0.41$ corresponds with $U/a = 1.66$.

When the speed of flow exceeds the local speed of sound stationary wavelets can exist at angle $M = \sin^{-1} (a^*/q)$ to the stream lines. This angle which might be called the "Local Mach angle" has been calculated in some cases for which the streamlines have been drawn, and the actual forms which stationary wavelets would assume have been drawn as dotted lines in fig. 14. In the case of the 60° cone it is only when $U/a > 1.66$ that the region for which $q > a^*$ extends to the surface, so that it is only when $U/a > 1.66$ that stationary wavelets are likely to be produced by irregularities on the surface of the solid cone.

Streamlines.—To trace the streamlines the angle $\phi = \tan^{-1} v/u$ is found for each value of θ and the direction of the element of streamline between θ and

$\theta + \delta\theta$ is traced. Beginning at some point on the shock wave the streamline is traced till it becomes so nearly parallel to the cone that it runs out of the portion of the field under consideration. Streamlines traced in this way are shown in fig. 14.

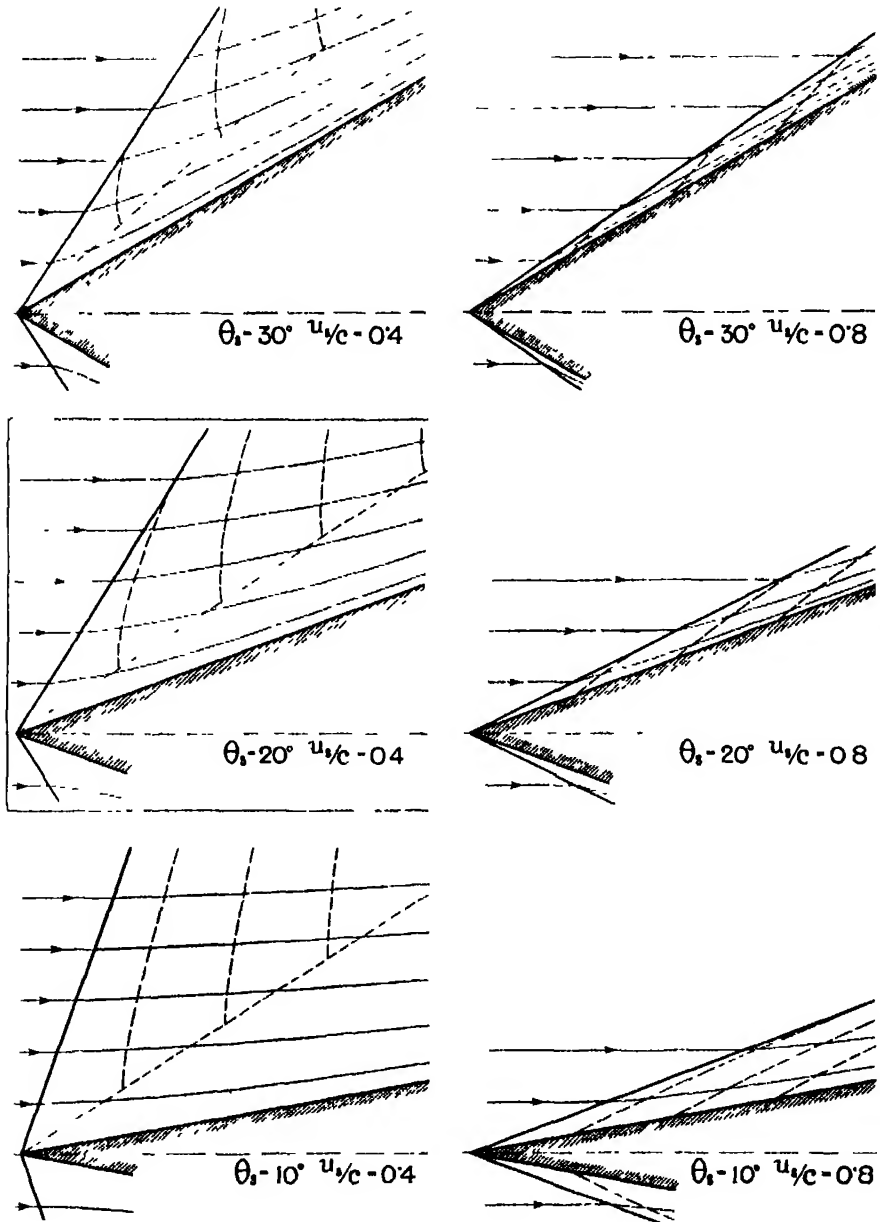


FIG. 14.

§ 6. *Limitations to the Application of the Solutions.*

The curves of fig. 12 which give the variations of $\frac{p_2 - p_1}{\rho_1 U^2}$ with U/a reveal a remarkable limitation to the applicability of the conical solution. As U/a decreases from large values, $\frac{p_2 - p_1}{\rho_1 U^2}$ gradually rises till at some critical value, namely, $U/a = 1.46$ for the 60° cone, 1.18 for the 40° cone and 1.035 for the 20° cone, a minimum possible value of U/a is reached. At speeds lower than this critical speed the conical regime cannot exist. If U/a is determined as it is in the case of a projectile with a conical head, moving at a given speed (greater than the critical speed), there are two mathematically possible regimes, one corresponding with the lower part of the curve of fig. 12 and one corresponding with the upper part. It seems unlikely that the second regime corresponding with the higher surface pressure would be realised under experimental conditions in front of a cylindrical body with a simple conical head.

The nature of regimes which could exist near the conical nose of a projectile moving at less than the critical speed into still air is discussed later in connection with photographs of bullets.

The Air Pressure on a Cone Moving at High Speeds.—II.

By G. I. TAYLOR, F.R.S., Yarrow Research Professor, and J. W. MACCOLL,
B.Sc., Ph.D.

[PLATES 3 and 4.]

§ 1 *Comparison with Experimental Results*

Though the calculations are concerned only with the flow in the neighbourhood of an infinite cone, it was thought that the flow near a finite cone or near the nose of a bullet with a conical head might be comparable with the calculations.

Accordingly, measurements of two kinds were undertaken. The surface pressures on cones were measured at the National Physical Laboratory, and photographs of a bullet with a 60° conical head were taken at various speeds by the Research Department at Woolwich.

Pressure Measurements.—These measurements were made at the National Physical Laboratory in the 3-inch high-speed wind tunnel designed by the late Sir Thomas Stanton.* The dimensions of the models and the position of the pressure holes are given in Table I with its explanatory sketch, fig. 1

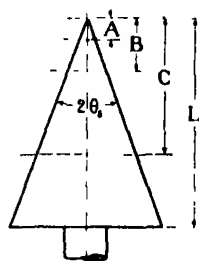


FIG. 1.

Table I —Dimensions of Cones in Wind Tunnel Experiments.

	Axial distance from vertex to pressure hole (in inches)			Total axial length of cone (in inches)
	A	B	C	
20° cone	0.078	0.185	0.508	0.74
40° cone	0.027	0.125	0.331	0.503
60° cone	0.039	0.076	0.188	0.304

* For description of the tunnel see 'Proc. Roy. Soc.,' A, vol. 131, p. 122 (1931).

In each case the pressure was measured at three distances from the vertex. Since the cones were small it was thought desirable to make the pressure holes as small as possible. Accordingly, to quote the N P.L. report:—

“ Nine cones were made of brass each being made in two parts, with a surface of separation at the section at which the pressure was required. before assembling, small scratches were made on the surfaces of separation and these scratches formed the pressure apertures. These apertures were triangular in shape and on measurement the largest dimension was found to be 0.0047-inch. The cone surfaces were finished smooth after assembling and on examination in a projection apparatus with a magnification of 50 diameters, no discontinuity of the surface was observed; the vertical angles of the 20° and 40° cones were correct, but all three of the 60° cones were one-third of a degree large.

“ After the completion of the first series of tests, the results of which appeared to be erratic, it was thought possible that microscopic irregularities in the conical surface, at the surface of separation, might account for the results, and it was suggested that a single piece cone with round pressure holes, even though these might be of greater magnitude than those formed by the scratches, might give more reliable results

“ An additional 60° cone, with three pressure holes of the smallest practicable diameter (0.012 to 0.014-inch) was, therefore, made and tested.

“ *Description of the Tests* — A suitable nozzle to give the required speed was fitted and a measurement was made of the pitot tube pressure and the static pressure, at the position to be occupied by the cone, for a known value of the pressure at the nozzle inlet. The cones were then each placed in the tunnel in turn and a measurement of pressure on the surface was made at the same inlet pressure. In all cases the pressures were measured by mercury columns balanced against the existing atmospheric pressure and the absolute pressure on the cone surface was deduced on the assumption that the static pressure in the tunnel during the test is the same as that measured when the tunnel was unobstructed.

“ The value of the ratio of the air velocity, U , to the local velocity of sound, a , was calculated from the initial measurements of pitot and static pressures, using Rayleigh's formula

“ Two series of tests were carried out with the original nine cones and tests at three air speeds were made with the single-piece drilled cone and the results of these tests, expressed as coefficients of $(p_s - p_1)/\rho_1 U^2$ given in Table II ”

It will be seen from Table II that there appears to be some variation between readings which should be nearly identical, particularly in the case of the 60° cone at speeds less than $1.8a$, but these variations are not sufficiently great to mask the general character of the results.

According to the theory of the conical regime the pressure at the surface of the cone is uniform. The observed distribution of pressure along the surface is shown in fig. 2, where it will be seen that it is nearly, though not quite, uniform.

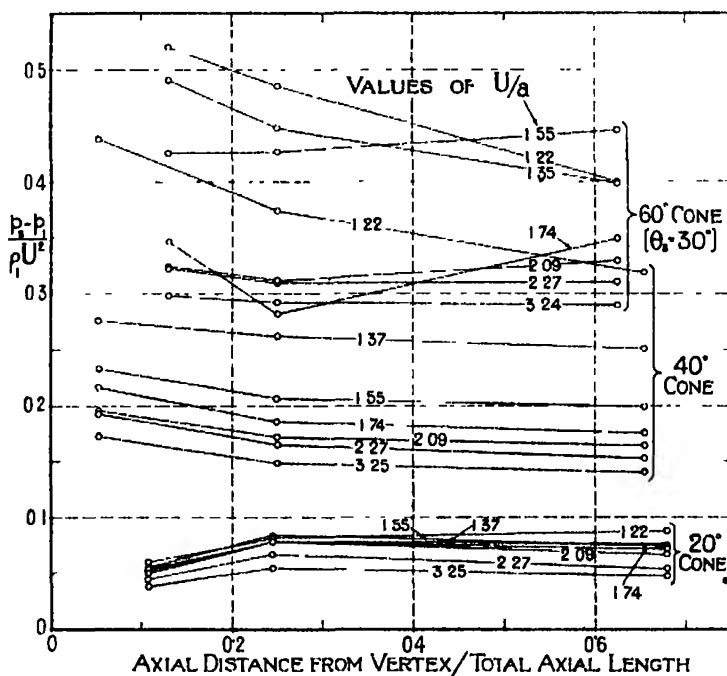


FIG. 2.

The comparison between the calculated and observed pressures at various speeds is shown in fig. 12, Part I. It will be seen that in the case of the 20° and 40° cones the agreement is good, and in the case of the 60° cone it is good over the whole range in which calculation predicts the existence of the conical regime. In the cases of the 40° and 60° cones $(p_s - p_1)/\rho_1 U^2$ rises rapidly with decreasing U/a as the critical velocities $1.18a$ and $1.46a$ are approached. It is only in the case of the 60° cone that measurements were made at speeds less than the critical speed, and it will be noticed that in these cases, i.e., at speeds $U = 1.22a$ and $1.35a$ there is a considerable decrease in pressure with increasing distance from the vertex. At all the speeds except

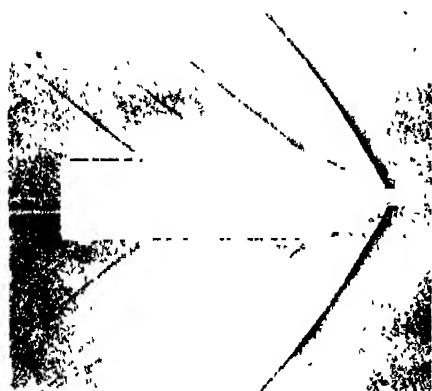


$V/Ua = 2.11$



$V/Ua = 2.11$

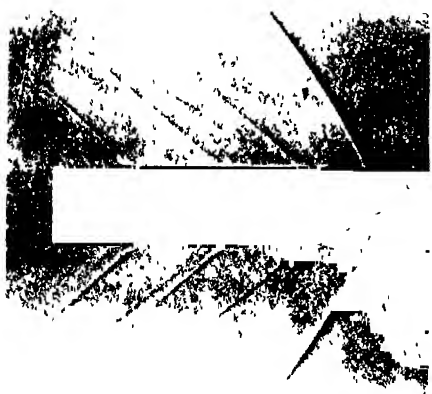
FIG. 5



B. U — 1.52a



C. U — 1.46a



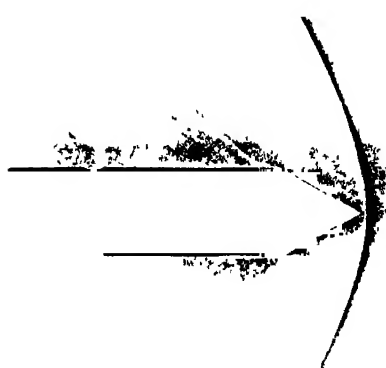
D. U — 1.44a



E. U — 1.42a



F. U — 1.35a



G. U — 1.26a

FIG. 6.

Table II.—Pressure Measurements expressed as Values of the Coefficient $(p_1 - p_2)/\rho_1 U^2$.

Vertical angle of cone = 60°.				Vertical angle of cone = 40°				Vertical angle of cone = 20°						
Value of U/a		Hole.			Value of U/a.		Hole			Value of U/a.		Hole.		
		A.	B.	C.			A.	B.	C.			A.	B.	C.
1.22	0.519	0.485	0.399	0.318	1.22	0.438	0.374	0.318	1.22	0.060	0.081	0.087		
1.37	0.496	0.460	0.410	0.250	1.37	0.276	0.262	0.250	1.37	0.050	0.078	0.074		
1.32*	0.484	0.434	0.385											
Mean 1.35	0.490	0.447	0.398											
1.56	0.394	0.376	0.423	0.180	1.56	0.223	0.200	0.180	1.56	0.045	0.087	0.076		
1.35	0.456	0.476	0.464	0.216	1.55	0.243	0.211	0.216	1.55	0.048	0.080	0.071		
Mean 1.55	0.425	0.426	0.445	0.198	Mean 1.55	0.233	0.206	0.198	Mean 1.55	0.055	0.083	0.073		
1.78	0.324	0.258	0.346	0.168	1.78	0.212	0.180	0.168	1.78	0.057	0.086	0.079		
1.70	0.367	0.303	0.331	0.180	1.70	0.219	0.190	0.180	1.70	0.050	0.070	0.063		
Mean 1.74	0.346	0.281	0.348	0.174	Mean 1.74	0.216	0.185	0.174	Mean 1.74	0.063	0.078	0.071		
2.09	0.321	0.293	0.318	0.154	2.09	0.202	0.175	0.154	2.09	0.055	0.076	0.063		
2.09	0.326	0.329	0.338	0.172	2.09	0.188	0.167	0.172	2.09	0.053	0.080	0.069		
Mean 2.09	0.324	0.311	0.328	0.163	Mean 2.09	0.195	0.171	0.163	Mean 2.09	0.064	0.078	0.066		
2.31	0.330	0.318	0.313	0.148	2.31	0.197	0.172	0.148	2.31	0.047	0.072	0.060		
2.24	0.315	0.303	0.306	0.155	2.24	0.186	0.159	0.155	2.24	0.041	0.062	0.047		
2.27*	0.321	0.306	0.309	0.132	2.27	0.186	0.159	0.132	2.27	0.044	0.067	0.053		
Mean 2.27	0.322	0.309	0.309		Mean 2.27	0.192	0.165		Mean 2.27					
3.24	0.266	0.302	0.282	0.141	3.24	0.176	0.162	0.141	3.24	0.038	0.055	0.049		
3.27	0.283	0.281	0.275	0.137	3.27	0.169	0.145	0.137	3.27	0.038	0.053	0.043		
3.22*	0.316	0.293	0.310	0.139	3.22	0.172	0.148	0.139	3.22	0.038	0.054	0.046		
Mean 3.24	0.298	0.292	0.289		Mean 3.25				Mean 3.25					

* Tests with single piece cone.

$U = 1.74a$ there seems to be no considerable systematic variation in pressure along the cone. Thus, the pressure measurements suggest that a regime approximating to the conical one is, in fact, set up at speeds higher than the critical speed $1.46a$. At $U = 1.74a$ the pressure at hole B falls considerably below that calculated, though the pressures at holes A and C are very near to the calculated value. In this connection it is worth noticing that $U = 1.74a$ happens to be very close to $1.66a$, for which the velocity at the surface of the cone is equal to the local speed of sound (see p. 295, Part I). Streams flowing with the speed of sound are in a condition where small disturbances can produce large variations in pressure. Small disturbances at the surface of the cone, such as might be produced in the boundary layer might, therefore, be expected to produce large disturbances in pressure when the speed is near $1.66a$. They would produce much smaller disturbances in pressure at higher and at lower speeds. This might well account for the anomaly in pressure at hole B when $U = 1.74a$.

Comparison with Instantaneous Photographs of Bullets in Flight.—The calculations indicate that a conical wave can exist at the nose of a pointed bullet provided that its speed is greater than a certain critical one. For a 60° conical head this critical speed is $1.46a$. At speeds less than this the conical wave cannot exist. When $a < U < 1.46a$, a wave of compression must be formed but it cannot, according to our calculations, be in contact with the point of the bullet. It must, therefore, have detached itself from the point and travel ahead of it. At the request, therefore, of the Ordnance Committee, the Research Department of Woolwich Arsenal was asked to take shadow-graphs of the shock waves produced by bullets with 60° conical heads at various speeds with a view to finding at what speed, if any, the shock wave leaves the point. A few preliminary photographs showed them, as they had expected, that at speeds only slightly higher than that of sound, the shock wave is detached from the bullet and at speeds of order $2a$ it is very definitely attached to it. There are, however, effects of refraction in the compressed air near the nose* which make it difficult to determine directly the exact position or shape of the nose from the photographs. The greatest distortion unfortunately always occurs at the nose.

On the other hand, the exact position of the shock wave is shown in the photographs, for rays of light which pass just in front of the wave are undeviated while those which just intersect or almost touch it are greatly deviated.

* These effects have been described by Quayle, 'Scientific Papers Bureau of Standards No. 508.

The sharply defined forward edge of the shadow of the shock wave therefore marks its true position.

The problem with which the Research Department was confronted was, therefore, to mark on the bullet shadowgraph the true geometrical shadow of the bullet. The method which they adopted to attain this end was the following

The shadowgraph was first enlarged to a suitable size for measurement. Before firing the bullets were measured on a travelling microscope and an enlarged outline was drawn on an old negative which was then "fixed." The scale of this outline was the same as that of the enlarged shadowgraph. To place the outline in its correct position on the shadowgraph, use was made of features on the bullet which were situated in regions where less refraction occurs than at the nose. The bullet had two shallow grooves, one between the main parallel portion and the conical head and the other, the "cannelure," about one-quarter of the length of the bullet from its base. It was found possible by means of the shadows of the cannelure and, when clearly defined, the angle where the base of the conical head joins the forward end of the forward groove, to fix the outline in position and thus to determine the position of the true geometrical shadow of the point of the bullet. In this way the relative position of the shock wave and the point of the bullet was found

To illustrate the application of this method the two photographs A and A', fig. 3, Plate 5, have been prepared. A is a slightly enlarged shadowgraph of the bullet and shock wave at speed $U = 2.11a$. A' shows the shadowgraph with the outline placed in position (white line) and with the shadow of the shock wave intensified to show its position more clearly. It will be seen that after this treatment the point of the shadow of the nose just coincides with the point of the forward edge of the shadow of the shock wave. The shock wave was, therefore, in contact with the nose when $U = 2.11a$.

Seven shadowgraphs were taken at speeds ranging from $2.11a$ down to $1.26a$. The data concerning them are given in Table III and six of them together with the superimposed outline of the geometrical shadow of the bullet are shown in fig. 6, Plate 4 (the seventh is that already discussed and shown in fig. 5).

Discussion of Shadowgraphs.—Inspection of these photographs shows that in A, fig. 5, $U = 2.11a$, the shadow of the shock wave is straight for a distance of about $1\frac{1}{2}$ diameters of the bullet from the axis. It is in contact with the nose and measurements of its semi-vertical angle made on the original enlarged negatives by the Research Department, Woolwich, gave the value $\theta_w = 47.25^\circ$

(see Table III). No calculations were made for the exact value $U = 2.11a$, but the curves of fig. 13, Part I, are capable of giving an interpolated value correct at any rate to one-fifth of a degree. This is $\theta_w = 46.6^\circ$. The agreement between the position of the shock wave determined by calculation and that observed in the shadowgraph is, therefore, very good, the difference only amounting to 0.65° . The agreement would have been still better if the calculations had been carried out for $\theta_s = 30.3^\circ$ which is the measured semi-vertical angle of the actual bullet used (see Table III).

In B, fig. 6, for which $U = 1.52a$ the shock wave is not truly conical except perhaps very near the nose. The point of the forward edge of the shock wave

Table III.—Details of Firings of Bullets with Conical Heads.

	Semi-vertical angle (deg.)	Atmospheric conditions			U (ft./sec.)	U/a	θ_w (degrees).	
		Dry bulb ($^\circ$ F.)	Wet bulb ($^\circ$ F.)	Barometric pressure (mm.)			Measured.	Calculated.
A	30.3	62	60	751.0	2374	2.11	47.25	46.6
B	30.2	70	66	763.2	1726	1.52	62.0	61.2
C	30.3	70	66	763.2	1659	1.46	64.7	66.0
D	30.4	75	69	757.4	1642	1.44	—	—
E	30.3	62	59.5	751.1	1593	1.42	—	—
F	30.3	62.5	60	749.0	1520	1.35	—	—
G	30.3	62.5	60	749.0	1419	1.26	—	—

coincides with the point of the outline of the bullet, but its shadow now consists of two lines which seem to be slightly curved. The measured value of semi-vertical angle of the shock wave at its point is 62° and that obtained from the curve of fig. 13, Part I, is 61.2° . Again the agreement is very good.

In C, fig. 6, for which $U = 1.46a$ the shock wave is still pointed, its point being coincident with the point of the outline of the bullet, but the curvature in the shock wave is now slightly greater than it was in the case of B. The measured value of the semi-vertical angle of the shock wave at the point is 64.7° while that obtained from the calculated curve of fig. 13 is 66° .

The three observed values of U/a and θ_w corresponding with bullets A, B and C are given in Table III and marked in fig. 13, so that the extremely good agreement between the calculated and measured positions of the shock wave may be appreciated.

In D, fig. 6, $U = 1.44a$, the shock wave passes through the nose of the bullet, but it is no longer pointed. At the point of the projectile it seems to be

sharply curved but continuous, its tangent plane being perpendicular to the axis of the bullet.

In E, $U = 1.42a$, the forward edge of the shadow of the shock wave is definitely forward of the point of the outline of the bullet so that the shock wave has become detached from the bullet and travels before it.

In F, fig. 6, $U = 1.35a$, the inner edge of the shadow of the shock wave is just clear of the outline of the bullet so that the shock wave has gone forward from the nose of the bullet through a distance equal to the thickness of the dark part of the shadowgraph of the shock wave.

In G, fig. 6, $U = 1.26a$, the shock wave has advanced to a still greater distance from the point of the bullet.

To sum up, it appears from these photographs that when $U/a > 1.46$ the shock wave is pointed and attached to the bullet at its point. When $U/a < 1.42$ the shock wave has no point and travels ahead of the bullet.

This result is in agreement with the theoretical result that if $U/a < 1.46$ a solid cone of 60° vertical angle cannot produce a conical shock wave.

The fact that the shock wave is truly conical for some distance from the nose in the case of bullet A while in cases B and C its section is more or less curved is to be expected. As has been pointed out already, it is only when $U/a > 1.66$ that the stream velocity is greater than the local velocity of sound throughout the space between the shock wave and the conical head. Under these circumstances the disturbance due to the change at the shoulder from the conical head to the parallel middle body cannot penetrate into this region so that the shock wave should be truly conical for some distance from the point. Thus a truly conical shock wave with section consisting of two straight lines extending to a finite distance from the nose is only to be expected in the case of bullet A for which $U/a = 2.11$. In cases B and C, which both fall within the range $1.46 < U/a < 1.66$, the speed of flow in part of the region between the shock wave and the conical head is less than the local speed of sound so that disturbances due to the finite size of the head can penetrate into it, causing the section or shadow of the shock wave to be more or less curved.

On the other hand, it seems clear that in the immediate neighbourhood of the point the conical regime must be set up in accordance with the equations, and this is verified in A, B and C by the remarkable agreement between the calculated semi-vertical angle of the shock wave and the observed angle in this region.

It is worth noticing that this line of argument would lead us to expect agreement between the calculated and observed pressure at all three pressure holes

A, B and C in the models tested at the National Physical Laboratory provided $U/a > 1.66$, but when $1.46 < U/a < 1.66$ the pressure might be expected to vary along the cone only attaining the calculated value close to the point. The only pressure measurements made at a speed within the range $1.46 < U/a < 1.66$ for the 60° cone were those at $U = 1.55a$.

The pressure coefficient at $U/a = 1.55$ is $\frac{p_2 - p_1}{\rho_1 U^2} = 0.378$. The measured pressures at hole A were (see Table II) 0.394 at $U/a = 1.56$, and 0.456 at $U/a = 1.55$, so that the difference between two measurements which should be practically identical is more than twice as great as the difference between the calculated value and the lower of the two observed values. The matter cannot, therefore, be tested by these measurements.

§ 2. Comparison between the Critical Speeds of Cone and Wedge.

The critical speeds at which the shock wave leaves the edge of a wedge can be found directly from the curves of fig. 7, Part I. For a wedge of angle $2(\beta - \alpha)$ moving along the bisector of its faces all possible values of y and the corresponding values of α are given by the intersections of the line $\beta - \alpha = \text{const}$ with the successive contours of y . Since U/a is the single-valued function of y given by equation (10B) all the points on the diagram of fig. 7 which correspond with the critical condition of minimum velocity for a given wedge or wedge of maximum angle for a given speed lie on the line which passes through the maximum values of $\beta - \alpha$ on each y contour. This line is shown dotted in fig. 7 and the corresponding values of $\beta - \alpha$, y and U/a are given in Table IV.

Table IV

y .	0	0.0005	0.006	0.02	0.05	0.10	0.15
θ , or $\beta - \alpha$ U/a	45.4 ∞	42.5 6.26	38.8 4.08	35.3 3.21	30.8 2.60	25.4 2.16	21.0 1.90
y .	0.20	0.25	0.30	0.35	0.40	0.45	0.50
θ or $\beta - \alpha$ U/a	17.1 1.71	13.6 1.56	10.3 1.43	7.2 1.32	4.5 1.22	2.2 1.13	0.4 1.045

These values are plotted in fig. 3 which shows the relationship between U/a and θ_s or $\beta - \alpha$ for a wedge. The corresponding points for a cone, namely $(\theta_s = 10^\circ, U/a = 1.035)$, $(\theta_s = 20^\circ, U/a = 1.18)$, $(\theta_s = 30^\circ, U/a = 1.46)$, are also marked in fig. 3 and joined by a curve

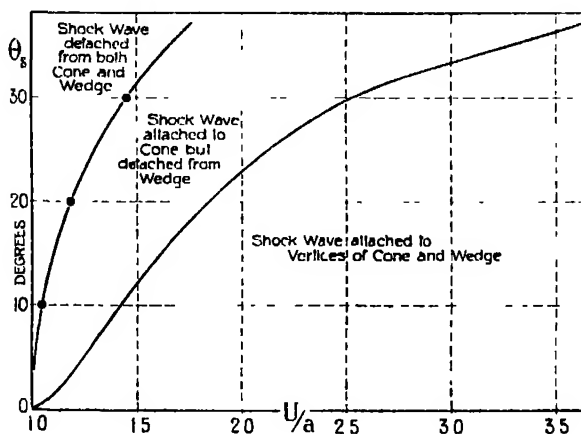


FIG. 3.

It will be seen that as the speed is reduced from high values the shock wave leaves the edge and travels ahead of a wedge long before it leaves the point of a cone having the same vertex angle

§3 Comparison with Approximate Theory of v Karman and Moore.

In a recent paper v Karman and Moore (*loc. cit.*, Part I) have given an approximate theory of the disturbances produced by a thin spindle-shaped body moving at speeds greater than that of sound. As an example of their general method they give the approximate solution for a cone of small angle. The motion which their solution presupposes is an irrotational one without shock waves. It is evident from the foregoing work that a shock wave necessarily exists in all cases where the conical regime exists, for our method would find solutions without shock waves if they could exist (In that case we would merely find that at the Mach cone $x = y$ and $z = 1$ would satisfy the required conditions)

When the angle of the cone is small it may occur that the change in pressure at the shock wave is small compared with the change in pressure between the shock wave and the solid surface. Denoting the ratio

$$\frac{\text{Pressure change in shock wave}}{\text{Total pressure change from undisturbed air to solid surface}} = \frac{p_3 - p_1}{p_2 - p_1}$$

by F, v. Karman and Moore's approximation might be expected to be valid if F is small compared with 1.0. The true value of F may be calculated in any given case from the figures given in Table II thus

$$\frac{p_2 - p_1}{p_1} = \frac{x}{y} - 1, \quad \frac{p_2 - p_1}{p_1} = \left(\frac{p_2 - p_1}{\rho_1 U^2} \right) \left(\gamma \frac{U^2}{a^2} \right)$$

and the values of each factor in F are given in the table. In the case $\theta_s = 10^\circ$ the values of F are given for various values of U/a in the following table.

Table V $-\theta_s = 10^\circ$.

U/a	1.09	1.04	1.07	1.22	1.39	1.81	2.39	3.33	5.46
F	0.69	0.37	0.12	0.13	0.17	0.26	0.38	0.58	0.84

It will be seen that from $U/a = 1.07$ to 1.39 , F is less than one-sixth, so that only one-sixth of the total change in pressure occurs in the shock wave, the remaining five-sixths occurring in the region of irrotational flow behind it. Outside this limited region F rapidly increases, so that at $U = 1.81a$ one-quarter of the total pressure change occurs in the shock wave. So far as the *distribution* of pressure is concerned, v. Karman's approximation can therefore only be said to give a good representation in a limited range extending approximately from $U/a = 1.07$ to 1.39 .

A similar conclusion might have been reached in a qualitative manner by inspection of fig. 13 or Table II, Part I. In that table it will be seen that the wave angle θ_w is within 1° of the Mach angle M over the range $U/a = 1.07$ to $U/a = 1.81$. At speeds greater than $1.81a$ the difference between them is greater than 1° . The difference between θ_w and M may be regarded as a rough measure of the intensity of the shock wave, so that in the case of the 20° cone the shock wave is weak in the range $U/a = 1.07$ to 1.81 .

In the case of the 40° cone θ_w does not differ from M by less than 7.0° in any part of the range, while in the case of the 60° cone the least value of this difference is 18.1° . Thus we may anticipate that the shock wave produced by the 40° cone is of considerable intensity at all speeds, and that that produced by the 60° cone is still more intense.

Though v. Karman and Moore's theory involves no sudden change in velocity or pressure at a shock wave, yet it does involve infinite values of the rates of change of these quantities at the cone whose semi-vertical angle is the Mach angle. The approximate solution might therefore still be a good approximation

even in cases like that of the 20° cone at $U/a = 1.81$ when the increase in pressure at the shock wave is a considerable fraction of the total pressure increase at the surface of the solid cone. A proper basis for comparison is to be found in the pressure at the surface. v. Karman and Moore give an expression for the pressure at any point in equation (27) of their paper. Transferring this formula into the notation adopted in the present investigation and applying it to give p_s we find

$$\frac{p_s - p_1}{\rho_1 U^2} = \frac{1}{2} \left(1 - \frac{u_s^2}{U^2} \right) \left\{ 1 + \frac{U^2}{4a^2} \left(1 - \frac{u_s^2}{U^2} \right) \right\}$$

where

$$\frac{1}{U} = \frac{\sec \theta_s \sqrt{\cot^2 \theta_s - \cot^2 M}}{\sqrt{\cot^2 \theta_s - \cot^2 M} + \tan \theta_s \cosh^{-1} (\cot \theta / \cot M)}$$

and

$$\sin M = a/U.$$

Using these formulæ $(p_s - p_1)/\rho_1 U^2$ was calculated for $\theta_s = 10^\circ, 20^\circ$ and 30° . These approximate values are shown as broken line curves in fig. 4 and the corresponding values obtained by our complete solution are also shown for

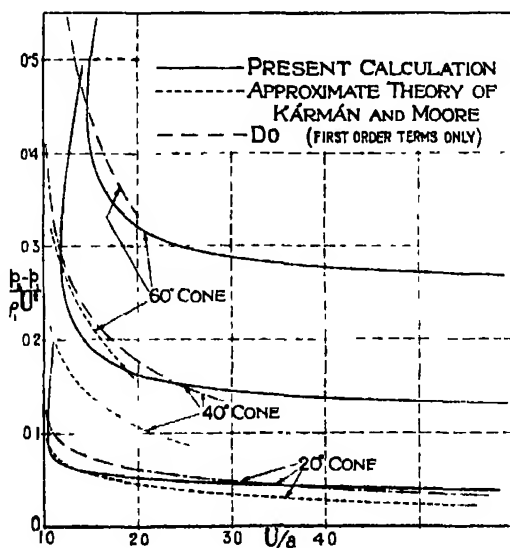


FIG. 4

comparison. It will be seen that in the case of the 20° cone ($\theta_s = 10^\circ$) the approximate solution agrees very well with the complete solution over the range $U = 1.05a$ to $U = 2.5a$. In the case of the 40° cone the approximation is rather badly wrong, the least error being about 25 per cent. In the case

of the 60° cone the approximate values are still further from the true values.

§ 4. We are indebted to the Ordnance Committee for arranging for the photographic and wind channel investigations undertaken to test the theory and for assistance in computation. Our thanks are due in particular to Dr. A. D. Crow and Mr. T. Harris, of the Research Department, Woolwich, for carrying out the photographic work, and to Dr. H. J. Gough and Mr. A. Bailey, of the National Physical Laboratory, for carrying out the wind channel work. We are also indebted to Mr. W. Stott for computing the functions from which figs. 6, 7 and 8, Part I, were prepared.

[*Note added December 18, 1932.*—Since writing this paper we have sent the diagram of fig. 4 to Professor v. Karman, who then reconsidered his theory in the light of the present calculations. He finds that his method of working out the second order terms is not quite logical, some of them having been neglected while others were retained. If only the first order terms are retained the agreement between our results and his is much improved. He has kindly calculated for us the first approximation to the values of $(p_2 - p_1)/\rho_1 U^2$ for our three cones and his results are shown by a third set of curves in fig. 4. The fact that the retention of some but not all, of the second order terms makes such a large difference to the results (as may be seen in fig. 4) shows that v. Karman and Moore's first order approximation cannot be regarded as mathematically justifiable outside the range where the first and second order approximations nearly coincide. This corresponds with the range where F (see Table V) is small compared with 1.0. On the other hand the excellent agreement between the first order approximation and the complete calculation over a large range for our three cones may perhaps justify its practical use for bodies which are not cones.]

Summary

A method is developed for calculating the air flow and pressure in the neighbourhood of a projectile with a conical head. The calculations are carried out for cones of vertical angle 20° , 40° and 60° . It is shown that the shock wave is attached to the point of the projectile provided its velocity is greater than $1.035a$ in the case of the 20° cone, $1.18a$ for the 40° cone and $1.46a$ for the 60° cone; a is the speed of sound. At lower speeds the shock wave is detached from the point and travels ahead of it. This conclusion is verified accurately in the case of the 60° cone by means of photographs of bullets in flight.

The calculated pressures on the head of the projectile are compared with those measured in a high speed wind tunnel and good agreement is found

The complete solution here developed is compared with v. Karman and Moore's approximate theory and good agreement is found in the case of the 20° cone over a limited range of speeds. The approximate theory does not apply to the cones of wider angle

A Theoretical Investigation of the Oxygen Atom in various States of Ionisation.

By D R HARTREE, F R S, and Miss M M BLACK

(Received October 7, 1932)

§ 1 *Introduction.*

An approximate description of a many-electron atom can be given by considering each electron to be in a stationary state in a suitable central field, and a method of calculating the wave functions of the different electrons, based on this description, has been developed by one of us† Further, in developing the theory of complex spectra Slater‡ has shown how to calculate approximate energies from such a set of one-electron wave functions in many cases, including a number in which more than one electron is in an incomplete group, so that a given distribution of electrons among the different groups gives rise to a number of different stationary states

The object of the work described in this paper is firstly the calculation of one-electron wave functions for the normal electron arrangements of O^{++} , O^{+} and neutral O ; secondly the use of Slater's results (slightly extended) and method for the calculation of the total energies of the various stationary states arising from the normal electron arrangements, and hence of the ionisation energies of those states, and thirdly the comparison with observation both of the absolute values of the ionisation energies so calculated (which correspond directly with the energies derived from the spectrum terms), and of the energy differences between the different terms arising from each electron arrangement (inter-multiplet separations).

† Hartree, 'Proc. Camb. Phil. Soc.', vol. 24, pp. 89, 111 (1928).

‡ Slater, 'Phys. Rev.', vol. 34, p. 1203 (1929) This paper will be referred to as Slater I.

The oxygen atom was chosen as the one for which to make calculations, as its spectra in several states of ionisation have been analysed in considerable detail, and reliable absolute values of the terms are available; it is a light atom so that spin and relativity effects are small; also the normal electron arrangements of O^{+1} , O^+ , and neutral O all give more than one stationary state, so that there are three ions for which to compare, with observation, the calculation of intermultiplet separations given by Slater's theory.

The present account is restricted to the normal electron arrangements only. Calculations for one electron in an excited state are in progress.

When this work was started, very few purely theoretical quantitative calculations of energies of many-electron atoms, or of inter-multiplet separations, had been made, and not many have appeared in the meantime.

The energy of the normal state of neutral He has been calculated by Gaunt† by a method which is essentially a simple case of that used here, and by Hylleraas,‡ using a much better type of approximation which, however, is perhaps hardly feasible for more complicated atoms. The latter has made precision calculations of the energies of the normal states of helium and helium-like ions, and of some excited states of helium, with notable success in obtaining agreement with the observed ionisation energy of neutral helium. Calculations of the normal states of atoms and ions in the first row of the periodic table have been made for Li by Guillemin and Zener,§ and for the other atoms by Zener,|| using an approximation of a different type from that used here, one which is in some aspects better and in others cruder (see further discussion § 8). Also McDougall¶ has used methods similar to those of this paper to calculate the optical terms of Si^{+3} ; the stationary states there calculated are essentially states of a series electron outside a core consisting of closed shells; the perturbation of the core by the series electron is then small and was neglected, so that the states of Si^{+3} were taken as an Si^{+4} structure with an additional wave function for the series electron, this resulted in important simplification of the work. The same simplification cannot be made in the present work; when, for example, a ($2p$) electron is removed from the normal O^+ ion to give a normal O^{++} ion, the wave functions of the ($2s$) and remaining ($2p$) electrons change quite appreciably, and the O^+ ion cannot be thought of as unperturbed O^{++} structure

† 'Proc. Camb. Soc.,' vol. 24, p. 332 (1928).

‡ Hylleraas, 'Z. Physik,' vol. 54, p. 347 (1929), vol. 65, p. 209 (1930), vol. 66, p. 453 (1930); Hylleraas and Undheim, 'Z. Physik,' vol. 65, p. 759 (1930).

§ 'Z. Physik,' vol. 61, p. 199 (1930).

|| Phys. Rev., vol. 36, p. 51 (1930).

¶ 'Proc. Roy. Soc.,' A, vol. 138, p. 550 (1932).

with an additional ($2p$) wave function. The result is that some terms in the energy formula which cancel in the approximation used by McDougall for Si^{+3} do not cancel here, and this makes the present calculations considerably more elaborate.

Of purely theoretical quantitative calculations of separations between different states arising from a given arrangement of electrons in incomplete groups there have been even fewer. The only ones of which we are aware are those of the singlet-triplet separations in helium by Heisenberg† for the nearly hydrogen-like terms, and Hylleraus (*loc cit*) for the S terms, and the inter-multiplet separations of the normal state of O^{+4} by Stevenson,‡ who used some preliminary numerical results obtained in the course of the present work. Stevenson works with Gaunt's extension of Dirac's wave equation, and is able to calculate spin separations within a single multiplet, as well as inter-multiplet separations: spin separations are outside the scope of the present paper.

§ 2. General Theory

It is well known that, for an atomic system whose Hamiltonian operator is H , the function Ψ which makes $\int \Psi^* H \Psi d\tau$ stationary, subject to $\int \Psi^* \Psi d\tau = 1$ ($d\tau$ being an element of the co-ordinate space of the system), are the wave functions of the stationary states of the system, and that the stationary values of $\int \Psi^* H \Psi d\tau$ are the energies of the corresponding states. As a result of the stationary property of $\int \Psi^* H \Psi d\tau$, it follows that a fair approximation to the correct wave function for the atomic system, however obtained, may, on evaluation of this integral, give a good approximation to the corresponding energy.

Now an approximate wave function can be obtained as follows. We think of each electron being in a stationary state; then representing each wave function by a Greek letter $\alpha, \beta, \gamma, \dots$, and the co-ordinates (including a spin co-ordinate) of an electron by a number 1, 2, 3, ..., the individual wave functions can be written $\psi(\alpha|1), \psi(\beta|2), \dots$, and a wave function for the whole atom is

$$\Psi = \psi(\alpha|1) \psi(\beta|2) \psi(\gamma|3) \dots \quad (1)$$

† 'Z. Physik,' vol. 39, p. 499 (1926)

‡ 'Proc. Roy. Soc., A,' vol. 137, p. 298 (1932).

But any permutation of the electrons between the wave functions gives a state of the same energy, and according to the general theory of such degenerate states, the wave function of a single stationary state is a linear combination of wave functions of the type (1) formed by such permutations; and to satisfy Pauli's principle the linear combination must be antisymmetrical in all pairs of electrons. that is to say, it must be determinant

$$\begin{aligned} \Psi = & \begin{vmatrix} \psi(\alpha|1) & \psi(\beta|1) & \psi(\gamma|1) \\ \psi(\alpha|2) & \psi(\beta|2) & \psi(\gamma|2) \\ \psi(\alpha|3) & \psi(\beta|3) & \psi(\gamma|3) \end{vmatrix} \end{aligned} \quad (2)$$

For an atomic (as distinct from molecular) system it is probably a good approximation to take, as is usually done, each one-electron wave function ψ to have the form of a wave function of an electron in a central field, that is

$$\psi(\alpha|j) = \frac{1}{r} P(n_a, l_a|r_j) S(l_a, m_a|\theta_j, \phi_j) \chi(s_a|s_j), \quad (3)$$

where $r_j, \theta_j, \phi_j, s_j$ are the spherical polar and spin co-ordinates of electron j , and n_a, l_a, m_a, s_a are the three spatial and one spin quantum numbers defining the wave function α , P is a function of r only,

$$S(l, m|\theta, \phi) = P_l^m(\cos \theta) e^{im\phi},$$

and χ is the spin wave function. For an atom consisting of complete groups of electrons only, Delbruck† has shown from consideration of spatial symmetry that if the complete wave function is of the form (2), the individual wave functions ψ must be of the form (3). In other cases the use of individual wave functions of the form (3) is only an approximation, a better approximation could be found by the variation method, but probably the approximation is trivial compared to that involved in the use of wave function of type (2) at all.

For an atom in which some electrons are in one or more incomplete groups, a further degeneracy arises, since there may be more than one set of wave functions $\alpha, \beta, \gamma, \dots$, giving a state of the same total energy, on account of the degeneracy of wave functions of the type (3) for given n, l and different m, s . This degeneracy, which we will call an m -degeneracy, gives rise to a set of stationary states of different energies whose wave functions are linear combinations of determinants of the type (2), involving the different degenerate sets of one-electron wave functions $\alpha, \beta, \gamma, \dots$. Slater (*loc. cit.*, I) has shown how

† 'Proc. Roy. Soc.' A, vol. 129, p. 686 (1930)

in many cases the energies of the various states of different total angular momentum quantum number L and total spin quantum number S can be written down without actually solving the secular perturbation equation and constructing the appropriate linear combinations of wave functions of the type (2), and we make considerable use of his method and results.

For any given atom or ion, approximate one-electron wave functions of the form (2) can be obtained by the method of the "self-consistent field" developed by one of us,[†] in which a set of functions $P(n, l|r)$ is found such that each wave function of the form (3) is that of an electron in the field of the nucleus and the spherical average of the distribution of charge of the other electrons. This method of obtaining the ψ 's was originally based on physical rather than on analytical arguments, and does not take into account the effects of interchange of electron between the one-electron wave functions, or Pauli's principle. It has been shown by Slater[‡] and Fock[§] that analytically it follows from the use of approximation (1) in the variation formulæ $\delta \int \Psi^* H \Psi d\tau = 0$,

$\delta \int \Psi \Psi^* d\tau = 0$ Slater indicated and Fock independently carried out the extension of the method using approximation (2) for the complete wave function, but the numerical solution of Fock's equations is considerably more difficult than that of the equations of the cruder self-consistent field, and we have been content to use the latter method.

There is no inconsistency in calculating the one-electron wave functions ψ by a method based on approximation (1) for the wave function Ψ of the whole atom, and then using approximation (2) to calculate the energy by evaluation of $\int \Psi^* H \Psi d\tau$. The determinant (2) represents an approximation to the wave function of the complete atom, however the one-electron wave functions ψ are obtained, whether by the solution of Fock's equations, or by the cruder method of the self-consistent field, or by the Ritz method as used by Zener. Those obtained by the method of the self-consistent field form one approximation to the best set of such one-electron wave functions, the solution of Fock's equations would provide a better approximation.

In the solution of the equations of the self-consistent field there occurs an energy parameter ϵ for each radial wave function $P(n, l|r)$: that is, for each

[†] Hartree, *loc. cit*

[‡] 'Phys. Rev.,' vol. 35, p. 210 (1929). This paper will be referred to as Slater II

[§] 'Z. Physik,' vol. 61, p. 126 (1930)

pair of quantum numbers n, l . This is formally the negative energy of an electron with this wave function in the field of the nucleus and the other electrons, treated as a static field, and is not the same as the energy required to remove an electron with this wave function (i.e., the positive energy of an atom lacking such an electron), although empirically there seems to be a very close agreement between the two quantities, at any rate for the deeper-lying X-ray levels. In particular the ionisation energy is not the value of ϵ for a wave function of the outer group, but must be found by the calculation of the total energy of the atom and that of the ion formed by removal of an electron with the wave function concerned, and subtraction of these values.

§ 3. Calculation of Wave Functions and Results.

The radial wave functions for the different electrons groups in the normal electron arrangement of O^{+++} , O^{++} , O^+ and O were calculated by the method of the self-consistent field. In these cases the outer group of electrons is not complete, so does not give a spherically symmetrical contribution to the field and the use of the central field wave equation may be a somewhat rougher approximation than for an atom consisting of complete groups only †

The numerical work was lightened to a considerable extent both in the calculation of radial wave functions and later in the evaluation of the necessary integrals involving them (see §§ 6, 7) by working in terms of *differences between the wave functions*, etc., for different states of ionisation, but to avoid accumulation of errors due to the use of a finite number of significant figures, all such differences were taken from one definite state of ionisation, not as difference between *successive* states

The normalised radial wave functions $P(\alpha|r)$ so calculated given in Table I; the accuracy of the numerical work is such that the fourth decimal place is not to be relied on, but is probably of some significance. The $(1s)$ wave function has only been calculated to this accuracy for O^{+++} and O neutral as the difference is small, and, as shown in § 8, if it is neglected the effect on the ionisation energies is considerably smaller than the probable random error due to the limited accuracy used in the evaluation of the integrals involved in them. The values of the integral $S = \int_{r=0}^{\infty} P(1s|r) P(2s|r) dr$, required for constructing

† The error involved in this approximation is of the same order as that involved in the neglect of interchange effects. See Slater (*loc. cit.*, II).

Table I.—Normalised One-electron Wave Functions for Normal Electron Arrangements of O^{1+} , O^{2+} , O^+ , O.

r	O^{1+}			O^{2+}		O^+		O.		
	1s.	2s.	2p	2s.	2p.	2s	2p.	1s.	2s.	2p.
0 00	0 0000	0 0000	0 0000	0 0000	0 0000	0 0000	0 0000	0 0000	0 0000	0 0000
0 01	0 3981	0 1065	0 0018	0 0907	0 0016	0 0952	0 0014	0 3981	0 0902	0 0013
0 02	0 7355	0 1964	0 0069	0 1839	0 0062	0 1738	0 0055	0 7354	0 1663	0 0050
0 03	1 0175	0 2713	0 0165	0 2541	0 0148	0 2401	0 0133	1 0174	0 2299	0 0118
0 04	1 2556	0 3329	0 0254	0 3619	0 0228	0 2947	0 0205	1 2554	0 2823	0 0182
0 06	1 6100	0 4216	0 0537	0 3950	0 0477	0 3734	0 0420	1 6098	0 3576	0 0381
0 08	1 8340	0 4717	0 0877	0 4421	0 0788	0 4180	0 0708	1 8338	0 4004	0 0630
0 10	1 9625	0 4911	0 1270	0 4607	0 1147	0 4356	0 1031	1 9622	0 4174	0 0917
0 12	2 0175	0 4862	0 1713	0 4564	0 1540	0 4318	0 1402	2 0172	0 4138	0 1233
0 14	2 0165	0 4619	0 2178	0 4341	0 1958	0 4110	0 1762	2 0162	0 3938	0 1568
0 16	1 9763	0 4226	0 2600	0 3977	0 2303	0 3760	0 2154	1 9750	0 3614	0 1917
0 18	1 9078	0 3716	0 3165	0 3505	0 2836	0 3323	0 2554	1 9074	0 3190	0 2273
0 20	1 8203	0 3118	0 3644	0 2950	0 3282	0 2805	0 2957	1 8199	0 2694	0 2632
0 25	1 5580	0 1385	0 4854	0 1341	0 4379	0 1291	0 3949	1 5577	0 1249	0 3521
0 30	1 2826	-0 0488	0 5981	-0 0402	0 5408	0 0349	0 4884	1 2825	-0 0319	0 4350
0 35	1 0286	-0 2330	0 6985	-0 2110	0 6333	-0 1969	0 5731	1 0286	-0 1867	0 5119
0 40	0 8100	-0 4041	0 7844	0 3722	0 7138	-0 3482	0 6474	0 8105	-0 3316	0 5793
0 45	0 6287	-0 5560	0 8558	-0 5852	0 7814	0 4837	0 7107	0 6295	-0 4616	0 6373
0 50	0 4822	-0 6862	0 9149	-0 6366	0 8364	0 6014	0 7631	0 4833	-0 5747	0 6858
0 6	0 2765	-0 8796	0 9828	-0 8254	0 9107	-0 7813	0 8371	0 2778	-0 7488	0 7568
0 7	0 1549	0 9914	1 0063	0 9386	0 9445	-0 8937	0 8764	0 1562	-0 8593	0 7977
0 8	0 0853	1 0369	0 9937	-0 9917	0 9465	0 9508	0 8880	0 0804	-0 9179	0 8152
0 9	0 0461	-1 0326	0 9550	-0 9991	0 9240	-0 9657	0 8789	0 0470	-0 9368	0 8150
1 0	0 0251	-0 9932	0 8980	-0 9737	0 8870	0 9499	0 8552	0 0257	-0 9268	0 8022
1 1	0 0134	-0 9310	0 8326	-0 9262	0 8383	-0 9133	0 8215	0 0138	-0 8967	0 7806
1 2	0 0071	-0 8557	0 7609	0 8649	0 7820	-0 8628	0 7811	0 0074	-0 8535	0 7531
1 4	0 0018	-0 6911	0 6161	-0 7241	0 6648	-0 7422	0 6904	0 0019	-0 7472	0 6880
1 6	0 0004	-0 5346	0 4830	-0 5828	0 5497	0 6100	0 5974	0 0004	-0 6347	0 6187
1 8	0 0001	-0 4007	0 3698	-0 4577	0 4452	-0 4995	0 5090	0 0001	0 5281	0 5507
2 0		0 2932	0 2776	-0 3496	0 3550	-0 3979	0 4287		-0 4334	0 4867
2 2		-0 2105	0 2052	-0 2637	0 2703	-0 3130	0 3574		0 3521	0 4281
2 4		0 1490	0 1497	-0 1962	0 2174	-0 2435	0 2958		0 2837	0 3741
2 6		-0 1040	0 1080	-0 1445	0 1676	-0 1880	0 2431		0 2273	0 3274
2 8		-0 0719	0 0772	-0 1056	0 1282	0 1439	0 1985		-0 1813	0 2850
3 0		0 0492	0 0547	0 0764	0 0973	-0 1096	0 1612		-0 1441	0 2477
3 2		-0 0335	0 0385	-0 0550	0 0734	0 0828	0 1303		-0 1141	0 2147
3 4		-0 0225	0 0269	0 0393	0 0551	0 0625	0 1050		-0 0901	0 1858
3 6		-0 0131	0 0187	-0 0280	0 0411	-0 0469	0 0842		-0 0710	0 1605
3 8		0 0101	0 0129	-0 0194	0 0302	-0 0351	0 0674		-0 0558	0 1384
4 0		-0 0067	0 0089	-0 0140	0 0226	-0 0260	0 0327		-0 0438	0 1191
4 5		-0 0023	0 0034	-0 0057	0 0105	-0 0124	0 0301		-0 0238	0 0811
5 0		-0 0008	0 0013	-0 0023	0 0048	-0 0058	0 0167		-0 0126	0 0552
5 5		-0 0003	0 0005	-0 0009	0 0022	-0 0027	0 0091		-0 0066	0 0372
6 0		-0 0001	0 0002	-0 0003	0 0010	-0 0012	0 0049		-0 0035	0 0240
6 5			0 0001	-0 0001	0 0004	-0 0005	0 0027		-0 0019	0 0166
7 0					0 0002	0 0002	0 0015		-0 0010	0 0111
8 0							0 0004		0 0003	0 0048
9 0							0 0001		-0 0001	0 0021
10 0										0 0009
11 0										0 0004
12 0										0 0002

orthogonal s wave functions needed for simplification of the energy formula (see § 5), are as follows:—

	O^{+++}	O^{++}	O^+	O
S . . .	0.0286	0.0278	0.0268	0.0258

On Schrödinger's interpretation of the wave function, the radial charge density for one electron with normalised wave function $P(\alpha|r)$ is given by $P^2(\alpha|r)$ (that is to say, $P^2(\alpha|r)dr$ is the charge lying in the spherical shell between radii r and dr). The total radial charge density for each of the ions is shown in fig. 1; and the contribution from one ($2p$) electron, $P^2(2p|r)$, for each ion is shown in fig. 2, to illustrate the contraction of the charge distribution of one electron with increasing ionisation, and therefore decreased screening of one ($2p$) electron by others of the group. A quantitative measure of this screening

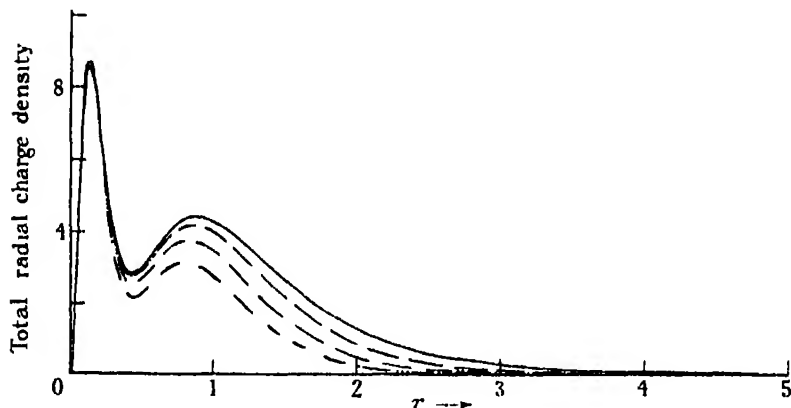


FIG. 1.— O^{+++} — · · · —; O^{++} — — — —; O^+ — · — —; O —

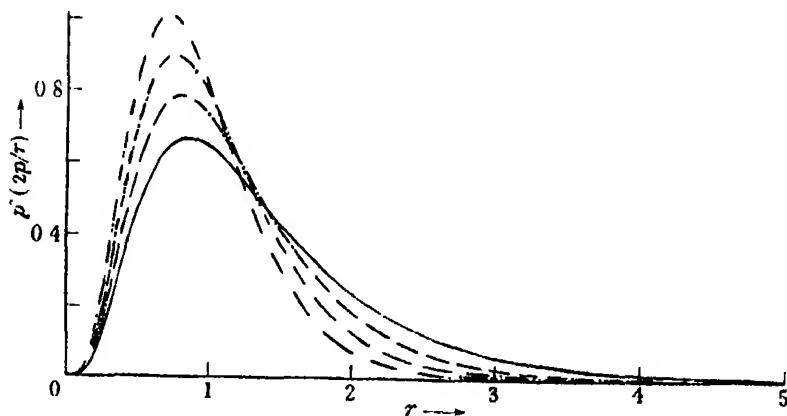


FIG. 2.— O^{+++} — · · · —; O^{++} — — — —; O^+ — · — —, O —

can be given in several ways, one of which is the following. If r_m is the radius of the maximum radial density, then $4/r_m$ is the nuclear charge for which a hydrogen-like ($2p$) electron has its maximum radial density at r_m , so that for oxygen $8 - 4/r_m$ is a measure of the screening of the nuclear charge by the other electrons. Values of r_m and $8 - 4/r_m$ are given in Table II; it will be seen that the screening of one ($2p$) electron by another, reckoned in this way, is about 0.30, but shows a consistent variation.

Table II.

	Electron arrangement	r_m	$8 - 4/r_m$
O^{+++}	$(1s)^3 (2s)^3 (2p)^1$	0.710	2.37
O^{++}	$(1s)^3 (2s)^3 (2p)^2$	0.756	2.71
O^+	$(1s)^3 (2s)^3 (2p)^3$	0.801	3.01
O	$(1s)^3 (2s)^3 (2p)^4$	0.847	3.29

It should be noted that the curves depart considerably from being replicas of the same curve on different linear scales; the proportion of the total charge lying outside r_m increases considerably with decreasing ionisation. This illustrates the roughness of the best approximation obtainable by considering each wave function as hydrogen-like in the field of some mean "effective nuclear charge," since a hydrogen-like ($2p$) wave function has only one adjustable constant, whose alteration represents a variation of linear scale.

For the more highly ionised atoms, the wave functions calculated are not at all sensitive to small variations in the assumed field, and the process of approximation to the self-consistent field is rapid. For example, the maximum differences between the estimated and calculated contributions to $Z[\equiv r^2 \times (\text{field at radius } r)]$ from the $(2p)^2$ group of O^{++} for the first, second, third and fourth trial fields were 0.42, 0.10, 0.02, 0.002 respectively.

§ 4. Formula for the Energy in Terms of Radial Wave Functions.

In evaluating integrals of the type $\int \Psi^* F \Psi d\tau$, that is to say, the diagonal matrix elements of a quantity F for the stationary states, with wave functions of the type (2), the work is greatly simplified if the one-electron wave functions ψ are mutually orthogonal, as then the majority of terms arising from the expansion of the two determinants vanish on integrating. This involves no restriction, since if the ψ 's are not all orthogonal, it is possible to replace

them by linear combinations which are orthogonal, without changing the value of the determinant, and therefore without changing the values of the matrix elements.†

If the one-electron wave functions ψ are of the form (3), the only sets which are not orthogonal are those with the same l, m, s and different n , since those for which l or m or s are different are already orthogonal by the properties of the spherical harmonic factors or spin wave functions. A set of orthogonal linear combinations of those with the same l and different n is easily constructed, and involves the radial functions P only (see § 5). We will assume this done, and will also assume the individual P 's normalised to $\int P^2 dr = 1$, and will indicate the P 's thus made normal and orthogonal by a suffix 0.

For an n -electron atom of atomic number N , the Hamiltonian operator in atomic units‡ is

$$H = \sum_{j=1}^n \left[-\frac{1}{2} \nabla_j^2 - \frac{N}{r_j} \right] + \sum_{j=1}^n \sum_{k=j+1}^n \frac{1}{r_{jk}}. \quad (4)$$

(neglecting spin and relativity contributions). Slater (*loc. cit.*, 1) has obtained a formula for $\int \Psi^* H \Psi d\tau$ when Ψ is given by a determinant of the form (2),

the individual ψ 's being of the form (3), assuming in addition that, as well as the individual ψ 's being orthogonal, each is the solution of the Schrödinger equation in a central field *the same for each*. This is not the case when the ψ 's are obtained by the self-consistent field, as the functions $P(n, l|r)$ for the same l and different n are calculated for different fields so are not orthogonal, and on making orthogonal linear combinations of them, the orthogonal functions $P_0(n, l|r)$ obtained are no longer each the solution of a one-electron wave equation. The modification of Slater's result is only a small one, and only affects the contribution from the first term in H .

We will write

$$I(\alpha) = -\frac{1}{2} \int P_0(\alpha|r) \left[\frac{d^2}{dr^2} + \frac{2N}{r} - \frac{l_a(l_a+1)}{r^2} \right] P_0(\alpha|r) dr \quad (5)$$

$$\rho(\alpha\beta|r) = P_0(\alpha|r) P_0(\beta|r)$$

† As far as we are aware, this was first explicitly stated by Delbrück (*loc. cit.*, see p. 601).

‡ That is, units such that the measures of the mass of an electron m , of the charge on electron e , and of $\hbar/2\pi$, are all 1. In these units, $a_H = \hbar^2/4\pi^2me^2$ has the value 1, so that the unit of length is the "radius of the first circular orbit" of the H atom; the measure of the velocity of light is 137. The unit of energy is *twice* the ionisation energy of the hydrogen atom.

and for generality

$$I_k(\alpha\beta; \gamma\delta) = \iint \rho(\alpha\beta|r) \rho(\gamma\delta|r_1) \frac{r_a^k}{r_b^{k+1}} dr dr_1 \quad (6)$$

$$= I_k(\gamma\delta; \alpha\beta),$$

where r_a and r_b are respectively the smaller and larger of r and r_1 , and all integrations are from 0 to ∞ , and as the integrals of type (6) which arise in the present work are either of the type $I_k(\alpha\alpha; \beta\beta)$ or $I_k(\alpha\beta; \alpha\beta)$ we will for brevity in these cases follow Slater's usage and write

$$I_k(\alpha\alpha; \beta\beta) = F_k(\alpha\beta), \quad I_k(\alpha\beta; \alpha\beta) = G_k(\alpha\beta) \quad (7)$$

Then Slater's formula for the value of the integral required, with the modification already mentioned, is

$$\int \Psi^* H \Psi d\tau = \sum_a I(\alpha) + \sum'_{\alpha\beta} \sum_k a_k(l_a, m_a; l_\beta, m_\beta) F_k(\alpha\beta) \\ - \sum''_{\alpha\beta} \sum_k b_k(l_a, m_a; l_\beta, m_\beta) G_k(\alpha\beta), \quad (8)$$

where the first summation is over all wave functions, the second over all pairs, and the third over all pairs for which the spins are the same, and the coefficients a_k, b_k are those tabulated by Slater.

When an m -degeneracy exists, the energies of the different stationary states arising from a given distribution of electrons in (nl) groups can be calculated according to Slater's paper, and are of the same form as (8) with different coefficients of the integrals F and G which involve the radial wave functions of the incomplete groups.

Thus when the wave functions $P(n, l|r)$ have been calculated by the method of self-consistent field (or any other method), we have the following steps in the calculation of an approximate value of the total energy:—

- (a) Construction of a set of normal and orthogonal functions $P_0(nl|r)$ from those of the same l and different n .
- (b) Evaluation of the integrals $I(\alpha)$.
- (c) Evaluation of the double integrals F and G

§ 5. Construction of Orthogonal Sets of Radial Wave Functions.

The construction of sets of orthogonal functions has already been treated by McDougall, and all we require here is a simple case of the results given by him.

In the case of the normal electron arrangement of oxygen, in all stages of ionisation considered here, the pair of functions $P(1s|r)$, $P(2s|r)$ is the only

set from which an orthogonal set has to be constructed. We will suppose these already normalised, and write

$$S = \int_{r=0}^{\infty} P(1s|r) P(2s|r) dr. \quad (9)$$

There is considerable liberty of choice in the way an orthogonal set of functions shall be constructed from a given non-orthogonal set. The most convenient way in this and similar cases is to take them in the order of increasing n , making a linear combination of each with those of smaller n such that the result is orthogonal to all those of smaller n , and normalised.

Thus in this case we take

$$\begin{aligned} P_0(1s|r) &= P(1s|r) \\ P_0(2s|r) &= (1 - S^2)^{-1} [P(2s|r) - SP(1s|r)] \end{aligned} \quad (10)$$

In the actual numerical work it is more convenient not to normalise the radial wave function $P(2s|r)$ before making it orthogonal to $P_0(1s|r)$, but to make an orthogonal linear combination first and then normalise this. Indeed, the experience of this work suggests that it would probably be more convenient to do the numerical work throughout with orthogonal *but not normalised* wave functions, and divide by the appropriate normalising factors as the last stage in evaluating each integral. This would save an appreciable amount of calculation, and would make it easier to make full use of the fact that, when the arbitrary multiplying constant in the solution of the differential equation is not fixed by the normalising condition, it can be taken so that, for small r , differences between the values of the wave functions with given (n, l) , for different states of ionisation, are very small.

§ 6. Evaluation of the Integrals $I(\alpha)$.

If the radial wave functions P have been calculated by the method of the self-consistent field, and $Z_p(\alpha|r)/r$ is the potential of the field used for calculating the α wave function, and $\epsilon(\alpha)$ is the energy parameter for this wave function, then $P(\alpha|r)$ satisfies

$$\left[\frac{d^2}{dr^2} + \frac{2Z_p(\alpha|r)}{r} - \epsilon(\alpha) - \frac{l_\alpha(l_\alpha + 1)}{r^2} \right] P(\alpha|r) = 0, \quad (11)$$

so that if $P(\alpha|r)$ is not modified by being made orthogonal to other P 's; that

is to say, if $P_0(\alpha|r) = P(\alpha|r)$, we have from (5), (11)

$$\begin{aligned} I(\alpha) &= -\frac{1}{2} \int P(\alpha|r) \left[\epsilon(\alpha) + 2 \frac{N - Z_p(\alpha|r)}{r} \right] P(\alpha|r) dr \\ &= -\frac{1}{2} \epsilon(\alpha) - \int P^2(\alpha|r) [N - Z_p(\alpha|r)] r^{-1} dr. \end{aligned} \quad (12)$$

[The coefficient $\frac{1}{2}$ in the first term arises because ϵ is taken as the negative energy parameter in units of the ionisation energy of the normal hydrogen atom, which is half an atomic unit.] The evaluation of the integral is a straightforward case of integration of a given function; there is no practical difficulty at $r=0$, as $P(\alpha|r)$ tends to 0 and $[N - Z_p(\alpha|r)]/r$ remains finite.

Further, if we write, as will be convenient for the discussion of the double integrals $I_k(\alpha\beta;\gamma\delta)$,

$$Z_k(\alpha\beta|r) = r^{-k} \int_{r_1=0}^r r_1^k \rho(\alpha\beta|r_1) dr_1 \quad (13)$$

$$Y_k(\alpha\beta|r) = Z_k(\alpha\beta|r) + r^{k+1} \int_{r_1=r}^{\infty} r_1^{-(k+1)} \rho(\alpha\beta|r_1) dr_1, \quad (14)$$

then $-Y_0(\alpha\alpha|r)/r$ is the contribution to the potential at radius r from the spherically averaged distribution of the charge of an electron with the orthogonalised wave function α^\dagger ; and since the basic idea of the self-consistent field is that $Z_p(\alpha|r)/r$ in equation (11) satisfied by $P(\alpha|r)$ should be the potential of the field of the nucleus and of the charge distributions of the electrons with wave functions other than α (spherically averaged in order to give a central field), we would have

$$Z_p(\alpha|r) = N - \sum_\beta Y_0(\beta\beta|r) + Y_0(\alpha\alpha|r), \quad (15)$$

the summation being over all occupied functions, if the wave functions were not affected by being mutually orthogonal.

Also since from the definitions of Y_k and I_k we have

$$I_k(\alpha\beta;\gamma\delta) = I_k(\gamma\delta;\alpha\beta) = \int_{r=0}^{\infty} [\rho(\alpha\beta|r) Y_k(\gamma\delta|r)/r] dr, \quad (16)$$

$\dagger Y_k(\alpha\beta|r)$ is similarly related to the potential of a distribution of charge having radial density $\rho(\alpha\beta|r) S_k(\theta, \phi)$ where S_k is a spherical harmonic of order k , and "radial density" for a distribution not uniform over the sphere means charge per unit radius per unit solid angle.

we could with the same proviso write (12) in the form

$$I(\alpha) = -\frac{1}{2}\epsilon(\alpha) - \sum_{\beta} F_0(\alpha\beta) + F_0(\alpha\alpha), \quad (17)$$

using the abbreviations (7).

Actually $Z_p(\alpha|r)$ is constructed from the non-orthogonal wave functions $P(\alpha|r)$, so that (15), (17) are not exactly correct. [McDougall (*loc. cit.*) has given some examples of the consequent modifications of (17).] Also in practice only an approximation of the self-consistent field may be obtained, so that the relation of consistency between the function $Z_p(\alpha|r)$ used in calculating $P(\alpha|r)$, and the solutions of the equations for the radial wave functions P , may not be exactly satisfied.

Though for both reasons (15) and so (17) may not be exact, we can make good use of the fact that they are approximately satisfied. If we write

$$D(\alpha|r) = N - Z_p(\alpha|r) - \sum_{\beta} Y_0(\beta\beta|r) + Y_0(\alpha\alpha|r) \quad (18)$$

then $D(\alpha|r)$ is small since (15) is approximately satisfied. Also

$$I(\alpha) = -\frac{1}{2}\epsilon(\alpha) - \sum_{\beta} F_0(\alpha\beta) + F_0(\alpha\alpha) - \int P^2(\alpha|r) D(\alpha|r) r^{-1} dr; \quad (19)$$

the function Y_0 and integrals F_0 concerned have to be calculated in any case, and the last integral is numerically small and easy to evaluate.

This result seems useful as an approximate *check* on the value of $I(\alpha)$, rather than as the formula to be used for calculating it, on account of the danger of the accumulations of numerical errors, first in the calculation of $D(\alpha|r)$ and then in the summation of the F_0 integrals, due to the use of a finite number of significant figures.

If the functions P_0 in (5) have to be formed by linear combination of the calculated radial wave functions P , which individually satisfy equations of the type (11) with different functions Z_p and different energy parameters ϵ , the substitution for d^2P/dr^2 from the differential equation for P gives rise to a rather less simple result, but one which is still useful.

For example, from (10) and the two equations of type (11) we have

$$\left[\frac{d^2}{dr^2} + \frac{2N}{r} \right] P_0(2s|r) = \left[2 \frac{N - Z_p(2s|r)}{r} + \epsilon(2s) \right] P_0(2s|r) \\ - \frac{8}{\sqrt{(1-S^2)}} \left[2 \frac{Z_p(2s|r) - Z_p(1s|r)}{r} + \epsilon(1s) - \epsilon(2s) \right] P_0(1s|r).$$

so that

$$I(2s) = -\frac{1}{2}\epsilon(2s) - \int \frac{N - Z_p(2s|r)}{r} P_0^2(2s|r) dr \\ + \sqrt{1 - S^2} \int \frac{Z_p(2s|r) - Z_p(1s|r)}{r} P_0(1s|r) P_0(2s|r) dr, \quad (20)$$

and the first two terms can be expressed in the form (19) as before, providing a similar numerical check on the value of the main integral in (20).

It is interesting to see that despite the linear combination of $P(1s|r)$ and $P(2s|r)$, only the energy parameter $\epsilon(2s)$ occurs in $I(2s)$. The third term in (20) is clearly the correcting term arising from the different fields for which the wave functions $P(1s|r)$ and $P(2s|r)$ are calculated. It is of the second order in the difference between these fields, as both S and the integrand vanish if the same field is taken for both $P(1s|r)$ and $P(2s|r)$.

In McDougall's work on the optical terms of Si^{+3} (*loc. cit.*) the evaluation of the I integrals was not necessary, as in that case, when the perturbation of the core wave functions on addition of the series electron could be neglected, the greater part of the contribution to the energy from the I integral for the series electron wave function was cancelled by contributions from F_0 integrals, on account of (19).

Here, however, when the wave function for the remaining $(2s)$ and $(2p)$ electrons are changed appreciably with each successive removal of a $(2p)$ electron to give O^+ , O^{1+} , O^{1+1} (*cf.* fig. 2), there is not the same cancellation, and the I integrals have to be evaluated.

§ 7. Evaluation of the Double Integrals.

The method of evaluating the double integrals of the type

$$I_k(\alpha\beta, \gamma\delta) = \iint \rho(\alpha\beta|r) \rho(\gamma\delta/r_1) \frac{r_a^k}{r_b^{k+1}} dr dr_1,$$

will be considered in rather more detail, both because they present a less familiar problem than the evaluation of the single integrals $I(\alpha)$, and also because similar integrals and functions of the type of Y_k (see (14)) used in evaluating them occur in other problems,† so it may be as well to give an account of the methods found best for evaluating them.

The introduction of the functions Y_k defined by (14) formally reduces the calculation of I_k to the evaluation of a single integral (16) which presents no

† For example, the functions Y_k appear in Fock's equations.

difficulty as in practical cases the integrand vanishes at $r = 0$ since both functions P are of order r at least and Y_k remains finite; so that the problem is reduced to the evaluation of Y_k . As already mentioned by McDougall (*loc. cit.*) in practice it often happens that this cannot conveniently be carried out directly by quadrature of the integrals in (14), especially for the higher values of k , and he has given an account of a method, originally devised in connection with the present work, for calculating Y_k ; this method consists essentially in replacing one or both direct integrations by differential equations whose numerical solution is practically easier than the evaluation of the integrals in Y_k directly by quadratures. Two slight modifications which appear to be improvements, and which have been used in the present work, will be indicated here.

From (13), (14) we obtain the equations

$$\frac{d}{dr} Y_k(\alpha\beta|r) = \frac{1}{r} [(k+1) Y_k(\alpha\beta|r) - (2k+1) Z_k(\alpha\beta|r)] \quad (21)$$

$$\frac{d}{dr} Z_k(\alpha\beta|r) = \rho(\alpha\beta|r) - \frac{k}{r} Z_k(\alpha\beta|r), \quad (22)$$

which are those given by McDougall; we can put these relations in two forms namely,

$$\frac{d}{dr} [r^{-(k+1)} Y_k(\alpha\beta|r)] = -(2k+1) [r^{-(k+2)} Z_k(\alpha\beta|r)] \quad (23)$$

$$\frac{d}{dr} [r^{-(k+2)} Z_k(\alpha\beta|r)] = r^{-(k+2)} \rho(\alpha\beta|r) - \frac{2(k+1)}{r} [r^{-(k+2)} Z_k(\alpha\beta|r)] \quad (24)$$

which are perhaps more convenient for small r , and

$$\frac{d}{dr} [r^k Y_k(\alpha\beta|r)] = \frac{2k+1}{r} [r^k Y_k(\alpha\beta|r) - r^k Z_k(\alpha\beta|r)] \quad (25)$$

$$r^k Z_k(\alpha\beta|r) = \int_{r_1=0}^r r_1^k \rho(\alpha\beta|r_1) dr_1 \quad (26)$$

which are perhaps more convenient for large r .

In the results of Slater's theory of complex spectra (or any derivable from them, *e.g.*, Fock's equations), k is never greater than $l_a + l_b$. Also $\rho(\alpha\beta|r)$ is $O(r^{l_a+l_b+2})$ at $r=0$, so $r^{-(k+2)}\rho(\alpha\beta|r)$ in (24) is at least $O(1)$, and $r^{-(k+2)}Z_k(\alpha\beta|r)$ is at least $O(r)$. For small r , it seems most convenient to calculate $r^{-(k+2)}Z_k(\alpha\beta|r)$ by numerical solution of (24), then the calculations of $r^{-(k+1)}Y_k$ is reduced to quadratures. For the start of the numerical

integration of (24) we require the value of $\frac{d}{dr} [r^{-(k+2)} Z_k(\alpha\beta|r)]$ at $r = 0$, which is easily found to be $\lim_{r \rightarrow 0} [r^{-(k+2)} \rho(\alpha\beta|r)] / (2k+3)$. This limit is 0 when $k < (l_\alpha + l_\beta)$, and is finite, and can be calculated from the data of the radial wave functions, when $k = l_\alpha + l_\beta$. For small r it is an advantage, rather than the reverse, to obtain directly values of Y_k multiplied by a *negative* power of r , provided the negative power is not so great that the product is infinite at $r = 0$, and the quadrature of $r^{-(k+2)} Z_k$ is very convenient practically.

For large r , $r^k Z_k(\alpha\beta|r)$ and $r^k Y_k(\alpha\beta|r)$ both tend to be constant $\int_{r_1=0}^{\infty} r_1^k \rho(\alpha\beta|r_1) dr_1$, so that the right-hand side of (25) tends to 0. Thus outside the region where ρ is large, in integrating (25) we are only integrating the small difference of $r^k Z_k$ from the constant value it would have if ρ were 0 outside that region, whereas Z_k varies with r even when $\rho = 0$, and in using (21) we are including this variation in our integration. The form (25), (26) of the relations between Y_k , Z_k , and ρ is not practically satisfactory for *small* r (especially for the higher values of k). For the calculations for oxygen here considered, it seemed best to change over from the use of (23), (24) to (25), (26) at about $r = 1$, but a considerable overlap was practicable and was used for checking purposes.

In any extensive numerical work, the question of checking the calculations is one of some importance. A check on the calculation of the I integrals has already been mentioned; a good check on the F_0 integrals can be obtained as follows.

We have

$$F_0(\alpha\beta) = \int \frac{\rho(\alpha\alpha|r) Y_0(\beta\beta|r)}{r} dr = \int \frac{\rho(\beta\beta|r) Y_0(\alpha\alpha|r)}{r} dr.$$

Now suppose, for example, we calculate $Y_0(2s, 2s|r)$ and $Y_0(2p, 2p|r)$, and calculate $F_0(2s, 2s)$ and $F_0(2p, 2p)$ by quadratures, then instead of calculating $F_0(2s, 2p)$ by quadratures directly, we calculate the *differences*

$$F_0(2s, 2p) - F_0(2s, 2s) = \int \frac{\rho(2s, 2s)}{r} [Y_0(2p, 2p|r) - Y_0(2s, 2s|r)] dr$$

$$F_0(2p, 2p) - F_0(2s, 2p) = \int \frac{\rho(2p, 2p)}{r} [Y_0(2p, 2p|r) - Y_0(2s, 2s|r)] dr$$

which are numerically much easier to evaluate as they are of much smaller

magnitude ; then we can obtain two values of $F_0(2s, 2p)$

$$\begin{aligned} F_0(2s, 2p) &= F_0(2s, 2s) + [F_0(2s, 2p) - F_0(2s, 2s)] \\ F_0(2s, 2p) &= F_0(2p, 2p) - [F_0(2p, 2p) - F_0(2s, 2p)] \end{aligned}$$

and the agreement between these checks all three F_0 integrals, and gives at least a partial check on the Y_0 functions, which are used in other integrals as well.

For example for O^{++} there were calculated :—

$$\left. \begin{aligned} F_0(2s, 2s) &= 0.8387 \\ F_0(2s, 2p) - F_0(2s, 2s) &= 0.0210 \end{aligned} \right\} \text{whence } F_0(2s, 2p) = 0.8597.$$

and

$$\left. \begin{aligned} F_0(2p, 2p) &= 0.8914 \\ F_0(2p, 2p) - F_0(2s, 2p) &= 0.0314 \end{aligned} \right\} \text{whence } F_0(2s, 2p) = 0.8600.$$

This difference is within the limits of accuracy of the numerical work, the probable error of each of the four integrals calculated being of the order of 0.0002.

Similar checks can be applied by using the differences between the different states of ionisation as well as differences between the different integrals.

§ 8. Calculation of Energies. Results.

The values of the relevant integrals, calculated for the normal electron arrangements of O^{+++} , O^{++} , O^+ , O from the wave functions tabulated in Table I, are given in Table III, and the coefficients of the various integrals in the formulæ for the energies of the stationary states, obtained by the method given in Slater's paper, are given in Table IV.

Table III —Values of F, G and I Integrals.

	O^{+++}	O^{++}	O^+	O
$-21(2s)$	14.713	14.321	13.947	13.620
$-21(2p)$	14.447	13.819	13.100	12.160
$F_0(1s, 2s)$	1.2322	1.1683	1.1151	1.0732
$F_0(1s, 2p)$	1.3584	1.2550	1.1510	1.0340
$F_0(2s, 2s)$	0.8884	0.8389	0.7956	0.7611
$F_0(2s, 2p)$	0.9257	0.8599	0.7953	0.7261
$F_0(2p, 2p)$		0.8912	0.8011	0.6972
$G_0(1s, 2s)$	0.0870	0.0762	0.0683	0.0621
$G_0(1s, 2p)$	0.1702	0.1398	0.1150	0.0921
$G_0(2s, 2p)$	0.5646	0.5288	0.4879	0.4401
$F_1(2p, 2p)$		0.4115	0.3598	0.3032

Table IV.—Coefficients of F, G and I Integrals in Expression for Total Energies of Normal States of O^{+1} , O^{+1} , O^{+1} , O .

	O^{+1}	O^{+1}	O^{+1}	O
I (2s)	2	2	2	2
I (2s)	2	2	2	2
I (2p)	1	2	3	4
$F_0(1s, 1s)$	1	1	1	1
$F_0(1s, 2s)$	4	4	4	4
$F_0(1s, 2p)$	2	4	6	8
$F_0(2s, 2s)$	1	1	1	1
$F_0(2s, 2p)$	2	4	6	8
$F_0(2p, 2p)$	0	1	3	6
$G_0(1s, 2s)$	-2	-2	2	2
$G_0(1s, 2p)$	$-\frac{1}{2}$	$-\frac{1}{2}$	-1	$-\frac{1}{2}$
$G_0(2s, 2p)$	$-\frac{1}{2}$	$-\frac{1}{2}$	-1	$-\frac{1}{2}$
$F_2(2p, 2p)$	${}^3P, 0$	${}^4P, -\frac{1}{2}$ ${}^1D, +\frac{1}{2}$ ${}^3S, +\frac{1}{2}$	${}^3S, -\frac{1}{2}$ ${}^1D, -\frac{1}{2}$ ${}^3P, 0$	${}^3P, -\frac{1}{2}$ ${}^1D, -\frac{1}{2}$ ${}^3S, 0$

The results of the first calculations made showed that the differences between calculated and observed ionisation energies were of the order 0.02 atomic units, but the numerical accuracy was not adequate to give a reliable second decimal in the calculated energy. It seemed desirable to carry out the calculations to a numerical accuracy higher than the accuracy of agreement between calculations and observation, to be sure that the differences were significant and that any good agreement was not spurious, and the calculations were revised with this object in view. This demanded the calculation of the I, F, G integrals to a considerable degree of numerical accuracy, as shown in the following paragraphs.

Apart from the effect of any undetected mistakes in the numerical work (of which it is hoped there are no serious ones which have escaped the fairly extensive checks applied) each integral is in error owing to the use of a finite number of significant figures at each stage of the calculation, possible cumulative errors of integration formulæ, etc.; the error arising from such causes may be termed the random error. The I integrals, being numerically larger than the F and G integrals (and so more affected by the random errors of the normalising integral) and more troublesome to calculate, are likely to have larger random errors than the F, G integrals, and random errors of the latter are likely to be all about the same. Using the term "probable error" in the sense in which it is used in the theory of errors, suppose x is the probable random error of an I integral and y that of a F or G integral, then δE_A , the probable error of a

calculated ionisation energy for the removal of an electron from an ion A to give ion A^+ , is given by

$$(\delta E_A)^2 = [\Sigma (C_x^2)_A + \Sigma (C_x^2)_{A^+}] x^2 + [\Sigma (C_y^2)_A + \Sigma (C_y^2)_{A^+}] y^2,$$

where C_x , C_y are the coefficients of the I, and of the F and G, integrals respectively. For the ionisation energy of O neutral this gives

$$(\delta E_{O, \text{neut}})^2 = 33x^2 + 295y^2 \quad (26)$$

(neglecting the contribution from (1s), see below), or if $x = 0.0007$, $y = 0.0003$,

$$\delta E_{O, \text{neut}} = 0.0065 \text{ approximately,}$$

so that in order that the second decimal in the ionisation energy should be significant, it is necessary that the fourth decimal in the integrals, if not reliable to a unit, should at least have some value. This is an unfavourable case; for the more highly charged ions the coefficients in the expressions corresponding to (26) are smaller; unfortunately O neutral, for which δE is largest, is also that for which E is smallest. It is not easy to give any very precise estimate of the numerical accuracy of the calculated values of I and F, but such estimates as can be made, and the results of checks such as the numerical example gives in § 6, suggest that the numerical accuracy attained is perhaps rather better than suggested by the values $x = 0.0007$, $y = 0.0003$, but is of that order, so that the probable error of the calculated value of the ionisation energy can be taken as about 0.007 for O neutral, and rather smaller for O^+ , O^{++} , O^{+++} .

For numerical reasons it is more convenient to calculate $2I(\alpha)$ than $I(\alpha)$, the values of $2I(\alpha)$ are given in Table III, and to three decimals only, as the probable error is greater than 10 in the fourth decimal, so that only three decimals are significant. The values of the integrals depending solely on $P(1s|r)$, that is $I(1s)$ and $F_0(1s, 1s)$, have not been calculated, as the change of $P(1s|r)$ with the state of ionisation is so small that the differences between the values, for successive states of ionisation, both of $I(1s)$ and of $F_0(1s, 1s)$ are negligible, and only these differences come into ionisation energy. The total difference of $F_0(1s, 1s)$ between O and O^{+++} is about 0.0013, so its contribution to the ionisation energy at any one stage is probably less than 0.0005, which is much smaller than the probable error of the ionisation energy; the change of $I(1s)$ is very difficult to estimate, as it depends on a third decimal in $\alpha(1s)$ which it is hardly possible to get, but it is likely to be of the same order as the change of $F_0(1s, 1s)$.

For the calculation of the other integrals involving P ($1s|r$), *e.g.*, $F_0(1s, 2s)$, the ($1s$) wave function for O^{++} has been used throughout, as this simplifies the numerical work, and the effect of the differences of the ($1s$) wave function from one ion to another is negligible; for example, the difference between the values of $F_0(1s, 2s)$ for O neutral, calculated using the ($1s$) wave function for O^{++} and using that for O neutral, is less than 0.0001.

Taking the lowest state of each ion as the zero of energy from which to calculate the negative energy of the states of the ion with one more electron, we obtain the values given in Table V for the ionisation energies of the different stationary states arising from the normal electron arrangements of the ions considered.

Table V.—Comparison of Calculated and Observed Ionisation Energies, and Inter-multiplet Separations.

		Calculated		Observed		Difference O — C.	
O ⁺	² P	1 988		2 025		0 037	
			0 099		0 091		-0 008
	¹ D	1 889		1 934		0 045	
			0 148		0 105		--0 043
	¹ S	1 741		1 829		0 088	
O ⁰	⁴ S	1 258		1 301		0 043	
			0 129		0 134		+ 0 005
	² D	1 129		1 167		0 038	
			0 087		0 062		-0 015
	² P	1 042		1 105		0 063	
O	² P	0 416		0 500		0 084	
			0 073		0 072		-0 001
	¹ D	0 343		0 428		0 085	
			0 109		0 081		--0 028
	¹ S	0 234		0 317		0 113	

In this table are also given the observed energies obtained from the respective spectra† as follows. The calculated energies contain no contribution from the spin interaction energy, while the energies derived from observed spectrum terms do contain such a contribution, so for comparison we want to derive from the observed multiple term a single energy value corresponding to the observed terms less the spin contribution to each.

† For terms, values used, and references to previous observations and analyses of the spectra see:—For O^{++} (Spectrum O III), Fowler, 'Proc. Roy. Soc.' A, vol. 117, p. 317 (1928). For O^+ (Spectrum O II), Russell, 'Phys. Rev.', vol. 31, p. 27 (1928). For O (Spectrum O I), Hopfield, 'Phys. Rev.', vol. 37, p. 160 (1931).

Now, according to the approximate theory of spin interaction given by Goudsmit,[†] the spin interaction energy of a term specified by quantum numbers L, S, j , is

$$A [j(j+1) - L(L+1) - S(S+1)],$$

where A depends on the details of atomic structure and is the same for terms of different j arising from a given electron arrangement. By choosing A to give the best fit with the spin separations between the observed terms, the spin interaction can be estimated and an observed energy "corrected for spin" obtained. The observed values given in the table are obtained thus. [The values in atomic units are obtained from the term values by dividing by $2R = 219474$.]

Comparing first the values of the ionisation energies, rather than the intermultiplet separations, the agreement between calculation and observation is satisfactory, particularly for O^{1+} and O^1 .

In the similar calculation of the ionisation energy of neutral helium,[‡] the difference between the calculated and observed ionisation energies was 0.04 atomic units. In the present case we are dealing with a more elaborate system and using the same type of approximation to the form of the wave function, and are making an additional approximation in the neglect of interchange terms in the equations for the one-electron wave functions (there are no such terms to neglect in the case of the normal helium atom). Moreover, for oxygen not all the one-electron wave functions are spherically symmetrical, and a further approximation has been made in taking a spherical average in calculating the contributions to the field acting on any electron from electrons in those wave functions which are not spherically symmetrical, while for the normal helium atom the one-electron wave function concerned is spherically symmetrical and this approximation is unnecessary.

So a better result than that obtained for the normal state of He would hardly be expected; in fact, it would hardly be expected even if the latter two approximations were not made (as would be the case if the one-electron wave functions were calculated by the solution of Fock's equations instead of by those of the self-consistent field), and it seems satisfactory that the differences between

[†] Goudsmit, 'Phys. Rev.', vol. 31, p. 945 (1927).

[‡] Gaunt (*loc. cit.*). Gaunt's $(O|G_0|O)$ is $F_0(1s, 1s)$ in the notation of this paper. There is an error in a numerical result calculated by one of us (D.R.H.), used by Gaunt; a revised calculation gives $F_0(1s, 1s) = 2.06$, calculated ionisation energy of He = 1.73 (observed 1.81), the unit of energy being the ionisation energy of H (which is half an atomic unit), as in Gaunt's paper.

calculation and observation are not larger. The differences for the ionisation energies of the states of lowest energy are 0.037, 0.043 and 0.084 for O^{++} , O^+ , O , comparing well with 0.04 for He.

It is not surprising that the difference between calculated and observed values is largest for the neutral O , since the neglected interchange terms in Fock's equations are probably of the same order in all cases, and are likely to make more difference to the more loosely bound wave functions of neutral O than to the more tightly bound ones of the ions. As the ionisation energy itself is smallest for O neutral, the larger difference between calculated and observed values shows up as a comparatively large *fraction* of the observed ionisation energy, but this is an unduly severe way of regarding the difference, as can be seen by considering the case of a negative ion of very small ionisation energy. As an illustration of the numerical difficulties it may be mentioned that the sum of the *magnitudes* of the terms from which the ionisation energy of O neutral was calculated is just over 100, so that in forming their algebraical sum which gives the ionisation energy 0.416 we have lost two whole significant figures and rather more, and the difference 0.084 between observed and calculated ionisation energies represents less than 0.1 per cent. of the sum of the magnitudes of the terms giving the calculated value.

The general agreement of the inter-multiplet separations is also satisfactory, especially for the separation of the lower two states in each case. To the approximation used in Slater's theory of complex spectra, on which the energy formulæ here used depend, the ratios of the inter-multiplet separations arising from a given electron arrangement are in simple cases (including all those which here appear) independent of their absolute values, so those ratios can be taken as a test of whether this approximation is adequate. As already noted by Slater, they indicate that it hardly is adequate, for example, for O^{1+} we have :—

$$\frac{{}^1D - {}^1S}{{}^3P - {}^3D} \quad \text{Calculated } \frac{3}{2}, \quad \text{observed } 1.04.$$

For an approximation which gives an error of this magnitude in the ratio, the general agreement between the absolute values of calculated and observed inter-multiplet separations is perhaps even rather surprising.

These inter-multiplet separations involve only the integral $F_2(2p)$ in these cases, so involve very much less calculation than the ionisation energies, and calculation of them in other cases, including particularly those in which the ratios agree better with Slater's theory, would probably give interesting results.

The only other theoretical calculations to compare with those of this paper are those of Guillerin and Zener (*loc. cit.*) who used the variation method with a determinant of type (2) for the wave function for the whole atom, with the one-electron wave functions ψ of a specified analytical form with parameters which were chosen to make $\int \Psi^* H \Psi d\tau$ stationary for variation of these parameters. The limitation of the one-electron wave functions ψ to a specified analytical form means that not so good an approximation to the actual wave function or energy can be obtained as if the form of these functions were left to be determined by the variation principle, as in the case of the method of the self-consistent field or Fock's development of it; on the other hand, it allows the interchange terms to be taken into account, as Fock's method does, but the self-consistent field does not, and is numerically simpler.

For oxygen, Zener only gives the calculated energy of the whole L shell $(2s)^2(2p)^4$ for the neutral atom, so that no direct comparison with the present work is possible. He says the agreement between the calculated value of this quantity and an estimate of the "observed" value (which depends on extrapolation of the ionisation energies in the higher stages of ionisation) is "decidedly worse" than for C, for which the difference is 0.095 atomic units, but gives no figures. Our total difference between calculated and observed values for the last three stages of ionisation is 0.17 atomic units, so that the differences are of the same order in the two methods. Zener states that the inter-multiplet separations calculated using his analytic wave functions were 1.5 to 2 times too large; here our wave functions show a considerable advantage,† the ratio calc./obs. being between 0.96 and 1.41. It would be very interesting to revise the present work, using the solutions of Fock's equations for the determination of the one-electron wave functions; this should give results better than ours or Zener's, but it must await the development of the numerical technique for solving Fock's equations.

§ 9. Summary.

One-electron wave functions for the three electron groups in the normal electron arrangement of each of the ions O^{+++} , O^{++} , O^+ , O have been calculated

† Zener uses hydrogen-like $(2p)$ wave functions. We have seen (§ 5 and fig. 2) that these cannot in all cases give a good approximation to the self-consistent field $(2p)$ wave function, and presumably not to the $(2p)$ wave function in the solution of Fock's equations. The inter-multiplet separations depend on the $(2p)$ wave function only, and it seems likely that our improvement on Zener's results is due to the freedom to use non-hydrogen-like wave functions.

by the method of the self-consistent field, and the results have been used to calculate the energies of the states arising from this electron arrangement (three states for each of O^{++} , O^+ and O and one for O^{+++} , apart from spin separations), and so the ionisation energies, and in particular the inter-multiplet separations, of these states, using Slater's theory of complex spectra, methods for calculating the necessary integrals, and for the necessary checking of the work are given.

The agreement with the observed values of the ionisation energies and inter-multiplet separations are satisfactory in view of the approximations necessary to make the problem amenable to quantitative treatment; the ionisation energies of O^{++} , and O^+ differ from the observed values by about the same amount as for the normal state of the neutral helium for which similar calculations involving rather less approximation have been made. For neutral O the difference is larger, as is to be expected since the approximations made are proportionally more important. The inter-multiplet separations, which are some of the first calculated purely theoretically for an atom of this degree of complication, are in satisfactory agreement with observation.

The numerical work is somewhat extensive; apart from the solution of the self-consistent field problem for each ion, and the construction of a normal orthogonal set of one-electron wave functions for each, 8 single integrals and 34 double integrals were required for the calculation of the energies, and a numerical accuracy of the order of 3 in 10,000 was required in each to make comparison with experiment significant. Actually about a third as many again were calculated for checking purposes.

The Corpuscular X-Ray Spectra of the Radio-Elements.

By C. D. ELLIS, F.R.S.

(Received November 2, 1932)

[PLATE 5.]

An interesting way in which an excited atom can emit its excess energy has been brought to light by the experiments of Robinson* and of Auger.† If, for example, an atom is ionised in the K state, then it may emit a quantum of radiation of some line of its K X-ray spectrum by means of a transition of an electron to the K level, but as an alternative method it may emit an electron instead, thus leaving the atom doubly ionised. One such process might be represented as $[L_I \rightarrow K, L_{II} \rightarrow \infty]$ and the energy E of the ejected electron would be given by $E = K_{atom} - L_{Iabs} - L_{IIabs} - \delta$, where δ is a small correcting term to take into account that the work required to remove an electron from an ionised atom is slightly greater than that necessary in the case of a normal atom. Processes of this kind are essentially different from those giving rise to radiation since two electrons instead of one are concerned in the transition. The entire process must be considered as occurring simultaneously, and, to take as an example the case already mentioned, it has no meaning to attempt to state whether it is an L_I electron which goes to the K state, and an L_{II} electron which is ejected or *vice versa*. Two points of interest in this phenomenon are the investigation of the magnitude of the correction term δ , and of the relative probabilities of the different types of transition. It will be seen later that the possible transitions are considerably more numerous than with single electron transitions which give rise to radiation.

This phenomenon has been studied by Robinson by analysing the ejected electrons with a magnetic field. A thin layer of the element under investigation is placed in the position of the source in the well-known semi-circular focussing apparatus, and is irradiated with X-rays of sufficiently high frequency to be able to eject electrons from the K state. There then follows a further electronic emission from these ionised atoms in the manner already described. Both sets of electrons are recorded photographically, and the various groups show up as lines or narrow bands on the photographic plate. A difficulty

* 'Proc. Roy. Soc.,' A, vol. 104, p. 455 (1923), and Young, *ibid.*, vol. 128, p. 92 (1930)

† 'J. Phys. Rad.,' vol. 6, p. 205 (1925).

inherent in the nature of the experiment is that the groups of homogeneous electrons become slightly diffuse in emerging from the target which must have a certain thickness in order to yield groups of reasonable intensity.

A convenient opportunity for investigating this phenomenon is provided by the radioactive elements. Many of these emit γ -rays from the nucleus in the course of the disintegration and certain of these γ -rays are absorbed in the K states of the actual emitting atom. This is the process known as internal conversion and which gives rise to the β -ray spectra. It, however, does not concern us here except that it provides the condition, ionisation of the K level, necessary for observing the corpuscular X-ray spectrum. It is clear that if a source of a radio-element is substituted for the target in Robinson's arrangement, its corpuscular X-ray spectrum should be recorded on the photographic plate. In addition to the interest of investigating a radio-element the great advantage of this method is that the lines can now be made narrow and sharply defined since the radio-element is present in only minute quantities and forms scarcely a monomolecular layer on its support. It has long been recognised that lines of about the expected energies occurred in the β -ray spectra of radium (B + C) and thorium (B + C), but a detailed investigation was made difficult by the complexity of the spectra in this region, by the necessity of determining which lines belonged to the B and which to the C bodies and by the possibility that certain of the lines might be true β -rays and due directly to low frequency γ -rays.

I have found it possible to decide with certainty which lines form the corpuscular X-ray spectrum by the simple method of comparing the β -ray spectra obtained from sources of radium (B + C) and thorium (B + C). The disintegrations that occur with a source of radium (B + C) are those of Ra B . C and Ra C . C', and, since the γ rays are emitted after the disintegration, the corpuscular X-ray spectra will be those of Ra C and Ra C', atomic numbers 83 and 84. With thorium (B + C), on the other hand, there will be corpuscular spectra resulting from the disintegrations Th B . C, Th C . C'', Th C'' . Pb and possibly Th C . C'; that is, spectra of atomic number 83, 81, 82 and possibly 84. From our knowledge of these β -ray spectra it is certain that the corpuscular spectra from the disintegrations Th C . C'' and Th C . C'; that is, of atoms of atomic number 81 and 84, will be extremely weak, and we should not even expect that from atomic number 82 (Th C'' . Pb) to be strong. The corpuscular X-ray spectra, determined entirely by the electronic part of the atom, will be similar for different radioactive isotopes, whereas any β -ray groups associated with γ -rays would be characteristic of the particular nucleus.

We can therefore conclude without any ambiguity that the groups common to both radium (B + C) and thorium (B + C) are X-ray groups from an atom of atomic number 83. On the other hand, groups occurring in radium (B + C) but not in thorium (B + C) might be either true β -rays or X-ray groups from atomic number 84, and *vice versa*, β -rays or X-ray groups from atomic number 82.

Experimental.

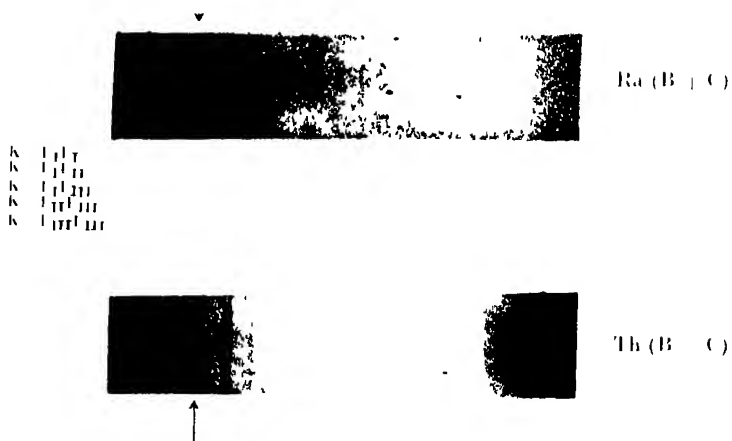
The application of this method was greatly simplified by the use of a large permanent magnet* for producing the analysing field. The magnetic field was kept throughout at one value and photographs were taken in turn of the corpuscular spectra from sources of radium (B + C) and thorium (B + C) deposited on platinum wires one-quarter of a millimetre in diameter. Since the positions of the two sources were usually practically identical direct inspection of the plates without measurement showed which lines were common to the two

Table I.

Ra (B + C)		Th (B + C).		Groups common to both sources
H ρ .	Estimated photographic intensity.	H ρ .	Measured photographic intensity.	H ρ
		968.3	0.1	
		962.2	0.1	
946.1	0.3	945.9	0.4	946.0
941.6	0.6	941.7	0.6	941.7
930.1	0.3	929.0	0.3	929.5
923.8	0.3	923.6	0.4	923.7
920.8	0.3	919.5†	0.4	920.8
890.8	0.9			
885.4	0.1			
872.1	0.9	871.0	0.8	871.5
867.2	0.15			
861.7	0.15			
854.9	1.2	854.2	1.4	854.5
849.8	0.9	849.2	0.8	849.5
844.0	0.45			
		841.5‡	0.3	
838.3	0.45			
		834.9‡	0.2	
832.8	1.2	831.9	1.0	832.3
827.9	0.9	826.4	0.6	826.6

† The H ρ value for this line is uncertain.

‡ These lines seemed diffuse and were difficult to measure.



sources. Reproductions of the photographs obtained with different sources are shown in Plate 5 and the great similarity in the spectra will be at once noticed.

Measurements of the absolute H_p of the groups were carried out with the same apparatus and in the same way as described in a previous paper.* In the next table is given a list of the lines from the two sources in the region where the corpuscular X-ray spectrum occurs. The thorium (B + C) values agreed excellently with those obtained previously,* and no reason was found to introduce any changes except for one line H_p 919.5.

The values for radium (B + C) are lower than those previously published.† It was pointed out in a previous paper that it was probable that all the published radium (B + C) values were about half per cent. too high and the present measurements appear to confirm this view. The intensities of the thorium (B + C) lines are those already published, while the values given for radium (B + C) were estimated from visual comparison of different photographs and are only very approximate. The values assigned to the strongest lines were made to agree approximately with the measured values for thorium (B + C).

It will be seen from the table that in many cases there is almost exact duplication of the lines in the two spectra, both as regards the H_p values and intensities. These lines must therefore be associated with the electronic structure of an atom of atomic number 83. The interpretation of these lines and the agreement with the calculated corpuscular X-ray spectrum is shown in Table II,

Table II.—Corpuscular X-ray Groups from Atomic Number 83.

H.	True intensity.‡	Energy volts $\times 10^5$.	Origin	Energy calculated volts $\times 10^5$.	$E_{calc} - E_{meas}$
946.0	0.7	0.7347	$K \rightarrow L_{III}M_{III}$	0.7342	—
941.7	1.0	0.7285	$K \rightarrow L_{II}N_I$	0.7269	—
929.5	0.6	0.7108	$K \rightarrow L_{II}M_{III}$	0.7112	—
923.7	0.7	0.7025	$K \rightarrow L_{II}M_{II}$	0.7047	—
920.8	0.7	0.6985	$K \rightarrow L_{II}M_{II}$	0.6994	—
871.5	1.5	0.6296	$K \rightarrow L_{III}L_{III}$	0.6320	0.0024
854.5	2.8	0.6066	$K \rightarrow L_{III}L_{III}$	0.6090	0.0024
849.5	1.6	0.5998	$K \rightarrow L_{II}L_{III}$	0.6025	0.0027
832.3	2.2	0.5770	$K \rightarrow L_{II}L_{II}$	0.5795	0.0025
826.6	1.2	0.5695	$K \rightarrow L_{II}L_{II}$	0.5730	0.0035

‡ The true intensities purport to represent the relative number of electrons in the groups. They are obtained from the photographic intensities by application of a factor giving the relative photographic action of electrons of different speeds (Ellis, *loc. cit.*). The correction makes little difference in the present case, but is introduced to make this table comparable with those already published.

* Ellis, 'Proc. Roy. Soc.,' A, vol. 138, p. 318 (1932).

† Ellis and Skinner, 'Proc. Roy. Soc.,' A, vol. 105, p. 60 (1924).

the symbol $K \rightarrow L_I L_{III}$, for example, meaning that an atom initially ionised in the K level makes a transition to a state where one electron is absent from the L_I level, and one from the L_{III} . The observed values for the five lower lines appear to be about 0.0025×10^5 volts; that is, 250 volts less than the calculated value. This energy difference, corresponding to about $1.7 \text{ H}\rho$, is only about twice the uncertainty in the measurement, but I think it is real since the measurements are more likely to be too high than too low. A difference between the measured and calculated values of this sign is also to be expected on theoretical grounds, since the calculated values for the final energy of the doubly ionised atom are obtained by using the two absorption energies (e.g., L_I and L_{III}) determined from X-ray spectra for singly ionised atoms. It appears likely from these measurements that it requires between 100 and 300 volts more energy to remove two electrons from the L state of the same atom than is needed to remove them from two separate atoms. The five upper lines in the table cannot be analysed with the same certainty, and it is not possible to be sure which M or N level is involved. No entries are therefore made in the last column.

Several points emerge from a consideration of the intensities. The transition $K \rightarrow L_I L_I$ gives rise to quite a strong line, and since both electrons come from the L_I state we can in this case specify the transition more exactly as ($L_I \rightarrow K$ and $L_I \rightarrow \infty$). The intensity of this transition is in sharp contrast to the non-existence of the single electron radiation transition $L_I \rightarrow K$. Robinson had previously noted the occurrence of $K \rightarrow L_I L_I$ lines, but they were so weak that measurement was very difficult. In the present experiments however, this line was among the stronger ones and can, in fact, be seen in the reproduction of the photographs in Plate 5 where it is marked with an arrow. This is direct evidence, if more were required, that we are here dealing with a non-radiation process involving two electrons simultaneously. It will be noticed that no line corresponding to $K \rightarrow L_{II} L_{II}$ was found, and if present its intensity must be put less than 0.2 on the above scale.

It has been already mentioned that the lines occurring in the radium (B + C) spectrum, but not in the thorium (B + C) spectrum would be either corpuscular X-ray lines of atomic number 84 or β -ray lines, and we may attempt to settle this ambiguity by using the information that has just been obtained about the characteristics of these corpuscular X-ray spectra. Table III shows five such lines that can be quite plausibly associated with atomic number 84. There is again a slight defect of energy of the same magnitude, 100 to 300 volts. The intensities, which, however, in this case depend only on visual

estimation, are not in entire agreement with those for atomic number 83, since in the present case the $K \rightarrow L_I L_I$ and $K \rightarrow L_I L_{II}$ transitions are considerably stronger than those for $K \rightarrow L_{II} L_{III}$ and $K \rightarrow L_{III} L_{III}$. This may

Table III.—Corpuscular X-ray Groups from Atomic Number 84.

H ρ	Estimated true intensity.	Energy volts $\times 10^{-5}$.	Origin	Energy calculated volts $\times 10^{-5}$	$E_{calc} - E_{meas}$ volts $\times 10^{-5}$
885.4	0.2	0 6480	$K \rightarrow L_{III} L_{III}$	0 6504	0 0015
867.2	0.3	0 6237	$K \rightarrow L_{II} L_{III}$	0 6260	0 0023
861.7	0.3	0 6163	$K \rightarrow L_I L_{II}$	0 6194	0 0031
844.0	0.0	0 5925	$K \rightarrow L_I L_{II}$	0 5950	0 0025
838.3	0.0	0 5849	$K \rightarrow L_I L_I$	0 5884	0 0035

be partly accounted for in the case of H ρ 838.3 by confusion with a weak $K \rightarrow L_{II} L_{II}$ transition of atomic number 83, which assumption would at the same time allow a possible explanation of the line H ρ 834.9 in thorium (B + C). However, it was very difficult to be sure of this line and the one next above it in the thorium (B + C) spectrum, and it is not worth while to pursue the matter further. It would appear that with these two exceptions, all the lines from thorium (B + C) are satisfactorily accounted for and no corpuscular X-ray spectrum was detectable under these conditions from Th C. C'' or Th C''. Pb, that is, atomic numbers 81 and 82. This is understandable from our general knowledge of the extent of the conversion of γ -rays in these two atoms.

There is one line, H ρ 890.8 from radium (B + C) which, both because of its intensity and because there is no analogous line in the corpuscular X-ray spectrum of atomic number 83, must be taken as a β ray associated with a γ -ray from either Ra B. C or Ra C. C'. The same argument applies to the top two lines in the thorium (B + C) spectrum given in Table I. For convenience these lines are collected in Table IV.

Table IV.— β -ray Groups in the Region of the Corpuscular X-ray Spectrum.

Ra (B + C)		Th (B + C)	
H ρ .	Energy volts $\times 10^{-5}$.	H ρ	Energy volts $\times 10^{-5}$
890.8	0 6592	968.3 962.2	0 7674 0.7587

It is very satisfactory to be able at last to clear up this region of the spectrum, and rather unexpectedly this investigation has yielded considerably more detailed information about these double electronic transitions than has been obtainable in the past by other methods. The slight energy defect owing to the double ionisation is too small to measure accurately, and is of minor importance, but the data about the intensities of the transitions appears much more interesting and it is hoped will provide material for checking a theoretical investigation of these processes.

I wish to acknowledge gratefully that much of the apparatus and radioactive material used in this research has been bought with grants from the Government Grant Committee of the Royal Society. I am also indebted to Professor Schlundt, of the University of Missouri, for the generous gift of some radio-thorium preparations which proved very useful in this work. I wish also to acknowledge the assistance I have received from Mr. R. Cole.

Summary.

By direct comparison, under suitable conditions, of the β -ray spectra of radium (B + C) and thorium (B + C) it has been found that certain lines are common to both. These must represent the corpuscular X-ray spectrum of an atom of atomic number 83, since the electronic structure of an atom of this atomic number is the only common feature in the two sources. The energies of these lines agree well with this hypothesis, and interesting data about the intensities of these double electronic transitions are obtained.

*The Concepts of Inverse Probability and Fiducial Probability,
Referring to Unknown Parameters.*

By R. A. FISHER, F.R.S

(Received November 3, 1932)

1 *Criticism of Dr. Jeffreys's Method*

In a paper published in these 'Proceedings'* Jeffreys puts forward a form of reasoning purporting to resolve in a particular case the primitive difficulty which besets all attempts to derive valid results of practical application from the theory of Inverse Probability

For a normally distributed variate, x , the frequency element may be written

$$df = \frac{h}{\sqrt{\pi}} e^{-h^2(x-\mu)^2} dx,$$

where μ is the mean of the distribution, and h the precision constant. For the convenience of the majority of statisticians who prefer to use the standard deviation, σ , of the distribution in place of the precision constant, we may note that

$$h^2 = \frac{1}{2\sigma^2}.$$

and that this substitution may be made at any stage of the argument.

Jeffreys considers the question. What distribution *a priori* should be assumed for the value of h , regarding it as a variate varying from population to population of the *ensemble* of populations which might have been sampled? He sets forth a proof to the effect that this distribution must be of the form

$$df \propto \frac{1}{h} dh \propto \frac{1}{\sigma} d\sigma. \quad (1)$$

That there should be a method of evolving such a piece of information by mathematical reasoning only, without recourse to observational material, would be in all respects remarkable, especially since the same principle of reasoning should, presumably, be applicable to obtain the distribution *a priori* of other statistical parameters. The proof can, however, scarcely in any case establish all that is claimed, since there is nothing to prevent our setting up an

* 'Proc. Roy. Soc.,' A, vol. 138, p. 48 (1932).

artificially constructed series of populations having any chosen distribution of h , such as

$$df = ae^{-ah} dh,$$

in which case Jeffreys's reasoning would certainly lead to a false conclusion. Moreover, Jeffreys himself seems to feel some doubt as to the general validity of the distribution (1), for he says: "The solution must break down for very small h . . . and for large h . . ."; though he does not indicate in what way his mathematical proof fails for these parts of the range.

The principle he uses rests on the fact that, if we have three independent observations from the same population, the probability that the last of the three shall be intermediate between the first two must be exactly $1/3$. This fact is sufficiently obvious if all three observations are made afresh for each test, but we may note at once that, for any particular population, the probability will generally be larger when the first two observations are far apart than when they are near together. This is important since, as will be seen, the fallacy of Jeffreys's argument consists just in assuming that the probability shall be $1/3$, *independently of the distance apart of the first two observations*.

Since the property used is possessed by all distributions, and therefore amongst others by normal distributions having all possible values of h , it might be argued *a priori* that its existence could not possibly be used to throw light upon the frequency distribution of h . It is, in fact, only the illegitimate inference stressed above which makes such further inferences appear to be possible.

Jeffreys's argument proceeds in four steps:—(a) the probability of the first two observations having assigned values is expressed in terms of the two parameters, the mean and the precision constant, of the population; (b) introducing the probability *a priori* of the two parameters having assigned values, their posterior probability of having them is obtained; (c) the probability of the third observation having an assigned value is found and integrated over all possible values of the parameters; (d) the expression so obtained is equated to $1/3$, *without averaging it for all possible pairs of initial observations*; had this essential step been taken, the equation would have degenerated to an identity for all possible distributions *a priori*.

The argument as developed involves the assumption of a particular distribution *a priori* of the mean; it will be advantageous, therefore, in order to make clear the exact point at which a fallacy is introduced to exhibit the analysis without this assumption.

Let the population sampled have mean μ , and precision constant h then the probability that the first two observations should lie in the ranges dx_1, dx_2 , is

$$\frac{h^2}{\pi} e^{-h^2[(x_1-\mu)^2 + (x_2-\mu)^2]} dx_1 dx_2$$

Let the larger of these observations be $u + v$ and the smaller $u - v$ then the frequency element may be re-written

$$\frac{2h^2}{\pi} e^{-2h^2[(u-\mu)^2 + v^2]} du dv$$

If now $f(h) dh$ is the prior probability that h lies in the range dh , the probability of assigned values for u, v and h will be

$$\frac{2h^2 f(h)}{\pi} e^{-2h^2[(u-\mu)^2 + v^2]} du dv dh,$$

and that for assigned values of u, v, h , and the third observation, x_3 , will be

$$\frac{2h^3 f(h)}{\pi^{3/2}} e^{-2h^2[(u-\mu)^2 + v^2] - h^2(x_3-\mu)^2} du dv dh dx_3.$$

Writing $x_3 = u + c$, since the magnitude of c determines whether or not the third observation lies between the others, we may now average over all values of u , by integrating with respect to that variate from $-\infty$ to ∞ . This gives

$$\frac{2h^2 f(h)}{\pi\sqrt{3}} e^{-2h^2 v^2 - h^2 c^2} dv dh dc, \quad (2)$$

in which μ , the mean of the population, has disappeared, showing that its value, and therefore its distribution, *a priori* is irrelevant. Equation (2) corresponds with Jeffreys's equation (3) (p. 49), save that the differential elements, dv and dc , have been retained.

For any given value of v , therefore, the probability of the third observation lying between the first two will be found by integrating (2) with respect to c and h , and evaluating the frequency with which c is less than v .

Writing

$$\alpha(x) = \frac{1}{\sqrt{\pi}} \int_{-x}^x e^{-t^2} dt,$$

the integral with respect to c from $-v$ to v is

$$\frac{2hf(h)}{\sqrt{2\pi}} \cdot \sigma(hv\sqrt{\frac{3}{2}}) e^{-2h^2 v^2} dv dh. \quad (3)$$

while the integral over all values is

$$\frac{2hf(h)}{\sqrt{2\pi}} e^{-2hv} dv dh, \quad (4)$$

it is by equating the integral of (4) with respect to h , to three times that of (3) for every possible value of v , that Jeffreys obtains a unique form for $f(h)$.

All that we really know, however, is that on the average of all values of v , the probability is exactly one-third. We should, therefore, integrate (3) and (4) with respect to v , over all values from 0 to ∞ . For (3) we have, as is also shown by Jeffreys (p. 50),

$$\frac{1}{3} f(h) dh,$$

and for (4),

$$f(h) dh,$$

so that the fact that the probability is just one-third is assured, irrespective of h , and therefore for every frequency element of that variate independently. It is merely because the substitution $f(h) = 1/h$ makes integration with respect to h equivalent to integration with respect to v , that this special distribution *a priori* satisfies Jeffreys's condition

2 The Method of the Fiducial Distribution.

An altogether different approach may perhaps make clear why the consideration of proportional rather than absolute increments in the variables h and σ should lead to simpler mathematical consequences. If from a series of n' observations, x , drawn from a normal population with standard deviation σ , or variance σ^2 , we make an estimate of this variance, based on the sum of the squares of the deviations of the observations from their mean, in the form

$$s^2 = \frac{1}{n' - 1} \sum (x - \bar{x})^2,$$

then the estimate s^2 is known* to be distributed, in random samples, in a manner, which depends only on the unknown parameter σ of the sampled population, and is specified by the formula

$$df = \frac{1}{\frac{n' - 1}{2}} \left\{ \frac{(n' - 1) s^2}{2\sigma^2} \right\}^{\frac{1}{2}(n' - 1)} e^{-\frac{(n' - 1) s^2}{2\sigma^2}} d \left\{ \frac{(n' - 1) s^2}{2\sigma^2} \right\}.$$

The distribution of the ratio s/σ is thus independent of all unknown parameters, and is calculable solely from the number of observations in the sample, or, to

* Fisher, 'Metron,' vol. 5, p. 90 (1926).

cover a more general class of cases, from the number of degrees of freedom of the residuals, from which the variance is estimated. From this distribution, which has been sufficiently tabulated, we can assert, without reference to any unknown quantities, or to their unknown probabilities *a priori*, with what frequency any particular value of the ratio s/σ will be exceeded in random samples; or, what is often more convenient, for any given probability, such as 0.99 or 0.01, what is the value of the ratio which will be exceeded with this probability. Thus for 10 degrees of freedom, such as we should have from a sample of 11 observations of a normally distributed variate, it is known that the ratio will exceed 2.3209 in 1 per cent. of cases,* and will fall short of 0.2558 in another 1 per cent. If, therefore, we designate by $s_{0.01}(\sigma)$ that value of s which, for a given σ , will be exceeded in exactly 1 per cent. of trials, we have the simple relationship

$$s_{0.01}(\sigma) = \sigma \times 2.3209,$$

and this value of s we may term the 1 per cent. value of s for the value of σ considered. If now we designate by $\sigma_{0.99}(s)$ that value of σ for which s is the 1 per cent. value, then evidently

$$\sigma_{0.99}(s) = s/2.3209,$$

and we may term this value of σ the 99 per cent. value of σ for the given value of s . Evidently where s is known this value of σ is also known. Moreover, the inequality

$$s > s_{0.01}(\sigma), \quad (5)$$

is equivalent to the inequality,

$$\sigma < \sigma_{0.99}(s), \quad (6)$$

since for any value of the probability chosen the corresponding values of s and σ increase together from 0 to ∞ .

Now we know that the inequality (5) will be satisfied in just 1 per cent. of random trials, whence we may infer that the inequality (6) will also be satisfied with the same frequency. Now this is a probability statement about the unknown parameter σ , easily translatable into an equivalent statement about the unknown parameter h , in terms of known quantities only. For example, if s is an estimate derived from 10 degrees of freedom we know that σ has a probability 0.01 of being less than $s/2.3209$, and in like manner we know its probability of falling between any other assigned limits. Probability statements of this type are logically entirely distinct from inverse probability

* Fisher, "Statistical Methods for Research Workers," Table III, 4th ed. (1932)

statements, and remain true whatever the distribution *a priori* of σ may actually be. To distinguish them from statements of inverse probability I have called them statements of fiducial probability. This distinction is necessary since the assumption of a given frequency distribution *a priori*, though in practice always precarious, might conceivably be true, in which case we should have two possible probability statements differing numerically, and expressible in a similar verbal form, though necessarily differing in their logical content. The probabilities differ in referring to different populations; that of the fiducial probability is the population of all possible random samples, that of the inverse probability is a group of samples selected to resemble that actually observed.

It is the lack of this distinction that gives a deceptive plausibility to the frequency distribution *a priori*

$$df = d\sigma/\sigma = d(\log \sigma).$$

For this particular distribution *a priori* makes the statements of inverse and of fiducial probability numerically the same, and so allows their logical distinctness to be slurred over. It is, moreover, as Jeffreys, by his references to large and small values of h , clearly perceives, an impossible distribution *a priori*, since it gives a zero probability *a priori* for h lying between any finite limits, however far apart. In the fiducial form of statement this difficulty does not occur.

3. Summary.

(1) The argument of Jeffreys in favour of a particular frequency distribution *a priori* for the precision constant of a normally distributed variate rests on the fallacy that the probability of the last of three observations, lying between the previous two, should be one-third, *irrespective of the distance apart of the two previous observations*.

(2) The apparent simplicity of the results of assuming this particular distribution *a priori* rests on the fact that the *inverse* and the *fiducial* probability statements about the unknown parameter are thereby made to coincide, though logically they are entirely distinct. This particular distribution *a priori* is, however, not only hypothetical but unacceptable as such, since it implies that all ranges of values of the parameter covering finite ratios, however great, are infinitely improbable.

On the Foundations of the Electron Wave Equation.

By S. R. MILNER, F.R.S.

(Received November 24, 1932.)

1. There are two problems which are fundamental to wave mechanics—that of deducing from first principles the properties of the wave field of ψ , by means of which, on modern theory, the mechanical properties of matter are to be described, and that of formulating a logical description of the properties of matter in terms of ψ . The former only of these problems is discussed in this communication. In spite of many valuable papers that have been published on the subject of Dirac's remarkable wave equation,* the derivation of the equation still seemed (to the present writer, at any rate,) to include some obscurities which could perhaps be removed. To some extent this is owing to the development of the equation, as a matter of historical necessity, having come about by successive extensions to classical mechanics; so that some difficulties have been produced by the fundamental relativity considerations having been introduced into the theory at a late stage, instead of in their proper place at the beginning. In what follows, by treating the problem from the beginning as a four-dimensional one, a deduction of the wave equation free from empirical steps is, I think, obtained, while also certain new features of the equation are brought to light.

2. *The Principle of Action.*—The method of four-dimensional mechanics is to assume that the motions of bodies in the world can be represented by "tracks," or curved lines, in a "fourfold." (This last term will be used here to mean a four-dimensional manifold with Euclidian geometry, i.e., in which†

$$ds^2 = dx_i^2 \quad (i = 1, \dots, 4). \quad (1)$$

Uniform motion in the world is represented by straight line tracks in the fourfold, and the "classical relativity" laws of motion are derived by formulating the simplest mathematical specification of curved tracks which will represent the non-uniform motions of bodies that are usually observed in the world.

Two courses are open to us. (1) We can modify the geometry assumed in equation (1), so that a mathematically straight track (i.e. its length obeys

* 'Proc. Roy. Soc.,' A, vol. 117, p. 610 (1928).

† The usual summation convention is employed up to equation (15)

a stationary principle) still continues to represent the non-uniform motion of a particle, this is the method of general relativity (2) We can retain the fourfold with unaltered geometry, and specify a curved track which represents the observed motion by weighting each element of its length so that the integral weighted length between two points is stationary; this is the method of "least action." Both these methods of describing the motions of bodies must be considered equally logical, when one remembers that a manifold (even when it is called "space-time") is not the actual world, but a mental concept, in which real phenomena are represented symbolically. One may indeed infer that equations resulting from the one method should be convertible into those of the other.

The second method is more suitable to the present object, and adopting it we naturally make the weighting function the simplest which will serve the purpose. In order of lessening simplicity we might take—

- (1) a scalar function of position in the fourfold, $U(x_1, \dots, x_4)$;
- (2) a function of position, and also of the angle made by the track s with a given direction σ , which is also a function of position. (Writing

$$s_k = \frac{dx_k}{ds} \quad (2)$$

for the direction cosines of the track, and σ_k for those of the given direction, the simplest form is $U\sigma_k s_k$. Here $\sigma_k s_k$ is the cosine of the angle between s and σ at each point);

- (3) a function of position and of the angles made by s with two varying directions, σ and ρ , given at each point, the simplest form being $U\sigma_k \rho_k s_k s_k$.

It appears that the second form is what is required to express the motion of a charged particle in an electromagnetic field. We separate it into two parts, postulating one constant (otherwise the development would not give rise to the idea of a particle), and write it

$$m + V_0 \sigma_k s_k = m + V_k s_k,$$

where V_k is a vector function of position.

The law of stationary action now takes the form

$$\delta A = 0, \quad (3)$$

where

$$A = \int_P^Q (m + V_k s_k) ds, \quad (4)$$

and in the variation, the metric (1) of the fourfold is understood to be unaltered. We get from (4)

$$\delta A = \int_P^Q \left\{ \frac{\partial V_k}{\partial x_i} s_k \delta x_i + V_i \delta s_i + (m + V_k s_k) \frac{d}{ds} (\delta s) \right\} ds,$$

in which (obtained by varying (2) and (1)) we have

$$\delta s_i = \frac{d}{ds} (\delta x_i) - s_i s_k \frac{d}{ds} (\delta x_k),$$

$$\frac{d}{ds} (\delta s) ds = \delta ds = s_i \frac{d}{ds} (\delta x_i) ds.$$

Substituting these respectively in the second and third terms, and integrating by parts all the terms containing d/ds , we get

$$\delta A = \left[(ms_i + V_i) \delta x_i \right]_P^Q + \int_P^Q \left\{ \frac{\partial V_k}{\partial x_i} s_k - \frac{dV_i}{ds} - \frac{d}{ds} [(ms_i)] \right\} \delta x_i ds. \quad (5)$$

For this to be zero, subject to no variation at the limits,

$$\frac{d}{ds} (ms_i + V_i) = s_k \frac{\partial V_k}{\partial x_i},$$

which may be written (since $\frac{dV_i}{ds} = \frac{\partial V_i}{\partial x_k} \frac{dx_k}{ds}$)

$$\frac{d}{ds} (ms_i) = s_k \left(\frac{\partial V_k}{\partial x_i} - \frac{\partial V_i}{\partial x_k} \right). \quad (6)$$

(6) expresses the classical law of motion of an electron in an electromagnetic field. It was first obtained (in another way) by Born* in 1909.

To reduce all formulæ in this paper to terms of space and time, write

$$\left. \begin{aligned} x_4 &= ict, \quad m = -im_0 c, \\ V_k &= \frac{e}{c} A_k \quad (k = 1, 2, 3), \quad V_4 = i \frac{e}{c} \phi, \end{aligned} \right\} \quad (7)$$

where m_0 is the rest-mass of the electron, A_k and ϕ are the vector and scalar potentials. We then get, for the action of a stationary electron at an electrostatic potential ϕ ,

$$A = \int (m_0 c^2 - e \phi) dt.$$

Our A is thus a positive quantity of dimensions [energy \times time].

* 'Ann. Physik,' vol. 28, p. 571 (1909).

3. *The Action Equation.*—If we arbitrarily fix the action to be zero over a hypersurface (three-dimensional region), which is taken as containing the starting points P of a family of tracks obeying (6), the actions A at the end points Q form a function of position which, by (5), satisfies the equation

$$\frac{\partial A}{\partial x_i} = ms_i + V_i. \quad (8)$$

As equations of this type are fundamental both in classical and in wave mechanics, the meaning and the use which is made of (8) merit a close consideration. We note :—

(1) It is an essential feature of (8) that A is a function of position, and that the right-hand side has been split up so as to express explicitly in it a vector ms_i of constant magnitude. ms_i is the "momentum vector," which defines the momentum and energy of a particle when it is describing a straight track, and strictly V_i is the vector representing the additional momentum and energy which have to be ascribed to the particle in virtue of the curvature of its track. If we write

$$g_i = ms_i + V_i,$$

(8) states only that the total momentum vector g_i of a moving particle is the gradient of a function of position, or that $g_i dx_i$ is a perfect differential. By choosing V_i suitably this could be made to apply to *any* track, so that, from this point of view, the equation contains no more than a definition of what has to be taken as the momentum vector in order to obtain a consistent mechanical scheme. In practice, however, (8) contains much more than a definition; it sums up a physical discovery, for it implies that when g_i is split up into a vector ms_i of suitably chosen constant magnitude m^2 , and the remainder V_i , V_i has not to vary from problem to problem to produce agreement with experiment, but remains the same simple function of position, and describes, in fact, an electromagnetic field.

(2) In this case, i.e., V_i being given, (8) is neither an equation of definition nor a real differential equation, but a relation between A and s_i which lays a restriction on the permissible corresponding values of each. On the one hand, $(ms_i + V_i)dx_i$ must be a perfect differential dA , and on the other, $\partial A/\partial x_i - V_i$ must be a vector of constant magnitude m^2 . This fixes both s_i and A.

(3) (8) sums up in one formula the equations giving the definition of action (4), the principle of stationary action (3), and the classical law of motion (6), for its substitution reduces each equation to an identity.

Since $s_i^2 = 1$, (8) may be transformed into a real differential equation (i.e., one expressing the gradient of A in terms of known functions) by squaring and adding the four component equations. This gives

$$\left(\frac{\partial A}{\partial x_i} - V_i \right)^2 = m^2. \quad (9)$$

In any particular solution of (9) A may be given an arbitrary value, say zero, over any chosen hypersurface, and when this is done its value becomes definite at every point of the fourfold. In some places this value will be real, but in others, since (9) is quadratic in the gradient of A, it will be complex.

There will be certain loci over which A is constant ; if A were real everywhere, these would, like the initial region, be hypersurfaces, but generally the existence of complex values for A restricts the loci to less extended regions. If τ stands for distance measured along the normal to a locus of constant action, so that τ is the line of the action gradient $dA/d\tau$, (8) may be written

$$ms_i = \frac{dA}{d\tau} \tau_i - V_0 \sigma_i,$$

and, in classical mechanics, the permissible tracks of particles can be constructed from this equation. (It is, of course, only applied where the A obtained by solving (9) is real.) We see that the tracks are not perpendicular to the loci of constant action, but have the direction of the resultant of $dA/d\tau$ along τ and $-V_0$ along σ .

It is now recognised that the ascription to particles of such determinate tracks does not succeed in giving an adequate account of their behaviour when they are very small, and we are faced with the problem of finding some other concept which will describe the phenomena in a more satisfactory way.

4 *The Wave Equation* (1).—In wave mechanics instead of the field of action A , a function ψ , which is regarded as forming a field of waves, is contemplated. It is therefore necessary to discuss the properties of a field of waves in a four-fold. Here, properties such as frequency and velocity clearly do not come in, they are non-invariant quantities manufactured to suit the space and time scales of a particular observer. A wave train must be considered as a disturbance which is a function of position, x_1, \dots, x_4 , only. Its essential feature (like that of the instantaneous view of a wave train in three dimensions) is that the "total disturbance" ψ at any point can be split up into two factors, the "non-harmonic disturbance" or *amplitude* ϕ , and the "harmonic factor" or *phase* χ . Thus in a field of waves

$$\psi = \phi \chi, \quad (10)$$

where ϕ and χ are also functions of position. There will be in the fourfold loci over which the phase is constant ; the line of action τ of the gradient of χ is normal to these loci, and, in passing along τ , χ varies harmonically, to return to its original value after a distance which, if the conditions were constant, would be called the wave-length λ . In general, however, the conditions will vary along τ , and the variation of χ must be expressed by a differential relation which involves only the conditions at the point in question. We therefore take as the fundamental relation defining λ (and also the properties of χ)

the equation

$$\frac{d\chi}{d\tau} = -\frac{2\pi i}{\lambda} \chi. \quad (11)$$

When λ is constant, this agrees with the usual definition, in general λ is a function of position, and also of the direction τ_i of the wave normal.* Integrating (11), and omitting the constant of integration, which can always be taken over into ϕ , we get

$$\chi = e^{-2\pi i \int \frac{d\tau}{\lambda}} = e^{-i\theta}, \text{ say.} \quad (12)$$

The postulation we have made that in a wave field χ , and therefore θ , must be a function of position requires that a stationary principle $\delta\theta = 0$ shall be satisfied for the line τ . The calculation of the consequences is exactly similar to that of section 2, and gives for the results corresponding to (8) and (9)

$$\frac{\partial\theta}{\partial x_i} = \frac{2\pi}{\lambda} \tau_i, \quad \left(\frac{\partial\theta}{\partial x_i}\right)^2 = \left(\frac{2\pi}{\lambda}\right)^2. \quad (13)$$

As regards the amplitude, while ϕ in simple cases might be considered to be a scalar function of position, in general it must be regarded as a vector. When ϕ is a vector, however, we must postulate that the same phase factor apply to each component, for if this were not so we should automatically decompose the field into a number of waves with different wave-lengths. We shall consequently write for the simplest wave disturbance, which cannot be further decomposed, the *vector* equation

$$\psi = \phi e^{-i\theta}. \quad (14a)$$

ψ is necessarily complex; its conjugate is

$$\bar{\psi} = \bar{\phi} e^{+i\theta}, \quad (14b)$$

where $\bar{\phi}$ is the conjugate of ϕ , which may also be complex.

A differential relation satisfied by ψ can now be obtained. From (14a) we get

$$\frac{\partial\psi}{\partial x_i} = \left(\frac{\partial \log \phi}{\partial x_i} - i \frac{\partial\theta}{\partial x_i}\right) \psi,$$

which may be written

$$i \left(\frac{\partial}{\partial x_i} - \frac{\partial \log \phi}{\partial x_i}\right) \psi = \frac{\partial\theta}{\partial x_i} \psi. \quad (15a)$$

* The latter assumption does not appear to be necessary for electron waves, and is therefore not made here.

Similarly from (14b),

$$-i \left(\frac{\partial}{\partial x_i} - \frac{\partial \log \bar{\phi}}{\partial x_i} \right) \bar{\psi} = \frac{\partial \theta}{\partial x_i} \bar{\psi}. \quad (15b)$$

We can eliminate $\partial \theta / \partial x_i$ by multiplying and summing, but since these equations will be used later in connection with matrices, where the summation convention is inconvenient, the convention will henceforward be dropped, to avoid confusion with the preceding formulæ, Greek letters will be used for suffixes. Let

$$\begin{aligned} r_\alpha &= i \left(\frac{\partial}{\partial x_\alpha} - \frac{\partial \log \phi}{\partial x_\alpha} \right), \\ \bar{r}_\alpha &= -i \left(\frac{\partial}{\partial x_\alpha} - \frac{\partial \log \bar{\phi}}{\partial x_\alpha} \right), \end{aligned} \quad (\alpha = 1, \dots, 4). \quad (16)$$

The point about these operators which becomes of importance later is that, when r_α acts on ψ and \bar{r}_α on $\bar{\psi}$, in each case the complex operation is equivalent to multiplication by the same factor. Thus, by (15),

$$r_\alpha \psi = \frac{\partial \theta}{\partial x_\alpha} \psi, \quad \bar{r}_\alpha \bar{\psi} = \frac{\partial \theta}{\partial x_\alpha} \bar{\psi}.$$

Taking the product and adding the four equations,

$$\Sigma_\alpha (\bar{r}_\alpha \bar{\psi}) (r_\alpha \psi) = \Sigma_\alpha \left(\frac{\partial \theta}{\partial x_\alpha} \right)^2 \bar{\psi} \psi = \left(\frac{2\pi}{\lambda} \right)^2 \bar{\psi} \psi \quad (17)$$

by (13). Let

$$r_5 = \bar{r}_5 = i \frac{2\pi}{\lambda}. \quad (18)$$

Then (17) can be written still more shortly

$$\Sigma_5 (\bar{r}_\alpha \bar{\psi}) (r_\alpha \psi) = 0, \quad (19)$$

the summation extending over the values 1, . . . 5 of α . In order to develop (19) further it will be useful to discuss first the geometrical meaning of complexity in the co-ordinates of vectors.

5. *Complex Co-ordinates.*—In geometry the idea of distance always makes its first appearance in the form of a scalar quantity, which is usually represented as a square, say s_0^2 . We shall here call s_0^2 (not s_0) the "magnitude" of the distance-vector; it is always real, and in space-time it may be positive or negative, depending on the direction of the vector with reference to the time axis. We can obtain from s_0^2 two "vector components," contravariant \bar{x} and covariant x , in an infinity of different ways, by considering it as the

product of two factors,

$$s_0^2 = \bar{x}x. \quad (20)$$

When s_0^2 is positive, the simplest type of factorisation is to choose the components equal, $\bar{x} = x = s_0$. When s_0^2 is negative, we have the choice of making \bar{x} and x real and of opposite sign, or imaginary and of the same sign. But the virtue of these is only that they are the simplest methods of decomposition. The choice of one component, say \bar{x} , may always be quite arbitrary, when it has been chosen x is fixed by the relation (20). There is, therefore, no logical difficulty in decomposing s_0^2 into a complex vector component and its conjugate, putting

$$s_0^2 = a^2 + b^2, \quad \bar{x} = a + ib, \quad x = a - ib,$$

where either a or b is arbitrary.* Further, seeing that in space-time we already have to admit the existence of real and imaginary vector components (space-like and time-like), there is no great extension of the imagination required to contemplate a component (or a line) as possessing part space-like and part time-like properties simultaneously, when it is useful to do so.

On the same lines, s_0^2 can also be still further decomposed into a sum of products, the factors of which are its "co-ordinate components." Thus

$$s_0^2 = \sum_4 x^a x_a,$$

where the x^a , x_a may be real and equal (Euclidian geometry), simple (*i.e.*, either real or imaginary) and unequal (this gives the geometry of the general relativity theory when they are infinitesimals), or complex. Geometrically considered, the fixing of the terms $x^a x_a$ associates the s_0^2 with a particular direction in the manifold. These remarks apply equally to vectors generally, *i.e.*, when the magnitude is not specifically associated with the idea of distance. When the vector components are complex, we shall write them \bar{V} (contravariant) and V (covariant), and the co-ordinate components \bar{V}_a and V_a , the magnitude being

$$V_0^2 = \bar{V}V = \sum_4 \bar{V}_a V_a. \quad (21)$$

6. *Complex Rotations.*—Taking for simplicity a plane, consider all the types of rotation of axes which can be imagined in it. A rotation may be defined as a transformation of co-ordinates of the form

$$\begin{aligned} x'^1 &= \{\cos \theta + f_1(x^1, x^2) \sin \theta\} x^1, \\ x'^2 &= \{\cos \theta + f_2(x^1, x^2) \sin \theta\} x^2, \end{aligned}$$

* The reason for putting the "conjugate stroke" on the factor with $+$, instead of on that with $-$ (as would be more natural) is to make the formulæ for ψ agree with the usual forms.

where θ is a real angle, and f_1, f_2 must be such that a rotation through θ followed by one through $-\theta$ leaves the co-ordinates unchanged. It is clear that no coefficient other than 1 can be attached to the $\cos \theta$, and that f_1, f_2 must be homogeneous functions of zero dimensions. We can apply the criterion about successive rotations to determine the possible values of f_1 and f_2 , and on doing so, and expanding f_1 and f_2 in powers of x^2/x^1 , we readily find that there are only four pairs of values permissible. These give the transformations labelled "contravariant" in the following table, in which c and s are written for $\cos \theta$ and $\sin \theta$. The corresponding covariant transformations are obtained from them by applying the usual tensor laws, viz

$$x'_\alpha = \sum_\beta \frac{\partial x^\beta}{\partial x'^\alpha} x_\beta$$

Contravariant.	Covariant	
$x'^1 = cx^1 + sx^2$	$x'_1 = cx_1 + sx_2$	} (i)
$x'^2 = cx^2 - sx^1$	$x'_2 = cx_2 - sx_1$	
$x'^1 = cx^1 + isx^2$	$x'_1 = cx_1 - isx_2$	} (ii)
$x'^2 = cx^2 + isx^1$	$x'_2 = cx_2 + isx_1$	
$x'^1 = (c + is)x^1$	$x'_1 = (c - is)x_1$	} (iii)
$x'^2 = (c - is)x^2$	$x'_2 = (c + is)x_2$	
$x'^1 = (c + is)x^1$	$x'_1 = (c - is)x_1$	} (iv)
$x'^2 = (c + is)x^2$	$x'_2 = (c - is)x_2$	

} (22)

The transformations (22) may be written in matrix form. Let

$$R_1 = \begin{bmatrix} 0 & -1 \\ 1 & 0 \end{bmatrix}, \quad R_2 = i \begin{bmatrix} 0 & 1 \\ 1 & 0 \end{bmatrix}, \quad R_3 = i \begin{bmatrix} 1 & 0 \\ 0 & -1 \end{bmatrix}, \quad R_4 = i \begin{bmatrix} 1 & 0 \\ 0 & 1 \end{bmatrix}. \quad (23)$$

Then the matrix equations

$$\left. \begin{aligned} [x'^1 \ x'^2] &= [x^1 \ x^2] (c + R_\mu s), \\ \begin{bmatrix} x'_1 \\ x'_2 \end{bmatrix} &= (c - R_\mu s) \begin{bmatrix} x_1 \\ x_2 \end{bmatrix} \end{aligned} \right\}, \quad (24)$$

give them all when μ is written successively 1, ... 4.* (24) applies to the rotation of any vector, its contravariant co-ordinate components being represented by a single row matrix, and its covariant by a single column one

* In matrix multiplication, $(ab)_{\mu\nu} = \sum_\sigma a_{\mu\sigma} b_{\sigma\nu}$, μ being the row, and ν the column suffix.

We may note about these rotations* :—

(1) If we start with the contravariant and covariant co-ordinates real and equal, the rotations (ii), (iii), (iv) convert them into complex co-ordinates conjugate to each other. It can readily be shown that this relation of conjugacy is unaffected by all further transformations by rotations (i), ... (iv), so that the assumption that contra- and co-variant components are conjugate complexes will always give consistent results. We may, therefore, write generally as the rotation transformation of conjugate vectors

$$\left. \begin{aligned} \bar{V}' &= \bar{V} (c + R_\mu s) \\ V' &= (c - R_\mu s) V \end{aligned} \right\}, \quad (25)$$

where \bar{V} and V stand respectively for the single row and single column matrices of \bar{V}_α and V_α .

(2) The matrix R_μ by itself indicates rotation through 90° . $R_{2, 3, 4}$ convert real axes into imaginaries, R_2 changes the direction as well. All four R_μ have the property

$$(R_\mu)^2 = -1, \quad (26)$$

so that in all cases a 90° rotation when repeated reverses the axes without other effects.

(3) In consequence of (26), (25) gives

$$\bar{V}'V' = \bar{V}V = V_0^2$$

The magnitude of a vector is unchanged by any rotation. It may be observed also that a rotation does not affect the metrical character of the plane (*e.g.*, whether its geometry is Euclidian or hyperbolic). The metric is fixed by the way in which the magnitude of the distance-vector $s_0^2 = \bar{x}x$ depends on direction, and this is not altered by a rotation.

(4) The first three matrices anti-commute, viz.,

$$R_\alpha R_\beta = -R_\beta R_\alpha \quad (\alpha, \beta = 1, 2, 3, \quad \beta \neq \alpha). \quad (27)$$

These are the "spin" matrices of Pauli; in Eddington's terminology, they form a "perpendicular set."

* The meaning of complex rotations can be seen in a better perspective by remembering that, as explained in section 5, co-ordinates are manufactured quantities, and a rotation of axes is simply a device, of which we make a geometrical picture, for changing them into a more convenient form. When vector components are assumed complex, with the result that their measures $a + ib$ may differ in "composition" (say, a/b) as well as in size and direction, the ordinary geometrical picture of a rotation has to be enlarged.

If we apply any one of the rotations R_μ to one co-ordinate plane (e.g., x^1x^4) of a fourfold, and a $+$ or $-$ rotation of the same type through an equal angle to the "dual" plane x^2x^3 , we obtain a set of transformation equations which again can be represented in matrix form. Doing this for all possible planes and for the four types of rotation, we arrive (putting $0 = 90^\circ$) at a set of the matrices E_μ ($\mu = 1, \dots 16$) which Eddington* discovered and introduced into the wave theory.

To represent these and show their relation to the R_μ , a shortened notation for a particular rotation matrix is used. The numbers of the columns in which the 1's occur in successive rows are written in order, with strokes placed above them when the signs of the 1's concerned are negative, e.g., the matrix

$$\begin{bmatrix} 0 & -1 & 0 & 0 \\ 1 & 0 & 0 & 0 \\ 0 & 0 & 0 & -1 \\ 0 & 0 & 1 & 0 \end{bmatrix} \text{ is written } (\bar{2}1\bar{4}3).$$

The notation gives a compact representation of covariant equations†; thus,

$$x' = (\bar{2}1\bar{4}3)x,$$

stands for

$$x_1' = -x_2, \quad x_2' = x_1, \quad x_3' = -x_4, \quad x_4' = x_3.$$

With this convention the following table shows the E_μ which are obtained by applying the plane rotations $R_1, \dots R_4$ to the three sets of dual planes in a fourfold.

Planes of simultaneous rotation	E_μ .	
	Rotation applied	
	R_1 .	R_2 .
$+14, +23$	$(\bar{4}3\bar{2}1) \quad ab$	$\bar{1}(43\bar{2}1) \quad bf$
$+14, -23$	$(\bar{4}321) \quad df$	$\bar{1}(\bar{4}321) \quad ad$
$+24, +31$	$(\bar{3}4\bar{1}2) \quad ac$	$\bar{1}(\bar{3}412) \quad ae$
$+24, -31$	$(\bar{3}412) \quad ef$	$\bar{1}(\bar{3}4\bar{1}2) \quad cf$
$+34, +12$	$(\bar{2}1\bar{4}3) \quad bc$	$\bar{1}(\bar{2}143) \quad cd$
$+34, -12$	$(\bar{2}143) \quad de$	$\bar{1}(\bar{2}1\bar{4}3) \quad be$
	R_3 .	R_4 .
$+14, +23$	$\bar{1}(12\bar{3}4) \quad af$	$\bar{1}(1234)$
$+14, -23$	$\bar{1}(1234) \quad bd$	$\bar{1}$
$+24, +31$	$\bar{1}(1234) \quad ce$	$\bar{1}$

† These matrices, as well as those corresponding to R_3 and R_4 rotations in other planes, are simply repetitions of the four enumerated.

* Eddington, 'Proc. Roy. Soc.,' A, vol. 121, p. 524 (1928)

† The same rule holds for the conjugate equations when the E_μ are imaginary (e.g., $\bar{x}' = \bar{x}(\bar{2}1\bar{4}3)$), but the signs of the $[\bar{x}_a]$ in the fully written equations must be reversed when the E_μ are real.

Eddington has shown that sets of five E_μ can be picked out which are mutually "perpendicular." There are six such sets; calling them $a, \dots f$, in the table the two sets to which each E_μ (except E_{16}) belongs are shown by the letters accompanying it. To distinguish the members of a perpendicular set from the remaining 11 E_μ , we shall use for them the suffixes α and β , so that in a set

$$E_\alpha E_\beta = -E_\beta E_\alpha \quad (\alpha, \beta = 1, \dots 5, \quad \beta \neq \alpha). \quad (28)$$

The general features of the E_μ are similar to those of the plane rotations R_μ . As with the R_μ ,

$$E_\mu^2 = -1 \quad (\mu = 1, \dots 16). \quad (29)$$

The E_μ and the R_μ each form an exhaustive list of rotations (of the type considered) which can be applied to the manifold without changing its metrical character. The number of perpendicular rotations exceeds by one the number of dimensions of the manifold in each case.

7. *A Theorem in Factorisation.*—Let P_0^2 and Q_0^2 be any real scalar functions of position. Decomposing P_0^2 into co-ordinate components, and Q_0^2 into vector components (these are equivalently single row (\bar{Q}) and single column (Q) four-term matrices), we can write

$$\left. \begin{aligned} \text{Let} \quad P_0^2 &= \Sigma_4 \bar{P}_\alpha P_\alpha, \quad Q_0^2 = \bar{Q} Q. \\ \bar{P}_5 &= P_5 = iP_0. \end{aligned} \right\} \quad (30)$$

Then the equation

$$\Sigma_5 \bar{P}_\alpha P_\alpha = 0, \quad (31)$$

and with it

$$\Sigma_5 \bar{P}_\alpha \bar{Q} P_\alpha Q = 0, \quad (32)$$

states a mere identity, equivalent to (30). The identity (32) is not affected by inserting, in each of the 5 terms, between \bar{Q} and P_α the product of any four-square matrix A_α and its reciprocal, hence

$$\Sigma_5 \bar{P}_\alpha \bar{Q} A_\alpha^{-1} A_\alpha P_\alpha Q = 0. \quad (33)$$

We now inquire into the conditions that (33) can be factorised, i.e., written in the form

$$(\Sigma_5 \bar{P}_\alpha \bar{Q} A_\alpha^{-1}) (\Sigma_5 A_\alpha P_\alpha Q) = 0. \quad (34)$$

A sufficient condition is that on multiplying out (34) the cross products of terms with different suffixes vanish. This will be the case if for each value of α and β ($\alpha \neq \beta$)

$$\bar{P}_\alpha \bar{Q} A_\alpha^{-1} A_\beta P_\beta Q + \bar{P}_\beta \bar{Q} A_\beta^{-1} A_\alpha P_\alpha Q = 0. \quad (35)$$

(35) will be satisfied if, on the one hand,

$$\bar{P}_\alpha \bar{Q} P_\beta Q = + \bar{P}_\beta \bar{Q} P_\alpha Q, \quad (36a)$$

and on the other,

$$A_\alpha^{-1} A_\beta = - A_\beta^{-1} A_\alpha. \quad (36b)$$

It is clear that, when the components of P_0^2 are *simple*, (36a) will always be satisfied, for \bar{P}_α and P_α are then equal multipliers, and each side reduces to $P_\alpha P_\beta \bar{Q} Q$. It will also be satisfied, however, when \bar{P}_α and P_α are complex and operators, if the results of the operations $\bar{P}_\alpha \bar{Q}$ and $P_\alpha Q$ are equivalent to simple multiplications of \bar{Q} and Q by the same factor. The second condition (36b) will be satisfied if

$$A_\alpha = B E_\alpha,$$

where B is any four-square matrix, and E_α a member of a perpendicular set, for then

$$\begin{aligned} A_\alpha^{-1} A_\beta + A_\beta^{-1} A_\alpha &= E_\alpha^{-1} B^{-1} B E_\beta + E_\beta^{-1} B^{-1} B E_\alpha \\ &= E_\alpha^{-1} E_\beta + E_\beta^{-1} E_\alpha \\ &= - E_\alpha E_\beta - E_\beta E_\alpha = 0, \end{aligned}$$

by (28) and (29).

When the conditions (36) hold, we can obtain from the original second degree equation, (31) or (32), an equivalent first degree one by equating either factor of (34) to zero. As we are concerned here only with obtaining the simplest equivalent equation we may take B to be unity,* and conclude that the equation

$$\Sigma_5 \bar{P}_\alpha \bar{Q} P_\alpha Q = 0 \quad (32)$$

is satisfied by *either*

$$\Sigma_5 E_\alpha P_\alpha Q = 0 \quad (37a)$$

or

$$\Sigma_5 \bar{P}_\alpha \bar{Q} E_\alpha^{-1} = 0, \quad (37b)$$

so long as P_α , \bar{P}_α are either simple and equal multipliers, or equivalent to such when operating on Q and \bar{Q} respectively.

The set of 4 simultaneous equations given by (37a) has as its eliminant

$$\Sigma_5 P_\alpha^2 = 0,$$

which is equivalent to the original identity (31) under the conditions applying to P_α . The equations require certain ratios, depending on the P_α , to exist between the co-ordinate components of Q , but are satisfied by any value for

* Multiplication of equation (37a) by a matrix B does not affect its meaning. It may be observed, however, that the matrices $B E_\alpha$ will not in general be perpendicular in the sense of (28). The essential condition (36b) is more general than (28).

the magnitude of this vector. They express, in fact, as they must, the original relations of identity, but in a restricted form, in which the vector Q , created from Q_0^2 , has an orientation determined by that of P . Similar remarks apply to the alternative form (37b).

8. *The Wave Equation* (2).—The method of factorisation described in the last section can be applied to the second degree wave equation

$$\Sigma_5 \bar{r}_a \bar{\psi} r_a \psi = 0 \quad (19)$$

by reason of the result proved in (15) that the complex operators r_a and \bar{r}_a , when acting on ψ and $\bar{\psi}$ respectively, behave as the simple multiplier $\partial\theta/\partial x_a$. We thus get as a first degree form either

$$\Sigma_5 E_a r_a \psi = 0, \quad (38a)$$

or

$$\Sigma_5 \bar{r}_a \bar{\psi} E_a^{-1} = 0. \quad (38b)$$

Introducing the value of r_a from (16) gives for (38a)

$$\Sigma_4 E_a \left(\frac{\partial}{\partial x_a} - \frac{\partial \log \phi}{\partial x_a} \right) \psi + E_5 \frac{2\pi}{\lambda} \psi = 0. \quad (39)$$

This is a linear differential equation satisfied by the ψ of an arbitrary wave field.* In such a field the five terms $\frac{\partial \log \phi}{\partial x_a}$ ($\alpha = 1 \dots 4$) and λ , may be regarded as five arbitrary functions of position.

If we now write

$$\frac{\partial \log \phi}{\partial x_a} = \frac{2\pi}{i\hbar} V_a, \quad (40a)$$

and

$$\lambda = \frac{h}{m}, \quad (40b)$$

where h is Planck's constant, and V_a and m are as defined in (7), then (39) becomes

$$\Sigma_4 E_a \left(\frac{i\hbar}{2\pi} \frac{\partial}{\partial x_a} - V_a \right) \psi + E_5 im\psi = 0. \quad (41)$$

(41) is Dirac's equation, in the symmetrical form first obtained by Eddington. To write down a specific equation we may take the five E_a of any perpendicular set in any order, and, since $-E_a$ satisfies the conditions equally with E_a ,

* By an arbitrary field is meant one in which the scalar magnitudes $\bar{\psi}\psi$ and λ are arbitrary functions of position; the vector ψ created from them is, as explained above, not arbitrary so far as its orientation is concerned.

give each term either a + or a - sign. An example is the equation (set e)

$$\{i(2\bar{1}43)q_1 - (2\bar{1}\bar{4}3)q_2 + i(123\bar{4})q_3 + (3\bar{4}12)q_4 - i(3412)q_5\}\psi = 0, \quad (42)$$

where

$$q_\alpha = \left(\frac{i\hbar}{2\pi} \frac{\partial}{\partial x_\alpha} - V_\alpha \right) \quad (\alpha = 1 \dots 4), \quad q_5 = im.$$

It may be reduced to a more usual form by writing it as four equations by the rule on p. 359, and expressing the q 's in terms of x, y, z, t, m_0 , etc., by (7). (42) will then be seen to be identical with the equations used by Darwin as the basis of his solutions for the hydrogen atom.*

9. *The Amplitude and Phase in an Electron Wave Field.*—The equations (40) express restrictions which are laid on the equation for an arbitrary wave to reduce it to the equation for an electron wave. They give us the specific assumptions on which the latter equation is founded. (40a) determines, V_α being assumed given, a relation which the amplitude ϕ has to satisfy. We cannot, however, get the relation directly from it, because the term $\frac{\partial \log \phi}{\partial x_\alpha}$, when ϕ is a matrix, is a symbolical expression, the algebraical meaning of which requires interpretation. This may be obtained by referring to (15), from which it is clear that, in all component equations derivable from it, the suffixes of ϕ and ψ in $\frac{\partial \log \phi}{\partial x_\alpha} \psi$ must be the same. Hence in (39), when it is written in full, any one of the corresponding terms will take the form $\frac{\partial \log \phi_\beta}{\partial x_\alpha} \psi_\beta$, and since this is equivalent to $\frac{\partial \phi_\beta}{\partial x_\alpha} e^{-i\theta}$, the terms can be gathered up into the matrix again, with ϕ a single column matrix like ψ . (39) may thus be written in the equivalent form

$$\Sigma_4 E_\alpha \frac{i\hbar}{2\pi} \left(\frac{\partial \psi}{\partial x_\alpha} - \frac{\partial \phi}{\partial x_\alpha} e^{-i\theta} \right) + E_5 \frac{i\hbar}{\lambda} \psi = 0.$$

Equating this to (41) gives us

$$\Sigma_4 E_\alpha \left(\frac{i\hbar}{2\pi} \frac{\partial \phi}{\partial x_\alpha} - V_\alpha \phi \right) + E_5 i \left(m - \frac{\hbar}{\lambda} \right) \phi = 0$$

as the actual equation which has to be satisfied by ϕ and λ . The simplest solution (not necessarily the only one) is given by the identification (40b) for

* Darwin, 'Proc. Roy. Soc.' A, vol. 118, p. 654 (1928), (Equations (2.2)).

λ , and the equation

$$\Sigma_a E_a \left(\frac{i\hbar}{2\pi} \frac{\partial}{\partial x_a} - V_a \right) \phi = 0 \quad (43)$$

for ϕ .

(43) is a set of differential equations between four dimensional vectors, and is of a recognised type, in contrast to the equation (41) for ψ , which with its five terms, apparently requiring five dimensions to accommodate them, has broken away in its form from the ordinary equations of physics.

The restriction of the λ of an arbitrary wave to the value h/m in the electron wave field requires a relation to be satisfied by the phase. If we write

$$0 = \frac{2\pi A'}{h}$$

and substitute this and (40b) in (13), we get the relation satisfied by the phase in the form of a differential equation for A' ,

$$\Sigma_a \left(\frac{\partial A'}{\partial x_a} \right)^2 = m^2. \quad (44)$$

A' is a quantity of the same dimensions as A , the action of the classical theory. It may be called the "action" of the wave, but it is not (except when $V_a = 0$) the same as A , which satisfies the different, although analogously built, equation (9). Since, expressed in terms of A' ,

$$\psi = \phi e^{-2\pi i A'/h},$$

we see that the phase is determined by h in such a way that an increase h of the wave action takes ψ through a complete cycle of its phase changes.

From the quadratic equation (44) a linear form may be derived by applying the factorisation process of section 7 directly to the equation, equivalent to (44),

$$\left\{ \Sigma_a \left(\frac{\partial A'}{\partial x_a} \right)^2 + (im)^2 \right\} \bar{\psi} \psi = 0$$

This gives

$$\Sigma_a E_a \frac{\partial A'}{\partial x_a} \psi + E_5 im \psi = 0. \quad (45)$$

(45) automatically satisfies (44), and otherwise serves to fix the orientation of ψ . That it is satisfied by the ψ of (41) may be concluded from the fact that it is effectively the wave equation (38a) in which the operators r_a have been replaced by the multipliers to which they are equivalent.

10. *Complex Manifolds.*—The matrix $E_{16} (= i(1234))$ is not included in any perpendicular set, but it has properties which are perhaps of even more interest than those of the others. The rotation of axes through an angle θ of the type which it defines has the effect of transforming each co-ordinate in the same proportion, thus

$$\left. \begin{aligned} x'_\alpha &= x_\alpha (\cos \theta + i \sin \theta) \\ x'_\alpha &= x_\alpha (\cos \theta - i \sin \theta) \end{aligned} \right\} (\alpha = 1, \dots 4). \quad (46)$$

Calling this rotation $R(\theta)$, we note that it is the only type possible in a one-dimensional manifold, that the matrix $R_4 (= i(12))$ is involved in its extension to a twofold, and E_{16} to a fourfold. Since all components are changed in the same proportion, the effect of $R(\theta)$ on a vector-distance, initially conceived as consisting of simple and equal directed components, ds_0 , is to change them into the complex conjugates

$$\overline{ds} = ds_0 (\cos \theta + i \sin \theta), \quad ds = ds_0 (\cos \theta - i \sin \theta)$$

without affecting the magnitude $(ds_0)^2$. It has already been pointed out that the metric of the manifold is not altered by the rotation $R(\theta)$, and this is certainly true so far as alterations can be detected by the usual physical methods of exploration of space-time, which, roughly, are confined to measurements by clock and scale of the way in which ds_0^2 varies with direction or position. Nevertheless in certain conditions a change in the geometry of the manifold can be supposed to be produced by $R(\theta)$ which may be of physical significance.

When θ is constant over the whole manifold, the effect of $R(\theta)$ on the component distances \overline{ds} , ds is clearly transformable away by a rotation $R(-\theta)$; the complexity of vectors in this case is solely due to a mathematical transformation of co-ordinates, and hence has no physical consequence. But suppose we find in our manifold that we can obtain a better correlation with phenomena by assuming that certain vectors are necessarily complex, and that their composition (ratio of real to imaginary part) varies with position. At any point by a suitable $R(\theta)$ the complexity may be transformed away, but since the θ required is a function of position, we cannot transform it away everywhere at once. There is now something fundamentally different in the geometry of this manifold from that of a Euclidian one in that complex co-ordinates *have* to be used in it somewhere. The state of things is exactly the same as that arising in the general relativity theory when the phenomena of gravitation require the use of a formula for ds_0^2 which can be transformed to the simple

formula of the special theory locally, but not everywhere at once by the same transformation.

Let us suppose then that, when we have chosen axes so that the vector components into which a magnitude is decomposable are simple at a given point P, we find that complex components are still necessary at a neighbouring point Q. The complexity at Q may be got rid of by making a suitable rotation $R(\theta)$ of axes, and, in the limit, by imagining a continuously varying θ as we trace out the vector, we can keep it continuously a simple quantity. The manifold now differs from the normal one in that it possesses, as an essential feature, a type of complex twist that can only be unravelled by a suitably varying local rotation of the axes. Alternatively we may perhaps more easily picture the effects by assuming the manifold as an undisturbed background, and a vector as something laid down in it which has the feature of having its contra- and co-variant components equally and oppositely twisted through angles which increase continuously as we pass along it. When the twist has become 2π the vector has acquired again its original composition. The two opposite twists produce no effect on the vector's magnitude ($\bar{V}V$), and more intimate properties of the field must be considered before they will reveal themselves. A suggestion as to what these may be is presented by the fact that, while a vector field may have a periodicity impressed on it through its being in a complex manifold, the wave vectors ψ and $\bar{\psi}$ possess, as an essential feature, a periodicity determined by Planck's constant.

11. The differential equation for the amplitude (43) has no reference to periodicity or wave-length in it, and the solutions of it giving fields of ϕ are not harmonic. By attributing to the fourfold in which the solution for ϕ is being displayed a complex character of the kind described in the last section, a periodicity may, however, be impressed on the field. In this section it is proposed to show that by following out this process the electron wave equation (41) for ψ may be decomposed into the separate equations (43) for the amplitude, and (45) for the phase, of the electron waves.

We suppose that the vector field representing the amplitude ϕ is laid down in a fourfold whose geometry is characterised by the complex twist $R(\theta)$. As has been shown the effect of the twist may be taken into account by considering, in a simple manifold, a vector ψ which is obtained from ϕ by rotating ϕ by the covariant transformation $R(\theta)$, where θ is a function of $x_1, \dots x_4$. We shall have, by (46),

$$\psi = \phi (\cos \theta - i \sin \theta). \quad (47)$$

Assuming that ψ satisfies the wave equation (41), and substituting (47) in this, we get

$$\Sigma_4 E_a \left\{ \frac{i\hbar}{2\pi} \left(\frac{\partial \phi}{\partial x_a} - i \frac{\partial \theta}{\partial x_a} \phi \right) - V_a \phi \right\} + E_5 i m \phi = 0.$$

Assume now that

$$0 = \frac{2\pi A'}{h}, \quad (48)$$

where A' satisfies the equation (45) which determines the phase. Then

$$\Sigma_4 E_a \left(\frac{i\hbar}{2\pi} \frac{\partial}{\partial x_a} - V_a \right) \phi + \Sigma_4 E_a \frac{\partial A'}{\partial x_a} \phi + E_5 i m \phi = 0. \quad (49)$$

Again, substituting (47) in (45) we have

$$\Sigma_4 E_a \frac{\partial A'}{\partial x_a} \phi + E_5 i m \phi = 0,$$

and on subtracting this from (49) the amplitude equation (43) is obtained.

It is true that the results of this section might have been obtained equally well from equation (14) (the definition of a wave), to which the transformation (47) is equivalent. It is, however, of interest to find that the enlarged geometry possessed by a complex fourfold provides room for getting into the picture the quantum periodicity in the field of ψ which is called for by wave mechanics, but for which there seems to be no room with simple geometry except by extending the number of dimensions.

12. *An Example.*—It is not easy to find accurate solutions of the wave equation, when the electromagnetic potentials are retained in it. Darwin (*loc. cit.*) has, however, obtained accurate solutions for the hydrogen atom, in which

$$V_{1,2,3} = 0, \quad V_4 = \frac{ze^2}{cr}, \quad (50)$$

$r = \sqrt{x_1^2 + x_2^2 + x_3^2}$ being the distance from the nucleus. His results strictly are not solutions of (42), but of that equation with the operator $\partial/\partial x_4$ replaced by a constant multiplier (the object being to obtain the stationary states), and his values of ψ are three dimensional functions only. It is not difficult to modify them into four dimensional functions which satisfy the wave equation. Let

$$\psi = \phi e^{-2\pi i A'/h},$$

where

$$\phi_1 = \gamma r^{\epsilon-2} (-ix_3), \quad \phi_2 = \gamma r^{\epsilon-2} (-ix_1 + x_2),$$

$$\phi_3 = (\epsilon + 1) r^{\epsilon-1}, \quad \phi_4 = 0,$$

$$A' = m(\gamma r + \epsilon x_4),$$

$$\gamma = \frac{2\pi e^2}{hc}, \quad \epsilon = \sqrt{1 - \gamma^2};$$

then it may be shown by direct substitution that ψ satisfies (41) and (45), ϕ satisfies (43), and A' satisfies (44) and (45), the E_a being those given in (42), and the V_a being given by (50). This solution corresponds to the ground state of the atom.

Summary.

The properties of (1) classical action, (2) a wave field, in a four-dimensional manifold are analysed. The discussion results in a derivation from first principles of the differential equation of an arbitrary wave field. By applying it to the electron wave field it is found that Dirac's equation for ψ can be decomposed into two equations, determining respectively the amplitude and the phase of electron waves in a given electromagnetic field.

Consideration of the meaning of complex co-ordinates shows that the geometry of a manifold can be enlarged by their use in such a way that the quantum periodic properties of ψ , and the 16 generalised rotations discovered by Eddington, can be accounted for geometrically in a manifold of 4 dimensions only.

The Internal Conversion of the γ -Rays and Nuclear Level Systems of the Thorium B and C Bodies.

By C. D. ELLIS, F.R.S., and N. F. MOTT.

(Received December 2, 1932)

§ 1. *Introduction.*

The problem of the internal conversion of γ -rays has long been the subject of theoretical investigation, but until recently it appeared impossible to obtain results in agreement with experiment. Recently, however, Hulme,* and Taylor and Mott,† using the relativistic wave equation of Dirac to describe the planetary electron, have carried out calculations on the assumption that the ejection of an electron is due to ordinary photoelectric absorption of the γ -ray. Excellent agreement with experiment was obtained for the γ -rays of Ra B . C and Ra C . C', on the assumption that the electromagnetic field of *some* of the rays is that of an oscillating dipole situated in the nucleus, and that the field of the other rays is that of a quadrupole. The calculations show that the internal conversion coefficients α , plotted against the frequency, should lie on two smooth curves, one for the dipole radiation, and one for the quadrupole. The calculated values of α depend on the atomic number Z, but should vary very little for the small range of Z considered in this paper. All the values of the internal conversion coefficient for Ra B . C and Ra C . C' measured by Ellis and Aston‡ lie, within experimental error, on one or other of the two curves. According to the usual wave mechanical theory (Taylor and Mott, *loc. cit.*, § 3) an atom radiates a dipole field in certain transitions, and a quadrupole field in others; it is reasonable to assume that this is true also for nuclei. In atoms transitions associated with the quadrupole or higher fields occur only with very small intensity; for nuclei, as was first pointed out by Gamow and Delbrück, it is quite possible that the quadrupole lines occur with intensity comparable to the dipole, owing to the fact that in a nucleus composed of α -particles only, the electrical centre coincides with the centre of mass, so that the dipole *moment* associated with any transition vanishes.

* 'Proc. Roy. Soc.,' A, vol. 138, p. 643 (1932).

† 'Proc. Roy. Soc.,' A, vol. 138, p. 665 (1932).

‡ 'Proc. Roy. Soc.,' A, vol. 129, p. 180 (1930).

The change of quantum number associated with the various transitions depends on the model assumed for the nucleus. If the γ -rays are due to transitions between excited states in which only one α -particle is excited, then the dipole field is radiated on transitions where the angular momentum $lh/2\pi$ of this particle changes by one quantum, and the quadripole field when l changes by two or zero. If transitions are involved in which more than one α -particle is excited, no such simple rule can be given. For the purpose of assigning quantum numbers we shall assume, as a working hypothesis, that the γ -radiation is due to a single excited particle making transitions in which the orbital angular momentum changes by multiples of $h/2\pi$; this assumption is naturally of a very provisional nature.

The information, which may thus be deduced from the internal conversion coefficient, clearly provides a new tool for investigating nuclear level systems, and in particular for classifying the levels and for assigning quantum numbers to them. It is possible that it may have in the future an importance similar to that of the Zeeman effect in classifying optical spectra. Just as it was possible to determine from the Zeeman effect to which series a given line belonged, so it may be possible to determine by the measurement of the internal conversion coefficient whether a given γ -ray corresponds to a change of angular momentum of 1 or 2 quanta. It may also be possible to find cases where there are three levels E, E', E'', such that the transitions E — E', E' — E'', are dipole and the transition E — E'' is quadripole.

Moreover, it is much more difficult to measure γ -ray intensities than to measure the intensities of the corresponding β -ray lines. Thus if the theory is right it gives us a means of estimating γ -ray intensities where these cannot be or have not been measured directly. A knowledge of the γ -ray intensities may decide for or against a proposed level scheme.

In view of these possibilities, it is important to test the theory as much as possible in the light of the available experimental evidence. An examination of the evidence from Th B and Th C lends considerable support to the hypothesis that the internal conversion coefficients of most rays lie on one or other of the two curves. The evidence from Ra B and Th B tends to suggest that the calculated values of the internal conversion for quadripole radiation, for the softer rays, are about 30 per cent. too low. This may be owing to experimental error; also it is possible that the calculated values are in error, owing to neglect of screening by the L electrons or to some other reason. We would emphasize, however, that the hypothesis that the values of α plotted against ν , lie on one or other of two curves, for all elements, is likely to be useful in ordering the

experimental data, whether or not the theory which suggested this hypothesis is ultimately shown to be true.

§ 2. *The Nuclear Level System of Th C . C''.*

Th C disintegrates by emitting an α -particle and becomes Th C'', and it is found that the α -particles fall into five (or possibly six) homogeneous groups. The relative intensities of these groups led Gamow* to propose the following mechanism. The Th C nucleus might either emit an α -particle of the maximum energy E_0 and nothing else, or instead an α -particle of one of the smaller energies E_r leaving the residual energy $E_0 - E_r$ as excitation energy in the Th C'' nucleus. This energy $E_0 - E_r$ would then be either emitted as a γ -ray or transferred to an electron by the process of internal conversion. This hypothesis has been investigated experimentally by Ellis† and found to fit the facts remarkably well. It is clear that the level system of Th C'', or as it is more usual to write, Th C . C'', starts at an energy E_0 and has levels at intervals above this equal to the energy deficits of the lower energy α -particle groups. This level system is shown in fig. 1. An equally important consequence for our present purpose is that the sum of the intensities of the transitions from any particular level, say α_s , must equal the number of α -particles in the corresponding sub-group.‡ The relative intensities of these α -particle groups as measured by Rosenblum and Valadres§ are given in Table I, and are expressed as Σp_r ; here, and elsewhere in this paper, we shall use p_{rq} to represent the true intensity or probability of a transition from the r th level to the q th level. Thus p_{rq} is the average number of quanta emitted per disintegration of frequency ν_{rq} .

Table I.

Name of level.	Excess energy volts $\times 10^{-6}$.	$\Sigma p_r \times 10^2$.
α_3	4.98	1.5
α_4	4.77	0.4
α_3	3.32	2.2
α_0	0.41	77
α_1	0	—

* 'Nature,' vol. 126, p. 396 (1930).

† 'Proc. Roy. Soc.,' A, vol. 136, p. 306 (1932).

‡ This assumes that the transitions of the type $\alpha_3 - \alpha_2$ are not important. This is supported by experiment.

§ 'C. R. Acad. Sci. Paris,' vol. 194, p. 967 (1932).

Ellis* has recently analysed the β -ray spectrum of Th (B + C) and detected the β -ray groups associated with the transitions shown in the next table. He also measured the intensities of these groups relative to that of the main Th B line, named F, of Hp 1386. Assuming Gurney's† value of 0.25 electrons per disintegration in this line we obtain the absolute intensities in electrons per disintegration shown in the next table, due regard, of course, being paid to the branching at Th C. If α represents the internal conversion coefficient, then these intensities clearly give the values of the quantity $p\alpha$. The values

Table II.

Transition.	$h\nu$ in volts $\times 10^{-5}$	Intensity of β -ray line $p\alpha \times 10^4$.	α (calculated)		p (calculated) $\times 10^2$	
			Quadrupole.	Dipole.	Quadrupole	Dipole
$\alpha_3 - \alpha_0$	4 57	2 2	0 029	0 0095	0.76	2.3
$\alpha_4 - \alpha_0$	4 36	2 2	0.032	0 0102	0.69	2 2
$\alpha_4 - \alpha_1$	4 77	0 9	0.027	0 0088	0.33	1 0
$\alpha_2 - \alpha_0$	2 91	28	0 113	0.0176	2 5	16
$\alpha_3 - \alpha_1$	3 32	6.1	0 075	0 0149	0 81	4 1

of the internal conversion coefficient calculated either for a quadrupole or dipole transition are shown in the next two columns, from which follows by division the calculated intensity, $p_{\text{calc.}}$, of the γ -transition according to the two assumptions. These values must now be compared with the experimental values given in Table I, and for this purpose we will take first the level α_2 . From Table I we see that the total transitions from this level, i.e., Σp , are 2.2×10^{-2} , whereas assumption of dipole transitions gives 20×10^{-2} and quadrupole gives 3.3×10^{-2} . It is obvious that there is a discrepancy by a factor of 9 if a dipole transition be assumed, whereas the discrepancy is only a factor of 1.5 if both transitions are quadrupole. Now from the point of verification of the theory it is significant that the values for the Ra B γ -rays showed much the same behaviour; a discrepancy of 30 to 40 per cent. in the same direction, if a quadrupole transition be taken, while with a dipole transition the disagreement amounts to a factor of 10. We shall leave it open for the moment whether this discrepancy lies in the experimental values, which are admittedly rather doubtful, or in the theoretical calculations, and we shall conclude, taking a broad view, that the calculations are in agreement as regards order of magnitude with the experiments and may therefore be

* 'Proc. Roy. Soc.,' A, vol. 138, p. 318 (1932).

† 'Proc. Roy. Soc.,' A, vol. 112, p. 380 (1926).

used to determine whether a transition is quadrupole or dipole. It follows that both $\alpha_2 - \alpha_0$ and $\alpha_2 - \alpha_1$ are quadrupole transitions. If we assign a quantum number $l = 0$ to the lowest state, then α_2 and α_0 must have $l = 2$, since $l = 0 \rightarrow l = 0$ is forbidden.

Considering now the level α_4 we note from Table I that Σp is 0.4×10^{-2} , while with quadrupole radiation for the transitions to both α_0 and α_1 it is calculated to be 1.0×10^{-2} , and with dipole radiation 3.2×10^{-2} . This is again somewhat the same behaviour as for α_2 , and taking into account the experimental difficulties of measuring the intensities of weak β -ray lines, we may conclude that both these transitions are quadrupole. On the same assumption as for α_2 we therefore put $l = 2$ for level α_4 .

The results for the level α_3 are indecisive, the calculated values for p are respectively 0.76×10^{-2} and 2.3×10^{-2} for quadrupole and dipole radiation, while the experimental value is 1.5×10^{-2} . Since the calculated intensities appear to be, from some as yet unknown cause, usually too high, there is a presumption that this is a dipole transition, but it would be well to await more accurate experimental data before reaching a decision.

The transition $\alpha_0 - \alpha_1$ corresponds to a powerful γ -ray but we are unable to include it in the present analysis since neither the intensity of the β -ray line has been measured nor has the conversion coefficient (L level) been calculated.

The l values that we have assigned to the various levels are shown in fig. 1.

l		Volts $\times 10^{-3}$
2 or 3	_____ α_3	4.98
2	_____ α_4	4.77
2	_____ α_2	3.32
2	_____ α_0	0.41
0	_____ α_1	0

FIG. 1.—Level system of Th C. C''

§ 3. Th C'' . Pb.

This is a β -ray disintegration and the γ -rays are emitted by an excited lead nucleus. According to Ellis' (*loc. cit.*) analysis of the β -ray spectra, we must take into account the γ -rays shown in Table III, which also shows his values for the intensities px of the β -ray groups arising by internal conversion. As before we give the values of the internal conversion coefficient for quadrupole

and dipole transition and hence the calculated intensities of the transitions on these two assumptions.

Table III.

Name of γ -ray.	$h\nu$ of γ -rays volts $\times 10^{-3}$.	Intensity of β -ray group $p\alpha \times 10^3$.	$\alpha \times 10^3$ (calc.).		p (calc.).	
			Quadripole.	Dipole.	Quadripole.	Dipole.
G	2 765	1 4	134	19 0	0.10	0.74
L	5 100	0.73	24 5	7.8	0.30	0.93
M	5.823	0 65	20.0	5.9	0.33	1.1
X	26.20	0 15	1.44	0.5	1.0	3 0

On the basis of these figures we must assume that γX is a quadripole transition, since we cannot have more than one quantum of given frequency emitted per disintegration, i.e., $p \ll 1$. The remaining transitions are more difficult to decide. The experiments of Thibaud* and also of Ellis† suggest γM is considerably more powerful than γL which, since the β -ray groups have nearly equal intensity, would lead one to infer that γM was dipole and γL quadripole. In support of this conclusion it may be pointed out that there is general evidence that the total γ -ray energy of Th C. C'' is about 3.8×10^6 volts per atom.‡ Subtracting 2.6×10^6 volts for γX which, as we have seen, appears to give one quantum per disintegration, we are left with 1.2×10^6 volts to be divided between γG , γL and γM . It is clear that this result is most easily achieved if at least γM is dipole and has therefore a large intensity. Provisionally it would seem justifiable to take γL and γX as quadripole transitions and γM as a dipole transition. The existing experimental evidence is on the whole against the large intensity of the ray γG , which would be implied by the assumption of a dipole transition. This is a point which we hope will soon be settled experimentally, and it serves as an illustration of the fruitfulness of these new ideas that they show how quite an approximate measurement of the intensity of a γ -ray can indicate clearly the type of transition to which it is due.

In further illustration of this point it is of interest to consider the various possibilities for the level system of Th C''. Pb. The intensities of γX and γM given in Table III show that these transitions must be sequent or, to use a

* 'Thesis,' Paris (1925).

† 'Conference on Nuclear Physics, Rome,' p. 117 (1931).

‡ See Rutherford, Chadwick and Ellis, "Radiations from Radioactive Substances," [Camb. Univ. Press], p. 500. The value given here allows for a slight emission from Th C. C' in accordance with Skobelczyn's results (see *infra*).

convenient phrase, in series, since for both $p \sim 1$, that is they occur once every disintegration. They are thus represented in figs. 2 (a) and 2 (b) which differ only in the position of γL . System 2 (a) is in good agreement with the present estimate of a total energy emission of 3.8×10^6 volts per disintegration, since the intensity of γX ($p \sim 1$) implies excitation to the top level for each atom, but it would also imply γL having the same intensity as γM , and being a dipole transition. We have mentioned that the existing evidence is against this, but this is a direct experimental point which can be tested more carefully. It will also be noted that a transition $C \rightarrow A$ would be quadripole and we should anticipate that it would be of considerable intensity, and being quadripole would give rise to a detectable β -ray line. Again, while at present the evidence is against the existence of this line, it is a point susceptible to test by experiment. For these reasons we prefer system 2 (b) although this gives an energy emission of only 3.2×10^6 volts per disintegration in disagreement with our estimate of 3.8×10^6 volts. On the other hand with this system we can allow γX , γM and γL to have the intensities which seem indicated by experiment, and the extra γ -ray predicted $D \rightarrow B$ would be a dipole transition of intensity equal to that of γL . The resulting β -ray line would be one-fifteenth of that of the K line from γX , and it is quite understandable that it has not yet been detected. It will again be noted that there are definite predictions which can be tested by experiment.

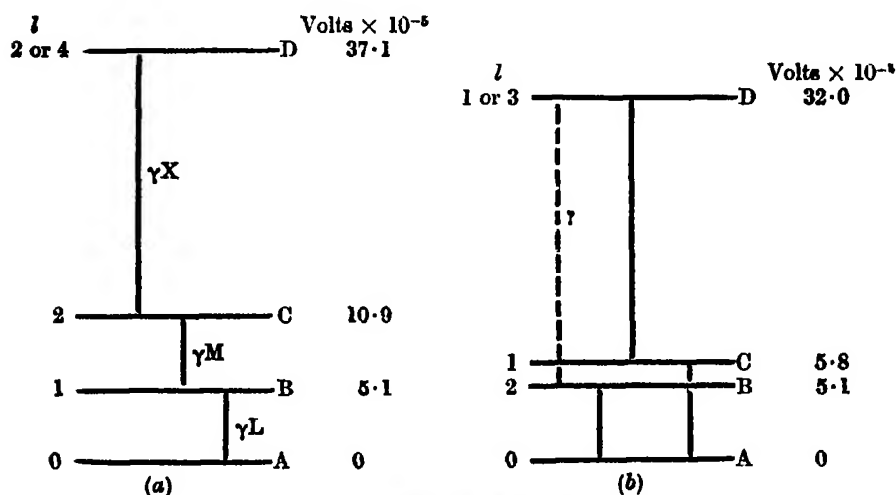


FIG. 2.—Possible levels of Th C'' . Pb.

With improvement in technique it should be possible to decide whether the l value of the top level D is 1 or 3. If it is 1 there should be a dipole γ -ray of

energy 32.0×10^6 volts, if it is 3 there should be no such γ -ray. There are, of course, analogous conclusions to be drawn from system (a). It does not seem unreasonable to hope that the level system of a body like Th C'' . Pb, where there is no assistance from α -ray evidence, may in time be ascertained by direct experiment on the β - and γ -rays.

§ 4. Th B . C.

The γ -rays of Th B . C as found by Ellis with the corresponding intensities of the β -ray lines due to the conversion are set out in the following table with the data about the calculated conversion coefficient for dipole and quadrupole transitions. In only one case, that of the extremely powerful γ -ray γF , can we come to any definite conclusion; and here the evidence is unambiguous that this transition is quadrupole since not more than one quantum of a given frequency can be emitted per disintegration. It will be noted that as

Table IV.

Name.	$h\nu$ in volts $\times 10^{-5}$.	Intensity of β -ray group $pa \times 10^4$.	a (calculated)		p (calculated).	
			Quadrupole.	Dipole.	Quadrupole	Dipole.
γDg	1 757	0.6	0.45	0 038	0 001	0.016
γE	1 147	24.2	0 6	0 05	0.04	0.43
γF	2 379	250	0 205	0 026	1 22	9.6
γFa	2 404	0 5	0.183	0 022	0 003	0.023
γH	2.990	9 0	0.104	0 017	0.009	0.53

in the case of Ra B the calculated quadrupole conversion coefficient appears to be about 25 per cent. too small. Ellis (*loc. cit.*) has suggested recently the level system for Th B . C shown in fig. 3.

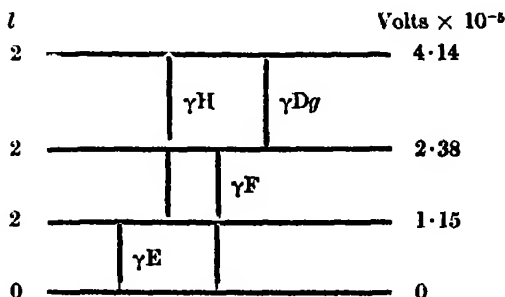


FIG. 3.—Levels of Th B . C.

Now we know that the γ -ray F is emitted nearly at every disintegration ($p \sim 1$, see Table IV) and it is therefore difficult to see how γ H and γ E could have the intensities of $p \sim 0.5$ predicted by dipole transitions. It appears more likely that these are both quadrupole transitions, and that the level system has relative l values as shown. It should not be difficult to settle this point experimentally since if γ E and γ H were dipole transitions these γ -rays would be sufficiently strong to be easily detectable. Experiments are being carried out on this point.

If these conclusions are correct it would appear that the top level is excited in 1 per cent. of the disintegrations, the next in nearly every disintegration, and the lowest level in 3 per cent. of the disintegrations. There is at present no evidence on which any statement can be made about γ Fa.

§ 5. Th C . C'.

The disintegration of Th C to Th C' is in many respects similar to that of Ra C to Ra C'. Both are of the β -ray type, both are followed by a very rapid α -ray disintegration, and both apparently leave the C' nucleus excited. This is shown by the occurrence of long range α -particle groups. The striking difference is that while Ra C . C' emits a great amount of γ -radiation, Th C . C' emits so little that it is only recently that it has been identified. In discussing this problem we shall deal only with the most prominent group of long range α -particles from Th C . C'. These have an energy of about 10.52×10^6 volts, and taking into account the energy of the recoiling nucleus, show the existence of an excited state in the Th C' nucleus 17.8×10^5 volts above the ground state. There are a surprising number of these long range α -particles: about 180 per million disintegrations, compared to between 1 and 10 per million in the long range groups of Ra C . C'. On the other hand, as mentioned above, the γ -radiation observed from Ra C . C' is much stronger than from Th C . C'. This at first sight seems surprising, in view of Gamow's theory of the connection between the long range α -particles and the γ -rays; the point will be discussed in this section.

With the exception of the γ -ray with 14.26×10^5 volts energy, all the chief γ -rays of Ra C . C' appear to be associated with quadrupole or dipole fields. The available evidence tends to show that the γ -ray 17.8×10^5 volts of Th C . C' is of the same type. Skobelzyn* using a source of radiothorium in equilibrium with the B and C bodies has detected a γ -ray of about this frequency. If we

* Skobelzyn, 'C. R. Acad. Sci. Paris,' vol. 194, p. 1486 (1932).

assume that this is the γ -ray associated with the Th C . C' disintegration it would appear from his measurements that it is emitted once in every 20 disintegrations (i.e., $p \sim 0.05$). The corresponding β -ray here is difficult to detect; its intensity is certainly no greater than 2×10^{-4} . These figures lead to a value of the conversion coefficient α , not greater than 4×10^{-3} . The calculated values for quadripole and dipole fields are 2.3×10^{-3} , 0.8×10^{-3} respectively. There is thus no evidence against the supposition that this line is of quadripole or dipole type.

We have seen that the long range α -particle corresponding to this line occurs 180 times per million disintegrations. Thus the ratio of the probability (a) of α emission to that of γ disintegration (g) is, using Skobelzyn's value of g

$$\frac{a}{g} = \frac{180 \times 10^{-6}}{5 \times 10^{-2}} = 3.6 \times 10^{-3}.$$

We compare this with the corresponding values for Ra C . C' as obtained by Rutherford and Ellis.†

Table V.

	Energy of disintegration in volts $\times 10^{-6}$.			a/g
	Long range α .	Normal α	γ -ray.	
Th C . C'	10.72	8.94	1.78	3.6×10^{-3}
Ra C . C'	8.43*	7.82	0.61	7×10^{-7}
	9.59*	7.82	1.77	2×10^{-6}
	10.03*	7.82	2.21	8×10^{-3}

* These figures are only intended for comparison with the Th C . C' value and do not necessarily represent the best experimental values.

We should not expect the value of g of Th C . C' to be very different from that of a line in Ra C . C' of the same energy, since we have seen that the *mechanism* of γ -radiation is probably the same for both. It follows that the probability a per unit time of α -disintegration is about 500 times more for Th C . C' than for the fastest ray shown above for Ra C . C'. Judging from the rate of increase of the a/g values for Ra C . C' with energy, the difference between 10.72×10^6 for Th C . C', and 10.07×10^6 for Ra C . C' should not affect a by more than about 10, if the potential barrier were the same for the two elements. We are inclined to conclude, therefore, that the potential

† 'Proc. Roy. Soc.,' A, vol. 132, p. 667 (1931).

barrier in Th C is lower than in Ra C. Since the decay constant, according to the Gamow theory, is very sensitive to the shape of the potential barrier, only a small difference is required. We conclude, therefore, that there is no difficulty in accounting for the large number of long range α -particles in Th C . C' along these lines.

Summary.

(1) The values of the internal conversion coefficient, recently calculated by Taylor and Mott, are compared with experimental evidence from the Thorium B and C elements. In the case of Th C . C'' the intensities of the various groups of short range α -particles measured by Rosenblum, together with the intensities of the β -ray groups converted in the K ring measured by Ellis, are found to lend definite support to the theory.

(2) The level schemes of Th C . C'', Th B . C and Th C'' . Pb are discussed. Quantum numbers l , giving the angular momentum of the excited particle, are suggested for the various levels. It is found that quadrupole transitions are more common than dipole, in marked contrast to Ra C . C', where at least three lines are dipole.

(3) The long range α -particles from Ra C . C' and Th C . C' are compared. The large number of particles from Th C . C', together with the weak γ -radiation, are seen to be explicable on the assumption that the potential barrier for Th C is slightly lower than for Ra C.

On the Arc Spectrum of Iodine.

By S. C. DEB, M.Sc.

(Communicated by M. N. Saha, F.R.S —Received October 22, 1931—Revised
May 23, 1932)

[PLATE 6]

1. *Introduction.*

Our knowledge of the arc spectrum of iodine is still very meagre, though it has been investigated by L. A. Turner* in the Schumann region for the fundamental transition. He found a set of strong lines with the frequency difference of 7600^{-1} cm. He showed that this is the frequency difference between the fundamental terms $^2P_{3/2}$, $^2P_{1/2}$ of the $5p^5$ -level. The correctness of this value has been indirectly supported by Franck and his co-workers,† from their study of the absorption spectra of alkali halides.

The main difficulty in the systematization of the arc lines is due to the extremely large difference between the value of the component terms arising from any particular electron combination. Owing to this fact, lines arising from the same multiplet lie in widely different parts of the spectrum. It is difficult to make any use of the intensity rules. Moreover it appears that the Russell-Saunders or normal coupling breaks down and the (*jj*)-coupling becomes operative.

The existing data were found to be very meagre and I had to supplement them by fresh experimental work. I photographed the entire spectrum from the infra-red (λ 9113·8) to the ultra-violet. After my work had been completed a paper on the same subject was published by Evans,‡ who extended the infra-red part of the spectrum beyond even 10,000 Å. (the largest wavelength measured being 10,481 Å.). Evans made an attempt to classify the lines, but a closer scrutiny of his paper shows that his analysis is, on the whole, incorrect. This will be apparent from the following discussions.

* 'Phys. Rev.,' vol. 27, p. 397 (1926).

† Franck, Kuhn and Rollefson, 'Z. Physik,' vol. 43, p. 155 (1927).

‡ 'Proc. Roy. Soc.,' A, vol. 133, p. 417 (1931).

2. The electron composition of iodine is given in Table I.

Table I.--Iodine At No 53.

$1s^2 2s^2 2p^6 3s^2 3p^6 3d^{10}$									
	4s	4p	4d	4f					
	2	6	10						
		5s	5p	5d	5f				
		2	6	(1)					
			6s	6p	6d	6f			
			(1)	(1)					
			7s	7p	7d	7f			
			(1)	(1)					
				8s	8p	8d			
				(1)	(1)				
					9s	9p			
					(1)	(1)			
						10s			
						(1)			

The expected terms are .—

Table II.--Electron Constitution of Iodine.

I ⁺ core	Coupling electron	Terms	
		J values	
	$5p^5$	$^2P_{3/2}$	$^2P_{1/2}$
$5p^4 \ ^3P_2$	$(\bar{5} \mid n)s$	$^4P_{5/2}$	$^2P_{3/2}$
$5p^4 \ ^3P_1$	$(\bar{5} \mid n)s$	$^4P_{3/2}$	$^2P_{1/2}$
$5p^4 \ ^3P_0$	$(\bar{5} \mid n)s$	$^4P_{1/2}$	
$5p^4 \ ^1D_2$	$(\bar{5} \mid n)s$	$^2D_{5/2}$	$^2D_{3/2}$
$5p^4 \ ^1S_0$	$(\bar{5} \mid n)s$	$^2S_{1/2}$	
$5p^4 \ ^3P_2$	$(\bar{5} \mid n)p$	X	$7/2, 5/2, 3/2, 1/2$
$5p^4 \ ^3P_1$	$(\bar{5} \mid n)p$	Y	$5/2, 3/2, 1/2$
$5p^4 \ ^3P_0$	$(\bar{5} \mid n)p$	Z	$3/2$
$5p^4 \ ^1D_2$	$(\bar{5} \mid n)p$	$7/2, 5/2, 3/2, 1/2$	$5/2, 3/2$
$5p^4 \ ^1S_0$	$(\bar{5} \mid n)p$	$3/2$	$1/2$
$5p^4 \ ^4P_5$	$(4 \mid n)d$	$9/2, 7/2, 5/2, 3/2, 1/2$	$7/2, 5/2, 3/2, 1/2$
$5p^4 \ ^4P_3$	$(4 \mid n)d$	$7/2, 5/2, 3/2$	$5/2, 3/2, 1/2$
$5p^4 \ ^4P_1$	$(4 \mid n)d$	$5/2$	$3/2$
$5p^4 \ ^1D_2$	$(4 \mid n)d$	$9/2, 7/2, 5/2, 3/2, 1/2$	$7/2, 5/2, 3/2, 1/2$

Explanations.—The I⁺-core has the fundamental electron constitution $5p^4$, and the different terms arising from this are 3P_2 , 3P_1 , 3P_0 , 1D_2 , 1S_0 . Though these terms are not known it can be safely predicted that the differences between them are very large, on account of the heaviness of the iodine nucleus. When an electron is brought to the I⁺-core in any one of the higher electron states $6s$ or $6p$, ... etc., the expected coupling will be of the (η)-type. Thus the symbol $5p^4 \ . \ ^3P_2 6s$ means that the I⁺-core is taken to be in the 3P_2 -state, and

an electron in the 6s state is coupled to it. This gives rise to terms having the inner quantum number 5/2 and 3/2. There can be no ambiguity regarding the term 5/2; it is ${}^4P_{5/2}$. Now $5p^4 \cdot {}^3P_1 \cdot 6s$ gives us two terms with $j = 3/2$ and $1/2$; $5p^4 \cdot {}^3P_0 \cdot 6s$ gives us a single term with $j = 1/2$. Thus two terms with $j = 3/2$ may arise either from 3P_2 or 3P_1 -core, and it is not certain whether the ${}^3P_2 \cdot 6s$ term approximates to ${}^4P_{3/2}$ or to ${}^2P_{3/2}$. From a comparison with the spectrum of F, Cl and Br (see below) I have assigned ${}^2P_{3/2}$ to ${}^3P_2 \cdot 6s$ and ${}^4P_{3/2}$ to ${}^3P_1 \cdot 6s$, and ${}^2P_{1/2}$ to ${}^3P_1 \cdot 6s$, ${}^1P_{1/2}$ to ${}^3P_0 \cdot 6s$.

3. Term Values

The value of the different term systems has now to be considered. Paschen,* in his celebrated paper on neon, showed that if we take the electron configuration $2p^5ms$ we get four terms s_2, s_3, s_4, s_5 with the inner quantum numbers 1, 0, 1, 2. To fix our ideas, we denote them by $2p^5 \cdot {}^2P_{3/2}ms, {}^3P_1$ and 3P_2 , and $2p^5 \cdot {}^2P_{1/2}ms, {}^1P_1, {}^3P_0$. He found that while the ${}^2P_{3/2}ms$ -terms follow the Rydberg sequence, ${}^2P_{1/2}ms$ -terms do not do so ordinarily, but if $\Delta\nu = 782 \text{ cm}^{-1}$ be added to the empirical term values, ${}^2P_{1/2}ms$ terms also follow a Rydberg sequence. It was later established by Russell, Compton and Boyce† that 782 is the difference between ${}^2P_{3/2}$ and ${}^2P_{1/2}$ of Ne^+ . The same phenomena has been observed in a number of other spectra, notably in Pb. The second fundamental terms arising from the electron configuration $6p.ms$ can be divided into two groups, ${}^3P_0, {}^3P_1$ and ${}^3P_2, {}^1P_1$. The former set arises when an "s" electron is coupled with $6p \cdot {}^3P_{1/2}$ state of Pb^+ , and the latter when it is coupled with $6p \cdot {}^2P_{3/2}$ state of Pb^+ . Sponer,‡ Sur,§ and others have shown that $(6p \cdot {}^2P_{1/2}ms) {}^3P_0, {}^3P_1$ terms follow a Rydberg sequence but the terms $(6p \cdot {}^2P_{3/2}ms) {}^3P_2, {}^1P_1$ fail to do so unless 14,000 is added to them. $\nu = 14,070 \text{ cm}^{-1}$ is known to be the difference between ${}^2P_{1/2}$ and ${}^2P_{3/2}$ terms of the fundamental state of Pb^+ .|| In the case of iodine as well, we expect that some such relation should occur amongst the terms as we see that the normal coupling is no longer operative.

An analysis of the data given by Turner (*loc. cit.*) shows that the lines given by him belong to the transition $5p^5 - 5p^46s$. The lines $5p^5 - 5p^45d$ will be

* 'Ann. Physik,' vol. 60, p. 405 (1919); vol. 63, p. 201 (1920)

† 'Proc. Nat. Acad. Sci. Wash.', vol. 14, p. 280 (1928)

‡ 'Z. Physik,' vol. 32, p. 19 (1925).

§ 'Phil. Mag.,' vol. 3, p. 736 (1927).

|| Gieseler, 'Z. Physik,' vol. 42, p. 265 (1927)

further up in the Schumann region. Further it is expected from the positions of the corresponding lines of chlorine and bromine that

$5p^46s \leftarrow 5p^46p$ should be partly beyond λ 9000.

$5p^46p \leftarrow 5p^46d$ should be in the extreme infra-red.

$5p^46s \leftarrow 5p^47p$ should be in the visible and in near infra-red.

Further it was thought necessary to make sure that Turner's lines were resonance lines by an absorption experiment; and also to supplement the existing data by taking an arc spectrum in the visible and in the infra-red.

4. Absorption by Iodine Atoms.

Iodine when vapourised is ordinarily diatomic, its heat of dissociation is small (34 kcal), and therefore it can be easily dissociated into atoms when moderately heated. Its thermal dissociation under varying temperatures and pressures has been studied by Bodenstein and Stark* and discussed from thermodynamical standpoint by Gibson and Heitler†. From their figures and applying the law of reaction isochore, it can be shown that at about 1500° C. and at a pressure of 1 atmosphere, about 90 per cent. of iodine is dissociated into atoms. If continuous light be passed through these dissociated atoms, the lines of Turner should appear in absorption. Several workers‡ studied the absorption of iodine vapour from the visible to the ultra-violet (2200 Å.), but none attempted to study absorption by atomic iodine. This experiment was tried as follows

Iodine was vaporised in the vacuum Acheson graphite furnace of the laboratory, which was heated to about 1500° C., and light from an under-water spark between two copper electrodes was passed through the furnace and photographed with an E₃-quartz spectrograph. Only two lines, viz., λ 2062.1 and λ 1830.4 were obtained in absorption. The other lines of Turner were either beyond the limit of our apparatus or had too small a probability to come in absorption. But the absorption of the two lines was fairly conclusive evidence that Turner's lines belong to the fundamental transition $5p^5 \leftarrow 5p^46s$.

* 'Z. Phys. Chem.,' vol. 10, p. 910 (1910).

† 'Z. Physik,' vol. 49, p. 465 (1928).

‡ Angerer and Joos, 'Ann. Physik,' vol. 74, p. 754 (1922); Zumstein and Fruth, 'Phys. Rev.,' vol. 25, p. 523 (1925); Fuchtbauer, Weibel and Holm, 'Z. Physik,' vol. 31, p. 523, (1925).

5. *Systematisation of the Fundamental Transition.*

If we compare the intervals between terms of the $(p^4.s)$ -combination of all the halogens, we observe an interesting case of transition from Russell-Saunders's coupling to (j) -coupling. In Table III we give a list of term values of F, Cl, Br and I

Table III.

	F	Cl	Br	I.
$^4P_{5/2}$	48547	33037	32120	30807
$^4P_{3/2}$	48272	32507	30649	24550
$^4P_{1/2}$	48112	32168	28072	19094
$^2P_{3/2}$	46221	30770	28373	29350
$^2P_{1/2}$	45896	30130	26586	23628

The gradual change in these terms as we pass from F to I is illustrated in fig. 1, which gives a qualitative idea of the changes involved.

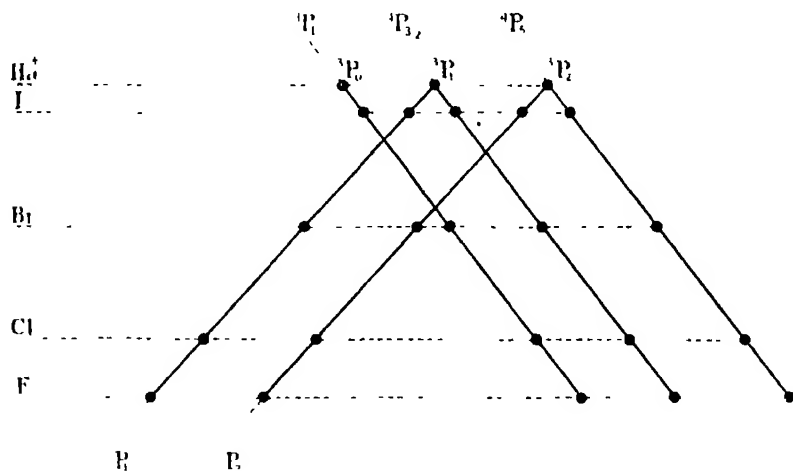


FIG. 1.

According to this scheme, every term of the fundamental state of Ha^+ i.e., 3P_2 , 3P_1 , 3P_0 split up due to s -coupling, into two terms with $j = (j' \pm \frac{1}{2})$, j' being the inner quantum number of any of the three P-terms of Ha^+ . Thus :

$(^3P_2)ms$ gives us two terms with $j = 5/2, 3/2$,

$(^3P_1)ms$ gives us two terms with $j = 3/2, 1/2$, and

$(^3P_0)ms$ gives us one term with $j = 1/2$.

We find that in F and Cl, where we expect (LS)-coupling, (${}^4P_{5/2}-{}^4P_{3/2}$) has nearly the same value as (${}^3P_2-{}^3P_1$), and (${}^4P_{3/2}-{}^4P_{1/2}$) nearly the same value as (${}^3P_1-{}^3P_0$) of the corresponding ions. In these cases (formation of ${}^4P_{5/2, 3/2, 1/2}$) the multiplicities are the same. If by $\phi(s_1, s_2)$ we denote the change in term values when the component ion and coupling electron have the spin vectors s_1 and s_2 respectively, we find that for all these terms ϕ has the same value, viz., $\phi(2/2, 1/2)$. The difference in term values is therefore primarily due to the difference in term-values of the states of the ions (${}^3P_{2, 1, 0}$). This is also illustrated in the differences ${}^2P_{3/2}-{}^2P_{1/2}$ of F and Cl, where ${}^2P_{3/2}-{}^2P_{1/2}$ is very nearly equal to ${}^3P_2-{}^3P_1$ of the component ions, for in this case for both the ${}^2P_{3/2}$, ${}^2P_{1/2}$ -terms the spin interaction energy is of the form $\phi(2/2, -1/2)$.

Table IV.

Ion	$^3P_2-^3P_1$	$^3P_1-^3P_0$	Atom	$^4P_{5/2}$	$^4P_{3/2}$	$^4P_{3/2}-^4P_{1/2}$	$\Delta^4P_{5/2, 1/2}/\Delta^4P_{3/2, 1/2}$	$^2P_{3/2}-^2P_{1/2}$
F [†]	344	147	F	275	160	5 2 900	325	
Cl [†]	692	300	Cl	530	339	5 3 198	640	
Br [†]	—	—	Br	1976	1470	5 3 72	1786	
I [†]	—	—	I	6257	5156	5 4 36	5722	

The F[†] and Cl[†] (${}^3P_{2, 1, 0}$)-differences are taken from values obtained by Dingle* and Bowen†.

If we compare the terms arising out of (3P_2)_{ms}, we find that the difference in their term value due to (s, s)-coupling would be $\phi(2/2, 1/2) - \phi(2/2, -1/2)$, and this is known to be nearly the same for light as well as for heavy elements. We get in the present case 2326 for F, 2268 for Cl, and this has the same order of value for the general (np). ($n+1$) s formation (*vide* the corresponding case in C, N, O, Ge, etc.). When we come to Br and I, we find that the ${}^3P_2-{}^3P_1$, ${}^3P_1-{}^3P_0$ differences of the core are of the same order of dimensions as the expected $s(2/2, 1/2) - s(2/2, -1/2)$ differences, hence there occurs an intermingling of the 4P and 2P -terms as we have sought to illustrate in fig. 1. The figure is drawn to show the ratio of the ${}^3P_2-{}^3P_1$, ${}^3P_1-{}^3P_0$ differences of the core to the $s(2/2, 1/2) - s(2/2, -1/2)$ differences. This is small for Cl and F (for in F, $s(2/2, 1/2) - s(2/2, -1/2) = 2326$ as measured by ${}^4P_{5/2}-{}^3P_{3/2}$ difference, while ${}^3P_2-{}^3P_1 = 344$). These are represented by the strips (${}^4P_{5/2}-{}^2P_{3/2}$), nearly unity for Br. and about 2 to 3 for I, which

* 'Proc. Roy. Soc.' A, vol. 128, p. 600 (1930)

† 'Phys. Rev.', vol. 31, p. 34 (1928)

shows clearly that we are passing from (LS) to (JJ)-coupling. Other cases have been treated by Laporte, Houston* and others for ps , ds , p^6s , d^9s -couplings.

In accordance with the considerations given above I have arranged Turner's lines in the multiplet in Table V.

Table V.

λ_{A}	$5p \rightarrow$	77844	85439
		$^2P_{1/2}$	$^2P_{3/2}$
29350	$^2P_{3/2}$	<u>48494</u> (10)	56089 (9)
23628	$^2P_{1/2}$	54216 (9)	61809 (6)
30807	$^4P_{5/2}$	—	<u>54632</u> (10)
24550	$^4P_{3/2}$	53293 (7)	60885 (7)
19094	$^4P_{1/2}$	58744 (8)	66342 (3)

The lines underlined were obtained in absorption

From this arrangement we can see why some of Turner's lines having larger wave-length than 1830 Å did not come in absorption. According to Maxwell's law, the fraction of iodine atoms in the metastable state $^2P_{1/2}$ is $\frac{1}{2}e^{-\frac{h\nu}{kT}}$, taking $\nu = 7595$ and $T = 1500^\circ$ (this ratio is 0.017, i.e., 1 ($^2P_{1/2}$ atoms) are about 60 times less numerous than the normal $^2P_{3/2}$ atoms. This, combined with the fact that the line $^2P_{1,2} \rightarrow ^2P_{1/2}$ ($\nu 54216$) lies very close to the limit of our spectrograph, probably prevented it from appearing in absorption.

6. Other Transitions.

To obtain the lines belonging to the transition $5p^46s \rightarrow 5p^46p$, a discharge tube of pyrex glass was prepared similar in pattern to that used in this laboratory for photographing the spectrum of chlorine† and of bromine‡. A bulb containing pure iodine, supplied by Kahlbaum, was attached to the side of the tube and heated whenever necessary. It was observed that like chlorine and bromine, iodine also acted upon the electrodes.

Photographs were taken with a 1-metre concave grating which had a dispersion of about 8 Å. per millimetre in the second order, and with a plane

* 'Handbuch der Astrophysik,' vol. 3, pt. 2, p. 651.

† Majumdar, 'Proc. Roy. Soc.,' A, vol. 127, p. 60 (1929).

‡ Deb, 'Proc. Roy. Soc.,' A, vol. 127, p. 108 (1930).

replica grating spectrograph designed by Majumdar, this latter was found particularly suitable for photographing the infra-red part of the spectrum. Infra-red spectrograms were taken on neocyanine plates prepared in this laboratory. The maximum wave-length recorded was 9113.9 Å. The time of exposure ranged from 25 to 80 hours.

The discharge tube was excited during the earlier part of the experiment by an induction coil and later by a 2.5 K.W. transformer. The colour of the discharge in the wider part of the tube was different from that in the capillary and when examined through a direct vision spectroscope it was found that the wider parts showed bands, while the capillary showed lines superposed upon bands or brilliant lines alone according to excitation. It was, however, not possible to keep the excitation always limited to that appropriate to the arc spectrum. We eliminated the spark lines by comparing different plates, and comparing the excitation in the different cases. We tried to eliminate probable foreign lines, and the only impurity lines that could be detected were the red lines of hydrogen.

7. The Recombination-spectrum.

The spark lines measured were mostly from the singly ionised state of the atom, they will be discussed in a future paper. An interesting feature of the spectrum was the appearance of a patch of continuous light extending from λ 3420 Å. to λ 3300 Å., this patch was most prominent when the excitation of the arc spectrum was most favourable. Similar patches were noted by Kiess and de Bruin for chlorine* and for bromine†. This continuous emission is explained as a recombination spectrum, owing to a combination of a free electron with I^1 in one of the excited states corresponding to the electron combination $5p^46s(^4P, ^2P)$ states. With chlorine as well as with bromine, Kiess and de Bruin observed two such separate bands at two different places on their spectrograms. These they interpreted as being due to the recombination in the two states 4P and 2P . In none of our spectrograms, on which we observed this continuous emission, could we detect two such bands. A photomicrogram of the patch was kindly taken by Dr. Banerji with the Zeiss micro-spectro-photometer of the Patna Physical Laboratory, and my warmest thanks are due to him, and to Professor Mukerji, the director of the laboratory. The photomicrogram is reproduced in Plate 6; it shows that the maximum intensity occurs at λ 3406 Å. corresponding to $\nu = 29351$

* 'Bur Stand. J. Res.', vol. 2, p. 1117 (1929).

† *Ibid.*, vol. 4, p. 667 (1930).

cm.⁻¹. This gave us the approximate value of ${}^3P_2 \cdot 6s \cdot {}^2P_{3/2}$. The maximum was assumed to correspond to ${}^3P_{3/2}$ from analogy with the spectrum of Cl and Br, where it was found that 2P -patch was stronger than 4P -patch.

8. The Classification of the Lines in the Visible and Infra-red Range.

The classification of the lines in the visible and infra-red range was next undertaken. If ${}^2P_{3/2} - 29351$, we have $5p^4 \cdot {}^4P_{5/2} = 30807$; we can then easily estimate the values of the other terms in the $5p^4 \cdot 6s$ -combination. These are shown in Table VII. The terms arising from $5p^4 np$ can be divided into five groups as shown in Table I. Of these, the six terms arising from $5p^4 \cdot {}^3P_2 np$ will be the first members of regular Rydberg sequence; the others arising from $5p^4 \cdot {}^3P_1 np \dots$ will be displaced, i.e., they will follow Rydberg sequence when ${}^3P_2 - {}^3P_1$, ${}^3P_2 - P_0$, etc., are respectively added to them, just as was first shown by Paschen for neon, and was found by Sponer for lead, and Meissner* for argon. It was calculated from the application of the Horizontal Comparison method† that $5p^4 \cdot {}^3P_2 6p \cdot X_{7/2}$ has roughly the value 19,000. The terms of the $6p \cdot X$ group are shown in Table VI. The Y-group arising from $5p^4 \cdot {}^3P_1 6p$ have also been found, and vary in value from 13845 cm.⁻¹ to 12637 cm.⁻¹. They are roughly Δv 6000 units smaller than the X-group. The Z-group arising from $5p^4 \cdot {}^3P_0 6p$ give two terms having values 7809 and 7603. The identification seems to be satisfactory.

In Table VI the terms arising from $5p^4 6p$ have been traced. The other parts of the table explain themselves. The terms of different groups of

Table VI -- Term Values of the p Sequence $5p^4 \cdot np$.

$5p^4 \cdot 1^+$	$5p^4 \cdot {}^3P_2 \cdot np$						$5p^4 \cdot {}^3P_1 \cdot np$					$5p^4 \cdot {}^3P_0 \cdot np$	
Series electron	5/2	7/2	5/2	3/2	3/2	1/2	3/2	5/2	3/2	1/2	1/2	3/2	1/2
6p	19270	18675	18379	17370	17113	16177	13845	13581	13515	13242	12637	7809	7603
7p	10476	10247	9822	9336	8740	8023	4455	4087	3900	3874	3706		
8p	6276	6123	5793	5649	5235	5015	- 340	- 336					
9p	4134	4035	4010	3755	3668								
10p	2916	2849											

* 'Z. Physik,' vol. 37, p. 238 (1926), vol. 39, p. 172 (1926).

† Saha and Majumdar, 'Ind. J. Phys.,' vol. 3, p. 67 (1928).

$5p^4 . 6p$ and their Rydberg sequences are also shown there. In $5p^4 . {}^3P_1 6p$ and $5p^4 . {}^3P_0 6p$, the terms tend to become negative after the second. Although there are several lines beyond λ 3400 Å. which may correspond to these negative terms, they are so much mixed up with spark lines that their separation is practically impossible until the spark lines of iodine are definitely known. Still I have tried to identify some of these negative terms. They are also included in Table VI. It can be shown that the terms in the second and third columns of Table VI follow the Rydberg sequences given below :—

(A) For the terms in the second column with $j = 5/2$

$$\frac{R}{(m + 0.111 + 1.1304/m^2)^2}$$

(B) For the terms in the third column with $j = 7/2$

$$\frac{R}{(m + 0.171 + 0.196/m - 0.311/m^2 + 1.86/m^3)^2}$$

The differences in values between the terms obtained from analysis and those calculated with the help of above formulæ are nowhere very great, the largest for the series A is -2 in the case of $8p$ and for the series B is 1 in the case of $10p$.

In Table VII the terms of the $5p^4 6s$ electron configuration and their Rydberg sequences will be found. In this case also terms arising from the $5p^4 . {}^3P_2 6s$

Table VII —List of Term Values of the “s” Sequence.

$5p^4 \quad I^+$	3P_4		3P_1		3P_0
Series electron	${}^4P_{5/2}$	${}^2P_{3/2}$	${}^4P_{7/2}$	${}^2P_{1/2}$	${}^4P_{1/2}$
6s	30807	20350	24550	23628	19014
7s	(13100)		(6900)		223.2
8s	(7250)		1851	990	(— 3800)
9s	4569	3622	(— 1700)		(— 6500)
10s	3452	2948	(— 3000)		(— 7800)

Terms within brackets are extrapolated

configuration follow a Rydberg sequence whereas the terms arising from $5p^4 . {}^3P_1 6s$ and $5p^4 . {}^3P_0 6s$ configurations follow the sequence when 6000 and 11,400 wave-number units are added to them respectively.

In Tables VIII and IX, we give the identified lines in tabular form, along with the terms from which they arise as well as their values.

Table VIII.

J values ↓	Term values ↓	No.	6s $^4P_{5/2}$ 30807	1457 $^2P_{3/2}$ 29350	4800 $^4P_{3/2}$ 24550	922 $^2P_{1/2}$ 23628	4534 $^4P_{1/2}$ 19094
$^3P_2, ^1P$	$6p$						
5/2	19270	1	(8) 11537 6				
7/2	18675	2	(10) 12132 4				
5/2	18379	3	(9) 12428 6	(7) 10909 2			
3/2	17570	4	(4) 13236 4	(4) 11781 2			
3/2	17113	5	(5) 13694 3	(7) 12237 2			
3/2	16177	6		(3) 13173 8			
$^3P_1, ^3P$							
3/2	13845	7	(8) 16961 8	(6) 15505 4	(2) 10708 3		
5/2	13581	8	(4) 17226 0	(6) 15768 6	(7) 10969 2		
3/2	13515	9	(3) 17292 6	(4) 15835 5	(5) 11036 4		
1/2	13242	10		(5) 16088 4	(4) 11286 8		
1/2	12637	11		(3) 16713 8	(4) 11910 9	(1) 10987 4	
$^3P_0, ^3P$							
3/2	7809	12	(5) 22998 3	(6) 21541 6	(4) 16740 6	(4) 15817 4	(3) 11285 3
1/2	7603	13		(4) 21748 4	(5) 16947 6	(2) 16024 4	(2) 11490 0
$^3P_2, ^1P$	$7p$						
5/2	10476	1	(16) 20331 0	(8) 18875 1	(4) 14075 3		
7/2	10247	2	(20) 20560 7				

Table VIII—(continued).

J values ↓	Term values ↓	No.	6s $^4P_{3/2}$ 30807	1457 $^2P_{3/2}$ 29350	4800 $^4P_{3/2}$ 24550	922 $^2P_{1/2}$ 23628	4534 $^4P_{1/2}$ 19094
$^3P_1, ^2P$	7p						
5/2	9822	3	(7) 20987.7	(12) 19528.2	(6) 14725.8		
3/2	9336	4	(4) 21468.6	(4) 20013.7	(3) 15214.6	(2) 14295.4	(3) 9758
3/2	8740	5	(2) 22067.8	(4) 20611.7	(3) 15812.5	(1) 14892.1	(1) 10356.7
1/2	8023	6		(3) 21327.7	(5) 16527.6	(1) 15606.4	?
$^3P_1, ^2P$							
3/2	4455	7	(3) 26352.4	(2) 24893.7	(1) 20096.1	(2) 19173.7	(2) 14641.5
5/2	4087	8	(4) 26718.4	(3) 25263.9	(4) 20465.9		
1/2	3990	9		(2) 25361.8	(4) 20561.4	(1) 19638.0	(2) 15102.3
3/2	3874	10	(4) 26934.5	(2) 25476.9	(3) 20675.1	(4) 19751.8	(0) 15215.6
1/2	3706	11		(2) 25644.0	(2) 20842.4	?	(2) 15389.8
$^3P_1, ^2P$	8p						
5/2	6276	1	(4) 24529.6	(3) 23072.2	(5) 18274.5		
7/2	6123	2	(5) 24683.8				
5/2	5793	3	(3) 25013.9	(1) 23558.2	(1) 18756.0		
3/2	5649	4	(2) 25158.0	(1) 23706.1	(3) 18903.2	?	(5) 13446.5
3/2	5235	5	(2) 25572.1	(2) 24114.1	(2) 19316.8	(5) 18392.5	(1) 13859.9
1/2	5013	6		(3) 24334.4	(2) 19533.5	(1) 18615.3	(2) 14080.5
$^3P_1, ^2P$							
3/2	-340	7	(2) 31147.5	(1) 29689.4	(3) 24886.7	(2) 23965.1	(0) 19430.2
5/2	-536	8	(2) 31342.7	(0) 29883.9	(2) 25082.9		

Table VIII—(continued).

J values ↓	Term values → ↓	No.	6s 30807	⁴ P _{3/2} 1457 20350	² P _{3/2} 4800 24550	922 23628	4534 10094
⁴ P _{3/2} ² P	9p						
5/2	4134	1	(2) 26672·0	(2) 25216 3	(5) 20415·9		
7/2	4035	2	(4) 26771 8				
5/2	4010	3	(2) 26796·2	(1) 25341 4	(1) 20540 5		
3/2	3758	4	(1) 27051 9	(3) 25596 1	(3) 20792 8	(2) 19871 6	(1) 15335 9
3/2	3668	5	(1) 27130 4	(3) 25681 7	(3) 20883 2	(2) 19961·1	(1) 15429 5
² P _{3/2} ² P	10p						
5/2	2916	1	(1) 27890 4	(2) 26435 3	(3) 21634 4		
7/2	2849	2	(3) 27957 6				

Table IX.

6p→ Series electron ↓	J→ Term	No → Term values→ ↓	5/2 1 19270	5p5 7/2 2 18675	296 3 18379	5/2 808 3/1 4 17570	458 3/2 5 17113	936 1/2 6 16177
7s	⁴ P _{1/2}	2232				(5) 15338 2	(4) 14879 4	(2) 13945·2
8s	⁴ P _{3/2}	1851	(4) 17418 8		(5) 16527 6	(2) 15721 2	(1) 15261 6	(0) 14326·3
	² P _{1/2}	990				(2) 16580 8	(4) 16123 2	(1) 15187 0
9s	⁴ P _{5/2}	4569	(4) 14699 7	(6) 14104 3	(3) 13812·4	(1) 13004 7	(2) 12546 0	
	² P _{3/2}	3622	(3) 15647·7		(4) 14759 2	(3) 13950 5	(4) 13489·3	9
10s	⁴ P _{5/2}	3452	(6) 15816 9	(8) 15224 7	(5) 14927 4	(2) 14119 7	(2) 13661 0	
	² P _{3/2}	2948	(6) 16320 6		(4) 15433 8	(2) 14625 0	(1) 14165 9	(3) 13229·6

9. Ionisation Potential of Iodine

From the peak of the continuous patch, the intensity curve of which is given in Plate 6, we fix the value of ${}^2P_{3/2}$ term of Gs level to be 29350 cm.^{-1} . Adding to it $56,089$, the frequency of the line ($5p^5\ {}^2P_{3/2} - 5p^4.6s\ {}^2P_{3/2}$), we find the value of the term $5p^5\ {}^2P_{3/2}$ to be $85,439\text{ cm.}^{-1}$. This gives the ionisation potential as 10.548 volts. Other estimations of the ionisation potential of iodine atom are due to Fruth* and Evans (*loc. cit.*). Evans gave the ionisation potential of iodine as 10.44 volts, but his analysis was not satisfactory, and the agreement can only be regarded as fortuitous. Fruth estimated the ionisation potential to be between 8 and 8.5 volts; this certainly is a very low estimate, and it is to be feared that he has not put the right interpretation on his experimental results. He subjected iodine vapour to electron bombardment, and found that arc is struck when the electron voltage reaches the value 8.5 volts. Apparently such an estimate is useless unless correction is made for the contact difference of potential, which does not appear to have been done. There are, however, other arguments in favour of the value given here. The ionisation potentials of consecutive elements from In to Xe are mostly known: they are shown in Table X. The elements whose ionisation potentials are unknown in this group are only Te and I, and it is well known that the values of ionisation potentials of successive elements form a linear sequence. Extrapolating in this way, the ionisation potential of iodine comes out to be 10.69 volts, which is in good agreement with our value.

Table X

At. No	Element.	Ionisation potential	References.
49	In	5.76	Fowler's Report, p. 158
50	Sn	7.37	Green and Loring, 'Phys. Rev.,' vol. 30, p. 575 (1927)
51	Sb	8.5	F. Charola, 'Phys. Z.,' vol. 31, p. 457 (1930).
52	Te	---	Not known.
53	I	(10.548)	Obtained in this paper.
54	Xe	12.078	Meggers, de Bruin and Humphreys, 'Bur. Std. J. Research,' vol. 3, p. 731 (1929)

* 'Phys. Rev.,' vol. 31, p. 622 (1928).

10 *Classified Lines.*

The lines which have been classified are collected in Table XI.

Table XI.—List of Classified Lines.

λ	I	ν (vac)	Combinations
*1507.3	3	66342	$5p\ ^2P_{3/2} - 6s\ ^4P_{1/2}$
*1617.9	6	61809	$5p\ ^2P_{3/2} - 6s\ ^2P_{1/2}$
*1642.5	7	60885	$5p\ ^2P_{3/2} - 6s\ ^4P_{3/2}$
*1702.3	8	58744	$5p\ ^2P_{1/2} - 6s\ ^4P_{1/2}$
*1782.9	9	56089	$5p\ ^2P_{3/2} - 6s\ ^2P_{3/2}$
†*1830.4	10	54632	$5p\ ^2P_{3/2} - 6s\ ^4P_{3/2}$
*1844.5	9	54216	$5p\ ^2P_{1/2} - 6s\ ^2P_{1/2}$
*1876.4	7	53293	$5p\ ^2P_{1/2} - 6s\ ^4P_{3/2}$
†*2062.1	10	48494	$5p\ ^2P_{1/2} - 6s\ ^2P_{3/2}$
3189.62	2	31342.7	$6s\ ^4P_{5/2} - 8p8_{5/2}$
3209.61	2	31147.5	$6s\ ^4P_{5/2} - 8p7_{3/2}$
3345.32	0	29883.5	$6s\ ^2P_{3/2} - 8p8_{5/2}$
3367.24	1	29689.4	$6s\ ^2P_{3/2} - 8p7_{3/2}$
3575.82	3	27957.6	$6s\ ^4P_{3/2} - 10p2_{7/2}$
3584.40	1	27890.4	$6s\ ^4P_{5/2} - 10p1_{5/2}$
3683.64	1	27139.4	$6s\ ^4P_{5/2} - 9p5_{3/2}$
3695.55	1	27051.9	$6s\ ^4P_{5/2} - 9p4_{3/2}$
3711.57	4	26934.4	$6s\ ^4P_{5/2} - 7p10_{3/2}$
3730.81	2	26796.2	$6s\ ^4P_{5/2} - 9p3_{5/2}$
3734.28	4	26771.8	$6s\ ^4P_{5/2} - 9p2_{7/2}$
3741.69	1	26718.4	$6s\ ^4P_{5/2} - 7p8_{5/2}$
3748.06	2	26672.9	$6s\ ^4P_{5/2} - 9p1_{5/2}$
3781.74	2	26435.3	$6s\ ^2P_{3/2} - 10p1_{5/2}$
3808.08	3	26352.4	$6s\ ^4P_{5/2} - 7p7_{3/2}$
3892.86	3	25681.7	$6s\ ^2P_{3/2} - 9p5_{3/2}$
3898.44	2	25644.0	$6s\ ^2P_{3/2} - 7p11_{1/2}$
3905.75	3	25596.1	$6s\ ^2P_{3/2} - 9p4_{3/2}$
3909.41	2	25572.1	$6s\ ^4P_{5/2} - 8p5_{3/2}$
3924.02	2	25476.9	$6s\ ^2P_{3/2} - 7p10_{3/2}$
3941.82	2	25361.8	$6s\ ^2P_{3/2} - 7p9_{1/2}$
3945.52	1	25341.4	$6s\ ^2P_{3/2} - 9p3_{5/2}$
3957.10	3	25263.9	$6s\ ^2P_{3/2} - 7p8_{5/2}$
3964.57	2	25216.3	$6s\ ^2P_{3/2} - 9p1_{5/2}$
3973.75	2	25158.0	$6s\ ^4P_{5/2} - 8p4_{3/2}$
3985.68	2	25082.9	$6s\ ^4P_{5/2} - 8p8_{5/2}$
3996.65	2	25013.7	$6s\ ^4P_{5/2} - 8p3_{5/2}$
4015.94	2	24893.7	$6s\ ^2P_{3/2} - 7p7_{3/2}$
4017.32	3	24886.8	$6s\ ^4P_{5/2} - 8p7_{3/2}$
4050.09	5	24683.8	$6s\ ^4P_{5/2} - 8p2_{7/2}$
4075.56	4	24529.6	$6s\ ^4P_{5/2} - 8p1_{5/2}$
4108.25	3	24334.4	$6s\ ^2P_{3/2} - 8p6_{1/2}$
4145.78	2	24114.1	$6s\ ^2P_{3/2} - 8p5_{3/2}$
4171.56	2	23965.1	$6s\ ^2P_{3/2} - 8p7_{5/2}$
4217.08	1	23706.4	$6s\ ^2P_{3/2} - 8p4_{3/2}$
4243.56	1	23558.2	$6s\ ^2P_{3/2} - 8p3_{5/2}$
4333.00	3	23072.2	$6s\ ^2P_{3/2} - 8p1_{5/2}$
4346.92	5	22998.3	$6s\ ^4P_{5/2} - 6p12_{3/2}$
4530.22	2	22067.8	$6s\ ^4P_{5/2} - 7p5_{3/2}$
4596.73	4	21748.6	$6s\ ^2P_{3/2} - 6p13_{1/2}$
4620.97	3	21634.4	$6s\ ^4P_{5/2} - 10p1_{5/2}$

* Turner's lines.

† Obtained in absorption.

Table XI—(continued).

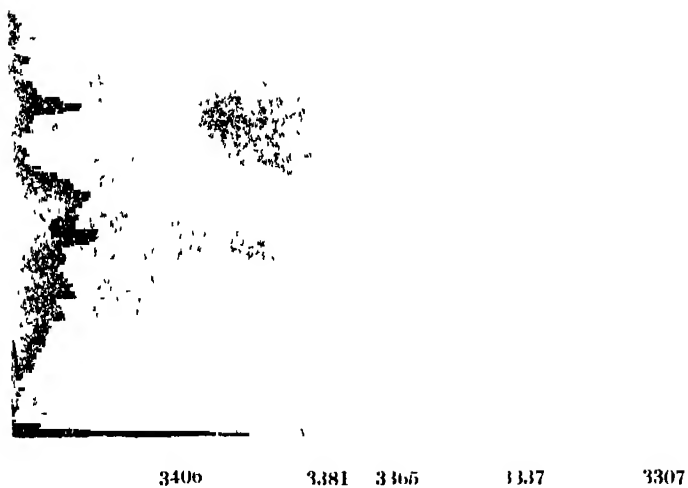
λ .	I.	ν (vac)	Combinations.
4640.88	6	21541 6	$6s^4P_{3/2} - 8p12_{3/2}$
4656 87	4	21468 6	$6s^4P_{3/2} - 7p4_{1/2}$
4687 43	3	21327 7	$6s^4P_{3/2} - 7p0_{1/2}$
4703 37	7	20987 7	$6s^4P_{5/2} - 7p3_{5/2}$
4787 21	3	20883 2	$6s^4P_{3/2} - 9p5_{3/2}$
4796 58	2	20842 4	$6s^4P_{3/2} - 7p11_{1/2}$
4808 02	3	20792 8	$6s^4P_{3/2} - 9p4_{3/2}$
4835 37	3	20675 1	$6s^4P_{3/2} - 7p10_{3/2}$
4850 26	4	20611 7	$6s^4P_{3/2} - 7p5_{3/2}$
4862 13	4	20561 4	$6s^4P_{3/2} - 7p9_{1/2}$
4862 30	20	20560 7	$6s^4P_{5/2} - 7p2_{1/2}$
4867 08	1	20540 5	$6s^4P_{3/2} - 9p3_{3/2}$
4884 82	4	20465 9	$6s^4P_{3/2} - 7p8_{3/2}$
4896 77	5	20415 9	$6s^4P_{3/2} - 9p1_{3/2}$
4917 23	16	20331 0	$6s^4P_{3/2} - 7p1_{3/2}$
4974 51	1	20096 1	$6s^4P_{3/2} - 7p7_{3/2}$
4995 15	4	20013 7	$6s^4P_{3/2} - 7p4_{3/2}$
5008 35	1	19961 1	$6s^4P_{1/2} - 9p5_{3/2}$
5030 90	2	19871 6	$6s^4P_{1/2} - 9p4_{3/2}$
5061 42	4	19751 8	$6s^4P_{1/2} - 7p10_{3/2}$
5090 76	1	19638 0	$6s^4P_{1/2} - 7p9_{1/2}$
5118 01	2	19533 5	$6s^4P_{3/2} - 8p6_{1/2}$
5119 38	12	19528 2	$6s^4P_{3/2} - 7p3_{5/2}$
5145 21	0	19430 2	$6s^4P_{1/2} - 8p7_{1/2}$
5175 40	2	19316 8	$6s^4P_{3/2} - 8p5_{3/2}$
5214 04	3	19173 7	$6s^4P_{1/2} - 7p7_{3/2}$
5288 65	3	18903 2	$6s^4P_{1/2} - 8p4_{3/2}$
5296 52	8	18875 1	$6s^4P_{3/2} - 7p1_{3/2}$
5330 16	1	18756 0	$6s^4P_{3/2} - 8p3_{5/2}$
5370 43	1	18015 3	$6s^4P_{1/2} - 8p6_{1/2}$
5435 48	5	18392.5	$6s^4P_{1/2} - 8p5_{3/2}$
5470 53	4	18274 7	$6s^4P_{5/2} - 8p1_{3/2}$
5739 34	4	17418 8	$6p1_{3/2} - 8s^4P_{3/2}$
5781 23	3	17292 6	$6s^4P_{3/2} - 6p9_{3/2}$
5803 58	4	17226 0	$6s^4P_{3/2} - 6p8_{3/2}$
5899.02	4	16947 6	$6s^4P_{3/2} - 6p13_{1/2}$
5893 06	8	16961 8	$6s^4P_{3/2} - 6p7_{3/2}$
5971.85	5	16740 6	$6s^4P_{3/2} - 6p12_{3/2}$
5981 42	3	16713 9	$6s^4P_{3/2} - 6p11_{1/2}$
6029 39	1	16580 8	$6p4_{3/2} - 8s^4P_{1/2}$
6048 72	5	16527 6	$\left\{ \begin{array}{l} 6p3_{3/2} - 8s^4P_{3/2} \\ 6s^4P_{3/2} - 7p6_{1/2} \end{array} \right.$
6125.53	6	16320 6	$6p1_{3/2} - 10s^4P_{3/2}$
6200 52	4	16123 2	$6p5_{3/2} - 8s^4P_{1/2}$
6213 91	5	16088 4	$6s^4P_{3/2} - 6p10_{1/2}$
6238 74	2	16024 4	$6s^4P_{1/2} - 6p13_{1/2}$
6313.12	4	15835 5	$6s^4P_{3/2} - 6p9_{3/2}$
6320 41	4	15817.4	$6s^4P_{1/2} - 6p12_{3/2}$
6320 60	6	15816 8	$6p1_{3/2} - 10s^4P_{3/2}$
6322.38	3	15812 5	$6s^4P_{3/2} - 7p5_{3/2}$
6338 97	6	15768 6	$6s^4P_{3/2} - 6p8_{3/2}$
6359 09	2	15721 2	$6p4_{3/2} - 8s^4P_{3/2}$
6388 94	3	15647 7	$6p1_{3/2} - 9s^4P_{3/2}$
6405 87	1	15606 4	$6s^4P_{1/2} - 7p6_{1/2}$
6444 51	6	15505 4	$6s^4P_{3/2} - 6p7_{3/2}$
6477 48	1	15433 8	$6p3_{5/2} - 10s^4P_{3/2}$
6478.94	1	15429 5	$6s^4P_{1/2} - 9p5_{3/2}$
6496.01	2	15389 4	$6s^4P_{1/2} - 7p11_{1/2}$
6517.88	3	15338 2	$6p4_{3/2} - 7s^4P_{1/2}$
6518.86	1	15335.9	$6s^4P_{1/2} - 9p4_{3/2}$

Table XI—(continued).

λ	I	ν (vac.).	Combinations.
6550.58	1	15261.6	$6p5_{3/2} - 8s^4P_{3/2}$
6566.45	8	15224.7	$6p2_{3/2} - 10s^4P_{3/2}$
6569.27	1	15218.2	$6s^4P_{1/2} - 7p10_{3/2}$
6570.81	3	15214.6	$6s^4P_{3/2} - 7p4_{3/2}$
6582.76	1	15187.0	$6p6_{1/2} - 8s^4P_{1/2}$
6619.70	2	15102.3	$6s^4P_{1/2} - 7p9_{1/2}$
6697.23	5	14927.4	$6p3_{3/2} - 10s^4P_{3/2}$
6713.13	1	14892.1	$6s^4P_{1/2} - 7p5_{3/2}$
6718.85	4	14879.4	$6p5_{1/2} - 7s^4P_{1/2}$
6773.56	1	14759.2	$6p3_{3/2} - 9s^4P_{3/2}$
6788.03	6	14725.8	$6s^4P_{3/2} - 7p3_{3/2}$
6801.00	4	14690.7	$6p1_{3/2} - 9s^4P_{3/2}$
6828.02	2	14641.5	$6s^4P_{1/2} - 7p7_{3/2}$
6835.70	2	14625.0	$6p4_{1/2} - 10s^4P_{3/2}$
6978.22	0	14326.3	$6p6_{1/2} - 8s^4P_{3/2}$
6993.35	2	14295.4	$6s^4P_{1/2} - 7p4_{3/2}$
7057.27	1	14165.9	$6p4_{3/2} - 10s^4P_{3/2}$
7080.34	3	14119.7	$6p4_{3/2} - 10s^4P_{3/2}$
7088.00	6	14104.3	$6p2_{7/2} - 9s^4P_{5/2}$
7100.16	2	14080.5	$6s^4P_{1/2} - 8p6_{1/2}$
7102.05	4	14075.3	$6s^4P_{3/2} - 7p1_{5/2}$
7166.47	3	13950.3	$6p4_{3/2} - 9s^4P_{3/2}$
7168.87	2	13945.2	$6p6_{1/2} - 7s^4P_{1/2}$
7213.11	1	13859.9	$6s^4P_{1/2} - 8p5_{3/2}$
7237.88	3	13812.3	$6p3_{3/2} - 9s^4P_{3/2}$
7300.30	4	13694.3	$6s^4P_{5/2} - 6p5_{3/2}$
7318.12	2	13661.0	$6p5_{3/2} - 10s^4P_{3/2}$
7411.25	4	13489.3	$6p5_{3/2} - 9s^4P_{3/2}$
7490.58	5	13446.5	$6s^4P_{1/2} - 8p4_{3/2}$
7554.25	5	13236.4	$6s^4P_{3/2} - 6p4_{3/2}$
7556.69	3	13220.6	$6p6_{1/2} - 10s^4P_{3/2}$
7588.70	3	13173.8	$6s^4P_{3/2} - 6p6_{1/2}$
7687.41	1	13004.7	$6p4_{3/2} - 9s^4P_{3/2}$
7969.54	2	12546.0	$6p5_{3/2} - 9s^4P_{3/2}$
8043.74	9	12428.6	$6s^4P_{5/2} - 6p3_{5/2}$
8169.51	7	12237.2	$6s^4P_{3/2} - 6p5_{3/2}$
8240.13	10	12132.4	$6s^4P_{3/2} - 6p2_{7/2}$
8393.42	4	11910.9	$6s^4P_{3/2} - 6p11_{1/2}$
8486.16	4	11781.2	$6s^4P_{3/2} - 6p4_{3/2}$
8664.93	8	11537.6	$6s^4P_{3/2} - 6p1_{3/2}$
8700.80	2	11490.0	$6s^4P_{1/2} - 6p13_{1/2}$
8857.46	4	11286.8	$6s^4P_{3/2} - 6p10_{3/2}$
8858.62	3	11285.3	$6s^4P_{1/2} - 6p12_{3/2}$
9058.38	5	11036.4	$6s^4P_{3/2} - 6p9_{3/2}$
9098.81	1	10987.4	$6s^4P_{1/2} - 6p11_{1/2}$
9113.88	9	10969.2	$\left\{ \begin{array}{l} 6s^4P_{3/2} - 6p3_{5/2} \\ 6s^4P_{3/2} - 6p8_{5/2} \end{array} \right.$
*9335.99	2	10708.3	$6s^4P_{3/2} - 6p7_{3/2}$
*9356.88	1	10356.7	$6s^4P_{1/2} - 7p5_{3/2}$
*10245	1	9758	$6s^4P_{1/2} - 7p4_{3/2}$

* Lines taken from Evans' paper.

The author wishes to express his indebtedness to Professor Saha, F.R.S., under whose direction and guidance this work has been carried out. His best



MICROPHOTOGRAM OF THE CONTINUOUS EMISSION

The wave-lengths marked in this plate are those of copper arc spectrum used for comparison, except 3406, which is marked to show the region of maximum in the continuous emission

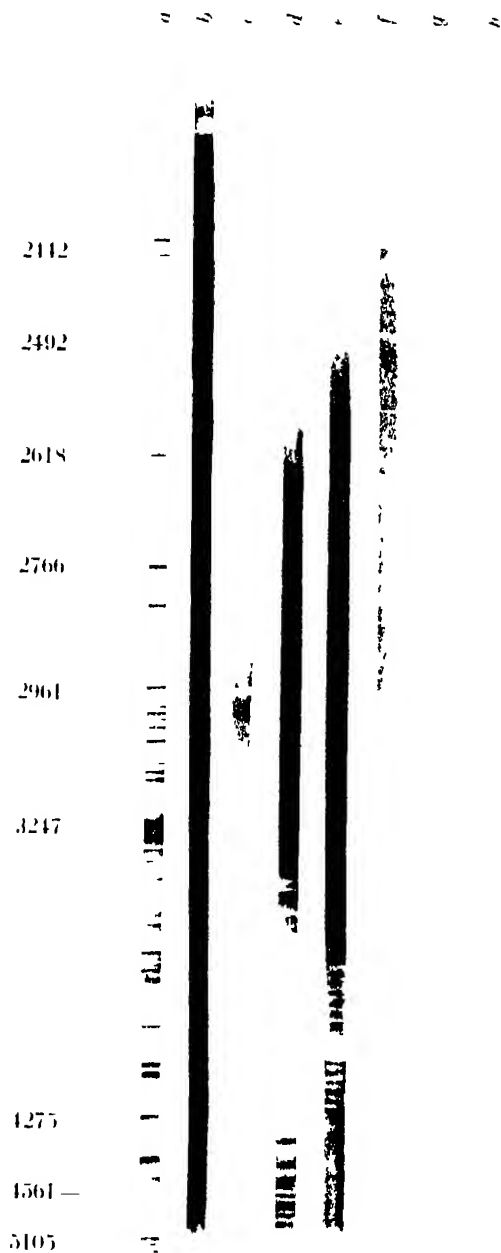


FIG. 5. a—comparison spectrum of copper

b—continuous spectrum

c, d, e—absorption spectra of N_2O , under different conditions, with NO_2 as impurityf, g, h—absorption spectra of NO_2 under different pressures. Compare the predissociation spectra of NO_2 with those obtained by Herz. Trans. Faraday Soc. vol. 25, p. 765 (1929).

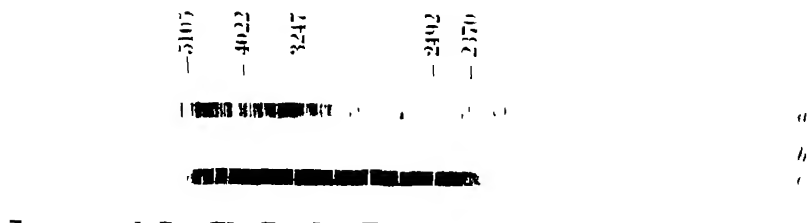


FIG. 6. *a*—comparison spectrum of copper,
b—absorption spectrum TeO_2 ,
c—continuous spectrum with scratches marked for comparison.

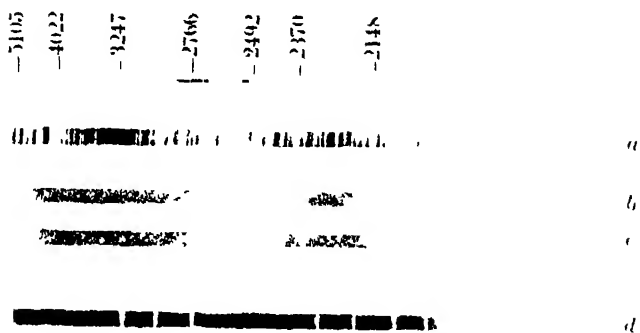


FIG. 7. *a*—comparison spectrum of copper,
b, c—absorption spectrum of MoO_3 at different temperatures,
d—continuous spectrum with scratches marked for comparison.

thanks are also due to Mr. D. G. Dhavale, M.Sc., who assisted him in photographing the infra-red and visible part of the spectrum.

11. Summary.

The spectrum of iodine has been photographed in the region λ 3200 to λ 9113 in emission, and in the region λ 2300 to λ 1800 in absorption. The transitions ($5p-6s$), ($6s-np$) and ($6p-ns$) have been identified from the data obtained by the author, from which the ionisation potential of iodine has been found to be 10.548 volts. Altogether 160 lines out of a total of 437 recorded lines have been classified.

On the Absorption Spectra of Some Higher Oxides.

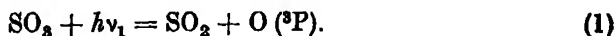
By ARUN K. DUTTA, M.Sc., and PRABHAT K. SEN GUPTA, M.Sc.,
Department of Physics, Allahabad University, Allahabad, India.

(Communicated by M. N. Saha, D Sc , F.R.S.—Received July 27, 1932.)

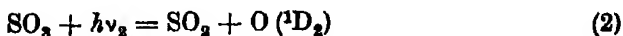
[PLATES 7 AND 8.]

Introduction.

Very little work has been done on the absorption spectra of the higher oxides, but recently, one of us* has found that SO_3 gives a continuous absorption, beginning from a long wave limit, and after retransmission of a patch of light absorption again sets in. It was postulated that the first long wave limit of absorption by SO_3 marks the photochemical dissociation into SO_2 and normal oxygen atom, according to the equation



From this formula the heat of dissociation of oxygen was obtained with the help of some thermochemical data. The second long wave limit of absorption was attributed to the dissociation of SO_3 into SO_2 and excited oxygen, according to the process,



the difference between the two beginnings of absorption giving approximately the energy of excitation of oxygen from ^3P to $^1\text{D}_2$ states.

* Dutta, 'Proc. Roy. Soc.,' A, vol. 137, p. 336 (1932).

In this paper we have studied the absorption spectra of a few more higher oxides, viz., N_2O_5 , TeO_3 , MoO_3 . As expected, all of them showed the same type of absorption as SO_3 . There was a first absorption on the long wavelength side, followed by a patch of retransmitted light, which was again succeeded by a second region of absorption. The methods of procedure are described below.

Experimental Procedure.

The first substance examined was N_2O_5 . Pure solid N_2O_5 was prepared* by adding the requisite quantity of phosphorus pentoxide to distilled nitric acid of high specific gravity. The mixture was distilled at a temperature of $32^\circ C.$, and crystalline N_2O_5 was obtained in the receiver, cooled in a freezing mixture. As is well known, it is very difficult to obtain N_2O_5 gas in a pure state, as it partially decomposes into NO_2 and O_2 . This decomposition is spontaneous and supposed to be monomolecular.† The crystalline solid was placed in a bulb attached to an absorption tube 50 cm. in length. The ends were sealed with quartz windows, and a ground glass stopper closed the side tube. In order to prevent decomposition as much as possible, the bulb was kept surrounded by freezing mixture, and the tube was kept cool by pouring cold water over it. Different pressures of the gas were obtained by varying the temperature of the bath surrounding the bulb. NO_2 , however, could not be completely eliminated, and its characteristic absorption bands also appeared in the spectrum. These bands could easily be identified and eliminated by comparison. For this some blank experiments were done by taking the absorption spectrum of NO_2 , which was prepared by heating lead nitrate. For a continuous source, the use of the hydrogen discharge tube run by a 2-kilowatt transformer has been found to be very convenient, as it gives a continuous spectrum from 5000 Å to 2000 Å with sufficient intensity. The spectrum was photographed in a quartz spectrograph of medium size.

The substances MoO_3 and TeO_3 have rather high melting points, $695^\circ C.$ and $795^\circ C.$ respectively, and to obtain sufficient vapour pressure, considerably higher temperatures were required, thus necessitating the use of a high temperature furnace. We found a Heræus furnace which could be electrically heated to be very convenient for MoO_3 . The furnace was 50 cm. long, and could be heated from the 220 volts D.C. mains, and by proper adjustment of resistances

* Our thanks are due to Dr. S. Dutta, Reader in Chemistry, Allahabad University, for kindly preparing the substance for us.

† Daniels and Johnston, 'J. Amer. Chem. Soc.', vol. 43, pp. 53, 72 (1921).

the temperature could be varied and maintained fairly constant for a considerable length of time. The absorption vessel was a seamless steel tube 90 cm. long, $3\frac{1}{2}$ cm. in diameter, the walls being 4 mm. thick. It was closed by quartz windows which were carried in water-cooled brass sockets. These were fixed to the tube by means of sealing wax. The substance was placed in a silica boat, the sides were sealed as described above, and the vessel was evacuated from a side tube, which was soldered to the iron tube. Diaphragms of iron were so placed as to obstruct the flow of vapour towards the quartz windows. These, combined with water cooling, completely prevented the deposit of the oxide on the quartz plates. Also as the diaphragms checked the flow of the gas, the conditions became nearer to that of a closed vessel, where variations of temperature gave rise to respective saturated vapour pressures. Thus different pressures of the gas were obtained by changing the temperature of the furnace. At high temperatures the tube was filled with N_2 to prevent rapid evaporation. In the case of MoO_3 the oxide was noticed to melt at dull red heat, but no appreciable vapour was visible, and plates taken at this stage indicated no absorption. As the temperature was increased beyond red heat, some smoky vapour was at first seen to rise from the molten mass, but again no appreciable absorption was found. On slightly increasing the temperature, the whole of the tube was filled with dense vapour, which almost completely obscured the light. Finally the vapour began to clear up till the transmitted continuous light became gradually more intense. At this stage the current in the furnace was found to be 17 amperes, this was gradually increased to about 20 amperes and different photographs were taken. From 18 to 20 amperes retransmissions, followed by reabsorption of light, were obtained very clearly on the plates. Exposures of 8 to 10 minutes were sufficient.

For TeO_3 , the vacuum graphite furnace of this laboratory was used.* TeO_3 decomposes slightly into TeO_2 and O_2 by heat. This was easily overcome by filling the vacuum chamber with excess of oxygen. In this process the graphite tube became rapidly oxidised, but it lasted for a sufficiently long time to enable us to obtain two photographs. The salt was contained in a silica tube open at both ends, and was placed inside the graphite furnace. The best condition of absorption was found to be at the start, when only a small amount of vapour was formed. The same hydrogen discharge tube was used as the continuous source, and the photographs were taken on an E_3 spectrograph. The copper arc spectrum was taken for comparison.

* Desai, 'Proc. Roy. Soc.,' A vol. 136, p. 76 (1932).

As eye estimations of absorption gives rather an inaccurate idea of the beginning of absorption, microphotographs of the plates were taken. For this, the microphotometer belonging to the Patna laboratory was used, and we take this opportunity of thanking Professor A. T. Mukherjee of the Patna Science College, for kindly allowing us the use of this apparatus. The procedure adopted to obtain the positions of the first and second beginnings of absorption is described later.

Discussion of Results.

N_2O_5 .—The absorption spectrum of N_2O_5 is shown in fig. 5, Plate 7. As N_2O_5 could not be obtained free from NO_2 , absorption spectra of pure NO_2 are also shown in fig. 5, to enable us to distinguish the spectrum of N_2O_5 from that of the contaminating NO_2 . It is seen that *f*, *g* and *h* (which show the absorption spectra of pure NO_2 under different pressures) contain a set of bands in the visible extending from λ 5000 to λ 2800, then the continuous spectrum is transmitted in full intensity and a second set of bands is observed beginning about λ 2500. We shall call these the first and second systems of NO_2 respectively. Measurements of the NO_2 bands have, however, been made by various workers.* It is to be noticed that in all conditions the second set of bands of NO_2 appear. But these bands do not appear in spectrum "c," where the light appears to be absorbed from λ 2800. This is apparently the second cut due to N_2O_5 . The tube in condition "c" contains NO_2 also, but the second system of bands of NO_2 cannot appear as light is already cut off by N_2O_5 at λ 2800.†

To obtain the position of the first cut due to N_2O_5 , a further scrutiny of the long wave side is required. An examination of the plates shows that the appearance of the first system of NO_2 bands is very sensitive to external conditions. When the pressure of the gas is high, only the violet end appears, the part on the red side seeming to be completely absorbed, but when the pressure

* Carwile, 'Astrophys. J.,' vol. 67, p. 184 (1928). Harris, 'Proc. Nat. Acad. Sci. Wash.,' vol. 14, p. 690 (1928); Henri, 'Nature,' vol. 125, p. 202 (1930).

† After this work was completed, our attention was drawn to a paper by Urey, Dawsey and Rice in the 'J. Amer. Chem. Soc.,' vol. 51, p. 3190 (1929), in which paper they state that they photographed the absorption spectrum of N_2O_5 and found that in addition to the usual band system which they ascribed to NO_2 , a continuous spectrum, due to N_2O_5 beginning from λ 3050 and extending to the Schumann region was obtained. Our result is at variance with this, and we cannot account for the discrepancy. The authors have not given details of their experiment, and particularly do not state the temperature at which the spectrum was taken. Possibly their use of O_2 had something to do with the complication of results. The matter requires further investigation.

is reduced the whole system of bands from violet to red end appears. In "c," however, we get both the violet and the red ends of the NO_2 bands, though there is complete absorption in the middle. This absorption is, therefore, not due to NO_2 , but to N_2O_5 . It is observed that the first absorption begins about λ 4500. We thus obtain for N_2O_5 a continuous absorption beginning at λ 4500, then a patch of transmitted light and a second absorption beginning at λ 2800.

MoO_3 and TeO_3 .—Figs. 6 and 7, Plate 8, show the absorption spectrum of MoO_3 and TeO_3 respectively. For comparison, a copper spectrum and a continuous spectrum were also taken on the same plate. The plates show a continuous absorption beginning from a long wave limit, a patch of transmitted light after it, and a second absorption. To obtain the correct positions of the beginnings of first and second absorption, microphotograms have been taken. These are shown in figs. 1 and 2 for MoO_3 and TeO_3 respectively. Each figure



FIG. 1.—(a) Microphotograph of the absorption spectrum of MoO_3 . (c) Microphotograph of the continuous spectrum with scratches marked on it.

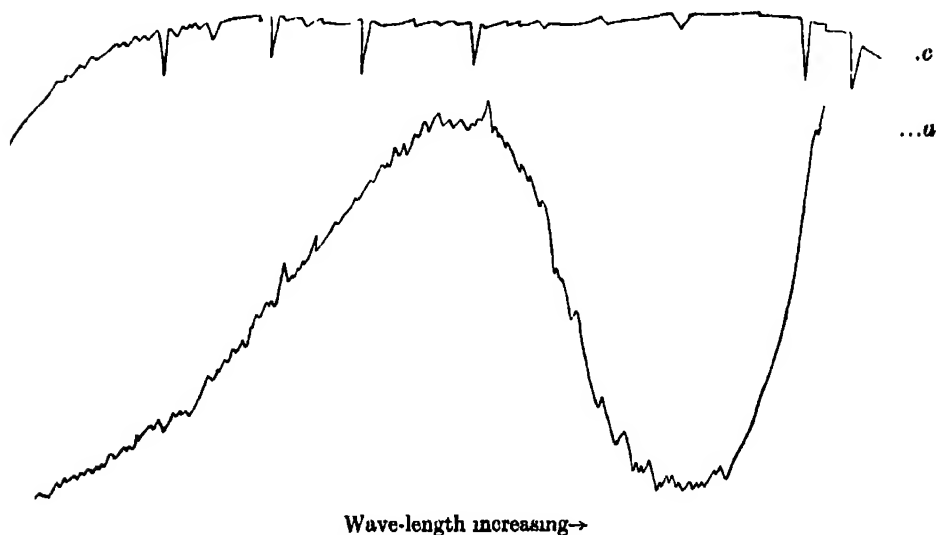


FIG. 2.—(a) Microphotograph of the absorption spectrum of TeO_3 . (c) Microphotograph of the continuous spectrum.

shows the microphotograph along the absorption spectrum and also along the continuous spectrum in which scratches were marked to indicate the wave-lengths. The intensity at different wave-lengths along a spectrum is shown by the respective heights of the microphotograph curve at corresponding points. The microphotograph of the continuous spectrum was recorded under less sensitive conditions. Apparently the falling off of the intensity after the first and second peaks in the absorption microphotograph represents the first and second beginnings of absorption. If, however, the regions of first absorption and second absorption overlap, as in the case of the halides* the positions thus determined will be subject to considerable error. Percentages of absorption at various wave-lengths obtained from the microphotograph curves show that the two regions of absorption are not superposed. This will be observed from the percentages of absorption curves shown in figs. 3 and 4 for TeO_3 and MoO_3 respectively. Evidently this is due to the fact that the second absorption

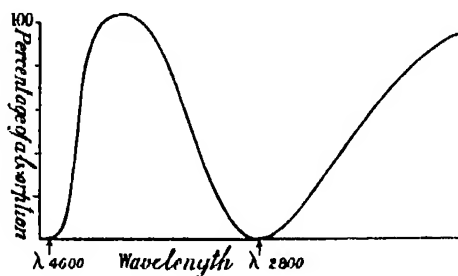


FIG 3.

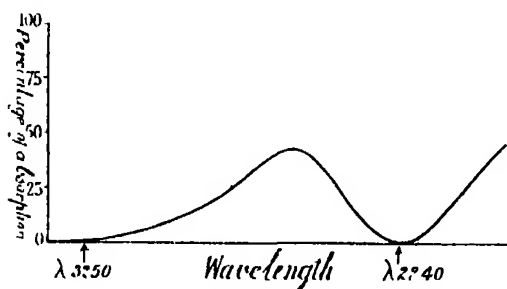


FIG 4

occurs after a sufficiently long energy interval from the first absorption. The absorption curves obtained in this case are, therefore, distinct and quite different in appearance from those obtained by Franck, Kuhn and Rollefson, (*loc. cit.*), in the case of the alkali halides, where they are intermingled with each

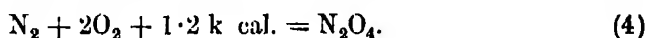
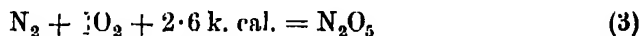
* Franck, Kuhn and Rollefson, 'Z. Physik,' vol. 43, p. 155 (1927).

other. The values obtained from the positions of the first and second beginnings of absorption are λ 3250 Å and 2240 Å for MoO_3 and λ 4600 Å. and, 3000 Å for TeO_3 .

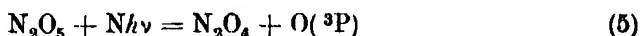
Interpretation of Results.

In the case of the absorption spectrum of SO_3 investigated by one of us (Dutta, *loc. cit.*), a similar result was obtained. As has been mentioned before, the first absorption corresponded to dissociation into SO_2 and normal oxygen atom, and the second absorption denoted dissociation into SO_2 and oxygen excited to the $^1\text{D}_2$ state. From the similarity of the absorption spectra investigated in the present paper with that of SO_3 and also in view of the similar nature of the molecules (all of these are higher oxide molecules) it was considered that the interpretation of the results might be similar. The following calculations show that there is a very good agreement between the experimental values and the values calculated from thermochemical data.

We have for N_2O_5 , thermochemically*



If N_2O_5 is decomposed, by absorption of light of frequency ν , into N_2O_4 and O (normal), we should have



where ν is the frequency of the first cut.

Taking the value of the heat of dissociation of oxygen as 128 k. cal.,† we get from (3), (4) and (5)



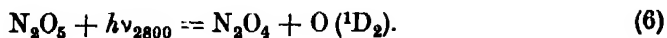
or, $N h \nu$ is equal to 62.6 k. cal. corresponding to λ 4560 Å. The observed beginning of the first absorption was at λ 4500 Å, thus the theoretically calculated limit agrees completely with the observed limit, on the assumption that D_{O_2} is 128 k. cal. Incidentally, this agreement may be taken to be a further confirmation of the view that the heat of dissociation of oxygen is 128 k. cal.

The second beginning of absorption takes place at λ 2800 Å, corresponding to 100.3 k. cal. As in the analogous case of SO_3 , we may suppose that this

* Landolt and Börnstein's Tables, 2nd ed., p. 1496.

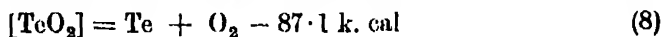
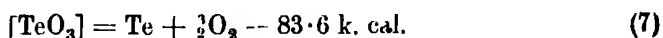
† Dutta, *loc. cit.*

marks the photodissociation of N_2O_5 into N_2O_4 and $O(^1D_2)$, according to the equation

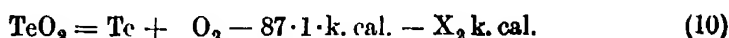
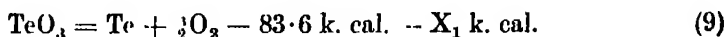


This gives the excitation energy of the 1D_2 -state of oxygen as $(100.3 - 63)$ k. cal., i.e., 1.6 volts.

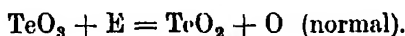
For TeO_3 , we have, thermochemically,



Hence,



The square brackets, in the above equations, signify the solid state of the substance, and X_1 , X_2 are the heats of vaporisation of TeO_3 and TeO_2 . The light energy required to dissociate TeO_3 into TeO_2 and O (normal) would be given by

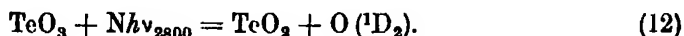


Substituting from (9) and (10), we get,

$$E = 60.5 \text{ k. cal.} + (X_1 - X_2) \text{ k. cal.}$$

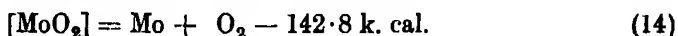
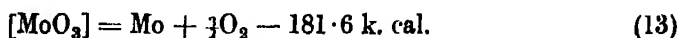
Experimentally, the first beginning of absorption was obtained at $\lambda 4600$, corresponding to 62.1 k. cal. Thus the value of $X_1 - X_2$ comes up as 1.6 k. cal. We could not find any data on the latent heats of evaporation of TeO_3 and TeO_2 , hence the conclusion could not be tested.

The second beginning of absorption at $\lambda 2800$ A, corresponds according to our assumption, to the process

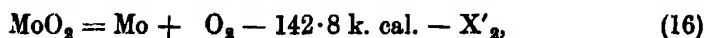
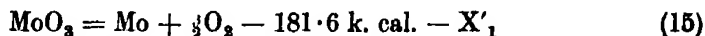


As $\lambda 2800$ corresponds to 100.3 k. cal., we obtain the energy required for exciting to the 1D_2 -state, given by 38.2 k. cal., i.e., 1.66 volts.

In the case of MoO_3 , the thermochemical data are,



When the compounds are considered to be in the vapour state, the corresponding equations are,



where X'_1 and X'_2 are the heats of evaporation of MoO_3 and MoO_2 respectively.

Arguing as above, we should have for MoO_3 , the equation



where $Nh\nu$ would be given by the relation

$$Nh\nu = 102.7 \text{ k. cal.} + (X'_1 - X'_2)$$

The experimental value for the beginning of the first absorption is λ 3250 Å, corresponding to 88 k. cal., so that $X'_1 - X'_2 = 14.7$ k. cal. The value of the heats of evaporation of the compounds MoO_3 and MoO_2 being unknown, quantitative verification could not be made.

The position at the beginning of the second absorption is λ 2240 Å, corresponding to 127.6 k. cal. Assuming the second absorption to denote dissociation into MoO_2 and O excited to the $^1\text{D}_2$ -state, the energy of excitation ($^3\text{P} - ^1\text{D}_2$) comes out as 39.8 k. cal., *i.e.*, 1.8 volts.

The values thus obtained for the excitation energy of the normal oxygen atom to the $^1\text{D}_2$ -state are not equal to each other and do not agree with Frerich's* value of 1.9 volts. Discussions and suggestions arising out of this anomaly will be made in a future paper.

Our thanks are due to Professor M. N. Saha, D.Sc., F.R.S., for his kind instructions during the course of this work.

Summary.

(1) Absorption spectra of N_2O_5 , TeO_3 and MoO_3 have been studied. In all cases there is a first absorption, followed by a retransmitted patch of light, and then a second absorption.

(2) The first absorption has been interpreted as corresponding to dissociation into N_2O_4 and O (^3P), TeO_2 and O (^3P), MoO_2 and O (^3P) respectively, and the second absorption as corresponding to N_2O_4 and O ($^1\text{D}_2$), TeO_2 and O ($^1\text{D}_2$), MoO_2 and O ($^1\text{D}_2$) respectively.

(3) Heat of dissociation of O_2 is found to be 128 k. cal. from absorption of N_2O_5 .

* Frerich's, 'Phys. Rev.', vol. 36, p. 398 (1930)

The Kinetics of Electrode Processes. Part II.—Reversible Reduction and Oxidation Processes.

By J. A. V. BUTLER, D.Sc., and G. ARMSTRONG, Ph D, University of Edinburgh

(Communicated by J. Kendall, F.R.S. —Received August 31, 1932.)

In Part I* the phenomena observed in the polarisation of platinum electrodes in hydrogen and oxygen saturated solutions were explained in terms of a theory of electrolytic depolarisation. In order to elucidate these effects and obtain further support for the equations put forward it seemed desirable to investigate the kinetics of processes in which depolarisers were present in the solution in known variable amounts. We have therefore studied the cathodic reduction of methylene blue solutions and the cathodic and anodic behaviour of solutions of quinhydrone at platinum electrodes.

In the investigation of electrolytic reductions and oxidations a transition phenomenon has frequently been observed.† In such cases the current voltage curve consists of three parts. (1) at low current densities electrolysis takes place at only a small displacement from the initial potential; (2) at higher current densities there is a transition region in which the potential changes continuously until a much greater displacement of the potential has been reached; (3) beyond this transition region a second current voltage curve is obtained which is not far removed from that obtained for the liberation of hydrogen at the cathode, or of oxygen at the anode. It was observed by Wilson and Youtz‡ in the case of the oxidation of ferrous salts that the transitional current density depended on the concentration of the oxidisable substance, and Ellingham§ has recently made a similar observation for the cathodic process in nitric acid solutions.

* 'Proc. Roy. Soc.,' A, vol. 137, p. 604 (1932).

† Cf., Ellingham and Allmand, 'Trans. Faraday Soc.,' vol. 19, p. 753 (1923).

‡ 'J. Ind. and Eng. Chem.,' vol. 15, p. 603 (1923).

§ 'J. Chem. Soc.,' p. 1565 (1932).

In the experiments described below the electrode was of bright platinum foil having an apparent area of 4.3 cm^2 . The experimental cell was similar to that described in Part I, the anode and cathode chambers being separated by a glass tube fitted with a tap which was normally kept closed, sufficient conduction being obtained round the barrel. Constant currents were obtained from a high tension battery with suitable resistances in the circuit. The reference electrode was a mercurous sulphate electrode in $\text{N, Na}_2\text{SO}_4$. In this paper the observed potentials are given with reference to this electrode. Their values on the standard hydrogen scale may be obtained by adding 0.66 volts. Slow changes of potential were determined by means of the Lindemann electrometer, one observer reading and calling out the values of the electromotive force, and the other noting and recording the time by means of a stop-watch. Rapid changes were recorded by means of the Einthoven string galvanometer.

Experiments with Methylene Blue Solutions.

The solutions were made by dissolving a good quality (bacteriological stain) methylene blue in $\text{M}/10$ sulphuric acid. The solution was not exhaustively freed from air, but before each experiment a stream of nitrogen from a cylinder was passed through the solution.

Fig 1 shows some typical curves of the change of potential with time in the cathodic polarisation of the electrode in a 0.04 per cent. methylene blue

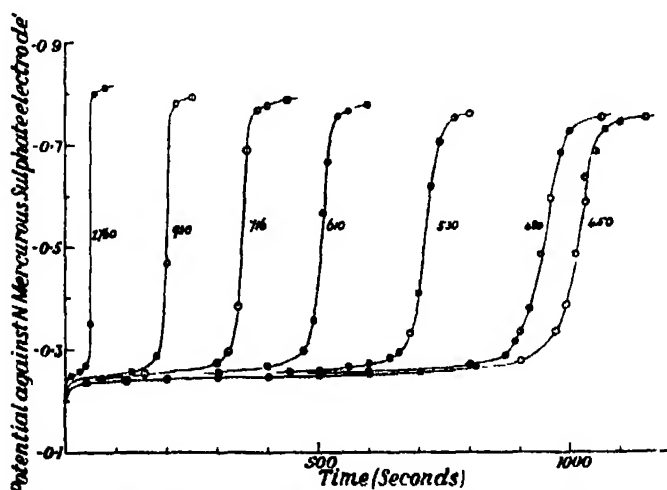


FIG. 1.—Cathodic polarisation of 0.04 per cent. methylene blue solution (currents, $\text{amp} \times 10^{-7}$)

solution. These curves are very closely reproducible if a stream of nitrogen is bubbled through the solution for 5 minutes between successive experiments. In this time the potential has returned to within a millivolt of its initial value. But if successive experiments are carried out after a short interval without stirring the solution in this way the final value of the potential is reached in a much shorter time. Occasionally the first polarisation of a new solution was anomalous, but when repeated once or twice under the conditions stated above a reproducible curve was soon obtained. It was immaterial in what order the curves were obtained. In some series we proceeded from high to low currents and in others we used the reverse order.

The curves all show the following features. (1) a small rapid rise of potential at the beginning, followed by (2), period of slow change which is shorter and occurs at somewhat more negative potentials the greater the current. This leads to (3), a rapid rise of potential to about -0.7 volts, and (4), the potential finally reaches a nearly steady value which is above the reversible hydrogen potential, but somewhat below the hydrogen overvoltage for the same current density. Similar curves were obtained with still higher currents, but they cannot conveniently be shown on the time scale of fig. 1.

The transition phenomenon occurs over the whole range of current density, but with high currents the changes are so rapid that only the final stage can be observed visually, while with low currents the transition occurs only after a long interval. It follows that if observations are made at a constant time interval from the starting of the current, a point on the slow stage (2) is observed with small currents and the final nearly constant value with large currents, while with intermediate currents points on the transition stage (3) may be obtained.

From a series of curves such as fig. 1, it is possible to construct a series of current-voltage curves each corresponding to a definite interval between the starting of the current and the time of observation, fig. 2. It is evident from these curves that the "transition current density" is a function of this interval; a variation of this time from 0.2 to 500 seconds leads to approximately a hundred-fold decrease in the value of the transition current.

We shall take as the *transition time* the time required to reach -0.5 volts, which is about midway on the transition stage. Table I shows how the transition times (t_{∞}) vary with the current density, and also gives the product it_{∞} , i.e., the number of coulombs required to effect the transition. It will be observed that this quantity approaches constancy at high current densities for the smaller concentrations.

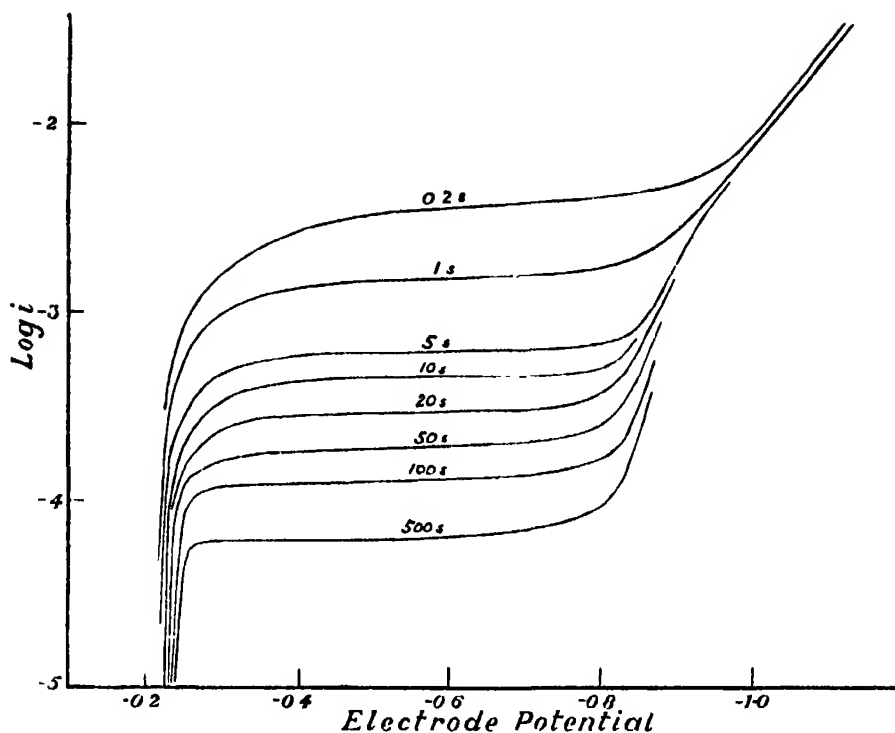


FIG. 2.—Cathodic polarisation of methylene blue solution. Curves show the variation of electrode potential with current at stated times (seconds) from the start.

Table 1.—Transition Times for Reduction of Methylene Blue Solutions.
(i , amps. $\times 10^{-7}$; t_{∞} , seconds, it_{∞} , Coulombs $\times 10^{-4}$.)

0.004 per cent. solution			0.04 per cent. solution			0.4 per cent. solution.		
t	t_{∞}	it_{∞}	t	t_{∞}	it_{∞}	t	t_{∞}	it_{∞}
50	1450	72	480	942	452	4620	710	3280
67	720	48	533	712	380	5660	370	2090
76	450	36	611	500	305	6960	220	1530
103	233	24	716	350	250	7990	160	1280
165	90	15	920	202	188	9280	120	1110
284	39	11	1762	54	95	14880	45	670
457	17	7.8	4280	11	47	25200	15	380
956	5.6	5.4	9110	2.8	25	40000	7	280
2680	1.4	3.7	16000	0.94	15	106800	0.86	90
6580	0.36	2.4	41700	0.15	6.3	153000	0.26	40
13060	0.13	1.7	76000	0.08	6.1			
			390000	0.02	7.8			

Discussion.

Solutions of methylene blue and its reduction product methylene white give well-defined reversible oxidation potentials. In these experiments the initial solution contained no methylene white, but in contact with the electrode and after a little reduction sufficient is formed to give a well-defined potential. We shall assume that the reversible potential is set up by the direct transfer of electrons between the electrode and the reduced and oxidised forms of the substance, by a mechanism similar to that suggested by Butler.* In most theories of electrolytic reduction it has been supposed that the primary process is the liberation of atomic hydrogen which subsequently reacts with the reducible substance. This may be the case in irreversible actions, but in the reversible processes with which we are concerned here it is probable that the primary process is the transfer of electrons from the electrode to molecules of the reversible depolariser, which may then unite with hydrogen ions to form the reduced product.

The rate of change of the potential during the passage of a current i , according to the theory of Part I, is governed by the equation

$$i - i' = B \cdot dV/dt, \quad (1)$$

where i' is the depolarisation current, or the rate of transfer of electrons across the electrode boundary in depolarisation processes, and B the capacity of the double layer. The depolarisation current is zero at the reversible potential V_0 . Except in the immediate vicinity of this value, where a "reverse term" which rapidly diminishes with the displacement of the potential is necessary,† it may be represented by the equation

$$i' = ke^{-a(V-V_0)}. \quad (2)$$

When the current is started the potential at first rises rapidly according to (1), i' being small, but as i' increases by (2), the rate of change diminishes and, when i' is equal to i , becomes zero. If V_0 remained constant the potential would now remain unchanged, but if the depolariser is reduced at the surface faster than it can be replaced by diffusion from the solution, its concentration near the electrode will diminish as the current continues and the reversible potential will vary, to a first approximation, according to the equation

$$V_0 = V_0^\circ - RT/zF \log q, \quad (3)$$

* 'Trans. Faraday Soc.,' vol. 19, p. 734 (1924).

† Butler, *loc. cit.*, and 'Trans. Faraday Soc.,' vol. 28, p. 379 (1932).

where q is its effective concentration at the electrode surface, and z the number of electrons required for the reduction of a molecule of depolariser. After the initial rapid rise the rate of change of potential is so slow that i' may be taken as equal to i , so that the difference between V and V_0 in (2) is constant, and the variation of the actual potential will be governed by the variation of q in (3). We will define q as the total amount of the depolariser, expressed as the quantity of electricity required for its reduction, within a certain short distance of the electrode. Then we may write

$$q = q_0 - it + f(c, t), \quad (4)$$

where q_0 is the initial value, it the amount reduced in the time t and $f(c, t)$, a function of the time and of the concentration of the depolariser in the bulk of the solution, the amount which has diffused into the specified region in the time t .

The times taken to reach a given value of V_0 are thus related to the current by the relation, $q_0 - it + f(c, t) = \text{const.}$ In estimating the transition times we shall make no great error by neglecting the displacement of the potential by the current (equation (2)), so that the times (t_∞) taken to reach the constant potential -0.5 on the transition stage are given by $q_0 - it_\infty + f(c, t_\infty) = \text{const.}$ Now the diffusion term $f(c, t_\infty)$ will be smaller the greater the current and the smaller the concentration, and we may suppose that for extreme values of these quantities it becomes negligible. Then we have $q_0 - it_\infty = \text{constant}$, or for a constant value of q_0 , $it_\infty = \text{constant}$. We have seen that the experimental values approach this relation at large current densities and small concentrations. With smaller current densities and greater concentrations the transition times are longer than those given by this relation, as is required by a positive value of $f(c, t)$.

It can be seen from Table I that for transition times longer than 100 seconds, the product it_∞ varies nearly linearly with t , and is closely represented by the following equations:—

$$\begin{aligned} 0.4 \text{ per cent.} \quad it_\infty &= 75 \times 10^{-3} + 3.5 \times 10^{-4} t_\infty, \\ 0.04 \text{ per cent.} : it_\infty &= 10.5 \times 10^{-3} + 3.8 \times 10^{-5} t_\infty, \\ 0.004 \text{ per cent.} : it_\infty &= 1.1 \times 10^{-3} + 5 \times 10^{-6} t_\infty, \end{aligned}$$

or, in general,

$$it_\infty = \alpha + \beta t_\infty. \quad (5)$$

The constants in these equations are to a first approximation proportional to the concentration of methylene blue.

In order to account for this relation, we may observe that when the amount of diffusion is considerable, q and q_0 in (4) are negligible compared with the other terms and we shall have $i = f(c, t)$, or for sufficiently long transition times, by (5)

$$f(c, t) = \alpha + \beta t. \quad (6)$$

A relation of this kind may be obtained if the diffusion process is supposed to consist of two stages, (1) the setting up of a uniform "diffusion layer," requiring the passage of α coulombs. Since α is proportional to the concentration this quantity will effect the reduction of the amount of methylene blue in a layer of approximately constant thickness, viz., 10^{-2} cm., round the electrode, and it follows that the diffusion layer must have approximately the same thickness in every case. When this layer has been established, (2) diffusion takes place at a practically constant rate β , which is also proportional to the concentration of methylene blue in the interior of the solution.

The rate of change of the potential after the establishment of the diffusion layer, obtained by inserting the values of (4) and (6) in (3) is now given by

$$V = \text{const.} - RT/2F \log (q_0 - it + \alpha + \beta t), \quad (7)$$

since for a given current V differs from V_0 by a constant amount (2). Since q_0 is negligible compared with the other terms, this equation may be tested for values of t greater than 100 seconds by plotting V against $\log_{10} (\alpha + \beta t - it)$ (fig. 3). The values of β were taken from the table given above, but in some cases a small modification was made in the average value of α , since it is essential for the testing of (7) that the relation $i_\infty = \alpha + \beta t_\infty$ should exactly hold. In some cases the observed data are not very suitable for testing this relation, since when making the measurements we were chiefly interested in the transition times, and in some of the experiments we noted comparatively few points on the slow stage. Sufficient cases are, however, available for an adequate test of the equation. Over a considerable part of their course the curves are straight line having slopes very near to the value $2.303 RT/2F = 0.029$ required by the theory. When the transition stage is approached the rate of change of the potential is in every case somewhat greater than that calculated. The curves of the very dilute 0.004 per cent. solution are not, however, in good agreement with this relation.

Experiments with Quinhydrone Solutions.

In order to obtain a confirmation of these relations for a reversible system in which both the oxidised and the reduced forms of the substance were

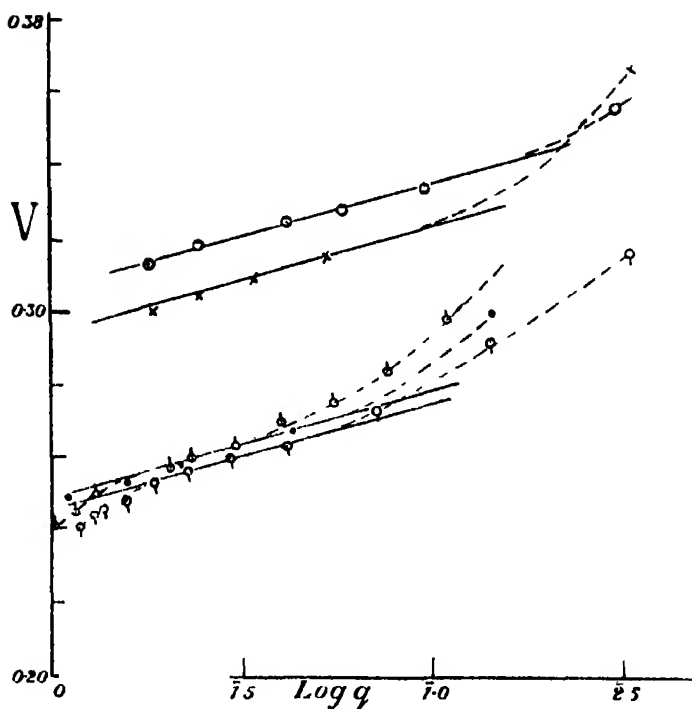


FIG. 3 — Variation of V with calculated value of $\log q$. (The full lines have the theoretical slope.)

0.4 per cent. solution—

⊙ $t = 6900$ 10^{-7} , $q = 76$ 10^{-1} , 3.5 $10^{-4} t - u$

△ $t = 4620$ 10^{-7} , $q = 75$ 10^{-1} , 3.5 $10^{-4} t - u$

0.04 per cent. solution—

● $t = 611$ 10^{-7} , $q = 11.5$ 10^{-1} , 0.38 $10^{-4} t - u$

○ $t = 533$ 10^{-7} , $q = 11.0$ 10^{-1} , 0.38 $10^{-4} t - u$

⊙ $t = 480$ 10^{-7} , $q = 9.4$ 10^{-1} , 0.38 $10^{-4} t - u$

initially present, we studied both the cathodic and the anodic polarisation of solutions of quinhydrone in M/10 sulphuric acid. The cathodic curves were similar in every way to those of methylene blue. The transition times (t_{∞} , $V = -0.5$) and the products u_{∞} are given in Table II. The product u_{∞} , which begins to approach a constant value in the weaker solution at high current densities, increases rapidly as the current is increased. The larger values are represented by (5), the constants having the values:—

	α	β
0.05 per cent.	350×10^{-4}	190×10^{-6}
0.005 per cent.	35×10^{-4}	19×10^{-6}

which are again proportional to the concentration of quinhydrone in the interior of the solution.

Table II.—Cathodic and Anodic Transition Times for Quinhydrone Solutions.
(i , amps. $\times 10^{-7}$; t_{∞} , seconds; it_{∞} , Coulombs $\times 10^{-4}$.)

Cathodic Polarisation.

0.05 per cent.			0.005 per cent.		
i	t_{∞}	it_{∞}	i	t_{∞}	it_{∞}
2810	355	998	291	360	105
3310	242	801	588	91	53
3820	196	750	982	30	29.5
4860	114	555	1840	9	16.6
6160	70	431	3800	2.1	8.1
7480	46	344	9320	0.48	4.4
9250	30	277	19500	0.14	2.7
12900	15	193			
17300	8.6	149			
19500	7	136			
35600	1.9	62			
88200	0.3	26			
370000	0.01	3.7			

Anodic Polarisation.

2600	330	858	308	132	49
4820	72	348	432	90	43
6670	40	267	448	80	36
7990	27	216	582	56	33
17400	5.6	97	721	10	20
35600	1.7	61	892	26	23
40400	1.3	52	1230	18	22
88100	0.28	25	2380	5	12
			4330	1.4	6.1
			12760	0.3	4.8

In the anodic polarisation of these solutions two depolarisation processes are observed. Fig. 4 shows a series of potential-time curves obtained with

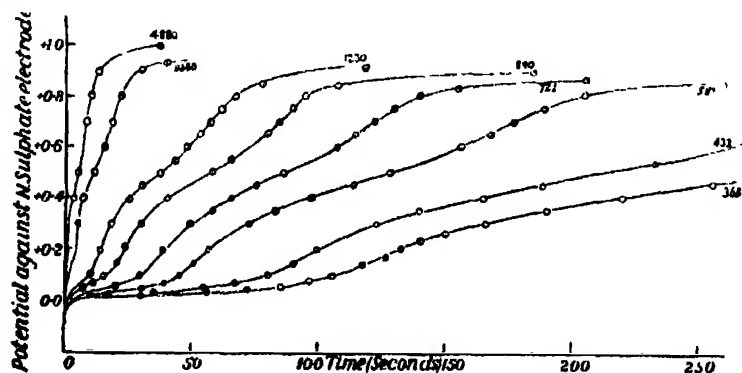


FIG. 4.—Anodic polarisation of 0.005 per cent. quinhydrone solution. (Currents; amps. $\times 10^{-7}$.)

0.005 per cent. quinhydrone solution. The initial rapid change is followed by a period of slow change at potentials between 0.05 and 0.1 volts more positive than the equilibrium potential. The depolarisation process taking place here is no doubt the transfer of electrons to the electrode from hydroquinone molecules, as represented by the equation $C_6H_4(OH)_2 = C_6H_4O_2 + 2H^+ + 2e$. The potential rises at a continuously increasing rate until between +0.3 and +0.5 a diminution of the rate of change indicates a second depolarisation process. This process occurs at the same potential (about $\epsilon_H = 1.1$) as that of the depolarisation effect observed in Part I in the anodic polarisation of platinum electrodes in sulphuric acid saturated with both hydrogen and oxygen, and is no doubt due to the same cause. We have ascribed it to the formation of an adsorbed film of oxygen, a process which can probably be effected with a smaller expenditure of energy than is required for the continuous discharge of negative ions in the solution. As this adsorbed layer becomes completed the potential rises and finally the potential at which the continuous formation of oxygen can occur is reached.

It is difficult to fix precisely the transition times of the first process because the second process has begun before the first is quite completed. We have taken as the transition times (t_∞), the times of the point of inflexion which occurs in the curves before the inception of the second process. These times, together with the corresponding values of it_∞ are given in Table II. For times above 75 seconds, it_∞ varies linearly with t_∞ , and the constants of (5) have the values :—

	α	β
0.05 per cent.	220×10^{-4}	190×10^{-6}
0.005 per cent.	22×10^{-4}	19×10^{-6}

The slope β is the same as for the cathodic process and α is somewhat less. Apart from this difference, which might possibly be due to the effect of traces of oxygen on the cathodic curves, it appears that the processes of reduction and oxidation in a reversible system are symmetrical and have similar mechanisms.

We wish again to express our appreciation of the Carnegie Teaching Fellowship held by the senior author, and the grant made by the Department of Scientific and Industrial Research to the junior author. We are also greatly indebted to the Committee of the Moray Research Fund, and to Imperial Chemical Industries, Ltd., for grants for the purchase of apparatus.

Summary.

The kinetics of the electrolytic reduction of methylene blue solutions, and of the reduction and oxidation of quinhydrone solutions at platinum electrodes have been investigated. A transition process has been observed over the whole range of currents and of concentrations, which has been ascribed to the depletion of the depolariser in the vicinity of the electrode. An expression for the rate of change of the concentration of the depolariser in the vicinity of the electrode has been obtained, which is in accordance with the facts.

The Stark Effect for Xenon.

By H. W. HARKNESS, Ph D., Associate Professor of Physics, Acadia University,
and J. F. HEARD, Ph.D., National Research Student, McGill University.

(Communicated by A. S. Eve, F.R.S.—Received September 9, 1932.)

[PLATES 9, 10, 11 AND 12]

Introduction.

Many leading features in the Stark effect are best illustrated by studies in the spectra of the rare gases. In each spectrum at least one phase of the Stark effect stands out prominently. Thus in helium* the Stark types for singlet lines are most clearly revealed, while in neon† an analogue of the Paschen-Back effect makes its appearance, together with some departures from the normal Stark patterns for parhelium. The present experiments with xenon constitute evidence in support of a quantum-mechanical explanation of the origin of Stark displacements and reveal new features concerning the nature of Stark patterns.

It was first observed in Stark displacements in helium that sharp and principal series lines were displaced very little in comparison with diffuse series lines. The relatively small displacements received an early explanation‡ on the grounds of an atomic model in which the *s*- and *p*- terms corresponded to electron orbits of high eccentricity which revolve rapidly in their planes. This action prevented the external field from producing an appreciable shift of the electrical centre from its normal position in the nucleus. Since the

* Foster, 'Proc. Roy. Soc.,' A, vol. 114, p. 47 (1927).

† Foster and Rowles, 'Proc. Roy. Soc.,' A, vol. 123, p. 80 (1929).

‡ Bohr, 'Phil. Mag.,' vol. 27, p. 506 (1914).

excess of the term in question over the hydrogen term of the same principal quantum number (the so-called hydrogen difference) measured the speed of revolution of the orbit, it seemed clear that hydrogen differences should serve as valuable guides to probable Stark displacements. Up to the present well organised data have appeared to support this view *

An indication that the hydrogen difference was not satisfactory as a criterion of Stark displacements to be expected in a given spectrum was first pointed out by Pauli† in his application of the Kramers-Heisenberg dispersion theory to the Stark effect. Pauli's analysis showed that the displacement of an energy level in an electric field depended upon its separations from certain other levels and upon the probabilities of transition between these levels and the given level. To a first approximation it is only necessary to consider levels which are related to the level in question (n, l, j, m) by $\Delta l = \pm 1, \Delta j = 0, \pm 1$. In this case the Pauli relation is :

$$\Delta E_{n, m, l, j} = \Delta E_{n, m, l, j}^{(1)} + \Delta E_{n, m, l, j}^{(2)}$$

where

$$\Delta E_{n, m, l, j}^{(1)} = -\frac{1}{2} F^2 \frac{1}{2h} \left[\frac{|\alpha_{n, m, l-1, j} \rightarrow n, m, l, j}|^2}{\nu_{n, m, l-1, j} \rightarrow n, m, l, j}} - \frac{|\alpha_{n, m, l, j} \rightarrow n, m, l-1, j}|^2}{\nu_{n, m, l, j} \rightarrow n, m, l-1, j}} \right]$$

and

$$\Delta E_{n, m, l, j}^{(2)} = -\frac{1}{2} F^2 \frac{1}{2h} \left[\sum_{n' > n, l' = l \pm 1, j' = j \pm 1} \frac{|\alpha_{n', m, l', j'} \rightarrow n, m, l, j}|^2}{\nu_{n', m, l', j'} \rightarrow n, m, l, j}} + \sum_{n' < n, l' = l \pm 1, j' = j \pm 1} \frac{|\alpha_{n, m, l, j} \rightarrow n', m, l', j'}|^2}{\nu_{n, m, l, j} \rightarrow n', m, l', j'}} \right]$$

That the later developments of quantum mechanics give support to this newer view can be illustrated by a particular example which has been chosen because of its simplicity. Consider the group of parhelium levels defined by $n = 3$ and $m = 1$. If H_1 and H_2 denote the hydrogen differences corresponding to P and D terms respectively, and W_1 denotes the excess of any perturbed level over the hydrogen level of principal quantum number 3, we have the following form‡ of the determinant for determining W_1 in a field of F volts per centimetre :—

$$\begin{vmatrix} W_1 - H_1 & -3kF \\ -3kF & W_1 - H_2 \end{vmatrix} = 0$$

* Stark, 'Hundbuch Exp. Physik,' vol. 21, p. 487 (1927)

† 'Handbuch der Physik.,' vol. 23, p. 147 (1926).

‡ Foster, 'Proc. Roy. Soc.' A. vol. 117, p. 137 (1927).

where k contains universal constants and has the value 6.46×10^{-4} . Expanding this and writing to a first approximation we have

$$W_1 = \frac{1}{2} (H_1 + H_2) + \frac{1}{2} (H_1 - H_2) \left[1 + \frac{6kF}{H_1 - H_2} \right]^2$$

In the case where $F = 0$, W_1 would have the values H_1 and H_2 ; that is, there would be no Stark effect. The displacement from the normal position in the helium spectrum, that is, the Stark effect, is given by the correction term, is the same for P and D levels and has the magnitude,

$$\Delta\nu_F = \frac{9k^2F^2}{H_1 - H_2}.$$

Thus, so long as the approximation assumed above is valid, (i.e., the fields are sufficiently small) the displacements will be proportional to the square of the field strength and inversely proportional to the separation $(H_1 - H_2)$, and not to any individual hydrogen difference.

On the basis of the Pauli theory it is easy to see why the hydrogen difference rule appeared to receive support from experimental results in many spectra. For, in most atoms, the hydrogen differences of the energy levels in a group, and the separation of these levels decrease together as one passes from groups of lower to higher principal quantum number. This regularity of grouping is well illustrated in helium and neon (Foster and Rowles, *loc. cit.*) and, indeed, their Stark displacements appear to obey the hydrogen difference rule. In contrast to this, the outstanding feature of the xenon atom is the random distribution of the energy levels. For this reason xenon provides an excellent medium for experiments which will give an unambiguous answer to the question of the true origin of Stark displacements.

Besides the magnitude of Stark displacements we have also to consider the nature and interpretation of the many Stark patterns which constitute one of the more striking features of the present observations.

If an individual line gives rise to a complicated pattern in the electric field we assume that the levels are split by the field into a number of perturbed levels specified by a quantum number m , very much as in Zeeman effect. However, the electric levels are not regularly spaced as are the corresponding magnetic levels, and positive and negative values of m specify the same electric levels, whereas positive and negative values of m specify magnetic levels equally spaced above and below the zero field position. The selection principles in the electrical case are the same as in the magnetic, i.e., $\Delta m = 0$ for parallel (π) components and $\Delta m = \pm 1$ for perpendicular (σ) components. The way

in which m values for various levels are limited is well understood for Zeeman effect but is not quite clear for Stark effect. The extent to which an analogy may be carried has been the subject of much discussion.

Foster* was able to organise completely the patterns which he observed in the parhelium spectrum, assuming that the perturbed levels of final states were not resolved by the fields. In this case the quantum number m was taken as the resolved part of the vector l in the direction of the field. Since electron spin was absent, this interpretation was analagous to that for the normal Zeeman effect. For this reason the Stark patterns of parhelium were called by Foster "normal" patterns.

Where electron spin does enter, that is to say, among individual members of multiplet series lines, one expects, by analogy to Zeeman effect, that Stark patterns will be of greater variety. Such patterns, however, in orthohelium Foster (*loc. cit.*, vol. 114) found to be "normal" as in parhelium. Again, in the neon spectrum, Foster and Rowles (*loc. cit.*) found that the patterns were, for the most part, "normal." The interpretation was that the ls coupling was broken down, and that the perturbed levels were specified by the quantum numbers m_l and m_s , the resolved parts of the vectors l and s respectively. And, since patterns were "normal," it appeared that any complexity among perturbed levels introduced by m_s values did not make its appearance in the patterns as observed. A few patterns of neon, however, could be interpreted as "abnormal" inasmuch as the quantum number m seemed to be the resolved part of the vector j , that is, the ls coupling was retained in the field, but such "abnormal" patterns comprised the exceptions to a general rule of "normal" patterns, and the authors expressed some uncertainty about this observation.

An investigation by Ladenburg† upon the inverse Stark effect for the sodium D lines and a similar investigation by Grotrian and Ramsauer‡ for certain of the principal series lines of potassium have indicated that these lines give rise to Stark patterns of a type which would be here termed "abnormal."

Briefly then, the Stark patterns of the helium and neon spectra have been characterised by the paucity of departures from the normal parhelium type and the absence of any patterns more complicated than the normal type, while, on the other hand, the alkali spectra have provided examples of abnormal patterns. It now appears that patterns of the diffuse series lines of the xenon spectrum represent a great range of complexity and, with a few exceptions,

* 'Proc. Roy. Soc.,' A, vol. 114, p. 47 (1927).

† 'Z. Physik,' vol. 28, p. 51 (1924).

‡ *Ibid.*, vol. 28, p. 846 (1927).

may be classified as abnormal. The exceptions are patterns which are classified as belonging to the normal parhelium type. Their importance lies in the fact that they provide a test for any hypothesis regarding the origin of Stark patterns. For example, the results lend no support to a suggestion made by Ladenburg* to the effect that m values in Stark effect are limited exactly as in Zeeman effect and that there is an exact electrical analogue to the Paschen-Back effect.

The Normal Spectrum of Xenon.

A description and analysis of the first spectrum of xenon is available in a paper by Meggers, de Bruin and Humphreys.† A further analysis, containing extensions and revisions, has since been made by these authors, and the lines recorded in the present investigation are described with reference to the revised data.‡

The normal state of the neutral atom is represented by (s^2p^6). The excited states arise from addition of s, p, d, f, \dots , electrons to the xenon ion (s^2p^6). The electron configuration of the ion gives rise to an inverted doublet term $^2P_{3/2, 1/2}$ with a separation of $10,540 \text{ cm.}^{-1}$.§ The j values of the excited electrons couple separately with the two j values of the core to produce two sets of theoretical s, p, d, f, \dots , terms, one converging to the higher limit, $^2P_{1/2}$, and the other to the lower limit, $^2P_{3/2}$. Theoretically there are four s -terms, 10 p -terms, 12 d -terms and 12 f -terms.

In Table I are given the terms which were recognised in the spectrum and the j value of each.

Table I.—Xenon Terms and j Values.

	Converging to higher limit, $^2P_{1/2}$.	Converging to lower limit, $^2P_{3/2}$.
s -term	$s_2(0), s_2(1)$	$s_1(1), s_1(2)$
p -terms	$p_1(0), p_2(1), p_4(1), p_2(2)$	$p_3(0), p_2(1), p_{10}(1), p_3(2), p_2(2), p_3(3)$
d -terms	$d_1'(1), d_1''(2), d_1'''(3), d_1''''(2)$	$d_3(0), d_2(1), d_1''(2), d_2(2), d_3(1), d_1'(3), d_4(3), d_4'(4)$
f terms		X(1), Y(2), V(2), U(3), W(3), Z(4), T(5).

* 'Phys. Z.', vol. 30, p. 367 (1929)

† 'Bur. Stand. J. Res.', vol. 3, p. 757 (1929).

‡ The new analysis is now being prepared for publication but Dr. Meggers has very kindly sent us the revised term table and permitted us to use it in our discussion. Our earlier reports upon the interpretation of patterns were based upon the original description of the spectrum.

§ 'Bur. Stand. J. Res.', vol. 6, p. 287 (1931).

Experimental.

The investigation was carried out in two stages. To obtain a general view of the Stark effect for xenon, an analysis was first made by means of a Hilger E1 spectrograph focussed for the visible region. These plates provided measurements of Stark displacements in the blue region of the spectrum and while the dispersion in the red region was poor they indicated that the red region of the spectrum was rich in displacements. A detailed study of the red region was subsequently undertaken using a 30-foot concave grating mounted stigmatically. The ruled surface of this grating is 5 inches wide and there are 15,000 lines per inch. The grating is exceptionally fast in the first order. In its present mounting it has a dispersion in the first order red region of approximately 3.8 Å per millimetre. Ghosts are strong.

The xenon was supplied by the Gesellschaft für Linde's Eismaschinen A.G., Munich, and by the Airco Company of New York.

The vacuum system was of a design as simple as was consistent with the requirements of the experiments. It was constructed entirely of Pyrex glass. Included in the system were reservoirs for helium and xenon, a pump for transferring these gases to and from the reservoirs, a McLeod gauge and a charcoal bulb. The discharge tube was of the Lo Surdo type as modified in this laboratory to give the highest fields with the greatest light intensity and to avoid the evils of sputtering*. The tube was connected to the vacuum system by means of two ground glass joints which facilitated the focussing of the light from the source upon the slits of the spectrographs.

The high potential source was capable of delivering a uniform potential of 10,000 volts and has been described in papers published from this laboratory.†

In general, it was difficult to obtain stable operation with high fields in xenon. With 25 to 50 per cent. of helium present the tubes operated satisfactorily when the pressure was 1.5 to 2 mm., terminal potential 9000 to 10,000 volts, and current 1 to 2 milliamperes. Hydrogen was always present as an impurity. The period of satisfactory operation was from 4 to 7 hours. During this time the tubes grew gradually softer, but if the terminal potential was maintained at a constant value the fields remained constant.

Light from the source was focussed upon the slits of the spectrographs by means of an F 2.7 Zeiss Tessar lens. Source and lens were arranged to give a magnification of 2.

* Foster, 'Proc. Roy. Soc.' A, vol. 114, p. 47 (1927)

† Foster, 'J. Franklin Inst.', vol. 209, p. 597 (1930)

When double image analysis was required a quartz Wollaston prism was interposed between the source of light and the condensing lens. Because the velocities of the two polarised beams are not the same within the prisms, both beams do not focus in the same plane. To make them do so to a greater degree it was necessary to tilt the double image prism. This cut down the light intensity on the slit, and it was found necessary to effect a compromise between sharp focus and best light intensity.

The photographic plates used for the visible region were Eastman 40 and Wratten and Wainwright panchromatic; for the region λ 5500– λ 6500 Wratten and Wainwright panchromatic and hypersensitive panchromatic; for the region λ 6500– λ 7500 Eastman 40 sensitised by bathing in a solution of di-cyanine A, as described by Dundon * and for the region λ 7500– λ 8400, Eastman 3P plates

Description of Plates 9, 10 and 11.

Plates 9, 10 and 11 represent selected portions of the spectrum as recorded by the grating spectrograph. The maximum field strength is 67,000 volts/cm. The upper image contains parallel components, the lower, perpendicular. Xe_I normal lines are accompanied by wave-lengths and notations, Xe_I combination lines by notations only and Xe_{II} lines by wave-lengths only.

Combination Lines.

A number of combination lines make their appearance on the photographs. It has been possible to identify only a limited number of these as arising from combinations between terms given by Meggers, de Bruin and Humphreys. The others, no doubt, arise from transitions from unknown f terms and g, h, \dots , terms, the values of which cannot be found from the visible region of the normal spectrum. Because these lines have large displacements and do not appear in low fields their wave-lengths at zero field cannot be estimated with any certainty. Consequently it was considered unwise to attempt any estimate of the corresponding values of g, h, \dots , terms.

Those combination lines which have been identified are included in Table II and are marked, in the wave-length column, with an asterisk, but since they do not actually appear at zero field the wave-lengths and displacements as recorded must be considered as only approximate.

* "American Photography," December, 1926.

It will be observed that pp combinations are the most numerous and are always of the form $2p_i - np_j$. The same was true of mercury combination lines observed by Hansen, Takamine and Werner,† and of neon combination lines observed by Foster and Rowles (*loc. cit.*).

Table II.—Stark Displacements and Patterns in the Xenon Spectrum
(Field strength = 67,000 volts/cm.)

Wave-length Å.	Notation	Displacements (cm ⁻¹).		Type of pattern
		π	σ .	
3685.91	$1s_5 - 5p_8$	-34	- 34	
3693.50	$1s_5 - 5p_8$	27	-27	
3809.90	$1s_5 - 5p_5$	12 8	-12 8	
3950.02	$1s_5 - 4p_8$	3 2	- 3 2	
3967.55	$1s_5 - 4p_8$	9 6	- 9 6	
4078.81	$1s_5 - 4p_5$	1 0	- 1 0	
4109.71	$1s_5 - 4p_5$	- 3 2	- - 3 2	
4193.51	$1s_5 - 4U$	Small (-)	Small (-)	
4203.69	$1s_5 - 4Y$	Small (-)	Small (-)	
4385.75	$1s_5 - 4X$	0	0	
4500.99	$1s_5 - 2p_2$	0	0	
4524.67	$1s_5 - 2p_1$	0	0	
4582.74	$1s_5 - 2p_1$	0	0	
4611.88	$1s_5 - 3p_7$	0	0	
4671.22	$1s_5 - 3p_8$	Small (-)	Small (-)	
4697.02	$1s_5 - 3p_9$	0	0	
4708.19	$1s_5 - 2p_2$	0	0	
4807.01	$1s_5 - 3p_5$	0	0	
4829.71	$1s_5 - 3p_7$	0	0	
4843.29	$1s_5 - 3p_6$	0	0	
4918.50	$1s_5 - 2p_4$	0	0	
4923.15	$1s_5 - 3p_5$	0	0	
5392.74	$1s_5 - 6X$	41	-41	
5594.21	$1s_5 - 5p_{10}$	-27	- 27	
5695.74	$1s_5 - 6Y$	39	-39	
5715.7*	$2p_{10} - 5s_5$	11 3	11.3	
5715.7*	$2p_{10} - 6V$	† 18	† 18	
5822.7*	$1s_5 - 5Y$		-12	
5823.89	$1s_5 - 5X$	12 4	-12 4	
5824.78	$2p_9 - 7d_4$		† 2 1	Abnormal
		† 4 3	† 4 3	
		† 8.5	† 8.5	
		† 20.7	† 20.7	
5875.02	$2p_{10} - 6d_3$	† 3.8	† 3.8	Abnormal
		† 5.3	† 5.3	
			† 11.0	
5894.99	$2p_{10} - 6d_5$		† 4.1	Normal
		† 12.5 (d)	† 12.5 (d)	
5925*	$2p_8 - 7d_2$	† 17	† 17	
		† 23	† 23	

* Combination line.

(d) Two components not resolved on the plate from which measurements have been made

† 'K. danske Vidensk. Selsk. Skr. Math-fisk.,' 'Medd. V.,' vol. 3 (1923).

Table II—(continued).

Wave-length A	Notation	Displacements (m. ¹).		Type of pitte. n.
		π	σ	
5931.23	$2p_{10} - 6d_8$	11 1	-11.1	Abnormal
5934.15	$2p_8 - 7d_4'$	-10 6	-10 6	Abnormal
		4 6	- 4 6	
		-20.7	-20 7	
		29 8 (d)	29 8 (d)	
5951 6*	$2p_{10} - 5p_{10}$	-29	-29	
5952.8*	$2p_8 - 6p_8$	-64	-64	
6111 82	$\left\{ \begin{array}{l} 2p_8 - 5s_5 \\ 2p_7 - 7d_1'' \end{array} \right.$	-11 0	-11 0	
		6 4	6 4	
		-14 8	-14 8	
		-19 1	-19 1	
6114 7		1 9	1.9	
			9 4	
6158*	$1s_2 - 5W$	13	-13	
6163.78	$1s_4 - 5V$	-18	-18	
6163.78	$2p_8 - 6d_1''$	1 1	- 1 1	Abnormal.
		5 3 (d)	5 3 (d)	
6178.30	$1s_2 - 5Y$	9 5	9 5	
		-12 5	-12.5	
6179 66	$1s_2 - 5\lambda$	-13 2	-13 2	
6182 41	$2p_8 - 6d_4$	- 0.9	- 0.9	Abnormal.
		0 2	0 2	
		3 5	3 5	
		7 0	7 0	
6197 3*	$2p_{10} - 5U'$	- 5 2	- 5 2	
6198 25	$2p_{10} - 4s_5$	-12.5	-12.5	
6200 86	$2p_4 - 7d_1'$	- 5 5	- 5 5	Abnormal
		+ 7 3	- 7 3	
		+11.5	+11 5	
		-14 9	-14.9	
6252*	$2p_8 - 5p_8$	large (-)	large (-)	
6292 62	$2p_8 - 6d_4$	- 0.9	- 0.9	Abnormal.
		+ 0.2	+ 0.2	
		3 2	3 2	
		6 6	6 6	
6318 08	$2p_8 - 6d_4$	- 4 0	- 4 0	Abnormal
		8 0	8.0	
		+15 6	+15 6	
		+21 1 (d)	+21 1 (d)	
6354*	$2p_8 - 5p_8$	-27	-27	
6355*	$3d_4' - 8d_1'$	-33	-33	
		-28	-28	
		-24	-24	
6407*	$3d_4' - 8d_8$	- 9 4	9 4	
6469.71	$2p_{10} - 5d_2$	Small (-)(d)	Small (-)(d)	Abnormal
			Small (+)	
6472 82	$2p_{10} - 5d_2$	- 0.1 (d)	- 0.1 (d)	Normal
6487.75	$2p_{10} - 5d_1''$	Small (+)(d)	Small (+)(d)	Abnormal
			+ 2 2	
6497.3	$3d_4' - 7W$	-41	41	

* Combination line.

(d) Two components not resolved on the plate from which measurements have been made

Table II—(continued).

Wave-length Å.	Notation	Displacements (cm ⁻¹)		Type of pattern
		π	σ	
6498.71	$2p_7 \rightarrow 6d_1''$	4.6 6.0 46 99	0.8 4.6 6.0 46	Abnormal
6500.4*	$3d_4' \rightarrow 7\Lambda$	46	46	
6504.16	$3d_4' \rightarrow 7T$	99	46	
6504.16	$1s_2 \rightarrow 4p_1$	2.2 0	2.2 0	
6521.50	$2p_7 \rightarrow 6d_3$	3.5 5.3	3.5 5.3 11.0	Abnormal.
6533.15	$2p_9 \rightarrow 4s_1$	2.5	2.5	
6542*	$2p_9 \rightarrow 5l$	4	4	
6543.32	$2p_9 \rightarrow 4s_1$	Single component (—) disappearing in high fields		
6595.54	$2p_8 \rightarrow 6d_1'$	0.4 2.1 5.1	4.5 0.4 2.1 5.1	
6632.43	$2p_8 \rightarrow 6d_1$	3.0 5.1 10.6	3.0 5.1 10.6	Abnormal
6666*	$2p_8 \rightarrow 5l$	5.1	5.1	
6666.95	$2p_8 \rightarrow 4s_2$	Single component (—) disappearing in high fields		
6668.93	$2p_{10} \rightarrow 5d_6$	1.7 6.8	1.7 6.8	Abnormal
6717*	$2p_{10} \rightarrow 4p_{10}$	11.4 (°)	11.4 (°)	
6728.0	$2p_{10} \rightarrow 5d_6$	13.5 1.7	13.5 1.7	Abnormal
6765*	$3d_5 \rightarrow 6W$	4.6 1.8	4.6 1.8	
6777.53	$3d_6 \rightarrow 6Y$	29	29	
6778.59	$3d_5 \rightarrow 6\Lambda$	43	43	
6818.30		0.8 1.7	0.8 1.7	
6827.3	$1s_3 \rightarrow 4\Lambda$	0	0	
6846.57	$2p_9 \rightarrow 5d_3$	0.5 0.3	0.5 0.3	Abnormal **
6848.73	$3d_4 \rightarrow 7Z$	2.0	2.0	
6860.16	$3d_4' \rightarrow 6W$	Large (—)		
6863.21		30	30	
6866.81	$2p_9 \rightarrow 5d_1''$	0.3 (d)	0.3 (d)	Abnormal
6872.10	$3d_4' \rightarrow 6T$	1.1 19 0.6 0.6	1.1 40 0.6 0.6	
6882.16	$2p_9 \rightarrow 5d_4$	0.5	0.5	Abnormal **
6910.80	$2p_7 \rightarrow 4s_4$	3.0	3.0	

* Combination line

† See p. 428.

** See p. 428.

(d) Two components not resolved on the plate from which measurements have been made

Table II—(continued).

Wave-length Å	Notation	Displacements (cm. ⁻¹).		Type of pattern.
		π	σ .	
6922*	2p ₇ — 5U	— 4.4	— 4.4	
6925 52	3d ₃ — 6U	Large (—) component and a (+) component which disappears in high fields		
6935.59	3d ₃ — 6Y	Large (—)	Large (—)	?
6976.17	2p ₈ — 5d ₁ '	— 0.6	— 0.6	
		+ 0.6 (d)	+ 0.6 (d)	
6982.04	2p ₈ — 5d ₃	Small (—)	Small (—)	Abnormal.**
		Small (+)	Small (+)	
7018 96	2p ₈ — 5d ₄	— 0.9	— 0.9	?
		+ 0.5 (d)	+ 0.5 (d)	
7035 53	2p ₈ — 4s ₃	— 2.2	— 2.2	
7045*	2p ₈ — 5U	— 5.0	— 5.0	
7047 34	2p ₈ — 4s ₄	Single component (—) disappearing in high fields		
7119 58	2p ₈ — 5d ₄ '		— 1.0	Abnormal
		+ 2.3	+ 2.3	
		+ 4.2	+ 4.2	
		+ 5.7 (d)	+ 5.7 (d)	
		— 1.7	— 1.7	
7244 8	3d ₄ — 6W	Large (—)	Large (—)	Abnormal
7257.94	3d ₄ — 6Z	— 0.6 (d)	— 0.6 (d)	
7262 5	2p ₇ — 5d ₃		+ 0.4	
7266 50	2p ₇ — 5d ₃	0.1 (d)	— 0.1 (d)	Normal.
			+ 2.2	
7283.95	1s ₃ — 4V	— 0.3	— 0.3	Abnormal.
7285 29	2p ₇ — 5d ₁ ''		— 0.3	
		+ 0.9 (d)	+ 0.9 (d)	
7316 28	1s ₂ — 4Y	0	0	
7321.46	1s ₂ — 4X	0	0	
7317*	2p ₁₀ — 3s ₄ '''	Small (—)	Small (—)	
7336 44	2p ₉ — 3s ₁ '''	— 0.4	— 0.4	
7355 54	3d ₆ — 5X	— 12.6	— 12.6	
7385 98	2p ₁₀ — 3s ₅	— 0.5	— 0.5	
7393.77	2p ₆ — 5d ₁ '		— 0.8	Abnormal.**
		+ 0.6	+ 0.6	
7400 38	2p ₆ — 5d ₃	— 0.4 (d)	— 0.4 (d)	Abnormal.
		+ 0.4	+ 0.4	
7424 0	2p ₆ — 5d ₁ ''	— 0.5 (d)	— 0.5 (d)	Abnormal
		+ 0.9	+ 0.9	
7471 94	3d ₅ — 5Y	Large (—)	Large (—)	
7474 05	3d ₅ — 5X	— 12	— 12	
7967.33	1s ₃ — 3p ₇	0	0	
8206 34	1s ₃ — 2p ₄	0	0	
8266.53	1s ₃ — 2p ₃	0	0	
8280.16	1s ₄ — 2p ₅	0	0	
8346.86	1s ₃ — 2p ₃	0	0	
8409 21	1s ₅ — 2p ₇	0	0	

* Combination line.

* See p. 428.

** See p. 428.

(d) Two components not resolved on the plate from which measurements have been made.

Patterns from Xenon Lines.

In Table II it will be noticed that lines of the sharp, principal and fundamental series seldom yield more than single unpolarised components. This may be interpreted to mean that all perturbed levels of both final and initial states are fused, that is to say, they are not resolved by the field strengths and spectrogram dispersions of the present investigation. Likewise combination lines, for the most part, yield single components. Since most of the combination lines involve *s*, *p* or *f*-terms as initial levels, this is in accord with the remark concerning sharp, principal and fundamental series lines.

On the other hand, diffuse series lines yield patterns of various degrees of complexity. For the most part, diffuse series lines give rise to patterns which are classified as *abnormal*. An abnormal pattern is here defined as one arising from perturbed levels (of both final and initial states) which are limited in number by *j* values. The perturbed levels of the final states are assumed to be unresolved. Since *j* values differ from term to term, abnormal patterns, of course, differ in character. This is best seen from fig. 1 which illustrates how a few typical abnormal patterns arise.

There are three exceptions to the rule of abnormal patterns for diffuse series lines, namely, $2p_{10}-6d_5$ (λ 5894.99), $2p_{10}-5d_2$ (λ 6472.82) and $2p_7-5d_2$ (λ 7266.50). These lines, in place of yielding abnormal patterns

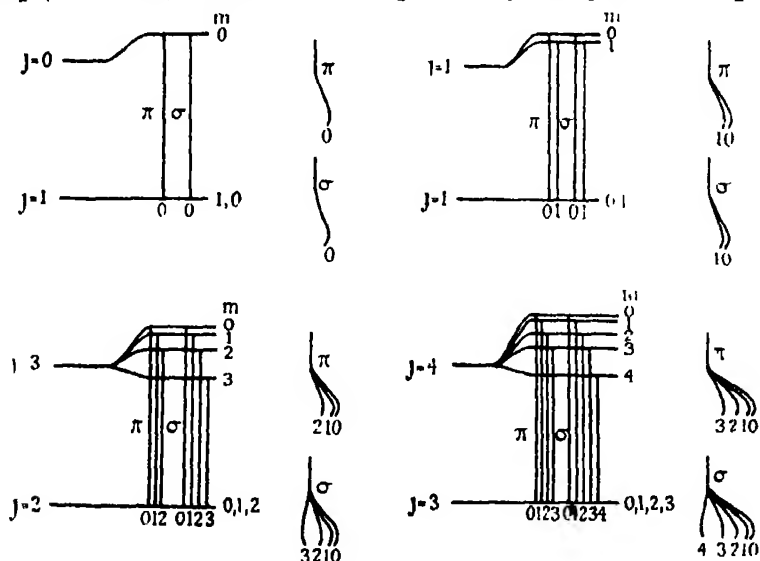


FIG. 1.

(which in these cases would have two parallel and two perpendicular components), appear to yield patterns having two parallel and three perpendicular

components. These patterns must then be classified as *normal*, the same as for diffuse series lines of parhelium.* Their interpretation requires that the perturbed levels of the individual states be limited in number by the l values.

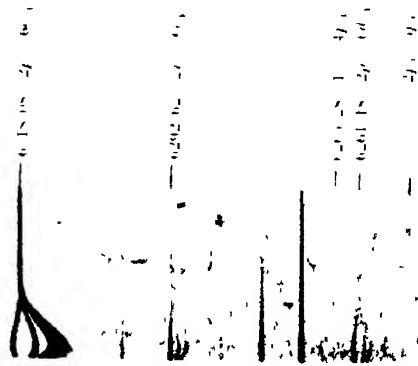
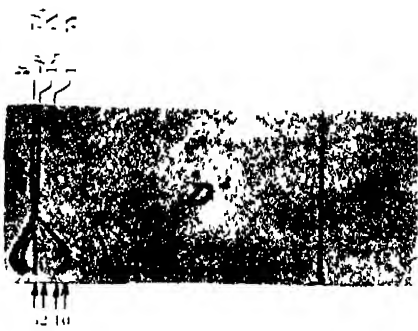
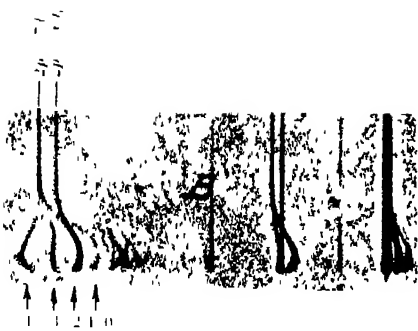
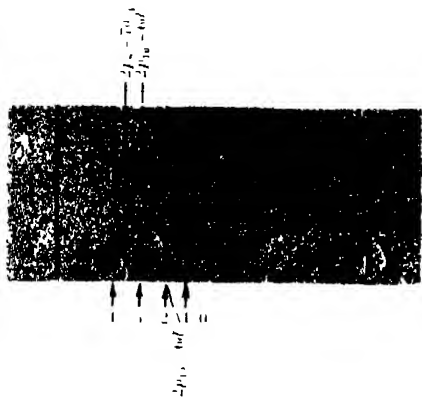
In Table II all the patterns of diffuse series lines which have been sufficiently well resolved have been classified as *normal* or *abnormal*. Those not sufficiently well resolved for classification have been indicated by an interrogation mark. Certain other patterns (indicated by **) are not well resolved but the *nature* of these patterns leaves no doubt concerning their classification. For example, although the displacements of $2p_9-5d_4$ (λ 6882.16) are very small and not clearly resolved, it is observed that the perpendicular components outnumber the parallel components by one. This can happen only if the perturbed levels of $5d_4$ ($j = 3$) outnumber the perturbed levels of $2p_9$ ($j = 2$) by one. But the perturbed levels of $2p_9$ (as deduced from clearly resolved patterns of other transitions to this state) are given by $m = 0, \pm 1, \pm 2$. So the perturbed levels of $5d_4$ must be given by $m = 0, \pm 1, \pm 2, \pm 3$, i.e., the values of m must be determined by the value of j . Since the values of m are likewise determined by j in the final state the pattern must be classified as abnormal. The same argument holds for the classification of $2p_8-5d'_1$ (λ 7393.77) and similar arguments for the classification of $2p_9-5d_3$ (λ 6846.57) and $2p_8-5d_3$ (λ 6982.04).

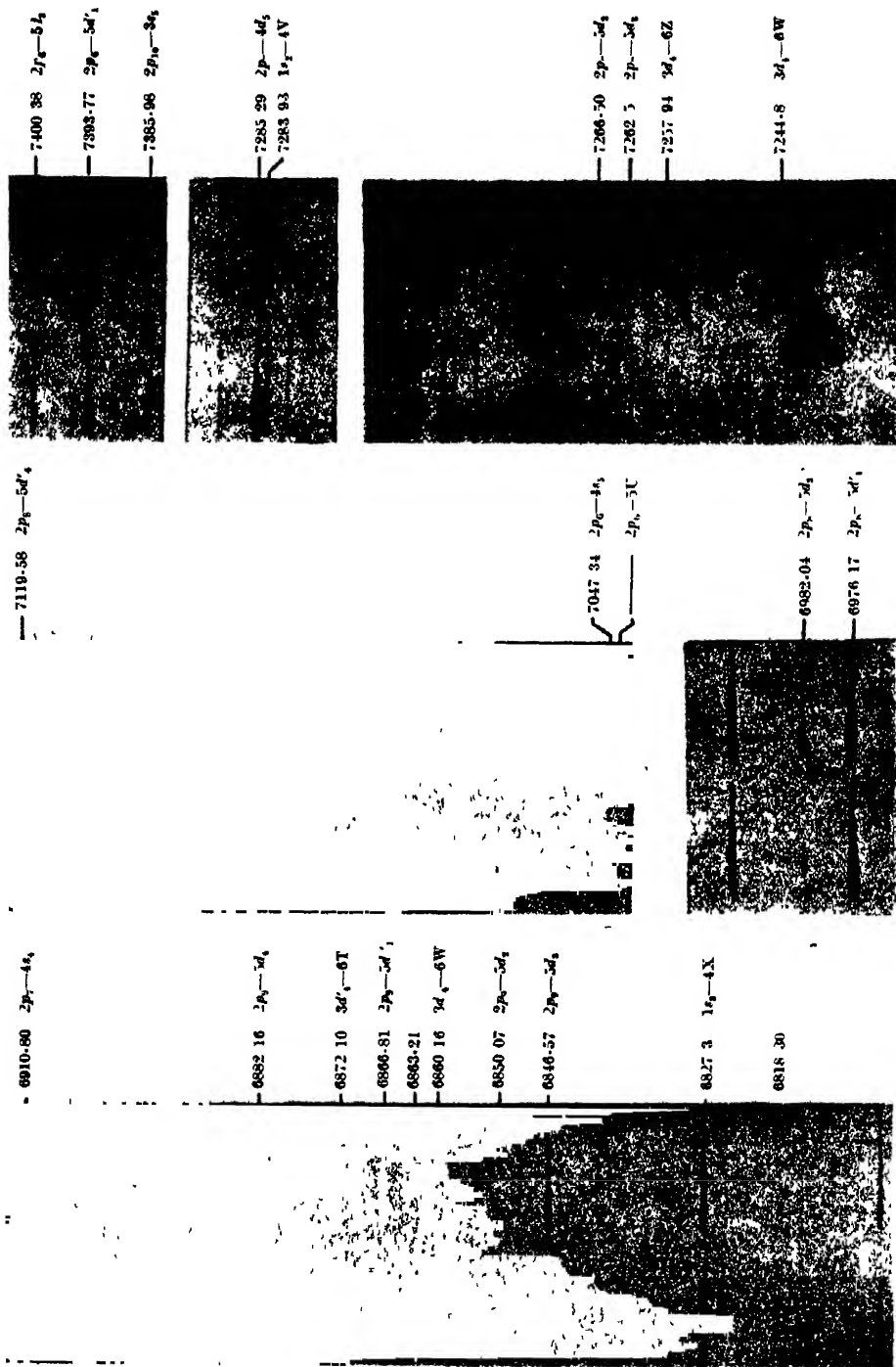
In the normal patterns of helium and neon the 0, 1 components (i.e., those arising from transitions from $m = 0$ and $m = \pm 1$ levels) are very often unresolved and appear as a single component. To some extent this is also true of xenon patterns, not only of the normal type but of the abnormal type as well. Wherever the 0, 1 components are indistinguishable for purposes of measurement, the fused component is indicated by a d in parenthesis. In such a case the double character of the component has been revealed either by its width or by its actual resolution on plates representing higher fields.

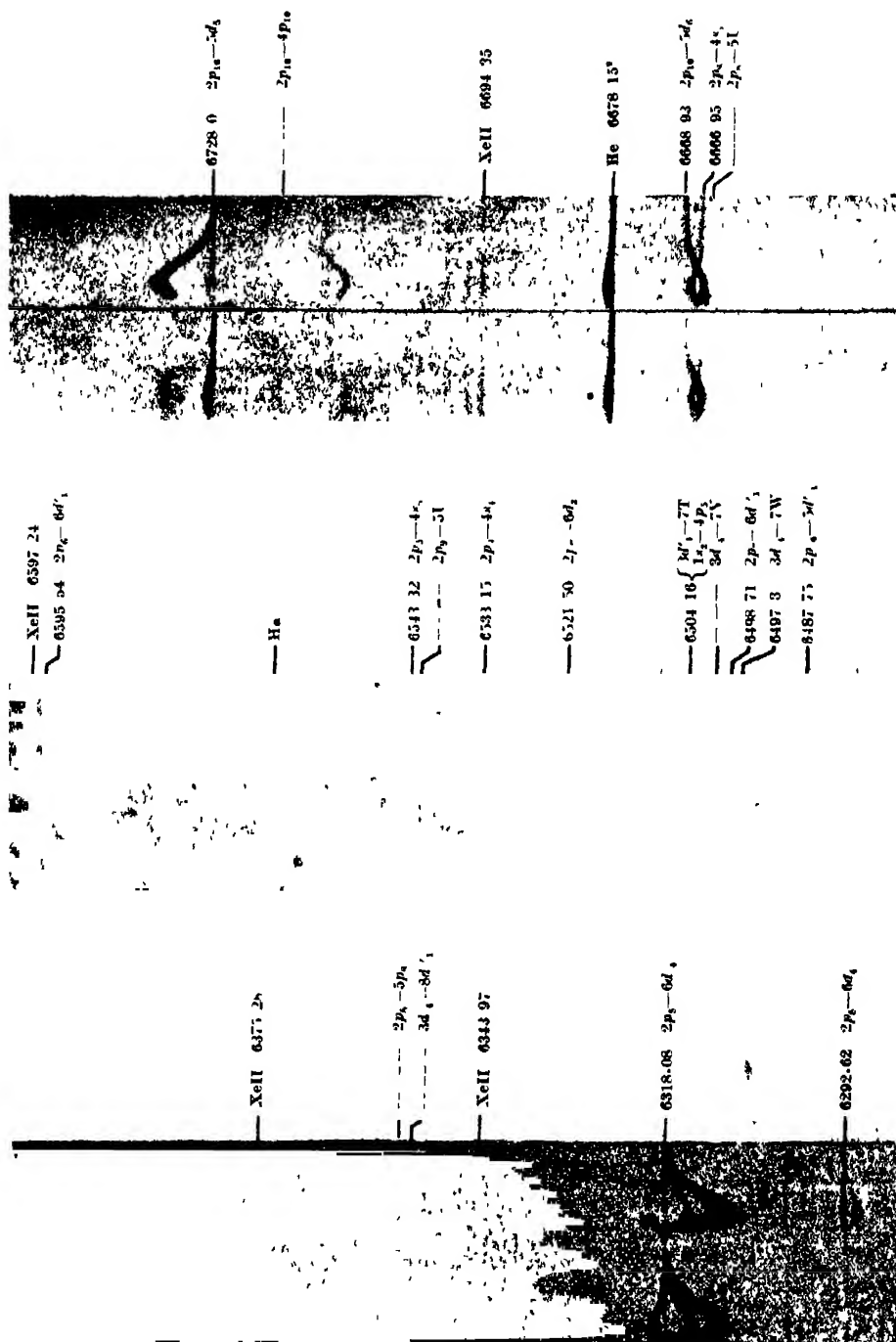
It may be remarked here that diffuse series lines from initial states of j value 2 to final states of j value 1 have patterns which may equally well be described as normal or abnormal. In Table II such lines have been described as abnormal.

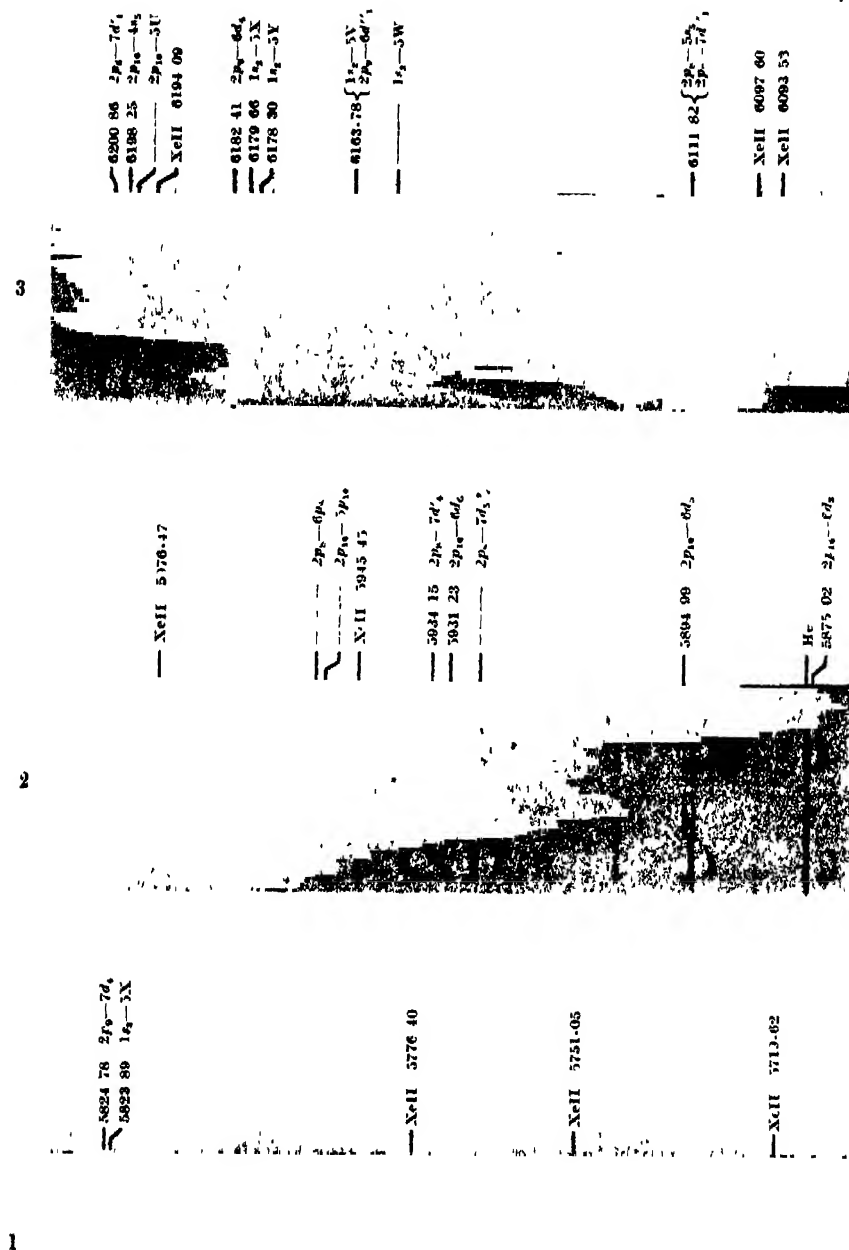
Having classified the diffuse series lines according to the type of pattern yielded, it is a simple matter to pick out those states in which the m values are specified by the j 's and those in which the m 's are specified by the l 's. Certain states, however, have $j = l$, viz., $2p_7, 2p_{10}$, ($j = 1$) and nd''_1, nd_3 ($j = 2$).

* Foster, *loc. cit.*, vol. 114.









Concerning these states, of course, nothing can be said as to how the m values are specified.

States whose perturbed levels are specified by j values are $2p_6$, $2p_8$, $2p_9$, $5d_6$, $6d_6$, $5d'_1$, $6d'_1$, $7d'_1$, $5d_4$, $6d_4$, $7d_4$, $5d'_4$, $6d'_4$, $7d'_4$. We must assume that these states are split in the electric field with reference to electron spin, i.e., that the ls coupling is undisturbed and the m values are the resolved parts of the j values.

States whose perturbed levels are specified by l values are $5d_2$ and $6d_8$. We must assume that these states are split in the field without reference to electron spin, i.e., the ls coupling is broken down and the m values are the resolved parts of the l values.

The importance of the existence of both types of splitting in the xenon spectrum lies in the fact that, if a simple hypothesis can explain why certain patterns are normal and others abnormal, then this spectrum must provide its verification.

Many authors have tacitly assumed that, as in Zeeman effect, if the multiplet separations are small with respect to displacements due to the electric field, then the ls coupling is broken down, and otherwise, retained. This hypothesis finds no support in the present results. For, on examination of the xenon energy chart, no systematic character of the multiplet separations of $5d_2$ and $6d_8$ is to be noticed. Moreover, upon observation of the normal patterns from zero field to 67,000 volts/cm., no suggestion is to be found of a transition from abnormal patterns at low fields to normal patterns at high fields

Displacement of Individual Terms.

It is now desirable to determine the extent to which the observed displacements may be attributed to shifts in the initial and final states respectively. An examination of lines involving the same initial state is helpful. In such a group the *number* of Stark components varies with the final state, but the *displacements* of individual components will vary—from member to member of the group—*only* if the different final states experience different displacements in the field. A number of groups of diffuse series lines with the same initial states are to be found in Table II. A careful examination of these groups indicates no variations of displacements within a group other than small irregular variations which may be attributed to errors in measurement.*

* It was reported earlier by one of us that there was evidence of the displacement of some final states in xenon. Observations of later plates obtained with the grating spectrograph have shown this to be an error.

Hence, one is forced to conclude that all final $2p$ levels are undisplaced in the field. The alternative conclusion, that they are all displaced exactly to the same extent is extremely unlikely. Other groups point to the same conclusion regarding final $1s$ and $3d$ states.

The splitting and displacement of individual terms at 67,000 volts/cm. are given in Table III on the assumption that final states help to determine the number of observed components, but have nothing to do with displacements. An attempt has been made to give the m_i or m_j values of the perturbed level of diffuse series terms. These are doubtful in many cases and are undoubted only in cases of highest m values—since the level of highest m value gives rise to the “extra” component appearing in many transitions. Perturbed levels whose m 's are undetermined, or which may consist of a number of fused levels are classified as *unknown*. In cases where small discrepancies occur among the measured displacements of lines with the same initial level the results of Table III represent average values. The table also includes the hydrogen difference of each term.

It is clear from this table that no simple relation exists between the displacements and the hydrogen differences. In seeking some explanation of the origin of these displacements, it is interesting to compare the general nature of displacements of diffuse series terms of xenon with those of helium and neon, as observed by Foster, and by Foster and Rowles respectively. In these latter atoms diffuse series terms have positive displacements which decrease in magnitude with increasing value of m . In xenon, on the other hand, the general rule for displacements of diffuse series terms is that they are negative for small m values and *increase* arithmetically with increasing m values, the displacement of the level with highest m value being positive. This is not, however, invariably the case. For a few diffuse series terms the opposite is true, i.e., displacements are positive for small m values and *decrease* arithmetically with increasing m value. This lends support to the view that the magnitude of displacements is governed, in part, by the distribution of the energy levels. In fact, the general rule of negative displacements for diffuse series terms finds a qualitative explanation in the Pauli formula. For, in the xenon energy chart, each group of d -levels with quantum number n lies near a group of p -levels with quantum number $(n - 1)$ and of slightly higher term values. According to the Pauli formula the mutual effect of these sets of terms will be to displace the d -terms negatively, and the p -terms positively. It will be observed in Table III that all initial p -terms have relatively large positive displacements. An excellent example is afforded in the case of the

$5d_5$ -term, whose term value is exceptional, being higher than any $4p$ -term. This level has a large positive displacement as would be expected. The hydrogen difference of this term is 1318.

Since the transition probabilities are unknown it is not possible to test the Pauli formula quantitatively. Throughout the spectrum, however, there is good qualitative agreement with the formula.

Table III.—Displacements of Initial Terms of the Xenon Spectrum in a Field of 67,000 volts/cm.

j.	Term.	Displacements (cm. ⁻¹).						Hydrogen difference.
		$m = 0.$	1.	2.	3.	4.	Unknown.	
2	$3s_3$						+ 0 5	—5161
2	$4s_3$						+ 12.5	—2420
1	$3s_2$						Small (—)	—5489
1	$4s_2$						+ 2 6	—2444
1	$4p_{10}$						+ 6 8	
							—11.4(?)	—1175
1	$5p_{10}$						+27	— 621
2	$3p_3$						0	—2708
2	$5p_3$						Large (+)	— 664
3	$3p_2$						Small (+)	—2825
3	$4p_2$						+ 9 6	—1287
3	$5p_2$						+27	— 689
3	$6p_2$						+64	— 410
1	$2p_7$						0	—8552
1	$3p_7$						0	—3101
2	$3p_6$						0	—3043
2	$4p_6$						+ 3.2	—1393
2	$5p_6$						+34	— 744
0	$2p_5$						0	—9715
0	$3p_5$						0	—3198
0	$4p_5$						+ 2 0	
							0	—1577
0	$5p_5$						+12 8	— 840
1	$2p_4$						0	—17975
2	$2p_3$						0	—18758
1	$2p_2$						0	—18875
0	$2p_1$						0	—19456
0	$5d_3$	— 4.7						+1186
0	$6d_3$	—11.1						+ 663
0	$8d_3$	+ 9.4						+ 319
1	$5d_2$						+13.5	
							+ 1.7	+1318
1	$6d_2$	—12.5	—12 5	— 4.1				+ 559
4	$5d_4$	— 5.7	5.7	— 4.2	— 2.3	+ 1.0		+1001
4	$6d_4$	—21.1	—21 1	—15 6	— 8 0	+ 4.0		+ 501
4	$7d_4$	—29.8	—29 8	—20.7	— 4 6	+10.6		+ 345
3	$5d_4$	— 0 5	— 0 5	— 0 5	+ 0 9			+ 800
3	$6d_4$	— 6 8	— 3.4	— 0 2	+ 0 9			+ 497
3	$7d_4$	—20.7	— 8.5	— 4.3	+ 0.9			+ 312
2	$5d_3$	+ 0.5	+ 0.5	— 0 4				+ 724
2	$6d_3$	— 3 4	— 5.2	—10 9				+ 501
1	$5d_2$	+ 0.1	+ 0 1	— 2 2				+ 732

Table III—(continued).

Displacements (cm ⁻¹)								Hydrogen difference.
<i>j</i> .	Term.	<i>m</i> = 0.	1	2.	3.	4	Unknown.	
2	5 <i>d</i> '' ₁	+ 0 4	+ 0 4	— 1 0				+ 767
2	6 <i>d</i> '' ₁	— 5 3	— 5 3	— 1 1				+ 447
2	8 <i>d</i> '' ₁						+33 +28 +24	+ 188
3	5 <i>d</i> ' ₁	— 0 6	— 0 6	— 0 6	+ 0 7			+ 712
3	6 <i>d</i> ' ₁	— 5 1	— 2 1	+ 0 4	+ 4 5			+ 417
3	7 <i>d</i> ' ₁	—14 9	—11 5	— 7 3	— 5 5			+ 260
1	4X						0	+ 138
1	5X						+12 6	+ 83
1	6X						+43	+ 52
2	4Y						0	+ 128
2	5Y						+ 12 5	
							+ 9 5	+ 80
2	6Y						—29	+ 50
4	6Z						Large (—)	+ 42
4	7Z						— 2 0	+ 27
5	6T						+ 0 6	
							+ 0 6	+ 42
5	7T						+99	+ 28
3	4U						Small (+)	+ 70
3	5U						+ 5 1	+ 44
3	6U						Large (—)	+ 29
2	4V						+ 0 3	+ 68
2	5V						+18	+ 41
2	6V						—18	+ 27
2	7V						+ 46	+ 18
3	5W						—13	+ 25
							Large (+)	
3	6W						— 1 8	+ 17
							— 4 6	
3	7W						+ 41	+ 12

Reversal of certain Components.

Several of the components observed in this investigation reveal a curious behaviour in the electric field. As the field increases from zero to a maximum each such component shows at first an increasing displacement toward the violet, and later a decreasing displacement. The result is an *s*-shaped component on the Lo Surdo photographs.

Certain components of the lines $2p_8-7d'_4$ and $2p_9-7d_4$ and the single component of $2p_{10}-6d_6$ exemplify this behaviour. Unfortunately all the features may not be observed clearly upon one photograph. However, Plate 9 serves to show all the features observed. *A* shows how the components "2" and "3" of $2p_8-7d'_4$ turn back in high fields, *B*, representing greater intensity but lower fields, shows more completely the pattern of this line, and also shows

how the single component of $2p_{10}-6d_8$ falls upon the "2" component of $2p_8-7d'_4$. It will be observed from *A* that the component of $2p_{10}-6d_8$ also turns back in highest fields. *C* shows the component "3" of $2p_9-7d_4$ turning back, while *D* (again lower fields, but greater intensity) shows the component "2" turning back and resolving itself from the component "1" which continues its increasing displacement to the violet.

The maximum field of *A* and *C* is 66,000 volts/cm. and that of *B* and *D* is 61,000 volts/cm.

These anomalous displacements may not be attributed to displacements of final levels, for other transitions to the levels $2p_8$, $2p_9$ and $2p_{10}$ yield displacements varying in the usual way with the square of the field strength. The phenomenon, then, must be attributed to an actual turning back of the initial levels $7d'_4$, $7d_4$ and $6d_8$ in higher fields.

Since the Pauli formula for displacements involves the field only in the term F^2 , it is not possible to interpret the above observations by this formula. Effectively the formula states that each level related to a given level by $\Delta l = \pm 1$, $\Delta j = 0, \pm 1$, $\Delta m = 0$ "repels" the given level, the consequent displacement being proportional to the square of the probability of transition

$$(|\alpha_{n,l,j,m \rightarrow n',l',j',m}|^2)$$

between the two levels, and inversely proportional to the separation of the levels ($\nu_{n,l,j,m \rightarrow n',l',j',m}$). The resultant displacement of a given level is the sum of the effects on the given level of all levels in the atom related to the given level by $\Delta l = \pm 1$, $\Delta j = 0, \pm 1$, $\Delta m = 0$. The obvious reason for the restriction upon Δl and Δj is that, ordinarily, the transition probability $|\alpha_{n,l,j,m \rightarrow n',l',j',m}|$ exists only if Δl and Δj are so restricted. Experiment shows, however, that in high fields these restrictions are no longer valid (viz., combination lines). A second order extension of the formula would necessarily include terms not involving these restrictions. In these terms the probability $|\alpha_{n,l,j,m \rightarrow n',l',j',m}|$ would be, clearly, a function of the field strength. It is suggested that the turning back, in high fields, of perturbed levels of $7d'_4$, $7d_4$ and $6d_8$ is to be attributed to the effect of levels of slightly smaller term values and such that transition probabilities between them and the given levels are zero in low fields, but reach appreciable values in higher fields.

Ishida* has observed certain pairs of displaced components in the helium spectrum which recede from each other at very high fields. This phenomenon is probably of the same nature as the one described above.

* 'Sci. Papers, Inst. Phys. Chem. Res.,' Tokio, No. 260 (1930).

Lines of the Type $2p_i-4s_5$ and $2p_i-5U$.

An interesting intensity feature is well illustrated by the line $2p_{10}-4s_5$ and the neighbouring combination line $2p_{10}-5U$, Plate 9, E. The sharp series line shows, at low fields, a displacement toward the red. In somewhat higher fields its intensity decreases greatly and at the same field the combination line appears with great intensity. This phenomenon persists throughout all lines of the form $2p_i-4s_5$ which have been observed here, namely $i = 10$ (λ 6198.25), $i = 9$ (λ 6543.32), $i = 8$ (λ 6666.95), $i = 6$ (λ 7047.34).

Ishida* first observed the same behaviour in connection with certain principal series lines and nearby *sd* combination lines in the ultra-violet region of the neon spectrum.

While these intensity changes might conceivably be due to changes in transition probabilities with increasing field, the authors believe that the persistence of this behaviour throughout the series $2p_i-4s_5$ and the juxtaposition of the terms $4s_5$ and $5U$ suggest a resonance explanation involving the relative number of atoms in the $4s_5$ and $5U$ states.

Double Lines Resolved by the Electric Field.

In the normal xenon spectrum Meggers, de Bruin and Humphreys failed to resolve certain pairs of lines which appear accidentally at the same wavelength. In two of these cases the electric field clearly resolves these lines because their Stark displacements are of decidedly different orders of magnitude. Thus in Plates 11 and 12 the displacements of $3d_4-7Z$ and $1s_2-5V$ break away from the normal line at much lower fields than do the displacements of $1s_2-4p_8$ and $2p_8-6d'_1$ respectively. (See λ 6504.16 and λ 6163.78.)

Lines of the Second Spectrum of Xenon.

Numerous lines belonging to the second spectrum of xenon (Xe_{II}) have been observed on the plates. None of these lines shows displacement in the electric field. They do, however, show considerable enhancement in the region of high fields due, no doubt, to the greater percentage of xenon ions there.

In conclusion the authors wish to express their deep indebtedness to Dr. J. S. Foster for his inspiration and guidance during the course of this work.

* 'Nature,' vol. 125, p. 970 (1930).

Summary.

(1) The Stark effect for xenon in the region λ 3500– λ 8400 has been examined, using the type of source developed in this laboratory. A Hilger E1 spectrograph and a 30-foot concave grating have been used for the analysis.

(2) Appreciable displacements have been observed for a total of 98 lines including a number of combination lines brought out by the field.

(3) The sharp, principal and fundamental series lines are, in general, displaced without splitting, while many of the diffuse series lines suffer large displacements and are split into a variety of patterns.

(4) The $5d_2$ and $6d_5$ terms are split without reference to electron spin, the resulting patterns being "normal" as in helium. On the other hand the action of the field upon the terms $2p_6$, $2p_8$, $2p_9$, $5d_6$, $6d_6$, $5d'_1$, $6d'_1$, $7d'_1$, $5d_4$, $6d_4$, $7d_4$, $5d'_4$, $6d'_4$, $7d'_4$ indicates that the ls coupling is retained, the m values being determined by the j 's.

(5) The displacements of observed xenon lines in the electric field are attributed to the displacements of initial states. The sign and magnitude of these displacements give no support to the prevalent idea that Stark displacements are governed by the hydrogen differences only. On the other hand these displacements find a qualitative explanation in the Pauli formula.

(6) The lines $2p_8$ – $7d'_4$, $2p_9$ – $7d_4$ and $2p_{10}$ – $6d_6$ have components with displacements which increase with the field up to a maximum value and then recede in higher fields. A possible explanation is suggested.

(7) As the electric field increases, displaced components of certain lines are observed to decrease greatly in intensity, this being accompanied by the enhancement of components arising from nearby lines. This unusual intensity relation is most clearly shown in the case of the groups $2p_i$ – $4s_5$ and $2p_i$ – $5U$, and persists for different values of i .

(8) Lines of the second spectrum of xenon have been observed. None of these shows displacement in the electric field.

The Efficiency of Secondary Electron Emission.

By Dr. S. RAMACHANDRA RAO, Annamalai University, Annamalainagar,
South India.

(Communicated by O. W. Richardson, F R.S. --Received September 12, 1932.)

1. *Introductum.*

The velocity distribution of the secondary electrons produced by bombarding a metallic face with a stream of primary electrons has been a matter of interest ever since the beginning of the study of secondary electron emission. As early as in 1908, Richardson* and von Baeyer† independently showed that slow moving electrons were copiously reflected from conducting faces. Farnsworth‡ showed that for primary electrons having velocities less than 9 volts, most of the secondary electrons had velocities equal to the primary. As the primary potential was increased, the percentage of the reflected electrons decreased gradually but was appreciable at 110 volts. Davisson and Kunsman§ obtained reflected electrons even at primary potentials of 1000 and 1500 volts in the cases of some metal faces. At higher potentials we have also the electrons that undergo the Davisson and Germer scattering|| from the many crystal facets on the bombarded targets. As the potential is increased, the number of electrons with low velocities increases steadily and at large applied potentials, we have a large percentage of these in the secondary beam. These conclusions followed as a result of the work of Farnsworth¶ who studied the distribution of velocities of the secondary electrons by the retarding potential method. He did not actually calculate the energy distribution from his curves but has drawn attention to the above conclusions.

A careful investigation of the velocity distribution of the secondary electrons from various conducting faces was made by Rudberg** at primary potentials ranging up to about 1000 volts. He adopted a magnetic deflection method

* 'Phil. Mag.,' vol. 16, p. 898 (1908), 'Phys. Rev.,' vol. 29, p. 557 (1909).

† 'Verh. deuts. phys. Ges.,' vol. 10, pp. 96, 953 (1908).

‡ 'Phys. Rev.,' vol. 20, p. 358 (1922); vol. 25, p. 41 (1925); and vol. 27, p. 413 (1926).

§ 'Phys. Rev.,' vol. 20, p. 111 (1922); vol. 22, p. 242 (1923).

|| 'Phys. Rev.,' vol. 30, p. 705 (1927).

¶ 'Phys. Rev.,' vol. 31, p. 405 (1928).

** Rudberg, 'K. svenska Vetensk Akad. Handl.,' vol 7, p. 1 (1929). See also 'Proc. Roy. Soc.,' A, vol. 127, p. 111 (1930).

similar to the one used in the analysis of the β rays and of the electrons excited by X-rays.* The method had indeed been used by previous workers for the study of secondary emission,† but Rudberg improved the technique considerably and obtained better focussing conditions. His results suggest that there are three groups of electrons in the secondary beam. The first group contains electrons returning with the same velocity as the primary. In the second group of electrons, we have those which undergo inelastic collisions with the orbital and structure electrons and hence are returned with some loss of energy. Richardson‡ has drawn attention to the well-marked minimum between the two groups in Rudberg's curves and infers that free electrons are not involved in the collisions. Finally there is the third group which contains the slow secondary electrons. The second and the third groups appear to be definitely connected with each other since they are both predominant at high primary potentials and become negligible at low primary potentials. Richardson suggests that the third group is the result of the excitation accompanying the inelastic collisions.

Several workers have also investigated the variation of the secondary current, per unit primary current, with the applied potential. Petry,§ Farnsworth,|| Krefft¶ and Ahearn** have studied the secondary electron emission from metal faces. Attention may also be drawn to the work of Hyatt and Smith†† who obtained similar secondary electron curves for molybdenum using a new method of investigation. The author‡‡ has carried out careful experiments on the secondary emission from a polycrystalline nickel target. Generally it is found that as the potential is increased from zero the ratio of the secondary to the primary current increases rapidly, attains a maximum in the neighbourhood of 3 volts, then decreases gradually up to about 20 volts, showing a few peaks in this part of the curve. The value then rises gradually and steadily, attaining a maximum value at a potential of about 500 volts and thereafter decreases very slowly. We do not consider here the small discontinuities in the secondary electron curves. In almost all the metals investigated, the

* For details see Rudberg, *loc. cit.*, p. 105.

† Cf. Brinsmade, 'Phys. Rev.', vol. 30, p. 494 (1927).

‡ 'Proc. Roy. Soc.,' A, vol. 128, p. 63 (1930); vol. 119, p. 531 (1928)

§ 'Phys. Rev.', vol. 28, p. 346 (1925) and vol. 28, p. 362 (1926).

|| *Loc. cit.*, and 'Phys. Rev.', vol. 31, pp 414, 419 (1928); vol. 34, p. 679 (1929).

¶ 'Phys. Rev.', vol. 31, p. 199 (1928); 'Ann. Physik,' vol. 84, p. 639 (1927).

** 'Phys. Rev.', vol. 38, p. 1858 (1931).

†† 'Phys. Rev.', vol. 32, p. 929 (1928).

‡‡ 'Proc. Roy. Soc.,' A, vol. 128, p. 41 (1930).

value of i_s/i_p (the ratio of the secondary to the primary current) becomes even greater than 1 at potentials more than about 200 volts. This means that there are more secondary electrons in the secondary beam than in the primary beam.

The author* has shown that if a single crystal of nickel with the 100 face be used, the value of i_s/i_p obtained at any potential (preferably greater than about 50 volts) is smaller than the corresponding value for the polycrystalline target. Some unpublished preliminary experiments on the 110 face of a nickel crystal show that the values of i_s/i_p obtained with this surface are still smaller. It was therefore a problem as to why there should be this difference in the total secondary emission when different faces of the same metal crystal were used for the experiments.

2. *Efficiency of Secondary Emission.*

At the time when the author was investigating the secondary emission from nickel in Professor Richardson's laboratories in King's College, London (from April, 1929, to June, 1930), he took careful readings of the distribution of velocities for the nickel targets by the method of retarding potentials in the manner adopted by Farnsworth.† Since, however, the interest of the experiment at that time was mostly with inflections in the secondary electron curves and their correlations with similar inflections in the soft X-ray excitation curves,‡ these results were not taken into consideration. However, the author has now gone back to the question and on carefully studying the problem, it is found that results of considerable importance ensue from the data. He has therefore decided to publish these figures and draw attention to the main conclusions. We have just said that there are three groups of electrons in the secondary emission. The ratio of their total kinetic energy to the kinetic energy of the primary beam may be considered as the efficiency of the secondary emission. Since $\frac{1}{2}mv^2 = eV$, we shall take the corrected applied potentials as proportional to the kinetic energy. Let us suppose that unit primary current is incident on the target. The kinetic energy may then be taken as proportional to V , the applied potential, since the incident beam may be assumed to consist of electrons having the velocity which corresponds to V .

If in the secondary beam, we find that a fraction f_1 has a velocity V_1 , we may then write down $\Sigma f_1 = i_s/i_p$, where the summation includes all the electrons having velocities ranging from 0 to V . The value of $\Sigma f_1 V_1$ similarly

* 'Proc. Roy. Soc., A, vol. 128, p. 57 (1930).

† 'Phys. Rev.,' vol. 31, p. 405 (1928).

‡ Richardson and Rao, 'Proc. Roy. Soc.,' A, vol. 128, pp. 16, 37 (1930).

extended to all values within V , is proportional to the kinetic energy of the secondary beam. The efficiency of the secondary emission will be equal to $\Sigma f_1 V_1 / V$.

3. Experimental Method.

The details of the experiment have been described,* and it is therefore unnecessary to repeat them here. However, the principle may be indicated by reference to fig. 1. Electrons from a glowing tungsten filament F_1 are directed through an electron gun G , on a metal target T screwed on a nickel cylinder C , which has been thoroughly outgassed with the help of a second filament F_2 . S is the shield around the target. The current from the filament

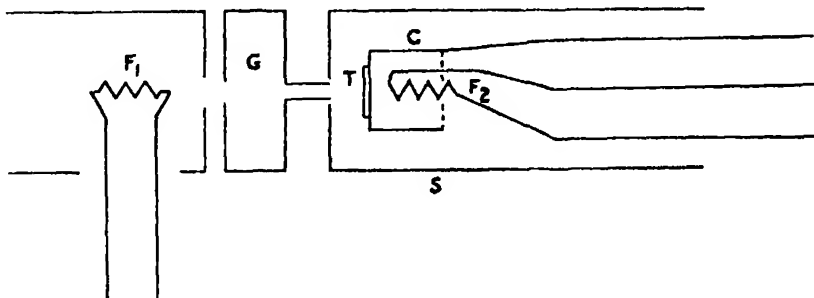


FIG. 1.

F_1 to the target measures the primary current i_p , and the current from the target to the shield S (which is maintained at 4 volts positive with respect to the target for measurements of the secondary ratio) the secondary current i_s . The potential on the primary electrons will, of course, be the potential of the target with respect to the filament F_1 , the gun G being also at the same potential as the target.

Applying a given potential to the primary beam, we can study the distribution of velocities in the secondary current by the application of a retarding potential to the shield. The secondary current is measured as the retarding potential is gradually increased from 0 to the value equal to the primary potential. The curves obtained for the nickel faces are shown in figs. 2 and 3. It can easily be shown that $\Sigma f_1 V_1$ for any potential is measured by the area enclosed between the curve and the X and Y axes. Since the primary current is taken as unity, V itself will be the energy of the primary current and hence the efficiency at any applied potential can be calculated.

* Rao, 'Proc. Roy. Soc.,' A, vol. 128, p. 41 (1930).

The necessary corrections were applied to the values of the primary potential. There are two more points which have to be mentioned here. The current reflected back through the opening in the shield C opposite the target will be

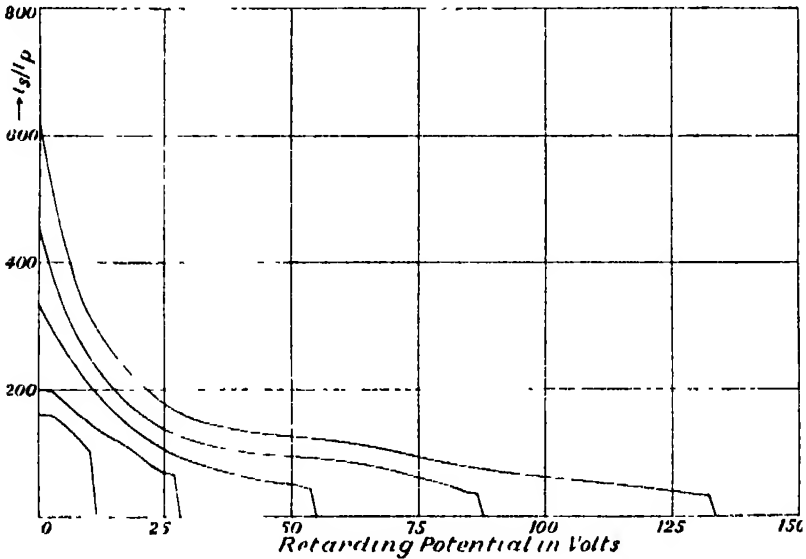


FIG. 2.

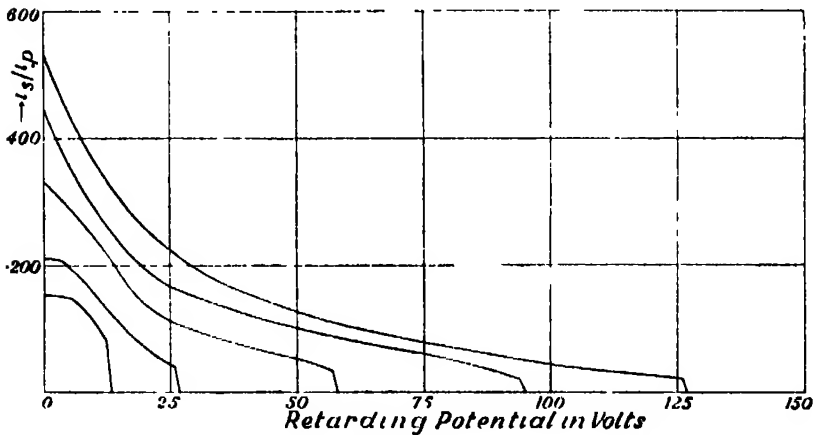


FIG. 3

lost, but since the solid angle subtended by the opening at the centre of the target was only 3 per cent. of the entire solid angle, this decrease will not be considerable; in comparative measurements, this will be of no consequence. There are also the electrons reflected and scattered from the shield C back to the target and cylinder. Since, however, it was found that even an additional

positive potential of 2 volts on the shield with respect to the target was enough to get a saturation value of the secondary current, it is believed that under the conditions of the experiment these could be neglected.

4. Results.

Before recording the results obtained by the writer with a polycrystalline nickel target and with the 100 face of a nickel crystal, it is instructive to consider the results of Farnsworth. A calculation has been made from his published curves and the results are given in Table I. The efficiency of the reflected (corresponding to the first group of electrons) and the scattered (corresponding to the second and third groups) electrons are given separately and the total efficiency is also tabulated.

Table I.

Metal	Primary potential in volts	Percentage efficiency of the first group of electrons	Percentage efficiency of the second and third groups of electrons	Total percentage efficiency of the secondary electrons	i_s/i_p
Copper	6.6	26.6	5.0	31.0	0.328
	8.5	25.0	5.6	30.6	0.332
	10.4	28.0	5.2	33.2	0.360
	24.3	16.0	8.3	24.3	0.320
	31.2	13.0	9.5	22.5	0.375
	41.2	11.0	11.9	21.9	0.460
	49.2	10.0	11.3	21.3	0.530
Iron	4.6	15.0	3.2	18.2	0.205
	8.4	14.5	5.4	19.9	0.240
	10.6	13.0	6.2	19.2	0.240
	12.5	12.0	6.0	18.0	0.235
	19.0	7.0	10.2	15.2	0.255
	34.0	5.0	9.9	14.9	0.330
	47.4	5.0	11.6	16.6	0.440
Nickel	6.2	12.0	2.6	14.6	0.163
	10.4	11.0	3.3	14.3	0.170
	18.6	9.0	5.8	14.8	0.210
	33.5	6.0	9.0	15.0	0.290
	50.0	5.0	11.5	16.5	0.440
Silver	10.6	20.0	3.9	23.9	0.250
	18.7	13.5	4.6	18.1	0.220
	33.5	9.5	7.1	16.6	0.240
	39.0	8.0	9.0	17.0	0.270
	50.0	7.0	10.3	17.3	0.320

In judging the significance of these results, it must be remembered that the disposition of the curves is very sensitive to gas adsorption. Without therefore

unduly emphasising the importance of individual figures, one can easily derive some interesting conclusions from the above table. The efficiency of the first group of full velocity electrons is nearly constant up to about 10 volts, then decreases with increasing voltages rapidly at first and slowly at higher potentials. The efficiency of the second and third group electrons is small at low primary potentials and then increases rapidly with increasing potentials. Above about 40 volts it is found that the increase becomes much less rapid.

These conclusions are indeed apparent from the work of Rudberg (*loc. cit.*) The above table, however, gives us some more information regarding the total efficiency of secondary electron emission from metal faces. Generally it is found that the total efficiency increases at low voltages until a maximum is reached in the neighbourhood of 10 volts, then decreases slowly attaining a broad minimum at about 35 volts and thereafter shows a slow and continuous rise. The actual values at which the maxima and minima occur depend on the nature of the metal.

The results obtained in this investigation and given in Table II, will now be considered.

Table II.

Metal surface.	Primary potential in volts.	Percentage efficiency of the first group of electrons	Percentage efficiency of the second and third groups of electrons.	Total percentage efficiency.	$\frac{1}{2}, \frac{1}{2}$.
Nickel poly-crystalline surface	11.2	10.1	2.8	12.9	0.160
	28.0	5.4	7.2	12.6	0.200
	55.2	4.2	8.8	13.0	0.350
	87.8	3.6	9.6	13.2	0.470
	133.5	3.0	11.0	14.0	0.640
Nickel single crystal face, 100	13.3	8.7	4.5	13.2	0.156
	26.8	4.0	9.0	13.0	0.210
	58.0	3.4	10.0	13.4	0.330
	95.0	2.2	11.6	13.8	0.450
	126.7	2.0	12.1	14.1	0.640

The values in Table II have been calculated from the curves shown in figs. 2 and 3. On comparing the nickel values in Table II with those in Table I, it is found that there is fairly good agreement. The author's values are in all cases slightly less than those calculated from Farnsworth's graphs. The results for the two nickel faces were obtained under the same conditions and

hence a comparison between these will be of interest. The following points are to be noted :—

- (a) The efficiency of the full velocity electrons is smaller uniformly for the single crystal than for the polycrystalline face
- (b) The efficiency of the scattered electrons is greater for the single crystal than for the polycrystalline target.
- (c) The values of i_s/i_p are different for the two surfaces, the departure being large at higher potentials. Attention has already been drawn to this point by the author.*
- (d) However the most interesting result is that the total efficiency is practically constant for both the surfaces.
- (e) The efficiency remains practically constant in the range below 60 volts, and shows a small rise as the potential is still further increased.
- (f) The general conclusions regarding the efficiencies of metal faces pointed out in reference to Table I are also verified.

5. Discussion.

(a) *Comparison of the Efficiency of Secondary Electron Emission with the Soft X-ray Excitation Efficiency.*—Richardson and Chalkin† made a preliminary calculation from their data of the relative efficiency of the soft X-ray excitation from more ordinary metals. Richardson and Robertson,‡ using a specially constructed quartz tube, determined the relative efficiencies of 14 metals and discovered that the efficiency for soft X-rays was a periodic function of the atomic number. Their results were obtained for different potentials ranging from 100 to 500 volts. L. P. Davies§ has also determined the efficiencies using different photoelectric targets and found no change in the relative values. Her applied potentials were above 300 volts. Nakaya|| has also compared the emission from different metal faces using cobalt as the material of the photoelectric plate, taking special care to degas the targets and the plate thoroughly. The results of these workers and the secondary electron efficiencies are tabulated in Table III.

* 'Proc. Roy. Soc.,' A, vol. 128, p. 57 (1930).

† 'Proc. Roy. Soc.,' A, vol. 110, p. 273 (1926).

‡ 'Proc. Roy. Soc.,' A, vol. 115, p. 280 (1927)

§ 'Proc. Roy. Soc.,' A, vol. 119, p. 543 (1928).

|| 'Proc. Roy. Soc.,' A, vol. 124, p. 616 (1929)

Table III.

(For soft X-ray excitation only relative values of the efficiencies are given.)

Metal	Soft X-ray excitation				Total secondary electron emission.	
	R & R * (100 volt)	R & R † (300 volt)	D (300 volt)	N. (150 volt)	R (Total efficiency at about 50 volt).	R. (Efficiency of the second and third groups of electrons).
Iron	2 718	—	5 82	0 715	16·6	11 6
Nickel	2 472	—	5 74	0 561	16 5	11 5
Copper	2 217	2 619	5 40	0 542	21 3	11 3
Silver	—	2 686	—	—	17·3	10 3

R & R, Richardson and Robertson D., Davies. N., Nakaya. R., Readings taken from Table I

* Readings taken on the same day, March 11, 1927. † Readings taken on the same day March 28, 1927

Although it must be admitted that the secondary electron emission values are not so precise as the soft X ray values, it is interesting to compare the two sets of values. The range of variation is nearly the same in both cases.

It is equally interesting to compare the efficiencies of the same metal at different voltages. Richardson and Robertson find that the efficiencies for soft X-rays increase gradually as the applied potential is increased. In both soft X-ray excitation and secondary electron emission, it must be remembered that the readings have been obtained under perfectly uniform conditions and hence are reliable. For nickel, they recorded the values given in Table IV. The values of the efficiencies of the total secondary electron emission and of the second and third group electrons are also given for comparison.

Table IV.

R & R			R		
Soft X rays			Secondary electron efficiency.		
Potential	Efficiency determined on		Potential	Total efficiency.	Efficiency of second and third group electrons.
	11 2 27	15 2 27.			
100	2 418	2 454	55 2	13 0	8 8
200	2 521	2 375	87 8	13·2	9 6
300	2·786	2 60	133 5	14 0	11 0

R & R, Richardson and Robertson. R., Ramachandra Rao.

It is inferred from Table IV that there is a similar correlation between the two efficiencies as the voltage is increased. With the existing data it is not possible to make more than a general statement like this, but it is interesting to note that, excepting for a small number of curves, the observations of Richardson and Robertson show that the soft X-ray efficiency increases slowly as the applied potential is increased. This is quite similar to the corresponding increase in the efficiency of the secondary electron emission.

It should be remembered that in the measurements of the soft X-ray efficiencies, we do not have a homogeneous beam of incident electrons as in the case of the secondary electron emission. However, since identical conditions hold good in the case of all the metals in the measurements of one efficiency or the other, and since we are considering only relative values and not comparing the two efficiencies directly with each other, this point will have no influence.

(b) *Comparison of the Soft X-ray Efficiency with the Secondary Electron Efficiency for the two Faces of Nickel.*—A reference to Table II shows clearly that in the case of polycrystalline and single crystal faces of nickel, the total efficiencies are nearly the same in both cases. But considering the efficiencies of the second and third group electrons, the values are uniformly greater for the 100 face than for the polycrystalline surface. In the same manner the soft X-ray efficiency for the 100 face is also greater than for the polycrystalline target in the range below 400 volts. In this respect the variation resembles that for increasing potentials for the same metal.

(c) *On the Saturation Effects in Soft X-ray and Secondary Electron Curves.*—Richardson and Robertson* found that the intensity of the soft X-radiation when measured by photoelectric methods increases with the applied potentials at ordinary potentials but at higher potentials, about 3000 volts, the intensity tends to show a saturation value. This observation was confirmed by Nakaya (*loc. cit.*). It is interesting to consider fig. 15 on p. 639 of Nakaya's paper, in which the intensity curves for manganese, iron, cobalt, nickel and copper are shown. The photoelectric plate was of cobalt. It is found that all the five elements give quite similar curves, nickel and manganese particularly showing almost identical curves as far as the effect of saturation is concerned. This strongly suggests that the cause of saturation is not in the target but in the photoelectric plate. Indeed, a similar resemblance can also be traced in the curves on p. 194 of Richardson and Robertson's paper. It has so happened

* 'Proc. Roy. Soc.,' A, vol. 124, p. 188 (1929).

that photoelectric plates used at these high voltages have been copper, nickel or cobalt. Soft X-ray excitation intensities for various metal faces should be investigated with elements having widely different atomic numbers—like C, Ni and W—as the photoelectric detectors.* These interesting questions may then get a definite answer.

According to Richardson, the radiation produced by the inelastic collisions of the second group of electrons acts on the metal itself and gives rise to the low velocity third group of secondary electrons. In the same way the soft X-radiation is incident on the photoelectric plate and gives rise to the low velocity photoelectrons.† Since the full velocity electrons (group I) have nearly constant efficiency at high potentials, the saturation effect and the subsequent fall in the total secondary electron curves should be due almost entirely to the second and third group electrons. It is probable that since the depth of penetration of the incident beam would have increased at higher potentials a part of the energy of the slower secondary electrons would be absorbed within the metal, but whatever be the ultimate cause, it is clear that there is a fall of i_s/i_p at higher voltages. There should then be a similar fall in the case of the photoelectric current, where the process is similar to a part of the mechanism in secondary electron emission. This is just what might be expected judging from the experimental results of Nakaya, and Richardson and Robertson. The actual difference in the voltages at which saturation is obtained in secondary electron emission and soft X-ray excitation can be explained easily by remembering the difference in the conditions and the fact that in the former the mechanism is more complicated than in the latter.

The experiments on the nickel faces were conducted in the laboratories of Professor O. W. Richardson in King's College, London. It is a pleasure to recollect the hospitality I enjoyed in those laboratories and my sincere thanks are due to him for his guidance and inspiration. I also wish to take this opportunity of expressing my thanks to Dr. Müller, of the Royal Institution, for his kindness in investigating for me the structure of the nickel crystals used in these and in the preceding experiments.

Summary.

The paper presents a new aspect of the study of the secondary electron emission from metal faces due to the bombardment by a beam of primary

* Nakaya has used C as the photoelectric detector and drawn curves with Co, Ni and Mn as the emitters, but the measurements are not enough to lead to any definite conclusions.

† Rudberg, 'Proc. Roy. Soc.,' A, vol. 120, p. 385 (1928).

electrons. The efficiencies of the secondary emission are calculated for several metal faces and at different potentials from the data of Farnsworth and it is shown that these show a good resemblance to similar efficiencies of soft X-rays. For a polycrystalline nickel face and the 100 face of a single crystal of nickel, the efficiencies calculated from the author's experiments are found to be nearly equal to each other at potentials below 150 volts. The significance of the observations is discussed and it is suggested that the observed saturation tendencies in the soft X-ray intensity curves at about 3000 volts may be due to the photoelectric methods of measurement.

The Beneficial Effect of Oxidation on the Lubricating Properties of Oil.

By R. O. KING.

(Communicated by H. T. Tizard, F.R.S. Received September 13, 1932.)

[PLATE 13.]

Part I.—Introduction.

Journal bearing friction experiments have been made generally at relatively low temperatures and otherwise in conditions tending to prevent oxidation of the lubricating oil. Thus Beauchamp Tower's experiments led Reynolds to the conclusion that fluid friction alone prevails in an oil film maintained by continuous rotation of the journal and that boundary conditions do not become sensible.* The more recent experiments by Stanton, undertaken after the Physical Society discussion of 1919, were made to verify the conclusion, and confirmed that especially for mineral oils, "the conditions were in all cases those of perfect lubrication (*i.e.*, complete fluid lubrication), no approximation to the hypothetical ones of boundary lubrication being observed,"† "the conditions of lubrication of a cylindrical journal being of the Reynolds' type right up to the seizing pressure."‡ Stanton's experimental conditions were such that oxidation effects were not obtained. The feed to the journal bearing was always by fresh, not circulated, oil and the temperature of the oil film was maintained at 51·6° C., *i.e.*, at least 50° lower than required to induce oxidation

* Reynolds, 'Phil. Trans.', vol. 177, p. 157 (1886).

† Stanton, 'Proc. Roy. Soc.', A, vol. 102, p. 241 (1922).

‡ Stanton, 'Proc. Inst. Mech. Eng.', vol. 2, pp. 1117–1145 (1922).

in a mineral oil particularly susceptible to the effect. The possibility that oxidation might lead to boundary conditions becoming a factor in the measurements was not considered. Oxidation of the oil used to lubricate internal-combustion engines cannot be avoided in the usual conditions of operation, and an investigation of the effect on lubricating value was begun, in connection with experiments made in association with Professor Callendar,* on the oxidation of the lighter oils used as engine fuel. The results of lubrication experiments made directly on engines were difficult to interpret. The friction measured is mainly that due to the reciprocating motion of the pistons in the cylinders and oxidation being uncontrolled, the resulting accumulation of semi-solid products leads to secondary friction effects greater in magnitude than the primary effect attributable to the fluid alone. The conditions of journal bearing lubrication, on the other hand, can be controlled and friction measured with full accuracy and it appeared therefore that the investigation could be continued most effectively by using journal bearing testing machines. Machines adapted to be run at the relatively high temperature required for the oxidation of mineral oils had been designed at the N.P.L. by Mr. C. Jakeman in association with whom the experiments were continued, by permission of the authorities concerned.

Part II.—Experimental Apparatus and Synopsis of Results.

The Jakeman machine was mentioned by Sir T. Stanton, B.A. meeting 1927, and a brief description with some diagrams was published earlier,† in connection with a report on the lubricating value of oils procured from coal. The machine differs from the familiar Thurston type in that the temperature of the oil film can be raised artificially by a gas flame, and load remaining constant a seizing temperature (S.T.) is obtained instead of a seizing pressure. The friction, in the circumstances, falls as the temperature of the oil film rises, a minimum value (μ min.) being obtained generally before the S.T. is reached, and the consequent sharp retardation of the journal motion throws the belt off the flat faced driven pulley of the journal. Many lubrication seizures can occur in this way without abrasion of the rubbing surfaces.

The fresh oil feed fitted to the machine as described was replaced by the circulatory oil supply system, shown by fig. 1, providing for a small quantity, maintained in a state of oxidation activity, to be used continuously for any

* Callendar, King, Mardles, Stern and Fowler, 'Aero. Res. Ctee. Rep. & Mem.,' No. 1062.

† 'Engineering,' 3 June, 1927.

period. The oil, supplied by force feed from a sump, after passing through the bearing, is in part thrown off the rotating journal as mist and spray into the oxidising mixture of air and hot products of combustion from the gas

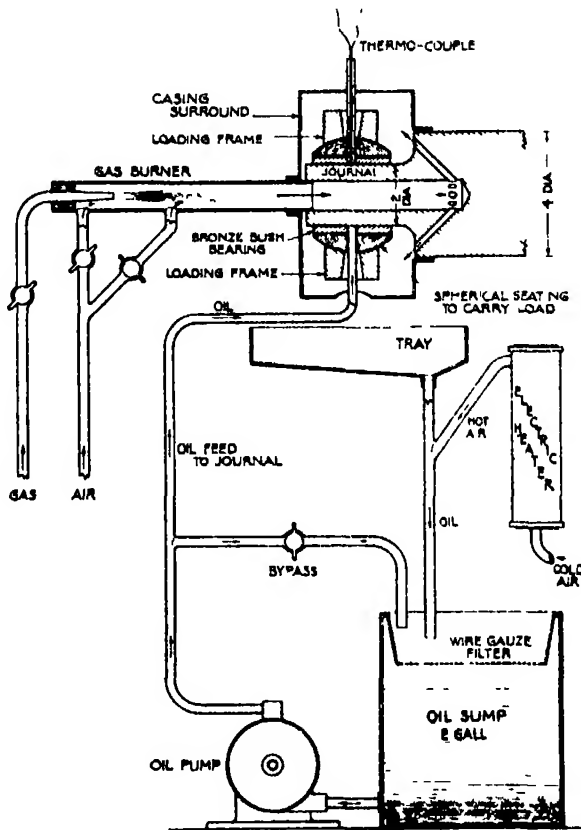


FIG. 1.—Journal heating and oil circulating systems.

burner contained in the casing surround. The oil running from the surface of the casing is collected in the open tray shown in the figure, and while draining to the sump, is further oxidised by exposure to a stream of air raised generally to 160°C . by the electric heater. No attempt was made to prevent contamination of the oil by the dust and dirt of the laboratory and adjoining workshop atmosphere, other than to provide a wire gauze filter over the top of the sump. The rate of circulation of the oil varied from about 4 to 30 ozs. per minute. A two-gallon sample was generally used, so on the basis of an average rate of circulation of 16 ozs. per minute, the whole sample passed

through the testing machine about eight times per hour. The rate of circulation was always in excess of that required for "bath" lubrication and was used to promote oxidation and assist temperature control.

Fig. 1 also shows the essential details of the machine other than the devices for applying the load and measuring the friction torque, described in the reference given. Referring to the figure, it will be seen that the hot gases from the burner after passing through the hollow journal, return by the inclined flues in the main shaft, to the casing enclosing the journal bearing. The arrangement tends to localise the heating at the journal end of the 4-inch shaft and to ensure uniformity of temperature over the length of the journal. When the temperature of the journal exceeds 250° C. heat conduction along the main shaft is excessive and liable to damage the near roller supporting bearing, not shown in the figure, nevertheless the temperature of the journal has been raised to over 300° C. for a short time without apparent ill-effect. A thermocouple set at the bottom of a small hole drilled into the top side of the bronze bush is used to indicate the approximate temperature of the oil film. The 2-inch diameter nickel chrome steel journal was lapped and polished after being smoothly lathe finished. The bronze bearing bushes were renewed as required but were always of the same quality, $2\frac{1}{4}$ inches long and the bore 0.0075 inch greater than the diameter of the journal. The load bearing area is small for a new bush but after "running in," extends over an arc of 80° to 100° . The use of a bronze bush was restricted to a limited period following the attainment of the normal arc of wear. The diameters of the journal and bush were measured and the arc of wear inspected before and after every trial. When the clearance had increased by 0.012 inch or the arc of wear extended beyond 120° , the bush was rejected.

The experiments were concerned mainly with the performance or lubricating value of oil in extreme conditions of use, that is, when because of a combination of heavy load and high temperature the film between the particular lubricated surfaces becomes extremely thin with seizure imminent. All of the experiments were made with a surface rubbing speed of 11.3 feet per second and a loading of 1000 lbs. per square inch of projected journal area, corresponding to a unit loading of 2000 lbs. approximately, taken on the normal arc of wear. The performance or useful lubricating value of a particular oil, in the circumstances, load being constant, is taken to be indicated by the coefficient of friction observed at the temperature of minimum friction, and the somewhat higher temperature at which, owing to a further decrease of film thickness, seizure actually occurs.

The experiments were begun with the bronze bushes lathe bored and finished with a broad tool fed through by the finest feed available. The finish obtained, described hereafter as an "A" surface, was considered to be such that complete fluid lubrication would prevail in the conditions of the experiments. The trial of a particular oil was continued as long as marked changes of μ min and S.T. were observed, and required the use of the testing machine for daily runs of about $7\frac{1}{2}$ hours, over a period of 1 to 2 weeks. A complete set of friction observations at temperatures over the range 40° to S.T. was taken daily.

Lubrication trials were made of many blends and single varieties of mineral oils and occupied a period of nearly 4 years. The lubricating value of any mineral oil in terms of μ min. and S.T. was found to depend in the first instance on the state of the lubricated surfaces and secondly on the time of use in the oxidising conditions of the experiments. The combined effect of the two factors is shown by fig 2 for oil M B, a proprietary blend of mineral oils in general use. The second "A" surface was obtained by dry polishing with

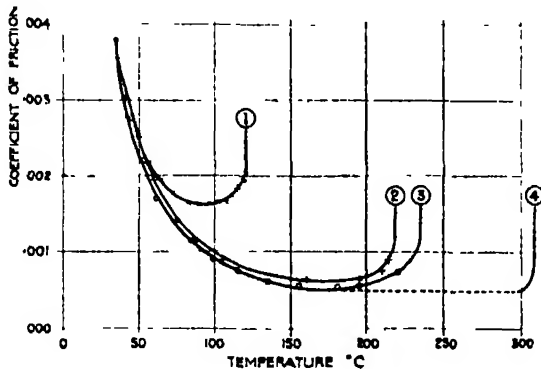


FIG. 2.—Surface state and optimum performances. Oil M.B (1) "A" surface bush (2) "A" surface bush polished, bush 32 (3) "B" surface, bush 36. (4) Bush 32 after use of doped castor.

fine emery cloth; the "B" surface by similarly polishing a more carefully lathe finished surface; the fourth surface by running in an "A" surface for a long period with castor oil containing lead tetra ethyl in the proportion of 7 c.c. per gallon. The initial performance of oil M.B. run with an "A" surface bush and not shown on the figure was represented by a μ min. of 0.002 and a S.T. of 90° C. Thus, referring to the figure it will be seen that the lubricating value of the one oil may vary from the minimum stated to an optimum represented by 0.00045 for μ min and 309° for S.T. The optimum performance was

of a remarkable character. The trial extended over a period of more than a month, representing about 200 hours' running time, the original 2-gallon sample being used throughout. The seizing temperature after 46 hours' running became too high to be observed with safety to the machine and an observation at 54 hours showing $307\frac{1}{2}^{\circ}$ for the S.T. was taken at some risk. The trial was continued, therefore, without attempting to attain seizure but at high running temperatures and at 61 hours, μ observed at the highest practicable temperature of observation had fallen to the record low value of 0.00045. It was expected that in the severe conditions, S.T. would fall soon to an observable value, but a further running time of 100 hours elapsed before this occurred. The relatively low value of 137° then observed seemed to indicate a somewhat accidental condition; the next set of observations showing a greatly improved performance. The trial was discontinued after 197 hours' running although over the 20 hours preceding, the S.T. was rising more rapidly than during any equal period of the early part of the trial when the oil was comparatively fresh. During the 100-hour period of the trial when seizing temperatures were above the safe limit of the testing machine, the running temperature was maintained over the range 175° to 190° and raised daily to the range 250° to 260° for short periods to invite seizure. A temperature of 260° corresponds to 500° F. and the flash point of M.B. oil is 430° F., so for many days the oil, while in a state of extreme oxidation activity, lubricated the journal bearing without seizure and with exceptionally low friction. The stream of smoke and steam rising from the circulating oil, which polluted the air of the laboratory and made necessary the fitting of extra ventilation, is shown by the photograph, fig. 3. Plate 13, taken while the running temperature was 250° .

When the lubricated surfaces were carefully finished and run in, preferably with doped castor oil, the results described above could be repeated with certainty. A maximum S.T. of 309° C. for example, was observed when using a second sample of oil M.B. drawn from bulk stock obtained after an interval of some months, and similar results were obtained for another and known blend. The constituents of the blend, tested singly, improved in lubricating value when used in oxidising conditions, but not to the same extent as the mixture.

Part III.—Interpretation of Experimental Results. Oxidation or Boundary Layer Surface Lubrication.

(1) *Introduction.*—Lubricating value expressed in terms of μ min. and S.T. and determined in oxidising conditions always improved with the progress

of an experiment, especially when trials were begun with surfaces already run in, or finely finished mechanically, and oxidation activity was promoted by raising the temperature of the air blown into the circulating oil. The improvement observed follows, therefore, from some change in the oil due to oxidation. The increase of viscosity known to accompany oxidation leads necessarily to an increase of friction in the fluid part of the oil film, therefore the observed *decrease of friction* arises from a change of boundary conditions effected by oxidation and is greater than the increase of fluid friction due to viscosity increase. The special lubricating value accompanying oxidation is described as oxidation lubrication for convenience of discussion.

(2) *Boundary Friction, Uniformity of Film Thickness and Friction Measurement.*—Boundary friction has long been recognised as a distinct type and as measured by Hardy on the adsorbed layer is determined by the chemical properties of the lubricant and the nature of the boundary surfaces. It will be described hereafter as adsorbed layer friction. The coefficient (static) using mineral oil on a steel surface is of the order of 0.15. It will be understood, therefore, that seizure would occur due to the rate of heat generation if this type of friction prevailed over any considerable part of the lubricated surfaces of a heavily loaded journal bearing running at high speed. Generally, however, lubrication performance in the circumstances and with *fresh mineral oil*, not in a state of oxidation, expressed in terms of μ min. and S.T., depends mainly on fluid friction. The persistence of this type, with increasing temperature, but in the absence of oxidation, load remaining constant, depends on how nearly uniformity of thickness is maintained as the film of oil becomes extremely thin. When surfaces are of the sort frequently used for trials the lubricating film is not of uniform thickness and the load tends to be carried on "high spots." The friction taken over the whole surface, being that measured, is affected by fluid friction varying with irregularity of film thickness, and adsorbed layer friction varying with the changing extent of the high spot area. Thus using *fresh M.B. oil* to lubricate the journal bearing of Part II at constant speed and load, the performance with a ground and polished journal and an "A" finished bronze bush was represented by an S.T. of 90° to 100° and a μ min. as high as 0.0020. This means that adsorbed layer friction was obtained over part of the rubbing surfaces while the average thickness of the oil film was relatively great, because by progressive improvement of the finish of the bronze bush surface to obtain more nearly uniform film thickness, but retaining the same material and fresh oil of the same variety, μ min. was reduced to 0.0010, and S.T. raised to 158°. Fluid lubrication then failed

again but might have persisted to higher temperatures and correspondingly thinner films, with oil of the viscosity of M.B. if the surfaces could have been made more nearly perfect.

(3) *Oxidation Lubrication, Oil M.B.*—The extent of the further improvement in the lubricating value of oil M.B. obtainable by oxidation is shown by the temperature-friction graphs of fig. 4, for $8\frac{1}{2}$, 23, 32, 54 and 61 hours of use in oxidising conditions. The graph for $8\frac{1}{2}$ hours represents approximately the performance of the oil at the beginning of activation by oxidation, that is, when viscosity remains the principal factor controlling friction and preventing seizure by maintaining separation of the lubricated surfaces. S.T. is then 158° and μ min, 0.0010. Viscosity changed little during the time covered by the graphs of fig. 4, as shown by the observed correspondingly small change

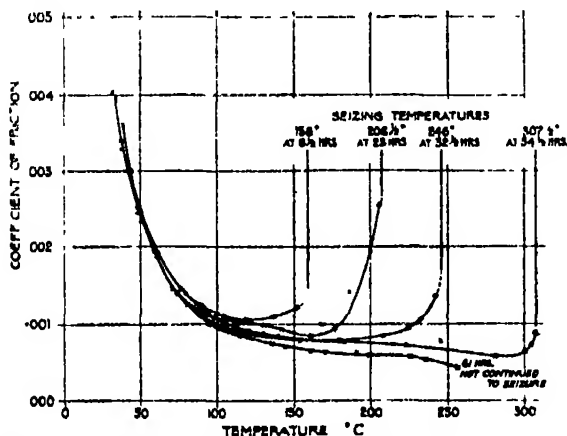


FIG. 4.—Rise of seizing temperature and decrease of friction with time of use. Oil M.B. Load on journal bearing 1000 lbs. per square inch of projected area. Air at 160°C . blown into circulated 2-gallon test sample of oil.

of μ 40° , and the subsequent rise of S.T. from 158° to 307° and the fall of μ min. from 0.0010 to 0.00045 is due to oxidation activity. The improvement of performance during the period cannot be due to an improvement of the surfaces during use. If this were the explanation, the improved performance would be maintained on replacing the partially oxidised oil by a fresh sample, but whenever this change was made the seizing temperature diminished, friction increased and the process of improvement began anew. Moreover, the journal bearing was "run in" for a long period on doped castor oil prior to the M.B. oil trial.

Reference again to fig. 4 will show that a decrease of friction with the progress of oxidation can be traced well into the lower range of temperature



FIG. 3. Smoke and steam (oxidation products) rising from journal bearing, running with lubricating oil film at 250°C [482°F].

corresponding to increasing film thickness. The separation of the temperature-friction curves at 100°, for example, can be measured easily and μ 100° diminished from 0.0013 to 0.00095 during the trial period 8½ to 61 hours while viscosity was rising slowly with the progress of oxidation. The curves cross in the region of 50° and at lower temperatures friction rises slowly but irregularly as viscosity increases, as shown for example by the change of μ 40°. The inference is that, in the conditions of the M.B. oil trial, the increase of friction at 50° due to the increasing viscosity, and possibly in part to adsorbed layer friction becoming sensible, is equal to the decrease of friction due to oxidation activity. It follows that oxidation lubrication persists to still lower temperatures and becomes a factor tending to reduce fluid friction in relatively thick and viscous films when the nature of the oil and the running conditions permit the existence of the effect.

The experimental evidence when considered in the light of Hardy's work supports the view that oxidation lubrication is determined by the chemical activity associated with the early stages of oxidation. If oxidation lubrication can be taken to be dependent on the formation of active (polar) molecules during the early stages of oxidation, the magnitude of the effect must depend on the previous history of the oil as well as on the nature of the constituents. Thus oxidation activity can be induced readily in a fresh oil containing unsaturated compounds and in suitable conditions the process will continue by autoxidation, the oil improving in oxidation lubrication value although not used. An improvement of the lubricating value of a blended mineral oil, on standing, was observed during the trials of Part II, but not made the subject of special experiments, and Kingsbury* observed "the change of body (oiliness) of a given fixed oil on exposure to the air for some time." Hardy and Nottage† have shown that the partial removal of polar molecules by percolation of an oil through a column of clean glass beads or silica chips generally decreases its lubricating value at room temperatures. In certain cases when the residual oil was allowed to stand for 10 to 15 days at room temperatures, it recovered some of its lubricating value if in contact with air but not if in contact with nitrogen. The inference is that the oil contains a friction reducing component yielded by the oxidation of some antecedent with which it is in labile equilibrium at room temperatures. Two percolations of the oil through glass beads completely removed the parent substance and henceforward recovery was impossible. The effect is analogous to the well-known tendency,

* 'J. Amer. Soc. Mech. Eng.,' p. 143 (1903).

† Dept. Sci. & Ind. Res., "Lubrication Research," Tech. Paper No. 1, pp. 9 and 19.

now attributed generally to peroxidation, of the lighter oils used for fuel to form gum on standing when the constituents are in part unsaturated compounds. When on the other hand, an oil has been used in severe conditions for a period so long that the more easily affected constituents have passed through the early stages of oxidation, the lubrication value attained would be expected to diminish on withdrawal of oxidation stimulation. The effect was observed during the trials of Part II, and on standing, M.B. oil failed to retain the exceptional oxidation lubrication value attained in a long trial. A sample used for confirmatory trials, for example, attained a lubricating value represented by a μ min. of 0.0005 and a S.T. of 309°, after 40 hours' running in the oxidation conditions of the experiment, but after the sample had remained out of use for 2 months the lubricating value was represented by a μ min. of 0.0008 and an S.T. 235°. The process of improvement then began anew on resuming the trial, as described for fresh oil, but proceeded less rapidly.

(4) *The Mechanism of Oxidation Lubrication.*—The curves of fig. 4 and the considerations advanced show that (1) separation of heavily loaded surfaces lubricated by M.B. oil at temperatures in excess of 158° is maintained in some way by oxidation processes; and (2) the coefficient (0.00045) of the minimum friction in conditions of active oxidation lubrication is less than the coefficient of viscous friction observed when using the most nearly perfect journal bearing surfaces yet described (Kingsbury, *loc. cit.*) although greater than the value calculated to be possible for mathematically exact surfaces. The statements being regarded as of experimental fact, lead to a possible explanation of the mechanism of oxidation lubrication based on the action of activated or polar molecules to affect the lubricating properties of a layer of oil in contact with a surface. Activated molecules are formed during the initial stage of the oxidation of mineral oils (hydrocarbons) by the attachment of an oxygen to an oil molecule. Activity persists until atomic separation occurs at a later stage of partial oxidation with the formation of steam, aldehydes and visible oxidation products. Activated molecules formed in the initial stages of oxidation tend to become attached by their active parts to the boundary surfaces, to the adsorbed layer or to the inactive parts of free molecules. Oxidation activity being sufficient, a boundary layer many molecules in thickness, but decreasing in rigidity in the direction of motion, is built up on each of the lubricated metals to a surface of slip on which motion can occur with little friction. Oxidation lubrication is obtained and the separation of the surfaces necessary to prevent seizure. The activated molecules not attaching themselves to the surfaces tend to form aggregates by attachment to others not already activated and

thereby increase viscosity. Thus the coincidence of oxidation lubrication with an increase of viscosity is explained. Friction and liability to seizure tend to become independent of viscosity as the fluid film decreases in thickness, and depend on the thickness and properties of the built up boundary layers. Two boundary layers, tending to corresponding surfaces of slip and tending to retain between themselves a fluid film, form in the lubricant. The thickness and friction reducing property, that is the degree of slip attained for either, although depending mainly on the rate of formation of activated molecules in the body of the lubricant is affected also by the known property of metal surfaces to promote or delay the early stages of oxidation in lubricating oils according to the nature of the metal and the oil and the temperature of the reaction. Copper and iron surfaces promote oxidation activity, but only slightly at temperatures below 175° , whereas tin has a strong inhibitory action even at 150° .* It would be expected, therefore, in similar conditions, that a boundary layer of activated molecules builds up to a greater thickness and degree of slip on a surface of copper or iron than on one of bronze; and for this reason at equal temperatures the coefficient of boundary or of adsorbed layer friction should be less with bearings of copper or iron than with those of bronze.

Further light on the mechanism of the process by which films of molecules activated by oxidation are built up on solid surfaces to a surface of slip, is obtained by reference to Hardy's† theory of the boundary state based on the experimental work on boundary lubrication carried out by himself and his assistants. Working with a plane slider at low pressures, and using pure chemical compounds as lubricants at room temperatures, Hardy and Bircumshaw‡ found that Amonton's Law, viz, that the coefficient of friction is independent of the pressure, holds good only for the adsorbed layer. Beyond this strongly attached layer there was found to be a layer several molecules in depth and of decreasing rigidity in which the resistance to tangential stress although greater than that obtaining in the interior of the fluid was less than

* Some preliminary experiments on the action of metal surfaces to delay or promote the formation of active oxidation compounds are described in "Dopes and Detonation," 'Aero Res. Ctee., Rep & Mem.' No. 1062, p. 18 (1926), 'Engineering,' February 4, *et seq.* (1927). The experiments were made with hexane-air mixtures and at the relatively high temperatures immediately preceding complete combustion. More recent experiments made in the Air Ministry Laboratory by Dr. Mardles indicate that of the common metals tin is unique in effecting the prevention of activated molecules in mineral lubricating oil at low temperatures. Iron, copper, aluminium and nickel appear to accelerate the effect.

† Hardy, 'Phil. Trans.,' A, vol. 230, p. 1 (1932).

‡ Hardy and Bircumshaw, 'Proc. Roy. Soc.,' A, vol. 108, p. 2 (1925).

that on the adsorbed layer. Hardy and Nottage* found that the tensile strength of joints formed by pure chemical compounds enclosed between two solid surfaces decreased as the thickness increased and was dependent upon the nature of both the chemical compounds and the enclosing surfaces, being always greater for steel than for copper. From these experiments Hardy concludes that while the direct influence of the attraction field of a solid embraces only the adsorbed layer in contact with it, the orientation and strain so produced in the molecules forming this layer induce orientation and strain in the molecules lying beyond them. The molecules are most firmly held and the orientation is most complete at the interface; it diminishes along the normal until ultimately it is destroyed by heat movements. The efficiency of a given lubricant increases with the degree of orientation. When the layer of lubricant is enclosed between the two solid surfaces, chains of highly polarised molecules are formed stretching through the liquid from one surface to the other. Each chain has little strength in shear, great strength in tension and, since the influence of each field diminishes as the distance from the solid face increases, the strength of the joint both in shear and in tension decreases as the chain lengthens.

Conclusion.—The experiments described show that boundary conditions in journal bearing lubrication are not “hypothetical” as generally supposed. Effective lubrication with extremely low friction, depending entirely on such conditions can prevail at temperatures greatly in excess of those possible when lubrication depends on a fluid film of oil maintained by the relative motion of the surfaces. When mineral oils are used in the circumstances mentioned the boundary conditions required for effective lubrication are induced by oxidation processes.

Summary.

The experiments were made in conditions promoting oxidation of the lubricating oil and at constant speed and load. Friction, in the circumstances, falls as the temperature is raised and generally passes through a minimum value (μ min.) at a temperature somewhat less than that of seizure (S.T.); lubricating value or performance is represented by the observed values of μ min. and S.T., which for a typical blended mineral oil were 0.0010 and 158° C. respectively at the beginning of oxidation. Viscosity was observed to increase with oxidation but the consequent increase of fluid friction was apparent at temperatures below 50° only, that is when the fluid film was relatively thick.

† Hardy and Nottage, ‘Proc. Roy. Soc.,’ A, vol. 118, p. 209 (1928).

Friction at higher temperatures decreased with the progress of oxidation and S.T. rose. Thus after about 60 hours of oxidation, μ min. diminished to 0.00045 and S.T. exceeded 300° C. The oil in a state of partial combustion remained an effective lubricant, μ being less than ever recorded for fluid friction, even with air as the lubricant. A safe region of high temperature lubrication was attained and experiments with various oils show that the extent of this region and the life of the oil depend on oxidation characteristics; friction is due neither to viscosity nor to the action of the adsorbed layer. It is suggested that the active or polar molecules formed during the early stage of oxidation build up to an appreciable thickness on the adsorbed layer and the friction observed is that on the surface of the built up layer. The surface diminishes in rigidity in the direction of motion as the thickness of the boundary layer increases and friction approaches zero as a surface of complete slip tends to be reached.

The Atomic Scattering Factor for X-Rays in the Region of Anomalous Dispersion.

By D. COSTER and K. S. KNOL, Groningen University.

(Communicated by W. L. Bragg, F.R.S. - Received October 1, 1932.)

The atomic scattering factor (f -factor) for X-rays is the ratio of the amplitude of the X-rays scattered by a given atom and that scattered according to the classical theory by one single free electron. It is given as a function of $\sin \vartheta/\lambda$, λ being the wave-length of the X-rays, 2ϑ the angle between the primary and the scattered radiation. It is assumed to be independent of the wave-length so long as $\sin \vartheta/\lambda$ remains constant.

Recently, however, it has been shown both theoretically and experimentally that the last assumption is no longer valid, when the scattered frequency is in the neighbourhood of one of the characteristic frequencies of the scattering element. The first to show the influence of the anomalous dispersion on the f -factor were Mark and Szilard,* who reflected strontium and bromine radiations by a rubidium bromide crystal. Theoretically the problem was dealt with by Coster, Knol and Prins† in their investigation of the influence of the

* 'Z. Physik,' vol. 33, p. 688 (1925).

† 'Z. Physik,' vol. 63, p. 345 (1930). See especially pp. 364-369.

polarity of zincblende on the intensity of X-ray reflection and later on once more by Glocker and Schäfer.*

Quite recently a beautiful experimental investigation of the atomic scattering factor of iron for various X-ray wave-lengths has been made by Bradley and Hope.† They used a method which had also been followed with analogous results by Wyckoff and his collaborators.‡ Powder photographs of FeAl were taken. The symmetry of FeAl is such (body-centred cubic) that the structure factors F are $F = f_{Fe} + f_{Al}$ or $F = f_{Fe} - f_{Al}$. This affords a method of comparing the f -factor for iron in the anomalous region with the f -factor for aluminium in the region, where the last behaves quite normally

It seems to us, however, that the last method needs a correction which might be of some importance on the short wave-length side in the neighbourhood of an absorption edge of the scattering element. As from recent experiments there seems to be some discrepancy between theory and experiment just in this region,§ we should like to call attention to this point.

Mathematically speaking we may say that the atomic factor is in general not a real quantity as was assumed by Wyckoff but a complex quantity of which not only the modulus but also the argument is a function of the wave-length and the angle ϑ .

A more detailed analysis is based on the following principles. We consider first the scattered radiation *for scattering angle zero*. By the action of the field of the primary ray an electric polarisation is induced in the atom. When we neglect the absorption, this polarisation is in phase with the electric vector for frequencies which are smaller than the characteristic frequency of the atom, whereas it has a phase difference of 180° , when the incident frequency is larger. To obtain the resultant scattered field we have to combine the fields due to all the atoms in a layer perpendicular to the beam. As we learn in elementary optics, this causes an additional phase difference of 90° , so that on the whole the phase difference between the direct beam and the scattered radiation is 90° (when the radiation has a smaller frequency than the characteristic frequency of the atom) or 270° (when the frequency of the radiation is larger). The scattered field thus far considered has no influence on the

* 'Z. Physik,' vol. 73, p. 289 (1932).

† 'Proc. Roy. Soc.,' A, vol. 136, p. 272 (1932).

‡ A. C. Armstrong, 'Phys. Rev.,' vol. 34, p. 931 (1929); Wyckoff, *ibid.*, vol. 35, p. 583 (1930); Morton, *ibid.*, vol. 38, p. 41 (1931).

§ R. Glocker and K. Schäfer, 'Z. Physik,' vol. 73, p. 289 (1932); D. Coster and K. S. Knol, 'Z. Physik,' vol. 75, p. 340 (1932).

absorption, it is only responsible for the dispersion. That part of the scattered radiation which is responsible for the absorption must have a phase opposite to that of the direct beam; it corresponds to a polarisation which has a phase difference of 90° with the incident ray.

In mathematical symbols we may formulate the same statements in the following way:

According to classical electrodynamics

$$n^2 = D/E = 1 + 4\pi P/E. \quad (1)$$

Here n is the complex refractive index, D the dielectric displacement, E the electric force, P the dielectric polarisation. In the X-ray region

$$n = 1 - \alpha - i\beta, \quad (2)$$

with α and β as quantities small relative to unity. $1 - \alpha$ is the (real) refractive index, $4\pi\beta/\lambda$ is the absorption coefficient.

From (1) and (2) results

$$4\pi P = -2(\alpha + i\beta)E. \quad (3)$$

The phase difference between the incident and scattered radiation is determined in the above way by the phase of the polarisation P . The quantities α and β may be taken from measurement; α , e.g., from a measurement of the maximum angle of total reflection which is $\sqrt{2\alpha}$; β from measurements of the absorption coefficient. The value of α obtained in that way is not very accurate.

We may also calculate α and β from a theory of the dispersion and absorption of X-rays. The method employed* is to replace the atom by classical oscillators, K-, L-, etc., oscillators. The K-oscillators are, for example, continuously distributed over the whole region of the K-absorption in such a way that the λ^3 -law of absorption is valid. The quantities α and β are composed of contributions of the K-, L-, etc., oscillators.

$$\begin{aligned} \alpha &= \alpha_K + \alpha_L + \dots \\ \beta &= \beta_K + \beta_L + \dots \end{aligned}$$

From simple semi-classical reasoning we obtain, apart from corrections which are small except in the immediate neighbourhood of the absorption edge†:

* Kramers, 'Nature,' vol. 113, p. 673 (1924); Krong, 'J. Opt. Soc. Amer.,' vol. 12, p. 547 (1926); Kallmann and Mark, 'Naturwiss.,' vol. 14, p. 648 (1926) and 'Ann. Physik,' vol. 82, p. 585 (1927); Bothe, 'Z. Physik,' vol. 40, p. 653 (1927); Prins, 'Z. Physik,' vol. 47, p. 479 (1928).

† See Prins, 'Z. Physik,' vol. 47, p. 479 (1928).

I.—On the long wave-length side of the K-edge—

$$\left. \begin{aligned} \alpha_K &= \frac{2\pi e^2}{m} \frac{N_K}{\omega_K^2} \frac{1}{x^2} \left[1 + \frac{\ln(1-x^2)}{x^2} \right] \\ \beta_K &= 0 \end{aligned} \right\} \quad (4)$$

II.—On the short wave-length side of the K-edge—

$$\left. \begin{aligned} \alpha_K &= \frac{2\pi e^2}{m} \frac{N_K}{\omega_K^2} \frac{1}{x^2} \left[1 + \frac{\ln(x^2-1)}{x^2} \right] \\ \beta_K &= \frac{2\pi e^2}{m} \frac{N_K}{\omega_K^2} \frac{\pi}{x^4} \end{aligned} \right\} \quad (5)$$

Here e and m are charge and mass of the electron, N_K is the total strength of all the K-oscillators in the unit of volume, ω_K the frequency of the K-edge, $x = \omega/\omega_K$, where ω is the incident frequency. Similar expressions are valid for the L-, M-, etc., oscillators.

From the value of $\alpha + i\beta$ we get the atomic factor in the direction of the primary beam by dividing through the amount that one free electron per atom would contribute to that quantity, namely,

$$\frac{2\pi e^2}{m} \frac{\rho}{A} \frac{1}{\omega^2},$$

where ρ is the density and A the atomic weight.

As yet we have only regarded the atomic factor for scattering angle zero. To calculate it also *for larger angles* we shall make the more or less arbitrary assumption (which seems to us, however, the most simple thing to do) that every oscillator separately scatters in every direction with the same intensity and the same phase. The oscillators which belong to one single atom are distributed respectively in the K-, L-, etc., region around the nucleus. Composing the waves emitted by the oscillators of the same electronic shell we have therefore to take into account the phase differences which are caused by differences in optical path as is done in the simple discussion of the dependence of the f -factor on the scattering angle.

The experimental results as yet available are all related to the anomalous f -factor in the region of the K-edge. In this case the following simple reasoning may be applied: The scattered frequency of the K-region is so far removed from the L-, M-, etc., edge, that we need not consider the corresponding oscillators of the last shells separately. We divide the atom factor in two parts, one which is due to the K-oscillators, the other to the rest of the atom:

$$f = f_K + f_R.$$

For the oscillators of the K-shell which are distributed at a distance from the nucleus which is small relative to the wave-length, we will assume that the above-mentioned difference in optical path may also be neglected for large values of $\sin \vartheta/\lambda$, so that f_K will be constant over all scattering angles.

It may be calculated from formulæ (4) or (5). We find on the long wave-length side of the K-edge :

$$f_K = n_K \left[1 + \frac{\ln(1-x^2)}{x^2} \right] \quad (6)$$

on the short wave-length side .

$$f_K = n_K \left[1 + \frac{\ln(x^2-1)}{x^2} \right] + i n_K \frac{\pi}{x^2}, \quad (7)$$

where $i = \sqrt{-1}$ and n_K is the total strength of the K-oscillators per atom.

It is a curious fact, indeed, that n_K is not equal to 2, the number of electrons in the K-shell, but that absorption as well as dispersion experiments have shown* that the best value for n_K in the region of Fe is about 1.3. A theoretical explanation of this fact has been given by Kronig and Kramers.†

For radiations with much larger frequencies than the characteristic absorption frequencies of the atom the f -factor may be considered as a nearly real quantity ; in this region its value has been determined both experimentally and theoretically.‡ In this same region $f_K = 1.3$, so that

$$|f_R| = |f| - 1.3. \quad (8)$$

When the scattered frequency is in the neighbourhood of the critical K-frequency, then it is far removed from the critical L-, M-, etc. frequencies. Thus we may assume that the L-, M-, etc., oscillators in this case behave quite normally, so that here also the corresponding atomic factor f_R may be found by subtracting 1.3 from the values as tabulated by James and Brindley for the normal region.

If we write

$$f_K = f'_K + i f''_K,$$

* Houstoun, 'Phil. Mag.', vol. 2, p. 512 (1926) ; Kronig, 'J. Opt. Soc. Amer.', vol. 12, p. 547 (1926) ; Richtmyer, 'Phil. Mag.', vol. 4, p. 1296 (1927) ; Prins, 'Z. Physik', vol. 47, p. 479 (1928).

† Kronig and Kramers, 'Z. Physik', vol. 48, p. 174 (1928).

‡ See Bragg and West, 'Z. Kristallog.', vol. 69, p. 118 (1929) ; James and Brindley, *ibid.*, vol. 78, p. 470 (1931).

where f'_K is the real part of the f_K -factor and if''_K the imaginary part, and neglect the small imaginary part of f_R , we find for modulus and argument of the complex atomic factor

$$\left. \begin{aligned} |f|^2 &= (f'_K + f_R)^2 + f''^2_K \\ \arg f &= \arctan \frac{f''_K}{f'_K + f_R} \end{aligned} \right\} \quad (9)$$

For much larger frequencies than the K-edge of the scattering element the argument of the f -factor is nearly zero and may be neglected. On the short wave-length side in the neighbourhood of the absorption edge, however, it may reach a rather large value. This is especially true for large values of $\sin \vartheta/\lambda$, as f'_K and f''_K are independent of the scattering angle, whereas f_R decreases considerably with increasing $\sin \vartheta/\lambda$.

This last peculiarity is clearly shown by Table I and fig. 1.

Table I.—Theoretical f -factors on the short wave-length side of the K-edge for Fe f_n is the f -factor as calculated by James and Brindley (*loc. cit.*) in the normal region.

$\sin \vartheta/\lambda$	f_n	$\lambda = 0.71$		$\lambda = 1.54$		$\lambda = 1.66$	
		$ f $	$\arg. f.$	$ f $	$\arg. f.$	$ f $	$\arg. f.$
0 0	26 0	26 3	1 30	25 0	7 20	23 5	9 0
0 1	23 1	23 4	1 40	22 1	8 20	20 6	10 15
0 2	19 1	19 4	2 10	18 1	10 10	16 8	12 40
0 3	15 6	15 9	2 30	14 7	12 40	13 4	16 0
0 4	13 4	13 7	2 50	12 5	14 50	11 3	19 0
0 5	11 7	12 0	3 20	10 9	17 10	9 7	22 20
0 6	10.2	10 5	3 50	9 5	19 50	8 4	26 20
0 7	8 9	9 2	4 20	8.3	22 50	7 4	30 40
0 8	7.9	8 2	4 50	7 4	25 50	6 4	35 30
0 9	7 1	7 4	5 20	6 7	28 50	5 7	40 0
1 0	6 4	6 7	5 50	6 1	32 10	5 2	45 0

The argument of the complex f -factor gives the phase difference of the scattered beam relatively to the beam scattered when the absorption might be neglected as is seen from Table I. In the case of the FeAl crystal on the short wave-length side of the Fe K-edge the argument of the f -factor of Fe may have a rather large value, whereas that for Al remains practically zero. The relation $F = f_{Fe} + f_{Al}$ or $F = f_{Fe} - f_{Al}$ remains only true when complex f -factors are considered. It may easily be estimated that in the case of Cu-radiation neglecting the complexity of f_{Fe} , as has been done by Bradley and

Hope, the value of this quantity comes only about 10 per cent. too high according to their calculation; for smaller values of $\sin \vartheta/\lambda$ the error is still less. On the long wave-length side of the K-edge, where Bradley and Hope found their most interesting results, the consideration of the complex f -factor as here proposed makes almost no difference at all to their results

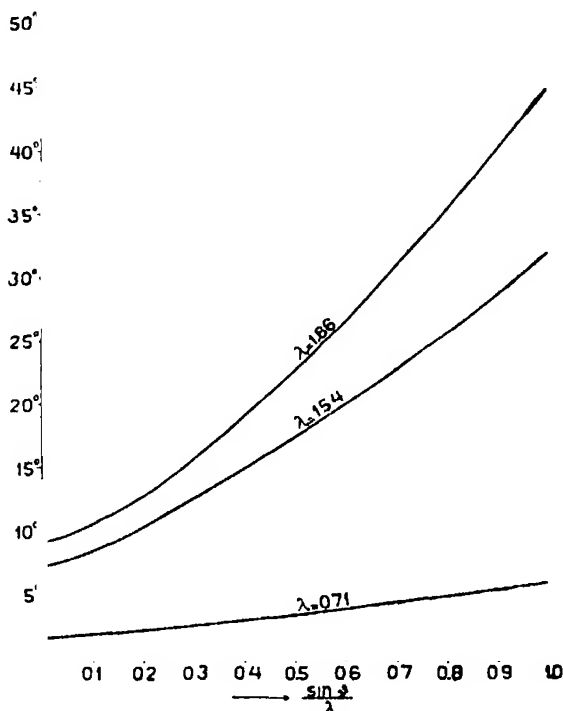


FIG. 1.—Phase difference between the radiation scattered by Fe and that scattered by Al as a function of $\sin \vartheta/\lambda$ for the wave-lengths 1.86 Å. ($\text{Ni K}\alpha$), 1.54 Å ($\text{Cu K}\alpha$) and 0.71 Å ($\text{Mo K}\alpha$).

If, however, in the experiments of Bradley and Hope $\text{Ni K}\alpha$ -radiation had been used, which lies still closer to the critical K-radiation of Fe, then the error involved by not considering the complexity of the f -factors would also have been larger: for $\sin \vartheta/\lambda = 0.5$, *e.g.*, the calculated f_{Fe} -factor in this case comes about 15 per cent. too high.

Summary.

A method is described of calculating theoretically the atomic factor for X-rays in the region of anomalous dispersion, especially in the neighbourhood of the K-edge of the scattering element. It is shown that not only the absolute

value of the atomic factor, but also its argument, i.e., the phase difference between the primary and the scattered beam, which is a function of λ and of $\sin \theta$, has to be taken into account. This phase difference assumes rather large values on the short wave-length side in the neighbourhood of the K-edge of the scattering element.

The Application of Quantum Mechanics to Chemical Kinetics.

By RONALD P. BELL.

(Communicated by C N Hinshelwood, F R S — Received October 5, 1932)

Much work has recently been done on the application of quantum mechanics to chemical reactions. In the majority of cases, however, the actual reaction processes have been considered as taking place according to the laws of classical mechanics, quantum-mechanical theory being only employed in calculating the interatomic forces. It has, however, been suggested by various authors* that the actual transition processes involved must be treated as non-classical. Some of these authors have claimed that this method of treatment is essential for the true explanation of chemical processes, just as in the case of radioactive disintegration, where it is well established that classical considerations are unable to explain the phenomena observed. It appears, however, to be the general consensus of opinion that for chemical processes the results obtained by a strict quantum-mechanical treatment would differ negligibly from the results of classical mechanics.† This opinion appears to be based only on approximate methods of treatment, and no actual figures have been published. The present paper is a contribution to a more exact knowledge of the problem.

According to modern views on reaction mechanism, the reacting system passes through a maximum of potential energy in passing adiabatically from the initial to the final state‡. The energy difference between the initial state

* Bourgin, 'Proc. Nat. Acad. Sci. Wash.,' vol. 15, p. 357 (1929); Langer, 'Phys. Rev.,' vol. 33, p. 290; vol. 34, p. 92 (1929); Roginsky and Rosenkewitsch, 'Z. phys. Chem.,' B, vol. 10, p. 47 (1930); vol. 15, p. 103 (1932). Similar ideas have been put forward for heterogeneous reactions by Born and Weisskopf, 'Z. phys. Chem.,' B, vol. 12, p. 206 (1931).

† See e.g., Hinshelwood, "Discussion on the Critical Increment of Homogeneous Reactions," p. 13, Chemical Society (1931); Kassel, 'Chem. Rev.,' vol. 10, p. 22 (1932).

‡ London, 'Z. Elektrochem.,' vol. 35, p. 552 (1929); Sommerfeld, 'Festschrift,' p. 194 (Hirzel, 1929).

and the maximum is the heat of activation for the reaction (E). As a simple type of chemical reaction we may take the system shown in fig. 1. A particle of mass m passes from a to b through a region of varying potential energy $V(x)$. Between a and b the potential energy reaches a maximum value E . The energy difference between a and b is Q , the heat of reaction.

If we consider a number of particles having varying energy W , they will according to classical mechanics fall into two distinct classes. If $W > E$, the particle will always pass over the potential energy barrier to b , while if $W < E$, it will invariably fail to do so. If we now assume that the statistical distribution of the particles with respect to their energies is given by

$$\frac{dN}{N_0} = \frac{1}{kT} \cdot e^{-W/kT} \quad (1)$$

the number of particles passing from a to b (which is identical with the number having $W > E$) is given by

$$\frac{N}{N_0} = e^{-E/kT}. \quad (2)$$

This is the well-known equation expressing the variation of reaction velocity with temperature in terms of the energy of activation.

According to quantum mechanics, however, the probability that the particle finds its way from a to b varies continuously with its energy, being finite for $W < E$, and only approaching unity for $W \rightarrow \infty$. The transit probabilities can easily be calculated for any barrier for which the Schrodinger equation

$$\frac{\partial^2 \psi}{\partial x^2} + \frac{8\pi^2 m}{h^2} \{W - V(x)\} \psi = 0 \quad (3)$$

is soluble (The barrier is treated as one-dimensional. This is permissible, since there is in general a definite direction of approach of two reacting molecules for which the activation energy is a minimum.) An exact solution of equation (3) has only been obtained in a limited number of cases, and various approximations have been used to obtain expressions for the permeability of potential barriers (i.e., the probability of transit). An expression frequently used is

$$G = \exp. - \frac{4\pi\sqrt{m}}{h} \int_{x_1}^{x_2} \sqrt{V(x) - W} \cdot dx, \quad (4)$$

where G is the permeability and x_1 and x_2 are the co-ordinates of the two

points for which $V(x) = W$. This expression is based upon Jeffreys's* approximate solution of equation (3), which fails for small values of $|W - V(x)|$. Thus while it is legitimate to employ equation (4) in some cases (*e.g.*, radioactive disintegration), it cannot be used for values of W in the neighbourhood of E , which is just the region which particularly interests us in the present case. Another simplification which has been introduced is to replace the actual continuous potential energy curve by a rectangular or wedge-shaped barrier. This again may be expected to give misleading results when W is not very different from E .

We are not at present able to express the actual potential barriers in chemical reactions by analytical expressions, and such expressions would in any case be very complicated. There exists, however, a class of curves of the general form shown in fig. 1 for which the exact solution of the Schrodinger equation has been obtained. Their general equation is

$$V(x) = \frac{Ae^{2\pi x/l}}{1 + e^{2\pi x/l}} + \frac{Be^{2\pi x/l}}{(1 + e^{2\pi x/l})^2} \quad (5)$$

The co-ordinates of the maximum in $V(x)$ are

$$x_m = \frac{l}{2\pi} \log \frac{B + A}{B - A}$$

$$V_m = E = \frac{(A + B)^2}{4B}$$

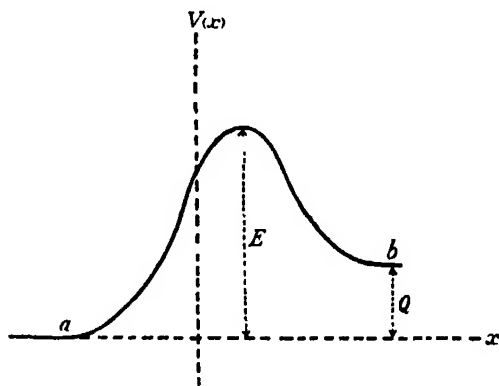


FIG. 1.

and the curve becomes horizontal at $x = -l$, $V(x) = 0$ and $x = +l$, $V(x) = A$. Eckart† has obtained the solution of the Schrodinger equation (3) when $V(x)$

* 'Proc. Math. Soc.', vol. 23, p. 428 (1924).

† 'Phys. Rev.', vol. 35, p. 1303 (1930).

is given by equation (5), and has calculated the permeability. As long as $B > \hbar^2/8ml^2$ (which is always true in the present case),

$$G = \frac{\cosh \{2\pi(\alpha + \beta)\} - \cosh \{2\pi(\alpha - \beta)\}}{\cosh \{2\pi(\alpha + \beta)\} + \cosh \{2\pi\delta\}} \quad (6)$$

where

$$\alpha = \frac{l}{\hbar} \sqrt{2mW}, \quad \beta = \frac{l}{\hbar} \sqrt{2m(W - A)}$$

$$C = \frac{\hbar^2}{8ml^2}, \quad \delta = \frac{1}{2} \left(\frac{B - C}{C} \right)^{\frac{1}{2}}.$$

It is therefore possible to calculate the transition probabilities for any given values of the heat of activation (E), the heat of reaction (A) and the distance between the initial and final positions of the particle ($2l$). These magnitudes are not in general known accurately, and we shall treat here an arbitrary case, which will, however, be typical of the magnitudes to be expected in practice. We shall for simplicity take the case in which the heat of reaction is zero and the potential barrier symmetrical (as for example in the transformation of ortho- to para-hydrogen) Equation (5) then becomes

$$V(x) = \frac{Be^{2\pi x/l}}{(1 + e^{2\pi x/l})^2}, \quad (7)$$

having a maximum value

$$V_m = E = \frac{B}{4},$$

and the permeability is (from equation (6)),

$$G = \frac{\cosh \{4\pi\alpha\} - 1}{\cosh \{4\pi\alpha\} + \cosh \{2\pi\delta\}} \quad (8)$$

The numerical values we have employed are

$$E = \frac{B}{4} = 1.0 \times 10^{-12} \text{ ergs.}$$

(corresponding to about 13,000 cal. per gram molecule).

$$l = 1 \text{ A. (width of barrier} = 2 \text{ A.)}$$

$$m = 1.66 \times 10^{-24} \text{ gm. (mass of H atom or proton).}^*$$

* The value of m for a particular reaction is the mass of the particle the transition of which initiates the chemical change. It will be shown later that a quantum-mechanical treatment of the transition is necessary only when this particle is a hydrogen atom or proton.

Since we are employing a symmetrical barrier, the width of the barrier is the distance between the initial position of the particle and the point on the other side of the barrier at which its potential energy is equal to that of the initial state. 2 A. is a reasonable value for this distance.

The following table contains some values of G calculated from equation (8) using these values.

$W \times 10^{12}$	1.0	2.0	3.0	5.0	7.0
G	3.7×10^{-11}	3.5×10^{-9}	1.2×10^{-7}	2.6×10^{-5}	2.8×10^{-3}

$W \times 10^{12}$	8.0	9.0	9.5	10.0	11.0	12.0	13.0
G	2.1×10^{-3}	0.12	0.27	0.45	0.85	0.96	0.99

These values are plotted in fig. 2, and it is seen that the departure from classical behaviour is considerable. If we now assume that the statistical

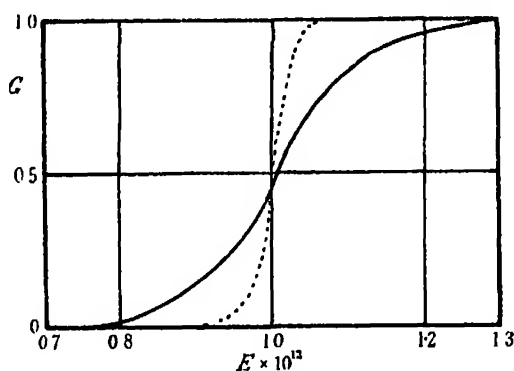


FIG. 2.

energy distribution is given by equation (1), the total number of particles passing the barrier is given by

$$\frac{N}{N_0} = \frac{1}{kT} \int_0^{\infty} G e^{-W/kT} dW. \quad (9)$$

This expression would be difficult to integrate analytically, but the integral can easily be evaluated graphically, since it converges to zero for $W = 0$ and $W > E$. This has been done for a number of different temperatures, and the curves for the lowest and highest temperatures are shown in fig. 3. The form and position of these curves is of interest: at 273° practically all the particles passing the barrier have energies lower than 1×10^{-12} ergs., the maximum of the curve lying at about 4×10^{-13} . At 673° the curve is displaced to the right, and the maximum occurs very little below 1×10^{-12} . The curves for the intermediate temperatures show a gradual transition between these two types.

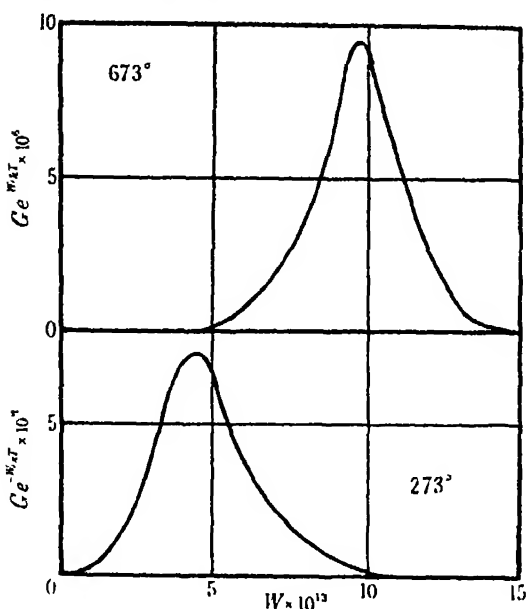


FIG. 3.

The values obtained for N/N_0 (see equation (9)) are given in the following table. The values obtained by treating the system classically ($e^{-E/AT}$, cf. equation (2)) are also given for comparison.

T.	N/N_0	$e^{-E/AT}$
273	7.0×10^{-10}	2.5×10^{-12}
323	1.2×10^{-9}	1.5×10^{-10}
373	3.1×10^{-8}	3.0×10^{-8}
473	7.3×10^{-7}	2.0×10^{-7}
573	6.4×10^{-6}	2.9×10^{-6}
673	3.4×10^{-5}	2.0×10^{-5}

In fig. 4 $\log_{10} N/N_0$ has been plotted against $1/T$. the dotted straight line is the same plot for $\log_{10} e^{-E/AT}$.

It is obvious from the table and the figure that considerable error is involved in a classical treatment of this system, especially at low temperatures. The same conclusion will apply to any system involving the passage of a hydrogen atom or a proton across a potential barrier of approximately the same dimensions, irrespective of whether the curve is symmetrical or can be exactly represented by an equation of the type of (5). It must, however, be emphasised

that all atoms heavier than helium behave, practically speaking, classically; expressions (6) and (8) being very sensitive to changes in m . (This may be seen from the dotted line in fig. 2, which represents the values of G for an oxygen atom, other conditions being the same.) The same will apply to barriers considerably wider than 2.0 Å. These restrictions still leave, however, a large number of reactions for which a classical method of treatment is inadequate.

These deviations from classical behaviour will affect our treatment of reaction kinetics in several ways, as follows.

(1) The value of the heat of activation calculated from the temperature coefficient and equation (2) (E') will be smaller than the actual height of the barrier (E) (This is obvious from fig. 4.) E , which we shall term the true

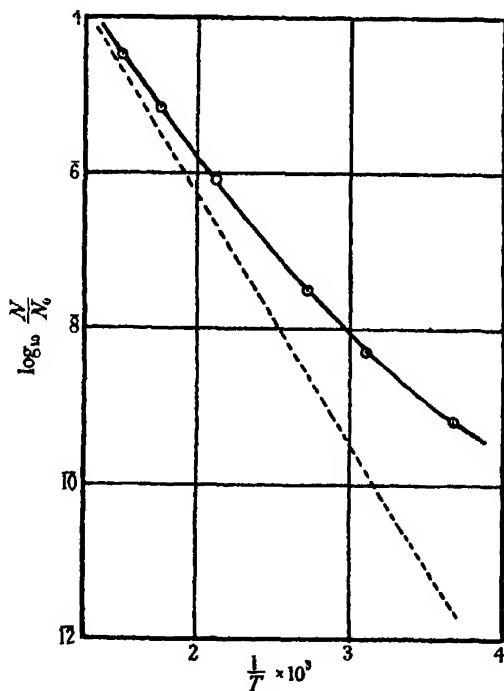


FIG. 4.

heat of activation, cannot be determined directly by experiment, but can be calculated approximately in a few simple cases according to modern theories of interatomic forces. The difference between E and E' is probably responsible for the discrepancy between the value calculated by Eyring and Polanyi* for

* 'Z. phys. Chem.,' B, vol. 12, p. 279 (1931).

the heat of activation in the transformation of ortho- to para-hydrogen (13 kg cal. per molecule), and the value observed by Geib and Harteck* (7.25 ± 0.25 kg. cal.).

(2) If the true heat of activation is known, it will be necessary to use quantum mechanics to calculate the absolute rate of the reaction. Thus the classical calculations of Pelzer and Wigner† on the absolute rate of the ortho-para-hydrogen transformation are probably in error, the agreement with experiment being fortuitous. (The authors themselves mention the neglect of quantum-mechanical effects as a probable source of error, but make no estimate of its magnitude.)

It should be remarked, however, that if the rate of a reaction is calculated from equation (2) using the experimental heat of activation E' , the error in using equation (2) instead of equation (9) is very nearly compensated by the error in using E' in place of E , so that the true rate is obtained. Thus the success of the collision theory of bimolecular reactions is not affected by the above considerations, except that the observed heat of activation need no longer possess any exact physical significance.

(3) It appears from fig. 4 that the plot of $\log N/N_0$ against $1/T$ should not give a straight line, especially at low temperatures, i.e., E' should vary with temperature. Actually, however, the plot over a limited temperature range may appear to be a straight line within the limits of experimental error, even when the divergence between the classical and quantum-mechanical treatments is large. No data at present available show with certainty the effect expected, the majority of cases of variation of E' being due to the occurrence of side reactions.‡

* 'Z. phys. Chem. Bodenstein Festband,' p. 849 (1931).

† 'Z. phys. Chem.,' B, vol. 15, p. 445 (1932).

‡ The accurate data of Bodenstein ('Z. phys. Chem.,' vol. 29, p. 295 (1899)) for the formation and decomposition of hydrogen iodide appear to show a very slight curvature in the expected direction when plotted in this way. (The corresponding variation in E' is about 10 per cent. for a temperature range of 200° .) It may be doubted, however, whether this effect is real. We should not expect to find a larger variation in E' on account of the high temperatures involved (cf. fig. 4.)

The transformation of ortho- to para-hydrogen can be followed at much lower temperatures, and might be expected to prove a favourable example. Unfortunately there is too much uncertainty in the experimental results and their interpretation to allow of a strict test. It may, however, be pointed out that the results are not incompatible with a large variation in E' .

There is a factor of uncertainty in the interpretation of the results of Geib and Harteck (*supra*) on account of the diffusion of the hydrogen atoms in the reaction tube. The authors calculate two sets of values, the first (A) assuming no diffusions,

The law of distribution of energy employed here (equation (1)) refers to any two non-quantised square terms, in particular the kinetic energy of relative motion of two molecules taking part in a bimolecular reaction. If the energy concerned is vibrational or rotational, and thus has discrete values, the problem becomes more complex and requires a knowledge of the exact values of the quantised energies of the initial and final states. As has previously been pointed out by Born and Weisskopf (*loc. cit.*), it is possible that under some conditions the majority of transitions may take place from a quantum state of the initial system having an energy lower than the true heat of activation.

Summary.

The majority of modern treatments of the mechanism of chemical reactions treat the transit involved as obeying the laws of classical mechanics. Previous statements that a quantum-mechanical treatment is unnecessary are based on approximations of doubtful validity.

The present paper gives a strict mathematical treatment of a simple system which is typical of the transits involved in chemical reactions. It is concluded that a quantum-mechanical treatment is necessary for any reaction involving the motion of a hydrogen atom or proton, while heavier atoms may be considered to behave classically.

It is shown that the departure from classical behaviour will in some cases lead to discrepancies between the experimental data and current theories of reaction kinetics. The data at present available do not permit of a strict test of these considerations, though several instances are quoted which appear to support the conclusions of the present paper.

and the second (B) assuming complete mixing, the true values lying somewhere between these two sets. On comparison with the values of Farkas for much higher temperatures* agreement was found between the (A) values and the values of Farkas on the assumption of a constant E^* of about 7 kg. cal. They therefore accept the (A) values as being nearly correct. If on the other hand the (B) values are combined with the values of Farkas, it is necessary to assume an apparent heat of activation varying from ca. 4 to ca. 10 kg. cal. Such a state of affairs when combined with the observation of Eucken and Hiller† that the homogeneous change persists at a measurable rate at very low temperatures, tallies very well with the considerations of the present paper, and the value of 13 kg. cal. obtained by Eyring and Polyani for the true heat of activation (*supra*).

* 'Z. phys. Chem.,' B, vol. 10, p. 419 (1930).

† 'Z. phys. Chem.,' B, vol. 4, p. 142 (1929).

On the Calculation of Stresses in Braced Frameworks.

By R. V. SOUTHWELL, F.R.S.

(Received September 17, 1932.)

Introduction.

1. Bending and twisting actions involve stresses which may range between wide limits, but in a straight bar subjected to tension or compression the stress has practically the same intensity at every point. Accordingly, in civil engineering, economy in material is attained by the use of skeletal or "framed" structures, built of straight members connected at their ends, and designed so that external forces (other than those arising from the weights of the members themselves) are applied only at the joints. Under these conditions, to a close approximation, every member is subjected to simple tension or compression.

"Simple" and "Redundant" Frameworks.

2. In estimating the actions of the constituent members, it is customary to neglect entirely the effects of fixity at the joints, and to substitute for the actual framework a "skeleton diagram" in which every member is replaced by a line of thrust or tension. The problem then presented may be soluble by purely statical methods, or it may involve the elastic properties of the members, according as the number of these (m) is related to the number (j) of the joints. In a "plane frame" (where the external forces, as well as the lines of thrust or tension, are coplanar) the actions will be statically determinate if

$$m = 2j - 3, \quad (1)$$

—as may be seen from the consideration that two equations of equilibrium can be written down for each joint, but that of the resulting $2j$ equations only $(2j - 3)$ are really independent, because three relations between the external forces are imposed by the conditions for equilibrium of the framework as a whole. In a "space frame," similar considerations show that the actions will be statically determinate if

$$m = 3j - 6. \quad (2)$$

A framework for which m and j are related by (1) or (2) is termed a "simple frame"; it has the least number of members which will suffice to ensure rigidity. When the number of members is in excess of this, so that

$$\left. \begin{aligned} m &= 2j - 3 + N \text{ (for a plane framework),} \\ &= 3j - 6 + N \text{ (for a space framework),} \end{aligned} \right\} \quad (3)$$

the framework is said to be "redundant," and N is termed the order of its redundancy. The actions in a redundant framework are not determined solely by statical conditions; in particular, they may have finite values even when no external forces are operative, if the length of any member is not exactly equal to the distance between the joints which it has to connect. In such circumstances the framework is said to be "self-strained."

"Pseudo-redundant" Frameworks.

3. On account of the simplicity of tension as compared with compression members, quadrilateral panels in a framework are often provided with two crossed diagonal members, each capable of sustaining tension but not compression, instead of one diagonal member capable of sustaining either tension or compression. In such instances the relevant formula (3) would indicate an order of redundancy greater than is really appropriate, because in general only one of the two diagonals will be in operation under any particular system of loading. Frameworks braced in this way are accordingly termed "pseudo-redundant," they call for special consideration in stress calculation.

Stress Calculation in Frameworks. Graphical and Analytical Methods.

4. It is not necessary here to give details of the procedure whereby, for a redundant framework, N equations (involving the elastic properties of the constituent members) can be obtained in addition to those afforded by statical considerations. The usual method depends upon Castigliano's celebrated "Theorem of Minimum Strain Energy," and deduces the N equations (in relation to a framework which is not initially self-strained) as conditions for a stationary value of U , the total elastic strain energy which is stored in the members. But essentially all the methods are identical, being based on the principle that load-systems may (by Hooke's Law) be superposed; and it may be added that all require, as a first step, the calculation of stresses in a "simple frame."

5. Problems which are presented in orthodox structural engineering can usually be treated as examples of plane frames. Here, in practice, graphical methods have considerable advantages, and for this reason (probably) stress calculation is taught, and presented in text-books,* almost entirely as a two-dimensional problem. But recent developments, more particularly in aero-

* A. J. S. Pippard's "Strain Energy Methods of Stress Analysis" is a noteworthy exception.

nautics, have introduced types of structure which can only be discussed as examples of "space frames," and for these graphical methods are not suitable. Not having been able to discover any satisfactory treatment of stress analysis in three dimensions, I proposed, some 12 years ago,* a systematic procedure which in application to aeronautics (and more especially to airships) has come into fairly general use. It involves the replacement (for simplicity) of resultant actions by "tension coefficients,"—the tension coefficient of any member being defined as its resultant action P (taken as positive if tensile) divided by its length L .

Outline of the Analytical Method.

6. If the member in question connects two joints A, B whose Cartesian co-ordinates are (x_A, y_A, z_A) , (x_B, y_B, z_B) , the force which it exerts on the joint A has a component, in the direction of x increasing, which is evidently given by

$$P_{AB} \cdot \frac{x_B - x_A}{l_{AB}} = T_{AB} (x_B - x_A) \quad \text{by definition,}$$

whereas the force in this direction which is exerted on the joint B is given by

$$T_{AB} (x_A - x_B).$$

Accordingly the notation is consistent (T_{AB} being a scalar quantity); and if B, C, ... K are the joints connected with A by members, the conditions for equilibrium of A are

$$X_A + T_{AB} (x_B - x_A) + T_{AC} (x_C - x_A) + \dots T_{AK} (x_K - x_A) = 0 \quad (4)$$

and two similar equations in y and z , where X_A, Y_A, Z_A are the components of the external force applied at A.

Equations of this type are readily formulated for every joint of a given framework; the use of Cartesian co-ordinates is convenient, in that quantities such as $(x_B - x_A)$, $(y_B - y_A)$, $(z_B - z_A)$ are easily read off from an ordinary engineering drawing. The tension coefficients (for a simple framework) can be deduced from the equations without great labour, the most that is involved being the solution of three simultaneous linear equations.

7. If u_A, v_A, w_A denote the component displacements of A under load, the fractional extension of AB is given by

$$e_{AB} = \frac{1}{l_{AB}^2} \{ (x_B - x_A)(u_B - u_A) + (y_B - y_A)(v_B - v_A) + (z_B - z_A)(w_B - w_A) \}. \quad (5)$$

* 'Engineering,' February 6, 1920.

Hence, if we define the elastic properties of the member AB by a quantity Ω_{AB} , such that Hooke's Law is expressed by the equation

$$P_{AB}/l_{AB} = T_{AB} = \Omega_{AB} \cdot l_{AB}^2 \cdot e_{AB}, \quad (6)$$

we have as an expression for the tension coefficient of AB in terms of joint displacements

$$T_{AB} = \Omega_{AB} \{ (x_B - x_A)(u_B - u_A) + (y_B - y_A)(v_B - v_A) + (z_B - z_A)(w_B - w_A) \}. \quad (7)$$

The strain energy stored in AB, when its tension coefficient has the value T_{AB} , is then given by

$$\begin{aligned} v_{AB} &= \frac{1}{2} P_{AB} (l_{AB} \cdot e_{AB}), \\ &= \frac{1}{2} T_{AB} \cdot l_{AB}^2 \cdot e_{AB}, \\ &= \frac{1}{2} \frac{T_{AB}^2}{\Omega_{AB}}, \quad \text{by (6)}. \end{aligned} \quad (8)$$

Using the formulæ (7) and (8), it becomes a straightforward matter to calculate the stresses in a redundant framework by purely analytical methods. Having selected N members to be classed as "redundant," we formulate equations of type (4) for the simple framework which is left when these are removed; and we solve these equations both for the specified system of external loads and for unit tension assumed to be exerted by each redundant member in turn. The tension coefficient of every member can now be expressed in terms of T_1, T_2, \dots, T_N , the (unknown) tension coefficients of the redundant members; and then, using (8), we can deduce an expression for the total elastic strain energy stored in the framework. This quantity (U) will be a quadratic function of the same N unknowns; making use of Castigliano's theorem, we equate to zero its partial differential coefficients with respect to T_1, T_2, \dots, T_N , and hence obtain N linear equations from which T_1, T_2, \dots, T_N may be calculated.

General Solutions obtainable by the Analytical Method.

8. Apart from its uses in application to "space frames," the analytical method has the advantage that it permits the discussion of general solutions relating to braced frameworks. In recent years I have published several papers dealing with this aspect*; in them solutions of a restricted kind

* 'Aero. Res. Ctee. Rep. and Mem.,' Nos. 737 (1921), 790, 791, 819 and 821 (1922), 1057 (1926) and 1427 (1931). The last of these papers was written in collaboration with Miss L. Chitty.

(analogous to those which St. Venant obtained for solid cylinders by means of his "semi-indirect" method*) were found for frameworks having redundancies of an order which would make the orthodox treatment quite impracticable. The present paper carries those investigations further, and obtains an exact and unrestricted solution of which their solutions appear as special cases. It relates to a tubular framework, fig. 1, which is divided by bulkheads into any number of similar bays; the bulkheads are taken to be of regular polygonal form, braced by wires which run from a central point to each corner of the polygon.† All longitudinal members are assumed to be identical in length and elastic properties, and similarly all the diagonal members which brace side panels, all the transverse (chord) members, and all

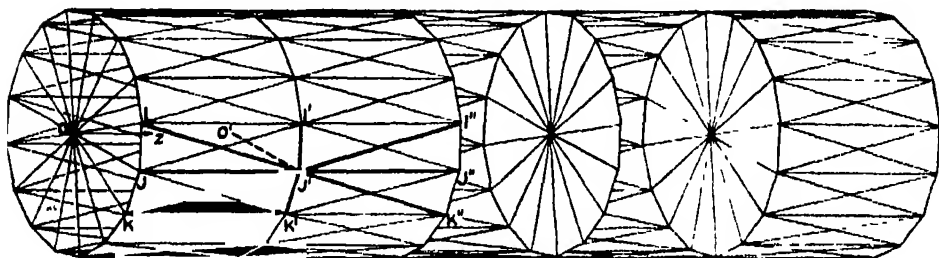


FIG. 1.

the radial members which brace the bulkheads, thus we have four "elasticity parameters" which may be varied severally:—

- Ω_l , a quantity defining the elastic properties of the longitudinals,
- Ω_d , a quantity defining the elastic properties of the diagonal bracing members,
- Ω_t , a quantity defining the elastic properties of the transverse members,
- Ω_r , a quantity defining the elastic properties of the members which compose the radial bulkhead bracing.

* Cf. Love, "Mathematical Theory of Elasticity," p. 19.

† This arrangement is generally representative (apart from taper) of the hulls of rigid airships; also of aeroplane fuselages of "monocoque" design, excepting that in these the diagonal panel bracing is replaced by thin metal sheet.

It is not essential to the analysis that the bulkheads shall in fact be braced with radial members in the manner shown: the results of this paper will hold provided that the behaviour of the polygonal ring, when loaded by radial forces, is such as can be represented by *equivalent* radial bracing.

In fig. 1, for clearness, the bulkheads and side panels of the framework have been drawn as though they were opaque, except at two intermediate bays, where the panels in the front of the framework have been removed.

All members are assumed capable of sustaining either tension or compression, and on this understanding a systematic procedure is developed, whereby exact solutions can be obtained for any specified system of loading (subject only to the conditions of equilibrium). According to (3), the order of redundancy for a tube of this kind having B bays and P sides to the polygonal cross-section is

$$N = P(2B - 1) + 6,$$

and so may be very large. But the difficulty (as distinct from the labour) of a solution by the methods here proposed does not increase with P or B .

9. The concluding section of the paper deals with a theorem having application to the problem of stressing a "pseudo-redundant" framework (§ 3). It is shown that the foregoing solution can still be utilized, when the diagonal bracings in the side panels are incapable of sustaining compression.

I desire to express my indebtedness to Miss L. Chitty for assistance given in the preparation of this paper, and for valuable suggestions, particularly in regard to questions of notation. She is engaged in applying its methods to certain practical problems, and it is hoped that her work will be published shortly. I have also to thank Mr. J. H. Lavery, B.Sc., and the Secretary of the Aeronautical Research Committee, for assistance in the preparation of the diagrams.

I.—THE DETERMINATION OF STRESSES IN A TUBULAR FRAMEWORK.

Formulation of the Conditions of Equilibrium for a Typical Joint.

10. The nature of our problem, and the assumptions made in regard to the tubular framework, have been explained in the introduction to this paper. In the first place we shall formulate the conditions of equilibrium for a typical joint of the framework, and use these to deduce systems of displacement which can be maintained by forces applied at the terminal bulkheads only. Subsequently (§§ 36-42) we shall show that these systems can be combined to form a solution of our problem in its most general case.

Let

l denote the length of a bay (i.e., of a longitudinal member) of the framework,

d denote the length of a diagonal member bracing one of the side panels,

t denote the length of a transverse member forming one side of a polygonal bulkhead,

r denote the length of a radial member in the bulkhead bracing.

Then if J' , fig. 1, is a joint in any intermediate bulkhead, the conditions for its equilibrium in the absence of any externally applied force can be expressed in the notation of "tension coefficients" (§ 5) as follows :—

Equilibrium in the radial direction ($O'J'$) requires that

$$t \sin \frac{\alpha}{2} [T_{J'K''} + T_{J'K'} + T_{J'K} + T_{J'I''} + T_{J'I'} + T_{J'I}] + r \cdot T_{O'J'} = 0; \quad (9)$$

equilibrium in the tangential direction (perpendicular to the plane $O'J'J''$) requires that

$$t \cos \frac{\alpha}{2} [T_{J'K''} + T_{J'K'} + T_{J'K} - T_{J'I''} - T_{J'I'} - T_{J'I}] = 0; \quad (10)$$

equilibrium in the axial direction ($J'J''$) requires that

$$l [T_{J'K''} - T_{J'K} + T_{J'I''} - T_{J'I} + T_{J'I'} - T_{J'I}] = 0. \quad (11)$$

We observe that nine members contribute to the equilibrium of J' , as indicated by thickened lines in the diagram. In the foregoing equations, α denotes the angle subtended at O' by a side of the polygonal bulkhead.

11. We define the displacement of O' , in the plane of its bulkhead,* by two components: a' , outward along the radius through some joint in its bulkhead which is taken as datum; and b' , perpendicular to this radius, in the direction given by positive rotation about the axis (z) of the tube. Then if J' is the j th joint (measured round the bulkhead, in this same direction) from the joint which is taken as datum, it is evident that the displacement of O' in the direction $O'J'$ will be given by

$$u_{O'J'} = a' \cos j\alpha + b' \sin j\alpha, \quad (12)$$

and we have

$$\alpha = \frac{2\pi}{N},$$

where N is the number of sides in the polygon.†

The displacement of any other joint in the bulkhead we define by three components u , v , w , directed respectively along and perpendicular to the

* To the first order of small quantities, an axial displacement of O' is without effect on the stresses.

† In the introduction a different significance was attached to N .

radius through the joint, and along the axis. Then from (7) we deduce, as the tension coefficient for a typical longitudinal

$$T_{J'J''} = \Omega_l \cdot l (w_{J''} - w_J);$$

as the tension coefficient for a typical diagonal

$$T_{J'K''} = \Omega_d \left[t \left\{ (u_{K''} + u_{J'}) \sin \frac{\alpha}{2} + (v_{K''} - v_{J'}) \cos \frac{\alpha}{2} \right\} + l (w_{K''} - w_{J'}) \right],$$

as the tension coefficient for a typical transverse member

$$T_{J'K'} = \Omega_t \cdot t \left\{ (u_{K'} + u_{J'}) \sin \frac{\alpha}{2} + (v_{K'} - v_{J'}) \cos \frac{\alpha}{2} \right\};$$

and as the tension coefficient for a radial member

$$T_{O'J'} = \Omega_r \cdot r (u_{J'} - u_{O'J'}).$$

(13)

12. Substituting expressions of the types (13) in the conditions (9)-(11) of equilibrium, and observing that

$$t = 2r \sin \frac{\alpha}{2},$$

we obtain the equations

$$\left. \begin{aligned} & \frac{1}{2} r \operatorname{cosec}^2 \frac{\alpha}{2} \Omega_r (u_{J'} - u_{O'J'}) + l \Omega_t \left\{ (u_{K'} + 2u_{J'} + u_{I'}) \sin \frac{\alpha}{2} \right. \\ & \qquad \qquad \qquad \left. + (v_{K'} - v_{I'}) \cos \frac{\alpha}{2} \right\} \\ & + l \Omega_d \left\{ (u_{K''} + u_K + 4u_{J'} + u_{I''} + u_I) \sin \frac{\alpha}{2} \right. \\ & \qquad \qquad \qquad \left. + (v_{K''} + v_K - v_{I''} - v_I) \cos \frac{\alpha}{2} \right\} \\ & + l \Omega_d (w_{K''} - w_K + w_{I''} - w_I) = 0, \\ & l \Omega_t \left\{ (u_{K'} - u_{I'}) \sin \frac{\alpha}{2} + (v_{K'} - 2v_{J'} + v_{I'}) \cos \frac{\alpha}{2} \right\} \\ & + l \Omega_d \left\{ (u_{K''} + u_K - u_{I''} - u_I) \sin \frac{\alpha}{2} \right. \\ & \qquad \qquad \qquad \left. + (v_{K''} + v_K - 4v_{J'} + v_{I''} + v_I) \cos \frac{\alpha}{2} \right\} \\ & + l \Omega_d (w_{K''} - w_K - w_{I''} + w_I) = 0, \\ & l \Omega_t \left\{ (u_{K''} - u_K + u_{I''} - u_I) \sin \frac{\alpha}{2} + (v_{K''} - v_K - v_{I''} + v_I) \cos \frac{\alpha}{2} \right\} \\ & + l \Omega_d (w_{K''} + w_K - 4w_{J'} + w_{I''} + w_I) \\ & \qquad \qquad \qquad + l \Omega_t (w_{J''} - 2w_{J'} + w_J) = 0, \end{aligned} \right\} \quad (14)$$

as conditions of equilibrium for the joint J'.

13. We now introduce a change of notation. First, in place (*e.g.*) of u_j , we write u'_j ,—this being the value of u for the j th joint (§ 11) in the bulkhead distinguished by dashes in fig. 1; and consistently with this usage we write (*e.g.*)

$$u''_{j+1}, u_{j-1} \quad \text{for} \quad u_{K''}, u_I.$$

Secondly, referring again to fig. 1, let x be the value assumed by some quantity at any joint in the bulkhead IJK, and x' , x'' the values assumed at the corresponding joints in the bulkheads I'J'K', I''J''K''. We write

$$x' - x = \Delta x,$$

so that Δx stands for the increase in x which occurs between one bulkhead and the next in the direction of z increasing; and consistently with this convention we write

$$\Delta^2 x = \Delta(\Delta x),$$

$$= \text{increase in } (x' - x) \text{ as we pass from one bay to the next in the direction of } z \text{ increasing,}$$

$$= (x'' - x') - (x' - x),$$

$$= x'' + x - 2x'.$$

Then we have the expressions

$$\left. \begin{aligned} x' &= \Delta x + x = [1 + \Delta]x, \\ x'' &= \Delta^2 x + 2x' - x, \\ &= [\Delta^2 + 2(\Delta + 1) - 1]x = [1 + \Delta]^2 x, \end{aligned} \right\} \quad (15)$$

in which Δ may be treated as a differential operator.

When these changes of notation are introduced, and the expression (12) substituted for $u_{O'J''}$, equations (14) assume the forms

$$\left. \begin{aligned}
 &4k_2 \sin \frac{\alpha}{2} [1 + \Delta] \{u_j - (a \cos j\alpha + b \sin j\alpha)\} \\
 &\quad + 2k_2 [1 + \Delta] \left\{ (u_{j+1} + 2u_j + u_{j-1}) \sin \frac{\alpha}{2} + (v_{j+1} - v_{j-1}) \cos \frac{\alpha}{2} \right\} \\
 &\quad + \left\{ [2 + 2\Delta + \Delta^2] (u_{j+1} + u_{j-1}) + 4[1 + \Delta] u_j \right\} \sin \frac{\alpha}{2} \\
 &\quad \quad + [2 + 2\Delta + \Delta^2] (v_{j+1} - v_{j-1}) \cos \frac{\alpha}{2} \\
 &\quad \quad + \frac{l}{t} [2\Delta + \Delta^2] (w_{j+1} + w_{j-1}) = 0, \\
 &2k_2 [1 + \Delta] \left\{ (u_{j+1} - u_{j-1}) \sin \frac{\alpha}{2} + (v_{j+1} - 2v_j + v_{j-1}) \cos \frac{\alpha}{2} \right\} \\
 &\quad + [2 + 2\Delta + \Delta^2] \left\{ (u_{j+1} - u_{j-1}) \sin \frac{\alpha}{2} + (v_{j+1} + v_{j-1}) \cos \frac{\alpha}{2} \right\} \\
 &\quad \quad - 4[1 + \Delta] v_j \cos \frac{\alpha}{2} \\
 &\quad \quad + \frac{l}{t} [2\Delta + \Delta^2] (w_{j+1} - w_{j-1}) = 0, \\
 &[2\Delta + \Delta^2] \left\{ (u_{j+1} + u_{j-1}) \sin \frac{\alpha}{2} + (v_{j+1} - v_{j-1}) \cos \frac{\alpha}{2} \right\} \\
 &\quad + \frac{l}{t} \left\{ [2 + 2\Delta + \Delta^2] (w_{j+1} + w_{j-1}) - 4[1 + \Delta] w_j \right\} \\
 &\quad \quad + 2k_1 \frac{l}{t} \Delta^2 w_j = 0,
 \end{aligned} \right\} \quad (16)$$

in which (for brevity) we have introduced symbols k_1, k_2, k_3 defined as follows :

$$k_1 = \frac{\Omega_t}{2\Omega_d}, \quad k_2 = \frac{\Omega_t}{2\Omega_d}, \quad k_3 = \frac{1}{16} \frac{\Omega_r}{\Omega_d} \operatorname{cosec}^4 \frac{\alpha}{2}.$$

Assumptions in regard to the Type Solutions.

14. Equations (16) are the conditions for equilibrium of the joint denoted by J' in fig. 1. Three equations of similar type hold for each of the other joints in the same bulkhead, so that each intermediate bulkhead provides $3N$ equations in all, where N is the number of joints in the polygonal transverse ring.

But on certain assumptions, leading to type solutions of a particular kind, we can ensure that every joint of every intermediate bulkhead will be in

equilibrium provided that three conditions, in all, are satisfied. Thus if we assume that u, v, w , in so far as they depend on j , have forms given by

$$\left. \begin{aligned} u_j &= U_n \cos (nj\alpha + \varepsilon), \\ v_j &= V_n \sin (nj\alpha + \varepsilon), \\ w_j &= W_n \cos (nj\alpha + \varepsilon), \end{aligned} \right\} \quad (17)$$

where n is integral and ε an arbitrary phase-constant, the conditions for equilibrium of the joint O will make a and b zero, in the first of (16), unless $n = 1$.* Accordingly, when we substitute from (17) in equations (16), for all values of n other than unity either $\cos (nj\alpha + \varepsilon)$ or $\sin (nj\alpha + \varepsilon)$ can be cancelled out of each equation, and we obtain

$$\left. \begin{aligned} [1 + \Delta] \left\{ 2k_3 U_n \sin \frac{\alpha}{2} + 2k_2 \left[(1 + \cos n\alpha) U_n \sin \frac{\alpha}{2} + \sin n\alpha V_n \cos \frac{\alpha}{2} \right] \right\} \\ + [\cos n\alpha \Delta^2 + 2(1 + \cos n\alpha)(1 + \Delta)] U_n \sin \frac{\alpha}{2} \\ + \sin n\alpha [2 + 2\Delta + \Delta^2] V_n \cos \frac{\alpha}{2} \\ + \frac{l}{i} \cos n\alpha [2\Delta + \Delta^2] W_n = 0, \\ 2k_2 [1 + \Delta] \left\{ \sin n\alpha U_n \sin \frac{\alpha}{2} + (1 - \cos n\alpha) V_n \cos \frac{\alpha}{2} \right\} \\ + [2 + 2\Delta + \Delta^2] \left\{ \sin n\alpha U_n \sin \frac{\alpha}{2} - \cos n\alpha V_n \cos \frac{\alpha}{2} \right\} \\ + 2[1 + \Delta] V_n \cos \frac{\alpha}{2} + \frac{l}{i} \sin n\alpha [2\Delta + \Delta^2] W_n = 0, \\ [2\Delta + \Delta^2] \left\{ \cos n\alpha U_n \sin \frac{\alpha}{2} + \sin n\alpha V_n \cos \frac{\alpha}{2} \right\} \\ + \frac{l}{i} [\cos n\alpha (2 + 2\Delta + \Delta^2) - 2(1 + \Delta)] W_n \\ + k_1 \frac{l}{i} \Delta^2 W_n = 0. \end{aligned} \right\} \quad (18)$$

* The conditions are

$$\Sigma [T_{Oj} \cos j\alpha] = \Sigma [T_{Oj} \sin j\alpha] = 0,$$

or, if we substitute for T_{Oj} from (13),

$$\Sigma [(u_j - u_{Oj}) \cos j\alpha] = \Sigma [(u_j - u_{Oj}) \sin j\alpha] = 0, \quad (1)$$

the summations extending to all values of j from 1 to N . But on this understanding, if u_j satisfies (17), we have

$$\Sigma [u_j \cos j\alpha] = \Sigma [u_j \sin j\alpha] = 0, \text{ unless } n = 1;$$

accordingly, if we substitute for u_{Oj} an expression of the form (12), we have

$$a = b = 0, \text{ unless } n = 1.$$

When $n = 1$, the conditions (i) require that $u_{Oj} = u_j$.

When $n = 1$, the footnote to this paragraph shows that $u_{0j} = u_j$; accordingly no term in k_3 will then appear in the first of (14) or (as a consequence) in the first of (16) or (18). It follows that we may take equations (18) as governing the type solutions for all values of n , if we adopt the convention that

$$k_3 = 0 \quad \text{when} \quad n = 1. \quad (19)$$

15. Again, we can eliminate the operator Δ if we assume that U_n, V_n, W_n in (17), in so far as they depend on the bulkhead in which the joint in question is situated, have forms given by

$$\left. \begin{aligned} U_n, V_n &\propto \cosh(\mu\beta + \eta), \\ W_n &\propto \sinh(\mu\beta + \eta), \end{aligned} \right\} \quad (20)$$

where β stands for the number of the bulkhead—reckoned from some datum bulkhead, in the direction of z increasing,— η is an arbitrary constant, and μ is a constant to be determined. For it is easily verified that*

$$\left. \begin{aligned} &[\Delta^2 - 2(\cosh \mu - 1)(1 + \Delta)]_{\sinh}^{\cosh}(\mu\beta + \eta) = 0 \\ \text{and} \quad &[2\Delta + \Delta^2]_{\sinh}^{\cosh}(\mu\beta + \eta) = 2 \sinh \mu [1 + \Delta]_{\cosh}^{\sinh}(\mu\beta + \eta), \end{aligned} \right\} \quad (21)$$

* According to the convention of § 13, we have

$$\begin{aligned} \Delta^2 \cosh(\mu\beta + \eta) &= \cosh\{\mu(\beta + 2) + \eta\} + \cosh(\mu\beta + \eta) \\ &\quad - 2 \cosh\{\mu(\beta + 1) + \eta\}, \\ &= 2(\cosh \mu - 1) \cosh\{\mu(\beta + 1) + \eta\}, \\ &= 2(\cosh \mu - 1)[1 + \Delta] \cosh(\mu\beta + \eta), \\ [2\Delta + \Delta^2] \cosh(\mu\beta + \eta) &= \cosh\{\mu(\beta + 2) + \eta\} - \cosh(\mu\beta + \eta), \\ &= 2 \sinh \mu \sinh\{\mu(\beta + 1) + \eta\}, \\ &= \sinh \mu [1 + \Delta] \sinh(\mu\beta + \eta). \end{aligned}$$

$\sinh(\mu\beta + \eta)$ can be treated similarly.

and accordingly equations (18) will be satisfied at all unloaded bulkheads, provided that

$$\left. \begin{aligned} & U_n \sin \frac{\alpha}{2} \{k_2 + k_2 (1 + \cos n\alpha) + 1 + \cos n\alpha \cosh \mu\} \\ & \quad + V_n \cos \frac{\alpha}{2} \sin n\alpha (k_2 + \cosh \mu) + \frac{l}{t} W_n \cos n\alpha \sinh \mu = 0, \\ & U_n \sin \frac{\alpha}{2} \sin n\alpha (k_2 + \cosh \mu) \\ & \quad + V_n \cos \frac{\alpha}{2} \{k_2 (1 - \cos n\alpha) + 1 - \cos n\alpha \cosh \mu\} \\ & \quad \quad \quad + \frac{l}{t} W_n \sin n\alpha \sinh \mu = 0, \\ & U_n \sin \frac{\alpha}{2} \cos n\alpha \sinh \mu + V_n \cos \frac{\alpha}{2} \sin n\alpha \sinh \mu \\ & \quad \quad \quad + \frac{l}{t} W_n \{\cos n\alpha \cosh \mu - 1 + k_1 (\cosh \mu - 1)\} = 0. \end{aligned} \right\} \quad (22)$$

16. Combining the assumptions stated in (17) and (20), we may say that a system of displacements which is specified by

$$\left. \begin{aligned} u_j &= U_n \cos (nj\alpha + \varepsilon) \cosh (\mu\beta + \eta), \\ v_j &= V_n \sin (nj\alpha + \varepsilon) \cosh (\mu\beta + \eta), \\ w_j &= W_n \cos (nj\alpha + \varepsilon) \sinh (\mu\beta + \eta), \end{aligned} \right\} \quad (23)$$

where U_n , V_n , W_n , n , μ , ε , η are constants, will satisfy the conditions of equilibrium at every joint of every intermediate (*i.e.*, unloaded) bulkhead, provided that U_n , V_n , W_n , n and μ are related by equations (22). Since ε and η are unrestricted, four distinct solutions are really given by (23), namely,

$$\left. \begin{aligned} u_j &= U_n [\cos nj\alpha \cosh \mu\beta, \quad \sin nj\alpha \cosh \mu\beta, \quad \cos nj\alpha \sinh \mu\beta, \\ & \quad \quad \quad \sin nj\alpha \sinh \mu\beta], \\ v_j &= V_n [\sin nj\alpha \cosh \mu\beta, \quad -\cos nj\alpha \cosh \mu\beta, \quad \sin nj\alpha \sinh \mu\beta, \\ & \quad \quad \quad -\cos nj\alpha \sinh \mu\beta], \\ w_j &= W_n [\cos nj\alpha \sinh \mu\beta, \quad \sin nj\alpha \sinh \mu\beta, \quad \cos nj\alpha \cosh \mu\beta, \\ & \quad \quad \quad \sin nj\alpha \cosh \mu\beta]. \end{aligned} \right\} \quad (24)$$

In order that equilibrium may be maintained at the terminal bulkheads, the forces which act there must be applied in some definite way, which has still to be investigated.

Condition for the Existence of a Type Solution. The Determinantal Equation.

17. Writing

$$\text{so that} \quad \left. \begin{aligned} \cosh \mu &= s, \\ \sinh \mu &= \sqrt{(s^2 - 1)}, \end{aligned} \right\} \quad (25)$$

we obtain, on elimination of U_n , V_n , W_n from (22), a relation which must be satisfied in order that those three equations may be compatible. This relation is

$$\begin{vmatrix} 1 + k_2(1 + \cos n\alpha) + k_3 + s \cos n\alpha, & \sin n\alpha(k_2 + s), & \cos n\alpha \sqrt{(s^2 - 1)}, \\ \sin n\alpha(k_2 + s), & 1 + k_2(1 - \cos n\alpha) - s \cos n\alpha, & \sin n\alpha \sqrt{(s^2 - 1)}, \\ \cos n\alpha \sqrt{(s^2 - 1)}, & \sin n\alpha \sqrt{(s^2 - 1)}, & -1 + k_1(s - 1) + s \cos n\alpha \end{vmatrix} = D = 0. \quad (26)$$

The determinant in (26) can be expanded as follows.—

$$\begin{aligned} -D &= (s - 1)^2 \{k_1(s - 1) + 2k_1(1 + k_2) + k_2(1 + \cos n\alpha)\} \\ &\quad + k_3[(1 + k_1 \cos n\alpha)(s - 1)^2 \\ &\quad - \{k_1(1 + k_2) - 2 + k_2 \cos n\alpha\}(1 - \cos n\alpha)(s - 1) \\ &\quad + (1 + k_2)(1 - \cos n\alpha)^2] = 0. \quad (27) \end{aligned}$$

In conformity with (19), the term k_3 is to be omitted when $n = 1$.

We can show that (27) has no root lying inside the range

$$-1 < s < 1.$$

For if s lies within this range, the part independent of k_3 , on the right-hand side of (27), is evidently positive; and the cofactor of k_3 can be seen to be also positive if we arrange it in the form

$$\begin{aligned} [(s - \cos n\alpha)^2 - k_1(s - 1)\{(1 - s \cos n\alpha) + k_2(1 - \cos n\alpha)\} \\ + k_2(1 - \cos n\alpha)(1 - s \cos n\alpha)]. \end{aligned}$$

Neither can $s = -1$ be a solution. But when $s = 1$ we have

$$-D = k_3(1 + k_2)(1 - \cos n\alpha)^2,$$

and therefore s can have the value 1 if either

$$\left. \begin{array}{l} \cos n\alpha = 1 \\ k_3 = 0. \end{array} \right\} \quad (28)$$

Accordingly s , if it is real, cannot be numerically less than 1; and it follows that purely imaginary values of μ cannot come from (26).

Nature of the Roots.

18. On account of the number of parameters which are involved in equation (27), it is useless to attempt a general solution; the roots can, of course, be calculated without difficulty when numerical values have been assigned to k_1, k_2, k_3, n . There will always be a real value of s lying in the range

$$-\infty < s < -(1 + 2k_3);$$

for when $s = -\infty$ the expression (27) for D is positive, and at the other end of the range it is

$$D = -(1 + \cos n\alpha)(1 + k_2) \left\{ 4k_2(1 + k_2) + k_3[1 + \cos n\alpha + 2\{k_1(1 + k_2) + (2 - \cos n\alpha)k_2\}] \right\},$$

which is clearly negative. This root (being negative and numerically greater than 1) will give a complex value for μ (cf. § 19).

Complex values for μ can also come from complex roots of (27), which evidently may occur. For example, when $n = \frac{1}{2}N$ equation (27) reduces to

$$-D = (s + 1 + 2k_2)[k_1(s - 1)^2 + k_3\{(1 - k_1)(s - 1) + 2\}] = 0,$$

and two of its roots will come from the quadratic equation

$$k_1(s - 1)^2 + (1 - k_1)k_3(s - 1) + 2k_3 = 0.$$

These will not be real if

$$(k_1 - 1)^2 k_3 < 8k_1,$$

or if

$$k_1 < 1 + \frac{4}{k_3} \left\{ 1 + \sqrt{1 + \frac{k_2}{2}} \right\}. \quad (29)$$

19. No difficulty arises in the interpretation of complex values of μ , if we observe that equations (14), since all the coefficients involved in them are real, must be satisfied by the real and imaginary parts, severally, of our solutions (24). The factors $\cosh \mu\beta$, $\sinh \mu\beta$, which are real when $s > 1$, may be

replaced by $(-1)^s (\cosh v\beta, \sinh v\beta)$ when s is real and $< (-1)$, v being defined by*

$$\cosh v = -s; \quad (30)$$

and the ratios V_n/U_n , W_n/U_n will be real when s is real, whether positive or negative.† When s is complex, it will lead to complex values for these ratios, and products such as $V_n \cosh \mu\beta$ must accordingly be multiplied out and separated into real and imaginary parts. Two distinct systems of displacement will thus be obtained, corresponding with any one of the four type solutions (24); but since complex roots of s will always appear as a conjugate pair, the same two systems, in every case, will be obtained from both; accordingly, *provided that the three roots in s are all different*, we shall have in every case *twelve* distinct solutions corresponding with any one value of n .

Two Special Cases.

20. When $s = 1$ we have $\mu = 0$, and terms in (24) which contain $\sinh \mu\beta$ will vanish. We have seen (§ 17) that s can be unity either if $\cos n\alpha = 1$ or if $k_3 = 0$, but not otherwise; in both circumstances, as may be seen from (27), $s = 1$ occurs as a repeated root, so that the proviso of the last paragraph is not satisfied.

According to the convention stated in (19), k_3 is to be treated as zero when $n = 1$. So we must give special consideration to the cases $n = 0$ and $n = 1$, and we go back for this purpose to the difference equations (18).

21. When $n = 0$ ($\cos n\alpha = 1$), equations (18) require that

$$\left. \begin{aligned} [\Delta^2 + 2(2 + 2k_2 + k_3)(\Delta + 1)] U_0 \sin \frac{\alpha}{2} + \frac{l}{i} [\Delta^2 + 2\Delta] W_0 &= 0, \\ \Delta^2 V_0 &= 0, \\ [\Delta^2 + 2\Delta] U_0 \sin \frac{\alpha}{2} + (1 + k_1) \frac{l}{i} \Delta^2 W_0 &= 0. \end{aligned} \right\} \quad (31)$$

The second of these equations gives a solution independent of those governed by the first and third. It may be integrated in the form

$$V_0 = P + Q\beta, \quad (32)$$

where P and Q are arbitrary constants, and β has the significance stated in § 15. The term in P (which makes v the same for every joint) represents a

* We have $\mu = v + i\pi$.

† We have seen (§ 17) that s , if real, will always be numerically greater than 1.

rotation of the framework as a whole, and involves no action in any member. The term in Q represents a uniform twist of the framework, whereby each bulkhead rotates by a constant amount in relation to the next.

22. Taking now the first and third of (31), we operate with $(1 + k_1) \Delta$ and $[\Delta + 2]$ respectively, and subtract to eliminate W_0 . Then we obtain

$$[k_1 \Delta^2 + \{4k_1 + 2(1 + k_1)(2k_2 + k_3)\}(\Delta + 1)] \Delta U_0 = 0. \quad (33)$$

A first solution of this equation is obtained if we write

$$\Delta U_0 = 0,$$

and then we have, from the third of (31),

$$\Delta^2 W_0 = 0.$$

This equation may be integrated in the form

$$W_0 = R + S\beta, \quad (34)$$

R and S being arbitrary constants, and β having the same significance as before. Then we have from the first of (31)

$$\begin{aligned} (2 + 2k_2 + k_3) U_0 \sin \frac{\alpha}{2} &= -\frac{l}{t} \Delta W_0, \\ &= -\frac{l}{t} S, \end{aligned} \quad (35)$$

so that U_0 is defined.

The term in R represents a displacement of the framework as a whole in the direction of z , since it makes w the same for every joint. The term in S , in (34) and (35), represents a uniform stretch of the framework, accompanied by contraction of every bulkhead.

23. The other solution of (33) can be seen to be of the type discussed in §§ 15–19, since on making the assumption (20) we find that (33) will be satisfied if

$$(s + 1)k_1 + (1 + k_1)(2k_2 + k_3) = 0. \quad (36)$$

The same value for s is given (when $n = 0$) by equation (27).

This solution does not involve V_0 , and hence (n being zero) it gives two, instead of the usual four, distinct systems of type (24). Two distinct systems have been found in § 21, and two in § 22; accordingly we have obtained six distinct systems, in all, for the case when $n = 0$.

24. When $n = 1$, k_3 must be omitted from the first of (18). Then, eliminating W_1 from the first two of those equations, we find that

$$\Delta^2 V_1 + 2(1 - \cos \alpha)(1 + k_2)[\Delta + 1](U_1 + V_1) = 0. \quad (37)$$

Again, if we multiply the first and second of (18) by $\cos \alpha$ and $\sin \alpha$ respectively, and add, we obtain

$$\Delta^2 U_1 + 2(1 + \cos \alpha)(1 + k_2)[\Delta + 1](U_1 + V_1) + \frac{1}{1 - \cos \alpha} \frac{l}{r} [\Delta^2 + 2\Delta] W_1 = 0, \quad (38)$$

since $t = 2r \sin \frac{\alpha}{2}$.

From the third of (18) we have

$$[\Delta^2 + 2\Delta] \{ \cos \alpha U_1 + (1 + \cos \alpha) V_1 \} + \frac{1}{1 - \cos \alpha} \frac{l}{r} [(\cos \alpha + k_1) \Delta^2 - 2(1 - \cos \alpha)(\Delta + 1)] W_1 = 0. \quad (39)$$

Adding (37) and (38), we have

$$[\Delta^2 + 4(1 + k_2)(\Delta + 1)](U_1 + V_1) + \frac{l}{1 - \cos \alpha} \frac{l}{r} [\Delta^2 + 2\Delta] W_1 = 0, \quad (40)$$

and on elimination of W_1 from (39) and (40) we have

$$\begin{aligned} & \left[k_1 \Delta^4 + 2\{2k_1(1 + k_2) + 2k_2 \cos \alpha - 1 + \cos \alpha\} \Delta^3 (\Delta + 1) \right. \\ & \quad \left. - 8(1 - \cos \alpha)(1 + k_2)(\Delta + 1)^2 \right] (U_1 + V_1) \\ & = [\Delta^2 + 2\Delta]^2 V_1, \\ & = -2(1 - \cos \alpha)(1 + k_2)[\Delta^2 + 4\Delta + 4][\Delta + 1](U_1 + V_1), \end{aligned}$$

by (37). We deduce that

$$[k_1 \Delta^2 + 2\{2k_1(1 + k_2) + k_2(1 + \cos \alpha)\}(\Delta + 1)] \Delta^2 (U_1 + V_1) = 0. \quad (41)$$

25. Corresponding with the operator in square brackets we have a solution of the type discussed in §§ 15-19, leading in the normal way to *four* distinct systems of displacement, of the type (24). For on making the assumption (20) we find that (41) will be satisfied if

$$k_1(s - 1) + 2k_1(1 + k_2) + k_2(1 + \cos \alpha) = 0, \quad (42)$$

and the same value of s is given (when $n = 1$, and k_3 accordingly = 0) by (27).

26. The other solutions come from the equation

$$\Delta^2 (U_1 + V_1) = 0, \quad (43)$$

which, by (40), requires that

$$4(1 - \cos \alpha)(1 + k_2)[\Delta + 1](U_1 + V_1) + \frac{l}{r}[\Delta^2 + 2\Delta]W_1 = 0. \quad (44)$$

From (37) and (43) we have

$$\Delta^4 V_1 = 0,$$

and can deduce the forms

$$\left. \begin{aligned} U_1 &= (1 - \cos \alpha)(1 + k_2)\{F\beta^2 + G\beta^2 + H\beta + K\} + 3F\beta + G, \\ -V_1 &= (1 - \cos \alpha)(1 + k_2)\{F\beta^3 + G\beta^2 + H\beta + K\}. \end{aligned} \right\} \quad (45)$$

Then from (39) and (44) we obtain

$$\begin{aligned} -\frac{l}{r}W_1 &= (1 - \cos \alpha)(1 + k_2)(3F\beta^2 + 2G\beta + F + H) \\ &\quad + 3F\{k_1(1 + k_2) + k_2 \cos \alpha\}, \end{aligned}$$

as the corresponding expression for W_1 .

27. In (45) we have four distinct solutions for the special case ($n = 1$), corresponding with the four independent constants

$$F, G, H, K.$$

Associated with any one of these we have two distinct systems of displacement, given by

$$\left. \begin{aligned} u_j &= U_1 [\cos j\alpha, \sin j\alpha], \\ v_j &= V_1 [\sin j\alpha, -\cos j\alpha], \\ w_j &= W_1 [\cos j\alpha, \sin j\alpha], \end{aligned} \right\} \quad (46)$$

so that eight distinct systems have been found. Adding the four systems found in § 25, we have in all *twelve* distinct systems, as in the normal case discussed in § 19.

In the solution associated with the constant K in (45),

$$U_1 : V_1 : W_1 = 1 : -1 : 0.$$

Evidently this represents a rigid-body translation of the framework as a whole.

In the solution characterized by H ,

$$U_1 : V_1 : W_1 = \beta : -\beta : -\frac{r}{l}.$$

Evidently this represents a rigid-body rotation of the framework as a whole, whereby its axis is inclined to its original position.

28. In the solution characterized by G we have

$$U_1 : V_1 : W_1 = \beta^2 + \frac{1}{(1 - \cos \alpha)(1 + k_2)} : -\beta^2 : -2\beta \frac{r}{l}. \quad (47)$$

This represents a uniform flexure of the framework under the action of terminal couples. Bulkheads remain plane, but are now distorted in their own planes ($U_1 + V_1$ does not vanish), owing to causes which produce similar effects in solid elastic cylinders. The central joints of the bulkhead bracings are displaced so as to lie on a parabolic curve, which is the usual approximation (in the theory of flexure) to the circular form.

29. Lastly, in the solution characterized by F we have

$$U_1 : V_1 : W_1 = \beta^2 + \frac{3\beta}{(1 - \cos \alpha)(1 + k_2)} : -\beta^2 : -\left\{ 3\beta^2 + 1 + \frac{3\{k_1(1 + k_2) + k_2 \cos \alpha\}}{(1 - \cos \alpha)(1 + k_2)} \right\} \frac{r}{l}. \quad (48)$$

This represents a uniform shearing of the framework, accompanied by flexure due to the uniformly varying bending moment which must accompany a constant shearing action. Bulkheads again remain plane but are distorted in their own planes, and the central joints of the bulkhead bracings are now displaced so as to lie on a cubic curve. Every feature of the distortion has an analogue in St. Venant's theory of flexure for solid elastic cylinders.

The Solutions Corresponding with a Repeated Root.

30. There remain for consideration cases in which equation (27) has a repeated root s_1 , other than unity: the argument of § 18 indicates that these cannot be excluded as impossible, and in relation to them we have still to demonstrate the existence of twelve independent systems of displacement, because the argument of § 19 will not apply.

An analogous question is presented in the theory of the vibrations of an elastic system, where one or more of the normal modes of vibration may have the same period. In that theory some mathematicians have erroneously concluded that time factors not of purely exponential type will then make an appearance*; but the correct conclusion is that no new consideration arises: there is the same number of distinct solutions of the standard type, whether

* Cf. Lamb's "Higher Mechanics," footnote to § 93, or Rayleigh, "Theory of Sound," vol. 1, § 87.

their associated frequencies are different or the same. In regard to our problem a similar conclusion might be expected to hold ; but in the particular case treated in § 18 (when $\cos n\alpha + 1 = 0$) it is found that only one solution—in which the constants U_n, V_n, W_n of (23) satisfy the equations

$$U_n \sin \frac{\alpha}{2} \sqrt{s^2 - 1} = 2 \frac{l}{l} W_n, \quad V_n = 0,$$

—corresponds with the repeated root of (27), when this exists.* Hence, if we restrict our solutions to those of type (20), we shall arrive at only eight, instead of twelve, distinct type solutions of the kinds represented by (24).

31. In the theory of vibrations, two distinct sets of ratios for the variables (corresponding with U_n, V_n, W_n in our problem) can be shown to satisfy the imposed equations when the conditions are such that the determinantal equation has a repeated root.† That is to say, the governing equations fail in these circumstances to define the ratios ; the reason being that every minor of the determinant vanishes when the repeated root is substituted, so that the three equations become (effectively) identical. But in our problem it appears that a repeated root will not necessarily involve the evanescence of every minor in the determinant D of equation (26), if the conditions are such that U_n, V_n, W_n are all finite. For example, the minor of the term $\sin n\alpha \sqrt{s^2 - 1}$, in the third column, is

$$\begin{vmatrix} 1 + k_2 (1 + \cos n\alpha) + k_3 + s \cos n\alpha, & (k_2 + s) \sin n\alpha \\ \cos n\alpha \sqrt{s^2 - 1}, & \sin n\alpha \sqrt{s^2 - 1} \end{vmatrix} \\ = \sin n\alpha \sqrt{s^2 - 1} (1 + k_2 + k_3),$$

and will not vanish unless either the repeated root is unity‡ or $\sin n\alpha = 0$. In either of the latter events one or other of U_n, V_n , as given by (22), will be zero.

There is no reason to believe that these are the only circumstances in which a repeated root will occur ; and in any case we have seen already (§§ 20–26) that when $n = 0$ or 1 they entail solutions which are not restricted to the types defined by (20). Accordingly we must make a new examination of the difference equations (18), to see in what circumstances solutions of an alternative type can exist.

* The conditions for a repeated root in this instance are discussed in § 35 (In very special circumstances all three roots of (27) may be equal, and then V_n is arbitrary ; but there will still be four type solutions missing.)

† Cf. Lamb. *op. cit.*, § 93.

‡ $(s + 1)$ cannot vanish : cf. § 17.

32. We have by definition (§ 13) of the operator Δ , when ϕ is *any* function of β ,

$$[\Delta + 1](\beta\phi) = [\Delta + 1]\beta \cdot [\Delta + 1]\phi = (\beta + 1)[\Delta + 1]\phi,$$

so that

$$[\Delta + 1]^2(\beta\phi) = [\Delta + 1](\beta + 1) \cdot [\Delta + 1]^2\phi = (\beta + 2)[\Delta + 1]^2\phi,$$

and so on. If then we assume that

$$\left. \begin{aligned} U_n \sin \frac{\alpha}{2} &= \beta P \cosh(\mu\beta + \eta) + P' \sinh(\mu\beta + \eta), \\ V_n \cos \frac{\alpha}{2} &= \beta Q \cosh(\mu\beta + \eta) + Q' \sinh(\mu\beta + \eta), \\ {}^l_t W_n &= \beta R \sinh(\mu\beta + \eta) + R' \cosh(\mu\beta + \eta), \end{aligned} \right\} \quad (49)$$

where $P \cosh(\mu\beta + \eta)$, ... etc. constitute the solution already found, substitution in (18) leads in each instance to a series of terms multiplied by the factor $(\beta + 1)$ —which series vanishes on account of the relations imposed on P, Q, R , — *plus* terms independent of β which come both from the terms in P, Q, R and from the terms in P', Q', R' . Making use of (21), we find that (49) will be a solution of the three equations (18), provided that

$$\left. \begin{aligned} &P' \{k_3 + k_2(1 + \cos n\alpha) + 1 + \cos n\alpha \cosh \mu\} \\ &\quad + Q' \sin n\alpha (k_2 + \cosh \mu) + R' \cos n\alpha \sinh \mu \\ &\quad + (P \cos n\alpha + Q \sin n\alpha) \sinh \mu + R \cos n\alpha \cosh \mu = 0, \\ &P' \sin n\alpha (k_2 + \cosh \mu) + Q' \{k_2(1 - \cos n\alpha) + 1 - \cos n\alpha \cosh \mu\} \\ &\quad + R' \sin n\alpha \sinh \mu + (P \sin n\alpha - Q \cos n\alpha) \sinh \mu \\ &\quad + R \sin n\alpha \cosh \mu = 0, \\ &P' \cos n\alpha \sinh \mu + Q' \sin n\alpha \sinh \mu + R' \{\cos n\alpha \cosh \mu - 1 \\ &\quad + k_1(\cosh \mu - 1)\} + (P \cos n\alpha + Q \sin n\alpha) \cosh \mu \\ &\quad + R(\cos n\alpha + k_1) \sinh \mu = 0, \end{aligned} \right\}$$

and if (for brevity) we write (26) in the form

$$D = \begin{vmatrix} a, & h, & g \\ h, & b, & f \\ g, & f, & c \end{vmatrix} = 0, \quad (50)$$

it may be seen that these conditions can be written in the forms

$$\left. \begin{aligned} aP' + hQ' + gR' + \frac{da}{d\mu}P + \frac{dh}{d\mu}Q + \frac{dg}{d\mu}R &= 0, \\ hP' + bQ' + fR' + \frac{dh}{d\mu}P + \frac{db}{d\mu}Q + \frac{df}{d\mu}R &= 0, \\ gP' + fQ' + cR' + \frac{dg}{d\mu}P + \frac{df}{d\mu}Q + \frac{dc}{d\mu}R &= 0. \end{aligned} \right\} \quad (51)$$

33. Since

$$\left. \begin{aligned} aP + hQ + gR &= 0, \\ hP + bQ + fR &= 0, \\ gP + fQ + cR &= 0, \end{aligned} \right\} \quad (52)$$

it is evident that the solution of (51) must be arbitrary to the extent that any multiples of P , Q , R may be added to P' , Q' , R' . Hence, without loss of generality (if $P \neq 0$), we may take P' as vanishing in equations (51).^{*} On this understanding, if A , B , C , F , G , H be written for the minors associated with a , b , c , f , g , h in the determinant of equation (50), we have on elimination of R' between successive pairs of the equations (51)

$$\left. \begin{aligned} -AQ' &= c\left(\frac{dh}{d\mu}P + \frac{db}{d\mu}Q + \frac{df}{d\mu}R\right) - f\left(\frac{dg}{d\mu}P + \frac{df}{d\mu}Q + \frac{dc}{d\mu}R\right), \\ -HQ' &= c\left(\frac{da}{d\mu}P + \frac{dh}{d\mu}Q + \frac{dg}{d\mu}R\right) - g\left(\frac{dg}{d\mu}P + \frac{df}{d\mu}Q + \frac{dc}{d\mu}R\right), \\ -GQ' &= f\left(\frac{da}{d\mu}P + \frac{dh}{d\mu}Q + \frac{dg}{d\mu}R\right) - g\left(\frac{dh}{d\mu}P + \frac{db}{d\mu}Q + \frac{df}{d\mu}R\right). \end{aligned} \right\} \quad (53)$$

Now the minors A , H , G are related by the condition

$$aA - hH + gG = D = 0, \quad (54)$$

and if $P \neq 0$ they cannot vanish unless B , F , C also vanish, because on elimination of P , Q , R from successive pairs of the equations (52) we have

$$\left. \begin{aligned} -Q \times (A, H, G) &= P(H, B, F), \\ R \times (A, H, G) &= P(G, F, C), \\ -Q \times (G, F, C) &= R(H, B, F). \end{aligned} \right\} \quad (55)$$

^{*} If P vanishes but Q is finite, we take Q' as zero, and so on. The argument will proceed on similar lines.

Accordingly, in order that the three equations (53) may be compatible with a finite value of Q' , we must have

$$0 = -H \left(\frac{da}{d\mu} P + \frac{dh}{d\mu} Q + \frac{dg}{d\mu} R \right) + B \left(\frac{dh}{d\mu} P + \frac{db}{d\mu} Q + \frac{df}{d\mu} R \right) \\ - F \left(\frac{dg}{d\mu} P + \frac{df}{d\mu} Q + \frac{dc}{d\mu} R \right),$$

and making use of (55) again we find that this condition may be written in the equivalent form

$$Q \frac{dD}{d\mu} = 0.$$

Hence, unless Q is zero, the condition for compatibility of the equations (51) is

$$\frac{dD}{d\mu} \left[= \sinh \mu \frac{dD}{ds} = \sqrt{(s^2 - 1)} \frac{dD}{ds} \right] = 0, \quad (56)$$

that is to say, either $s = 1$ must be a root of the equation ($D = 0$),—and if so, we have seen in § 20 that it will be a repeated root,—or we must have

$$\frac{dD}{ds} = 0 = D,$$

—which again is the condition for a repeated root. If $Q = 0$, we can arrive at the same conclusion by eliminating Q' , instead of R' , between successive pairs of the equations (51).

34. Elimination of Q' from the last two of equations (53) leads to the relation

$$g \left\{ A \left(\frac{da}{d\mu} P + \frac{dh}{d\mu} Q + \frac{dg}{d\mu} R \right) - H \left(\frac{dh}{d\mu} P + \frac{db}{d\mu} Q + \frac{df}{d\mu} R \right) \right. \\ \left. + G \left(\frac{dg}{d\mu} P + \frac{df}{d\mu} Q + \frac{dc}{d\mu} R \right) \right\} = 0,$$

as the condition for a finite value of Q' . The expression on the left-hand side may, by (55), be thrown into the form

$$gP \frac{dD}{d\mu},$$

and accordingly the condition is satisfied already, in virtue of (56). A similar argument will show that P' , R' are both finite when the determinantal equation has a repeated root; accordingly we have demonstrated the validity in these circumstances of our trial solution (49).

We have assumed in this demonstration that the minors A, H, G do not all vanish. The contrary, as we have seen (§ 33), would require B, C, F also to vanish, so that we should have the circumstances contemplated in the theory of vibrations (*cf.* § 31). In our problem these circumstances cannot arise unless either $s = 1$ or $\sin n\alpha = 0$; for we have seen (§ 31) that the minor here denoted by F cannot otherwise vanish.

35. Of the circumstances in which the minors of D can vanish severally, we have discussed all excepting those mentioned in § 31, when $\cos n\alpha + 1 = 0$. Here the condition for a repeated root (*cf.* § 18) is

$$k_3 (k_1 - 1)^2 = 8k_1,$$

and can always be satisfied; the repeated root is given by

$$s = s_1 = 1 + \frac{4}{(k_1 - 1)},$$

and the remaining root gives a solution in which $U_n = W_n = 0$. We require a second solution corresponding with the repeated root.

Under the conditions stated, we may substitute in (51) the expressions

$$h = f = 0,$$

$$a = \frac{k_1 + 1}{k_1 - 1} (s_1 - 1), \quad \frac{du}{d\mu} = -\sqrt{(s_1^2 - 1)},$$

$$g = -\sqrt{(s_1^2 - 1)}, \quad \frac{dg}{d\mu} = -s_1.$$

$$c = 2, \quad \frac{dc}{d\mu} = (k_1 - 1)\sqrt{(s_1^2 - 1)},$$

and (*cf.* § 30)

$$2R = P\sqrt{(s_1^2 - 1)}.$$

The first and third of equations (51) are then seen to be independent of the second, and identical with one another. They require that

$$-\sqrt{(s_1^2 - 1)} P' + 2R' + (2 + s_1) P = 0,$$

and will be satisfied if we take

$$P' = 0,$$

$$-2R' = P(2 + s_1).$$

We observe that the solution is arbitrary in regard to the value of P' , for reasons which have been explained in § 33.

Satisfaction of Imposed Conditions at the Terminal Bulkheads.

36. (1) *Displacements Specified.*—In the simplest case of our general problem, u, v, w have specified values at joints of the terminal bulkheads, and it is required to find their values at other joints. We shall show that our solutions are adequate for this purpose.

Let N denote the number of joints in a bulkhead.* Then the displacement u , being specified at N joints of one terminal bulkhead, can be represented by a series of N terms as follows :—

$$u_j = A_0 + A_1 \cos j\alpha + \dots + A_n \cos nj\alpha + \dots \\ + B_1 \sin j\alpha + B_2 \sin 2j\alpha + \dots + B_n \sin nj\alpha + \dots \quad (57)$$

where

$$\left. \begin{aligned} A_0 &= \frac{1}{N} \Sigma_j [u_j], \\ A_n &= \frac{2}{N} \Sigma_j [u_j \cos nj\alpha] \quad (0 < n < \frac{1}{2}N), \\ A_{\frac{1}{2}N} &= \frac{1}{N} \Sigma_j [u_j \cos j\pi], \\ B_n &= \frac{2}{N} \Sigma_j [u_j \sin nj\alpha], \end{aligned} \right\} \quad (58)$$

and Σ_j denotes a summation extending to all integral values of j from 1 to N . The number of coefficients involved in (57) will in all cases be N ; for when N is odd we have distinct solutions corresponding with

$$A_0, A_1, A_2, \dots, A_{\frac{1}{2}(N-1)}, \\ B_1, B_2, \dots, B_{\frac{1}{2}(N-1)},$$

and when N is even we have distinct solutions corresponding with

$$A_0, A_1, A_2, \dots, A_{\frac{1}{2}N}, \\ B_1, B_2, \dots, B_{\frac{1}{2}N-1}.$$

At the other terminal bulkhead we shall have, similarly, N specified values of u which may be represented by the series

$$\bar{u}_j = \bar{A}_0 + \bar{A}_1 \cos j\alpha + \dots + \bar{A}_n \cos nj\alpha + \dots \\ + \bar{B}_1 \sin j\alpha + \bar{B}_2 \sin 2j\alpha + \dots + \bar{B}_n \sin nj\alpha + \dots, \quad (59)$$

* In the Introduction (§ 8) this number was denoted by P , because the symbol N had been employed (§ 2) to represent the order of redundancy.

in which the coefficients can be calculated from expressions analogous with (58).

37. The displacements v and w can be similarly represented. Hence, fixing attention on the terms which involve $\sin n_j\alpha$ or $\cos n_j\alpha$, we may say that a system of displacements is required in which—

at one terminal bulkhead (say, the left-hand bulkhead of fig. 1)

$$\left. \begin{aligned} u_j &= A_n \cos n_j\alpha + B_n \sin n_j\alpha, \\ v_j &= C_n \sin n_j\alpha + D_n \cos n_j\alpha, \\ w_j &= E_n \cos n_j\alpha + F_n \sin n_j\alpha, \end{aligned} \right\}$$

and at the other (right-hand) terminal bulkhead

$$\left. \begin{aligned} u_j &= \bar{A}_n \cos n_j\alpha + \bar{B}_n \sin n_j\alpha, \\ v_j &= \bar{C}_n \sin n_j\alpha + \bar{D}_n \cos n_j\alpha, \\ w_j &= \bar{E}_n \cos n_j\alpha + \bar{F}_n \sin n_j\alpha, \end{aligned} \right\}$$

(60)

—the constants A_n, B_n, \dots etc., having specified values.

On reference to our type solutions (24), we see that six distinct solutions (involving three distinct values of μ) will normally be available, in all of which

$$\begin{aligned} u_j, w_j &\propto \cos n_j\alpha, \\ v_j &\propto \sin n_j\alpha. \end{aligned}$$

Accordingly, if we attach suitable constants to these solutions, we can use them in combination to satisfy the six conditions imposed by $A_n, C_n, E_n, \bar{A}_n, \bar{C}_n, \bar{E}_n$ in (60). There will also be six distinct solutions in which

$$\begin{aligned} u_j, w_j &\propto \sin n_j\alpha, \\ v_j &\propto \cos n_j\alpha, \end{aligned}$$

and these can be used, similarly, to satisfy the six conditions imposed by $B_n, D_n, F_n, \bar{B}_n, \bar{D}_n, \bar{F}_n$ in (60).

38. A solution can thus be obtained in the normal case, when the determinantal equation corresponding with n has three different roots; and in the case of a repeated root, although we have seen that a new type solution (49) makes its appearance, the same number of independent solutions is available, and the same procedure (in principle) is required.

These remarks include the special case ($n = 1$) which was treated in §§ 24–29. When $n = 0$, so that all terms involving $\sin n_j\alpha$ are zero, the procedure is the

same, but we have in all six, instead of twelve, imposed conditions, and six (instead of twelve) distinct solutions whereby they may be satisfied.*

39. (2) *Forces Specified*.—In another case of our problem, specified *forces* (instead of displacements) are imposed at the terminal bulkheads. We shall show that a solution can be obtained by the same procedure as before.

Referring to fig. 1, in which J' is a typical joint of the framework, we can write down expressions in the notation of § 13 for the tension coefficients of the members $J'I''$, $J'J''$, $J'K''$. Then *in relation to any one of our standard type solutions*, where

$$u_j, w_j \propto \cos (nj\alpha + \epsilon), \quad v_j \propto \sin (nj\alpha + \epsilon),$$

it is an easy matter to deduce the expressions

$$\left. \begin{aligned} T_{J'K''} + T_{J'I''} &= 2\Omega_d \left\{ t \sin \frac{\alpha}{2} (u'_j + \cos n\alpha u''_j) \right. \\ &\quad \left. + \cot (nj\alpha + \epsilon) t \cos \frac{\alpha}{2} \sin n\alpha v''_j, \right. \\ &\quad \left. + l(\cos n\alpha w''_j - w'_j) \right\}, \\ T_{J'K''} - T_{J'I''} &= -2\Omega_d \left\{ \tan (nj\alpha + \epsilon) t \sin \frac{\alpha}{2} \sin n\alpha u''_j, \right. \\ &\quad \left. + t \cos \frac{\alpha}{2} (v'_j - \cos n\alpha v''_j) \right. \\ &\quad \left. + \tan (nj\alpha + \epsilon) l \sin n\alpha w''_j \right\}, \\ T_{J'J''} &= \Omega_t \cdot l(w''_j - w'_j), \end{aligned} \right\} \quad (61)$$

in which u'_j, v'_j, w'_j relate to the joint under consideration, and u''_j, v''_j, w''_j to the corresponding joint in the next bulkhead on the side of z increasing.

40. Now if J' is a joint on the terminal bulkhead in the direction of z increasing, the forces which would have been exerted by $J'I''$, $J'J''$ and $J'K''$ must (if our solution is to hold) be supplied as externally applied forces. So the force required at J' must have components R'_j, T'_j, Z'_j , acting in the radial, tangential and axial directions respectively, which are given by

$$\left. \begin{aligned} -R'_j &= t \sin \frac{\alpha}{2} (T_{J'K''} + T_{J'I''}), \\ T'_j &= t \cos \frac{\alpha}{2} (T_{J'K''} - T_{J'I''}), \\ Z'_j &= l(T_{J'K''} + T_{J'J''} + T_{J'I''}). \end{aligned} \right\} \quad (62)$$

* Cf. § 23

The other terminal bulkhead may be considered similarly. Without going further into details, we can see from (61) that in so far as they depend on j we may write

$$\left. \begin{aligned} R'_j &\propto \cos (nj\alpha + \epsilon), \\ T'_j &\propto \sin (nj\alpha + \epsilon), \\ Z'_j &\propto \cos (nj\alpha + \epsilon); \end{aligned} \right\} \quad (63)$$

that is to say, in any one of our standard type solutions R'_j , T'_j , Z'_j will vary from joint to joint of a terminal bulkhead in the same manner as u'_j , v'_j , w'_j . It follows that the procedure described in §§ 36-38, in relation to specified displacements, will also deal with specified forces.

41. (3) *Other Forms of the Terminal Conditions.*—Equally it is clear that the same procedure can deal with cases of our problem in which specified forces are imposed on the joints of one terminal bulkhead and specified displacements on those of the other. It is not necessary here to multiply the number of cases considered; in general we may say that either forces or the corresponding displacements, *but not both*, may be specified at any joint.

The General Problem of a Loaded Framework.

42. We must, however, sketch the procedure required in order to adapt the foregoing analysis to the treatment of our problem in its most general form; that is, when specified forces (subject only to the conditions of equilibrium) act at *every* joint.

Referring again to fig. 1, and now taking J' to represent a typical joint *in a framework of infinite length*, it is clear from what has been said that we can find a solution, applicable to the semi-infinite framework on the right of the bulkhead $I'J'K'$, in which w vanishes at this bulkhead, and in which no tangential force is required for the maintenance of equilibrium. The displacements u and v will in general be finite, and axial forces of types R and Z , in equations (62), must be presumed to act at joints of the bulkhead $I'J'K'$; we can arrange that both, so far as they depend on j , contain the factor $\cos (nj\alpha + \epsilon)$.

If now we assume that a similar solution holds in respect of the semi-infinite framework on the left of the bulkhead $I'J'K'$, we shall have a solution for the complete framework which involves no forces at this bulkhead of the types T or Z (because the longitudinal force required by each semi-infinite framework is supplied by the other), but which requires, on the other hand, radial forces

for the maintenance of equilibrium, because in this respect the requirements of the two semi-infinite frameworks are *additive*.

Using similar methods, we can also find solutions which require either tangential or longitudinal forces only (*i.e.*, forces of type T or type Z only) to act at the joints of the bulkhead I'J'K': and in any one of the three solutions we can arrange that the forces so required involve j as a factor $\cos nj\alpha$ or $\sin nj\alpha$. We thus have solutions for an infinite tube which can be used in cases where forces of these types are specified as acting at any intermediate bulkhead in a framework; and since any distribution of applied forces can be analysed (on the lines indicated in § 36) into series of such types, we are in a position to deal with problems in which arbitrary distributions are specified.

In dealing with a framework of finite length, we must first dispose in this way of the forces at the intermediate bulkheads, and calculate the forces which our solutions entail at the terminal bulkheads. The problem then reduces to one in which forces are specified at the end bulkheads only; and it can be completed by methods which have already been described.

II. —A THEOREM RELATING TO PSEUDO-REDUNDANT FRAMEWORKS.

43. It has been assumed in this investigation that every member of the framework can sustain either tension or compression. But in practice it may happen (*e.g.*, in the hulls of rigid airships) that wires instead of stiff compression members (struts) are employed for bracing the rectangular panels of a tubular framework, and then we have the problem mentioned in § 3,—of stress determination in a pseudo-redundant framework.

We observe, in the first place, that the stresses given by our solution may (on the basis of Hooke's Law) be superposed on any stresses which are present initially as the result of self-straining (§ 2). When crossed wires are employed as bracing members, they can be easily strained to any desired tension; and if in any wire this initial tension is greater than the compressive action which is imposed by the external loads, the resultant action will still be tensile, and the wire will continue to function.* When the compressive action is known, the requisite initial tension can be deduced and applied; it is, of course, necessary to take account, in design, of the stresses which this process of initial self-straining will impose on other members.

44. But the problem of the "pseudo-redundant" framework (in which self-straining has not been employed) still remains for discussion. Its difficulty

* Cf. 'Aero. Res. Ctee. Rep. and Mem.,' No. 800, § 6; also No. 1057, § 3.4 *et seq.*

lies in the fact that usually we cannot say in advance which of a given pair of diagonal wires will slacken (as being unable to sustain compression) under a given system of loading.

To meet this difficulty I suggested in 1924* a procedure which has come to be known as the "device of the separate panel." Let us suppose that we have a panel ABCD, fig. 2, of which the diagonals AC and BD are flexible wires, and that a solution obtained on the lines (*e.g.*) of the present paper indicates a compressive action in the wire BD. Actually this compressive action cannot be sustained, and accordingly there will be a readjustment of stresses, which in general will extend to every member of the framework, the procedure suggested was to assume (as an approximation) that the readjustment is confined to those members which form the braced panel ABCD.

On this understanding, the failure of BD to withstand a compressive action P (which evidently has the same effect as the imposition of equal and opposite forces P tending to bring B and D together) is to be taken into account by making compressive additions to the calculated actions in AB, BC, CD, DA, and a tensile addition to the calculated action in AC. The necessary additions are easily calculated; when the panel is rectangular (as in the problem of this paper), and if the compressive action which our solution would predict for BD is represented by a (negative) tension coefficient T for that member, the additions to the tension coefficients for AB, BC, CD, DA are given by T (*i.e.*, they are compressive) and the addition to the tension coefficient for AC is $-T$ (*i.e.*, it is tensile).

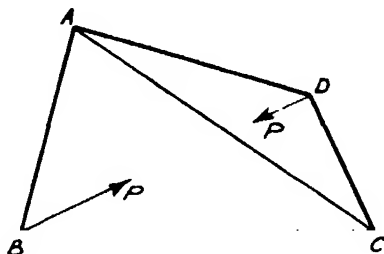


FIG. 2.

45. We now consider the accuracy of this approximate solution; that is to say, the accuracy with which we can say that members of the framework other than those comprising the panel ABCD will be unaffected by the readjustment of stress. It is evident that the other members would in fact be unaffected if the readjustment involved no change in the lengths of AB, BC, CD, DA, AC, therefore our procedure would lead to exact results if, simultaneously with the readjustment (which causes AB, BC, CD, DA to shorten and AC to lengthen), the side members of the panel were lengthened, and the diagonal member AC were shortened, by suitable amounts.

* Cf. 'R. and M.' No. 1057, § 3.6.

For any member the amount in question is, by (6) of § 7,

$$le = \frac{T}{l\Omega},$$

this being the extension which it undergoes when subjected to an action which imposes a tension coefficient T . Knowing Ω for every member, we can thus estimate the accuracy of our assumption in terms of the changes in length which it (virtually) ignores.

46. Considering the question in this way, we can arrive at an important conclusion. The greater the number of panels to which our suggested procedure is applied, the more nearly does the resulting framework reduce to a "simple frame"; and in a simple (*i.e.*, a statically determinate) frame small changes in the lengths of the constituent members (such as we considered in the last paragraph) are without effect on the stresses. Accordingly the "device of the separate panel," although it may lead to sensible inaccuracies if only partially applied, can be employed with some confidence to predict the occurrences in a framework when many wires have gone slack, as will happen when the framework is close to failure. It has the further merit that it can be applied in conjunction with generalized solutions, such as have been obtained in the first part of this paper.

Summary.

Stress determination in frameworks has been developed mainly by graphical methods, and in consequence there has been a tendency to fix attention on problems in two dimensions. An alternative (analytical) method of treatment has been found useful in relation to the structural problems of aeronautics, which are largely three-dimensional; it has the further advantage that problems can be treated in a general manner, and solutions of wide applicability obtained.

An example is given in this paper; exact solutions can be found for a tubular framework (generally representative of a rigid airship hull, or of a fuselage of "monococque" construction) when definite (self-equilibrating) forces are specified as acting on the joints. This problem (on account of the high order of redundancy of the framework) would be quite intractable by conventional methods; but here no appeal is made to considerations of strain-energy, solutions being constructed by synthesis from "type solutions" which are fully investigated.

In the concluding section of the paper a procedure is described whereby its solutions may be extended to "pseudo-redundant" frameworks, in which some of the constituent members are incapable of sustaining compression. It is shown that the procedure will give sufficiently accurate results under the conditions which immediately precede failure,—namely, when many such members have become inoperative.

Fluorescent Excitation of Mercury by the Resonance Frequency and by Lower Frequencies.—V.*

By Lord RAYLEIGH, For Sec R S.

(Received December 6, 1932.)

[PLATE 14.]

§ 1. *Introduction.*

It was shown at an early stage of the present work† that the characteristic fluorescence of mercury could be generated by wave-lengths much longer than the resonance line λ 2537; indeed, its excitation was traced as far as λ 3450. It was found also that the primary excitation by atomic absorption (core of the resonance line) could be distinguished from excitation by molecular absorption (wing of the resonance line).

Although in the case of the longer waves it appears certain that the excited systems produced in the first instance by absorption are molecules and not atoms, yet it is possible that subsequent dissociation, or excitation by collision might lead to the formation of excited atoms in a secondary way.

In examining the persistent luminosity produced by core excitation, it was found that large numbers of $2\ ^3P_0$ atoms, and, what was very surprising, $2\ ^3P_2$ atoms as well, were present,‡ and it was thought very probable that the long life of $2\ ^3P_0$ atoms was the cause of persistent luminosity in this case, whatever might be the nature of the subsequent transformations. It is obviously impor-

* I, 'Proc. Roy. Soc.,' A, vol. 125, p. 1 (1929); II, 'Proc. Roy. Soc.,' A, vol. 132, p. 650 (1931); III, 'Proc. Roy. Soc.,' A, vol. 135, p. 617 (1932); IV, 'Proc. Roy. Soc.,' A, vol. 137, p. 101 (1932).

† I, p. 5.

‡ IV, pp. 106–110.

tant to examine whether this persistence occurs when we excite well away from the resonance line, and to determine definitely whether or not excited atoms take any part in the process.

Some may be tempted to rule out at once the possibility that 2^3P_1 atoms can be formed when the exciting frequencies are less than corresponds to the excitation potential of these atoms. Since finding that the resonance line λ 2537 can excite Wood's bands 2345, etc., the "forbidden" line λ 2270, and also the complete line spectrum,* I have felt that such questions should be cautiously approached.

If 2^3P_1 atoms were formed at all at any stage of the changes which follow on absorption, some of them might perhaps have a complex career, taking part in the formation of metastable atoms or of excited molecules. Others would die an early death in radiating the resonance line λ 2537·52, thereby indicating the presence of their species. The presence or otherwise of this line will therefore be the test of whether 2^3P_1 atoms enter into the question or not.†

§ 2. *Excitation of the Mercury Resonance Line by Iron Lines in the Neighbourhood.*

It was found in earlier work that the iron arc, unfiltered, can give rise to the resonance line in mercury vapour.‡ It was also found that if the iron line 2536·82 was filtered out by a preliminary mercury vapour cell, the resonance line was still obtained, the nearest remaining iron line being 2537·18, 0·66 Å. from the resonance line. These experiments clearly proved, contrary to what had been supposed up to then, that the resonance line could be excited, whether by a direct or indirect process, without accurate coincidence with the exciting frequency. Beyond this point the investigation was not then pushed. Further work is now to be described, showing what are the limits.

In order to remove progressively the iron lines, nearest the resonance line, a mercury vapour filter was used. This was in a cylindrical cell with flat ends 3·5 cm. apart. It was placed in a heating coil wound on a tube considerably longer than the cell itself, and was kept free from condensed mercury by

* III, pp. 623, 625; IV, p. 110.

† Under certain circumstances, e.g., in the presence of hydrogen, 2^3P_1 atoms may be so quickly de-excited by collision that they cannot show their presence by emitting λ 2537·52. Since in the present case this radiation *can* appear when excitation is near the resonance line we may fairly conclude that there is nothing in the conditions to invalidate the test.

‡ I, pp. 6 and 7. Also Plate 1, facing p. 16, reproductions IX and X.

making it permanently hotter than the lateral tube containing the supply of liquid mercury. The temperature of the latter was controlled by an independent heating circuit. By varying the measured current in this circuit the extent of the absorption band could be controlled, and brought back again to a former value. It was not necessary to attempt any actual measurement of temperature. The cell contained hydrogen gas at 30 cm. pressure measured at room temperature. The advantage of adding hydrogen is that it makes the absorption band more symmetrical, so as to cut out some of the iron lines near the mercury resonance line on the short wave side. It is desirable to avoid any possible complication from these lines, even though none would be expected.

In this particular experiment, it is not necessary to take precautions against stray light from the walls of the vessel, since we are only looking for light of the mercury line. This line is not present in the source. There is no trouble in this region of the spectrum from fluorescence of the silica walls, and the mercury vapour filter provides a dark gap in the spectrum, free for the mercury line to appear in even if there is a good deal of stray light. On the other hand it is desirable to have no dead space of unilluminated mercury vapour for the secondary radiation to pass through. The conditions are met by a silica flask with a small tubulus, its sealed end blown clear (fig. 1). The flask contained a little mercury boiling under an atmosphere of nitrogen at 2 cm. pressure. The tubulus was kept warm enough to prevent condensation. For this purpose a *very* small hydrogen flame was placed some way below it. The image of the iron arc was focussed on the end of the tubulus, and the spectrum photographed laterally with a small instrument, taking the light from near the end where the beam enters. Preliminary experiments without the mercury filter proved that a pressure of about 2 cm. of mercury gave the resonance line most brightly under the conditions, and this pressure was used throughout.

The behaviour of the mercury vapour filter was tested directly in an inde-

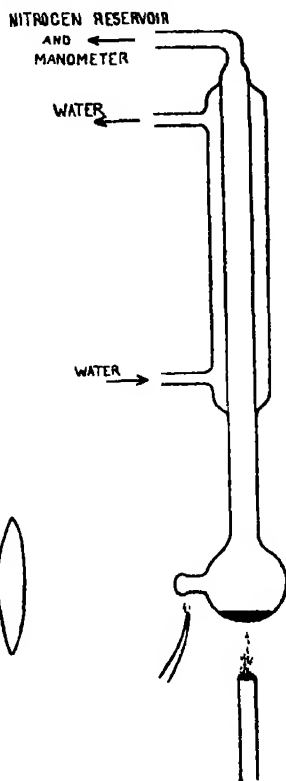


FIG. 1.

pendent experiment by taking the spectrum of the iron arc through it with a medium size Hilger spectrograph. The results of the experiment were as below.

Heating current.	Iron line next to resonance line.		Resonance line.
	Short wave side.	Long wave side.	
amps. 2.1 2.6	A. 2.9 5	A. 2.3 8	Strong, 16 minutes exposure Absent, 1 hour exposure

It will be understood, of course, that the line is very much stronger still when the mercury filter cell is not in use at all.

We may conclude then that while 2^3P_1 atoms are formed to some extent when excitation is at 2.3 A. on the long wave side of the resonance line, they are not formed in appreciable numbers when the interval is increased to 8 A. Since the green fluorescence can be detected as much as 900 A. from the resonance line it appears that over nearly the whole of this range we have nothing to do with 2^3P_1 atoms.

Another consideration pointing strongly in the same direction is that the green visual fluorescence excited by the iron arc is not extinguished or apparently affected by the addition of hydrogen gas even in large amount.* Now hydrogen certainly destroys 2^3P_1 and 2^3P_0 atoms very effectively.† It would seem, therefore, that neither of these kinds of atoms can enter into the matter to any appreciable extent. Further evidence on the point will follow later in this paper.

§ 3. *Persistence of Luminosity in Molecular Excitation. The Maximum at λ 3300.*

It was shown‡ that in a moving current of vapour the fluorescence is carried away from the point of excitation and along the vapour stream, somewhat similarly, whether the cooled mercury lamp (core excitation, atomic excitation) or the hot lamp (wing excitation, molecular excitation) was used. In these experiments, however, the active wave-lengths were not more than 1 A. in excess of the resonance wave-length. As we have seen 2^3P_1 atoms are

* II, p. 653.

† E. Meyer, 'Z. Physik.,' vol. 37, p. 639 (1926).

‡ I, pp. 15-16. Also Plate 2 of the same paper.

produced in this region of excitation.* To examine the purely molecular phenomena without any complication, it is desirable to work considerably further off from the line.

The difficulty of this is that denser vapour is needed, because of the rapidly falling absorption for longer waves; and the arrangements hitherto used do not lend themselves to experimenting with dense vapour.

High linear velocities and considerable density of vapour are by no means incompatible, but the necessary conditions require attention. To attain high velocity the vapour must be allowed to expand to, say, one-half of its original density. This expansion should occur at a short narrow passage or nozzle separating the high from the low pressure regions, so as to avoid frittering away the kinetic energy generated.†

In this nozzle the optical excitation may be applied, for then the density will still be high and the motion is becoming rapid. Since the amount of exciting light utilized by absorption will depend on the mass of vapour traversed, the vapour issues in the form of a jet into the lower part of the casing when it can be observed through the casing walls. The casing is prolonged below in a round silica tube 2 cm. in diameter. This is connected by a large rubber tube to a pyrex glass flask, to receive the condensed mercury. A side tube leads to pump and manometer so that the pressure of gas (nitrogen) under which the mercury condenses can be regulated. Condensation is in the vertical tube. This and the rubber joint are wrapped round with lead pipe 1.5 mm. inside diameter, through which a stream of cold water passes.‡

It was necessary to guard against premature condensation in the silica connecting tube between the flask and the nozzle. This tube§ was wound with nichrome wire and lagged, so that it could be kept warm by a small electric current. If it was desired to superheat the issuing vapour this current could be increased so as to raise the connecting tube to a full red heat, or more.

To prevent condensation on the walls of the square casing, a ring of small

* They do not, however, move with the stream to the same extent as the green fluorescence.

† The highest velocities are realized by de Laval's expanding nozzle, but this refinement is not necessary or convenient of application in the present case.

‡ The rubber joint in the actual construction gave occasional trouble, but if the silica tube had been prolonged to say 20 cm. instead of only 7 cm., most of the heat would have been taken out before the rubber was reached, and the latter would not have been liable to get overheated.

§ This tube is shown in the main figure as coming away in a plain parallel to the sides of the square nozzle and casing. This is only for convenience of representation; the connecting tube and boiler were in reality placed diagonally, as represented in plan in the inset.

hydrogen flame was arranged round the silica tube just below the casing as shown. The hot gases rising from these produced the desired result, while the light from the flames was almost inappreciable.

Using these arrangements, and exciting with the iron arc filtered through 15 cm. length of chlorine and 6 cm. of bromine vapour, a green jet of luminous mercury vapour could be observed issuing from the nozzle into the square casing below. This jet preserved its diameter without showing much tendency to get lost in the surrounding vapour space, and is seen well away from the

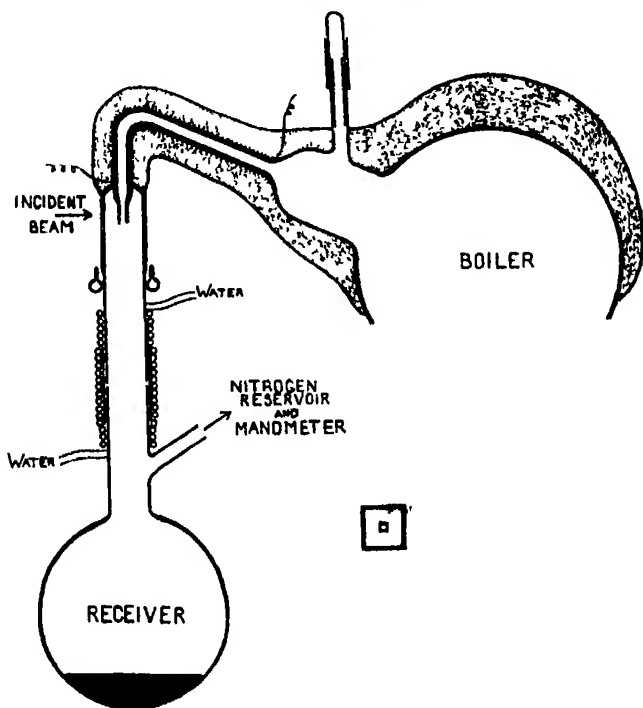


FIG. 2.

surrounding silica walls. This last feature is of special advantage for avoiding false light.

The issuing jet of vapour may be with or without a periodic structure along its length. Figs. 4 and 5 on Plate 14 (actual size) show the distinction, though they are given for a different purpose, and are not taken under conditions otherwise comparable. The periodic structure is only developed when the pressure behind the jet is more than about double* the pressure of

* The exact ratio is given by $\left(\frac{2}{\gamma-1}\right)^{\frac{\gamma}{\gamma-1}}$, when γ is the ratio of specific water. The value is 1.90 for air, and 2.05 for mercury.



FIG. 4



FIG. 5

the outside atmosphere into which the jet emerges. In such a case the velocity of the jet will be the velocity of sound under the prevailing conditions, and stationary sound waves appear, causing alternate swellings and contractions along the length of the jet.

It was found that the output of vapour from the boiler was enough to give a jet with periodic structure if the outside pressure was 3 cm., and by pushing the heat it would doubtless have been possible to go somewhat further; but a pressure of 1 cm. was the most suitable for this phenomenon. When, as occasionally happened, there was momentarily an abnormal density of vapour due to percussive boiling ("bumping"), the periodic luminous column appeared to be stretched, the linear period being for the moment increased. On increasing the gas pressure in the receiver or diminishing the heat under the boiler, the jet lost its periodic structure as in fig. 5, Plate 14. For a further discussion of these periodic phenomena, a paper by my father, the late Lord Rayleigh, may be consulted*. In the present work they are only of casual interest, though the method of exhibiting them by a self luminous vapour is a pleasing one. In experimenting with an air jet the shadow method has been used to show the periodic structure.

To examine the phenomenon of persistence as dependant on the excitation frequency, the exciting beam was filtered through the hot mercury cell (see above, § 2) in addition to the chlorine and bromine filters. Keeping the nitrogen pressure in the receiving vessel at 7 cm. of mercury, the green luminosity of the issuing jet was quite bright, and perceptible even in a fully lighted room. The mercury in the filter cell was then made denser, until the absorption extended 8 Å. from the resonance line towards long waves; the issuing vapour still showed strongly by its green light.

The vapour was then superheated by raising the silica tube from the boiler to bright redness. This caused the green luminosity due to the continuous maximum 4850 to fade out, the issuing jet becoming nearly or quite invisible. Although invisible the jet could be photographed using a filter of 6 cm. of bromine vapour combined with 1 mm. of blue uviol glass over the camera lens. This compound filter is completely opaque to the visual maximum 4850, and indeed to all visible light except the extreme red. It is designed to transmit the spectral region of the continuous maximum 3300. The exposure was 4 minutes, using an aperture of $f/12$. The result is shown in fig. 5, Plate 14.

There was little doubt, considering the circumstances of the experiment, that

* 'Phil. Mag.', vol. 32, p. 177 (1916); 'Collected Sci. Papers,' vol. 6, p. 407.

the invisible jet thus photographed did in fact reveal itself by the light of the continuous maximum λ 3300. To make certain, a spectrum of the issuing jet was taken, placing the slit of the spectrograph horizontally, and allowing a narrow reduced image of the jet to pass perpendicularly across it. The radiation of the invisible jet was thus found to consist of the continuous maximum 3300 as expected.

It is proved then that 3300 shows persistence even when the excitation is 8 A. or more away from the resonance wave-length, and under conditions when 4850 does not appear at all.

§ 4. Persistence of the Green Visual Fluorescence, when Excited by Long Waves.

As already mentioned the green fluorescence (4850) and the maximum 3300 can be excited with waves very much longer than those used in the above experiments, but the experimental difficulties of demonstrating persistence increase rapidly with the wave-length. I have, however, been able to go further with 4850. This work was done earlier, and with different apparatus, not adequate to the continuous working which is necessary for photography. The general principle was the same, but the nozzle which was directed upwards, consisted of a hole of 1.5 mm. diameter in an iron plate. This plate closed

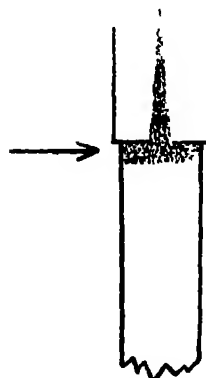


FIG. 3.

the end of a silica tube 5 mm. in diameter. The iron plate was bent as shown (fig. 3) so as to screen the issuing vapour from the exciting light coming from the left. The latter was focussed on the wall of the silica tube inside which the vapour was at the higher pressure. The mercury was raised to boiling point while a nitrogen pressure of 1 atmosphere was kept in the outer space. On reducing the outside pressure (usually from 76 to about 56 cm.) a jet of vapour squirted up from the hole and showed the green fluorescence. In successive experiments the excitation frequency was progressively lowered by suitable filters. The green jet was still observed to come out when the source was filtered by benzene in alcohol, giving a minimum

wave-length of about 2650, and by "vita" glass, giving about 2850. In the latter case it was faint, though not at all doubtful. With a sheet of ordinary glass, cutting at about 3200, the green fluorescence could no longer be seen.

These experiments show that the visual fluorescence is persistent, even when

the excitation is 300 Å. on the long wave side of the resonance line. The persistence of 3300 has only been traced 8 Å. away from this line; but naturally the difficulty of working with invisible radiation is greater. In all probability its behaviour is the same as that of 4850 throughout.

§ 5. *Direct Test for 2^3P_0 Atoms in the Jet.*

Reasons for considering that excited atoms are not concerned in these cases have already been explained in § 2. It was thought of interest, however, to apply the test for 2^3P_0 metastable atoms which succeeded so well in the case of persistently luminous vapour produced by core excitation.* In that case it was found that the jet of vapour was locally enhanced in luminosity when light of wave-length 4047 Å. from a supplementary source (mercury arc with violet filter) was focussed upon any part of it. The enhancement consisted of monochromatic green light of wave-length 5461,† and the interpretation of it is that 2^3P_0 atoms were initially present and had been further excited to the level 2^3S_1 by absorption of the violet line.

In the same way 2^3P_1 atoms when present are raised to 2^3S_1 by absorption of the blue line.

The method was applied in the present case, using the arrangements as above described, and bringing in the supplementary illumination from the right. The tests were carried out at pressures in the casing ranging from 20 mm. down to 2·5 mm. both without superheat, and with enough superheat to extinguish the green luminosity. The results were entirely negative, no trace of the enhancement being even suspected. Since both the violet and blue lines were in use the negative result indicates the absence of a sensible number of either 2^3P_0 or 2^3P_1 atoms.

§ 6. *General Conclusions*

The work described seems to establish satisfactorily that when mercury is made fluorescent by wave-lengths more than a very few Angstroms longer than the resonance line, the processes occurring do not at any stage involve free excited atoms, metastable or otherwise. The excited systems are molecules, and molecules only.

* IV, p. 108 and reproductions Nos. VIII and IX.

† No doubt 5461 was accompanied by the other numbers 4358 and 4047 of the triplet, though these are visually much less conspicuous, and were not looked for.

If we adopt the view that 3300 is the radiation from 2^3P_1 molecules, which has been urged especially by H. Kuhn,* it would follow that molecules of this kind can travel several centimetres under gaseous pressure before their life is over. The velocity is necessarily less than that of sound, and the life in the excited state of the order of 10^{-4} seconds, a duration which has generally been considered to belong only to metastable states. The corresponding state of the atom is, of course, not metastable, and its duration is estimated at about 10^{-7} seconds.†

It might possibly be attempted to avoid this conclusion by urging that the long life really resides in 2^3P_0 molecules, which, according to the theory mentioned, are the radiators of the green visual light belonging to the maximum usually called 4850. 2^3P_1 molecules would then be regarded as generated only at the last moment, and some auxiliary hypothesis would be necessary to explain the increase of potential energy involved in the transformation. But apart from this difficulty, any view of the kind seems to be excluded by the condition of the actual experiment as described in § 3. By keeping the vapour hot, the emission of 4850 was prevented, and presumably also the formation of the kind of molecules which emit this radiation. We have only to do with molecules which emit 3300. The conclusion that these molecules are of long duration appears to be unavoidable even if it is difficult to reconcile with their assignment to the state 2^3P_1 .

§ 7. *Summary.*

On exciting mercury vapour to fluorescence by wave-lengths longer than the resonance line, it is found that this line is emitted to some extent when the nearest exciting wave-length is 2·3 Å. longer than the resonance line, but not when it is 8 Å. longer. In the latter case 2^3P_1 atoms are not formed either initially or in the course of subsequent changes. 2^3P_0 atoms are also shown to be absent. It is concluded, therefore, that with this kind of excitation the mechanism of fluorescence producing the 3300 and 4850 maxima is concerned solely with excited mercury molecules.

It is shown that in this case of molecular excitation both the maxima are "persistent" that is to say the gas remains luminous long enough to travel under a pressure gradient several centimetres away from the place of excitation. When the vapour is considerably superheated, 3300 alone is emitted, and shows persistence. Without superheat, 4850 appears with little of 3300,

* 'Z. Physik,' vol. 72, p. 462 (1931).

† Ladenburg and Wolfssohn, 'Z. Physik,' vol. 65, p. 207 (1930).

and this too is persistent. If as has been supposed, these maxima are attributable to 2^3P_0 and 2^3P_1 states of the molecule respectively, it is clear that persistence cannot be peculiar to the states which in the atom are metastable, but occur also in the 2^3P_1 molecule.

Incidentally, it is shown that self-luminous mercury vapour issuing through a nozzle from a region of high to low pressure, with the velocity of sound, shows very beautifully the stationary vibrations which are usually investigated by a shadow method, using an air jet.

On the Refractivity of Para-Hydrogen.

By CLIVE CUTHBERTSON, O.B.E., F.R.S., and MAUDE CUTHBERTSON.

(Received December 9, 1932.)

In the paper by K. F. Bonhoeffer and P. Harteck* published in 1929, on para-hydrogen, no mention is made of the refractive index of the new modification, and, so far as we can find, no experiments on this subject have hitherto been published. It may, therefore, be presumed that, on the hypothesis which led to the discovery of the para-form, no change of index was expected, and, on any theory, it seemed probable that the change would be very small. It appeared worth while, however, to make use of a Jamin interferometer already set up for other purposes to test this point experimentally and the following paper records the result of the investigation.

Para-hydrogen was prepared by adsorbing ordinary hydrogen, purified by previous adsorption in palladium, in charcoal at the temperature of liquid oxygen ($-183^\circ \text{C}.$). After $1\frac{1}{2}$ to 2 hours the gas was allowed to warm up, and should then consist of approximately 50 per cent. ortho- and 50 per cent. para-hydrogen. In order to test whether this was actually so Schleiermacher's method of measuring the thermal conductivities of the two forms, as described in Bonhoeffer and Harteck's paper, was followed. In their case a Wollaston wire (0.01 mm. diameter) was stretched in a narrow cylindrical tube immersed in liquid hydrogen, and the change in the resistance of the wire, which was electrically heated to 200° absolute, was observed when para- was substituted for ordinary hydrogen at the same pressure (40 mm.). In these circumstances the resistance varied between 111.85 ohms for ordinary hydrogen to 106.25 for hydrogen containing 99.7 per cent. para-hydrogen.

* 'Z. phys. Chem.,' B., vol. 4, p 113 (1929)

When liquid air was used for cooling both the charcoal and the measuring tube the resistance varied from 112.96 ohms for ordinary hydrogen from a cylinder to 111.13 for a mixture containing about 50 per cent. para-hydrogen, a change of 1.62 per cent.

In our apparatus the diameter of the wire was 0.02 mm. and in other respects the dimensions were different from those of Bonhoeffer and Harteck. Liquid hydrogen not being readily available liquid oxygen was employed, and the resistance of the wire was measured over a range of pressures from 2 to 10 cm. The resulting graphs of resistance plotted against pressure, though not pretending to a high degree of accuracy showed a reduction of resistance, when the adsorbed gas was substituted for ordinary hydrogen, of 1 part in 70, or 1.43 per cent. Whether the difference between this ratio and that obtained by Bonhoeffer and Harteck (1.62) is due to differences in the dimensions of our apparatus or to failure to obtain as high a percentage of para-hydrogen as they did we do not decide. Possibly the use of liquid oxygen instead of liquid air accounts for the difference. But, in any case, our values indicate the presence of about 47 per cent. of para-hydrogen in the gas employed, and this sufficed for our purpose.

In the refractivity measurements freshly prepared para-hydrogen 47/53 was allowed to warm to the temperature of the room and measurements were immediately made of its refractive index. The refractometer tubes were 103.9 cm. long, the approximate pressure change during an experiment was 35 cm. of mercury and the approximate number of bands counted 120. With these data, and with pressures read to 0.1 mm., temperatures to 0.1° C. and bands to 0.1 it should be possible to measure the refractivity of a gas to 1 part in 1400, *i.e.*, to determine the fourth significant figure of the refractivity (0.0001396). To obtain the fifth figure accurately would involve an amount of labour incommensurate with the present value of the result; but by taking the mean of a number of experiments a fair approximation may be obtained.

The refractivity of ordinary hydrogen has often been measured, and some of the more recent results for the green mercury line are shown below :—

Date.	Observer.	($\mu - 1$) 10^8 .
1896	Perreau	13925
1907	Scheel	13916
1909	C. and M. Cuthbertson	13971
1912	J. Koch	13966
1921	Kirn	13965
1923	Schackerl	13965

From these figures it appears certain that the true value lies between $(1396)10^{-7}$ and $(1397)10^{-7}$ and J. Koch's value $(13966)10^{-8}$ may be accepted as very nearly correct.

Numerous observations were made by us, both with the short glass tubes mentioned above and with brass tubes (length 274.06 cm.) previously used for measuring the refractive index of neon. For ordinary hydrogen the mean of 14 double experiments (pressure falling and rising) was $(13964)10^{-8}$, a result sufficiently near to Koch's value to test the accuracy of the experimental arrangements and the purity of the gas.

For freshly prepared para-hydrogen a preliminary series of 14 double experiments gave the mean value of $(13971)10^{-8}$. A final series of six experiments, which we consider much more trustworthy than the preliminary series, gave the following values.—

$(\mu - 1)10^8.$		$(\mu - 1)10^8$
13963		13971
13963		13960
13977		—
13959	Mean	13965
		—

The difference between this value and Koch's value for ordinary hydrogen is within the limits of experimental error, and we conclude that if there is any difference between the refractivities of ordinary hydrogen and hydrogen recently adsorbed in charcoal at the temperature of liquid oxygen, and containing about 47 per cent. of para-hydrogen it does not exceed 2 or 3 parts in 14,000.

In these experiments the gas came into contact with mercury, tap grease, brass (in the early experiments) and cotton wool (in the bore of a tap). The light used was a mercury arc in quartz, but covered by a thick glass plate.

It was, therefore, necessary to enquire whether any of these materials could have retransformed the para-hydrogen into ordinary hydrogen before the refractivity measurements could be completed and so rendered the experiments futile.

With regard to the mercury arc Senftleben* states that, in the presence of a trace of mercury, irradiation by the mercury line (λ 2537) quickly transforms para- to ortho-hydrogen. Glass is opaque to this wave-length, but in order to test whether any of the light to which it is transparent could have had the same

* 'Z. phys. Chem.,' vol. 4, p. 169 (1929).

effect in our experiments a thermal conductivity experiment was made, first with freshly prepared para-hydrogen and, later, with the same gas after it had been illuminated by the shielded mercury arc for 15 minutes. No change of resistance in the wire was observed.

The absence of any catalytic effect in cotton wool was proved by allowing the gas used in one of the refractivity experiments to flow into the tube without passing through the tap in question. No difference was observed. The possible influence of brass tubes is disposed of by the observation that the early series of experiments with brass tubes did not give different results from those in which brass was not used.

Tap grease was evidently used in the German experiments without detrimental results, and the gas used in our thermal conductivity experiments, which gave positive results, passed through two or three greased taps.

It was considered whether it would be desirable to repeat these experiments with gas adsorbed in charcoal at the temperature of liquid hydrogen, containing 99.7 per cent. of para-hydrogen. But in the absence of any positive result in this research it was not thought worth while to pursue the matter further at present.

Our thanks are due to the Director of the Davy-Faraday Research Laboratory and the Managers of the Royal Institution for permission to carry out the work in that laboratory, and to the staff of the laboratory for much help. We have also to thank Dr. H. Lowery of the College of Technology, Manchester, for suggesting the subject of this interesting investigation.

Summary.

Para-hydrogen was prepared by adsorption of pure hydrogen in charcoal at the temperature of liquid oxygen, and the refractive index of a mixture of about 47 per cent para- to 53 per cent. ortho-hydrogen was measured.

It was found that, at the temperature of the room, for the green mercury line, the index does not differ from that of ordinary hydrogen. The limits of error of the experiments were about 3 parts in 14,000.

The Combination of Hydrogen and Oxygen in a Silver Vessel.

By C. N. HINSHELWOOD, F.R.S., E. A. MOELWYN-HUGHES and A. C. ROLFE.

(Received December 13, 1932.)

As is now well known, reaction chains may play a prominent part in the combination of hydrogen and oxygen. The region of temperature in which the chain processes are important is limited. Below it, the combination takes place exclusively on the walls of the vessel, while above it the reaction is so rapid that it ceases to be isothermal in any sense and passes into explosion.

In vessels of silica or porcelain* the development of a non-explosive reaction in the gas phase occurs between about 540° and 600° C. The characteristics of this reaction are first, a very pronounced dependence of rate upon pressure—for example under some circumstances the rate may vary as the cube of the hydrogen concentration; secondly, sensitiveness to the accelerating influence of inert gases, including steam; and thirdly, an extremely marked increase in rate as the diameter of the vessel is increased.

The last two characteristics show that the chains propagating this particular mode of reaction are terminated principally at the wall of the vessel. The action of the walls depends upon the deactivation of active molecules, or more probably upon the destruction in a definite chemical reaction of certain species normally responsible for continuing the chains. As examples of possible reactions we may take the decomposition of hydrogen peroxide, or the recombination of hydrogen atoms or of hydroxyl radicals. All these processes would be very sensitive to surface catalysis. If the vessel wall actively promotes them the rate of the reaction in the gas will be kept small.

The chain breaking power of metals is probably very different from that of silica or porcelain; thus a correspondingly changed development of the gas reaction must be anticipated. The experiments described below show that in a silver vessel there is little sign of effective chain propagation in the gas up to 700° C. Above this temperature the rate of the surface reaction is too great for further investigation to be possible. The chain-breaking efficiency of silver appears therefore to be very high, a result which is not surprising, when the possible chemical reactions between silver oxide and hydrogen atoms or hydrogen peroxide are taken into consideration.

In silica or porcelain vessels from about 450° C. upward a peculiar kind of

* Hinshelwood and Thompson, 'Proc. Roy. Soc.,' A, vol. 118, p. 170 (1928); Gibson and Hinshelwood, *ibid.*, vol. 119, p. 591 (1928).

explosion occurs if the pressure of the hydrogen-oxygen mixture lies between two definite limits.* Outside these limits, at the lower temperatures at least, the rate of reaction is very slow indeed. Explanations of the phenomenon in terms of the theory of "branching chains" have been suggested, and account satisfactorily for the known facts. It is interesting to note that in the silver vessel this explosion does not occur at all.

The apparatus used for the experiments was similar to that described in previous papers, except for the silver vessel. This was cylindrical, of length 10 cm., diameter 5 cm., and with a narrow neck about 20 cm. long, ending in a flange to which a corresponding ground-glass flange could be cemented. Below the flange was a small cooling jacket, welded to the neck. Through this was circulated water at such a temperature that heat conducted from the furnace did not disturb the cementing of the flanges and steam produced in the reaction did not condense in the neck of the vessel. The whole arrangement was perfectly vacuum tight.

The catalytic activity of the smooth silver surface was small enough to allow working up to 700°, and differed qualitatively as well as quantitatively from that of the active preparations of silver used by Benton and Elgin† at lower temperatures. This difference is not at all surprising in the light of the observations of Chapman and others on the complex and varied behaviour of silver-silver oxide surfaces. As was to be expected the catalytic efficiency of the bulb varied with use. But throughout the investigation this was controlled by "blank" experiments under standard conditions, as will be evident from the tables of results.

At 650° where the rates in a silica vessel would usually be far too great to measure, the reaction was still fairly slow; even at 700° it was easily measurable. The figures in Table I show the course of a typical experiment.

Table I.—700° C. Initial pressure of hydrogen 200 mm., initial pressure of oxygen 100 mm.

Time in seconds.	Change of pressure in mm.
26	10
37	15
48	20
75	30
102	40
137	50
177	60

* Thompson and Hinshelwood, 'Proc. Roy. Soc.,' A, vol. 122, p. 610 (1929).

† 'J. Amer. Chem. Soc.,' vol. 48, p. 3027 (1926).

For each experiment a curve was drawn from which the initial rate of reaction, expressed as millimetres pressure change per minute, was read off.

Both at 650° and at 700° the rate is almost independent of the concentration of hydrogen, and is nearly directly proportional to the concentration of oxygen.

The experiments in Table II are recorded in the order in which they were made.

Table II.—Temperature 700°.

Initial pressure of hydrogen mm.	Initial pressure of oxygen mm.	Initial rate. mm per min.
201	99	29.8
202	196	52.5
202	100	30.0
301	100	27.6
200	103	28.9
400	100	26.3
200	100	26.8
202	53	14.2
200	100	30.0
197	28	6.7
202	98	26.6

From these numbers Table III can be compiled.

Table III.

p_{O_2} constant at 100 mm.		p_{H_2} constant at 200 mm		
p_{H_2}	Rate.	p_{O_2}	Rate.	Rate/ p_{O_2}
201	28.7	196	52.5	0.268
301	27.6	100	28.7	0.287
400	26.3	53	14.2	0.268
		28	6.7	0.239

Table IV.—Temperature 651°.

p_{O_2} constant at 101 mm.		p_{H_2} constant at 201 mm.	
p_{H_2}	Rate.	p_{O_2}	Rate.
201	7.95	99	7.10
404	9.55	197	12.7
202	7.35		
299	7.90		

There is no sign of the appearance of the high order reaction which becomes prominent in silica or porcelain vessels of corresponding dimensions at temperatures as low as 540°.

Neither steam nor nitrogen have the accelerating influence which they exert under conditions where the effective development of chains is possible. The action of steam is somewhat to retard the combination.

Table V.—Temperature 700°.

p_{H_2}	p_{O_2}	p_{N_2O}	Rate.
200	100	0	27.3, 29.0, 25.8, 26.8
202	99	25	25.0
202	100	50	22.8
200	96	53	19.7
198	98	100	23.7

The rate is not seriously altered by the presence of nitrogen. In three experiments at 650° with 200 mm. hydrogen and 60 mm. oxygen the initial rates were 16.2, 15.6 and 13.2 mm./min. while in two experiments with 234 and 254 mm. nitrogen respectively, and alternating with the "blanks," the rates were 13.2 and 17.4. A similar excess of nitrogen would increase the rate of the chain reaction in a silica vessel by several hundred per cent.

Mixing hydrogen and oxygen in the vessel at a relatively high pressure and then slowly evacuating failed to reveal any sign of the "low pressure" explosion. The experiment was repeated at a number of different temperatures. Since in silica vessels it is apparently the surface which gives rise to the first centres necessary for chain propagation,* the experiment was next made by placing a thin silica rod in the silver vessel. There was still no sign of an explosion at any temperature between 530° and 650°. As far as it goes this experiment seems to show that the absence of explosion in the silver vessel can be explained by the great deactivating influence of the silver-silver oxide surface, without assuming inability of the silver to provide the right kind of centres for starting the reaction.†

* Alyea and Haber, 'Z. phys. Chem.,' B, vol. 10, p. 193 (1930).

† The mode of action of centres on the surface, in particular the question of the extent to which they can be regarded as isothermal, is being discussed in another paper, dealing with the explosion phenomena in vessels of alumina and other materials. For this reason discussion of the influence which the thermal conductivity of the silver may exert, is postponed.

The next series of experiments consisted in the introduction of silver and other metal wires into a silica vessel to see whether they would prevent explosion. They often did prevent it, but unfortunately this result proved to be ambiguous. The catalytic action of the wires was great enough to give rise to appreciable amounts of steam during the time of an experiment, and steam itself can stop the explosion.* Thus little weight can be given to this particular result. Nevertheless it is perhaps as well that the experiment should be recorded.

We are indebted to the Royal Society and to Imperial Chemical Industries, Ltd., for grants with which apparatus for these experiments was obtained.

Summary.

The combination of hydrogen and oxygen in a silver vessel shows the characteristics of a surface reaction up to 700°. There is no sign of the development of reaction chains in the gas. The inhibition of the gas reaction is attributed to the catalytic destruction at the silver-silver oxide surface of the active species which would normally propagate the chains.

* Garatang and Hinshelwood, 'Proc. Roy. Soc.,' A, vol. 130, p 640 (1931).

X-Ray Study of Copper-Cadmium Alloys.

By Professor E. A. OWEN, M.A., D.Sc., and LLEWELYN PICKUP, M.Sc. (Lond.),
Ph.D. (Wales), University College of North Wales, Bangor.

(Communicated by Sir William Bragg, F.R.S — Received September 28, 1932.)

[PLATES 15 AND 16.]

The most recently published accounts of experimental data relating to the copper-cadmium alloy system are the thermal investigation of Jenkins and Hanson* who mapped out the equilibrium diagram, and the X-ray work of Bradley and his collaborators† on the structure of the δ -phase. The present paper gives an account of an attempt to apply X-ray analysis to the whole series, particular attention being paid to alloys in the α -phase, the parameters of which have been measured to a high degree of accuracy.

The X-ray methods employed took two forms, namely, powder spectrum analysis and precision camera measurements. The former has been used to make a general survey over the whole range of composition, and the latter, to study in detail the α -phase.

Where the early data used for obtaining equilibrium diagrams have been found later to be erroneous, the chief source of error has been traced to the fact that the samples examined were not in their true equilibrium condition. Particular attention has therefore been given in the present work to heat treatment. Annealing treatments were carried out on small fragments (about 1 c.c.) and on filings of the alloys. For X-ray methods, only a comparatively small quantity of material (maximum about 0.5 gm.) is required; this is less than that necessary for thermal analysis and microscopical examination. Should it therefore prove possible to bring about the true equilibrium condition in these small samples easier and quicker than in the comparatively large masses required for other methods, this in itself would be an advantage.

The X-ray method of analysis, provided the desired samples are available, has been shown to give accurate determinations of the phase boundaries in the copper-zinc system,‡ so that errors are much more likely to arise through inadequate heat treatment than through faulty experimental X-ray technique.

* Jenkins and Hanson, 'J. Inst. Met.', vol. 31, p. 257 (1924).

† Bradley and Thewlis, 'Proc. Roy. Soc.,' A, vol. 112, p. 678 (1926); Bradley and Gregory, 'Phil. Mag.,' vol. 12, p. 143 (1931).

‡ Owen and Pickup, 'Proc. Roy. Soc.,' A, vol. 137, p. 397 (1932).

The nomenclature of the equilibrium diagram of Jenkins and Hanson has been adopted and the distribution of the phase fields suggested in this diagram has, in general, been corroborated by these X-ray researches. Precision measurements of the parameters of the α -phase alloys show that a modification is necessary in the position of the $(\alpha) - (\alpha + \beta)$ boundary, and as only alloys rich in copper have been found of service in industry, such a modification may have important bearing on the working and treatment of these industrial alloys.

Experimental Procedure.

The alloys were prepared from electrolytic copper and pure cadmium, supplied by Messrs. Johnson Matthey, London. The melting was carried out in salamander crucibles in an electric resistance furnace. A basis alloy containing about 50 per cent. copper (by weight) was first made and the alloys of different compositions were prepared by adding either copper or cadmium, melting the higher melting-point component first. Each step in the alloying process was carefully noted and timed; this procedure, together with chemical analysis,* enabled the melting losses to be ascertained fairly accurately. Such losses were then allowed for, when alloys of definite composition were being made. Temperatures were kept as low as possible, and powdered charcoal was used as a covering material. The ingots prepared, which weighed about 30 gm., were either sawn or broken in two and examined for porosity and homogeneity, before using for subsequent work.

Temperatures were measured by means of a nickel-nichrome thermo-couple, which was calibrated up to 800° C. with the usual standard materials. At 500° C. and below, the insulated couple wires were sheathed in tubes of glass or pyrex. Above this temperature, iron tubes were used.

As only a small quantity of filings off the ingots were required for annealing, it was convenient to heat these in evacuated tubes, about 0.5 cm. in diameter. Up to 500° C. glass tubes were used; between 500° and 650° C. pyrex tubes; and for higher temperatures and for all quenching experiments, thin walled silica tubes. Evacuation was carried out by means of a Hyvac oil pump. For annealing these tubes in the furnace, a steel block, about 4.5 cm. square, 18.0 cm. long and having a series of deep holes drilled into one rectangular face, was used. The object of this block was to prevent any confusion of the samples when a number were annealed together, and to eliminate any small

* Copper was estimated by a volumetric method, see "The Analysis of Non-ferrous Alloys," Ibbotson and Aitchison, p. 68.

fluctuations in temperature inside the furnace. When lumps about 1 c.c. were to be annealed, large bore pyrex tubes were used to make suitable containers, which could be readily evacuated and sealed up. These containers were wrapped in asbestos cloth for annealing in the furnace.

When it was desirable to quench after annealing, the sample, sealed in a silica tube, was attached to a piece of stiff nichrome wire, which passed through a hole in the lid of a furnace with its tube lining vertical. The sample and the "hot-junction" were arranged together in the centre of the furnace lining, the lower end of which passed through a hole in a wood box, which supported the furnace. A bung of asbestos cloth closed this lower end, under which was placed the quenching medium. By removing the bung quickly and plunging the sample by means of the nichrome wire into the cooling medium, the cooling was carried out very rapidly.

The X-ray tube used was of the "gas" type* fitted with a copper anti-cathode and operated on a Schall transformer. The pumping system was the usual mercury condensation pump, backed by a Hyvac oil pump. The tube was run at about 35–40 KV. and 10 milliamperes. For powder-spectrum work, the time of exposure was 8 to 12 hours, and for precision camera photographs, $1\frac{1}{2}$ to 2 hours.

Powder-Spectrum Analysis.

(a) *Method.*—After several preliminary experiments had been conducted, the arrangement and procedure finally adopted was as follows. When using the Bragg relation, $n\lambda = 2d \sin \theta$, it is necessary to determine the angle θ experimentally, whence knowing the wave-length λ , the spacing d is found. A glass fibre of uniform diameter (0.6 mm.) was very thinly coated with seccotine, and the sample in the form of the finest powder obtainable, was then used to make a uniform over-all diameter of 0.75 mm. These dimensions were found to be such that faint spurious reflection lines at small values of θ were eliminated. The coated fibre was inserted into a steel pillar so as to coincide with the axis of the brass cylindrical camera frame. This camera, of Hilger design, had a radius of about 3.0 cm. and carried a film about 16 cm. long and 2 cm. wide. By passing the X-ray beam from the tube, first through a brass slit system and then through a slip of lead glass 3 mm. thick, having a fine hole about 0.5 mm. diameter, an approximately parallel beam of small cross-section was caused to fall on the coated fibre. Although this arrangement increased the time of exposure, the sharp narrow reflection lines which

* Owen and Preston, 'J. Sci. Inst.,' vol. 4, p. 1 (October, 1926).

resulted, enabled the measurement of the arcs to be made more accurately than would have been possible with a more divergent beam.

Owing to the uncertainty of the various corrections to be applied to measurements of photographs obtained with this form of X ray camera, it was decided to calibrate the camera by means of accurately known parameter values, such as those of pure copper, aluminium and silver. Powder spectrum photographs were therefore made of well annealed filings of these metals and the arcs of the lines measured. Knowing the true lattice spacing corresponding to each set of reflecting planes and the wave-length λ of the radiation, the true value of $\sin \theta$ for these planes was calculated. The relation between "the true $\sin \theta$ " and the "actual arc measured" was obtained by plotting on a large scale the values of these quantities for each set of planes. The advantages of such a procedure were (1) a separate correction for the fibre diameter was not necessary provided that the coated fibre was always of a constant diameter (0.75 mm.); (2) errors in the measuring instrument scale were eliminated; and (3) provided the film took the same contour in the camera for each exposure, this need not be circular. Correction for film shrinkage was made, by having fiducial marks registered on each film by small V-shaped slots in the edges of the camera frame.

By annealing the filings to eliminate the lattice distortion, the reflection lines were fine enough to show sharp resolution of the $K\alpha_1$ and $K\alpha_2$ reflections near the ends of the film. Determining the mean values of the parameter of the α -phase in an alloy containing 88.8 per cent. copper, by this procedure, and comparing with the value obtained by the precision camera, the former method gave 3.632 Å. and the latter 3.631₅ Å. This accuracy was considered very satisfactory for powder-spectrum photographs, since where high accuracy was required, the precision camera was used.

(b) *Results.*—A survey was made by taking photographs of alloys of different compositions. Filings from these alloys were annealed to remove lattice distortion produced by the filing process; for alloys down to 27 per cent. copper, at 500° C.; and below this composition, at 300° C. owing to their becoming liquid above this temperature. The compositions were decided upon after consulting the diagram by Jenkins and Hanson. In fig. 1, Plate 15, a reproduction is given of the X-ray photographs of the 18 alloys examined.

As a general conclusion, it may be said that the main divisions of the phase regions of the diagram are confirmed in these photographs. Owing to the simple arrangement of the α -phase lines, these can be traced down to 67.7 per cent. copper, and the expansion of the copper lattice with the solution of

cadmium in it, can be just traced down to 96.7 per cent. copper, after which the lines show a constant α -phase parameter.

The β -phase reflection lines in the alloy containing 53.3 per cent. copper, show a complex structure, but a noticeable feature in their sequence is the apparent gap after about the first 10 lines. A similar feature is shown in the photographs of both the γ - and ϵ -phases.

The alloy representing the γ -phase, contained 43.2 per cent. copper, but the photograph contained so many reflection lines that its structure could not be found or solved satisfactorily from this type of photograph alone.

The δ -phase, represented by an alloy containing 27.1 per cent. Cu, gives a more even distribution of lines. The structure was found to be a body-centred cube, having a mean parameter value of 9.59, Å. Table I contains details of the measurement of eight lines, having glancing angles between 35° and 68°, given by a spectrum photograph of this alloy.

Table I.

Plane and λ .	Log sin θ .	Log $\sqrt{\frac{1}{\Sigma h^2}}$.	Parameter in Å.
721 α_1	1.7692	1.13380	9.610
752 α_1	1.8499	1.05395	9.592
770 α_1	1.8986	1.00439	9.610
10.22 α_1	1.9207	2.98329	9.590
871 α_1	1.9323	2.97155	9.592
963 α_1	1.9540	2.94981	9.594
963 α_2	1.9552	2.94981	9.589
972 α_1	1.9676	2.93645	9.590
Mean parameter value 9.59, Å.			

The density of this alloy was found to be 9.166 gm. per cubic centimetre. These data are consistent with the view that the body-centred structure contains 4 molecules having the formula Cu_5Cd_3 per unit cell. We have here an independent confirmation of the conclusion of Bradley and his co-workers that this phase is analogous to γ -brass.

The ϵ -phase alloy containing 15.6 per cent. copper, also gave a photograph too complex to effect a solution of its structure. From a comparison with other analogous alloy systems, one would expect this structure to be close-packed hexagonal, but this could not be definitely established.

From these photographs we are led to conclude that the analogy sometimes stated to exist between the Cu-Cd system and the Cu-Zn, Ag-Cd, and Ag-Zn systems, is by no means as good as that between these last three systems

amongst themselves. From a cursory glance at the equilibrium diagrams, the Cu-Cd system appears to show some "abnormal" features. There does not appear to be any phase in this system possessing a body-centred structure similar to those of the β -phases in the other systems above mentioned.

Precision Camera Analysis.

(a) *Lattice Distortion and Annealing.*—The technique of the X-ray precision camera having already been described,* it is proposed to describe here the study which has been made of the effect of annealing treatments on the production of reflection lines and their appearance, from the α -phase of copper-cadmium alloys.

The high resolution obtainable with this camera makes it essential to work with samples free from lattice distortion. It is seen therefore that the annealing treatment must produce a uniformity of structure as well as a uniformity of composition. The lattice distortion encountered in alloys is mainly due to some form of cold working, such as filing in the present investigation. Two forms of annealing treatment were carried out. The first, called here "lump annealing" consisted in heating small fragments, about 1 cm. cube of "as cast" alloy in evacuated pyrex tubes. The second, called here "powder annealing" was the annealing in evacuated tubes of filings taken off either "as cast" ingots or "lump annealed" samples. The effects of these two types of annealing need not necessarily be the same. Unless precautions are taken to ensure a very prolonged cooling from the liquid state, the resulting ingot, when cast, is in a heterogeneous condition, so that when filings are taken from it, different particles may have different compositions. Annealing such filings will produce equilibrium in each particle, but unless there is interdiffusion of components between one particle and another, distinct from that between the components of the same fragment, the mass as a whole will still be heterogeneous. Before, however, the existence of this distinction between these two types of annealing processes could be determined, it was essential to ascertain the effect of the rate of cooling from the annealing temperature and of the possible change in composition due to volatilization of cadmium.

With the copper-zinc alloys a homogeneous condition was obtained by simply annealing the "as cast" filings, but it was necessary with the copper-cadmium alloys, as will be shown below, to submit them to prolonged "lump annealing" to produce homogeneous samples. From this, it may be concluded that the

* Owen and Pickup, *loc. cit.*

rate of interdiffusion of copper and zinc was much greater than that of copper and cadmium.

In the initial stages of developing the application of the precision camera to this work, samples containing between 96 and 98 per cent. copper, in the form of thin foils, (0.5 mm. thick) were made. These were annealed at 800° C. for 2 hours and quenched in cold water. Precision photographs of these showed very irregular and "spotty" reflection lines, from which accurate measurements could not be made. Even if satisfactory reflections were obtained from foil samples, this procedure would be limited to samples which could be made into this form. Filings were therefore mounted in a uniform layer on thin aluminium foil, using seccotine as an adherent; by this means brittle samples could be prepared equally well for mounting in the camera. Fig. 2, Plate 16, shows typical forms of the reflection lines from foil and powder. All the subsequent photographs were therefore obtained with annealed filings.

(b) *Rate of Cooling*.—Filings of an alloy, containing 94.6 per cent. Cu, were annealed at 500° C. for 6 hours. One sample was cooled in air and gave an α -phase parameter value of 3.620₈ A.; another was water-quenched and gave a parameter value of 3.621₈ A.; the third was quenched in liquid air and gave a parameter value of 3.620₄ A., so that there is no difference in parameter value by the three methods of cooling. Next three different alloys were taken and annealed at 400° C., one series was water-quenched and the other air-cooled. From one alloy (88.8 per cent. Cu) further samples were treated at 600° C. Table II shows the results obtained.

Table II.

Approximate ingot composition.	Annealing temperature	Method of cooling.	α -phase parameter A.
97.4	° C 400	W.Q. A.C.	3.612 ₈ 3.612 ₈
93.9	400	W.Q. A.C.	3.612 ₈ 3.613 ₈
88.8	400	W.Q. A.C.	3.613 ₈ 3.614 ₄
88.8	600	W.Q. A.C.	3.626 ₈ 3.628 ₈

W.Q. denotes water-quenched. A.C. denotes air cooled. (*)

* The glass tubes were cool enough to handle in about half a minute after removal from the furnace.

Except when the annealing was carried out at 600° C. the parameter differences after the two methods of cooling for each alloy, are considered to be within experimental error, especially since no chemical analysis on the actual samples photographed were made. Therefore it was decided to quench into iced-water only the samples, which were annealed at temperatures above 500° C.

(c) *Volatilization of Cadmium during Annealing.*—Table III is a summary of parameter values of the α -phase of (i) filings taken from an "as cast" alloy, (91.2 per cent. Cu) and (ii) filings taken from the same alloy which had been lump-annealed at 450° C. for 700 hours.

Table III.—Ingot Composition 91.2 per cent. Copper.

Condition of filings.	Filings annealed at		
	400° C.	500° C.	600° C.
As cast	3 614 ₀	3 621 ₀	3 627 ₀
Lump annealed	3 611 ₀	3 617 ₀	3 621 ₀

Since at each temperature the parameter is lower in the lump-annealed samples than that in the "as cast" samples, some volatilization of cadmium had taken place—a lower parameter indicates a higher copper concentration since solution of cadmium in the copper lattice increases its parameter value.

The amount of volatilization, which took place, from alloys in the α -phase during the annealing of filings of these alloys in evacuated glass tubes was shown to be comparatively small by annealing filings taken from an alloy containing 88.8 per cent. Cu, for different times, ranging from 1 minute to 6 hours at 500° C. From Table IV, showing these data, it is seen that annealing for 1 or 2 minutes only is necessary at 500° C., to eliminate lattice distortion, though stronger reflection lines are obtained after about 1 hour's annealing.

Table IV.—Alloy (88.8 per cent. Cu) annealed at 500° C.

Time annealed	α -phase parameter A.
1 minute	3.619 ₀
2 minutes	3 621 ₁
4 minutes	3 620 ₀
15 minutes	3.621 ₀
30 minutes	3.620 ₀
1 hour	3.620 ₀
2 hours	3.622 ₀
4½ hours	3.623 ₁
6 hours	3.620 ₀

At 300° C., it was necessary to anneal for 1 hour to produce measurable reflection lines, and by annealing for 6 hours stronger lines giving the same parameter values were obtained.

No reflection lines were produced even after prolonged annealing at 200° C., but it was found later that by annealing at about 300° C. and above, followed by slow cooling down to 200° C. and continuing the annealing for some hours at 200° C., reflection lines corresponding to the thermal conditions at this latter temperature, were obtained.

These results were then used as a guide to determine the minimum annealing time, so as to reduce the amount of volatilization of cadmium, when preparing samples of filings for photographing.

(d) *The α -phase Parameters of "as cast" Alloys.*—The lines in the precision photographs from all these alloys were reflections of the $K\alpha_1$ and $K\alpha_2$ copper radiation by the (420) planes. A doublet from the (331) planes was also registered by some alloys, but beyond a certain copper content this disappeared off the end of the film. This doublet was therefore ignored in measuring, as its arc was, in any case, too great to use for accurate parameter measurements.

Filings from the alloys used were annealed at 300°, 400°, 500° and 600° C. for a fixed time of 6 hours, as the results of the experiments dealing with the time of annealing were not available at this stage of the work. The precaution was, however, taken to analyse chemically most of the samples photographed.

Alloys, with less than about 88 per cent. copper, did not show good reflection lines, owing to the diminishing amount of α -phase present below this composition. The filings of the alloys, below 96 per cent. copper, adhered together, when annealed at 600° C.; the liquid phase present at this temperature accounted for this. It was possible, however, with alloys down to about 88 per cent. copper, to break up the mass gently enough so as not to obliterate the reflection lines by the small amount of cold work done.

Some of the experimental results obtained with these alloys appeared somewhat erratic, but in Table V the parameter values and compositions for each annealing temperature have been chosen from the batch of data, which are considered to represent best their apparent relation.

The parameter of annealed electrolytic copper was found to be 3.607, Å. These results are plotted in fig. 3, and it is seen that, after a certain composition for each temperature, the parameter value tends to become constant. As this constant value becomes greater with increasing temperature, it suggests that more cadmium can enter the α -phase lattice with increasing temperature. If this conclusion be true, then the $(\alpha) - (\alpha + \beta)$ boundary cannot be parallel

Table V.—“ As Cast ” Copper-Cadmium Alloys.

Annealing temperature ° C.	α -phase parameter A.	Per cent. copper in sample.
300	3 609 _a	99.3
	3.610 _a	96.7
	3 610 _a	93.9
	3.610 _a	88.8
400	3 610 _a	99.3
	3.612 _a	97.4
	3 612 _a	96.7
	3.613 _a	93.9
	3 613 _a	88.8
500	3.612 _a	99.3
	3.618 _a	98.1
	3.619 _a	96.1
	3.620 _a	93.9
	3 620 _a	88.8
600	3 613 _a	99.3
	3 621 _a	98.1
	3 625 _a	96.7
	3 626 _a	93.9
	3 626 _a	88.8

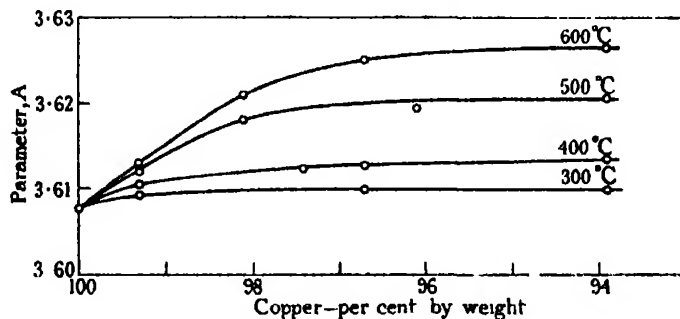


FIG. 3.—Copper-cadmium “ as cast ” alloys.

to the temperature axis. From the shape of these curves, it was impossible to ascertain with any accuracy the position of this boundary; but it was suspected from the shape of the curves that the alloys were not in the true thermal equilibrium conditions. The investigation was then continued with this point in view by working on lump-annealed alloys.

(e) *The α -phase Parameters of “ Lump-Annealed ” Alloys.*—The possible effects of “ powder annealing ” and “ lump annealing ” have already been discussed, so that fragments of “ as cast ” ingots were lump annealed for prolonged periods. As the actual ingots prepared were between 20 and 30 gm.,

and were cooled fairly rapidly, some heterogeneity was inevitable. As demonstrated by Genders and Bailey* with copper-zinc alloys, the true thermal equilibrium condition can often be more readily obtained by annealing alloys in the most unstable condition. As the "as cast" lumps were to some extent in this condition, it was thought very possible that the true equilibrium condition would be obtained in this manner.

As prolonged annealing was likely to cause volatilization of cadmium, it was necessary to investigate the variation in composition from the surface inwards after lump annealing. From each of four alloys which had been lump annealed at 500° C. for 600 hours, two batches of filings were taken; (1) filings taken near the surface, and (2) filings taken at least 1 mm. below the surface. A determination was made of the α -phase parameter and of the composition by chemical analysis on each sample after photographing. These results are given in Table VI.

Table VI.

(All filings annealed at 500° C. for 10 minutes to remove lattice distortion.)

Approximate ingot composition	Surface filings.		Filings 1 mm. below.	
	Composition	Parameter A.	Composition.	Parameter A.
99.5	97.6	3.612 ₀	99.1	3.611 ₀
98.6	95.9	3.613 ₀	96.0	3.620 ₀
97.5	97.0	3.615 ₁	96.7	3.621 ₅
96.5	95.9	3.615 ₁	96.1	3.622 ₀
93.0	—	—	97.7	3.616 ₀

This table shows interesting features. The compositions of the surface filings are lower in copper content than those 1 mm. below the surface, for each alloy. Plotting these results in fig. 4 it is shown that the data of filings

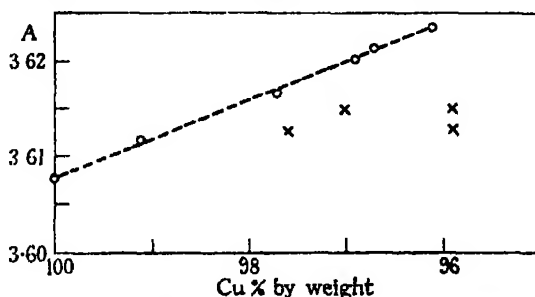


FIG. 4.—Cu-Cd Alloys, lump annealed. × Surface metal; ○ Metal 1 mm. below surface.

* Genders and Bailey, 'J. Inst. Met.', vol. 33, p. 213 (1925).

taken 1 mm. below the surface show a linear relation, while those of the surface metal are erratic. The excessive amount of volatilization in the alloy, with ingot of composition 93.0 per cent. copper, was due to the fact that the container broke during the lump annealing. In spite of this, when the composition and parameter value of the metal 1 mm. below the surface, are taken, they are consistent with the linear relation mentioned. It must therefore be concluded that only at least 1 mm. below the surface a true homogenous condition exists. The reflection lines from the surface metal are little, if any, broader, or in any way different from those giving the regular parameters, and hence neither can the reflecting α -phase be heterogeneous nor can its lattice be distorted in the surface metal. An explanation of these lines can be given if we assume that apart from volatilization, some of the cadmium oxidizes and remains on the surface. Since only a pure α -phase can reflect the lines produced and since the copper is not likely to be oxidized, the copper determined by chemical analysis is entirely in the α -phase with less cadmium in it, by the amount present as oxide. The parameter found, therefore, corresponds to an α -phase composition richer in copper than that indicated by chemical analysis. The irregular points in fig. 4 being to the right of the line support this explanation.

Therefore when treating alloys of various compositions, which had been lump annealed, to obtain data to determine the $(\alpha) - (\alpha + \beta)$ boundary, the following precautions were taken: (1) only filings at least 1 mm. below the surface were used, (2) chemical analysis for copper content was carried out on the actual sample photographed, and (3) the time of annealing was made as short as possible consistent with the production of good reflection lines for measurement purposes, so as to minimize volatilization of cadmium.

The lump-annealing consisted in heating the samples at 500° C. for 500 hours continuously, fluctuations temperature being estimated as $\pm 20^\circ$ C. during the night periods.

In Table VII, the time and temperature of annealing the filings, the α -phase parameter value, and the composition are given.

These figures are plotted graphically in fig. 5. Apart from alloys annealed at 600° C., the relations between composition and parameter value in the pure α -region are approximately linear. From a comparison of fig. 3 with fig. 5, it is evident that the lump annealing, followed by annealing the filings, has produced the true equilibrium condition in these alloys. It has already been shown* that (1) when the parameter value remains constant over

* Owen and Pickup, *loc. cit.*

Table VII.—Copper-Cadmium Alloys Lump Annealed at 500° C. for 500 hours.

Filings annealed.		α -phase parameter A.	Per cent. copper in sample.
Temperature.	Time.		
° C. 300	6 hours air cooled	3.611 _a	99.5
		3.610 ₇	98.6
		3.611 ₁	97.5
		3.610 ₇	93.2
400	1 hour air cooled	3.612 _a	99.2
		3.613 _a	97.9
		3.613 _a	97.2
		3.613 _a	95.8
500	10 minutes air cooled	3.612 _a	99.2
		3.618 _a	98.1
		3.620 _a	96.0
		3.620 _a	95.3
		3.620 _a	94.5
600	5 minutes water quenched	3.620 _a	92.4
		3.613 _a	99.2
		3.618 _a	98.1
		3.622 _a	97.2
		3.624 _a	96.2
		3.625 _a	95.8
		3.626 _a	93.7
		3.627 _a	92.4

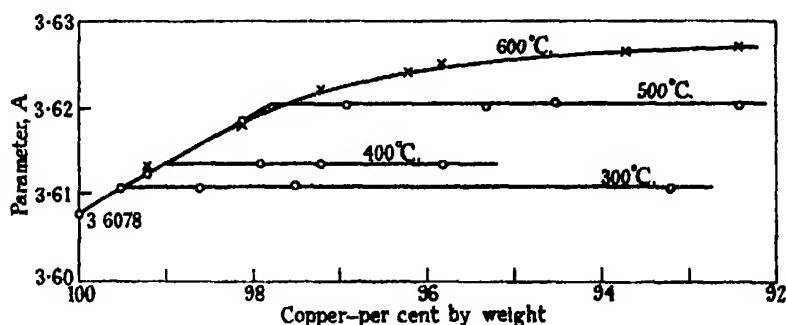


FIG. 5.—Copper-cadmium alloys lump annealed.

a range of composition for the same temperature, a two-phase region is indicated at this temperature, and (2) when the parameter value at all temperatures for one composition remains constant, this composition is in a one-phase region.

From the data in fig. 5 relating to the (α) and ($\alpha + \beta$) regions of the copper-cadmium system, the boundary at 300°, 400° and 500° C. can be read off

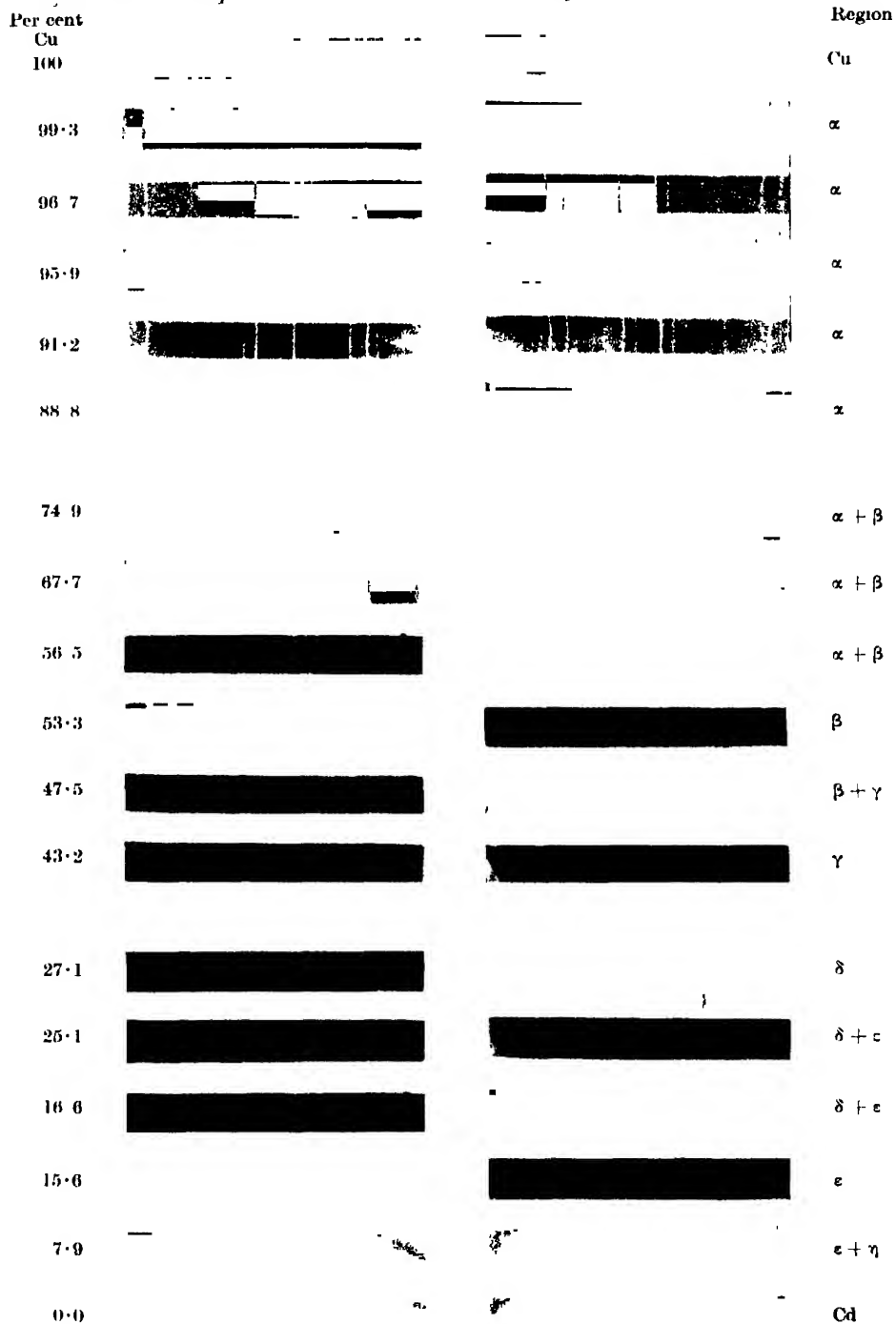


FIG. 1.

Foil

Powder

Fig. 2

93 per cent Cu lump annealed

300° C



400° C



500° C

600° C

Fig. 6A

89 per cent Cu as cast



300° C

400° C

500° C



600° C



Fig. 6B.

Annealed at 500° C



100 per cent
Cu



99.5 per cent



98.6 per cent



97.5 per cent

96.8 per cent



Fig. 6c.

accurately. It is found that this boundary is at 99.5 per cent. copper at 300° C., 99.0 at 400° C., and 97.8 at 500° C. The curve representing the results at 600° C. after coinciding with the other curves from pure copper to about 98 per cent. copper shows that the α -phase parameter still increases but more slowly with decreasing copper content. We believe that the position of the solidus boundary at 549° C.* accounts for this gradual increase in parameter, the extent of the coincidence of the 600° C. curve with the other curves representing the extent of the pure solid α -phase at 600° C. The point of deviation at 98.2 per cent. copper approximately must define the limit of this solid phase at 600° C., that is, the solidus boundary at this temperature.

The assumption rather than the deduction of Jenkins and Hanson that "this solubility (at 97.8 per cent. copper at 500° C.) is not appreciably different at lower temperatures" cannot be maintained in view of the above X-ray data.

In figs. 6a and 6b, Plate 16, the reproduction of photographs shows clearly the change in the parameter value (corresponding to solid solubility) of the α -phase with change of temperature in the $(\alpha + \beta)$ region. Fig. 6c, Plate 16 shows the change of the α -phase parameter value with composition after annealing at 500° C., and the constant parameter in the $(\alpha + \beta)$ region.

Fig. 7 gives the modification suggested here to the $(\alpha) - (\alpha + \beta)$ boundary, together with the previously determined boundary. Since only alloys in this range of composition have been put to industrial use, owing to their containing no appreciable amount of the brittle β -constituent, the modification suggested may have a marked influence on the manufacture and properties of these industrial alloys.

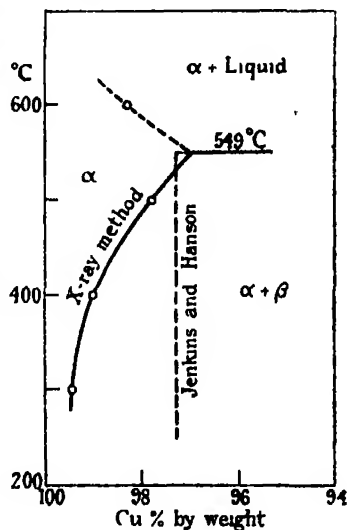


FIG. 7.

Conclusions.

1. The division of the phase regions in the copper-cadmium system, from 100 to 30 per cent. copper at 500° C., and those below this composition at

* See Jenkins and Hanson's diagram, *loc. cit.*

300° C., are found by X-ray powder-spectrum analysis, to be similar to that given by the equilibrium diagram of Jenkins and Hanson.

2. The structures of the pure β , γ and ϵ -phases are found to be too complex to solve satisfactorily by powder-spectrum photographs alone.

3. The δ -phase structure is confirmed to be similar to that of γ -brass, having a body-centred cubic structure with 4 molecules (Cu_5Cd_9) per unit cell.

4. The annealing of filings taken from small "as cast" ingots does not produce the true equilibrium state, but results in some volatilization and oxidation of cadmium.

5. The true thermal equilibrium condition is produced by annealing small lumps of "as cast" alloy for a prolonged period, discarding at least 1 mm. of the surface layer, and annealing filings from the interior of the metal for comparatively short times depending on the temperature of annealing.

6. The saturation of copper with cadmium in the α -phase changes with temperature, becoming less with decreasing temperature. A modification is therefore made in the previously accepted $(\alpha) - (\alpha + \beta)$ boundary.

We wish to express our thanks to the Royal Society for a grant which enabled us to carry out the work.

Summary.

Alloys covering the whole range of the copper-cadmium system have been examined by X-ray powder methods. The technique of powder-spectroscopy is described which gives fine, well-defined reflection lines and eliminates the uncertain corrections inherent in this type of X-ray analysis. The phase regions of the diagram due to Jenkins and Hanson have been confirmed by these investigations. The β , γ , and ϵ -phase structures were too complex to solve from the photographs taken, but the δ -phase structure was confirmed to be similar to that of γ -brass. The close analogy, which has been suggested by some workers between the corresponding phases of the copper-cadmium system and the analogous systems, copper-zinc, silver-zinc, and silver-cadmium, is not supported by the present X-ray data.

Special attention is given to annealing treatments, the effects of which are studied by precision camera analysis. While lattice distortion in filings is shown to be completely eliminated by a simple annealing, such annealing may not, and does not with these alloys, bring about the true thermal equilibrium. Alloys were therefore annealed in lump form for prolonged periods, which, when followed by a comparatively short annealing of the filings depending on

the temperature, produced equilibrium. Volatilization of cadmium was found to take place during the annealing treatments, but, by discarding 1 mm. depth of the surface metal from the lump-annealed samples and analysing chemically the actual samples after using them to obtain precision photographs, this source of error was eliminated.

The data obtained relating the α -phase parameter, composition and temperature of samples in the equilibrium state, show that the solid solubility of cadmium in the copper lattice decreases with decreasing temperature. The limits of solubility were found to be at 97.8 per cent., copper at 500° C., 99.0 per cent. at 400° C., and 99.5 per cent. at 300° C. A modification is therefore suggested in the (α) — ($\alpha + \beta$) boundary of the equilibrium diagram given previously by Jenkins and Hanson. This change in the boundary is considered to be of importance in the working of the industrial alloys of this system, which are mostly confined to this copper-rich region, where there is no appreciable amount of the brittle β -constituent.

The Photochemistry of Phosphine.

By H. W. MELVILLE.

(Communicated by J. Kendall, F.R.S. -Received October 1, 1932.)

Introduction.

In the previous paper in this investigation* the first part (I) dealt with the mercury photo-sensitized decomposition of phosphine, and the second (II) with the sensitized photo-oxidation. Certain calculations and conclusions in that paper had to be left unfinished, until data on the direct photochemical reaction became available. The present paper, therefore, is devoted to the absorption spectrum, the direct decomposition and the photochemical oxidation of phosphine. The experiments are to some extent confirmatory of those involving excited mercury atoms but, owing to the simpler conditions obtaining in the direct reaction, it is possible to extend the calculations on the results to yield more information about the mechanism of the reactions.

* 'Proc. Roy. Soc.,' A, vol. 138, p. 374 (1932).

PART III.

The Absorption Spectrum of Phosphine.

The absorption spectrum has been photographed by Purvis* using a condensed cadmium spark. In a 10 cm. tube absorption begins at 223 m μ at room temperature, and at 100° C. the limit is raised to 224 m μ . No bands were observed.

Owing to the discontinuous nature of the cadmium spectrum, it was deemed advisable to photograph the absorption spectrum, using a continuous source of radiation.

The source of light was a water-cooled hydrogen tube consuming about 2 kw., while the spectroscope was a small Hilger instrument giving the region 200–800 m μ on a quarter-plate. Two absorption tubes were used, one 110 cm. long of glass and fitted with quartz windows, the other entirely of fused silica 15 cm. long. Exposures ranged from 1 minute to 1 hour, using Wellington Anti-screen plates.

A series of exposures of about 1 hour was made at room temperature with pressures of phosphine from 0.01 mm. to 760 mm. with the 110 cm. tube. At atmospheric pressure absorption was continuous beyond 225 m μ as far as 185 m μ , the limit of the spectroscope. Preceding this continuous absorption, four very weak diffuse absorption bands could be observed at wave-lengths of 228, 229.5, 232 and 236 m μ . The breadth of the bands was 1–2 m μ , but no fine structure was evident. The dispersion of the spectroscope was sufficient to show structure, had there been any present, for the rotational lines in the Schumann O₂ bands could be distinguished. When the pressure of the phosphine was reduced to 20 mm. the limit of continuous absorption had moved to about 217 m μ , while all trace of the bands observed at atmospheric pressure had disappeared. Upon reducing the pressure to 0.01 mm., the absorption limit became rather indefinite, but no light was transmitted beyond 195 m μ . No bands appeared on the plates except those belonging to the O₂ molecule.

Using the 15 cm. tube the absorption spectrum was photographed at 300° C., at which temperature the limit of continuous absorption shifted slightly—1–2 m μ —towards the red, while all traces of band absorption observed at room temperatures had disappeared.

These experiments would therefore indicate that the absorption spectrum of phosphine is of the predissociation type and similar to that of ammonia.

* 'Proc. Camb. Phil. Soc.,' vol. 21, p. 566 (1923).

The Direct Photochemical Decomposition. Materials and Apparatus.

The phosphine and other gases used in these experiments were prepared as described in I.

The apparatus is shown diagrammatically in fig. 1. It consisted of a McLeod gauge (M) attached to a liquid air trap (T_4) provided with a tap and a reaction bulb of silica (R_1), 7 cm. in diameter. This bulb was connected to the apparatus by a silica-glass ground joint so that the bulb could be rotated. When working

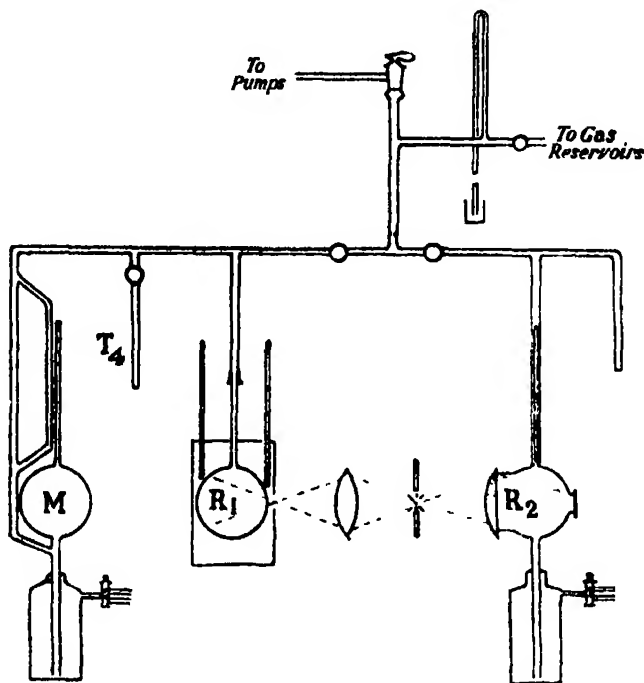


FIG. 1.

at temperatures above 15°C . the bulb was surrounded by an electric furnace provided with a small window. Two silica thermometers were used for reading temperatures. To the other end of the vacuum line another McLeod gauge, fitted with a liquid air trap was sealed. The bulb of this gauge functioned as a reaction tube and was fitted with a quartz lens 6 cm. in diameter and focal length (for yellow light), 10 cm. at one side and a quartz plate at the other. The whole was placed in a brass box fitted with a suitable window for observing the capillary so that, if necessary, water at a constant temperature could be circulated through it. The reasons for constructing the gauge in this manner were (1) compactness and ease of temperature control, (2) economy

of quartz plates and lenses, (3) sensitivity, owing to the fact that no expansion takes place from the reaction tube into the bulb of the McLeod gauge. The bulb of this gauge was about 300 c.c. in volume.

The apparatus was exhausted by a mercury condensation pump backed by an oil pump. The spark was placed in between R_1 and R_2 : it was fed from a 10 K.V.A. 6600 volt transformer with suitable condensers across the secondary. The electrodes were of zinc and aluminium, and were kept cool by a strong blast of air. The spark voltage was usually about 3000 when a current of about 1 amp. passed across the spark gap.

The gauge (R_2) was used as a photometer, using ammonia as photometric gas, while R_1 served as the phosphine reaction vessel. Then, assuming that the distribution of light from the spark remains sensibly constant, a check is kept on the energy emitted and therefore corrections for variation in spark intensity can easily be applied when making a long series of experiments in R_1 .

Trouble was experienced with red phosphorus being deposited on the walls of R_1 . R_1 had to be standardized against R_2 before and after every experimental run. As this process was rather lengthy an alternative method was employed. Immediately in front of R_1 a piece of sheet iron, with an aperture 2×1 cm., was set up, and after each experiment R_1 was turned on its axis so as to present a clear portion of the bulb behind the aperture. In this way about 15 exposures could be made without having to remove the bulb for cleaning.

Products of Decomposition.

First of all, it was necessary to determine the percentage of hydrogen produced during the photochemical decomposition. If the percentage approached that required by the equation $4PH_3 = P_4 + 6H_2$ then it would be reasonable to assume that no other hydrides of phosphorus were formed. Table I is a record of a series of experiments carried out at room temperature with a zinc spark, the exposure time being about 20 minutes.

Table I.

PH_3 , mm.	$PH_3 + P_4$, after exposure.	PH_3 \pm 0.0085 mm.	PH_3 , decomp.	H_2 , per cent. of theory.
0.1455	0.1465	0.0123	0.0028	91
0.0788	0.0815	0.0207	0.0087	93
0.1245	0.1290	0.0263	0.0133	90
0.0645	0.0690	0.0235	0.0105	95
0.0930	0.0980	0.0275	0.0140	91
0.1345	0.1465	0.0495	0.0290	95
Average				93

0.0085 mm. is the vapour pressure of phosphine, measured by the McLeod gauge, at the temperature of the liquid air employed in this series. The slightly low value of the percentage of hydrogen is, no doubt, due to adsorption of the hydrogen atoms by the walls of the reaction tube. The phosphorus is deposited as a brownish-red film. In view of the probability that the reactions subsequent to the primary fission of the PH_3 molecule take place on the walls (see below), it would appear that no phosphorus vapour is produced. It is important to observe that 93 per cent. agrees well with 95 per cent. found in the photo-sensitized reaction, thus yielding evidence, that the secondary reactions in both cases are similar. It may be concluded, therefore, that the result of the decomposition process is expressed by the equation given above.

Quantum Efficiency.

The measurement of the quantum yield depends on determining the pressure of hydrogen produced. Therefore it was necessary to find if molecular hydrogen had any effect on the course of the reaction. On illuminating 0.0785 mm. of PH_3 in R_1 for 20 minutes 0.0045 mm. of hydrogen were obtained. On adding 0.0660 mm. of hydrogen and giving the same exposure, 0.0040 mm. (accuracy of pressure readings ± 0.0005 mm.) of H_2 were produced. That is, H_2 had practically no effect, although the pressure was equal to that of the PH_3 . In the experiments to be described below the pressure of H_2 was invariably a very small fraction of the PH_3 pressure.

Since Warburg's value for the quantum yield of the decomposition of NH_3 has recently been confirmed,* it was decided to measure the quantum yield for PH_3 in terms of that of NH_3 as the band absorption limits are almost identical for the two gases. The group of lines near 210 m μ emitted by the zinc spark is absorbed completely by NH_3 and by PH_3 if the pressure is sufficiently high.

Preliminary experiments were made to ascertain when NH_3 or PH_3 in R_1 began to transmit the zinc lines appreciably; it was found that at about 30 mm. incomplete absorption became noticeable. Pressures of 100 mm. were therefore employed. R_1 and R_2 were filled with NH_3 at 100 mm. and an exposure of 10-20 minutes given, after which the pressure of $\text{N}_2 + \text{H}_2$ was determined by condensing out the NH_3 with liquid air. PH_3 at 100 mm. was then put into R_1 and the same procedure repeated. Table II gives three series of experi-

* Wlig and Kistiakowski, J. Amer. Chem. Soc., vol. 54, p. 1906 (1932).

ments with the 7 cm. bulb for R_1 at room temperature, while Table III is a record of two series with a 2 cm. cylindrical tube 15 cm. long.

Table II.

Spark.	Gas in R_1	p in R_1 (mm.)	$p_{H_2+N_2}$ (R_2)	γ .
Al	NH ₃	0.0143	0.0412	—
	PH ₃	0.0145	0.0250	0.61
	PH ₃	0.0190	0.0250	0.60
	PH ₃	0.0183	0.0369	0.52
Zn	NH ₃	0.0125	0.0203	—
	PH ₃	0.0185	0.0209	0.47
	PH ₃	0.0195	0.0203	0.57
	PH ₃	0.0180	0.0203	0.53
Zn	NH ₃	0.0770	0.0209	—
	PH ₃	0.0686	0.0119	0.53
	NH ₃	0.1290	0.0459	—

In the third series of Table II the bulb was not rotated. This series was carried out after an interval of 6 months, during which time the bulb had been in continuous use. Another series of experiments also carried out at a different time yielded the results $\gamma = 0.57, 0.57, 0.50$. For the 7 cm. bulb the average value of γ is 0.56.

Table III.—2 cm. Cylindrical Tube. Temperature 18° C. Zn spark.

Gas in R_1 .	$p_{H_2+(N_2)}$ in R_1 .	$p_{H_2+N_2}$ in R_2 .	γ .
NH ₃	0.0790	0.0152	} 0.47
PH ₃	0.0940	0.0244	
NH ₃	0.0130	0.0304	
NH ₃	0.0975	0.0292	} 0.52
PH ₃	0.0520	0.0143	
NH ₃	0.0455	0.0351	
NH ₃	0.1560	0.0298	} 0.47
PH ₃	0.0915	0.0167	
NH ₃	0.0505	0.0188	

In the experiments recorded in Table III rotation of the tube was not practicable, so that ammonia calibration experiments were made before and after every phosphine experiment. The mean of the ammonia experiments was used for calculating the quantum yield. The insolation tube was cleaned

out with bromine water after each series in order to remove the film of red phosphorus deposited on the window.

It will be observed that the quantum yield in the smaller vessel is a little less than that in the 7 cm. bulb, thus confirming the results of the photo-sensitized experiments.

A possible criticism may be levelled against the interpretation of the increase in the rate of the photo-sensitized decomposition in wider tubes. In a recent paper on the mean life (τ) of the mercury atom in the 2^3P_1 state, Garrett* finds that the pressure of the mercury vapour in a tube 3 cm. in diameter has quite a large influence on the *apparent* mean life. The apparent mean life is the life measured by the apparatus employed by Garrett. For example, at 10^{-4} mm. τ is 1.43×10^{-7} second, and at 10^{-5} mm., 1.08×10^{-7} second. This increase in life is due to part of the resonance radiation being reabsorbed by the mercury vapour before escaping out of the tube in which the mercury atoms are excited. Extrapolation of Garrett's results to 0.001 mm., which pressure was used in the photo-sensitized experiments, gives a value of τ approximately equal to 5×10^{-7} seconds. At 0.001 mm. therefore, the apparent mean life of Hg 2^3P_1 will increase with the diameter of the tube, but as k_3 (see I) is inversely proportional to τ , the ratio k_1/k_3 will increase with diameter. Hence the observed increase in k_1/k_3 may possibly be due to this increase in apparent life by reabsorption of resonance radiation. Garrett's results, however, only apply to pure mercury vapour; that is, when gas phase deactivation occurs by radiation alone. When phosphine is present, the *effective* mean life is much smaller and is proportional to $1/(k_1[\text{PH}_3] + k_3)$. In the 2 cm. tube $k_1/k_3 = 2.7$, while the pressures used for determining the ratio k_1/k_3 were in the range 0.5–10 mm. At the low pressure of 1 mm. then, the mean life is $k_3/(k_1[\text{PH}_3] + k_3) = 1/4$ that in absence of phosphine, or 10^{-7} second. The effective life is thus equal to the mean life at low pressure ($< 10^{-5}$ mm.) of mercury vapour so that little reabsorption of resonance radiation could occur.

Furthermore, had appreciable reabsorption of resonance radiation taken place, the line obtained by plotting the reciprocal of the reaction rate ($1/R$) against the reciprocal of the phosphine pressure should have become concave to the $1/p_{\text{PH}_3}$ axis at high values of $1/p_{\text{PH}_3}$, owing to the increase in $[\text{Hg}^1]$. The line in fig. 5 of Paper I shows no such deviation. In order to settle the matter, more accurate data than the extrapolated value used above would be

* 'Phys. Rev.,' vol. 40, p. 779 (1932).

required on the apparent mean life in mercury vapour at 0.001 mm. in a 2-cm. cylindrical tube.

Effect of Pressure on γ .

The range of pressures which could be used with the experimental method described above was rather restricted, since the pressure of the phosphine had to be of such a magnitude that there was complete absorption of the zinc lines at 210 m μ . The following method, however, allows of the calculation of quantum yields down to very low pressures.

Table IV contains the record of a series of experiments using different pressures of phosphine with the same time of exposure and intensity of spark.

Table IV.—Room temperature 15° C., 2 cm. cylindrical tube.

p_{PH_3} (mm.).	Rate (mm./min.).	Calculated rate.
760	0.0022	---
44	0.0022	---
5	0.0011	---
0.226	0.00033	0.00037
0.072	0.00012	0.00020
0.0365	0.000065	0.00008

The quantum yield is independent of pressure between 44 and 760 mm. If the reduction in rate below 44 mm. pressure is owing wholly to incomplete absorption, then the variation in rate with pressure is simply expressed by the equation

$$R = R_{\infty} (1 - e^{-kp}),$$

where R_{∞} is the rate when absorption is complete, R that at pressure p mm. and k is a constant depending only on the dimensions and shape of the insolation tube and the extinction coefficient of phosphine for the wave-lengths in the region of 210 m μ . k was obtained from the experiment at 5 mm. using R_{∞} from the experiments at 44 and 760 mm. and assuming that the quantum yield at 5 mm. is the same as that at 44 mm. The third column of Table IV was calculated from this value of k . The agreement is reasonably good in view of the exponential factor governing R ; however, it is sufficient to show that the quantum yield is independent of pressure from 0.04 to 760 mm.

Effect of Temperature on γ .

Preliminary experiments were made to find when thermal dissociation becomes appreciable with this type of apparatus. At 340° C., the phosphine

pressure being 40 mm., 0.0315 mm. of hydrogen were produced in 30 minutes, at 290°, 0.0015 mm. Photochemical experiments were therefore impossible at temperatures much above 300° as the photo-reaction yielded about 0.05 mm. hydrogen in 10 minutes.

In order to reduce pressure readings at high temperatures to 15° C., hydrogen was admitted to the McLeod gauge and R_1 to a pressure of 0.05 mm. R_1 was then heated up to 300° C., pressure readings being taken at suitable temperature intervals. At pressures of the order of 0.05 mm. of hydrogen, thermal effusion is appreciable so that the reduction of the pressure readings by calculation is difficult to carry out accurately.

In these experiments phosphine was used as the photometric gas in R_2 . Owing to deposition of red phosphorus on the lens of R_2 , calibration experiments were made at the beginning and end of each run. Table V gives two series of experiments, where it is seen that the quantum yield is practically independent of temperature.

Table V.—Pressure of PH_3 , 40 mm. 7 cm. bulb. Zn spark.

p_{H_2} in R_1 (mm.)	p_{H_2} in R_2 (mm.)	Temperature (° C.)	p_{H_2} in R_1 reduced to 15°	γ rel. to 15° C
0.0165	0.0430	25	0.0162	1.0
0.0283	0.0273	267	0.0232	1.1
0.0300	0.0351	212	0.0254	0.9
0.0197	0.0220	176	0.0171	0.9
0.0131	0.0167	117	0.0118	0.8
0.0178	0.0161	73	0.0166	1.0
0.0145	0.0131	30	0.0141	1.0
0.0270	0.0215	25	0.0265	1.0
0.0457	0.0191	324	0.0304	1.6
0.0425	0.0244	232	0.0361	1.1
0.0255	0.0173	208	0.0215	0.9
0.0390	0.0220	140	0.0345	1.1
0.0363	0.0208	90	0.0333	1.1
0.0257	0.0173	33	0.0250	1.0

Discussion of Reaction Mechanism.

The experiments described above corroborate those using excited mercury atoms for dissociation of the phosphine molecule, in those cases where comparison can be made. The effect of atomic hydrogen may be mentioned again, as the experimental data in I provide direct proof that the photochemical decomposition is inhibited by hydrogen atoms. The low quantum yield, in this case also, is probably owing to recombination of PH_2 and H on the walls.

It is rather surprising to find that temperature has no appreciable influence on γ . This means that temperatures up to 300° C. do not alter the relative probabilities of the reactions $\text{PH}_2 + \text{PH}_2 = \text{P}_2 + 2\text{H}_2$, $\text{H} + \text{H} = \text{H}_2$ and $\text{PH}_2 + \text{H} = \text{PH}_3$. If these reactions require only small energies of activation the result is to be expected. Unfortunately, experiments could not be extended to 400–500° C. where adsorption of molecular hydrogen begins on silica surfaces.* At these temperatures the altered surface might well exert a large influence on the secondary reactions.

At high phosphine pressures, there is the possibility that the secondary reactions postulated above may go through the medium of ternary collisions. It is therefore of importance, first of all, to calculate the stationary concentration of hydrogen atoms, and then find if a hydrogen atom can collide with another of its kind and a third molecule before reaching the wall of the reaction tube. When the concentration of hydrogen atoms is stationary,

$$- \frac{d[\text{H}]}{dt} = \frac{1}{T} [\text{H}],$$

where T is the time required for a hydrogen atom to diffuse to the walls, assuming that this is the only way in which hydrogen atoms are removed from the gas. $d[\text{H}]/dt$ may easily be obtained from the experimental data and amounts to about 10^{-5} mm. per second. T may be obtained from the diffusion coefficient (D) of hydrogen atoms through phosphine by means of the Einstein equation $r^2 = 2DT$, r being the radius of R_1 . Taking the radius of the hydrogen atom as 0.5×10^{-8} cm., D , on calculating from the Stefan-Maxwell equation $D = \kappa/\sigma_{12}^2(1/M_1 + 1/M_2)^{1/2}$, amounts to 1.1 for phosphine at 760 mm. T is therefore 10 seconds and $[\text{H}] = 10^{-4}$ mm. Now one hydrogen atom makes about 10^{10} collisions per second with phosphine molecules at 760 mm.; it will therefore make 10^3 collisions per second with hydrogen atoms. If a phosphine molecule is also involved in the collision between the two hydrogen atoms, there will be between 1 and 10 ternary collisions before the hydrogen atom reaches the walls, if the ratio of the number of bimolecular collisions to that of ternary collisions is as the diameter of the hydrogen atom to its mean free path in phosphine.

The hydrogen atom takes 10 seconds to reach the walls if it is generated in the middle of the bulb. At 760 mm., however, absorption of light at 210 m μ is practically complete in a layer less than 1 cm. in thickness, so that the time required for the atom to reach the walls is more nearly 1 second instead of 10

* Bone and Wheeler, 'Phil. Trans.,' A, vol. 206, p. 1 (1906).

seconds. Hence there is slight balance in favour of the hydrogen atom (or the PH_2 radical) reaching the walls rather than making a ternary collision. At pressures less than 760 mm. collisions with the walls are very much more probable. It may be concluded that, in the experiments described above, the secondary reactions in the photochemical decomposition of phosphine take place mainly on the walls of the reaction tube, thus explaining the negligible influence of pressure on the quantum yield. It would be interesting to know, if the concentration of hydrogen atoms and PH_2 radical were increased by adding inert gas to a pressure of several atmospheres and/or increasing the intensity of the incident radiation, whether the ternary collisions, which would take place under these conditions, would have any effect on the quantum yield.

Having now obtained quantum yields of the direct reaction and also the relative efficiency of the photo-sensitized decomposition of NH_3 and of PH_3 , an estimate may be made of the square of the effective collision radii (σ_P^2) of the PH_3 molecule and the 2^3P_1 mercury atom. This estimate is based on the assumption that the secondary reactions in the direct and photo-sensitized reactions are identical. Such an assumption has been substantiated for ammonia (see I) and is probably true for phosphine. σ_P^2 is given by the equation

$$\frac{R_{\text{NH}_3}}{R_{\text{PH}_3}} = \frac{\gamma_{\text{NH}_3}}{\gamma_{\text{PH}_3}} \frac{\sigma_N^2 (1/M_{\text{Hg}} + 1/M_{\text{NH}_3})^{\frac{1}{2}}}{\sigma_P^2 (1/M_{\text{Hg}} + 1/M_{\text{PH}_3})^{\frac{1}{2}}}.$$

In the 2 cm. tube $R_{\text{NH}_3}/R_{\text{PH}_3} = 0.073$, $\gamma_{\text{NH}_3} = 0.25$, $\gamma_{\text{PH}_3} = 0.49$, $\sigma_N^2 = 2.94 \times 10^{-16} \text{ cm.}^2$,* so that the value of σ_P^2 is $27.5 \times 10^{-16} \text{ cm.}^2$

No data for the quenching of resonance radiation by PH_3 are yet available. If subsequent experiment gave σ_P^2 of the order $27.5 \times 10^{-16} \text{ cm.}^2$, then it may be concluded that every collision involving deactivation of the mercury atom results in dissociation of the phosphine molecule. According to the calculations in I, this appears to be the case for ammonia, so that it would be of importance to find whether phosphine behaves in the same way.

It has been pointed out by Zemanski* and by Bates† that those simple molecules which possess large quenching radii have a vibration band in which the energy associated with the quantum corresponds closely to the difference in energy between the 2^3P_1 and 2^3P_0 states of the mercury atom, which amounts to 0.218 volts. For example, CO_2 has a σ^2 of $2.48 \times 10^{-16} \text{ cm.}^2$,

* Zemanski, 'Phys. Rev.', vol. 36, pp. 919, 930 (1930).

† 'J. Amer. Chem. Soc.', vol. 54, p. 569 (1932).

the nearest vibration band being at 0.253 volts; while for NO, $\sigma^2 = 24.7 \times 10^{-16}$ cm.² and a band at 0.235 volts. Although σ^2 for PH₃ is of the same magnitude as that for NO, there is no vibration band close to 0.218 volt, the nearest band at 4.2 μ^* corresponding to 0.29 volts. The exchange of energy between Hg 2³P₁ and PH₃ cannot, therefore, resemble the process suggested by Zemanski.

The mechanism of the photochemical decomposition of phosphine, so far as it is revealed by these experiments and calculations, may be summarized as follows: PH₃ is dissociated into PH₂ and H, which diffuse to the walls. These radicals undergo secondary reactions at the walls such that the net quantum yield is about 0.5 in a 2-cm. tube. The three main secondary reactions would appear to be PH₂ + PH₂ = P₂ (red phosphorus) + 2H₂, H + H = H₂, PH₂ + H = PH₃. The reaction PH₂ + H is slightly favoured by increase of surface and by an increase in the number of hydrogen atoms adsorbed on the walls. Temperatures up to 300° C. have little effect, so that the heats of activations of the surface reactions are probably small.

PART IV.

The Photochemical Oxidation of Phosphine.

It has been shown in II that oxygen strongly accelerates the photo-sensitized decomposition of phosphine, while the subsequent addition of argon still further increases the rate of oxidation. The latter influence of argon is indicative of the intervention of a chain mechanism. Quantitative experiments are, however, not easy with the photo-sensitized reaction, as it is difficult to estimate the extent of the deactivation of the mercury atoms by oxygen and by argon. With the direct photochemical reaction, conditions are rather simpler, so that it is possible to make more detailed calculations and finally to obtain quantum yields of the oxidation process, so that the length of the reaction chains may be calculated.

The experimental procedure was as follows: R₁ was filled with PH₃, the pressure being about 0.05 mm. With the ammonia photometer (R₂) in use an exposure was made in order to measure the rate of decomposition of the PH₃. R₁ was again filled with phosphine to the same pressure, the PH₃ was condensed out with liquid air and then oxygen added (about 0.05 mm.). The PH₃ was evaporated and the mixture illuminated, R₂ measuring the

* Robertson and Fox, 'Proc. Roy. Soc.,' A, vol. 120, p. 128 (1928).

intensity of the spark as before. After condensing out the residual PH_3 into a liquid air trap provided with a tap (having a volume of about 10 c.c. compared with 600 c.c. of R_1 + McLeod) the pressure of residual gas was measured. The tap on the liquid air trap was then closed, the non-condensable gases pumped off and the pressure of the remaining phosphine determined. From these measurements, which are given in Table VI, after making a small correction for pumping off a little phosphine with the non-condensable gas, the amount of PH_3 decomposed was easily calculated.

Table VI.—Temperature $18^\circ \pm 1^\circ \text{C}$. Zn spark. 7 cm. bulb.

P_{PH_3} initial.	P_{O_2} added	P_{uncond} + 0.0085 mm.	P_{PH_3} residual.	P_{PH_3} decom- posed	$P_{\text{H}_2 + \text{N}}$ in R_2 .	Chain length observed.	Chain length calculated.
0.0970	—	0.0103	—	0.0014	0.0232	—	
0.0900	0.0670	0.0585	0.0505	0.0365	0.0226	265	1100
0.1235	—	0.0113	—	0.0021	0.0214	—	
0.1210	0.0600	0.0545	0.0635	0.0490	0.0179	240	1310
0.1235	0.1055	0.1055	0.0610	0.0545	0.0116	270	2350
0.0715	—	0.0093	—	0.0006	0.0217	—	
0.0685	0.0570	0.0450	0.0200	0.0400	0.0113	1150	663
0.0650	0.0955	0.1040	0.0255	0.0310	0.0086	550	1110
0.0705	—	0.0197	—	0.0084	0.0480	—	
0.0645	0.0165	0.0305	0.0315	0.0245	0.0232	—	
0.0705	0.0535	0.0520	0.0170	0.0450	0.0191	180	818
0.0695	0.0805	0.0775	0.0120	0.0490	0.0161	190	1010
0.1035	—	0.0217	—	0.0100	0.0440	—	
0.1020	0.0155	0.0315	0.0675	0.0260	0.0155	—	
0.1025	0.0560	0.0575	0.0445	0.0495	0.0173	59	1030
0.0995	0.0820	0.0765	0.0265	0.0645	0.0155	190	1480
0.0610	—	0.0153	—	0.0050	0.0410	—	
0.0515	0.0540	0.0530	0.0083	0.0347	0.0179	250	500
0.0520	0.0790	0.0785	0.0055	0.0380	0.0167	205	740
0.0570	—	0.0135	—	0.0038	0.0393	—	
0.0550	0.0435	0.0360	0.0167	0.0297	0.0107	215	430
0.0605	0.0570	0.0495	0.0220	0.0300	0.0071	265	620
0.0605	0.0770	0.0780	0.0215	0.0305	0.0095	160	840

0.0085 mm. is the vapour pressure of the PH_3 .

After the third set of experiments R_1 was taken down and cleaned.

In the penultimate column of the table the results are multiplied by $1/\gamma$ since the quantum yield in the 7 cm. tube is less than unity.

The third column in Table VI shows that the pressure of non-condensable gas is approximately equal to the initial pressure of oxygen although the amount of phosphine decomposed is quite large. The same observation was

made during the experiments on the photo-sensitized oxidation. In the present case also, it would appear that the main oxidation reaction is $\text{PH}_3 + \text{O}_2 = \text{H}_2 + \text{HPO}_2$, the HPO_2 being deposited on the walls. All subsequent calculations about chain lengths will therefore be based on the assumption that the reaction takes place according to this equation.

In suggesting a mechanism for the reaction it will be supposed that the phosphine molecule is decomposed according to the equation $\text{PH}_3 + h\nu = \text{PH}_2 + \text{H}$. The PH_2 radical reacts on colliding with the first oxygen molecule it encounters. During this collision some molecule or radical is produced which is able, by virtue of its energy content or chemical unsaturation, to initiate a chain reaction between PH_3 and O_2 . At 0.1 mm. of PH_3 according to the estimates made on p. 550, the hydrogen atom could make 10^6 collisions per second with O_2 molecules. As the H atoms would diffuse to the wall in about 10^{-4} seconds, the formation of excited H_2O or of OH by the ternary collision $\text{H} + \text{H}_2 + \text{O}_2 = \text{H}_2\text{O} + \text{H}$ is improbable, so that the possibility of H_2O or OH starting a chain may be excluded.

It has been shown that with small pressures of phosphine the rate of the photochemical decomposition is proportional to the pressure so that

$$\frac{d[\text{PH}_3]}{dt} = kI^1 [\text{PH}_3], \quad (1)$$

and for the photo-oxidation

$$-\frac{d[\text{PH}_3]}{dt} = kIK [\text{PH}_3]^2 [\text{O}_2] \{1 + \mu [\text{H}_2]/([\text{PH}_3] + [\text{O}_2])\}, \quad (2)$$

where k is a constant, I and I^1 are the intensities of the incident radiation. K is another constant depending on the chain characteristics of the oxidation. The factor including H_2 represents the inert gas effect, μ being a constant.

If a and b are the initial concentrations of PH_3 and O_2 respectively and x the concentration of PH_3 decomposed, then from (1)

$$\frac{dx}{dt} = kI^1 (a - x)$$

or

$$kI^1 t = \ln \frac{a}{a - x} \quad (3)$$

where t is the time of illumination. Now Table VI shows that the amount of PH_3 decomposed is nearly equivalent to the amount of O_2 used up and to the amount of hydrogen formed so that (2) becomes

$$\frac{dx}{dt} = kIK (a - x)^2 (b - x) \{1 + \mu x/(a + b - 2x)\}. \quad (4)$$

The integration of (4) is considerably simplified for it is probable that μ is of the order of 0.1^* so that the inert gas factor may, to a first approximation, be neglected. Upon integrating the simplified form of equation (4)

$$kIt \cdot K = \frac{1}{a(b-a)} \frac{x}{a-x} + \frac{1}{(b-a)^2} \ln \frac{b(a-x)}{a(b-x)}. \quad (5)$$

If the chain is unbranched, the chain length ν is given by

$$\nu = K[\text{PH}_3][\text{O}_2]. \quad (6)$$

From the experiments on the photo-dissociation and the readings of the photometer $\ln a/(a-x)$ and It and therefore k can be calculated. Similarly the experiments on the photo-oxidation yield the value of $k \cdot K$ by means of (5). Hence K is obtained and from (6) the chain length.

The number of links ν^1 in a straight chain assuming reaction at every collision is given by the formula†

$$\nu^1 = \frac{ab}{(a+b)^2} \cdot \frac{1.5 d^2}{\lambda^2},$$

where d is the average distance a chain diffuses to the walls where it is supposed to be broken. λ is the mean free path of the chain in centimetres at pressure $(a+b)$. In the present case λ is difficult to estimate, since the nature of the chain carriers is not known, but at 0.1 mm. pressure $\lambda = 10^{-1}$ cm. is not an unreasonable estimate. If $a = b = 0.05$ mm. and $d = 3.5$ cm., $\nu^1 = 450$. Using this value the last column of Table VI has been constructed.

The calculated and observed values of ν are of the same order of magnitude, although the calculated results are higher consistently by a factor of 2–5. The simplest interpretation of this approximate agreement would be that the chains are straight, reaction occurring at every collision of the chain carrier with O_2 or with PH_3 , according to the nature of the carrier, and that every chain which reaches the wall terminates there. The low value of the observed chain length is probably due to deactivation in the gas phase—a phenomenon which becomes very marked at higher pressures (*cf.* Dalton and Hinshelwood, *loc. cit.*).

Phosphine and oxygen mixtures are, however, spontaneously inflammable if the pressure is raised to a sufficient degree. The chain theory interprets this as an indication of branched chains. Suppose, therefore, that the phosphine

* Melville, 'Trans. Faraday Soc.', vol. 28, p. 814 (1932).

† Semenov, 'Z. Physik,' vol. 48, p. 109 (1927); Dalton and Hinshelwood, 'Proc. Roy. Soc.' A, vol. 125, p. 294 (1929).

oxygen chain branches at every cycle. Let n be the average length of any chain from the starting point to the end of the branch, then v the total number of molecules of PH_3 decomposed per initial chain centre (which is the length of a straight chain) is given by

$$\begin{aligned} v &= 1 + (2 + 2^2 + 2^3 + \dots \text{to } n \text{ terms}) \\ &= 1 + 2^{n+1} - 2. \end{aligned}$$

From Table VI $v \doteq 200$, so that $n = 7$. Therefore if branching does occur at every cycle, the chain is so short that it will not reach the wall. But as an increase in the diameter of the reaction tube increases the chain length, the chains must reach the wall and therefore the probability of branching must be less than 1 in 200.

If the agreement between calculated and observed chain lengths obtained in Table VI is regarded as purely fortuitous, and if the chains are reflected from the wall, then the probability of branching must be even smaller than 5×10^{-3} . That the condition of the walls does alter the probability of termination has been demonstrated,* but the effect is less than an order of magnitude, and thus does not alter the significance of the above discussion to any great extent. In order to settle the matter unequivocally, experiments would require to be devised in which the probability of branching and the probability of termination could be separately determined.

The author wishes to thank Dr. E. B. Ludlam and Professor Kendall for their interest and encouragement during the progress of these experiments. Thanks are also due to the Carnegie Trustees for a scholarship and to the Imperial Chemical Industries, Ltd., for a grant towards the cost of the apparatus.

Summary.

The absorption spectrum of phosphine has been photographed at room temperature. It consists of a region of continuous absorption beginning at $230 \text{ m}\mu$, which is preceded by four weak diffuse bands. At 300°C . the bands disappear and the limit moves towards the longer wave-lengths.

The photo decomposition of phosphine by light from zinc and aluminium sparks has been studied. The reaction is $4\text{PH}_3 = \text{P}_4 + 6\text{H}_2$, the phosphorus being deposited as the red variety. The quantum yield (γ) is 0.56 in a 7 cm.

* Hinshelwood and Clusius, 'Proc. Roy. Soc.,' A, vol. 129, p. 589 (1930); also Part II of this investigation.

bulb, falling to 0.49 in a 2 cm. cylindrical tube. Temperatures up to 300° C. do not influence γ . Molecular hydrogen has no effect, but atomic hydrogen decreases γ . The mechanism of the reaction is discussed and compared with the photo-sensitized reaction.

On adding oxygen to PH_3 and illuminating, a stable chain reaction occurs, and with pressures of $\text{PH}_3 = \text{O}_2 = 0.05$ mm. $\gamma = 200$. The significance of the value is discussed in relation to the theory of branched chains. It is concluded that the probability of branching at any one cycle is not more efficient than 5×10^{-3} .

A compact and sensitive form of combined reaction tube and McLeod gauge is described.

The Relationship between Viscosity, Elasticity and Plastic Strength of a Soft Material as Illustrated by some Mechanical Properties of Flour Dough.—II.

By ROBERT KENWORTHY SCHOFIELD and GEORGE WILLIAM SCOTT BLAIR.

(Communicated by Sir John Russell, F.R.S.—Received October 1, 1932.)

In an earlier communication* Maxwell's "time of relaxation" was given an extended and more general definition so that the conception might be used in describing the behaviour of plastic substances. From a study of such materials in steady flow it is well known that the viscosity defined as the ratio of the shearing stress, S , to the velocity gradient or rate of shear, G , is not a constant but usually decreases as S increases. The time of relaxation, t_r , is related to the viscosity, η , thus

$$t_r = \eta/n,$$

n being the rigidity modulus. Since n is normally independent of the stress,† t_r and η show parallel variations.

For ordinary fluids t_r is very small and no way has yet been devised for measuring it. In flour dough, however, we have a material in which high viscosities are combined with a low rigidity modulus, and consequently the relaxation of internal stress is slow enough to be easily followed experimentally.

* 'Proc. Roy. Soc.,' A, vol. 138, p. 707 (1932).

† p. 566.

Observations made on cylinders of dough which had been stretched to various extents showed that the relaxation time (and hence the viscosity) depends on the degree of stretching as well as on the stress.



FIG. 1.

It appeared desirable to obtain confirmation of this double dependence of viscosity on the extent of shearing as well as on the shearing stress by a more direct method. For this purpose, a study was made of the rate of elongation of cylinders of unyeasted dough hung vertically by their upper ends and allowed to extend under the action of gravity. In carrying out these observations it has been found convenient to mark on the dough cylinders a series of fine parallel lines accurately spaced 1 mm. apart. The marks were made by successive turns of a fine wire wrapped round a frame, which are wetted with enamel, the marks remaining wet long enough to be subsequently printed off on to a strip of duplicator paper. This method has the advantage of enabling an instantaneous record to be made of the deformation of a series of elements throughout the length of the dough cylinder. The recording is rapid and permanent, and the print (which may be called a rheogram) is available for whatever analysis appears suitable, fig. 2.

In obtaining the data which is about to be discussed, a number of precautions were taken :—

- (1) *Moisture Content.*—The doughs used had a moisture content such that when they were pressed firmly on to a glass plate they just did not stick appreciably to it. At the first mixing, slightly insufficient salt solution—strength 2.5 per cent.—was added to the flour, and after half an hour a little more was kneaded in so as to produce the desired condition. If, on thoroughly kneading at the end of a further half-hour, the moisture condition was judged to be correct, the dough was considered to be satisfactory for testing. In order to prevent drying during the test, the shaping, and marking of the cylinders was carried out as quickly as possible and while extending under gravity they were hung inside large boiling tubes containing a little water, see fig. 1.
- (2) *Shaping the Cylinders.*—Each of the pieces into which the dough was divided was forced through a short metal tube attached to a wider tube fitted with a plunger. In order to prevent avoidable straining, the “gun” was held vertically, the cylinders being extended downwards. Each cylinder as it was formed was detached and held by its

upper end which was then pressed firmly on to the support provided, see fig. 1. The diameter of these cylinders, about 7 mm., was surprisingly uniform except for a "blob" at the end, which was always cut off. The length used for the test depended on the nature of the dough, and on the time allowed for the extension, the aim being to use the longest cylinder that would not break off prematurely. In practice the lengths varied from 4 to 12 cm.

- (3) *Elastic Deformation*.—So long as the dough cylinder is hanging vertically, it is subject not only to plastic flow, but also to an elastic deformation which could be recovered by placing it horizontally. This recovery will only proceed to completion on a frictionless support like a mercury bath. It was found convenient to apply the marker and also to print off the rheogram with the dough lying horizontally on the wooden back B, but in neither case is the elastic deformation recovered owing to the tendency of the dough to stick lightly to the back as soon as it touches it. The elastic deformation was generally small compared with the plastic deformation, and as it was present both at marking and at printing, it cannot appreciably have affected the results.

- (4) *Printing the Rheograms*.—As a certain degree of pressure is needed when printing the rheograms which somewhat flattens the cylinder it was feared that the marks on the print might not faithfully reflect the state of affairs before the paper touched the dough. Such fears are, however, allayed by an examination of the rheograms themselves, fig. 2. The clearness

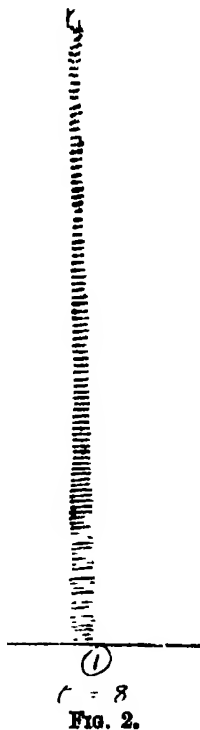


Fig. 2.

of the impression makes it evident that no movement of the surface of the dough occurs once it has touched the paper. Before printing off, a line is ruled on the paper which is placed against the lower end of the dough cylinder when taking the print. This line provides the zero for computing the stress.

Although the apparatus and procedure are simple, care is needed in the manipulation lest the test cylinder be accidentally strained at some stage. So easy is it to spoil an experiment that the cylinders were usually tested in

triplicate. In the case of the data about to be discussed, one of each of the three sets had to be discarded leaving only duplicate rheograms for the final analysis.

When analysing the rheograms it is not necessary to know the dimensions of the cylinders, provided that they were initially of uniform cross-section. Except within a few millimetres of the support, the behaviour of any element is governed exclusively by the original length of the dough which hung below it. The top two or three marks are usually distorted and are always disregarded. In evaluating the shear and the shearing stress, use is made of the well-known principle (already employed in the earlier paper) that an elongation of a material which does not change its volume may be expressed as the resultant of two shears each equal in magnitude to the elongation, while the corresponding shearing stresses are equal to one-third of the tensile stress per unit area. The extensions involved here are sometimes several-fold, so that it appears better to express the elongation, and hence the shears, in an element of which the original length, l_0 , has increased after time, t , to l ; as $\log_e l/l_0$ rather than as $l - l_0/l_0$ (although, of course, the two expressions are equal for small elongations). The tensile stress per unit area acting over the meridian cross-section of this element was equal to $g\rho L_0$ where ρ is the density and L_0 the (initial) distance of the section from the lower end of the cylinder. This distance can still be ascertained after the elongation has taken place by counting up the markings. The elongation is accompanied by a proportional shrinkage of the cross-sectional area, so that the tensile stress at time t is $g\rho L_0 l/l_0$. Hence the mean shearing stress equals $\frac{1}{3} g\rho L_0 (1 + l/l_0)$ under which the dough suffers a mean rate of shear of $\frac{1}{t} \log_e l/l_0$.

In fig. 3 the mean rate of shear is plotted against the mean shearing stress for three times-of-hanging of cylinders all formed from pieces of the same dough and tested in rapid succession. The flour was a good bakers' mixture. A value of 5 mm. was selected for the length, l_0 , of an element, and l was found by determining the distance between each mark and its fifth neighbour. Each point is the result of a measurement of this kind. Two rheograms were obtained for each of the three times-of-hanging, and the points from all six are shown.

The lack of coincidence between the three sets of points shows that the rate of shear under a given stress is not uniform but diminishes as the shearing proceeds. It is very important to bear this fact in mind when seeking to interpret the curves. Apart from this fact their negative curvature, which is

particularly marked for the 8 min. curve, would be very surprising, involving an increase of viscosity with increase of stress. This curvature is the result of the double dependence of viscosity on stress and shear. The position emerges more clearly if sets of points corresponding to equal shears are picked out on the three curves. One such set is connected by the broken curve. This evidently leaves the axis of the abscissa at about $S = 800$ (since below this

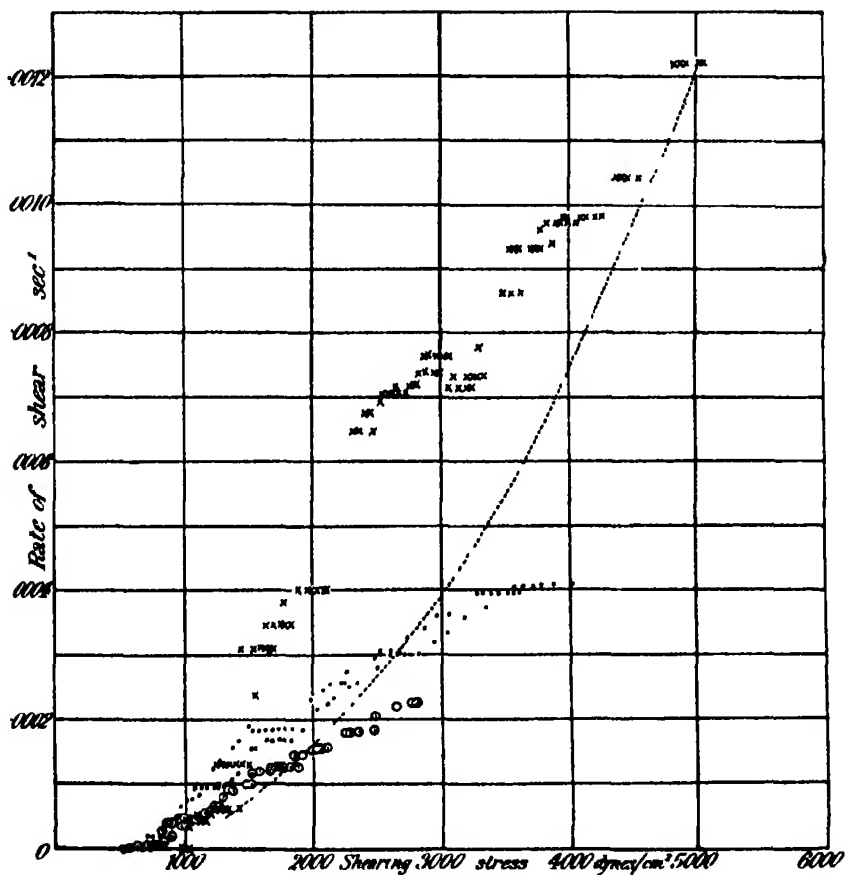


FIG. 3.—○ $t = 64$; ● $t = 32$; × $t = 8$ minutes.

stress the shear is zero for all three times) and thence shows a consistent upward curvature. A family of such curves could be drawn each having the same form.

In order to evaluate the viscosities, the variation of shear with time for a series of constant mean stresses has been traced in fig. 4, the positions of the points being obtained by interpolating on fig. 3. The slope of one of these

at any particular point, gives the rate of shear under that stress after a shear measured by the ordinate has taken place. The figures given in the table for shears of 2.5, 4.1, and 7.0 were obtained in this way by dividing each

Shear.	0.25	0.41	0.70	0.58
Stress dynes/mm. ² .	Viscosities from rheograms.			Viscosity from relaxation times.
15	1.6×10^7	2.4×10^7	—	2.1×10^7
20	0.9×10^7	1.7×10^7	—	1.4×10^7
25	0.7×10^7	1.6×10^7	2.3×10^7	1.1×10^7
30	—	1.2×10^7	2.1×10^7	0.8×10^7
35	—	0.9×10^7	1.8×10^7	0.6×10^7
40	—	0.8×10^7	1.6×10^7	0.5×10^7

shearing stress by the corresponding rate of shear. These viscosities are of the same order of magnitude and show the same kind of variation with stress and shear as those deduced in Part I, fig. 5. A detailed comparison shows,

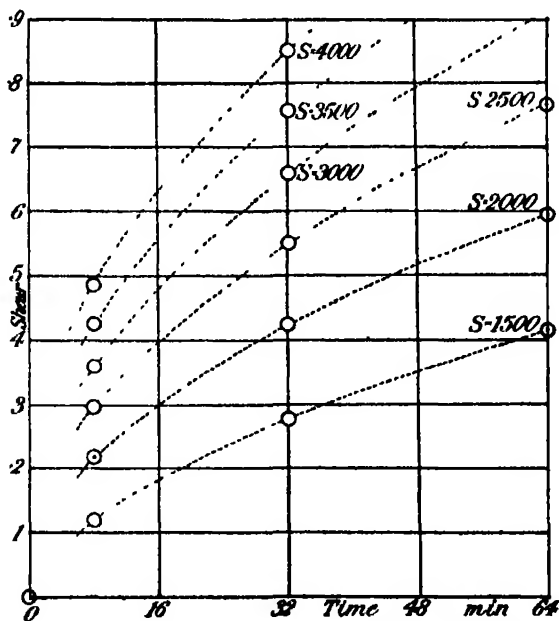


FIG. 4.

however, that the values obtained by the earlier method are consistently lower. As the new flour, though very similar, was not identical with that used in the former experiments, a set of observations of the relaxation of stress was

carried out on a dough cylinder made from the new flour (the old flour being no longer available). The measurements were carried out in the way described in Part I (*loc. cit.*) and the viscosities which are given in the last column of the table were obtained by finding the relaxation times $\left(= \frac{1}{d(\log_e S)/dt} \right)$ for a series of stresses, and multiplying by the rigidity modulus $(= \frac{1}{3}$ Young's modulus). An extension of 80 per cent. was used, which falls between those used in obtaining the curves of fig. 5 of Part I. The corresponding shear of 0.58 also lies within the range covered by the rheogram figures.

The new values fall into line with the old. As will be seen they are only about half what would be obtained by interpolating between the figures for shears of 0.41 and 0.70. They rest, it is true, on the use of 2×10^4 as the rigidity modulus. This is admittedly a "round" figure, but it is unlikely to be in error by as much as a factor of 2*. There are other experimental and computational uncertainties, but none appears serious enough to account for the difference. When it is noted that the viscosities vary threefold for only modest variations of stress and shear it will be realized that the values are very sensitive to changes in the condition of the dough. It may be that the results differ because the shearing recorded in the rheograms was slow and steady in contrast to the rapid preliminary shearing given to the cylinders in the earlier method. As was noted in Part I a considerable proportion of the elastic recovery of a dough which has been strained for a long time is of the nature of a creep while the whole of the recovery from a short strain is comparatively rapid, indicating that during long periods of strain internal adjustments occur which take some time to readjust when the external stress is removed. It may be that these internal adjustments, which would have more opportunity of taking place in the rheogram method, have as much to do with the variations of viscosity as the shear associated with the alteration of external form, but such a hypothesis requires further test before it can be advanced with confidence. While reserving this point for further investigation we appear justified in taking the general concordance of the two sets of figures as substantiating the correctness of the relationship

$$\eta = t_r \cdot n.$$

In a general way the results from the rheograms show an interesting correspondence with those of Trouton† for pitch, though there are contrasts in the

* *Note.*—p. 566.

† 'Proc. Roy. Soc.' A, vol. 77, p. 426 (1906).

magnitudes concerned. The stresses used by Trouton were considerably larger, and the rate of shear for a given stress approached constancy after a much smaller degree of shearing. Trouton stated that after the lapse of about half an hour under a constant stress a steady rate of shear was reached, but the data shown in his fig. 2, p. 428, are consistent with the view that a decrease was going on during the whole of the experiment. It is also interesting to compare his fig. 3, p. 429, with our fig. 3. Although he draws a straight line in his graph, his points indicate a negative curvature just as do ours in the case of dough. In both cases the curvature is only negative above a certain stress limit. For the dough, the curves start from the origin and remain practically coincident with the axis of the abscissa until somewhere between $S = 600$ and $S = 1000$, they then take a very steep upward bend after which the gentle negative curvature sets in. The upward bend marks the yield value, the corresponding stress measuring the shearing strength of the material under the conditions of the experiment. Below this stress no detectable flow takes place during the time of the experiment, and the material behaves like a solid.

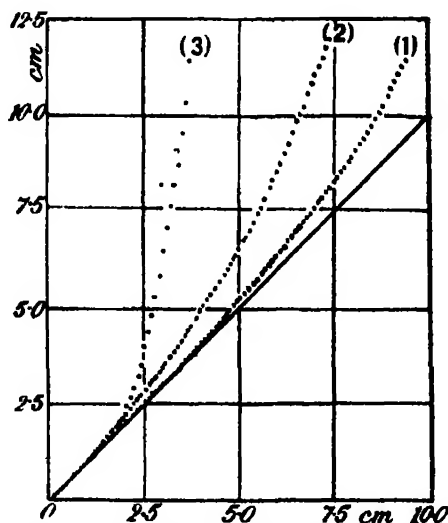


FIG. 5.—(1) Manitoba flour; (2) Baker's mixture; (3) English flour.

Although the foregoing analysis is needed to ascertain the factors upon which the rate of flow of a dough depends, a much less elaborate treatment suffices in many cases to distinguish doughs by their flow properties. Fig. 5 has been constructed by placing each of the three rheograms in turn along the axis of the ordinate and plotting the marks in turn against successive millimetre divisions along the abscissa. If no flow had taken place the result

would have been a line from the origin, of slope unity, and the aggregate flow in 20 minutes is shown by the departure of points from this line. This way of plotting easily differentiates the three flours in question, but the capacity of the method to distinguish the small differences which are of importance in baking has still to be determined. The outlook in this direction is, however, distinctly hopeful, as, from the point of view of the stresses used and their times of application, the conditions of the test correspond closely to those ruling inside a dough that is distending under the action of yeast.



FIG. 6.

The hardening of a dough by shearing was independently demonstrated by a simple experiment. Three doughs were made up *with yeast* and kneaded well. Each was then pulled out and folded over a number of times, care being taken that the elongation and folding were always made in the same direction. The final fold was made so as to give the dough a form as nearly cubic as possible, finishing touches being given by slight pressure of the thumb and fingers. As the photograph, fig. 6, shows, the swelling was uneven, the smaller expansion occurring in the direction in which the dough had previously been stretched, as shown by the arrow. Dough B was at the standard moisture content, A being a little wetter, and C a little dryer.

Summary.

The dependence of the viscosity of a flour dough on the shear which has taken place as well as on the shearing stress is brought out by a series of observations on the rate of shear in cylinders of unyeasted dough hung vertically and allowed to elongate under the action of gravity.

The deformations were recorded by marking a millimetre scale in enamel on the surface of the dough cylinders, and, after elongation had proceeded for a measured time, printing the deformed scale off on to a strip of duplicator paper. The print has been called a rheogram.

The agreement between the viscosities determined directly in this way and those obtained indirectly in Part I is satisfactory as substantiating the theory that the viscosity is equal to the product of the rigidity modulus and the relaxation time.

The conditions of test correspond closely with those ruling inside a dough distending under the action of yeast, but whether the method is capable of distinguishing the small differences which are of importance in baking has still to be determined.

[*Note added in proof, January 11th, 1932.*—Further work, of which the results have been submitted for publication as Paper III of this series, has shown that, although n is far less variable than η , it is not exactly constant. (cf p. 557, lines 9 and 10.) Since writing the statement on p. 563 to the effect that the value of 2×10^4 for the rigidity modulus used to compute viscosity from relaxation time "is unlikely to be in error by as much as a factor of 2," the authors have concluded that 2×10^4 , although a good mean value, is not that most appropriate for this computation. Using the value which the latest experiments have shown to be applicable to the conditions of stress relaxation, a close agreement is found between the viscosities calculated from the relaxation times and those obtained from the rheograms.]

The Parent of Protactinium.

By O. A. GRATIAS and C. H. COLLIE.

(Communicated by F. A. Lindemann, F.R.S.—Received October 4, 1932)

Introduction.

Although protactinium was discovered by Hahn and Meitner* and Soddy and Cranston† in 1918, no direct experimental evidence as to its parent element has yet been obtained.

Theoretical speculations as to its parent have been published by Russell,‡ but the most commonly accepted suggestion is that protactinium is formed from uranium Y (UY). This is in agreement with the displacement rule, according to which the product of UY must be a homologue of tantalum (ekatantalum), and the approximate equality of the UY/UX, Pa/U ratios.§

However, as various workers|| have pointed out, this is merely a convenient hypothesis; there is no unambiguous experimental reason why the parent of protactinium could not be a β -ray emitting body of atomic number 90 with a long half-value period. Such an element would almost certainly have escaped detection.

The simplest way of settling this question is to investigate directly the product of uranium Y. When uranium Y decays, as far as is known, it must form an element isotopic with protactinium which cannot be strongly radioactive since otherwise its presence would have been detected by other workers. We have to devise an experiment to isolate the daughter element formed from the decay of uranium Y, and then to examine it to see whether it emits α particles.

If a negative result is obtained then the protactinium which grows in uranium minerals must have another origin.

If a positive result is obtained one must find out whether the particles are emitted by the known radioactive element (protactinium). This is most easily done by showing that it is isotopic with protactinium by an examination of its

* 'Phys. Z.,' vol. 19, p. 208 (1918).

† 'Proc. Roy. Soc.,' A, vol. 94, p. 384 (1918).

‡ Russell, 'Nature,' vol. 111, p. 703 (1923).

§ Kirsch, 'SitzBer. Akad. Wiss. Wien,' vol. 129, p. 309 (1920), St. Meyer, 'SitzBer. Akad. Wiss. Wien,' vol. 129, p. 483 (1920).

|| Cf. Fajans, "Radioelements and Isotopes," chap. 1.

chemical behaviour and by measuring its decay constant. Identification by measurement of the range is very difficult when the source is weak.

Since the decay constants of uranium Y and protactinium are known it is possible to calculate how much uranium nitrate must be taken in order to give an unambiguous result.

The number of uranium Y atoms formed in 24 hours* (the half-value period) in 1 kilogram of uranium assuming 3 per cent. branching is 2.15×10^{10} , and these would produce 0.9 α particles per minute.

But not all these particles can be relied on to contribute to the number measured in the apparatus, for the following reasons :—

- (a) During the isolation and purification of the source of uranium Y several chemical separations have to be carried out, some of them on a large scale which cannot be expected to give 100 per cent. yields.
- (b) The source is adsorbed on a small quantity of tantalic acid so that some of the α particles will be absorbed and not enter the ionization chamber.
- (c) The final source must be supported on a metal disc so that one half of the α particles are emitted into the base instead of into the ionization chamber.

A careful consideration of all the factors involved, based on known measurements for the separate processes, showed that from 10 kg. of uranium used as starting material one would expect to get one α particle a minute due to protactinium in the ionization chamber.

Experiment showed that it was difficult to obtain an ionization chamber which showed a natural contamination of less than one α particle a minute, so that to obtain definite results one requires 10 α particles a minute effective in the chamber. Thus by separating the uranium Y grown from 10 kg. of uranium every 24 hours for a period of 2 to 3 weeks, allowing it to decay for 7 to 10 days and adding it together, one might expect to have about 10 recorded α particles a minute due to protactinium. Thus about 25 kg. of the uranium nitrate ($\text{UO}_2(\text{NO}_3)_2 \cdot 6\text{H}_2\text{O}$) are needed for the source of uranium Y.

Experimental.

Throughout this work weak α particle sources were measured with a six-stage resistance capacity coupled amplifier. The source, which was usually a small platinum dish covered with a thin film of the active material, was placed in the base of a vertical ionization chamber whose design was essentially

* Gratias and Collie, 'Proc. Roy. Soc.,' A, vol. 135, p. 299 (1932).

similar to the one used in previous work on the chemistry of ekatantalum.* The α particles were counted on a telephone exchange counter operated by the anode current of a thyratron. This proved very satisfactory for the weak sources used (less than one α particle per second) and once it had been adjusted, apart from an occasional recharging of the high tension accumulators, required no attention.

The experimental part may be divided into two parts :—

- (a) The preparation of the source of uranium Y free from ekatantalum.
- (b) The separation of the ekatantalum formed from the uranium Y and the determination of its decay constant.

(a) *Preparation of the Uranium Y.*—The method used was essentially the improvement of Crookes' method used by us in some work on the period of uranium Y,† modified so as to make it suitable for use with larger quantities of material. The principle of this method is that if uranium nitrate is dissolved in ether and the ethereal solution extracted with a little water, most of the uranium X and uranium Y are concentrated into the aqueous layer from which they can be isolated by adsorption on to a precipitate of cerium fluoride.

The chief difficulty was that the volume of aqueous layer separated from the ether solution was too large to be worked up in a platinum dish, while the short average life of uranium Y made it essential to work expeditiously. The problem was solved by evaporating the aqueous layer nearly to dryness under reduced pressure (10 mm.), dissolving the anhydrous nitrate in about 400 c.c. of ether and again extracting with water. The second extract which contained most of the uranium Y was transferred to a platinum dish and worked up as before. To the acid solution was then added 0.001 mg. of thorium nitrate,‡ a few milligrams of ammonium carbonate and 4 c.c. of standard

* Gratias and Collie, 'J. Chem. Soc.,' vol. 1, p. 987 (1932).

† Gratias and Collie, 'Proc. Roy. Soc.,' A, vol. 135, p. 299 (1932).

‡ This thorium was added in order to reduce the adsorption of the uranium X_1 by the tantalum precipitate. In one day the amount of uranium X_1 from 10 kg of uranium

$$\frac{10^4 \times 6.06 \times 10^{23} \times 4.8 \times 10^{-18} \times 9 \times 10^4}{238} = 1.2 \times 10^{13} \text{ atoms.}$$

The adsorption of uranium X_1 was about 3 per cent. in preliminary experiments, so in order to reduce this to a negligible amount (0.03 per cent.) we need one hundred times as much thorium or 10^{15} atoms. But 10^{15} atoms

$$= \frac{10^{15} \times 232}{6.06 \times 10^{23}} = 4 \times 10^{-7} \text{ gm.} = 0.0004 \text{ mg.}$$

of thorium or 0.001 mg. of thorium nitrate. This amount of thorium even in 12 runs would produce only $1.2 \times 10^{15} \times 1.3 \times 10^{-18} \times 60 = 0.94$ particles per minute.

potassium tantalate solution (1 mg. Ta_2O_5 per cubic centimetre); the precipitated tantallic acid was filtered off leaving the solution free from protactinium.

In this way the uranium Y from the 28 kg.* of uranium nitrate used as the starting material could be concentrated into a solution containing only a few milligrams of cerium nitrate in 6 hours.

(b) *Separation of Ekatantalum*.—After the decay of the uranium Y the solution contains the ekatantalum formed from the uranium Y together with the original cerium, uranium X and ionium.

It was hoped that it would be possible to separate the ekatantalum from this solution by depositing it on a lead plate, the method originally used by Fajans and Göhring† to separate UX_2 from such a solution. Although many experiments were carried out under varying conditions the method had to be abandoned as the deposition of the ekatantalum on the lead plate was found to be far from quantitative. It is well known that protactinium is adsorbed very markedly by tantallic acid, and experiments were therefore made to see under what conditions it could be quantitatively adsorbed by tantallic acid in the very small concentrations to be expected.

It was found that adsorption was quantitative in dilute acid solution in the presence of ammonium salts and that the protactinium followed the tantallic acid on solution in hydrofluoric acid, but not on fusion with alkali.

Thus on adding a known quantity of standard potassium tantalate to the solution containing the ekatantalum formed from the UY, at least 90 per cent. of the ekatantalum was separated on a base of inactive tantallic acid.

Actually two series of experiments were carried out. The first in order to see whether the ekatantalum formed was actually an α particle body which gave a sufficient number of α particles to be counted; after a positive result had been obtained the experiment was repeated with the refinement that the quantity of uranium Y allowed to decay each day was measured on a calibrated electroscope so that a fairly accurate measurement of the half value period of the, as yet, unidentified ekatantalum could be made.

Series 1.—In the interval November 22 to December 7 the uranium Y was separated 14 times in the way described at intervals of 24 hours; each source was kept in a separate covered beaker in a cupboard free from dust. Three

* Messrs. Hopkin and Williams very kindly undertook the crystallization and spinning of the uranium nitrate, and our thanks are due to them for the very friendly way in which they met our somewhat exacting requirements as to purity.

† 'Phys. Z.,' vol. 14 p. 877 (1913).

days after the last separation (December 10) the sources were combined evaporated to about 100 c.c., 20 c.c. of standard tantalate added and the tantalic acid filtered off (ppt. A). A further 20 c.c. of tantalate were added to the filtrate and the precipitation repeated (ppt. B). Both these precipitates adsorbed less than one half of 1 per cent. of the total β -ray activity of the solution. Precipitate A contains the ekatantalum formed from the uranium Y together with adsorbed uranium X and ionium, while precipitate B has only adsorbed uranium X and ionium. Since uranium X and ionium are isotopes the ratio of

$$\frac{\text{Ionium in A}}{\text{Ionium in B}} = \frac{\beta\text{-ray activity of A}}{\beta\text{-ray activity of B}}.$$

The actual activities found were :—

Source A = 18.9 d.p.m.

Source B = 7.4 d.p.m.

It is seen from this that A has adsorbed more than twice as much ionium as B, so that even if there were no ekatantalum in A it will show a greater α particle activity.

The tantalic acid precipitates (A and B) were dissolved in strong hydrofluoric acid, and the solutions evaporated to dryness in small flat platinum dishes (L and O respectively) so as to give films weighing 2 to 3 mg. per cm.².

On examining these dishes in the amplifier the following results were obtained :—

Dish L gave	14.40	α particles per minute.
Blank for dish L	1.2	„ „
Therefore precipitate A gave	13.2	„ „
Dish O gave	3.6	„ „
Blank for dish O	1.4	„ „
Therefore precipitate B gave	2.2	„ „

The α particles in precipitate B are due entirely to ionium so that to a first approximation the ionium in precipitate A contributes $18.9/7.4 \times 2.2 = 5.6$ α particles per minute leaving $13.2 - 5.6 = 7.6$ α particles per minute due to the ekatantalum formed from the decay of uranium Y.

Series 2.—For this series 12 separations of uranium Y were made in 13 days (February 5 to 18), and after the uranium Y had decayed the solutions

were combined and tantalic acid precipitated in them to give two precipitates C and D, the former containing the ekatantalum.

The difference between this series and the former set of experiments was that after the preparation of each source an aliquot portion was removed and the amount of uranium Y in it measured with an electroscope.

The electroscope used had a $1\ \mu$ aluminium foil base and the source could be placed on a small table a constant distance below it. One cubic centimetre of the solution to be measured was evaporated to dryness in a watch glass so as to give a uniform film. The activity measured was due to uranium Y and uranium X, but after 10 days the activity was due only to uranium X; thus a simple calculation gives the activity due to uranium Y in the original preparation. The electroscope was calibrated by making a quantitative separation of the uranium Y in equilibrium with a weighed quantity of uranium (278 gm. of uranium nitrate).

The result of the calibration was that each d.p.m. of activity due to UY shown on the electroscope corresponded to 1.59×10^8 atoms of uranium Y.

The measurements of the amount of uranium Y in the second series of experiments is given in Table I.

Table I.

Date of separation.	Volume of solution in c.c.	Activity of UY + UX ₁ of 1 c.c. in d.p.m.	Activity of UX ₁ 10 days later.	Activity of UX ₁ at separation.	Activity of UY.	Total UY activity in d.p.m.
February 5	29 0	83.9	50 2	66.8	17.1	495.9
" 6	30.5	71.2	39.7	52.9	18.3	558.1
" 8	30 0	85.2	49 5	66.5	18.7	729.3
" 9	29 0	77.7	46 8	62.3	15.4	446.4
" 10	29.0	72.6	38 2	50.9	21.7	629.3
" 11	34.0	65.0	35 0	46.6	18.4	625.6
" 13	47.8	65.3	36 0	48.0	17.3	825.2
" 14	34 0	52.7	34 0	45.3	7.2	244.8
" 15	29 0	32.5	17.8	23.8	8.7	252.3
" 16	34 0	51.3	29 3	39.1	12.2	414.8
" 17	34 0	45.7	24.8	33.1	12.6	428.4
" 18	30 0	52.6	29.0	38.7	13.9	417.0

The total uranium Y activity amounted to 6067.1 d.p.m. and corresponded to $6067.1 \times 1.59 \times 10^8 = 9.64 \times 10^{11}$ atoms.

The two tantalic acid precipitates showed the following β -ray activities due to adsorption :—

Source C = 20.0 d.p.m.

Source D = 49.2 d.p.m. .

The tantalic acid was dissolved in hydrofluoric acid as before and evaporated so as to give thin films in the small platinum dishes. The numbers of α particles emitted were as follows :—

Dish O gave	11.3 α particles per minute.
Blank for dish O.....	1.0 " "
Thus source C gave	10.3 " "
Dish L gave	13.8 " "
Blank for dish L	.. .	1.0 " "
Thus source D gave	.. .	12.8 " "

The α particles from source C are due to ekatantalum and ionium while those from source D are due only to adsorbed ionium. Thus to a first approximation the adsorbed ionium contributes $12.8 \frac{\beta\text{-ray activity of C}}{\beta\text{-ray activity of D}} = 5.2$ α particles per minute to source A, leaving 5.1 α particles per minute due to ekatantalum.

A more accurate determination of the number of α particles due to the ekatantalum was carried out by a direct experiment in which the ionium was separated from the ekatantalum. This experiment confirmed the supposition that these excess α particles from the precipitates containing the ekatantalum were really due to a body isotopic (if not identical) with protactinium. The two precipitates C and D were dissolved in warm hydrofluoric acid in a large platinum dish (specially cleaned and shown to have no adsorbed protactinium on it) and a solution added containing 6 mg. of cerium nitrate. The cerium fluoride, and with it the ionium, was filtered off using paraffin coated vessels and the filtrate containing the tantalum was again evaporated so as to give a thin film in the platinum dish (L).

The results obtained were :—

Dish containing tantalic acid and ekatantalum gave 8.1 α particles per minute.

Blank for dish = 1.1 α particles per minute.

Thus the ekatantalum gave 7.0 particles per minute by direct measurement, in agreement with the 5.1 α particles per minute obtained by difference.

Previous experiments had shown that under the conditions of the last separation :—

(a) No ionium would be adsorbed by the tantalic acid.

(b) At least 90 per cent. of the protactinium would be found with tantalic acid precipitate.

Discussion of the Results.

It is clear from the experiments which have been described that when uranium Y decays it forms a radioactive element which has similar chemical properties to protactinium and emits α particles. This substance must either be protactinium itself in agreement with the usually accepted scheme, or a new radioactive element. Consideration of the number of α particles emitted by the unknown substance enables its decay constant to be determined and compared with the known decay constant of protactinium.

Owing to the many approximations which have to be made and the difficulty of controlling chemical separations in which so small a number as 10^{12} atoms are concerned, no very great accuracy can be expected. On the other hand the very wide range of decay constants exhibited by even closely related radioactive elements justifies the identification of a radioactive element by means of an approximate determination of its decay constant.

The results obtained in the two series of experiments which have been described are in substantial agreement, and for the purpose of the discussion the directly determined figure of 7 α particles per minute will be taken as the basis of the calculation.

The ekatantalum was adsorbed in a film of tantalic acid of appreciable stopping power so that the actual number of α particles emitted is larger than the number recorded. The film weighed 40 mg. and was formed in a platinum dish 4 cm. in diameter, so that the film weighed 3.2 mg. per cm.².

Since the stopping power of compounds is an additive property it is possible to calculate the stopping power of such a film in terms of that of air by means of the relation* for equivalent thickness, i.e., $\rho d/\sqrt{A} = \text{constant.}$, where ρ , d and A are respectively the density, thickness and atomic weight of the element under consideration. In this case this film is the same as an air film weighing 1.28 mg. per sq. cm.² and has an air equivalent of 1.0 cm.

If $n\alpha$ particles of range R are emitted per unit volume of the film, a layer of unit cross section, and thickness dx , situated x cm. below the surface of the film will emit ndx α particles of which only $ndx/2 [1 - x/R]$ penetrate the surface.

Thus the total number emitted from a film whose thickness is 1.0 cm. is

$$\int_0^{1.0} \frac{n}{2} \left(1 - \frac{x}{R}\right) dx = \left[\frac{nx}{2} \left(1 - \frac{x}{2R}\right) \right]_0^{1.0} = \frac{N}{2} \left(1 - \frac{1.0}{2R}\right),$$

where N is the total number of α particles. This expression is not very sensitive

* Meyer and Schweidler, "Radioaktivität," p. 103.

to the value of R and for the purpose of calculation R has been assumed to equal 3.39 cm. (mean range of Pa at 0°C.),* so that the fraction $[\frac{1}{2}(1 - 1.0/2R)]$ of particles getting out of the film is 0.43. Actually, therefore, at least $7/0.43 = 16.3 \alpha$ particles are emitted by the ekatantalum per minute. This is a minimum figure since all departures from the ideal uniform film assumed in the calculation increase the number stopped in the film.

The number of uranium Y atoms which disintegrated was 9.6×10^{11} , leaving an equal number of ekatantalum atoms in their place. Thus if λ is the decay constant of the ekatantalum, we have $\lambda 9.6 \times 10^{11} = 16.3/60$ disintegrations per second, whence $\lambda = 2.8 \times 10^{-13} \text{ sec.}^{-1}$, corresponding to a half value period of 7.8×10^4 years.

This again is a maximum value since it assumes that both separations of the ekatantalum were quantitative. It is in sufficiently good agreement with the accepted value† 3.2×10^4 years to establish the identity of the ekatantalum formed from UY with protactinium.

Conclusions.

(a) The disintegration product of uranium Y is a radio element which emits α particles; the element has a chemistry similar to that of protactinium as was to be expected from the displacement rule.

(b) The half value period of this element obtained by direct measurement is 7.8×10^4 years, a value so close to the accepted value of protactinium (3.2×10^4 years) that in the absence of direct evidence to the contrary the element must be assumed to be protactinium itself.

Thus the commonly accepted view that uranium Y is the parent of protactinium is supported for the first time by direct experiment evidence.

In conclusion we have to thank Professor Lindemann for his interest and advice throughout the work, and also for extending to us the facilities of his laboratory.

Summary.

By using a valve amplifier it has been shown that the product of uranium Y is an α particle emitting radio element whose chemical behaviour is similar to that of protactinium.

The half-value period of this radio element obtained by direct measurement is 7.8×10^4 years, a value sufficiently close to that of protactinium (3.2×10^4 years) to identify the daughter element of uranium Y with protactinium.

* Gamow, "Atomic Nuclei and Radioactivity," p. 33.

† Grosse, 'Naturwiss,' vol. 20, p. 505 (1932).

Thermal Decomposition and Detonation of Mercury Fulminate.

By W. E. GARNER and H. R. HAILES, Department of Physical Chemistry,
Bristol University.

(Communicated by Sir Robert Robertson, F.R.S.—Received October 5, 1932.)

Introduction.

Mercury fulminate decomposes when heated below its ignition temperature in vacuum, giving (1) a gas which is mainly carbon dioxide and (2) a brown insoluble residue.* This residue either has a very complex constitution or else is a mixture of several substances, for the gaseous products contain only 60 per cent. of the original oxygen in the fulminate. According to the experiments of Langhams,† the residue behaves towards chemical reagents as if it were a mixture of $\text{Hg}(\text{OCN})\text{CN}$ with a little mercuric oxide. It follows, therefore, that the reaction which occurs on heating must be complex in character and occur in several stages.

There is a very marked initial quiescent period in the decomposition of fulminate which is followed by a rapid acceleration of the decomposition. Farmer ascribes this acceleration to the production of a solid auto-catalyst. Also, since he found that finely powdered fulminate decomposed more rapidly than larger crystals, he concluded that the gas evolution is probably due to surface decomposition,‡ although the increase in the rate of decomposition due to grinding was not so great as would have been expected from the increase in surface.

Mercury fulminate explodes shortly after the end of the quiescent period if heated above a critical temperature. Lafitte and Patry§ in some experiments in which fulminate crystals were heated in air, determined the length of the quiescent period before detonation for the range of temperatures 135° C. to 277° C. Their values are in general agreement with those reported in this paper. The minimum temperature of explosion varies with the experimental conditions. It is higher when a mass of small crystals is heated in air (187° C. according to Berthelot, 190°, Wöhler and Matter, and 137°, Hoitzema) than when single crystals are heated in vacuum (105°–115° C. present experiments).

* Farmer, 'J. Chem. Soc.,' vol. 121, p. 174 (1922).

† 'Z. ges. Schiess. u. Sprengstoffw.,' vol. 17, p. 9 (1922).

‡ Cf. Robertson, 'J. Chem. Soc.,' vol. 119, p. 15 (1921).

§ 'C. R. Acad. Sci. Paris,' vol. 193, p. 171 (1931).

Farmer employed 1-2 gm. of fulminate in his experiments on thermal decomposition, and this quantity contained a large number of individual crystals of which the surface area was unknown. It is desirable that his work should be extended by experiments on single crystals of known area.* For the study of the initiation of explosion, it is advantageous to examine the behaviour of single crystals, for the flash point is less sharp with a mass of small crystals since ignition started in one crystal is not necessarily communicated to the rest. This is shown by the curves in fig. 1, which give the pressure of the gas evolved from a large number of individual crystals near their flash point. The decomposition is discontinuous, each burst of gas corresponding to the incipient explosion of a portion of the mass.

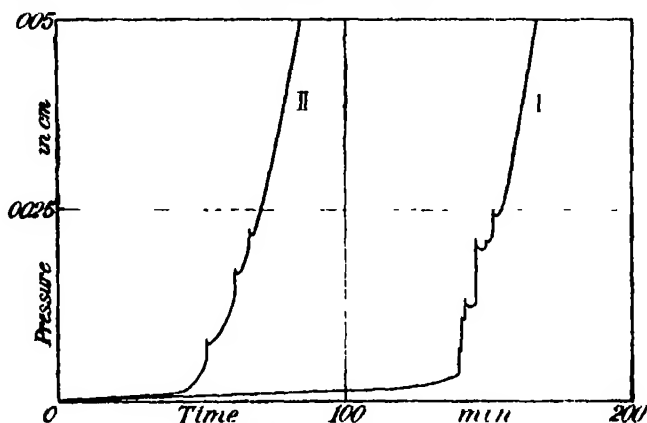


FIG. 1.—I. 120° C. (recrystallized). II. 125° C. (technical).

The present investigation had for its aim the examination of the conditions under which the thermal decomposition of fulminate passes into detonation. Since the thermal decomposition of fulminate had not been exhaustively studied, it was first necessary to make as complete an examination as possible of the decomposition below the ignition temperature. The method adopted was that of the measurement of the rate of evolution of gas from single crystals, 0.001 to 0.005 gm. in weight, when suspended in a high vacuum.

Experimental.

Crystals of Mercury Fulminate.—Mercury fulminate crystallizes in the orthorhombic system. Miles† gives the crystallographic details of fulminate

* Cf. Garner and Tanner, 'J. Chem. Soc.,' p. 47 (1930); Garner and Gomm, *ibid.*, p. 2123 (1931).

† 'J. Chem. Soc.,' p. 2539 (1931).

crystals as far as they are known from his own and other work, and describes methods of preparing them so as to obtain crystals several millimetres in length. Our first measurements were made on two samples, kindly supplied by Nobel's, Limited, (1) well-formed, thin plates of purity 99.4 per cent. as analysed by a modification of the method of Philip* ; (2) irregular crystalline masses, slightly yellow, with a purity 98.05 per cent. Five other batches of crystals were prepared subsequently by the crystallization of commercial fulminate from its solution in alcoholic ammonia, by the method described by Miles. Experiments were carried out on batches (IV), (V) and (VI). (IV) and (VI) were colourless crystals, but (V) was slightly yellow, purity 98.0 per cent.

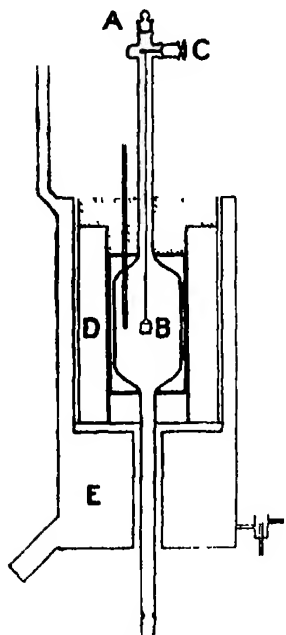


FIG. 2.

Apparatus.—This has been previously described (Garner and Gomm, *loc. cit.*) and since only slight modifications have been made in the experimental technique, the apparatus employed need be only briefly described here. The reaction chamber, together with its furnace, is shown in fig. 2. This was made of pyrex glass and had a ground joint, A, at the top for the introduction of a crystal. The crystal, lying flat on the bottom of a platinum bucket B, 8 mm. in diameter and 1 cm. long, was lowered into the reaction vessel by means of thin platinum wire from the spindle attached to a second ground joint C. In later experiments, the crystal in the bucket was covered with a thin sheet of platinum. From the bottom of the reaction chamber, tubes led to a jacketed McLeod gauge and a water jacketed Pirani gauge. The latter was

used in conjunction with a Moll galvanometer, and was calibrated against the McLeod.† The total volume of the reaction chamber and both gauges at room temperature was 993 c.c. The furnace D was electrically heated, and was contained in a copper steam bath E, which served to maintain the radiation losses independent of the temperature of the room. Before each experiment, the reaction vessel was heated at the temperature of the experiment for 24 hours under a vacuum of 10^{-6} cm. in order to reduce the evolution of gas from

* 'Z. ges. Schiess. u. Sprengstoffw.,' vol. 7, p. 181 (1912).

† With the gas produced by the decomposition.

the walls. The bucket and the crystal were suspended during this period in a part of the apparatus which was at room temperature.

Thermal Decomposition of Fulminate below the Flash Point.

Quiescent Period.—In agreement with the work of Farmer, it was found that there was a quiescent period over which the volume of gas liberated was very small. The rate is of the same order as that emitted from the walls and from the platinum bucket, so that it could not be determined accurately. The pressure change due to the liberation of gas from the walls was in general $1-2 \times 10^{-6}$ cm. per hour, and that from the bucket was of the same order. It is estimated that about one-half to two-thirds of the gas evolution comes from the crystals. On lowering the crystal into the reaction vessel, there is a very small burst of gas at first, very probably due to gas adsorbed on the external and internal surfaces of the crystal. The pressure then increases at a linear rate throughout the remainder of the quiescent period. At this stage 80 per cent. of the gas evolved is carbon dioxide.

Concurrently with the emission of gas, the crystal becomes browned. When examined under a microscope the coloration is seen to occur in strips and patches when viewed by either transmitted or reflected light. If at the end of the quiescent period the crystal be broken, most of the fragments are coloured yellow, although some colourless ones can be picked out. The coloration, however, is mainly superficial, but the quantity of decomposition product formed on the external surface at this stage is so small that its thickness cannot be observed under the microscope. Nevertheless, the decomposition appears to extend some distance into the crystal, possibly over the surfaces of microscopic cracks. The yellow decomposition product has no structure resolvable under the microscope.

In Table I is given the length of the quiescent period for crystals of batches I and IV.

Table I.

Temperature, ° C.	Period in minutes	
	I.	IV.
100	685	615
105	360, 360	360, 410
109	—	270
110	240	220
115	150, 145	—

Period of Marked Acceleration of the Reaction.—At the end of the quiescent period, the reaction is accelerated. (Typical curves at 100°, 105° and 110° are given in fig. 3.) This acceleration continues until the pressure of the gas above the crystal is 1/5 to 2/5 of the final pressure, after which, for a short period of time, the rate of gas evolution is constant. Before the end of the period of acceleration the crystal is browned throughout, although at this stage the major part of the fulminate is undecomposed. A hypothesis was sought which would give the correct mathematical form for the acceleration of the reaction and at the same time would account for the penetration of the coloration into the interior of the crystal. This assumed for its physical basis the penetration of the reaction along Smekal cracks into the interior (see p. 588).

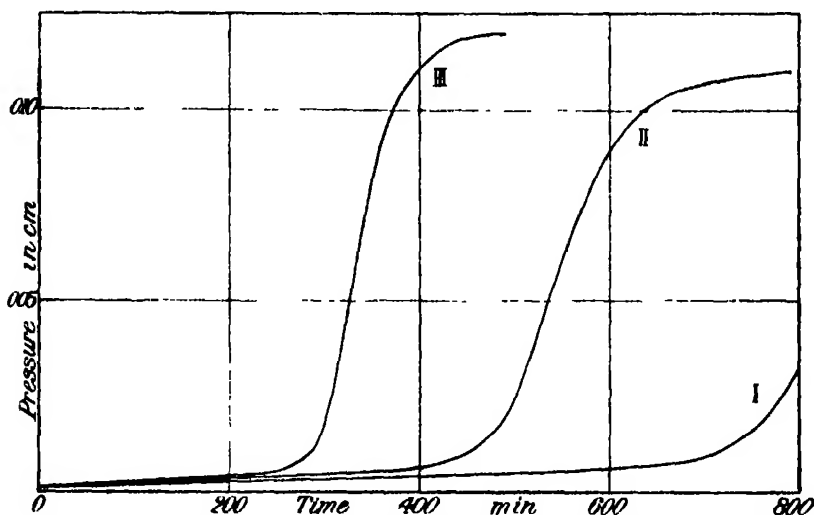


FIG. 3.—I. 100° C. 2.0 mg. ; II. 105° C. 2.0 mg. ; III. 110° C. 2.0 mg.

The equation (1), $\log (dp/dt - dp_0/dt) = k_1 t + \text{const.}$ was derived (p. 588) and found to fit the experimental results up to 1/5 decomposition. dp/dt is the total rate of increase of pressure at any time, and dp_0/dt is the linear rate of evolution of gas during the quiescent period. The equation probably holds back to the beginning of the reaction, but on account of the small value of dp/dt cannot be tested in the early stages. Typical plots of $\log (dp/dt - dp_0/dt)$ against time are given in fig. 5. Equation (1) was found subsequently to be applicable to the initial stages of the decomposition of barium azide* and lead styphnate except that for these substances dp_0/dt vanishes.

* Dr. F. E. Harvey (unpublished).

The values obtained for the range 100° to 115° C. in the case of fulminate batch I are given in Table II.

Table II.

Temperature ° C.	Integration constant.	k_1 .	Critical increment of k_1 .
100	2.4×10^{-12}	0.017	32,200
105	9.4×10^{-12}	0.032	
	1.4×10^{-11}	0.030	
	3.3×10^{-12}	0.032	
110	5.5×10^{-12}	0.055	
	1.0×10^{-11}	0.052	
115	2.7×10^{-12}	0.084**	

** Detonation.

The plot of $\log k_1$ against $1/T$ gives a straight line and a critical increment of 32,200 cal.

Measurements of the period of half decomposition* were also made on this batch of crystals and $\log t$ plotted against $1/T$. A straight line was obtained for the results below the flash point (115°–120° C.). The value for the critical increment of the time of half change was 30,350 calories.†

Table III.

Time of half change (minutes)	1080	543	333	191½	73½	29½	14½	8	2½
Temperature ° C.	100	105	110	115	125	135	145	155	180

Final Stage in the Decomposition.—The volume of the total gas evolved in c.c./gm. lies between 52 and 55 c.c. Farmer, working at higher pressures and lower temperatures with 1–2 gm. of fulminate, finds 45 c.c./gm. After the time of half decomposition, the rate is proportional to the amount of fulminate undecomposed, that is, the equation for reactions of the first order (2),

$$k_2 = \frac{1}{t} \log_e \frac{p_{\text{final}}}{p_{\text{final}} - p_t},$$

holds for the velocity of the reaction. t is the time in minutes from some zero value found by extrapolation. Table IV shows the degree of constancy obtained

* By the period of half decomposition is meant the time at which the pressure is one-half of the final pressure.

† From Farmer's results a value of 27,700 cal. can be obtained.

for the velocity constant k_2 for crystals of batch I at 100° and 105° C. and for a crystal of batch IV at 109° respectively.

Table IV.

		Temperature = 100° C.				
Time		1040	1080	1120	1160	1200
k_2		0 00213	0 00216	0 00209	0 00216	0 00220
Time		1240	1280	1330	1420	
k_2		0 00225	0 00216	0 00215	0 00206	
		Temperature = 105° C.				
Time		540	560	580	600	620
k_2		0 00672	0 00632	0 00619	0 00635	0 00644
		640	660	680	680	680
		0 00647	0 00642	0 00640		
		Temperature = 109° C.				
Time		360	370	380	390	400
k_2		0 00906	0 00889	0 00920	0 00931	0 00939
Time		410	420	430	440	450
k_2		0 00932	0 00970	0 00901	0 00909	0 00872

That the rate of decomposition at this stage is proportional to the amount of fulminate left undecomposed can be understood if the mass after half decomposition were composed of disconnected crystallites, and the rate of decomposition were dependent only on the rate of formation of reaction centres on their surfaces. Hume and Colvin* suggest that this is the case for the transition,

monoclinic sulphur \longrightarrow rhombic sulphur,

which also obeys the unimolecular law. β -azide (Garner and Gomm, *loc. cit.*), lead styphnate, and barium azide crystals obey the same law, towards the end of the period of their decomposition.

The values of k_2 for crystals of batches I and IV were determined over the range 100°–110° C. and are given in Table V. The temperature coefficient of k_2 is appreciably greater than that of k_1 .

The experimental conditions were the same for the two batches of crystals except that with batch IV, the flat crystals were contained between two platinum plates.

Decomposition of Lead Styphnate.

The relation, $\log(dp/dt - dp_0/dt) = k_1t + \text{const.}$, which was found to hold for fulminate in the region of acceleration of the reaction, fits the experimental curves for explosives which contain water of crystallization, in particular

* 'Phil. Mag.', vol. 8, p. 589 (1929).

Table V.

Batch.	Temperature °C.	k_1 .	k_2 .
I	100	0.017	0.00214
I	105	0.032	0.00573
I	110	0.055	0.00777
IV	100	0.022	0.00295
IV	105	0.054	0.00639
IV	105	0.053	0.00624
IV	109	0.076	0.00884
IV	110	0.080	0.01531
V	105	0.038	
V	105	0.038	
V	108	0.061	0.01057
II	105	0.023	0.00430

those for lead styphnate, $C_6H(NO_2)_3O_3Pb \cdot H_2O$.* In the case of this explosive dp_0/dt is negligible. Lead styphnate loses its water very readily above $100^\circ C$., and the loss is complete before the substance has appreciably decomposed. A pseudomorph of the original crystal is left behind if the dehydration occurs slowly, but at $225^\circ C$. the crystal breaks into fragments. If crystals be studied as previously described for lead azide, with the addition to the apparatus of a trap surrounded by solid carbon dioxide to remove water vapour, then the p , t curves show no quiescent period, acceleration of the rate commencing immediately the crystal is lowered into the furnace. Equation (1) holds up to the time of half change, and equation (2) for the later stages of the reaction. Details of these experiments will be published elsewhere.

As a result of the loss of water, the lead styphnate before decomposition must possess a large internal surface. Presumably after dehydration the anhydrous salt consists of crystallites joined together by unorganized matter, as is the case for copper sulphate pentahydrate when it has lost water.† Since equation (1) holds for both styphnate and fulminate crystals, it is reasonable to enquire if crystals of the latter are composed of aggregates of crystallites. The fact that the decomposition of fulminate in its later stages obeys the first order equation certainly indicates that the fulminate at half decomposition is disintegrated into a large number of separate fragments. This fragmentation possibly exists in the unheated crystal as Smekal blocks. It is thus of

* Barium azide behaves similarly.

† Cf. Topley, 'Proc. Roy. Soc.,' A, vol. 136, p. 413 (1932).

interest to examine the mode of decomposition of crushed and ground fulminate for on pulverization the structure will be profoundly modified.

*Effect of Grinding and Crushing Fulminate Crystals.**

Crystals of batch IV were used for this series of experiments. Single crystals of average weight 2.5–5 mg., thickness 0.02 cm., were placed in the flat bottom of a platinum bucket and covered with a thin sheet of platinum. This served to reduce the self heating of the crystal to a minimum (see later). Six experiments were performed, (1) two with whole crystals; (2) two with crystals crushed in the bucket by gently rotating a glass rod on the thin sheet of platinum; and (3) two with similar weights of fulminate ground in an agate mortar. In figs. 4 and 5 are given the p , t and $\log dp/dt$, t curves respectively.

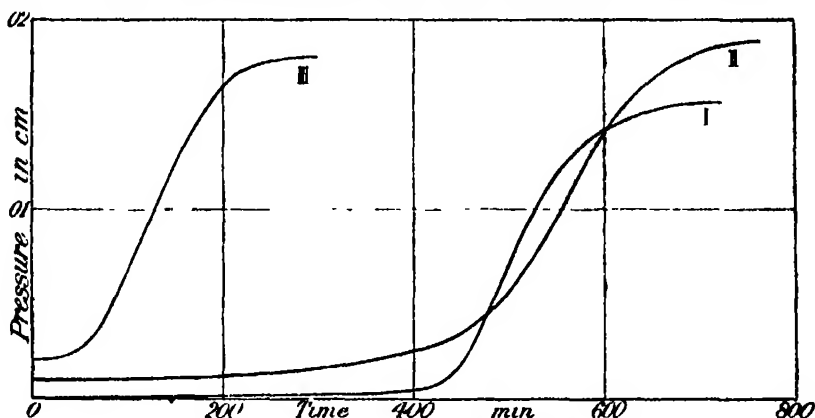


FIG. 4.—I, whole crystal; II, crushed crystal; III, ground crystal.

It is clear from fig. 4 that with ground fulminate the quiescent period has disappeared, and equation (1), p. 580, holds practically from the beginning of the decomposition, but here $dp_0/dt = 0$. The same is true for crushed fulminate although on account of the low values of dp/dt in the early stages, this is not evident from fig. 4. The values of k_1 , the acceleration constant, and k_2 , the monomolecular constant are given in Table VI.

The acceleration constant, k_1 , for the whole crystal is somewhat greater than that for the ground crystal, and considerably greater than that for the crushed crystal. In consequence of this, the maximum rates of decomposition are little affected by grinding, but appreciably reduced by crushing, fig. 4. This is a surprising result in view of the enormous increase in surface that has occurred.

* In this and the following section the McLeod gauge was used to measure the pressures.

The unimolecular constant, k_2 , is slightly reduced on crushing, and about doubled on grinding the crystal. If, as seems likely, the rate for the final stage of the reaction is determined by the superficial area of the fulminate fragments,

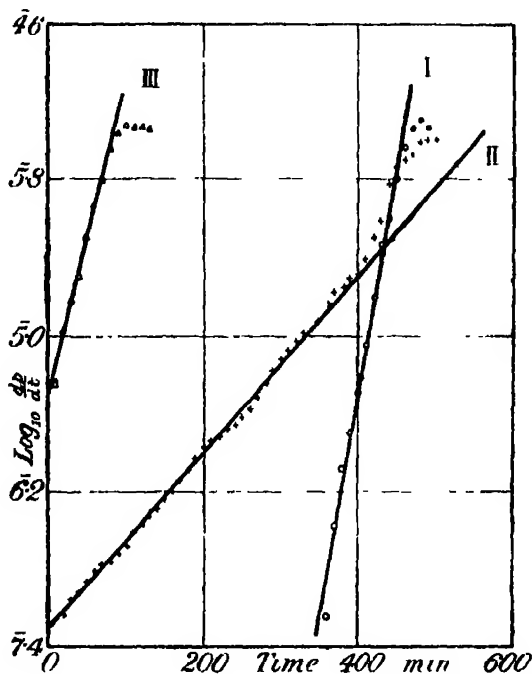


FIG. 5.—I, whole crystal ; II, crushed crystal ; III, ground crystal.

Table VI.—Temperature = 105° C.

	Weight in mg.	Thickness cm.	Total area cm ² .	Integration constant.	k_1 .	k_2 .
Whole crystal	4.15	0.0174	0.1278	8×10^{-16}	0.054	0.00639
	3.513	0.0169	0.1172	3×10^{-16}	0.053	0.00624
Crushed crystal	4.387	—	—	3.2×10^{-7}	0.010	0.00528
	2.593	—	—	3.3×10^{-7}	0.010	0.00537
Ground crystal	7.053	—	—	6.6×10^{-6}	0.045	0.01396
	3.748	—	—	4.7×10^{-6}	0.039	0.01104

then it follows that grinding and crushing fulminate crystals does not appreciably affect the area of the ultimate units into which the crystal is disintegrated. This is readily understandable if the ultimate units are Smekal blocks.

Experiments carried out at 120° C. have confirmed the general effect observed with crushed and ground crystals at 105°.

Effect of Self Heating on the Values of k_1 and k_2 .

Calculations have been made of the rise in temperature of a crystal, from the rate at which heat is liberated for all stages of the chemical reaction and assuming black body emission. The results for a crystal of area 0.08 sq. cm. and various rates of evolution of gas are given in Table VII for 115°.

Table VII.—Volume of apparatus, 511 c.c. Total volume gas/gm.=45 c.c.

Rate in centimetres pressure per minute.	Heat liberated in cal./sec.	Rise in t°.
3.24×10^{-5}	3.2×10^{-5}	0.13
1.42×10^{-5}	1.37×10^{-5}	0.55
5.68×10^{-5}	5.49×10^{-5}	2.08
2.27×10^{-4}	2.20×10^{-4}	8.2

No rates greater than these were actually measured in the present experiments. The effect of the rise in temperature on the rate of decomposition would be negligible during the quiescent period and during the early part of the region of acceleration, but rises of 2° to 8° may occur when the crystal decomposes at its maximum rate. No account has, however, been taken in the above calculation of the loss of heat by conduction to the platinum bucket, nor of the convection of heat from the crystal to the platinum as a result of molecular bombardment, so that the above are maximum values.

Since the rate of reaction trebles for a rise in temperature of 10° C. it is evident that the values for k_2 and to a lesser extent for k_1 would be vitiated if these rises in temperature actually occurred. It was on this account that the crystal was placed between two platinum plates not more than 0.02 cm. apart. These will serve to facilitate the transference of heat from the crystal, for the molecules of the gaseous products must collide many times with the two plates before escaping into free space.

In order to test the efficiency of this arrangement for the reduction of the self heating, the experiments (see above) were repeated in an atmosphere of hydrogen, 10^{-3} cm. pressure, Table VIII.

The effect on k_1 is practically negligible in the case of the crushed and ground crystals over the range of rates of reaction for which equation (1) holds. This is an important observation for it proves that the acceleration of the reaction

Table VIII.—Temperature = 105°

	Weight in mg.	Thickness cm.	Total area cm ²	Integration constant.	k_1	k_2
Whole crystal	0.37	0.0288	0.1246	2.3×10^{-12}	0.037	0.00795
	4.99	0.0220	0.1268	2.0×10^{-11}	0.030	0.00739
Crushed crystal	2.93			2.2×10^{-7}	0.010	0.00473
	3.71			6.8×10^{-8}	0.014	0.00579
Ground crystal	1.837			1.7×10^{-6}	0.040	0.00698
	1.867			1.0×10^{-6}	0.044	0.00578
	1.517			2.2×10^{-6}	0.022	0.00665

found in these cases is not in any way connected with self heating. There is a lowering of k_1 for the whole crystal from 0.054 to 0.034. If this were due to self heating, it would mean that the hydrogen had lowered the temperature of the crystal by 5° C. Against this, it is found that the plot of $\log dp/dt$ against t is always linear up to a rate of $dp/dt = 1.35 \times 10^{-4}$ cm. per minute. This could not hold if the crystal had become self heated to the extent of 5°. The lowering may be caused by a specific action of hydrogen in breaking energy chains.

The unimolecular constant, on the other hand, is the same in the case of crushed fulminate, decreased for ground fulminate and increased for the whole crystal. Since the whole crystal is the most likely to self heat because it gives a thicker film between the platinum plates, the increase in k_2 on surrounding the crystal by an atmosphere of hydrogen gas is significant. It is an effect in the opposite direction to that expected if self heating had occurred to an appreciable extent. In explanation of the effect, it is conceivable that the hydrogen facilitates the starting of new centres of reaction by carrying energy from one place to another, thereby increasing k_2 and also the integration constant (see Tables VI and VII). There must also be present the opposite effect in the case of ground fulminate, the removal of energy from the zone of reaction, for the velocity constant is in this case reduced. Whether or no an inert gas increases the chance of formation of new centres of reaction on the surfaces of fragments will obviously depend on the distances between them.

Discussion of the Thermal Decomposition of Fulminate.

In the majority of cases of solid decomposition, visual and microscopical examination shows that the reaction commences at centres formed on the

external surfaces of the solid, or on the surfaces of microscopic cracks. Researches on solid explosives have, however, revealed the existence of another type of decomposition which penetrates the solid along surfaces not visible under the microscope. For decompositions of the second type, the rate in the initial stages of the reaction is given by the law, (1), $\log (dp/dt - dp_0/dt) = kt + \text{constant}$; and then, for the later stages of the decomposition, it is proportional to the mass of the explosive remaining undecomposed. These laws are obeyed by whole crystals of fulminate, crushed and ground fulminate crystals, β -azide crystals,* and dehydrated crystals of lead styphnate and barium azide.

The surfaces at which decomposition occurs are probably (1) for whole crystals of fulminate—Smekal cracks; (2) for crushed and ground fulminate—gliding planes; and (3) for dehydrated salts—the surfaces of crystallites. It is reasonable to assume that the reaction commences at centres lying in the non-crystalline matter which cements the grains of crystal together, and that there are channels between the grains along which the gaseous products of decomposition can escape †

Equation (1) may be derived as follows. Only a fraction of the CNO ions along the cracks will occupy sufficiently open positions for decomposition to be possible. The removal of these ions by decomposition will uncover others which can decompose in turn, so that if the reaction commences in cracks at a few centres, each centre will lead to a chain of decomposition. This chain will probably be of a branching type, for occasionally the decomposition of one CNO ion will uncover two or more others. Let N_0 be the number of chains started per minute, and let the chains branch K times per minute, then

$$(3) \quad \frac{dN}{dt} = N_0 + KN,$$

where N is the total number of chains still in existence at a time t . On integration,

$$(4) \quad N = \frac{N_0}{K} (e^{Kt} - 1),$$

and when e^{Kt} is large compared with unity,

$$(5) \quad \log_e N = Kt + \log_e \left(\frac{N_0}{K} \right)$$

* The acceleration in the case of this reaction has not been fully investigated.

† Smekal ('Phys. Z.', vol. 26, p. 707 (1925); 'Z. Physik,' vol. 45, p. 871 (1927)) concludes that in ionic crystals the ions move over the boundaries of the mosaic structure of the crystal under the action of an electric field.

If dp/dt is proportional to N ,

$$(1) \quad \log \frac{dp}{dt} = k_1 t + \text{const}$$

This equation will only hold as long as there is no appreciable interference and overlapping of the chains.

Since the period of acceleration of the reaction may be as long as 160 minutes for a crystal of a 2 mg. in weight, it is evident that the reaction is not composed of ordinary branching reaction chains in which the energy of decomposition of one ion becomes the energy of activation of the next.* There will be appreciable intervals of time between successive links in the chain. Branching occurs when two or more CNO ions are left uncovered by the decomposition of one CNO ion. The number of times branching occurs in unit time will depend on the structure of the unorganized matter along the cracks, and this explains why k_1 varies for whole crystals, crushed, and ground crystals. The time interval between successive links of the chain, which is proportional to the probability of decomposition of the CNO ions, will decrease with increasing temperature; thus the critical increment of k_1 will be a measure of the activation energy of a CNO group. This is about 30,000 k. cal

The reaction occurring during the period of acceleration is not confined to the cracks, but must extend to the Smekal blocks as fast as they are uncovered. The number of blocks uncovered will, however, be proportional to the number of centres of reaction started in the cement, so that it would be expected that equation (1) would hold for the acceleration of the reaction. When all of the blocks remaining have been uncovered then the reaction will follow the first order law as previously explained.

From Table VI it will be seen that the probability of branching, K , has been reduced from 0.54 to 0.10 on crushing the crystal, whereas the integration constant in equation (1), which is dependent on N_0/K , is 100 million times smaller for the whole crystal than for crushed crystal. It is clear, therefore, that N_0 , the number of centres started per minute, must be enormously increased by crushing; a somewhat larger increase in N_0 occurs on grinding. On this account, we conclude that the apparent induction period met with in the decomposition of fulminate is caused by a low value of N_0 . This induction

* [Note added in proof, January, 14, 1933.—The reaction can be interrupted by cooling to room temperature without affecting rate on return to high temperature. This shows that the chains are not energy chains.]

period disappears very largely on crushing and grinding because of the marked increase in the number of centres of reaction formed.*

Detonation of Fulminate Crystals.

Single crystals of fulminate do not explode violently on heating in vacuum at temperatures below 250° C. The platinum bucket in which they are contained remains intact after the explosion, although the thin sheet of platinum placed above them is blown out of the bucket. This behaviour is in marked contrast with the behaviour of lead azide and lead styphnate which, on heating to the ignition temperature, shatter the bucket to pieces. This is in accord with the well-known comparative slowness with which fulminate attains its maximum speed of detonation.

A crystal of fulminate on heating in a platinum bucket in air decomposes with more violence, the crystal breaking up into pieces which are projected through the platinum to the sides of the reaction vessel and there leave traces of metallic mercury on the glass walls. These traces when formed on a plain surface are approximately straight lines. The process is similar to that which occurs on the explosion of a barium azide crystal by heat. These crystals ignite on a hot plate and the luminous decomposing fragments are projected along a straight or slightly curved path into the air, often to a distance of several metres. The fragments are like rockets, being propelled forward by the emission of the gaseous decomposition products behind them. This scattering of the crystal, which occurs during an explosion, makes it difficult to ensure that the whole of the explosive is consumed. Consequently, the volume of gases evolved on explosion of fulminate crystals varies within wide limits. The volume in vacuum varies from 30 to 90 c.c./gm., whereas on thermal decomposition without explosion a constant value of 52–55 c.c./gm. is obtained.

When explosion occurs, the rate of rise of pressure is too rapid to measure on a Pirani gauge, and the explosion arises out of thermal decomposition with practically no warning. The pressure-time curve is like a thermal decomposition curve up to the point of explosion. At the higher temperatures of the reaction vessel, above 125°, the explosion occurs at the beginning of the period of acceleration of the reaction. At the lower temperatures, especially near the flash point, the explosion may occur when the crystal is 1/5 decomposed

* Washing a partially decomposed crystal with acetone and water (Farmer, *loc. cit.*) reduces the rate of reaction, very probably because these solvents remove the more active CNO ions from the interface, and thus these experiments cannot be adduced in favour of the autocatalysis theory.

but not when it is decomposed to a greater extent than this. If a crystal is heated until it is more than $1/5$ decomposed at a temperature below the flash point, it is impossible to cause the crystal to detonate at temperatures above the flash point. No explosion has been observed outside the region where the rate of evolution is given by equation (1). There is thus every reason to conclude that the processes occurring during the period of acceleration of the reaction are responsible for the explosion.

Minimum Temperature of Explosion and Duration of Heating before Explosion

—The minimum temperature of explosion of a crystal of fulminate in vacuum varies between 105 and 115°C ., the temperature depending on the purity of the fulminate and to some extent on the size and crystal form. The duration of the heating before explosion also depends on the same factors

The duration is somewhat variable at constant temperature (Table IX) for crystals of weight 1 to 5 mg. In spite of this variation, if the log of the duration is plotted against $1/T$, a reasonably good straight line is obtained. The slope is nearly the same for all batches of crystals so far examined, fig. 6, although

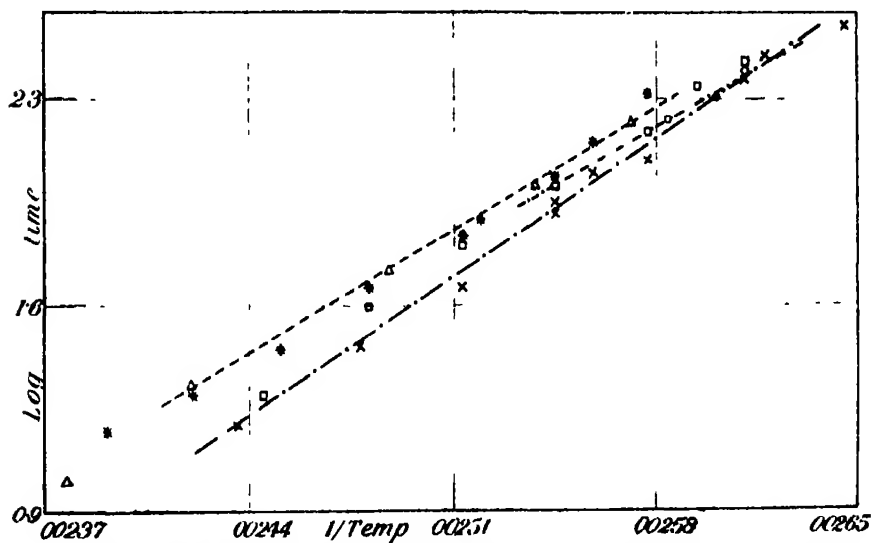


FIG. 6.—* batch I; □ batch II; ○ batch IV; × batch V; Δ batch VI.

the curves for the different batches are not coincident. Batches I and II were examined in small buckets without the covering slip of platinum, so that the curves for batches I and II, and those for batches IV–VI are not strictly comparable. At 105° the covering slip of platinum increased the time from 97 to 102 minutes on an average. The following critical increments were

obtained for the various batches of crystals, (I) 27,900; (II) 30,600; (IV) 26,700; (V) 30,300; (VI) 28,100 calories. These increments are very close to the values obtained for the thermal decomposition.

Table IX.

°C.	Batch.	Time in minutes.	°C.	Batch.	Time in minutes.
110	(IV)	248	124	(I)	77.3
111.5	(IV)	200	125	(I)	68.3
114	(IV)	169.5	130	(I)	45.7
115	(I)	208	135	(I)	28, 32.5
118	(I)	141	140	(I)	19.5
120	(I)	107.5, 100, 99.5	145	(I)	14.5
	(IV)	See Table XI			

Of these batches, (I) and (IV) were colourless, well-formed rhombs, which gave approximately the same times (Table IX). Batches II and V were yellow crystals and probably contained basic fulminate due to hydrolysis during crystallization. The crystals were always yellow if the process of crystallization from alcoholic ammonia was unduly prolonged; they contained only 98 per cent. of fulminate; the times are shorter and it was possible to obtain ignition at somewhat lower temperatures. The yellow-coloured crystals are distinctly more sensitive to heat than the colourless crystals. For batch V it was possible to obtain explosion at 105° C. after 352 minutes. The period of acceleration in this case could be followed over 70 minutes. Batch VI consisted of colourless pyramidal crystals (98.4 per cent. fulminate). These gave almost identical times with those of batch I.

Effect of Crystal Size. The duration of the period of thermal decomposition before explosion was determined at 120° for crystals ranging in weight from 0.4 to 6.73 mg (Table X).

Table X —Temperature 120° C.

Weight mg	Area cm ²	Time mins	Weight mg.	Area cm. ²	Time mins.
6.73	0.138	99	2.10		97.3
6.32	0.171	93.5	1.148	0.0147	112.5
5.71	0.178	105.6	0.788	0.0130	121.5
4.68	0.106	114.3	0.377	0.0129	130.5
3.62	0.096	113.9	Very small crystals, 0.05 to 0.25 mg.		
2.85	0.075	103.1	Crushed crystal		
2.74	0.082	105.0	Ground crystal		
2.55	—	97		—	∞
2.45	0.074	108.3		—	∞
2.19	—	96			

The times vary between 96 to 114 minutes for crystals 0.1 to 0.7 mg. in weight. The variation is erratic over this range and not related to the size or area of the crystal or to irregularities in the bath temperature. It thus appears that the favourable circumstances, which cause detonation, are to some extent governed by chance. For crystals of weight less than 1 mg., the times are sensibly longer, and crushed and ground fulminate cannot be made to explode at this temperature, though the crushed fulminate can be made to explode at 140° C. At this temperature, it gives rise to a series of small explosions between 10 to 21 minutes after the beginning of the acceleration. On the other hand, ground fulminate did not appear to explode even at 160° C.

The rate of explosion immediately preceding explosion, viz., 4×10^{-6} — 2×10^{-5} cm. per minute is small, and hence the long times obtained with small crystals, 130–140 minutes, cannot be ascribed to a decrease in the self heating of the crystal as a whole. It must, however, be borne in mind that local high temperatures can occur if the reaction on the surfaces of the grains follows a chain mechanism.

Effect of Hydrogen and Helium Atmosphere on the Explosion Time.—The results are given in Table XI.

Table XI.—Temperature 120° C. Batch V.

Weight mg	p_{H_2} cm. $\times 10^2$	Time mins.	Weight mg.	p_{H_2} cm. $\times 10^2$	Time mins.
5.47	0	81	3.98	1.177	88.1
3.89	0	80.8	3.74	1.221	88.4
4.30	0	89.8	3.91	1.122	84.9
4.42	0	80.5			
3.84	1.176	93.3			
4.64	1.171	98.8			
4.14	1.086	102.2			
3.30	2.205	110.5			

A pressure of 1.2×10^{-2} cm. H_2 causes an average delay of 15 minutes in the time to detonation, and the same pressure of helium a delay of 4 minutes. The hydrogen probably smooths out the local differences in temperature within the crystal.

Discussion on Detonation.

Detonating substances decompose with the liberation of heats of reaction greater than the measured activation energies, so that chain reactions may be

expected in the solid state. For lead azide, the heat of detonation is 106 k. cal./mol. and the critical increment 47.6 k. cal. For fulminate the heat of detonation is 113 k. cal. and the critical increment appears to be about 30 k. cal.

The N_3 and metal ions in azides are arranged in alternate layers.* For potassium azide, the linear N_3 ions are so arranged that one of its products of decomposition must be projected into the centre of an adjacent ion. There is thus every facility for the occurrence of a chain mechanism which may consume all of the ions within a single layer of the mosaic structure. On account of the similarity between N_3 and CNO ions, what is true of the azides will probably be true of fulminates also.

Since the main reaction which occurs during the period of acceleration lies within the crystal boundaries, it is reasonable to conclude that the centres of detonation are initiated in the interior of the crystal. Under favourable circumstances, the reaction will consume layers of CNO ions on adjacent surfaces of two crystal grains. The local heating produced will depend on the distances separating the two surfaces, which will be greater for the whole crystal than for crushed or ground fulminate. Thus with the whole crystal there is a greater probability that the reaction will spread across the layers of mercury ions and cause the onset of detonation.

The times which elapse between the commencement of the heating and the occurrence of detonation are erratic; this indicates that conditions favourable to detonation depend on chance. This chance, according to the above hypothesis, is that of the simultaneous decomposition of two CNO layers on the surface of two adjacent crystallites.

This hypothesis is in accord with the observation that it is not possible to bring about detonation in a crystal which has been decomposed to a greater extent than one-fifth. At this stage, the crystallites will be surrounded with a comparatively thick film of decomposition product, and consequently the local rises of temperature caused by the simultaneous decomposition of two layers of CNO groups will be smaller than in the earlier stages of the period of acceleration.

We wish to express our thanks to Messrs. Nobels, Ltd., for a grant which has made it possible for us to carry out this investigation.

* Hendricks and Pauling, 'J. Amer. Chem. Soc.', vol. 47, p. 2904 (1925).

Summary

Single crystals of mercury fulminate have been heated in vacuum at temperatures between 100° and 150° C. and a detailed examination made of the decomposition which ensues. In vacuum the thermal decomposition passes into detonation at 105°–115° C. The conditions which govern the inception of detonation have been investigated

The thermal decomposition occurring below the ignition temperature occurs in three stages, (1) a quiescent period during which there is a slight browning of the crystal, the decomposition being mainly superficial; (2) a period of acceleration of the rate of reaction for which the relation $\log (dp/dt - dp_0/dt) = kt + \text{const.}$ holds; and (3) a region where the equation of the first order applies. Stages 2 and 3 have also been shown to occur in the decomposition of crushed and ground fulminate and in the decomposition of lead styphnate. These results have been interpreted as due to the commencement of thermal decomposition in the Smekal cracks of the fulminate crystal and the spread of the reaction to crystallites isolated by the destruction of the cementing material. The critical increment of the thermal reaction is approximately 30 k. cal.

Detonation occurs during the period of acceleration of the reaction and probably arises within the crystal on the surfaces of the Smekal cracks.

On the Diffuse Double Layer.

By Dr. J. LENS, Sir William Ramsay Laboratories of Physical and Inorganic Chemistry.

(Communicated by F. G. Donnan, F. R. S. —Received October 13, 1932.)

§ 1. The formulæ derived by Gouy* for the diffuse double layer hold only in the case of a single surface in an infinite amount of medium. In practice they are not very suitable, for very frequently we have to deal either with capillaries, as in streaming potential measurements, or with colloidal particles which may be near enough to influence one another. In these cases it is too difficult to calculate the effect of the mutual influence of two double layers, though in less complicated systems it is possible.

Suppose we have two plane parallel surfaces separated by a distance $2h$ and charged both to the same potential, in a solution of an electrolyte. If the dimensions of the surfaces are large compared with the distance h there will be no drop of potential between the two. We therefore need to make the assumption (which was superfluous in Gouy's case) of a specific adsorption by the surface of one or more of the ions in the solution, otherwise there will be no double layer at all; the same effect will also be obtained if ions of the surface dissolve.

Suppose we have a solution containing a mixture of ions with the valencies $v_c, v'_c, v''_c, \dots, v_a, v'_a, v''_a, \dots$.

We use the index c for cations and a for anions. The concentrations of these ions at the distance h from the surfaces when equilibrium is reached are $N_c, N'_c, N''_c, \dots, N_a, N'_a, N''_a, \dots$. At the distance x from one surface the concentrations are $N_c U_c, N'_c U'_c, N''_c U''_c, \dots, N_a U_a, N'_a U'_a, N''_a U''_a, \dots$. U is a function of x . One could object that the surface might give off an ion which the original mixture did not contain, and which is not present at the distance h . This does not disturb our calculations; it simply means that there is one cation whose N -value is zero and whose U -value is infinite except in h , and as we shall see later this objection has no validity.

§ 2. The electric density ρ in x will be :

$$\rho = \sum N_c U_c v_c - \sum N_a U_a v_a, \quad (1)$$

* 'J. Phys.,' vol. 9, p. 457 (1910).

and the attraction A of the unit of charge :

$$A = \frac{2\pi}{K} \left(\int_0^x \rho dx - \int_1^h \rho dx \right), \quad (2)$$

where K is the D.E.C. of the solution.

A must be zero if $x = h$.

Further we know

$$\int_0^h \rho dx - \int_1^{2h} \rho dx = \int_0^h (\Sigma N_c U_c v_c - \Sigma N_a U_a v_a) dx = -2F, \quad (3)$$

$-2F$ represents therefore the total amount of electricity present in excess in the liquid due to adsorption of anions by the surface or cations dissolved from it.

Equation (2) can be written

$$A = \frac{4\pi}{K} \left(-F - \int_1^h \rho dx \right) = \frac{4\pi q}{K} \quad (4)$$

Hence from equation (4) we get the same derivations for our formulæ as Gouy

$$U_c \frac{1}{v_c} = U'_c \frac{1}{v'_c} \quad , \quad U_a \frac{1}{v_a} = U'_a \frac{1}{v'_a} \quad (5)$$

and

$$\Sigma N_c (U_c - 1) + \Sigma N_a (U_a - 1) = \frac{2\pi q^2}{KRT}. \quad (6)$$

§ 3.—(a) Equation (5) shows that if an ion is present in the neighbourhood of the surface it is present as well at h and the assumed objection made in § 1 is therefore proved to be wrong

(b) Gouy's equations agree with the results deduced above for two double layers under each others influence.

(c) These equations enable us to throw some light on a rather peculiar behaviour of a mixture of two colloids.

Suppose one of the cations in the solution is a very large one and has a valency of, say, 100, other cations present are all univalent ; then at a distance x the concentration of the 100-valent ion will be

$$N_{100} U_{100} = N_{100} U_1^{100}$$

In order to get a univalent ion at the same concentration in x , its concentration in h has to be

$$N_1 = N_{100} U_1^{99}. \quad (7)$$

For a bivalent ion we get

$$N_2 = N_{100} U_2^{48}. \quad (8)$$

Generally an ion with a valency 100 will be colloidal so that we have only a very rough approximation of what really happens, since such an ion has a surface itself and the ionic places cannot move freely over that surface. Furthermore, the dimensions of such a particle cannot be neglected, but nevertheless a qualitative effect in the same sense may be expected, and has indeed been found.

The two surfaces are supposed to be the surfaces of two colloidal particles, and we add colloidal ions of opposite sign. These ions with their high valency will be strongly adsorbed in the double layer; much more strongly than the ordinary ions with valencies generally not higher than six. But if these other ions are present in a large amount (that is to say, if N_{100} is very small compared with N_1 for instance) it is possible to get both ions, the colloidal one and the other, present in the double layer in the same concentration. Then by increasing the electrolyte concentration it is even possible to make the electrolyte ion concentration in the boundary the dominating one, hence, on addition of electrolyte, the adsorption of colloidal ions in the layer becomes smaller and smaller. Equations (7) and (8) show that with ions of different valency one will find the Schulze-Hardy rule valid.

These deductions are in perfect agreement with the results obtained by Bungenberg de Jong and Dekker* who found the Schulze-Hardy rule to be valid for both positive and negative ions in the same system. To explain this fact we have to interchange the rôle of the two colloids; if we take the other one as surface, we get the Schulze-Hardy rule for the ions with the opposite sign.

§ 4. We take a system containing a mixture of uni-uni-valent electrolytes and a n -uni-valent electrolyte, both present in h , so that

$$N_n = N'_n N_1,$$

where N_1 = the sum of the concentrations of the uni-valent cations. That is to say, N_1 is taken as unit for N_n . Then

$$q = \sqrt{\frac{N_1 KRT}{2\pi}} \left(N'_n U_1^n + U_1 + \frac{n N'_n + 1}{U_1} - (n + 1) N'_n - 2 \right)$$

* 'Biochem. Z.', vol. 221, p. 403 (1930).

Hence

$$\frac{dq}{dx} = \sqrt{\frac{N_1 KRT}{8\pi}} \frac{nN'_n U_1^{n+1} + 1 - \frac{nN'_n + 1}{U_1^2}}{\sqrt{N'_n U_1^n + U_1 + \frac{nN'_n + 1}{U_1} - (n+1)N'_n - 2}} \quad (9)$$

So $dq/dx = 0$ if

$$nN'_n U_1^{n+1} + U_1^2 = nN'_n + 1$$

If $U_1 = 1$, then $\frac{dq}{dx} = \frac{0}{0}$, hence the curve for q in terms of x shows a discontinuity for this value of U_1 . In Gouy's case this happens only at an infinite distance from the surface, here certainly at the distance h and we will assume that it happens at another distance too

Then we have two possibilities, firstly $U_1 = 1$ in every point, which means that there is no double layer at all. Secondly, $U_1 = 1$ at the distances x and h and not at other points. Between x and h the curve has then to go through a maximum or minimum or shows a discontinuity. For the first assumption dq/dx must be zero for a certain value of U_1 , corresponding to a point between x and h . But this will never be the case, for if $U_1 \geq 1$, we have

$$nN'_n U_1^{n+1} + U_1^2 \geq nN'_n + 1.$$

The curve for q never shows a maximum or minimum.

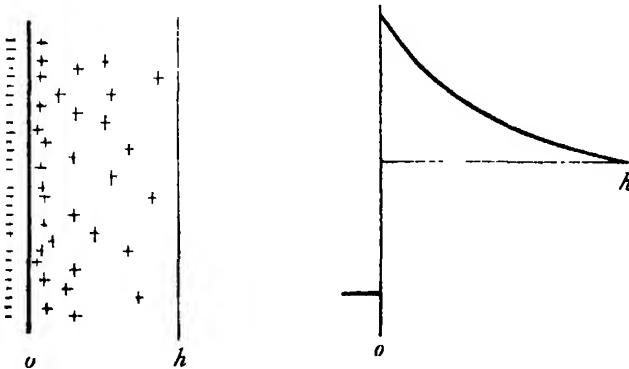


FIG. 1.

Accordingly the only possibility for the case is a discontinuity in the curve. It could happen on the surface itself, where certainly a discontinuity exists. The ion distribution over the medium will be roughly as indicated in fig. 1.

Hence, coming from h , U first increases, but falls off suddenly if we come into the surface itself, where the ions of opposite sign dominate.

We therefore conclude that the q/x curve for a mixture of ions C_1, C_n, A_1 , does not show maxima or minima between the surface and h , and that there are discontinuities in this curve in the surface and at h .

We also come to the same conclusion if the mixture is supposed to contain the ions $C_2, C_n, A_2; C_1, C_n, A_2; C_3, C_n, A_1$; etc.

§ 5. Further on we make the same simplifications as Gouy.* The liquid is supposed to contain only two kinds of ions, one of which is identical with that from the surface. The charge is so small that U does not differ very much from 1.

So we get in the same way

$$x = \frac{1}{2m} \sqrt{\frac{KRT}{\pi C (v_o + v_a)}} \log \frac{r_o}{r} + C \text{ (constant),}$$

or

$$x = a \log \frac{r_o}{r} + C$$

where we call

$$r = - \int_x^h \rho dx$$

And from equation (4)

$$x = a \log \frac{\frac{4\pi q_o}{K} + F}{\frac{4\pi q}{K} + F} + C$$

or, if

$$F' = \frac{KF}{4\pi}$$

$$x = a \log \frac{q_o + F'}{q + F'} + C. \quad (10)$$

If $x = 0$ then $q = q_o$, and the constant is zero.

We obtain the same equation as Gouy, differing only by the additional factor F' .

§ 6. If $x = h, q = 0$, hence

$$h = a \log \frac{q_o + F'}{F'}$$

giving us q_o in terms of h if F' is known.

Substituting this value for q_o in (10)

$$x = h + a \log \frac{F'}{q + F'}$$

* In Gouy's paper there is obviously a misprint, instead of $V_o/V_a = n$ one has to read $V_a/V_o = n$.

or

$$q = F' (e^{\frac{h-x}{a}} - 1).$$

Now the "centre of gravity" of the field is at a distance ε from the surface

$$\varepsilon = \frac{1}{q_0} \int_0^h q dx = \frac{1}{\frac{h}{e^{\frac{h}{a}} - 1}} \int_0^h (e^{\frac{h-x}{a}} - 1) dx$$

$$a = \frac{h}{\frac{h}{e^{\frac{h}{a}} - 1}}.$$

Hence $\varepsilon \rightarrow a$ if $h \rightarrow \infty$ and $\varepsilon \rightarrow 0$ if $h \rightarrow 0$

§7.—(a) If C is, for instance, 1 m. equivalent per L., then $a = 9.6 \mu\mu$ and ε may be calculated as a function of h , as is done in Table I

Table I

h in $\mu\mu$	ε in $\mu\mu$
38.4	8.0
19.2	6.6
9.6	4.0
4.8	2.2

Certainly an analogy will exist between this system and the particles in a sol, so one may expect quantitatively the same effect there as a function of the particle distance. When electrolyte is added the value for a decreases and hence the effect becomes smaller, sols with as low an electrolyte content as possible will show the largest alteration in charge on varying the sol concentration. This is in perfect agreement with the author's own (unpublished) experiments on lyophilic sols.

(b) Furthermore one sees that the impossibility of increasing the concentration of a lyophobic sol is not only necessarily due to the increasing amount of impurities present. The double layers are getting less and less diffuse under each others influence, and this alone may already be sufficient to make the concentrated sol unstable.

(c) Neither q_0 nor F' have any influence on ε .

§ 8. This brings us to a closer description of the difference between the ε and ζ potential, a point in nomenclature which in this case is rather confusing.

For if F and the distance ε of the centre of gravity from the surface are related to the ζ potential, the relation between the ε potential (which may depend on F only) and the ζ potential is clear

One may ask now how the mechanism of the ϵ and ζ potential can be explained; actually the Freundlich theory gives an explanation of this difference. ϵ can be expressed with the aid of the Nernst formula in the ordinary way or with the aid of other formulæ for diffusion potentials, a subject which lies beyond the range of this paper.

The only fact we need to know is that there is a surplus of ions in the liquid dissolved from the surface, or caused by adsorption of the oppositely charged ions from the solution, which was our first assumption.

Hence, as the q/x curve never shows a minimum or maximum the curve as constructed by Freundlich is purely schematic, provided there are no other influences. The Freundlich curve is shown in fig. 2A, and as modified by our assumptions, fig. 2B, the part AB in the surface layers being only an example of a possible form.

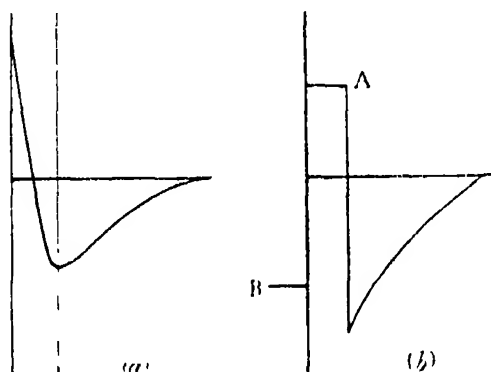


FIG. 2.

The curve in the simplest case is as shown in fig. 1. It starts in the solid, and may be negative; in the surface it suddenly goes up, then down again with a discontinuity, and does not end asymptotically at h . If there is an adsorption layer on the surface or if the surface has a composition other than that of the solid itself, as frequently happens, we obtain the more complicated curves shown in fig. 3A and fig. 3B.

At any rate the potential drop from the adsorbed layer to the liquid is always discontinuous, as we have shown in this paper. Furthermore one sees that in the last instances cited the ζ potential is not at all related to the ϵ potential. In the first, fig. 3, if $\epsilon = 0$, ζ is bound to be zero, and ϵ and ζ have opposite signs: this is not necessarily true in the last instance.

Finally we once more draw attention to the fact that all our deductions are

made by starting from certain assumptions and therefore all our conclusions hold only if these assumptions are fulfilled.

My thanks are due to Professor F. G. Donnan, F.R.S., for his interest in this work.

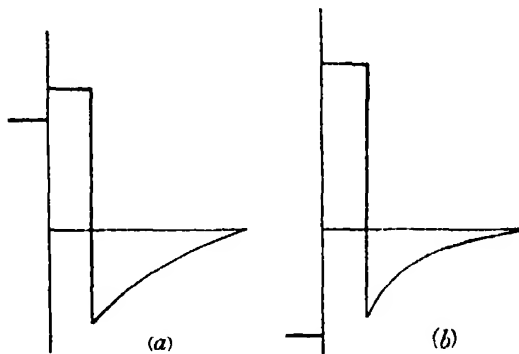


FIG. 3.

Summary.

§§ 1, 2 —An extension is given of the original theory of Gouy for two double layers under each others influence.

§ 3.—The so obtained formulæ make more understandable the effects, found by Bungenberg de Jong and Dekker in a mixture of two sols with oppositely charged particles under the influence of electrolytes.

§ 4.—The properties of the double layers are discussed in terms of these formulæ.

§§ 5, 6, 7.—An equation is derived for the relation between the position of the “centre of gravity” of the double layers between two surfaces and the distance of these surfaces.

The centre of gravity is not affected by the potential of the surfaces, but depends only on the valency and the amount of ions in the solution and on the distance of the two surfaces.

§ 8.—The relation between ϵ and ζ potential is discussed.

The Positive Ion Work Function of Tungsten for the Alkali Metals.

By R. C. EVANS, B.A., B.Sc., Denman Baynes Research Student, Clare College, Cambridge.

(Communicated by Lord Rutherford, O.M., F.R.S.--Received December 13, 1932)

Introduction.

The evaporation of positive ions of potassium from a hot tungsten surface has been investigated qualitatively by Moon and Oliphant.* In their experiments a beam of positive ions, the energy of which could be varied from 0 to 6000 volts, was allowed to fall on a tungsten strip heated to a desired temperature. A collector maintained at a negative potential with regard to the strip collected the positive ions which re-evaporated from it. When an equilibrium state had been reached such that the beam of ions evaporating was equal to the incident beam, the incident beam was suddenly cut off and the decay of potassium ions from the target followed by means of an oscillograph. The results of these experiments, which were of a purely qualitative nature, showed that when the energy of the incident ions was low or the temperature of the target was high the current from the target decayed exponentially with time, but that when the target temperature was low or the energy of the ions high, the decay began to depart appreciably from the exponential form, becoming much more complex in nature. The interpretation of the experiments indicated that an explanation of the evaporation of the fast ions must be sought in processes taking place within the body of the metal, whereas with slow ions the behaviour could probably be explained in terms of phenomena at the surface.

The experiments described in the present paper were carried out to investigate from a *quantitative* point of view the simpler case of the evaporation of slow ions.

Apparatus.

The apparatus used is illustrated in fig. 1.

The portion T of the tube acted as a source of positive ions, and was separated from the rest of the apparatus by the glass partition P into which was sealed a nickel disc D. In this disc a slit 6×0.32 mm. was cut, this slit thus forming the only communication between T and the rest of the apparatus. Parallel

* 'Proc. Roy. Soc.,' A, vol. 137, p. 463 (1932).

to the slit and about 0.5 mm. from it was mounted a tungsten strip W, $10 \times 1 \times 0.05$ mm., the strip being fixed to two stout nickel supports welded to heavy current pinches. The strip was heated by alternating current to about 1400° K. The side tube K, into which the potassium was finally put,

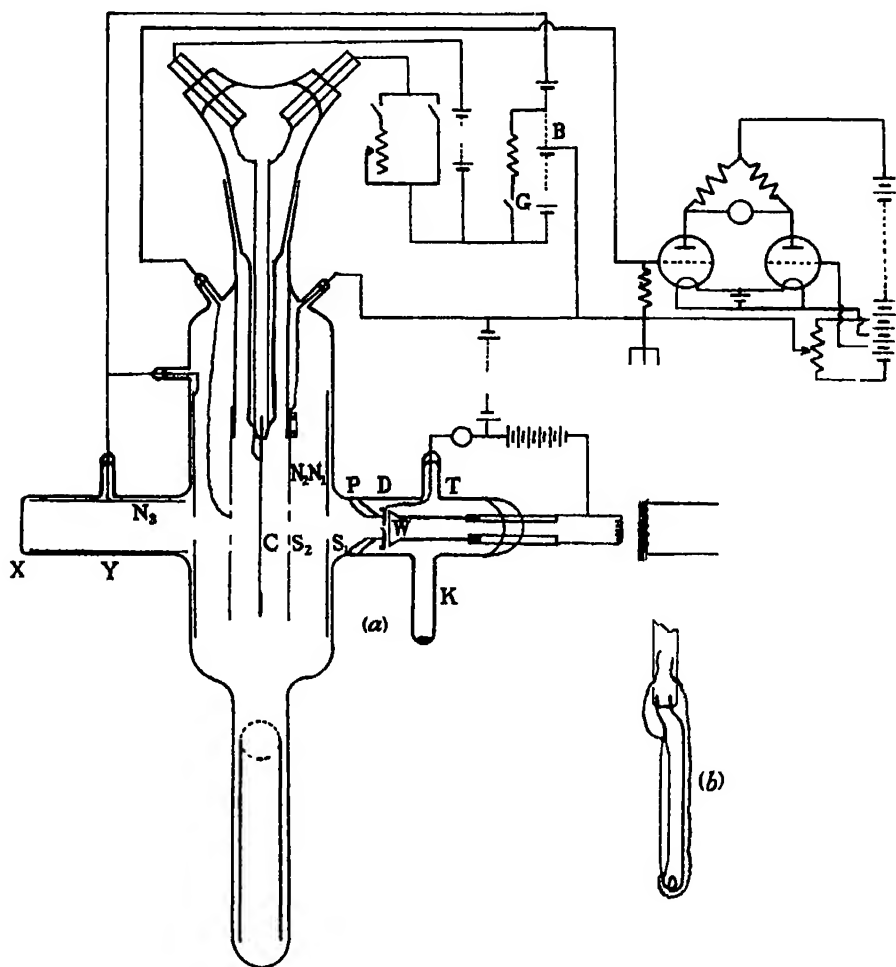


FIG. 1.

originally ended in a series of four stills, the first of which projected outside the furnace used to outgas the apparatus. After baking, the potassium was distilled into the successive bulbs, each of which was removed in turn, until finally a quantity of potassium was in the side tube at K. The potassium at K produced a concentration of atoms in the region T of the tube, and some of these

atoms passed through the slit in the disc D. Since, however, the tungsten strip occupied a very large part of the field of view of the slit as seen from the other side, the great majority of the atoms passing through the slit must have struck the strip. If this strip was maintained at a temperature above about 1200° K., most of these atoms became ionized, since the work function of tungsten (4.6 volts) exceeds the ionization potential of potassium (4.32 volts).*

The current that can be obtained in this way is clearly limited by the vapour pressure of potassium at the temperature of the side tube. In order to obtain sufficiently large currents it was necessary to heat the side tube to about 100° C. by means of a small oven that could be slipped over it. The temperature of the main tube in the region T was maintained slightly higher by the heat radiated from the tungsten strip. The total emission obtained was of the order of 30×10^{-8} amperes. If the disc D was maintained at a negative potential with regard to the strip an ionic beam, representing a few per cent. of the total emission, passed through the slit, while if this potential was reversed, positive ions were prevented from reaching D and a small atomic beam passed through the slit. The arrangement could thus be used as a very convenient source of either an ionic or an atomic beam. Experiments were made with both atomic and ionic beams.

The beam which passed through the slit in D was further defined by a narrow slit S_1 5×0.3 mm., 30 mm. from D, cut in the nickel cylinder N_1 . The narrow beam thus obtained passed through a very much wider and longer slit S_2 in the nickel cylinder N_2 , and fell on the target C. This target, shown in detail in fig. 1, *b*, consisted of a strip of tungsten $60 \times 3 \times 0.05$ mm., mounted axially in the main portion of the apparatus. The strip was slightly channelled to add rigidity, and was tapered slightly at each end in order to make the temperature distribution along it more uniform.

The target was surrounded by a concentric cylindrical collector N_3 , constructed on the guard ring principle, so that the measured currents came only from the central portion of the target, the temperature of which was sensibly uniform. Some form of guard ring device is essential in such experiments as these, for although the beam only falls on to a small region of the target, evaporation may take place from a large area due to the surface migration of the adsorbed alkali metal.†

* Langmuir and Kingdon, 'Proc. Roy. Soc.,' A, vol. 107, p. 61 (1925).

† Langmuir and Taylor, 'Phys. Rev.,' vol. 40, p. 463 (1932).

The temperature of that portion of the target on which the beam fell, and from which the evaporation current was measured, was determined with the aid of a disappearing filament optical pyrometer sighted on the back of the target through the plane polished window X, and appropriate holes in N_1 and N_2 . On account of the large size of the target, its image occupied a very large fraction of the total field of view of the pyrometer thus affording a good ground against which to adjust the instrument. The pyrometer was calibrated against a standard instrument, and it was found possible, with practice, to measure the temperature of the target to within 4° C. The usual emissivity correction was applied.* With the arrangement used temperature measurements could be made continuously throughout the experiment, the temperature being always determined directly, and not in terms of the target current.

In order to eliminate any possibility of disturbance of the field at the target by ions which might fail to strike it, and collect on the walls of the apparatus, the window X was fixed at the end of the tube Y the sides of which were shielded by the nickel cylinder N_3 . The field at T due to any charge that might have collected on X was negligible.

The target strip was heated by a battery of accumulators, about 10 amperes being required to heat it to 1000° K. and 30 amperes to flash to 2700° K. The currents from the target to the central portion of the collector were measured with the bridge system and oscillograph shown, identical with that used by Moon and Oliphant, details of which will not be given here. The deflections of the oscillograph were recorded photographically on a moving strip of bromide paper. The overall sensitivity was about 3×10^{-9} amperes per millimetre at 25 cm. The bridge system was very sensitive to electromagnetic disturbances, and it and all the apparatus connected to it were enclosed in earthed shields.

The nickel cylinder N_1 was maintained a few volts positive with regard to the collector N_2 in order to prevent any secondary electrons liberated from the slit S_1 by the incident beam from reaching the collector. In the majority of experiments an atomic beam was used, and then the disc D was kept about 40 volts positive with respect to the source strip. A slightly larger potential was then applied between D and N_1 to prevent thermionic electrons from the source strip from passing through S_1 . The field between the target and collector was provided by the battery B, and was normally so directed that positive ions could not pass from the target to the collector. By depressing

* "Handbuch der experimental Physik," vol. 13, p. 331, Leipzig (1928).

the key G, however, part of this battery could be short circuited through a high resistance thus instantaneously reversing the field at the surface of the target.* The remainder of the electrical connections call for no particular mention.

The whole of the apparatus was constructed of pyrex glass, and after the introduction of the potassium into the first still, was outgassed by baking at 480° C. for an hour. The potassium was then distilled from bulb to bulb and finally into the side tube K. The lower part of the apparatus constituted a mercury trap cooled in liquid air, and this was connected by a short length of wide tubing to a mercury diffusion pump. Under the conditions which obtained during the experiments a McLeod gauge connected to the apparatus registered a "sticking vacuum."

Experimental Procedure.

The experiments were performed in the following manner.

The target was flashed to 2700° K. for a few seconds, the key G being depressed in order to allow any positive ions on the surface to evaporate, and to prevent a large thermionic current from passing through the oscillograph. The target was then allowed to cool to the experimental temperature T of the order of 1000° K., and the key G was released. The only way in which potassium could permanently leave the target under these conditions was in the atomic state, and the surface concentration thus went on increasing until the atomic evaporation rate was equal to the rate of deposition from the incident beam, when an equilibrium state was established. The field between the target and the collector was then suddenly reversed by depressing the key G, and the excess concentration of ions allowed to evaporate. We should thus expect the current to the collector, zero before reversing the field, to assume a large value immediately after reversing, and to decay from this value to a limiting value corresponding to a new surface concentration for which the evaporation rate in the atomic and ionic states together equals the arrival rate. It was this decaying evaporation current that was measured with the oscillograph, and fig. 2 shows the general form of the records obtained in the experiments. We may anticipate the full discussion of the results by stating that in all the experiments using a tungsten target, it was found that at all the temperatures at which measurements could be made the curves obtained

* [Note added in proof, January 14, 1933.—There is a slight error in fig. 1. The connection from the target circuit should be taken to the upper end of the resistance and the key G should be placed between this point and the battery B. The lower end of the resistance should be connected to the negative end of B.]

were closely exponential from B to C, and that the final steady current AO was always small compared with AB. It was further found that the time constant of the exponential curve was independent of the intensity of the incident beam, being a function only of the temperature of the target.

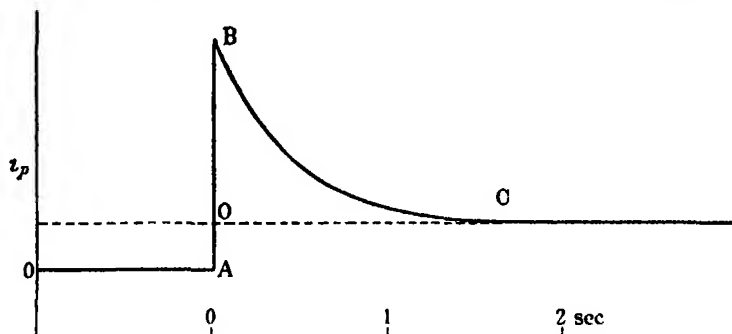


FIG. 2.

Theory of Evaporation.

In order to investigate the significance of the exponential decay curves obtained experimentally we must enquire into the mechanism of the evaporation of adsorbed atoms and ions. The general theory has been developed from somewhat different viewpoints by Langmuir and Kingdon (*loc. cit.*) and by Becker,* but the two treatments yield essentially the same results. Becker's treatment, which, perhaps, gives a more physical picture of the processes involved, lends itself better to the discussion of these experiments, and will be followed here. This treatment is based on the assumption that atoms and ions can co-exist independently adsorbed on a metal surface with surface concentrations N_a and N_p respectively, the relative concentrations being given by the Boltzmann equation

$$N_p/N_a = e^{-I_s / kT}, \quad (1)$$

in which I_s is the surface ionization potential. If the surface concentrations are sufficiently small for the atoms and ions to evaporate independently of their neighbours, the atomic and ionic evaporation rates will be proportional to N_a and N_p respectively, and we may write for these evaporation rates,

$$E_a = a N_a, \quad \text{and} \quad E_p = b N_p. \quad (2)$$

In all the experiments described in this paper the maximum total surface

* 'Trans. Amer. Electrochem. Soc.,' vol. 55, p. 153 (1929).

concentration never exceeded 1 per cent. of a monatomic layer, and the assumption that the atoms and ions evaporate independently of their neighbours seems justified. It is in fact proved by the experimental observation that the time constant on the exponential curves obtained is a function only of the target temperature, and is quite independent of the intensity of the incident beam used.

Becker's treatment is strictly only applicable to equilibrium conditions under which N_a and N_i are not changing. Such conditions will be realized, for example, when positive ions are drawn from a hot wire in potassium vapour, but they will not obtain when the current from the target is varying as in the present experiments. During the period in which the surface concentrations are falling from their initial non-equilibrium value to their final equilibrium value, equation (1) will not necessarily hold, and to apply it is to assume that the rate of attainment of equilibrium between atoms and ions on the surface is indefinitely large. An extension of the theory to take account of finite rates of interchange between adatoms and adions is given elsewhere,* and will not be repeated here. In that treatment it is shown that the experimentally observed facts:—

(a) that the decay curves are closely exponential; and

(b) that the final equilibrium value OA, fig. 2, of the positive ion current is small compared with the instantaneous value at the moment of reversing the field, lead to the conclusions:

(a) that the majority of adsorbed particles exist on the surface as ions;

(b) that the probability of an adatom being converted into an adion is very much greater than the probability of either an adatom or an adion evaporating as such. This is equivalent to the statement that the rate at which atoms are converted into ions on the surface is large compared with the rate at which atoms and ions evaporate from the surface; and

(c) that the variation of positive ion current with time after the reversal of the field is given by an equation of the form

$$i_p = \alpha Q (1 + \beta e^{-bt}), \quad (3)$$

where α and β are constants, and Q is the intensity of the incident beam. The current thus decays exponentially from an initial value $\alpha Q (1 + \beta)$ to a final value αQ . The important point about the decay, however, is that the time constant contains only the quantity b so that the time rate of decay of the

* Evans, 'Proc. Camb. Phil. Soc.,' vol. 29, 1933.

current is the same as that which would obtain if positive ions alone existed on the surface and evaporated at a rate given by (2). From the experimental decay curves we can thus find b at any temperature.

We must now investigate the variation of b with temperature. For the rate of evaporation of positive ions over a narrow range of temperatures we may write (Becker, *loc. cit.*)

$$E_p = Me^{-\phi_p e/kT},$$

where M is a constant proportional to the surface concentration, but independent of temperature, and ϕ_p is the work required to remove a positive ion from the surface to infinity. Dividing by N_p , we have

$$E_p/N_p = b = Ne^{-\phi_p e/kT}, \quad (4)$$

where N is a constant for all conditions of surface concentration and temperature. It follows from this equation that if this treatment is correct a straight line should be obtained when the logarithm of b is plotted against the reciprocal of the target temperature, the slope of this line being a measure of ϕ_p .

Results.

The experiments were performed in the manner already described. The deflections of the oscillograph were recorded photographically on a drum camera, a time base being simultaneously recorded by imposing an A.C. wave of standard frequency on the zero line before the field was reversed to make the experiment. The temperature of the target was measured with the pyrometer within a few seconds of making the experiment, although in practice it was found that the temperature remained very steady for long periods of time. The photographic records, each of the general form of fig. 2, were analysed by plotting the logarithm of the deflection, measured from OC as zero, against the time, the slope of the resulting straight line being a measure of the quantity b from (3). Each exponential curve thus gave one value of b . A second graph was then prepared by plotting the logarithm of b against the reciprocal of the corresponding target temperature, and this was found to be a straight line within the limits of the experimental error, thus justifying a formula of the form of (4).

Experiments were made with potassium, rubidium, and caesium, these being the only alkali metals whose ionization potentials are lower than the work function of tungsten.

Potassium.—The results for potassium are shown in fig. 3, line K. The extreme range of target temperatures over which measurements could be made was about 120° C., the half period of the evaporation curves changing in this interval from about 2 to 0.1 seconds, and these being the limits of decay rate that it was convenient to measure with the oscillograph. It will be seen that no point lies further from the straight line than a distance corresponding to an error in temperature measurement of 4° C., which was found to be

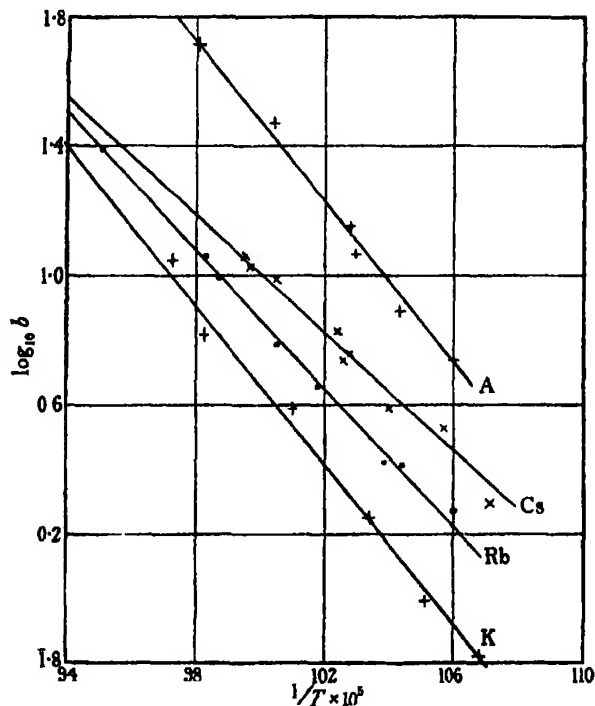


FIG. 3.

approximately the accuracy with which pyrometer readings could be reproduced.

In the experiments with potassium it was at first found to be impossible to obtain reproducible values of b until it was discovered that b changes, after flashing, with time of exposure to the beam, falling rapidly at first and finally tending to a limit after about 2 minutes exposure. This effect would be that obtained if the temperature were falling during this time, but observations with the pyrometer showed that the temperature in all cases became sensibly steady 15 seconds after flashing, whereas b was still decreasing. Fig. 4 shows the way in which b varies with time for two values of the incident beam,

the target temperature being the same in each case ; it will be seen that with the smaller beam the time to reach equilibrium is greater, but that the final equilibrium value is the same in each case. The most remarkable feature of this change in b , however, is that if all the experiments be made the same time after flashing the points on fig. 3 lie above those corresponding to equilibrium conditions, but nevertheless on a straight line *very closely parallel* to the equilibrium line. This is illustrated by line A which is also for potassium on tungsten, the exposure to the beam being in this case only 30 seconds. Although the evaporation rate at any given temperature is for line A about six times that for the equilibrium line K, the two are very nearly parallel. This effect was also obtained with the other alkali metals.

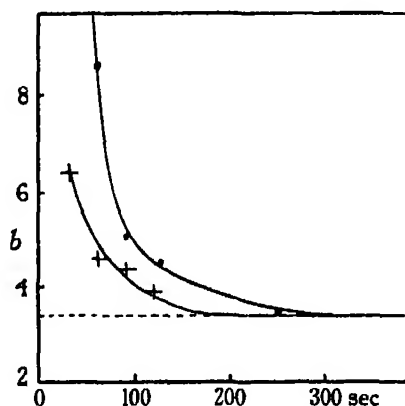


FIG. 4

The value of the positive ion work function deduced from line K is 2.4_3 volts.

Rubidium.—Rubidium was introduced into the apparatus in the same way as potassium, a small quantity of the metal being available.

Curve Rb, fig. 3, shows the results obtained. In this case the evaporation rate at 1000° K. was about twice that of potassium, although the temperature rate of change was slightly smaller, giving a value for the work function of 2.1_4 volts.

Cæsium.—With cæsium the metal was introduced into the apparatus in the following manner. A further side tube was connected on to K and in it was placed a nickel cylinder containing about 0.1 gm. of a mixture of misch metal and cæsium chromate. This was heated to a dull red heat by an eddy current heater when a vigorous reaction set in, cæsium being liberated and distilling out of the cylinder. The metal was distilled once into K, and the

subsidiary side tube was removed. The vapour pressure of caesium at room temperatures is such as to give a beam of convenient magnitude, so that no heating of the side tube was required.

The results obtained are shown on line Cs, fig. 3, and it will be seen that the evaporation rate at 1000° K. is about twice that of rubidium, but that it has a slightly lower temperature coefficient giving a value for the work of 1.8_1 volts.

Discussion of Results.

In the experiments of Moon and Oliphant (*loc. cit.*) a rough value of 4.4 volts for the positive ion work function for potassium evaporating from tungsten was found by the same method as that used in the present experiments. Little significance, however, is attached to the discrepancy between this and the present value of 2.43 volts, since in Moon and Oliphant's experiments no provision was made for the accurate measurement of temperature, and indeed the experiments were not intended to be of a quantitative nature.

A significant check on the experimental values for work function for the three alkali metals can, however, be made by comparing them with the work required to remove a positive ion from the surface of a metal against the attraction of its image charge, starting at a distance equal to its radius, and neglecting the action of neighbouring ions on each other. For this purpose we may take as the radii of the ions the values obtained by Goldschmidt* from the X-ray analysis of polar salts. These values are in close agreement with those given by Slater.† Table I shows the values of the work function thus calculated compared with the experimental values.

It will be seen that in all cases the experimental values are about 10 per

Table I.

Ion	Radius	Work function.	
		Calculated.	Observed.
K	cm. 1.33×10^{-8}	volts 2.69	volts. 2.43
Rb	1.49	2.40	2.14
Cs	1.75	2.03	1.81

* 'Trans. Faraday Soc.,' vol. 25, p. 253 (1929).

† 'Phys. Rev.,' vol. 36, p. 57 (1930).

cent. lower than the calculated values. Goldschmidt's values of the ionic radii are, however, probably only correct to a few per cent., and on account of polarization, do in fact vary by several per cent. from salt to salt. Moreover, while the approximate agreement between the calculated and observed values suggests that the greater part of the work required to evaporate an ion represents work done against the image force, there is no doubt that very close to the surface other forces are operative.

Further insight into the processes of surface ionization may be obtained by applying the Born cycle to the phenomenon, as has been done by Günterschulze* and Becker (*loc. cit.*). Let us suppose that we start with an atom on the surface. Then we can imagine the following reversible process. Let us ionize the atom on the surface, thus doing an amount of work I_s . Let the ion and the electron be now evaporated independently and let them recombine in free space, the atom thus produced returning to the surface. From this cycle we see at once that with an obvious notation,

$$\phi_s + \phi_a - I = \phi_a - I_s. \quad (5)$$

Inserting the measured values of ϕ_s and the known values of the electron work function of tungsten and of the ionization potentials of the alkali metals in the left-hand side, we obtain as the values of $(\phi_a - I_s)$ for potassium, rubidium, and caesium, 2.64, 2.54 and 2.46 volts respectively. Unfortunately there are available no reliable measurements of ϕ_a or I_s . Langmuir and Kingdon (*loc. cit.*) quote a value of $\phi_a = 4.63$ volts for caesium evaporating from tungsten, but recently Langmuir† has given a formula for the rate of evaporation of adsorbed caesium which, for dilute films, gives a value for ϕ_a of 2.76 volts. The experimental methods followed in deriving the formula are not given. If this value is correct, comparison with the value found for $(\phi_a - I_s)$ in the present experiments gives a value of I_s of about 0.3 volts. This, however, is not consistent with the observations that the majority of adsorbed particles are ionized, for it follows from (1) that in this case I_s must be negative. Indeed a rough estimate of the order of magnitude of I_s can be made from these experiments in the following way.

Before reversing the field, the surface concentration of adsorbed particles increases until it reaches a value such that the *atomic* evaporation rate is equal to the rate of deposition from the incident beam. The ion current appropriate to such a concentration is that which obtains at the instant of reversing the

* 'Z. Physik,' vol. 31, p. 507 (1925).

† 'J. Amer. Chem. Soc.,' vol. 54, p. 1252 (1932).

beam, namely, AB, fig. 2. After the new equilibrium conditions have been established, the ionic current AO, and a very small atomic current, together equal the incident beam, so that we may take AO as a rough measure of this beam, and therefore of the atomic evaporation current under the conditions when the evaporation of positive ions is not allowed. It follows that at any surface concentration, the ratio of the ionic to the atomic currents is roughly equal to the ratio AB/AO, and if we denote this by R , we have from (2),

$$R = b N_p / a N_a. \quad (6)$$

Now we have seen that in all the experiments R was large, but on most of the curves the current AO was nevertheless measurable, so that we can safely say that $100 > R > 10$. If now we assume for the moment that a and b are of the same order of magnitude, we may say $100 > N_p/N_a > 10$, and from this it follows by equation (1), since N_p/N_a is very sensitive to small variations in I_p , that I_p lies between about -0.2 and -0.4 volts for all the alkali metals. The values of ϕ_a necessary to make the Born cycle close are then about 2.3, 2.2, and 2.1 volts for potassium, rubidium, and caesium respectively, and this is consistent with our assumption that a and b are of the same order of magnitude, for just as b is given by an equation of the form (4), so a will be given by a similar equation in which ϕ_a replaces ϕ_p .

We thus see that the atom work functions of the three metals lies much closer together than the positive ion work functions.

It is a great pleasure to me to express my thanks to Professor Lord Rutherford, F.R.S., and to Dr. J. Chadwick, F.R.S., for their interest and advice, and to Dr. M. L. E. Oliphant and to Dr. P. B. Moon for very many most valuable suggestions and discussions. I have also to express my thanks to the Department of Scientific and Industrial Research for a maintenance grant.

Summary.

The experiments described in the present paper give a very simple method of investigating the problem of the evaporation of ions of the alkali metals from a metal surface, under the conditions most susceptible to theoretical treatment, namely, when the surface concentrations are very small, and the particles are deposited on the surface with low kinetic energy. By artificially creating a state of non-equilibrium on the surface, in which the concentration of adsorbed particles is very much larger than the equilibrium value, and by following by means of an oscillograph the positive ion current from the surface

as the equilibrium state is attained, the rate of evaporation of ions, as a function of the ionic concentration, is determined. The temperature coefficient of this rate of evaporation is a measure of the positive ion work function, the work required to remove an ion from the surface to infinity.

Experiments have been made with ions of potassium, rubidium, and caesium evaporating from clean tungsten, and give for the work functions the values $2\cdot4_3$, $2\cdot1_4$ and $1\cdot8_1$ volts respectively. By considering these values in terms of the Born cycle it is concluded that the surface ionization potential of all three elements is about $-0\cdot3$ volts, and the *atomic* work function about $2\cdot2$ volts.

Analysis of α -Rays by an Annular Magnetic Field. .

By Lord RUTHERFORD, O.M., F.R.S., C. E. WYNN-WILLIAMS, Ph.D.,
W. B. LEWIS, B.A., and B. V. BOWDEN, B.A.

(Received December 27, 1932.)

[PLATE 17.]

In previous papers* an account has been given of a new counting method for analysing the groups of α -rays emitted by radioactive substances, and for measuring directly their mean range in air. In the course of these experiments, we showed that the long range groups of α -particles from radium C' are very complex, consisting of at least nine groups, with mean ranges lying between $7\cdot7$ and $11\cdot6$ cm. of air. As it is believed that the energies of these long range groups are intimately connected with those of the γ -rays from radium C',† it has become of great importance to determine the energies of these groups of particles with precision. As, however, the seven groups with ranges between $9\cdot5$ and $11\cdot6$ cm. differ so little in velocity that they can only be partially resolved in range measurements, it was very difficult in our experiments to determine the mean ranges with accuracy. Moreover, there has been considerable uncertainty as to the precise relation between the range and velocity of such long range particles.

A much greater resolving power can be obtained by a direct velocity deter-

* Rutherford, Ward and Wynn-Williams, 'Proc. Roy. Soc.,' A, vol. 129, p. 211 (1930); Rutherford, Ward and Lewis, 'Proc. Roy. Soc.,' A, vol. 131, p. 684 (1931); Rutherford, Wynn-Williams and Lewis, 'Proc. Roy. Soc.,' A, vol. 133, p. 351 (1931); Lewis and Wynn-Williams, 'Proc. Roy. Soc.,' A, vol. 136, p. 349 (1932)

† Rutherford and Ellis, 'Proc. Roy. Soc.,' A, vol. 132, p. 667 (1931).

mination, using a magnet to bend the α -rays into a circle. The great Paris electromagnet has been used in this way by Rosenblum,* who photographed the α -ray spectra produced by the well-known focussing method. He has demonstrated the complexity of a number of α -ray groups, and has measured their velocities with an accuracy of at least 1 in 1000.

The intensity of several of the long range groups of particles from radium C' is about 1 in 10^6 of the main group, and this is probably too small to allow of their analysis by this photographic method; yet the high resolving power of the apparatus, and the possibility it offers of a direct determination of the velocity of the particles, make this general method very advantageous for α -ray analysis. It was therefore decided to combine the advantages of the direct method of electrical counting of α -particles already developed† with the high resolution obtainable by the magnetic focussing method.

A laboratory type of electromagnet,‡ of reasonable dimensions and cost was kindly designed for us by Dr. Cockcroft, and constructed by Metropolitan Vickers, Ltd.§ This magnet produces an annular field, in which the swiftest α -rays can be bent into a circle of 40 cm. radius.

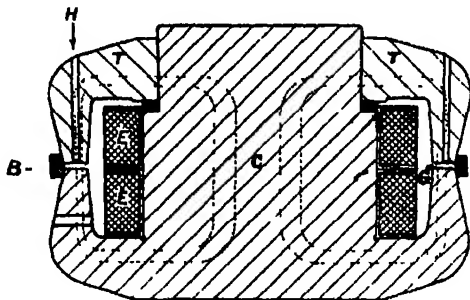


FIG. 1.

Magnet.

A sectional drawing of this magnet is shown in fig. 1. The energizing coils, E, are wound round the central core, C, so that the magnetic circuit is formed

* Rosenblum, 'C. R. Acad. Sci. Paris,' vol. 190, p. 1124 (1930) and succeeding papers.

† Wynn-Williams and Ward, 'Proc. Roy. Soc.,' A, vol. 131, p. 391 (1931); Wynn-Williams, 'Proc. Roy. Soc.,' A, vol. 136, p. 312 (1932).

‡ An account of the electromagnet has been given by Dr. Cockcroft 'J. Sci. Instr.' vol. 1, No. 3, March (1933).

§ We are much indebted to Metropolitan Vickers for the great care taken in the construction of the electromagnet, which has proved admirable for its purpose; and for the presentation to us of one of their oil diffusion pumps to obtain the necessary high vacuum in the interior of the magnet.



FIG. 3.

as indicated by the broken lines. With a dissipation of only 200 watts, a field of 10,000 gauss is produced in the annular gap, G, of width 5 cm., the pole faces being 1 cm. part. The field was explored by means of a large search coil (11,800 sq. cm. turns) connected to a fluxmeter, and the top, T, was rotated until the circumferential variations of the field over the semicircle to be used were less than 4 parts in 10,000. The positions of source, counter and defining slit are shown in plan in fig. 2. The beam of particles focussed on the counter

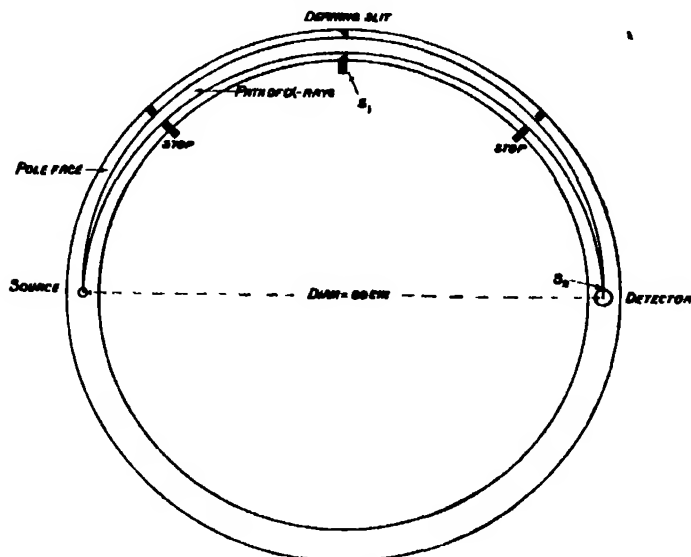


FIG. 2.

slit is defined by the central slit, S_1 . It has been found possible to allow a maximum width of 3 cm. for this slit, but owing to the falling off of the field at the edge of the gap, the focus deteriorates if a wider beam is employed.

Vacuum.

During an experiment the whole of the interior of the electromagnet—of volume about 20 litres—is evacuated to a low pressure. In order that there should be no sensible reduction of the velocity of the α -particles in their long path of 126 cm. it is essential that the residual pressure of air should not be higher than about 0.001 mm. mercury. A very convenient method of sealing the outer edge of the gap, which facilitates alteration of the slits and stops, has been adopted. A stout rubber band is stretched round the outside of the gap and held in position by a brass band, B (figs. 1 and 3). A special low vapour

pressure grease* is applied to make a seal between the rubber and the magnet. All other joints are sealed with a special plasticine*. The magnet is evacuated continuously during an experiment by means of an oil* diffusion pump, which has proved very satisfactory for this purpose.

When the apparatus was first set up, it was not possible to obtain a very good vacuum owing to the great quantity of water and other vapours released within the magnet, but after a few days pumping, it was found possible, under normal conditions, to reduce the pressure to about 0.001 mm. mercury within a few minutes of switching on the pumps. In order to avoid letting air into the apparatus when the radioactive sources are introduced, the latter are inserted through an air lock which is separately evacuated. If, however, adjustment of the slit system has necessitated the removal of the rubber band and admission of air to the whole apparatus, about an hour is required to reach the working pressure of 0.001 mm. mercury.

Ionization Chamber.

The counter slit (S_2 , fig. 2) is covered by a mica window through which the α -particles pass into the ionization chamber, C. This chamber is of the parallel plate type, as shown in fig. 4.

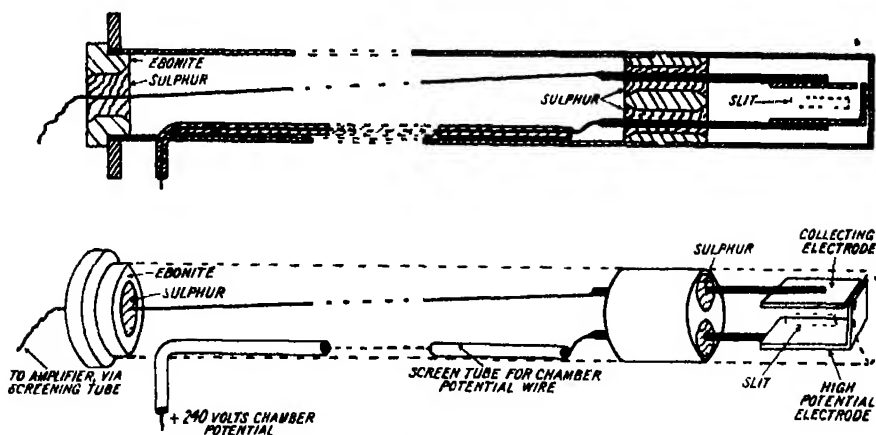


FIG. 4.

A hole (H, fig. 1) 1.9 cm. in diameter, was bored through the upper casting of the magnet, through which the counter was inserted so as to occupy its correct position in the gap, and in order to facilitate its removal without intro-

* Apiezon low vapour pressure compounds, "M," "Q," "J," and "K" made by Shell Mex, Ltd.

ducing air into the magnet a "well" was permanently fitted into the magnet. This consists of a tube, closed at its lower end, and passing through the hole in the top casting into the gap. The section in the gap, which carries the counter slit, is of brass; the upper section is of steel in order to avoid undue distortion of the magnet field, and for the same reason the diameter of this tube is kept as small as possible. The joint between the projecting upper end of this well and the top of the upper casting is sealed with plasticine so that it is a simple matter to change the counter slit by substituting a different well. Mica absorbing screens can be brought in front of the chamber window by means of a concentric brass tube situated between the "well" and the tube of the counting chamber. In this way one can ensure that only particles of the correct range are counted, by arranging that the peak of their ionization curve lies in the counting chamber. Other particles, which enter the chamber by scattering or otherwise are thus rejected.

Counting Apparatus.

The collecting lead of the chamber is connected with an amplifying system of the kind previously used. The first valve (D E.V type) had to be shielded from the stray magnetic field by mounting it in an iron box (D, in fig. 3, Plate 17) 5 mm. thick situated about 30 cm. above the top of the magnet. The rather large grid-earth capacity involved by the long grid lead, the smallness of the counting chamber, and the necessity of using a small diameter screening tube, made it desirable to collect ions from about 5 mm. of track, instead of about 3 mm. as in our previous experiments.

The voltage impulses in the output from the amplifier are applied to a valve filter circuit which rejects impulses below a certain magnitude, and amplifies the remainder still further. The impulses are then applied to a "scale of two" thyatron counting circuit which enables direct counts to be made on mechanical meters at speeds up to 1600 particles per minute, and which is able to count separately two particles arriving $1/1250$ th second apart. In order to facilitate the experimental procedure and quicken the working, auxiliary relay apparatus was devised and installed, which carries out, entirely automatically, a series of routine operations associated with the timing of counts, switching of thyatron circuits, and resetting of meters, etc., This allows the observers to concentrate their attention on other experimental details, so that it is possible to take as many as 50 two-minute runs with a decaying radium (B + C) source in the course of 2 hours.

Measurement of Magnetic Field.

In the present experiments, since the counter and source are fixed, and groups of α -rays are brought on to the counter slit by variation of the magnetic field, it is essential that the relative values of the field should be determined with accuracy at the moment of each experimental count. We have not, as yet, attempted to determine the absolute values of the magnetic fields, but have taken as standard the value of the velocity of the main radium C' α -rays, accurately measured by Briggs,* and more recently by Rosenblum.† The value of $H\rho$ for this group is taken as $3.993_0 \times 10^5$ gauss cm. It is desirable that the relative values of the magnetic field should be measured with the highest possible accuracy. A special method has been devised which has proved very satisfactory for the purpose.

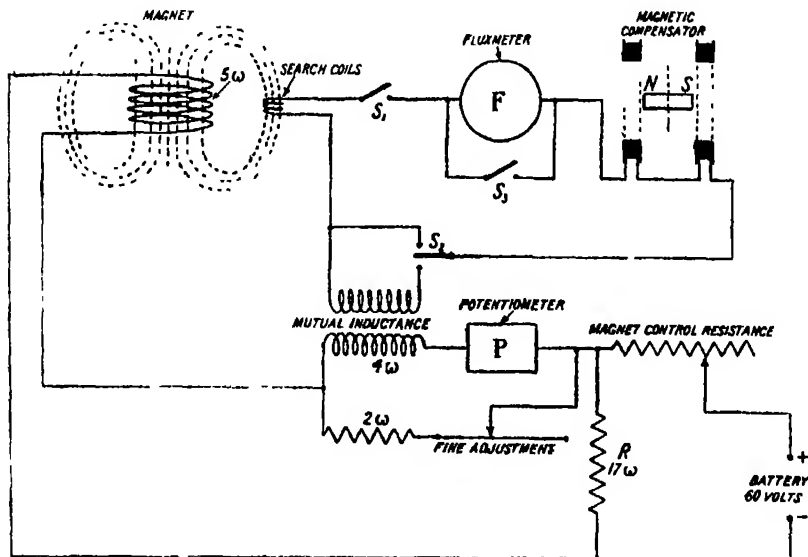


FIG. 5.

Two large search coils are permanently fixed in the gap, and are connected to a fluxmeter as shown in fig. 5. The secondary of a large mutual inductance and a "magnetic compensator" are also included in the circuit. The fluxmeter is used as a null instrument, which integrates small changes of flux in the circuit over long periods of time. The fluxmeter is provided with a mirror, and its movements are observed by a lamp and scale, adjustments being made

* 'Proc. Roy. Soc.,' A, vol. 118, p. 549 (1928).

† Rosenblum and Dupouy, 'C. R. Acad. Sci. Paris,' vol. 194, p. 1919 (1932).

so that the spot of light is always kept as close as possible to its natural zero. The sensitivity is such that a deflection of 1 mm., which is easily observed and corrected, corresponds to a change of 1 part in 50,000 in the main field. The changes of flux through the search coil are balanced by an opposing change of flux through the mutual inductance, the magnetic compensator being used for fine adjustments. The balance is substantially preserved during a change of field by arranging that a certain fraction of the main energizing current passes through the primary of the mutual inductance. When it is desired to maintain the field constant, the mutual inductance is removed from circuit by the switch S_2 , and the fluxmeter spot is kept at its zero by fine adjustment of the magnetizing current.* If a small change of field is required, the magnetizing current is changed, and the fluxmeter spot is still kept at its zero by making simultaneous changes of the compensator, with which it is possible to balance small changes of flux through the search coils. This compensator consists of a bar magnet which can be rotated between a pair of coils. A graduated circle is provided so that the compensator may be calibrated in terms of gauss in the magnet gap, by comparison with the mutual inductance. The scale of the compensator covers the equivalent of a change of about 200 gauss in the main field; if the end of the calibrated portion of the scale is reached, and a greater change of field is required, it is practicable and convenient to wait until the field is perfectly steady, and, after shortcircuiting the fluxmeter, to reset the compensator to the other end of its scale. It has been found that five or six such changes may be made in succession without introducing an error of more than about half a gauss. In order to measure large changes in the field, however, the mutual inductance is switched into circuit, and the flux changes in the search coil are opposed by the change of the current in the mutual inductance primary. This current is measured with an accuracy of 1 part in 20,000 by a potentiometer. To calibrate the apparatus it is necessary to determine the current corresponding to a known magnetic field. This magnetic field is determined by means of a standard group as follows. The magnet is first demagnetized so that the residual field at the search coil is not more than about 1 gauss, and can be measured approximately by rotating a search coil outside the gap. The fluxmeter circuit is then completed—the mutual inductance being included—and the magnet field is slowly increased until the particles from the main radium C' group, or some previously measured group, enter the counting

* A special mercury resistance has proved very satisfactory for adjusting the current with the required precision. This consists of a spiral groove of 12 metres total length, containing mercury, the resistance of which is about 0.8 ohm.

chamber. The current through the primary of the mutual inductance is then measured by the potentiometer, and the secondary is switched out of circuit. The group is then explored by counting the number of particles per minute entering the chamber at a series of neighbouring values of the field, the small changes being measured by the compensator. In this way it is possible to determine the exact relation between the current in the mutual inductance primary and the corresponding magnetic field. This calibration is repeated at intervals to determine small changes in the characteristics of the mutual inductance or the search coils. The difference in field between two groups can now be determined by switching in the mutual inductance and proceeding as before.

The above process of increasing the field from zero can be completed in 6 or 7 minutes. The deflections of the fluxmeter are kept small by adjustment of the compensator and if necessary by small adjustments of the shunt across the mutual inductance. The resistance R , is included to minimize the deflections. This is a low resistance (17 ohms) connected across the primary of the mutual inductance and the energizing coils of the magnet. The time constant (L/R) of the circuit formed in this way is of the order of 1 second, and any sudden changes in the external circuit produce relatively slow changes in the current through the magnet and mutual inductance.

Analysis of Observations.

Figs. 6, 7, 8 and 9, in which the number of particles counted per minute is plotted against the corresponding magnetic field are typical of the results obtained. A homogeneous group of α -particles produces a peak the shape of which is determined by the width of source, counter and defining slits. The narrow peaks shown in figs. 6 and 7 were obtained using sources deposited on wires 0.125 mm. diameter, a defining slit 2 cm. wide and a counter slit 0.43 mm. wide. It will be noted that the width of these peaks is of the order of 12 gauss in a total field of about 10,000 gauss. The peaks in fig. 9 were obtained using wider slits. It must be emphasized that the width of the peaks shown is mainly determined by the width of the counter slit; in the case of the 0.43 mm. slit a change of field of about 5 gauss would displace a group of particles by a distance equal to the width of the slit. Computation, based on the dimensions of the apparatus and the measured variation of the field, radially across the gap, shows that some of the observed peaks can be explained without assuming any inhomogeneity in the velocity of emission of

the α -particles, and when the source is prepared under the most favourable conditions, such as the preparation of a radium C' source by the method of recoil from radium A, it seems certain that the inhomogeneity in velocity cannot exceed 2 parts in 10^4 . When a very clean source cannot be prepared, however, the observed peaks are always broadened, and show that a considerable number of retarded particles are present in the beam.

Measurements are made to the point one-third the height of the peak on the high velocity side. It appears that this point is very little affected by imperfection of the sharpness of the peak.

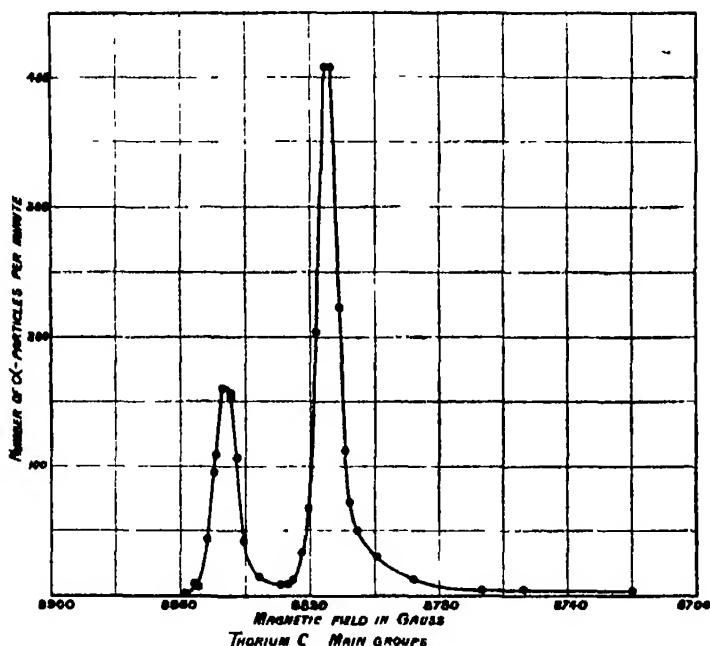


FIG. 6.

It will be seen in fig. 6 that the two main peaks from thorium C, which differ in velocity by 3 parts in 1000, are completely resolved. Under favourable circumstances the complexity of a beam of particles consisting of two homogeneous groups differing in velocity by 1 in 5000 would be detected.

The very high resolving power of the apparatus is well illustrated in fig. 7, which shows the effect of accelerating or retarding the α -particles by a potential of 1000 volts applied to the source. The energy of the α -particles which is about 8.8×10^6 electron volts is thereby increased or diminished by 1 part in 4400 (i.e., 1 part in 8800 in velocity) and this produces a very large effect

on the number counted when the magnetic field is maintained constant on the steep slope of the peak.

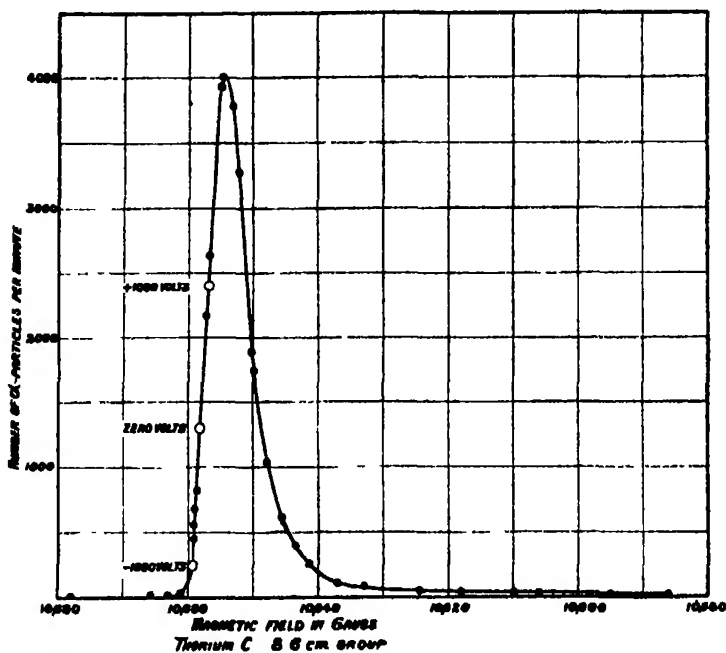


FIG. 7.

Accuracy of Results.

Since a very considerable accuracy is claimed for these measurements, it is desirable to discuss the principal sources of error which have been considered. Some of these errors are inherent in the method, and others we hope to reduce in future work.

It has already been mentioned that all absolute values depend on the assumed value of H_p for radium C' measured by Briggs and by Rosenblum (*loc. cit.*); the probable error in this is about 1 in 2000. In calculating energies it is also necessary to assume the value of E/M for the α -particle. We have assumed that the energy of the α -particle emitted by radium C' is $7.683_0 \times 10^6$ electron volts.* Absolute values of energy and energy difference depend on this quantity, which may be in error by 1 in 1000.

Our relative measurements, however, will be much more accurate than this. The calibration of the mutual inductance previously described is always repeated

* For a discussion of probable values for velocity and energy, see Rutherford, Chadwick and Ellis, "Radiations from Radioactive Substances," Camb. Univ. Press (1930), pp. 47, 86.

to within 1 in 5000. Slow variations over a period of weeks may be greater than this, but are detected by frequent calibrations. The *difference* of field between two groups is always measured directly, and the difference from polonium to radium C', or from radium C' to the swiftest long range particles is less than 20 per cent. of the total field, so the uncertainty in the calibration of the mutual inductance will not introduce an error in the ratio of the velocities of more than 20 per cent. of 1 in 5000, that is, 1 in 25,000. The scale of the compensator can be read to about a fifth of a gauss, and the error in calibration is of the same order of magnitude. Both these errors would be reduced by improvement in the design of the compensator.

In any fluxmeter there is a slight residual restoring torque. If, therefore, the spot were displaced while the field remained constant, the gradual drift of the spot towards its natural zero would be interpreted as a change of field, which would be corrected by adjusting the magnet current. For this reason it is necessary in practice to keep the spot at a point as close as possible to its natural zero. In practice there is usually a residual error which gives rise to a slow drift of the magnet field, but under normal good conditions this does not amount to more than 6 gauss in 2 hours. Moreover, this drift can readily be determined by returning to a previously observed group, and the values of the fields are corrected accordingly.

As already mentioned there is a slight circumferential variation of the field over the semicircle traversed by the α -particles. We find that this variation is not proportional to the field and attribute this to very slight differences of permeability in the iron. It is therefore necessary to apply a small correction to the measured field through the search coil. We have calculated this, using the formula obtained by Hartree* in conjunction with our measurements. As our measurements of the variation have only been approximate, we are aware that the estimate of this correction may be subject to a slight error, which may introduce an uncertainty of as much as 1 in 8000 in our determinations of the long range groups. A rather elaborate investigation will be necessary before this uncertainty can be eliminated, in view of the fact that the variation may depend to some extent on the previous magnetic history of the iron.

Other possible sources of error lie in the potentiometer readings, the possible variation of the position of the source, and the differences in the thermal expansion of the magnet, search coils and mutual inductance. These are all

* 'Proc. Camb. Phil. Soc.,' vol. 21, p. 746 (1923).

involved in the calibrations of the mutual inductance, which, as already mentioned, are consistent to 1 in 5000.

In the intercomparison of groups the errors would be smaller. Where possible, comparisons are made between sources deposited on the same button or wire to avoid change in the position of the source, but even when this is done it cannot be assumed that the two deposits are similarly distributed on the surface of the button, and we believe that this is one of the more important sources of error in the present experiments. The evidence for this is that we can intercompare thorium C and thorium C' with greater consistency than thorium C' and radium C'. A further point is that when the sources are not perfectly clean the resultant broadening of the peak may be different for the two deposits, and this may introduce an appreciable error. This error is practically negligible in the intercomparison of two groups from the same deposit.

It may be repeated that the measurements made in practice are of the difference of magnetic field between two groups. Since the velocities of most of the known groups of α -particles lie within ± 20 per cent. of that of radium C' it will be realized that if these measurements of difference are correct to 1 in 1000 the accuracy of the relative velocities will be correct to 1 in 5000, even for widely separated groups. The relative velocities are, however, often of less importance than the difference of energy between two α -particle groups. Our experiments indicate that it will be very difficult to determine any energy difference closer than about 200 electron volts, or in any case to measure any difference with greater accuracy than 1 in 1000. The application of these two limits may be illustrated by particular examples; thus, the two main groups from thorium C differ in energy by about 40,000 electron volts. This difference can be found to ± 200 electron volts, a probable error of 1 in 200. For widely separated groups on the other hand, such as the radium C' and the main thorium C group where the energy difference is about 1.6×10^6 electron volts, an error of 1 in 1000 corresponds to 1600 electron volts.

The resulting experimental error in relative velocity of the main groups, as estimated from the consistency with which results may be repeated is about 1 in 5000, but the relative velocity of close groups is known with greater accuracy than this.

Results.

Thorium C.—The first experiments to be undertaken were chosen so that the results obtained would be of interest even if the accuracy of measurement were not as great as it is hoped ultimately to attain. The complexity of the

α -rays from thorium C was examined, and a very substantial confirmation of Rosenblum's results was obtained, the only point of difference being that we could make no measurement of the group α_4 which appears very definitely in Rosenblum's photographs. We therefore conclude that this group must be of

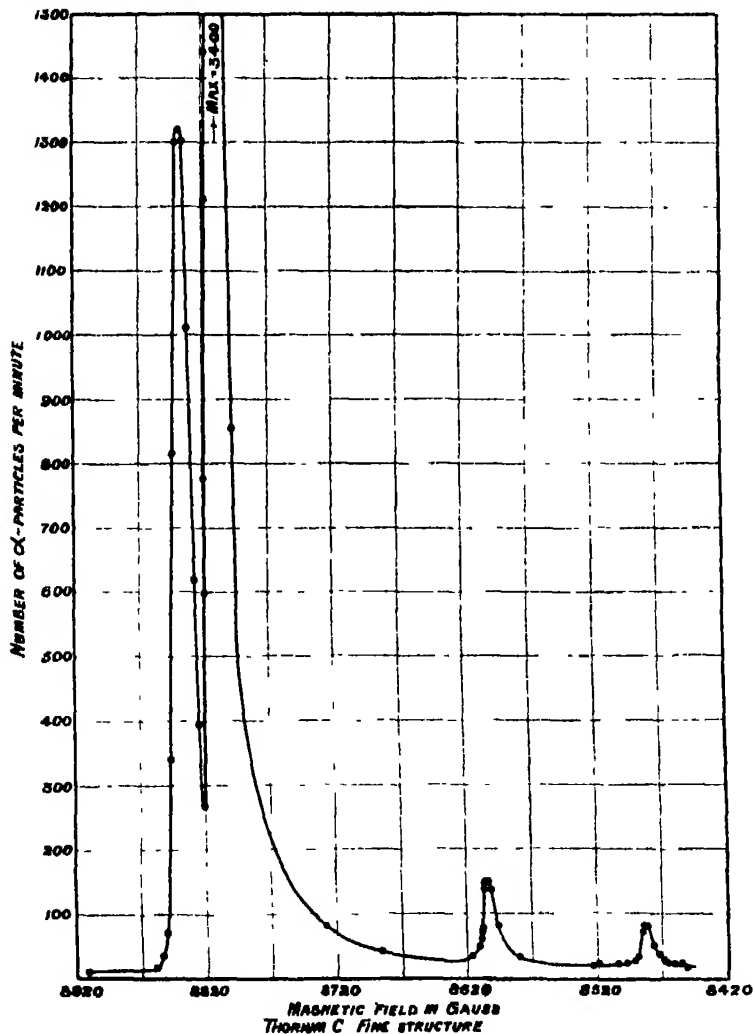


FIG. 8.

less than one-third of the originally assigned intensity (i.e., 0.5 per cent. of the main group), and Rosenblum's later results* confirm this conclusion. Our results are illustrated by fig. 8. We hope to repeat these measurements now that the accuracy of measurement has been increased.

* Rosenblum, "Origine des Rayons Gamma," p. 19 (Hermann et Cie., Paris) (1932).

Radium C.—Indirect evidence had led to the deduction that radium C disintegrates in two ways. The majority of the atoms emit a β -particle and produce radium C', which in turn disintegrates emitting a swift α -particle having a range of about 7 cm. in air. About 1 in 3500 of the radium C atoms, however, break up with the emission of an α -particle which has a range of about 4 cm. in air. Attempts by earlier investigators to observe these particles failed owing to the background of stray α -particles. In 1930,* however, when the differential counting chamber was developed, definite evidence of the presence of this group of α -particles was obtained. The background was reduced to about the height of the observed peaks by using the cleanest sources it was possible to prepare by the method of recoil from radium A. It was expected, that with the greater resolving power of the magnet, these particles would stand out clearly above the background, even when the necessary strong sources (50 mgm.) were used. It was found, however, that the background was unexpectedly large, and the utmost precautions were necessary to reduce it to a minimum. Sources deposited on wires produced a very large background so the wires were replaced by flat plates of polished stainless steel (3.5 mm. wide). The plates were inclined so that the α -particles reaching the counter left the plate at an angle to its surface of about 10° ; any smaller angle increased the number of retarded particles forming the background. The projected width of the source plate was thus only about 0.6 mm., and the resolving power of the apparatus was not unduly reduced.

The results of these experiments are shown in fig. 9. It will be seen that there are two nearly equal groups, each containing about 1/10,000 of the number in the main radium C' group. The velocities of these groups have been measured and the difference in disintegration energy between the two groups is found to be 62,000 electron volts. From the curve connecting range and velocity given in fig. 10, it can be estimated that the ranges in air are 4.043 and 3.973 cm. at 15° C. and 760 mm. These ranges are in good accord with the main range observed in our early experiments.

We were unable to detect any further groups by the magnetic method, and conclude that any such group, if it exists, must be less than 1/40,000 of the main radium C' group. It may be, however, that other weak groups are present which would bring the total number of particles into better agreement with our previous estimate.

Main Groups. Radium C', Thorium C', Thorium C and Polonium.—Very accurate intercomparisons between these groups have been made. Three

* Rutherford, Ward and Wynn-Williams, *loc. cit.*

polonium sources have been prepared by deposition from dilute hydrochloric acid solution on to polished silver buttons. On one plate it is just possible to detect signs of the deposit in bright daylight, on another the polish of the button appears dulled, and on the third a distinct tarnish is visible. The measurements made with these three sources agree to within 1 in 5000. The polonium group has been compared with thorium C, a small amount of thorium active deposit being obtained on the source. The best polonium source has also been compared direct with radium C', deposited on the same button by recoil from radium A.

The main radium C', thorium C' and thorium C groups have also been intercompared, using recoil sources of radium C and clean sources of thorium

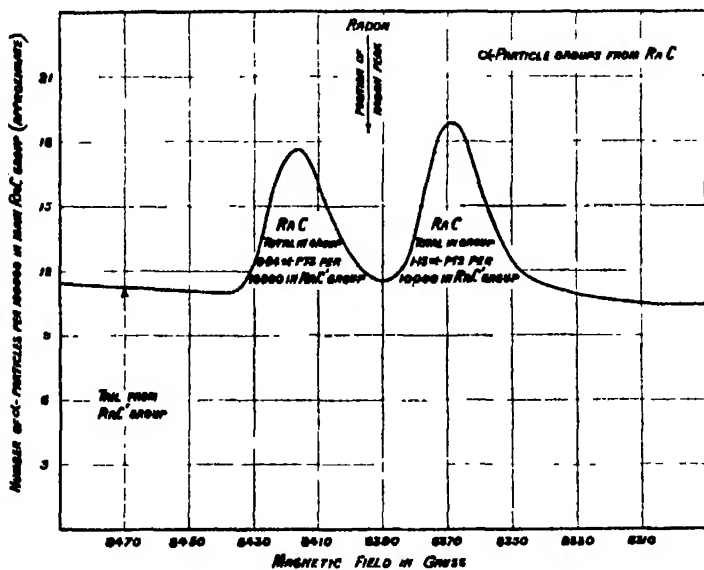


FIG. 9.

active deposit, prepared by short exposure to thorium emanation. The polish of such sources remains perfect, and no trace of a deposit is visible.

Radium A and Radon.—In the radium C experiments, the difference between the two groups and the thorium C group was measured. At the beginning of an experiment there was sufficient radium A on the source for the velocity of this group to be measured, and three consistent measurements of the difference between this group and the main thorium C group were made during the course of these experiments.

It was noted that the velocity of the radon group as deduced from our range determination lay between the two radium C groups, and it was therefore

necessary during the measurements of these groups to make careful observation of the decay of the groups found, in order to make certain that there was no appreciable amount of radon on the source. The observed decay was not always quite as calculated, but it was concluded that there was no evidence for the presence of radon. Nevertheless an experiment was undertaken to fix accurately the position of the radon group. A radon source was prepared by exposing to the emanation overnight a source button, covered with an almost invisible film of grease. This source was not very satisfactory, but it was possible to make measurements of the radium A and radon groups, from which their relative velocities have been deduced with an accuracy of about 1 in 2000. It was thus found that the radon group falls about midway between the two radium C peaks, confirming that the radium C sources had not been contaminated with radon.

It may be worth noting that though in both the thorium and the actinium series the main emanation group has a velocity greater than the main C group, the reverse is true in the radium series. Another point of difference between the series is thus established.

During the course of these measurements M. Rosenblum published the results of his measurements of the velocity of the radon and radium groups. Our results agreed with his to within 1 in 2000, which was probably within the accuracy of either measurement. Recently we have made a more accurate determination of the velocity of the radon group. It happened that some of our strong sources of radium B + C (of about 130 mgm.) used for measurement of the long range groups from radium C', absorbed a measurable amount of radon on the surface, and we were able to use these to redetermine the relative velocities of the radium A and radon groups. The results we obtained agree well with the previous measurements, but are considered somewhat more accurate, and are included in the table of results.

Long Range Particles.—The experiments to determine the velocities of the long range groups from thorium C' and radium C' were quite straightforward. The sources used were as clean and as strong as could be obtained, but the rate of counting was very slow, so that counts had to be taken for a period of 3 or 4 minutes. It was very difficult to obtain a sufficiently strong and clean source to observe the long range particles of thorium C', but by using a stainless steel button, and limiting the exposure time to 18 hours, satisfactory sources have been obtained, from which we counted about four particles a minute in the 9.7 cm. group, and twenty per minute in the larger 11.7 cm. group.

The main (9 cm.) group of long range particles from radium C' was readily

located. A small amount of thorium B + C is first deposited on the button to be used for the radium B + C source. A very accurate intercomparison can then be made between the 9 cm. group and the main thorium C' 8.6 cm. group. Subsequently, when the radium C has decayed sufficiently, the difference between the thorium C' and the main 7 cm. group of particles from radium C' is measured on the same source.

Some of the weak long range groups from radium C' have now been measured, but much remains to be done before a complete analysis is made. The result for the small 7.8 cm. group is included in the table.

Discussion. Range-velocity Relation.

In our previous experiments where we measured the mean ranges of a number of groups of α -particles the corresponding velocities were deduced from a correction curve showing the departures from Geiger's law $V^3 = kR$. In this curve the correction

$$\frac{\Delta V}{V_0} = \frac{V}{V_0} \left(\frac{R}{R_0} \right)^{1/3}$$

is plotted against range. V_0 and R_0 are the velocity and mean range of the α -particles from radium C' which are taken as standard. It was pointed out* that the form of the curve was very uncertain owing to the disagreement between the velocity measurements of different observers for the same group of particles. Further it was stated that more accurate velocity data was expected to be available in the near future. We are now able to give the more accurate curve, fig. 10, which differs very markedly from that previously published. In the first place Rosenblum,† to whom most of the previous velocity measurements were due, has corrected all his values in such a way that the velocities of the thorium C and C' groups agree more closely with the previous measurements of Laurence.‡ In the second place the accuracy of our own relative velocity measurements is such that little uncertainty about the form of the curve remains. It is satisfactory to note that the points obtained lie very close to a smooth curve, which confirms the accuracy claimed for both the range and velocity measurements apart from systematic errors. In view of this greater accuracy the velocities of the α -particles have been recalculated

* Lewis and Wynn-Williams, *loc. cit.*

† Rosenblum and Dupouy, *loc. cit.*

‡ 'Proc. Roy. Soc.,' A, vol. 122, p. 543 (1929).

Table.

	Mean range, cm. of air at 15° C. 760 mm.	Extra-polated ionization range cm. of air 15° C. 760 mm.	V/V ₀			Energy of α -particle e. volts $\times 10^{-4}$	Energy of disintegration e. volts $\times 10^{-4}$	Measurement used as basis for energy calculation.
			New magnet.	Rosenblum.	Deduced from range			
Radon	4.014	4.060	0.8448 ₆	0.844 ₄	0.8452	5.479 ₆	5.579 ₆	M.
Radium A	4.620	4.673	0.8837 ₄	0.8836 ₆	0.8837	5.996 ₆	6.108 ₆	M.
Radium C—								
a	(4.043)	(4.089)	0.8471 ₆	—	—	5.509 ₆	5.614 ₆	M.
a ₁	(3.973)	(4.019)	0.8425 ₆	—	—	5.448 ₆	5.552 ₆	M.
Radium C'	6.870	6.945	1.0000	1.0000	1.0000	7.683 ₆	7.829 ₆	—
Long range radium C'—								
7.8 cm.	7.755	7.830	1.0381	—	1.0379	8.280 ₆	8.438 ₆	M.
9 cm.	(9.000)	(9.093)	1.0861 ₆	—	—	9.068 ₆	9.240 ₆	M.
Polonium	3.805	3.848	0.8312 ₆	0.8308 ₆	0.8309	5.303 ₆	5.406 ₆	M.
Thoron	4.967	5.023	—	0.904 ₆	0.9042	6.278	6.394	R.
Thorium A	5.601	5.664	—	0.938 ₆	0.9388	6.769	6.897	R.
Thorium C—								
a ₁	(4.729)	(4.783)	0.8903 ₆	0.8904 ₆	—	6.086 ₆	6.203 ₆	M.
a	(4.681)	(4.734)	0.8874 ₆	0.8876 ₆	—	6.047 ₆	6.163 ₆	M.
Thorium C (mean)	4.693	4.746	0.8882 ₆	0.888 ₆	0.8882	—	—	—
Thorium C'	8.533	8.623	1.0686 ₆	1.069 ₆	1.0687	8.778 ₆	8.947 ₆	M.
Long range thorium C'—								
9.7 cm.	9.677	9.775	1.1103 ₆	1.109 ₆	1.1104	9.479 ₆	9.661 ₆	M.
11.5 cm.	11.633	11.644	1.1705 ₆	1.170 ₆	1.1705	10.638 ₆	10.740 ₆	M.
Actinon—								
a	5.655	5.718	—	0.941 ₆	0.9417	6.811	6.937	R.
a ₁	(5.30 ₁)	(5.36 ₁)	—	0.923 ₆	—	6.54 ₇	6.66 ₆	Ros.
a ₂	(5.13 ₁)	(5.18 ₆)	—	0.913 ₆	—	6.41 ₁₁	6.53 ₆₁	Ros.
Actinon a ₁ and a ₂ (mean)	5.203	5.262	—	—	0.9175	—	—	—
Actinium A	6.420	6.491	—	0.980 ₆	0.9794	7.368	7.508	R.
Actinium C—								
a	5.392	5.453	—	0.928 ₆	0.9278	6.611	6.739	R.
a ₁	4.947	5.003	—	0.904 ₆	0.9030	6.262	6.383	R.
Actinium C'	6.518	6.590	—	0.984 ₆	0.9839	7.437	7.581	R.

1. The ranges given in brackets in the second and third columns have been deduced from the measured velocities by means of the correction curve of fig. 10. All other ranges have been measured directly.

2. In the last column, the measurement used as a basis for the calculation of the energies is indicated. M = velocity measured with the new magnet, R = mean range; Ros. = velocity measured by Rosenblum.

3. The values of V/V_0 , the ratio of the velocity of the α -particle to the velocity of the α -particles from Ra. C' obtained by the three methods, are given. Most of the values attributed to Rosenblum are calculated from the velocities published by Rosenblum and Dupouy (*loc. cit.*). Others have been deduced from earlier publications, applying a systematic correction to bring them into line with these latest values where the inhomogeneity of his magnetic field has been more exactly allowed for.

4. All the velocity ratios and energies have been corrected for relativity effects.

5. The value of the velocity ratio V/V_0 determined by the magnet for the 9 cm. group of long range particles from radium C' has been used to calculate the range of this group, and this is found to be 9.00 cm., which is very little less than the mean range previously measured (*viz.*, 9.018 cm. on this scale) (Rutherford, Ward and Lewis, *loc. cit.*). It seems probable that this slight discrepancy is caused by the application of too great a correction for the tarnish on the source in the range measurements. If the range of the 7.8 cm. group is also reduced by 0.018 cm., the mean range becomes 7.755 cm., as given in the table. It will be noted that the value of V/V_0 deduced from this range is in good agreement with that directly determined with the magnet.

6. The complexity of the actinon group was established by our range measurements with the differential counting chamber (Lewis and Wynn-Williams, *loc. cit.*). Later, Curie and Rosenblum ('C. R. Acad. Sci. Paris,' vol. 194, p. 1232 (1932)) concluded that the lower velocity group consisted of two close components (actinon a_1 and a_2). The measurement of range thus corresponds to a mean of these two groups.

from the measured ranges in those cases in which we have not as yet made direct velocity determinations. These results are given in the table.

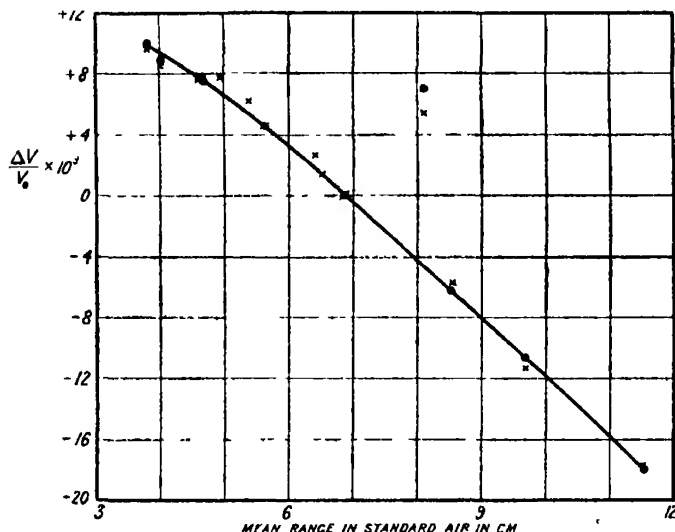


FIG. 10.

All the points shown in fig. 10 depend on our measurements of mean range. Those indicated by circles depend also on our determinations of relative velocity. Points calculated using velocities given by Rosenblum, combined with our range measurements, are indicated by crosses. A slight increase in velocity, or decrease in range, would displace a point upwards in the figure.

Relation between α -rays and γ -rays.

In previous papers attention has been drawn to the importance of determining with precision the energies of the α -particles corresponding to the various groups of long range α -particles from radium C', as these give us the energies of the α -particle levels in the excited nucleus. γ -rays should arise owing to the transition of an α -particle from the higher level to the normal level and also to transitions between levels in the excited nucleus.

In the present paper accurate measurements have been made by the magnet of the energies of the α -particles corresponding to the first two groups of ranges 7.8 cm. and 9.0 cm. It will be seen from the table that the energy released in a transition of an α -particle in the first group to the normal level is 6.09×10^5 electron volts, and from the second level to the normal 14.11×10^5 electron volts.*

* The values given in our earlier paper, viz., 6.3×10^5 and 14.6×10^5 were too high. The difference was mainly due to the use of an incorrect extrapolation curve to determine the velocity from the range. The correct curve is given in fig. 10.

It seems certain that these two transitions account for the presence of two of the most prominent γ -rays (or β -rays) in the spectrum of radium C'. In the original measurements of Ellis and Skinner, the energies of the γ -rays were found to be 6.12×10^5 and 14.26×10^5 volts. These values have been redetermined during the present year by Ellis* by the same method used for the measurements of the magnetic spectrum of thorium products. He informs us that he has found the corresponding values 6.07×10^5 and 14.14×10^5 volts, agreeing closely with our measurements of the energy differences 6.09×10^5 and 14.11×10^5 and within the limit of experimental error. We estimate our probable error to be about 1/150 for the 6.09 difference and about 1/400 for the 14.11. On account of the small number of α -particles in the first group—about 1 in 2 million of the main group—it is difficult to measure the velocity of the α -particle with the same precision as for a strong group.

The agreement between these measurements of the α -rays and the γ -rays thus strongly confirms the hypothesis that these two γ -rays have their origin in transition of an α -particle from an excited level to the normal level. When we have more completely explored the long range groups of α -particles from radium C', we hope to discuss in more detail the bearing of our measurements on the origin of the γ -rays emitted from radium C'.

We have already referred to the discovery of two groups of α -particles emitted from the product radium C. Since the difference between the disintegration energies of the α -particles in these groups is 62,000 volts, from analogy with the case of the α -particle groups from thorium C and actinium C, we should expect that a γ -ray of energy 62,000 volts should be emitted following the escape of an α -particle from radium C. Since, however, these particles constitute only about 1 in 5000 of the main group from radium C', the γ -ray should be very weak and probably undetectable under normal conditions.

We have measured accurately the energies of the two long range groups of α -particles from thorium C' of ranges 9.8 cm. and 11.6 cm. The transitions of the α -particle in the two cases to the normal level should give rise to γ -rays of energies $7.12 \pm 0.05 \times 10^5$ and 17.93×10^5 volts. Ellis (*loc. cit.*) has observed weak β -rays corresponding to a γ -ray of energy 7.26×10^5 volts in the magnetic spectrum of the products thorium C, C'. The difference between the α -ray and γ -ray energies is probably outside the experimental errors. It may be that the γ -ray arising from the transition is too weak to observe. Probably for the same reason no γ -ray has been observed corresponding to the energy difference 17.93×10^5 volts.

* 'Proc. Roy. Soc.,' A, vol. 138, p. 318 (1932).

We wish to express our thanks to the British Thomson Houston Company for their kindness in presenting us with thyratrons for use in the counter. Our thanks are also due to the Laboratory staff for their assistance in the installation of the apparatus, and, in particular, to Mr. G. R. Crowe, for his help in the preparation of the radium sources.

We are indebted to the Board of Education and to the Department of Scientific and Industrial Research for grants to two of us

Summary.

Experiments are described in which the velocities of a number of α -particle groups have been measured by a new method. A laboratory electromagnet has been constructed which produces a uniform annular field in which the α -rays are bent into a circle of 40 cm. radius, which enables the well-known focussing properties to be used. The interior of the whole magnet is exhausted to a low pressure. The particles are emitted from a source placed in the gap, and are detected by a small ionization chamber situated at the other end of the diameter. The ionization chamber is connected to an amplifier and individual α -particles are counted by a system of thyratrons.

The analysis is carried out by adjusting the magnetic field so as to bring groups of different velocities successively on to the slit of the ionization chamber. It is necessary to measure the magnetic field with great accuracy during the experiments. A very satisfactory method has been developed for this purpose and we have been able to determine the relative velocities of a number of important α -particle groups with an accuracy of about 1 in 5000. We have been able to show that the weak group of α -rays from radium C, numbering only 1 in 4000 of the main radium C' group, comprises two distinct components. Further, we have been able to observe the main long range groups from thorium C' and radium C', and experiments are now in progress to complete the examination of the weaker groups from radium C'. It has been found that the differences of energy between the main group and two of the long range groups from radium C', deduced from our measurements, are in close accord with the energies of γ -rays found by Ellis.

The Relative Velocities of the Alpha-Particles from Thorium X and its Products and from Radium C'.

By G. H. BRIGGS, Ph.D., The University of Sydney.

(Communicated by Lord Rutherford, O.M., F.R.S.—Received December 27, 1932.)

During the last few years determinations of the velocities of emission of α -particles have been made by Briggs,* Laurence† and by Rosenblum and his co-workers.‡ The discrepancies between the values obtained for the relative velocities of thorium C, thorium C' and radium C', which are collected in this paper in Table VIII, indicate the uncertainty that existed as to the correct values of α -ray velocities.

Much of this uncertainty has been removed by the recent determination by Rosenblum and Dupouy§ of the absolute velocities of the α -particles of radium C' and polonium, and the velocities relative to them of the α -particles of thorium C_a, thorium C', actinium C_a, actinium C_a, and radium A. These measurements were made after a new exploration of the field of the large electro-magnet of the Academy of Sciences which enabled the accuracy of measurement to be increased to 1 or 2 in 2000 and appears to have removed a systematic source of error in the earlier velocity determinations made with this magnet in the course of the investigation of the fine structure of α -ray spectra.

The present paper describes measurements by the direct magnetic deflection method of the relative velocities of the α -particles from thorium X, thoron, thorium A, thorium C (mean), thorium C' and radium C'; the probable error in the results is 1 in 20,000. Preliminary results, correct to about 1 in 2000, are also given for the relative velocities of radium A and radon. Where the results are comparable with those of Rosenblum and Dupouy they agree to well within the experimental error in their work.

The results obtained here have been combined with the range measurements of Lewis and Wynn-Williams|| to give a new correction curve to the Geiger relation $V^3 = kR$ for ranges between 8.6 cm. and 4 cm. and from this curve the velocities of the other groups of α -particles whose ranges have been

* 'Proc. Roy. Soc.,' A, vol. 118, p. 549 (1928).

† 'Proc. Roy. Soc.,' A, vol. 122, p. 543 (1919).

‡ Rosenblum, 'C. R. Acad. Sci. Paris,' vol. 190, p. 1124 (1930), vol. 193, p. 848 (1931); Rosenblum and Valdares, *ibid.*, vol. 194, p. 967 (1932); Rosenblum and Chamié, *ibid.*, vol. 194, p. 1154 (1932).

§ *Ibid.*, vol. 194, p. 1919 (1932).

|| 'Proc. Roy. Soc.,' A, vol. 136, p. 349 (1932).

measured by Lewis and Wynn-Williams have been deduced; the error in the velocity ratios so determined depends on the range measurements and appears to be not greater than 1 in 2000.

For ranges greater than 5 cm. the relation between range and velocity is found to be given accurately by the equation $V^{3.26} = kR$.

Experimental Method.

The magnetic deflections of the α -particles were produced by a large permanent magnet, described elsewhere,* which gives a field of about 5000 gauss over an area of 26 cm. by 8 cm. in a gap of 1.2 cm. The vacuum exposure box between the poles had sides of mild steel accurately machined to $\frac{1}{4}$ -inch thickness. The usual arrangement† of an activated wire, a slit, and a photographic plate, mounted on a rigid bar, was employed, but the usual single slit was replaced by two, mounted in a plane parallel to the plate, so that a set of lines was obtained from each. The slits were made of thick copper, the opposing edges which define the beam of α -particles being formed of accurately ground and polished surfaces meeting at an angle of about 120° . The widths of the slits were 0.05 mm. and 0.06 mm. and their distance apart 2.75 mm. The narrower slit, which will be referred to as slit A, was set on the perpendicular from the source of α -particles to the plate. The distance from source to slits was 11.6 cm. and that from slits to plate 12.1 cm. approximately. The active wire was 0.10 mm. in diameter and about 1.1 cm. long. It was clamped at the ends in a pair of V-cuts and stretched taut.

The method of double deflections was used throughout, the bar carrying the plate, source, and slits, being merely turned upside down in order to obtain lines at the other end of the plate. During an exposure the box was maintained at a hard X-ray vacuum by charcoal immersed in a 5-litre flask of liquid air.

The first part of the experimental work was the determination of the relative velocities of the α -particles from thorium X, thoron, thorium A, thorium C and thorium C' using sources which gave these groups of particles simultaneously. These sources, which decayed with the half value period of thorium X, 3.64 days, were so feeble that four wires, each exposed for one week, were required for each plate, two wires being used for each direction of the deflection. On some of the plates radium C' lines were obtained by using

* Briggs, 'J. Sci. Inst.,' vol. 9, p. 5 (1932).

† Rutherford, Chadwick and Ellis, "Radiations from Radioactive Substances," Camb. Univ. Press, p. 42 (1930).

an additional wire activated with radium B + C, but the velocities relative to radium C' thus obtained showed small irregular errors, which might have been due to slight differences in the positions of the radium B + C and of the thorium X sources, or to small diurnal or secular changes in the field of the magnet. To avoid this difficulty a new series of exposures was made with wires each activated with thorium B + C and radium B + C in order to obtain the velocities of the thorium group relative to radium C'. For this a new and particularly rigid carrier for the plate, slits, and source, was made with an improved source holder shown in fig. 1. With this holder the active wire was placed immediately behind a slit, against which it was pressed by a metal tongue. The width of the slit was about 0.8 of the diameter of the wire.

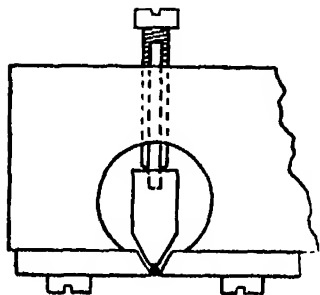


FIG 1

The chief advantage of this form of source holder is the increase in accuracy of the positioning of the active wire. There is also a slight advantage in the elimination of the α -particles shot out nearly tangentially from the wire. With the radium B + C, thorium B + C sources six wires were used for each plate, three in each direction of the deflection; the total length of exposure was 6 days.

The magnitude of the double deflections was about 3.95 cm. for thorium X and 3.19 cm. for thorium C'. The photographic plates were Ilford process; others which were tried proved unsatisfactory owing to the drying during the prolonged exposure causing frilling and peeling of the emulsion in development.

Preparation of the Sources.

(a) *The Thorium X Sources.*—The writer has shown* that it is possible to collect thorium X by recoil from a thin layer of radio-thorium with an efficiency of recoil of a few per cent. This method was used in the present work; the activation apparatus for the thorium X sources is shown in fig. 2. A solution of radio-thorium equivalent in γ -ray activity to about 2 mg. of radium was spread on a sheet of gold the surface of which had been slightly etched with *aqua regia*. This sheet was placed inside a brass cylinder 5 cm. in diameter and open at the top; the length of wire to be activated was exposed at the centre of the apparatus as shown in the diagram. The activation was carried out in dry hydrogen at 5 cm. pressure and was allowed to continue for one

* Briggs, 'Phil. Mag.', vol. 50, p. 600 (1925).

week. The sources prepared in this way had an initial γ -ray activity equivalent to that of 0.06 to 0.07 mg. of radium and gave α -particles from thorium X, thoron, thorium A, thorium C and thorium C'. A very small quantity of radio-thorium was also liberated from the activated gold surface and collected on the wire, but the barely detectable lines produced by it were too faint for accurate measurement.

When the plates were photometered it was found that, taking the intensity of the thorium X line as unity, the intensities of the thoron and thorium A

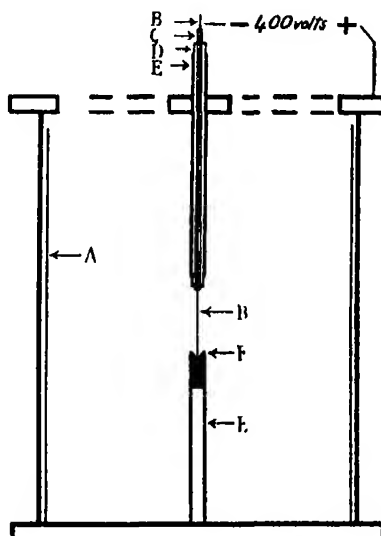


FIG. 2—Thorium X activation apparatus. A, gold sheet coated with radio-thorium; B, platinum wire; C, gold tube 0.8 mm. external diameter; D, glass tube; E, brass tube; F, glass insulator.

lines were approximately 0.9 and 0.8, and the sum of the branching products thorium C and thorium C' was 1.0. This excess of thorium C + C' was due to the collection of thorium A and thorium B directly from the radio-thorium preparation and from free thoron in the activation apparatus. The intensities of the lines show that the sources lost by recoil only about 10 per cent of the thoron formed from the thorium X. This, however, was sufficient to produce serious fogging of the plates during the exposure, and although various means were tried to eliminate it no satisfactory cure was found and the best that could be done was to protect, by means of an aluminium diaphragm, the half of the plate which was not being exposed. The activated wires were all slightly discoloured by a pale yellow deposit which was seen, under a micro-

scope, to consist of a smooth transparent layer which had not altered the surface of the platinum. From a comparison of the conditions under which the thorium B + C, and radium B + C sources were prepared it seems likely that this deposit was due to the action of the radiations on tap grease vapour in the presence of hydrogen. It is probable that very clean sources of thorium X could have been prepared, but it is doubtful whether they would have been satisfactory sources of α -particles from thoron and thorium A, and it is probable that contamination, owing to thoron recoiling from the source, would have made the experiments much more difficult.

(b) *The Thorium B + C, Radium B + C Sources.*—The sources used for the second series of experiments were prepared by collecting thorium B + C on a platinum wire, as an active deposit from thoron which diffused from some radio-thorium spread on gold as in the earlier work. The activation was carried out in dry hydrogen and the wire was so arranged that the active deposit was collected on one side only. The wires after an exposure of 24 hours had activities up to 0.06 mg. radium equivalent. After this activation the wire was exposed for 10 to 30 minutes to radium emanation in a capillary tube, following the method described by Rosenblum.* The time of exposure was chosen so that about 1.5 to 3 mg. radium equivalent of radium B + C was collected on each wire. This double activation was carried out with every wire used in this part of the work because such a procedure is more likely to eliminate errors than if the radium C' lines had been obtained, as could readily have been done, from a single activated wire. These wires were quite free from any surface deposit such as was found on the thorium X sources. A small amount of thorium X was probably present as well as the thorium B + C, but was too small to produce any measurable lines in these exposures and there was no fogging from contamination by thoron.

Measurement of the Deflections.

The distances between the lines on the photographic plates were measured with a photoelectric microphotometer of the Dobson-Skinner type which was constructed in this laboratory and which will be described elsewhere. The instrument has an accurate screw which was calibrated against a standard glass scale for variation in pitch and for periodic error. The photometer was used as a null instrument, the density being compared with an adjustable

* 'C. R. Acad. Sci. Paris,' vol. 188, p. 1549 (1929).

optical wedge; readings on the plates were taken at intervals of 0.005 mm. across the lines. The photometer is capable of measuring deflections of the order of those obtained in this work to an accuracy of about 1 in 10; greater errors arose on account of irregularities in the lines, but all purely instrumental errors in the measurements were quite negligible.

In fig. 3 the groups of lines obtained from the thorium X sources, together with the radium C' lines, are shown diagrammatically and in fig. 4 a typical

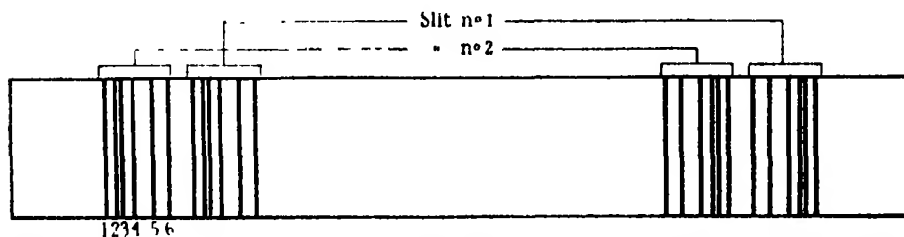


FIG. 3.—Diagram of plate showing lines for the two slits deflected in either direction 1, Th X, 2, Th C; 3, Thoron; 4, Th A, 5, Ra C', 6, Th C'.

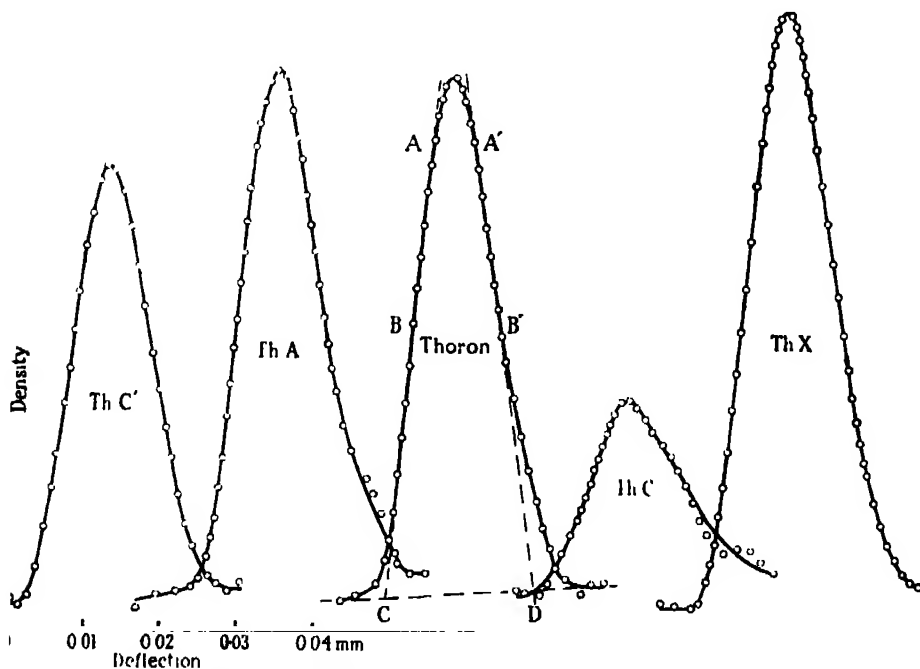


FIG. 4.—Examples of photometer curves for the thorium group. Direction of deflection left to right. The slope of the bases, e.g., CD is due to a steady rise in the background density. The curves are shown overlapping for convenience of reproduction.

set of photometer curves for the thorium group. The lines on the thorium X plates had distinct tails on the low velocity side, owing to absorption in the deposit on the source; the curves in fig. 4 illustrate the maximum asymmetry found; on some of the plates this asymmetry was smaller. With such lines there are a number of methods which might be used for determining the deflection. After considerable experience with lines slightly unsymmetrical as in this work, and with perfectly symmetrical lines obtained in other work in progress, the writer prefers to determine the position of a line by taking the mean of the mid-points of widths such as AA' and BB' averaged over a region AB. This method makes the maximum use of the steepest parts of the density curves and the result obtained, which will be called the "peak" reading, could usually be determined to 0.0005 mm.

As the thorium C and thorium C' lines were rather feeble the positions of all the lines were also determined from the mid-points of the bases, indicated by CD in the diagram. Owing to the asymmetry of the lines there were small systematic differences between the deflections obtained by these two methods. The correction for this, together with the general question of correction for loss of velocity at the source, will be discussed later.

The lines on the thorium C'—radium C' plates showed no sign of tails, but the slopes of the two sides of the lines differed slightly. This is to be expected because of the presence of the slit in front of the source, for the rays reaching the plate are emitted from the curved surface of the wire at an angle to the plane of the jaws and so the source is, in effect, stronger at one edge than the other. This might produce an appreciable error in an absolute measurement of velocity but can be shown to be quite negligible in these relative measurements.

Each plate was photometered in two independent positions and the velocity ratios were calculated independently for the deflections measured between the peaks and between the mid-points of the bases. The deflection readings were carefully weighted and each of the observed ratios shown in Tables II, III and V represents the weighted mean of the four independent observations.

The double deflections for slit B were slightly greater than those for A and it was convenient to apply corrections so that the radii of curvature could be calculated from the well-known formula which applies to a slit on the normal from the source to the plate. These corrections are purely geometrical and can be calculated by an extension of a method given in a previous paper.*

* Briggs, 'Proc Roy Soc.,' A, vol. 114, p. 313 (1927).

They are nearly proportional to the deflections and for thorium X amount to 2.30×10^{-2} mm. and for thorium C' to 1.86×10^{-2} mm.

Before discussing the results certain corrections and possible sources of error must be considered.

Corrections for the Loss of Velocity due to Absorption at the Source.

The difficulty of preparing and maintaining a clean source of α -particles is well known, and loss of velocity often occurs owing to the collection of foreign material on the source, or to the recoil of the active material into the surface on which it is deposited.

In the thorium X experiments both of these causes operated. As the correction for this amounted, for some of the velocity ratios, to twelve times the probable error in the final result it required most careful consideration.

To determine the average reduction in velocity of any group of α -particles in escaping from the wire it is necessary to know :—

- (a) The thickness of the deposit on the wire and its stopping power ;
- (b) The distribution of each substance in this layer and in the platinum, for, as a result of successive recoils, there will be a redistribution of each product throughout the layer, part of the product escaping from the surface and part being buried in the platinum ,
- (c) The effect of the curvature of the surface of the wire.

In order to determine the mass per unit area of the deposit a light beam micro-balance with quartz fibre suspensions was made. This had a sensitivity of 2.5×10^{-8} gm per millimetre deflection ; the deflection being observed on a scale at a distance of a metre. A large number of wires which had been used in the experiments were weighed before and after removing the deposit and the mean loss of weight was found to be 7.7×10^{-7} gm.

Although the composition of the deposit on the thorium X sources is not known it almost certainly consists for the most part of light atoms including some hydrogen, and no appreciable error will be made if it is assumed that its stopping power for α -particles and recoil atoms is equal to that of air. From the diameter of the wire the mean air equivalent of the layer on the source wires was calculated to be 0.20 mm.

We may assume that this layer was built up continuously throughout the seven days activation of the wire, and, since the half value period of thorium X is 3.64 days, the distribution of thorium X at the end of activation, and through-

out the exposure of the plate, will fall off exponentially from a maximum at the surface of the deposit to about 0.25 of this at the surface of the platinum. The distribution of thoron, thorium A and thorium C + C', may then be calculated by considering the effect of the successive recoils. The details of these calculations need not be given here. It was assumed :—

- (i) That a thin layer of a radioactive substance within a solid medium becomes, after an α -ray recoil, uniformly distributed throughout a layer having a total thickness of twice the mean range of recoil. This assumption would be strictly correct if all the recoil atoms from any one substance had exactly the same range.
- (ii) That the mean range of recoil in air of thoron, thorium A and thorium B may be taken as 0.08, 0.08 and 0.10 mm. respectively. In calculating these values the range of radium B recoiling from radium A is taken as 0.12 mm. and it is assumed that the mean range is about 0.7 of the range as usually measured.

An exact knowledge of the range of recoil in platinum is not essential. Wertenstein* found the range in silver to be 20×10^{-6} mm. and Rief† found the mean range in both nickel and copper to be 10×10^{-6} mm. From these results the mean range in platinum was estimated to be 4.0×10^{-6} mm.

With these data the distribution with depth of the successive products of thorium X was determined graphically and incidentally the loss from the wire by recoil for each product. These losses agreed satisfactorily with the observed falling off in the areas of the density curves of the lines for the successive products thorium X, thoron, and thorium A.

The distribution of thorium C + C' requires special consideration for it consists of two parts, one originating from the thorium X on the wire, the other the product of thorium A or thorium B collected from the gas or from the plate coated with radio-thorium. Of the thorium C + C' originating in the latter way only that collected near the end of the activation period will be left to contribute to the photographic effect. Hence this thorium C + C' will be situated near the outer surface of the deposit and the resulting α -particles will experience a comparatively small loss of velocity. The relative contribution to the thorium C and thorium C' lines from these two parts was estimated from the decay curves of the activated wires, and independently from the areas of the density curves for thorium C and thorium C' as com-

* 'Ann. Physique' vol. 1, p. 347 (1914).

† 'SitzBer. Akad. Wiss. Wien,' vol. 130, p. 293 (1921).

pared with the other lines. It was found that the thorium C + C' originating from the thorium X on the wire produced two-thirds of the total intensity.

The above data would be sufficient to enable the reduction in velocity $\delta V/V$ to be calculated for a flat source, with normal emission of α -particles, from the relation between velocity and range. With a wire source, however, the effect of the curvature of the surface of the wire must be considered. In fig. 5 let OA be the radius of the wire, AB the depth of the deposit on the wire, y the density of distribution of an α -radiating substance in a layer CDE of thickness dx and at a depth $BC = x$ below the surface of the deposit. Then the average thickness of absorbing material traversed by particles emitted parallel to OA from the part of the source included between $\theta = 0$ and $\theta = \theta_{\max}$ is :-

FIG. 5.

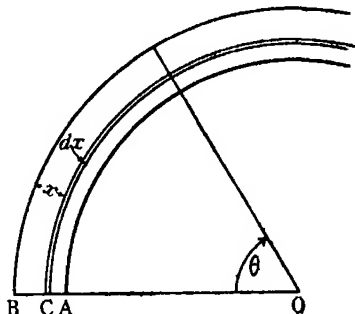


Fig. 8.

$$\delta R = \frac{\int_{r=0}^{r_{\max}} \int_{\theta=0}^{\theta_{\max}} xy \sec \theta \, d\theta \, dx}{\int_{x=0}^{x_{\max}} \int_{\theta=0}^{\theta_{\max}} y \, d\theta \, dx}. \quad (1)$$

As θ_{\min} approaches zero, the factor $\frac{\int \sec \theta d\theta}{\int d\theta}$, which is introduced on account

of the curvature of the wire, approaches unity, and the expression reduces to that for a flat source. This obliquity factor increases slowly until θ_{\max} approaches $\pi/2$; it has, for example, a value of 2.04 at 85° and becomes infinite when $\theta_{\max} = \pi/2$. This means that particles emitted from within the layer at points corresponding to θ nearly equal to $\pi/2$ may be so much reduced in velocity that they are deflected completely outside the band observed on the photographic plate. We may, however, use the above equation to calculate δR if we exclude all particles for which the reduction in velocity, and therefore the increase in deflection, is greater than a certain amount. To determine this limiting amount an artificial line was built up by compounding the contributions from all parts of the wire without any limit to θ , and taking into consideration the finite size of the source and the slit. The line so constructed is shown in *fig. 6*; it reproduces quite satisfactorily the shape of a typical observed line.

It was found that the observed shift of the peak of this line agreed with that calculated by equation (1) if the limit of θ was such that the increase of deflection of particles for which $\theta = \theta_{\max}$ is 0.41 ± 0.02 of the width of the line. This limit determines for each value of x a maximum value of θ to be used in equation (1).

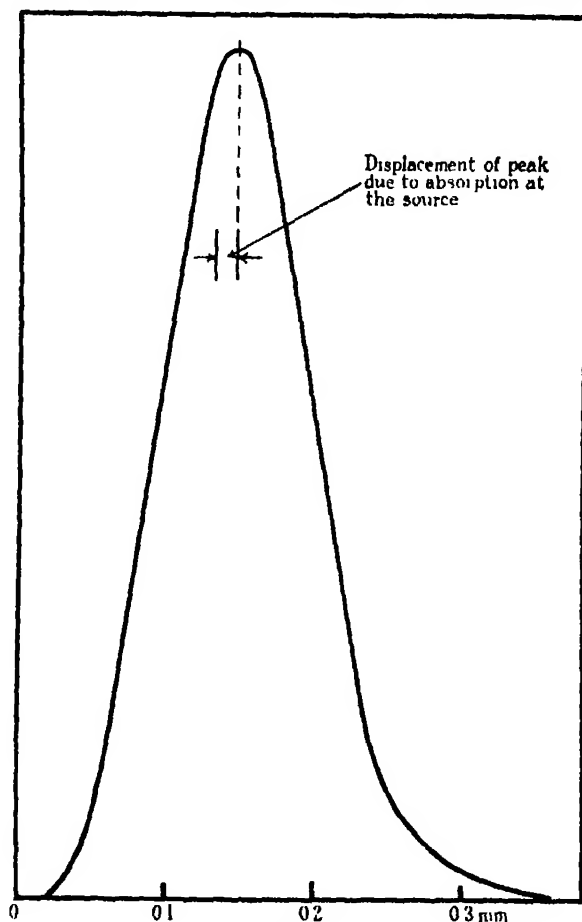


FIG. 6.

From the values of δR the correction for each group of α -particles can be calculated most conveniently from the equation

$$\frac{\delta V}{V} = \frac{1}{p} \frac{\delta R}{R}. \quad (2)$$

According to the Geiger relation $p = 3$, but this relation is known to be inaccurate. The values of p for the various velocities were calculated from the correction curve to the Geiger relation which will be discussed later. Table I

gives the values of δR , p , $\delta V/V$, and of the corrections to the velocity ratios for the thorium X plates.

Table I.—Corrections for Absorption at the Source.

	δR (mm)	p	$\frac{\delta V}{V}$	Correction to velocity relative to thorium C'	Correction to velocity relative to thorium C.
Thorium X	0.134	3.15	9.93×10^{-4}	3.97×10^{-4}	0.17×10^{-4}
Thoron	0.160	3.17	10.15	4.19	0.39
Thorium A	0.179	3.21	9.95	3.99	0.19
Thorium C	0.144	3.16	9.76	3.80	--
Thorium C'	0.166	3.26	5.96	—	—

No detectable deposit was found on the thorium C + C', radium C' wires even when the time of activation was seven times longer than usual, so, only the effect of recoil into the platinum has to be considered. Applying the general method described above the corrections, expressed as parts in 10,000 were found to be

$$\frac{\text{thorium C}}{\text{radium C'}} = 0.30, \quad \frac{\text{thorium C'}}{\text{radium C'}} = -0.04, \quad \frac{\text{thorium C}}{\text{thorium C'}} = 0.34,$$

and are therefore almost negligible.

Besides producing a shift of the peaks of the lines the deposit on the thorium X plates gave rise to the previously mentioned tails in the low velocity sides of the lines, and it was found that the distance between a pair of lines measured from peak to peak was slightly less than if measured between the mid-points of the bases. The artificial line shown in fig. 6 was used to determine the difference to be expected between the two measurements of the deflection, and it was concluded that this difference (0.0056 mm. for thorium C) would be approximately proportional to the correction $\delta V/V$ already calculated. When these corrections, which were of the order of 0.4×10^{-4} , were made there was no systematic difference between the velocity ratios calculated from the deflections measured in the two ways.

In his work on the velocity of the α -particles from thorium C and thorium C' Laurence (*loc. cit.*) determined the position of a line by producing the straight parts of the sides upwards to intersect. If the line is asymmetric owing to absorption at the source this method will automatically produce a slight correction. It was found, however, that for lines having the degree of asymmetry of those in fig. 4 the correction thus produced is only one-tenth of that required.

Absorption at the source readily explains the low results found by Briggs for the relative velocity $\frac{\text{thorium C}}{\text{radium C'}}$ and by Laurence for $\frac{\text{polonium}}{\text{radium C'}}$. In each case the sources were tarnished and broadened lines were found. The velocities were calculated from the position of the least deflected edges of the lines. The present investigation shows that this method does not eliminate the error, which may be large if the velocities being compared differ considerably.

Correction for the Complexity of Thorium C.

As a result of the work of Rosenblum the α -particles from thorium C are known to be highly complex. The thorium C line obtained in the present work may be considered to consist only of the two strong components for which the ratio of the velocities* is 1 : 1.0032 and the ratio of the intensities† 1 : 0.3. Since these are unresolved it is desirable to give as the velocity for thorium C a value which corresponds to the weighted mean of these two components. As the separation of the components is about one-third of the width of the observed line the measured deflection may not correspond exactly to the weighted mean velocity. To test this a complex line was built up by compounding two lines whose relative intensities and separation corresponded to those found by Rosenblum. The shape of these component lines was that to be expected from a consideration of the other lines on the plates; and since the lines on the thorium C + C' plates were narrower than those on the thorium X plates and also were free from tails the operation was carried out independently for both sets of plates. In both cases it was found that the mid-point of the base of the complex line coincided with the centre of gravity of the mid-points of the bases of the components. The peaks, however, gave deflections which were too great by 3.30×10^{-4} for the radium C' plates and by 0.72×10^{-4} for the thorium X plates. This difference was due to the broadening of the lines on the thorium X plates due to absorption at the source. When these corrections were applied the relative velocities determined from the peaks and from the mid-points of the bases agreed completely.

It may be mentioned that these corrections are not greatly affected by uncertainties in the relative velocities and intensities of the components. For example an error of 10 per cent. in the relative intensities of the components

* Rosenblum and Valadares, *loc. cit.*

† Rosenblum, *loc. cit.*

would produce an error of only 1 in 80,000 in the mean velocity as determined here.

Possible Sources of Error.

(i) *The Constancy of the Magnetic Field.*—We are concerned both with the uniformity of the field in the region traversed by the α -particles and with its constancy during the time of the exposure. Since relative velocities are being measured the field need be investigated only for variations normal to the paths of the α -particles. Such variations were found to be negligible for 0.7 of the total path starting from the source. Nearer the plate the variation increased to 4 gauss per centimetre, but as the effect of such change on the observed relative velocity of two substances varies inversely as the distance from the slit and directly as the distance between the two paths the total effect is only of the order of 1 in 10^5 for $\frac{\text{thorium X}}{\text{thorium C'}}$ which is the worst case.

There appears to be a seasonal change in the field of the magnet amounting to 1 in 500 from winter to summer. However, in the thorium X exposures of one month each no error results since the α -particles for the various substances are produced simultaneously. In the exposures with the thorium B + C and radium B + C sources the possibility of error owing to the differences in the rates of decay and to the effect of the diurnal changes of temperature had to be considered, but it was found that the error on this account is not likely to be greater than 2 in 10^5 .

(ii) *Movement of the Photographic Image in Development and Drying of the Plates.*—This source of error is well known and is due chiefly to the swelling of the gelatine in development and its contraction in drying. Cooksey and Cooksey* found movements up to 0.009 mm. with double-coated Eastman X-ray plates. The gelatine on the plates used in the present work expands comparatively little in development and serious trouble was not expected. The magnitude of the shifts was found by exposing plates of the same size as those used in the experiments under a stencil made by ruling, with a dividing engine, very fine lines, 1 mm. apart, on a piece of silvered plate-glass. The developed images were examined through the stencil with a microscope. Six plates were examined and it was found that close to the ends of the plate there was generally a comparatively large outward movement of 0.01 to 0.02 mm. which ceased about a millimetre from the edge. At distances between 1 and 5 mm. from the edge there was usually a systematic movement of 0.002

* 'Phys. Rev.', vol. 36, p. 80 (1930).

to 0.003 mm. away from the edge of the plate. Over the rest of the plate there might be irregular movements up to 0.002 mm.

The lines near the ends of the plates are most likely to be affected as they approached to about 5 mm. from the end, but in the 5 mm. which represents the spread of each group of thorium lines, a change of more than 0.001 mm. in the movement of the emulsion was very seldom found. It is concluded that these emulsion shifts cannot produce any systematic error in the relative velocities greater than 2 in 10^5 .

Results.

The results of the measurements are collected in Tables II to VI. The results for thorium X and its products are based on four plates: plates 1, 2 and 3 were obtained with the source wire stretched between V-cuts as described earlier, and plate 4 with the source wires placed behind the slit source holder.

Table II.—Velocities of α -particles from Thorium X, Thoron, and Thorium A, relative to those from Thorium C' and Thorium C.

Plate.	Slit	Velocities relative to Thorium C'						Velocities relative to Thorium C.					
		Thorium X Thorium C'	Wt.	Thoron Thorium C'	Wt.	Thorium A Thorium C'	Wt.	Thorium X Thorium C	Wt.	Thoron Thorium C	Wt.	Thorium A Thorium C	Wt.
1	A	0 804752	3	0 846127	2	0 878669	3	0 968826	1	1 018621	1	1 057537	1
	B	788	2	230	2	616	2	710	1	525	1	665	1
2	A	879	1	194	3	814	1	781	2	456	1	861	1
	B	945	1	030	2	694	1	935	2	609	2	919	2
3	A	763	3	158	3	544	3	795	3	628	2	635	2
	B	709	3	0 845987	3	490	3	719	2	407	2	558	2
4	A	684	2	0 846199	2	594	2	—	—	—	—	—	—
	B	871	1	018	1	558	1	—	—	—	—	—	—
Weighted mean		0 80477		0 84612		0 87860		0 96880		1.01854		1.05767	
Corrected for absorption at source		0 80513		0 84650		0 87895		0 96882		1 01858		1 05769	

The results for the ratios $\frac{\text{thorium C}}{\text{radium C'}}$ and $\frac{\text{thorium C'}}{\text{radium C'}}$ were based on three plates and are shown in Table III.

The velocities of the α -particles from thorium X, thoron, and thorium A, calculated relative to those from radium C' using the results given in Table III for $\frac{\text{thorium C'}}{\text{radium C'}}$ and $\frac{\text{thorium C}}{\text{radium C'}}$ are given in Table IV.

Table III.—Relative Velocities of α -particles from Thorium C, Thorium C' and Radium C'.

Plate	Slit	$\frac{\text{Thorium C'}}{\text{Radium C'}}$	Weight	$\frac{\text{Thorium C}}{\text{Radium C'}}$	Weight.
7	A	1 068659	3	0 888092	3
	B	494	2	7977	1
8	A	787	3	8082	3
	B	754	3	8015	4
9	A	749	3	8141	0 5
	B	837	3	8156	3
Weighted mean		1 06872		0 88808	
Corrected for absorption at the source		1 06872		0 88811	

Table IV.

	$\frac{\text{Thorium X}}{\text{Radium C'}}$	$\frac{\text{Thoron}}{\text{Radium C'}}$	$\frac{\text{Thorium A}}{\text{Radium C'}}$
Derived from the thorium C' ratios	0 86042	0 90465	0 93936
„ „ thorium C „	0 86042	0 90462	0 93935
Weighted mean	0 86042	0 90464	0 93935

Values for the $\frac{\text{thorium C}}{\text{thorium C'}}$ ratio were obtained from the two sets of plates with the exception of plate 4 on which the thorium C lines were too faint for accurate measurement. In addition values for $\frac{\text{thorium C}}{\text{thorium C'}}$ are included which were obtained from some of the preliminary plates.

From the relative velocities the absolute velocities and energies of the α -particles and the disintegration energies have been calculated using 1.922×10^9 cm. sec.⁻¹ for the velocity of the α -particles from radium C'. This is based on the value $1.921_8 \times 10^9$ cm. sec.⁻¹ found by Rosenblum and Dupouy, and 1.922×10^9 cm. sec.⁻¹ which is calculated from the measurement of Briggs when the necessary changes are made in the constants used in deducing the velocity from the observed value of $H\rho$.

Discussion of the Accuracy of the Results.

In considering the accuracy of the relative velocities the following points may be noted. The direct magnetic deflection method of measuring relative

Table V.—Relative Velocities of α -particles from Thorium C and Thorium C'.

From the Thorium X plates.				From the Thorium C + C', Radium C' plates.			
Plate.	Slit.	Thorium C Thorium C'	Weight.	Plate.	Slit	Thorium C Thorium C'	Weight
1	A	0 830709	2	5	A	0 830919	0.5
	B	844	1		B	1021	1
2	A	712	2	6	A	0917	0.5
	B	698	2		B	1035	1
3	A	631	3	7	A	1061	1
	B	713	3		B	1068	1
				8	A	0894	2
					B	0950	2
				9	A	1198	0.5
					B	0940	3
Weighted mean		0 83070				0 83098	
Corrected for absorption at source		0 83104				0 83101	
Final mean			0 83102				

Table VI.

	Velocity cm. sec ⁻¹ $\times 10^{-9}$	Energy of particle, electron-volts $\times 10^{-4}$	Disintegration energy electron-volts $\times 10^{-6}$
Thorium X	1 653 ₇	5 682 ₈	5 785 ₈
Thoron	1 738 ₇	6 283 ₈	6 399 ₈
Thorium A	1 805 ₈	6 775 ₈	6 903 ₈
Thorium C	1 707 ₆	6 055 ₁	6 171 ₈
Thorium C'	2 064 ₁	8 777 ₆	8 956 ₁

velocities is very insensitive to lack of uniformity of the magnetic field because of the small separation of the paths over most of the distance. In the method of double deflections, compared with the method of single deflection, error due to the residual field of the magnet does not arise, and any error due to the plate not being exactly normal to the undeflected beam is practically eliminated. The use of a number of small sources for each plate tends, in the experiments with the thorium B + C, radium B + C sources, to average out errors due to non-uniform distribution of the active material on the wire. In the thorium X experiments it tends to average out the effect of variations in the thickness of the surface deposit.

For the velocities of the α -particles from thorium X, thoron, and thorium A the accuracy depends chiefly on the accuracy with which the correction for loss of velocity at the source can be estimated.

The probable error in the mean thickness of the surface deposit is believed to be not greater than 10 per cent. The effect of this and of other uncertainties in the data used in calculating these corrections has been carefully investigated, and as the corrections increase less rapidly than the thickness of the absorbing layer it is considered that the error in these corrections does not exceed 10 per cent. For the case where the correction is largest this introduces an error of only 1 in 40,000 in the final result. This view is supported by the agreement of the $\frac{\text{thorium C}}{\text{thorium C'}}$ ratios found on the two sets of plates, where for the thorium X plates the correction is large and for the radium C' plates it is almost negligible.

Taking all these factors into consideration it appears that these corrections have been fairly accurately estimated. The probable errors in the uncorrected velocity ratios range from 1 in 30,000 to 1 in 60,000 for the different ratios. It is concluded that the probable error in the final results is for none of the ratios greater than 1 in 20,000; for the velocity of thorium C' relative to radium C' where all corrections are negligible it is estimated to be 1 in 30,000.

Relation between Velocity and Range.

Using the measurements of the mean ranges given by Lewis and Wynn-Williams the departures from the Geiger relation, $V^3 = kR$, have been calculated from the equation used by Rutherford, Ward and Lewis.*

$$\frac{\Delta V}{V_0} = \frac{V}{V_0} - \left(\frac{R}{R_0}\right)^{\frac{1}{3}}$$

The correction curve is shown in fig. 7, curve I. The following preliminary results from some work by the author on the relative velocities of the α -particles from radon, radium A, and radium C' are included in the calculation of the correction curve :—

$$\frac{\text{radon}}{\text{radium C'}} = 0.8455 \pm 0.0003, \quad \frac{\text{radium A}}{\text{radium C'}} = 0.8839 \pm 0.0002.$$

The error given by Lewis and Wynn-Williams for their range measurements, 0.05 mm., produces an uncertainty of 0.0003 in $\Delta V/V$ and is sufficient to account for the scattering of the points about the curve.

If the relation between range and velocity is taken to be

$$V^{3.26} = kR,$$

* 'Proc. Roy. Soc.,' A, vol. 131, p. 684 (1931).

and the corresponding correction curve is calculated from the equation

$$\frac{\Delta V}{V_0} = \frac{V}{V_0} - \left(\frac{R}{R_0}\right)^{\frac{1}{20}},$$

curve 2, fig. 7, is obtained. It is seen that for ranges between 5 and 9 cm. this equation accurately expresses the relation between V and R , and it appears that this law will hold for much longer ranges.

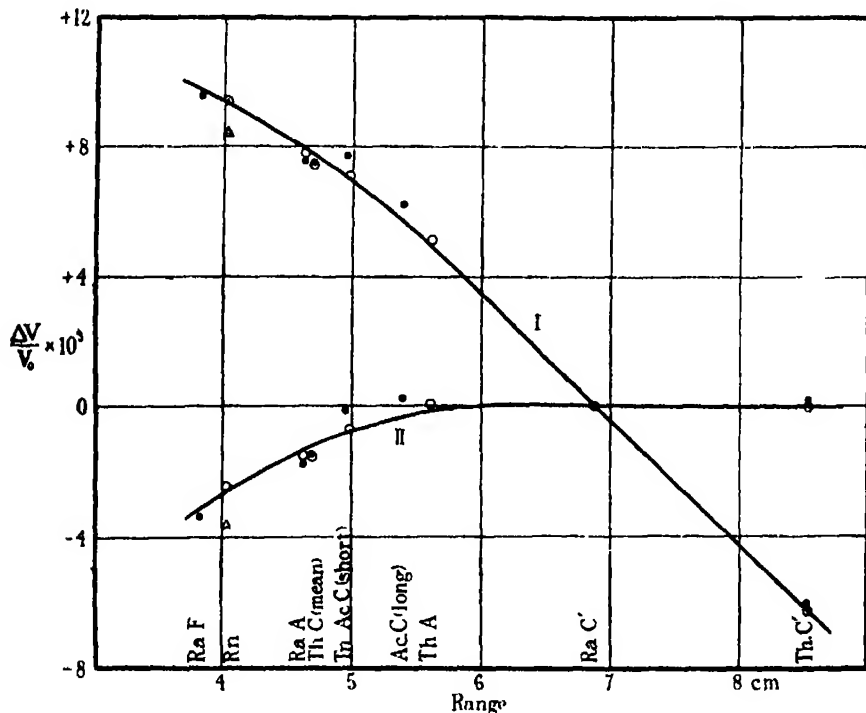


FIG. 7.—○ Briggs; ● Rosenblum and Dupouy; △ Rosenblum.

The velocities and energies of the other α -particles the ranges of which were measured by Lewis and Wynn-Williams have been deduced from the correction curve and are given in the following table.

The maximum error in the relative velocities depends on the range measurements and is 0.001 for actinon, 0.0006 for polonium and 0.0004 for actinium A, C and C'. The table also includes the energies calculated from the author's preliminary results for radon and radium A.

The mean range of α -particles from thorium X calculated from the velocity is found to be 4.243 ± 0.005 cm. and the extrapolated range 4.291 cm. The

Table VII.

	Range, cm	Velocity relative to radium C'.	Velocity cm. sec ⁻¹ $\times 10^{-6}$	Energy of α -particle, electron-volts $\times 10^{-6}$	Disintegration energy, electron-volts $\times 10^{-6}$
Actinon (short)	5 203	0 9179	1 764	6 469	6 590
Actinon (long)	5 655	0 9420	1 811	6 814	6 941
Actinium A	6 420	0 9795	1 883	7 360	7 509
Actinium C' (short)	4 947	0 9034	1 736	6 266	6 387
Actinium C (long)	5 392	0 9282	1 784	6 616	6 743
Actinium C'	6 518	0 9841	1 891	7 439	7 583
Polonium	3 805	0 8310	1 597	5 300	5 403
Radon	-	0 8455	1 625	5 487	5 587
Radium A	-	0 8839	1 699	5 998	6 110

latter is in agreement with the value 4 29 cm. recently found by I. Curie† using the Wilson cloud method and confirms her conclusion that the previously accepted value was too low

Comparison with the Results of other Observers.

The uncertainty that existed in the earlier α -ray relative velocity measurements and the subsequent increase in precision is illustrated by the results obtained by various observers for the relative velocities of α -particles for thorium C, thorium C' and radium C' collected in Table VIII.

Table VIII.

	Date	Thorium C' (mean) Radium C'	Thorium C' Radium C'	Thorium C (mean) Thorium C'
Biggs	1928	0 886	1 068	0 8306
Laurence	1929	0 8885	1 0679	0 8321
Rosenblum	1930	0 886*	1 0706	0 8278
Rosenblum and Valadares	1932	0 8870*	1 0682	0 8304
Rosenblum and Dupouy	1932	0 8882†	1 0690	0 8309
Biggs	1932	0 88811	1 06872	0 83101

* The thorium C (mean) velocity has been deduced from the velocities of the components and the ratio of intensities 1 0 3

† Mean velocity deduced by assuming the same relative velocity of components as was found by Rosenblum and Valadares.

The discrepancy between the author's previous value for the relative velocity of thorium C and that given here has already been discussed. The systematic

differences between the earlier results of Rosenblum obtained in the course of his experiments on the fine structure of α -particles and those found in this work are to be ascribed to the non-uniformity of the field of the magnet used. The velocities found by Rosenblum and Dupouy after a new exploration of the field of the magnet are in good agreement with those found here.

The velocities of the α -particles from thorium X, thoron, and thorium A have been measured recently by Rosenblum and Chamié. The values for the absolute velocities given by them are systematically lower by about 1 in 600 than those given here, a result that is consistent with the other velocity measurements made with the magnet of the Academy of Sciences before the above-mentioned re-exploration of the field by Rosenblum and Dupouy.

In Table IX the relative velocities deduced from the range measurements of Lewis and Wynn-Williams and the preliminary values for radon and radium A are compared with the relative velocities deduced from the measurements of Rosenblum and Dupouy.

Table IX.—Velocities Relative to Radium C'.

	Ac C (long).	Ac C' (short).	Ra F.	Ra A.	Rn.
Rosenblum and Dupouy	0.9286	0.9040	0.8308	0.8837	0.8444
Calculated from the range	0.9282	0.9034	0.8310	—	—
Briggs	—	—	—	0.8839	0.8455

I have much pleasure in expressing my thanks to the Trustees of the Commonwealth Science and Industry Endowment Fund for a grant towards the cost of the permanent magnet used in this work, and to E. D. Briggs for her assistance in the photometry of the plates and in the calculations. I also wish to thank Mr. J. Thompson for his assistance in the experiments.

Summary.

The relative velocities of the α -particles from thorium X, thoron, thorium A, thorium C (mean), thorium C', and radium C' have been measured with a probable error of 1 in 20,000.

Preliminary results for the relative velocities of radon and radium A, accurate to about 1 in 2000 have been given.

These results have been combined with the range measurements of Lewis and Wynn-Williams to give the relation between velocity and the range for α -particles of ranges between 4 and 9 cm.

It is found that for ranges greater than 5 cm. this relation is accurately given by

$$V^{3.26} = kR.$$

The corrections for loss of velocity due to absorption at the source have been fully discussed.

*The Maximum Energy of the β -Rays from Uranium X
and other Bodies.*

By B. W. SARGENT, M.A., Queen's University, Kingston, Ontario.

(Communicated by C. D. Ellis, F.R.S.—Received December 28, 1932.)

1. *Introduction.*

It is now generally accepted that the disintegration electrons from radioactive nuclei have a continuous distribution with energy. The end-points of these distribution curves, representing the maximum kinetic energies carried by the β -rays, have been determined in a considerable number of cases and appear to be quite definite. The purpose of this paper is twofold. First, new experimental work on the β -rays from uranium X will be presented in sections 2, 3 and 4. This includes a determination of the end-point of its normal β -ray spectrum, which was found to be 2.32 million volts, and a search for β -rays having energies from 3 to 7 million volts. None were found, and an upper limit on their number was determined. Secondly, a critical survey of the data on the end-points of a number of β -ray spectra with a list of preferred values will be given in section 5. It will then be shown, in section 6, that a relation between the maximum energy emitted in a spectrum of β -rays and its disintegration constant appears to exist

2. *Methods of Determining the End-points of Continuous Spectra.*

Three methods have been used to find the maximum energies in β -ray spectra. One direct method, carried out principally by Madgwick* and Gurney,†

* 'Proc. Camb. Phil. Soc.,' vol. 23, p. 982 (1927).

† 'Proc. Roy. Soc.,' A, vol. 109, p. 540 (1925); *ibid.*, vol. 112, p. 380 (1926).

consists of analysing the β -rays with the usual semicircular focussing in a magnetic field, and determining, from the field strength and the radius of curvature of the path, the velocity of the fastest particles that can be detected by electrical methods.

A more recent method, used by Terroux and Alexander,* and Champion,† is to photograph the tracks of the β -particles in an expansion chamber, and from the curvature produced by a magnetic field a distribution with velocity can be found. So far, this method has only been applied to the fast β -rays, with the hope of deciding whether the high velocity end-points are real or not. It seems to the writer that it is very difficult to choose an adequate criterion for rejecting those tracks whose curvatures have been appreciably affected by scattering. More satisfactory results might be obtained if the air in the expansion chamber was replaced by hydrogen to diminish scattering, and if stronger magnetic fields were applied. This method suffers from the common fault of all statistical ones in that a large number of particles have to be registered, and so the work involved is enormous. If it were extended to give the complete distribution of the β -rays with velocity the variation of the efficiency of registration of tracks with velocity during the time of expansion would have to be carefully investigated.

The high velocity limit of a β -ray spectrum can be determined in yet another way. The effective range of the β -rays is found in paper or aluminium, and this is usually ascribed to the fastest particles in the spectrum. The velocity of these may then be obtained by comparing their range with the extrapolated ranges of initially homogeneous β -rays. This procedure was followed by Chalmers‡ for thorium active deposit and by the writer§ for actinium active deposit. In order to avoid certain difficulties in interpretation, Feather|| preferred to find the end-point of the spectrum of mesothorium 2 by comparing his value of the range with the ranges of the β -rays of radium E, thorium C and radium C, whose maximum energies are known approximately from magnetic analyses.

The first and third methods especially agree where comparison can be made, as in the cases of thorium B, thorium C, radium E, and radium C. This agreement may be partly fortuitous, because the interpretation of the experimental

* Terroux, 'Proc. Roy. Soc.,' A, vol. 131, p. 90 (1931); Terroux and Alexander, 'Proc. Camb. Phil. Soc.,' vol. 28, p. 115 (1932).

† 'Proc. Roy. Soc.,' A, vol. 134, p. 672 (1932).

‡ 'Proc. Camb. Phil. Soc.,' vol. 25, p. 331 (1929).

§ 'Proc. Camb. Phil. Soc.,' vol. 25, p. 514 (1929).

|| 'Phys. Rev.,' vol. 35, p. 1559 (1930).

results by the third method is somewhat uncertain for reasons that will be given later. The experiments in the range method are, however, very simple and can be performed even with rapidly decaying sources. To find the range of the β -rays, the ionization caused by the β - and γ -rays which have passed through absorbing screens of different thicknesses, is measured in an electro-scope. The β - and γ -ray effects may be separated by using a magnetic field as Douglas* and the writer† have done. The range may then be found from the absorption curve of the β -rays alone. Alternatively, the range may be found from the curve obtained by plotting the combined β - and γ -ray ionization against the mass per unit area of the absorbing screen. This curve is always composed of two main parts, a rapidly falling one, where the ionization is mostly due to the β -rays, and a second part at large thicknesses of absorber, where the ionization is due entirely to the γ -rays. The effective range of the β -rays, or the thickness of absorber which reduces their intensity to a quantity too small to be detected, is then fairly evident. This procedure was adopted for finding the range and thereby the end-point of the β -ray spectrum of uranium X.

3. *Experimental Results*

An active preparation of uranium X ($= X_1 + X_2$) on a piece of filter paper was placed in a cavity, 2.5 cm. diameter and 4 mm. deep, drilled in a wooden block. This preparation was covered with another filter paper and a piece of gummed paper. The block was placed 4 cm. below the paper base of an iron electro-scope, 13 cm. cube. Absorption sheets of carbon and cardboard or of aluminium were placed over the source, and readings of the ionization due to the β - and γ -rays were taken.

Very consistent readings were obtained, and sets taken on different days agreed to 2 parts in 300 when allowances were made for the decay of the source and variations in atmospheric pressure. Averages listed in Tables I and II are probably correct to 1 part in 300. The results are plotted in fig. 1, where the effective range of the β -rays is seen to be 1.06 gm./cm.². A preliminary set of measurements using a brass electro-scope yielded 1.05 gm./cm.².

To the value 1.06 gm./cm.² must be added the mass per unit area of the filter paper and the gummed paper over the source, also of the paper base of the electro-scope. This correction amounts to 0.041 gm./cm.², making the effective range 1.10 gm./cm.² in aluminium and carbon. Fajans and Gohring‡

* 'Trans. Roy. Soc. Can.', III, vol. 16, p. 113 (1922).

† 'Proc. Camb. Phil. Soc.', vol. 25, p. 331 (1929).

‡ 'Phys. Z.', vol. 14, p. 877 (1913).

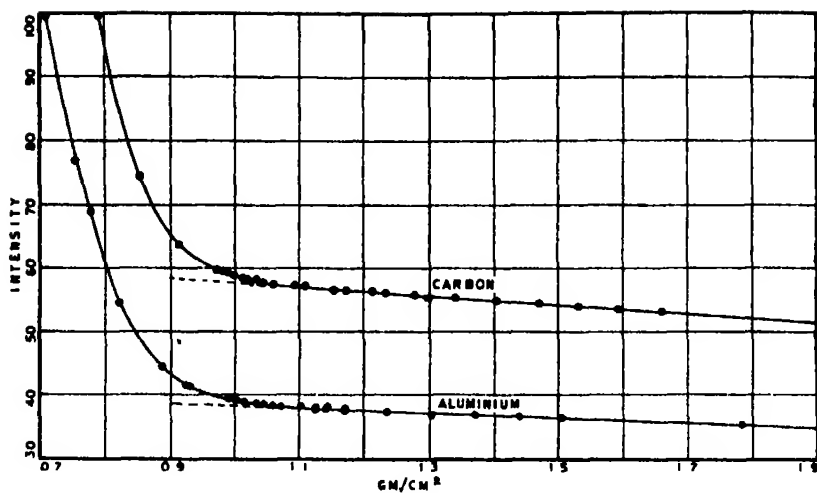


FIG. 1.

Table I.—Absorption of β -rays of $U(X_1 + X_2)$ in Carbon + Cardboard.

Carbon. (gm /cm ²)	Total (gm /cm ²)	Intensity. ($\beta + \gamma$)	Carbon. (gm./cm. ²)	Total. (gm /cm ²)	Intensity. ($\beta + \gamma$)
0.785	0.792	100	0.785	1.156	56.6
0.785	0.855	74.4	0.785	1.174	56.6
0.785	0.916	63.8	0.785	1.216	56.2
0.785	0.974	59.9	0.785	1.237	56.0
0.785	0.983	59.6	0.785	1.280	55.8
0.785	0.987	59.2	0.785	1.343	55.2
0.785	1.000	58.9	0.785	1.407	55.0
0.785	1.013	58.4	0.785	1.471	54.3
0.785	1.020	58.3	0.785	1.534	53.9
0.785	1.026	57.9	0.785	1.598	53.3
0.785	1.034	58.1	0.785	1.662	53.0
0.785	1.047	57.8	1.618	1.943	53.0
0.785	1.060	57.5	2.360	2.685	50.7
0.785	1.095	57.4	3.193	3.518	47.6
0.785	1.110	57.3			

Table II.—Absorption of β -rays in $U(X_1 + X_2)$ in Aluminium.

Aluminium. (gm./cm ²)	Intensity. ($\beta + \gamma$)	Aluminium. (gm /cm ²)	Intensity. ($\beta + \gamma$)
0.710	100	1.074	38.3
0.779	65.9	1.104	38.2
0.821	54.6	1.129	37.8
0.888	44.7	1.147	38.0
0.926	41.7	1.172	37.7
0.931	41.5	1.238	37.2
1.005	39.2	1.306	36.9
1.018	38.9	1.374	36.8
1.035	38.7	1.441	36.5
1.048	38.6	1.508	36.3
1.060	38.5	1.785	36.2

and others* have shown that uranium X_1 emits slow β -rays and uranium X_2 fast ones, so this range must be ascribed to the latter. If Varder's† and Madgwick's‡ values of the extrapolated ranges of homogeneous β -rays in aluminium may be applied, we find $H\rho$ 9700 (Varder) and 8800 (Madgwick) as estimates of the end-point of this β -ray spectrum. The mean value, $H\rho$ 9250, corresponds to an energy of 2.31 million volts. Feather's (*loc. cit.*) empirical equation,

$$R = 0.511 E - 0.091,$$

connecting the range R of a β -ray spectrum with its maximum energy E , leads to 2.33 million volts for the end-point.

It should be pointed out that the absorption curves are really smooth, and no definite "kink" is evident at the range. The value 1.10 gm./cm.^2 may be regarded as correct to 2 per cent. with the present source. The β -ray intensity at the range was not greater than 0.2 div. per minute, and the initial intensity of the source was estimated at 10,000 div. per minute. That is, the ionization of the β -rays has been reduced to 2 parts in 100,000, which is about the same order of reduction as in some previous experiments with other β -ray bodies

It is well known that, unless the initial activity of the source is very large, the range may be underestimated. Feather§ has examined this and other points in detail. An underestimation of the range is the inevitable result of the finite sensitivity of the electroscope, and the fact that those rays, whose range we wish to measure, form only a small fraction of the whole spectrum. In fact with weak sources of actinium (B + C) the writer (*loc. cit.*) found it necessary to separate the β - and γ -ray effects with a magnetic field, and to extrapolate the absorption curve of the β -rays. The smallest intensity of β -rays that could be measured was 0.1 per cent. of the initial one. When the logarithm of the β -ray intensity was plotted against the mass per unit area of absorbing screen, it was possible to extrapolate the curve obtained in a reasonable way, with the purpose of avoiding the error just considered. On the other hand, if sufficiently active sources were available, it would be possible to over-estimate the range, even if the spectrum had an end-point beyond which there were no β -rays whatever. Owing to straggling within the absorbing material

* Fleck, 'Phil. Mag.,' vol. 26, p. 529 (1913), Hahn and Meitner, 'Phys. Z.,' vol. 14, p. 758 (1913).

† 'Phil. Mag.,' vol. 29, p. 725 (1915).

‡ 'Proc. Camb. Phil. Soc.,' vol. 23, p. 970 (1927).

§ 'Proc. Camb. Phil. Soc.,' vol. 27, p. 430 (1931).

the effective range of a spectrum of β -rays would not be the extrapolated range of the fastest ones, as defined by Varder (*loc. cit.*) and Madgwick (*loc. cit.*), so their data would not be applicable for a determination of the end-point. It seems, therefore, that the good agreement among the end-points obtained by direct and indirect methods may be due, in part, to a fortunate choice of activity of the sources.

The early experimenters were mainly interested in finding the absorption coefficients of the β -rays in different materials, and so it was unnecessary to carry out the measurements to large thicknesses of absorber. There is, therefore, very little previous information about the end-point of the β -ray spectrum of uranium X. Levin's* absorption curve in aluminium shows the effective range to be about 0.95 gm/cm.², but this is only a rough estimate since his curve has not been carried quite far enough.

Many years ago Schmidt† published a rough ionization distribution curve of the β -rays using magnetic analysis. The curve indicated an end-point at H_p 9000, but little weight should be attached to this value because the focussing was poor and no attempt was made to allow for scattered radiation.

4 β -rays of Very High Energy.

Of the continuous spectra containing the primary electrons due to the normal mode of disintegration, only one, radium C, has an upper limit of energy greater than 3 million volts, while four others have limits near 2 million volts (see latter). Evidence has been accumulating which seems to show that certain β -ray bodies occasionally emit electrons possessing energies of the order of 7 million volts. Indication of their presence was first given by feeble traces on photographic plates exposed in a magnetic spectrograph. While these diffuse traces may be caused by secondary electrons produced by penetrating γ -rays, at present it seems most reasonable to consider most of them, in fact those above H_p 12,000, to be from primary electrons arising from an abnormal and infrequent mode of disintegration.‡ The evidence for such high-speed β -rays has been summarized by Rutherford, Chadwick and Ellis (*loc. cit.*), and also by d'Espine.§ Experiments by J. A. Gray and O'Leary,|| Cave,¶

* 'Phys. Z.', vol. 8, p. 585 (1907).

† 'Phys. Z.', vol. 10, p. 6 (1909).

‡ Rutherford, Chadwick and Ellis, "Radiations from Radioactive Substances," pp. 381-384.

§ 'Ann. Physique,' vol. 16, p. 5 (1931).

|| 'Nature,' vol. 123, p. 568 (1929).

¶ 'Proc. Camb. Phil. Soc.,' vol. 25, p. 222 (1929).

Cave and Gott,* Champion (*loc. cit.*), and Wang† agree in showing that in particular experiments the number of high-speed β -rays forms an extremely small fraction of those emitted in the usual spectrum. Clearly β -rays having energies of 10 million or even of 4 million volts are of great interest. While no evidence of such high-speed β -particles from uranium X has ever been given, an investigation seemed opportune when the end-point of its continuous spectrum was being determined.

The experimental arrangement was that described in section 3, and an absorption method was used. Ionization measurements were carried out until the mass of carbon and cardboard between the source and the electro-scope was 3.52 gm./cm.². Relative values of the transmitted radiation are given in column 2 of Table III. At each stage the radiation issuing from the absorber was tested by passing it through a lead foil of 0.0975 gm./cm.². The percentages transmitted by the foil are given in column 3, Table III. It

Table III.

Mass of carbon, etc (gm /cm ²)	Transmission by carbon, etc	Transmission by lead foil (0.0975 gm /cm ²)
		per cent
0.792	100	51.3
0.855	74.4	62.5
0.919	63.8	70.7
0.983	59.6	73.8
1.046	58.1	74.3
1.110	57.3	74.2
1.174	56.6	74.3
1.237	56.0	74.2
2.085	50.7	74.5
3.518	47.6	74.3

is seen that after 1.046 gm./cm.² of carbon the transmission remains constant for this foil at 74.3 per cent. to 1 part in 300. This shows that the radiation remains unchanged in quality. Below 1.046 gm./cm.² the presence of β -rays in the radiation issuing from the carbon absorber is well shown by the larger absorption in the lead foil.

From what follows we conclude that the radiation penetrating thicknesses of carbon greater than 1.06 gm./cm.² must be almost entirely of the γ -ray type. Its mass absorption coefficient in the lead foil is 3.05, while 2.4 gm./cm.² of carbon diminishes it to 83 per cent. of its value at 1.11 gm./cm.², or μ/ρ in

* *Vide* "Radiations from Radioactive Substances," p. 383.

† 'Z. Physik,' vol. 74, p. 744 (1932).

carbon is about 0.077. That is μ/ρ in lead is 39.6 times μ/ρ in carbon.* Only a γ -radiation can have this property, for with β -rays the mass absorption coefficient in lead is only about 1.5 times that in carbon. Without going into cumbersome details we estimate that if 0.2 div. per minute of the radiation issuing from 1.11 gm./cm.² carbon were of the β -ray type it could just have been detected by these absorption measurements. This estimate is supported by an inspection of the absorption curves in fig. 1, and it provides an upper limit on the ionization produced by β -rays having ranges between 1.11 and 3.52 gm./cm.² carbon. If the equivalence of carbon and aluminium is assumed we find that β -rays require energies of 2.5 and 7.0 million volts to penetrate these two thicknesses.

In order to set a limit on the fraction of high-speed β -rays the intensity of the source with no absorber in position must be known. This was roughly estimated from the ionization measurements given in Table IV. These have

Table IV.

Absorber (gm /cm ²)		β -ray activity (div /min)
Carbon.	Lead	
0.438	—	700
0.458	0.0975	235
Lead plate containing small hole over source.		
—	—	220
	0.0975	59.0
0.458	0.0975	3.90

* The effective wave-length of the γ -rays issuing from 1.1 gm./cm.² carbon or aluminium can be approximately calculated. The mass absorption coefficients measured with the experimental arrangement were 0.075 (carbon), 0.088 (aluminium), 0.140 (cardboard) and 3.05 (lead foil). These when corrected for the oblique passage of some of the γ -rays through the absorption sheets become 0.068, 0.079, 0.126 and 2.68 respectively. For this correction a formula given by W. and F. M. Soddy and Russell ('Phil. Mag.', vol. 19, p. 725 (1910)) was used. Since much of the radiation scattered in the forward direction enters the electroscope a further correction has to be applied, particularly for the light substances in which the photoelectric absorption is small. Compton's formula ('Phys. Rev.', vol. 21, p. 483 (1923)) for the distribution of scattered radiation with angle, regarded as satisfactory for these wave-lengths, was used. The mass absorption coefficient in carbon then becomes 0.144, which corresponds to an effective wave-length of 0.093 Å. The coefficient in lead, 2.68, corresponds to 0.083 Å. It is believed that the lead foil contains a fairly high percentage of impurity so that $\lambda = 0.083$ is probably too small. It should be noticed that the apparent absorption coefficient in cardboard is about twice that in carbon. The cardboard must contain a considerable amount of heavy materials in order that the photoelectric absorption can be appreciable.

been corrected for γ -rays. The first two were obtained by using the whole source. A lead plate containing a small hole was then placed over the source in order that the intensity of the β -rays coming through could be directly measured. The initial β -ray intensity of the whole source is $220 \times 235/3.90$ or 13,200 div. per minute. It is also seen that 0.458 gm./cm.² carbon cuts down the intensity from 59.0 to 3.90 div. per minute, i.e., to 6.6 per cent. The second estimate of the initial activity is therefore $700 \times 100/6.6 = 10,600$ div. per minute. It was found later by using a thin layer of the active material that 0.458 gm./cm.² carbon transmits 7.1 per cent. of the β -radiation incident on it. This agrees with 6.6 and with figures obtained in another connection, 6.1 per cent. for the same mass per unit area of paper and 5.75 for cardboard. If 7.1 per cent. is taken the initial activity is 9800 div. per minute. These estimates are accurate enough for the present purpose, and a round figure 10,000 div. per minute is adopted as the final value of the initial β -ray activity.

The conclusion reached is that out of a total of 10,000 div. per minute less than 0.2 penetrate 1.11 gm./cm.² carbon. The ionization of the fast β -rays has been diminished by this carbon, and at this point it is necessary to assume a value for their initial energy. If we take 7 million volts, Madgwick's* curves show that about 55 per cent. of the initial intensity is transmitted. On the other hand, if we take 3 million volts as the energy of the β -rays, in passing through 1.11 gm./cm.² carbon their ionization is reduced to 18 per cent. of its initial value. The initial intensity of the fast β -rays is therefore either 0.36 or 1.10 div. per minute in a total of 10,000, i.e. either 1 in 28,000 or 1 in 9,000. The ionizing power of the fast β -rays is less than that of the average ones (average energy 820,000 volts). Allowing for this we find that uranium X emits less than one β -ray of 3 million volts energy in 6,500 normal ones, and less than one β -ray of 7 million volts energy in 15,000 normal ones.

5. *Collected Results for several β -ray Bodies.*

Uranium X₁.—Absorption curves obtained by Levin (*loc. cit.*), Schmidt (*loc. cit.*), Fajans and Gohring (*loc. cit.*), and Hahn and Rothenbach† for the β -rays of uranium ($X_1 + X_2$) show a group of very absorbable β -rays to be present. Their range lies between 0.014 and 0.021 gm./cm.² aluminium, and the mean 0.018 gm./cm.² is here chosen. These β -rays must come from uranium X₁. Using Schonland's‡ and Varder's (*loc. cit.*) values for the ranges of homo-

* 'Proc. Camb. Phil. Soc.,' vol. 23, p. 970 (1927).

† 'Phys. Z.,' vol. 20, p. 194 (1919).

‡ 'Proc. Roy. Soc.,' A, vol. 104, p. 235 (1923); vol. 108, p. 187 (1925).

geneous β -rays, we find that this range corresponds to H_p 1300, or 130,000 volts energy. Meitner,* in her magnetic analysis of the line spectrum, found a band extending from 108,000 to 124,000 volts. If this contains the disintegration electrons its maximum energy agrees very well with that found from the range.

Radium B.—From Schmidt's† absorption curve the range of the β -rays of radium B is estimated at 0.216 gm./cm.² of aluminium. This corresponds to H_p 3380 (Varder) or to H_p 3170 (Madgwick). The mean, H_p 3280, should be compared with Gurney's (*loc. cit.*) value H_p 3470, obtained by magnetic deflection.

Radium C.—A number of estimates, ranging from H_p 11,000 to H_p 16,000, of the end-point of the β -ray spectrum of radium C have been made. Madgwick and Gurney‡ found H_p 12,000 by magnetic analysis when care was taken to eliminate scattered β -rays. D'Espine§ found the end-point to lie between H_p 11,000 and H_p 12,000 from photographic plates exposed in a magnetic spectrograph. The range of these β -rays is estimated at 1.62 gm./cm.² from Schmidt's§§ absorption curve, which yields H_p 12,500 as the end-point. Feather|| has determined this range very carefully and found 1.54 ± 0.02 gm./cm.², which corresponds to H_p 12,000.

Radium E.—Many range estimates have been made and are best shown in a table (V). Choosing 0.475 gm./cm.² as the range to which Varder's and Madgwick's data may be applied we find that H_p 5100 is the end-point of the β -ray spectrum.

Kovarik and McKeehan¶ have obtained a distribution curve of the rays of radium E by using magnetic deflection and a point-counter. This curve falls rapidly towards H_p 5500 but extends as far as H_p 8000. The latter is probably due to scattered β -rays. It should be noticed that for radium C they found a similar extension of the distribution curve to H_p 16,000. Madgwick** gives H_p 5000 for the end-point of the ray spectrum of radium E, although his distribution curve would justify choosing a slightly higher value. Champion (*loc. cit.*) finds the end-point to be about H_p 5500, using magnetic deflection and an expansion chamber.

* 'Z. Physik,' vol. 17, p. 54 (1923).

† 'Ann. Physik,' vol. 21, p. 609 (1906).

‡ 'Phys. Z.,' vol. 8, p. 361 (1907); vol. 10, p. 929 (1909).

§ 'Proc. Roy. Soc.,' A, vol. 87, p. 487 (1912).

|| 'Phys. Rev.,' vol. 35, p. 1559 (1930).

¶ 'Phys. Rev.,' vol. 8, p. 574 (1916).

** 'Proc. Camb. Phil. Soc.,' vol. 23, p. 982 (1927).

Table V.

Observer	Effective range (gm./cm. ²)				
	Paper.	Aluminium	Copper	Tin	Lead
H. W. Schmidt*	—	0.50	0.48	0.47	0.45
J. A. Gray†	0.477	—	—	—	—
Douglas‡	0.474	0.460	0.432	0.395	0.354
G. H. Aston§	—	—	—	—	0.40
Feather	0.475	—	—	—	—
Wang¶	—	—	0.47	—	—

* 'Phys. Z.,' vol. 8, p. 361 (1907); vol. 10, p. 929 (1909)

† 'Proc. Roy. Soc.,' A, vol. 87, p. 487 (1912).

‡ 'Trans. Roy. Soc. Can.,' III, vol. 16, p. 113 (1922).

§ 'Proc. Camb. Phil. Soc.,' vol. 23, p. 935 (1927)

|| 'Phys. Rev.,' vol. 35, p. 1559 (1930).

¶ 'Z. Physik,' vol. 74, p. 744 (1932).

Thorium C''.—Chalmers' (*loc. cit.*) range measurements, 0.79 gm./cm.² in paper and aluminium, gives $H\rho$ 7200 for the end-point. The writer has obtained an absorption curve in paper for the β -rays of thorium C'', which was carried out until the transmitted intensity was 3 per cent. of the initial one. The intensities I for thicknesses X will be given elsewhere. These values were plotted, logarithm I against X , and the curve fitted, by adjusting the abscissæ, to a similar one for the β -rays of radium E, obtained by Douglas (*loc. cit.*). This can be done quite accurately since the absorption curves have the same shape. The range 0.84 gm./cm.² in paper is found to be comparable with 0.475 gm./cm.² for the β -rays of radium E. The corresponding end-point of the spectrum of thorium C'' is $H\rho$ 7550, in fair agreement with Chalmers.

Recently Terroux and Alexander (*loc. cit.*) find $H\rho$ 9400 to be the end-point with an expansion chamber. This method is apt to give too high a value, for the reasons given in section 2, and also since a few recoil and photoelectrons due to the γ -rays of 2.6×10^6 volts are apt to be included with the disintegration electrons.

In a recent paper,* Chalmers suggests, as an empirical rule, that the mass range of a β -ray spectrum is given by $7.5 \rho/\mu$, where μ/ρ is the mass absorption coefficient. This is satisfactory for uranium X₂, radium B, radium C, radium E, mesothorium 2 and thorium B. It is interesting to note that the ranges† found for the β -rays of actinium C'', thorium C'' and thorium C, using this

* 'Proc. Camb. Phil. Soc.,' vol. 28, p. 319 (1932).

† Chalmers (*loc. cit.*) concludes that the range of the β -rays of actinium C'' should be as low as 0.49 gm./cm.² through choosing an incorrect absorption coefficient.

rule and the generally accepted coefficients§ 10·7, 8·0 and 5·35 respectively, are 0·70, 0·94 and 1·40 gm./cm.². These should be compared with the experimental ones, 0·62, 0·79 or 0·84, and 0·98. The end-points corresponding to the calculated values are respectively H_p 6600, 8200 and 11,000. This argues against the end-point of the thorium C'' spectrum being as high as H_p 9400, but the disagreement of H_p 11,000 with similar results for thorium C in Table VI is very striking. It seems desirable to redetermine these end-points.

Table VI contains a summary of the end-points of β -ray spectra, as determined by the three principal methods. The values in column 2 were found from the effective ranges of the β -rays. In order to give uniform values of H_p it was necessary to decide on a set of ranges of homogeneous β -rays. The means of Varder's and Madgwick's values have been used throughout; this gives good agreement between the end-points obtained by the range and electrical methods. The order of reduction of the initial intensity of β -rays, forming an extended spectrum, by an absorbing screen of thickness equal to the range, is about the same for many of the β -ray bodies included in Table VI. This minimizes the effect of straggling and makes the ranges of these bodies closely comparable with each other. It seems, therefore, that the relative values of the end-points collected here must be more accurate than their

Table VI.

Element	End-point					Average energy (volts $\times 10^{-5}$)
	H _p Range method.	H _p Magnetic analysis.	H _p Expansion chamber	H _p "Preferred."	Energy (volts $\times 10^{-5}$)	
UX ₁	(1300)	(1300)	—	(1300)	(1·3)	—
UX ₂	9250	(9000)	—	9250	23·2	8·2
RaB	3280	3470	—	3470	6·5	2·3
RaC	12000	12000	—	12,000	31·5	7·4
RaD	—	—	(650)*	(650)	(0·35)*	—
RaE	5100	5000	5500	5500	12·2	3·4
MsTh ₂	8350	6800†	—	8350	20·5	5·6
ThB	2500	2330	—	2330	3·6	0·89
ThC	8450	8900	—	8900	22·0	8·0
ThC''	7550	—	9400	7550	18·2	5·8
AcB	(2100)‡	—	—	(2100)	(3·0)	—
AcC''	6140	—	—	6140	14·0	4·8

* O. W. Richardson, 'Proc. Roy. Soc.,' A, vol. 133, p. 367 (1931).

† Yovanovitch and d'Espine, 'J. Phys. Rad.,' vol. 8, p. 276 (1927).

‡ New measurement, details of which are in course of publication elsewhere.

The values in brackets are regarded as less reliable than the others.

absolute values; for completeness a number of values* for the average energy in the spectrum is also included.

6. A Relation between the Disintegration Constant of a β -ray Body and the High Energy Limit of its Spectrum.

When the logarithms of the disintegration constants† are plotted against the logarithms of the maximum energies emitted in the β -ray spectra, fig. 2, it is seen that, with the exception of actinium B, the twelve β -ray bodies given

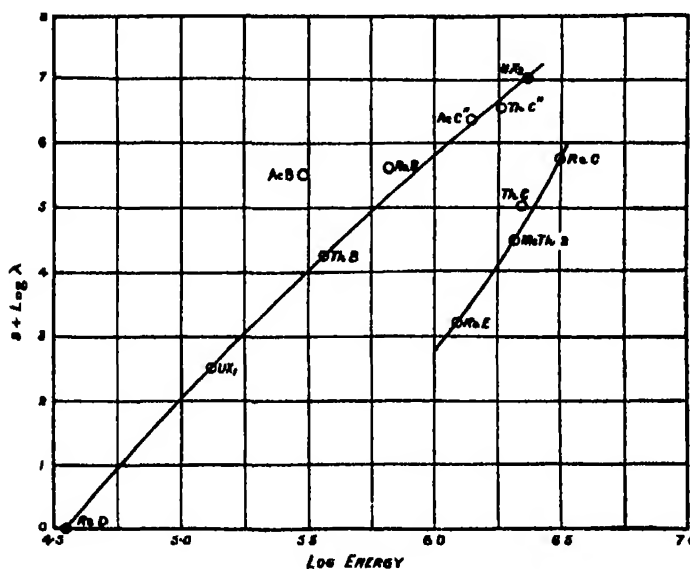


FIG. 2.

in Table VI fall into two distinct groups. (The same grouping is obtained if the maximum energy is replaced by the average energy emitted in each spectrum.)

Group I.—RaD, UX₁, ThB, RaB, AcC'', ThC'' and UX₂.

Group II.—RaE, MsTh2, ThC and RaC.

With the exception of uranium X₂ the ones in Group I are the first β -ray members of the $\alpha\beta\alpha$ sequences and those of the $\alpha\beta\alpha\beta$ sequences. Group II contains the second β -ray members of the $\alpha\beta\alpha$ sequences. (While the end-point of the spectrum of actinium B is rather uncertain, it definitely lies off

* Sargent, 'Proc. Camb. Phil. Soc.,' vol. 24, p. 538 (1932).

† For thorium C account has been taken of the fact that only 65 per cent. of the atoms emit β -rays.

the curve. Perhaps a third curve should be added for actinium B and actinium C".) It is interesting to note that if the maximum energy of the thorium C spectrum is really 2.5 instead of 2.2 million volts the agreement in fig. 2 is improved. Slight evidence already given indicates that this experimental value is too low. If the relation indicated in fig. 2 applies to all β -ray bodies then the end-points of additional spectra may easily be found from their decay constants. For example, radium C" would be expected to have an upper limit of energy at 2.2 million volts.

Certain similarities tend to separate the β -ray bodies into groups as shown here. For instance, radium C and thorium C stand at the beginning of branches. The spectral distribution of radium C is rather unlike that of most other β -ray substances. The distribution curve* of its disintegration electrons with momentum has a maximum at Hp 2600 and then extends as far as Hp 12,000. This general result could have been inferred long ago from absorption measurements, since it was found that these β -rays were not absorbed exponentially in aluminium with a single absorption coefficient but at least two exponential terms were necessary. Similar information about the distribution of the β -rays of mesothorium 2 can be inferred from absorption measurements by Hahn and Meitner.† These indicate that many slow electrons are emitted and the fast ones form a tail to the distribution curve. In this respect mesothorium 2 is similar to radium C and is expected to belong to the same group.

A comparison of the relation here suggested with the Geiger-Nuttall rule for α -particles is interesting. The α -particles have energies between 4 and 8.8 million electron volts while the transformation constant λ (sec.⁻¹) ranges from about 10^{20} to 10^{-18} . If the Geiger-Nuttall rule is expressed as $\lambda \propto (\text{energy})^x$ we find that x varies from 65 to 100. The maximum energies of the β -ray spectra range from 35,000 to 3,150,000 volts, while the transformation constant varies from 10^{-2} to 10^{-9} . For the curves of fig. 2, x lies between 3 and 7. At present the significance of this general relation is not apparent.

In conclusion, the writer wishes to express his thanks to Dr. J. A. Gray, F.R.S., and Dr. C. D. Ellis, F.R.S., for their kind interest in this work, to Mr. C. W. Clapp, B.Sc., for preparing the very active source required, and to Professor D. M. Jemmett for permission to carry out the experiments in one of the Engineering Laboratories at Queen's University.

* Gurney, 'Proc. Roy. Soc.,' A, vol. 109, p. 540 (1925).

† 'Phys. Z.,' vol. 9, p. 321 (1908).

Summary.

The range of the β -rays of uranium X_2 was found to be 1.10 gm./cm.^2 in carbon and in aluminium. The corresponding end-point of its spectrum is 2.32 million volts. A search was made for β -rays of very high energy, but none were found. It was estimated that uranium X emits less than one β -ray for 3 million volts energy in 6500 normal ones and less than one β -ray of 7 million volts energy in 15,000 normal ones.

Collected results for the high energy end-points and average energies of twelve β -ray spectra are given. While the absolute definiteness of the end-point of a β -ray spectrum can never be proved experimentally, many experiments, designed to determine its value and to set an upper limit on the fraction of β -rays that have greater energies, in particular cases, afford a strong indication that the end-point is one of the characteristics of the spectrum. An apparent relation between the transformation constant and the maximum energy emitted in the β -ray spectrum is pointed out.

The Hyperfine Structure of the Lines of the Arc Spectrum of Rubidium.

By D. A. JACKSON.

(Communicated by F. A. Lindemann, F.R.S.—Received December 12, 1932.)

The structure of the lines of the arc spectrum of rubidium was investigated with a reflexion echelon grating of high resolving power, the light source being a tube containing helium neon mixture at about $\frac{1}{2}$ mm. pressure and a small quantity of rubidium; this tube was fitted with external electrodes and excited with an oscillator of very high frequency. The two resonance lines—7947 and 7800—were found to possess the same fine structure, and each possessed four components: at 0.00, -0.09 , -0.19 and -0.23 cm.^{-1} ; the two outer components, 0.00 and -0.23 cm.^{-1} , are weak and the two inner components are strong. The lines 4215 and 4201 were found to possess three components; at 0.00, -0.09 and -0.20 cm.^{-1} . The line at the latter point was slightly broadened. This was presumed to correspond to the same structure as that observed in the resonance lines, the broadened line corresponding to -0.19 and -0.23 unresolved. This observed structure is

explained as arising from the $5S_{1/2}$ level; the two outer, weak, components arising from the isotope 87 and corresponding to a separation into two levels, 0.23 cm.^{-1} apart, in the $5S_{1/2}$ level; while the two inner, stronger, components arise from the other isotope, 85, and correspond to a similar separation of 0.10 cm.^{-1} . The centre of gravity of the levels of Rb 85 is displaced about 0.02 cm.^{-1} from that of the levels of Rb 87. Measurements on the intensities of the components of 4201 show that the probable value for the nuclear moment of Rb 85 is $3/2$, but the accuracy is not sufficiently high to enable the value for the scarcer isotope Rb 87 to be determined with certainty; the probable value is, however, $5/2$. The magnetic moment of the nucleus of Rb 87 is shown to be approximately two and a half times as great as that of Rb 85.

Experimental.—The spectroscope of high resolving power used was a reflexion echelon of fused silica mounted according to the method previously described.* The light source was a discharge tube fitted with external electrodes and excited by means of a high frequency oscillator, capable of an output of $\frac{1}{2}$ k.w. The discharge tube was filled with a mixture of helium and neon at about $\frac{1}{2}$ mm. pressure; it also contained a small quantity of pure rubidium. The two ends of the tube, around which external electrodes of thin sheet copper were wrapped were 5 cm. in diameter and 7 cm. in length, and the capillary portion was 5 cm. long and with an internal diameter of 7 mm. A small quantity of rubidium was allowed to run into the capillary, and the tube was placed in a horizontal position. On excitation the spectra of neon and helium appeared, but after the heat of the discharge had increased the temperature of the tube the lines 4215 and 4205 of rubidium appeared. In order to prevent the temperature increasing further, the tube was cooled by means of a powerful fan. The cooling was arranged so that the violet lines of rubidium were of the same order of intensity as the 4481 line of helium. Under these conditions the infra-red resonance lines of rubidium could be photographed with an exposure of about a quarter of an hour. The plates used were the new Ilford infra-red sensitive plates, which do not require any hypersensitizing by bathing in ammonia. Each of the resonance lines was found to possess four components, the positions of which are given in Table I. The intensities of these lines could not be measured quantitatively on account of the great change in sensitivity of the infra-red plates with small changes in wave-length; so rapid is this change that the sensitivity at 8000 Å. is twice as great as that at 7800 Å., with the result that the long wave-length resonance line, although only half as strong as the other, requires the same exposure. Moreover, the

* Jackson, 'Proc. Roy. Soc.,' A, vol. 128, p. 508 (1930).

self absorption of the resonance lines when the vapour pressure of the rubidium is sufficiently high to make the lines strong enough to photograph in the infra-red is very great, so that the relative intensities of the components are altered, the weaker lines gaining in intensity. This difficulty has been overcome for indium,* gallium† and thallium‡ by using the chlorides of the metals when the only free atoms present are the excited atoms (free atoms are removed by condensation on the walls of the tube in an extremely short time, the mean free path being comparable with the diameter of the tube, and the vapour pressure of the metal very much lower than that of the chloride). The chloride of rubidium could not be used because it is very much less volatile than the metal.

The lines 4201 and 4215 were photographed simultaneously. The exposure required for these lines varied between 3 minutes and 1 hour, according to the vapour pressure of the rubidium. The pressure of the air surrounding the grating was adjusted so that the components of 4201 were in the weak double order position (the total separation of the structure is only 0.2 cm.^{-1} or about a quarter of the spectral range). Under these conditions, by a fortunate coincidence the components of the weaker line 4215 were in the stronger single order position, so that although the intensity of the components of the weaker line is only half that of the other, they required approximately the same exposure.

Both of these lines were found to possess three components; that of longest wave-length was somewhat broader than the others. It evidently corresponded to the two components of longest wave-length of the four observed in the infra-red lines; these very close lines being no longer resolved (the resolving power required to separate two lines 0.04 cm.^{-1} apart is 350,000 at 8000 Å. and 600,000 at 4200 Å., and the Doppler width, $d\lambda$, of the line is equal to $\lambda/500,000$). It was found that the relative intensities of these components varied according to the pressure of the rubidium, the intensity ratios becoming smaller as the vapour pressure was increased. By measuring the intensities at a number of different pressures it was, however, possible to extrapolate to the values at infinitesimal pressure; the manner in which this was done is described below. Table I gives the results of the measurements on the fine structure.

Determination of Intensities.—As has already been stated the infra-red plates were not suitable for intensity measurement, the line 4201 on the other

* Jackson, 'Z. Phys.' vol. 80, p. 59 (1933).

† *Ibid.*, vol. 74, p. 291 (1932).

‡ *Ibid.*, vol. 75, p. 223 (1932).

Table I.

Line.	Components in cm. ⁻¹	Intensities and origin.	
$5S_{1/2}-5^2P_{1/2}$ (7947 Å.)	0.00	Weak	Rb 87
	-0.09	Strong	Rb 85
	-0.19	Strong	Rb 85
	-0.23	Weak	Rb 87
$5S_{1/2}-5^2P_{3/2}$ (7800 Å.)	0.00	Weak	Rb 87
	-0.09	Strong	Rb 85
	-0.19	Strong	Rb 85
	-0.23	Weak	Rb 87
$5S_{1/2}-6^2P_{1/2}$ (4215 Å.)	0.00	1	Rb 87
	-0.09	3	Rb 85
	-0.20 (broad)	6	Rb 85
			Rb 87
$5S_{1/2}-6^2P_{3/2}$ (4201 Å.)	0.00	1	Rb 87
	-0.09	3	Rb 85
	-0.20 (broad)	6	Rb 85
			Rb 87

hand was particularly suitable for accurate measurements. In the first place it is possible to make very accurate measurements of intensity of a line in this part of the spectrum; and in the second place it is possible, by suitably adjusting the pressure of the air surrounding the grating, to get the components in such a position in the echelon spectrum that the greatest apparent intensity ratio to be measured is about 2:1, this greatly reduces the difficulties of measurement. The method* of measuring intensities of lines in the echelon spectrum has already been fully described; it will suffice here to state that the density-intensity curve is determined separately for each photographic plate, and that the intensity curve of the grating is measured directly, the calculated value being somewhat different from the experimental values. The relative intensities of the three components was found to vary with the pressure of the rubidium in the tube; this was to be expected as the line 4201 has as its lower state the unexcited atom. The unexcited atoms have a very strong absorption for the components of this line, and consequently as the vapour pressure increases and the self absorption becomes greater, the relative intensities approach equality. In order to determine the true intensity ratios (the intensities at extremely low pressures where there is no appreciable self absorption) it is necessary to make measurements at a number of known vapour pressures, and from these values to calculate the values which are approached as the pressure approaches zero. Accordingly the method of

* Jackson, 'Z. Physik,' vol. 80, p. 59 (1933).

using the discharge tube was modified ; the whole of the rubidium was brought into one end of the tube, which was now run in a vertical position, the lower end (containing all the metal) being immersed in an oil bath, which could be kept at any desired temperature. On running the tube with the oil bath cold the lines of helium and neon alone could be seen, all the rubidium being condensed in the lower end of the tube. When the oil bath was heated the vapour pressure of the rubidium increased, being equal to the value appropriate to the temperature of the oil bath. As the discharge kept the capillary part of the tube at a slightly higher temperature than the end of the tube, it was impossible for any metal to condense in it ; the level of the oil was up to that part of the tube where the capillary started, and the spectrum of the discharge in the capillary just above this was photographed. Under these conditions the vapour pressure of rubidium in the part of the capillary observed was equal to that in the lower end of the tube. Measurements of intensities were made at four different temperatures, and the vapour pressures corresponding to these temperatures were calculated from the figures given by Scott.* In this method of measuring the intensity the brightest point in each line is measured ; for the width of the slit of the photometer (0.02 mm.) is narrow compared with the width of the lines (0.10 mm.). The intensities thus measured give the relative intensities of the lines, only if all the lines are the same width. The line at -0.20 cm.^{-1} , however, was considerably wider than the other two, as it is composed of a line at -0.19 cm.^{-1} and another line at -0.23 cm.^{-1} not quite resolved ; the half value width of a single line is about 0.05 cm.^{-1} and the separation of the unresolved components is 0.04 cm.^{-1} . Consequently the effect of the weaker component (0.23 cm.^{-1}) is not so much to increase the intensity of the centre of the blend, as to increase the width. Accordingly the widths of the simple lines (0.00 cm.^{-1} and -0.09 cm.^{-1}) and the blend were measured. They were found to be 0.50 cm.^{-1} and 0.63 cm.^{-1} respectively. In determining the relative intensities, the intensities of the maxima were, therefore, multiplied by $63/50$ for the broad blend.

The table of measurements, Table II, shows the variation of the relative intensities with the temperature of the tube. It can be seen that with increasing temperature the stronger lines lose in intensity, but the changes are not great. From this it follows that the effects of self absorption are observable but relatively small. Now in this case the loss in intensity of a line through self absorption will be approximately proportional to the average number of layers

* 'Phil. Mag.,' vol. 47, p. 49 (1924).

Table II.

Temperature.	Intensity ratios of lines 0.00 -0.09 -0.20.		Vapour pressure in mm Hg (<i>p</i>)	$N=0.35 \cdot \sqrt[3]{2.7 \times 10^{19} \times p/760}.$
	Individual plates	Average.		
123	1 2 5 4 5 1.2 3 4 5	1.2 4 4.5	5.2×10^{-4}	900
136	1.2 3.4 2 1.2 3.4 1	1.2 3 4 2	1.1×10^{-3}	1250
147	1.2 2 3 0 1.2 3.3 9 1.1 9 3 3	1.2 1 3 7	2.0×10^{-3}	1500
165	1.1 8 3.0 1.1 9 3.1 1.2 0.3 5	1.1 9 3 2	5.2×10^{-3}	2000

of atoms through which the light has to pass before it emerges from the tube. This quantity, *N*, is equal to half the thickness of the tube, in centimetres, multiplied by the cube root of the number of atoms per cubic centimetre in

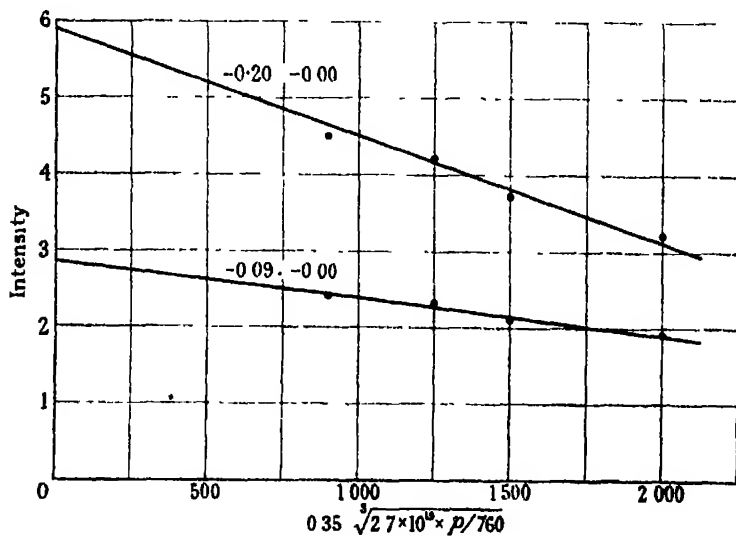


FIG. 1.

rubidium vapour, at the pressure corresponding to the temperature of the tube ; it is given in the last column of Table II. In fig. 1 the measured intensities

are plotted against N . It can be seen that all the points for both intensity ratios $-0.20 \text{ cm.}^{-1} : 0.10 \text{ cm.}^{-1}$ and $-0.09 \text{ cm.}^{-1} : 0.00 \text{ cm.}^{-1}$ lie very nearly on straight lines. Extrapolation to $N = 0$ gives the relative intensities when the effects of self absorption have been completely eliminated. The graph shows that the self absorption losses are relatively small, but as expected they are greater for the strongest line, yet even for this line, at the highest pressure at which measurements were made, the loss is not much in excess of one-third. The condition that self absorption losses are relatively small is therefore fulfilled, and the linear extrapolation to zero can be regarded as reliable. The intensity ratio at zero for the lines 0.20 cm.^{-1} and 0.00 cm.^{-1} is $5.9 : 1$ and for the lines 0.09 cm.^{-1} and 0.00 cm.^{-1} $2.8 : 1$. It is difficult to estimate the accuracy of these extrapolated values; it is probably not better than 5 per cent., nor worse than 10 per cent.

Discussion.—The observed structure of the lines of the principal series of the arc spectrum of rubidium can be satisfactorily explained by the assumption that each isotope (Rb 85 and Rb 87) has its $5S_{1/2}$ level split up into two levels. The fact that the same structure is observed for all four lines $5S_{1/2} - 5^2P_{1/2}$, $5S_{1/2} - 5^2P_{3/2}$, $5S_{1/2} - 6^2P_{1/2}$ and $5S_{1/2} - 6^2P_{3/2}$ (if it is assumed that the broadened component observed in the last two lines at -0.20 cm.^{-1} corresponds to the components -0.19 and -0.23 cm.^{-1} observed in the first two lines, not resolved) show that the structure of these lines is independent of the upper (P) levels and consequently may be assumed to arise from the $5S_{1/2}$ level, which is common to all of these lines. None of the P levels possesses any observable structure; if there is any structure the total separation must be less than 0.02 cm.^{-1} . The isotopes of rubidium are present in the proportion of $3.0 : 1$, the lighter isotope being the more plentiful. The two outer components of the resonance lines are very much weaker than the two inner components. The former are therefore ascribed to Rb 87 and the latter to Rb 85. The separation of the levels of Rb 87 is 0.23 cm.^{-1} , and that of Rb 85 0.10 cm.^{-1} . The observed doubling of the S level of each isotope is explained by ascribing a quantized nuclear moment to each atom. In order to determine the values of the nuclear moments (the only level with any resolvable structure being the $5S_{1/2}$ level), it is necessary to ascertain the intensity ratios of the lines composing the doublets. This was not possible for the resonance lines. It was, however, possible to make determination of the intensities of the observed components of the line 4201 ($5S_{1/2} - 6^2P_{3/2}$) in the manner described above.

It was found that the components 0.00 cm.^{-1} , -0.09 cm.^{-1} and -0.20 cm.^{-1} possessed the intensity ratio $1 : 2.8 : 5.9$. Now 0.00 cm.^{-1} is the shorter

wave-length component of the doublet arising from Rb 87 while -0.09 cm.^{-1} is the corresponding component of Rb 85. The strongest line, -0.20 cm.^{-1} , represents the components of longer wave-length of both Rb 85 and Rb 87 unresolved. But from a knowledge of the proportions in which the two isotopes are present, it is possible to calculate in what ratio the two isotopes contribute to the unresolved line. The ratio of the sum of the intensities of the two components of Rb 85 to that of the two components of Rb 87 may be assumed to be equal to the ratio in which the atoms of Rb 85 and Rb 87 are present; according to Aston* this is 3.0 : 1, which figure is in good agreement with the atomic weight determinations. Of the total (9.7) therefore one-quarter must come from Rb 87 and three-quarters from Rb 85. The sum of the intensities of the doublet of Rb 87 is thus 2.4. Of this 1 is supplied by the line 0.00 cm.^{-1} , so that the remaining 1.4 must be supplied by the unresolved line at 0.20 cm.^{-1} . The remainder of this line is equal to 4.5 and corresponds to the intensity of the stronger component of the doublet due to Rb 85. The intensity ratios of the four components, found in the above manner, are given in Table III.

Table III.

Line	0.00 cm.^{-1}	-0.09 cm.^{-1}	-0.20 cm.^{-1}	
Intensities	1	2.8	5.9	
Component and origin	0.00 Rb 87	-0.09 Rb 85	-0.19 Rb 85	-0.23 Rb 87
Intensities of 4 components from observed intensities and known proportions of Rb 85 and Rb 87	1	2.8	4.5	1.4

From this table it is clear that the intensity ratio of the two lines comprising the doublet due to Rb 85 is 1.6 : 1. This is in good agreement with the value (1.67) required by theory for a nuclear moment, I , of $3/2$. The values required for $I = 1/2$ and $I = 5/2$ are respectively 3 : 1 and 1.40 : 1. Of these the former is definitely excluded, lying well beyond the limits of error, while the latter lies only just outside the limits. It is therefore concluded that the nuclear moment of Rb 85 has the probable value $3/2$, although $5/2$ is just possible. The corresponding intensity ratio for Rb 87 is 1.40 : 1, this agrees with the value required by theory for a value of I of $5/2$. This cannot be

* F. W. Aston, 'Proc. Roy. Soc.,' A, vol. 134, p. 575 (1932).

regarded as at all certain, for the value corresponding to $I = 7/2$ lies well within the limits of accuracy, and that corresponding to $3/2$ is not definitely outside them.

Fig. 2 shows the energy levels of the $5S_{1/2}$ level of rubidium. The levels of the isotope Rb 85 are on the left, and those of Rb 87 on the right; the deeper levels (those of greater negative energy) are placed lower in the diagram. (The diagram is not drawn accurately to scale) The dotted lines show the positions of the centres of gravity of the two levels for each isotope. It can be seen that there is an appreciable isotope shift; the centre of gravity of the levels of Rb 85 is 0.2 cm.^{-1} higher than that of the levels of Rb 87. Similar isotope shifts have been observed in the spectra of thallium,* mercury† and lead.‡ It is impossible to give any exact explanation of the cause of these shifts, but probably it is owing to a difference in the deviation from the Coulomb law of force, in the neighbourhood of the nucleus for the two isotopes.

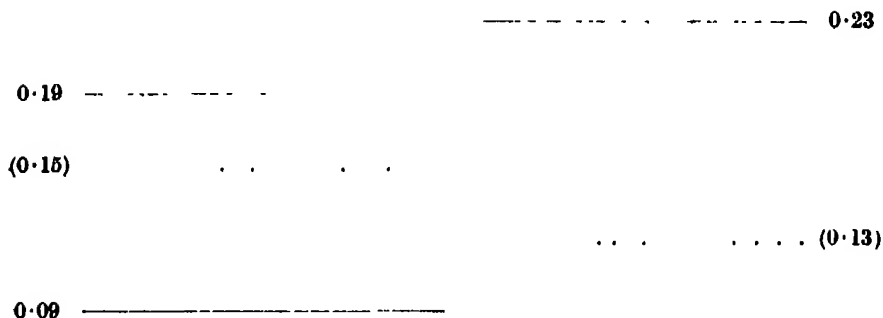


FIG. 2.—The structure of the $5S_{1/2}$ level of the arc spectrum of rubidium.

Another point of great interest is a comparison of the magnetic moments of the two isotopes of rubidium. It has been shown that the splitting of a term through interaction with a nuclear moment I is given by the formula§

$$\Delta W = \mu H_{(0)} \frac{2I + 1}{I},$$

where ΔW is the splitting of the term, μ is the magnetic moment of the nucleus

* Jackson, 'Z. Physik,' vol. 75, p. 223 (1932).

† Schüller and Jones, 'Z. Physik,' vol. 72, p. 631 (1932).

‡ Schüller and Jones, 'Z. Physik,' vol. 76, p. 14 (1932).

§ Kallmann and Schüller, 'Ergebn. Exa. Naturwiss,' vol. VII, p. 138 (1932).

and $H_{(0)}$ is the magnetic field at the nucleus due to the valency electron in the orbit corresponding to the term. In the case of the $5S_{1/2}$ terms of Rb 85 and Rb 87, $H_{(0)}$ is very nearly the same for both atoms, so that from the observed values of ΔW and I it is possible to make a comparison of the nuclear magnetic moments. The value of ΔW is 0.10 cm.^{-1} for Rb 85 and 0.23 cm.^{-1} for Rb 87. I is $3/2$ for Rb 85, but for Rb 87 it is not known with certainty. Table IV shows the ratio of the magnetic moments of the two isotopes, $\mu_{\text{Rb } 87} / \mu_{\text{Rb } 85}$

Table IV.

Nuclear moment of Rb 87 ($I_{\text{Rb } 87}$)	3/2	5/2	7/2
Ratio of magnetic moments of Rb 87 and Rb 85 ($\mu_{\text{Rb } 87} / \mu_{\text{Rb } 85}$)	2.3	2.5	2.6

for values of I between $3/2$ and $7/2$ for Rb 87. It can be seen that for the lowest value of $I_{\text{Rb } 87}$ the ratio is $2.3 : 1$, while for the highest it is $2.6 : 1$. The fact that the nuclear moment of Rb 87 is not known with certainty is therefore not of much consequence in the calculation of the ratio of the magnetic moments. The most probable ratio is that corresponding to $I = 5/2$ for Rb 87, and is $2.5 : 1$. The magnetic moment of Rb 87 is thus shown to be about two and a half times as great as that of Rb 85. This is of the greatest interest, for it shows that the nuclei of the two isotopes must be very different in structure. The existence of a resolvable isotope shift in the $5S_{1/2}$ levels of the isotopes of rubidium also indicates a more than usually great difference in the nuclear structure. In the $7S_{1/2}$ level of thallium, which corresponds to a very much deeper orbit than the $5S_{1/2}$ level of rubidium (this can be seen from the greater separation caused by the magnetic moment of the nucleus) there is no resolvable isotope shift; the difference in structure between the isotopes of rubidium must be far greater than that of the isotopes of thallium. It appears, therefore, that, both from the point of view of the difference in magnetic moments and the difference in nuclear structure giving rise to isotope shift, the isotopes of rubidium must be considered to possess very different nuclear structures.

*The Broadening of the Ultraviolet Absorption Bands of Xenon
under Pressure.*

By J. C. McLENNAN, F.R.S., and R. TURNBULL, M.A.,* The McLennan
Laboratory, Department of Physics, University of Toronto.

(Received January 3, 1933.)

[PLATES 18-20.]

Introduction.

By a series of experiments reported in a previous publication of the authors,† it was shown that for the monatomic gas xenon, the absorption at the resonance wave-length λ 1469 Å. (1S_0 — $^3P^{\circ}_1$) exhibited an unusually large broadening with increase of pressure. With the gas at a pressure of 2 mm. mercury, in a cell with fluorite windows spaced 2 mm. apart, the absorption appeared as a sharp line at λ 1469 Å. As the pressure of the xenon was increased at a constant temperature of 12° C. the absorption rapidly widened out into a continuous band. At a pressure of 50 atmospheres, the band was 156 Angstroms wide and extended from λ 1484 Å. to λ 1428 Å. The spreading out was definitely asymmetrical towards the longer wave-lengths. The shift of the long wave-length absorption limit corresponded to an energy change of 0.7 volts, and that of the short wave-length limit to 0.3 volts.

The type of absorption obtained with xenon was found to be similar to that obtained with the vapours of zinc, cadmium and mercury.‡ In all spectra the absorption occurred at the resonance lines (1S_0 — $^3P^{\circ}_1$, 1S_0 — $^1P^{\circ}_1$) and developed asymmetrically to the longer wave-lengths. It is significant that all these atoms have similar characteristics. Xenon, as well as the metal vapours, is known to approximate closely to the ideal monatomic gas. The normal state of each of the atoms by virtue of completed electron shells, is a 1S_0 . The first excited state to which the atoms can be raised by absorption of light is the $^3P^{\circ}_1$ of the $^3P^{\circ}_{012}$ group and the next higher state is the $^1P^{\circ}_1$ associated with the triplet group. The transitions 1S_0 — $^3P^{\circ}_1$ and 1S_0 — $^1P^{\circ}_1$ from these two states to the normal state give rise to the resonance lines, the latter of which has the shorter wave-length. For the metal vapours the

* Student of the National Research Council of Canada.

† 'Proc. Roy. Soc.,' A, vol. 129, p. 266 (1930).

‡ R. W. Wood, 'Astrophys. J.,' vol. 26, p. 41 (1907); McLennan and Edwards, 'Trans. Roy. Soc. Can.,' vol. 9, p. 167 (1915).

shorter resonance line is the more absorbed, and has a much greater development of an associated absorption band.

In the previous paper (*loc. cit.*, p. 281) it was suggested that the effect could be explained by a displacement of the atomic energy levels during collision between two or more atoms when the interaction of atomic electromagnetic fields would be most effective. Because of the continuous distribution of velocities in a gas there would be an infinite number of ways in which the atoms could influence each other when colliding. The absorption of light by this wide variety of collision aggregates would necessarily constitute a continuous spectrum. Increase of pressure would cause a greater frequency of collisions. Therefore, as greater pressures were employed the region of complete absorption would extend farther from the resonance line. Though this process would account, in a measure, for the continuous absorption band and its broadening with pressure the explanation, on account of its vagueness, was not considered altogether acceptable.

The explanation offered by Franck* of the occurrence of analogous bands in the spectrum of mercury at λ 2536 Å. and λ 1840 Å. was more convincing and would appear to be applicable to the present case. Franck represents the effect of the interaction between two colliding atoms in the normal and the excited state of the individual atoms by potential energy curves as developed theoretically by Born and Franck.† From the experiments of Franck and Grotrian‡ on the change of the absorption of the mercury band λ 2540 Å. with temperature a very low energy of dissociation (about 0.1 volt) was ascribed to the normal Hg_2 molecule. This corresponded to a small minimum in the potential curve for two normal atoms. In order to explain the asymmetry of the absorption band originating in a transition from the normal curve to the curve for one normal and one excited atom, Franck assumed that the latter curve had a pronounced minimum. The significance was that the chemical binding between two mercury atoms increased with the excitation of one of the atoms.

Winans§ and Hamada|| have applied Franck's theory to the (1S_0 — 1P_1) bands of zinc, cadmium and mercury to explain their form, and from the results estimated the stability of the normal and excited molecules. As a typical

* 'Trans. Faraday Soc.', vol. 21, p. 536 (1926); 'Z. physik. Chem.', vol. 120, p. 144 (1926).

† 'Z. Physik', vol. 31, p. 411 (1925).

‡ 'Z. techn. Phys.', vol. 3, p. 194 (1922).

§ 'Phil. Mag.', vol. 7, p. 555 (1929); 'Phys. Rev.', vol. 37, p. 897 (1931).

|| 'Phil. Mag.', vol. 12, p. 50 (1931).

example the potential curves for the cadmium band λ 2288 Å. is shown in fig. 1 from the work of Winans. In accordance with the Franck-Condon principle the frequencies corresponding to wave-lengths in the band spectrum are given by the lengths of vertical lines between the two curves. Transitions are most probable when the relative velocity of the colliding atoms is least. The vertical line (a) gives the frequency of the atomic transition, (c) gives the frequency of the short wave-length limit of the band, and lines shorter than (a) to the left of (c), such as (d), represent wave-lengths on the long wave-length side of the resonance line. For vapour pressures of the order of 10 mm. the transition (c) is revealed in absorption as a separate faint band owing to the presence of loosely bound normal molecules.

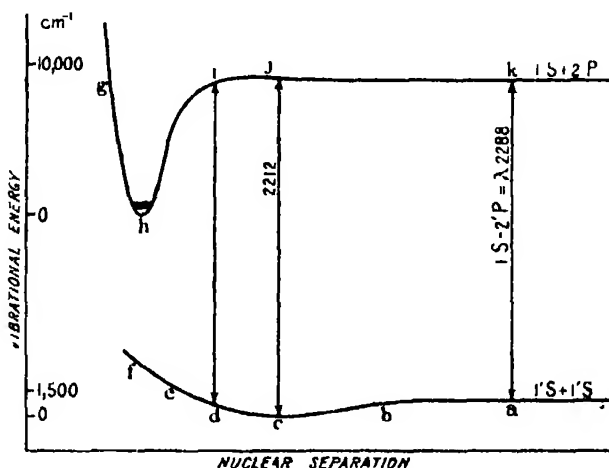


FIG. 1.—Potential energy curves for the cadmium molecule.

Our earlier results can be explained in part at least in a similar manner. However, to formulate a more complete explanation of the earlier results and those reported in this paper, the theory must be extended to include many body collisions as qualitatively suggested by us, and more definitely by Franck.*

The new experiments on gaseous xenon and their interpretation are presented in the following order. The first part of the paper shows how the absorption coefficient for various wave-lengths in the band varies with pressure. The results indicate the pressures at which collisions between more than two atoms become effective in the absorption. The second part describes a temperature effect, and in the third part results are presented which indicate the relative

* 'Naturwiss.,' vol. 10, p. 217 (1931).

broadening of the bands associated with λ 1295.6 Å. (1S_0 — $^1P^{\circ}_1$) and λ 1469.6 Å. (1S_0 — $^3P^{\circ}_1$).

I. *The Effect of Pressure on the Absorption with Cells of Different Lengths.*

(a) *Experimental.*—In our present investigation the light from a gold spark operating in an atmosphere of pure hydrogen, passed through the absorption cell and illuminated the slit of a fluorite spectrograph. The spectrograph and spark chamber were those described in our previous communication, and the absorption cell was of the type shown in fig. 2. The body of the cell was constructed of brass with ground tapered surfaces (a) and (b) which fitted similar attachments on the spectrograph and spark chamber making airtight

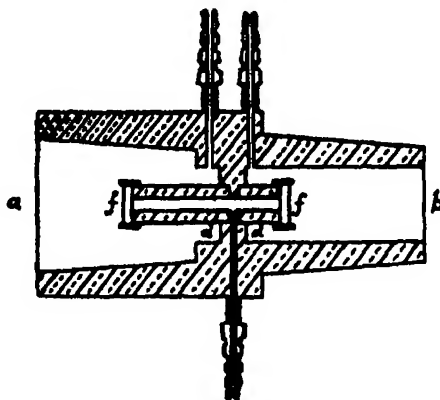


FIG. 2.

seals when greased. Plates (f) of clear fluorite were fastened with a hard red wax in the main body of the cell at (d). The length of the cell could be changed by using tubes of different lengths. With this construction it was not necessary to alter the distance between the source and the spectrograph slit whenever a change was made in the cell length.

Photographs of the absorption spectrum of various columns of gaseous xenon corresponding to cell lengths of 0.2, 1.0, 2.0, 5.0, 7.0 and 10.0 cm. and to a number of pressures between 10 and 800 mm. mercury were taken on Schumann plates. During exposures all other factors which would influence the absorption were kept constant. The temperature was kept at 18° C. and the time of exposure was 60 minutes for all photographs. Further, to insure a fairly constant intensity of illumination during the exposures, cells of identical cross-section were used, the current exciting the source was kept

constant, the spark gap was set at 3 mm. and as pointed out before, the distance between the source and spectrograph slit was maintained the same for all cell lengths.

Spectroscopically-pure xenon was used in these experiments. Before each exposure it was purified in a pyrex bulb by an arc discharge between a tungsten electrode and a pool of melted potassium heated by the arc. The xenon was passed from the purifier to the absorption cell through a U-tube immersed in methyl alcohol at -100° C. which prevented any mercury vapour from an attached manometer from entering the cell.

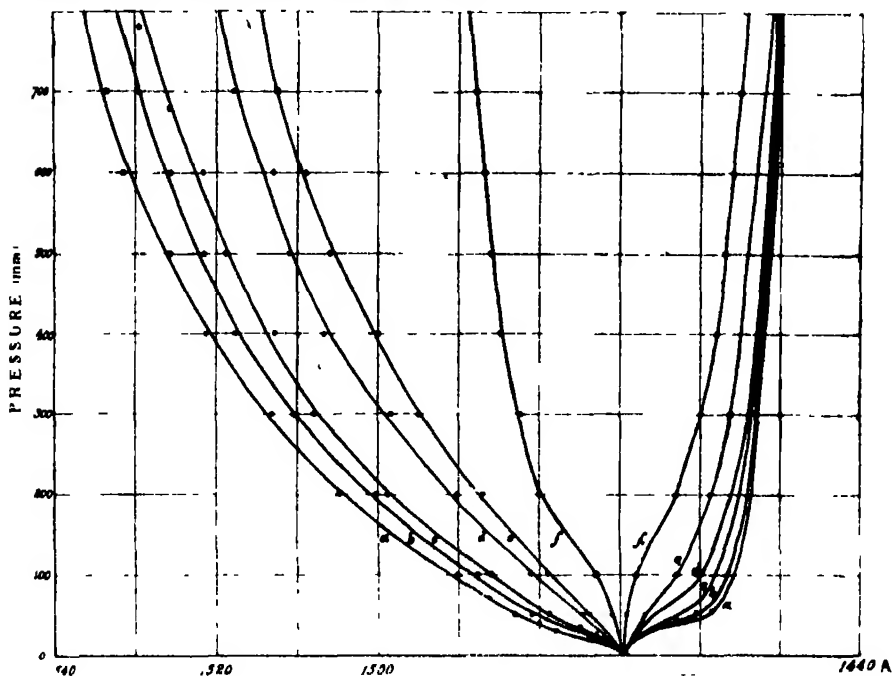


FIG. 9.

(b) *Results.*—The complete results are given by a graphical method in fig. 9. However, to facilitate the interpretation of this figure, reproductions of a number of the original spectrograms are first presented in figs. 3 to 8, Plates 18 and 19. Each figure shows how the absorption band broadens with pressure for a particular cell length. The lowest strip in each set of prints is the gold spark spectrum transmitted by the empty cell. The second strip shows the narrow part (at λ 1469.6 Å.) of this spectrum absorbed by xenon at 10 mm. pressure. The remaining seven strips show how the absorption broadens as the pressure is raised by equal steps from 100 to 700 mm.

Fig. 9 is composed of data from all the spectrograms. In it the wave-lengths of the band edges, such as shown in figs. 3 to 8, are plotted as abscissae against the corresponding pressures as ordinates. The wave-length of a band edge is taken as the wave-length of the last spark line of average normal intensity recorded on the photographic plate. The points corresponding to the same cell length fall approximately on a smooth curve. The curve for each cell length is drawn in heavily and designated a and a_1 for the 10 cm. cell, b and b_1 for the 7 cm. cell, c and c_1 for the 5 cm. cell and so on.

These curves show qualitatively the nature of the absorption. The asymmetrical development of the band to the long wave side is quite obvious. Further, it may be seen that the development to the short wave side is rapid at first but becomes slower and slower until beyond λ 1451 Å. further development is barely perceptible.

(c) *Discussion.*—For any particular cell length, the spreading of the absorption with pressure is due to two possible causes, increase in the frequency of collisions (if the phenomenon depends on atomic interactions) and increase in the number of atoms in the absorption path. If collisions are not involved the broadening of the absorption should depend only on the number of atoms present. That is, the absorption in cells with different lengths and pressures but with the same number of atoms should be identical. However, if collision frequency is involved the absorption by the same number of atoms will change with pressure if the temperature is kept constant. It is thus imperative to separate out these two effects. This can readily be done by considering the data given in fig. 9. From the curves three appropriate tables are constructed. For each table the product cell-length-times pressure is constant. This is the condition, since the temperature was constant, for having the same number of atoms in all the cells cited in a table. Thus, any variation in the absorption limits shown in columns 3 and 4 of a table must be due to variation in collision frequency with pressure. The data in these columns show quite definitely that the process is one of absorption of light during collisions. This is in contrast with those cases of the ultraviolet absorption bands of the normally stable molecules of the hydrogen-halides, alkali-halides, etc., where there is no broadening of the absorption bands with pressure when the number of atoms is kept constant.

Information as to the type of collisions can be obtained by evaluating the absorption coefficient and finding how it varies with pressure. According to Lambert's law of absorption

$$I = I_0 e^{-k l},$$

where

I_0 = intensity of unabsorbed light.

I = intensity of light after passing through a thickness L of the absorptive medium.

k' = the absorption coefficient.

Table I.—Cell-length \times Pressure = 140.

Cell length.	Pressure.	Long wave limit.	Short wave limit.
cm.	mm.	A.	A.
7 0	20	1473	1468
5.0	28	1474	1468
2 0	70	1477	1466
1.0	140	1482	1466
0.2	700	1488	1455

Table II.—Cell-length \times Pressure = 700.

Cell length.	Pressure.	Long wave limit.	Short wave limit.
cm.	mm.	A.	A.
10 0	70	1487	1458
7.0	100	1488	1457
5.0	140	1491	1457
2.0	350	1503	1453
1.0	700	1513	1452

Table III.—Cell-length \times Pressure = 3500.

Cell length.	Pressure.	Long wave limit.	Short wave limit.
cm.	mm.	A.	A.
10.0	350	1517	1452
7.0	500	1522	1451
5.0	700	1526	1451

In our experiments the law is applied to selected lines of the same intensity estimated visually from the unabsorbed spectrum. In addition it is assumed that the sensitivity of the Schumann plate is constant for the wave-length region over which the absorption extends. For this assumption and for constant conditions of exposure, I , the intensity after absorption of any of

these selected lines that is just capable of producing a record will be the same for all spectrograms. Thus for an absorption limit

$$\left. \begin{aligned} I/I_0 &= \text{constant} = e^{-kL} \\ k &= c/L; c = \text{constant.} \end{aligned} \right\}$$

The reciprocal of the cell length then gives a measure of the absorption coefficient for the wave-length of an absorption limit.

To show how the absorption coefficient varies with pressure and with wave-length the results given in fig. 9 are re-arranged. First, as an intermediate step, the curves in fig. 10 are constructed. For each curve which corresponds to a constant pressure the cell length (L) is plotted against the wave-length (λ) of a limit of the absorption band. The values used in constructing these curves were taken from the smooth curves in fig. 9. Using the curves to interpolate cell length (L), values of k ($= 1/L$) proportional to the absorption coefficient k' ($= c/L$) for various wave-lengths can be calculated for different pressures. Tables IV and V show typical relative values k of the absorption coefficient derived in this manner.

Table IV.—Pressure of Xenon = 200 mm.

Wave-length.	Absorption coefficient.	Wave-length.	Absorption coefficient.
A.	k .	A	k .
1485	1.7	1463	5.0
1487	1.14	1460	1.41
1490	0.63	1457	0.68
1495	0.29	1454	0.13
1500	0.167		
1504	0.103		

Table V.—Pressure of Xenon = 400 mm.

Wave-length.	Absorption coefficient	Wave-length.	Absorption coefficient
A.	k .	A.	k .
1495	1.9	1460	5.0
1500	1.06	1457	1.64
1505	0.58	1454	0.67
1510	0.294	1452	0.14
1515	0.176		
1520	0.108		

These tables are quoted simply to show the order of magnitude of the variation in the absorption coefficient with wave-length and with pressure.

The data in fig. 10 indicate the types of collisions involved in the absorption process. In this figure the variation with pressure of the absorption coefficient for a particular line can be traced. For example consider $\lambda 1475$ A. The cell lengths, which, for the pressures marked on the curves, produce an absorption limit at this wave-length, are given by the ordinates of the intersection of the vertical line through $\lambda 1475$ A. with the different pressure curves. The reciprocals of these cell lengths give values of k proportional to the absorption

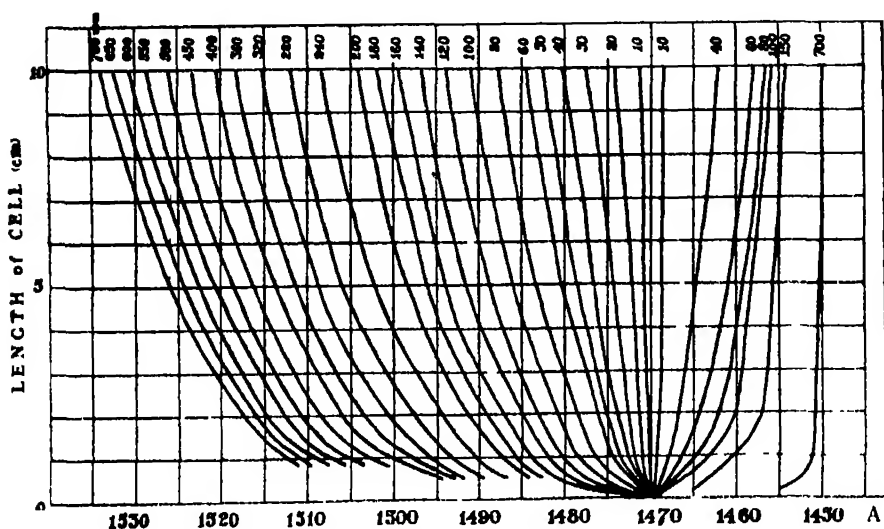
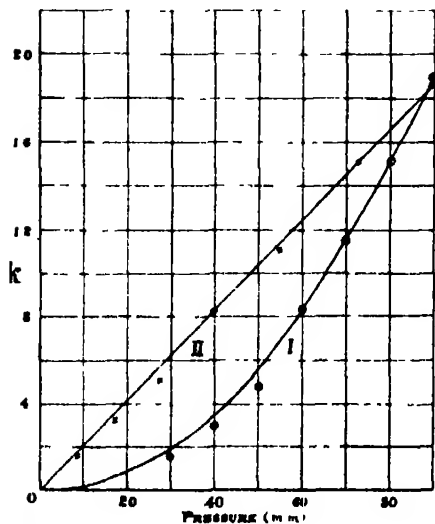
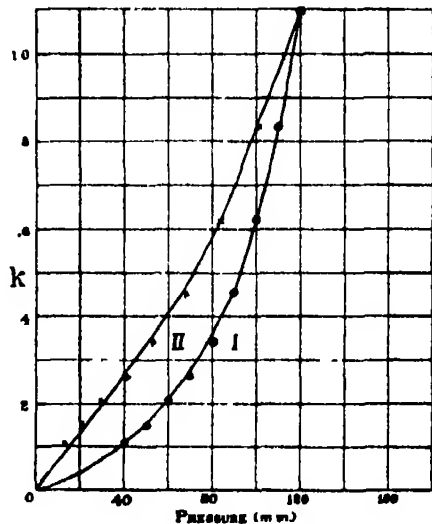
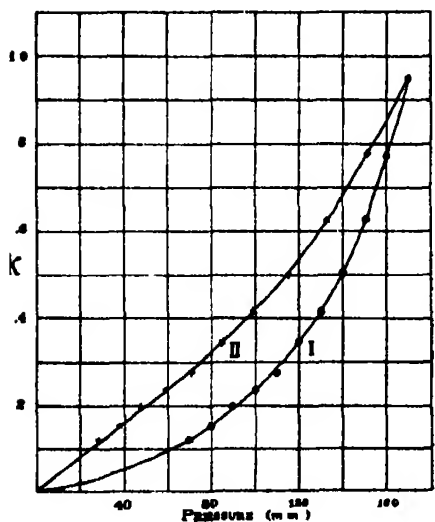
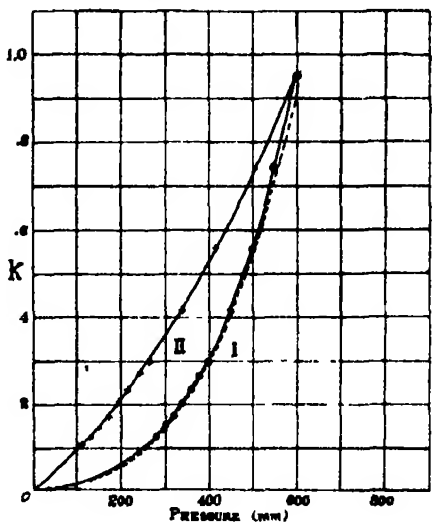


FIG 10.

coefficients for $\lambda 1475$ A. for the various pressures. The variation with pressure of these numbers k is shown by curve I in fig. 11. [Since $\lambda 1475$ A. is near the resonance line the observations are limited to pressures below 90 mm. The shape of curve I suggests that the law is parabolic; this is confirmed by curve II in the same figure which shows a linear relation between k and p^2 . In fig. 12 similar curves are given for $\lambda 1480$ A. However, in this figure, curve II shows that the parabolic relation between absorption coefficient and pressure holds only for pressure up to 90 mm. Above this pressure the slope of the p^2k curve increases showing that a single quadratic term is no longer sufficient. Figs. 13 and 14 for $\lambda 1485$ A. and $\lambda 1510$ A. respectively show that for still higher pressures the slopes of the p^2k curves continue to increase. The same general shape of these curves II definitely shows that for pressures above 90 mm. the absorption coefficient depends also on additional pressure terms of powers higher than the second.

The dependency of the absorption coefficient upon pressure can be explained on the assumption that the absorption occurs during atomic collisions. The results show that for pressures below 90 mm. the absorption coefficient varies

FIG. 11.—Absorption coefficient for λ 1475.FIG. 12.—Absorption coefficient for λ 1480.FIG. 13.—Absorption coefficient for λ 1485.FIG. 14.—Absorption coefficient for λ 1510.

as the square of the pressure. According to the kinetic theory of gases the frequency of two-body collisions per unit volume also varies as the square of the pressure. Since by definition k' , the absorption coefficient, is proportional

to the number of absorbers per unit volume, and since it is improbable that the absorption efficiency (molecular absorption coefficient) of two-body collision aggregates* varies appreciably with pressure, it appears that the variation in the absorption coefficient is entirely owing to the change in the number of these two-body aggregates. Above 90 mm. the relation between k' and p includes in addition to the square term, higher power terms in p . This is consistent with the collision mechanism of absorption. By the kinetic theory the frequency of three-body collisions would be proportional to p^3 and the number of three-body aggregates relative to the number of two-body aggregates would be appreciable at the higher pressures. Further, it is possible that higher terms representing many-body collisions will become effective at still higher pressures, especially near liquefaction points.

The absorption of xenon then can be explained as primarily due to absorption during collision when the atomic energy levels are perturbed by mutual interactions. At lower pressures mainly two-body collisions are effective, while at pressures above 90 mm., and at room temperature, our results show that collisions between three or more atoms occur frequently enough to affect appreciably the absorption, as suggested by Franck (*loc. cit.*).

Attempts have been made to analyse the pk curves and to determine the relative frequency of occurrence of two- and three-body collisions. As an example this is done for the curve of λ 1510 which has a fairly wide range of pressures. The agreement between the continuous observed curve and the dotted synthetic curve is fair. The relation between k and the pressure (p) may be expressed

$$k = 6.9 \times 10^{-7} p^2 + 3.1 \times 10^{-9} p^3.$$

The values of each term give approximately the relative frequency of two- and three-body collisions. However, our method of determining the absorption coefficient is such that these values cannot be considered very accurate.

The above considerations show that for low pressures two-body collisions mainly are involved, and the question arises as to the possibility of two colliding normal atoms uniting to form a weakly bound molecule. During our research a faint detached band was looked for. Although no separate band was found, the shape of the absorption curves in fig. 9 suggests that one exists. The failure to observe this as a detached band was probably owing to the masking by the broadening resonance line. The repetition of this experiment at lower temperatures and pressures would be more favourable for detecting a detached

* A convenient term for a system of two atoms interacting during collision.

band. However, by interpreting the sudden short wave-length shift apparent in the band at low pressures, fig. 9, as caused by feebly bound normal diatomic molecules, the maximum value of the stability of such loose van der Waals combinations is estimated as 0.07 volts. This is only an approximation because of the uncertainty in considering the short wave-length shift as entirely caused by the normal diatomic molecule.

II. *The Effect of Temperature.*

The absorption of gaseous xenon at different temperatures between 100° C. and -100° C. was studied with the cell shown in fig. 15. Fluorite windows (*f*) were waxed 2 cm. apart in the brass body of the cell, which was heat insulated

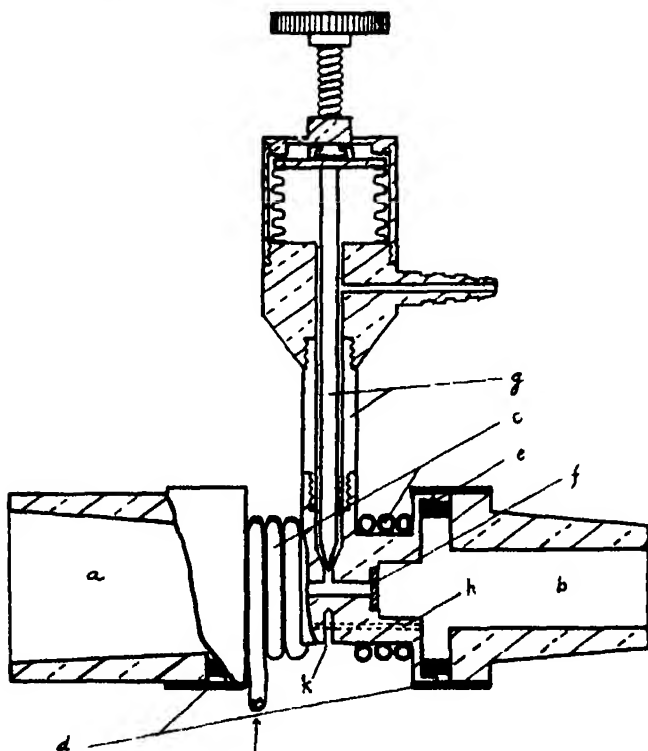


FIG. 15.

from the tapered ground brass fittings (*a*) and (*b*) by the flat rings of German silver (*d*) and the bakelite rings (*e*). The spindle and sheath (*g*) of the needle valve were also of German silver. The valve was of the packless type with the spindle movable within an airtight copper bellows. All metal to metal joints in the cell were soldered except the waxed connections between the flat

German silver rings and the brass tapers fitting to the spectrograph and spark chamber.

The temperatures below that of the room were obtained by a flow of cold hydrogen through copper coils (c) about the brass cell. The hydrogen was cooled by passing it through a copper spiral immersed in liquid air, and after circulating the cell coils was returned to a gasometer at atmospheric pressure. By controlling the flow of hydrogen various temperatures down to -100°C . could be maintained. Hydrogen was employed here because of its high heat conductivity and the ease with which it can be dried. Temperatures in the neighbourhood of 100°C . were obtained by passing steam through the cell coils. The temperature of the cell was determined by means of a thermocouple placed at (k).

These experiments were performed with a constant mass of gas in the absorption cell. This condition was obtained by applying to the xenon pressures calculated to give at the various temperatures the constant mass of gas desired in the cell. As a check on this method of assuring constant mass (and density) the experiments were repeated with the chosen mass of gas fixed by a pressure of 300 mm. mercury and temperature 20°C sealed in the cell by the needle valve. The results from each method were the same.

The arrangement of source, cell and spectrograph was that described in the first part of this paper.

The results of the temperature investigation are shown in fig. 16, Plate 20. The wave-lengths of the absorption limits are plotted against temperatures for the range from -100° to 100°C . For these temperatures the variation in the position of the long wave-length limit was quite small. This limit shifted slightly towards the longer wave-lengths as the temperature was increased. The short wave limit of the band, however, showed a distinct shift towards the shorter wave-lengths with decreasing temperatures. This latter shift became noticeable at about -75°C . as shown by the right-hand curve of fig. 16.

In Part I of this paper it has been definitely shown that the width of the band depends on frequency of collision. For this experiment, performed with the gas at constant mass and density, collision frequency increases as the square root of the absolute temperature, consequently one expects off hand that the band will broaden with increasing temperatures. A consideration of the pressure curve for a 2 cm. cell in fig. 9 shows that the shift produced by a change in collision frequency corresponding to a 200° change in temperature above that of the room is quite small. In particular the change in temperature from 18° to 100°C . increases the collision frequency by a factor of

$373/291 = 1.13$. Consider the 300 mm. pressure point on curve *d*, fig. 9, 18° C. The value to which the pressure will have to be increased from 300 mm. to increase the collision frequency by 1.13 can be calculated considering two- and three-body collisions, and the relation between collision frequency (proportional to *k*) and pressure established in Part I.

$$6.9 \times 10^{-7} p^2 + 3.1 \times 10^{-9} p^3 = k = 0.146 \text{ for } p = 300 \text{ mm.}$$

We wish to find the value of *p* for which $k = 0.146 \times 1.13 = 0.165$. This is given by the equation

$$6.9 \times 10^{-7} p^2 + 3.1 \times 10^{-9} p^3 = 0.165,$$

whence, by trial, $p = 315$ mm. The broadening produced by the pressure change from 300 mm. to 315 mm. then should be equal to the broadening produced by the temperature change from 18° to 100° C. provided the only effect of temperature is to increase the frequency of collision.

Similar considerations show that a pressure change from 271 to 300 mm. should produce the same change in band width as the temperature change from -100° to 18° C. The experimental curves *dd*₁ show that the change in band width for a pressure change from 271 to 315 mm. is quite small. Consequently if the only effect of temperature is to change the frequency of collision, no large change in the band width is anticipated for the temperature change from -100° to 100° C. for the cell length and density of gas used.

Our observations in regard to the long wave-length edge of the band are in complete agreement with the above predictions. The variation in position of the short wave-length band limit is also negligible down to -75° C. However, at this temperature a rapid shift to shorter wave-lengths starts. This shift is much larger and is in the opposite sense to that expected for the effect of decreasing temperature on the frequency of collision. Since it is inconceivable how the decreasing temperatures, giving less available energy of agitation, can modify the potential energy of two colliding atoms, the effect cannot be explained by absorption during collision. It is quite probable that the effect is due to the absorption by relatively stable many-body aggregates which absorb the shorter wave-lengths. Although from -75° to 100° C. the probability of formation of many-body aggregates decreases, the actual number may increase owing to the smaller probability of dissociation by thermal agitation.

It is significant that the effect is observed only when the temperature is near the point of liquefaction (B.P. = -109° C.). If the above interpretation

is tenable the experiment indicates that the formation of aggregates is involved in the process of liquefaction. A study of the short wave-length absorption when the xenon is changed continuously from gas to liquid is under consideration. Further, an investigation of the variation of the absorption coefficient with pressure at low temperatures is contemplated in order to detect the presence of aggregates stable near liquefaction points. Absorption by stable aggregates would be revealed by a linear pressure term in the expression for the absorption coefficient.

III. *Comparison of the Bands at λ 1469.6 Å. and λ 1295.6 Å.*

For the vapours of zinc, cadmium and mercury the band absorption about the shorter resonance line ($^1S_0-^1P_1$) is much broader than that about the longer resonance line ($^1S_0-^3P_1$). It is of interest to see if the above feature is also characteristic of xenon. Accordingly the band absorption about the shorter resonance line λ 1295.6 Å. was investigated.

The spectrograph used for the investigation in the region $\lambda\lambda$ 1250–1850 Å. was a one-metre vacuum grating giving a dispersion of 17.4 Angstroms per millimetre. The background spectrum used in this absorption experiment was produced by passing a low potential discharge of 40 milliamperes through a mixture of hydrogen and carbon monoxide, contained in a 3 mm. pyrex capillary tube 20 cm. long. The absorption cell consisted of a pyrex tube 7.5 cm. long and 1 cm. in diameter closed at the ends by two clear fluorite plates. A side tube fused into the wall of the pyrex cylinder connected the cell to the gas system which was essentially that used in the experiment described in Part I. Each end of the cell was waxed into a brass tapered mounting. One of these fitted a cone on the spectrograph and held the cell directly in front of the slit; the other, at the end of the cell remote from the spectrograph, was tapered so that the discharge tube could be coaxially attached to the absorption cell. With this arrangement the light had only to traverse two fluorite windows in passing from the source through the cell to the slit of the spectrograph. The first fluorite plate sealed the discharge tube from the absorption cell, and the second plate formed a vacuum seal separating the cell from the spectrograph.

With this equipment the variation of the absorption with pressure was studied for a range of pressures between 10 and 720 mm. at room temperature. The series of spectrograms taken when the cell contained xenon are practically all too faint for favourable reproduction of the region about λ 1295.6 Å. However, on visual inspection the original plates definitely show the variation

in the absorption at λ 1295.6 Å. The band develops with increasing pressure and the greater spread is to the long wave side of the resonance line λ 1295.6 Å. In this respect the band is similar to that about λ 1469.6 Å. The width of the band about λ 1295.6 Å., however, is smaller than the width of the band about λ 1469.6 Å. For example, at 180 mm. pressure for which we have a clear plate, the total width of the λ 1295.6 Å. band is 20 Angstroms. Under the same experimental conditions the width of the λ 1469.6 Å. band which appears on the same plate is 53 Angstroms. Although for higher pressures the exact limits of the absorption about λ 1295.6 Å. cannot be traced, however, at no pressure up to 720 mm. was λ 1330 Å. absorbed. Thus for 720 mm. pressure, fig. 17, Plate 20, the long wave shift of the λ 1295.6 Å. band cannot be more than 35 Angstroms ($\lambda\lambda$ 1330–1295 Å.). The long wave-length spread of the λ 1469.6 Å. band from the same plate is 75 Angstroms ($\lambda\lambda$ 1544–1469 Å.). At these two pressures (180 and 720 mm.) the shifts are decidedly larger for the band of longer wave-length, and it appears quite probable that this is characteristic at all intervening pressures.

Xenon, since its upper absorption band shows a larger spread than its lower, then stands in contrast to the vapours of zinc, cadmium and mercury where the reverse is the case. The potential energy curves representing the initial state for both bands are identical, since they both arise from absorption of light by colliding normal atoms. The difference in the behaviour of the bands is then owing to a characteristic difference in the potential energy curves representing the excited states. In the case of the λ 1469.6 Å. band the excited state of the aggregate involves one of the atoms in the excited 3P_1 state. For the λ 1295.6 Å. band the excited aggregate involves an atom in the excited 1P_1 state. Since the latter band is the narrower it appears, according to the accepted theory of Born and Franck, that for the case of the rare gas xenon, aggregates involving an atom in the 1P_1 state are less stable than those aggregates involving an atom in the 3P_1 state.

In conclusion, the authors wish to thank the National Research Council of Canada for a scholarship awarded to one of them, R. Turnbull. They are also indebted to Mr. M. F. Crawford for valuable assistance received from him during the investigation, and to Messrs. The Adam Hilger Company for a contribution made towards the purchase of the xenon used.

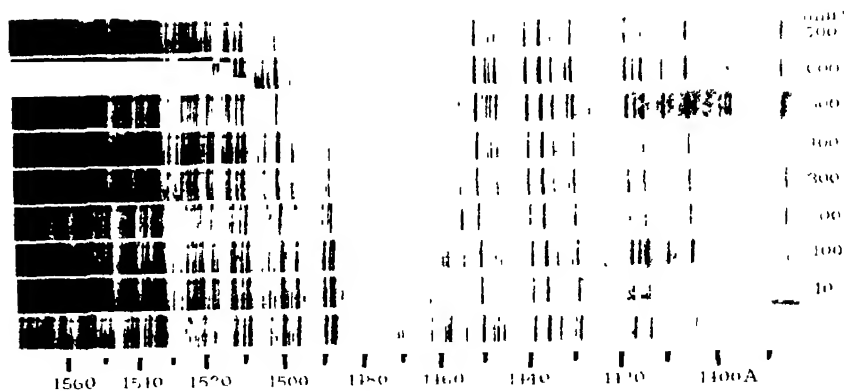


FIG. 3.—Cell length 0.2 cm.

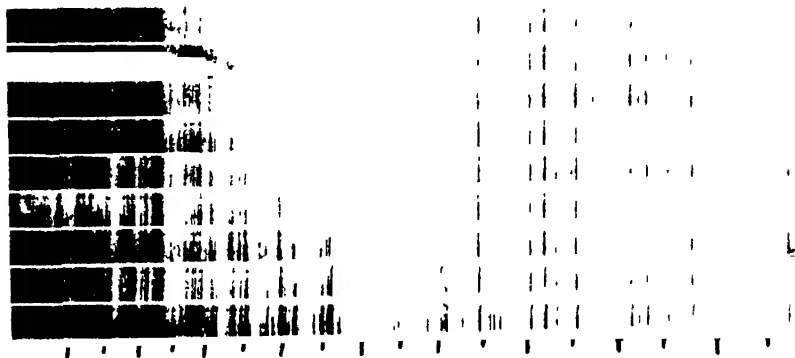


FIG. 4.—Cell length 1.0 cm.

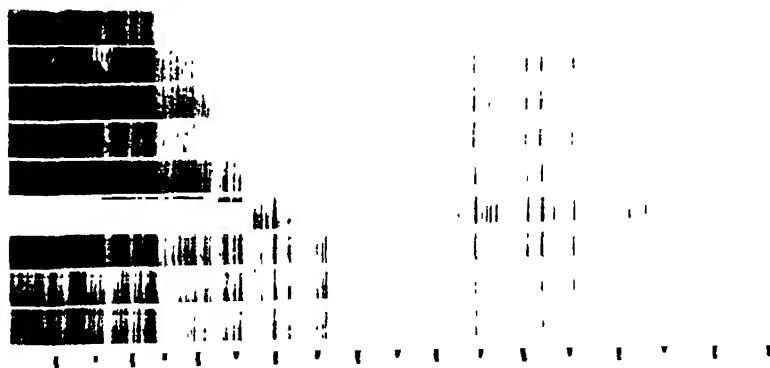


FIG. 5.—Absorption of Xenon. Cell length 2.0 cm.

(Facing p. 698)

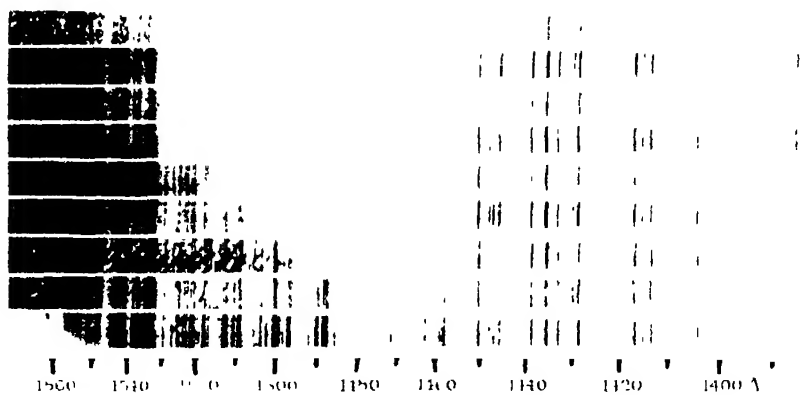


FIG. 6. Cell length 5.0 cm.

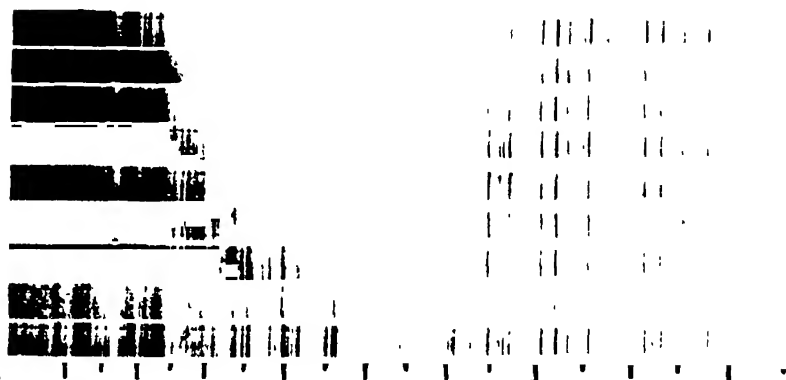


FIG. 7. Cell length 7 cm.



FIG. 8. Absorption of Xenon. Cell length 10 cm.

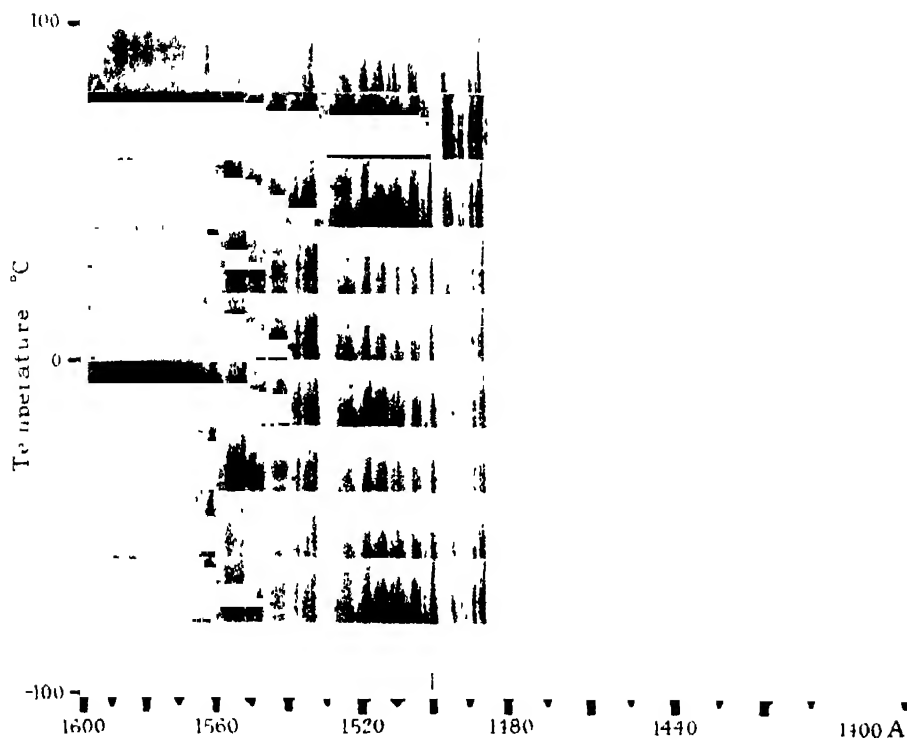


Fig 16

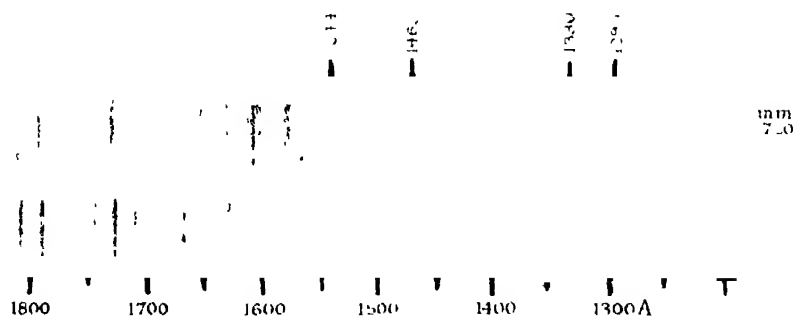


Fig 17

Some Photographs of the Tracks of Penetrating Radiation.

By P. M. S. BLACKETT and G. P. S. OCCHIALINI, The Cavendish Laboratory,
Cambridge University.

(Communicated by Lord Rutherford, O.M., F.R.S. —Received February 7, 1933.)

{PLATES 21-24 }

1. The Experimental Method.

We have recently developed a method by which the high speed particles associated with penetrating radiation can be made to take their own cloud photographs.* By this means it is possible to obtain these photographs very much more speedily than by the usual method of making expansions at random. For when this latter method is used it is only on a small fraction of the photographs that a track will be found. The average number of photographs required to obtain one track will depend on the size and orientation of the chamber and on the effective time of expansion. The latter is not likely to be more than 1/20 second. From measurements with counters it is known that about 1.5 fast particles fall, from all directions, on 1 sq. cm. per second. Roughly consistent with these figures are the results found with cloud chambers. Skobelzyn† has obtained as many as one track every ten expansions, but in the work of Anderson‡ the number of tracks which were long enough to be suitable for energy measurements was only about 1 in 50 photographs. By our method, tracks are found on 80 per cent. of the photographs. We intend to give a full account of the technique of this method of photography in a separate paper, confining ourselves here to a rough outline only §

A cloud chamber of diameter 13 cm. and depth 3 cm. is arranged with its plane vertical and two Geiger-Muller counters, each 10 cm. by 2 cm. are placed one above and one below the chamber so that any ray which passes straight through both counters will also pass through the illuminated part of the chamber, fig 2. An alternative arrangement is described on p. 719. The

* 'Nature,' vol. 130, p. 363 (1932).

† 'C. R. Acad. Sci. Paris,' vol. 195, p. 315 (1932)

‡ 'Phys. Rev.,' vol. 41, p. 405 (1932).

§ Mott-Smith and Locher 'Phys. Rev.,' vol. 38, p. 1399 (1931); vol. 39, p. 883 (1932) have found a correlation between the occurrence of these tracks and the discharge of a counter, and Johnson, Fleischer and Stroet, 'Phys. Rev.,' vol. 40, p. 1048 (1932) have used coincidences to operate the illuminating flash of a continuously working closed chamber.

counters are connected to a valve circuit arranged to record only simultaneous discharges of the two counters.*

The piston of the chamber is a light aluminium disc attached to the rest of the chamber by means of a rubber diaphragm and so free to move sufficiently to make the expansion. Before an expansion the piston is in equilibrium under the pressure of gas in the chamber, about 1.7 atmospheres, and the same pressure of air below it. The expansion is caused by opening a valve which allows the air under the piston to escape to the atmosphere. The sequence of events during operation is as follows. When a coincidence occurs the grid of a thyratron connected to the amplifier becomes positive, so that the thyratron short circuits a small magnet, which had previously held up a light armature against a spring. The armature flies off and moves a catch which releases the valve under the piston, and so causes the expansion. By careful attention to the detailed design of the various parts it has been possible to make the total time from the discharge of the counters to the end of the expansion as small as 1/100 second. In this time the ions produced by an ionizing particle only diffuse a short distance from the position where they are formed: the resulting tracks have a breadth in oxygen at 1.7 atmospheres of only 0.8 mm. and this breadth, though of course much larger than that of tracks formed by particles passing through at the end of the expansion, is small enough to allow very accurate measurements. The observed breadth is in good agreement with that calculated from the known rate of diffusion of the ions.†

About 1/100 second after the expansion the illuminating flash begins. This lasts about 1/30 second and is produced by passing a large transient current from a 4000-volt transformer through a capillary mercury lamp.

The whole chamber is placed in a water cooled solenoid capable of maintaining a field of 3000 gauss over the whole chamber. Two cameras are employed, one with its axis coincident with the axis of the chamber and so parallel to the magnetic field, and one with its axis making an angle of 20° with this direction. The two photographs of a track were not viewed stereoscopically, as the angle of 20° is too large for this, but the plates were replaced in the cameras and illuminated from behind, so as to throw two images back into the object space. Wire models of the tracks could thus be built up full size in the object space. This method of stereoscopic reprojection is essentially that used by Curtiss,‡ and by Williams and Terroux.§ It is of the utmost

* Rossi, 'Nature,' vol. 125, p. 636 (1930).

† Blackett and Occhialini, *loc. cit.*

‡ Curtiss, 'Bull. Stand., J. Res.,' vol. 4 p. 663 (1930).

§ Williams and Terroux, 'Proc. Roy. Soc. A,' vol. 126, p. 280 (1930).

importance to use two cameras, to give two photographs from different directions, for one photograph alone gives little definite information.

The average time of waiting from the moment of making ready to the first coincidence was found to be about 2 minutes, which is in agreement with the observed *rate* of about two coincidences a minute.

Over 700 photographs have been made in this way and on over 500 of these are found the tracks of particles of high energy

In order to investigate the interaction of these particles with matter, plates of various metals were in many experiments placed across the middle of the chamber. Anderson* has used a lead plate in this way and we have used in addition to lead both copper and tungsten plates. In some recent experiments thick metal blocks have been placed immediately over the upper counter (B 1, fig. 2) to investigate the nature of the secondary particles produced by various metals

2. The Photographs

About 75 per cent. of the successful photographs show a single track caused by a particle which has passed through both counters. The majority of these are not appreciably deflected in a magnetic field of 2000 gauss. Since the minimum deflection which we could consider significant was a little over one degree, they must have therefore a radius of curvature greater than about 500 cm. and so an Hp greater than 10^6 gauss-cm. Since the energy E of an electron, expressed in electron volts, is given approximately by $E = 300 \text{ Hp}$ (provided $E \gg mc^2 \sim \frac{1}{2} \times 10^6$ volts), the mean energy of the undeflected particles, assuming them to be electrons, is greater than about 300 million volts. Many curved tracks are also observed, corresponding to electrons of lower energy.†

By using magnetic fields up to 18,000 gauss, both Millikan and Anderson,‡ and Kunze§ have been able to deflect nearly all the particles. The results of the two investigations do not appear to be in complete agreement, but both find that deflections in either direction occur with comparable frequency. The distribution seems roughly continuous up to a maximum Hp of about 7×10^6 gauss-cm. corresponding to an electron energy of 2×10^9 volts.

The remaining 25 per cent. of the photographs show either a single track not

* Anderson, *loc. cit.*

† An electron must have an energy greater than about 5×10^6 volts in order to be able to pass through the 5 mm. glass walls of the chamber and the 1 mm. brass walls of the counters.

‡ 'Phys. Rev.', vol. 40, p. 325 (1932); Anderson, *loc. cit.*

§ 'Z. Physik,' vol. 79, p. 203 (1932).

passing through both counters or else they show the groups of two or more tracks, which were first discovered by Skobelzyn* and which are now so well known a feature of penetrating radiation. The occurrence of these multiple tracks is clearly related to the various secondary processes occurring when penetrating radiation passes through matter. The investigation of these secondary particles by means of counters was first carried out by Rossi† and later by Johnson and Street.‡

A most striking result of the present work has been to reveal the astonishing variety and complexity of these multiple tracks. Already 18 photographs have been obtained on which are the tracks of more than 8 particles of high energy and four photographs show more than 20 tracks.

Thirteen photographs are reproduced on Plates 21 to 24, and a detailed description is given of each.

A very lengthy investigation will certainly be required before it will be possible to give a complete interpretation of the extraordinarily complex atomic phenomena which are responsible for these groups of tracks. In this paper a preliminary and mainly qualitative account will be given of some of the more striking phenomena observed in the photographs, leaving almost all the details and the measurements for subsequent reports.

The most noticeable feature which is common to many of these multiple tracks is the occurrence of a group of several tracks diverging, mainly downwards, from some region in the material surrounding the chamber (Nos 1 and 2, 3, and 4, 8, 9, 10, 11, 12 and 13, Plates 21 to 24). Sometimes a group of these tracks appear to diverge fairly accurately from a single point; sometimes two or more such radiant points can be detected and often there are stray tracks not obviously related to the main groups. The majority of the tracks forming these groups are not appreciably deflected by the magnetic field of 2000 gauss. When such a shower of particles is seen to have entered the top of the chamber, it is not infrequently found that a subsidiary radiant point occurs in the metal plate, which in some of the experiments is placed across the chamber (Nos. 8, 11). When this occurs it is sometimes found that particles of great energy are thrown backwards in a direction nearly opposite to that of the incident shower (No. 11).

* Skobelzyn, 'Z. Physik,' vol. 54, p. 686 (1929), 'C. R. Acad. Sci. Paris,' vol. 194, p. 118 (1932); Auger and Skobelzyn, 'C. R. Acad. Sci. Paris,' vol. 189, p. 55 (1929); Mott-Smith and Locher, *loc. cit*

† 'Phys. Zt.' vol. 33, p. 304 (1932); 'Acad. Lincei,' vol. 15, p. 734 (1932).

‡ 'Phys. Rev.,' vol. 40, p. 635 (1932)

3. The Nature of the Particles in the Showers.

To begin to unravel these complexities it is first necessary to identify the particles producing the tracks. It is not always easy to do this as the evidence furnished by the photographs is often inconclusive. But it will be shown that it is necessary to come to the same remarkable conclusion that has already been drawn by Anderson* from similar photographs. This is that some of the tracks must be due to particles with a positive charge but whose mass is much less than that of a proton.

The most important measurement is the curvature of the track by the magnetic field, as expressed by the product $H\rho$, of the magnetic field by the radius of curvature of the track.

In addition the ionization density along the track can be roughly estimated, and, in some cases, the direction of motion of the particles can be inferred. In rare cases a particle stops in the gas of the chamber so that its range can be measured, and even when this is not so, the knowledge that the range is greater than a definite amount is sometimes of decisive importance.

Now the ionization density due to a fast particle depends only on its charge and velocity, but not on its mass. But the velocity of a particle of given $H\rho$ depends on its mass, so two particles *with the same $H\rho$ but different masses* will ionize differently.† Consequently the simultaneous observation of the $H\rho$ of a track and the ionization along it allow, in principle, the mass of the particle to be determined.

Now the variation of ionization density along the track of a β -particle has been determined experimentally‡ for values of v/c up to 0.95, and can be estimated theoretically for higher values. For our purpose it is convenient to take the values for the rate of loss of energy obtained theoretically by Bethe.§ The two curves, fig. 1, show the energy loss along the track of an electron and a proton as a function of $\log_{10}(H\rho)$. It can be seen that there is little difference between the ionization due to the two kinds of particles when their $H\rho$ is greater than about 1.5×10^6 gauss-cm. But for smaller values of $H\rho$, the

* 'Science,' vol. 76, p. 238 (1932).

† The relation between the velocity v and $H\rho$ is

$$\frac{v}{c} = H\rho \left/ \left\{ \left(\frac{mc^2}{e} \right)^2 + (H\rho)^2 \right\}^{\frac{1}{2}} \right.$$

where m is the mass and e the charge in e.s. units.

‡ Williams and Terroux, *loc. cit.*

§ 'Ann. Physik,' 'Z. Physik,' vol. 76, p. 293 (1932).

heavier particle, in consequence of its smaller velocity, ionizes much more readily. Consequently, if a track is observed to have an $H\rho$ less than, say, 1.0×10^6 , it is easily possible to decide if the mass is of the order of that of an electron or that of a proton. In a similar way the observation of the $H\rho$

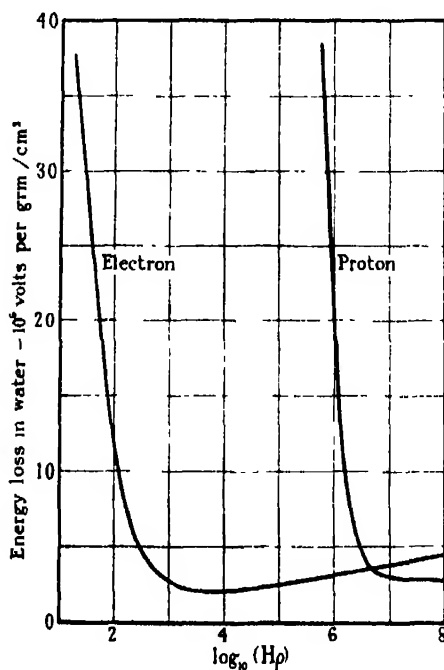


FIG 1

of a track and its *range* allows the mass of the particle to be estimated. In Table I are given the ranges and velocities* of protons and alpha-particles of given $H\rho$.

Table I.—Relation between $H\rho$, Velocity and Range of Protons and Alpha-Particles.

$H\rho \times 10^{-4}$ gauss-cm		0.5	1.0	2.0	3.0	4.0
Protons—						
Velocity $\times 10^{-9}$ cm./sec.		0.48	0.96	1.92	2.87	3.83
Range, cm. air 15°C		0.19	1.0	6.9	25.7	69.7
Alpha-Particles—						
Velocity $\times 10^{-9}$ cm/sec	0.24	0.48	0.96	1.45	1.93	0.49
Range, cm air 15°C	0.13	0.35	1.09	2.91	7.0	0.35
						0.72
						0.64
						0.97
						1.1

704, Table I. Last two rows of Table I should read :—

* Blackett, 'Proc. Roy. Soc.,' A. vol. 135, p. 132 (1932).

Anderson reports having found several tracks which must be attributed to positively charged particles of small mass, and discusses these photographs in detail, though the photographs themselves are not reproduced. In one the direction is given by the change of curvature in going through a lead plate, in another two tracks curved in opposite directions appear to leave the plate, and in a third two particles appear to leave the plate with a curvature corresponding to a positive charge. For all these, Anderson states that the ranges and specific ionization show that positively charged particles must be present with a mass much less than that of a proton.

To decide the sign of the charge of a particle it is necessary to know in which direction it was moving. There are four ways of obtaining this information from a photograph. (a) If a particle passes through a metal plate, which is thick enough to cause it to lose an appreciable part of its energy, then the particle must have moved from the side of greater H_p to that of less, since the possibility that the particle has gained energy in the plate may be neglected. If the particle is quite slow it may be possible to detect the change of H_p owing to the loss of energy while passing through the gas. (b) Again, if a particle produces a secondary of sufficient energy by collision with, say, a free electron, then the direction of the secondary will indicate the direction of motion of the particle. (c) If a group of tracks diverge from some point or some small region of space, then there is a high probability, but no certainty, that any one particle did actually move away from this region. (d) If a track is observed in a nearly vertical direction, then it is more probable that the particle has moved downwards than upwards. The evidence for this last assumption is the fact that the ionization from penetrating radiation increases upwards. It is hard, however, to estimate these probabilities numerically, as the frequency of such events as in No. 11, Plate 23, where at least one particle of high energy is thrown upwards, is unknown.

Now on photographs 3 and 4 the majority of the tracks are undeflected ($H_p > 10^6$), but there are some which are definitely curved and of these some are curved in one direction and some in the other.* The appearance of the whole group strongly suggests that the particles have diverged downwards, and if this is assumed true, those bent to the left are negatively charged and those bent to the right are positively charged. There are two of the latter,

* A single nearly vertical track will be said to have a positive curvature if curved as for a positive charge moving downwards. A track which forms part of a shower will be said to have a positive curvature if curved as for a positive charge moving away from the apparent region of divergence of the shower. Similarly for negative curvatures.

with values of H_p of 0.4×10^5 and 1.5×10^5 gauss-cm. If these two tracks were due to protons their ranges could only be 0.2 cm. and 3 cm., in air, whereas their actual lengths *in the chamber* are about 12 cm. of air at N.T.P. So these tracks are certainly not due to protons, but to particles of much smaller mass. Two similar tracks can be seen in photographs 1, 2, one in 9, one in 10 and probably two in 13.

The study of the ionization density along the tracks entirely confirms these conclusions.

It is strikingly evident from their appearance that the ionization density along the positively curved tracks in the photographs mentioned is very nearly the same as that along the undeflected and negatively curved tracks. It is, unfortunately, not possible to make a precise count of either the primary or the total ionization along these tracks without special experiments,* but rough counts have shown that the ionization density common to all these tracks is approximately that to be expected for fast electrons. Further, by comparing the appearance of an undeflected track with that of a slow secondary β -particle of known energy, it becomes clear that any track, along which the ionization is about three times greater than this, can be easily recognized. (See description of No. 11.) Consequently it is legitimate to conclude that these tracks cannot possibly be due to protons. If they were due to protons the ionization would be between 10 and 100 times as heavy, and the tracks would look like that in No. 14 where there is an undoubted proton track of $H_p \sim 3 \times 10^5$ gauss-cm.

The only possible conclusion of the argument both from the range and from the ionization is that these tracks are due to positively charged particles with a mass comparable with that of an electron rather than with that of a proton. It is, of course, conceivable that some of these tracks are caused by negative electrons moving upwards, which only by chance pass through the region from which the other tracks appear to diverge. It is difficult to estimate this chance numerically, but the presence of these positively curved tracks is so common a feature of these showers that this explanation can hardly be maintained for them all.

Altogether we have found 14 tracks occurring in showers which must almost certainly be attributed to such positive electrons, and several others which are less certain.

* This can be done by working with H_2 or He, as has been done by Anderson and the writers, or by introducing a time delay into the mechanism so as to allow the ions time to diffuse away from each other.

Until larger fields are available it will not be possible to find the ratio of the number of the positive and negative particles in the showers, but there seems some slight evidence that in some showers at least the numbers are about equal. Of the tracks which are appreciably deflected in photographs 1, 2, Plate 21, and 3, 4, Plate 22, about equal numbers go to the right and to the left. In general however, negative particles are more frequent

Additional evidence, independent of the showers, for the existence of a positively charged particle with a mass comparable with that of an electron is found in photograph No. 7. In this, the particle passes through a 4 mm. lead plate. The track is seen to be more curved below the plate than above, so the particle must have moved downwards unless it be assumed that it gained energy in traversing the plate, hence it had a positive charge. Corresponding to the final $H\rho$ of 1.2×10^5 gauss-cm it would only have had a range of 1.5 cm. in air if it had been a proton and it would have ionized more than 100 times as much as a fast electron. Its range is certainly greater than 5 cm. and it ionizes just like a fast electron.

Several tracks have been observed in which the presence of a secondary formed in the gas indicates the direction of motion of the particle passing through both counters, and in most cases the direction indicated is downwards as is to be expected. But on photograph No. 14, Plate 24, a track is seen which can only be due to a positive electron, if the evidence of the secondary is to be trusted. There is always, however, the possibility that such a slow secondary (about 35,000 volts) may have been deflected by a subsequent collision so that its apparent direction of projection is not its original one. So not much weight can be put on this one track.

No. 5 shows a secondary produced in the plate indicating a downward direction of motion and one of the two tracks below shows a positive curvature, which, though small, does seem to be considerably greater than any possible fictitious curvature owing to distortion by movement of the gas.

It is unfortunate that in our experiments the magnetic field was not sufficient to deflect appreciably the majority of the tracks, either those appearing singly or those in showers. But, as has already been mentioned, the measurements of Anderson and of Kunze were made with much larger fields, and though not in complete agreement with each other show conclusively that about equal numbers are deflected either way, and this is also true of those tracks in our photographs which are appreciably deflected. Anderson and Kunze find respectively that 30 per cent. and 60 per cent. are positively deflected.

Now it is certainly possible that almost all the single tracks are due

to particles which have originated as part of showers, which have occurred higher up in the atmosphere or in other material far above the chamber. If this is so, one would expect to find about the same ratio of the numbers of positive and negative particles amongst the single tracks as are found in the showers. What experimental evidence is available suggests that this may be so.

But the evidence of such photographs as No. 11, Plate 23, shows that fast particles are sometimes projected upwards, so that it is certain that a few of the single tracks are due to particles moving upwards and not downwards.* It is impossible, therefore, to be certain of the sign of the charge of the particle, producing a particular single track, from the curvature alone, unless other evidence of its direction is available. Still it is certainly safe to conclude that the majority of the positively curved tracks are due to positive particles moving downwards.

However, it is not easy to agree with Anderson and Kunze that the positively curved tracks are mainly due to protons. For, as already mentioned, it is a striking feature of our photographs that the great majority of the tracks have almost the same specific ionization. Now Kunze finds that the mean energy of the protons (for this he assumes the positively curved particles to be) is about 4×10^8 volts. Protons of this energy ($H_p \sim 3.5 \times 10^6$ gauss-cm.) ionize not very differently from electrons (see fig. 1). But if such fast protons are present, then there must also be some slower ones present, for the stream of descending particles must certainly be fairly heterogeneous at the bottom of the atmosphere, whatever it may be at the top, and these slower tracks will ionize more strongly and so produce noticeably denser tracks. Four tracks have been found showing the character of proton tracks of which two are on No. 14 and one on 13, but in no case are they to be classified with the main group of downward moving particles, but rather with some local nuclear disintegration process. Further, all the single tracks which do show marked positive curvature have nearly the same specific ionization as the undeflected ones, so are either negative electrons going up, or positive electrons coming down. By a positive electron is meant a particle with unit positive electronic charge and with a mass very much less than that of a proton.

So the conclusion seems justified that the main beam of downward moving particles consists chiefly of positive and negative electrons. Some protons are probably also present.

* Skobelzyn has also shown the existence of such particles 'C. R. Acad. Sci. Paris,' vol. 195, p 315 (1932).

4. The Frequency of the Showers

It seems plausible to assume that the showers of particles arise from some nuclear disintegration process stimulated by particles or protons of high energy associated with the penetrating radiation. The fact that most of the showers diverge downwards makes this probable.

It is possible that these showers of particles are related to the occurrence of the bursts of ionization found originally by Hoffmann* and studied by Stemke, Schindler, Messerschmidt, and others. These have been definitely shown to be correlated with the intensity of the penetrating radiation by experiments in deep mines. It is hoped to investigate in a similar way the frequency of the showers by means of multiple coincidence counting. It is, however, conceivable that some part of the phenomena of the showers may be of spontaneous nuclear origin.

These showers are certainly much rarer in comparison with the single tracks than their frequency of occurrence on our photographs would seem to indicate. For the frequency of occurrence of a given type of track depends on the product of its actual frequency of occurrence multiplied by the probability that when it occurs both counters will be operated. This last probability is very different for showers and single particles. We find about one shower to every *thirty* single tracks. But the actual ratio of the number of showers crossing the chamber to single tracks is certainly much less than this. For if a single particle crosses the *chamber*, there is only a small chance (about one in 200) that it will pass through both *counters*, while if a shower of many particles passes through the chamber there may be quite a high chance, perhaps as high as 1 in 5, that a coincidence will result. So the ratio of showers to single tracks on our photographs may be forty times greater than the ratio of their actual occurrence.

The showers appear to originate indifferently in any of the material surrounding the chamber. Since the chamber is nearly surrounded by the copper solenoid the majority originate in the copper, but radiant points have also been located in the glass walls and roof of the chamber, in the aluminum piston and in the air of the room. When plates of lead and copper have been placed across the centre of the chamber groups of tracks have been found to radiate from points in the plate. A tungsten plate has also been used for a few photographs, but nothing of special interest has been found with it.

* Full references are given by Hoffmann, 'Phys. Z.', vol. 17, p. 633 (1932), Stemke and Schindler, 'Z. Physik,' vol. 75, p. 115 (1932), 'Naturwiss.', vol. 26, p. 491 (1932), Messerschmidt, 'Z. Physik,' vol. 78, p. 668 (1932).

It is of interest to make a rough estimate of the frequency of these showers in relation to the number of nuclei in the surrounding material. One coincidence occurs every 2 minutes, and one shower with more than 8 tracks about every thirty coincidences; that is, once every hour. These come predominantly from the part of the copper solenoid above the chamber, say from a mass of 10 kg of copper. Taking the chance to be 1 in 5 that a shower which has originated in this copper will set off the counters we get that one shower originates in 10 kg. of copper about every 10 minutes. Expressed in the form of a mean life one finds a value of about 10^{18} years.

Alternatively we can obtain a rough lower limit for the effective area of a copper nucleus for the production of such showers by assuming that all the incident fast particles are effective. Since there are about 1.5 of these per sq. cm. per minute, we find the effective area of a copper nucleus to be about 10^{-27} sq cm.

It is possible to make a rough estimate of the amount of ionization which would be produced in an ionization chamber of the type used by Steinke and Schindler by such a shower as that in photographs Nos. 1 and 2. The photographs show about 20 tracks with energies very much more than sufficient to pass right across such an ionization chamber. Taking the air equivalent depth of the ionization chamber as 240 cm., and allowing 80 ion pairs per centimetre of path, we get for the total ionization produced about 4×10^5 ion pairs. Though this is less than the value of 3×10^6 given by Messerschmidt (*loc. cit.*) for the lower limit of the ionization bursts, there are almost certainly, in the showers, many more particles than actually pass through the cloud chamber, and some of these may be of greater mass and charge and so have a larger specific ionization. The evidence of Nos. 14 and 15 shows that some protons at least are produced. And there may be still other particles with still greater ionizing power which only rarely succeed in entering the gas of the chamber so as to become visible.

It must be remembered that the chance that an ionizing particle, which originates at some random point in the walls of the chamber or the surrounding material, should be observed as a track, is proportional to its range and so is inversely proportional to its ionizing power. In general, heavily ionizing particles will not reach the chamber at all and so will not be observed. It is not impossible therefore that such short range particles are produced along with the penetrating ones in the processes giving rise to the showers.

It seems, therefore, likely that the phenomena of the showers in a cloud chamber and these ionization bursts are related, though the latter are both

rarer and show greater ionization than any showers that we have yet observed.

The total energy of the particles crossing the chamber in photographs Nos. 1 and 2 is more than 2×10^9 volts, this is obtained by assuming 20 tracks of 100×10^6 volts each.

5. *The Mechanism of the Showers.*

The showers are almost certainly due to some process that involves the interaction of particles or photons of high energy with atomic nuclei. Existing theory appears to be able to deal approximately with the interaction of such particles and photons with the extra-nuclear electrons, and Heisenberg* has recently collected the relevant results for comparison with such experiments as these on penetrating radiation. We intend to study the frequency of occurrence, on our photographs, of the scattering processes and of the production of secondaries, both by particles and photons. Photograph No. 5, Plate 22 shows the production, by a fast particle, of a secondary particle of energy about 60 million volts.

The effective area of cross-section for the collision of an electron or proton of very high energy with a free particle of mass m and unit electronic charge

$$2\pi e^4/mc^2\epsilon, \quad (1)$$

where ϵ is the energy given to the particle initially at rest. The direction of projection θ of this particle is given by

$$\tan^2 \theta = 2mc^2/\epsilon. \quad (2)$$

It will be noticed that the mass of the incident particle does not enter into these expressions. Several collisions, in which this last relation is approximately satisfied, have been photographed.

From (1) we find that the free path in lead for the production of a secondary electron with energy of 100 million volts is about 16 cm, our experiments confirm this as regards order of magnitude. It is clear from this figure that the chance of two or more secondaries being produced independently nearly at the same point is very small. So when one track is seen to branch at one point into three or more tracks, it is impossible to resist the conclusion that some nuclear interaction has taken place. If an incident photon is considered the same argument is valid.†

* 'Ann. Physik,' vol. 13, p. 430 (1932), 'Naturwiss.,' vol. 21, p. 365 (1932).

† Millikan and Anderson, *loc. cit.*, Skobelzyn, *loc. cit.*

It is clear that there are several distinct processes giving rise to the complex tracks. In a few cases the processes seem fairly simple. An incident particle probably a negative or positive electron ejects three or more particles presumably from a single nucleus. No. 15 shows probably that an incident particle has ejected two electrons (both with $E_e \sim 13$ million volts) from a copper nucleus together with one proton. Other particles may have been ejected also, but may have had too small a range to escape from the plate. No. 11 shows two electrons ($E_e \sim 10$ and 13 million volts) ejected downward from a lead nucleus and two tracks of greater energy ($E_e > 100$ million volts) directed upwards. It is possible that one of the latter represents the incident particle causing the disintegration and that the other is an ejected particle moving upwards, or that both are ejected particles, in which case the disintegration must be attributed to some non-ionizing agency.

But these two cases are comparatively simple compared with the complexity of the larger showers. In these, the typical process seems to be the simultaneous ejection of a number of particles of high energy. These particles seem usually to be projected in directions lying within a fairly narrow cone, but there are occasions (No. 10) when the cone is fairly wide. It seems reasonable to seek the explanation of the narrow cone of projection in the momentum imparted by the collision of some incident particle of very high energy. It is not possible, as yet, to tell the nature of all the particles, but negative and positive electrons seem to predominate and there is some slight indication that in some cases they occur with about equal frequencies.

The origin of these particles is of great interest, particularly as they certainly often arise in materials of low and medium atomic weight, since radiant points have been located in air, glass, aluminium and copper. Now on recent views* of nuclear structure there are no free negative electrons in such light nuclei. Yet at least seven positive and negative electrons have been found diverging from a single point in glass, copper and lead (Nos. 10, 9 and 8), and presumably therefore from single nuclei.

There are three possible hypotheses that can be made about the origin of these particles. They may have existed previously in the struck nucleus, or they may have existed in the incident particle, or they may have been created during the process of collision. Failing any independent evidence that they existed as separate particles previously, it is reasonable to adopt the last

* Heisenberg, 'Z. Physik,' vol. 77, p. 1 (1932); Iwanenko, 'Phys. Z. Soviet Union,' vol. 1, p. 820 (1932); Mandel, 'Phys. Z. Soviet Union,' vol. 2, p. 286 (1932); Perrin, 'C. R. Acad. Sci. Paris,' vol. 195, p. 236 (1932).

hypothesis. Further, in view of the well-known difficulties* in treating electrons in a nucleus as independent mechanical entities, the last hypothesis becomes perhaps the most convenient. One would then describe these showers (in common with ordinary β -ray disintegrations) as involving a creation of particles.

This question is intimately bound up with that of the constitution of the neutron.† On the view that a neutron is a complex particle, the negative electrons in the showers might be produced by the disintegration of neutrons into negative electrons and protons, but this picture gives no explanation of the origin of the positive electrons. It also leads one to expect more proton tracks on the photographs than are actually observed.

On the view that the neutron is an indivisible particle and that there are no free negative electrons in light nuclei, it follows that both the negative and positive electrons in the showers must be said to have been created during the process. If, however, the conservation of electric charge is to be fulfilled, then positive and negative electrons must be produced in equal numbers, for there can hardly be many protons created on account of the large energy ($E \sim Mc^2 = 940$ million volts), required to create one |

In this way one can imagine that negative and positive electrons may be born in pairs during the disintegration of light nuclei. If the mass of the positive electron is the same as that of the negative electron, such a twin birth requires an energy of $2mc^2 \sim 1$ million volts, that is much less than the translational energy with which they appear in general in the showers.

Though one of the ultimate objects of the experiments must be to obtain the evidence on which to draw up a balance sheet of number of particles and of mass and energy, this will certainly prove exceedingly difficult to do. To attempt this, it will certainly be necessary to obtain a shower which originates in the gas of the chamber, so that the tracks of all the particles can be observed.

The fact that some of the showers show groups of nearly parallel tracks suggests at once a possible relation to the prediction by C. T. R. Wilson§ that "run away" electrons and protons of high energy are produced by the electric field of a thunderstorm. But if these particles, which certainly must exist,

* Bohr, "Report of Congress in Rome," (1931), 'J. Chem. Soc.', p. 349 (1932).

† Chadwick, 'Proc. Roy. Soc.,' A, vol. 136, p. 693 (1932).

‡ Another possible way in which electric charge may be conserved during a process involving the emission of an electron from a nucleus has been suggested to us by Professor Dirac. This is that a neutron may be converted into a proton simultaneously with the creation of a negative electron.

§ 'Proc. Camb. Phil. Soc.', vol. 22, p. 534 (1925), 'Proc. Phys. Soc.', vol. 31, 32D (1925).

appeared in the chamber, one might expect to find groups of widely spaced parallel tracks of varying breadth, owing to their having been formed at varying times before and during the expansion. Now it is characteristic of the showers that the tracks are almost always slightly diverging, that they are bunched together and that they have appreciably the same breadth, indicating that the particles passed through the chamber within a time small compared with the time of expansion (1/100 second). So it is certain that the showers are not themselves due to groups of "run away" electrons.

6 *The Hypothetical Properties of the Positive Electron*

The existence of positive electrons in these showers raises immediately the question of why they have hitherto eluded observation. It is clear that they can have only a limited life as free particles since they do not appear to be associated with matter under normal conditions.

It is conceivable that they can enter into combination with other elementary particles to form stable nuclei and so cease to be free, but it seems more likely that they disappear by reacting with a negative electron to form two or more quanta.

This latter mechanism is given immediately by Dirac's theory of electrons.* In this theory all but a few of the quantum states of negative kinetic energy, which had previously defied physical interpretation, are taken to be filled with negative electrons. The few states which are unoccupied behave like ordinary particles with positive kinetic energy and with a positive charge. Dirac originally wished to identify these "holes" with protons, but this had to be abandoned when it was found that the holes necessarily have the same mass as negative electrons.† It will be a task of immediate importance to determine experimentally the mass of the positive electrons by accurate measurements of their ionization and $H\beta$. At present it is only possible to say that no difference between the ionization from the tracks of negative and positive electrons of the same $H\beta$ has been detected so that provisionally their masses may be taken as equal.

On Dirac's theory the positive electrons should only have a short life, since it is easy for a negative electron to jump down into an unoccupied state, so filling up a hole and leading to the simultaneous annihilation of a positive and negative electron, the energy being radiated as two quanta.

* 'Proc. Roy. Soc.,' A, vol. 126, p. 360 (1930); A, vol. 133, p. 60 (1931).

† H. Weyl, "Gruppentheorie und Quantenmechanik," 2nd ed., p. 234 (1931).

We are indebted to Professor Dirac not only for most valuable discussions of these points, but also for allowing us to quote the result of a calculation made by him of the actual probability of this annihilation process. The area of cross-section for annihilation is*

$$\phi = \frac{\pi e^4}{m^2 v^4} f(\gamma), \quad (3)$$

where

$$f(\gamma) = \gamma + 1 - \frac{\gamma^2 + 4\gamma + 1}{\gamma^2 - 1} \log \{ \gamma + \sqrt{\gamma^2 - 1} \} - \frac{1}{\sqrt{\gamma^2 - 1}}$$

and $\gamma = 1/\sqrt{1 - v^2/c^2}$ and v is the velocity of the positive electron.

Dirac has computed the following values for the mean free path in water for annihilation. This is $\lambda = 1/n\phi$, where n is the number of extra-nuclear electrons per unit volume.

Table II.--Free Path for Annihilation and Range of Positive Electron.

E Energy in million volts	200	100	50	20	10	5	2	1	1/10
λ cm. H ₂ O	833	471	270	133	78.8	47.6	25.9	17.5	7.2
R Range, cm. H ₂ O	52	28	16	7.7	4.3	2.2	0.9	0.45	0.05

In the last row of the table is given the range of an electron in water. The values for energies below 2 million volts are experimental† and the rest theoretical.‡

If the chance that a positive electron will disappear in this way while decreasing in energy from E_1 to E_2 is denoted by $\Phi(E_1, E_2)$, then it is easily shown that

$$\log [1 - \Phi(E_1, E_2)] = \int_{E_2}^{E_1} dR/\lambda,$$

when dR is an element of its path and λ is the mean free path for annihilation of a particle of energy E .

A rough numerical integration using the figures in the table, given for the probability of annihilation of a positive electron, while decreasing in energy from 200 million volts to 100,000 volts, the value

$$\Phi(E_1, E_2) = 0.36$$

* Dirac, 'Proc. Camb. Phil. Soc.', vol. 26, p. 361 (1930).

† Rutherford, Chadwick and Ellis, "Radiation from Radioactive Substances," p. 443.

‡ Heisenberg, *loc. cit.*

If the probability of annihilation in water *per unit time* is evaluated, it is found that this probability increases as the energy decreases and reaches a constant value of $2.5 \times 10^6 \text{ sec.}^{-1}$, for energies less than 100,000 volts. So those positive electrons which live till they reach this energy will then die according to a probability law, exactly analogous to a radioactive decay, except that their mean life is proportional to the concentration of negative electrons. In water, their mean life is 3.6×10^{-10} second.

When the behaviour of the positive electrons have been investigated in more detail, it will be possible to test these predictions of Dirac's theory. There appears to be no evidence as yet against its validity, and in its favour is the fact that it predicts a time of life for the positive electron that is long enough for it to be observed in the cloud chamber but short enough to explain why it had not been discovered by other methods.

It should be possible to find evidence on the photographs of positive electrons which have entered a metal plate but which do not emerge again owing to their annihilation while traversing the metal. It is also possible that the gamma-ray annihilation spectrum may be detectable by observations of the Compton recoil electrons. According to Dirac's theory, this spectrum should have a lower limit at an energy of 0.5×10^6 volts and should extend through a maximum at a slightly greater energy to a steadily decreasing intensity for high energies.

It is not unlikely that positive electrons may be produced otherwise than in association with the penetrating radiation. Perhaps the anomalous absorption of gamma-radiation* by heavy nuclei may be connected with the formation of positive electrons and the re-emitted radiation with their disappearance. The re-emitted radiation is, in fact, found experimentally to have an energy of the same order as that to be expected for the annihilation spectrum.

Again the hypotheses of the existence of positive electrons amongst the secondary particles produced by neutrons, would provide an explanation of the curious fact discovered by Curie and Joliot† that fast electron tracks are found with a curvature indicating a negative electron moving *towards* the neutron source.

7. *The Non-ionizing Links and the Secondary Radiant Points.*

It is not possible to explain the appearance of the showers without assuming the existence in the showers of some non-ionizing agency. For it is not

* Gray and Tarrant, 'Proc. Roy. Soc.,' A, vol. 136, p. 662 (1932); Meitner and Hupfield, 'Naturwiss.,' vol. 19, p. 775 (1931); Chao, 'Phys. Rev.,' vol. 36, p. 1519 (1931).

† "Exposé de Physique Théorique," p. 21 (1933).

unusual to find that one or more tracks appear to originate in the plate without any track to correspond to an incident particle. To explain these secondary radiant points it is necessary to postulate that there exist in the showers non-ionizing particles or photons.

Now when two or more distinct radiant points are found above the chamber as in No. 1, it is reasonable to assume that one represents a secondary process caused by the other, or that both are secondary to some initial process. In either case, a surprisingly short free path for a further interaction must be

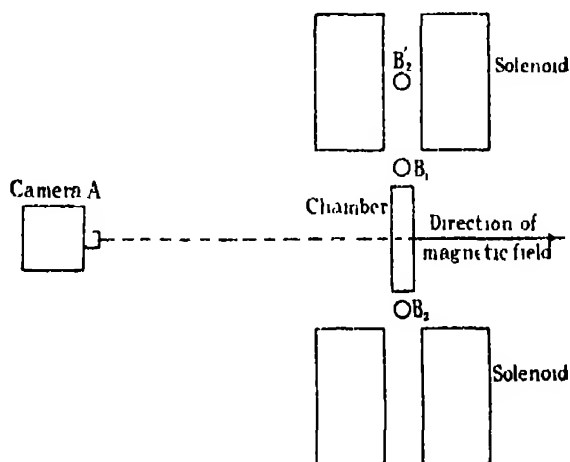


FIG 2

postulated for the particle or photon causing the secondary process. It can be seen from the photographs that when one shower occurs there is a surprisingly large chance that another will occur a short way below it. It will be of great interest to discover if this high probability can be explained by means of the assumption that the non-ionizing links are neutrons or photons.

The cost of the solenoid for producing the magnetic field was met by a grant from the Government Grant Committee of the Royal Society. One of us (G. P. S. O.) is indebted to the National Research Council of Italy for a grant to enable him to work in the Cavendish Laboratory.

We wish to express our appreciation of the skilful assistance given us by Mr. R. Aves, both in the construction of the apparatus and in the conduct of the experiments. We wish also to thank Mr. C. W. Gilbert, of Christ's College, for his invaluable assistance in the latter part of the investigations.

Summary.

(1) A short description is given of a method of making particles of high energy take their own cloud photographs.

(2) The most striking features of some 500 photographs taken by this method are described, and the nature of the showers of particles producing the complex tracks is discussed.

(3) A consideration of the range, ionization, curvature and direction of the particles leads to a confirmation of the view put forward by Anderson that particles must exist with a positive charge but with a mass comparable with that of an electron rather with that of a proton.

(4) The frequency of occurrence of the showers is discussed, and also their possible relation to the bursts of ionization observed by Hoffman, Steinke and others.

(5) The origin of the positive and negative electrons in the showers is discussed, and the conclusion is reached that they are best considered as being created during a collision process.

(6) The subsequent fate of the positive electrons is discussed in the light of Dirac's theory of "holes."

(7) The probable existence of non-ionizing links in the processes giving rise to the multiple showers is discussed.

DESCRIPTION OF PLATES

All the photographs were taken with the magnetic field at right angles to the chamber and directed *away* from the cameras, fig. 2. Consequently a downward descending particle will be deflected to the *right* as seen in the photographs if positively charged and to the *left* if negatively charged. Alternatively a positively charged particle will describe an anti-clockwise and a negatively charged particle a clockwise path, as viewed from the camera or in the photograph.

The photographs are reproduced 0.9 times the actual size of the tracks in the chamber. The gas in the chamber was in all cases oxygen, at an initial pressure of 1.7 atmospheres. An electric field of 3 to 4 volts per centimetre was maintained between top and bottom of the chamber. The expansion used was usually between 1.29 and 1.31.

Two cameras were used, (A) with its axis parallel to the magnetic field, (B) with its axis making an angle of 20° with this direction. Of the photographs reproduced, Nos. 1 and 2 are (stereoscopic) pairs, so are Nos. 3 and 4. All the rest are single photographs, either (A) or (B), depending on which showed the better detail.

The counters were usually arranged at positions B_1 and B_2 , fig. 2, but sometimes the lower counter was removed from B_2 and placed at B'_2 . Nos. 10 and 13 were taken with the latter arrangement, all the rest with the usual one. The usual position (B_1 , B_2) gives the better yield of tracks, but the other position (B_1 , B'_2) allows the photography of tracks which do not pass right through the chamber and the metal plate.

The angle between the axes of the cameras (20°) is too great for stereoscopic viewing and is so chosen as to give greater accuracy in reconstruction. Full size models of the complicated tracks were made with wire and plasticene by a method of stereoscopic reprojection.

In the description of the photographs the following abbreviations will be made.—

$H\rho$ = $H\rho$ gauss-cm = product of magnetic field by the radius of curvature of the track.

E_e = energy calculated from $H\rho$ assuming mass to be that of an electron.

MV = million volts

(A) or (B) indicates photograph from camera A or B

On some photographs there is a noticeable distortion and broadening of the tracks owing to mass movement of the gas (see Nos. 8 and 11 on the right-hand side, and No. 15 in the centre). This distortion impairs the accuracy of observation. But in general it is concluded that a curvature of $\rho \sim 500$ cm. is significant when there is no plate in the chamber and one of $\rho \sim 200$ cm. when there is a plate.

PLATE 21.

PHOTOGRAPH 1 (B) } Pair of photographs showing about 23 separate tracks. 4 mm. lead
 PHOTOGRAPH 2 (A) } plate. $H = 2200$ gauss.

A group of tracks appear in the upper part of the chamber diverging downwards and somewhat forward from some region, in the copper solenoid. A second fairly distinct group appears on the right-hand side of the photograph.

Most of the tracks pass through the lead plate, but there are so many of them that it is difficult to identify them all separately in the two images. Several secondary processes, scattering, etc., take place in the plate.

The majority of the tracks are nearly straight corresponding to electron energies greater than 100 MV. But two tracks in the middle of the upper part of the chamber are bent to the left with $H_p \sim 2 \times 10^5$, and so $E \sim 60$ MV. These tracks are almost certainly due to electrons.

There are also two tracks plainly bent to the right with $H_p \sim 0.7$ and 0.5×10^5 , and so with $E_e \sim 20$ and 15 MV. Since these tracks diverge from the same direction as the others they must be caused by positively charged particles. Since the ionization along them does not differ appreciably from that along the electron tracks, they must be due to particles with a mass comparable with that of an electron. The white blob is probably due to some heavily ionizing particle (if a contamination alpha-particle) passing through before the expansion.

The broad white band on the left of photograph B is caused by the reflection of the illuminated glass cylinder in the piston. It is very difficult to avoid this, but it does not appear in photograph A.



PLATE 22

PHOTOGRAPH 3 (B) } Pair of photographs showing about 10 separate tracks. $H = 3100$
 PHOTOGRAPH 4 (A) } gauss

The divergent point of the shower is again in the copper coils. On the left are two negative electron tracks with $H_p \sim 0.5 \times 10^6$ and so $E_e \sim 15$ MV.

On the right are two tracks curved markedly to the right, which must be due to positive electrons, with $H_p \sim 0.4$ and 1.5×10^6 , and so $E_e \sim 12$ and 45 MV.

Some of the other tracks are slightly curved, some one way, and some the other. Most of the nearly straight tracks seem to diverge from the same point, but the more bent ones probably diverge from a secondary radiant point lower down.

PHOTOGRAPH 5 (B) $H = 2200$ gauss. 4 mm. lead plate.

A single particle of too great energy to give a measurable curvature ($H_p > 3 \times 10^6$, $E_e > 100$ MV), passes through the lead plate and produces a secondary (?). Below the plate one track is appreciably straight and the other is curved for a positive charge with $E_e \sim 60$ MV.

PHOTOGRAPH 6 (A). $H = 2200$ gauss. 4 mm lead plate

Two particles one of which passes through the plate and is straight above the plate $E_e > 100$ MV, but curved negatively below $E_e \div 30$ MV. The apparent energy loss is too great for normal absorption, for Anderson has found an energy loss of 35 MV per centimetre lead.

PHOTOGRAPH 7 (B). $H = 2200$ gauss. 4 mm lead plate

A track showing deflection at plate and a greater positive curvature below than above. The direction must therefore be downwards, and hence the charge positive. Above plate $E_e \sim 60$ MV. Below, $E_e \sim 22$ MV. Energy loss too great again, but this is not unexpected since energy may well have been lost in the collision causing the deflection.

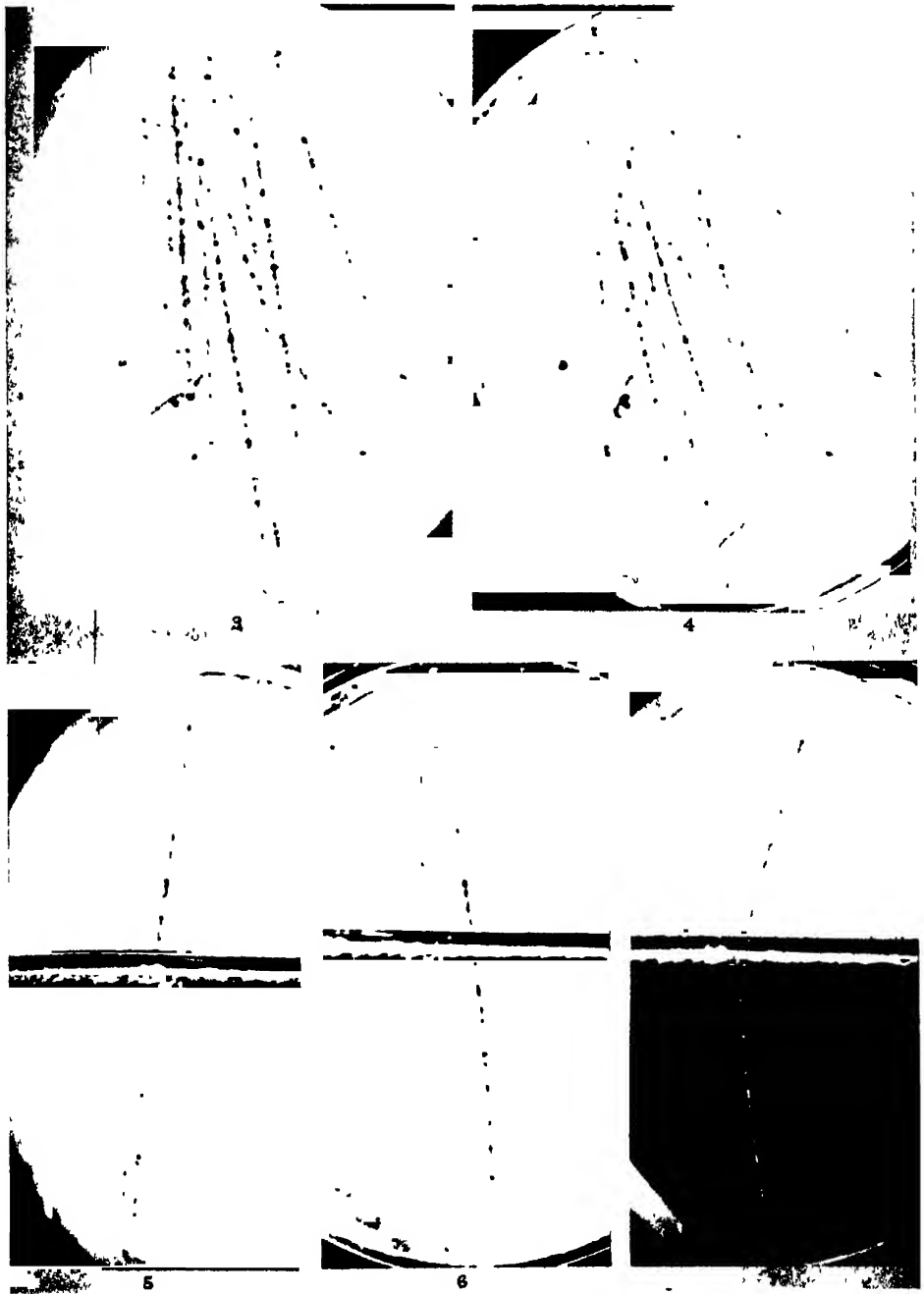


PLATE 23.

PHOTOGRAPH 8 (A). $H = 2200$ 4 mm lead plate.

A shower of about seven tracks comes through the roof of the chamber, radiating probably from the copper solenoid. A secondary radiant point occurs in the lead plate, from which a group of about six tracks diverge. From a careful study by stereoscopic reprojection it seems, but it is not quite certain, that no track of the primary shower passes through the point of origin of the secondary shower. If this is the case, it indicates that the secondary shower is produced by some non-ionizing agency in the primary shower. Below the plate, one track is negatively curved. The rest are nearly straight. Above the plate some tracks are broadened by distortion.

PHOTOGRAPH 9 (B). $H = 2200$ gauss.

A shower of four particles comes inclined through the top of the chamber.

Three more straight tracks diverge from a point in the glass roof. Above and to the left is a track curved to the left and in the middle is another track, coplanar with the former, curved to the right—probably a positive electron. These two tracks do not come from the same point as the three others, but from a neighbouring point.

The spiral track is a negative electron of energy about 130,000 volts, and may be due to the photoelectric absorption of a photon.

Several apparently unrelated tracks are to be noticed.

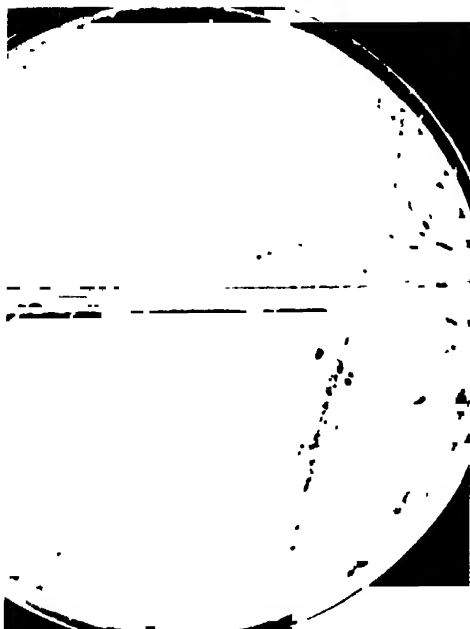
PHOTOGRAPH 10 (A) $H = 700$ gauss 6 mm. copper plate.

Seven tracks diverge from a point in the glass roof of the chamber. The curved track diverges accurately from the same point as the other six and so the particle producing it probably actually came from the point. The sign of the curvature then indicates a positive charge. $E_e \sim 120,000$ volts.

This track is the lowest energy positive-electron track so far observed. Several other, apparently unrelated, tracks are present.

PHOTOGRAPH 11 (A). $H = 2200$ 4 mm lead plate.

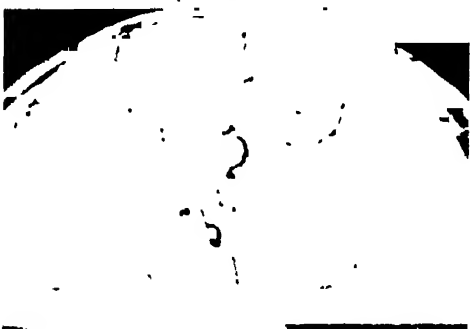
From a point in the lead two negative electrons of energy 13 and 10 MV diverge downwards, and two straight tracks diverge upwards. It is possible to assume (a) that one of the two latter is caused by a particle moving downwards and that the other is projected almost directly backwards and upwards, or (b) that both are projected upwards, in which case the disintegration process must be attributed to a non-ionizing agency. On either assumption the projection of at least one particle of high energy upwards is proved. This draws attention to the danger of assuming that all the penetrating radiation particles are moving downwards. On hypothesis (a) one of the particles can be considered as part of a primary shower from above the chamber, of which two other members are visible. Note secondary electron, $E_e \sim 5 \times 10^4$ volts, originating in gas. Such an electron ionizes between 2 and 3 times as much as a fast electron. Note great difference in appearance.



8



9



10



11

PLATE 24.

PHOTOGRAPH 12. $H = 2200$ gauss 4 mm. lead plate

Shower of four tracks from copper solenoid. One track is deflected by plate and one produces a secondary with negative curvature

PHOTOGRAPH 13. $H = 2200$ gauss

A complicated collection of curved tracks, three curved negatively and three positively, neglecting the lower short one. There appears to be a radiant region in the glass roof from which two negative and two positive electrons diverge, but it is not possible to say for certain that one of the positively curved tracks may not be due to a negative particle moving upwards

PHOTOGRAPH 14. $H = 3000$ gauss

Two proton tracks and two electron tracks. The thick horizontal track has an H_p of 3×10^6 and is curved as for a positive charge moving to the right. It is almost certainly due to a proton. For this H_p a proton would have a range of about 26 cm in air at N.T.P. and would ionize about 100 times as much as a fast electron. This

Page 726, Description of Photograph 14, fifth line. "0.6 cm." should read "2.9 c.m."

The two negatively curved tracks in the bottom of the photograph are the two long proton tracks, but the assumption that they *come* from the same point is made doubtful by the appearance of the slow secondary near the bottom, which appears to indicate a motion upwards and so a positive charge

PHOTOGRAPH 15. $H = 2200$ gauss 6 mm. copper plate

Presumably an incident particle which disintegrates a copper nucleus with the emission of two electrons $E_0 \sim 12$ and 14 MV, and one heavier particle, which is either a proton or an alpha particle. Unfortunately the tracks are badly distorted near the plate by the swirling of the air. Another track seems to be thrown backwards, but the distortion is too great to be certain. The resemblance of this photograph to No. 11 is marked except for the absence, in the latter, of the proton track. But it is quite probable that such particles are produced also in No. 11 and many other photographs, but that they do not have sufficient range to emerge from the plate. In any case the chance that a proton will emerge from the plate with just sufficient energy to stop in the gas as it has done in No. 15 is very small.



14

15

INDEX TO VOL. CXXXIX. (A.)

- Adam (N. K.) *See* Guggenheim and Adam
Adsorption at surface of solutions (Guggenheim and Adam), 218
Alpha-particles, products from radium C' (Briggs), 638.
Alpha-particles, relative velocities from thorium X (Briggs), 638.
Alpha-rays, analysis by annular magnetic field (Rutherford and others), 617.
Armstrong (G.) *See* Butler and Armstrong.

Barrell (H.) *See* Sears and Barrell.
Barometer, new primary standard (Sears and Clark), 130
Bell (R. P.) *The Application of Quantum Mechanics to Chemical Kinetics*, 466.
Beta-rays, maximum energy from uranium X (Sargent), 659
Black (M. M.) *See* Hartree and Black.
Blackett (P. M. S.) and Occhialini (G. P. S.) *Some Photographs of the Tracks of Penetrating Radiation*, 699.
Blair (G. W. S.) *See* Schofield and Blair
Bone (W. A.), Newitt (D. M.) and Townend (D. T. A.) *Gaseous Combustion at High Pressures*, XIV, 57.
Bowden (B. V.) *See* Rutherford and others.
Briggs (G. H.) *The Relative Velocities of the Alpha-Particles from Thorium X and its Products and from Radium C'*, 638.
Butler (J. A. V.) and Armstrong (G.) *The Kinetics of Electrode Processes*, II, 406.

Cadmium lamp radiations, comparison with Michelson lamp (Sears and Barrell), 202
Clark (J. S.) *See* Sears and Clark.
Collie (C. H.) *See* Gratias and Collie.
Collisions, inelastic, general theory (Massey and Mohr), 187.
Collisions, method of impact parameter (Williams), 163.
Combustion at high pressures, XIV, XV, XVI (Bone and others), 57, 74, 83
Concepts of inverse probability (Fisher), 343.
Cone moving at high speeds, air pressure on (Taylor and Maccoll), 278
Copper-cadmium alloys, X-ray study (Owen and Pickup), 526
Coster (D.) and Knol (K. S.) *The Atomic Scattering Factor for X-Rays in the Region of Anomalous Dispersion*, 459.
Crystal-photoeffect (Teichmann), 105.
Cuthbertson (C.) and Cuthbertson (Maude) *On the Refractivity of Para-Hydrogen*, 517.

Dob (S. C.) *On the Arc Spectrum of Iodine*, 380
Double layer, diffuse (Lens), 596.
Dutta (A. K.) and Sen Gupta (P. K.) *On the Absorption Spectra of some Higher Oxides*, 397.

Electric current, flow in semi-infinite stratified media (King), 237.
Electrode processes, kinetics (Butler and Armstrong), 406.
Electromagnetic fields due to variable electric charges (Schott), 37.

- Electron emission, secondary (Rao), 436.
 Electron scattering in helium (Werner), 113.
 Electrons, slow, collision with atoms (Massey and Mohr), 187.
 Electron wave equation, foundations (Milner), 349.
 Ellis (C D) The Corpuscular X-Ray Spectra of the Radio-Elements, 336.
 Ellis (C D) and Mott (N. F.) The Internal Conversion of the γ -Rays and Nuclear Level Systems of the Thorium B and C Bodies, 369.
 Ergosterol, surface potentials of unimolecular films (Fosbinder), 93.
 Evans (R. C.) The Positive Ion Work Function of Tungsten for the Alkali Metals, 604.
 Fisher (R. A.) The Concepts of Inverse Probability and Fiducial Probability Referring to Unknown Parameters, 343.
 Fosbinder (R. J.) On the Surface Potentials of Unimolecular Films of Ergosterol.—The Photochemical Formation of Vitamin D, 93.
 Frameworks, braced, calculation of stresses (Southwell), 475.
 Gamma-rays, internal conversion (Ellis and Mott), 369.
 Garner (W. E.) and Hailes (H. R.) Thermal Decomposition and Detonation of Mercury Fulminate, 576.
 Gaseous combustion at high pressures (Bone and others), 57, 74, 83.
 Gratias (O. A.) and Collie (C. H.) The Parent of Protactinium, 567.
 Griffiths (J. G. A.) See Norrish and Griffiths.
 Guggenheim (E. A.) and Adam (N. K.) The Thermodynamics of Adsorption at the Surface of Solutions, 218.
 Hailes (H. R.) See Garner and Hailes.
 Harkness (H. W.) and Heard (J. F.) The Stark Effect for Xenon, 416.
 Hartree (D. R.) and Black (M. M.) A Theoretical Investigation of the Oxygen Atom in various States of Ionisation, 311.
 Heard (J. F.) See Harkness and Heard.
 Helium, electron scattering (Werner), 113.
 Hinshelwood (C. N.), Moelwyn-Hughes (E. A.) and Rolfe (A. C.) The Combination of Hydrogen and Oxygen in a Silver Vessel, 521.
 Hopkins (Sir F. Gowland) Address at Anniversary Meeting, 1.
 Hydrogen and oxygen, combination in silver vessel (Hinshelwood and others), 521.
 Hydrogen and oxygen combination photosensitised by nitrogen peroxide (Norrish and Griffiths), 147.
 Iodine, arc spectrum (Deb), 380.
 Jackson, (D. A.) The Hyperfine Structure of the Lines of the Arc Spectrum of Rubidium, 673.
 King (L. V.) On the Flow of Electric Current in Semi-Infinite Stratified Media, 237.
 King (R. O.) The Beneficial Effect of Oxidation on the Lubricating Properties of Oil, 447.
 Knol (K. S.) See Coster and Knol.
 Lamont (F. G.) See Newitt and Lamont.
 Lens (J.) On the Diffuse Double Layer, 596.
 Lewis (W. B.) See Rutherford and others.

- Maccoll (J. W.) *See* Taylor and Maccoll.
- Massey (H. S. W.) and Mohr (C. B. O.) The Collision of Slow Electrons with Atoms, II, 187.
- McBain (J. W.) and McBain (M. E. L.) Sedimentation Equilibrium in the Ultracentrifuge; Types Obtained with Soap Solutions, 26
- McLennan (J. C.) and Turnbull (R.) The Broadening of the Ultraviolet Absorption Bands of Xenon under pressure, 683.
- Melville (H. W.) The Photochemistry of Phosphine, 541
- Mercury, fluorescent excitation (Rayleigh), 507.
- Mercury fulminate, thermal decomposition (Garner and Hailes), 576
- Michelson lamp radiations, comparison with cadmium lamp (Sears and Barrell), 202
- Milner (S. R.) On the Foundations of the Electron Wave Equation, 349
- Moelwyn-Hughes (E. A.) *See* Hinshelwood and others
- Mohr (C. B. O.) *See* Massey and Mohr
- Mott (N. F.) *See* Ellis and Mott
- Newitt (D. M.) *See* Bone and others.
- Newitt (D. M.) and Lamont (F. G.) Gaseous Combustion at High Pressures, XVI, 83.
- Norrish (R. G. W.) and Griffiths (J. G. A.) The Combination of Hydrogen and Oxygen Photosensitised by Nitrogen Peroxide, 147.
- Occhialini (G. P. S.) *See* Blackett and Occhialini
- Oil, lubricating properties (King), 447.
- Outridge (L. E.) *See* Townend and Outridge.
- Owen (E. A.) and Pickup (L.) X-Ray Study of Copper-Cadmium Alloys, 526
- Oxygen and hydrogen, combination in silver vessel (Hinshelwood and others), 521
- Oxygen atom, theoretical investigation (Hartree and Black), 311
- Para-hydrogen, refractivity (Cuthbertson and Cuthbertson), 517
- Penetrating radiation, photographs of tracks (Blackett and Occhialini), 699
- Phosphine, photochemistry (Melville), 541
- Pickup (L.) *See* Owen and Pickup
- Presidential address, 1
- Protactinium, parent (Gratias and Collie), 567
- Probability inverse and fiducial (Fisher), 343.
- Quantum mechanics, application to chemical kinetics (Bell), 466
- Radiation, penetrating photographs of tracks (Blackett and Occhialini), 699.
- Radiations emitted by new cadmium and Michelson lamp (Sears and Barrell), 202
- Rao (S. R.) The Efficiency of Secondary Electron Emission, 436.
- Rayleigh (Lord) Fluorescent Excitation of Mercury by the Resonance Frequency and by Lower Frequencies, V, 507
- Rolfe (A. C.) *See* Hinshelwood and others
- Rutherford (Lord), Wynn-Williams (C. E.), Lewis (W. B.) and Bowden (B. V.) Analysis of α -Rays by an Annular Magnetic Field, 617
- Sargent (B. W.) The Maximum Energy of the β -Rays from Uranium X and other Bodies, 659.

- Schofield (R. K.) and Blair (G. W. S.) The Relationship between Viscosity, Elasticity and Plastic Strength of a Soft Material as Illustrated by some Mechanical Properties of Flour Dough, II, 557.
- Schott (G. A.) On the Electromagnetic Fields due to Variable Electric Charges and the Intensities of Spectrum Lines According to the Quantum Theory, 37.
- Sears (J. E.) and Barrell (H.) Interferential Comparison of the Red and other Radiations emitted by a New Cadmium Lamp and the Michelson Lamp, 202.
- Sears (J. E.) and Clark (J. S.) A New Primary Standard Barometer, 130.
- Sedimentation equilibrium in the ultracentrifuge (McBain and McBain), 26
- Sen Gupta (P. K.) See Dutta and Sen Gupta.
- Southwell (R. V.) On the Calculation of Stresses in Braced Frameworks, 475
- Spectra, absorption of some higher oxides (Dutta and Sen Gupta), 397.
- Spectrum arc of iodine (Deb), 380.
- Spectrum, arc, of rubidium (Jackson), 673.
- Spectrum lines, intensities according to quantum theory (Schott), 37.
- Stresses in braced frameworks, calculation (Southwell), 475.
- Taylor (G. I.) and Maccoll (J. W.) The Air Pressure on a Cone Moving at High Speeds, I, 278.
- Teichmann (H.) The Theory of the Crystal-Photoeffect, 105.
- Thermodynamics of adsorption at surface of solutions (Guggenheim and Adam), 218.
- Townend (D. T. A.) See Bone and others.
- Townend (D. T. A.) and Outridge (L. E.) Gaseous Combustion at High Pressures, XV, 74.
- Tungsten, positive ion work function for alkali metals (Evans), 604.
- Turnbull (R.) See McLennan and Turnbull.
- Viscosity of soft materials (Schofield and Blair), 557.
- Vitamin D, photochemical formation (Fosbinder), 93
- Werner (S.) Electron Scattering in Helium. Absolute Measurements at 90° and 45°, 113.
- Williams (E. J.) Applications of the Method of Impact Parameter in Collisions, 163.
- Wynn-Williams (C. E.) See Rutherford and others
- Xenon, stark effect (Harkness and Heard), 416
- Xenon, ultraviolet absorption bands (McLennan and Turnbull), 683.
- X-ray spectra of the radio-elements (Ellis), 336.
- X-ray study of copper-cadmium alloys (Owen and Pickup), 526.
- X-rays, atomic scattering factor (Coster and Knol), 459.

IMPERIAL AGRICULTURAL RESEARCH
INSTITUTE LIBRARY
NEW DELHI

Date of issue.	Date of issue.	Date of issue.
16.3.42		
18.8.42		
18.1.42		
20.1.42		
7-12-61		
16-12-80		